Transition Metal Catalyzed Carbon-Heteroatom Bond Formations

Dissertation

der Mathematisch-Naturwissenschaftlichen Fakultät

der Eberhard Karls Universität Tübingen

zur Erlangung des Grades eines

Doktors der Naturwissenschaften

(Dr. rer. nat.)

vorgelegt von

Regina Michaela Oechsner

aus Ingolstadt

Tübingen

2023

Gedruckt mit Genehmigung der Mathematisch-Naturwissenschaftlichen Fakultät der Eberhard Karls Universität Tübingen.

Tag der mündlichen Qualifikation:	13.09.2023
Dekan:	Prof. Dr. Thilo Stehle
1. Berichterstatterin:	Prof. Dr. Ivana Fleischer
2. Berichterstatter:	Prof. Dr. Martin E. Maier
3. Berichterstatter:	Prof. Dr. Marko Hapke

Preface

The following cumulative thesis describes two strategies for mild transition metal catalyzed carbon-heteroatom bond formations, including C-S bonds *via* cross-coupling, and C-I bonds *via* epimerization. An introduction and literature overview, as well as a summary of published and unpublished results, in addition to the published scientific articles with their corresponding supporting information are included.

This work has been carried out at the Institute of Organic Chemistry at the University of Tubingen, Germany, from August 2019 to August 2023, under the supervision of Prof. Dr. Ivana Fleischer. The epimerization project was carried out at the Institute of Chemistry at the University of Toronto, Canada, in the Group of Prof. Dr. Mark Lautens. Funding has been gratefully received from the German Academic Exchange Service (DAAD).

Acknowledgements

First and foremost, I would like to express my profound gratitude to Prof. Dr. Ivana Fleischer. Thank you for all the support, encouragement and trust. You have never failed to do your best for us, even under challenging circumstances. Your open door policy and your genuine interest in our research, but also into us, not just as your PhDs, but as private individuals, has made it a privilege to work on my dissertation in your group. I am glad beyond words that you are now a Professor in Tuebingen. My sincere gratitude also goes to the examination committee, Prof. Dr. Martin E. Maier the second assessor, Prof. Dr. Reiner Anwander and Prof. Dr. Holger F. Bettinger.

Now to the working group, including former and current members. I had the incredible luck to share most of my time as a PhD student with Dr. Valentin Geiger as co-worker. Your remarkable work ethic, even or especially in face of challenging and ungrateful research results, has always been an inspiration and highly motivating to me. Your broad knowledge and excellent advice in chemistry, as well as our discussions about work and private life have brightened up even the most demanding work days. Thank you for a great time. In addition, I would like to express my gratitude to Alexandru Căciuleanu for the insightful discussions about chemistry, as well as the highly educating information about Romanian folklore. Savva Ponomarev, who worked on his PhD during a rather challenging time, the way you dealt with it and continued moving forwards impressed me immensely. Anne Haupt for all you did for the working group. Robert Richter for the interesting experience synthesizing the pre-catalyst and preceptive conversations in the office and of course, Ivo H. Lindenmaier. It was my privilege and luck to supervise you during your internship in our group and later have you as a master student and PhD co-worker. Your help on the triflate project was invaluable, and it was a pleasure to see you follow your own path. I look forward to reading your future publications. Additionally, I would like to thank Dr. Paul H. Gehrtz for the opportunity to continue his research, Dr. Benjamin Ciszek for introducing me into the Fleischer group during a research internship, Dr. Prasad Kathe for the plentiful discussions and musical accompaniment in the laboratory and Dr. Marlene Böldl, for reminding us to not only think about work.

My gratitude also goes to the research internship, as well as Bachelor and Master students I had the opportunity to supervise including Miriam Abbas, Markus Fröhlich, Stefan Clewing, Robin Scholl, Alexander Huber and Adrian Ott.

The Analytics Department, the Metal Workshop and the Glass Shop of the University of Tuebingen have my gratitude for their excellent work and kind as well as helpful support.

Furthermore, my sincerest gratitude goes to Prof. Dr. Mark Lautens and the Lautens Group at the University of Toronto for the opportunity to work with and learn from them, as well as the German Academic Exchange Service (DAAD) for the research scholarship.
Additionally, I want to express my profound gratitude to all my friends, especially Theresa Rieser and Arne Kobalt, as well as the inspiring individuals I had the privilege to meet in the InOne Consult, for accompanying me on this journey.

And finally, the most important people, my family. I want to thank them for their unfailing support, unconditional love and continues encouragement throughout my years of studies and the PhD. They were a solid rock to stand on in turbulent times and I feel incredibly proud and thankful to have them in my life.

Summary

The following thesis focuses on the development of mild reaction conditions for previously challenging or unreported transformations with an emphasis on mechanistic insights. Transition metal catalysis enables a plethora of transformations, generating valuable synthetic products. One example is the C-S cross-coupling of aryl and alkenyl (pseudo)halides with alkyl thiols, generating thioethers, a compound class with widespread application in materials, agrochemicals and pharmaceuticals. An efficient synthesis of these high value compounds, by employing the air-stable, low-cost pre-catalyst XantphosNi(*o*-tolyl)Cl **Ni1** and KOAc as base in a mild, fast and convenient reaction, is the first part and main focus of this thesis. The developed methodology overcomes previous challenges in the field, including the utilization of tertiary alkyl thiols.

The first project focused on the coupling of aryl chlorides as challenging, but commercially available substrates, showcasing a scope of 50 examples with excellent yields and functional group tolerance (Scheme 1). A variety of alternative aryl (pseudo)halides, such as (ArI, ArBr, ArOTf) could be employed as electrophiles, demonstrating the versatility of the system. Chemoselective functionalization of di-substituted aryl (pseudo)halides enabled selective mono-coupling as well as sequential multi-functionalization. Subsequently, in the second project, the methodology was expanded to aryl and alkenyl triflates, synthesized in a straight-forward, one-step procedure from abundant phenols and ketones, with a scope of 38 examples, exhibiting superior reactivity and yields. Additionally, the applicability of the catalytic system for late stage functionalization of pharmaceutically active or biorelevant compounds was demonstrated.

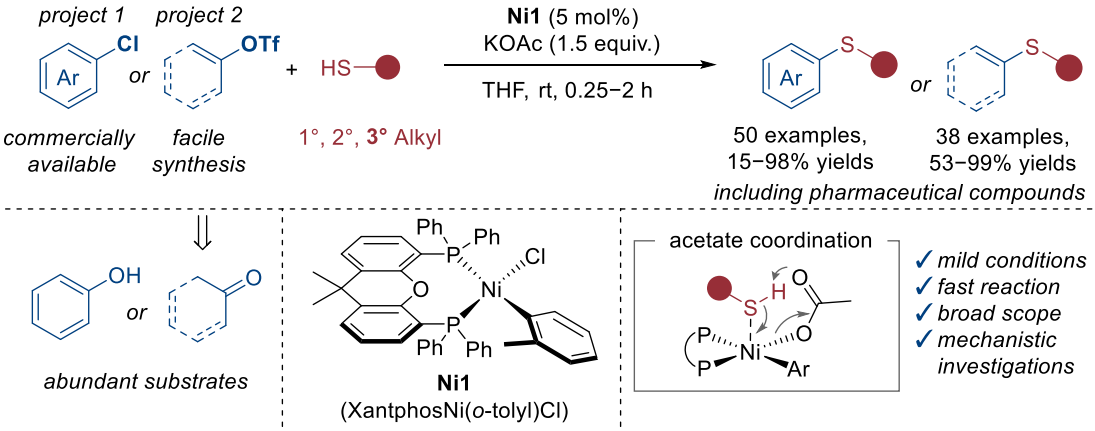

Scheme 1. Developed C-S cross-coupling of aryl and alkenyl (pseudo)halides with alkyl thiols utilizing the air-stable one-component pre-catalyst **Ni1** and KOAc as base under mild reaction conditions.

Extensive mechanistic investigations, including kinetic and NMR-studies, as well as DFT calculations, supporting a Ni(0)/Ni(II) catalytic cycle, were conducted. Several factors were identified as important for the reaction, including the hemilabile nature and adaptable coordination modes of Xantphos. An initial π-coordination of the aryl (pseudo)halide, such as ArCl to the active Ni(0) catalyst, facilitating the oxidative addition and generation of the corresponding Ni(II) complex XantphosNi(Ar)Cl, which acts as resting state of the catalytic cycle, in addition to an acetate coordination with subsequent acetate facilitated thiolate complex formation *via* internal deprotonation were postulated as key steps. The comparison of various LNi(Ar)X pre-catalysts identified generation of the active catalytic species LNi(0) as an important step for one-component pre-catalytic systems and showcased that the influence of ligand L has to be analyzed separately from catalyst activation (influence of Ar and X).

Preliminary experiments enabled mono-selective coupling of a prochiral di-chloro-biaryl model substrate in excellent yield with $Ni(cod)_2$/DPEPhos as catalytic system and showed potential for the developed system to generate thioether-based atropisomers after identification of suitable chiral ligands.

The second part of this thesis utilized stereochemical C-I bond editing in a palladium catalyzed epimerization under blue light irradiation (465 nm LED) from the *exo* to *endo* face of norbornene model compounds with 17 examples and *endo* selectivity up to > 20:1 (Scheme 2). Mechanistic studies and DFT calculations support a reversible C-I bond formation through a thermodynamically driven epimerization. Stochiometric experiments showcased a C-Br bond formation through reductive elimination under blue light irradiation from an isolated LPd(alkyl)Br complex, acting as conceptual proof and indicating the applicability of palladium catalysis under blue light irradiation for future carbobromination reactions.

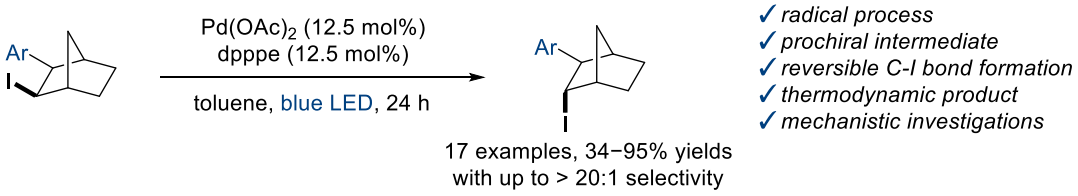

Scheme 2. Developed mild and base free palladium catalyzed epimerization under blue light irradiation *via* reversible C-I bond formation yielding the thermodynamic *endo* product.

Zusammenfassung

Übergangsmetallkatalyse ermöglicht eine Vielzahl von Reaktionen durch welche wertvolle Produkte synthetisiert werden können. Ein Beispiel hierfür ist die C-S Kreuzkupplung von Aryl- und Alkenyl(pseudo)halogeniden mit Alkylthiolen. Die entstandenen Thioether sind eine verbreitete Verbindungsklasse in der Material-, Agro- und pharmazeutischen Chemie. Eine effiziente Synthese dieser Verbindungen unter Verwendung des luftstabilen und kostengünstigen Ni(II)-Präkatalysators XantphosNi(*o*-tolyl)Cl **Ni1** und KOAc als Base, in einer milden Reaktion ist der erste Teil und Schwerpunkt dieser Arbeit. Die entwickelte Methode überwindet vorherige Limitationen auf dem Gebiet, wie beispielsweise die Verwendung von tertiären Alkylthiolen. Das erste Projekt konzentrierte sich auf die Kupplung von Arylchloriden als anspruchsvolle, aber kommerziell erhältliche Substrate. 50 Thioether mit ausgezeichneter funktioneller Gruppentoleranz konnten isoliert werden (Schema 1). Weitere Aryl(pseudo)halogenide (ArI, ArBr, ArOTf) welche erfolgreich als Elektrophile eingesetzt werden konnten demonstrieren die Vielseitigkeit des Systems. Darüber hinaus ermöglichte die chemoselektive Funktionalisierung von disubstituierten Aryl(pseudo)halogeniden selektive Monokupplung und sequentielle Multifunktionalisierung. Im zweiten Projekt wurde die Methode auf Aryl- und Alkenyltriflate ausgeweitet, welche durch eine einfache Ein-Schritt Synthese aus in der Natur zahlreich vorhandenen Phenolen und Ketonen synthetisiert werden konnten. 38 Aryl und Alkenyl Thioether wurden isoliert und wiesen eine überlegene Reaktivität und Ausbeute im Vergleich zu Arylchloriden auf. Zudem konnte das katalytische System für die Funktionalisierung von pharmazeutisch aktiven oder biorelevanten Verbindungen verwendet werden.

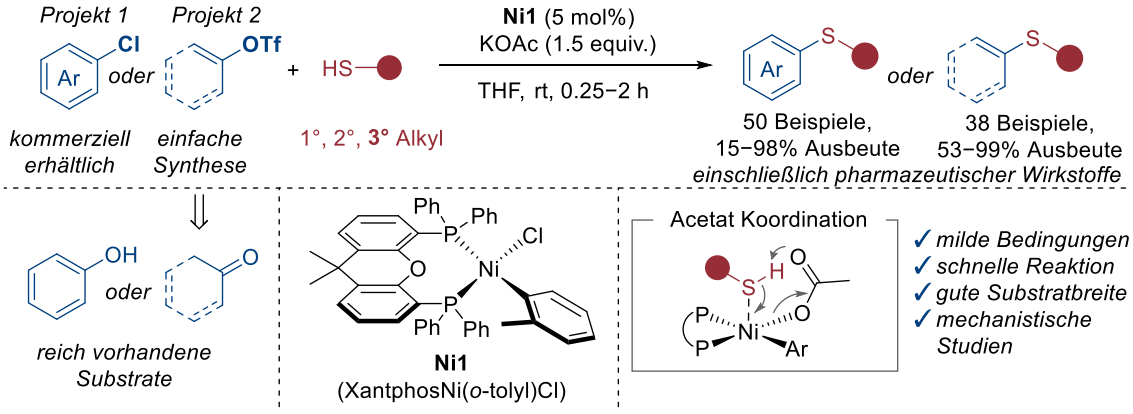

Schema 1. C-S Kreuzkupplung von Aryl- und Alkenyl(pseudo)halogeniden mit Alkylthiolen unter Verwendung des luftstabilen Präkatalysators **Ni1** und milden Reaktionsbedingungen.

Umfassende mechanistische Untersuchungen, einschließlich kinetischer und NMR-Studien, sowie DFT-Rechnungen wurden durchgeführt und unterstützen einen Ni(0)/Ni(II) Katalysezyklus. Mehrere Faktoren wurden als wichtig für die Reaktion identifiziert. Eine initiale π-Koordination von Aryl(pseudo)halogeniden (z.B. ArCl) an den aktiven Ni(0) Katalysator erleichtert die oxidative Addition und die Bildung des entsprechenden Ni(II) Komplexes XantphosNi(Ar)Cl, welcher als Ruhezustand des Katalysezyklus fungiert. Zudem wird eine Acetat Koordination mit anschließender Acetat unterstützter Thiolat-Komplexbildung über eine interne Deprotonierung postuliert. Die anpassungsfähigen Koordinationsmodi und hemilabile Natur von Xantphos ist ein weiterer wichtiger Aspekt. Im Hinblick auf die Verwendung von Ein-Komponenten Präkatalystoren LNi(Ar)X, wurde beim Vergleich verschiedener Strukturen festgestellt, dass die Erzeugung des aktiven LNi(0) Katalysators ein wichtiger Schritt ist und der Einfluss des Liganden L getrennt von der Aktivierung (Einfluss der Liganden Ar und X) betrachtet werden sollte. Vorläufige Experimente ermöglichten die monoselektive Kopplung eines prochiralen Dichlor-Biaryl Substrat in ausgezeichneter Ausbeuten mit $Ni(cod)_2$/DPEPhos als katalytisches System und zeigten Potenzial für die zukünftige Synthese von Thioether basierten Atropisomeren, wenn geeignete chirale Liganden identifiziert werden können.

Das zweite Thema dieser Arbeit ist die Editierung der C-I Bindung in einer palladiumkatalysierten Epimerisierung unter Blaulichtbestrahlung (465 nm LED) von der *exo* zur *endo* Seite in Norbornen-Verbindungen mit 17 Beispielen und einer *endo* Selektivität von bis zu > 20:1 (Schema 2). Mechanistische Studien und DFT-Rechnungen zeigen eine reversible C-I Bindungsbildung durch eine thermodynamisch getriebene Epimerisierung. Stöchiometrische Experimente unterstützen eine C-Br Bindungsbildung unter Blaulichtbestrahlung durch eine reduktive Eliminierung von einem isolierten LPd(alkyl)Br Komplex. Dies fungiert als konzeptioneller Beweis und Indiz für die Anwendbarkeit der Palladiumkatalyse unter Blaulichtbestrahlung in zukünftigen Carbobromierungsreaktionen.

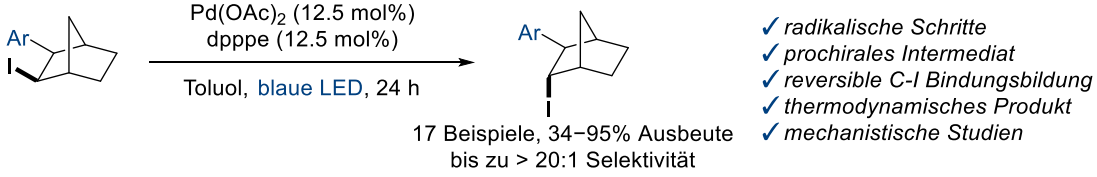

Schema 2. Milde und basenfreie palladiumkatalysierte Epimerisierung unter Blaulichtbestrahlung über eine reversible C-I Bindungsbildung generiert das thermodynamische *endo* Produkt.

Publications

Publications incorporated into this thesis:

Paper I Acetate Facilitated Nickel Catalyzed Coupling of Aryl Chlorides and Alkyl Thiols
R. M. Oechsner, J. P. Wagner, I. Fleischer
ACS Catal. **2022**, *12*, 2233-2243
https://doi.org/10.1021/acscatal.1c04895

Paper II Nickel Catalyzed Cross Coupling of Aryl and Alkenyl Triflates with Alkyl Thiols
R. M. Oechsner[†], I. H. Lindenmaier[†], I. Fleischer
Org. Lett. **2023**, *25*, 1655-1660
https://doi.org/10.1021/acs.orglett.3c00218

Paper III Flipping the Switch on Palladium-Catalyzed Carboiodination: Accessing Kinetic and Thermodynamic Products
R. Arora, R. M. Oechsner, C. Jans, B. Mirabi, A. D. Marchese, M. Lautens
ACS Catal. **2023**, *13*, 6562-6567
https://doi.org/10.1021/acscatal.3c01055

Poster Presentation:

Poster I Acetate Facilitated Nickel Catalyzed Cross Coupling of Aryl Chlorides and Alkyl Thiols
R. M. Oechsner, J. P. Wagner, I. Fleischer

Personal Contribution

Paper I:

All reactions were designed and carried out by R. M. Oechsner, including optimization of the reaction conditions, catalytic reactions and collection of the analytical data. DFT calculations were carried out and the corresponding paragraph in the manuscript was written by J. P. Wagner. The manuscript and supporting information were written by R. M. Oechsner and corrected by I. Fleischer.

Paper II:

The reactions were designed by R. M. Oechsner and the substrates were synthesized by I. H. Lindenmaier. Product yielding catalytic reactions were performed, the analytical data collected and the supporting information written by R. M. Oechsner with support from I. H. Lindenmaier. The manuscript was written by R. M. Oechsner and corrected by I. Fleischer.

Paper III:

The initial hit was observed by R. Arora and A. D. Marchese. Experiments were designed by R. Arora, A. D. Marchese and R. M. Oechsner. Substrate synthesis and product yielding catalytic reactions, as well collection of analytical data was conducted by R. Arora, R. M. Oechsner and C. Jans. R. M. Oechsner and R. Arora isolated the catalytic intermediates and designed mechanistic experiments with support from A.D. Marchese. DFT calculations were conducted by B. Mirabi. The manuscript was written by R. Arora and A.D. Marchese, finalized with input from B. Mirabi and R. M. Oechsner and corrected by M. Lautens.

Copyright

Parts of this thesis are included in the Master thesis of I. H. Lindenmaier and A. Huber, which were initiated and closely supervised by R. M. Oechsner.

Objective

The following thesis will discuss two general themes, detailing mild and efficient transition metal catalyzed carbon-heteroatom bond formations. The first theme and main focus is the synthesis of thioethers *via* nickel catalyzed C-S cross-coupling of alkyl thiols with a variety of aryl and alkenyl (pseudo)halides, with an emphasis on aryl chlorides for the first, and aryl as well as alkenyl triflates for the second project. The second theme consist of a palladium catalyzed epimerization under blue light irradiation as a method for C-I bond editing.

After an initial introduction into catalysis and cross-coupling, a literature overview of transition metal catalyzed thioether synthesis *via* C-S cross-coupling is followed by a short introduction into stereochemistry and stereochemical editing *via* epimerization. Subsequently, a summary of the published and unpublished results is presented and the published scientific articles are included with their corresponding supporting information.

Table of Contents

Chapter 1

INTRODUCTION

1. Introduction

1.1. Catalysis

"A catalyst is a substance which increases the rate at which a chemical reaction approaches equilibrium without becoming itself permanently involved"[1]

This modern definition of catalysis could be specified through the contributions of countless scientists over the past centuries. Understanding of the concept started in the 18th century, with Berzelius coining the term catalysis in 1835 and key contributions by Ostwald.[2] Catalysis has played an intriguing role in the development of humanity since ancient times and remains essential until today. Millenia ago, many early societies unknowingly utilized enzyme catalysis in the production of various goods, such as alcoholic beverages (7000 BCE),[3] cheese (5400 BCE)[4] or soap (2200 BCE).[5] Harnessing the potential of catalysis for the chemical industry started in the 18th century, when the first catalytic processes were employed in industrial applications,[6] while understanding of the concept as a whole took until the 19th century. Since then, catalysis has developed into an irreplaceable tool in synthetic chemistry, academic research and industrial applications.[7] The majority of industrial chemicals today are produced *via* catalysis, from fuels and bulk chemicals to fine chemicals, such as pharmaceutical compounds.[6] While catalysts do not influence thermodynamics and therefore the equilibrium of a chemical reaction, they can influence kinetics and increase the reaction rate through an energetically favorable, but more complex mechanism which decreases the required activation energy E_A (Figure 1). During the reaction a catalyst is not consumed and can be regenerated afterwards.[7]

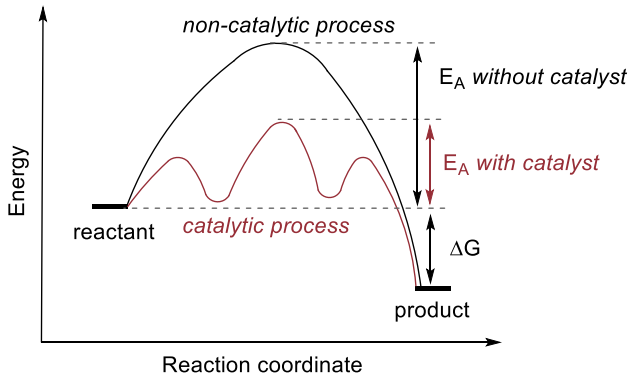

Figure 1. Simplified energy surface for catalytic and non-catalytic transformations.[7]

Catalysis can be categorized into heterogeneous and homogeneous reactions. Heterogeneous catalysis describes reactions in distinct, differing physical phases (e.g. solid phase catalyst and gas phase reactant), with the reaction commonly occurring at the interface, on the surface of a solid catalyst, through the continuous creation of active catalytic sites.[8] While the employed catalyst and resulting mechanism are typically complex, the phase boundary between reactants/products and catalyst enables facile separation and recycling, which is important for an efficient process on large scales. Heterogeneous catalysis is therefore predominantly employed in industrial applications for the production of materials, chemicals and fuels.[9] An important example is the energy intensive Haber Bosch process, which produces nitrogen-based fertilizer for agriculture.[10] This thesis will concentrate solely on homogeneous catalysis, in which substrate and catalyst are in the same, commonly liquid, phase. While separation of homogeneous catalysts from a reaction mixture is more challenging, the high catalytic activity and selectivity (chemo-, regio-, diastereo- and enantioselectivity) permit previously unprecedented transformations. This is enabled through the defined transition metal complexes, in which the metal center is coordinated by ligands. Through varying the metal and adapting the ligand sphere, characteristics and therefore reactivity of the catalyst can be modified and controlled.[1, 7]

1.2. Cross-Coupling

The importance of homogeneous catalysis has been recognized by several Nobel Prizes in the 21st century, including the 2010 Nobel Prize in chemistry, received by Negishi, Suzuki and Heck for the development of key reactions in the field of palladium catalyzed cross-coupling reactions.[11] As an important and rapidly developing discipline with a plethora of reactions and publications, cross-coupling chemistry has led to essential discoveries in a variety of fields, such as materials, agrochemicals and pharmaceuticals.[12] A specific application example is the synthesis of the blood pressure medication Losartan, which includes a late-stage Suzuki-Miyaura coupling (Scheme 3).[13] Cross-coupling is one of the most important and versatile tools in synthetic organic chemistry for the construction of carbon-carbon (C-C) and carbon-heteroatom (C-Heteroatom) bonds through the connection of two organic reagents.[14] The exclusive and selective formation of the cross-coupling products, with limited homo-coupling, is crucial for an efficient transformation. Due to the significant C-C and C-Heteroatom bond strength in some reactants, cleavage can be difficult to achieve in one step, requiring harsh reaction conditions to overcome the high activation barrier.

Catalytic reactions, such as cross-coupling, open up an alternative reaction pathway through a multiple step mechanism with smaller activation barriers *via* the generation of catalytic intermediates (in which molecules involved in the reaction coordinate to the metal complex in a stepwise process, Figure 1),[15] leading to an increase of the reaction rate, even under milder reaction conditions.

The transition metal catalyzed covalent bond formation between two reagents, such as a reaction of aryl, alkyl or alkenyl (pseudo)halides as electrophile with varying organometallic, alkene, alkyne or heteroatom (pseudo)nucleophilic coupling partners are commonly classified depending on the nature of the nucleophile (Scheme 3).[12d, 14] Examples for carbon-based nucleophiles include Grignard reagents (Kumada-Corriu),[16] organoboronic acids (Suzuki-Miyaura),[17] organozinc reagents (Negishi),[18] organotin reagents (Stille),[19] alkenes (Mizoroki-Heck)[20] and alkynes (Heck-Cassar-Sonogashira).[21] In addition to C-C, a variety of C-Heteroatom,[12c] such as C-N (Buchwald-Hartwig)[22] and C-S (Migita)[23] bonds can be generated.

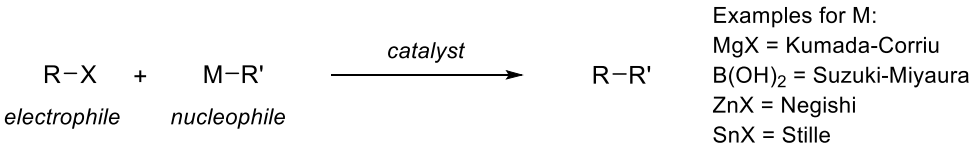

Scheme 3. Examples for cross-coupling reactions classified by the nucleophile.[14]

Palladium is the most frequently utilized catalyst, especially in industrial applications.[11-12] Its popularity is based on multiple factors, including the intensively studied and well understood mechanism with predictable reaction pathways, as well as the exceptionally optimized transformations with low catalyst loading and excellent control over the ligand sphere enabled by well-studied privileged ligands, allowing for challenging and highly selective transformations.[24]

A variety of cross-coupling reactions proceed through a classic Pd(0)/Pd(II) catalytic cycle (Scheme 4). After activation of the catalyst, the mechanism commonly involves three elementary steps, with an initial oxidative addition of the electrophile to the active catalyst $L_nPd(0)$, a subsequent transmetalation of the nucleophile, followed by a reductive elimination to yield the corresponding product and regenerate the active catalyst.[14] While the classic catalytic cycle does not represent all cross-coupling reactions, a variety, such as Kumada-Corriu, Suzuki-Miyaura, Negishi and Stille are generally accepted to follow it, while others, such as Heck, Sonogashira and Buchwald-Hartwig diverge after the initial oxidative addition.

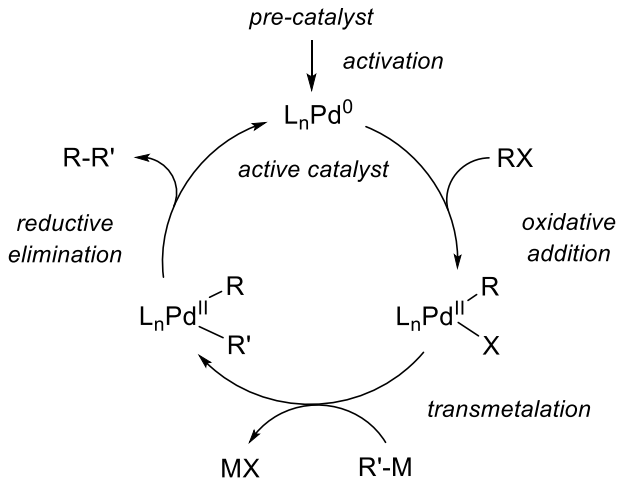

Scheme 4. General mechanism for cross-coupling reactions with a Pd(0)/Pd(II) catalytic cycle.[14, 24]

Cross-coupling reactions have been an intensely researched field for the last 50 years, but new developments are continuously pushing the boundaries of possible transformations. The developments include control over the ligand sphere and utilization of abundant low-cost transition metal catalysts (e.g. Ni, Cu, Fe), extending the substrate scope to non-activated, challenging electrophiles and nucleophiles, as well as chemo-, regio-, diastereo- and enantioselective transformations under mild and convenient reaction conditions. Furthermore, classic cross-coupling has inspired new transformations, such as cross-electrophile and cross-nucleophile coupling, as well as electrochemical and photocatalytic reactions, which open up alternative reaction pathways *via* a radical mechanism.[25]

New challenges for the chemical industry in the 21st century include a shortage of energy and fossil fuels, as well as an increasing overall sustainability-consciousness and subsequently stricter environmental regulations. Therefore, in addition to stability, activity and selectivity, new factors, such as sustainability, environmental impact (toxicity and biocompatibility e.g. biomass as alternative feedstock for substrates), as well as energy efficiency (e.g. mild reaction conditions) have gained importance for the development of new catalytic systems.[25]

In the following chapters, selected features of catalytic coupling reactions, including aryl and alkenyl (pseudo)halides as electrophiles, catalyst precursors with Ni(0) and Ni(II) examples, as well as ligands, concentrating on bidentate phosphines, will be discussed.

1.2.1. Aryl and Alkenyl (Pseudo)halides as Electrophiles

While the nucleophile is essential and often name-defining in cross-coupling reactions (Scheme 3), the electrophile is of equal importance. Aryl and alkenyl (pseudo)halides, including aryl and alkenyl halides (ArI, ArBr, ArCl) as well as sulfonates (ArOTf, ArOTs, ArOMs), herein referred to as pseudohalides, are commonly employed as electrophilic coupling partners.[12c] While the electrophile would therefore be a poor choice for classification, it has an important influence on the overall reaction.

Aryl halides present valuable building blocks utilized in organic chemistry and are commonly employed as substrates in a variety of cross-coupling reactions. Inversely proportional to the C-X bond strength, which is approximated by the bond dissociation energy (BDE, Figure 2), the reactivity of aryl halides and ease of oxidative addition to an active Pd/Ni(0) catalyst commonly decreases from PhI > PhBr > PhCl.[26] This reactivity order was experimentally observed by Fitton and Rick in 1971 for the oxidative addition of the corresponding aryl halides to palladium.[27]

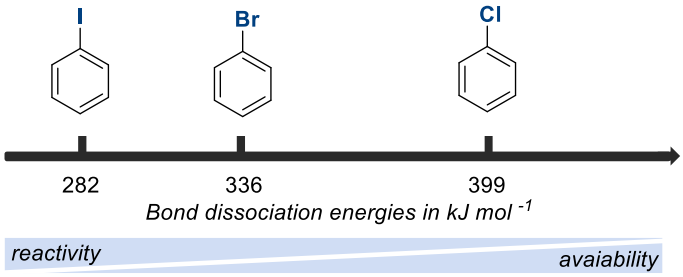

Figure 2. Bond dissociation energy (BDE) of aryl iodide, bromide and chloride, including reactivity as well as commercial availability trends.[28]

Until the 1990s[29] aryl and alkenyl iodides as well as bromides were primarily employed as competent electrophiles and coupling partners due to their weaker bond strength and high reactivity. Later, the development of novel ligands and reactive catalytic systems enabled the cross-coupling of comparatively stable aryl chlorides (Figure 3), giving access to a vast range of low-cost substrates.[30] Although aryl halides are excellent electrophiles, their accessibility is limited if they are not commercially available. Synthesizing aryl or alkenyl halides may require multiple steps, forcing reaction conditions with a limited functional group tolerance and highly toxic chemicals.[31] In contrast, aryl and alkenyl pseudohalides, such as triflates (ROTf), tosylates (ROTs) and mesylates (ROMs) are easily accessible in a straightforward one-step procedure from the corresponding phenols[32] and ketones[33] respectively (Scheme 6).

Phenols and ketones exist ubiquitously in nature and are present in organic compounds with a wide range of functionalities, rendering the oxygen based electrophiles derived from them versatile building blocks useful for the synthesis of complex or pharmaceutically active compounds.[29, 34]

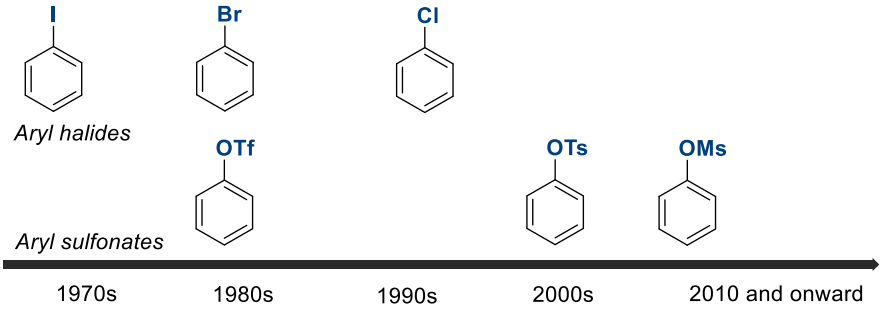

Figure 3. Development timeline for the utilization of certain aryl (pseudo)halides as electrophiles in cross-coupling reactions.[29]

Triflates are among the most reactive aryl and alkenyl pseudohalides due to the strong electron-withdrawing ability of the trifluoromethylsulfonyl group. They were first employed in cross-coupling reactions at a similar time to aryl bromides and often show a comparable reactivity, undergoing facile oxidative addition.[35]

While alkenyl halides are sparsely commercially available and challenging to synthesize, alkenyl triflates are an attractive, comparatively easy to access alternative.[33] Their synthetic potential as substrates and intermediates is showcased through a multitude of high impact publications reporting the transformation of alkenyl triflates to the corresponding alkenyl halides, which can be seen as a preferable synthetic route compared to direct access (Scheme 5).[36]

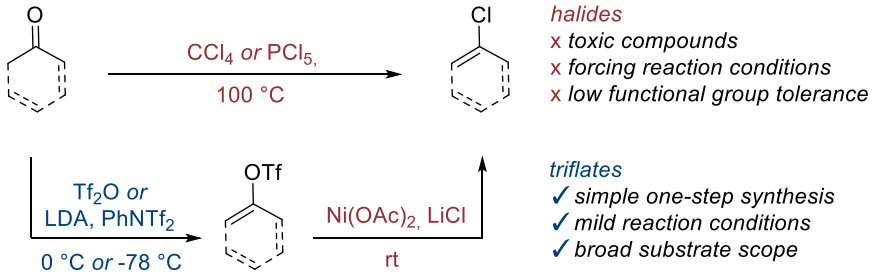

Scheme 5. Direct synthesis of alkenyl chlorides[31b, 31c] from ketones compared to the facile synthesis *via* alkenyl triflates[33] as attractive intermediates and electrophiles.[36]

Although triflates, as highly reactive pseudohalides, are attractive substrates, they have certain disadvantages. They may require long term storage under inert conditions or low temperatures, especially for alkenyl compounds and while their synthesis is straight-forwards and preferable to aryl and alkenyl halides, reagents such as triflic anhydride (Tf_2O), lithiumdiisopropylamid (LDA) or lithium bis(trimethylsilyl)amide (LiHMDS) are air-sensitive (Scheme 6).

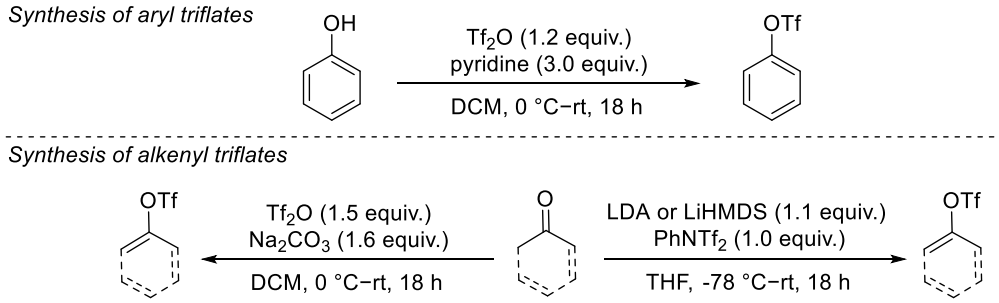

Scheme 6. Synthesis of aryl triflates with Tf_2O[32] and synthesis of alkenyl triflates with Tf_2O,[33b, 33c] or $PhNTf_2$ utilizing LDA or LiHMDS.[33d]

In the 2000s, aryl tosylates and later mesylates have emerged as alternative aryl pseudohalides (Figure 3), which can be synthesized *via* low-cost and air-stabe tosyl- and mesyl-chloride generating thermally stable solids.[29] Due to their higher stability, the C-O bond cleavage (e.g. oxidative additon) can be more challenging and may require harsher reaction conditions, partially migating the advantage of their synthesis and rendering catalytic systems which can activate such bonds desirable.[37]

The selectivity and therefore preferential reaction of aryl pseudohalides is less consistent and more fluid than for aryl halides, with a high dependence on the employed catalytic system, including metal, ligands, substrates and reaction conditions (in particular solvent polarity/coordinating ability).[26] While further studies are required to analyze and decode the influence, a variety of (chemo)selective Pd[38] and Ni[39] catalyzed cross-coupling reactions with various aryl (pseudo)halides have been reported. For palladium catalyzed reactions *via* a bis-ligated complex, I > Br ≈ OTf > Cl, with the relative order of Br and OTf dependent on the reaction conditions is a common, but not exclusive pattern.[26, 40]

Exemplary for solvent influence is the Pd/P^{t}Bu$_3$ catalyzed Suzuki coupling, which in coordinating solvents undergoes a preferential oxidative addition of triflate through a bis-ligated, solvent coordinated, transition state LPd(solvent), while in non-coordinating solvents the inverse order was observed with preferential oxidative addition of chloride *via* a mono-ligated transition state LPd.[40]

So while for bis-ligated palladium catalysts a preferential reaction of ArOTf > ArCl and for mono-ligated ArCl > ArOTf has been observed,[40] the selectivity in nickel catalyzed reactions is more complex.[26] Although the steric and electronic properties of electrophile and ligand influence the ease of oxidative addition to Ni(0) and therefore the selectivity, more studies are required to define general rules.[39]

Examples for nickel include the selective cross-Ullmann coupling *via* a two-catalyst system (Pd and Ni) by Weix and co-workers. The Pd/bidendate phosphine catalyst was observed to react preferentially with ArOTf > ArCl, while Ni/bidentate bipyridine, such as bpy, reacted preferentially with ArBr or ArCl > ArOTf.[41] Nickel catalyzed intermolecular competition experiments by Neufeldt and co-workers showcased that for monodentate small phosphine ligands, such as PCy_3, PPh_3, PMe_3 a preferential reaction of ArOTf > ArCl occurs. In regards to toslyates, the ligands PCy_3, PPh_3 (ArCl > ArOTs) and PMe_3 (ArOTs > ArCl) demonstrated a reverse selectivity order.[39]

1.2.2. Catalyst Precursors

While the oxidative addition, transmetalation and reductive elimination are three common elementary steps in a Pd/Ni(0)/(II) catalytic cycle (Scheme 4) a forth step, which is generally seen as outside the catalytic cycle, the generation of the active catalytic species, can have a strong influence on the performance of a catalytic system.[42] Generation of the active catalyst $L_nPd/Ni(0)$ is dependent on a variety of factors, such as nature and oxidation state of the metal, the coordinated ligands and reaction conditions. Activation can be induced or facilitated in various ways, including a metal reductant, substrate, base or (partial) dissociation of an ancillary ligand.

A popular method in catalysis is the *in-situ* generation of the catalyst *via* combination of metal source and ligand in a highly modular system, which is convenient for ligand screening, but requires coordination of the ligand to the metal source for generation of the active catalytic species. One option are the stable and comparatively low-cost Ni/Pd(II) salts (e.g. $Ni/PdCl_2$, $Ni/Pd(OAc)_2$, Table 1), which are less reactive and commonly require a reduction to generate the active catalytic species. Another option are air-sensitive and high-cost Ni/Pd(0) sources (e.g. $Ni(cod)_2$, $Pd_2(dba)_3$, Table 1). They are highly reactive and do not require reducing agents for activation, which is advantageous for rapid ligand screening, but storage under inert conditions is necessary. Due to the high price of $Ni(cod)_2$ utilizing it as catalyst precursor partially negates the advantage of nickel as low-cost alternative to palladium. Additionally, labile ligands such as cod have been observed to diminish catalytic activity by coordinating to and therefore stabilizing the active catalyst.[43]

Table 1: Price of catalyst precursors (Sigma-Aldrich, comparable batch sizes, see Chapter 6, Table 6).

	$NiCl_2$	$PdCl_2$	$Ni(OAc)_2$	$Pd(OAc)_2$	$Ni(cod)_2$	$Pd_2(dba)_3$
Price per 1 g	2.50 €	71.20 €	0.28 €	63.20 €	64.40 €	83.80 €

Well-defined and air-stable one-component Ni/Pd(II) pre-catalysts present an attractive alternative.[44] A variety of them have been developed and successfully employed in cross-coupling reactions, including commercially available examples (Figure 4).[45] A common structure for such pre-catalysts is LNi(Ar)Cl, with a variety of examples for phosphine-containing Ni(II) complexes developed by Jamison and co-workers,[46] including XantphosNi(*o*-tolyl)Cl **Ni1**, which can be conveniently synthesized from low-cost $NiCl_2$.

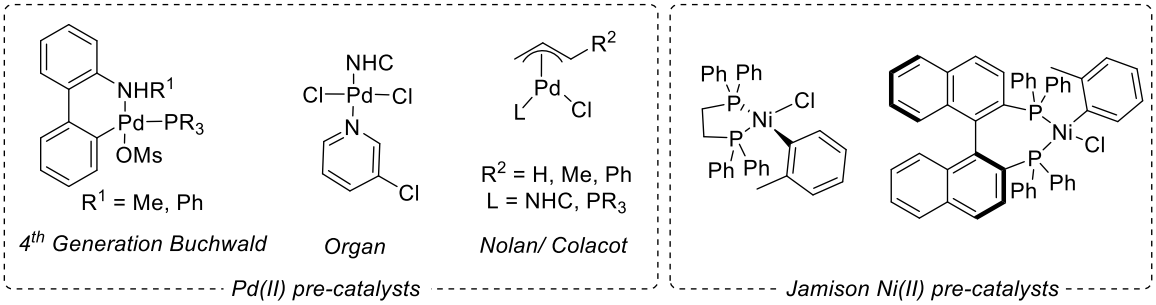

Figure 4. Selected examples of commercially available, air-stable and mono-ligated Pd(II)[45] and Ni(II)[46] pre-catalysts utilized in cross-coupling reactions (NHC = N-hetereocyclic carbene).

The system presents several advantages. In addition to convenient storage under air, the ligand is pre-coordinated and the catalyst can therefore be directly activated. This is possible *via* multiple pathways, such as a reaction with the cross-coupling nucleophile (see Chapter 2.1) or an external reductant. Additionally, the fixed 1:1 metal to ligand ratio in defined pre-catalysts of bidentate phosphines is ideal for the generation of mono-ligated and active LPd/Ni(0) species. The bis-ligated species for bidentate phosphine ligands L_2Pd has been reported to act as catalyst sink,[47] rendering an excess of ligand leading to a dimeric coordination disadvantageous. The development and application of such convenient and low-cost one-component pre-catalysts has gained importance during the last years and enabled reactions under mild reaction conditions (see Chapter 1.3).[37]

1.2.3. Ligands including Bidendate Phosphines

Transition metal catalysts commonly consist of a metal center surrounded by a ligand sphere, which is defined through the electronic and steric properties (motif, denticity and bonding properties) of the coordinated ligands.[24a] They have an essential influence on the structure of the catalyst and can therefore enable control over reactivity as well as selectivity (chemo-, regio-, diastereo- and enantioselectivity). The utilization of novel ligands has led to substantial progress in transition metal catalyzed cross-coupling reactions during the last decades and expanded the substrate scope to previously challenging substrates.[14] Developing ligands which facilitate specific elementary steps, such as oxidative addition or reductive elimination, can influence the rate determining step, the slowest step of the catalytic cycle which limits and therefore defines the overall reaction rate, and increase it. Although the potential of a ligand is dependent on the reaction (metal, substrates, reaction conditions) and there is no generic solution, specific ligand classes have shown potential in a variety of transformations.

Phosphines, which are frequently utilized in transition metal catalysis, are such a ligand class. They have played a significant role in the development of Pd and Ni catalyzed cross-coupling reactions over the past decades. With highly adaptable electronic and steric properties, they can generate stable complexes, as well as active Pd/Ni(0) catalytic species, which react in a controlled and selective manner. As strong σ-donor ligands phosphines donate two electrons to the metal center and as π-acceptor ligands they withdraw electron density from the metal center through a π back-bonding *via* the anti-bonding σ* orbital (Figure 5).[1, 24a]

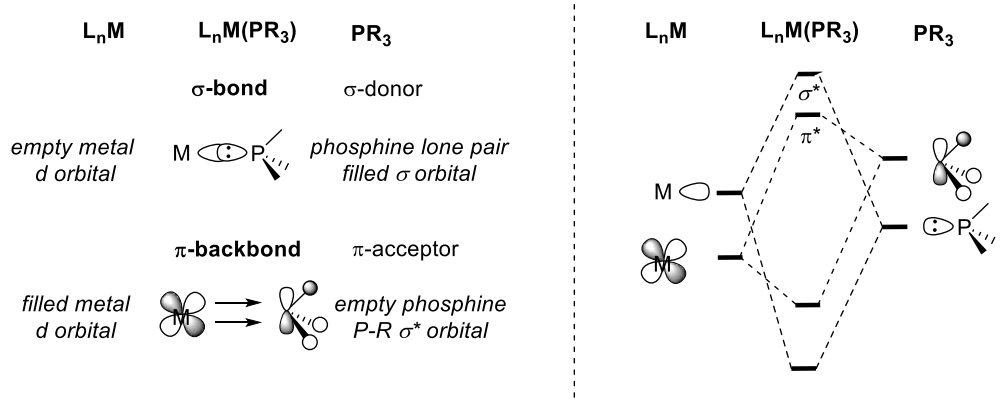

Figure 5. Phosphines as σ-donor and π-acceptor ligands with a simplified molecular orbital depiction.[1, 24a]

Since the 1990s, the development of novel electron-rich and sterically demanding phosphine ligands has progressed and gained importance. Bidentate ligands consisting of two phosphines connected through a backbone have enabled selective transformations in high yields and are therefore commonly utilized in cross-coupling reactions.[48] As electron donating ligands they increase the reactivity for an oxidative addition on the metal center, while the steric strain, induced through the wide bite angle, facilitates the reductive elimination, promoting both steps of the catalytic cycle. The generated complexes typically have a full coordination sphere and valence shell. While the dissociation of one phosphine and generation of highly active catalytic intermediates is possible, facile reassociation (due to the kinetic chelate effect) inhibits catalyst deactivation or off-cycle reactions (side-product formation), generating stable complexes.[48]

A wide variety of bidentate phosphine ligands have been successfully utilized in catalytic cross-coupling reactions (Figure 6).[1] Xantphos with a bite angle of 111°[49] and rigid backbone, as well as DPEPhos with a bite angle of 102°[49] and flexible backbone are examples of such ligands.

Their hemilabile nature enables the POP-type ligands to coordinate in a mono-, bi- and tridentate fashion through their versatile κ1, κ2 and κ3 coordination modes.[50] This gives rise to the unique ability to adapt the coordination mode to the requirements in the catalytic cycle, including varying oxidation states and steric needs. While the classic coordination is bidentate κ2, the oxygen of the ether linkage can coordinate in a κ3 pincer like fashion to stabilize intermediates with an unsaturated metal center. In addition, monodentate κ1 coordination, through a partial and reversible dissociation of one phosphine ligand can generate temporarily unsaturated and highly reactive catalytic intermediates.[50]

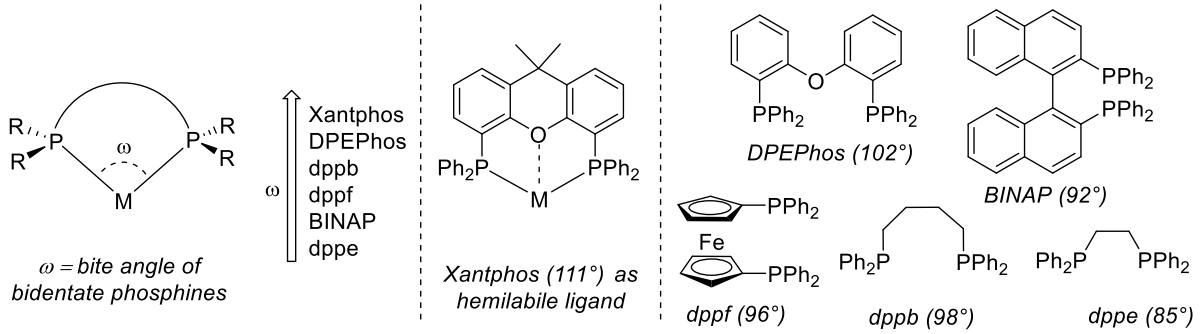

Figure 6. Depiction of the bite angle for a variety of bidentate phosphine ligands, including the hemilabile ligands Xantphos and DPEPhos.[1]

Catalytic systems are often developed through extensive screening and optimization experiments. While rational ligand design is ideal, it is not always realistically feasible. Predicting a ligands influence is challenging, due to the manifold of factors which influence the catalytic cycle and elementary steps. A trial and error method, consisting of predictions derived from literature reports for the influence of ligands and their electronic as well as steric adaptations, in combination with a transition metal-, ligand-, followed by reaction condition screening is commonly utilized to identify the ideal catalytic system and reaction conditions. Newer strategies, which have emerged in recent years, include machine learning and artificial intelligence as powerful tools that contribute toward a data-driven analysis,[51] allowing for more accurate yield and selectivity predictions (through the prediction of kinetic and thermodynamic properties).[52]

1.3. Synthesis of Thioethers *via* C-S Cross-Coupling

1.3.1. Thioethers

Sulfur containing compounds are abundant in nature and functionally important in a vast quantity of biomolecules. They are relevant in the active sites of proteins, essential for protein folding and involved in the biosynthesis of biologically active compounds. Examples are cofactors such as the vitamins biotin and thiamine, the amino acid cysteine, iron-sulfur clusters in proteins and the essential coenzyme Acetyl-CoA (Figure 7).[53]

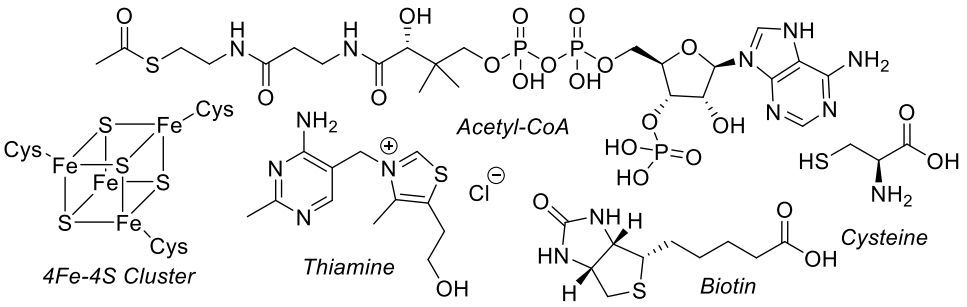

Figure 7. Examples of biologically active sulfur containing compounds.[53]

One of sulfurs functional groups are thioethers. The versatile structural class has found widespread application in material science, agrochemicals, as well as pharmaceutical compounds (Figure 8).[54] Pharmaceutically active sulfur compounds are abundant, with 25% of the top 200 FDA approved drugs in the USA (in 2014) containing sulfur, 11% of which were thioethers.[54a, 55]

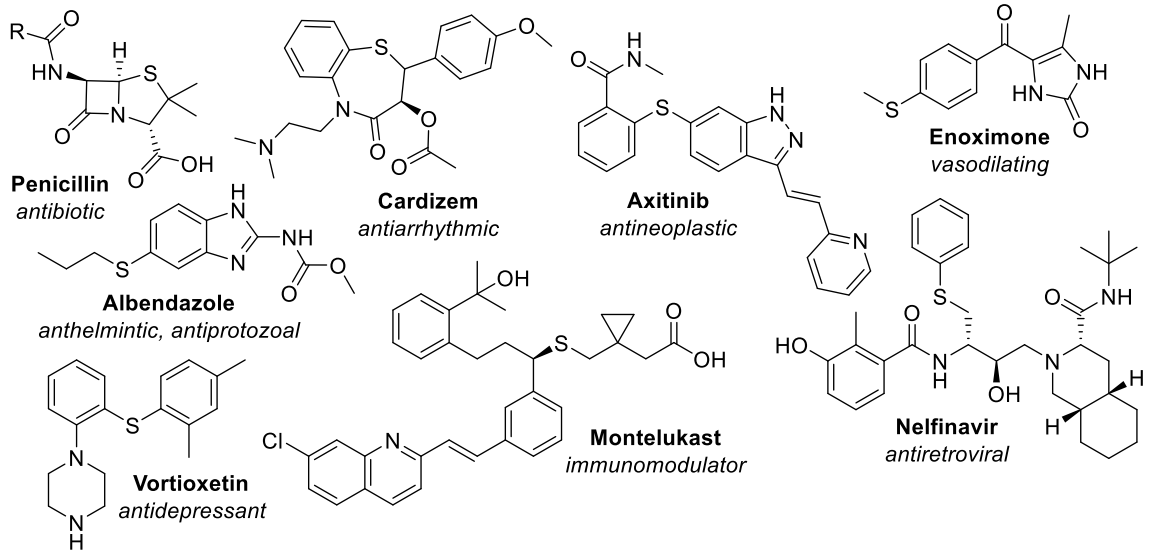

Figure 8. Examples of sulfur compounds, such as thioethers, with their pharmaceutical application.[56]

In medicinal chemistry thioethers can be employed as bioisosteres of oxoethers due to their higher lipophilicity,[57] which can increase membrane and therefore cell permeability and additionally has an effect on absorption, metabolism and target selectivity.[58]

A variety of methods are known to synthesize thioethers, such as simple, non-catalytic nucleophilic substitution or addition reactions, as well as nucleophilic aromatic substitution (limited to electron poor substrates).[59] While sulfur compounds commonly act as nucleophiles, the arylation of electrophilic S-reagents, such as N-chlorosuccinimide has been reported.[60] Additionally, various radical reactions have been utilized, including the coupling of diazoniumsalts.[61] One of the most versatile methods to synthesize thioethers is the transition metal catalyzed C-S coupling of thiols with electrophiles such as aryl and alkenyl (pseudo)halides or with nucleophiles such as boronic acid derivatives in a cross-nucleophile coupling (Scheme 7).[62]

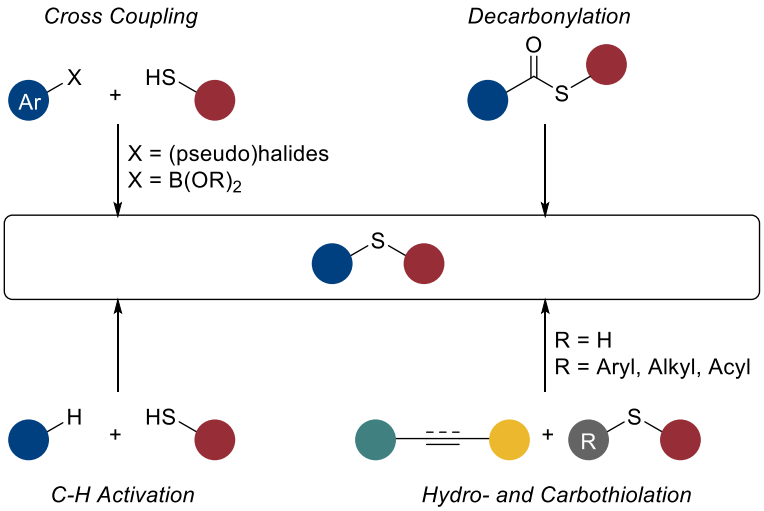

Scheme 7. Examples of transition metal catalyzed coupling reactions for the synthesis of thioethers.[62]

Other methods to access thioethers include the decarbonylation of carboxylic acid derivatives, such as thioesters,[63] C-H activation,[64] hydro- and carbothiolation,[65] as well as reversible arylation *via* C-S single-bond metathesis.[66] In addition to classic transition metal catalysis, a variety of electrochemical[67] and photocatalytic[68] strategies have been developed.

Due to their versatile application and common use in pharmaceutical compounds, efficient methods for the synthesis of thioethers are essential. The previously detailed non-catalytic routes, such as S_N2 or S_NAr reactions,[69] have a limited functional group tolerance and generally require harsh reaction conditions, rendering transition metal catalyzed cross-coupling an attractive alternative.

A multitude of reviews detailing C-S cross-coupling for a variety of transition metals[62, 70] or focusing on Pd,[71] Cu[72] and Fe,[73] including electrochemical[67] and photocatalytic[68] methods, have been published. In the following section a literature overview for transition metal catalyzed coupling reactions of aryl as well as alkenyl (pseudo)halides and thiols, with an emphasis on Pd and Ni, is presented. While electrochemical and photocatalytic transformations have been utilized, this chapter will concentrate on classic transition metal catalysis.

1.3.2. Historical Development

By harnessing the potential of transition metal catalysis, the C-S cross-coupling, more specifically for this work, the coupling of aryl (pseudo)halides and thiols, has developed into a versatile and powerful method for the synthesis of thioethers.

The pioneering work was published by Migita and co-workers in the 1978,[23a] and further explored in 1980,[23b] coining the term Migita coupling for the transformation. $Pd(PPh_3)_4$ was utilized as catalyst and NaO^tBu as base in DMSO or an alcoholic solvent at 100 °C or reflux conditions respectively to yield a variety of diary as well as a limited scope of aryl alkyl thioethers (Scheme 8). Aryl iodides and bromides reacted efficiently, whereas less reactive and more challenging aryl chlorides only provided moderate yields. The typical mechanism for palladium catalyzed C-S coupling reactions is postulated to consist of a Pd(0)/Pd(II) catalytic cycle *via* an initial oxidative addition to the active Pd(0) species, followed by a transmetalation or halide/thiolate ligand exchange and subsequent reductive elimination to yield the corresponding thioether as product and regenerate the active catalyst.

While the Migita coupling can refer to catalysis by various transition metals, the Ullmann type coupling refers specifically to copper catalyzed coupling of aryl halides and thiols, which was first reported in 1984 (see Chapter 1.3.5).[74] Although the original work from Migita was developed more than 40 years ago, the reaction conditions, employing precious metal catalysts, reactive and air-sensitive reagents, as well as high temperatures and long reaction times have remained common. Newer methods and current optimization focus on low-cost transition metal catalysis and mild reaction conditions, rendering the transformation economically feasible and more sustainable.

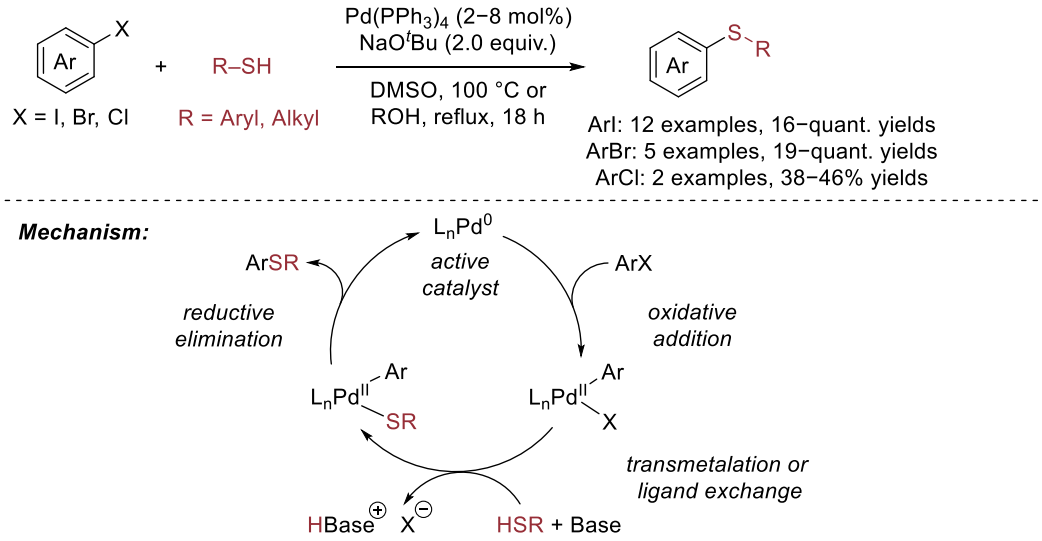

Scheme 8. Pioneering C-S cross-coupling of aryl halides and thiols by Migita and co-workers[23] and an overview of a typical postulated Pd(0)/Pd(II) catalytic cycle for the transformation.

1.3.3. Palladium Catalysis

Up to 40% of all cross-coupling reactions in the industrial synthesis of pharmaceutical compounds are palladium catalyzed.[12a] Despite the low natural abundance and high cost, the precious metal is still one of the most commonly employed catalysts, due to the predictable nature, which enables control over selectivity and reactivity patterns.[11]

A highly efficient palladium catalyzed C-S cross-coupling was published by Hartwig and co-workers in 2006,[75] employing a catalyst loading of $Pd(OAc)_2$ as low as 0.001 mol%. The Josiphos ligand **L1** and NaO^{t}Bu as base at 110°C enabled the coupling of a variety of aryl halides (ArCl, ArBr, ArI) and aryl as well as alkyl thiols (Scheme 9). Aryl pseudohalides (ArOTf, ArOTs) required a higher catalyst loading, longer reaction time and K_2CO_3 or Na_2CO_3 as base.

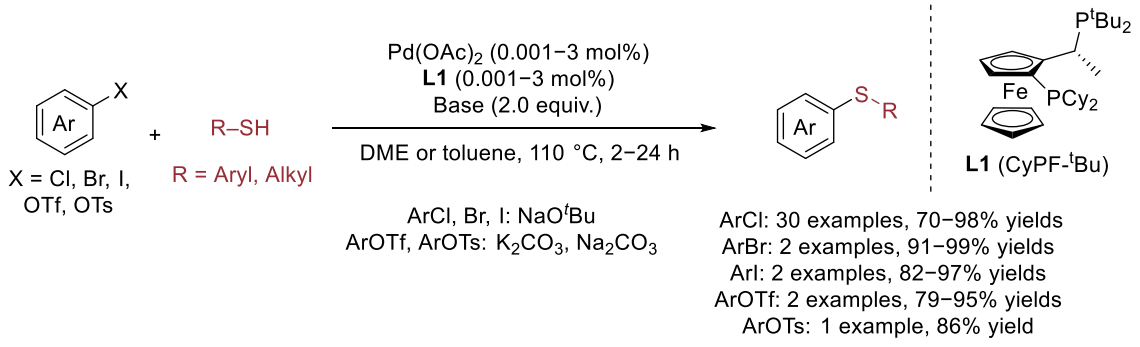

Scheme 9. Efficient palladium catalyzed C-S coupling of various aryl (pseudo)halides and thiols.[75]

A variety of catalytic systems for the palladium-catalyzed C-S cross-coupling with aryl (pseudo)halides have been developed since then, extending the functional group tolerance, increasing the substrate scope and exploring various ligands as well as reaction conditions. Bidentate phosphines (see Chapter 1.2.3) were identified in earlier reports as excellent ligands for the thioether synthesis *via* palladium catalyzed C-S cross-coupling with a strong base under high temperatures.[76] They were postulated to increase the stability and reactivity of the catalytic system under forcing reaction conditions, as they are challenging to displace by thiolate, rendering coordination and therefore poisoning of the catalyst, generation of off-cycle catalytic species, or β-hydride elimination, less likely. Additionally, reductive elimination and subsequent product formation is generally favored for such wide bite angle ligands due to the induced steric strain. Palladium catalyzed C-S cross-coupling with Xantphos as wide bite angle, bidentate phosphine ligand has been utilized in a variety of multiple step synthesis of pharmaceutical compounds,[77] such as fused thioglycosyls[77a] and 5-lypoxygenase inhibitors.[77b]

The often utilized harsh reaction conditions (high temperature, reactive and air-sensitive reagents) limit the functional group tolerance for pharmaceutically relevant compounds, such as protic heterocycles, and restrict the substrate scope for alkyl thiols, which readily undergo homocoupling. Alternative strategies, with milder conditions, include the use of one-component pre-catalysts, with bulky monodentate phosphine ligands on Pd(II)[47] or dimeric Pd(I) complexes,[78] as well as N-hetereocyclic carbene (NHC) ligands on Pd(II),[79] enabling a facile catalyst generation and circumventing the need for *in-situ* ligand coordination (see Chapter 1.2.2).

One example by Buchwald and co-workers[47] utilized the bulky monodentate phosphine ligands **L2** (^{t}BuXPhos) and **L3** (^{t}BuBrettPhos) in a one-component pre-catalyst **Pd1**, in combination with the soluble base Et_3N to enable the C-S coupling at room temperature (Scheme 10). Heteroaryl bromides could be coupled with aryl and alkyl thiols generating the corresponding thioether in excellent yields with a high functional group tolerance. Aryl thiols required a modified catalyst and LiHMDS, while aryl chlorides could not be employed as substrates in the reaction. The superior activity of sterically challenging monodentate biaryl phosphines, in comparison to the well-established bidentate phosphine ligands, was further investigated through mechanistic experiments, including NMR studies. Based on the observations it was postulated that at room temperature, with only a weak base, displacement of the ligand through thiol coordination was not a crucial problem and did not limit the efficiency of the catalytic system.

The low yield observed for bidentate phosphine ligands in this transformation is postulated to be due to the formation of stable and unreactive off-cycle PdL_2 species, in case of Xantphos, the generation of $Pd(Xantphos)_2$, which acts as catalyst sink.

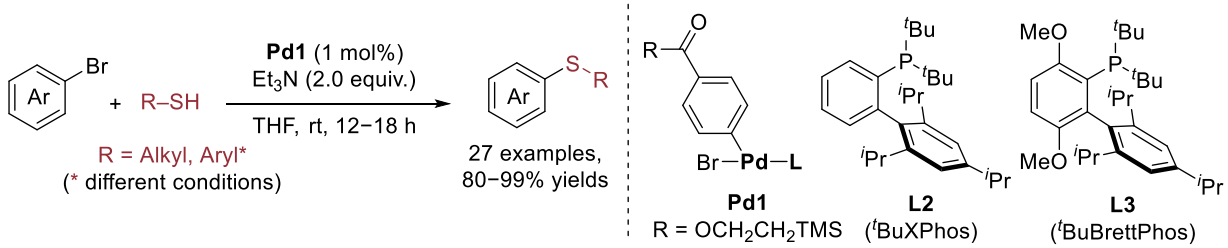

Scheme 10. Coupling of aryl bromides and thiols under mild reaction conditions catalyzed by one-component pre-catalyst **Pd1** with sterically challenging monodentate phosphine ligands **L2** and **L3**.[47]

In another notable contribution, a dimeric Pd(I) complex **Pd2** was developed by Schoenebeck and co-workers[78] for the selective thiolation of aryl bromides and iodides with sodium thiolates under moderate reaction conditions (Scheme 11). The air- and moisture-stable $[P^tBu_3Pd(\mu\text{-}I)]_2$ **Pd2** was found to be less susceptible to off-cycle deactivation by thiol and could be recovered, as well as recycled, with no loss in activity or efficiency for up to 5 rounds. Additionally, chemoselective thiolation of C-Br in the presence of C-OTf and C-Cl bonds was demonstrated. The mechanism was postulated to follow a Pd(I)/Pd(III) catalytic cycle starting with a ligand exchange.

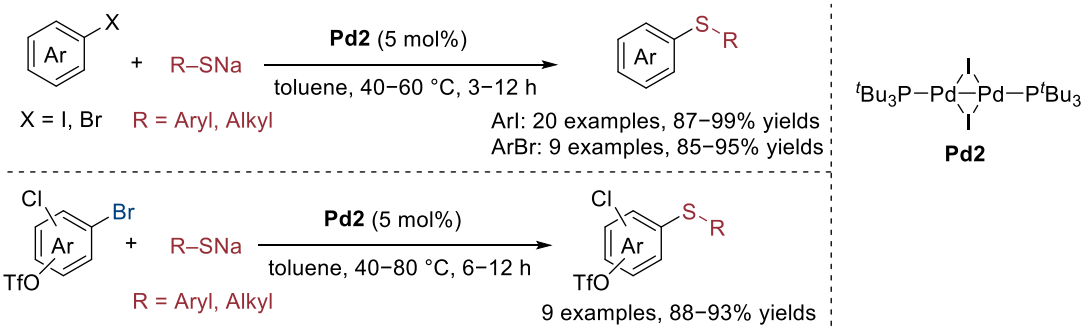

Scheme 11. Coupling of aryl bromides and iodides with sodium thiolates catalyzed by a dimeric Pd(I) pre-catalyst **Pd2**, including chemoselective C-Br bond thiolation in presence of C-Cl and C-OTf.[78]

One-component Pd(II)-NHC complexes, such as **Pd3**, reported by Organ and co-workers,[79a] have been successfully employed in a mild mechanochemical C-S cross-coupling *via* ball-milling developed by Browne and co-workers (Scheme 12).[79b] A variety of aryl bromides and iodides could be coupled with aryl and alkyl thiols under ambient, solvent-free and aerobic conditions. For alkyl thiols the addition of 2.5 equiv. zinc was essential and was postulated to prevent disulfide formation.

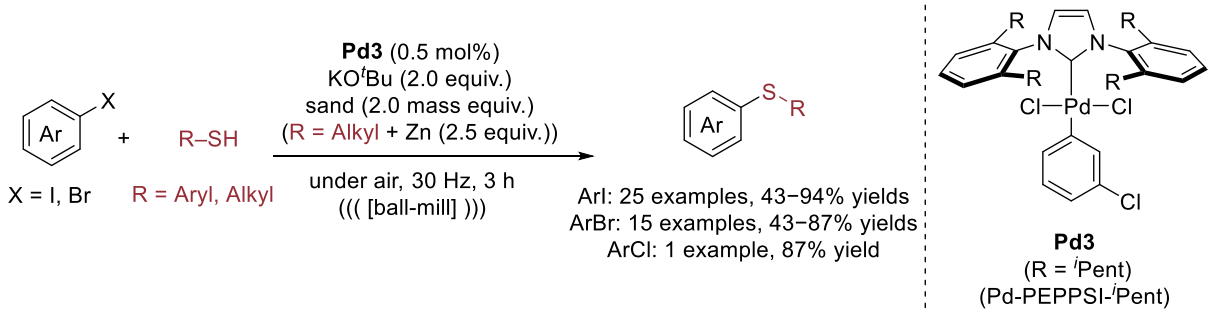

Scheme 12. Mechanochemical C-S cross-coupling using a ball-mill under ambient, solvent-free, aerobic conditions employing a one-component Pd(II)-NHC complex **Pd3**.[79b]

Aryl chlorides, as less reactive and more stable electrophiles (see Chapter 1.2.1) could not be coupled efficiently in a variety of transformations in the past, but more recent studies focus on the vastly commercially available substrates. The combination of not activated aryl chlorides and mild reaction conditions, such as a transformation at room temperature is highly desirable, but has remained elusive for palladium catalysis so far. A limited scope of activated heteroaryl chlorides, such as purine, pyrimidine and ribonucleosides were coupled with thiols at 50°C by Kapdi, Schulzke and co-workers,[80] employing $Pd(OAc)_2$/**L4** as catalytic system (Scheme 13). The catalytic system has been used prior successfully for C-N cross-coupling.[81]

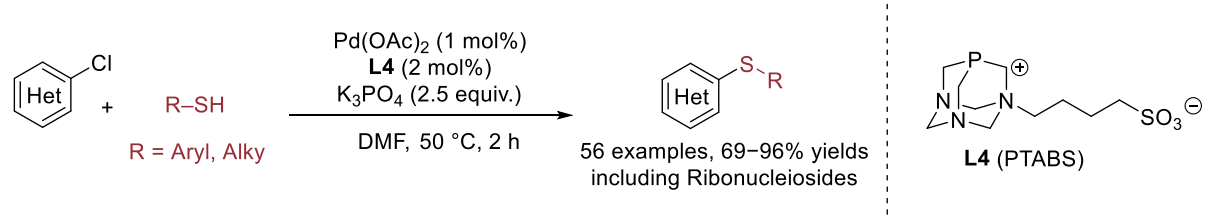

Scheme 13. Palladium catalyzed C-S cross-coupling of activated heteroaryl chlorides and thiols.[80]

Alternative sulfur containing compounds, including thioacetates[82] and 1,3-dithianes,[83] were utilized as substrates in thioether yielding palladium catalyzed C-S cross-coupling reactions with aryl chlorides and aryl bromides respectively.

In addition to aryl halides, aryl and alkenyl pseudohalides, such as triflates, have shown potential as electrophiles. They are easily accessible from ketones and phenols, rendering them attractive substrates for the synthesis of pharmaceutically relevant compounds (see Chapter 1.2.1). Although they can be competent electrophiles in C-S cross-coupling reactions, with palladium as most represented catalyst,[75-76, 84] publications solely on the coupling of aryl pseudohalides have remained rare, with limited examples in publications which focus primarily on the coupling of aryl halides.

In general, bidentate ligands such as Xantphos or BINAP, as well as elevated temperatures are common requirements. An early report, published by Zheng and co-workers[84a] in 1998, solely concentrates on the coupling of aryl triflates and n-butanethiol, utilizing $Pd(OAc)_2$/**L5** (Tol-BINAP) as catalytic system with NaO^tBu as base at 80°C (Scheme 14).

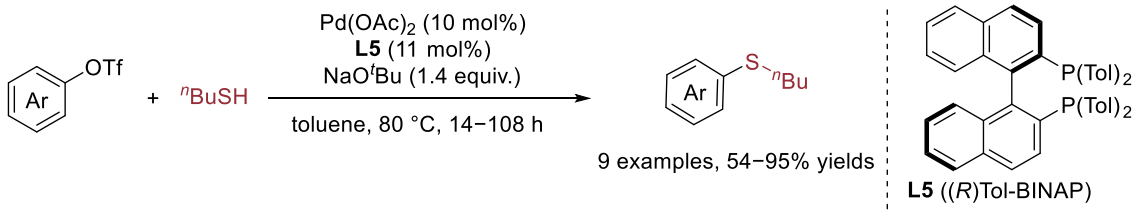

Scheme 14. Palladium catalyzed C-S cross-coupling of aryl triflates and n-butanethiol.[84a]

A vareity of aryl bromides and a limited scope of aryl triflates were coupled with aryl and alkyl thiols by Itoh and Mase,[76] employing $Pd_2(dba)_3$/**L6** (Xantphos) as catalytic system under reflux conditions (Scheme 15). Beslin and co-workers[84b] employed a similar catalytic system, with $Pd_2(dba)_3$/**L6** (Xantphos), K_2CO_3 as base at 140°C, coupling a variety of aryl bromides and a limited scope of aryl triflates and chlorides. In addition to aryl and alkyl thiols alternative sulfur containing compounds, such as triisopropylsilanethiol have been employed to synthesize thioethers in a C-S coupling of aryl halides and triflates.[84d]

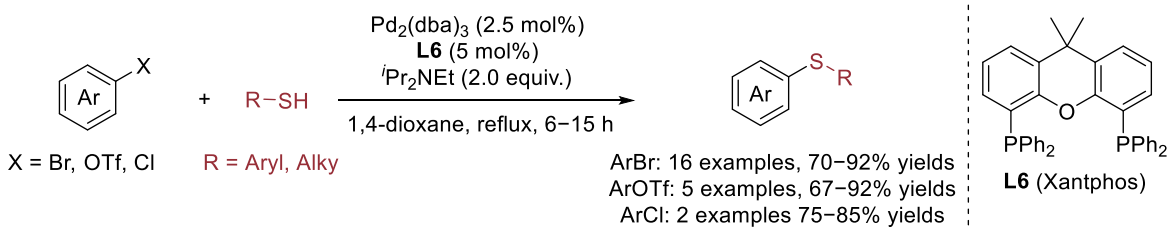

Scheme 15. Palladium catalyzed cross-coupling of aryl bromides, triflates and chlorides with thiols.[76]

Alkenyl (pseudo)halides represent valuable building blocks,[70a] but are a less explored substrate class in C-S cross-coupling compared to aryl (pseudo)halides, despite the synthetic potential of alkenyl thioethers, which are structural motifs common in pharmaceutical compounds.[85] The palladium catalyzed literature overview will concentrate on alkenyl pseudohalides, due to the limited availability and inconvenient synthesis of alkenyl halides (see Chapter 1.2.1). Only few examples for alkenyl triflates[86] and tosylates,[87] requiring forcing reaction conditions under reflux, have been published.

One of the first examples focusing on alkenyl triflates was reported by Martinez and co-workers in 1994,[86] utilizing lithiumthiolates, $Pd(PPh_3)_4$ as catalyst and LiCl as additive under reflux conditions (Scheme 16).

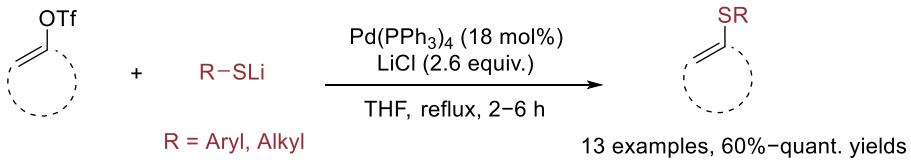

Scheme 16. Palladium catalyzed C-S cross-coupling of alkenyl triflates and lithiumthiolates.[86]

Decades later, in 2018, Fernandez-Rodriguez and co-workers utilized 0.1 mol% $Pd_2(dba)_3$/**L7** (dppf) as catalytic system for the coupling of alkenyl bromides with aryl and alkyl thiols in the presence of LiHMDS at 110 °C (Scheme 17).[87] Changing the ligand to **L1** (CyPF^{t}Bu) and increasing the catalyst loading to 5 mol% enabled the coupling of less reactive alkenyl chlorides and tosylates for the first time.

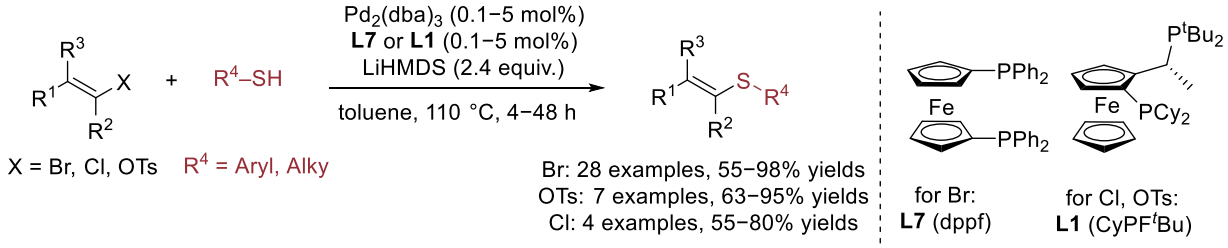

Scheme 17. Palladium catalyzed C-S cross-coupling of alkenyl bromides and first example for the coupling of alkenyl chlorides and tosylates with thiols.[87]

An alternative strategy, coupling thioesters and N-tosylhydrazones with $Pd(OAc)_2$ (10 mol%), P^{t}Bu$_3$ (20 mol%) and LiO^{t}Bu as base at 60°C was employed by Yamaguchi and co-workers.[88] Since Migita's original work various other transition metals, including Ni, Cu and Fe were utilized as catalysts in C-S cross-coupling reactions and will be discussed in the following chapters.

1.3.4. Nickel Catalysis

Nickel is an abundant, low-cost, and versatile transition metal able to catalyze a variety of transformations. The unique reactivity, which can be hard to control, enables new reaction pathways.[15] This contrast of potential and challenges has first been described over a century ago in 1922 by Paul Sabatier, a Nobel Prize laureate, who wrote:

"it can be compared to a spirited horse, delicate, difficult to control"[89]

The intriguing reactivity of nickel can be explained through the wide variety of readily available oxidation states, ranging from Ni(0) to Ni(IV),[15, 37, 90] which enables classic Ni(0)/Ni(II), as well as Ni(I)/Ni(III) catalytic cycles, in addition to those including SET (single-electron transfer) steps. The facile radical reactions, due to nickels relatively stable open shell configurations, can be utilized in photoredox catalysis and electrochemistry. Therefore, nickel catalysis has permitted access to new products *via* previously difficult transformations, inaccessible with palladium catalysis. Defining properties, in comparison to palladium, are the smaller atomic radius,[91] as well as the lower electronegativity[92] and reduction potential,[93] which enable diverse reactivity patterns and lead to a less facile β-hydride elimination, expanding the scope to alkyl substrates.[90a] Although palladium and copper have been predominantly employed in earlier reported C-S cross-coupling reactions of aryl iodides and bromides, less reactive substrates, such as aryl chlorides have been challenging, whereas nickel, which readily undergoes oxidative addition, has shown great potential. The high reactivity of nickel towards inert substrates can be explained through a relative weak metal-carbon bond in comparison to other group 10 metals, with Ni-C < Pd-C < Pt-C for the corresponding BDE.[15, 94] Due to the weaker metal-carbon bond the oxidative addition has a comparatively lower E_A, which enables the facile reaction of an electron-rich Ni(0) complex with traditionally inert or less reactive electrophiles.[37, 90a, 90b]

The high activity of nickel has not only tremendous potential, but also challenging drawbacks, rendering nickel catalysts difficult to control with at times unpredictable reaction pathways, leading to the generation of side products and off-cycle catalytic species, which has impeded the progress and application of nickel catalysis in the past. To harness the potential and gain control, monodentate and especially bidentate phosphines, N-hetereocyclic carbenes, as well as bidentate nitrogen ligands have been utilized.

One of the first nickel catalyzed C-S cross-coupling reactions was reported by Cristol and co-workers in 1981.[95] Aryl bromides and *in-situ* generated sodium thiolates were coupled with the one-component pre-catalyst (dppbz)$NiBr_2$ **Ni2** at 200 °C (Scheme 18).

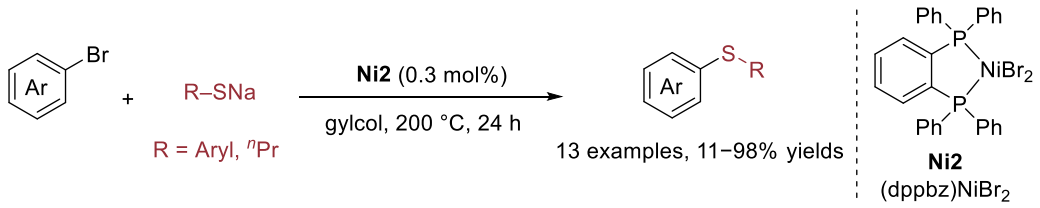

Scheme 18. Nickel catalyzed C-S cross-coupling of aryl bromides and sodium thiolates.[95]

Since then, a variety of publications and reviews have been reported for the nickel-catalyzed C-S cross-coupling and the corresponding mechanisms were discussed.[90a, 90b] The low-cost nickel has developed into a commonly employed metal in homogeneous catalysis,[15, 37, 90b] but much less research was conducted in the field of C-S cross-couplings compared to palladium. Most reactions in the past showcase the coupling of aryl bromides and iodides, which are still frequently employed in recent reports.[96] Reaction conditions, such as high temperatures, stochiometric additives or air-sensitive reagents are often required for a facile transformation. To enable mild reaction conditions, utilizing one-component pre-catalysts is a common strategy not only in palladium catalysis but also applicable for nickel. One example reported by Stefan and co-workers,[97] utilized the air- and moisture-stable, well-defined α-diimine Ni(II) **Ni3** and Pd(II) **Pd4** pre-catalysts for the coupling of aryl bromides with aryl and alkyl thiols, KOH or NaOH as base at 40-60°C (Scheme 19). The sterically strained dinuclear complex **Ni3** outperformed the best palladium complex **Pd4**, showcasing the potential of nickel catalysis.

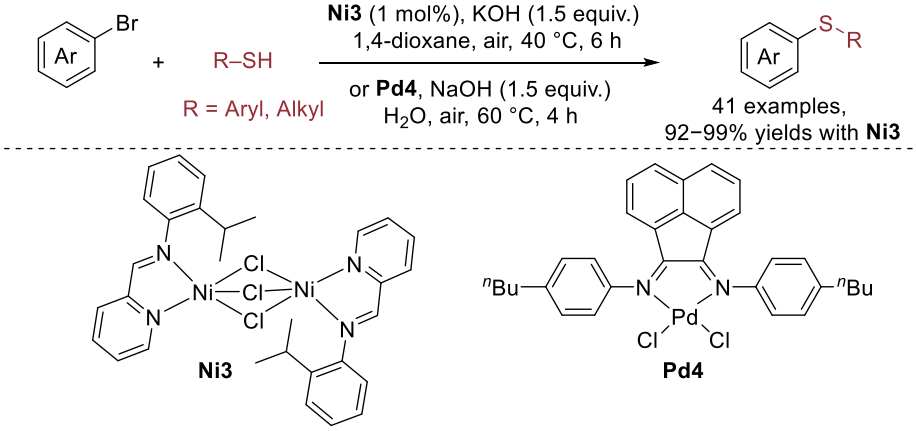

Scheme 19. One-component α-diimine Ni(II) **Ni3** and Pd(II) **Pd4** pre-catalysts enable (relative) mild C-S cross-coupling of aryl bromides and thiols.[97]

An alternative, more sustainable method for C-S bond formation was developed by Lipshutz and co-workers,[98] employing the one-component pre-catalyst $(phen)_2NiBr_2$, a substochiometric amount of zinc, K_3PO_4, Cs_2CO_3 or KO^{t}Bu as base in a 2 wt% TPGS-750-M (α-tocopherol-methoxypoly-ethylenglycol-succinate) aqueous solution (Scheme 20). In this inexpensive micellar catalysis, pure water was a competitive solvent for a limited amount of water-soluble substrates, while the surfactant TPGS-750-M proved essential to emulsify insoluble substrates.

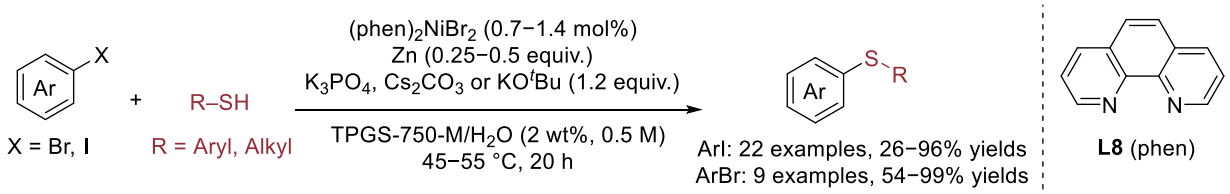

Scheme 20. Alternative micellar catalysis utilizing pre-catalyst $(phen)_2NiBr_2$ in a C-S bond formation.[98]

In recent years aryl chlorides, as challenging but readily accessible substrates, were intensely researched. A variety of alternative routes have been explored concentrating on mild reaction conditions enabled by the high reactivity and facile oxidative addition of nickel catalysts. One notable example is the coupling of aryl and heteroaryl chlorides in a trifluoromethylthiolation reported by Schoenebeck and co-workers (Scheme 21).[43] $Ni(cod)_2$/**L7** (dppf) was employed as catalytic system with $(Me_4N)SCF_3$ as coupling partner at 45 °C to generate the corresponding trifluoromethyl sulfides, which represent high-value pharmaceutical compounds. Prior to this report only aryl iodides and bromides could be trifluoromethylthiolated *via* nickel catalysis.[43] Beside the demonstration of synthetic applications in a broad substrate scope, including pharmaceutically relevant compounds, mechanistic investigations and DFT calculations support a Ni(0)/Ni(II) catalytic cycle. Additionally, the Ni(I) complex (dppf)NiCl was identified as a readily formed off-cycle deactivation product *via* comproportionation and biaryl formation from the *in-situ* generated Ni(II) precursor. Further studies by the same group observed and explained the unexpected reactivity order of electrophiles ArCl > ArBr > ArI *via* deactivation of the catalyst through formation of the off-cycle Ni(I) species, which shows the inverse order for a facile generation with ArI > ArBr > ArCl.[99] The transformation required bidentate ligands with wide bite angles, which lead to the formation of reactive, mono-ligated LNi(cod) as resting state, contrary to bidentate ligands with a smaller bite angle (e.g. dppe) or monodentate ligands, which form bis-ligated L_2Ni complexes as more stable and less reactive resting states.

Additionally, MeCN was identified to increase the catalyst activity and therefore substrate scope, especially in regards to less reactive electron rich aryl chlorides, by acting as a more labile ligand compared to cod. The resulting *in-situ* generated complex LNi(MeCN) undergoes oxidative addition more readily and the overall energetic span (δG_{max}, energy difference of the highest and lowest point of the reaction path) was reduced (Scheme 21). In contrast to bidentate phosphine ligands, which favor a Ni(0)/Ni(II) mechanism, bidentate N,N-ligands were postulated to enable the product formation *via* a Ni(I)/Ni(III) pathway.[43]

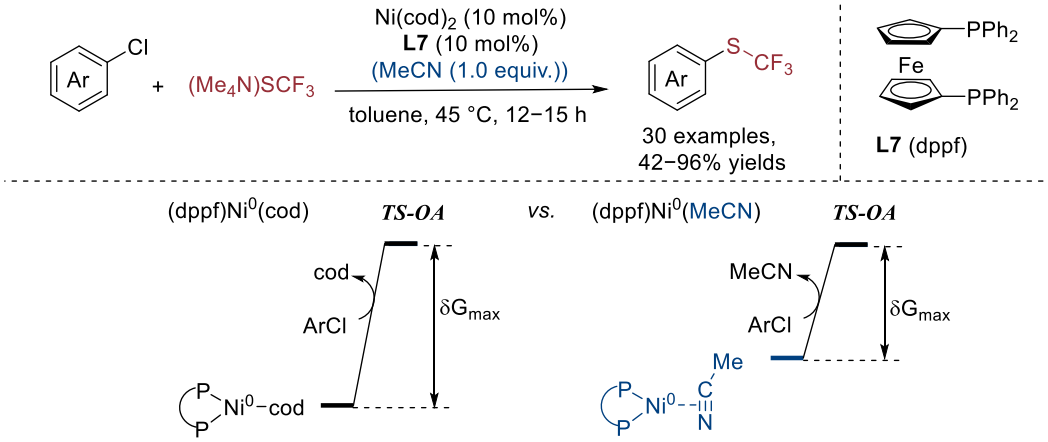

Scheme 21. Nickel catalyzed trifluoromethylthiolation of aryl chlorides and a comparison of the oxidative addition step with cod and MeCN as labile ligands.[43] (TS-OA = transition state of the oxidative addition).

Later, the substrate scope was extended to a variety of electron rich and electron poor aryl and heteroaryl chlorides, which were coupled with aryl thiols by Stewart and co-workers, utilizing $Ni[P(O\textit{p}\text{-tolyl})_3]_4$ and **L6** (Xantphos) as catalytic system, KO^{t}Bu or Cs_2CO_3 as base at 110 °C under reducing conditions with stochiometric amounts of zinc (Scheme 22).[100] The challenging alkyl thiols were unsuitable coupling partners for aryl chlorides (one example, 20% yield) but showed moderate yields up to 62% for the coupling of more reactive aryl bromides.

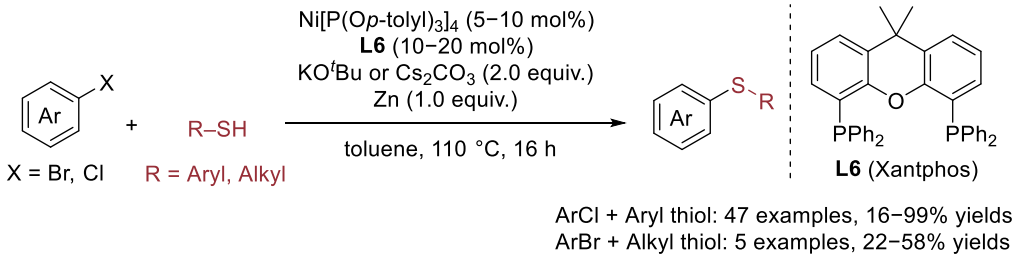

Scheme 22. Nickel catalyzed cross-coupling of aryl bromides and chlorides with thiols.[100]

The reactivity of alkyl thiols with aryl chlorides was improved in a contribution by our group employing the air-stable one-component pre-catalyst XantphosNi(*o*-tolyl)Cl **Ni1** at room temperature or 60 °C, however air-sensitive organomagnesium or -zinc reagents were required as base and activating agent (Scheme 23). [101] A broad range of aryl chlorides could be successfully coupled, with an adaptation of the catalyst to DPEPhosNi(mesityl)Br **Ni4** for *ortho*-substituted aryl chlorides. While primary and secondary alkyl thiols were coupled efficiently, tertiary examples reacted only in low yields up to 26%. The coupling of aryl thiols required a modified procedure with more forcing reaction conditions in comparison to alkyl thiols due to a competing Kumada coupling.

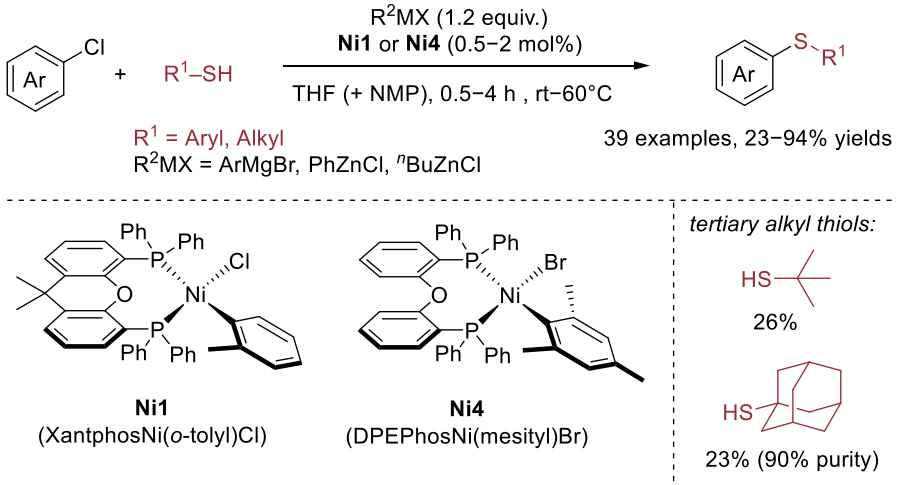

Scheme 23. C-S cross-coupling of aryl chlorides with aryl and alkyl thiols catalyzed with one-component pre-catalysts **Ni1** and **Ni4** under moderate reaction conditions.[101]

Alternative sulfur containing compounds, such as disulfides[102] and phenyldithiocarbamates[103] could be employed as substrates in thioether yielding C-S cross-coupling reactions with aryl iodides, requiring stochiometric amounts of zinc and high temperatures.

While limited examples for the palladium catalyzed coupling of aryl pseudohalides have been reported (see Chapter 1.3.3), nickel catalyzed methods are even rarer, with only few examples for the coupling of thiols and aryl mesylates,[104] as well as tosylates,[105] but no examples, with an extensive substrate scope, for aryl triflates.

One of the first nickel catalyzed publications concentrating solely on the coupling of aryl mesylates[104] was published in 1995 and utilized sodium thiolates with (dppf)$NiCl_2$ (10 mol%) and **L7** (dppf) (20 mol%) as catalytic system, stochiometric amounts of zinc as reducing agent at 80 °C in generally low yields (3 examples, 20–32%), with only diphenyl thioether showcasing high yields.

Decades later, Nicasio and co-workers[105] employed the Ni(II) pre-catalysts **Ni5**/**Ni6** and LiO^{t}Bu as base to couple aryl tosylates and various aryl halides with aryl and alkyl thiols (Scheme 24).

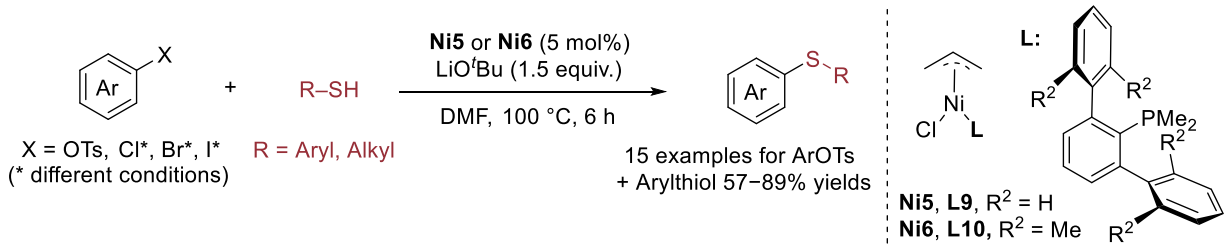

Scheme 24. Nickel catalyzed cross-coupling of aryl (pseudo)halides, including tosylates with thiols.[105]

Nickel catalyzed C-S cross-coupling reactions yielding alkenyl thioethers are even more underrepresented.[106] For palladium catalysis, solely coupling reactions of alkenyl pseudohalides were discussed. For nickel catalysis examples with alkenyl halides are included due to the limited scope of alkenyl pseudohalides.

The utilization of alkyl phosphite ligands has been a successful strategy for the coupling of alkenyl iodides and bromides. First, the stereospecific synthesis of alkenyl thioethers *via* a coupling of (*E*)-alkenyl iodides and bromides with aryl as well as alkyl thiols utilizing a triethyl phosphite nickel complex Ni[P(OEt)$_3$]$_4$ **Ni7** was reported by Tekeda and co-workers (Scheme 25).[106a] While (*E*)-alkenyl halides yielded the alkenyl thioether, (*Z*)-alkenyl halides led to formation of alkynes.

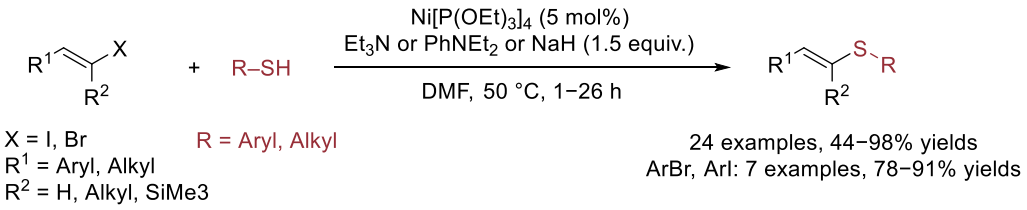

Scheme 25. Nickel catalyzed C-S cross-coupling of (*E*)-alkenyl iodides and bromides with thiols.[106a]

Later, alkenyl thioethers were synthesized by Lautens and co-workers[106b] through the coupling of alkenyl bromides and aryl thiols utilizing NiI$_2$/P(O^{i}Pr)$_3$ as catalytic system with DIPEA as base (Scheme 26). This system is stereospecific for each isomer, and while (Z)-alkenyl bromides can be coupled, the reaction rate is slower, presumably due to steric hinderance.

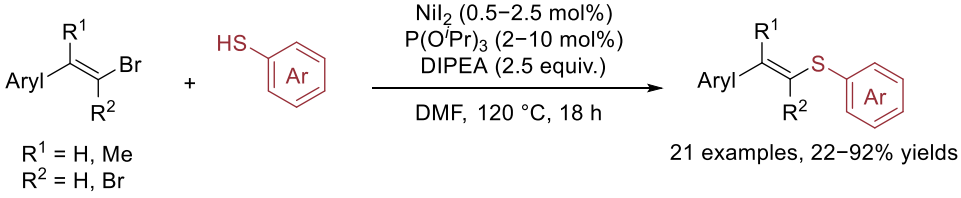

Scheme 26. Nickel catalyzed C-S cross-coupling of alkenyl bromides and aryl thiols.[106b]

A recent and highly relevant nickel catalyzed coupling of alkenyl triflates with thiols, reported by Pan and co-workers,[106c] will be the only electrochemically promoted reaction referenced and included in this thesis, due to its importance on the topic. $Ni(cod)_2$/**L11** (bpy) was utilized as catalytic system with Bu_4NOAc as base under mild reaction conditions (Scheme 27). A broad substrate scope in respect to aryl thiols, but a limited scope with two examples in moderate yields for alkyl thiols, was demonstrated.

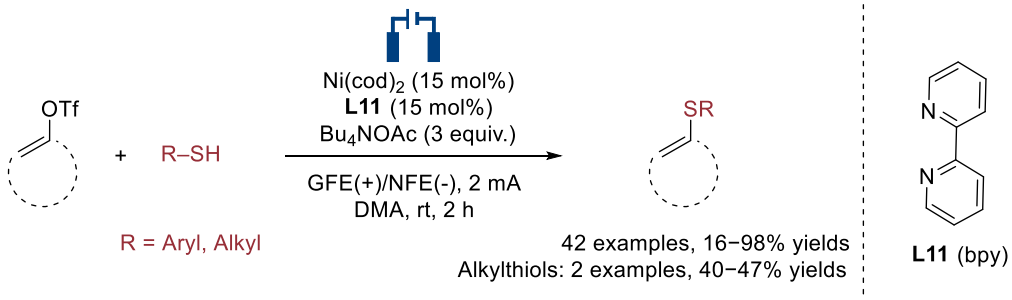

Scheme 27. Electrochemically promoted nickel catalyzed cross-coupling of alkenyl triflates and thiols.[106c]

The inefficient and low-yield coupling of alkyl thiols, especially sterically challenging tertiary examples, has been a typical limitation in C-S cross-coupling reactions for the coupling of aryl and alkenyl (pseudo)halides.

1.3.5. Copper Catalysis

Another alternative low-cost transition metal, which has shown potential in homogeneous catalysis, is copper. The first copper-catalyzed coupling of thiols with aryl halides to generate thioethers, referred to as Ullmann type coupling,[107] was published in 1984.[74] Thiophenol and aryl bromides or iodides were coupled with metallic copper as catalyst at 240-300 °C in an autoclave. Later research led to the development of catalytic variants performed at comparatively lower temperatures (~100 °C). These methods typically employed Cu(I) salts, either under ligand free conditions, or with N-containing ligands, such as bidentate amines.[108] In contrast to palladium and nickel, copper catalyzed ligand free coupling reactions can generate excellent yields. Additionally, only a limited amount of publications for the cross-coupling of aryl (pseudo)halides with thiols, but a variety of reactions with alternative sulfur sources and thiol surrogates have been reported.

While aryl iodides and thiols were coupled efficiently by Anilkumar and co-workers with CuI/DABCO as catalytic system and K_2CO_3 as base at 120 °C, aryl bromides had moderate and chlorides low yields.[109] An alternative, ligand free catalytic system employing CuI as catalyst and KO^{t}Bu as base for the coupling of aryl iodides with (hetero)aryl thiols was reported by Patil and co-workers (Scheme 28).[110]

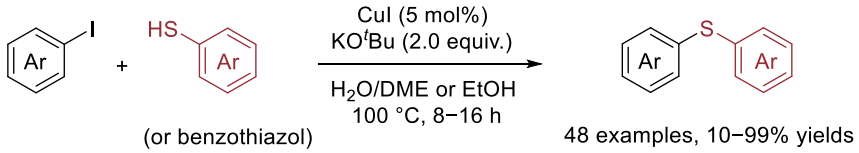

Scheme 28. Ligand free CuI catalyzed coupling of aryl iodides and (hetero)aryl thiols.[110]

Expanding the substrate scope, the coupling of aryl bromides as well as less reactive aryl chlorides with aryl and alkyl thiols utilizing CuI and the oxalic diamide ligands **L12**/**L13**, in addition to KO^{t}Bu as base, was investigated by Lee and co-workers (Scheme 29).[111]

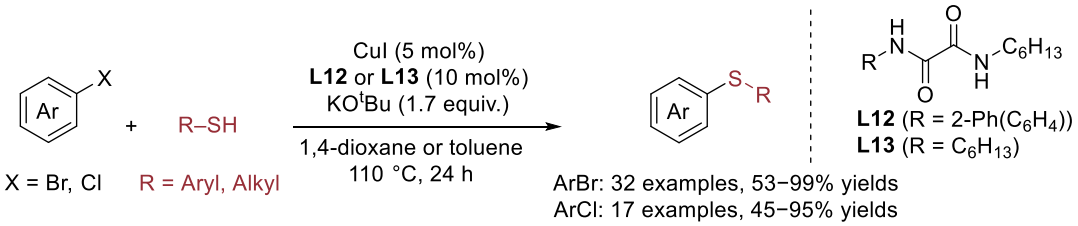

Scheme 29. Coupling of aryl halides with aryl and alkyl thiols utilizing CuI and oxalic diamide ligands.[111]

Due to the versatile nature of copper a variety of alternative sulfur sources (which only deliver one sulfur atom into the target structure) and sulfur surrogates (which are coupled with the aryl halide and fully integrate into the generated thioether) have been employed in copper catalysis. These include elemental sulfur (S_8),[112] xanthate,[113] sodium thiosulfate,[114] potassium thioacetate,[115] sulfoxide,[116] and sodium sulfinate[117] (Figure 9).

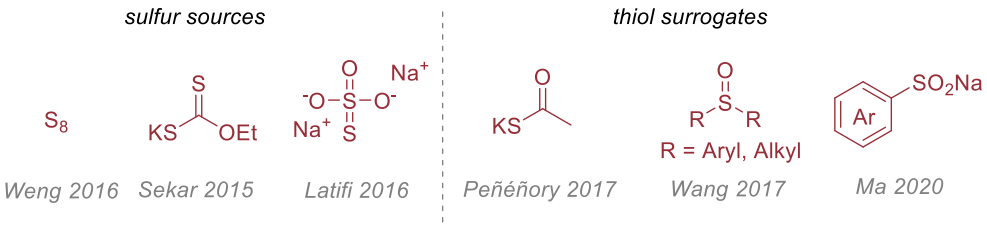

Figure 9. Examples of alternative sulfur sources and sulfur surrogates employed in the copper catalyzed synthesis of thioethers.[112-117]

The first two sulfur sources will be discussed in greater detail. Utilizing CuI/**L8** (phen) as catalytic system and $NaBH_4$ as reducing agent, a reductive trifluoroethylthiolation of aryl iodides and bromides with elemental sulfur (S_8) was published by Weng and co-workers (Scheme 30).[112]

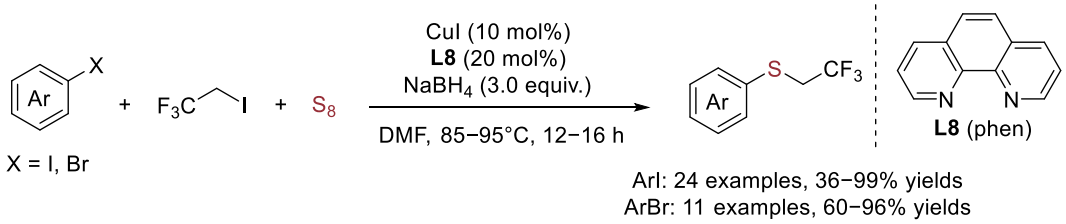

Scheme 30. Reductive coupling for the copper catalyzed synthesis of fluorinated thioethers.[112]

Xanthate, as odorless sulfur source, was utilized by Sekar and co-workers in a ligand and base free, $Cu(OAc)_2$ catalyzed tandem reaction with 2-iodo and 2-bromochalcones to synthesize thioflavanones (Scheme 31).[113] The proposed mechanism consists of a C-S coupling, followed by C-S bond cleavage and ring formation *via* an intramolecular Michael addition.

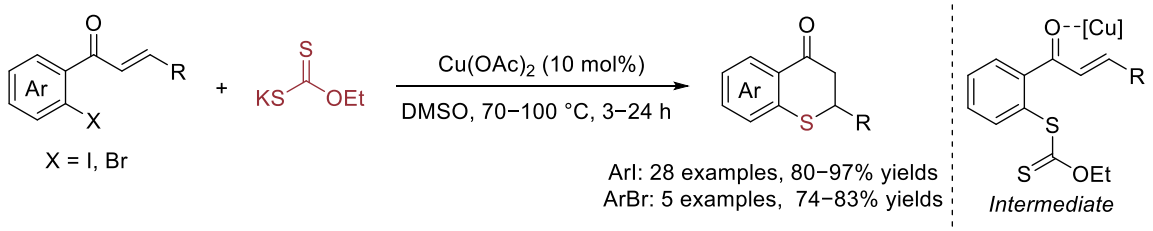

Scheme 31. Tandem reaction including a copper catalyzed C-S bond formation.[113]

A limited amount of copper catalyzed methods to synthesize alkenyl thioethers have been reported for the coupling of alkenyl iodides and bromides.[118] The Cu(I) one-component pre-catalyst **Cu1** and K_3PO_4 as base were employed to couple a variety of alkenyl iodides and aryl as well as alkyl thiols yielding the corresponding thioethers (Scheme 32).[118a] Both (*E*)- and (*Z*)-isomers were tolerated with a retention of stereochemistry. In addition to pre-catalyst **Cu1**, CuI/**L8** (phen) could be employed as catalytic system for the C-S cross-coupling.

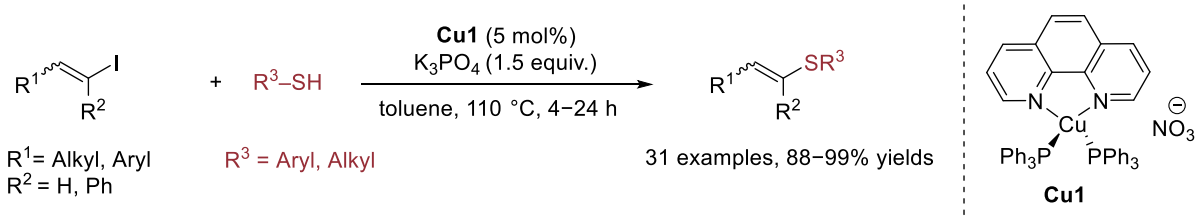

Scheme 32. Copper catalyzed coupling of alkenyl iodides and thiols with pre-catalyst **Cu1**.[118a]

The stereospecific reaction was further developed and the substrate scope was extended by Cook and co-workers[118b] in a coupling of alkenyl iodides and aryl as well as alkyl thiols with CuI/**L14** (*cis*-1,2-cyclohexanediol) as catalytic system and K_3PO_4 as base under milder reaction conditions (Scheme 33).

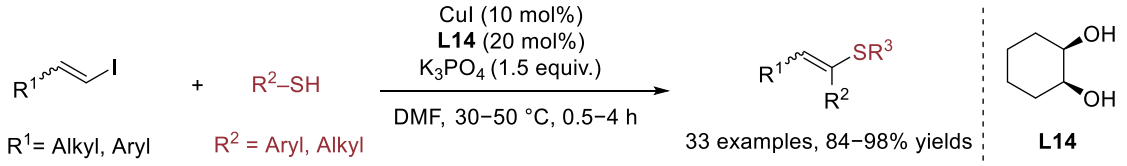

Scheme 33. Copper catalyzed coupling of alkenyl iodides and thiols under milder reaction conditions.[118b]

Later the substrate scope of alkenyl halides was extended by Kao und Lee[118c] to enable the coupling of alkenyl bromides and alkenyl chlorides in addition to the commonly employed alkenyl iodides. For alkenyl iodides Cu_2O (0.5 mol%) as catalyst, under ligand free conditions, with KOH as base at 110°C was sufficient, whereas the more stable alkenyl bromides and chorides required Cu_2O (5 mol%), ligand **L8** (phen) (10 mol%) and longer reaction times to yield the thioeter.

1.3.6. Iron Catalysis

Iron, as abundant low-cost transition metal with comparatively low toxicity, has been utilized as catalyst in a variety of C-Heteroatom, including C-S cross-coupling reactions.[73]

The first iron catalyzed Migita type coupling was published by Bolm and co-workers in 2008 (Scheme 34).[119] Aryl iodides and aryl thiols were coupled with $FeCl_3$ and **L15** (DMEDA) as bidentate ligand at high temperatures. However, Buchwald and Bolm reported later that copper contamination in non-high-purity commercial batches of iron precursor salts (< 99.99%) were likely to be responsible for the cross-coupling activity, as only low yields were observed with the pure precursor without contaminant.[120] This study highlights the importance of high purity precursors for iron catalysis and the pitfalls of accidental trace metal catalysis.

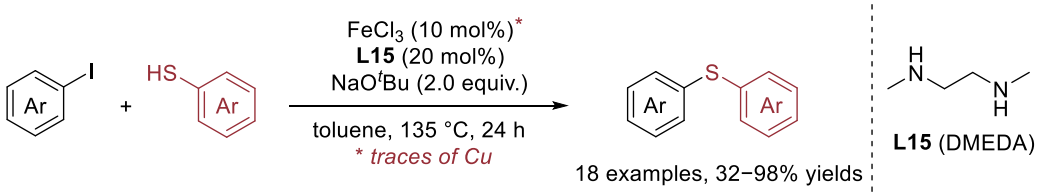

Scheme 34. Iron catalyzed coupling of aryl iodides and thiols with a copper contaminated precursor.[119-120]

Several reports on iron catalyzed C-S cross-coupling reactions followed, although the presence of copper cannot always be excluded, partially due to a lack of control experiments. Among more recent contributions, a $FeCl_3$/proline catalytic system was employed for the coupling of thiophenols and aryl halides.[121] Additionally, the iron catalyzed C-S bond formation has been utilized as useful tool in sequential ring closing reactions for the synthesis of heterocycles. A variety of phenothiazines were synthesized by Hu and Zhang through a tandem C-S/C-N cross-coupling of 1,2-diarylhalides with protected 2-mercaptoanilines *via* a $FeSO_4$/**L8** (phen) catalytic system and KO^{t}Bu as base (Scheme 35).[122]

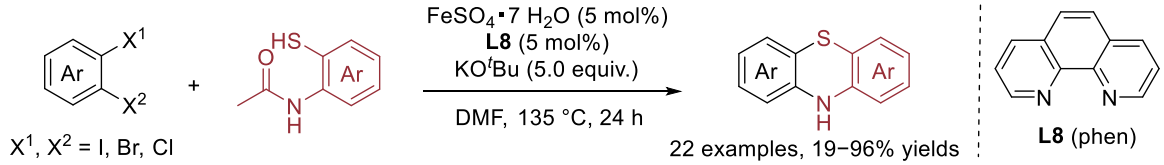

Scheme 35. Iron catalyzed synthesis of phenothiazines *via* sequential C-S and C-N cross-coupling.[122]

Another example is the synthesis of benzothiazoles by Xu and co-workers,[123] in a $Fe(OAc)_2$/**L16** catalyzed transformation of benzyl mercaptans with 2-iodo and 2-bromoanilines *via* a sulfur directed C-H amination followed by a C-S cross-coupling (Scheme 36).

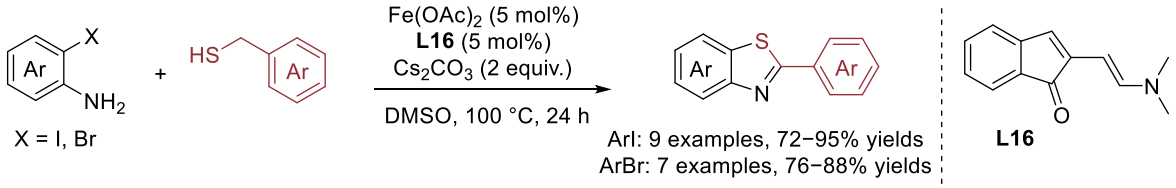

Scheme 36. Tandem C-S coupling and C-H amination to access benzothiazoles.[123]

The coupling of alkenyl iodides, bromides and chlorides with aryl and alkyl thiols was reported by Lee and co-workers,[124] employing $FeCl_3$/**L6** (Xantphos) as catalytic system (Scheme 37).

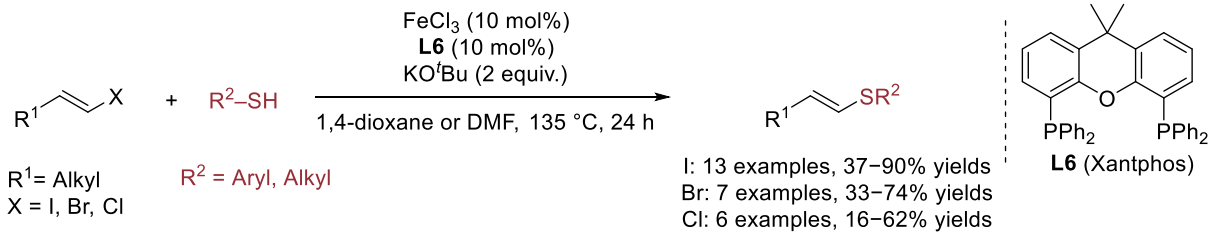

Scheme 37. Iron catalyzed coupling of alkenyl halides and thiols.[124]

Challenges in iron catalysis are the facile off-cycle disulfide formation as well as the reduction or poisoning of iron through thiol coordination. Until today high temperatures and long reaction times are required for a facile iron catalyzed C-S cross-coupling

1.3.7. Other Metals

Other metals, such as Co,[125] Mn,[126] In[127] and Zn[128] were less frequently employed for the coupling of aryl and alkenyl (pseudo)halides with thiols. Hayashi and co-workers utilized disulfides as alternative sulfur containing compounds in a ruthenium catalyzed coupling of alkenyl triflates with **Ru1**/**L17** as catalytic system and stochiometric amounts of zinc as reducing agent yielding the corresponding alkenyl thioethers (Scheme 38).[129]

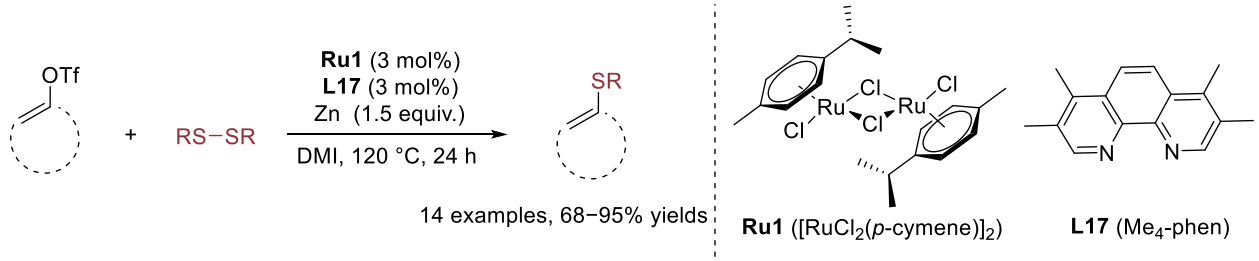

Scheme 38. Ruthenium catalyzed coupling of alkenyl triflates and disulfides.[129]

1.4. Stereochemistry

"Since most molecules are three-dimensional, it pervades all of chemistry. It is not so much a branch of the subject as a point of view, and whether one chooses to take this point of view in any given situation depends on the problem one wants to solve and the tools available to solve it."[130]

Stereochemistry describes chemistry in a three dimensional space. This subdiscipline, which focuses on the relationship between different stereoisomers, is essential for the understanding of chemistry in general, from organic, inorganic, physical, analytical to biochemistry. Stereoisomers, also referred to as spatial isomers have the same constitution but a diverging three-dimensional orientation of their atoms in space. They can be differentiated in enantiomers and diastereomers (Figure 10).[130] Enantiomers, also referred to as optical isomers, are chiral compounds with one single stereocenter. They exist in two forms as non-superimposable mirror images, one left- and one right-handed. Diastereomers, stereoisomers with two or more stereocenters, are not mirror images of each other.[131] When two diastereomers differ in only one of their stereocenters, they are called epimers. While enantiomers share the same physical and chemical properties in an achiral environment, whereas in a chiral environment their properties differ, diastereomers have different physical and chemical properties independent of the environment.

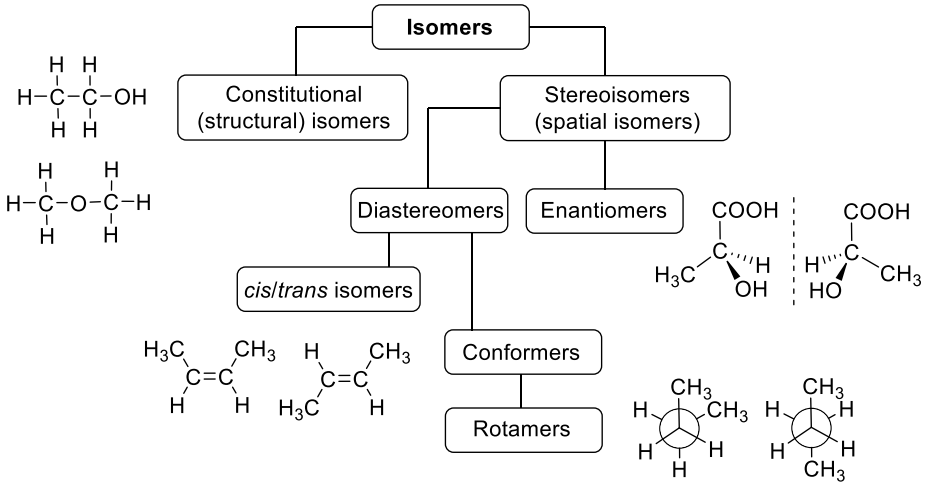

Figure 10. Overview of isomers, concentrating on stereoisomers.[130, 132]

The historic origin of stereochemistry can be found in the early 19th century when Malus first discovered the polarization of light through optically active crystals. 50 years later Louis Pasteur, considered today as the father of molecular chirality (although he called it dissymmetry) revolutionized organic stereochemistry, by extending the concept of optical activity from crystals to single molecules and molecular structures.[133] He succeeded in the historically first artificial chiral resolution of enantiomers, through separation of the distinct enantiomorphic crystals of the (+) and (-) sodium-ammonium salt of tartaric acid from a racemic mixture, by hand. While Le Bel and van't Hoff independently described the asymmetric tetrahedral structure of carbon atoms, laying the foundation for (modern) organic stereochemistry, the term chirality was coined by Lord Kelvin in the late 19th century.[133]

Chirality is an essential concept not only in stereochemistry and biochemistry but more generalised in life, as chiral molecules in living organisms predominantly exist as one enantiomer. This can be seen explementary by life's molecular building blocks L-amino acids and D-carbohydrates, which build more complex fundamental biological structures, such as proteins and DNA. The homochirality of biological molecules is essential for molecular recognition and leads to the chiral environment of the human body.[134] In such a chiral environment two enantiomers can have different properties (*via* distinct interactions with chiral receptors, such as enzymes and proteins) and can therefore be metabolized differently, which is of relevance for chiral pharmaceutical compounds. The 1960s Thalidomide scandal has led to awareness of this critically important factor.

While the (*R*)-enantiomer of Thalidomide was marketed for treating morning sickness in pregnant women and indeed acts as a sedative, the (*S*)-enantiomer is teratogenic and led to severe birth defects, such as limb deficiencies, in infants.[135] Thalidomide was sold as racemate, but even the enantiopure (*R*)-compound is dangerous, as the isomers readily interconvert *in vivo*.[136] A less severe example is Ibuprofen, in which the (*S*)-enantiomer is effective, whereas the (*R*)-enantiomer is ineffective, but does not cause side effects and can interconvert *in vivo* (Figure 11).[137]

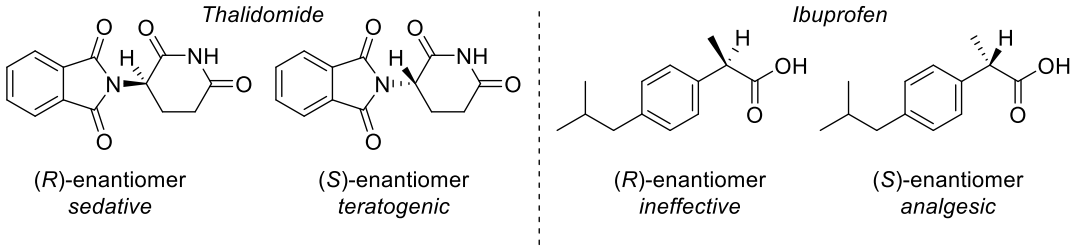

Figure 11. (*R*)- and (*S*)-enantiomers for the pharmaceutical compounds Thalidomide and Ibuprofen with the corresponding effects *in vivo*.[135, 137]

Today, the two enantiomers of chiral pharmaceutical compounds are therefore considered two separate drugs, unless proven otherwise, as diverging chemical and pharmacological behaviour can be expected in the human body (e.g. toxicity, bioavailability, potency, metabolism rate, metabolites and receptor selectivity).[138] As a consequence the isolation of enantiopure compounds is essential in drug development, as well as of interest for the agriculture, flavour and fragrance industry.

The isolation can be enabled *via* a variety of methods, including chiral resolution of a racemic mixture through separation of enantiomers (chiral HPLC, crystallization of diastereomeric adducts or kinetic resolution), by utilizing a chiral pool precursor (chiral building blocks from natural products), *via* stochiometric enantioselective synthesis (chiral reagents or chiral auxiliaries in a diastereoselective reaction) or through asymmetric catalysis (e.g. prochiral substrates generate an enantioenriched product mixture utilizing a chiral catalyst).[139]

The importance of chiral catalysis and asymmetric synthesis was recognized with a Nobel Prize awarded to Knowles, Sharpless and Noyori in 2001 for their pioneering work on asymmetric hydrogenation reactions.[140]

A variety of stereogenic elements can lead to chirality. The most common is a chiral carbon stereocenter in an organic compound exhibiting four distinct and different substituents in a tetrahedral geometry. Further options are axial chirality, generated through a stereogenic axis (e.g. BINOL), planar chirality (e.g. trans-cyclooctene) as well as inherent chirality, such as helical chirality, which arises from curvature or twisting of a molecule in space (e.g. DNA).[132]

1.4.1. Atropisomers

Atropisomers are stereoisomers, more specifically rotamers, which exhibit axial chirality. The hindered rotation about a σ-bond, usually due to steric strain, creates an energy barrier high enough to allow isolation of different conformers. The half-life $t^{1/2}$ for atropisomers, which by definition do not readily interconvert, is > 10^3 s at any given temperature, with a minimum free energy barrier dependent on the temperature.[141] LePen defined classes of atropisomers based on the half-life of racemisation at 37 °C. Class 1: ($t^{1/2}$ < 60 s), class 2: (60 s > $t^{1/2}$ < 4.5 years), class 3: ($t^{1/2}$ > 4.5 years). Class 1 atropisomers have a too low rotational barrier and half-life to be defined as classic atropisomers, but they are abundant in FDA-approved small-molecule drugs, and although they interconvert fast, they have been observed to bind targets exclusively in one of their chiral conformations. Class 3 atropisomers are considered stable enantiomers and can be employed for chiral drug development.[142]

In the beginning of the 20th century axial chirality was first described correctly and in 1933 Kuhn coined the term atropisomerism. Atropisomers are important structural motifs, represented in nature,[143] with numerous applications in catalyst design, as well as drug discovery.[144] The most common form, biaryl compounds bearing *ortho* substituents, are used as privileged bisphosphine ligands,[145] such as BINAP,[146] and can be found among pharmaceutical compounds.[141] In the past, enantiopure atropisomers were primarily isolated *via* racemic (optical) resolution. Other alternative methods, which yield enantiopure or enantioenriched atropisomers include the (dynamic) kinetic resolution of racemic mixtures, the *de novo* aryl ring synthesis (construction of aromatic rings), the construction of a chiral axis, as well as the desymmetrization through functionalization of an aromatic ring, such as a prochiral biarly (Figure 12).[147] The latter can be exemplary achieved *via* site-selective asymmetric cross-coupling.

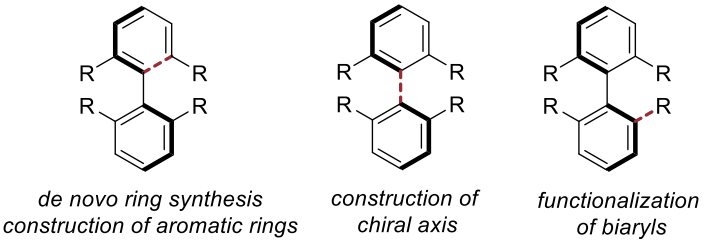

Figure 12. Examples of methods for the synthesis of atropisomeric biaryls.[147]

The stereoselective synthesis of atropisomers in modern drug discovery and ligand development has been of interest during the last decade. Sulfur containing atropisomers are an attractive target structure, because of their potential as pharmaceutical compounds, as well as their use as ligands (axial chiral biaryl thioethers are a privileged ligand class, Figure 13),[148] but their synthesis is challenging with multiple-step procedures reported.[149]

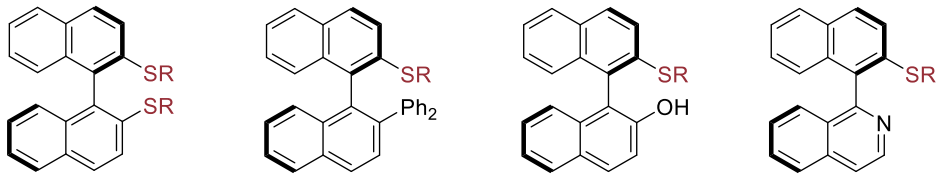

Figure 13. Examples of axial chiral ligands containing thioethers.[148-149]

While the synthesis of atropisomers *via* palladium catalyzed C-C bond formation is comparatively common, generation of C-Heteroatom bonds has remained rare, with limited examples for atropselective C-N[150] and C-P[151] coupling reactions. For the C-S bond construction only highly specific copper catalyzed ring opening reactions in a desymmetrization of cyclic diaryliodoniumsalts (five membered bridged biaryl structures), utilizing BOX (bis(oxazoline)) ligands with a limited substrate scope have been reported (Scheme 39).[152] A fast isomerization between the conformers of the diaryliodoniumsalts, as well as the release of torsion strain enable the reaction under mild conditions and low temperatures.[153]

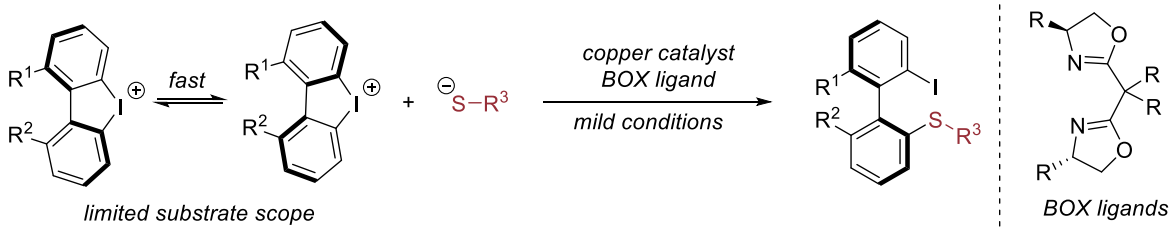

Scheme 39. Atropisomers containing thioethers synthesized *via* C-S bond construction from cyclic diaryliodoniumsalts *via* copper catalysis utilizing chiral BOX ligands under mild reaction conditions.[152]

Gu and co-workers utilized $Cu(CH_3CN)_4PF_6$ and **L18** (PhBOX) as catalytic system in an enantioselective ring opening of diaryliodonium salts with potassium thiocarboxylates as nucleophiles at -20 °C to generate a variety of axial chiral thioesters in high yield and ee (Scheme 40).[152a] The reaction has been previously utilized to couple amines as well as diarylphosphines.[150b]

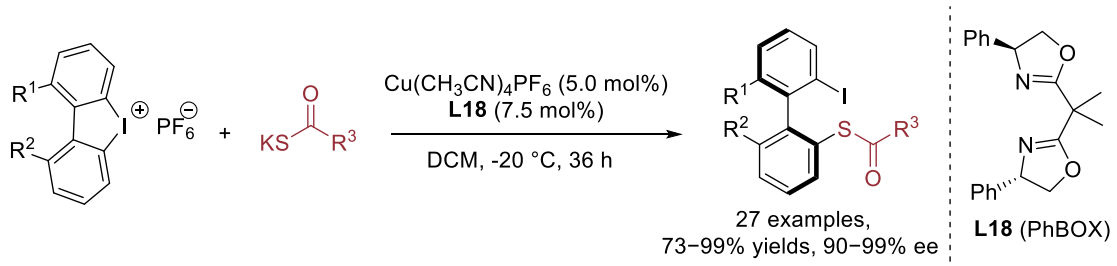

Scheme 40. Enantioselective ring-opening reaction of cyclic diaryliodoniumsalts with potassium thiocarboxylates.[152a]

The alternative BOX ligand **L19** and $Cu(OAc)_2$ as copper source with Na_2CO_3 as base was utilized by Zhang and co-workers[152b] in a similar desymmetrization, employing heteroaryl thiols, such as 2-mercaptobenzoxazole and 2-mercaptobenzothiazole derivatives as nucleophiles, to generate the corresponding product in good to excellent yields and ee (Scheme 41).

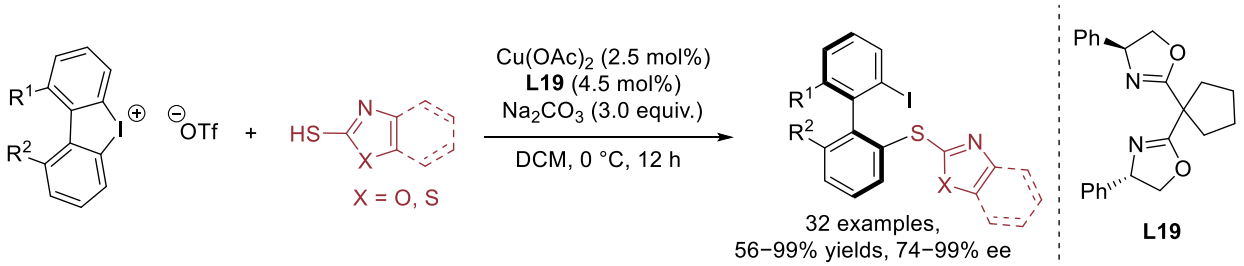

Scheme 41. Enantioselective desymmetrization of diaryliodoniumsalts with heteroaryl thiols.[152b]

1.4.2. Epimers

Epimers are diastereomers with multiple stereocenters that differ in the configuration of only one of them. The interconversion of one epimer into the diastereomeric counterpart is called epimerization.[154] Common examples of such epimers are carbohydrates. For D-glucose, the C2 epimer is D-mannose, while the C4 epimer is D-galactose (Figure 14).[155]

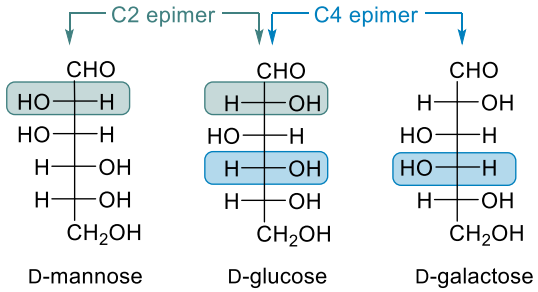

Figure 14. D-glucose, D-mannose (C2 epimer) and D-galactose (C4 epimer).[155-156]

1.5. Palladium Catalyzed Epimerization of Iodides under Visible Light Irradiation

1.5.1. Stereochemical Editing *via* Epimerization

The stereochemistry of molecules has a defining influence on their properties, with diverging chemical as well as biological effects for different isomers (see Chapter 1.4).[130, 157] Controlling and adapting the stereochemistry of organic compounds, which is possible *via* a variety of enantio- and diastereoselective reactions, is therefore of importance to harness their unique characteristics.[158]

A well-established method to access organic molecules with defined stereocenters is retrosynthesis, commonly *via* strategic bond-formation and stereo-induction steps, in which the precise stereochemical control is essential. Possible strategies include the utilization of accessible enantiopure starting materials from the chiral pool as well as selective stereochemical transformations. As both are limited, the stereoselectivity defining step commonly dictates and restricts possible reaction pathways, rendering the synthesis of some stereoisomers easier than others.[159] This can be seen explementary for 8α(H)-drimane, which is accessible *via* a selective one-step reduction from the chiral pool precursor drimene through a conventional hydrogenation, while the synthesis of 8β(H)-drimane from the same starting material initially required four steps (Scheme 42).[159-160] Although later an elegant copper-mediated reduction, which accessed the desired 8β(H)-drimane directly was published, it required the development of a new reaction (Scheme 43).[161]

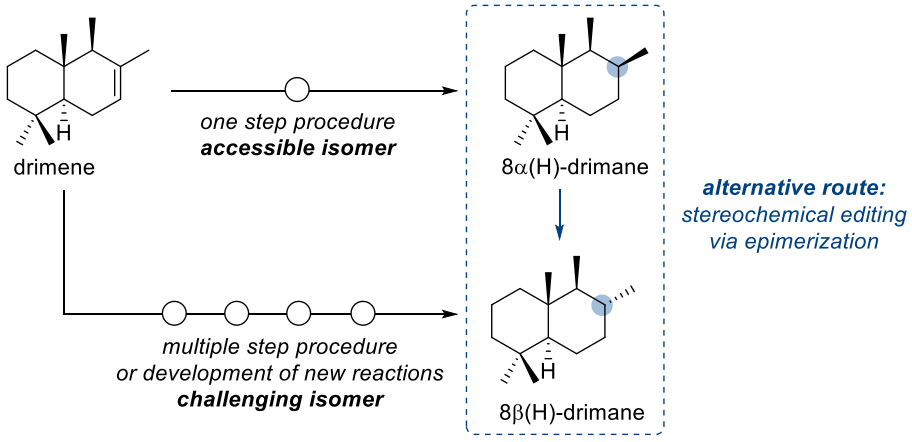

Scheme 42. Stereochemical editing *via* epimerization as alternative route to access isomers, which cannot be derived in a straight forward manner from chiral pool precursors or known stereoselective reactions.[159]

An alternative method to access different stereoisomers, which can be used to extend the scope of classic retrosynthesis, is stereochemical editing.[162] With this strategy the stereocenter of an organic molecule can be modified, simplifying the synthesis of challenging isomers and allowing for late stage functionalization (Scheme 43).[162-163] It enables flexibility in the choice of retrons (e.g. chiral pool precursors) and reactions (selective high yielding transformations), opening up new synthetic routes in which the stereoselectivity is decoupled from the bond forming step.[159] Stereochemical editing can be viewed as a complementary method which enables distinct (retro)synthetic options, simplifying access to stereoisomers which do not yet have a straight forward way of synthesis, without the need for novel and time intensive reaction development.

One form of stereochemical editing is epimerization. Here the method is leveraged to access different diastereomers (epimers), through a common, generally prochiral intermediate. The potential of this transformation can be seen on the previous example for the synthesis of 8β(H)-drimane, which is synthesized in a simple one-step epimerization from the accessible 8α(H)-drimane. A similar strategy can be utilized to access the challenging isomer of the steroid derived from (+)-cholic acid in a simple esterification and epimerization sequence, while the synthesis previously required seven steps (Scheme 43).[164]

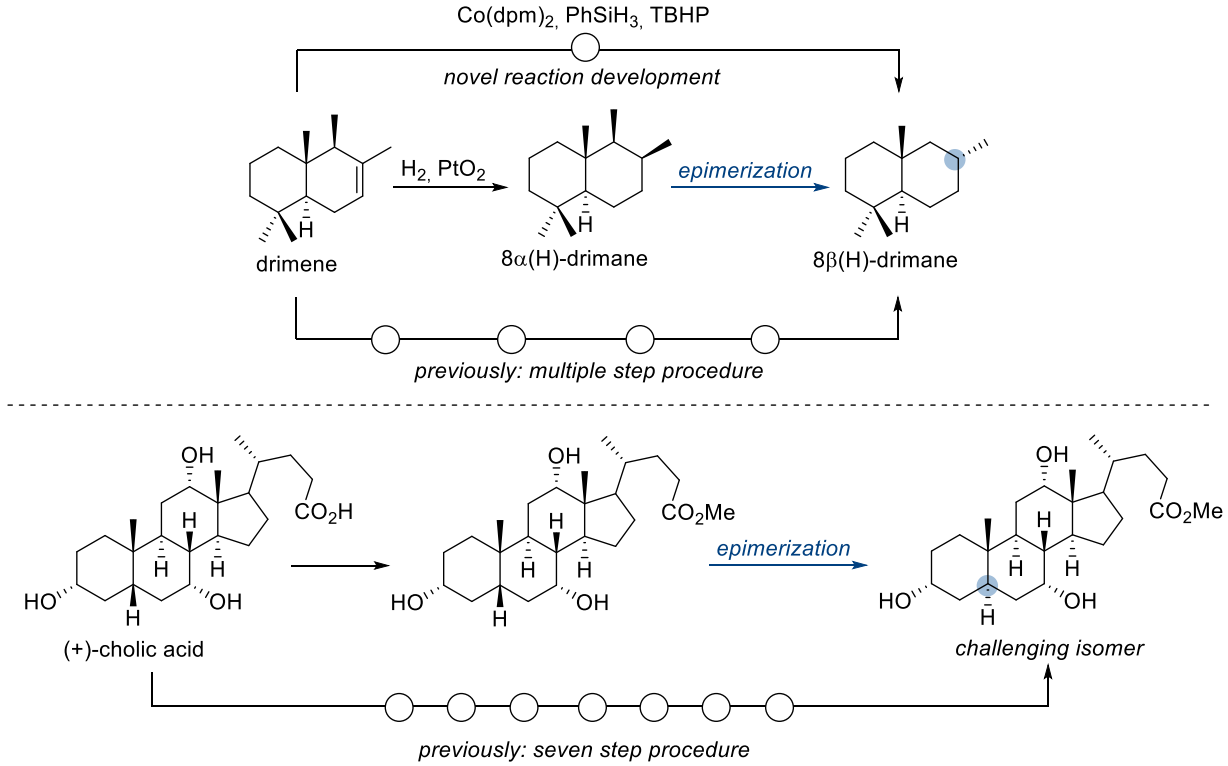

Scheme 43. Examples in which stereochemical editing *via* epimerization enables facile access to stereoisomers that would otherwise require multiple step synthesis or novel reaction development.[159]

While the revision of stereocenters *via* epimerization is a deceptively simple and often employed strategy, it may require multiple steps and can have a limited substrate scope. A variety of examples, reported by Wendlandt[159, 165] and MacMillan,[166] independently showcase the potential of photocatalytic epimerization to edit a carbon center *via* the *in-situ* formation of a prochiral radical intermediate for carbohydrates[165a] and cyclic 1,2-diols[165b, 166] (Scheme 44).

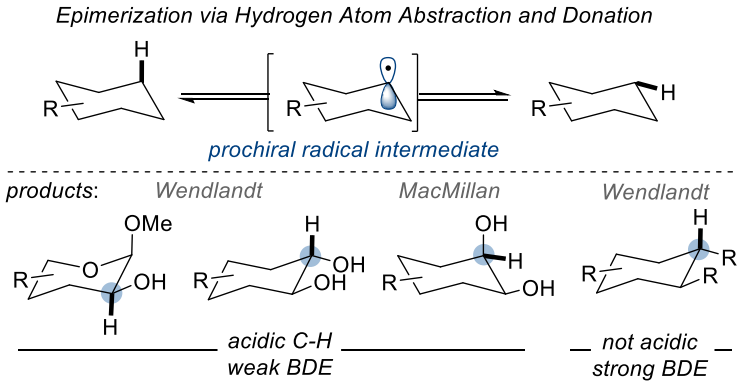

Scheme 44: Recent examples of stereochemical editing through a photocatalytic epimerization *via* hydrogen atom transfer and prochiral radical intermediates for acidic[165-166] and not acidic C-H bonds.[159]

In the transformations, initially weak C-H bonds in close proximity to a secondary alcohol could be broken and reformed selectively in a sequential C-H bond abstraction and donation *via* radical mediated reactions.[162] While Wendlandt and co-workers isolated the *trans*-diequatorial 1,2-diol as thermodynamic product, utilizing an iridium photocatalyst and triphenylsilanethiol, which promotes kinetically efficient reversible H atom transfer,[165b] McMillan and co-workers utilized dynamic epimerization under transient thermodynamic control, selectively stabilizing an otherwise thermodynamically disfavored isomer, generating the *cis*-diol.[166] Methylboronic acid acted as selectivity defining chelating agent during the reaction. Due to the reversible boronic ester formation and ring strain on the *trans*-boronic ester intermediate, the dynamic system generated *cis*-boronic ester as stable intermediate, yielding the *cis*-diole after workup (Scheme 45).

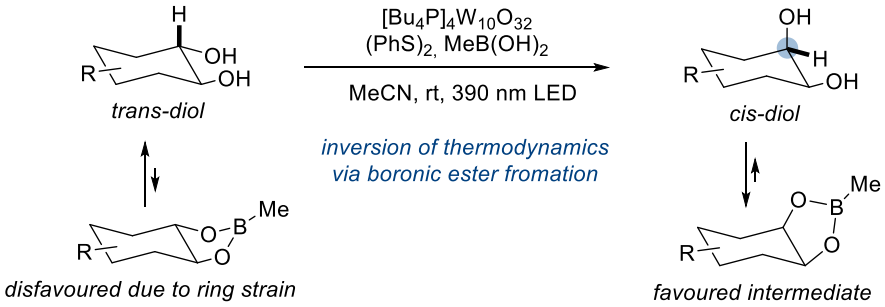

Scheme 45. Dynamic epimerization of *trans*- to *cis*-diols *via* boronic ester intermediates.[166]

The photocatalytic epimerization was initially limited to reactive and acidic protons at the corresponding stereocenter of interest, which enabled facile C-H bond abstraction and donation. Wendlendt and co-workers extended the substrate scope to non-activated tertiary stereocenters, utilizing a decatungstate photocatalyst and disulfide additive to facilitate the isomerization.[159] The reaction enabled access to otherwise challenging structures and late-stage functionalization of complex molecules, such as the previously presented examples for 8β(H)-drimane and the challenging steroid isomer (Scheme 43), as well as reduced Diels-Alder cycloaddition products (Scheme 46), expanding the stereospecific reaction outcome.

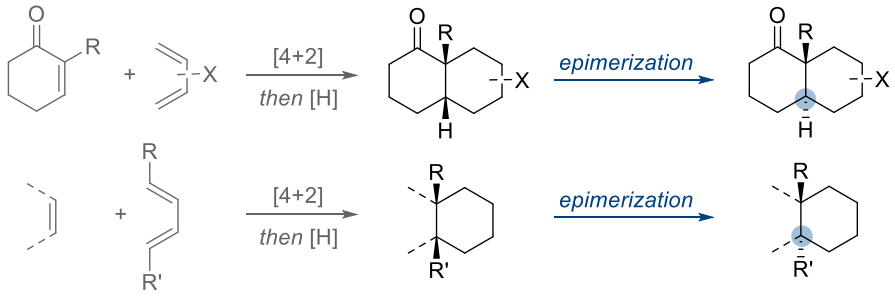

Scheme 46. Stereochemical editing of reduced Diels-Alder cycloadducts *via* epimerization. Inversion of stereocenters defined by the dienophile or diene.[159] [4+2] cycloaddition, [H] = H_2, Pd/C.

While the reported photocatalytic epimerization reactions are often limited to C-H bonds, employing the strategy of stereochemical editing on a wider variety of functionalized carbons, such as C-X bonds, and further expanding the substrate scope is of interest.

1.5.2. Palladium Catalysis under Visible Light Irradiation

Palladium, although expensive and relatively rare compared to other transition metals, is still the most commonly employed catalyst for C-C/C-X bond formations. During the last years visible light induced transition metal catalysis has developed into a useful tool in organic synthesis, by enabling reactions under mild conditions, which previously required high temperatures.[167] Palladium has shown tremendous potential in this area, since the first visible light induced exited state palladium catalyzed reaction *via* an aryl Pd(I) radical hybrid species was published by Gevorgyan and co-workers in 2016.[168]

While the common ground state palladium catalysis often proceeds through a Pd(0)/Pd(II) catalytic cycle (see Chapter 1.2), the new method generates exited state palladium complexes *via* visible light irradiation of $L_nPd(0)$ (Scheme 47), which can undergo single electron transfer to generate Pd(I) radical hybrid species that exhibits radical, as well as classic Pd-type reactivity.[167, 169]

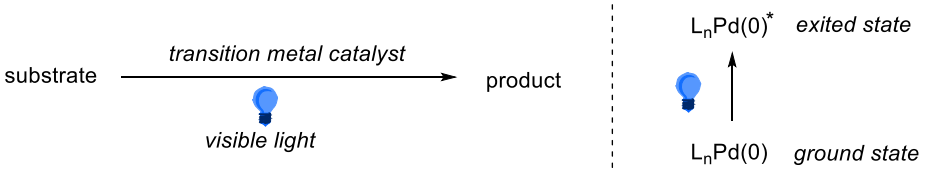

Scheme 47. Visible light induced exited state palladium catalysis enables new reaction pathways.[169]

The *in-situ* generated palladium radical species enables facile and less explored one-electron transformations through reaction pathways including H atom-, single electron-, and triplet energy-transfer[163] in addition to classic two-electron transformations.[167]

1.5.3. Carboiodination

Organic halides, such as aryl, alkyl and alkenyl iodides are important synthetic intermediates and versatile, reactive substrates employed in a variety of transformations. Installing C-X, such as C-I bonds in a stereoselective manner can be challenging due to the forcing reaction conditions typically required (see Chapter 1.2.1). Transition metal catalysis, such as palladium or nickel catalyzed carboiodination,[170] which represents a method for selective C-I bond formation, typically *via* reductive elimination from a Pd(II) $L_nPd(R)I$ complex, is an attractive alternative. Lautens and co-workers[170-171] published a multitude of carboiodination reaction during the last decades. An often utilized strategy is the intramolecular C-I bond transfer across a π-system to access complex iodo-heterocycles.[171a, 172] One of the earlier works by Newman et al. showcases such a palladium catalyzed intramolecular carboiodination of alkenes, utilizing $Pd(QPhos)_2$ as catalyst at 100 °C, in addition to an intermolecular carboiodination of norbornene with aryl iodides, utilizing $Pd(P^tBu_3)_2$ as catalyst and yielding the di-substituted *exo (syn)* iodo-norbornyl product (Scheme 48).[173] For high temperature palladium catalyzed carboiodination reactions, bulky phosphine ligands, favoring the C-I bond reductive elimination through a release of steric strain, have shown promise. The reaction was postulated to follow a classic 2-electron mechanism with an initial oxidative addition of the aryl iodide to Pd(0).[172a]

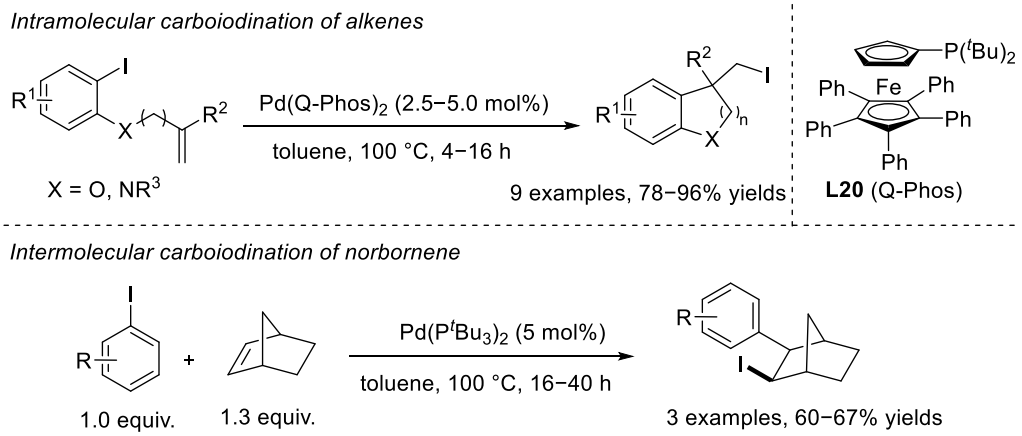

Scheme 48. Palladium catalyzed intramolecular carboiodination of alkenes and intermolecular carboiodination of norbornene with aryl iodides at 100 °C.[173]

Combining the potential of palladium catalysis under visible light irradiation and carboiodination, Marchese et al. recently published a palladium catalyzed blue light promoted intramolecular carboiodination with $[Pd(allyl)Cl]_2$/**L21** (DPEPhos) as catalytic system generating primary alkyl iodides. The mechanism is postulated to include a blue light induced reversible C-I bond formation *via* a radical one-electron pathway (Scheme 49).[174]

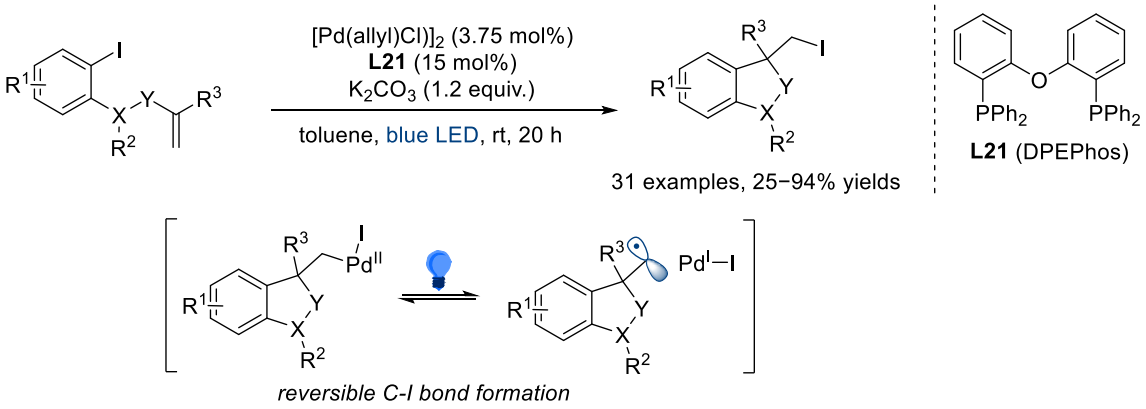

Scheme 49. Palladium catalyzed and blue light promoted intramolecular carboiodination *via* reversible C-I bond formation. [174]

Chapter 2

SUMMARY OF PUBLISHED RESULTS

2. Summary of Published Results

2.1. Acetate Facilitated Nickel Catalyzed Coupling of Aryl Chlorides and Alkyl Thiols

Aim of this work was to enable a mild, low-cost and convenient C-S cross-coupling of aryl chlorides with primary, secondary and tertiary alkyl thiols.[175] Previously the reaction was limited to aryl iodides and bromides with few examples for the less reactive aryl chlorides. Additionally, relative high temperatures and air-sensitive, reactive reagents were commonly required to enable the transformation. While aryl thiols could be coupled efficiently, alkyl thiols, especially sterically challenging tertiary examples remained challenging (see Chapter 1.3).

This gap was closed and a mild transformation was enabled through the combination of nickel as catalyst, Xantphos as ligand and KOAc as base. The high reactivity and facile oxidative addition of nickel catalysts renders them an excellent option for the transformation of challenging electrophiles, such as aryl chlorides (see Chapter 1.3.4). Nickels potential was controlled with the help of Xantphos, a bidentate phosphine ligand, which has been shown to reduce catalyst deactivation, stabilize active catalytic species and promote reductive elimination through steric strain. The hemilabile nature of Xantphos renders it versatile by enabling κ1, κ2 and κ3 coordination with the three possible donors (phosphines and oxygen ether linkage). This adaptability of the coordination mode to the properties required (such as oxidation state or free coordination space) gives rise to the opportunity to stabilize intermediates (κ3 – coordination) or generate reactive and unsaturated intermediates through temporary partial ligand dissociation (κ1-coordination) (see Chapter 1.2.3). The advantages of nickel and Xantphos were combined in the air-stable one-component pre-catalyst XantphosNi(*o*-tolyl)Cl **Ni1**, first synthesized by Jamison and co-workers,[46] which has previously shown potential in C-S cross-coupling reactions.[101] Due to the facile activation of the pre-catalyst, in addition to the crucial role of KOAc facilitating the reaction, a previously unreported, mild and convenient catalytic system for the coupling of aryl chlorides and challenging tertiary alkyl thiols has been developed.

To realize the goal of mild and low-cost reaction conditions, first *via* circumventing the need for air-sensitive and reactive reagents, a base screening was conducted with aryl chloride **1a** and secondary alkyl thiol **2a** at 50 °C. Surprisingly, a variety of simple inorganic salt reagents enabled the coupling in low to good yields (Table 2, entries 1–6).

Sodium acetate (entry 7) showed the highest yield, which led to a screening of alkali metal acetates (entries 8–11). For the coupling of tertiary alkyl thiol **2b** at room temperature no or low reactivity was observed with lithium and sodium acetate, whereas potassium and cesium acetate generated excellent yields after 2 h. Under cost considerations potassium acetate (KOAc) was chosen as base for further screening experiments.

Table 2. Selected examples for the preliminary base and alkali metal acetate screening for the coupling of aryl chloride **1a** and alkyl thiols **2a** and **2b**. R = CO_2Et, GC-FID yields calibrated against pentadecane.

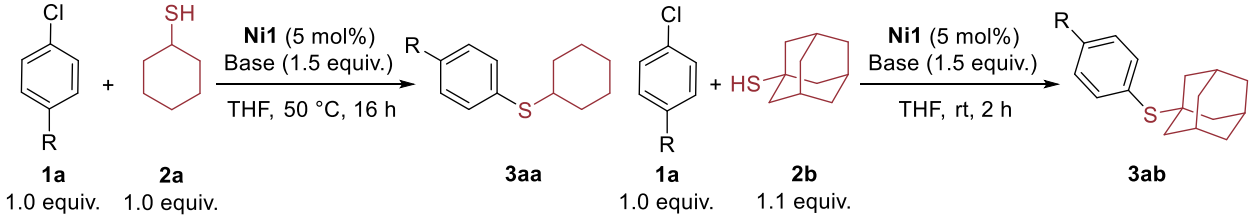

Entry	Base	Yield [%]
1	NaO^{t}Bu	62
2	Na_2CO_3	56
3	K_2CO_3	52
4	$Zn(OAc)_2$	54
5	Na_2HPO_4	62
6	Sodium citrate	42
7	NaOAc	85
8	LiOAc	none
9	NaOAc	14
10	KOAc	95
11	CsOAc	93

Optimization of the reaction conditions, including temperature, catalyst loading as well as substrate and base equivalent screenings (see Chapter 5) were conducted, which identified 1.0 equiv. aryl chloride **1**, 1.1 equiv. alkyl thiol **2**, 5 mol% pre-catalyst XantphosNi(*o*-tolyl)Cl **Ni1** and 1.5 equiv. KOAc in THF at room temperature for 0.5–2 h as ideal reaction conditions (Scheme 50).

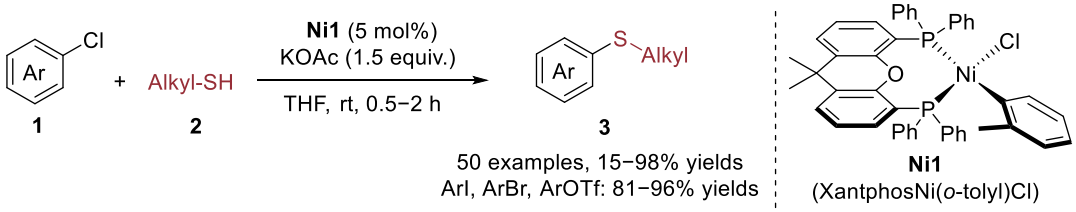

Scheme 50. Optimized reaction conditions for the coupling of aryl chlorides **1** and alkyl thiols **2**.

The optimized reaction conditions were applied to a broad substrate scope. For aryl chlorides **1a-z**, a variety of electron-neutral, -rich and -deficient *meta*- and *para*-substituents with various functional groups, such as esters, nitrile **3ab**–**3kb** amide **3mb** and hydroxy **3nb**, as well as heterocycles **3qb**–**3wb** and pharmaceutical compounds, such as Fennofibrat **3xb**, Loratidin **3yb** and Indometacin ethyl ester **3zb** generated the thioether in good to excellent yields (Scheme 51).

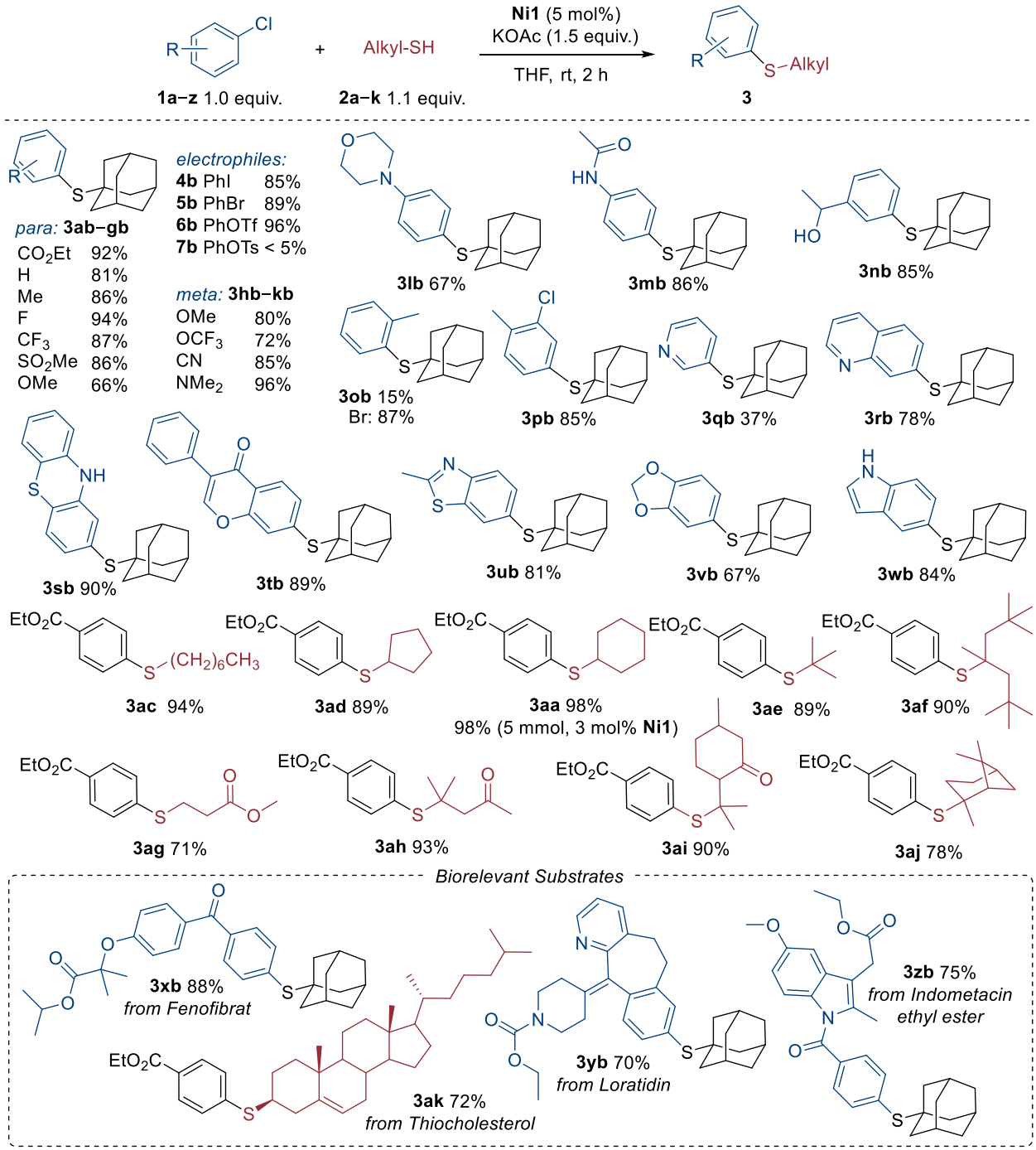

Scheme 51. Selected examples for the substrate scope with respect to aryl chlorides **1a**–**z** and alkyl thiols **2a**–**k**, as well as aryl iodide **4b**, bromide **5b**, triflate **6b** and tosylate **7b** as alternative electrophiles.

Additionally, primary, secondary and a large scope of sterically challenging tertiary alkyl thiols could be coupled **3ac**–**3ak**, tolerating functional groups such as ester **3ag** and ketone **3ah**, **3ai**. For secondary alkyl thiol **2a**, an upscale of the reaction (5 mmol), while simultaneously reducing the catalyst loading (3 mol%) showed the potential of this reaction for larger scale applications. While for aryl chlorides *ortho*-substituents presented a challenge **3ob**, for alkyl thiols amines, acid groups and aryl as well as benzyl substituents were not tolerated (see Chapter 5).

Further expanding the substrate scope, a variety of aryl (pseudo)halides, including aryl iodides, bromides, and triflates (PhI **4b**, PhBr **5b**, PhOTf **6b**) could be coupled in excellent yields under standard conditions, whereas aryl tosylates (PhOTs **7b**) required elevated temperatures and longer reaction times. Kinetic experiments were conducted regarding aryl (pseudo)halides and alkyl thiols to gain further insights (Figure 15). The reaction profiles for aryl (pseudo)halides depict an increasing induction period from PhOTf < PhI < PhBr < PhCl (presumably the time required to activate the pre-catalyst), while the reaction rate decreased from PhOTf > PhBr > PhCl > PhI. Aryl triflates could be identified as ideal substrates and were further investigated in the second publication (see Chapter 2.2). Aryl iodides, as an exception, did not follow the classic ease of oxidative addition correlating to the BDE for aryl halides (see Chapter 1.2.1). This can be explained through the facile generation of paramagnetic off-cycle Ni(I) species, which has been previously observed and described by Schoenebeck[99] (see Chapter 1.3.4) and could be shown for this system through NMR experiments. Primary **2c** and secondary **2a** alkyl thiols behaved similarly, with a comparable reaction rate and induction period of ~ 5 minutes, whereas the sterically challenging tertiary alkyl thiol **2b** required ~ 15 minutes induction period and had a slightly lower reaction rate. This showcases the influence of thiols, especially on the activation of the catalyst.

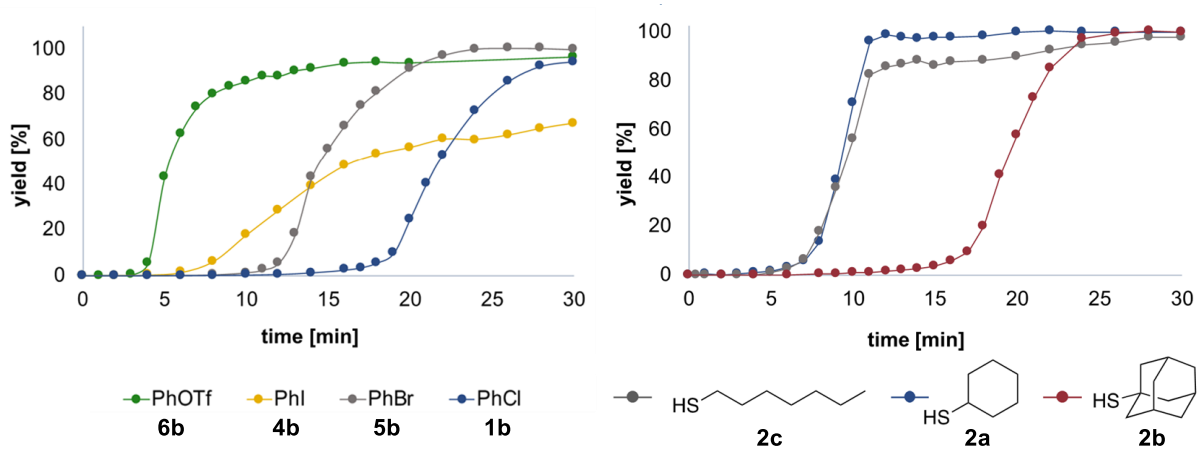

Figure 15. Reaction progress for different aryl (pseudo)halides coupled with tertiary alkyl thiol **2b** and reaction progress for different alkyl thiols coupled with aryl chloride **1a** under standard conditions.

To further explore the reactivity of different aryl (pseudo)halides, with the goal to enable chemoselective functionalization of bis-electrophiles, inter- as well as intramolecular selectivity experiments were conducted for a variety of C-X bonds (X = Cl, Br, I, OTf, OTs), identifying a reactivity order of PhOTf > PhI > PhBr > PhCl >> PhOTs (Scheme 52). Chemoselective reactions of substrates with two or more (pseudo)halide functionalities are a versatile and elegant tool to synthesize high value products. Selective mono-substitution yields products with reactive functional groups intact, while controlled, sequential reactions enable the synthesis of complex multi-functionalized molecules. For the mono-substitution between two different halides in di-substituted aryl (pseudo)halides (C-Cl *vs*. C-Cl, C-Br and C-I **9ab**–**9cb**) low to moderate selectivity was observed, while chemoselective mono-substitution of C-OTf in presence of C-Cl **9db**, as well as C-Cl **9eb** and C-OTf **9fb** in presence of C-OTs was possible in excellent yields.

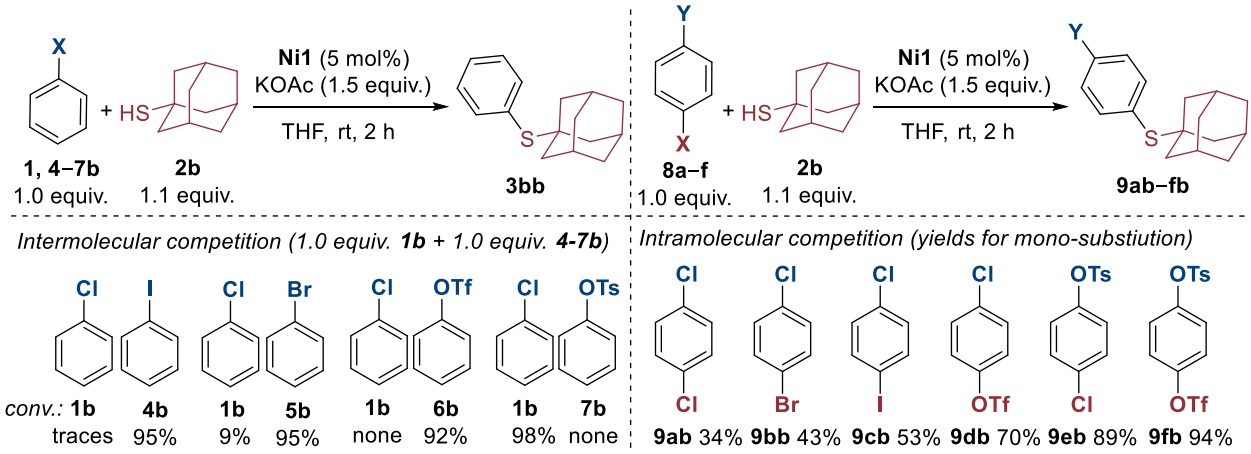

Scheme 52. Intermolecular competition experiments of two aryl (pseudo)halides (1.0 equiv. each) with the corresponding conversion depicted (GC-FID yields) and intramolecular competition experiments of various di-substituted aryl (pseudo)halides with the corresponding isolated yields for the mono-substituted product.

The preferential reactivity order was utilized to enable sequential one-pot C-S cross-coupling of di-substituted aryl (pseudo)halides for OTf/Cl **8d** and Cl/OTs **8f** combinations to generate the bis-functionalized thioether **10** (Scheme 53).

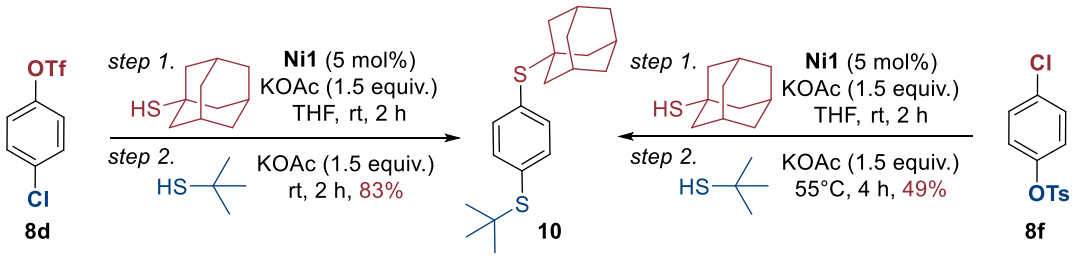

Scheme 53. Chemoselective one-pot multi-functionalization of bis-electrophiles **8d** and **8f**.

A variety of mechanistic studies were conducted, including Hammett analysis, NMR studies, radical scavenger experiments, as well as DFT calculations, to elucidate the mechanism. The postulated mechanism (Scheme 54) derived from the conducted mechanistic studies consists of a Ni(0)/Ni(II) catalytic cycle, with an initial activation of the one-component pre-catalyst XantphosNi(*o*-tolyl)Cl **Ni1** to generate the active Ni(0) complex **I**, followed by an oxidative addition of aryl chloride **1**, generating XantphosNi(Ar)Cl **II**, which acts as resting state of the catalytic cycle. An acetate coordination (ligand exchange *via* salt metathesis) to **III** and subsequent acetate facilitated formation of the thiolate complex **V** *via* internal deprotonation, similar to a CMD mechanism in **IV** (concerted metalation-deprotonation, known for C-H activation/arylation in Pd/Xantphos systems[176]), followed by a reductive elimination yields the thioether **3** and regenerates the active catalyst **I**.

Activation of the one-component pre-catalyst XantphosNi(*o*-tolyl)Cl **Ni1** to XantphosNi(0) **I** and on-cycle catalysis (reaction from the oxidative addition complex **II** to regeneration of the active catalyst XantphosNi(0) **I**) share the same mechanistic steps, rendering it an elegant way of catalyst activation.

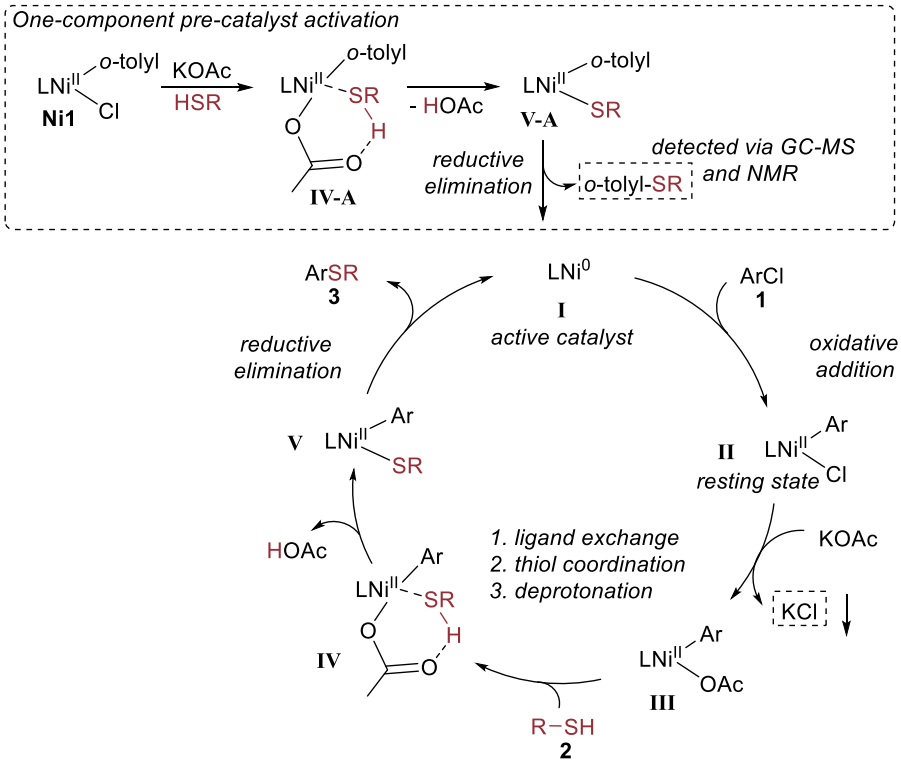

Scheme 54. Postulated mechanism with a Ni(0)/Ni(II) catalytic cycle, including the activation pathway for one-component pre-catalyst **Ni1**. For simplification the ligand Xantphos is abbreviated as L.

DFT calculations were conducted by Dr. J. Philipp Wagner (Figure 16, 17). They identified the role acetate plays, in addition to the versatile coordination modes of Xantphos, as well as the π-coordination of aryl chloride to the active Ni(0) catalyst **I-ArCl** prior to the oxidative addition, as key elements in the mechanism. η^1 and η^2 coordination of acetate could be calculated for the XantphosNi(Ar)OAc intermediate **III**. In the less stable and therefore more reactive η^2 coordination, one phosphor atom of the ligand is less tightly bound (elongation of the bond to a distance of 2.4 Å, in comparison to 2.2 Å for both phosphor atoms in the more stable η^1 coordination). This partial dissociation of Xantphos allows for the thiol **2** to attack trans on the metal and a subsequent deprotonation (acetate facilitated formation of the thiolate complex *via* internal deprotonation) are postulated to occur, yielding the intermediate XantphosNi(Ar)SR **V**. This is followed by a reductive elimination of the thioether, which is initially still bound to the generated XantphosNi(0) complex **I-Thiol**, but replaced by a π-coordinated aryl chloride to generate complex **I-ArCl**. The initial π-coordination facilitates the subsequent oxidative addition and generation of the oxidative addition intermediate XantphosNi(Ar)Cl **II**, which acts as resting state of the catalytic cycle (supported by NMR experiments, see Chapter 5). The current hypothesis as to why aromatic thiol compounds do not represent competent substrates for the catalytic system is that they could poison the active Ni(0) catalyst, similar to the π-coordination of aryl chloride, in an irreversible fashion. It is important to notice that the DFT calculations were conducted with methyl thiol as substrate. For larger alkyl thiols, such as tertiary examples, which increase the steric strain on the thiolate intermediate XantphosNi(Ar)SR **V**, reductive elimination most likely has a smaller activation barrier.

During NMR studies and stochiometric experiments, $Ni(Xantphos)_2$ was observed to act as catalyst sink. Although crystallization and full characterization are pending, the results are supported by previous reports on $Pd(Xantphos)_2$ (see Chapter 1.3).[47]

Kinetic studies (Hammett analysis) including electronic modifications of the electrophile (aryl chloride) and ligand (Xantphos), as well as steric modifications of the nucleophile (alkyl thiol) were conducted, analyzing the initial periods, reaction rates and overall yields (for graphs of the Hammett analysis see Chapter 5). Steric modification of the alkyl thiol (Figure 15) has an insignificant influence on the reaction rate, whereas tertiary alkyl thiols have a three times longer induction period (5 *vs* 15 minutes). One possible explanation for this observation is the role thiol plays during activation of the catalyst. A further increase in steric strain to generate

XantphosNi(*o*-tolyl)SR **V-A** from pre-catalyst XantphosNi(*o*-tolyl)Cl **Ni1** is disfavored due to the steric strain already induced by the *ortho*-tolyl group. This theory is supported by the low yields observed for *ortho*-substituted aryl chlorides **3ob** (for which on-cycle catalysis faces similar steric constraints as catalyst activation) and the short induction period < 2 minutes observed for the reaction with an *in-situ* generated catalyst from $Ni(cod)_2$/Xantphos, which only requires coordination of the ligand and no thiol interference for activation. Although the reaction rate is diminished, which can be explained by the stabilizing effect cod coordination has on the active catalytic species, rendering it less reactive (see Chapter 1.2.2).[43] Additionally, modifications of the aryl chloride, *p*-substituents with varying electronic properties (-OMe, -Me, -H, $-CO_2Et$, $-CF_3$), were analyzed. While electron withdrawing substituents were observed to slightly increase the reaction rate, with a mostly linear correlation to the σ_p Hammett constant ($\rho = 0.46$, $R^2 = 0.96$), the low ρ value shows an overall small influence, which is in agreement with the DFT calculation, indicating that the oxidative addition is unlikely to be the rate determining step.

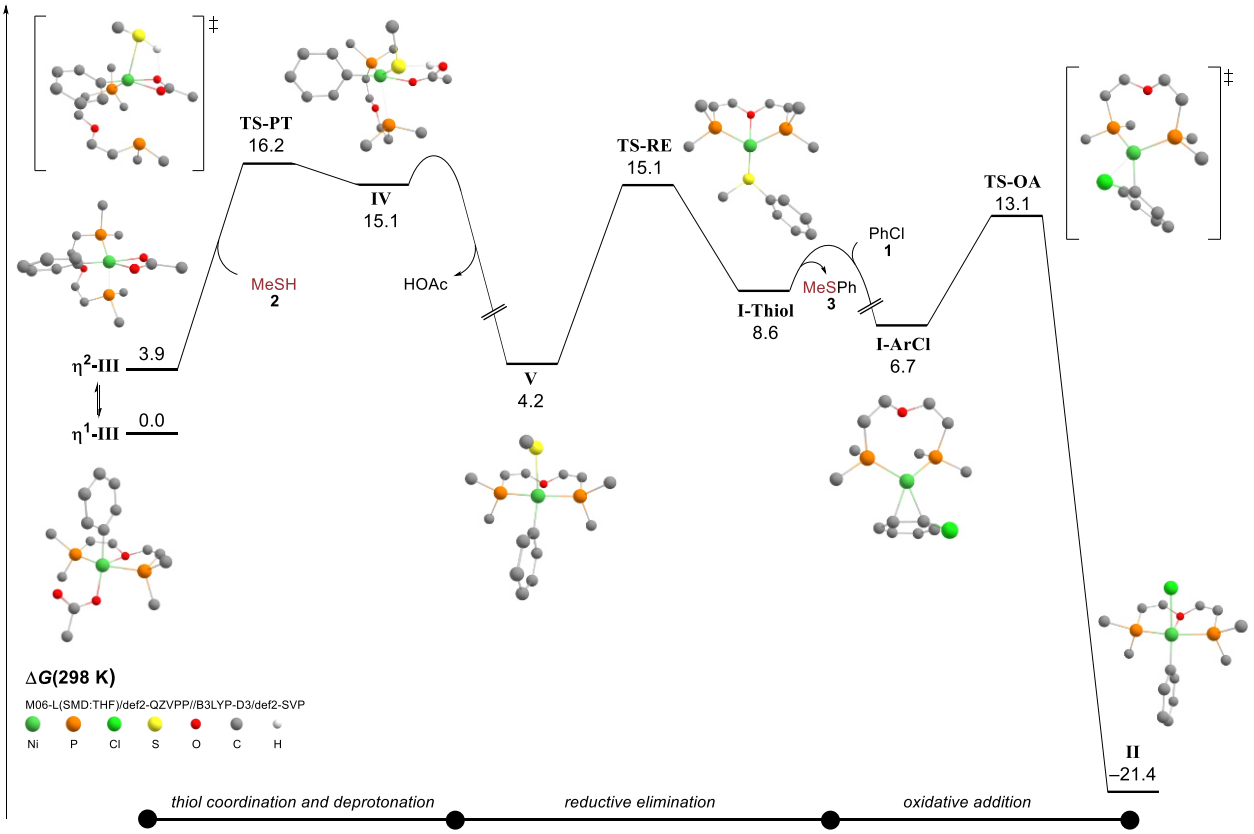

Figure 16. Free energy surface for the nickel catalyzed coupling of methanethiol as model nucleophile and PhCl as electrophile at the M06-L(SMD:THF)/def2-QZVPP//B3LYP-D3/def2-SVP level of theory. Only selected atoms of the Xantphos ligand are displayed and all carbon-bound hydrogens are omitted for clarity. Transition state is abbreviated as TS.

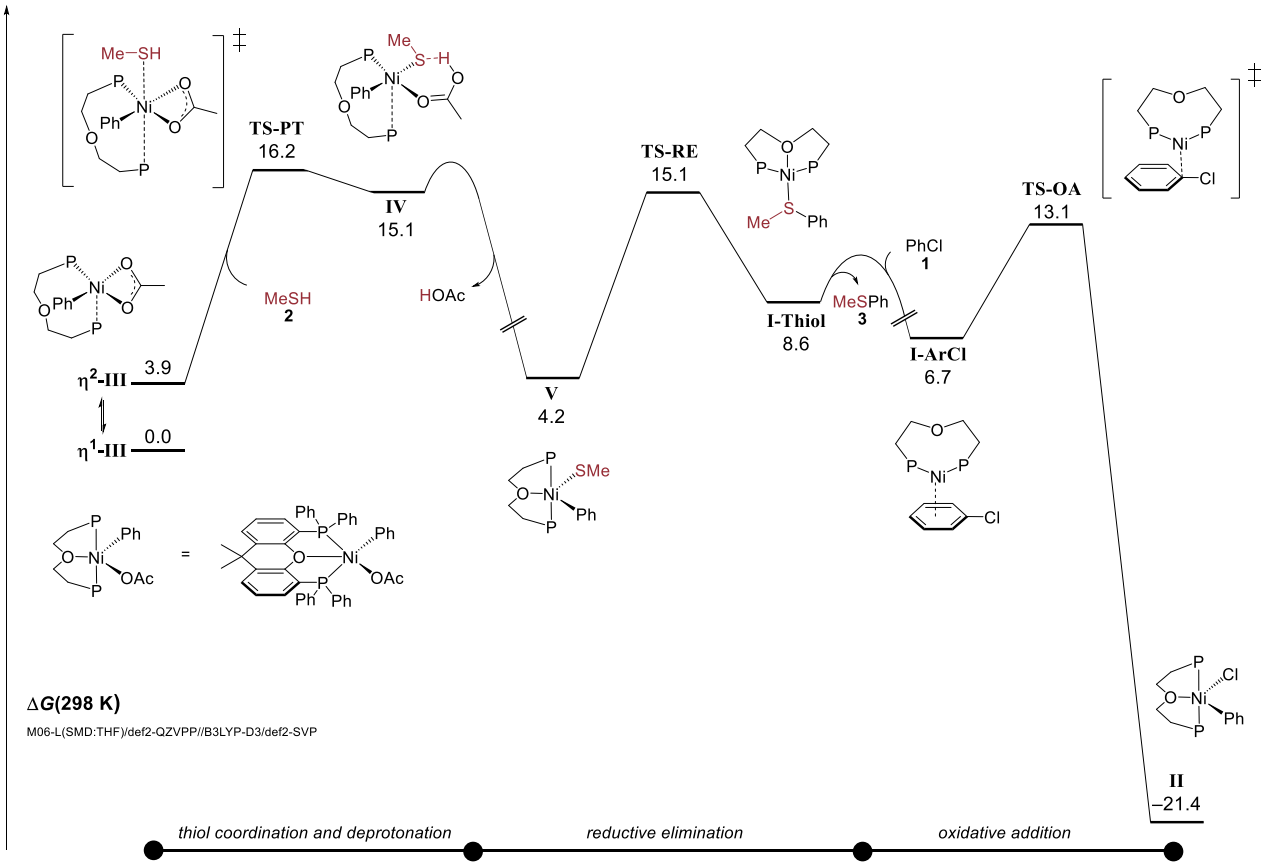

Figure 17. Free energy surface of Figure 16 with graphic depiction of the chemical structures.

In conclusion, a mild, fast and operationally simple catalytic system for the coupling of aryl chlorides with primary, secondary as well as previously challenging tertiary alkyl thiols in excellent yields, using the air-stable pre-catalyst XantphosNi(*o*-tolyl)Cl **Ni1** and KOAc as base at room temperature, was developed (Scheme 55). An excellent functional group tolerance and functionalization of complex pharmaceutical compounds, as well as chemoselective mono- and di-substitution of bis-electrophiles were demonstrated in addition to insights into the mechanism through mechanistic studies including kinetic, DFT and NMR experiments.

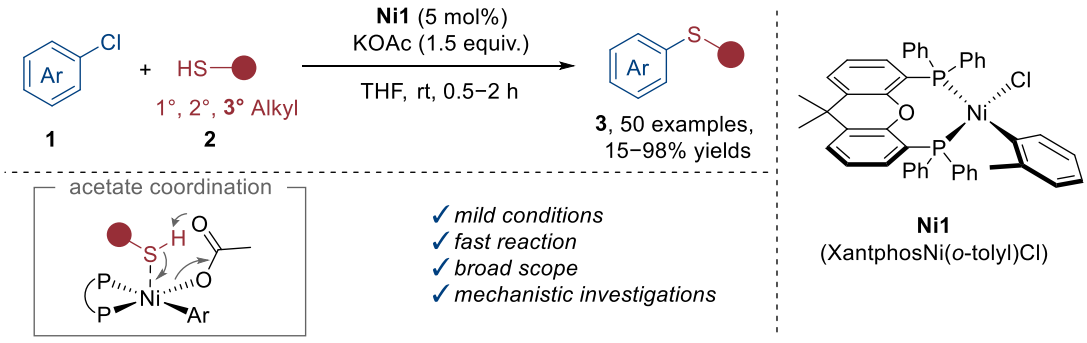

Scheme 55. Developed mild nickel catalyzed C-S cross-coupling of aryl chlorides **1** and alkyl thiols **2**.

2.2. Nickel Catalyzed Cross Coupling of Aryl and Alkenyl Triflates with Alkyl Thiols

Aim of this work was to utilize the previously developed catalytic system for the C-S cross-coupling of alkyl thiols and aryl halides, by expanding the substrate scope to aryl and alkenyl triflates, which have been identified as ideal substrates during previous electrophile screening experiments (see Chapter 2.1, Figure 15).[177] Aryl and the less investigated alkenyl thioethers are valuable structural motifs present in materials, agrochemicals and pharmaceutical compounds (see Chapter 1.3.1).[85] Aryl halides, in particular aryl chlorides, are abundant, low-cost substrates, when commercially available. Otherwise, the synthesis of aryl and alkenyl halides may require multiple steps and forcing reaction conditions.[31] On the other hand, the synthesis of aryl and alkenyl triflates is a simple one step procedure under mild reaction conditions with a broad functional group tolerance, from phenols[32] and ketones[33] respectively, rendering them excellent alternative substrates and versatile building blocks (see Chapter 1.2.1).

The previously developed catalytic system (see Chapter 2.1) consisting of XantphosNi(*o*-tolyl)Cl **Ni1**[46] as air-stable pre-catalyst and KOAc as low-cost base could be utilized for the coupling of aryl and alkenyl triflates with alkyl thiols, concentration on challenging tertiary examples, without further adaptations, showcasing the diverse potential and applicability of the system.

First a variety of aryl triflates were explored together with Ivo H. Lindenmaier, showcasing an excellent functional group tolerance and overall higher yields than previously observed for aryl chlorides. Electron-neutral, -rich and -deficient aryl triflates could be coupled, including a variety of functional groups **11ab**–**11hb**, such as ester **11ab**, nitrile **11eb**, amide **11kb** and methoxy **11hb**, in addition to various heterocycles **11lb**–**11nb**. Especially for sterically challenging electrophiles, such as *ortho*-methyl **11ib** and 1-napthyl based aryl compound **11jb**, aryl triflates were superior, generating excellent yields, whereas for aryl chlorides only low yields were observed (**3ob**, Scheme 51). The high reactivity of triflates enabled chemoselective mono-coupling of bis-electrophiles, through a C-OTf functionalization in presence of C-OTs **11fb** and in presence of C-Cl **11gb** in excellent yields. Late stage functionalization of pharmaceutically relevant compounds was exemplary shown on triflates derived from Ezetimibe **11pb** and Estrone **11qb** (Scheme 56).

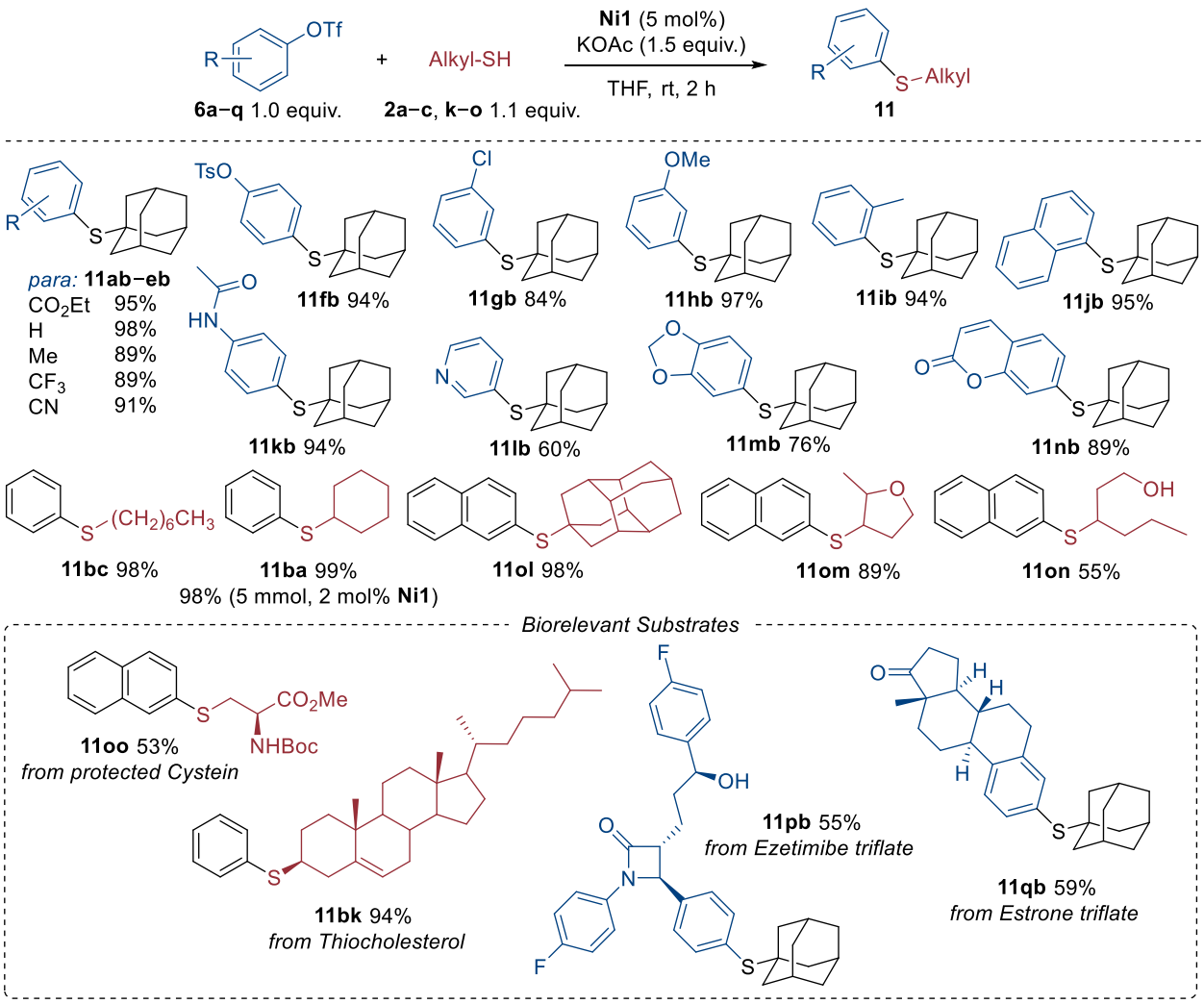

Scheme 56. Selected examples for the substrate scope with respect to aryl triflates **6a**–**q** and alkyl thiols.

Furthermore, a variety of primary, secondary as well as tertiary alkyl thiols, such as diadamantanethiol **11ol**[178] could be coupled in excellent yields, tolerating functional groups such as ether **11om** and hydroxy **11on**. The functionalization of protected cysteine **11oo** and thiocholesterol **11bk** showcased the facile coupling of biorelevant thiols. An upscale of the reaction to 5 mmol and simultaneous reducing of the catalyst loading to 2 mol% **11ba** shows the applicability of this system for low-cost, larger scale transformations.

In addition to aryl triflates, a variety of alkenyl triflates could be coupled in excellent yields (Scheme 57). Cyclic 6-membered alkenyl moieties, including functional groups such as ester **13bb** and heterocycles **13cb**, **13db** were tolerate. 5- and 7- membered cycloalkenyl triflates **13fb**, **13gb** and fused benzene rings **13hb**, **13ib**, as well as acyclic compound **13jb** in addition to the cholestane 3-one derived triflate **13eb** were coupled in excellent yields.

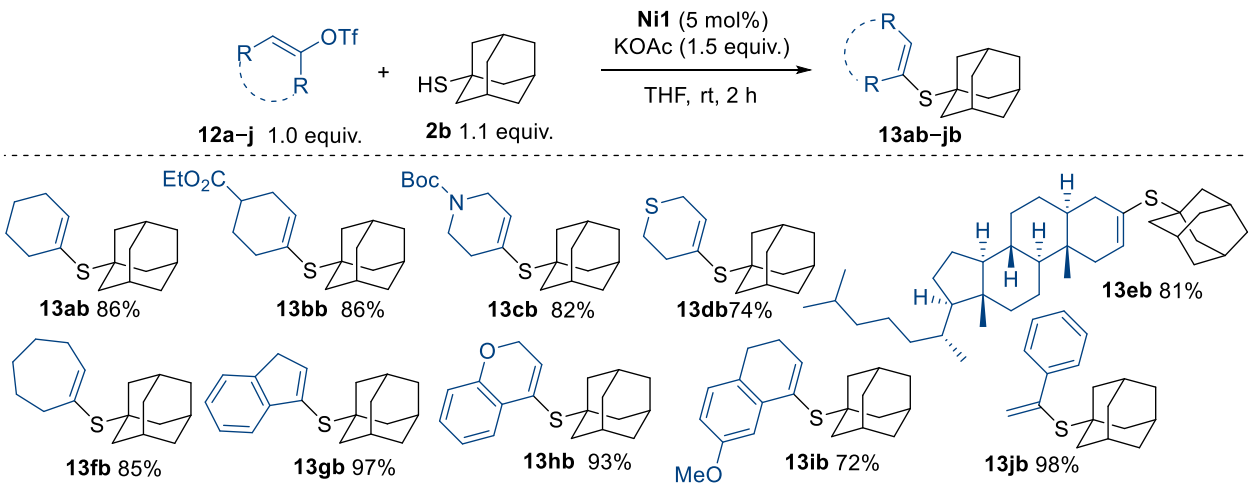

Scheme 57. Selected examples for the substrate scope with respect to alkenyl triflates **12a**–**j**.

The mechanism is postulated to conform to the reaction with aryl chlorides, in a Ni(0)/Ni(II) catalytic cycle (see Chapter 2.1, Scheme 54). Further kinetic studies were conducted to compare the reaction profile and reactivity of aryl halides to aryl and alkenyl triflates (Figure 18). The induction period increases from PhOTf < AlkenylOTf ≈ PhBr < PhCl and the reaction rate decreases from PhOTf > PhBr > PhCl > AlkenylOTf. While the kinetic profiles of the aryl (pseudo)halides (PhOTf, PhBr, PhCl) are similar, aryl triflates can be identified as most reactive electrophiles, showcasing the shortest induction period and highest reaction rate. This observation could indicate a comparatively facile oxidative addition, enabling a fast activation of the catalyst (short induction period) and on-cycle catalysis (high reaction rate), which is supported by the facile coupling of challenging *ortho*-substituted compounds.

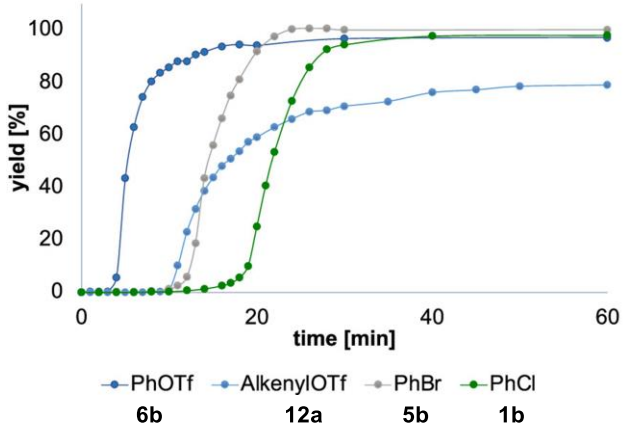

Figure 18. Reaction progress for the C-S cross-coupling of different aryl and alkenyl (pseudo)halides with tertiary alkyl thiol **2b** under standard reaction conditions.

While the short induction period of aryl triflates, in comparison to aryl halides has yet to be researched further, it indicates that the (pseudo)halide has an influence on the catalyst activation, possibly due to an equilibrium between (pseudo)halide and acetate coordination (see Chapter 2.1, Scheme 54, equilibrium between **II** and **III**) prior to the reaction with alkyl thiol. In palladium catalysis such an equilibrium has previously been postulated and the weak bonding of the triflate anion was observed to enable a more facile ligand exchange with acetate in comparison to halides, rendering the reaction and therefore catalyst activation faster.[179]

In comparison to aryl triflate **6b**, alkenyl triflate **12a** has a longer induction period, as well as a lower reaction rate and overall yield. The current explanation for the superiority of aryl over alkenyl triflates is the π-coordination of the aryl (pseudo)halide to the activated Ni(0) catalyst (supported by DFT calculations for the reaction with aryl chlorides, see Chapter 2.1, Scheme 16, 17, **I-ArCl**) facilitating the oxidative addition by decreasing the required activation energy.[175]

To further study the influence of the aryl(pseudo)halide and acetate on the catalytic system XantphosNi(*o*-tolyl)X (X = OTf, Br, I, OAc) could be synthesized and isolated, to analyze if the induction period for a reaction with aryl chlorides would be decreased. Alternative aryl moieties to *ortho*-tolyl may be required to isolate a stable complex, which could render a direct comparison challenging. Additionally, various (pseudo)halide salt reagents could be added to the reaction mixture to test the influence on the catalyst activation (induction period) and overall reaction rate.

In conclusion, a mild, low-cost and convenient C-S cross-coupling of aryl and alkenyl triflates with alkyl thiols utilizing the one-component pre-catalyst XantphosNi(o-tolyl)Cl **Ni1** and KOAc as base at room temperature for 0.25–2 h was developed (Scheme 58), showcasing an excellent functional group tolerance. Late stage functionalization of bioactive or pharmaceutically relevant compounds enabled the synthesis of complex aryl and previously underdeveloped alkenyl thioethers. The versatile reactivity with a variety of aryl (pseudo)halides indicates potential of the catalytic system for future nickel-catalyzed cross-electrophile coupling reactions.

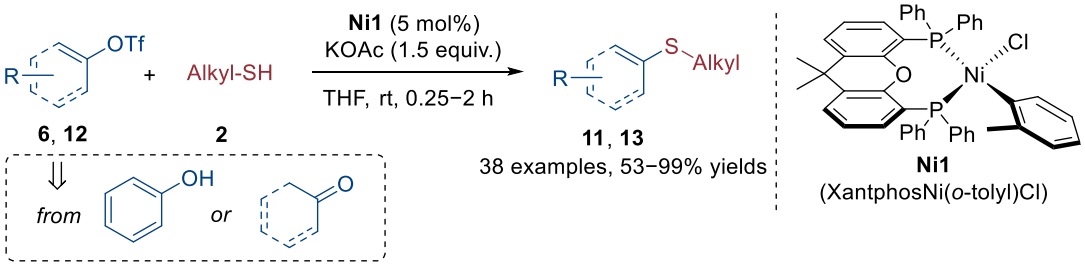

Scheme 58. Developed mild nickel catalyzed C-S cross-coupling of aryl **6** and alkenyl **12** triflates, derived from low-cost phenol and ketones, with alkyl thiols **2**.

2.3. Flipping the Switch on Palladium Catalyzed Carboiodination: Accessing Kinetic and Thermodynamic Products

Aim off this work was to synthesize the *endo (anti)* carboiodination product of stereogenic iodides. While direct access proved challenging, an epimerization of the *exo (syn)* isomer could be utilized to generate the desired product in excellent yield and selectivity.[180] Epimerization can be employed as a powerful tool for stereochemical editing, granting convenient access to different diastereomers (see Chapter 1.5.1). While previous reports[159, 165-166] focused on C-H bond epimerization, the substrate scope could be expanded to C-I bonds.

Norbornene was chosen as model compound due to the sterically differentiated *exo* and *endo* faces. While the thermal intermolecular carboiodination of norbornene with aryl iodides has been reported to yield the *exo (syn)* product[173] **14**, an initial screening for a palladium catalyzed intermolecular carboiodination under blue light irradiation yielded the *endo (anti)* product **15** (Scheme 59). Although the palladium catalyzed carboiodination under blue light irradiation is not efficient yet (an excess of 4.0 equiv. norbornene is required, yielding up to 55%) the possibility to access the *endo (anti)* product, in combination with the previously postulated reversible C-I bond formation (see Chapter 1.5.3, Scheme 49),[174] inspired the alternative pathway: to utilize stereochemical editing and access the *(endo) anti* isomer *via* epimerization of the *exo (syn)* isomer in a palladium catalyzed reaction under blue light irradiation (Scheme 59). This project was a cooperative work with Ramone Arora, Clara Jans, Bijan Mirabi and Dr. Austin D. Marchese.

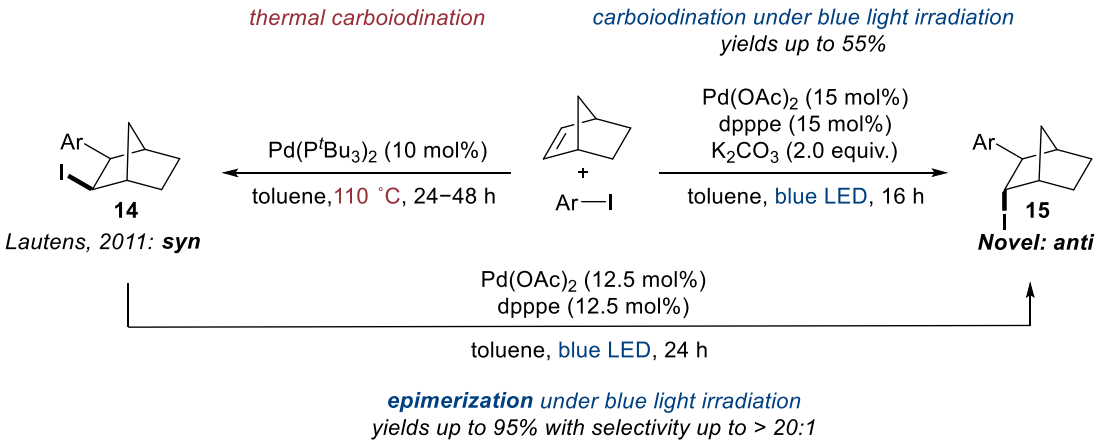

Scheme 59. Thermal carboiodination of norbornene yielding the *exo (syn)* isomer **14**,[173] carboiodination under blue light irradiation yielding the *endo (anti)* isomer **15** and palladium catalyzed epimerization under blue light irradiation from the *exo (syn)* **14** to the *endo (anti)* isomer **15**.

An initial reaction conditions screening (palladium source, ligand, solvent, catalyst and ligand loading in addition to temperature and time studies, see Chapter 5) identified 12.5 mol% $Pd(OAc)_2$ and dpppe **L22** in toluene at room temperature under blue light irradiation (465 nm LED) for 24 h as ideal, generating the product in high yield and selectivity (83% yield with > 20:1 selectivity, Table 3, entry 1). Lowering the catalyst loading to 10 mol% did not impact the yield, but decreased the *endo*:*exo* ratio significantly (10:1 selectivity, entry 2). High stereoselectivity was considered more important than low catalyst loading in this conceptual study. When utilizing $Pd(OAc)_2$/dpppe as catalytic system, the base K_2CO_3 had no impact (entry 3), while for $Pd(PPh_3)_4$ as catalyst only low yields (38% with 1:1 selectivity, entry 4) without, while with base 80% yield and 8:1 selectivity were observed (entry 5). No product was formed under UV light irradiation (entry 6), which is known to induce C–I bond homolysis,[154] showcasing the necessity of the catalytic system.

Table 3. Selected examples for screening of the catalytic system, base and irradiation for the epimerization of *exo* isomer **14a** to *endo* isomer **15a**. ^{1}H NMR-yields with internal standard 1,3,5-trimethoxybenzene.

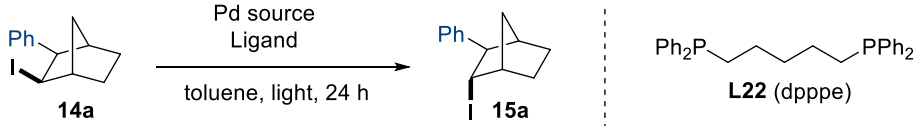

Entry	Catalytic system		K_2CO_3 [equiv.]	Light	Yield [%]	*endo*:*exo*
1	$Pd(OAc)_2$/ dpppe	12.5 mol%	-	465 nm	83	>20:1
2	$Pd(OAc)_2$ /dpppe	10.0 mol%	-	465 nm	81	10:1
3	$Pd(OAc)_2$ /dpppe	12.5 mol%	2.0	465 nm	80	>20:1
4	$Pd(PPh_3)_4$	10.0 mol%	-	465 nm	38	1:1
5	$Pd(PPh_3)_4$	10.0 mol%	2.0	465 nm	80	8:1
6	-		-	270 nm	none	-

After optimization, the substrate scope was analyzed (Scheme 60). A variety of electron-neutral, -rich and -deficient *meta*- and *para*-substituents, including methoxy **15b**, hydroxy **15c**, nitro **15d** and cyano **15e**, as well as the heterocyclic iodo-indole **15l** were tolerated in good to excellent yield and selectivity. Chemoselective mono-functionalization was observed for di-halides, coupling preferentially on the iodo-group, generating the corresponding chloro-, bromo-, iodo- and fluoro-substituted products **15g**–**15j**. While an *ortho*-methyl substituent was tolerated **15f**, *ortho*-^{i}Pr led to no product formation, showcasing a limitation to steric strain on the *ortho* position, possibly due to a challenging oxidative addition into the alkyl-iodide bond.

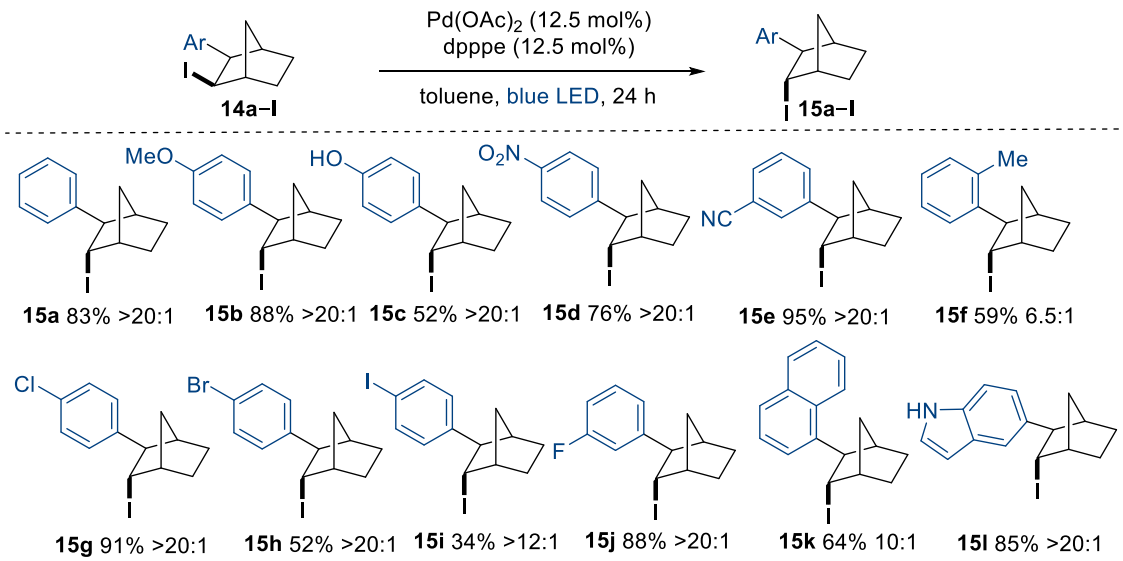

Scheme 60. Selected examples of the substrate scope for the epimerization of *exo (syn)* isomers **14a-l**.

Mechanistic studies, including isolation of catalytic intermediates, DFT calculations and radical scavenger experiments were conducted and the following mechanism was postulated (Scheme 61). After *in-situ* generation of LPd(0) **I**, two pathways for the reaction with the *exo* isomer **14a** could occur. Either a classic two-electron oxidative addition into the alkyl-iodide bond, generating intermediate **II**, followed by a blue light mediated bond homolysis yielding the corresponding radical pair **III**, or a blue light mediated excited state LPd(0)* **I*** undergoes a one-electron oxidative addition, abstracting the halide and generating the radical pair **III**. Product formation, presumably *via* reversible stereoinvertive reductive elimination through a halide abstraction from the radical LPd(I)iodide species **III** yields the *endo (anti)* isomer **15a** while LPd(0) **I** is regenerated.

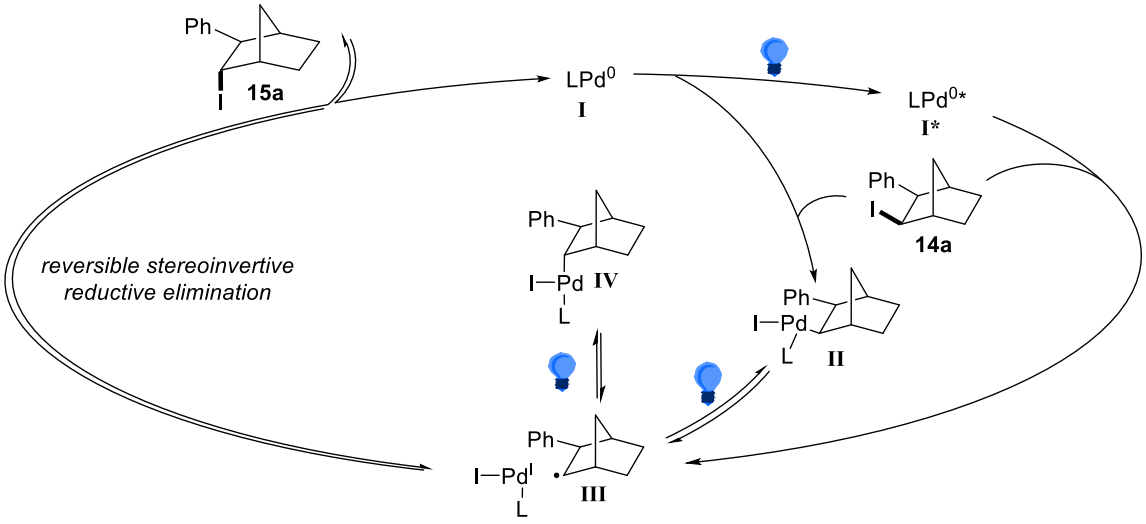

Scheme 61. Postulated mechanism for the palladium catalyzed epimerization under blue light irradiation. For simplification the ligand is abbreviated as L.

The radical LPd(I)iodid species **III** can presumably recombine reversibly with palladium, generating the *anti* oxidative addition complex **IV**. This equilibrium is postulated, due to the observation of β-hydride elimination product **17a** in the crude product mixture.

To enable a facile isolation and crystallization of catalytic intermediates, $Pd(PPh_3)_4$ which has proven to be a competent catalyst for the reaction, although generating lower yields (Table 3), was utilized as a simplified model compound. The analogue of intermediate **II**, complex $PPh_3Pd(alkyl)I$ **Pd5-I** was isolated and crystalized, confirming the *syn* isomer. Under thermal conditions, at 100 °C insignificant product formation was observed from $PPh_3Pd(alkyl)I$ **Pd5-I**, while under blue light irradiation the *endo (anti)* product **15m** was generated *via* reductive elimination in similar yields to the epimerization catalyzed with $Pd(PPh_3)_4$ (Scheme 62 and Table 3, entry 4). Additionally, the catalytic competence of intermediate **II** could be confirmed, by employing complex $PPh_3Pd(alkyl)I$ **Pd5-I** successfully as catalyst for the epimerization (40% yields were generated, see Chapter 5).

Isolation and blue light irradiation of the bromine analogue of intermediate **II**, complex $PPh_3Pd(alkyl)Br$ **Pd5-Br** yielded the brominated *endo (anti)* product **16a** in 20% (Scheme 62). Although a low yield, requiring further optimization, it acts as conceptual proof for a $C(sp^3)$–Br bond formation *via* reductive elimination from an isolated LPd(alkyl)Br complex, showcasing the potential of the catalytic system for palladium catalyzed carbobromination reactions under blue light irradiation. While radical scavenger experiments support a radical mechanism, DFT calculations by Bijan Mirabi confirmed that the *endo (anti)* isomer is the thermodynamically favored product by 1.71 kcal/mol^{-1} (see Chapter 5).

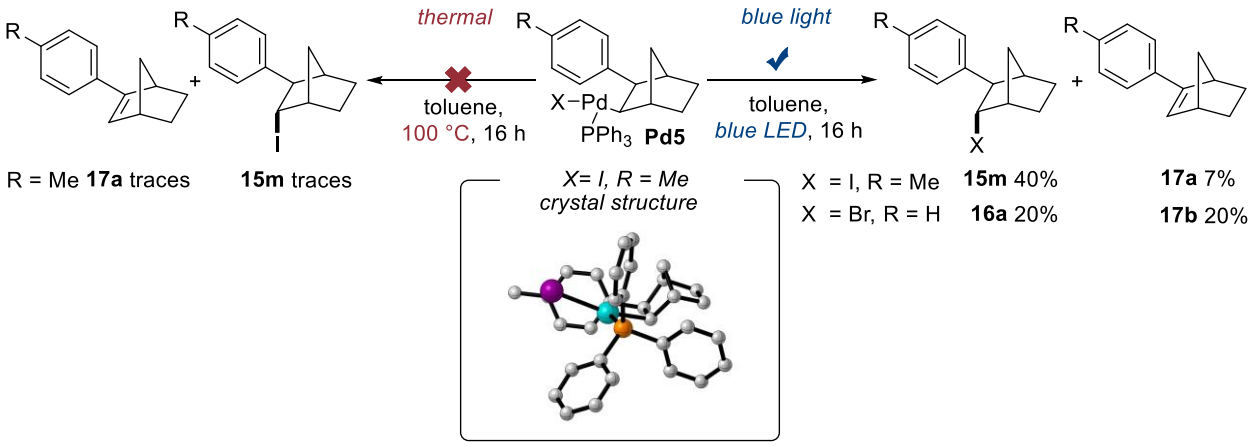

Scheme 62. Crystal structure for complex $PPh_3Pd(alkyl)I$ **Pd5-I** with product formation *via* reductive elimination under blue light irradiation and insignificant product formation at 100 °C. ^1H NMR-yields with internal standard 1,3,5-trimethoxybenzene.

In conclusion, a mild, base free palladium catalyzed epimerization of stereogenic iodides under blue light irradiation from the *exo* **14** to the *endo* **15** phase in norbornene model compounds was developed (Scheme 63). Mechanistic studies and DFT computations support a thermodynamically driven reaction generating the *endo (anti)* product *via* reversible C-I bond formation. Conceptual proof for a C(sp^3)–Br bond formation *via* reductive elimination from an isolated P(II) complex LPd(alkyl)Br **Pd5-Br** indicates the applicability of palladium catalyzed carbobromination under blue light irradiation for future studies.

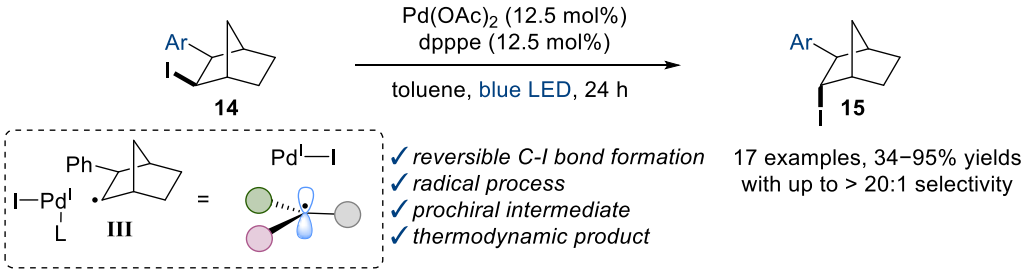

Scheme 63. Developed mild and base free palladium catalyzed epimerization under blue light irradiation *via* reversible C-I bond formation yields the thermodynamic product, *endo (anti)* isomer **15**.

Chapter 3

UNPUBLISHED RESULTS

3. Unpublished Results

3.1. Further Investigations into Nickel Catalyzed C-S Cross-Coupling

In the quest to enable a facile C-S cross-coupling with previously challenging tertiary alkyl thiols, preliminary screening experiments of ligands, additives and reaction conditions, while utilizing the air-sensitive transmetalation reagent PhZnCl, identified DPEPhos (one-component pre-catalyst DPEPhosNi(mesityl)Cl **Ni4** or *in-situ* generation of the catalyst *via* $Ni(cod)_2$/DPEPhos **L21**) as superior ligand to Xantphos (one-component pre-catalyst XantphosNi(*o*-tolyl)Cl **Ni1** or *in-situ* generation of the catalyst *via* $Ni(cod)_2$/Xantphos **L6**). DPEPhos, a hemilabile ligand similar to Xantphos, but more flexible and less sterically demanding with a smaller bite angle (see Chapter 1.2.3) could decrease the steric strain on the catalytic system, rendering the coupling of tertiary alkyl thiols possible. While DPEPhosNi(mesityl)Cl **Ni4** enabled the coupling of tertiary alkyl thiol **2e** in 76% and **2b** in 67% yield, primary **2c** and secondary **2a** alkyl thiols only generated low yields (Scheme 64, conditions A), presumably due to a lack of steric strain. For XantphosNi(*o*-tolyl)Cl **Ni1** the order was reversed with primary **2c** and secondary **2a** alkyl thiols showcasing excellent and tertiary alkyl thiols **2e**, **2b** low yields. Therefore, the steric strain on the catalytic system, induced by the thiol or ligand, is postulated to be a limiting factor in the transformation.

Despite extensive optimization experiments, the yields could not be further improved, which led to the initial base screening (see Chapter 2.1, Table 2). KOAc was identified as ideal base for this transformation, enabling the reaction under mild conditions. Optimization experiments, substrate scope as well as mechanistic studies can be seen in the original publication and supporting information (see Chapter 5). In this chapter additional experiments which were conducted, but not included in the publication are summarized.

For the new catalytic system with KOAc as base at room temperature, XantphosNi(*o*-tolyl)Cl **Ni1**, outcompetes DPEPhos(mesityl)Br **Ni4** for primary **2c**, secondary **2a** as well as tertiary alkyl thiols **2e**, **2b** (Scheme 64, conditions B). This behavior diverges from the old system with PhZnCl, in which XantphosNi(*o*-tolyl)Cl **Ni1** was superior for primary **2c** and secondary **2a**, whereas DPEPhos(mesityl)Br **Ni4** was superior for tertiary alkyl thiols **2e**, **2b** (Scheme 64, conditions A).

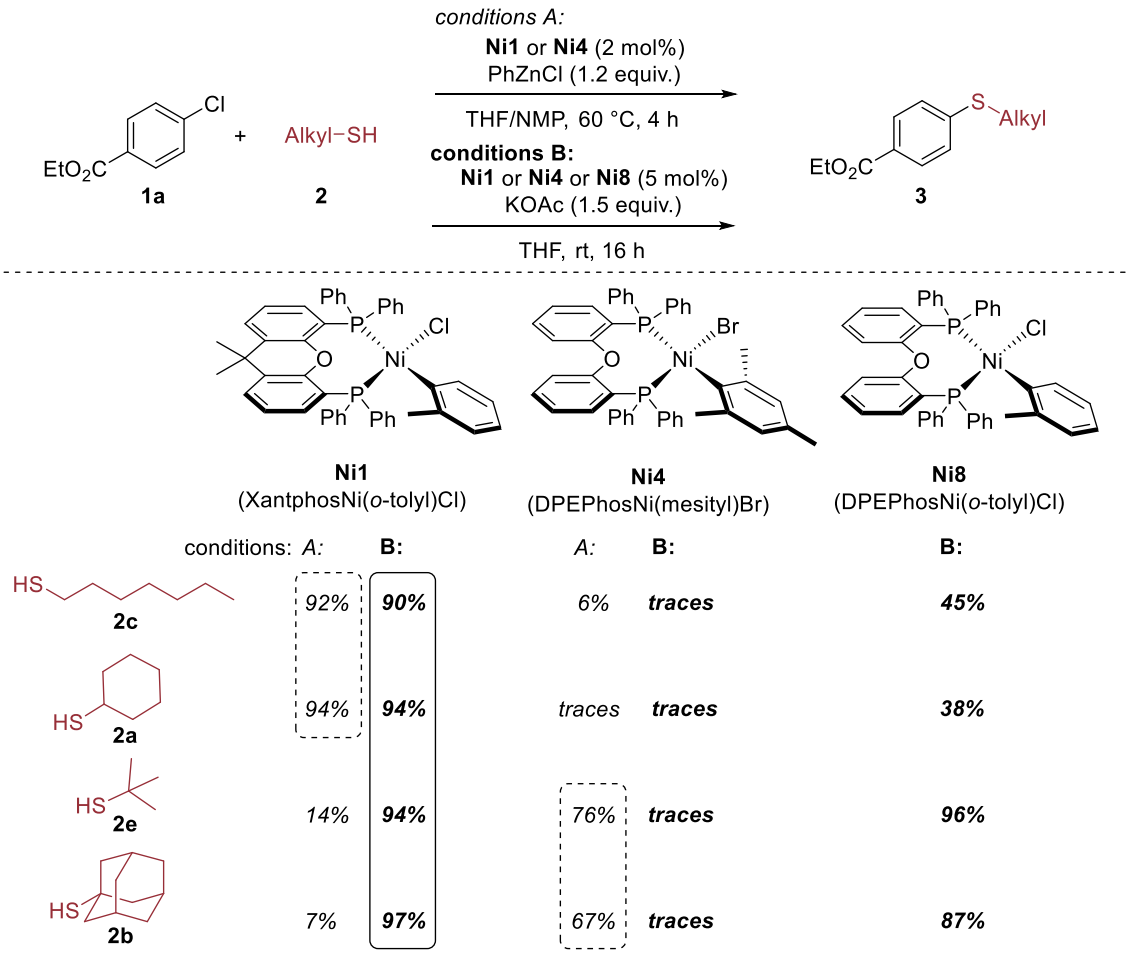

Scheme 64. Influence of pre-catalyst XantphosNi(*o*-tolyl)Cl **Ni1**, DPEPhosNi(mesityl)Cl **Ni4** and DPEPhosNi(*o*-tolyl)Cl **Ni8** on the coupling of aryl chloride **1a** and primary **2c**, secondary **2a**, as well as tertiary **2e**, **2b** alkyl thiols for the catalytic system utilizing PhZnCl (conditions A) or KOAc (conditions B). GC-FID yields calibrated against pentadecane.

Another difference between the two catalytic systems is that for PhZnCl, the one-component pre-catalyst **Ni1**/**Ni4** and the corresponding *in-situ* generated catalyst from $Ni(cod)_2$ and Xantphos/DPEPhos generate comparable yields for the reaction with secondary thiol **2a**, while for KOAc as base, the yields with Xantphos are comparable (Table 4, entry 1: 94% *vs* entry 6: 97%), whereas the yields for DPEPhos diverge (Table 4, entry 2: traces *vs* entry 7: 46%). This indicates that in addition to Xantphos and DPEPhos, the aryl (*o*-tolyl *vs* mesityl) and halide (Cl *vs* Br) ligands, which are involved in the activation of the pre-catalyst, have an increased influence. Therefore, the diverging yields with PhZnCl as more reactive and KOAc as milder, less reactive system, are dependent on two different influences, which have to be viewed separately.

1. One-component pre-catalyst activation (*o*-tolyl *vs* mesityl) and (Cl *vs* Br)
2. Ligand influence (Xantphos *vs* DPEPhos)

For activation of the pre-catalyst, not Xantphos and DPEPhos, but the coordinated aryl and halide species (*o*-tolyl)Cl and (mesityl)Br are of importance. To generate the active catalytic species, the one-component pre-catalyst undergoes a ligand exchange, followed by thiol coordination and reductive elimination of the thioether (*o*-tolyl)SR and (mesityl)SR respectively, generating Xantphos/DPEPhosNi(0) (see Chapter 2.1, Scheme 54). To enable a direct comparison of Xantphos and DPEPhos pre-catalysts, without the influence of different aryl (*o*-tolyl *vs* mesityl) and halide (Cl *vs* Br) ligands, DPEPhosNi(*o*-tolyl)Cl **Ni8** was synthesized. The pre-catalyst could couple primary **2c** and secondary **2a** alkyl thiols in moderate, whereas tertiary alkyl thiols **2e**, **2b** were coupled in excellent yields (Scheme 64, conditions B), correlating with the control experiments for $Ni(cod)_2$/DPEPhos (Table 4, entry 7). A systematic investigation of the aryl as well as halide influence on the pre-catalyst DPEPhos or XantphosNi(aryl)X, by varying the aryl as well as halide (and alternative pseudohalide) substituents, is to be conducted to gain further detailed insight.

$Ni(cod)_2$ is commonly employed as nickel source in coupling reactions due to a multitude of reasons. The highly reactive Ni(0) source is commercially available and can be utilized efficiently in ligand as well as reaction condition screenings, generating the active catalytic species, without requiring additional reducing agents (see Chapter 1.2.2). Disadvantageous are the high costs and the air-sensitive nature, which necessitates storage and reaction set-up under inert conditions.

In addition to the air-stable one-component pre-catalysts, low-cost and air-stable Ni(II) salts are an alternative nickel source, which commonly require reducing agents and harsher reaction conditions. A variety of these nickel sources ($Ni(OAc)_2$, $Ni(acac)_2$, $NiCl_2$) were screened for the coupling of secondary alkyl thiol **2a**, requiring 1 equiv. of zinc and 50 °C for a facile transformation (Table 4, entry 8–15).

Interestingly, zinc, which is often employed as reducing agent, facilitates the reaction catalyzed with DPEPhosNi(mesityl)Br **Ni4**, providing excellent yields and therefore rendering the influence of the coordinated aryl halide *o*-tolylCl or mesitylBr insignificant, presumably by enabling an alternative activation pathway for the pre-catalyst *via* a facile reduction from Ni(II) to Ni(0) (Table 4, entry 4,5, Table 5, entry 4,5).

Table 4. C-S cross-coupling of aryl chloride **1a** and secondary alkyl thiol **2a** with various catalytic systems and reaction conditions, including Ni(II) sources, such as one-component pre-catalyst **Ni1**, **Ni4**, **Ni8**, nickel salts and the Ni(0) source $Ni(cod)_2$, with Xantphos **L6** or DPEPhos **L21** as ligand. GC-FID yields calibrated against pentadecane.

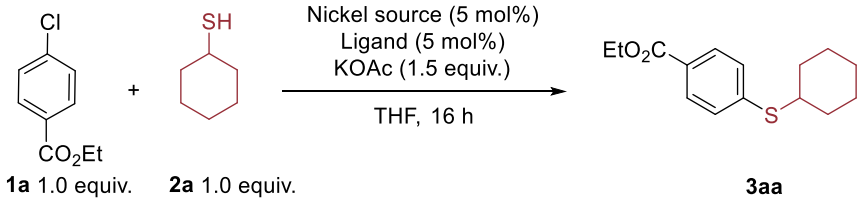

1a 1.0 equiv. **2a** 1.0 equiv. **3aa**

Entry	Nickel source	Ligand	Zn [equiv.]	temp. [°C]	Yield [%]
1	**Ni1** XantphosNi(*o*-tolyl)Cl		-	rt	94
2	**Ni4** DPEPhosNi(mesityl)Br		-	rt	traces
3	**Ni8** DPEPhosNi(*o*-tolyl)Cl		-	rt	38
4	**Ni1** XantphosNi(*o*-tolyl)Cl		1	rt	94
5	**Ni4** DPEPhosNi(mesityl)Br		1	rt	96
6	$Ni(cod)_2$	Xantphos	-	rt	97
7	$Ni(cod)_2$	DPEPhos	-	rt	46
8	$Ni(OAc)_2$	Xantphos	1	rt	traces
9	$Ni(OAc)_2$	Xantphos	-	50	traces
10	$Ni(OAc)_2$	Xantphos	1	50	96
11	$Ni(OAc)_2$	DPEPhos	1	50	91
12	$NiCl_2$	Xantphos	1	50	91
13	$NiCl_2$	DPEPhos	1	50	6
14	$Ni(acac)_2$	Xantphos	1	50	82
15	$Ni(acac)_2$	DPEPhos	1	50	none

Additionally, an impact of acetate on the influence of the Xantphos/DPEPhos ligand was observed. For $NiCl_2$ and $Ni(acac)_2$ as Ni(II) sources, a strong ligand effect is seen for the coupling of secondary alkyl thiol **2a**, with Xantphos generating excellent yields, whereas for DPEPhos only trace amounts of product can be observed. When $Ni(OAc)_2$ is employed as nickel source, both Xantphos and DPEPhos led to excellent yields, showcasing the diminished influence of the ligand with acetate precoordinated to the nickel source (Table 4, entries 10–15).

This effect is not observable for the coupling of tertiary alkyl thiol **2e** (Table 5, entries 8–12), presumably due to the increased steric strain, which favors DPEPhos as ligand.

Furthermore, a variety of transition metals were screened and the superiority of nickel and acetate salts for the reaction was demonstrated. While Cu, Fe and Co sources, such as $Cu(OAc)_2$, $CuCl_2$, CuCl, $CoCl_2$, $FeCl_2$ yielded no product with DPEPhos as ligand, palladium sources generated low to moderate yields with 48% for $Pd(OAc)_2$ (Table 5, entries 13–14).

Table 5. C-S cross-coupling of aryl chloride **1a** and tertiary alkyl thiol **2e** with various catalytic systems and reaction conditions, including one-component pre-catalyst **Ni1**, **Ni4**, **Ni8**, $Ni(cod)_2$ and Ni/Pd(II) salts with Xantphos **L6** or DPEPhos **L21** as ligands. GC-FID yields calibrated against pentadecane.

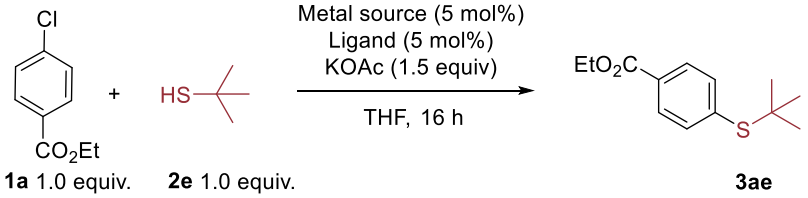

1a 1.0 equiv. **2e** 1.0 equiv. **3ae**

Entry	Metal source	Ligand	Zn [equiv.]	temp. [°C]	Yield [%]
1	**Ni1** XantphosNi(*o*-tolyl)Cl		-	rt	94
2	**Ni4** DPEPhosNi(mesityl)Br		-	rt	traces
3	**Ni8** DPEPhosNi(*o*-tolyl)Cl		-	rt	96
4	**Ni1** XantphosNi(*o*-tolyl)Cl		1	rt	94
5	**Ni4** DPEPhosNi(mesityl)Br		1	rt	96
6	$Ni(cod)_2$	Xantphos	-	rt	94
7	$Ni(cod)_2$	DPEPhos	-	rt	97
8	$Ni(OAc)_2$	Xantphos	1	50	54
9	$Ni(OAc)_2$	DPEPhos	1	50	92
10	$Ni(OAc)_2$	-	1	50	none
11	$NiCl_2$	Xantphos	1	50	64
12	$NiCl_2$	DPEPhos	1	50	82
13	$Pd(OAc)_2$	DPEPhos	1	50	48
14	$PdCl_2$	DPEPhos	1	50	traces

3.2. Towards Atropselective C-S Cross-Coupling

Atropisomers are rotamers with hindered rotation about a σ-bond. Commonly due to steric strain a rotational barrier is created with a sufficient energy difference to enable isolation of the conformers. As atropisomers are structural motifs common in ligands and pharmaceutical compounds, their enantiopure synthesis is of interest. While cross-coupling *via* palladium catalyzed C-C bond formation is an often utilized method, C-Heteroatom bond formation has remained rare. For C-S bond construction only copper catalyzed asymmetric ring opening reactions of cyclic diaryliodoniumsalts, which are highly limited in their substrate scope, have been reported (see Chapter 1.4.1).[152] Therefore, expanding the substrate scope to aryl (pseudo)halides and thiols *via* C-S cross-coupling, more specifically a selective mono-functionalization of prochiral di-chloro-biaryl substrates **18** in a mild nickel catalyzed reaction was envisioned (Scheme 65).

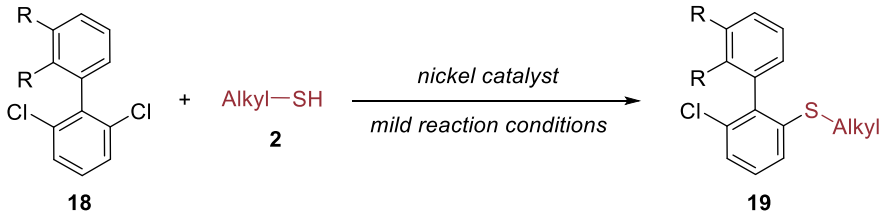

Scheme 65. Atropisomer synthesis *via* selective mono-functionalization of prochiral di-chloro-biaryl **18**.

Prochiral di-chloro-biaryl **18a** was chosen as model substrate and synthesized in excellent yields (Scheme 66). The aryl zinc chloride reagent **22** was generated in a selective lithiation of **20** and subsequent reaction with $ZnCl_2$,[181] followed by a Negishi coupling with the corresponding aryl iodide **23** yielding the product **18a** in 89%.[182]

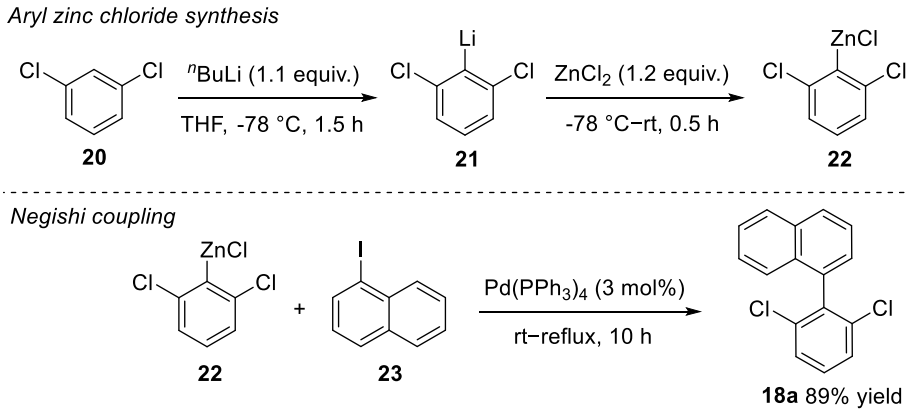

Scheme 66. Synthesis of the aryl zinc chloride reagent **22**,[181] followed by a Negishi coupling[182] with aryl iodide **23** to generate the prochiral biaryl 1-(2,6-dichlorophenyl)naphthalene **18a**.

Subsequently, a variety of phosphine ligands were screened *via in-situ* generation of the catalyst with $Ni(cod)_2$ as nickel source (Scheme 67). The initial experiments identified DPEPhos **L21** as promising ligand for the mono-selective coupling of di-chloro-biaryl **18a**. The other achiral and chiral mono- or bidentate ligands generated insignificant yields for the mono-coupled product or did not couple selectively on one, but on both coupling sites.

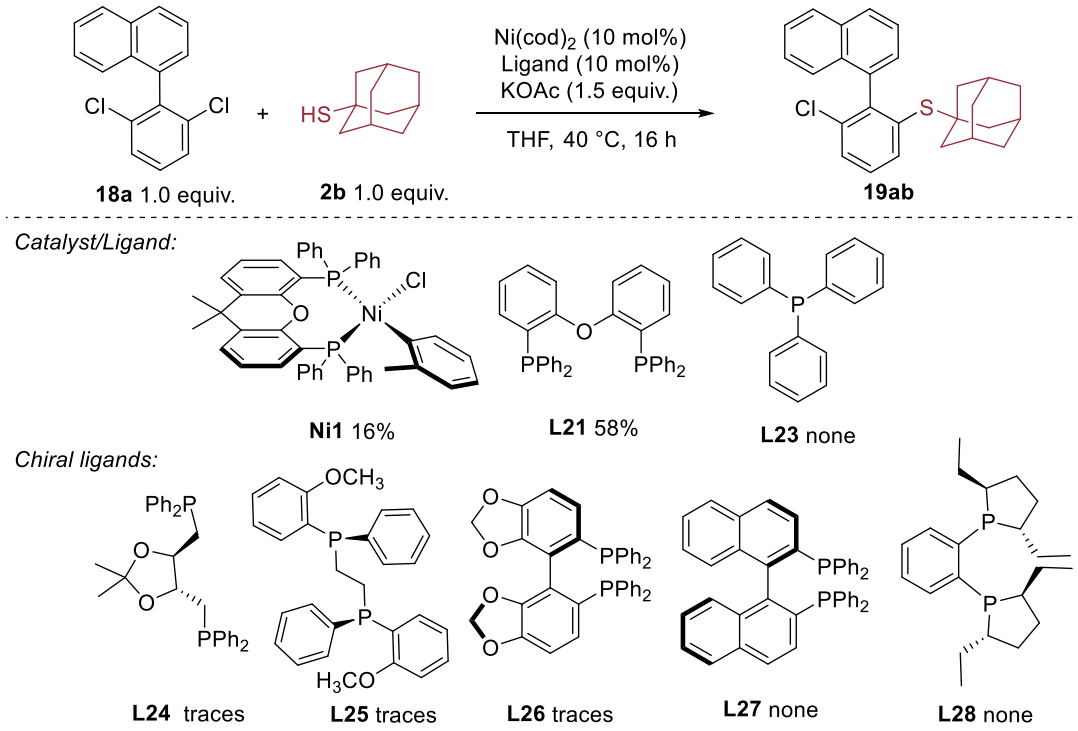

Scheme 67. Screening of pre-catalyst XantphosNi(*o*-tolyl)Cl **Ni1**, as well as achiral and chiral ligands with $Ni(cod)_2$ as nickel source for the synthesis of atropisomer **19ab**. Approximated GC-MS yields for **19ab**.

The identified catalytic system consisting of $Ni(cod)_2$/DPEPhos **L21** enabled the coupling of prochiral di-chloro-biaryl **18a** mono-selectively in 78% yield (Scheme 68). Preliminary screening experiments by Alexander Huber for the commercially available, chiral DPEPhos ligand **L29** showed low yields < 5% and 32% ee for the desired product **19ae**.

Chiral HPLC and GC columns to sperate the racemate have been identified, which will simplify the chiral ligand screening in the future. For HPLC the columns CHIRALPAK IJ (n-heptane/isopropanol as mobile phase) and CHIRALPAK IB-N (n-heptane/MTBE as mobile phase) were identified by Daical chiral technologies. And for GC-FID the column CP-Chirasil-Dex was identified by the Analytics Department of the University of Tuebingen.

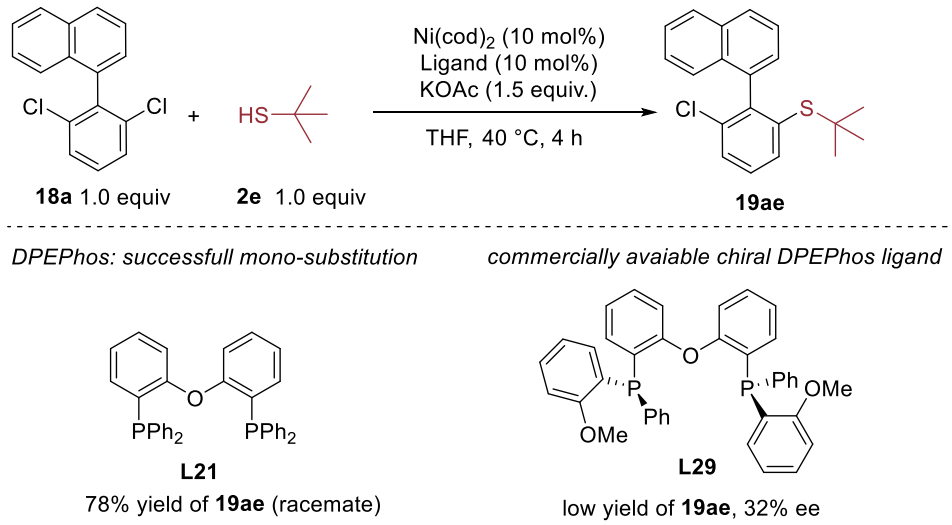

Scheme 68. Selective mono-coupling of di-chloro-biaryl **18a** with tertiary alkyl thiol **2e** in excellent yield for $Ni(cod)_2$ and DPEPhos **L21** as ligand and with low yield and 32% ee for the commercially available chiral DPEPhos ligand **L29**.

Further screening is necessary to identify a chiral ligand for the enantioselective coupling in high yields and ee. While the hemilabile nature of Xantphos and DPEPhos has proven to be an important factor for the catalytic system, methoxy groups have previously been challenging for the coupling of aryl chlorides (Scheme 51, **3gb**), rendering alternative substituents, such as *ortho*-methyl, -ethyl, -^{i}Pr, -Ph or -naphthyl on a chiral DPEPhos, 5-ring or alternative POP-style ligand more promising (Figure 19). Chiral amino-phosphine ligands, which have shown promise in asymmetric coupling reactions,[145] or the utilization of a chiral base to induce stereoselectivity could be tested, in addition to the screening of further aryl (pseudo)halide substrates, such as more reactive aryl bromides or aryl triflates, which did not show the same limitations for methoxy substituents (Scheme 56, **11hb**).

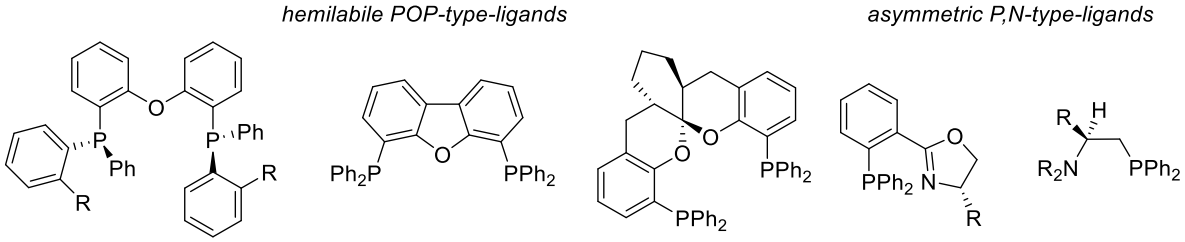

Figure 19. Potential ligands for future enantioselective C-S cross-coupling reactions generating thioether based atropisomers, including hemilabile POP-type and asymmetric P,N-type ligands.

Chapter 4

BIBLIOGRAPHY

4. Bibliography

[1] P. W. N. M. van Leeuwen, *Homogeneous Catalysis: Understanding the Art*, Springer Science & Business Media, **2006**.

[2] W. Ostwald, *Über Katalyse (G. Bredig, Hrsg.), Ostwald's Klassiker der exakten Wissenschaften*, Akademische Verlagsgesellschaft, Leipzig, **1923**.

[3] P. E. McGovern, J. Zhang, J. Tang, Z. Zhang, G. R. Hall, R. A. Moreau, A. Nuñez, E. D. Butrym, M. P. Richards, C. S. Wang, G. Cheng, Z. Zhao, C. Wang, *PNAS* **2004**, *101*, 17593-17598.

[4] M. Salque, P. I. Bogucki, J. Pyzel, I. Sobkowiak-Tabaka, R. Grygiel, M. Szmyt, R. P. Evershed, *Nature* **2013**, *493*, 522-525.

[5] K. L. Konkol, S. C. Rasmussen, in *Chemical Technology in Antiquity, Vol. 1211*, American Chemical Society, **2015**, pp. 245-266.

[6] J. N. Armor, *Catal. Today* **2011**, *163*, 3-9.

[7] I. Chorkendorff, J. W. Niemantsverdriet, *Concepts of Modern Catalysis and Kinetics*, John Wiley & Sons, **2017**.

[8] R. Schlögl, *Angew. Chem. Int. Ed.* **2015**, *54*, 3465-3520.

[9] J. J. Bravo-Suárez, R. V. Chaudhari, B. Subramaniam, in *Novel Materials for Catalysis and Fuels Processing*, **2013**, pp. 3-68.

[10] V. S. Marakatti, E. M. Gaigneaux, *ChemCatChem* **2020**, *12*, 5838-5857.

[11] C. C. C. Johansson Seechurn, M. O. Kitching, T. J. Colacot, V. Snieckus, *Angew. Chem. Int. Ed.* **2012**, *51*, 5062-5085.

[12] a) J. Magano, J. R. Dunetz, *Chem. Rev.* **2011**, *111*, 2177-2250; b) J. D. Hayler, D. K. Leahy, E. M. Simmons, *Organometallics* **2018**, *38*, 36-46; c) K. M. Korch, D. A. Watson, *Chem. Rev.* **2019**, *119*, 8192-8228; d) S. L. Buchwald, *Acc. Chem. Res.* **2008**, *41*, 1439-1439.

[13] R. D. Larsen, A. O. King, C. Y. Chen, E. G. Corley, B. S. Foster, F. E. Roberts, C. Yang, D. R. Lieberman, R. A. Reamer, D. M. Tschaen, *J. Org. Chem.* **1994**, *59*, 6391-6394.

[14] N. Miyaura, S. L. Buchwald, *Cross-Coupling Reactions: A Practical Guide, Vol. 219*, Springer, **2002**.

[15] V. P. Ananikov, *ACS Catal.* **2015**, *5*, 1964-1971.

[16] a) K. Tamao, K. Sumitani, M. Kumada, *J. Am. Chem. Soc.* **1972**, *94*, 4374-4376; b) R. Corriu, J. Masse, *J. Chem. Soc., Chem. Commun.* **1972**, 144a-144a.

[17] N. Miyaura, K. Yamada, A. Suzuki, *Tetrahedron Lett.* **1979**, *20*, 3437-3440.

[18] E. Negishi, A. O. King, N. Okukado, *J. Org. Chem.* **1977**, *42*, 1821-1823.

[19] D. Milstein, J. Stille, *J. Am. Chem. Soc.* **1978**, *100*, 3636-3638.

[20] R. F. Heck, J. Nolley Jr, *J. Org. Chem.* **1972**, *37*, 2320-2322.

[21] a) K. Sonogashira, Y. Tohda, N. Hagihara, *Tetrahedron Lett.* **1975**, *16*, 4467-4470; b) L. Cassar, *J. Organomet. Chem.* **1975**, *93*, 253-257; c) a. H. Dieck, F. Heck, *J. Organomet. Chem.* **1975**, *93*, 259-263.

[22] a) A. S. Guram, R. A. Rennels, S. L. Buchwald, *Angew. Chem. Int. Ed.* **1995**, *34*, 1348-1350; b) J. Louie, J. F. Hartwig, *Tetrahedron Lett.* **1995**, *36*, 3609-3612.

[23] a) M. Kosugi, T. Shimizu, T. Migita, *Chem. Lett.* **1978**, *7*, 13-14; b) T. Migita, T. Shimizu, Y. Asami, J. Shiobara, Y. Kato, M. Kosugi, *Bull. Chem. Soc. Jpn.* **1980**, *53*, 1385-1389.

[24] a) R. Lundgren, M. Stradiotto, in *Ligand Design in Metal Chemistry: Reactivity and Catalysis*, John Wiley & Sons, **2016**, pp. 1-14; b) S. J. Firsan, V. Sivakumar, T. J. Colacot, *Chem. Rev.* **2022**, *122*, 16983-17027.

[25] L. C. Campeau, N. Hazari, *Organometallics* **2019**, *38*, 3-35.
[26] E. K. Reeves, E. D. Entz, S. R. Neufeldt, *Chem. Eur. J.* **2021**, *27*, 6161-6177.
[27] P. Fitton, E. A. Rick, *J. Organomet. Chem.* **1971**, *28*, 287-291.
[28] Y.-R. Luo, *Comprehensive Handbook of Chemical Bond Energies*, CRC press, **2007**.
[29] C. M. So, F. Y. Kwong, *Chem. Soc. Rev.* **2011**, *40*, 4963-4972.
[30] A. F. Littke, G. C. Fu, *Angew. Chem. Int. Ed.* **2002**, *41*, 4176-4211.
[31] a) G. Wiley, R. Hershkowitz, B. Rein, B. Chung, *J. Am. Chem. Soc.* **1964**, *86*, 964-965; b) N. S. Isaacs, D. Kirkpatrick, *J. Chem. Soc., Chem. Commun.* **1972**, 443-444; c) K. V. Axenov, C. M. Mömming, G. Kehr, R. Fröhlich, G. Erker, *Chem. Eur. J.* **2010**, *16*, 14069-14073.
[32] a) L. J. Goossen, N. Rodríguez, C. Linder, *J. Am. Chem. Soc.* **2008**, *130*, 15248-15249; b) Z. Huang, Z. Liu, J. Zhou, *J. Am. Chem. Soc.* **2011**, *133*, 15882-15885.
[33] a) J. Duan, Y.-F. Du, X. Pang, X.-Z. Shu, *Chem. Sci.* **2019**, *10*, 8706-8712; b) A. M. Olivares, D. J. Weix, *J. Am. Chem. Soc.* **2018**, *140*, 2446-2449; c) A. G. Martínez, A. Herrera, R. Martínez, E. Teso, A. García, J. Osío, L. Pargada, R. Unanue, L. R. Subramanian, M. Hanack, *J. Heterocycl. Chem.* **1988**, *25*, 1237-1241; d) J. E. Mc Murry, W. J. Scott, *Tetrahedron Lett.* **1983**, *24*, 979-982; e) X. Su, H. Huang, Y. Yuan, Y. Li, *Angew. Chem. Int. Ed.* **2017**, *56*, 1338-1341.
[34] A. Corma, S. Iborra, A. Velty, *Chem. Rev.* **2007**, *107*, 2411-2502.
[35] W. J. Scott, G. T. Crisp, J. K. Stille, *J. Am. Chem. Soc.* **1984**, *106*, 4630-4632.
[36] a) J. L. Hofstra, K. E. Poremba, A. M. Shimozono, S. E. Reisman, *Angew. Chem. Int. Ed.* **2019**, *58*, 14901-14905; b) E. Shirakawa, Y. Imazaki, T. Hayashi, *Chem. Commun.* **2009**, 5088-5090; c) X. Shen, A. M. Hyde, S. L. Buchwald, *J. Am. Chem. Soc.* **2010**, *132*, 14076-14078; d) Y. Imazaki, E. Shirakawa, R. Ueno, T. Hayashi, *J. Am. Chem. Soc.* **2012**, *134*, 14760-14763; e) J. Pan, X. Wang, Y. Zhang, S. L. Buchwald, *Org. Lett.* **2011**, *13*, 4974-4976.
[37] S. Z. Tasker, E. A. Standley, T. F. Jamison, *Nature* **2014**, *509*, 299-309.
[38] a) T. Scattolin, E. Senol, G. Yin, Q. Guo, F. Schoenebeck, *Angew. Chem. Int. Ed.* **2018**, *57*, 12425-12429; b) S. T. Keaveney, G. Kundu, F. Schoenebeck, *Angew. Chem. Int. Ed.* **2018**, *57*, 12573-12577.
[39] E. D. Entz, J. E. A. Russell, L. V. Hooker, S. R. Neufeldt, *J. Am. Chem. Soc.* **2020**, *142*, 15454-15463.
[40] E. K. Elias, S. M. Rehbein, S. R. Neufeldt, *Chem. Sci.* **2022**, *13*, 1618-1628.
[41] a) L. K. G. Ackerman, M. M. Lovell, D. J. Weix, *Nature* **2015**, *524*, 454-457; b) L. Huang, L. K. G. Ackerman, K. Kang, A. M. Parsons, D. J. Weix, *J. Am. Chem. Soc.* **2019**, *141*, 10978-10983.
[42] J. Nasielski, N. Hadei, G. Achonduh, E. A. B. Kantchev, C. J. O'Brien, A. Lough, M. G. Organ, *Chem. Eur. J.* **2010**, *16*, 10844-10853.
[43] G. Yin, I. Kalvet, U. Englert, F. Schoenebeck, *J. Am. Chem. Soc.* **2015**, *137*, 4164-4172.
[44] J. D. Shields, E. E. Gray, A. G. Doyle, *Org. Lett.* **2015**, *17*, 2166-2169.
[45] a) N. C. Bruno, M. T. Tudge, S. L. Buchwald, *Chem. Sci.* **2013**, *4*, 916-920; b) M. G. Organ, G. A. Chass, D.-C. Fang, A. C. Hopkinson, C. Valente, *Synthesis* **2008**, *17*, 2776-2797; c) O. Navarro, H. Kaur, P. Mahjoor, S. P. Nolan, *J. Org. Chem.* **2004**, *69*, 3173-3180.
[46] E. A. Standley, S. J. Smith, P. Müller, T. F. Jamison, *Organometallics* **2014**, *33*, 2012-2018.
[47] J. Xu, R. Y. Liu, C. S. Yeung, S. L. Buchwald, *ACS Catal.* **2019**, *9*, 6461-6466.
[48] A. L. Clevenger, R. M. Stolley, J. Aderibigbe, J. Louie, *Chem. Rev.* **2020**, *120*, 6124-6196.

[49] P. C. J. Kamer, P. W. N. M. van Leeuwen, J. N. H. Reek, *Acc. Chem. Res.* **2001**, *34*, 895-904.
[50] G. M. Adams, A. S. Weller, *Coord. Chem. Rev.* **2018**, *355*, 150-172.
[51] a) J. Panteleev, H. Gao, L. Jia, *Bioorganic Med. Chem. Lett.* **2018**, *28*, 2807-2815; b) K. A. Carpenter, D. S. Cohen, J. T. Jarrell, X. Huang, *Future Med. Chem.* **2018**, *10*, 2557-2567; c) X. Yang, Y. Wang, R. Byrne, G. Schneider, S. Yang, *Chem. Rev.* **2019**, *119*, 10520-10594.
[52] W. L. Williams, L. Zeng, T. Gensch, M. S. Sigman, A. G. Doyle, E. V. Anslyn, *ACS Cent. Sci.* **2021**, *7*, 1622-1637.
[53] H. Beinert, *Eur. J. Biochem.* **2000**, *267*, 5657-5664.
[54] a) X. Jiang, *Sulfur chemistry*, Springer Nature, **2019**; b) F. Z. Dörwald, *Lead Optimization for Medicinal Chemists: Pharmacokinetic Properties of Functional Groups and Organic Compounds*, John Wiley & Sons, **2012**.
[55] K. A. Scott, J. T. Njardarson, *Top. Curr. Chem.* **2018**, *376*, 5.
[56] a) P. Annamalai, K.-C. Liu, S. Singh Badsara, C.-F. Lee, *Chem. Rec.* **2021**, *21*, 3674-3688; b) E. A. Ilardi, E. Vitaku, J. T. Njardarson, *J. Med. Chem.* **2014**, *57*, 2832-2842; c) M. Feng, B. Tang, S. H. Liang, X. Jiang, *Curr. Top. Med. Chem.* **2016**, *16*, 1200-1216; d) Y. Hai, M.-Y. Wei, C.-Y. Wang, Y.-C. Gu, C.-L. Shao, *Mar. Life Sci. Technol.* **2021**, *3*, 488-518.
[57] G. A. Patani, E. J. LaVoie, *Chem. Rev.* **1996**, *96*, 3147-3176.
[58] a) T. L. Lemke, D. A. Williams, V. F. Roche, S. W. Zito, *Foyes Principles of Medicinal Chemistry, Vol. 7*, Wolters Kluwer, **2012**; b) İ. M. Han, G. Ş. Küçükgüzel, *Curr. Drug Targets.* **2022**, *23*, 170-219.
[59] S. Oae, *Organic Chemistry of Sulfur*, Springer New York, **1977**.
[60] J.-H. Cheng, C. Ramesh, H.-L. Kao, Y.-J. Wang, C.-C. Chan, C.-F. Lee, *J. Org. Chem.* **2012**, *77*, 10369-10374.
[61] a) R. Leuckart, *J. prakt. Chem.* **1890**, *41*, 179-224; b) D. Koziakov, M. Majek, A. J. von Wangelin, *Org. Biomol. Chem.* **2016**, *14*, 11347-11352.
[62] V. J. Geiger, R. M. Oechsner, P. H. Gehrtz, I. Fleischer, *Synthesis* **2022**, *54*, 5139-5167.
[63] V. Hirschbeck, P. H. Gehrtz, I. Fleischer, *Chem. Eur. J.* **2018**, *24*, 7092-7107.
[64] a) J. Liu, L. Zheng, *Adv. Synth. Catal.* **2019**, *361*, 1710-1732; b) M. Iwasaki, Y. Nishihara, *Dalton Trans.* **2016**, *45*, 15278-15284; c) W. Ma, N. Kaplaneris, X. Fang, L. Gu, R. Mei, L. Ackermann, *Org. Chem. Front.* **2020**, *7*, 1022-1060.
[65] a) S. W. M. Crossley, C. Obradors, R. M. Martinez, R. A. Shenvi, *Chem. Rev.* **2016**, *116*, 8912-9000; b) R. Castarlenas, A. Di Giuseppe, J. J. Perez-Torrente, L. A. Oro, *Angew. Chem. Int. Ed. Engl.* **2013**, *52*, 211-222; c) A. Massi, D. Nanni, *Org. Biomol. Chem.* **2012**, *10*, 3791-3807.
[66] T. Delcaillau, A. Bismuto, Z. Lian, B. Morandi, *Angew. Chem. Int. Ed.* **2020**, *59*, 2110-2114.
[67] Z.-W. Chen, R. Bai, P. Annamalai, S. S. Badsara, C.-F. Lee, *New J. Chem.* **2022**, *46*, 15-38.
[68] A. Wimmer, B. König, *Beilstein J. Org. Chem.* **2018**, *14*, 54-83.
[69] J. Yin, C. Pidgeon, *Tetrahedron Lett.* **1997**, *38*, 5953-5954.
[70] a) T. Kondo, T.-a. Mitsudo, *Chem. Rev.* **2000**, *100*, 3205-3220; b) C. C. Eichman, J. P. Stambuli, *Molecules* **2011**, *16*, 590-608; c) I. P. Beletskaya, V. P. Ananikov, *Chem. Rev.* **2011**, *111*, 1596-1636; d) C.-F. Lee, Y.-C. Liu, S. S. Badsara, *Chem. Asian J.* **2014**, *9*, 706-722; e) A. Ghaderi, *Tetrahedron* **2016**, *72*, 4758-4782; f) P. Bichler, J. A. Love, in *Organometallic Approaches to Carbon–Sulfur Bond Formation, C-X Bond Formation*,

Springer **2010**, pp. 39-64; g) J. Li, S. Yang, W. Wu, H. Jiang, *Org. Chem. Front.* **2020**, *7*, 1395-1417.
[71] J. Li, S. Yang, W. Wu, H. Jiang, *Org. Chem. Front.* **2020**, *7*, 1395-1417.
[72] a) A. Sujatha, A. M. Thomas, A. P. Thankachan, G. Anilkumar, *Arkivoc* **2014**, *2015*, 1-28; b) S. V. Ley, A. W. Thomas, *Angew. Chem. Int. Ed.* **2003**, *42*, 5400-5449.
[73] J. Zhang, S. Wang, Y. Zhang, Z. Feng, *Asian J. Org. Chem.* **2020**, *9*, 1519-1531.
[74] a) T. Yamamoto, Y. Sekine, *Can. J. Chem.* **1984**, *62*, 1544-1547; b) J. Lindley, *Tetrahedron* **1984**, *40*, 1433-1456.
[75] M. A. Fernández-Rodríguez, Q. Shen, J. F. Hartwig, *J. Am. Chem. Soc.* **2006**, *128*, 2180-2181.
[76] T. Itoh, T. Mase, *Org. Lett.* **2004**, *6*, 4587-4590.
[77] a) R. A. A. Al-Shuaeeb, G. Galvani, G. Bernadat, J.-D. Brion, M. Alami, S. Messaoudi, *Org. Biomol. Chem.* **2015**, *13*, 10904-10916; b) B. Chekal, D. Damon, D. LaFrance, K. Leeman, C. Mojica, A. Palm, M. St. Pierre, J. Sieser, K. Sutherland, R. Vaidyanathan, J. Van Alsten, B. Vanderplas, C. Wager, G. Weisenburger, G. Withbroe, S. Yu, *Org. Process Res. Dev.* **2015**, *19*, 1944-1953.
[78] T. Scattolin, E. Senol, G. Yin, Q. Guo, F. Schoenebeck, *Angew. Chem. Int. Ed.* **2018**, *57*, 12425-12429.
[79] a) J. L. Farmer, M. Pompeo, A. J. Lough, M. G. Organ, *Chem. Eur. J.* **2014**, *20*, 15790-15798; b) A. C. Jones, W. I. Nicholson, H. R. Smallman, D. L. Browne, *Org. Lett.* **2020**, *22*, 7433-7438.
[80] S. S. M. Bandaru, S. Bhilare, J. Cardozo, N. Chrysochos, C. Schulzke, Y. S. Sanghvi, K. C. Gunturu, A. R. Kapdi, *J. Org. Chem.* **2019**, *84*, 8921-8940.
[81] S. S. Murthy Bandaru, S. Bhilare, N. Chrysochos, V. Gayakhe, I. Trentin, C. Schulzke, A. R. Kapdi, *Org. Lett.* **2018**, *20*, 473-476.
[82] T. Zhao, F. Liang, M. Cai, J. Chen, C. Kang, H. Wang, Q. Wu, *Asian J. Org. Chem.* **2020**, *9*, 214-217.
[83] N. Abidi, J. R. Schmink, *J. Org. Chem.* **2015**, *80*, 4123-4131.
[84] a) N. Zheng, J. C. McWilliams, F. J. Fleitz, J. D. Armstrong, R. P. Volante, *J. Org. Chem.* **1998**, *63*, 9606-9607; b) C. Mispelaere-Canivet, J.-F. Spindler, S. Perrio, P. Beslin, *Tetrahedron* **2005**, *61*, 5253-5259; c) F. Ma, J. Li, S. Zhang, Y. Gu, T. Tan, W. Chen, S. Wang, H. Xu, G. Yang, R. A. Lerner, *ACS Catal.* **2022**, *12*, 1639-1649; d) M. Kreis, S. Bräse, *Adv. Synth. Catal.* **2005**, *347*, 313-319.
[85] a) H. S. Sader, D. M. Johnson, R. N. Jones, *Antimicrob. Agents Chemother.* **2004**, *48*, 53-62; b) E. Marcantoni, M. Massaccesi, M. Petrini, G. Bartoli, M. C. Bellucci, M. Bosco, L. Sambri, *J. Org. Chem.* **2000**, *65*, 4553-4559; c) P. Johannesson, G. Lindeberg, A. Johansson, G. V. Nikiforovich, A. Gogoll, B. Synnergren, M. Le Grèves, F. Nyberg, A. Karlén, A. Hallberg, *J. Med. Chem.* **2002**, *45*, 1767.
[86] A. G. Martínez, J. O. Barcina, A. de Fresno Cerezo, L. R. Subramanian, *Synlett* **1994**, *7*, 561-562.
[87] N. Velasco, C. Virumbrales, R. Sanz, S. Suárez-Pantiga, M. A. Fernández-Rodríguez, *Org. Lett.* **2018**, *20*, 2848-2852.
[88] K. Ishitobi, K. Muto, J. Yamaguchi, *ACS Catal.* **2019**, *9*, 11685-11690.
[89] P. Sabatier, *Catalysis in Organic Chemistry*, D. Van Nostrand Company, **1922**.
[90] a) J. Diccianni, Q. Lin, T. Diao, *Acc. Chem. Res.* **2020**, *53*, 906-919; b) J. B. Diccianni, T. Diao, *Trends Chem.* **2019**, *1*, 830-844; c) C. Zhu, H. Yue, J. Jia, M. Rueping, *Angew. Chem. Int. Ed.* **2020**, 17810-17831; d) M. E. Greaves, E. L. B. Johnson Humphrey, D. J. Nelson,

Catal. Sci. Technol. **2021**, *11*, 2980-2996; e) C.-Y. Lin, P. P. Power, *Chem. Soc. Rev.* **2017**, *46*, 5347-5399.
[91] S. Nag, K. Banerjee, D. Datta, *New J. Chem.* **2007**, *31*, 832-834.
[92] J. B. Mann, T. L. Meek, E. T. Knight, J. F. Capitani, L. C. Allen, *J. Am. Chem. Soc.* **2000**, *122*, 5132-5137.
[93] S. S. Batsanov, *Inorg. Mater.* **2001**, *37*, 871-885.
[94] S. A. Macgregor, G. W. Neave, C. Smith, *Faraday Discuss.* **2003**, *124*, 111-127.
[95] H. J. Cristau, B. Chabaud, A. Chêne, H. Christol, *Synthesis* **1981**, *11*, 892-894.
[96] a) N. P. N. Wellala, H. Guan, *Org. Biomol. Chem.* **2015**, *13*, 10802-10807; b) F.-J. Guo, J. Sun, Z.-Q. Xu, F. E. Kühn, S.-L. Zang, M.-D. Zhou, *Catal. Commun.* **2017**, *96*, 11-14.
[97] M. M. Talukder, J. T. Miller, J. M. O. Cue, C. M. Udamulle, A. Bhadran, M. C. Biewer, M. C. Stefan, *Organometallics* **2021**, *40*, 83-94.
[98] T. Y. Yu, H. Pang, Y. Cao, F. Gallou, B. H. Lipshutz, *Angew. Chem. Int. Ed.* **2021**, *60*, 3708-3713.
[99] I. Kalvet, Q. Guo, G. J. Tizzard, F. Schoenebeck, *ACS Catal.* **2017**, *7*, 2126-2132.
[100] K. D. Jones, D. J. Power, D. Bierer, K. M. Gericke, S. G. Stewart, *Org. Lett.* **2018**, *20*, 208-211.
[101] P. H. Gehrtz, V. Geiger, T. Schmidt, L. Srsan, I. Fleischer, *Org. Lett.* **2019**, *21*, 50-55.
[102] J. M. Serrano-Becerra, H. Valdés, D. Canseco-González, V. Gómez-Benítez, S. Hernández-Ortega, D. Morales-Morales, *Tetrahedron Lett.* **2018**, *59*, 3377-3380.
[103] X. Liu, Q. Cao, W. Xu, M.-T. Zeng, Z.-B. Dong, *Eur. J. Org. Chem.* **2017**, *38*, 5795-5799.
[104] V. Percec, J.-Y. Bae, D. H. Hill, *J. Org. Chem.* **1995**, *60*, 6895-6903.
[105] M. T. Martín, M. Marín, C. Maya, A. Prieto, M. C. Nicasio, *Chem. Eur. J.* **2021**, *27*, 12320-12326.
[106] a) Y. Yatsumonji, O. Okada, A. Tsubouchi, T. Takeda, *Tetrahedron* **2006**, *62*, 9981-9987; b) A. D. Marchese, B. Mirabi, E. M. Larin, M. Lautens, *Synthesis* **2020**, *52*, 311-319; c) F. Zhang, Y. Wang, Y. Wang, Y. Pan, *Org. Lett.* **2021**, *23*, 7524-7528.
[107] a) L. Chen, A. Noory Fajer, Z. Yessimbekov, M. Kazemi, M. Mohammadi, *J. Sulphur Chem.* **2019**, *40*, 451-468; b) C.-F. Lee, *Phosphorus Sulfur Silicon Relat Elem.* **2019**, *194*, 678-681; c) C. Sambiagio, S. P. Marsden, A. J. Blacker, P. C. McGowan, *Chem. Soc. Rev.* **2014**, *43*, 3525-3550.
[108] a) A. V. Kalinin, J. F. Bower, P. Riebel, V. Snieckus, *J. Org. Chem.* **1999**, *64*, 2986-2987; b) C. Palomo, M. Oiarbide, R. López, E. Gómez-Bengoa, *Tetrahedron Lett.* **2000**, *41*, 1283-1286; c) C. G. Bates, R. K. Gujadhur, D. Venkataraman, *Org. Lett.* **2002**, *4*, 2803-2806.
[109] A. M. Thomas, S. Asha, K. S. Sindhu, G. Anilkumar, *Tetrahedron Lett.* **2015**, *56*, 6560-6564.
[110] S. P. Bakare, M. Patil, *New J. Chem.* **2022**, *46*, 6283-6295.
[111] C.-W. Chen, Y.-L. Chen, D. M. Reddy, K. Du, C.-E. Li, B.-H. Shih, Y.-J. Xue, C.-F. Lee, *Chem. Eur. J.* **2017**, *23*, 10087-10091.
[112] S. Chen, M. Zhang, X. Liao, Z. Weng, *J. Org. Chem.* **2016**, *81*, 7993-8000.
[113] S. Sangeetha, P. Muthupandi, G. Sekar, *Org. Lett.* **2015**, *17*, 6006-6009.
[114] N. Nowrouzi, M. Abbasi, H. Latifi, *Chinese J. Catal.* **2016**, *37*, 1550-1554.
[115] S. M. Soria-Castro, D. M. Andrada, D. A. Caminos, J. E. Argüello, M. Robert, A. B. Peñéñory, *J. Org. Chem.* **2017**, *82*, 11464-11473.
[116] L. Cao, S.-H. Luo, H.-Q. Wu, L.-Q. Chen, K. Jiang, Z.-F. Hao, Z.-Y. Wang, *Adv. Synth. Catal.* **2017**, *359*, 2961-2971.
[117] Y. Liu, L. Y. Lam, J. Ye, N. Blanchard, C. Ma, *Adv. Synth. Catal.* **2020**, *362*, 2326-2331.

[118] a) C. G. Bates, P. Saejueng, M. Q. Doherty, D. Venkataraman, *Org. Lett.* **2004**, *6*, 5005-5008; b) M. S. Kabir, M. L. Van Linn, A. Monte, J. M. Cook, *Org. Lett.* **2008**, *10*, 3363-3366; c) H. L. Kao, C. F. Lee, *Org. Lett.* **2011**, *13*, 5204.
[119] A. Correa, M. Carril, C. Bolm, *Angew. Chem. Int. Ed.* **2008**, *47*, 2880-2883.
[120] S. L. Buchwald, C. Bolm, *Angew. Chem. Int. Ed.* **2009**, *48*, 5586-5587.
[121] K. S. Sindhu, T. G. Abi, G. Mathai, G. Anilkumar, *Polyhedron* **2019**, *158*, 270-276.
[122] W. Hu, S. Zhang, *J. Org. Chem.* **2015**, *80*, 6128-6132.
[123] F.-F. Duan, S.-Q. Song, R.-S. Xu, *Chem. Commun.* **2017**, *53*, 2737-2739.
[124] Y.-Y. Lin, Y.-J. Wang, C.-H. Lin, J.-H. Cheng, C.-F. Lee, *J. Org. Chem.* **2012**, *77*, 6100-6106.
[125] Y.-C. Wong, T. T. Jayanth, C.-H. Cheng, *Org. Lett.* **2006**, *8*, 5613-5616.
[126] T.-J. Liu, C.-L. Yi, C.-C. Chan, C.-F. Lee, *Chem. Asian J.* **2013**, *8*, 1029-1034.
[127] V. P. Reddy, K. Swapna, A. V. Kumar, K. R. Rao, *J. Org. Chem.* **2009**, *74*, 3189-3191.
[128] A. P. Thankachan, K. S. Sindhu, K. K. Krishnan, G. Anilkumar, *RSC Advances* **2015**, *5*, 32675-32678.
[129] Y. Imazaki, E. Shirakawa, T. Hayashi, *Tetrahedron* **2011**, *67*, 10212-10215.
[130] E. L. Eliel, S. H. Wilen, *Stereochemistry of Organic Compounds*, John Wiley & Sons, **1994**.
[131] G. Q. Lin, Q.-D. You, J.-F. Cheng, *Chiral Drugs: Chemistry and Biological Action*, John Wiley & Sons, **2011**.
[132] S. K. Talapatra, B. Talapatra, *Basic Concepts in Organic Stereochemistry*, Springer Nature, **2023**.
[133] a) H. Flack, *Acta Cryst.* **2009**, *65*, 371-389; b) G. Vantomme, J. Crassous, *Chirality* **2021**, *33*, 597-601; c) C. A. Challener, *Chiral Drugs*, John Wiley & Sons, **2001**.
[134] B. Kasprzyk-Hordern, *Chem. Soc. Rev.* **2010**, *39*, 4466-4503.
[135] H.-U. Blaser, *Rend. Fis. Acc. Lincei* **2013**, *24*, 213-216.
[136] T. Eriksson, S. Björkman, B. Roth, P. Höglund, *J. Pharm. Pharmacol.* **2000**, *52*, 807-817.
[137] K. C. Duggan, D. J. Hermanson, J. Musee, J. J. Prusakiewicz, J. L. Scheib, B. D. Carter, S. Banerjee, J. Oates, L. J. Marnett, *Nat. Chem. Biol.* **2011**, *7*, 803-809.
[138] J. M. Daniels, E. R. Nestmann, A. Kerr, *Drug Inf. J.* **1997**, *31*, 639-646.
[139] C. Kaya, K. Birgül, B. Bülbül, *Chirality* **2023**, *35*, 4-28.
[140] R. Noyori, *Angew. Chem. Int. Ed.* **2002**, *41*, 2008-2022.
[141] G. Bringmann, A. J. Price Mortimer, P. A. Keller, M. J. Gresser, J. Garner, M. Breuning, *Angew. Chem. Int. Ed.* **2005**, *44*, 5384-5427.
[142] M. Basilaia, M. H. Chen, J. Secka, J. L. Gustafson, *Acc. Chem. Res.* **2022**, *55*, 2904-2919.
[143] M. C. Kozlowski, B. J. Morgan, E. C. Linton, *Chem. Soc. Rev.* **2009**, *38*, 3193-3207.
[144] S. R. LaPlante, L. D. Fader, K. R. Fandrick, D. R. Fandrick, O. Hucke, R. Kemper, S. P. Miller, P. J. Edwards, *J. Med. Chem.* **2011**, *54*, 7005-7022.
[145] W. Tang, X. Zhang, *Chem. Rev.* **2003**, *103*, 3029-3070.
[146] R. Noyori, H. Takaya, *Acc. Chem. Res.* **1990**, *23*, 345-350.
[147] J. Wencel-Delord, A. Panossian, F. R. Leroux, F. Colobert, *Chem. Soc. Rev.* **2015**, *44*, 3418-3430.
[148] M. Mellah, A. Voituriez, E. Schulz, *Chem. Rev.* **2007**, *107*, 5133-5209.
[149] A. M. Masdeu-Bultó, M. Diéguez, E. Martin, M. Gómez, *Coord. Chem. Rev.* **2003**, *242*, 159-201.
[150] a) P. Ramírez-López, A. Ros, A. Romero-Arenas, J. Iglesias-Sigüenza, R. Fernández, J. M. Lassaletta, *J. Am. Chem. Soc.* **2016**, *138*, 12053-12056; b) K. Zhao, L. Duan, S. Xu, J. Jiang, Y. Fu, Z. Gu, *Chem* **2018**, *4*, 599-612.

[151] a) V. Bhat, S. Wang, B. M. Stoltz, S. C. Virgil, *J. Am. Chem. Soc.* **2013**, *135*, 16829-16832; b) P. Ramírez-López, A. Ros, B. Estepa, R. Fernández, B. Fiser, E. Gómez-Bengoa, J. M. Lassaletta, *ACS Catal.* **2016**, *6*, 3955-3964.
[152] a) M. Hou, R. Deng, Z. Gu, *Org. Lett.* **2018**, *20*, 5779-5783; b) K. Zhu, Y. Wang, Q. Fang, Z. Song, F. Zhang, *Org. Lett.* **2020**, *22*, 1709-1713.
[153] J. A. Carmona, C. Rodríguez-Franco, R. Fernández, V. Hornillos, J. M. Lassaletta, *Chem. Soc. Rev.* **2021**, *50*, 2968-2983.
[154] J. Clayden, N. Greeves, S. Warren, *Organic Chemistry*, Oxford University Press, **2012**.
[155] V. S. R. Rao, *Conformation of Carbohydrates*, CRC Press, **1998**.
[156] E. Generalic, *Epimer*, Chemistry Dictionary & Glossary, **2022**.
[157] a) W. H. Brooks, W. C. Guida, K. G. Daniel, *Curr. Top. Med. Chem.* **2011**, *11*, 760-770; b) A. Calcaterra, I. D'Acquarica, *J. Pharm. Biomed. Anal.* **2018**, *147*, 323-340.
[158] V. Andrushko, N. Andrushko, *Stereoselective Synthesis of Drugs and Natural Products*, John Wiley & Sons, **2013**.
[159] Y.-A. Zhang, V. Palani, A. E. Seim, Y. Wang, K. J. Wang, A. E. Wendlandt, *Science* **2022**, *378*, 383-390.
[160] M. González-Sierra, M. de los Angeles Laborde, E. A. Rúveda, *Synth. Commun.* **1987**, *17*, 431-441.
[161] K. Iwasaki, K. K. Wan, A. Oppedisano, S. W. Crossley, R. A. Shenvi, *J. Am. Chem. Soc.* **2014**, *136*, 1300-1303.
[162] G. Tan, F. Glorius, *Angew. Chem. Int. Ed.* **2023**, *62*, e202217840.
[163] P.-Z. Wang, W.-J. Xiao, J.-R. Chen, *Nat. Rev. Chem.* **2023**, *7*, 35-50.
[164] K. M. Bhattarai, V. del Amo, G. Magro, A. L. Sisson, J.-B. Joos, J. P. H. Charmant, A. Kantacha, A. P. Davis, *Chem. Commun.* **2006**, 2335-2337.
[165] a) H. M. Carder, Y. Wang, A. E. Wendlandt, *J. Am. Chem. Soc.* **2022**, *144*, 11870-11877; b) Y.-A. Zhang, X. Gu, A. E. Wendlandt, *J. Am. Chem. Soc.* **2022**, *144*, 599-605.
[166] C. J. Oswood, D. W. C. MacMillan, *J. Am. Chem. Soc.* **2022**, *144*, 93-98.
[167] a) K. P. S. Cheung, S. Sarkar, V. Gevorgyan, *Chem. Rev.* **2022**, *122*, 1543-1625; b) W.-J. Zhou, G.-M. Cao, Z.-P. Zhang, D.-G. Yu, *Chem. Lett.* **2019**, *48*, 181-191.
[168] M. Parasram, P. Chuentragool, D. Sarkar, V. Gevorgyan, *J. Am. Chem. Soc.* **2016**, *138*, 6340-6343.
[169] P. Chuentragool, D. Kurandina, V. Gevorgyan, *Angew. Chem. Int. Ed.* **2019**, *58*, 11586-11598.
[170] a) D. A. Petrone, C. M. Le, S. G. Newman, M. Lautens, in *New Trends in Cross-Coupling, Pd(0)-Catalyzed Carboiodination: Early Developments and Recent Advances*, Royal Society of Chemistry, **2014**, pp. 276-321; b) H. Yoon, A. D. Marchese, M. Lautens, *J. Am. Chem. Soc.* **2018**, *140*, 10950-10954.
[171] a) D. A. Petrone, J. Ye, M. Lautens, *Chem. Rev.* **2016**, *116*, 8003-8104; b) D. A. Petrone, H. Yoon, H. Weinstabl, M. Lautens, *Angew. Chem. Int. Ed.* **2014**, *53*, 7908-7912; c) A. D. Marchese, L. Kersting, M. Lautens, *Org. Lett.* **2019**, *21*, 7163-7168; d) A. D. Marchese, F. Lind, Á. E. Mahon, H. Yoon, M. Lautens, *Angew. Chem. Int. Ed.* **2019**, *58*, 5095-5099; e) A. D. Marchese, T. Adrianov, M. F. Köllen, B. Mirabi, M. Lautens, *ACS Catal.* **2021**, *11*, 925-931; f) X. Chen, J. Zhao, M. Dong, N. Yang, J. Wang, Y. Zhang, K. Liu, X. Tong, *J. Am. Chem. Soc.* **2021**, *143*, 1924-1931.
[172] a) A. D. Marchese, E. M. Larin, B. Mirabi, M. Lautens, *Acc. Chem. Res.* **2020**, *53*, 1605-1619; b) D. Bag, S. Mahajan, S. D. Sawant, *Adv. Synth. Catal.* **2020**, *362*, 3948-3970.
[173] S. G. Newman, M. Lautens, *J. Am. Chem. Soc.* **2011**, *133*, 1778-1780.

[174] A. D. Marchese, A. G. Durant, C. M. Reid, C. Jans, R. Arora, M. Lautens, *J. Am. Chem. Soc.* **2022**, *144*, 20554-20560.
[175] R. M. Oechsner, J. P. Wagner, I. Fleischer, *ACS Catal.* **2022**, *12*, 2233-2243.
[176] A. A. Ruch, S. Handa, F. Kong, V. N. Nesterov, D. R. Pahls, T. R. Cundari, L. M. Slaughter, *Org. Biomol. Chem.* **2016**, *14*, 8123-8140.
[177] R. M. Oechsner, I. H. Lindenmaier, I. Fleischer, *Org. Lett.* **2023**, *25*, 1655-1660.
[178] B. A. Tkachenko, N. A. Fokina, L. V. Chernish, J. E. P. Dahl, S. Liu, R. M. K. Carlson, A. A. Fokin, P. R. Schreiner, *Org. Lett.* **2006**, *8*, 1767-1770.
[179] M. Kalek, M. Jezowska, J. Stawinski, *Adv. Synth. Catal.* **2009**, *351*, 3207-3216.
[180] R. Arora, R. M. Oechsner, C. Jans, B. Mirabi, A. D. Marchese, M. Lautens, *ACS Catal.* **2023**, 6562-6567.
[181] L. Peng, L. T. Scott, *J. Am. Chem. Soc.* **2005**, *127*, 16518-16521.
[182] C.-C. Hsiao, Y.-K. Lin, C.-J. Liu, T.-C. Wu, Y.-T. Wu, *Adv. Synth. Catal.* **2010**, *352*, 3267-3274.

Chapter 5

PUBLICATIONS

ACS Catalysis

pubs.acs.org/acscatalysis Research Article

Acetate Facilitated Nickel Catalyzed Coupling of Aryl Chlorides and Alkyl Thiols

Regina M. Oechsner, J. Philipp Wagner,* and Ivana Fleischer*

Cite This: ACS Catal. 2022, 12, 2233−2243 Read Online

ACCESS | Metrics & More | Article Recommendations | Supporting Information

ABSTRACT: We report a mild, fast, and convenient catalytic system for the coupling of aryl chlorides with primary, secondary, as well as previously challenging tertiary alkyl thiols using an air-stable nickel(II) precatayst in combination with the low-cost base potassium acetate at room temperature. This catalytic system tolerates a variety of functional groups and enables the generation of thioethers for a wide range of substrates, including pharmaceutical compounds in excellent yields. Chemoselective functionalization of disubstituted substrates was demonstrated. Kinetic and NMR studies, as well as DFT computations support a Ni(0)/Ni(II) catalytic cycle and identify the oxidative addition product as the resting state. Acetate coordination and subsequent acetate facilitated formation of a thiolate complex via internal deprotonation play a key role in the catalytic cycle.

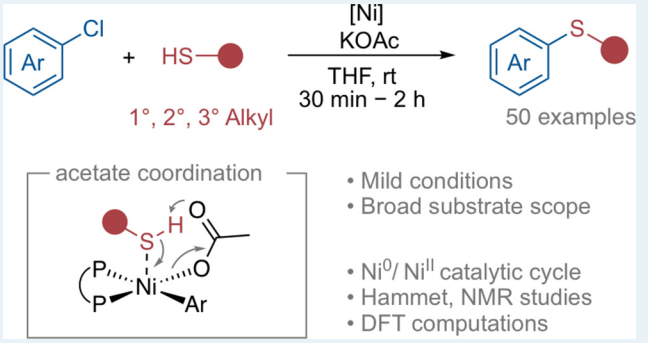

KEYWORDS: *cross coupling, nickel catalysis, thioether, aryl chloride, acetate*

INTRODUCTION

The metal catalyzed C−S cross-coupling of aryl (pseudo)-halides and thiols under basic conditions, known as the Migita reaction, provides efficient access to thioethers.[1] The more lipophilic bioisosters of ethers are an attractive structural motif in pharmaceutical compounds, agrochemicals, and materials design.[2] Most academic research in the past focused on palladium-catalyzed reactions,[3] and the same was true for industrial applications,[4] but low-cost nickel catalysts can replace the precious metal. This, as well as its intriguing and versatile reactivity patterns,[5] are the reason why nickel has evolved into an intensively researched and popular metal for homogeneous catalysis.

While most nickel-catalyzed C−S couplings were developed for the transformation of more reactive aryl bromides and iodides,[6] the reactions of aryl chlorides remained rare until recently (Scheme 1a).[7] Aryl chlorides are comparatively more challenging to couple, but they are readily accessible compounds with a vast range of commercially available substrates, which renders them invaluable for organic synthesis. Apart from a few exceptions such as the trifluorothiomethylation by Schoenebeck and co-workers,[7b] the scope of nickel-catalyzed couplings of aryl chlorides is often limited; higher catalyst loadings and temperatures, stoichiometric additives, or sensitive organometallic bases are required. The latter was also the case in our report on the coupling of aryl chlorides with thiols in the presence of organomagnesium or -zinc reagents as bases and activating agents.[8] Primary and secondary alkyl thiols were coupled efficiently, but tertiary thiols reacted with low yields.

The coupling of tertiary thiols remains a challenge in nickel catalysis, regardless of the employed coupling partner.[9] It is performed under harsh conditions in most cases, and typically, only a few substrates are shown, without systematic investigation. Notable exceptions are reports showing couplings of aryl bromides by the groups of Stefan[9j] and Stewart[7a] as well as the work by Morandi and co-workers on metathesis of thioanisols.[9h]

Nevertheless, to the best of our knowledge, there is no published efficient coupling of aryl chlorides and tertiary alkyl thiols with high yields under mild reaction conditions. Therefore, our goal was to develop a general method for the nickel-catalyzed coupling of aryl chlorides with primary, secondary, and especially tertiary aliphatic thiols. We achieved this by employing the precatalyst (Xantphos)Ni(*o*-tolyl)Cl (**C1**; Xantphos = (9,9-dimethyl-9*H*-xanthene-4,5-diyl)bis-(diphenyl-phosphane)), first reported by Jamison et al.[10] as an air-stable, easily synthesized Ni(II) precursor,[11] together with potassium acetate as a low-cost and air-stable base at

Received: October 25, 2021
Revised: January 13, 2022
Published: January 31, 2022

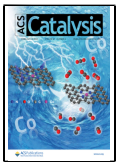

Scheme 1. Current Challenges for the Nickel-Catalyzed C–S Cross-Coupling and Our Approach to Tackle them

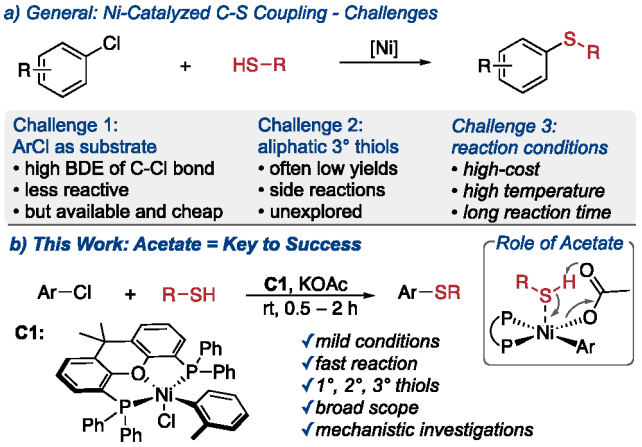

room temperature (Scheme 1b). We present the results of our investigation on the substrate scope together with mechanistic studies, which uncovered the plausible role of acetate in the catalytic cycle.

RESULTS AND DISCUSSION

We began our investigation with the overall goal to find a simple and economical catalytic system to render air-sensitive transmetalation reagents and high temperatures redundant, by using precatalyst **C1** and examining various bases (Table 1 and Table S1 in the SI). At first, the easier to couple secondary cyclohexanethiol (**2a**) and aryl chloride **1a** were tested. To our surprise, a large variety of screened bases were successful in the cross-coupling at 50 °C, generating thioether **3aa** in low to moderate yields (entries 1–11). Sodium acetate could be identified as a suitable base for the C–S cross-coupling providing a high yield of **3aa** (entry 12).

Intrigued by the efficiency of sodium acetate, we continued screening different counterions in the arylation of the more challenging adamantanethiol (**2b**) at room temperature (Table 2). While no or low reactivity was observed after 2 h using lithium and sodium acetates (entries 1, 3), potassium and cesium acetates showed excellent performance (entries 5, 6). A prolonged reaction time of 16 h led to increased yield with sodium acetate, while lithium acetate still performed poorly (entries 2, 4). Low-cost potassium acetate was chosen as the optimal base over the cesium salt for further optimization of the reaction conditions (temperature, catalyst loading, and substrate equivalents; see SI Tables S2–S4). Upon optimization, 1 equiv of aryl halide, 1.1 equiv of thiol, 5 mol % **C1**, and 1.5 equiv of KOAc in THF at room temperature were identified as ideal reaction conditions.

Table 1. Base Screening for the Coupling of the Aryl Chloride 1a with Secondary Thiol 2a[a]

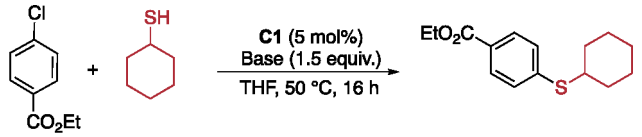

entry	base	conversion (%)[b]	yield (%)[b]
1	NaO^{t}Bu	81	62
2	Li_2CO_3	13	10
3	Na_2CO_3	60	56
4	K_2CO_3	56	52
5	Cs_2CO_3	12	9
6	$Zn_5(CO_3)_2(OH)_6$	68	66
7	$Zn(OPiv)_2$	34	33
8	$Zn(OAc)_2$	60	54
9	$Na_4P_2O_7$	6	4
10	Na_2HPO_4	65	62
11	sodium citrate	44	42
12	NaOAc	89	85

[a]Reaction conditions: ethyl 4-chlorobenzoate (350 μmol, 1.0 equiv), cyclohexanethiol (350 μmol, 1.0 equiv), base (1.5 equiv), **C1** (5 mol %), THF (1 mL), 50 °C, 16 h. [b]GC-FID yields using pentadecane as an internal standard.

Table 2. Comparison of Acetates in the Coupling of the Aryl Chloride 1a with Tertiary Thiol 2b[a]

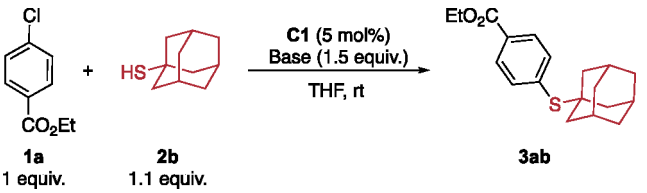

entry	base	time (h)	conversion (%)[b]	yield (%)[b]
1	LiOAc	2	4	0
2	LiOAc	16	5	2
3	NaOAc	2	20	14
4	NaOAc	16	86	83
5	KOAc	2	95	95
6	CsOAc	2	95	93

[a]Reaction conditions: ethyl 4-chlorobenzoate (350 μmol, 1.0 equiv), adamantanethiol (385 μmol, 1.1 equiv), acetate (1.5 equiv), **C1** (5 mol %), THF (1 mL), rt. [b]GC-FID yields using pentadecane as internal standard.

Subsequently, the substrate scope as well as functional group tolerance were explored with potassium acetate under optimized conditions. First, adamantanethiol was used as a benchmark substrate to test a variety of aryl chlorides (Table 3). A wide range of electron-neutral, electron-rich, and electron-deficient *meta*- and *para*-substituted aryl chloride derivatives could be coupled in good to excellent yields. Various functional groups like ethers **3eb**, ketones **3fb**, esters **3ab**, amides **3jb**, and nitriles **3nb** were tolerated. The sulfone **4cb** was obtained after oxidation of **3cb** with *m*-CPBA. For *ortho*-substituents, only low yields of **3rb** could be obtained (15%) by employing the aryl chloride, whereas the bromide was converted in excellent yield (87%), showcasing the more facile oxidative addition. The low reactivity of chloride **1r** was used for a selective functionalization of dichloride **1s** to furnish monothioether **3sb** by steric discrimination.

Heterocycles, which are important motifs in pharmaceuticals and agrochemicals, like pyridine, quinoline, indole, thiazole, dioxole, phenothiazine, or 4*H*-chromen-4-one, were tolerated and afforded the corresponding products **3ub-Bb** in good to excellent yields. Moreover, the successful sulfenylation of pharmaceutically active compounds or their derivatives like loratidine (**3Cb**, allergy medication), indometacine ethyl ester

https://doi.org/10.1021/acscatal.1c04895
ACS Catal. 2022, 12, 2233–2243

Table 3. Substrate Scope with Respect to Aryl Chlorides[a]

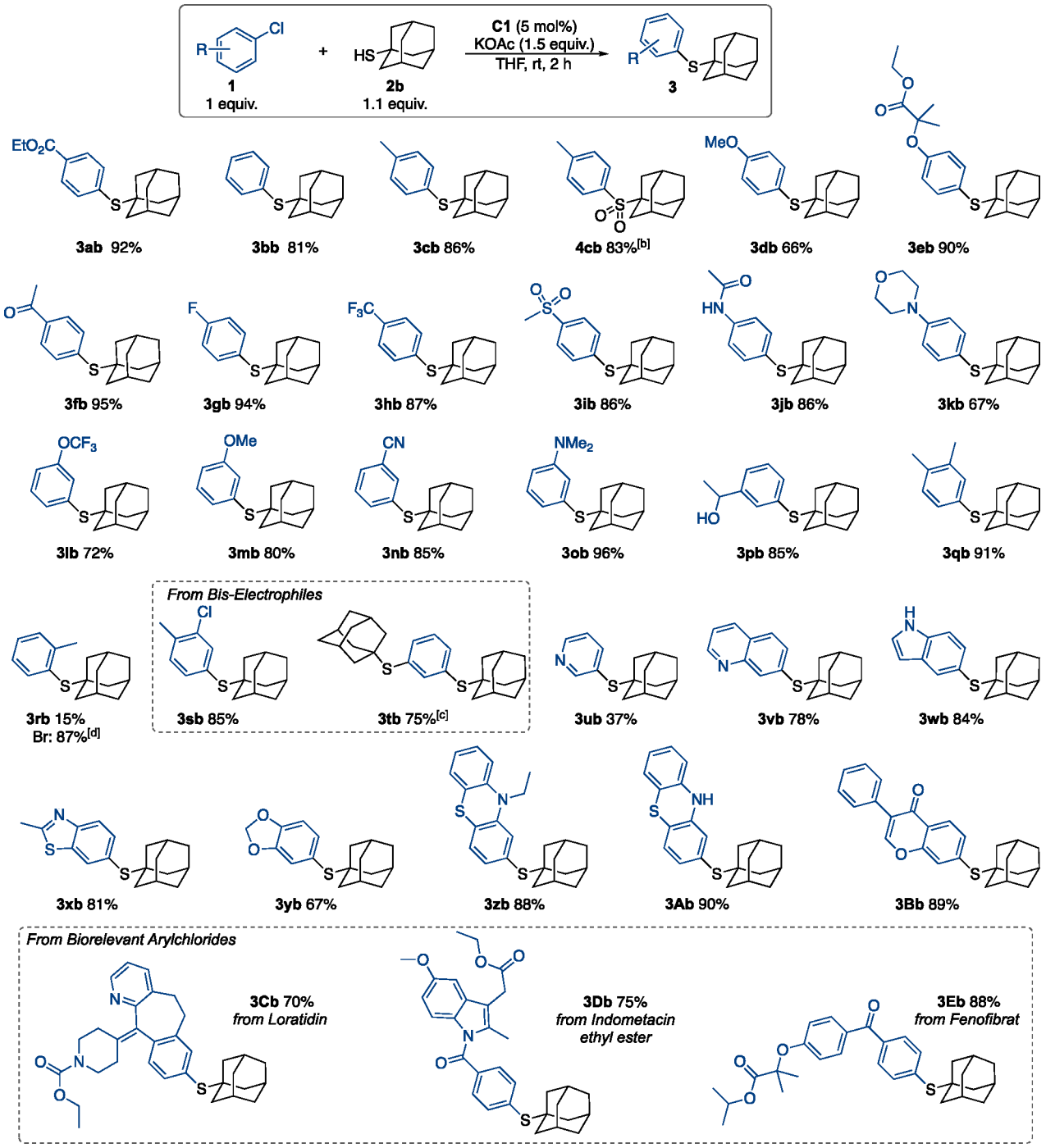

[a]Standard reaction conditions: **1** (1.0 equiv), **2b** (1.1 equiv), KOAc (1.5 equiv), **C1** (5 mol %), THF (3 mL), rt, 2 h. Yields of isolated products unless stated otherwise. [b]Isolated as sulfone after oxidation with *m*-CPBA (yield over two steps). [c]With 2.1 equiv of **2b**. [d]GC-FID yields using pentadecane as internal standard.

(**3Db**, anti-inflammatory drug), and fennofibrat (**3Eb**, a drug against cardiovascular disease) demonstrates the potential of this reaction for the derivatization of bioactive molecules and highlights the scope and applicability of the methodology in a pharmaceutical context. Notable limitations are aldehyde, acid, or primary amine functionalities (see SI, section 7).

The substrate scope with regard to the thiol was evaluated next, with a focus on the previously challenging tertiary thiols (Table 4). Ethyl-4-chlorobenzoate (**1a**) was used as a standard electrophile. Primary, secondary, and a variety of sterically challenging tertiary alkyl thiols were coupled providing the desired thioether in good to excellent yields. Functional groups such as ketone **3al**, **3am**, and ester **3an** were tolerated. Thiocholesterol as a large, bioactive model thiol could be converted to **3ap** in 72% yield. Moieties like amines and acid groups as well as aryl, benzyl, and homobenzyl thiols were not tolerated so far. The inhibition by thiols containing an aryl moiety in certain distances from the sulfur atom might be

https://doi.org/10.1021/acscatal.1c04895
ACS Catal. 2022, 12, 2233−2243

Table 4. Substrate Scope with Respect to Alkyl Thiols[a]

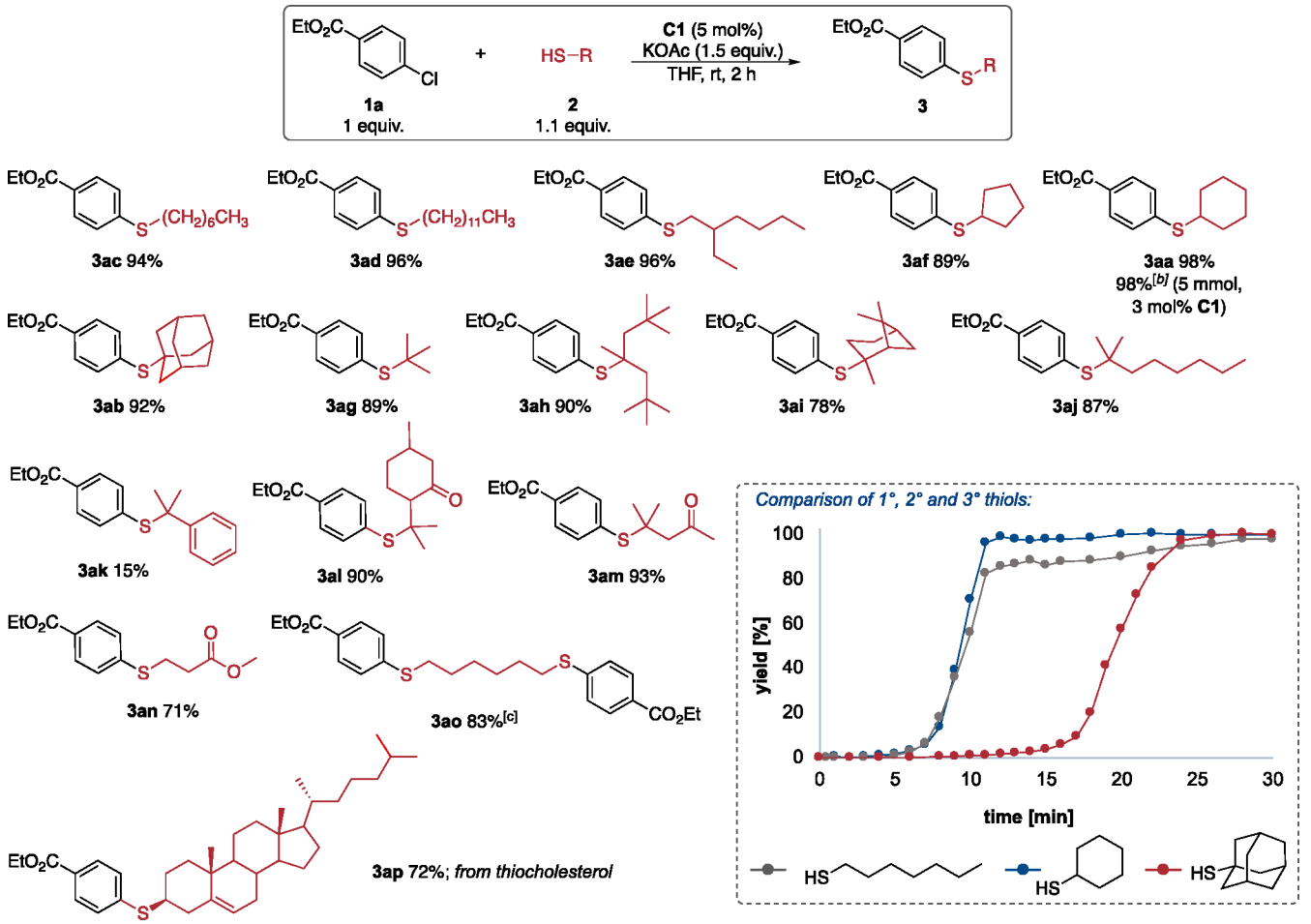

[a]Standard reaction conditions: **1a** (1.0 equiv), **2** (1.1 equiv), KOAc (1.5 equiv), **C1** (5 mol %), THF (3 mL), rt, 2 h. Yields of isolated products unless stated otherwise. [b]5 mmol, C1 (3 mol %), rt, 30 min. [c]With 2 equiv of **1a**.

explained by a bidentate coordination of these compounds, since arenes can act as ligands for Ni(0) species.[12] Comparison of the reaction progress for representatives of primary (heptane-), secondary (cyclohexane-), and tertiary (adamantane-) thiols showed similar reaction rates but a significantly longer induction period for the tertiary adamantanethiol (1°, 2° ≈ 5 min; 3° ≈ 15 min). This period might arise from the involvement of the thiol in the activation of **C1**, which will be discussed later.

Air stability and low cost of the reaction components are advantageous for the developed system. The reaction is operationally simple, and solids can be weighed under benchtop conditions before using inert conditions during the reaction. The coupling is fast (30 min to 2 h) and takes place at room temperature. Upscaling of the reaction in the synthesis of **3aa** while lowering the catalyst loading (5 mmol, 3 mol % **C1**, 30 min), as well as the ability to couple pharmaceutical compounds in good to excellent yields, render this method interesting for possible industrial use. Another advantage is the high selectivity with little to no side reactions. Conversion and yield correlate for most substrates with a maximum 5% difference.

The identified reaction conditions are versatile and can be applied to a variety of electrophiles in addition to aryl chlorides. Phenyl bromide, iodide, as well as triflate reacted in excellent yields (Scheme 2a). Interestingly, tosylates performed poorly. To assess the reactivity in greater detail, we subsequently undertook inter- and intramolecular competition experiments comparing the reactivity of different C–X (X = Cl, Br, I, OTf, OTs) bonds. Intermolecular competition experiments between the electrophiles showed that every electrophile except tosylate reacted preferably to phenyl chloride, with the order PhOTf > PhBr > PhI > PhCl when yields were compared after 2 h (Scheme 2b).

The reaction profiles of different electrophiles (Scheme 2c) showed an increase of the induction period from PhOTf < PhI < PhBr < PhCl and the reaction rate decreasing as follows: PhOTf > PhBr > PhCl > PhI, with phenyl iodide as an unexpected exception. Otherwise, the results roughly correlate with the expected ease of oxidative addition. The lower reactivity of PhI could be explained with Schoenebeck's[13] observation that, for nickel-catalyzed reactions with aryl iodides, more off cycle Ni(I) species are formed and the catalysis is slower.

Intrigued by the intermolecular selectivity and inspired by literature reports on chemoselective Pd-[14] and Ni-catalyzed[15] couplings, we decided to examine if related transformations are possible with our system. Introducing substrates with two or more (pseudo)halide functionalities can enable selective, sequential reactions to generate complex functionalized target

https://doi.org/10.1021/acscatal.1c04895
ACS Catal. 2022, 12, 2233–2243

Scheme 2. Reactivity of Electrophiles and Intermolecular Competition Experiments[a]

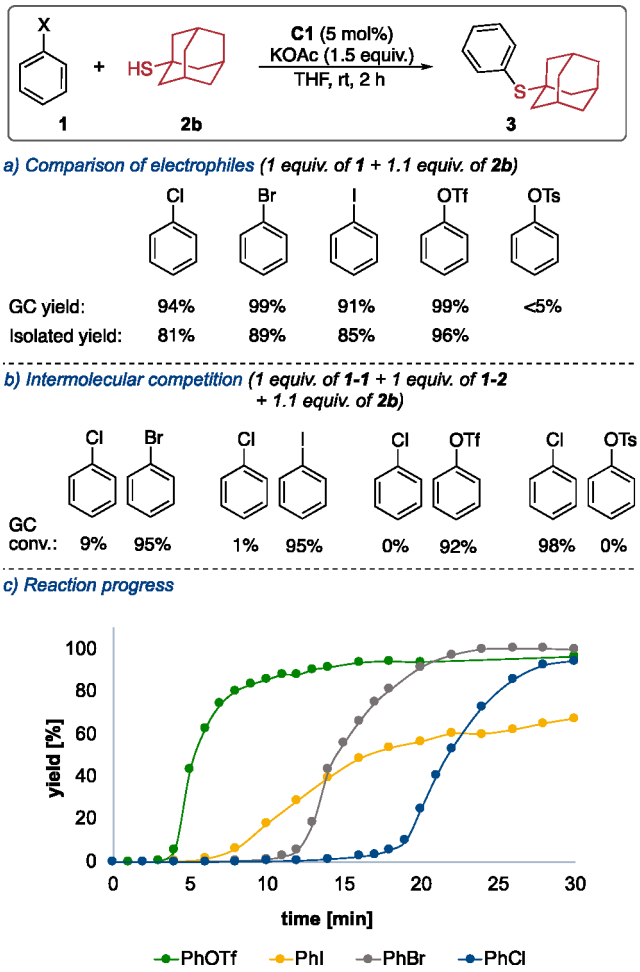

[a]GC-FID yields with pentadecane as internal standard.

compounds or products with an intact and reactive functional group. Therefore, several 1,4-dielectrophilic substrates were subjected to intramolecular competition experiments (Scheme 3a).

No significant selectivity for monofunctionalization was observed between two different halides, C−Cl vs C−Cl, C−Br, and C−I. The difference in reactivity was not sufficient enough under standard conditions, although the more reactive C−X bond was functionalized preferentially (only **3-X** as mono-substituted product, no **3-Y** can be observed), following the typical reactivity order of arylhalides toward oxidative addition with ArI > ArBr > ArCl. Unfortunately, the difunctionalized product **3-XY** was obtained as well, explaining the lower conversion of electrophile **1**.

In contrast, a higher chemodivergent selectivity could be observed in a C−OTf selective functionalization in the presence of C−Cl bonds. Under standard reaction conditions, monofunctionalization at the C−OTf site yielded thioether **3Fb** (70%) in a mixture with the difunctionalized product (14%) and remaining starting material (16%). Additionally, chemoselective couplings of C−Cl (89%) and C−OTf (94%) bonds in the presence of a tosylate substituent, which is relatively inert under the employed reaction conditions, generated the corresponding monothioether in excellent isolated yields. In these cases, the GC-FID analysis of the

Scheme 3. Intramolecular Competition Experiments of Biselectrophiles and Application in Sequential Transformation[a]

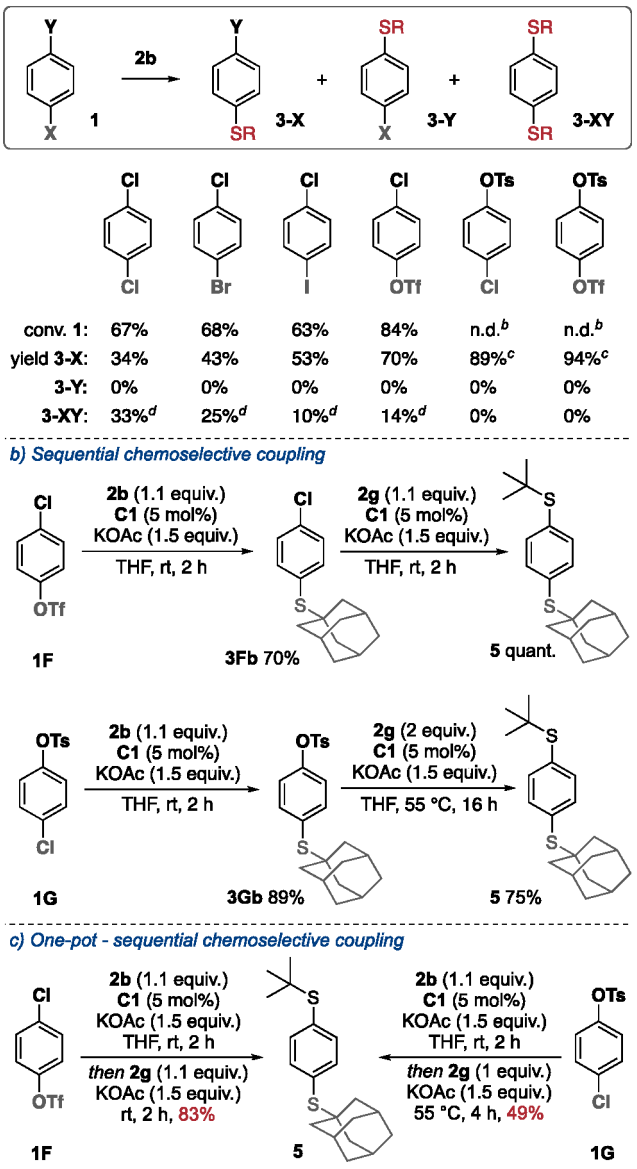

[a]GC-FID yields with pentadecane as an internal standard, unless otherwise noted. [b]Not determined due to detection difficulties by GC-FID. [c]Isolated yields. [d]Caluclated yields/GC-MS.

crude mixture was hampered by detectability of the substrates and monosubstituted products, but no disubstituted compound nor the product of single C−OTs sulfenylation were observed after isolation or on GC-MS. C−Cl selectivity in the presence of C−OTs bonds is typical for Ni(0).[16] The usefulness of the preferential activation of one particular C−X bond was further demonstrated in two sequential C−S couplings of the biselectrophilic substrates **1F** and **1G** (Scheme 3b). Surprisingly, tosylate could be converted under higher temperatures with a longer reaction time in 75% yield. The sequence was also successfully performed in one-pot fashion for both substrates. No additional catalyst was needed in the second step (Scheme 3c).

https://doi.org/10.1021/acscatal.1c04895
ACS Catal. 2022, 12, 2233−2243

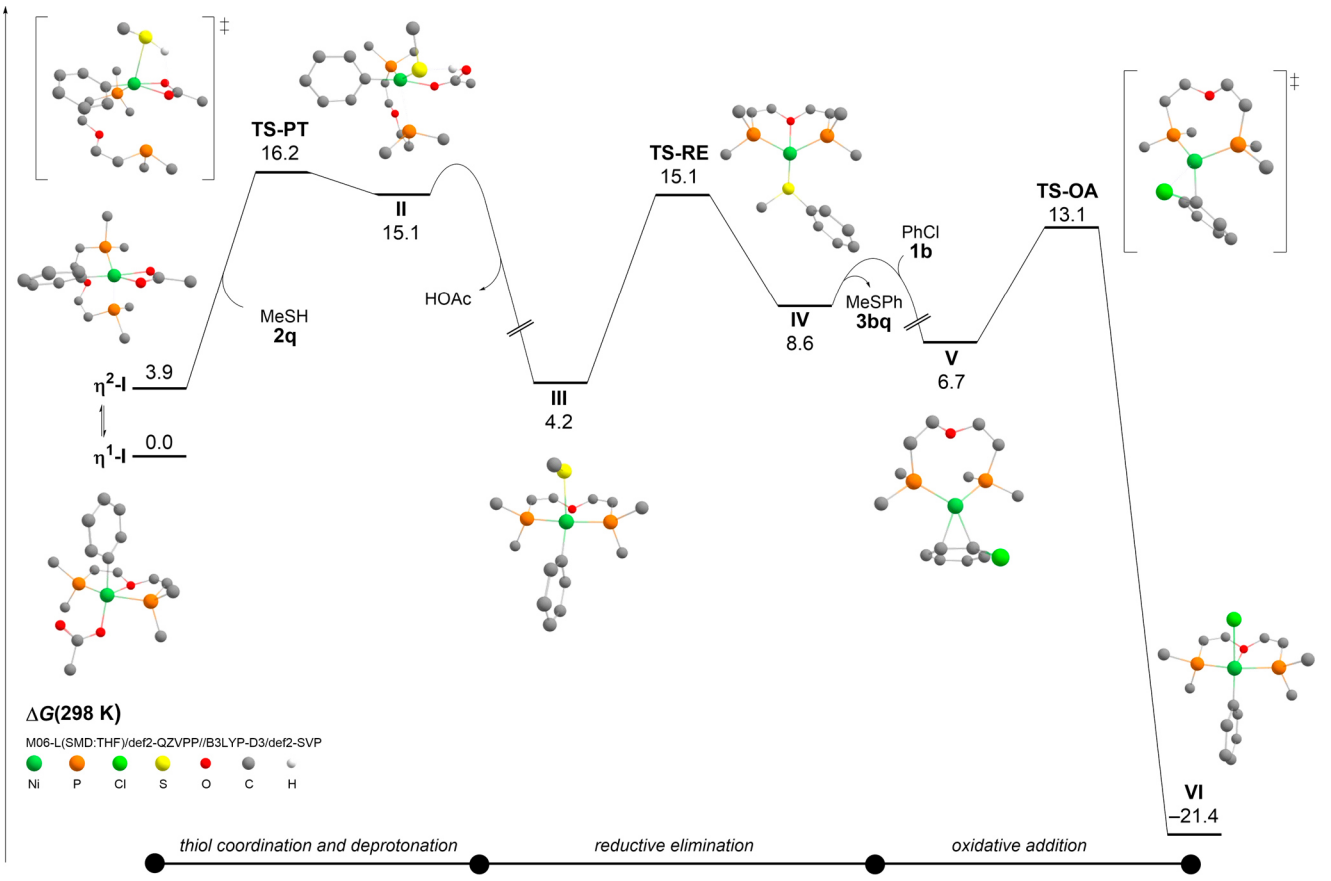

Figure 1. Free energy surface of the Ni-catalyzed cross-coupling reaction with methanethiol as a model nucleophile and chlorobenzene as the electrophile at the M06-L(SMD:THF)/def2-QZVPP//B3LYP-D3/def2-SVP level of theory. Only selected atoms of the Xantphos ligand are displayed, and all carbon-bound hydrogens are omitted for clarity.

Next, we pursued mechanistic investigations of our catalytic reaction. Several experiments with radical scavengers (2 equiv) were performed (see SI, Scheme S3). The reaction was suppressed in the presence of TEMPO (2,2,6,6-tetramethylpiperidinyloxyl) and the galvinoxyl radical, which are also known to react directly with Ni(0) species.[17] On the other hand, reactions with BHT (butylated hydroxytoluene) and 9,10-dihydroantracene proceeded smoothly, providing 82% and 85% yields of thioether product, respectively. These observations as well as the lack of paramagnetic signals in NMR experiments (see SI section 6.2) led to the assumption that a two-electron mechanism with a Ni(0)/Ni(II) catalytic cycle is more likely. Cycles proceeding via alternative pathways, including single electron transfer steps cannot be ruled out completely, but they were not further considered.

In order to better understand the mechanism and the unique role the acetate plays,[18] we performed DFT computations with the ORCA 4 electronic structure code.[19] All structures were optimized with the B3LYP(VWN-3) hybrid density functional[20] in combination with Grimme's D3-dispersion correction (with zero-damping)[21] and a def2-SVP basis set,[22] which treats all electrons explicitly (without an effective core potential). Furthermore, the electronic energies were refined by computing M06-L single point energies[23] with the prodigious def2-QZVPP basis set, and solvation effects were accounted for implicitly using the SMD model[24] with THF as a solvent. Comparable levels of theory have previously been employed for the computational assessment of other Ni-catalyzed reactions.[7b] The obtained results are displayed in Figure 1.

We were particularly interested in the role of the acetate both during the activation of the one-component Ni(II) precatalyst **C1** and during the active catalytic cycle. **C1** and the on-cycle oxidative addition product **VI** have a similar structural motive [LNi(II)ArCl]; therefore activation of the catalyst and on-cycle catalysis share the same steps. Assuming the involvement of the metal during the deprotonation step and ligand exchange, Ni(II) complexes with acetate as a ligand were optimized.[25] Two isomeric complexes, η^1-**I** and η^2-**I** [LNi(II)ArOAc], were localized, in which the acetate acts as a mono- and bidentate ligand, respectively. The η^1-**I** complex roughly assumes a distorted square-pyramidal geometry, in which both phosphorus atoms occupy equatorial positions across from each other at almost equal distances (~2.2 Å), while the oxygen atom of Xantphos sits in the apical position. In contrast, this oxygen atom is unbound in the 3.9 kcal mol^{-1} less stable η^2-**I** complex, and one of the phosphorus donors is less tightly bound at a distance of 2.4 Å. This opens the possibility for the thiol coupling partner to attack the metal center *trans* to the loosely bound phosphorus arm of the ligand. Using methanethiol as a model nucleophile, we were able to localize the transition state **TS-PT** at an energy of 16.2 kcal mol^{-1}. The reactive mode of the transition state mainly corresponds to a contraction of the Ni−S distance and an elongation of one of the Ni−O bonds to the acetate. As confirmed with the help of intrinsic reaction coordinate (IRC) computations, the reactive motion is consistent with an

https://doi.org/10.1021/acscatal.1c04895
ACS Catal. 2022, 12, 2233−2243

insertion of the SH-moiety into an Ni−O bond. However, we were unable to localize a minimum energy structure, in which the proton is still bound to the sulfur atom when thiolate and acetate are both coordinated to the nickel center, suggesting that the transition state structure **TS-PT** corresponds to a metal-mediated proton transfer reaction. The resulting complex **II** is approximately square-planar, and the second P donor is remote from the coordination center (3.2 Å). Rebinding of the latter and dissociation of acetic acid in a not further elucidated order of events affords thiolate complex **III** [LNi(II)ArSMe] at an energy of 4.2 kcal mol^{-1}. Therefore, the generation of thiolate complex **III** is modestly uphill but provides the possibility of product formation. The presumably interfering production of phenyl acetate by reductive elimination in **I** is not competitive since this process is associated with a prohibitive activation barrier of 44.0 kcal mol^{-1}. However, the reductive elimination of the thioether product **3bq** from complex **III** is activated by only 10.9 kcal mol^{-1} in another uphill reaction step. The thioether is initially still bound to the resulting Ni(0) complex **IV** but can be replaced by chlorobenzene (**1b**). From there, facile oxidative addition under formation of complex **VI** provides a sizable 28.1 kcal mol^{-1} of driving force to the reaction. The generation of complex **I** from **VI** and potassium acetate is difficult to describe computationally since it might involve the precipitation of potassium chloride in a salt metathesis reaction.

The corresponding proposed catalytic cycle is depicted in Scheme 4. After activation of precatalyst **C1**, generation of the active Ni(0) species (shown without the coordinated electrophile), and oxidative addition of the aryl halide, the intermediate **VI** is formed. It further undergoes a ligand exchange with potassium acetate generating **I** and precipitating KCl via salt metathesis. Subsequent acetate promoted deprotonation of the metal precoordinated thiol leads to intermediate **III** [LNi(II)ArSR]. This step (via intermediate **II**) is analogous to the CMD (concerted metalation-deprotonation) mechanism occurring in C−H activation processes.[26] Finally, **III** undergoes reductive elimination to yield the product and to regenerate the active Ni(0) catalyst.

Scheme 4. Postulated Mechanism via Acetate-Assisted Catalysis

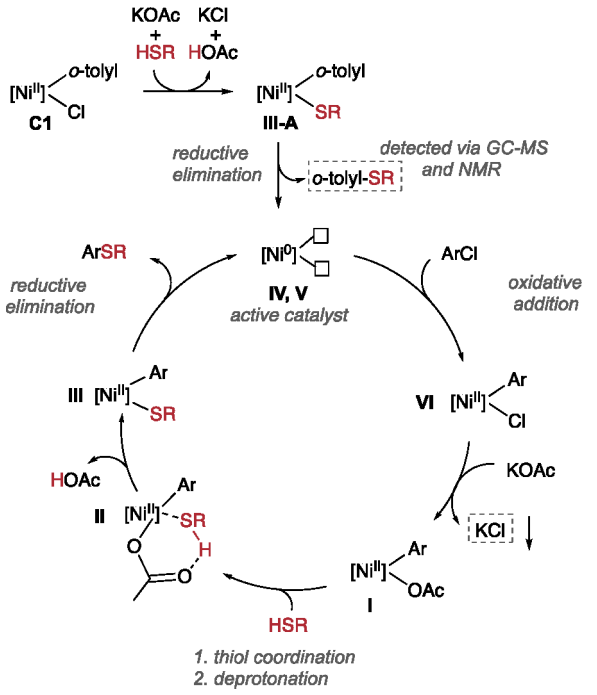

Several kinetic studies were conducted with electronic modifications of the electrophile (aryl chloride) and ligand, as well as steric modifications of the nucleophile (thiol) in order to analyze and compare initial periods, reaction rates, and overall yields. The reaction profiles of varying thiols are depicted within Table 4. Similar reaction rates for primary, secondary (both k_{rel} = 0.95), and tertiary thiols (k_{rel} = 1.0, see SI, section 6.1) indicate that the thiol is not relevant during the rate-determining step or that its steric adaptations do not have any influence. However, a significantly longer initial period was observed for the tertiary thiol (1°, 2° = 5 min; 3° = 15 min), which can be explained through the involvement of thiol during the activation of precatalyst **C1**. Due to the *ortho*-substituent on the aryl coordinated to nickel in **C1**, an increase in steric strain could disfavor the formation of **III-A** [LNi(II)ArSR], especially with a tertiary thiol. The low yield observed for the *ortho*-methyl substituted aryl chloride **3rb**, in which the on-cycle intermediate **III** equals the activation intermediate **III-A**, supports this theory.

Another hint supporting the hypothesis that the activation of **C1** is responsible for an increase of the initial period is the use of Ni(cod)$_2$ and Xanthphos as a catalyst system, for which only a short induction period (<2 min, Figure 2c in blue) was observed. The thiol is not involved in the in situ generation of the active catalyst from a nickel(0) source.

In order to gain further insight into the mechanism and rate limiting step, Hammett studies were performed analyzing the influence that varying substituents on the ligand and on electrophile have on the reaction rate after the induction period (Figure 2, see SI section 6.1).[27] The series of experiments with modified aryl chlorides (*p*-OMe, *p*-Me, *p*-H *p*-CO$_2$Et, *p*-CF$_3$) showed an impact of electronic properties on the reaction rate (Figure 2a,b). Excluding the CF$_3$-substituent, a linear correlation with the σ_p Hammett constant was observed (ρ = 0.46, R^2 = 0.96) indicating that electron-withdrawing substituents increase the reaction rate to a specific point. The low ρ value is in agreement with the DFT computation, indicating that the oxidative addition is not the rate-determining step. The reaction rate decreased for a highly electron deficient trifluoromethyl-substituted substrate (ρ = −3.71), which indicates a change in mechanism, the rate-determining step, or different overall contributions.

The second Hammett study included adaptations of the electronic properties of the Xantphos ligand (*p*-OMe, *p*-Me, *p*-H, *p*-CF$_3$), which were tested with Ni(cod)$_2$ as a catalyst precursor via *in situ* catalysis (Figure 2c,d). Electron-donating substituents on the ligand increased the reaction rate (ρ = 1.68, R^2 = 0.83), but the *p*-CF$_3$-substituted ligand did not yield any product. Electron-donating ligands are known to stabilize higher oxidation states and promote the oxidative addition,[28] but the interpretation is complicated due to multiple factors. The reaction performed with defined catalyst **C1** is faster compared to the Xanthphos/Ni(0) system. The lower reaction rate for Ni(cod)$_2$ can be explained by the presence of cod, which was found to suppress oxidative addition during catalysis by coordinating and stabilizing the active Ni(0) catalyst, rendering it less reactive.[7b,29] Therefore, the result of the Hammett analysis with Ni(cod)$_2$ as a nickel source might not be completely adaptable to our catalytic system, as the

https://doi.org/10.1021/acscatal.1c04895
ACS Catal. 2022, 12, 2233−2243

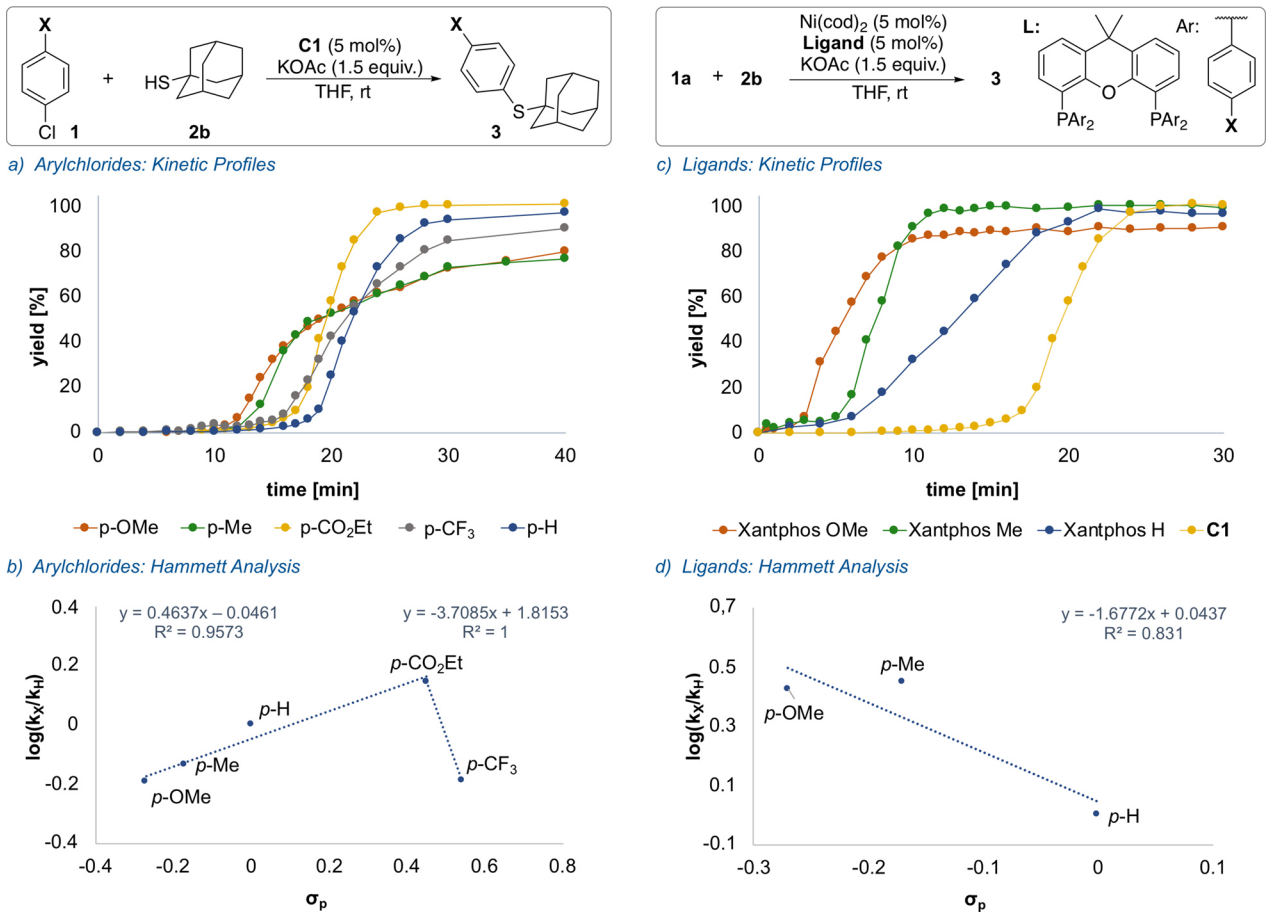

Figure 2. Kinetic and Hammett analysis. For reaction conditions, see SI, section 6.1.

additional cod might change rates of the elemental steps and disfavor the oxidative addition.

To gain further insight into the mechanism, the standard reaction of **1a** with **2b** was followed by $^{31}P\{H\}$ NMR (Figure 3, SI section 6.2). After 5 min, signals of the employed precatalyst **C1** (two different geometries, 6.55 and 1.43 ppm),[10] free Xantphos (−18.20 ppm), and a new signal at 7.02 ppm were detected, which can be assigned to the oxidative addition intermediate **VI** [LNiArCl]. The signal could be reproduced from a mixture of $Ni(cod)_2$, Xantphos, and **1a** (Figure 3, spectrum 2). After about 30 min, two broad doublets appeared at 9.31 and 8.24 ppm, presumably the $Ni(Xanthphos)_2$ complex. The signal was reproduced by the addition of $Ni(cod)_2$ and 2 equiv of Xantphos (Figure 3, spectrum 7). The complex has not yet been characterized in the literature, but it was previously identified as a catalyst sink.[30] In our case, it might form at a low substrate concentration, due to a lack of stabilization of Ni(0) species. Corresponding data for the analogous Pd complex are known from the literature and show similar signals.[31]

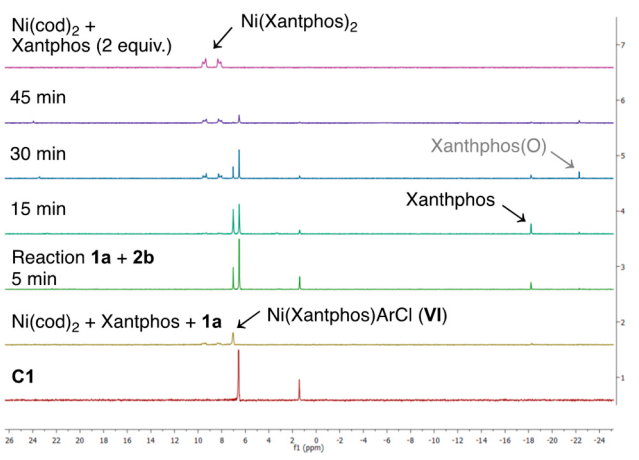

Figure 3. $^{31}P\{H\}$ NMR spectra for the reaction progress of a standard reaction with **1a** and **2b** (3−6). With additional comparison spectra (1, 2, 7).

The isolation of the catalytic intermediates and $Ni(Xanthphos)_2$ was not successful, yet. However, we were able to follow and compare the formation of a series of oxidative addition complexes **VI** [LNiArCl] in the catalytic transformation of three electron-poor aryl chlorides (Figure 4). Variation of para-substituents on the aryl chloride for the on-cycle generation of the oxidative addition product shows a shift in the $^{31}P\{H\}$ signals correlating to the Hammett value (CO_2Et σ_p = +0.45, 7.02 ppm; CF_3 σ_p = +0.54, 7.47 ppm; SO_2Me σ_p = +0.73, 7.69 ppm). These signals could be reproduced in a reaction of $Ni(cod)_2$, Xantphos and the corresponding aryl chloride. The experiments suggest that the oxidative addition product is the resting state of the catalytic cycle, which is in line with previous observations and our DFT computations (for further NMR spectra, see SI section 6.2.).

https://doi.org/10.1021/acscatal.1c04895
ACS Catal. 2022, 12, 2233−2243

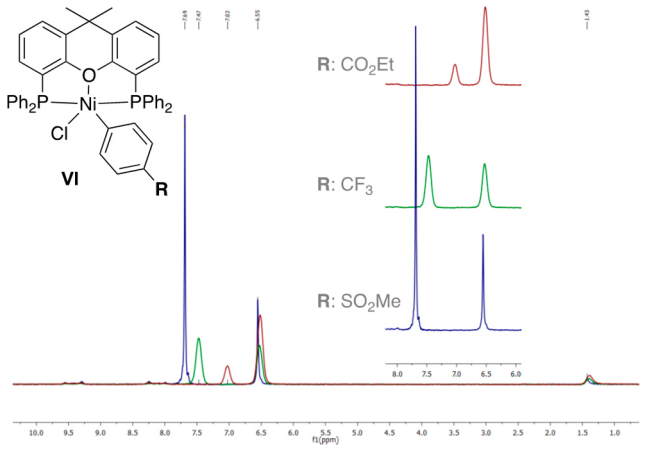

Figure 4. $^{31}P\{H\}$ NMR spectra of oxidative addition intermediates detected in the catalytic transformation of various electrophiles with **2b**. Signals at 6.55 and 1.43 ppm correspond to **C1**.

CONCLUSION

An operationally simple and mild nickel-catalyzed coupling of aryl chlorides with aliphatic thiols at room temperature was developed. The key feature is the combination of a defined air-stable Ni(II) precatalyst and potassium acetate as a base, without the need for further additives. A large variety of functional groups was tolerated, and complex pharmaceutically relevant compounds were functionalized. Chemoselective coupling of tertiary thiols with triflates in the presence of C−Cl and C−OTs bonds, as well as with chlorides in the presence of C−OTs bonds, was achieved. The conducted kinetic and NMR studies as well as DFT computations support a Ni(0)/Ni(II) catalytic cycle with the oxidative addition product as the resting state and acetate playing a key role in the formation of a thiolate complex via internal deprotonation.

ASSOCIATED CONTENT

Supporting Information

The Supporting Information is available free of charge at https://pubs.acs.org/doi/10.1021/acscatal.1c04895.

General procedures, analytical data, NMR spectra, computational data (PDF)

AUTHOR INFORMATION

Corresponding Authors

Ivana Fleischer − *Institute of Organic Chemistry, Faculty of Science, Eberhard Karls University Tübingen, 72076 Tübingen, Germany;* orcid.org/0000-0002-2609-6536; Email: ivana.fleischer@uni-tuebingen.de

J. Philipp Wagner − *Institute of Organic Chemistry, Faculty of Science, Eberhard Karls University Tübingen, 72076 Tübingen, Germany;* orcid.org/0000-0002-1433-0292; Email: philipp.wagner@orgchem.uni-tuebingen.de

Author

Regina M. Oechsner − *Institute of Organic Chemistry, Faculty of Science, Eberhard Karls University Tübingen, 72076 Tübingen, Germany*

Complete contact information is available at: https://pubs.acs.org/10.1021/acscatal.1c04895

Author Contributions

The manuscript was written through contributions of all authors. All authors have given approval to the final version of the manuscript.

Funding

This work was supported by the University of Tübingen and the FCI (Fonds der Chemischen Industrie).

Notes

The authors declare no competing financial interest.

ACKNOWLEDGMENTS

We thank M. Abbas, A. Huber, and S. Clewing for their synthetic contributions to the project during research internships and the analytics department of the University of Tübingen for their excellent work. Financial support from the University of Tübingen and the FCI (Liebig Fellowship J. P. W.) is gratefully acknowledged. J.P.W. is grateful to Prof. Holger Bettinger for his generous support.

REFERENCES

(1) Migita, T.; Shimizu, T.; Asami, Y.; Shiobara, J.-i.; Kato, Y.; Kosugi, M. The Palladium Catalyzed Nucleophilic Substitution of Aryl Halides by Thiolate Anions. *Bull. Chem. Soc. Jpn.* **1980**, *53*, 1385−1389.

(2) (a) Scott, K. A.; Njardarson, J. T. Analysis of US FDA-Approved Drugs Containing Sulfur Atoms. *Top. Curr. Chem.* **2018**, *376*, 5. (b) Hill, H. W., Jr.; Brady, D. G. Properties, environmental stability, and molding characteristics of polyphenylene sulfide. *Polym. Eng. Sci.* **1976**, *16*, 831−835. (c) Hilton, H. W.; Nomura, N. S.; Yauger, W. L.; Kameda, S. S. Absorption, translocation, and metabolism of metribuzin (BAY-94337) in sugarcane. *J. Agric. Food Chem.* **1974**, *22*, 578−582.

(3) For selected examples, see: (a) Li, G. Y. The First Phosphine Oxide Ligand Precursors for Transition Metal Catalyzed Cross-Coupling Reactions: C-C, C-N, and C-S Bond Formation on Unactivated Aryl Chlorides. *Angew. Chem., Int. Ed.* **2001**, *40*, 1513−1516. (b) Fernández-Rodríguez, M. A.; Shen, Q.; Hartwig, J. F. A General and Long-Lived Catalyst for the Palladium-Catalyzed Coupling of Aryl Halides with Thiols. *J. Am. Chem. Soc.* **2006**, *128*, 2180−2181. (c) Murata, M.; Buchwald, S. L. A general and efficient method for the palladium-catalyzed cross-coupling of thiols and secondary phosphines. *Tetrahedron* **2004**, *60*, 7397−7403.

(4) For selected examples, see: (a) Chekal, B.; Damon, D.; LaFrance, D.; Leeman, K.; Mojica, C.; Palm, A.; St. Pierre, M.; Sieser, J.; Sutherland, K.; Vaidyanathan, R.; Van Alsten, J.; Vanderplas, B.; Wager, C.; Weisenburger, G.; Withbroe, G.; Yu, S. Development of the Commercial Route for the Manufacture of a 5-Lipoxygenase Inhibitor PF-04191834. *Org. Process Res. Dev.* **2015**, *19*, 1944−1953. (b) Chekal, B. P.; Guinness, S. M.; Lillie, B. M.; McLaughlin, R. W.; Palmer, C. W.; Post, R. J.; Sieser, J. E.; Singer, R. A.; Sluggett, G. W.; Vaidyanathan, R.; Withbroe, G. J. Development of an Efficient Pd-Catalyzed Coupling Process for Axitinib. *Org. Process Res. Dev.* **2014**, *18*, 266−274.

(5) For selected reviews on nickel catalysis, see: (a) Ananikov, V. P. Nickel: The "Spirited Horse" of Transition Metal Catalysis. *ACS Catal.* **2015**, *5*, 1964−1971. (b) Tasker, S. Z.; Standley, E. A.; Jamison, T. F. Recent advances in homogeneous nickel catalysis. *Nature* **2014**, *509*, 299−309. (c) Diccianni, J. B.; Diao, T. Mechanisms of Nickel-Catalyzed Cross-Coupling Reactions. *Trends Chem.* **2019**, *1*, 830−844.

(6) (a) Takagi, K. Nickel(0)-catalyzed Synthesis of Diaryl Sulfides from Aryl Halides and Aromatic Thiols. *Chem. Lett.* **1987**, *16*, 2221−2224. (b) Zhang, Y.; Ngeow, K. C.; Ying, J. Y. The First N-Heterocyclic Carbene-Based Nickel Catalyst for C-S Coupling. *Org. Lett.* **2007**, *9*, 3495−3498. (c) Iglesias, M. J.; Prieto, A.; Nicasio, M. C. Well-Defined Allylnickel Chloride/N-Heterocyclic Carbene [(NHC)-

Ni(allyl)Cl] Complexes as Highly Active Precatalysts for C-N and C-S Cross-Coupling Reactions. *Adv. Synth. Catal.* **2010**, *352*, 1949−1954. (d) Martin, A. R.; Nelson, D. J.; Meiries, S.; Slawin, A. M. Z.; Nolan, S. P. Efficient C−N and C−S Bond Formation Using the Highly Active [Ni(allyl)Cl(IPr*OMe)] Precatalyst. *Eur. J. Org. Chem.* **2014**, *2014*, 3127−3131. (e) Cristau, H. J.; Chabaud, B.; Chêne, A.; Christol, H. Synthesis of Diaryl Sulfides by Nickel(II)-Catalyzed Arylation of Arenethiolates. *Synthesis* **1981**, *1981*, 892−894. (f) Talukder, M. M.; Miller, J. T.; Cue, J. M. O.; Udamulle, C. M.; Bhadran, A.; Biewer, M. C.; Stefan, M. C. Mono- and Dinuclear α-Diimine Nickel(II) and Palladium(II) Complexes in C−S Cross-Coupling. *Organometallics* **2021**, *40*, 83−94. (g) Yu, T.-Y.; Pang, H.; Cao, Y.; Gallou, F.; Lipshutz, B. H. Safe, Scalable, Inexpensive, and Mild Nickel-Catalyzed Migita-Like C-S Cross-Couplings in Recyclable Water. *Angew. Chem., Int. Ed.* **2021**, *60*, 3708−3713. (h) Liu, D.; Ma, H. X.; Fang, P.; Mei, T. S. Nickel-Catalyzed Thiolation of Aryl Halides and Heteroaryl Halides through Electrochemistry. *Angew. Chem., Int. Ed. Engl.* **2019**, *58*, 5033−5037.

(7) (a) Jones, K. D.; Power, D. J.; Bierer, D.; Gericke, K. M.; Stewart, S. G. Nickel Phosphite/Phosphine-Catalyzed C−S Cross-Coupling of Aryl Chlorides and Thiols. *Org. Lett.* **2018**, *20*, 208−211. (b) Yin, G.; Kalvet, I.; Englert, U.; Schoenebeck, F. Fundamental Studies and Development of Nickel-Catalyzed Trifluoromethylthiolation of Aryl Chlorides: Active Catalytic Species and Key Roles of Ligand and Traceless MeCN Additive Revealed. *J. Am. Chem. Soc.* **2015**, *137*, 4164−4172. (c) Martín, M. T.; Marín, M.; Maya, C.; Prieto, A.; Nicasio, M. C. Ni(II) Precatalysts Enable Thioetherification of (Hetero)Aryl Halides and Tosylates and Tandem C-S/C-N Couplings. *Chem.—Eur. J.* **2021**, *27*, 12320−12326.

(8) Gehrtz, P. H.; Geiger, V.; Schmidt, T.; Srsan, L.; Fleischer, I. Cross-Coupling of Chloro(hetero)arenes with Thiolates Employing a Ni(0)-Precatalyst. *Org. Lett.* **2019**, *21*, 50−55.

(9) (a) Guan, P.; Cao, C.; Liu, Y.; Li, Y.; He, P.; Chen, Q.; Liu, G.; Shi, Y. Efficient nickel/N-heterocyclic carbene catalyzed C-S cross-coupling. *Tetrahedron Lett.* **2012**, *53*, 5987−5992. (b) Xu, X.-B.; Liu, J.; Zhang, J.-J.; Wang, Y.-W.; Peng, Y. Nickel-Mediated Inter- and Intramolecular C-S Coupling of Thiols and Thioacetates with Aryl Iodides at Room Temperature. *Org. Lett.* **2013**, *15*, 550−553. (c) Venkanna, G. T.; Arman, H. D.; Tonzetich, Z. J. Catalytic C-S Cross-Coupling Reactions Employing Ni Complexes of Pyrrole-Based Pincer Ligands. *ACS Catal.* **2014**, *4*, 2941−2950. (d) Jouffroy, M.; Kelly, C. B.; Molander, G. A. Thioetherification via Photoredox/Nickel Dual Catalysis. *Org. Lett.* **2016**, *18*, 876−879. (e) Oderinde, M. S.; Frenette, M.; Robbins, D. W.; Aquila, B.; Johannes, J. W. Photoredox Mediated Nickel Catalyzed Cross-Coupling of Thiols With Aryl and Heteroaryl Iodides via Thiyl Radicals. *J. Am. Chem. Soc.* **2016**, *138*, 1760−1763. (f) Guo, F.-J.; Sun, J.; Xu, Z.-Q.; Kuhn, F. E.; Zang, S.-L.; Zhou, M.-D. C-S cross-coupling of aryl halides with alkyl thiols catalyzed by in-situ generated nickel(II) N-heterocyclic carbene complexes. *Catal. Commun.* **2017**, *96*, 11−14. (g) Cavedon, C.; Madani, A.; Seeberger, P. H.; Pieber, B. Semiheterogeneous Dual Nickel/Photocatalytic (Thio)etherification Using Carbon Nitrides. *Org. Lett.* **2019**, *21*, 5331−5334. (h) Delcaillau, T.; Bismuto, A.; Lian, Z.; Morandi, B. Nickel-Catalyzed Inter- and Intramolecular Aryl Thioether Metathesis by Reversible Arylation. *Angew. Chem., Int. Ed.* **2020**, *59*, 2110−2114. (i) Rodriguez-Cruz, M. A.; Hernandez-Ortega, S.; Valdes, H.; Rufino-Felipe, E.; Morales-Morales, D. C-S cross-coupling catalyzed by a series of easily accessible, well defined Ni(II) complexes of the type [(NHC)Ni(Cp)(Br)]. *J. Catal.* **2020**, *383*, 193−198. (j) Talukder, M. M.; Miller, J. T.; Cue, J. M. O.; Udamulle, C. M.; Bhadran, A.; Biewer, M. C.; Stefan, M. C. Mono- and Dinuclear α-Diimine Nickel(II) and Palladium(II) Complexes in C-S Cross-Coupling. *Organometallics* **2021**, *40*, 83−94. (k) Isshiki, R.; Kurosawa, M. B.; Muto, K.; Yamaguchi, J. Ni-Catalyzed Aryl Sulfide Synthesis through an Aryl Exchange Reaction. *J. Am. Chem. Soc.* **2021**, *143*, 10333−10340.

(10) Standley, E. A.; Smith, S. J.; Müller, P.; Jamison, T. F. A Broadly Applicable Strategy for Entry into Homogeneous Nickel(0) Catalysts from Air-Stable Nickel(II) Complexes. *Organometallics* **2014**, *33*, 2012−2018.

(11) For catalysis using **C1** catalyst, see: (a) Beattie, D. D.; Schareina, T.; Beller, M. A room temperature cyanation of (hetero)aromatic chlorides by an air stable nickel(II) XantPhos precatalyst and Zn(CN)2. *Org. Biomol. Chem.* **2017**, *15*, 4291−4294. (b) Gehrtz, P. H.; Kathe, P.; Fleischer, I. Nickel-Catalyzed Coupling of Arylzinc Halides with Thioesters. *Chem.—Eur. J.* **2018**, *24*, 8774−8778. For related Ni complexes, see: (c) McGuire, R. T.; Paffile, J. F. J.; Zhou, Y.; Stradiotto, M. Nickel-Catalyzed C−N Cross-Coupling of Ammonia, (Hetero)anilines, and Indoles with Activated (Hetero)aryl Chlorides Enabled by Ligand Design. *ACS Catal.* **2019**, *9*, 9292−9297. (d) Morrison, K. M.; McGuire, R. T.; Ferguson, M. J.; Stradiotto, M. CgPhen-DalPhos Enables the Nickel-Catalyzed O-Arylation of Tertiary Alcohols with (Hetero)Aryl Electrophiles. *ACS Catal.* **2021**, *11*, 10878−10884.

(12) Brauer, D. J.; Krueger, C. Bonding of aromatic hydrocarbons to nickel(0). Structure of bis(tricyclohexylphosphine)(1,2-.eta.2-anthracene)nickel(0)-toluene. *Inorg. Chem.* **1977**, *16*, 884−891.

(13) Kalvet, I.; Guo, Q.; Tizzard, G. J.; Schoenebeck, F. When Weaker Can Be Tougher: The Role of Oxidation State (I) in P- vs N-Ligand-Derived Ni-Catalyzed Trifluoromethylthiolation of Aryl Halides. *ACS Catal.* **2017**, *7*, 2126−2132.

(14) (a) Scattolin, T.; Senol, E.; Yin, G.; Guo, Q.; Schoenebeck, F. Site-Selective C-S Bond Formation at C-Br over C-OTf and C-Cl Enabled by an Air-Stable, Easily Recoverable, and Recyclable Palladium(I) Catalyst. *Angew. Chem., Int. Ed.* **2018**, *57*, 12425−12429. (b) Keaveney, S. T.; Kundu, G.; Schoenebeck, F. Modular Functionalization of Arenes in a Triply Selective Sequence: Rapid C(sp2) and C(sp3) Coupling of C-Br, C-OTf, and C-Cl Bonds Enabled by a Single Palladium(I) Dimer. *Angew. Chem., Int. Ed.* **2018**, *57*, 12573−12577.

(15) (a) Reeves, E. K.; Entz, E. D.; Neufeldt, S. R. Chemodivergence between Electrophiles in Cross-Coupling Reactions. *Chem.—Eur. J.* **2021**, *27*, 6161−6177. (b) Entz, E. D.; Russell, J. E. A.; Hooker, L. V.; Neufeldt, S. R. Small Phosphine Ligands Enable Selective Oxidative Addition of Ar−O over Ar−Cl Bonds at Nickel(0). *J. Am. Chem. Soc.* **2020**, *142*, 15454−15463.

(16) Russell, J. E. A.; Neufeldt, S. R. C−O-Selective Cross-Coupling of Chlorinated Phenol Derivatives. *Synlett* **2021**, *32*, 1484−1491.

(17) Greaves, M. E.; Ronson, T. O.; Lloyd-Jones, G. C.; Maseras, F.; Sproules, S.; Nelson, D. J. Unexpected Nickel Complex Speciation Unlocks Alternative Pathways for the Reactions of Alkyl Halides with dppf-Nickel(0). *ACS Catal.* **2020**, *10*, 10717−10725.

(18) Kalek, M.; Jezowska, M.; Stawinski, J. Preparation of Arylphosphonates by Palladium(0)-Catalyzed Cross-Coupling in the Presence of Acetate Additives: Synthetic and Mechanistic Studies. *Adv. Synth. Catal.* **2009**, *351*, 3207−3216.

(19) Neese, F. Software Update: the ORCA Program System, Version 4.0. *Wiley. Interdiscip. Rev. Comput. Mol. Sci.* **2018**, *8*, No. e1327.

(20) (a) Becke, A. D. Density-Functional Thermochemistry. III. The Role of Exact Exchange. *J. Chem. Phys.* **1993**, *98*, 5648−5652. (b) Stephens, P. J.; Devlin, F. J.; Chabalowski, C. F.; Frisch, M. J. Ab Initio Calculation of Vibrational Absorption and Circular Dichroism Spectra Using Density Functional Force Fields. *J. Phys. Chem.* **1994**, *98*, 11623−11627.

(21) Grimme, S.; Antony, J.; Ehrlich, S.; Krieg, H. A Consistent and Accurate Ab Initio Parametrization of Density Functional Dispersion Correction (DFT-D) for the 94 Elements H-Pu. *J. Chem. Phys.* **2010**, *132*, 154104.

(22) Weigend, F.; Ahlrichs, R. Balanced Basis Sets of Split Valence, Triple Zeta Valence and Quadruple Zeta Valence Quality for H to Rn: Design and Assessment of Accuracy. *Phys. Chem. Chem. Phys.* **2005**, *7*, 3297−3305.

(23) Zhao, Y.; Truhlar, D. G. A New Local Density Functional for Main-Group Thermochemistry, Transition Metal Bonding, Thermochemical Kinetics, and Noncovalent Interactions. *J. Chem. Phys.* **2006**, *125*, 194101.

https://doi.org/10.1021/acscatal.1c04895
ACS Catal. 2022, 12, 2233−2243

(24) Marenich, A. V.; Cramer, C. J.; Truhlar, D. G. Universal Solvation Model Based on Solute Electron Density and on a Continuum Model of the Solvent Defined by the Bulk Dielectric Constant and Atomic Surface Tensions. *J. Phys. Chem. B* **2009**, *113*, 6378−6396.
(25) Li, Z.; Zhang, S.-L.; Fu, Y.; Guo, Q.-X.; Liu, L. Mechanism of Ni-Catalyzed Selective C-O Bond Activation in Cross-Coupling of Aryl Esters. *J. Am. Chem. Soc.* **2009**, *131*, 8815−8823.
(26) For selected examples on CMD mechanism, see: (a) Stuart, D. R.; Fagnou, K. The Catalytic Cross-Coupling of Unactivated Arenes. *Science* **2007**, *316*, 1172−1175. (b) Gorelsky, S. I.; Lapointe, D.; Fagnou, K. Analysis of the Concerted Metalation-Deprotonation Mechanism in Palladium-Catalyzed Direct Arylation Across a Broad Range of Aromatic Substrates. *J. Am. Chem. Soc.* **2008**, *130*, 10848−10849. (c) Bugaut, X.; Glorius, F. Palladium-Catalyzed Selective Dehydrogenative Cross-Couplings of Heteroarenes. *Angew. Chem., Int. Ed.* **2011**, *50*, 7479−7481. (d) Zhang, S.; Shi, L.; Ding, Y. Theoretical Analysis of the Mechanism of Palladium(II) Acetate-Catalyzed Oxidative Heck Coupling of Electron-Deficient Arenes with Alkenes: Effects of the Pyridine-Type Ancillary Ligand and Origins of the meta-Regioselectivity. *J. Am. Chem. Soc.* **2011**, *133*, 20218−20229.
(27) (a) Hansch, C.; Leo, A.; Taft, R. W. A survey of Hammett substituent constants and resonance and field parameters. *Chem. Rev.* **1991**, *91*, 165−195. (b) Hammett, L. P. The Effect of Structure upon the Reactions of Organic Compounds. Benzene Derivatives. *J. Am. Chem. Soc.* **1937**, *59*, 96−103.
(28) Xiong, B.; Li, Y.; Wei, Y.; Kramer, S.; Lian, Z. Dual Nickel-/Palladium-Catalyzed Reductive Cross-Coupling Reactions between Two Phenol Derivatives. *Org. Lett.* **2020**, *22*, 6334−6338.
(29) Bajo, S.; Laidlaw, G.; Kennedy, A. R.; Sproules, S.; Nelson, D. J. Oxidative Addition of Aryl Electrophiles to a Prototypical Nickel(0) Complex: Mechanism and Structure/Reactivity Relationships. *Organometallics* **2017**, *36*, 1662−1672.
(30) Clevenger, A. L.; Stolley, R. M.; Staudaher, N. D.; Al, N.; Rheingold, A. L.; Vanderlinden, R. T.; Louie, J. Comprehensive Study of the Reactions Between Chelating Phosphines and Ni(cod)2. *Organometallics* **2018**, *37*, 3259−3268.
(31) Klingensmith, L. M.; Strieter, E. R.; Barder, T. E.; Buchwald, S. L. New Insights into Xantphos/Pd-Catalyzed C-N Bond Forming Reactions: A Structural and Kinetic Study. *Organometallics* **2006**, *25*, 82−91.

https://doi.org/10.1021/acscatal.1c04895
ACS Catal. 2022, 12, 2233−2243

Acetate Facilitated Nickel Catalyzed Coupling of Aryl Chlorides and Alkyl Thiols

SUPPORTING INFORMATION

Regina M. Oechsner, J. Philipp Wagner,* and Ivana Fleischer*

Institute of Organic Chemistry, Faculty of Science, Eberhard Karls University Tübingen, Auf der Morgenstelle 18, 72076 Tübingen, Germany

*ivana.fleischer@uni-tuebingen.de; philipp.wagner@orgchem.uni-tuebingen.de

Table of Contents

1. General information

1.1. Chemicals and General Techniques

All cross-coupling reactions were carried out under an argon atmosphere using standard Schlenk techniques or an argon atmosphere Glovebox (GS MEGA E-Line, Glovebox Systemtechnik) and pre-dried glassware, unless noted otherwise. Dry THF was distilled over Na/benzophenone, stored over 3 Å MS and degassed. Solvents for reactions were dry and degassed unless otherwise noted.
Solvents for chromatography were distilled prior to use. Column chromatography was carried out either manually or by a Puriflash system (Interchim XS420) using silica gel (0.04–0.063 mm) from Machery&Nagel. Thin Layer Chromatography was performed on silica gel coated glass plates (0.25 mm) with fluorescence indicator UV254 (Macherey-Nagel, TLC plates SIL G-25 UV254). For detection of spots, irradiation of UV light at 254 nm was used. Chemicals were purchased from abcr, Acros, Alfa Aesar, BLDChem, Carbolution Chemicals, Carl Roth, Fluorochem, Sigma-Aldrich or TCI. Inorganic, temperature stable solid bases were dried prior to use at 110 °C under high vacuum. The substrates Indometacine-*o*-ethylester and 2-chloro-10-ethylphenothiazine were synthesized following literature procedures.[1]

1.2. Analytical Techniques

NMR spectra were recorded using Bruker Avance III HD 400 or Bruker Avance III HDX 600 at room temperature (400 MHz for ^{1}H experiments; 101 MHz for ^{13}C experiments; 162 MHz for ^{31}P experiments; 376 MHz for ^{19}F experiments) in commercially available deuterated solvents. ^{13}C-NMR and ^{31}P-NMR experiments were performed in proton-decoupled mode. Chemical shifts (*δ)* are reported in ppm relative to the residual NMR solvent signals[2] (chloroform: ^{1}H 7.26 ppm and ^{13}C 77.16 ppm; THF ^{1}H 1.73 ppm, 3.56 ppm and ^{13}C 25.2 ppm, 67.4 ppm). The coupling constants (*J* values) are given in Hz and spin multiplicity with the usual designations for splitting patterns (s = singlet, d = doublet, t = triplet, q = quartet, m = multiplet).

HR-MS (ESI, APCI, EI) measurements were carried out by the mass spectrometry department of the Institute of Organic Chemistry, University of Tübingen. Measurements were carried out using maXis 4G from Bruker (ESI, APCI) or by a MAT95 from Finnegan (EI). The molecular ion [M]+, [M+H]+, [M+K]+ and [M+Na]+ respectively are given in m/z units.

GC-LR-MS (EI) analysis was carried out on an Agilent 7820A system using dry hydrogen as carrier gas and an Agilent 190915-433UI column (30 m × 250 µm × 0.25 µm). Program: heating from 50 °C to 280 °C within 15 minutes. Samples were also measured by the MS-department of the University of Tübingen with an 8890 GC system and 5977B MSD. For these measurements, temperature program started by holding 3 min at 40 °C, then heating to 320 °C within 32 min and holding for 10 min at the same temperature.

GC-FID (flame ionization detection) analysis was carried out on an Agilent 7820A system using dry hydrogen as carrier gas. An Agilent 19091J-431 column (30 m × 320 µm × 0.25 µm) was used. Program 50-280M15: heating from 50 °C to 280 °C within 15 minutes. Conversion and yield were determined via calibration against the internal standard pentadecane.

Melting point determination was achieved by using a Büchi B-540 machine with a visual detection (heating rate 5 °C/min). FT-IR spectra were recorded using a Cary 630 FTIR by applying the sample neat on a diamond ATR sampler.

1.3. Computational Methods

All reported computations were performed with the ORCA 4 program package.[3] Geometries were fully optimized at the B3LYP-D3(0)/def2-SVP level of theory employing the RIJCOSX approximation and tight integration grids (GRID6, FINALGRID7, GRIDX6) and convergence criteria (VeryTightSCF, VeryTightOpt).[4-6] Analytical frequency computations were undertaken in order to assure the nature of the stationary point with minima exhibiting zero and transition states exactly one imaginary mode. Free energies were computed using a rigid-rotor-harmonic-oscillator model in a variation reported by Grimme.[7] Free energies were corrected for the one-molar standard state by adding 1.89 kcal mol^{-1} to each structure's energy. In addition, M06-L/def2-QZVPP single point energies were computed on top of each structure utilizing the SMD solvation model with THF as a solvent.[8, 9]

2. Optimization studies

Table S1: Preliminary base and reaction condition screening for the cross-coupling of cyclohexanethiol.

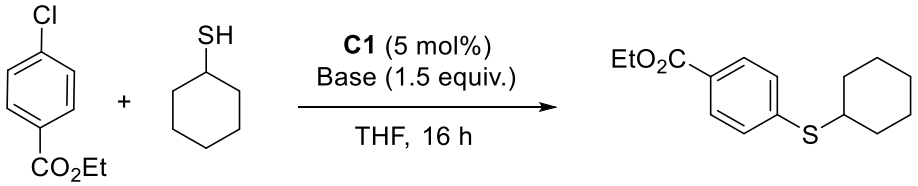

1a 1 equiv. + **2a** 1 equiv. → **3aa**

Entry	Base	Additive	Temp. [°C]	Conv. [%]	Yield [%]
1	NaO^tBu		50	81	62
2	Li_2CO_3		50	13	10
3	Na_2CO_3		50	60	56
4	K_2CO_3		50	56	52
5	Cs_2CO_3		50	12	9
6	K_2CO_3	Zn (1.0 equiv.)	50	100	61
7	Na_2CO_3	Zn (0.2 equiv.)	50	74	70
8	Na_2CO_3	Zn (0.2 equiv.)	rt	85	79
9	Na_2CO_3		rt	31	25
10	$Zn_5(CO_3)_2(OH)_6$		50	68	66
11	$Zn(OPiv)_2$		50	34	33
12	$Zn(OAc)_2$		50	60	54
13	Sodiumdiphosphate		50	6	4
14	Na_2HPO_4		50	65	62
15	Sodiumcitrate		50	44	42
16	NaOAc		50	89	85
17	KOAc		50	99	95

Conditions: ethyl 4-chlorobenzoate (350 µmol, 1.0 equiv.), cyclohexanethiol (350 µmol, 1.0 equiv.), base (525 µmol, 1.5 equiv.), **C1** (5 mol%), THF (1 mL) at rt for 16 h. Conversion and yield determined via GC-FID calibrated against the internal standard pentadecane. Temperature stable solid bases were dried prior to use at 110 °C under high vacuum.

Table S2: Reaction conditions screening for base equivalents and different alkali metal acetates.

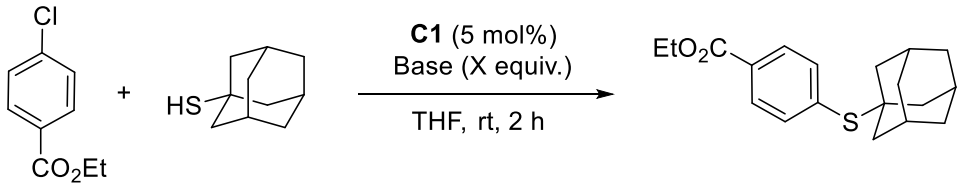

1a 1 equiv. **2b** 1.1 equiv. **3ab**

Entry	Base	[equiv.]	Time [h]	Conv. [%]	Yield [%]
1	LiOAc	1.5	2	4	0
2	LiOAc	1.5	16	5	2
3	NaOAc	1.5	2	20	14
4	NaOAc	1.5	16	86	83
5	KOAc	1.5	2	95	95
6	CsOAc	1.5	2	95	93
7	KOAc	0.5	2	44	41
8	KOAc	1	2	75	72
9	KOAc	1.5	2	99	98
10	KOAc	2	2	98	97

Conditions: ethyl 4-chlorobenzoate (350 µmol, 1.0 equiv.), adamantanethiol (385 µmol, 1.1 equiv.), base (X equiv.), **C1** (5 mol%), THF (1 mL) at rt for 2 h. Conversion and yield determined via GC-FID calibrated against the internal standard pentadecane.

Table S3: Thiol equivalent screening with ^{t}BuSH **2g**.

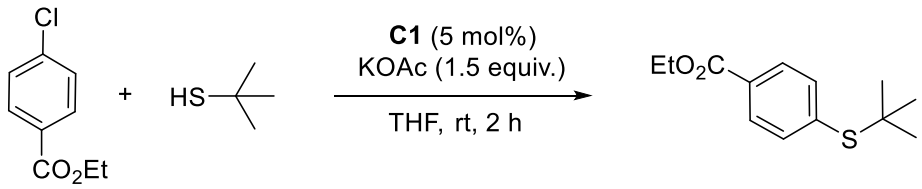

1a 1 equiv. **2g** X equiv. **3ag**

Entry	2g [equiv.]	Conv. [%]	Yield [%]
1	1.0	87	88
2	1.05	94	97
3	1.1	96	98

Conditions: ethyl 4-chlorobenzoate (350 µmol, 1.0 equiv.), 2-Methyl-2-propanthiol (X equiv.), KOAc (1.5 equiv.), **C1** (5 mol%), THF (1 mL) at rt for 2 h. Conversion and yield determined via GC-FID calibrated against the internal standard pentadecane.

Table S4: Reaction condition screening for catalyst loading with adamantanethiol.

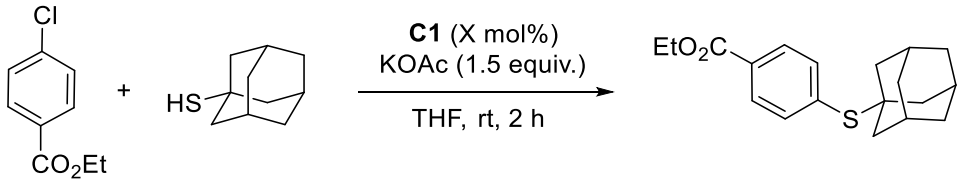

1a 1 equiv. **2b** 1.1 equiv. **3ab**

Entry	C1	Time [h]	Conv. [%]	Yield [%]
1	0.5 mol%	0.5	6	1
		1	6	1
		2	6	1
2	1 mol%	0.5	2	2
		1	4	4
		2	4	8
3	3 mol%	0.5	17	11
		1	90	73
		2	90	70
4	5 mol%	0.5	93	89
		1	94	94
		2	94	90

Conditions: ethyl 4-chlorobenzoate (350 µmol, 1.0 equiv.), adamantanethiol (385 µmol, 1.1 equiv.), KOAc (1.5 equiv.), C1 (X mol%), THF (1 mL) at rt for 2 h. Conversion and yield determined via GC-FID calibrated against the internal standard pentadecane.

Table S5: Reaction condition screening for catalyst loading with cyclohexanethiol.

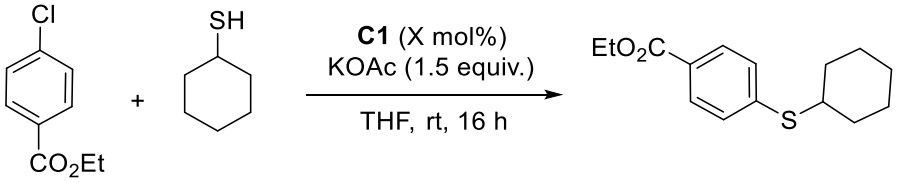

1a 1 equiv. **2a** 1.1 equiv. **3aa**

Entry	C1	Conv. [%]	Yield [%]
1	0.5	4	1
2	1	8	3
3	3	97	95

Conditions: ethyl 4-chlorobenzoate (350 µmol, 1.0 equiv.), cyclohexanethiol (385 µmol, 1.1 equiv.), KOAc (1.5 equiv.), C1 (X mol%), THF (1 mL) at rt for 16 h. Conversion and yield determined via GC-FID calibrated against the internal standard pentadecane.

3. Additional screening

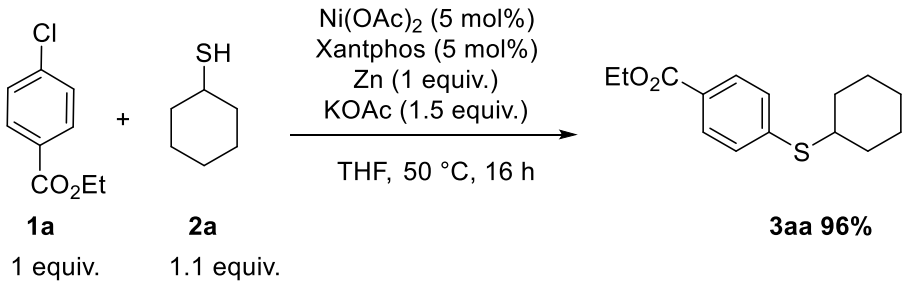

Scheme S1: In-situ generation of the active nickel catalyst from Ni(OAc) $_2$.

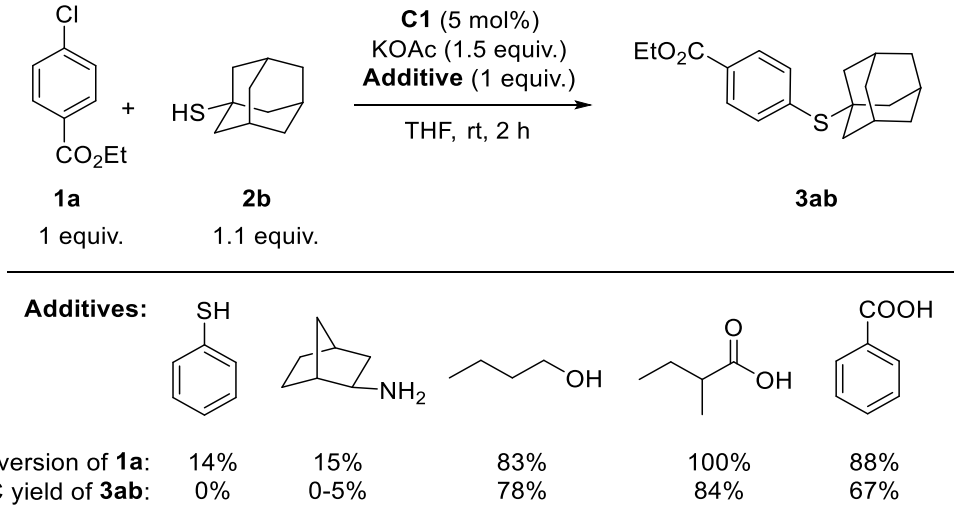

GC conversion of **1a**:	14%	15%	83%	100%	88%
GC yield of **3ab**:	0%	0-5%	78%	84%	67%

Scheme S2: Test of catalyst poisoning by certain functional groups.

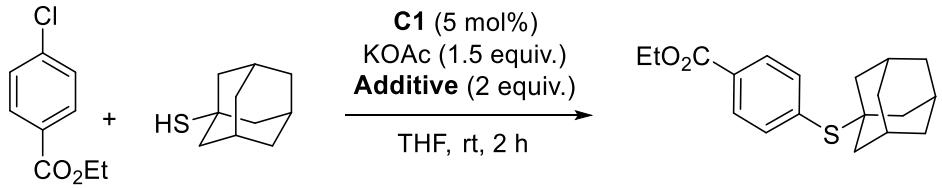

1a 1 equiv. + **2b** 1.1 equiv. → **3ab**

Additive:

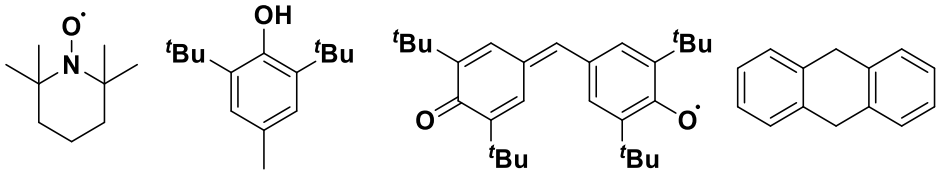

GC conversion of **1a**:	5%	83%	9%	86%
GC yield of **3ab**:	1%	82%	2%	85%

Scheme S3: Radical trapping experiments.

4. General Procedures

General Procedure A (GP-A): Xantphos ligand synthesis.

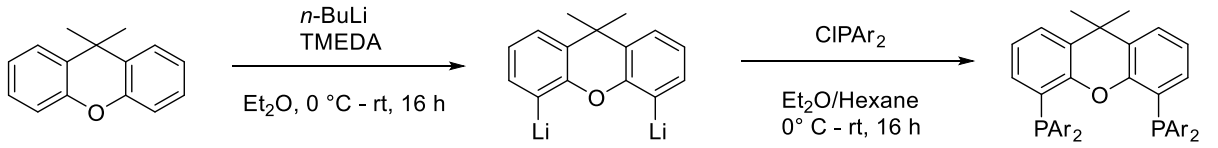

Ar = Ph (71%)
Ar = *p*-Me-C_6H_4 (50%)
Ar = *p*-OMe-C_6H_4 (66%)
Ar = *p*-CF_3-C_6H_4 (43%)

The ligands were synthesized following modified literature procedure.[10] At room temperature 9,9-dimethylxanthene was placed in an oven and flame-dried septum-capped 25 mL Schlenk-tube with stirring bar. After dissolving in dry, degassed Et_2O (5 mL) dry, degassed TMEDA (2.5 equiv.) was added. The reaction mixture was cooled to 0 °C and *n*-BuLi (1.6 M in Hexanes, 2.5 equiv.) was added dropwise under stirring over 30 min. The reaction mixture was slowly warmed to room temperature and stirred for another 16 h.

The colored suspension was cooled to 0 °C and a solution of the corresponding chlorodiphenylphosphane (2.5 equiv.) in dry and degassed *n*-hexane (4 mL) was added dropwise over 45 min. The reaction mixture decolorized, and a beige precipitate was formed. After stirring for 16 h the reaction mixture was diluted with degassed DCM (6 mL) and hydrolyzed with 4 mL of a degassed mixture of brine and 1 M HCl (1:1 v/v). The workup was done under inert conditions. The water phase was removed and washed with DCM (3 × 5 mL). The combined organic phases were dried over $MgSO_4$, the solvent removed in vacuo and the resulting residue was washed with *n*-Hexane (3 mL) and crystallized.

General Procedure B (GP-B): Nickel-catalyzed C-S cross-coupling of arylhalides and thiols for product isolation.

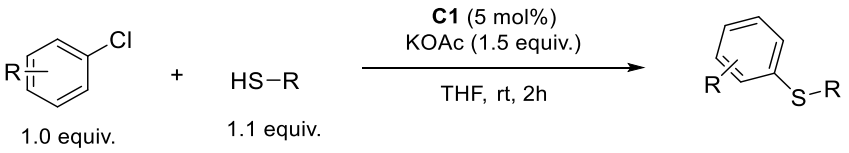

A 25 mL inert, flame-dried and septum-caped Schlenk-tube equipped with a stirring bar was charged with KOAc (1.5 mmol, 1.5 equiv.) and catalyst **C1** (5 mol%). After addition of the respective thiol (1.1 mmol, 1.1 equiv.), and corresponding aryl chloride (1.0 mmol, 1.0 equiv.) the mixture was dissolved in THF (3 mL) under stirring. After 2 h at room temperature the reaction mixture was quenched with brine (3 mL) and diluted with EtOAc (8 mL). After phase separation, the organic phase was washed with brine (5 mL) and the combined aqueous phases were re-extracted with EtOAc (3 × 5 mL). The combined organic phases were dried over $MgSO_4$, followed by solvent removal in vacuo. The product was isolated by flash column chromatography.

General Procedure C (GP-C): Nickel-catalyzed C-S cross-coupling of electrophiles (arylhalides) and thiols for GC-FID analysis (screening).

A 10 mL inert, flame-dried and septum-caped Schlenk-tube equipped with a stirring bar was charged with KOAc (0.53 mmol, 0.53 equiv.) and catalyst **C1** (5 mol%). After addition of the respective thiol (0.39 mmol, 0.39 equiv.), and corresponding aryl chloride (0.35 mmol, 0.35 equiv.) the mixture was dissolved in THF (1 mL) under stirring. After 2 h at room temperature the internal standard *n*-pentadecane (50 µL) was added, the reaction mixture was quenched with brine (1 mL) and diluted with EtOAc (3 mL). A sample of the organic phase was filtered (celite, Al_2O_3 and Mg_2SO_4) and analyzed via GC-FID. Yields and conversion were determined through the internal standard method for quantitative analysis.

General Procedure D (GP-D): Reaction Progress of nickel-catalyzed C-S cross-coupling of electrophiles (arylhalides) and thiols (kinetic studies).

A 10 mL inert, flame-dried and septum-caped Schlenk-tube equipped with a stirring bar was charged with KOAc (1.5 mmol, 1.5 equiv.) and catalyst **C1** (5 mol%). After addition of the internal standard n-pentadecane (100 µL), the respective thiol (1.1 mmol, 1.1 equiv.), and corresponding aryl chloride (1.0 mmol, 1.0 equiv.) the mixture was dissolved in THF (3 mL) under stirring. The time was started with the addition of THF. After defined intervals (e.g. 1, 2, 3, 5 min) 0.1 µL samples of the reaction mixture were removed from the reaction mixture with inert syringes. The probes were diluted with EtOAc and quenched with brine. A sample of the organic phase was filtered (celite, Al_2O_3 and Mg_2SO_4) and analyzed via GC-FID. Yields and conversion were determined through the internal standard method for quantitative analysis.

5. Analytical Data

5.1. Ligands and C1

Xantphos (L1)

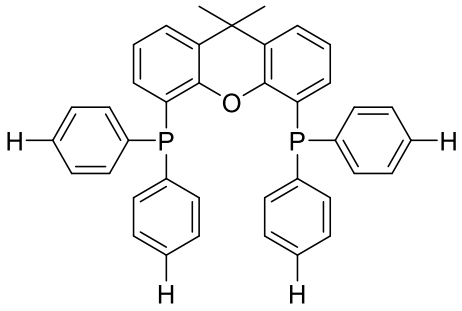

L1

$C_{39}H_{32}OP_2$ (578.63 g/mol)

Following GP-A, the ligand **L1** was synthesized using *n*-BuLi (1.6 M in hexanes, 2.25 mL, 3. 60 mmol, 2.5 equiv.), 9,9-dimethylxanthene (303 mg, 1.40 mmol, 1.00 equiv.), TMEDA (544 µL, 3.60 mmol, 2.5 equiv.) and chlorodiphenylphosphane (685 µL, 3.60 mmol, 2.5 equiv.). Purification by crystallization from DCM/EtOH afforded **L1** as colorless crystals (596 mg, 1.03 mmol, 71%). Conforms to reported analytical data.[11]

^{1}H-NMR (400 MHz, $CDCl_3$, δ): 7.40 (dd, J = 7.8, 1.5 Hz, 2H), 7.26 – 7.15 (m, 20H), 6.96 (d, J = 15.3 Hz, 1H), 6.55 (dd, J = 7.5, 1.8 Hz, 2H), 1.65 (s, 6H).

^{13}C-NMR (101 MHz, $CDCl_3$, δ): 152.7 (m), 137.5, 134.1 (m), 132.2, 130.0, 128.3 (dd, J = 7.0, 3.6 Hz), 126.5, 123.5, 34.6, 32.0.

^{31}P-NMR (162 MHz, $CDCl_3$, δ): -18.03.

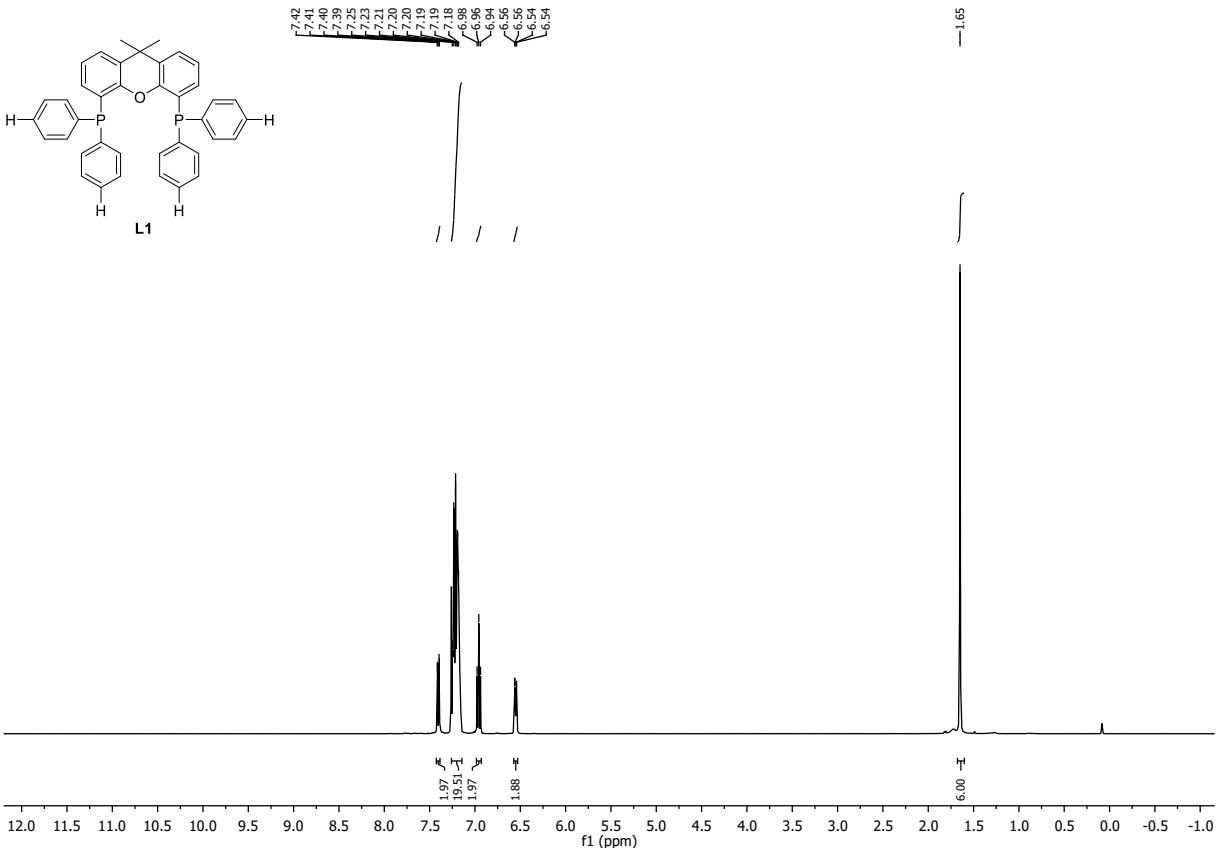
L1
7.42
7.41
7.40
7.39
7.25
7.23
7.21
7.20
7.20
7.19
7.19
7.18
6.98
6.96
6.94
6.56
6.56
6.54
6.54
1.65
1.97
19.51
1.97
1.88
6.00
f1 (ppm)

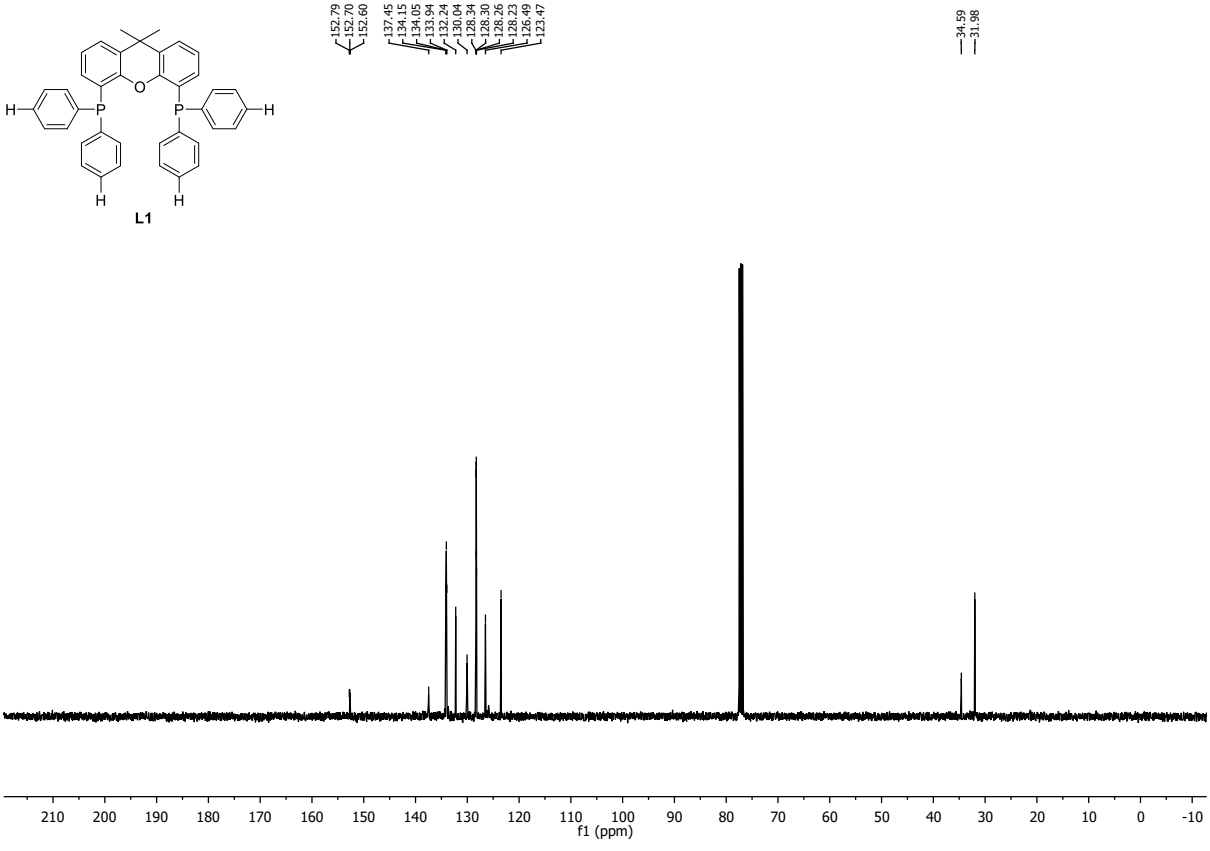
L1
152.79
152.70
152.60
137.45
134.15
134.05
133.94
133.24
130.04
128.34
128.30
128.26
128.23
126.49
123.47
34.59
31.98
f1 (ppm)

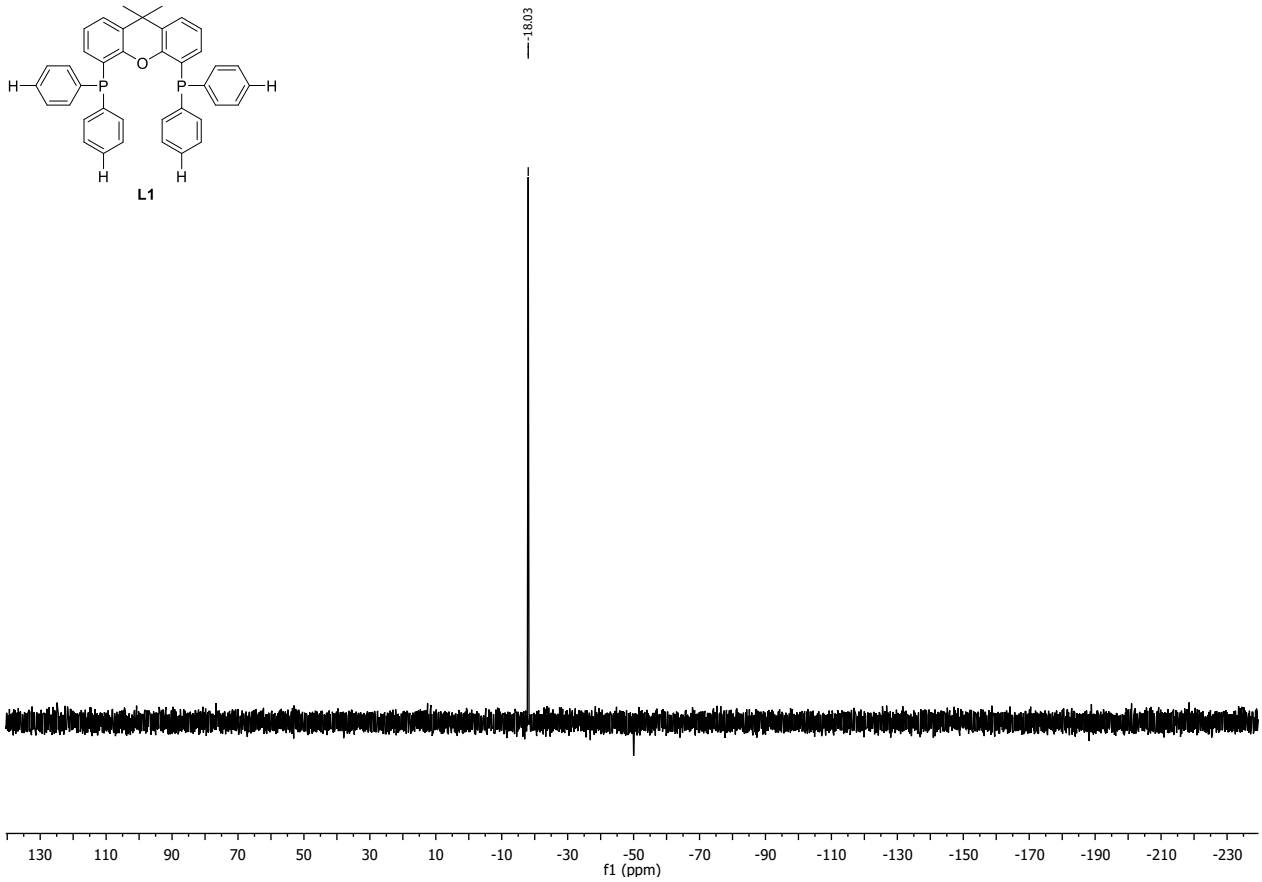
-18.03
H
P
O
P
H
H
H
L1
130
110
90
70
50
30
10
-10
-30
-50
-70
-90
-110
-130
-150
-170
-190
-210
-230
f1 (ppm)

9,9-dimethylxanthene-4,5-bis(di-p-tolylphosphine) (L2)

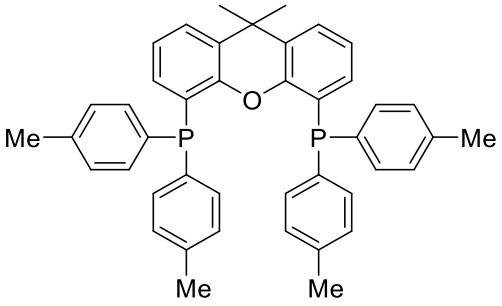

L2

$C_{43}H_{40}OP_2$ (634.74 g/mol)

Following GP-A, the ligand **L2** was synthesized using *n*-BuLi (1.6 M in Hexanes, 1.26 mL, 2.00 mmol, 2.5 equiv.), 9,9-dimethylxanthene (169 mg, 0.80 mmol, 1.0 equiv.), TMEDA (303 µL, 2.01 mmol, 2.5 equiv.) and chlorodi(*p*-tolyl)phosphane (431 µL, 2.01 mmol, 2.5 equiv.). Purification by crystallization from DCM/EtOH afforded **L2** as colorless crystals (255 mg, 0.40 mmol, 50%). Conforms to reported analytical data.[12]

1H-NMR (400 MHz, $CDCl_3$, δ): 7.37 (dd, *J* = 7.7, 1.5 Hz, 2H), 7.08 – 7.02 (m, 8H), 7.01 (s, 5H), 6.99 (s, 3H), 6.93 (t, *J* = 7.6 Hz, 2H), 6.55 (dq, *J* = 7.5, 1.6 Hz, 2H), 2.31 (s, 12H), 1.63 (s, 6H).

^{13}C-NMR (101 MHz, $CDCl_3$, δ): 137.9, 134.0 (t, *J* = 10.4 Hz), 132.1, 130.0, 129.0 (t, *J* = 3.5 Hz), 126.2, 123.3, 31.9, 21.5.

^{31}P-NMR (162 MHz, $CDCl_3$, δ): -19.67.

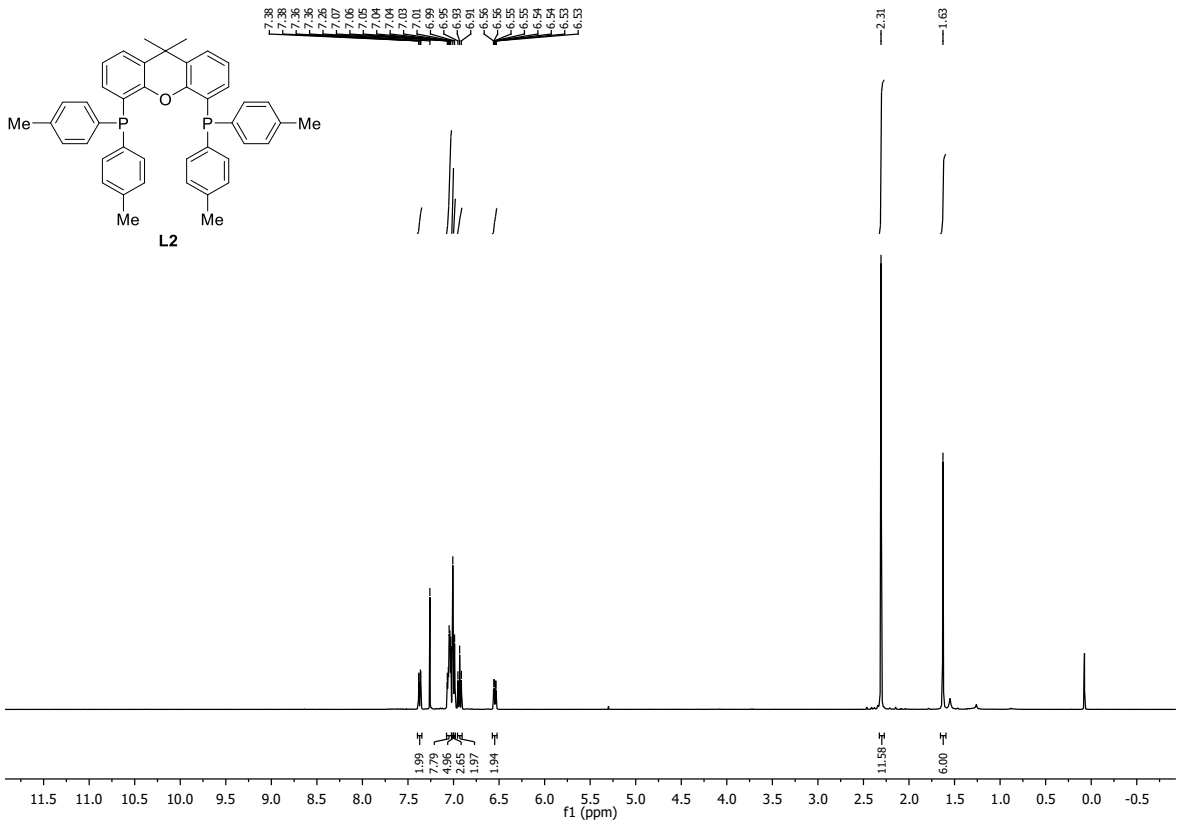
Me
P
O
P
Me
Me
Me
L2
7.38
7.38
7.36
7.36
7.26
7.07
7.06
7.05
7.04
7.04
7.03
7.01
6.99
6.95
6.93
6.91
6.56
6.56
6.55
6.55
6.54
6.54
6.53
6.53
2.31
1.63
1.99
7.79
4.96
2.65
1.97
1.94
11.58
6.00
f1 (ppm)

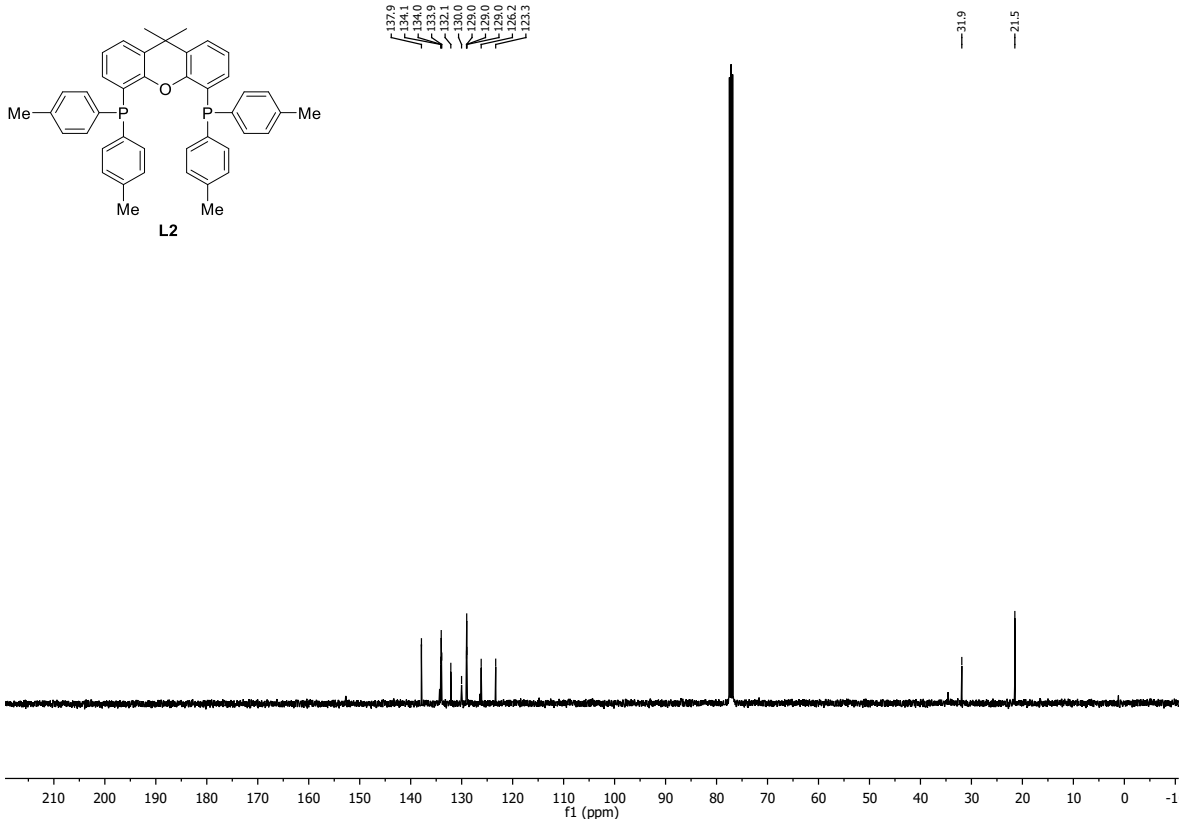
Me
P
O
P
Me
Me
Me
L2
137.9
134.1
134.0
133.9
132.1
130.0
129.0
129.0
129.0
126.2
123.3
31.9
21.5
f1 (ppm)

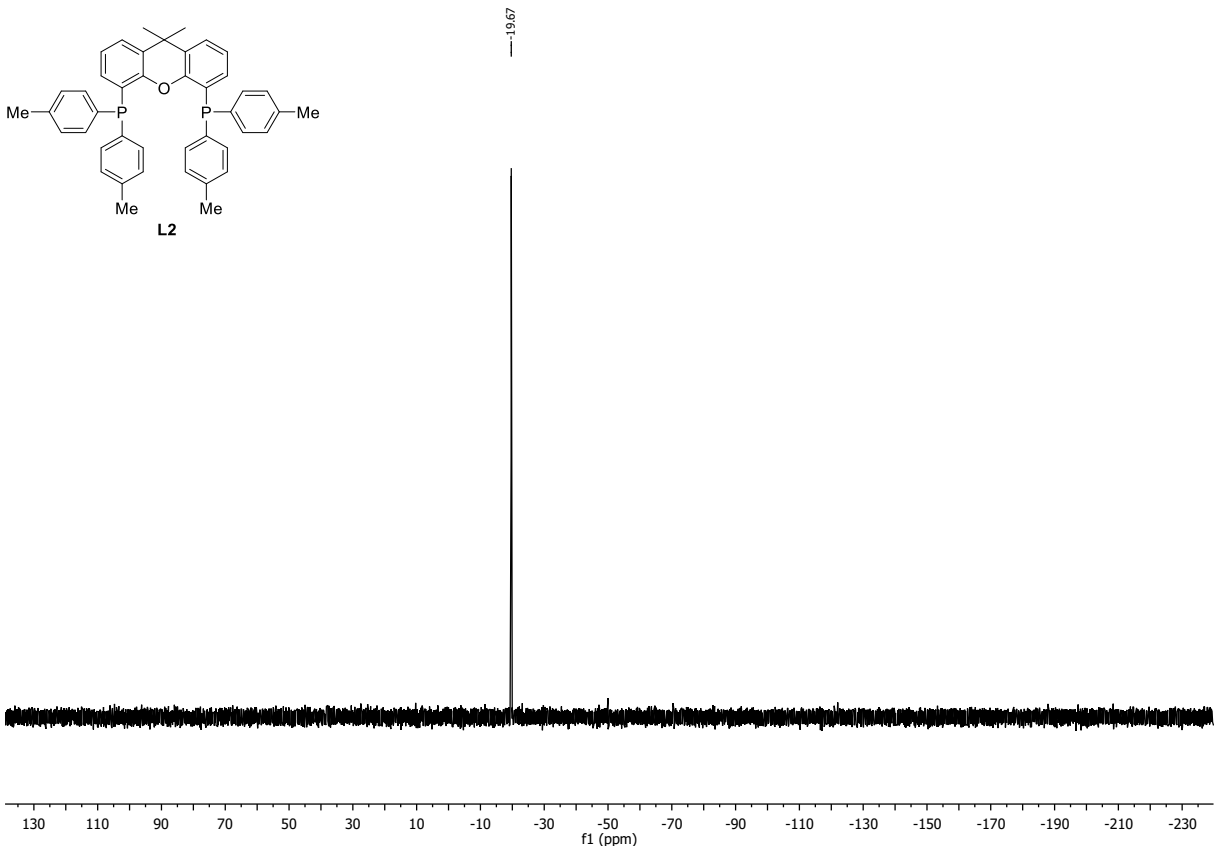
-19.67
Me
P
O
P
Me
Me
Me
L2
130
110
90
70
50
30
10
-10
-30
-50
-70
-90
-110
-130
-150
-170
-190
-210
-230
f1 (ppm)

9,9-dimethylxanthene-4,5-bis(di(4-methoxyphenyl)phosphine) (L3)

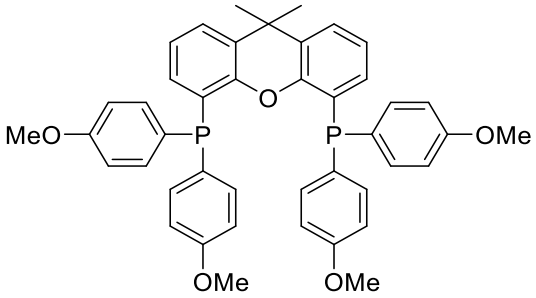

L3

$C_{43}H_{40}O_5P_2$ (698.74 g/mol)

Following GP-A, the ligand **L3** was synthesized using *n*-BuLi (1.6 M in Hexanes, 1.11 mL, 1.78 mmol, 2.5 equiv.), 9,9-dimethylxanthene (150 mg, 0.71 mmol, 1.0 equiv.), TMEDA (269 µL, 1.78 mmol, 2.5 equiv.) and chlorobis(4-methoxyphenyl)phosphane (500 mg, 1.78 mmol, 2.5 equiv.). Purification by crystallization from DCM/Hexane afforded **L3** as colorless crystals (327 mg, 0.47 mmol, 66%). Conforms to reported analytical data.[12]

^{1}H-NMR (400 MHz, $CDCl_3$, δ): 7.38 (dd, *J* = 7.8, 1.5 Hz, 2H), 7.10 – 7.03 (m, 8H), 6.94 (t, *J* = 7.6 Hz, 2H), 6.73 (d, *J* = 8.5 Hz, 8H), 6.54 – 6.49 (m, 2H), 3.77 (s, 12H), 1.63 (s, 6H).

^{13}C-NMR (101 MHz, $CDCl_3$, δ): 159.8, 135.3 (t, *J* = 10.9 Hz), 132.0, 130.0, 128.8 (t), 126.1, 123.4, 113.9 (t, *J* = 3.8 Hz), 55.1, 34.6, 31.9.

^{31}P-NMR (162 MHz, $CDCl_3$, δ): -20.43.

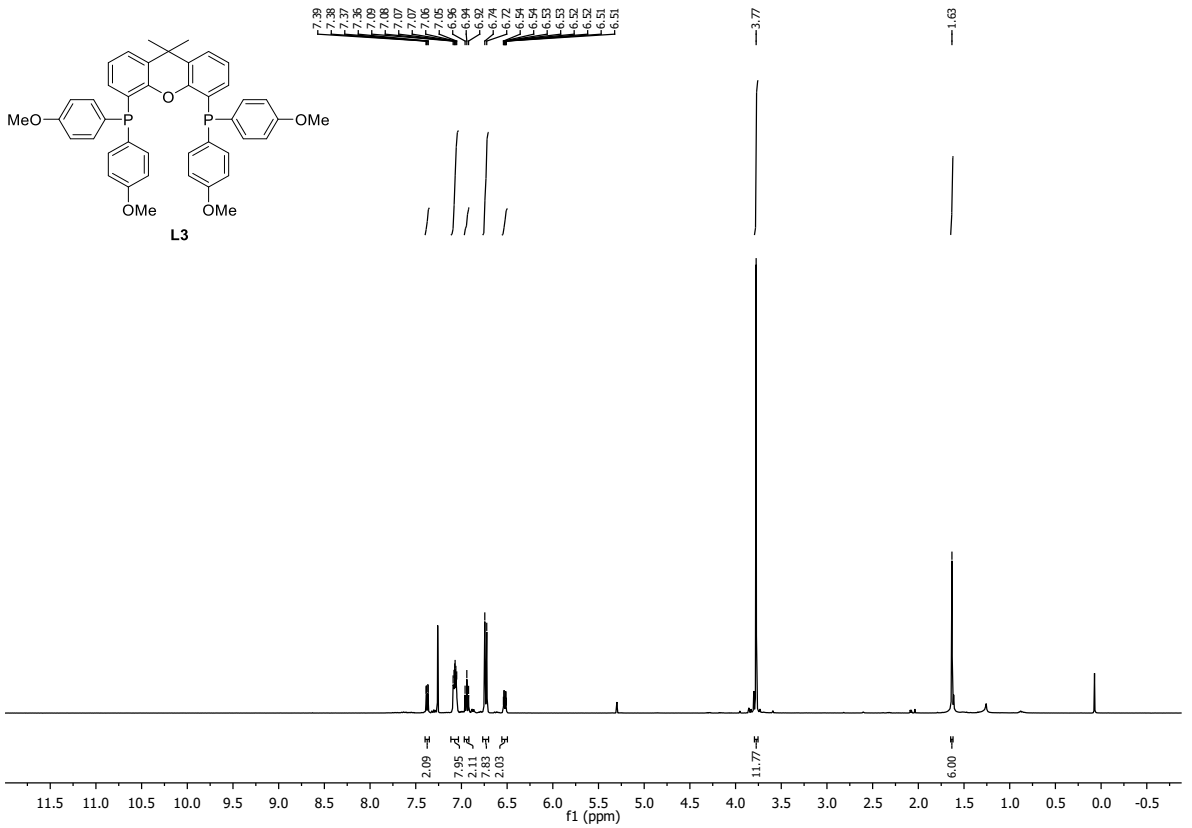
MeO
OMe
OMe
OMe
OMe
L3
7.39
7.38
7.37
7.36
7.09
7.08
7.07
7.07
7.06
7.05
6.96
6.94
6.92
6.74
6.72
6.54
6.54
6.53
6.52
6.52
6.51
6.51
3.77
1.63
2.09
7.95
2.11
7.83
2.03
11.77
6.00
f1 (ppm)

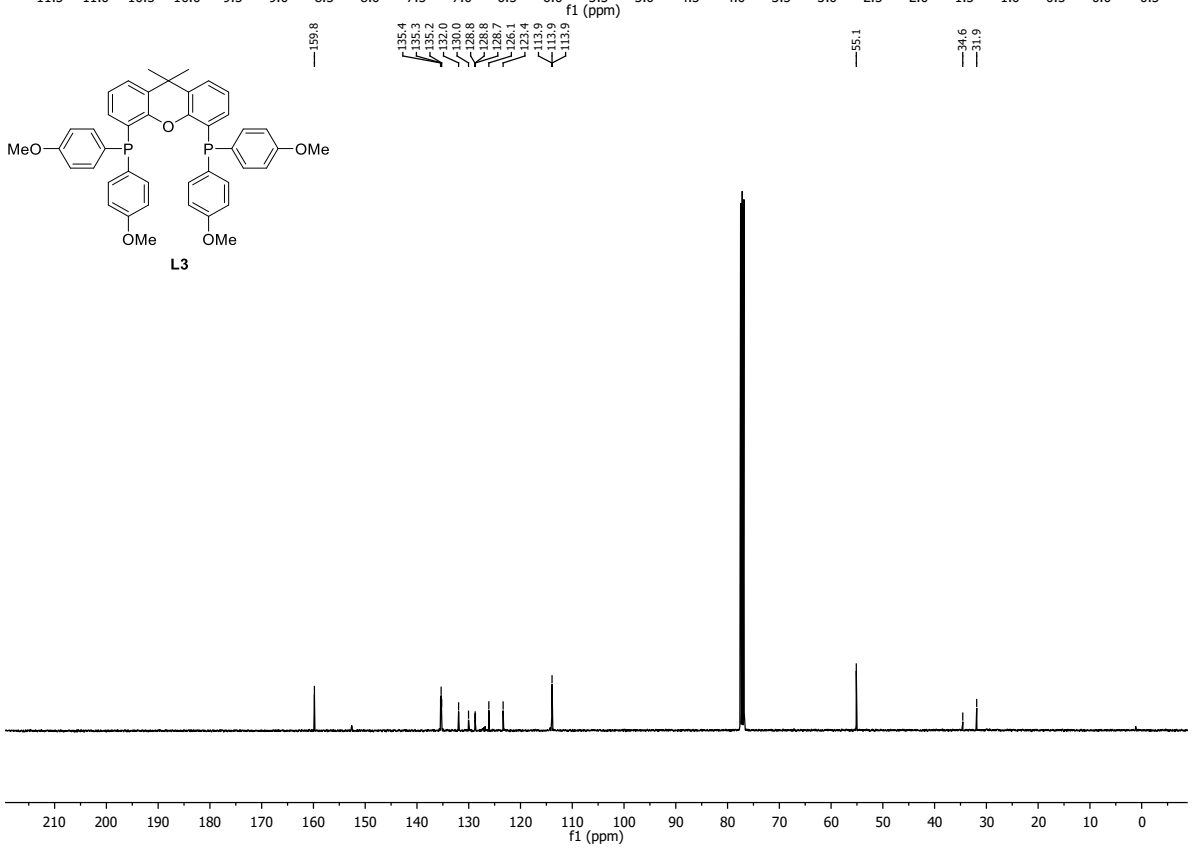
MeO
OMe
OMe
OMe
OMe
L3
159.8
135.4
135.3
135.2
132.0
130.0
128.8
128.8
128.7
126.1
123.4
113.9
113.9
113.9
55.1
34.6
31.9
f1 (ppm)

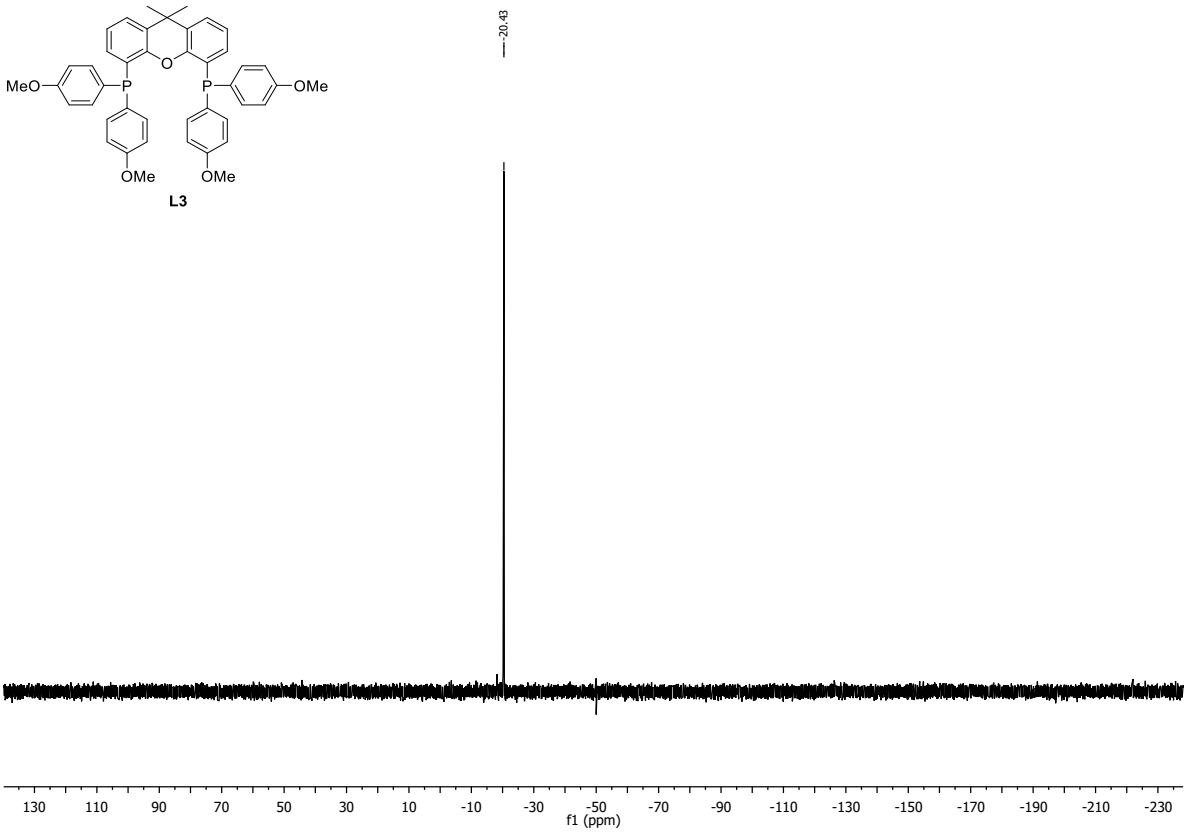
MeO
P
P
OMe
OMe
OMe
O
L3
-20.43
130
110
90
70
50
30
10
-10
-30
-50
-70
-90
-110
-130
-150
-170
-190
-210
-230
f1 (ppm)

9,9-dimethylxanthene-4,5bis(di(4(trifluoromethyl)phenyl)phosphine) (L4)

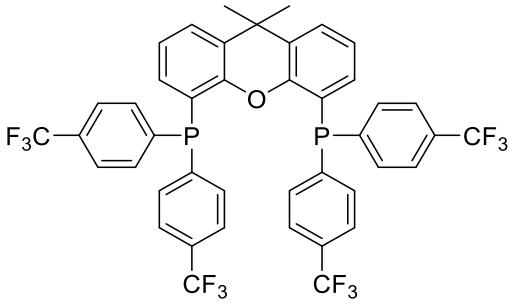

L4

$C_{43}H_{28}FOP_2$ (850.62 g/mol)

Following GP-A, the ligand **L4** was synthesized using *n*-BuLi (1.6 M in Hexanes, 876.25 µL, 1.4 mmol, 2.5 equiv.), 9,9-dimethylxanthene (117.92 mg, 0.6 mmol, 1.0 equiv.), TMEDA (211.59 µL, 1.4 mmol, 2.5 equiv.) and chlorobis[4-(trifluoromethyl)phenyl]phosphine (500 mg, 1.4 mmol, 2.5 equiv.). Purification by crystallization from EtOH at -4 °C afforded **L4** as colorless crystals (204 mg, 0.24 mmol, 43%). Conforms to reported analytical data.[12]

^{1}H-NMR (400 MHz, $CDCl_3$, δ): 7.53 – 7.46 (m, 10H), 7.31 – 7.20 (m, 6H), 7.03 (t, *J* = 7.7 Hz, 2H), 6.47 (dq, *J* = 7.6, 1.8 Hz, 2H), 1.68 (s, 6H).

^{13}C-NMR (101 MHz, $CDCl_3$, δ):[13] 152.0 (t, J = 9.5 Hz), 141.5 (t, J = 7.7 Hz), 134.1 (t, J = 10.5 Hz), 132.0, 130.8 (t, J = 30.7 Hz), 127.5 (s), 124.3 (s), 125.5 (q, J = 8.6 Hz), 124.3, 122.8, 120.1, 34.8, 31.9.

^{31}P-NMR (162 MHz, $CDCl_3$, δ): -17.57.

^{19}F-NMR (376 MHz, $CDCl_3$, δ): -62.80.

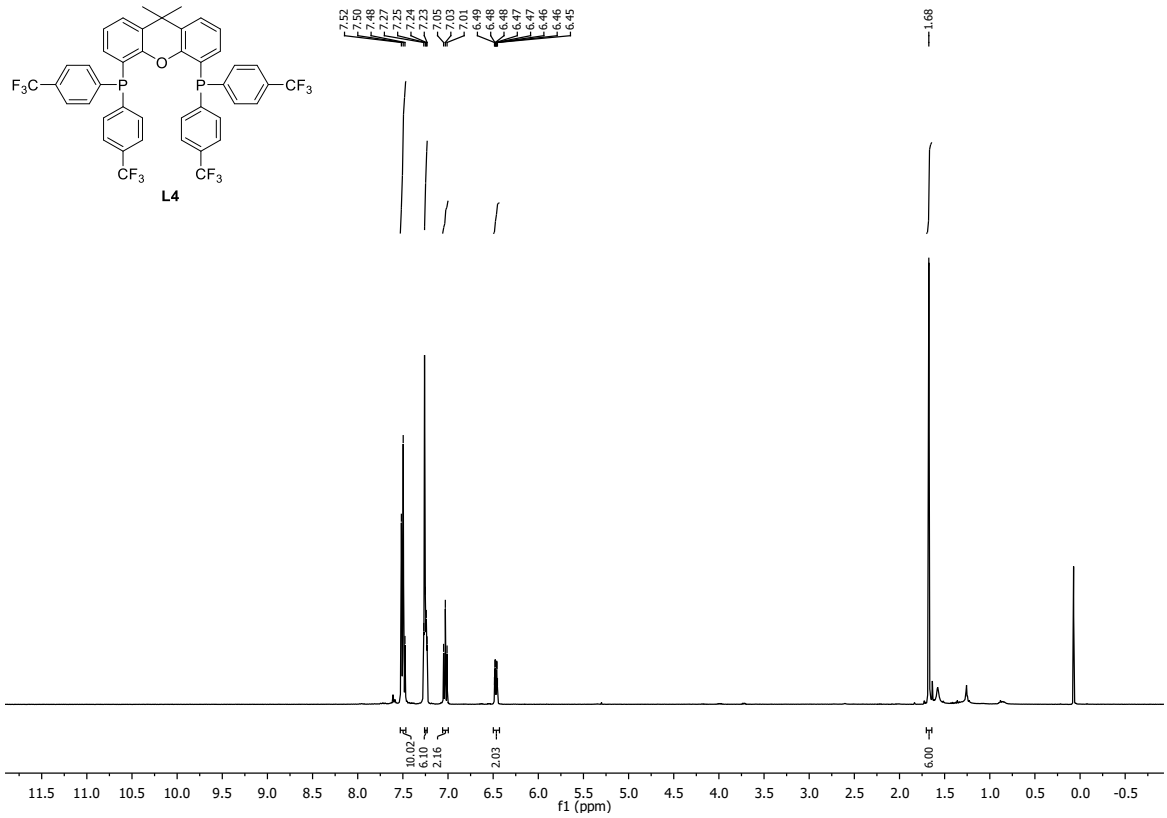
L4
7.52
7.50
7.48
7.27
7.25
7.24
7.23
7.05
7.03
7.01
6.49
6.48
6.48
6.47
6.47
6.46
6.46
6.45
1.68
10.02
6.10
2.16
2.03
6.00
f1 (ppm)

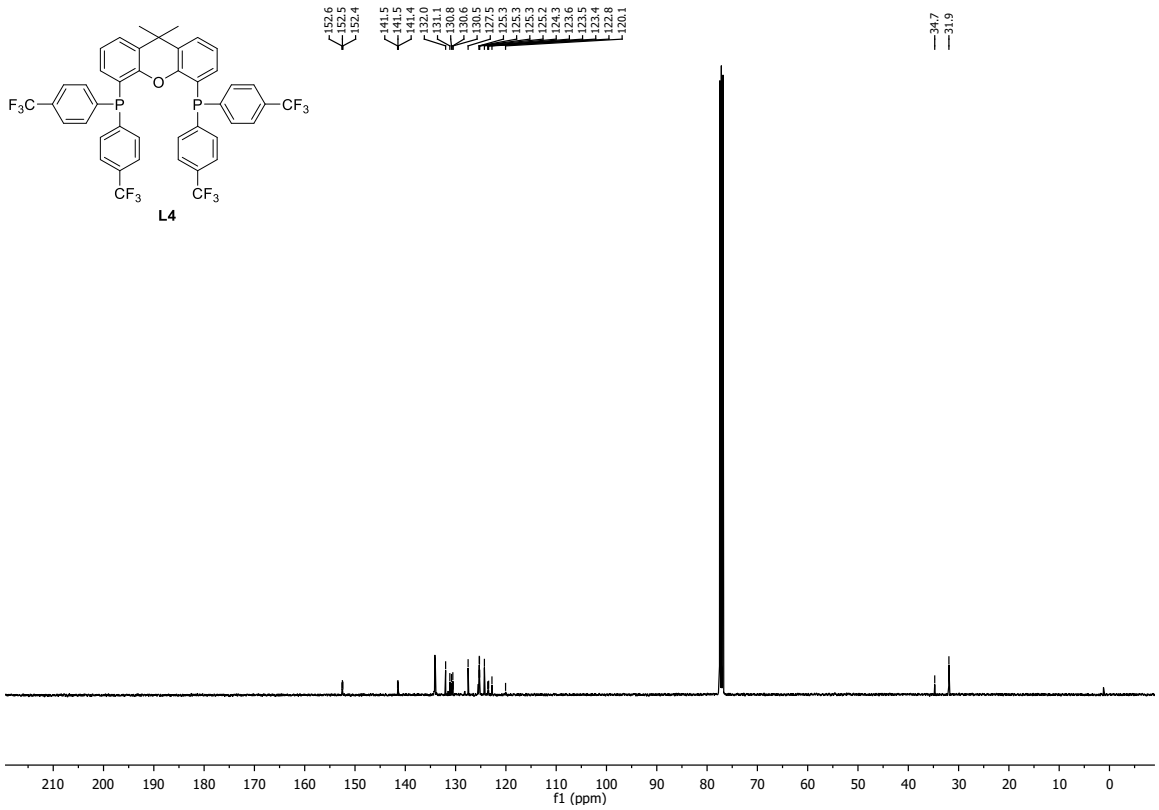
L4
152.6
152.5
152.4
141.5
141.5
141.4
132.0
131.1
130.8
130.6
130.5
127.5
125.3
125.3
125.3
125.2
124.3
123.6
123.5
123.4
122.8
120.1
34.7
31.9
f1 (ppm)

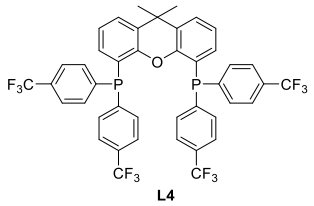

L4

-17.57
130
110
90
70
50
30
10
-10
-30
-50
-70
-90
-110
-130
-150
-170
-190
-210
-230
f1 (ppm)

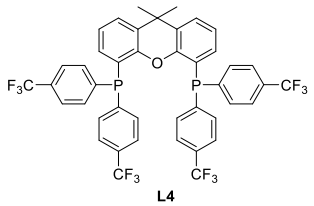

L4

-62.80
10
0
-10
-20
-30
-40
-50
-60
-70
-80
-90
-100
-110
-120
-130
-140
-150
-160
-170
-180
-190
-200
-210
f1 (ppm)

(Xantphos)Ni(*o*-tolyl)Cl (C1)

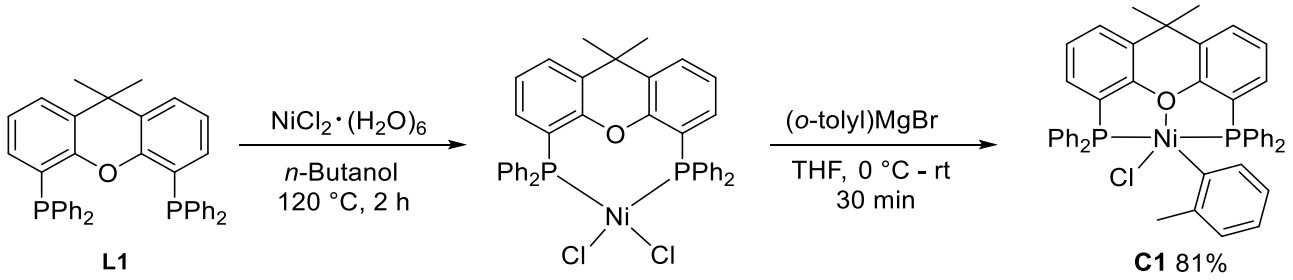

$C_{46}H_{39}ClNiOP_2$ (763.91 g/mol)

Step1: Synthesis of (Xantphos)$NiCl_2$

The catalyst was synthesized following a literature procedure.[14] $NiCl_2$ hydrate (513 mg, 2.16 mmol, 1.0 equiv.) was placed in an inert and flame-dried septum-capped 100 mL round bottom flask equipped with a stir bar. *N*-Butanol (20 mL) was added, the bright green solution was sparged with argon for 20 minutes and added to Xantphos (1.25 g, 2.16 mmol, 1.00 equiv.), which was placed in an oven and flame-dried three necked round bottom flask equipped with a stir bar and reflux condenser. The reaction mixture was heated to 120 °C for 2 h. The purple-grey suspension was cooled to room temperature and shortly before filtration to 0 °C. The product was filtered with an inert Schlenk frit and placed under high vacuum. The grey-purple solid, which was presumed to be (Xantphos)$NiCl_2$ (1.38 g, 1.94 mmol, 90%) was carried on to the next step without further analysis.

Step2: Synthesis of (Xantphos)Ni(*o*-tolyl)Cl

(Xantphos)$NiCl_2$ (1.38 g, 1.94 mmol, 1.0 equiv.) was placed in an inert and flame-dried septum-capped 100 mL round bottom flask equipped with a stir bar, suspended in dry THF (30 mL) and cooled to 0 °C. While stirring vigorously a freshly titrated *o*-tolylmagnesium chloride (1.15 M in THF/Toluene from Acros, 1.69 mL) was added dropwise. During the addition the color changed to dark red. Once the addition was completed the reaction mixture was stirred for 15 minutes at 0 °C and the solvent was removed by vacuum evaporation using a tepid water bath. The orange-red residue was suspended in MeOH (5 mL, HPLC grade, 15 min sparged with argon), cooled to 0 °C and filtered with an inert Schlenk frit. The orange filter cake was washed with cold Et_2O (2 x 15 mL, -20 °C) and dried in high vacuum to yield (Xantphos)Ni(*o*-tolyl)Cl (1.19 g, 1.94 mmol, 81%) as a fine orange powder. Conforms to reported analytical data.[14]

^{1}H-NMR (400 MHz, THF-D_8, δ): 8.32 – 8.24 (m, 4H), 7.64 (dd, *J* = 7.4, 1.5 Hz, 2H), 7.42 – 7.36 (m, 2H), 7.35 – 7.28 (m, 4H), 7.12 – 7.02 (m, 4H), 6.94 (t, *J* = 7.4 Hz, 2H), 6.72 (t, *J* = 7.7 Hz, 4H), 6.31 – 6.24 (m, 5H), 6.01 – 5.95 (m, 1H), 5.20 (d, *J* = 3.8 Hz, 2H), 3.40 (s, 3H), 1.94 (s, 3H), 1.63 (s, 3H).

^{31}P-NMR (162 MHz, THF-D_8, δ): 6.56 (s, major), 1,41 (s, minor).

^{31}P-NMR (162 MHz, Tol-D_8, δ): 7.18 (s, major), 1.83 (s, minor).

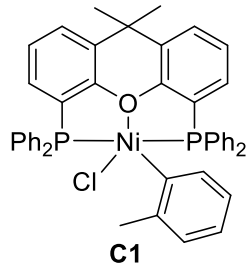
O
Ph2P
Ni
PPh2
Cl

C1

8.30
8.29
8.27
8.26
7.66
7.65
7.64
7.63
7.33
7.32
7.09
7.07
6.72
6.29
6.28
6.27
6.25
5.98
5.97
5.87
5.20
5.19
3.40
1.94
1.63
3.94
2.17
2.06
4.18
3.94
2.09
4.02
5.14
1.02
1.97
2.81
3.09
2.86
f1 (ppm)

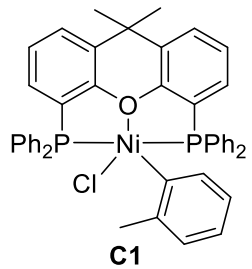
O
Ph2P
Ni
PPh2
Cl

C1

6.56
1.41
f1 (ppm)

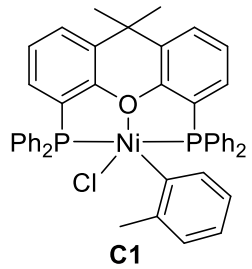
O
Ph2P
Ni
PPh2
Cl

C1

7.20
1.84
9 8 7 6 5 4 3 2 1 0 -1
f1 (ppm)
50 45 40 35 30 25 20 15 10 5 0 -5 -10 -15 -20 -25 -30 -35
f1 (ppm)

5.2. Substrates

4-chlorophenyl trifluoromethanesulfonate (1F)

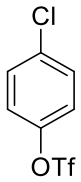

1F

$C_7H_4ClF_3O_3S$ (260.61 g/mol)

4-Chlorophenol (1.19 g, 10.0 mmol, 1.0 equiv.) was diluted in DCM (20 mL). Pyridine (1.6 mL, 20 mmol, 2 equiv.) was added and the stirred solution was cooled to 0 °C. Trifluoromethansulfonic anhydride (2.02 mL, 12.0 mmol, 1.2 equiv.) was added dropwise. The reaction mixture was allowed to warm to room temperature and stirred for 5 h. After dilution with DCM (20 mL), aqueous HCl (1M, 15 mL) was added and the mixture was washed with H_2O (15 mL), saturated aqueous solution of $NaHCO_3$ (15 mL) and brine (15 mL). The organic phase was dried over $MgSO_4$, concentrated under reduced pressure and the crude product was purified via column chromatography (Hex:EtOAc 100:0 to 95:5) to afford **1F** as colorless liquid (1.49 g, 5.72 mmol, 57%). Conforms to reported analytical data.[15]

R_f: 0.29 (Hexane)

^{1}H-NMR (400 MHz, $CDCl_3$, δ): 7.45-7.41 (m, 2H), 7.25-7.21 (m, 2H).

^{13}C-NMR (101 MHz, $CDCl_3$, δ): 148.0, 134.4, 130.5, 122.9, 118.8 (q, *J* = 320.8 Hz).

^{19}F-NMR (376 MHz, $CDCl_3$, δ): -72.7.

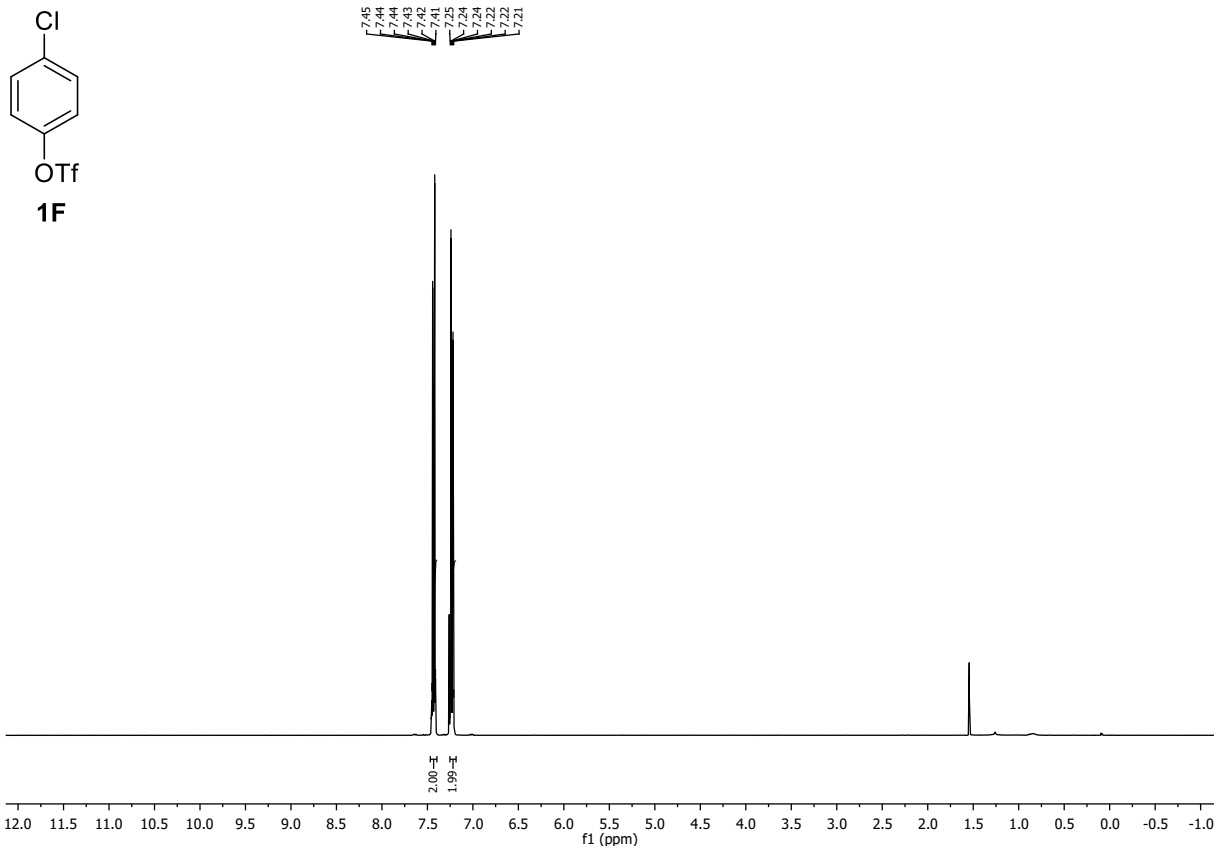
Cl
OTf
1F
7.45
7.44
7.44
7.43
7.42
7.41
7.25
7.24
7.24
7.22
7.22
7.21
2.00
1.99
12.0 11.5 11.0 10.5 10.0 9.5 9.0 8.5 8.0 7.5 7.0 6.5 6.0 5.5 5.0 4.5 4.0 3.5 3.0 2.5 2.0 1.5 1.0 0.5 0.0 -0.5 -1.0
f1 (ppm)

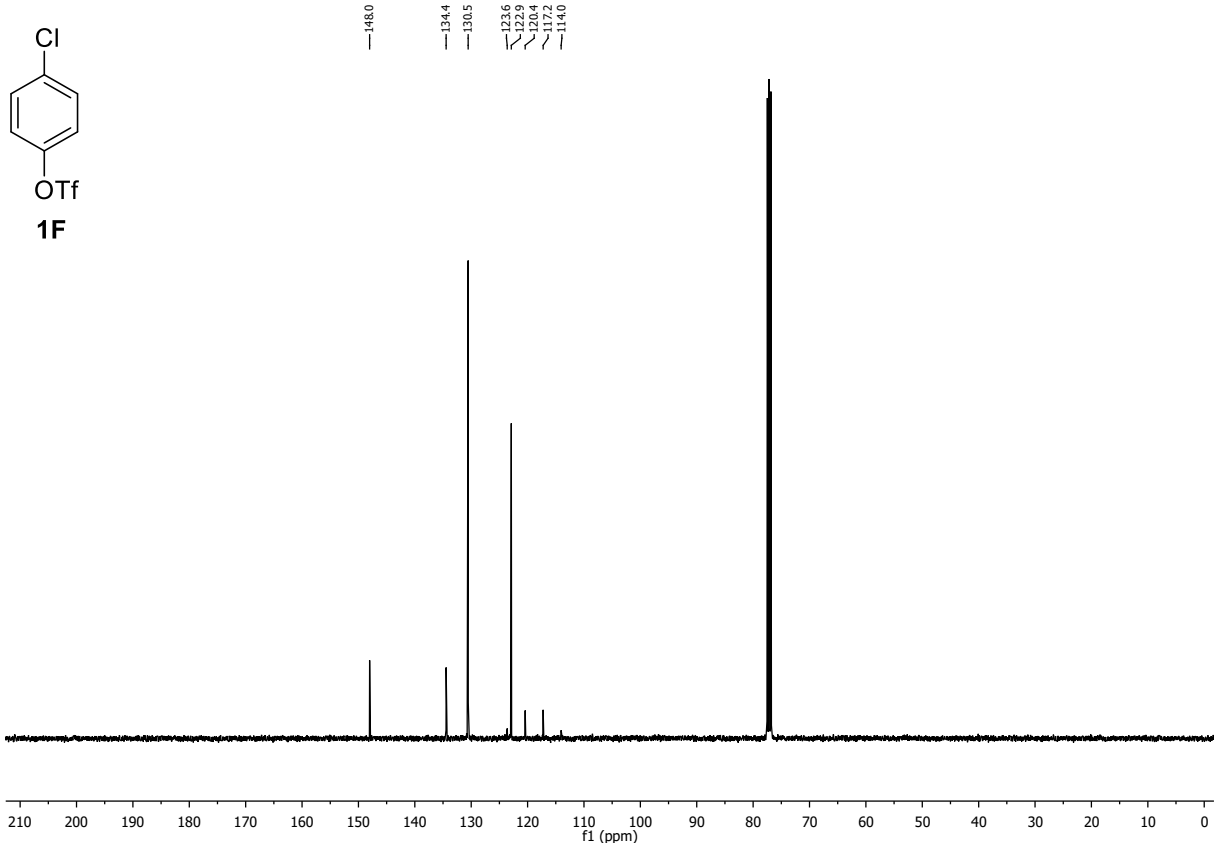
Cl
OTf
1F
148.0
134.4
130.5
123.6
122.9
120.4
117.2
114.0
210 200 190 180 170 160 150 140 130 120 110 100 90 80 70 60 50 40 30 20 10 0
f1 (ppm)

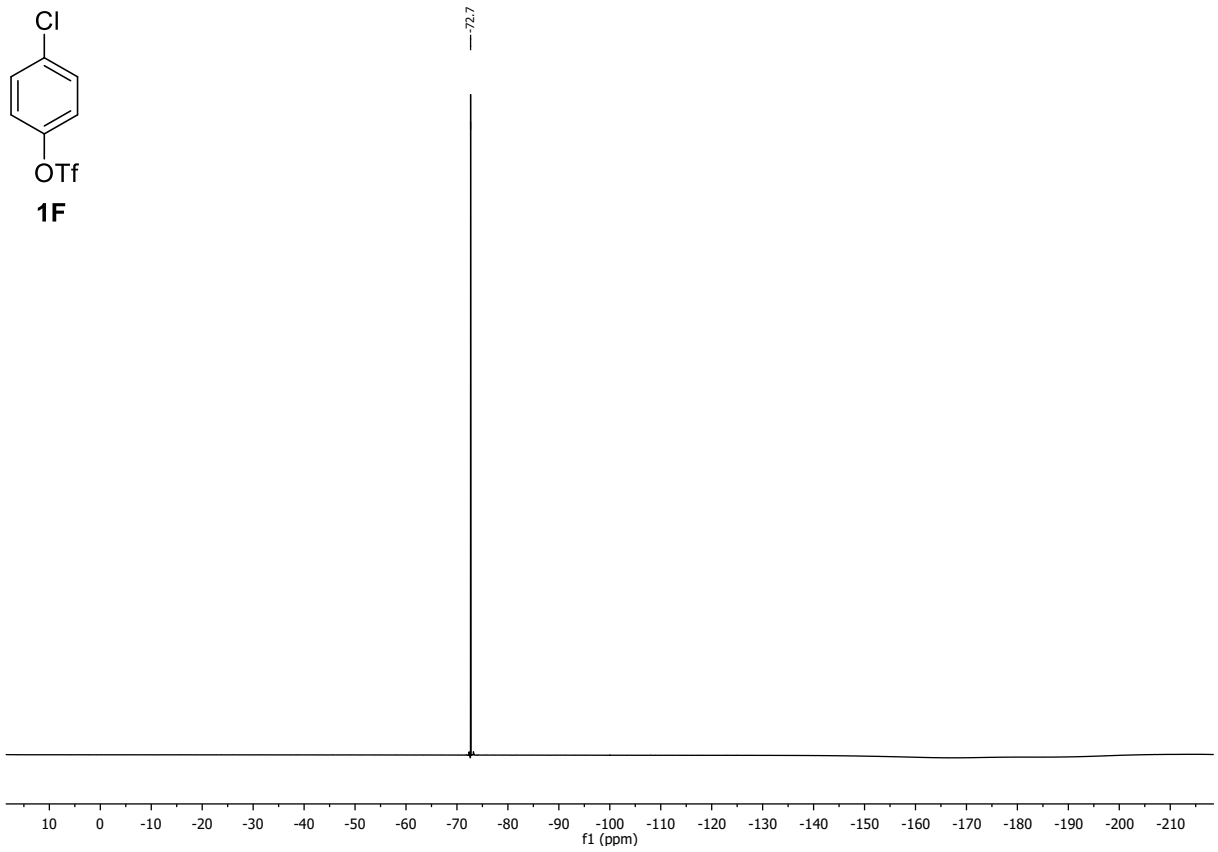
Cl
OTf
1F
-72.7
10
0
-10
-20
-30
-40
-50
-60
-70
-80
-90
-100
-110
-120
-130
-140
-150
-160
-170
-180
-190
-200
-210
f1 (ppm)

4-chlorophenyl-4-methybenzenesulfonate (1G)

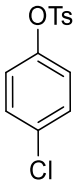

1G

$C_{13}H_{11}ClO_3S$ (282.74 g/mol)

To a solution of 4-chlorophenol (2.00 g, 15.6 mmol, 1.0 equiv.) in pyridine (20 mL), 4-toluenesulfonyl chloride (5.06 g, 26.5 mmol, 1.7 equiv.) was added portion wise and the mixture was stirred at 45 °C for 16 h. After cooling to room temperature, water (15 mL) was added and stirred at room temperature for 1 h. The reaction mixture was diluted with toluene (100 mL) and washed with water (10 mL), aqueous HCl (1M, 2 $\times$ 25 mL), saturated aqueous solution of $NaHCO_3$ (25 mL) and brine (25 mL). The combined organic phases were dried over $MgSO_4$, followed by solvent removal in vacuo providing a colorless solid. Recrystallization from EtOAc/Hexane afforded **1G** (3.31 mg, 11.7 mmol, 75 %) as colorless crystals. Conforms to reported analytical data.[16]

R_f: 0.29 (Hex:EtOAc 95:5)

^{1}H-NMR (400 MHz, $CDCl_3$, δ): 7.75-7.67 (m, 2H), 7.35-7.30 (m, 2H),7.29-7.23(m,2H), 6.96-6.90 (m, 2H), 2.47 (s, 3H).

^{13}C-NMR (101 MHz, $CDCl_3$, δ): 148.2, 145.8, 132.9, 132.1, 130.0, 129.9 128.7, 123.9, 21.9.

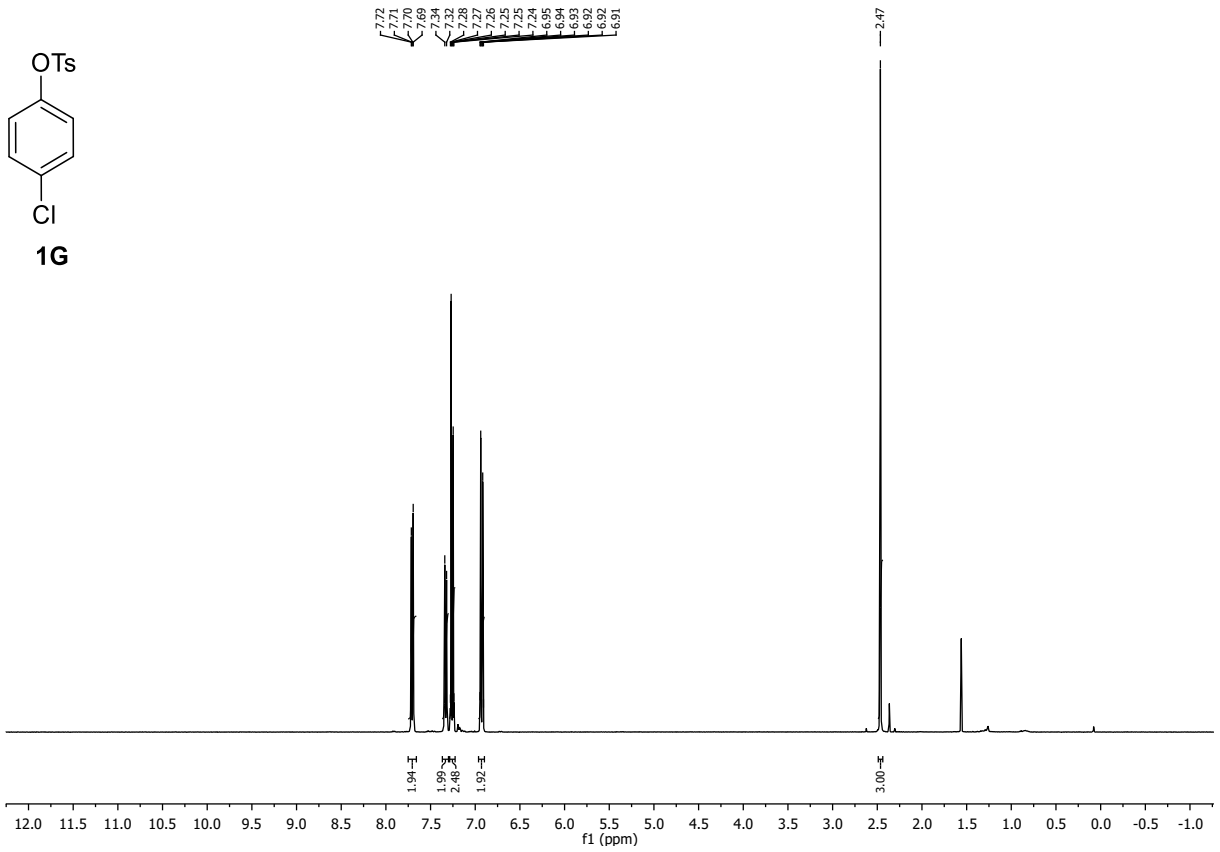
OTs
Cl
1G
7.72
7.71
7.70
7.69
7.34
7.32
7.28
7.27
7.26
7.25
7.25
7.24
6.95
6.94
6.93
6.92
6.92
6.91
2.47
1.94
1.99
2.48
1.92
3.00
12.0 11.5 11.0 10.5 10.0 9.5 9.0 8.5 8.0 7.5 7.0 6.5 6.0 5.5 5.0 4.5 4.0 3.5 3.0 2.5 2.0 1.5 1.0 0.5 0.0 -0.5 -1.0
f1 (ppm)

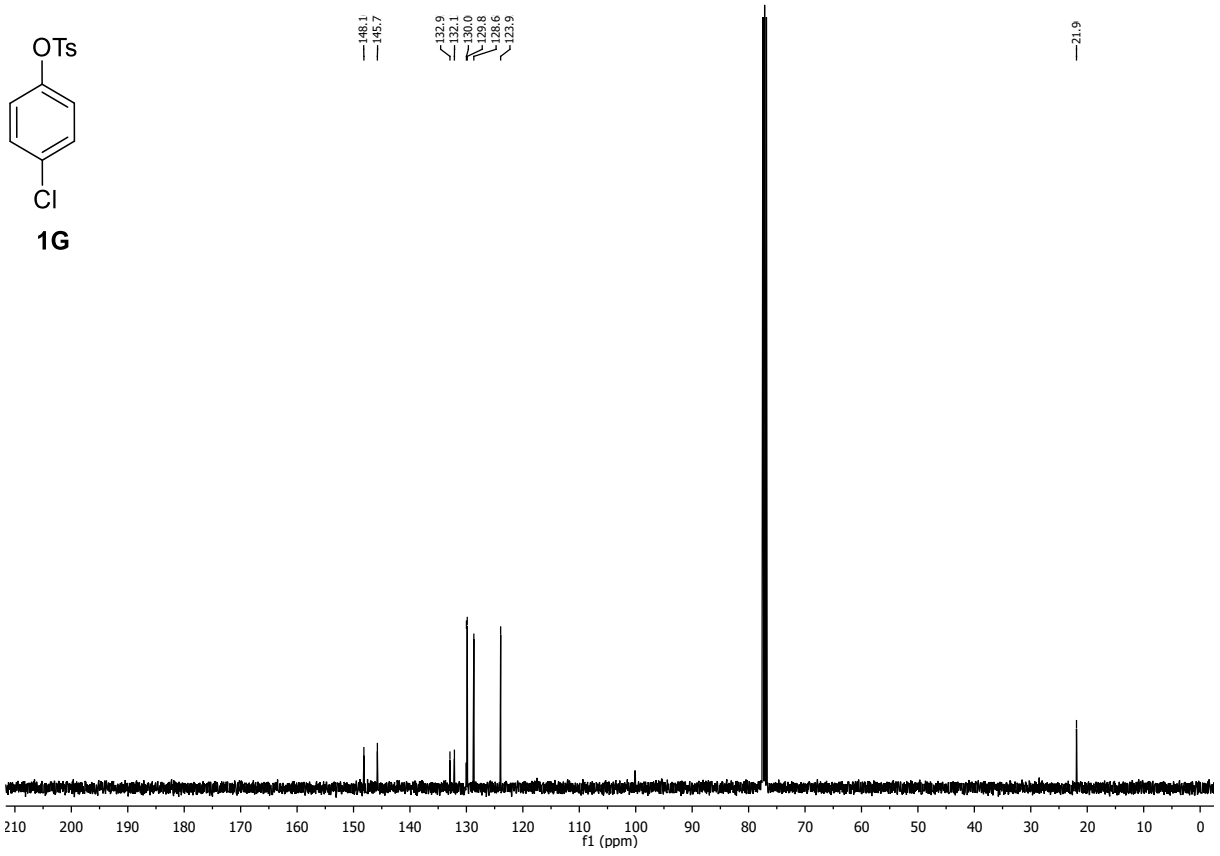
OTs
Cl
1G
148.1
145.7
132.9
132.1
130.0
129.8
128.6
123.9
21.9
210 200 190 180 170 160 150 140 130 120 110 100 90 80 70 60 50 40 30 20 10 0
f1 (ppm)

4-chlorophenyl-4-methylbenzenesulfonate (1H)

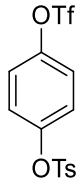

1H

$C_{14}H_{11}F_3O_6S_2$ (396.35 g/mol)

1H was synthesized following modified literature procedure.[16-18] Hydrochinone (1,1 g, 10 mmol, 1.0 equiv.) was dissolved in dry DCM (20 mL). Analytical grade pyridine (1.6 mL, 20 mmol, 2.0 equiv.) was added and the stirred solution was cooled to 0 °C. Trifluoromethanesulfonic anhydride (1.7 mL, 10 mmol, 1.0 equiv.) dissolved in dry DCM (10 mL) was added dropwise to the reaction mixture. After the addition was finished the reaction mixture was slowly warmed up to room temperature and stirred for 5 h. After dilution with DCM (15 mL) quenching with aqueous HCl (1M, 10 mL) the reaction mixture was washed with H_2O (10 mL), saturated aqueous solution of $NaHCO_3$ (10 mL) and brine (10 mL). The organic phase was dried over $MgSO_4$, concentrated under reduced pressure and the crude product was purified via column chromatography (Hex:EtOAc 9:1) to afford the 4-hydroxyphenyl trifluoromethanesulfonate as colorless liquid (928 mg, 3.83 mmol, 38%)

To a stirred solution of 4-hydroxyphenyl trifluoromethanesulfonate (928 mg, 3.83 mmol, 1.0 equiv.) in DCM (1.5 mL) and triethylamine (1.5 mL) a solution of 4-toluenesulfonyl chloride (731 mg, 3.83 mmol, 1.0 equiv.) in DCM (1 mL) was added and the reaction mixture was stirred at room temperature for 16 h. Water (5 mL) was added and the reaction mixture was extracted with DCM (3 x 5 mL). The combined organic phases were washed with brine (5 mL), dried over $MgSO_4$ and concentrated under reduced pressure. The purification by FC (SiO_2, gradient to 8:2 Hex:EtOAc over 20 CV) afforded the **1H** (1.15 g, 2.90 mmol, 76%) as colorless solid. Conforms to reported analytical data.[19]

R_f: 0.25 (Hex:EtOAc 9:1)

^{1}H-NMR (400 MHz, $CDCl_3$, δ): 7.70 (d, *J* = 8.3 Hz, 2H), 7.34 (d, *J* = 8.0 Hz, 2H), 7.24 – 7.19 (m, 2H), 7.11 – 7.06 (m, 2H), 2.46 (s, 3H).

^{13}C-NMR (101 MHz, $CDCl_3$, δ): 149.0, 147.7, 146.1, 131.9, 130.1, 128.7, 124.5, 122.8, 120.4, 117.2, 21.9.

^{19}F-NMR (376 MHz, $CDCl_3$, δ): -72.7.

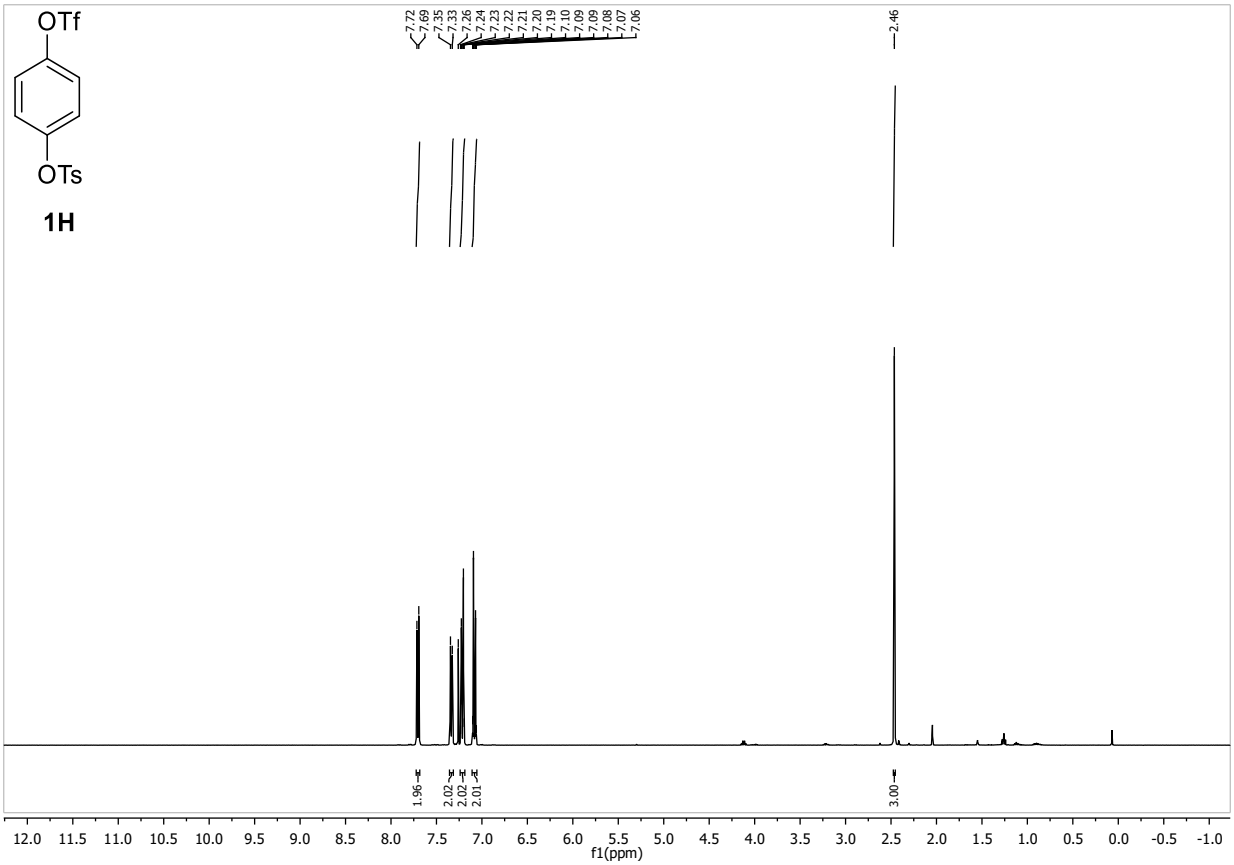
OTf
OTs
1H
7.72
7.69
7.35
7.33
7.26
7.24
7.23
7.22
7.21
7.20
7.19
7.10
7.09
7.09
7.08
7.07
7.06
2.46
1.96
2.02
2.02
2.01
3.00
f1(ppm)

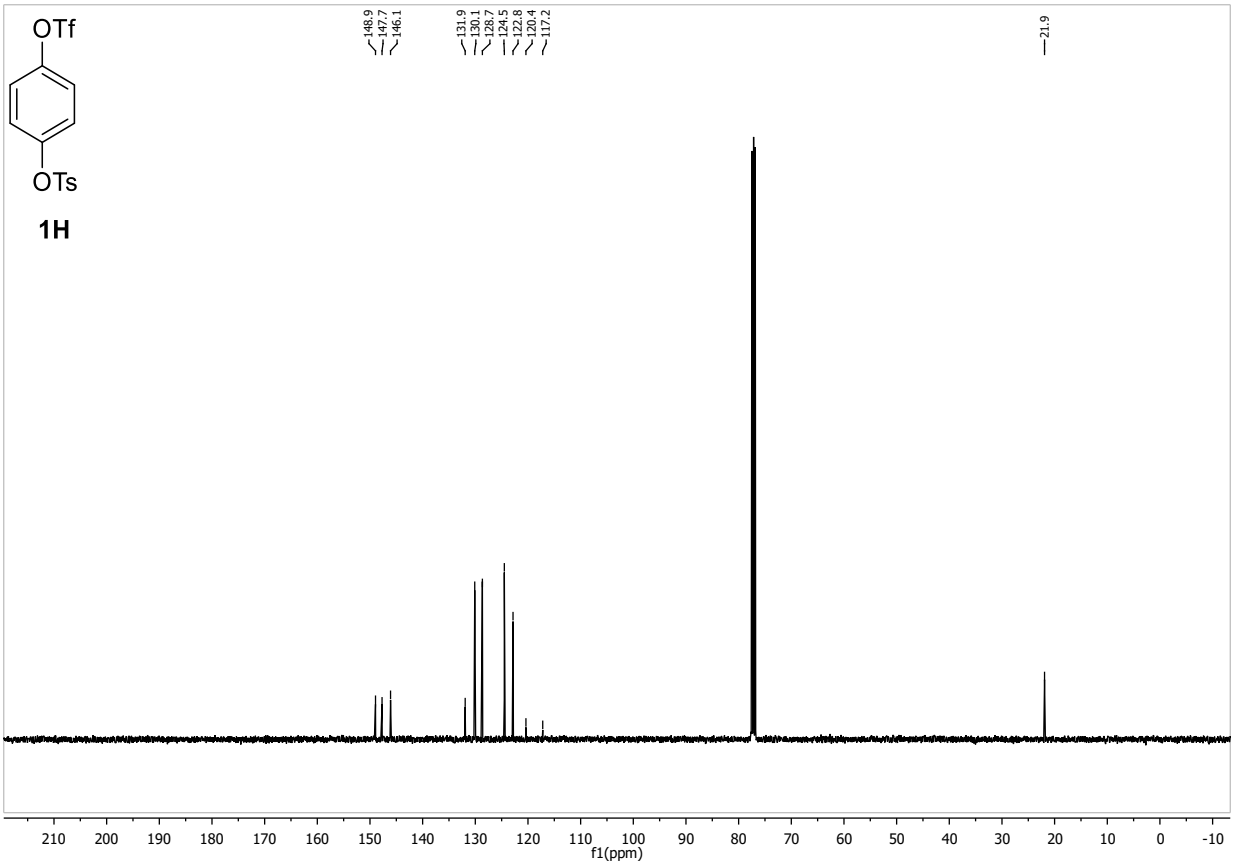
OTf
OTs
1H
148.9
147.7
146.1
131.9
130.1
128.7
124.5
122.8
120.4
117.2
21.9
f1(ppm)

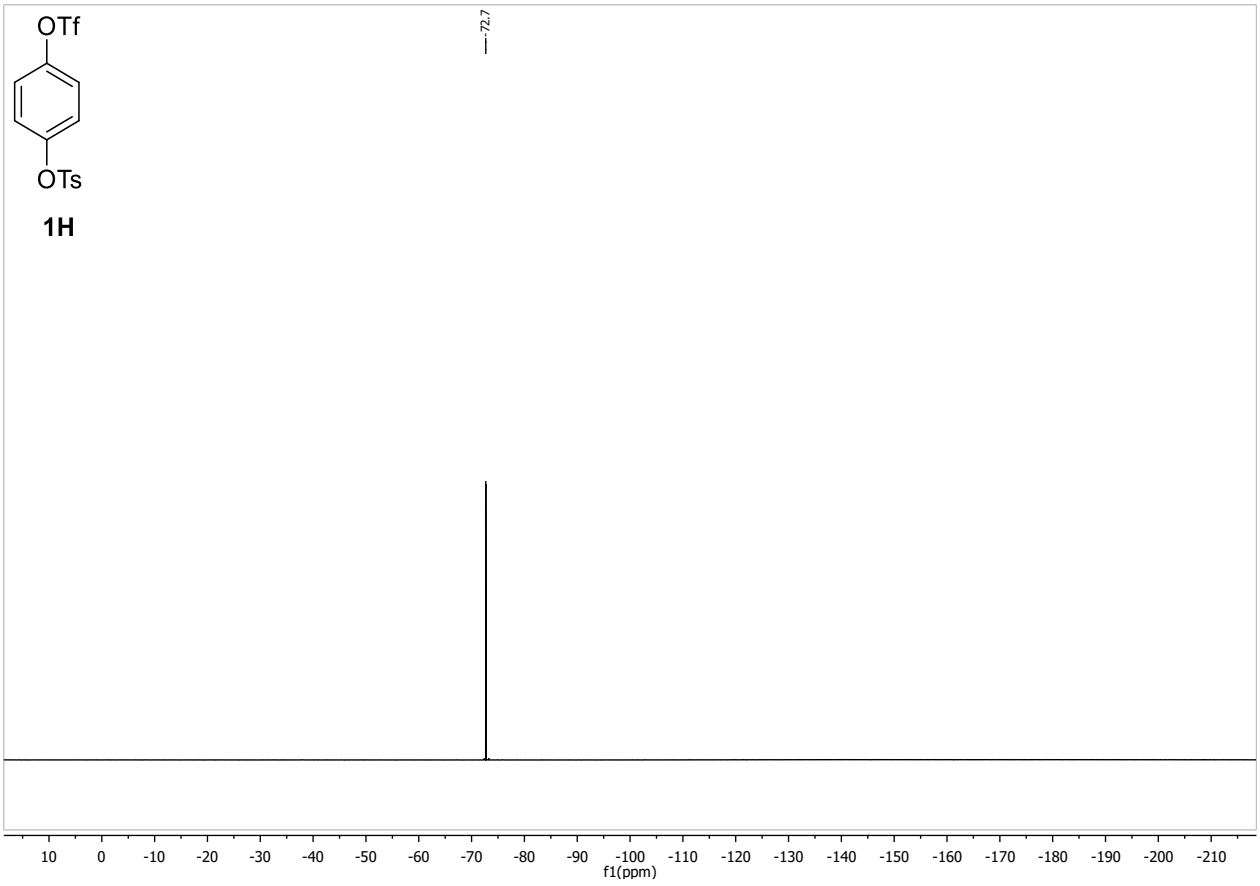
OTf
OTs
1H
-72.7
10
0
-10
-20
-30
-40
-50
-60
-70
-80
-90
-100
-110
-120
-130
-140
-150
-160
-170
-180
-190
-200
-210
f1(ppm)

5.3. Products

Ethyl 4-(((3s,5s,7s)-adamantan-1-yl)thio)benzoate (3ab)

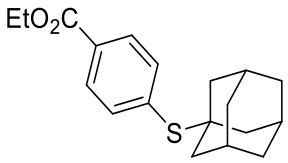

3ab

$C_{19}H_{24}O_2S$ (316.46 g/mol)

Following GP-B, **3ab** was synthesized using ethyl 4-chlorobenzoate (157 µL 1.00 mmol, 1.0 equiv.) and 1-adamantanethiol (185 mg, 1.10 mmol, 1.1 equiv.) Purification by FC (SiO_2, 5 CV Hex, gradient to 90:10 Hex:EtOAc over 15 CV) afforded **3ab** (290 mg, 915 µmol, 92%) as colorless solid. Conforms to reported analytical data.[1]

R_f: 0.64 (Hex:EtOAc 9:1)

m.p.: 68 – 70 °C

^{1}H-NMR (400 MHz, $CDCl_3$, δ): 7.97 (d, J = 8.3 Hz, 2H), 7.56 (d, J = 8.3 Hz, 2H), 4.38 (q, J = 7.1 Hz, 2H), 2.08 – 1.96 (m, 3H), 1.82 (d, J = 2.9 Hz, 6H), 1.62 (q, J = 12.1 Hz, 3H), 1.39 (t, J = 7.1 Hz, 3H).

^{13}C-NMR (101 MHz, $CDCl_3$, δ): 166.5, 137.3, 136.9, 131.0, 129.4, 61.3, 49.1, 43.9, 36.2, 30.2, 14.5.

HR-MS (ESI): m/z calc. for $[M+Na]^+$ 339.13892, found 339.13934.

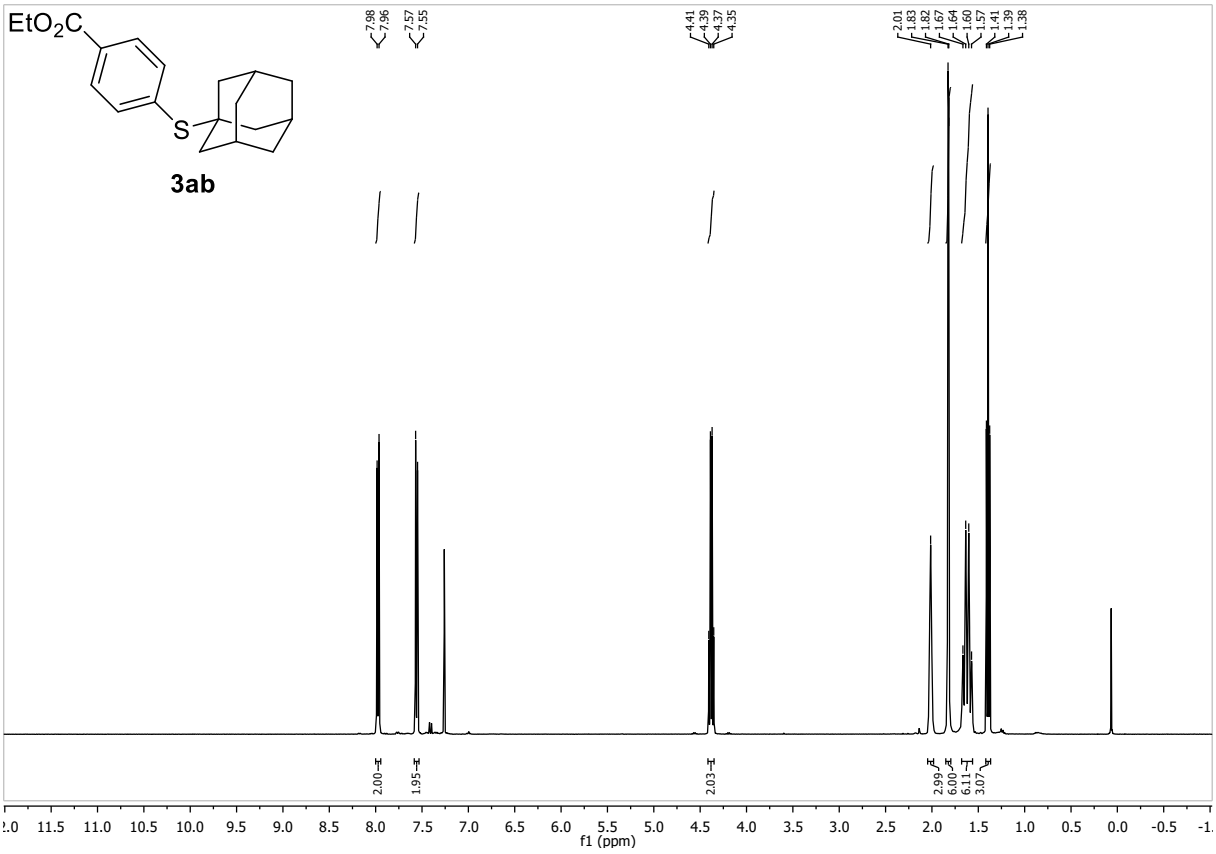
EtO2C
S
3ab
7.98
7.96
7.57
7.55
4.41
4.39
4.37
4.35
2.01
1.83
1.82
1.67
1.64
1.60
1.57
1.41
1.39
1.38
2.00
1.95
2.03
2.99
6.00
6.11
3.07
f1 (ppm)

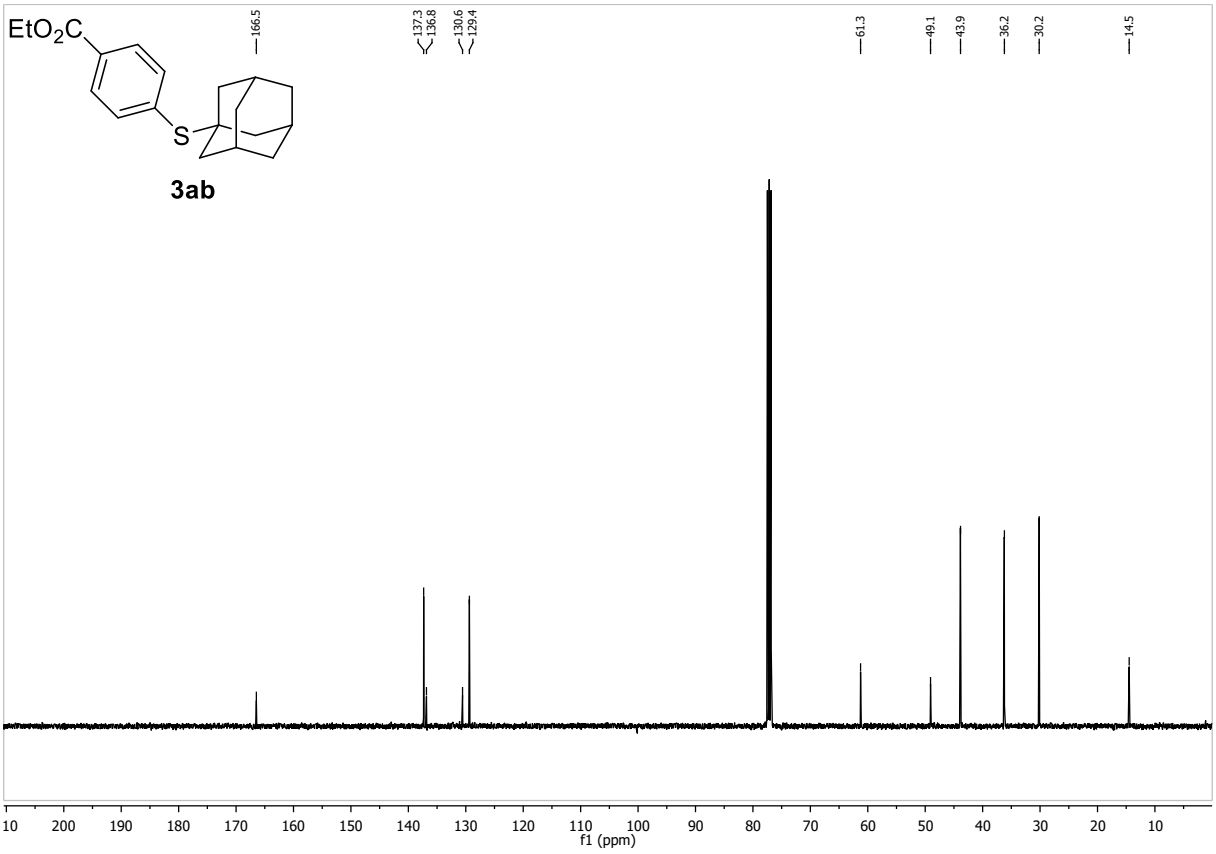
EtO2C
S
3ab
166.5
137.3
136.8
130.6
129.4
61.3
49.1
43.9
36.2
30.2
14.5
f1 (ppm)

((3s,5s,7s)-adamantan-1-yl)(phenyl)sulfane (3bb)

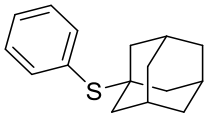

3bb

$C_{16}H_{20}S$ (244.40 g/mol)

Following GP-B, the **3bb** was synthesized using chlorobenzene (101 µL, 1.00 mmol, 1.0 equiv.) and 1-adamantanethiol (185 mg, 1.10 mmol, 1.1 equiv.). Purification by FC (SiO_2, gradient to 9:1 Hex:EtOAc over 20 CV) afforded **3bb** (189 mg, 811 µmol, 81%) as colorless solid. Conforms to reported analytical data.[20]

R_f: 0.78 (Hex:EtOAc 9:1)

m.p.: (Lit. 73.9 – 74.9)

^{1}H-NMR (400 MHz, $CDCl_3$, δ): 7.53 – 7.48 (m, 2H), 7.38 – 7.29 (m, 3H), 2.01 (s, 3H), 1.81 (d, *J* = 2.6 Hz, 6H), 1.62 (q, *J* = 12.3 Hz, 6H).

^{13}C-NMR (101 MHz, $CDCl_3$, δ): 137.83, 130.64, 128.70, 128.42, 47.98, 43.74, 36.30, 30.11.

HR-MS (EI): m/z calc. for $[M]^+$ 244.128022, found 244.12727.

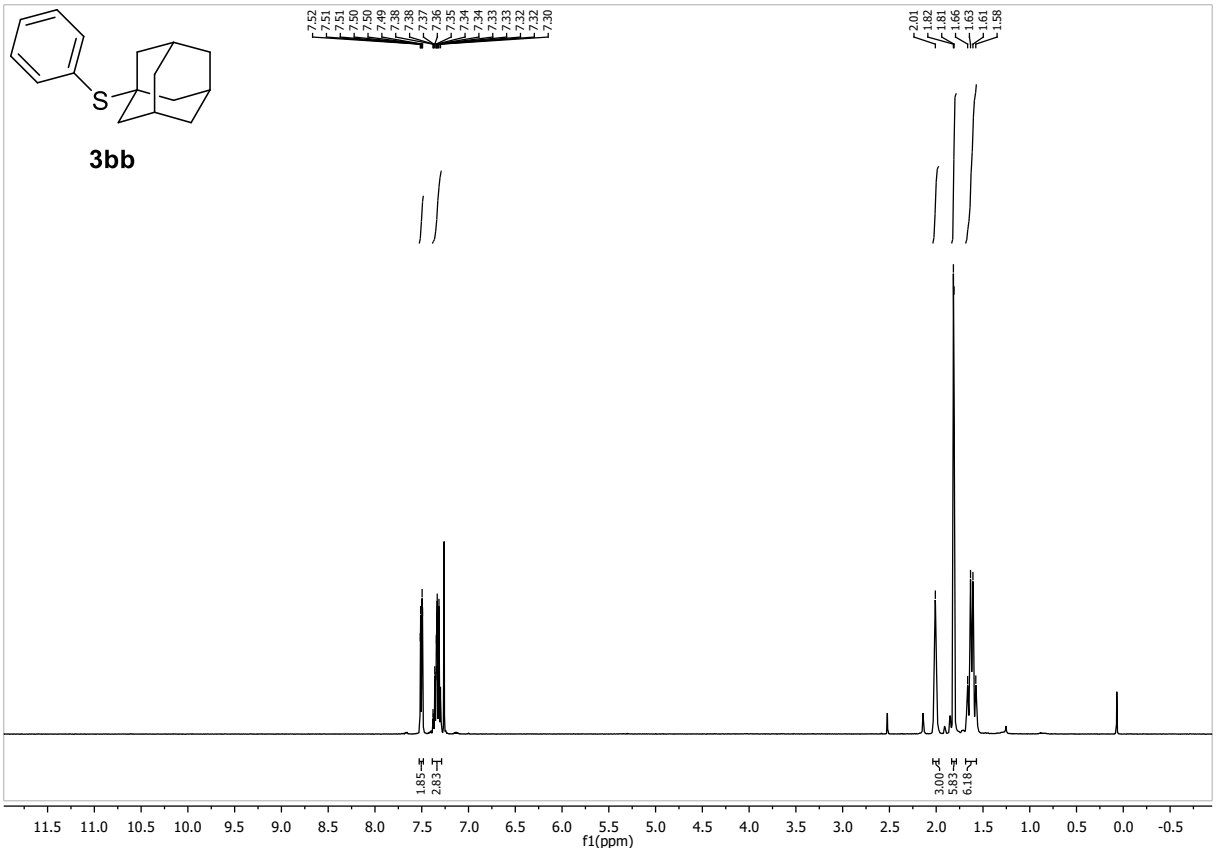
S
3bb
7.52
7.51
7.51
7.50
7.50
7.49
7.38
7.38
7.37
7.36
7.35
7.34
7.34
7.33
7.33
7.32
7.32
7.30
2.01
1.82
1.81
1.66
1.63
1.61
1.58
1.85
2.83
3.00
5.83
6.18
f1(ppm)

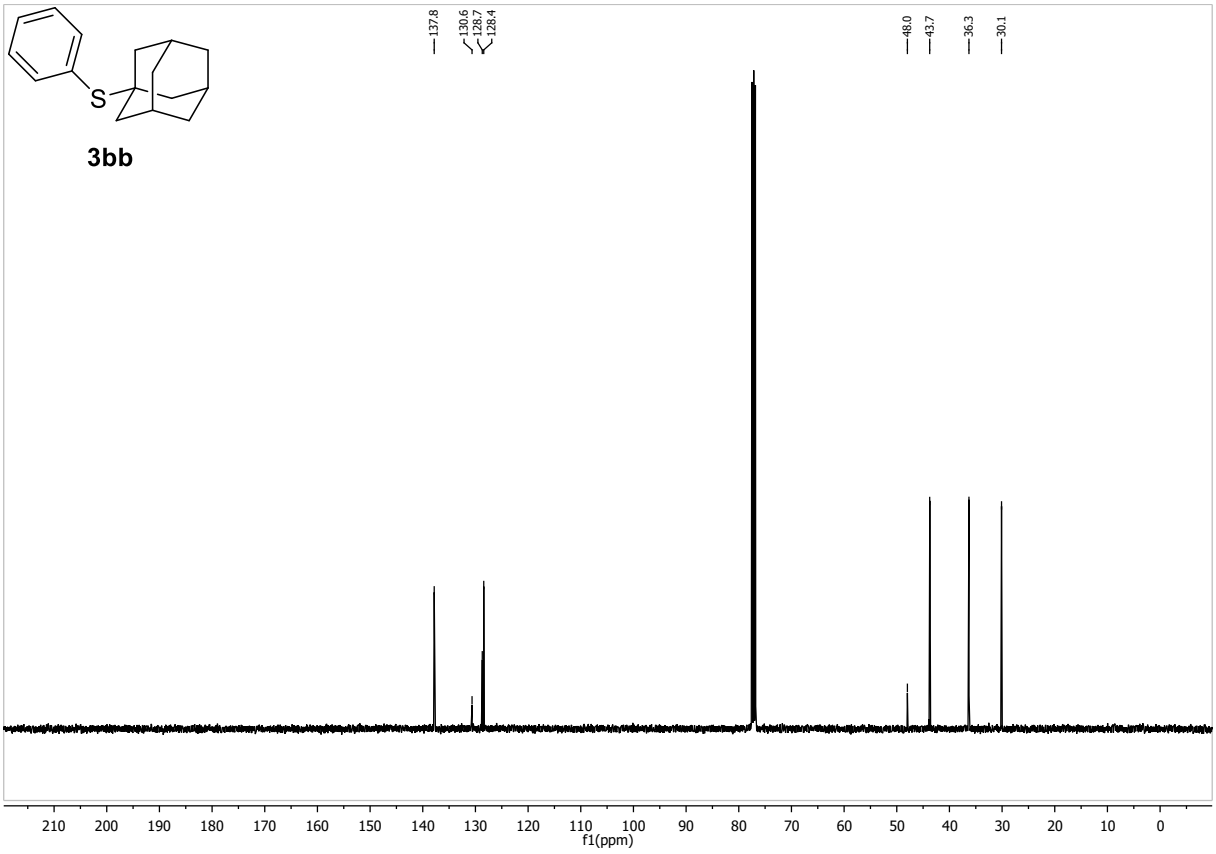
S
3bb
137.8
130.6
128.7
128.4
48.0
43.7
36.3
30.1
f1(ppm)

((3s,5s,7s)-adamantan-1-yl)(p-tolyl)sulfane (3cb)

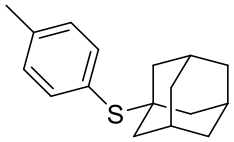

3cb

$C_{17}H_{22}S$ (258.42 g/mol)

Following GP-B, the **3cb** was synthesized using 4-chlorotoluene (119 µL 1.00 mmol, 1.0 equiv.) and 1-adamantanethiol (185 mg, 1.10 mmol, 1.1 equiv.) Purification by FC (SiO_2, gradient to 9:1 Hex:EtOAc over 20 CV) afforded **3cb** (221 mg, 855 µmol, 86%) as colorless solid. Conforms to reported analytical data.[21]

R_f: 0.80 (Hex:EtOAc 9:1)

^{1}H-NMR (400 MHz, $CDCl_3$, δ): 7.38 (d, *J* = 8.0 Hz, 2H), 7.12 (d, *J* = 8.0 Hz, 2H), 2.36 (s, 3H), 2.00 (s, 3H), 1.80 (d, *J* = 2.9 Hz, 6H), 1.69 – 1.54 (m, 6H).

^{13}C-NMR (101 MHz, $CDCl_3$, δ): 138.7, 137.7, 129.3, 127.1, 47.7, 43.7, 36.3, 30.1, 21.4.

HR-MS (EI): m/z calc. for $[M]^+$ 258.143672, found 258.14282.

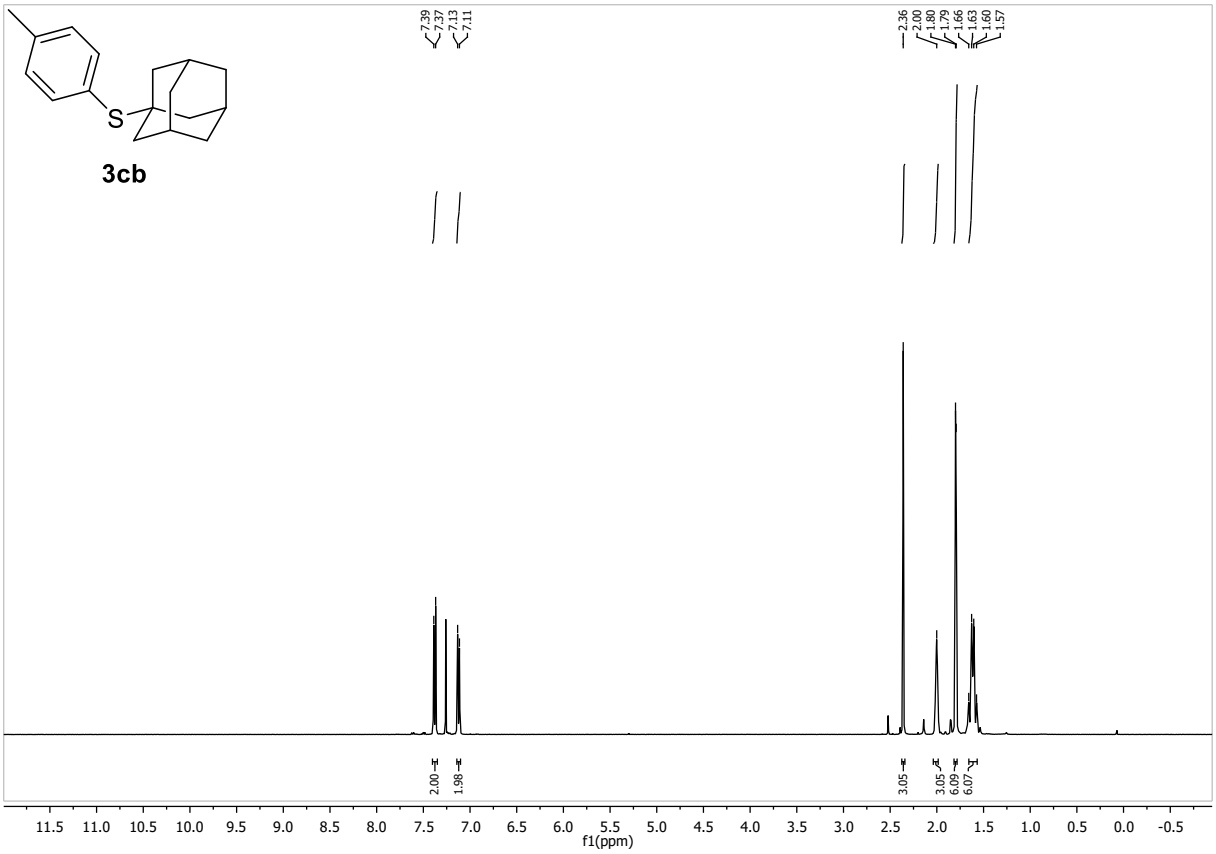
3cb
7.39
7.37
7.13
7.11
2.36
2.00
1.80
1.79
1.66
1.63
1.60
1.57
2.00
1.98
3.05
3.05
6.09
6.07
f1(ppm)

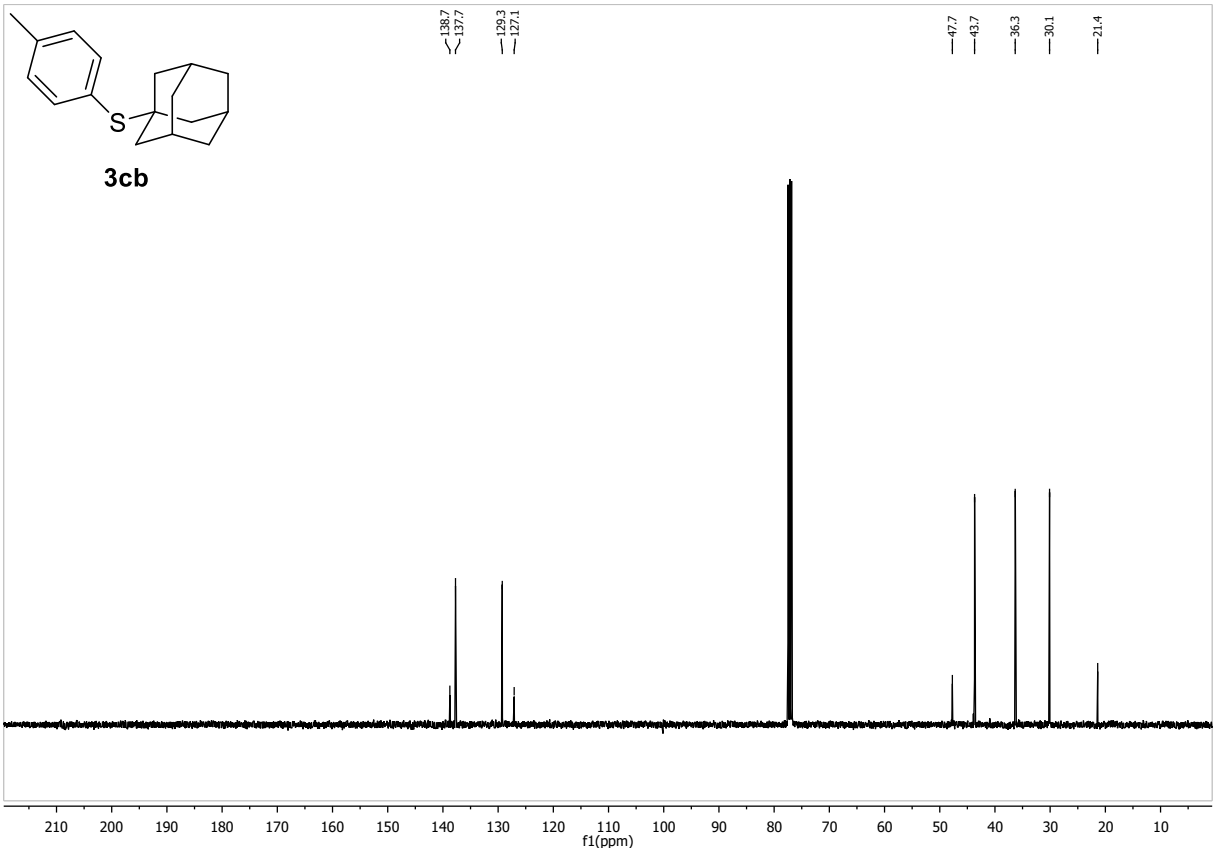
3cb
138.7
137.7
129.3
127.1
47.7
43.7
36.3
30.1
21.4
f1(ppm)

(3s,5s,7s)-1-tosyladamantane (4cb)

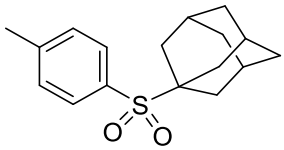

4cb

$C_{17}H_{22O2}S$ (290.42 g/mol)

Following GP-B, the **4cb** was synthesized using 4-chlorotoluene (119 µL 1.00 mmol, 1.0 equiv.) and 1-adamantanethiol (185 mg, 1.10 mmol, 1.1 equiv.). The crude product and 3-chlorobenzoperoxoic acid (690 mg, 4.00 mmol, 4.0 equiv.) were solved in DCM and stirred at rt for 12 h. Purification by FC (SiO_2, gradient to 8:2 Hex:EA over 15 CV) afforded **4cb** (241 mg, 831 µmol, 83%) as white solid.

R_f: 0.13 (Hex:EA 9:1)

m.p.: 118.5 – 120.1 °C

^{1}H-NMR (400 MHz, $CDCl_3$, δ): 7.70 (d, *J* = 8.2 Hz, 2H), 7.33 (d, *J* = 8.0 Hz, 2H), 2.45 (s, 3H), 2.10 (s, 3H), 1.92 (d, *J* = 2.7 Hz, 6H), 1.72 – 1.55 (m, 6H).

^{13}C-NMR (101 MHz, $CDCl_3$, δ): 144.5, 131.7, 130.6, 129.4, 60.8, 35.9, 35.0, 28.3, 21.8.

HR-MS (ESI): m/z calc. for [M + Na^+] 313.12327, found 313.12326.

IR (ATR, $\tilde{\nu}$, [cm^{-1}]): 2909 (m), 2850 (w), 1593 (w), 1483 (w), 1448 (w), 1400 (w), 1347 (w), 1284 (s), 1180 (w), 1138 (s), 1100 (m), 1038 (m), 971 (w), 934 (w), 833 (w), 807 (m), 770 (w), 707 (m).

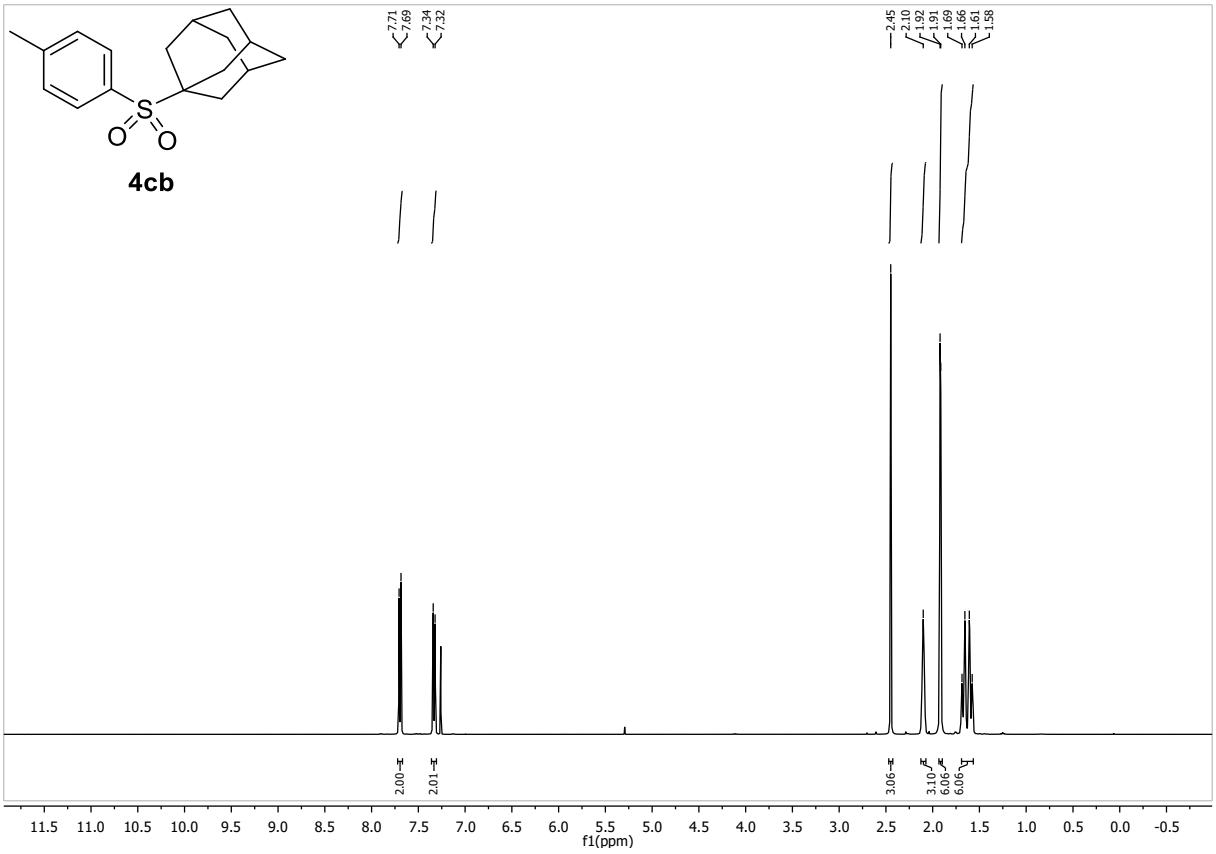
4cb
7.71
7.69
7.34
7.32
2.45
2.10
1.92
1.91
1.69
1.66
1.61
1.58
2.00
2.01
3.06
3.10
6.06
6.06
f1(ppm)

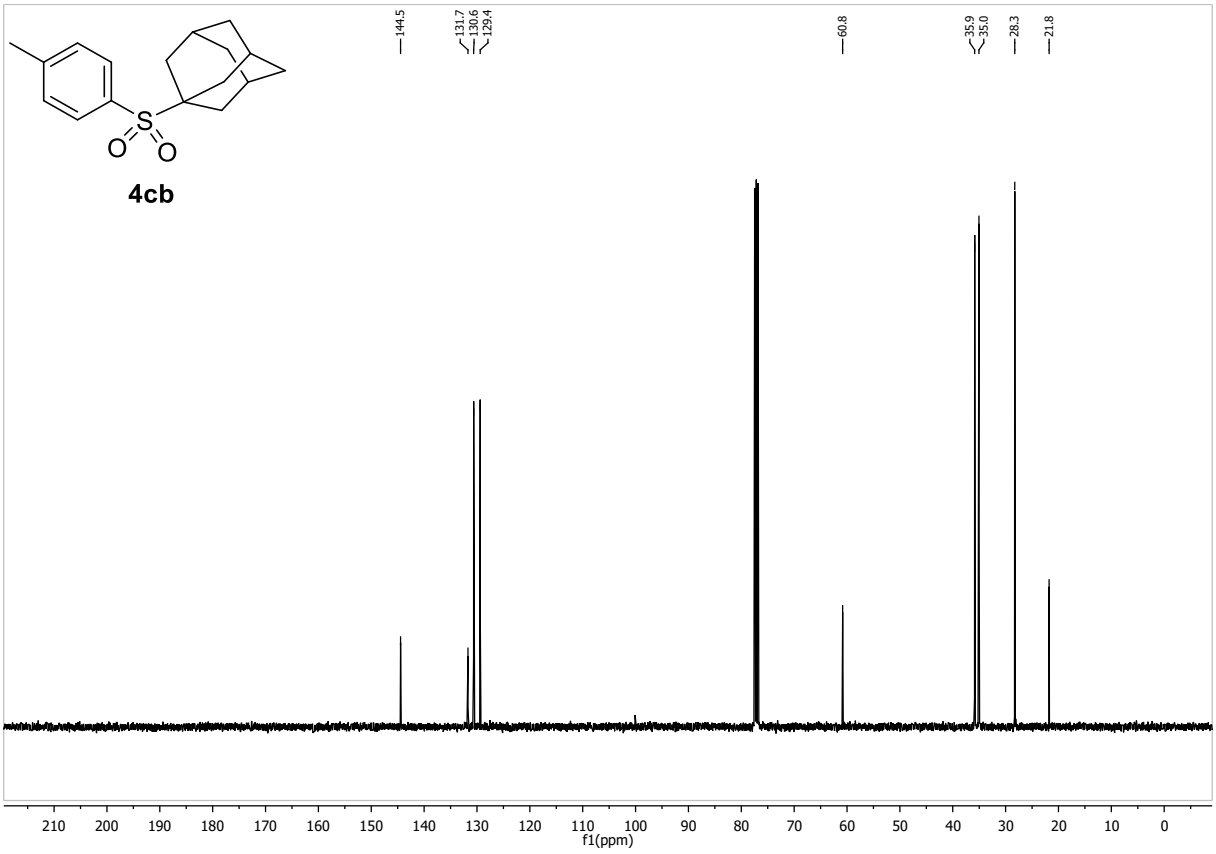
4cb
144.5
131.7
130.6
129.4
60.8
35.9
35.0
28.3
21.8
f1(ppm)

((3s,5s,7s)-adamantan-1-yl)(4-methoxyphenyl)sulfane (3db)

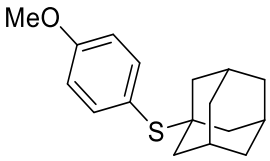

3db

$C_{17}H_{22}0S$ (274.42 g/mol)

Following GP-B, the **3db** was synthesized using 4-chloroanisole (122 µL 1.00 mmol, 1.0 equiv.) and 1-adamantanethiol (185 mg, 1.10 mmol, 1.1 equiv.) Purification by FC (SiO_2, gradient to 9:1 Hex:EtOAc over 20 CV) afforded the product **3db** (182 mg, 661 µmol, 66%) as colorless solid. Conforms to reported analytical data.[21]

R_f: 0.62 (Hex:EtOAc 9:1)

m.p.: 66.8 – 68.0 °C

^{1}H-NMR (400 MHz, $CDCl_3$, δ): 7.41 (d, *J* = 8.7 Hz, 2H), 6.85 (d, *J* = 8.7 Hz, 2H), 3.82 (s, 3H), 2.00 (q, *J* = 3.0 Hz, 3H), 1.78 (d, *J* = 2.9 Hz, 6H), 1.67 – 1.55 (m, 6H).

^{13}C-NMR (101 MHz, $CDCl_3$, δ): 160.3, 139.1, 121.5, 113.9, 55.4, 47.6, 43.6, 36.3, 30.1.

HR-MS (EI): m/z calc. for $[M]^+$ 274.138587, found 274.14124.

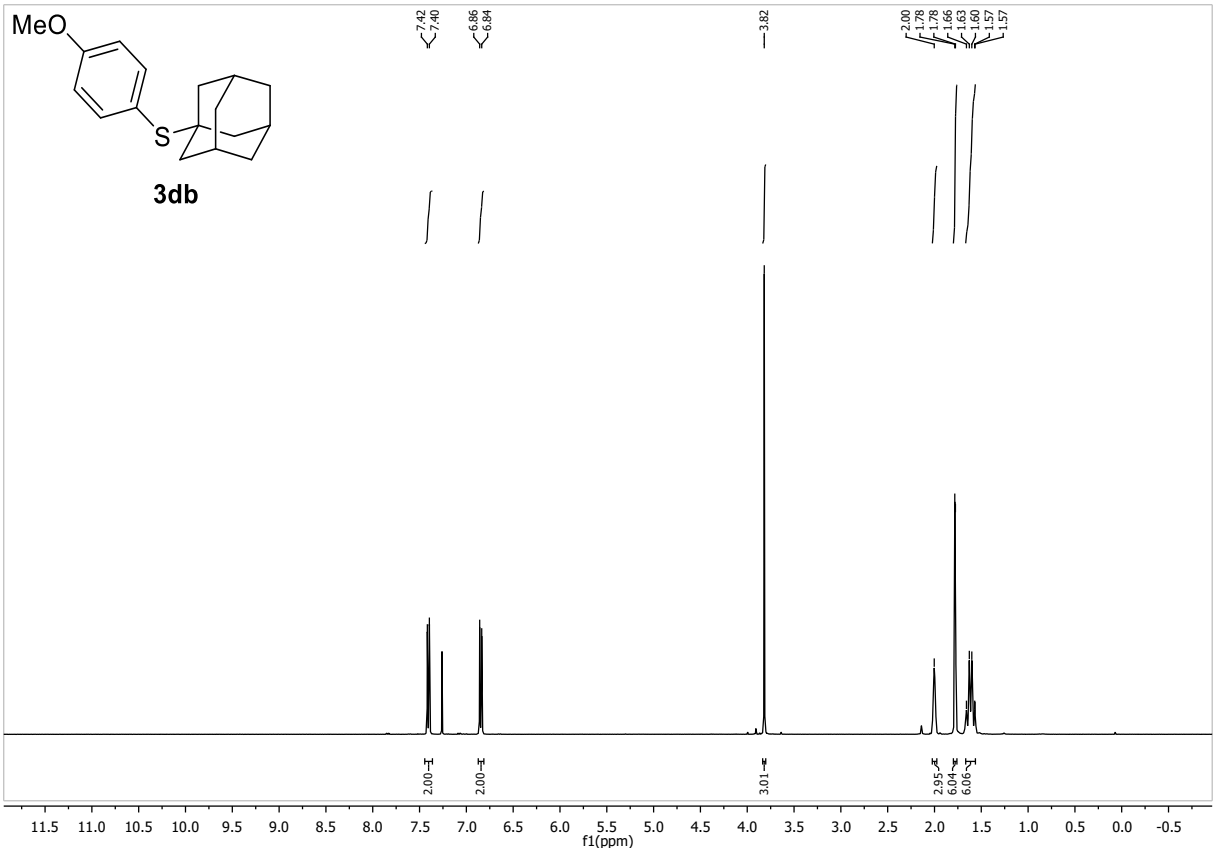
MeO
S
3db
7.42
7.40
6.86
6.84
3.82
2.00
1.78
1.78
1.66
1.63
1.60
1.57
1.57
2.00
2.00
3.01
2.95
6.04
6.06
11.5 11.0 10.5 10.0 9.5 9.0 8.5 8.0 7.5 7.0 6.5 6.0 5.5 5.0 4.5 4.0 3.5 3.0 2.5 2.0 1.5 1.0 0.5 0.0 -0.5
f1(ppm)

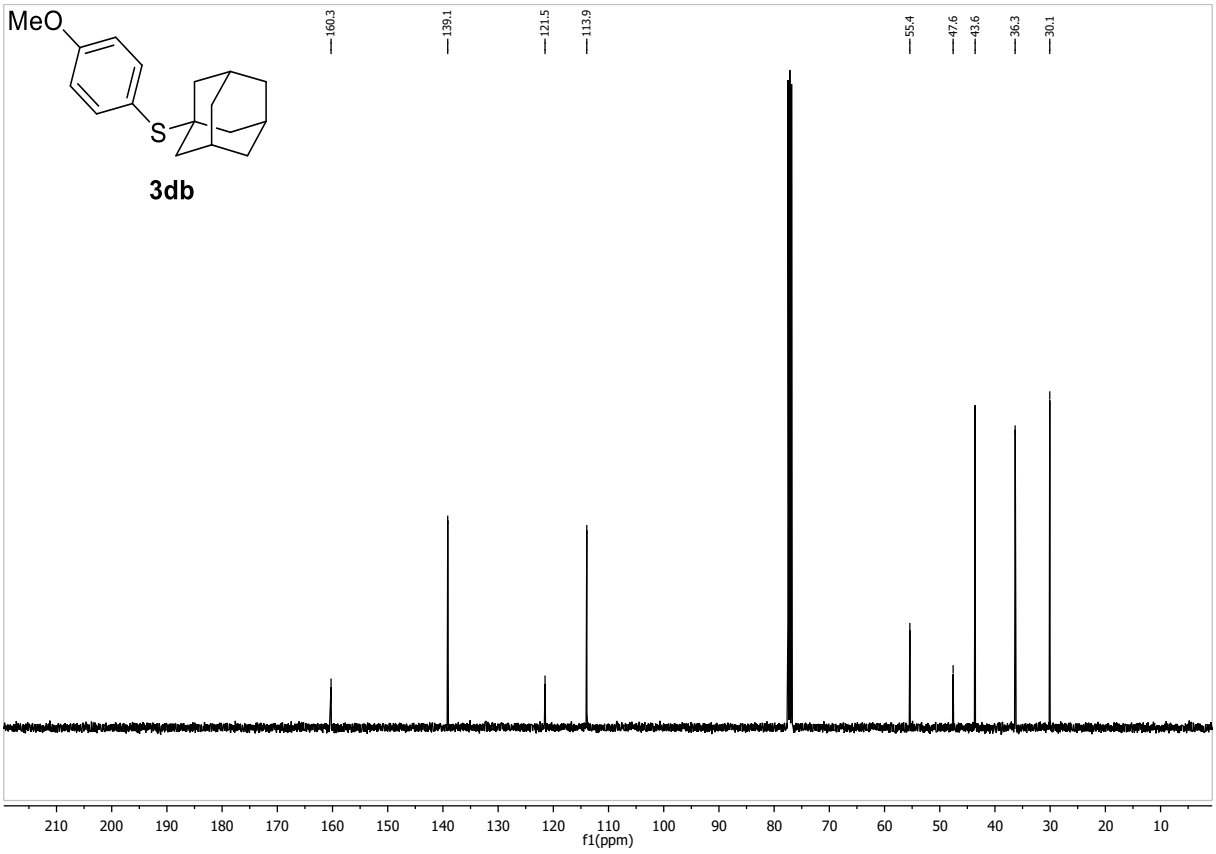
MeO
S
3db
160.3
139.1
121.5
113.9
55.4
47.6
43.6
36.3
30.1
210 200 190 180 170 160 150 140 130 120 110 100 90 80 70 60 50 40 30 20 10
f1(ppm)

Ethyl 2-(4-(((3s,5s,7s)-adamantan-1-yl)thio)phenoxy)-2-methylpropanoate (3eb)

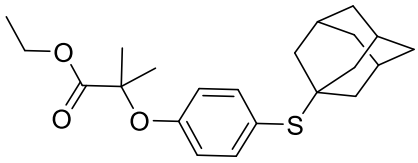

3eb

$C_{22}H_{30}O_3S$ (374.54 g/mol)

Following GP-B, the **3eb** was synthesized using Clofibrat (122 mg, 500 µmol, 1.0 equiv.) and 1-adamantanethiol (93 mg, 0.55 mmol, 1.1 equiv.). Purification by FC (SiO_2, gradient to 9:1 Hex:EtOAc over 20 CV) afforded the **3eb** (168 mg, 448 µmol, 90%) as colorless solid.

R_f: 0.62 (Hex:EtOAc 9:1)

m.p.:62.1 – 63.5 °C

^{1}H-NMR (400 MHz, $CDCl_3$, δ): 7.37 – 7.31 (m, 2H), 6.78 – 6.73 (m, 2H), 4.23 (q, *J* = 7.1 Hz, 2H), 1.99 (s, 3H), 1.76 (d, *J* = 2.9 Hz, 6H), 1.61 (s, 12H), 1.22 (t, *J* = 7.1 Hz, 3H).

^{13}C-NMR (101 MHz, $CDCl_3$, δ): 174.2, 156.3, 138.8, 122.9, 118.4, 79.2, 61.6, 47.7, 43.6, 36.3, 30.1, 25.6, 14.2.

HR-MS (EI): m/z calc. for [M] 374.191017, found 374.18967.

IR (ATR, $\tilde{\nu}$ [cm^{-1}]): 2989 (w), 2899 (m), 2849 (w), 1728 (s), 1586 (w), 1483 (m), 1448 (w), 1378 (w), 1353 (w), 1347 (w), 1283 (s), 1232 (m), 1206 (w), 1202 (w), 1172 (s), 1139 (s), 1105 (m), 1029 (m), 967 (m), 919 (w), 837 (m), 811 (w), 770 (w), 718 (w), 675 (w).

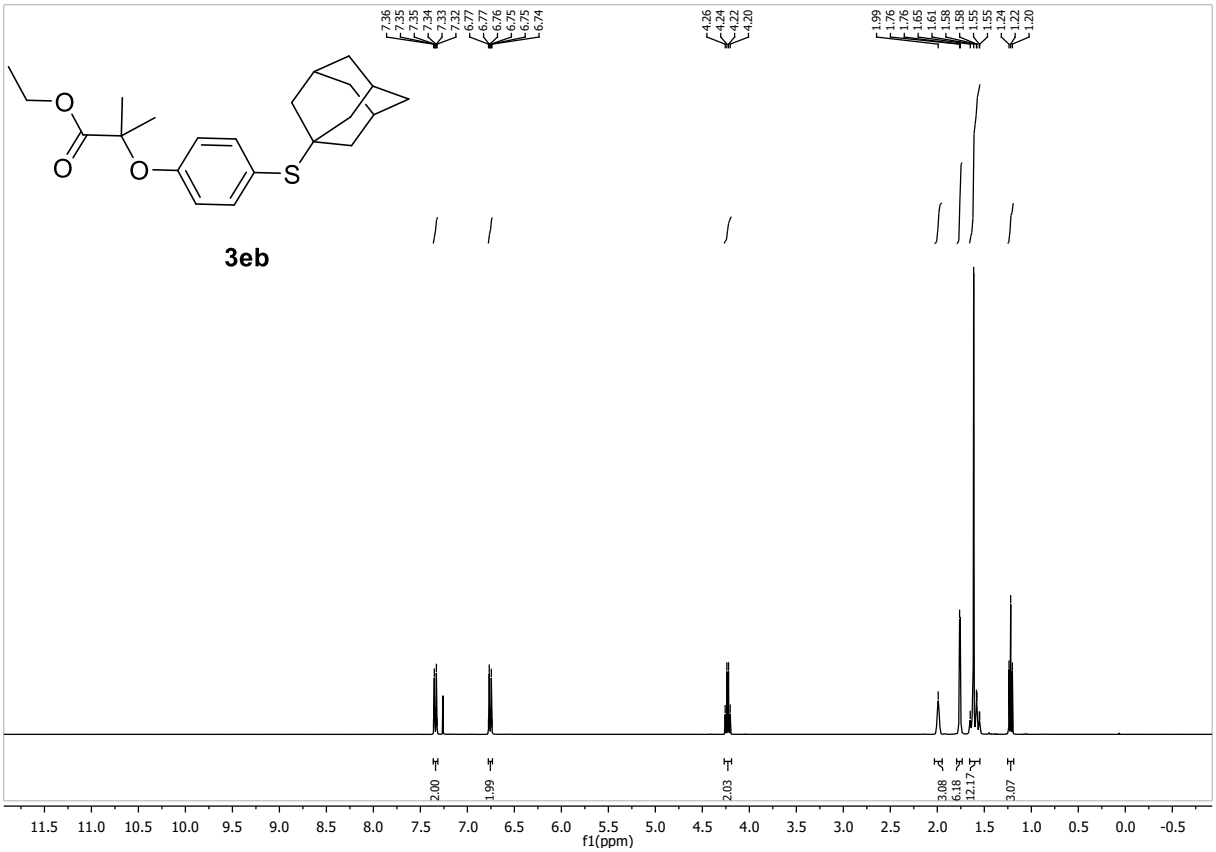
7.36
7.35
7.35
7.34
7.33
7.32
6.77
6.76
6.75
6.75
6.74
4.26
4.24
4.22
4.20
1.99
1.76
1.76
1.65
1.61
1.58
1.58
1.55
1.55
1.24
1.22
1.20
O
O
O
S
3eb
2.00
1.99
2.03
3.08
6.18
12.17
3.07
11.5 11.0 10.5 10.0 9.5 9.0 8.5 8.0 7.5 7.0 6.5 6.0 5.5 5.0 4.5 4.0 3.5 3.0 2.5 2.0 1.5 1.0 0.5 0.0 -0.5
f1(ppm)

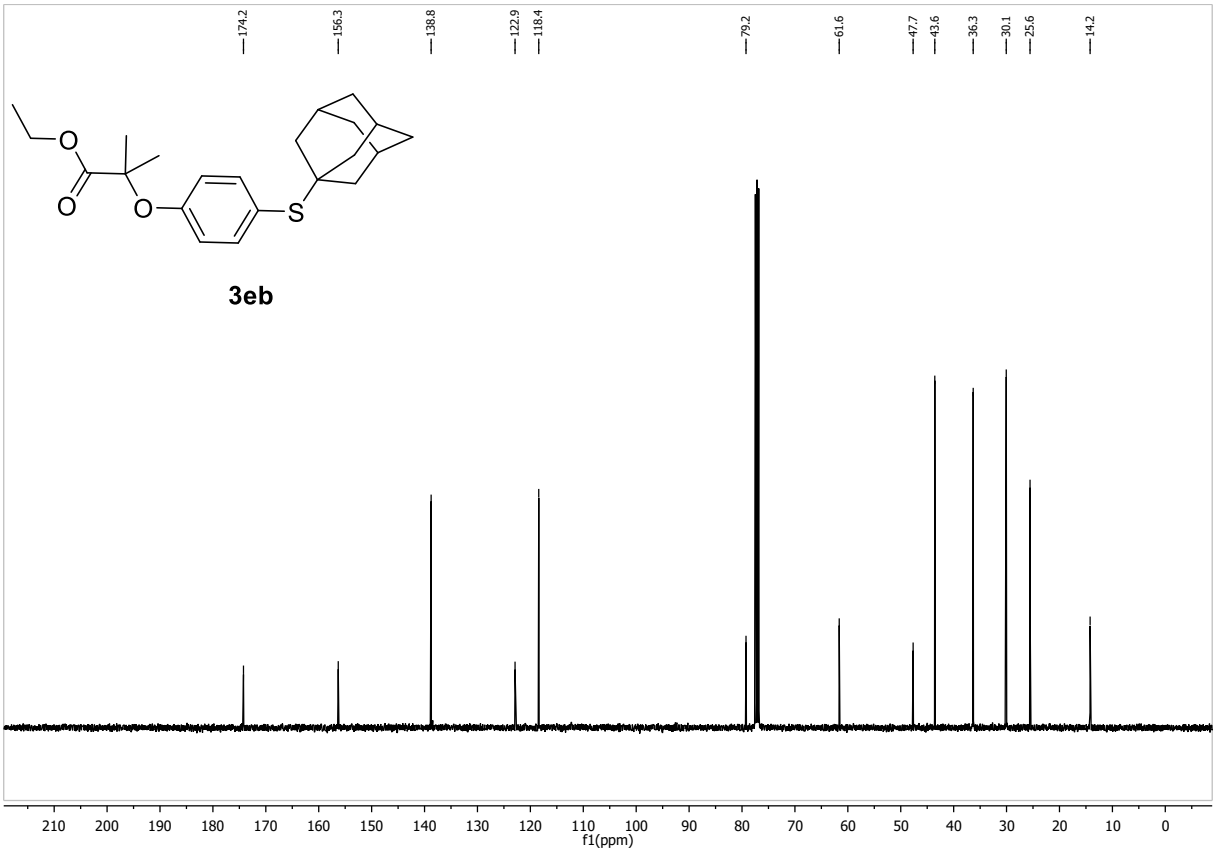
174.2
156.3
138.8
122.9
118.4
79.2
61.6
47.7
43.6
36.3
30.1
25.6
14.2
O
O
O
S
3eb
210 200 190 180 170 160 150 140 130 120 110 100 90 80 70 60 50 40 30 20 10 0
f1(ppm)

1-(4-(((3s,5s,7s)-adamantan-1-yl)thio)phenyl)ethan-1-one (3fb)

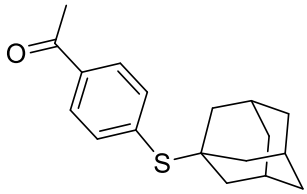

3fb

$C_{18}H_{22}OS$ (286.43 g/mol)

Following GP-B, the **3fb** was synthesized using 4-chloroacetophenone (155 mg, 1.00 mmol, 1.0 equiv.) and 1-adamantanethiol (185 mg, 1.10 mmol, 1.1 equiv.). Purification by FC (SiO_2, gradient to 9:1 Hex:EtOAc over 20 CV) afforded the product **3fb** (271 mg, 947 µmol, 95%) as colorless solid.

R_f: 0.42 (Hex:EtOAc 9:1)

m.p.: 99.1 – 101.3 °C

^{1}H-NMR (400 MHz, $CDCl_3$, δ): 7.88 (d, *J* = 8.3 Hz, 2H), 7.58 (d, *J* = 8.3 Hz, 2H), 2.61 (s, 3H), 2.02 (s, 3H), 1.83 (d, *J* = 3.0 Hz, 6H), 1.62 (q, *J* = 12.3 Hz, 6H).

^{13}C-NMR (101 MHz, $CDCl_3$, δ): 197.8, 137.4, 137.4, 136.9, 128.1, 49.2, 43.9, 36.2, 30.1, 26.8.

HR-MS (ESI): m/z calc. for $[M + Na]^+$ 309.12836, found 309.12852.

IR (ATR, $\tilde{\nu}$ [cm^{-1}]): 2901 (m), 2846 (w), 1675 (s), 1586 (m), 1553 (w), 1519 (w), 1448 (w), 1426 (w), 1389 (m), 1348 (m), 1299 (w), 1254 (s), 1176 (w), 1102 (w), 1034 (m), 1009 (m), 952 (m), 826 (s), 762 (w), 725 (w), 684 (w).

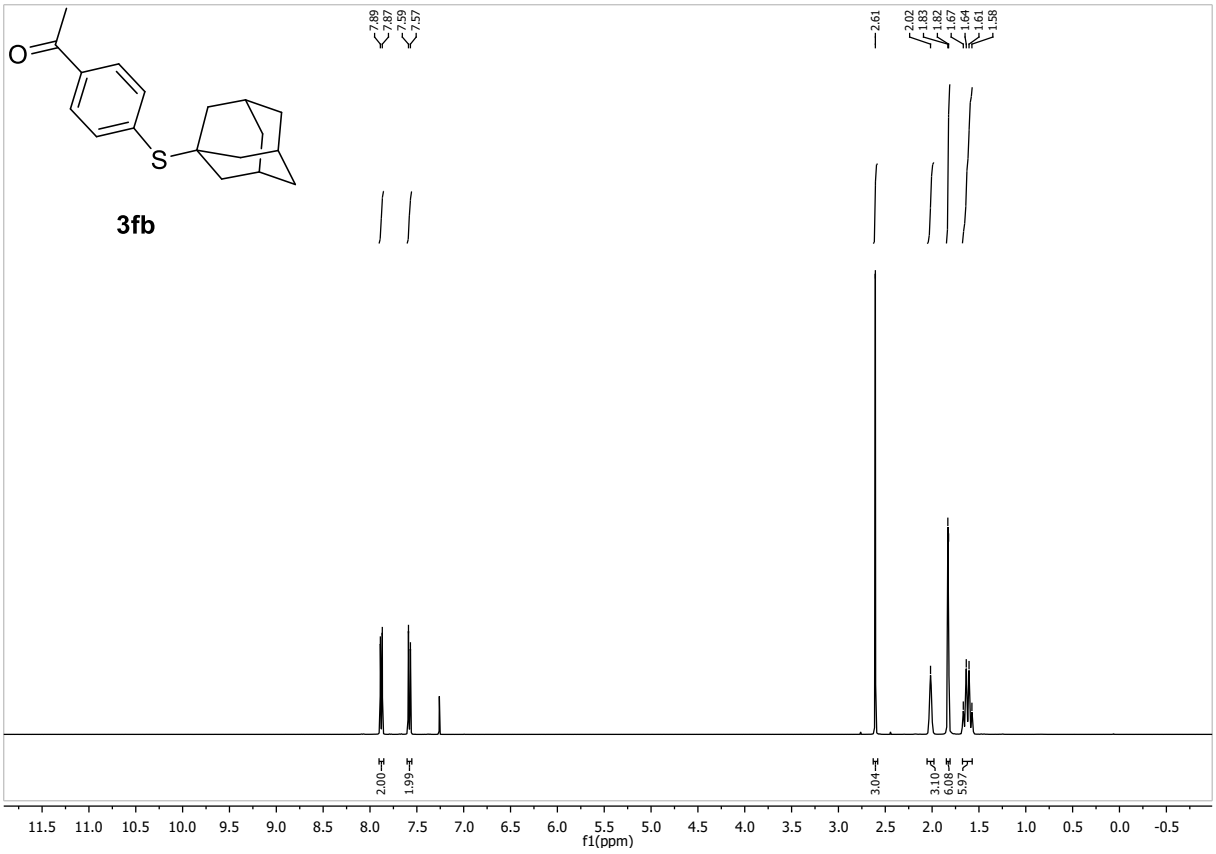
O
S
3fb
7.89
7.87
7.59
7.57
2.61
2.02
1.83
1.82
1.67
1.64
1.61
1.58
2.00
1.99
3.04
3.10
6.08
5.97
f1(ppm)

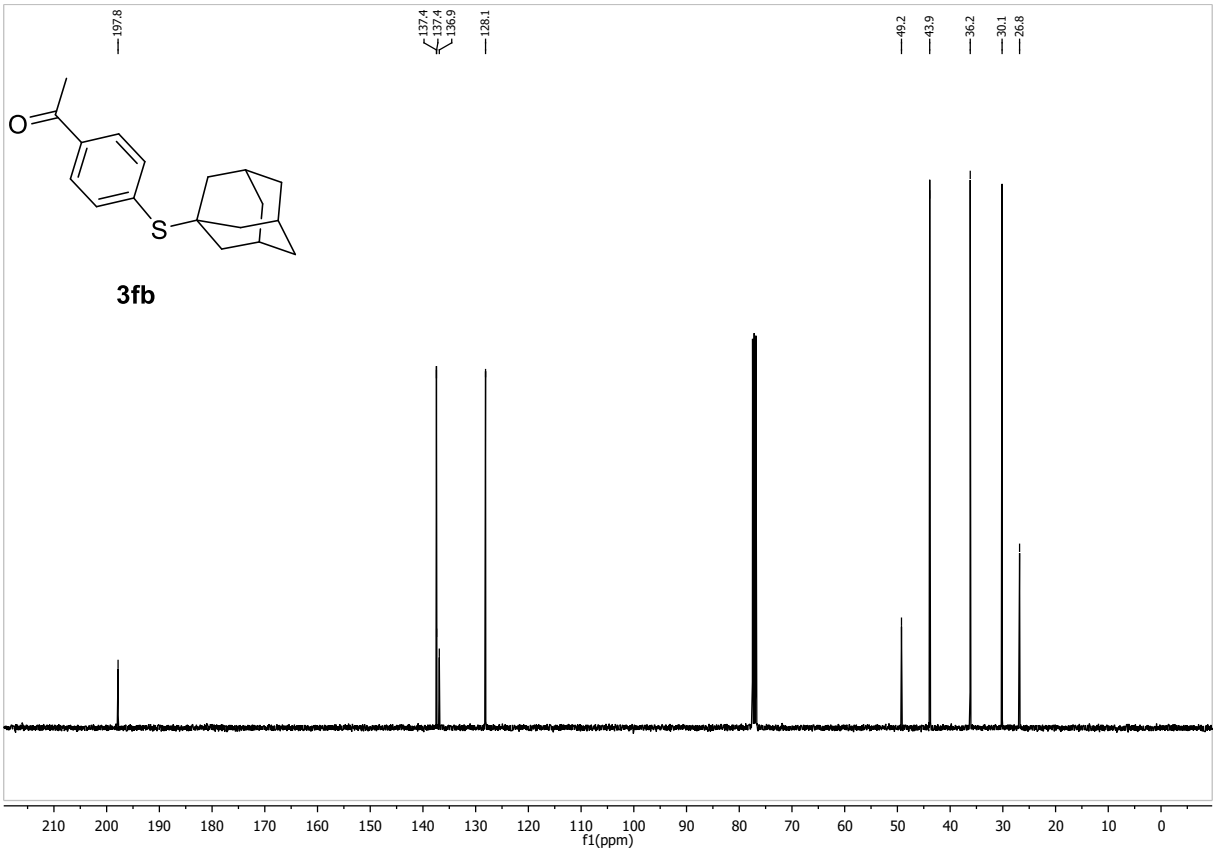
O
S
3fb
197.8
137.4
137.4
136.9
128.1
49.2
43.9
36.2
30.1
26.8
f1(ppm)

((3s,5s,7s)-adamantan-1-yl)(3-fluorophenyl)sulfane (3gb)

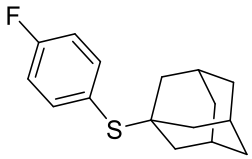

3gb

$C_{16}H_{19}FS$ (262.39 g/mol)

Following GP-B, **3gb** was synthesized using 1-chloro-4-fluorobenzene (131 mg, 1.0 mmol, 1.0 equiv.) and 1-adamantanethiol (185 mg, 1.10 mmol, 1.1 equiv.). Purification by FC (SiO_2, gradient to 9:1 Hex:EtOAc over 20 CV) afforded **3gb** (246 mg, 938 µmol, 94%) as colorless solid.

R_f: 0.78 (Hex:EtOAc 9:1)

m.p.: 98.8 – 101.0 °C

^{1}H-NMR (400 MHz, $CDCl_3$, δ): 7.42 – 7.35 (m, 2H), 6.97 – 6.90 (m, 2H), 1.94 (s, 3H), 1.71 (d, *J* = 2.6 Hz, 6H), 1.55 (q, *J* = 12.3 Hz, 6H).

^{13}C-NMR (101 MHz, $CDCl_3$, δ): 163.35 (d, *J* = 248.5 Hz), 139.45 (d, *J* = 8.3 Hz), 125.83 (d, *J* = 3.4 Hz), 115.41 (d, *J* = 21.4 Hz), 47.8, 43.5, 36.2, 30.0.

^{19}F-NMR (376, $CDCl_3$, δ): -113.04 (ddd, *J* = 14.2, 8.8, 5.6 Hz).

HR-MS (EI): m/z calc. for [M] 262.118600, found 262.11972.

IR (ATR, $\tilde{\nu}$ [cm^{-1}]): 3054 (w), 2915 (m), 2893 (s), 2846 (m), 1582 (m), 1482 (m), 1448 (m), 1393 (w), 1340 (w), 1292 (w), 1239 (w), 1210 (s), 1158 (m), 1093 (w), 1038 (m), 1016 (w), 967 (w), 841 (s), 811 (s), 755 (w), 713 (w), 684 (w).

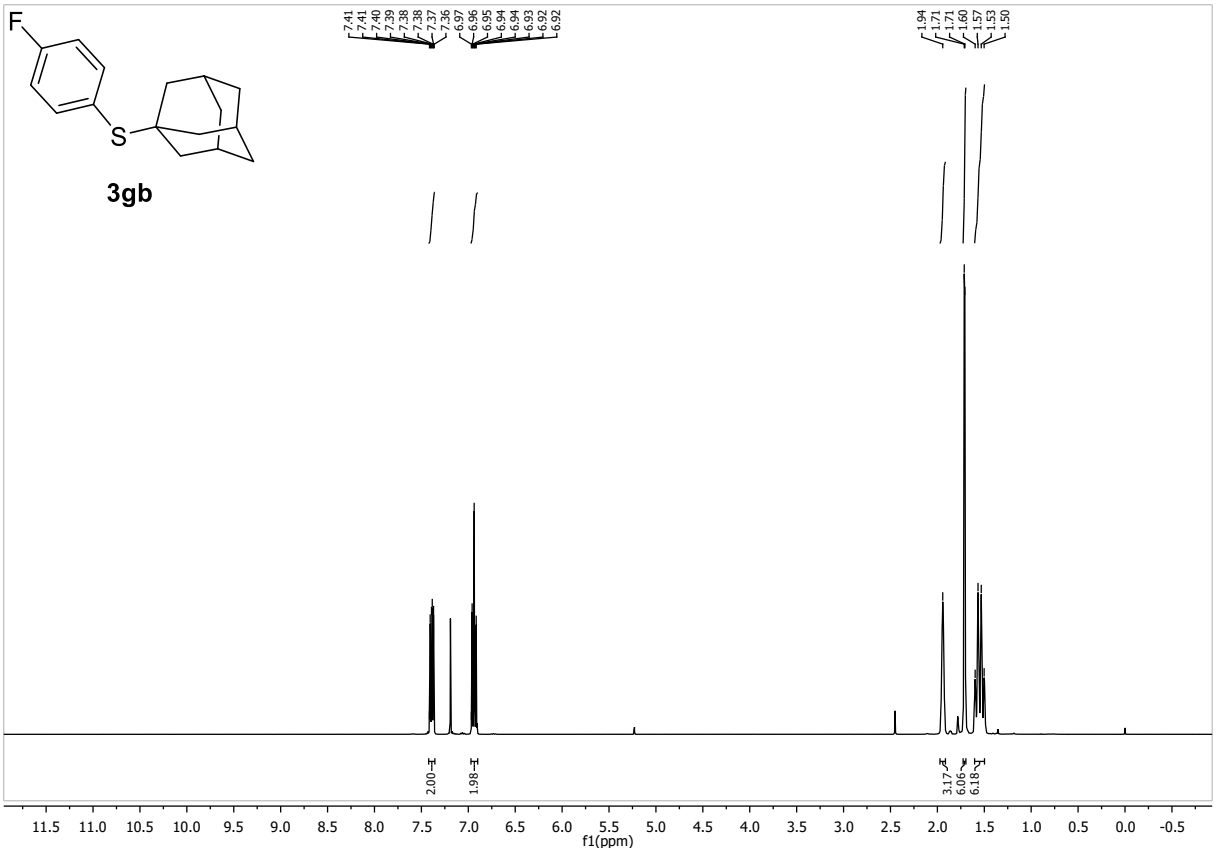
F
S
3gb
7.41
7.41
7.40
7.39
7.38
7.38
7.37
7.36
6.97
6.96
6.95
6.94
6.94
6.93
6.92
6.92
1.94
1.71
1.71
1.60
1.57
1.53
1.50
2.00
1.98
3.17
6.06
6.18
11.5 11.0 10.5 10.0 9.5 9.0 8.5 8.0 7.5 7.0 6.5 6.0 5.5 5.0 4.5 4.0 3.5 3.0 2.5 2.0 1.5 1.0 0.5 0.0 -0.5
f1(ppm)

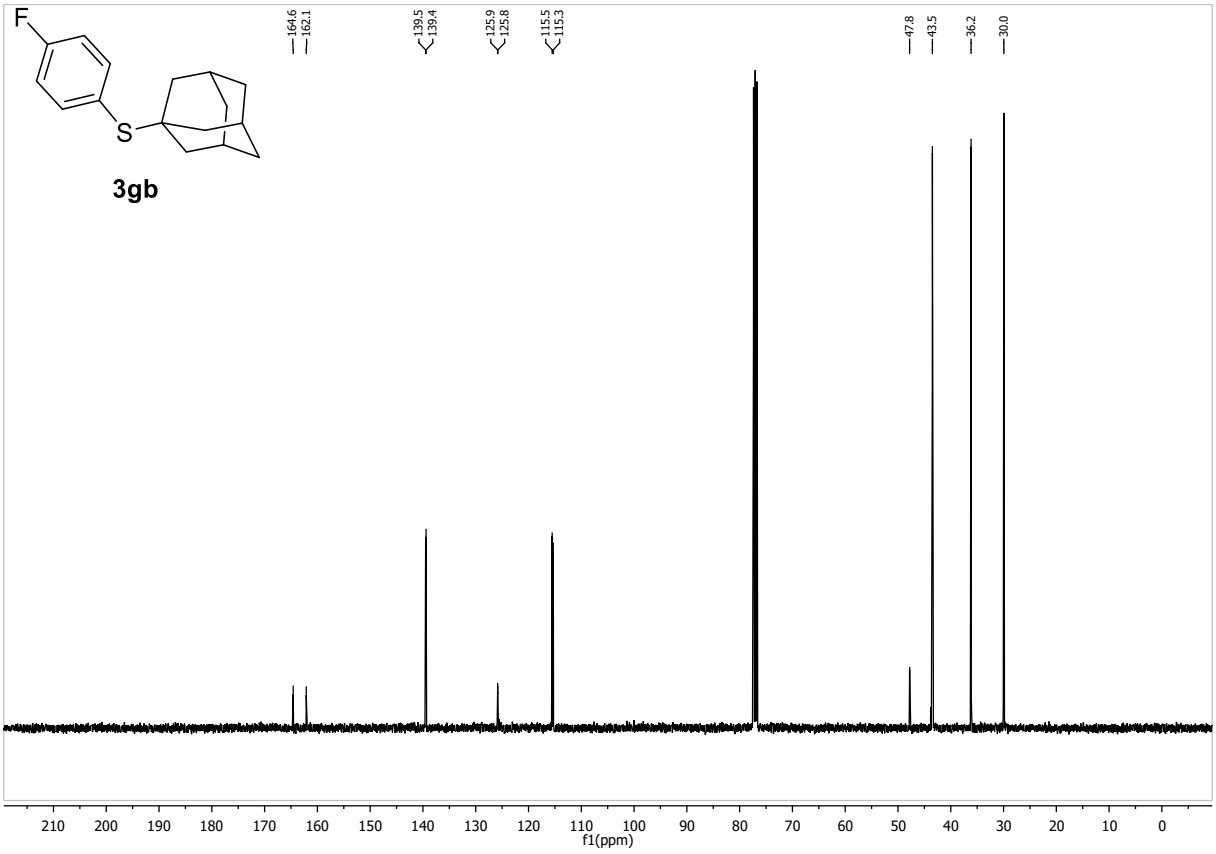
F
S
3gb
164.6
162.1
139.5
139.4
125.9
125.8
115.5
115.3
47.8
43.5
36.2
30.0
210 200 190 180 170 160 150 140 130 120 110 100 90 80 70 60 50 40 30 20 10 0
f1(ppm)

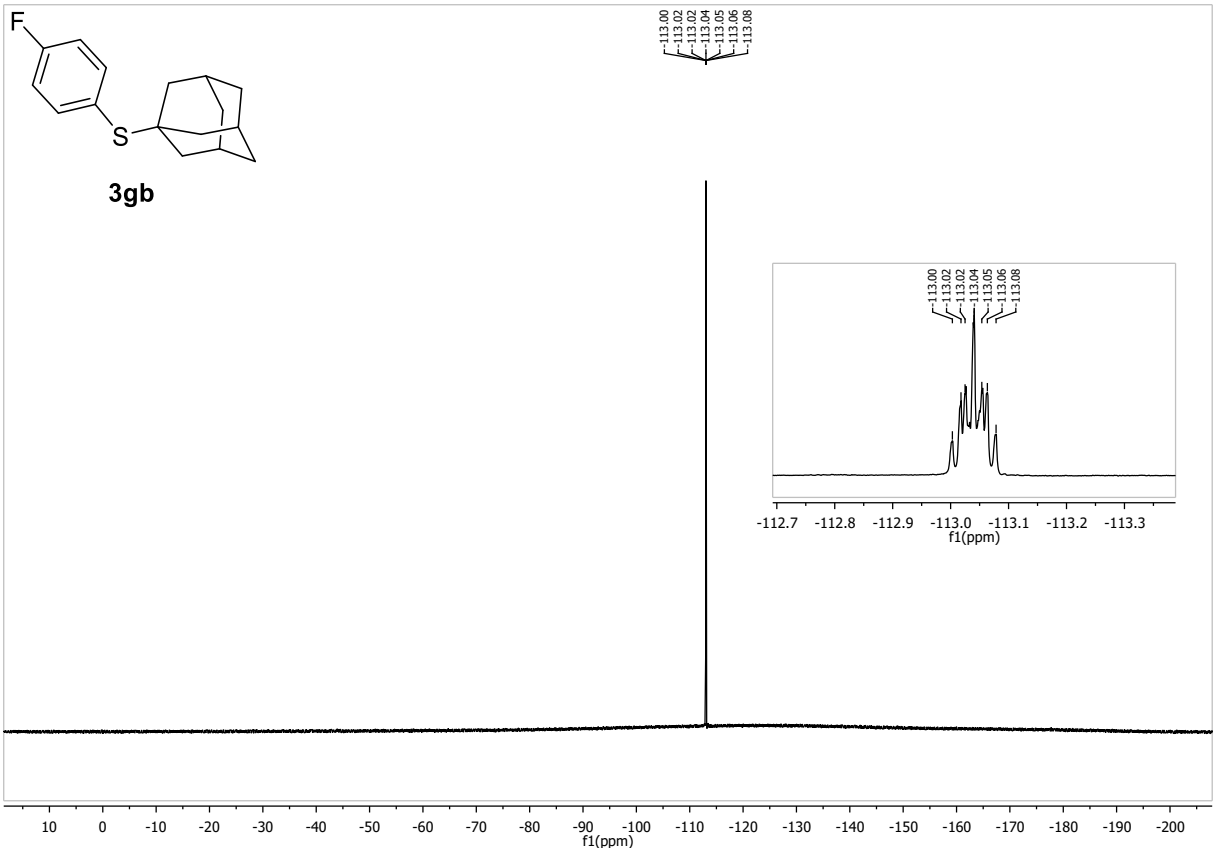
F
S
3gb
-113.00
-113.02
-113.02
-113.04
-113.05
-113.06
-113.08
-112.7
-112.8
-112.9
-113.0
-113.1
-113.2
-113.3
f1(ppm)
10
0
-10
-20
-30
-40
-50
-60
-70
-80
-90
-100
-110
-120
-130
-140
-150
-160
-170
-180
-190
-200
f1(ppm)

((3s,5s,7s)-adamantan-1-yl)(4-(trifluoromethyl)phenyl)sulfane (3hb)

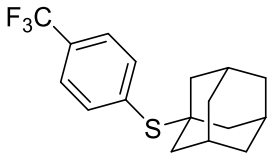

3hb

$C_{17}H_{19}F_3S$ (312.39 g/mol)

Following GP-B, the **3hb** was synthesized using 4-chlorobenzotrifluoride (134 µL, 1.00 mmol, 1.0 equiv.) and 1-adamantanethiol (185 mg, 1.10 mmol, 1.1 equiv.) Purification by FC (SiO_2, 5 CV Hex, gradient to 8:2 Hex:EtOAc over 15 CV) afforded **3hb** (272 mg, 872 µmol, 87%) as colorless solid. Conforms to reported analytical data.[22]

R_f: 0.82 (Hex:EtOAc 9:1)

^{1}H-NMR (400 MHz, $CDCl_3$, δ): 7.61 (d, *J* = 8.2 Hz, 2H), 7.56 (d, *J* = 8.2 Hz, 2H), 2.03 (s, 3H), 1.82 (d, *J* = 2.6 Hz, 6H), 1.63 (q, *J* = 12.3 Hz, 6H).

^{13}C-NMR (101 MHz, $CDCl_3$, δ): 137.76, 135.66, 130.68 (q, *J* = 32.5 Hz), 125.21 (q, *J* = 3.7 Hz)., 122.88, 48.97, 43.80, 36.19, 30.13.

^{19}F-NMR (376 MHz, $CDCl_3$, δ): - 62.6.

HR-MS (EI): m/z calc. for $[M]^+$ 312.115407, found 312.11863.

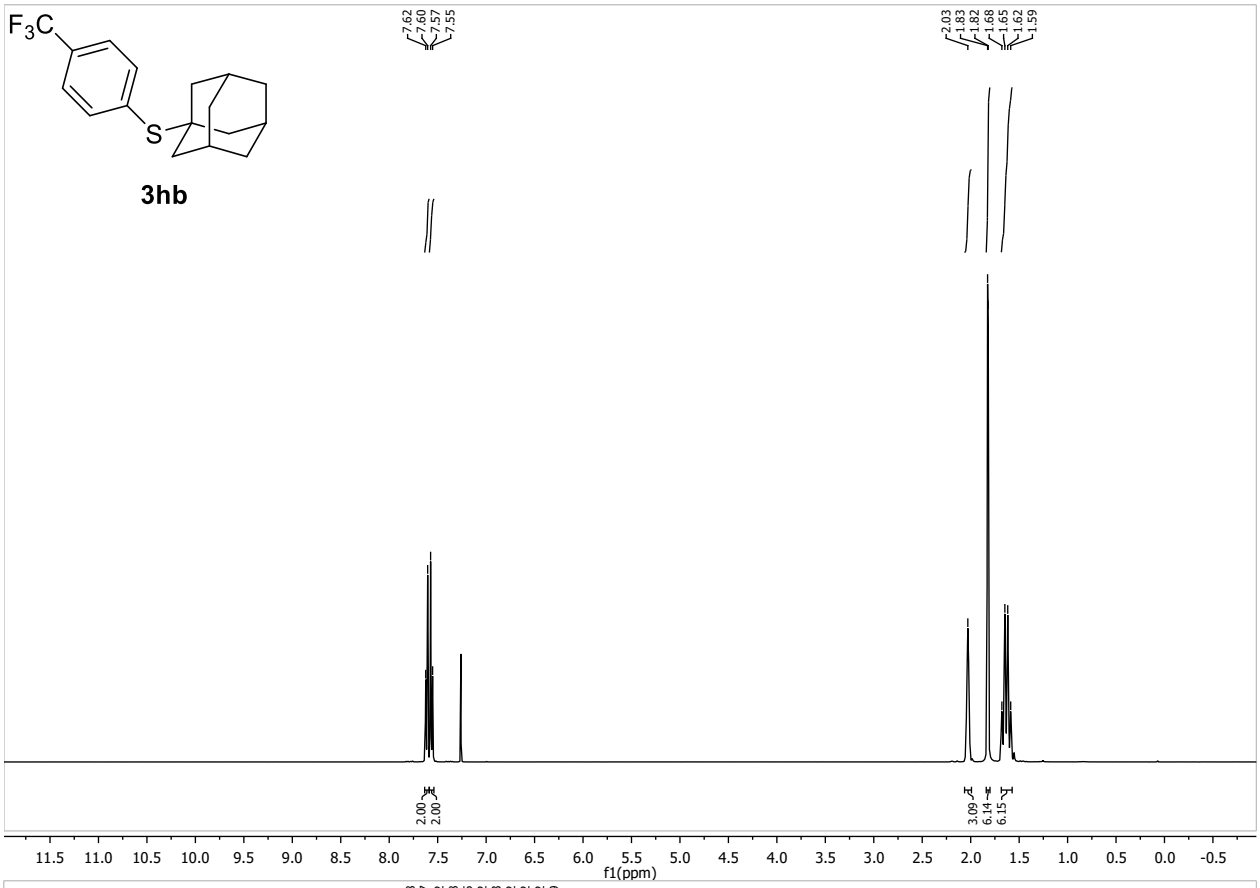
F3C
S
3hb
7.62
7.60
7.57
7.55
2.03
1.83
1.82
1.68
1.65
1.62
1.59
2.00
2.00
3.09
6.14
6.15
11.5 11.0 10.5 10.0 9.5 9.0 8.5 8.0 7.5 7.0 6.5 6.0 5.5 5.0 4.5 4.0 3.5 3.0 2.5 2.0 1.5 1.0 0.5 0.0 -0.5
f1(ppm)

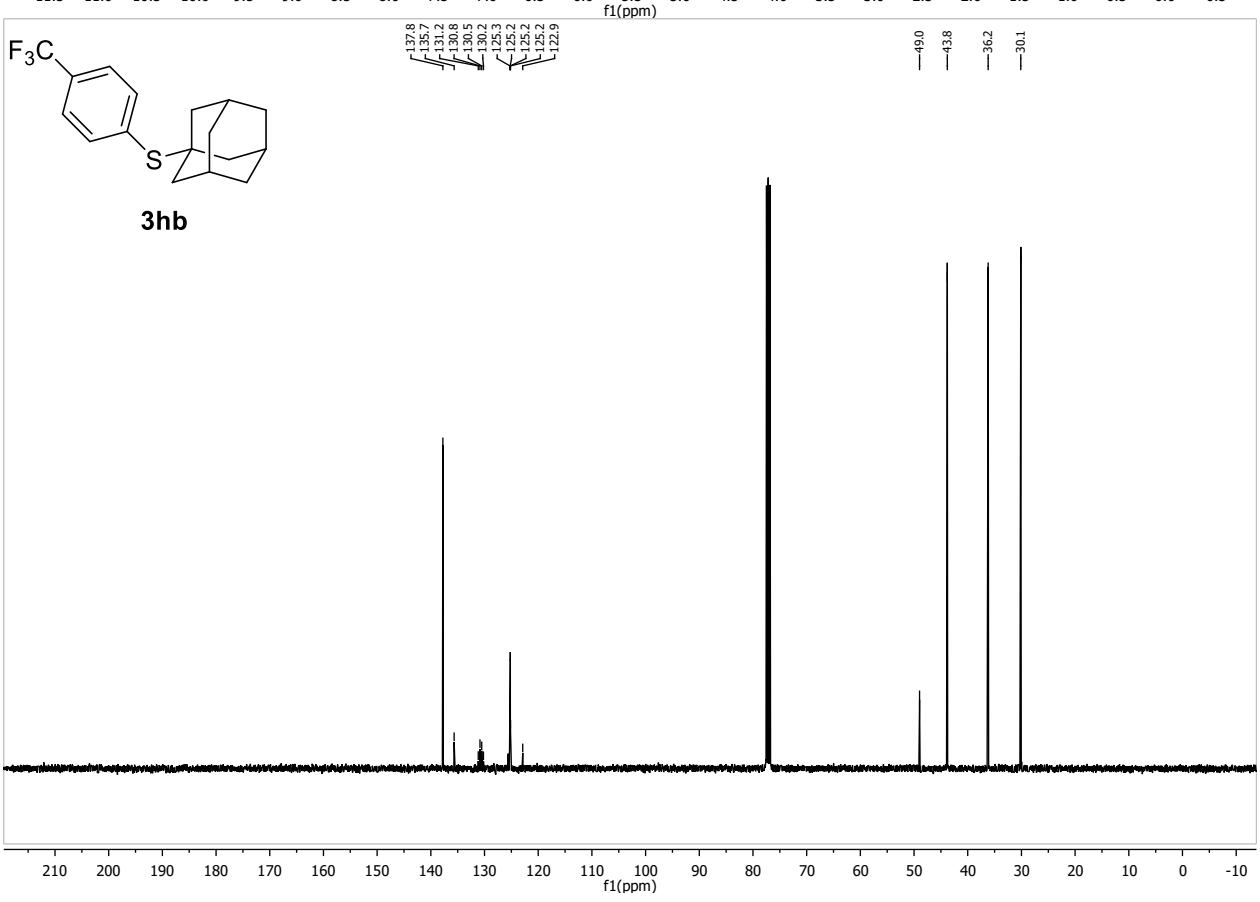
F3C
S
3hb
137.8
135.7
131.2
130.8
130.5
130.2
125.3
125.2
125.2
125.2
125.2
122.9
49.0
43.8
36.2
30.1
210 200 190 180 170 160 150 140 130 120 110 100 90 80 70 60 50 40 30 20 10 0 -10
f1(ppm)

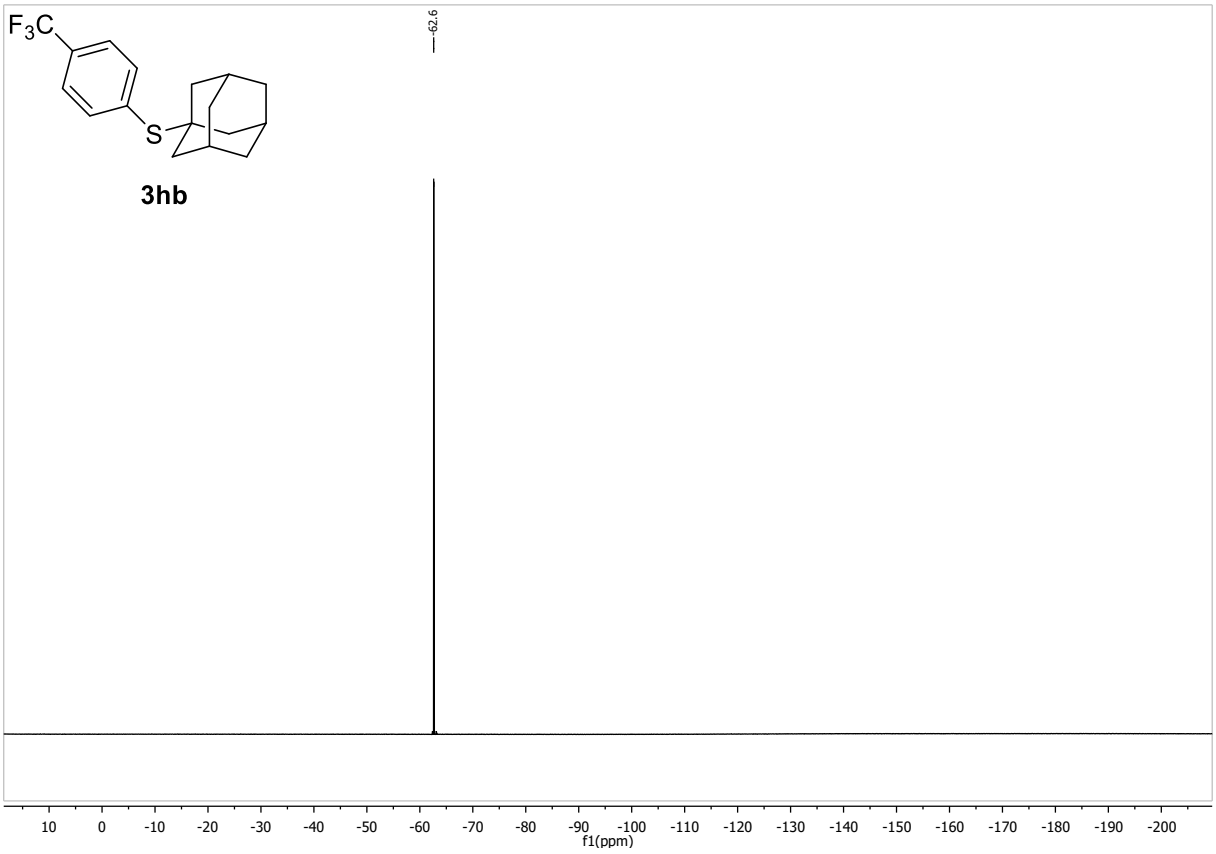
F3C
S
3hb
-62.6
10
0
-10
-20
-30
-40
-50
-60
-70
-80
-90
-100
-110
-120
-130
-140
-150
-160
-170
-180
-190
-200
f1(ppm)

((3s,5s,7s)-adamantan-1-yl)(4-(methylsulfonyl)phenyl)sulfane (3ib)

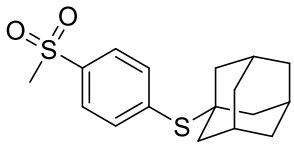

3ib

$C_{17}H_{22}O_2S_2$ (283.43 g/mol)

Following GP-B, **3ib** was synthesized using 1-chloro-4-(methylsulfonyl)benzene (191 mg, 1.00 mmol, 1.0 equiv.) and 1-adamantanethiol (185 mg, 1.10 mmol, 1.1 equiv.). Purification by FC (SiO_2, gradient to 8:2 Hex:EtOAc over 20 CV) afforded **3ib** (276 mg, 857 µmol, 86%) as colorless solid. Conforms to reported analytical data.[23]

R_f: 0.27 (Hex:EtOAc 9:1)

m.p.: 147.8 – 149.2 °C

^{1}H-NMR (400 MHz, $CDCl_3$, δ): 7.87 (d, *J* = 8.4 Hz, 2H), 7.68 (d, *J* = 8.4 Hz, 2H), 3.08 (s, 3H), 2.04 (s, 3H), 1.83 (d, *J* = 2.5 Hz, 6H), 1.63 (q, *J* = 12.2 Hz, 6H).

^{13}C-NMR (101 MHz, $CDCl_3$, δ): 140.4, 138.8, 137.9, 127.2, 49.7, 44.6, 43.9, 36.1, 30.1.

HR-MS (ESI): m/z calc. for [M + Na^+] 345.09534, found 345.09570.

IR (ATR, $\tilde{\nu}$ [cm^{-1}]): 2902 (m), 2849 (w), 1575 (w), 1448 (w), 1381 (w), 1348 (w), 1304 (s), 1269 (m), 1176 (w), 1146 (s), 1088 (m), 1034 (m), 1012 (w), 952 (s), 830 (m), 770 (s), 740 (m), 710 (w), 684 (w).

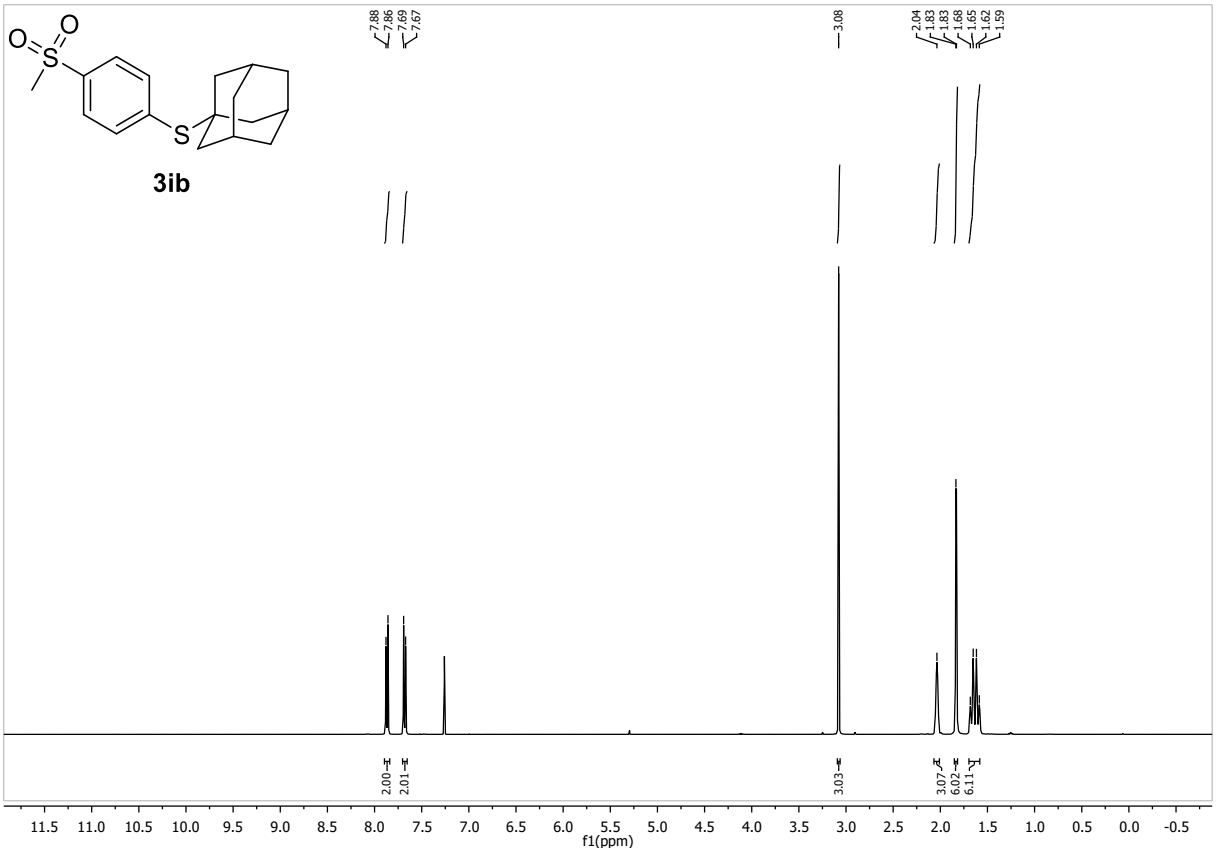
3ib
7.88
7.86
7.69
7.67
3.08
2.04
1.83
1.83
1.68
1.65
1.62
1.59
2.00
2.01
3.03
3.07
6.02
6.11
f1(ppm)

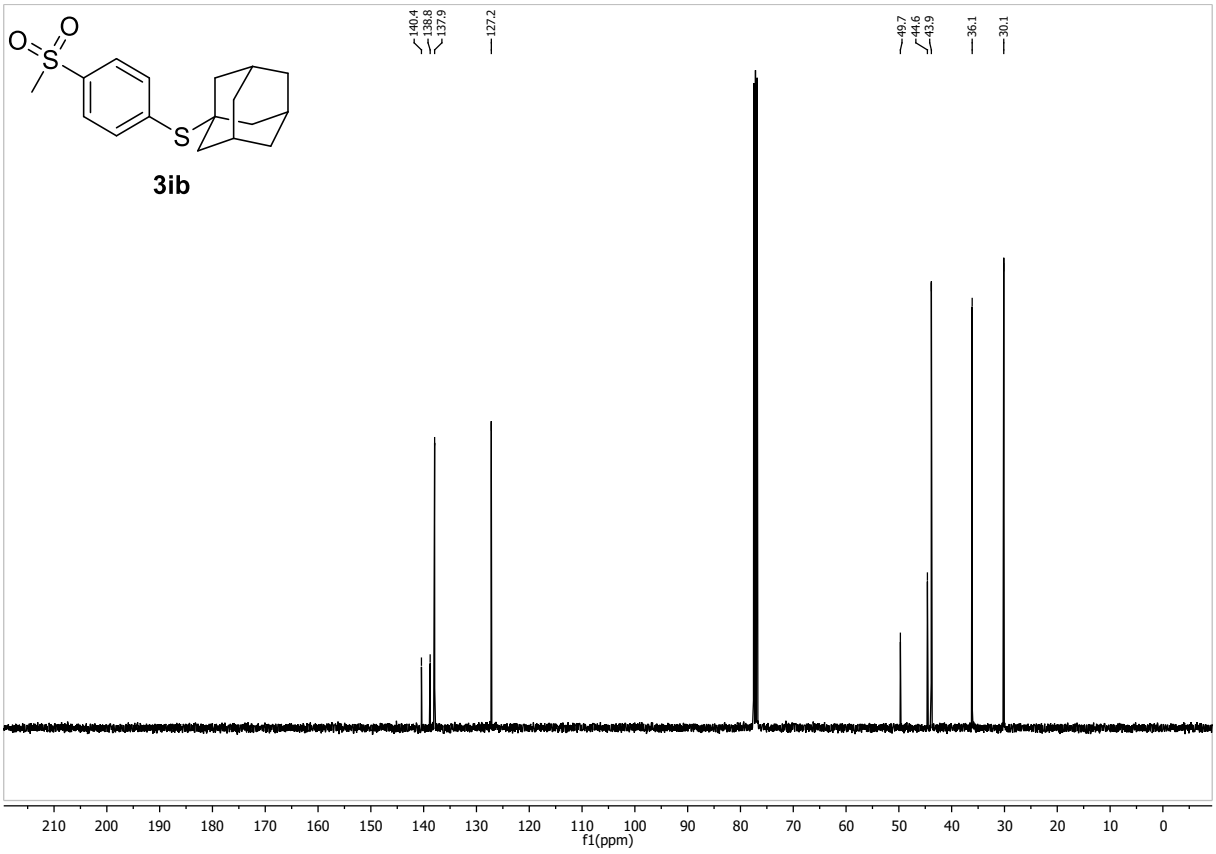
3ib
140.4
138.8
137.9
127.2
49.7
44.6
43.9
36.1
30.1
f1(ppm)

N-(4-(((3s,5s,7s)-adamantan-1-yl)thio)phenyl)acetamide (3jb)

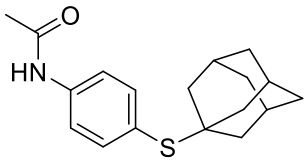

3jb

$C_{18}H_{23}NOS$ (301.45 g/mol)

Following GP-B, **3jb** was synthesized using N-(4-chlorophenyl)acetamide (170 mg, 1.00 mmol, 1.0 equiv.) and 1-adamantanethiol (185 mg, 1.10 mmol, 1.1 equiv.). Purification by FC (SiO_2, gradient to 5:5 Hex:EtOAc over 20 CV) afforded **3jb** (259 mg, 857 µmol, 86%) as colorless solid.

R_f: 0.38 (Hex:EtOAc 5:5)

m.p.: 188.0 – 189.8 °C

^{1}H-NMR (400 MHz, $CDCl_3$, δ): 7.54 (br. s, 1H), 7.47 (d, *J* = 8.6 Hz, 2H), 7.42 (d, *J* = 8.6 Hz, 2H), 2.18 (s, 3H), 1.99 (s, 3H), 1.78 (d, *J* = 2.5 Hz, 6H), 1.60 (q, *J* = 12.2 Hz, 6H).

^{13}C-NMR (101 MHz, $CDCl_3$, δ): 168.6, 138.5, 138.5, 125.7, 119.5, 48.0, 43.6, 36.3, 30.1, 24.8.

HR-MS (ESI): m/z calc. for [M + Na^+] 324.13926, found 324.13955.

IR (ATR, $\tilde{\nu}$ [cm^{-1}]): 3230 (w), 2901 (w), 2846 (w), 1657 (m), 1582 (m), 1523 (m), 1485 (m), 1448 (w), 1389 (m), 1370 (m), 1349 (w), 1303 (m), 1250 (m), 1176 (w), 1101 (w), 1035 (m), 1008 (w), 967 (w), 888 (w), 822 (m), 750 (m), 688 (w).

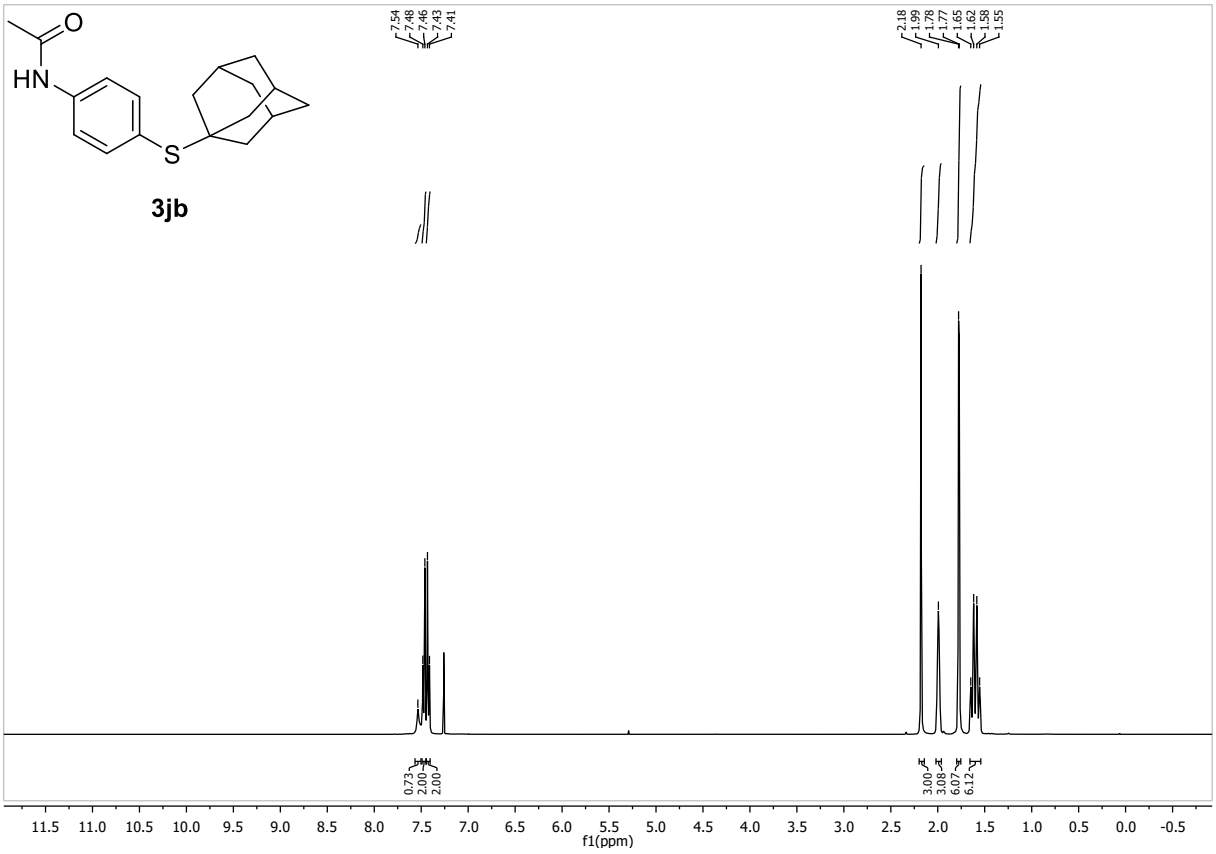
O
HN
S
3jb
7.54
7.48
7.46
7.43
7.41
2.18
1.99
1.78
1.77
1.65
1.62
1.58
1.55
0.73
2.00
2.00
3.00
3.08
6.07
6.12
11.5 11.0 10.5 10.0 9.5 9.0 8.5 8.0 7.5 7.0 6.5 6.0 5.5 5.0 4.5 4.0 3.5 3.0 2.5 2.0 1.5 1.0 0.5 0.0 -0.5
f1(ppm)

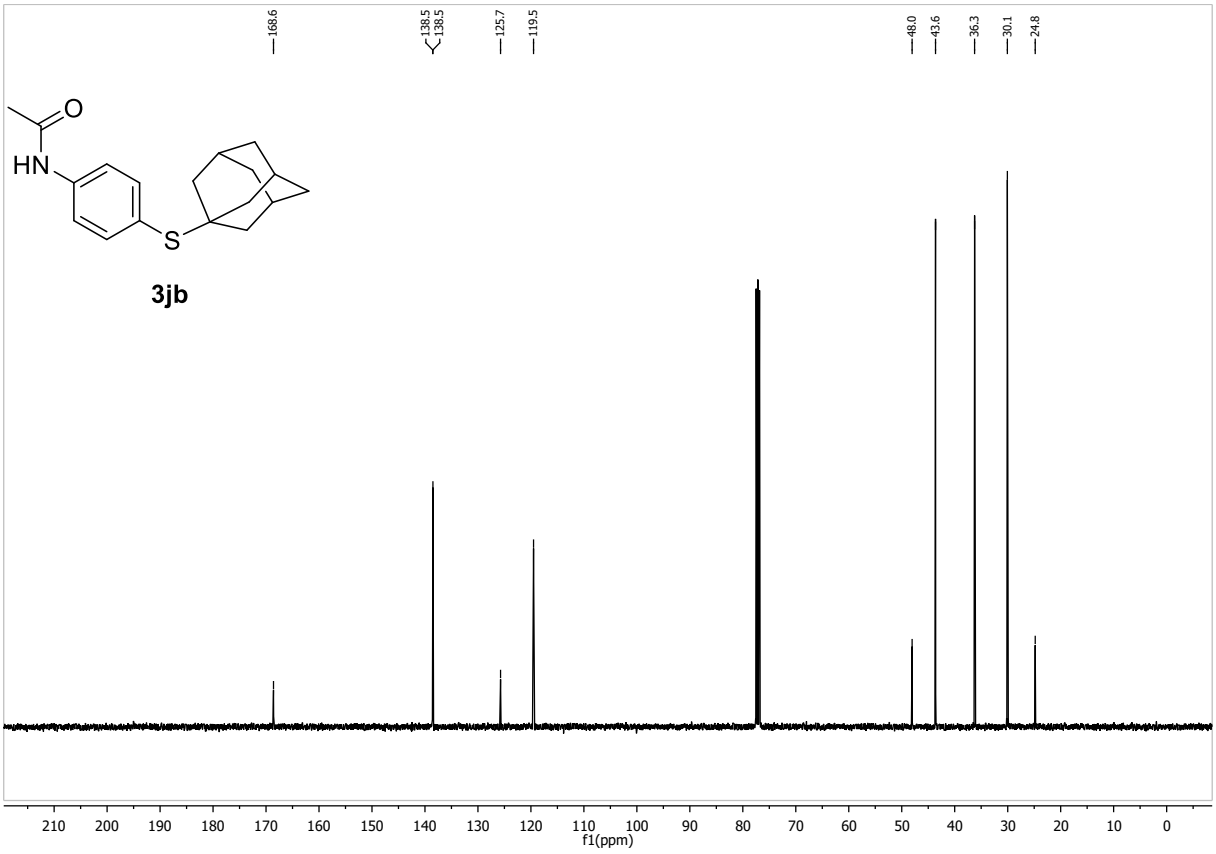
O
HN
S
3jb
168.6
138.5
138.5
125.7
119.5
48.0
43.6
36.3
30.1
24.8
210 200 190 180 170 160 150 140 130 120 110 100 90 80 70 60 50 40 30 20 10 0
f1(ppm)

4-(4-(((3s,5s,7s)-adamantan-1-yl)thio)phenyl)morpholine (3kb)

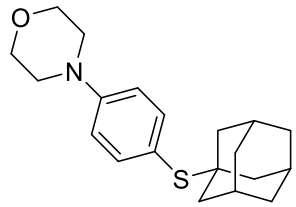

3kb

$C_{20}H_{27}NOS$ (329.50 g/mol)

Following GP-B, **3kb** was synthesized using 4-(4-chlorophenyl)morpholine (198 mg, 1.00 mmol, 1.0 equiv.) and 1-adamantanethiol (185 mg, 1.10 mmol, 1.1 equiv.). Purification by FC (SiO_2, gradient to 8:2 Hex:EtOAc over 20 CV) afforded **3kb** (221 mg, 672 µmol, 67%) as colorless solid.

R_f: 0.25 (Hex:EtOAc 9:1)

m.p.: 125.9 – 127.4 °C

^{1}H-NMR (400 MHz, $CDCl_3$, δ): 7.38 (d, *J* = 8.7 Hz, 2H), 6.83 (d, *J* = 8.7 Hz, 2H), 3.90 – 3.83 (m, 4H), 3.22 – 3.15 (m, 4H), 2.00 (s, 3H), 1.78 (d, *J* = 3.0 Hz, 6H), 1.61 (q, *J* = 12.3 Hz, 6H).

^{13}C-NMR (101 MHz, $CDCl_3$, δ): 151.4, 138.8, 120.2, 115.0, 66.9, 48.8, 47.6, 43.6, 36.3, 30.1.

HR-MS (ESI): m/z calc. for $[M+H]^+$ 330,18861, found 330,18895.

IR (ATR, $\tilde{\nu}$ [cm^{-1}]): 2898 (m), 2846 (w), 1590 (m), 1492 (m), 1445 (m), 1374 (w), 1332 (m), 1303 (m), 1232 (s), 1176 (w), 1113 (s), 1038 (m), 975 (w), 922 (s), 867 (w), 810 (s), 721 (w), 673 (m).

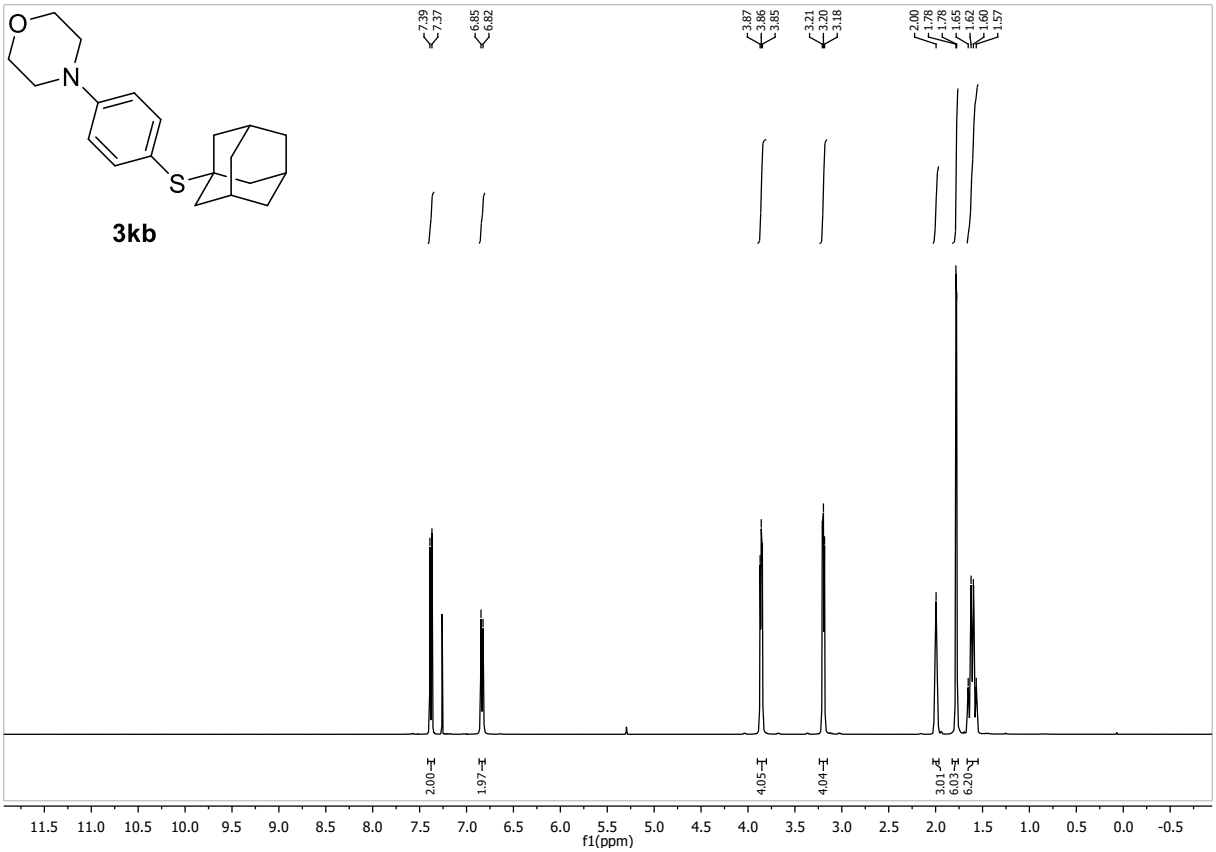
3kb
7.39
7.37
6.85
6.82
3.87
3.86
3.85
3.21
3.20
3.18
2.00
1.78
1.78
1.65
1.62
1.60
1.57
2.00
1.97
4.05
4.04
3.01
6.03
6.20
f1(ppm)

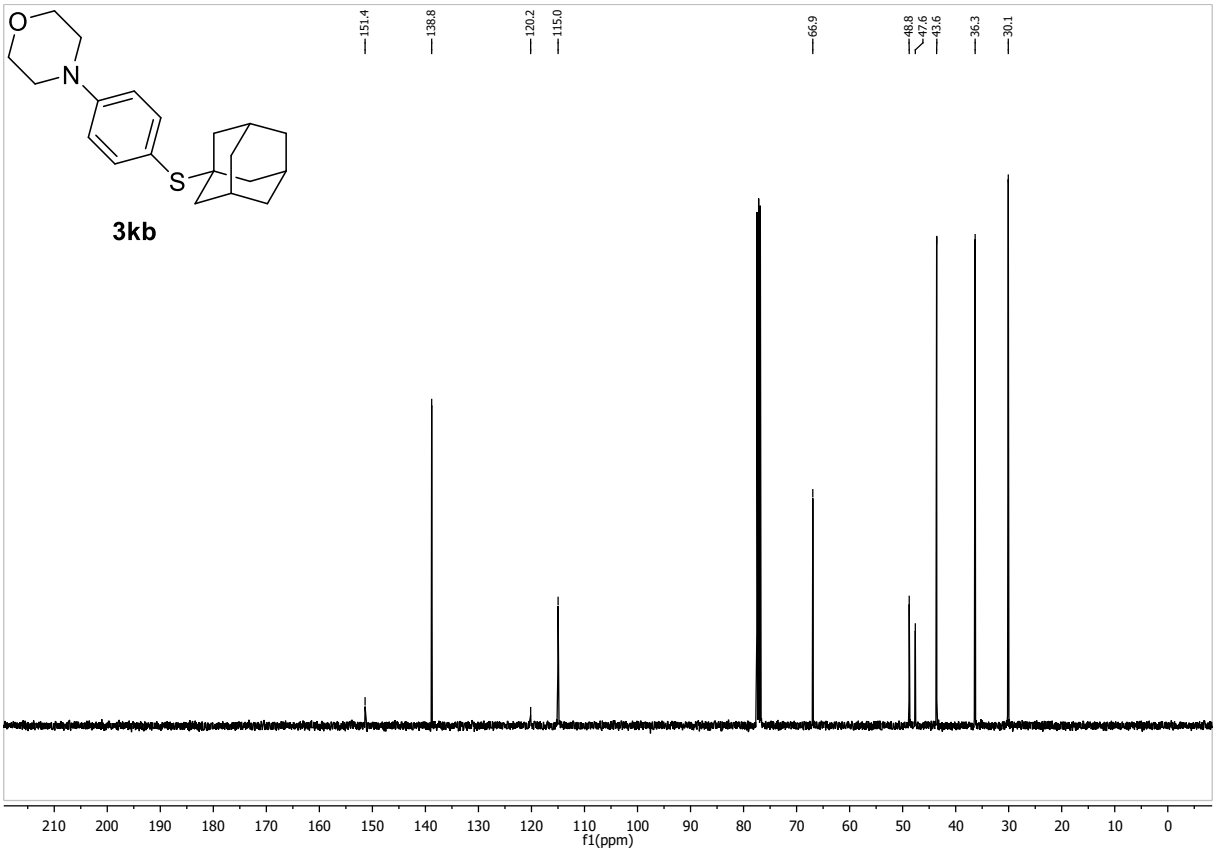
3kb
151.4
138.8
120.2
115.0
66.9
48.8
47.6
43.6
36.3
30.1
f1(ppm)

((3s,5s,7s)-adamantan-1-yl)(4-(trifluoromethoxy)phenyl)sulfane (3lb)

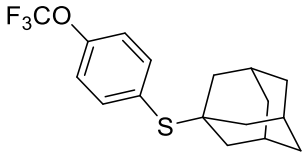

3lb

$C_{17}H_{19}F_3OS$ (328.39 g/mol)

Following GP-B, **3lb** was synthesized using 1-chloro-4-(trifluoromethoxy)benzene (144 µL 1.00 mmol, 1.0 equiv.) and 1-adamantanethiol (185 mg, 1.10 mmol, 1.1 equiv.). Purification by FC (SiO_2, gradient to 9:1 Hex:EtOAc over 20 CV) afforded **3lb** (235 mg, 716 µmol, 72%) as colorless solid.

R_f: 0.42 (Hex:EtOAc 9:1)

m.p.: ambient temperature

^{1}H-NMR (400 MHz, $CDCl_3$, δ): 7.53 – 7.49 (m, 2H), 7.15 (d, J = 7.9 Hz, 2H), 2.02 (s, 3H), 1.80 (d, J = 2.4 Hz, 6H), 1.68 – 1.59 (m, 6H).

^{13}C-NMR (101 MHz, $CDCl_3$, δ): 149.8 (q, *J* = 1.8 Hz), 139.2, 129.3, 120.5 (q, *J* = 257.7 Hz), 48.3, 47.7, 43.7, 36.2, 30.1.

^{19}F-NMR (376 MHz, $CDCl_3$, δ): 57.7.

HR-MS (EI): m/z calc. for [M] 328.110322, found 328.11073.

IR (ATR, $\tilde{\nu}$ [cm^{-1}]): 2905 (s), 2850 (m), 1586 (w), 1485 (w), 1448 (w), 1344 (w), 1251 (vs), 1206 (vs), 1158 (vs), 1097 (s), 1038 (s), 1016 (m), 975 (w), 923 (w), 893 (w), 839 (m), 807 (m), 770 (w), 766 (w), 732 (w), 671 (w).

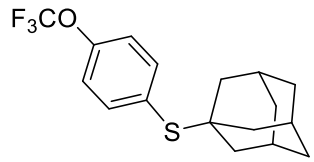
F3CO
S

3lb

7.53
7.52
7.52
7.51
7.50
7.49
7.16
7.14
2.02
1.80
1.79
1.67
1.64
1.61
1.88
1.87
3.21
6.00
6.19
f1 (ppm)

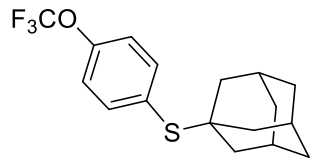
F3CO
S

3lb

149.9
149.9
149.8
149.8
139.2
129.3
124.4
121.8
120.6
119.2
116.7
48.3
47.7
43.7
36.2
30.1
f1 (ppm)

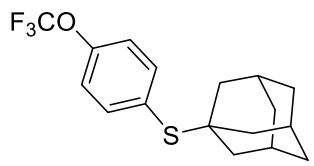
F3CO
S

3Ib

-57.7
10
0
-10
-20
-30
-40
-50
-60
-70
-80
-90
-100
-110
-120
-130
-140
-150
-160
-170
-180
-190
-200
-210
f1 (ppm)

((3s,5s,7s)-adamantan-1-yl)(3-methoxyphenyl)sulfane (3mb)

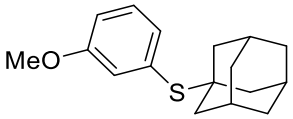

3mb

$C_{17}H_{22}OS$ (274.42 g/mol)

Following GP-B, **3mb** was synthesized using 3-chloroanisole (123 µL, 1.00 mmol, 1.0 equiv.) and 1-adamantanethiol (185 mg, 1.10 mmol, 1.1 equiv.). Purification by FC (SiO_2, gradient to 9:1 Hex:EtOAc over 20 CV) afforded **3mb** (218 mg, 795 µmol, 80%) as colorless solid.

R_f: 0.53 (Hex:EtOAc 9:1)

m.p.: 47.9 – 49.5 °C

^{1}H-NMR (400 MHz, $CDCl_3$, δ): 7.25 – 7.20 (m, 1H), 7.09 (dt, *J* = 7.6, 1.2 Hz, 1H), 7.07 – 7.04 (m, 1H), 6.91 (ddd, *J* = 8.2, 2.6, 1.0 Hz, 1H), 3.81 (s, 3H), 2.01 (s, 3H), 1.83 (d, *J* = 2.9 Hz, 6H), 1.62 (q, *J* = 12.4 Hz, 6H).

^{13}C-NMR (101 MHz, $CDCl_3$, δ): 159.2, 131.7, 130.1, 129.1, 122.9, 114.6, 55.5, 48.2, 43.8, 36.3, 30.1.

HR-MS (EI): m/z calc. for [M] 274.138587, found 274.13497.

IR (ATR, $\tilde{\nu}$ [cm^{-1}]): 2891 (m), 2846 (w), 1567 (m), 1459 (m), 1418 (m), 1343 (w), 1280 (s), 1224 (s), 1179 (w), 1101 (w), 1075 (w), 1038 (s), 975 (w), 878 (m), 848 (w), 822 (w), 774 (s), 688 (s).

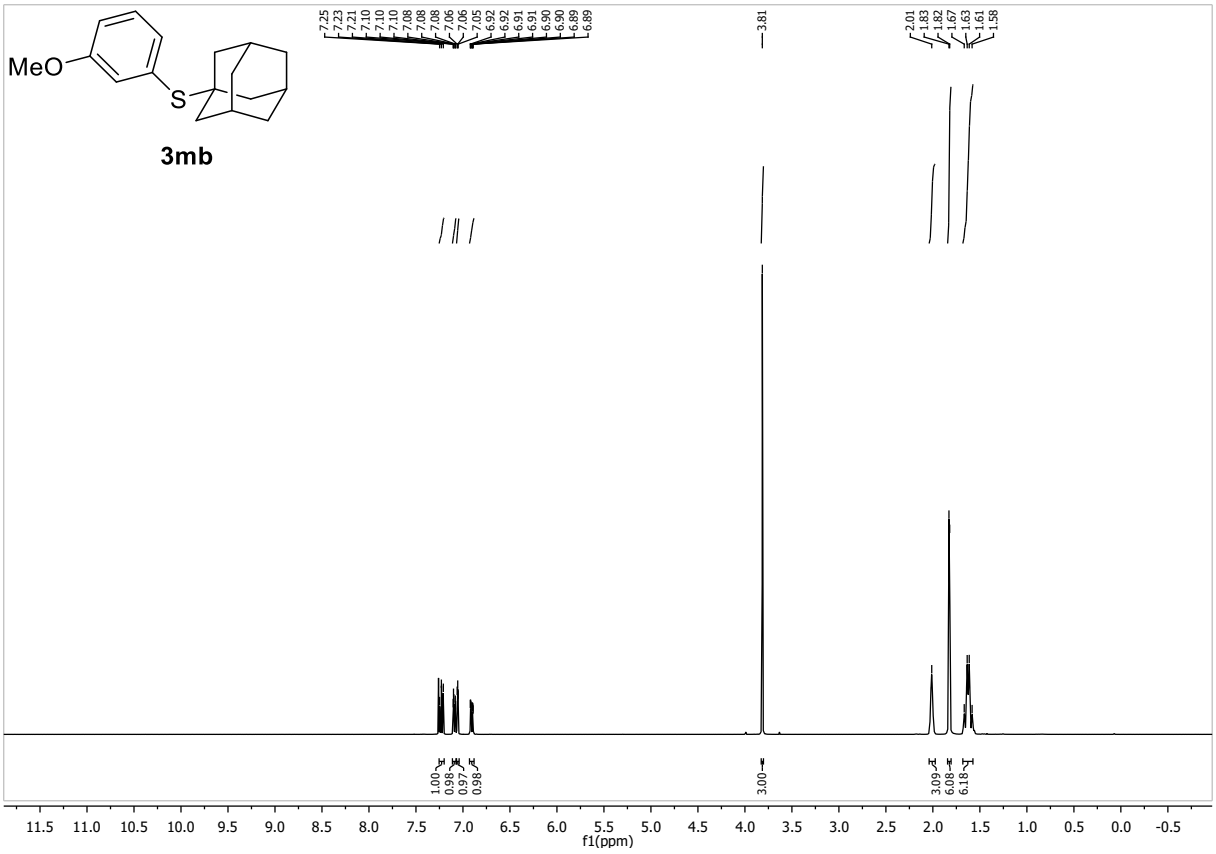
MeO
S
3mb
7.25
7.23
7.21
7.10
7.10
7.10
7.08
7.08
7.08
7.06
7.06
7.05
6.92
6.92
6.91
6.91
6.90
6.90
6.89
6.89
3.81
2.01
1.83
1.82
1.67
1.63
1.61
1.58
1.00
0.98
0.97
0.98
3.00
3.09
6.08
6.18
11.5 11.0 10.5 10.0 9.5 9.0 8.5 8.0 7.5 7.0 6.5 6.0 5.5 5.0 4.5 4.0 3.5 3.0 2.5 2.0 1.5 1.0 0.5 0.0 -0.5
f1(ppm)

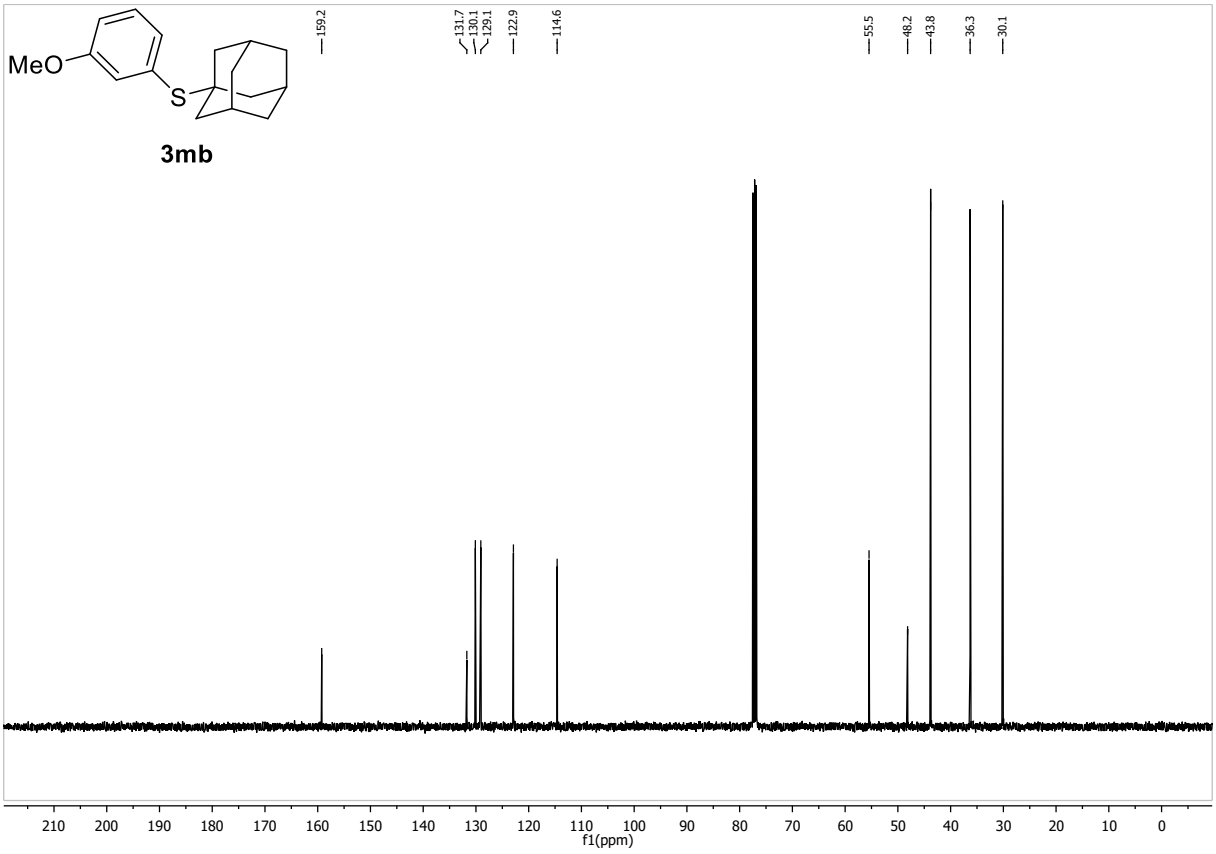
MeO
S
3mb
159.2
131.7
130.1
129.1
122.9
114.6
55.5
48.2
43.8
36.3
30.1
210 200 190 180 170 160 150 140 130 120 110 100 90 80 70 60 50 40 30 20 10 0
f1(ppm)

3-(((3s,5s,7s)-adamantan-1-yl)thio)benzonitrile (3nb)

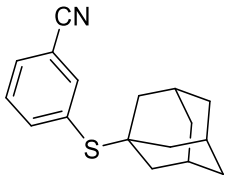

3nb

$C_{17}H_{19}NS$ (269.41 g/mol)

Following GP-B, **3nb** was synthesized using 3-chlorobenzonitril (121 µL 1.00 mmol, 1.0 equiv.) and 1-adamantanethiol (185 mg, 1.10 mmol, 1.1 equiv.). Purification by FC (SiO_2, gradient to 9:1 Hex:EtOAc over 20 CV) afforded **3nb** (229 mg, 848 µmol, 85%) as colorless solid.

R_f: 0.53 (Hex:EtOAc 9:1)

m.p.: 80.0 – 81.2 °C

^{1}H-NMR (400 MHz, $CDCl_3$, δ): 7.78 (t, *J* = 1.7 Hz, 1H), 7.72 (dt, *J* = 7.8, 1.7 Hz, 1H), 7.64 (dt, *J* = 7.8, 1.7 Hz, 1H), 7.43 (t, *J* = 7.8 Hz, 1H), 2.03 (s, 3H), 1.79 (d, *J* = 2.9 Hz, 6H), 1.69 – 1.55 (m, 6H).

^{13}C-NMR (101 MHz, $CDCl_3$, δ): 142.0, 140.7, 132.9, 132.2, 129.2, 118.5, 112.7, 49.1, 43.7, 36.1, 30.1.

HR-MS (ESI): m/z calc. for $[M+Na]^+$292.11304, found 292.11332.

IR (ATR, $\tilde{\nu}$ [cm^{-1}]): 2913 (m), 2883 (m), 2850 (m), 2223 (w), 1724 (w), 1560 (w), 1455 (m), 1396 (m), 1344 (w), 1295 (m), 1258 (w), 1232 (w), 1188 (w), 1098 (w), 1034 (m), 978 (w), 930 (w), 889 (w), 822 (w), 796 (s), 744 (w), 684 (s).

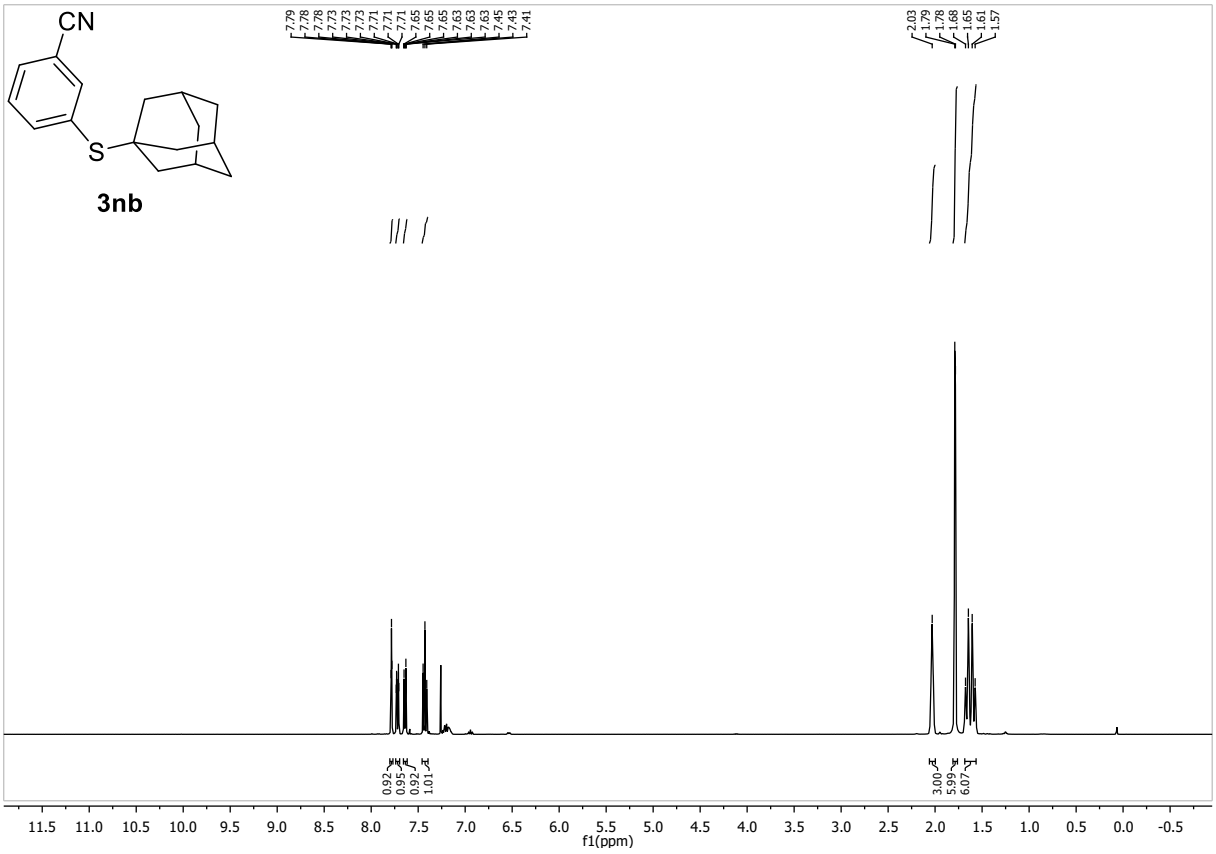
CN
S
3nb
7.79
7.78
7.78
7.73
7.73
7.73
7.71
7.71
7.71
7.65
7.65
7.63
7.63
7.45
7.43
7.41
2.03
1.79
1.78
1.68
1.65
1.61
1.57
0.92
0.95
0.92
1.01
3.00
5.99
6.07
11.5 11.0 10.5 10.0 9.5 9.0 8.5 8.0 7.5 7.0 6.5 6.0 5.5 5.0 4.5 4.0 3.5 3.0 2.5 2.0 1.5 1.0 0.5 0.0 -0.5
f1(ppm)

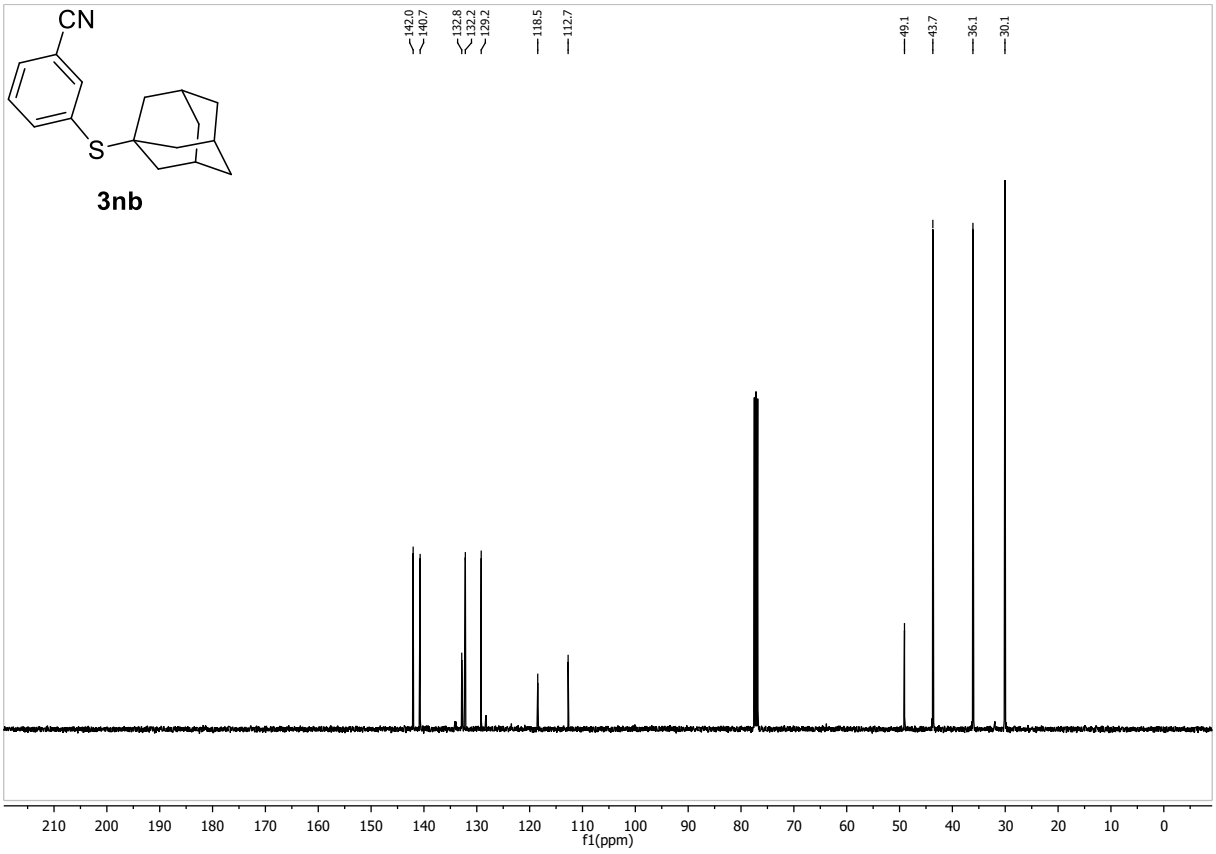
CN
S
3nb
142.0
140.7
132.8
132.2
129.2
118.5
112.7
49.1
43.7
36.1
30.1
210 200 190 180 170 160 150 140 130 120 110 100 90 80 70 60 50 40 30 20 10 0
f1(ppm)

3-(((3s,5s,7s)-adamantan-1-yl)thio)-N,N-dimethylaniline (3ob)

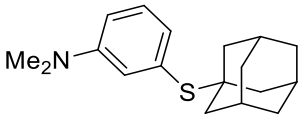

3ob

$C_{18}H_{25}NS$ (287.47 g/mol)

Following GP-B, **3ob** was synthesized using 3-chloro-N,N-dimethylaniline (139 µL 1.00 mmol, 1.0 equiv.) and 1-adamantanethiol (185 mg, 1.10 mmol, 1.1 equiv.) Purification by FC (SiO_2, 5 CV Hex, gradient to 95:5 Hex:EtOAc over 15 CV) afforded **3ob** (275 mg, 955 µmol, 96%) as off-white solid.

R_f: 0.56 (Hex:EtOAc 9:1)

m.p.: 94.7 – 96.4 °C

^{1}H-NMR (400 MHz, $CDCl_3$, δ): 7.18 (t, *J* = 7.8 Hz, 1H), 6.90 – 6.85 (m, 2H), 6.73 (d, *J* = 7.8 Hz, 1H), 2.96 (s, 6H), 2.01 (s, 3H), 1.84 (d, *J* = 3.0 Hz, 6H), 1.68 – 1.56 (m, 6H).

^{13}C-NMR (101 MHz, $CDCl_3$, δ): 150.5, 131.0, 128.8, 125.9, 121.9, 112.8, 47.8, 43.9, 40.8, 36.3, 30.2.

HR-MS (ESI): m/z calc. for $[M+Na]^+$ 288,17805, found 288,17819.

IR (ATR, $\tilde{\nu}$ [cm^{-1}]): 2891 (m), 2846 (w), 2801 (w), 1586 (m), 1485 (m), 1440 (m), 1404 (w), 1347 (m), 1292 (m), 1229 (m), 1176 (w), 1098 (w), 1064 (w), 1038 (m), 986 (m), 956 (w), 878 (w), 837 (m), 807 (w), 769 (m), 744 (w), 688 (m).

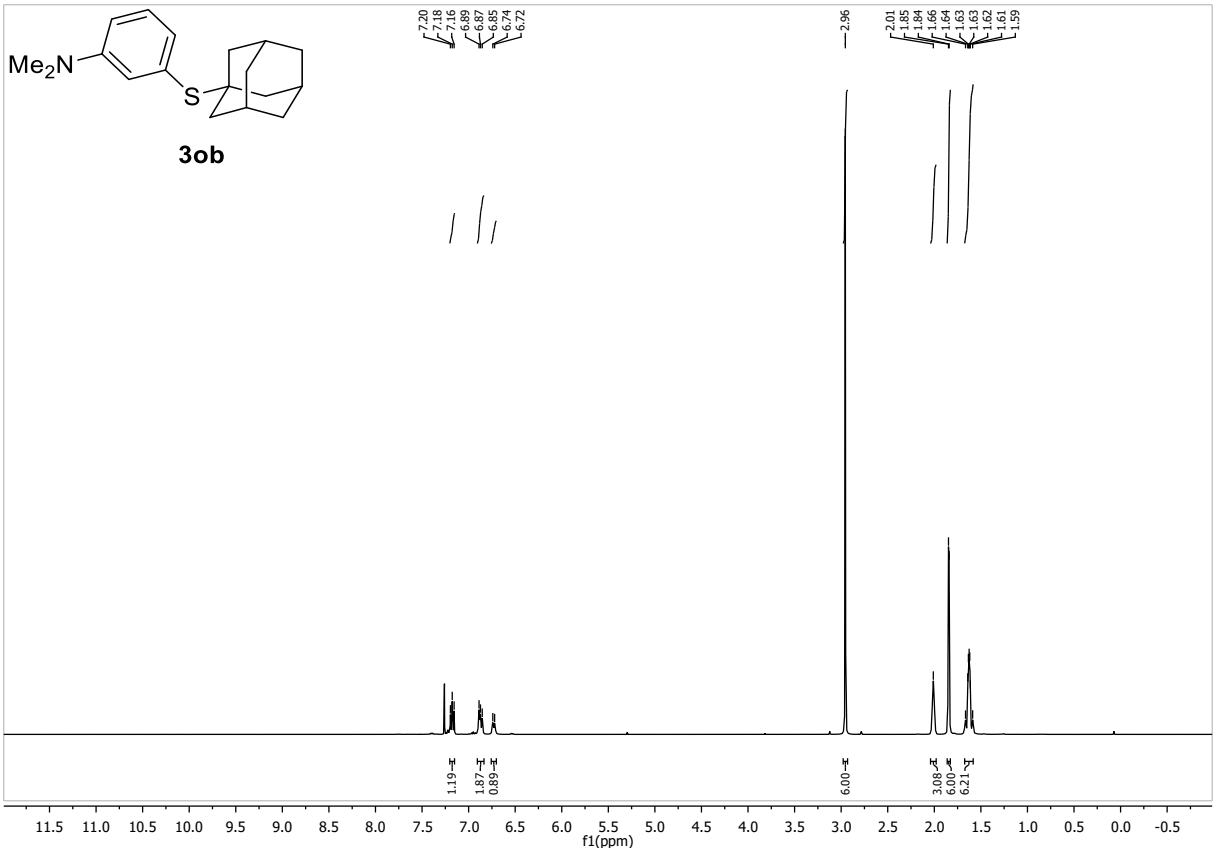
Me2N
S
3ob
7.20
7.18
7.16
6.89
6.87
6.85
6.74
6.72
2.96
2.01
1.85
1.84
1.66
1.64
1.63
1.63
1.62
1.61
1.59
1.19
1.87
0.89
6.00
3.08
6.00
6.21
11.5 11.0 10.5 10.0 9.5 9.0 8.5 8.0 7.5 7.0 6.5 6.0 5.5 5.0 4.5 4.0 3.5 3.0 2.5 2.0 1.5 1.0 0.5 0.0 -0.5
f1(ppm)

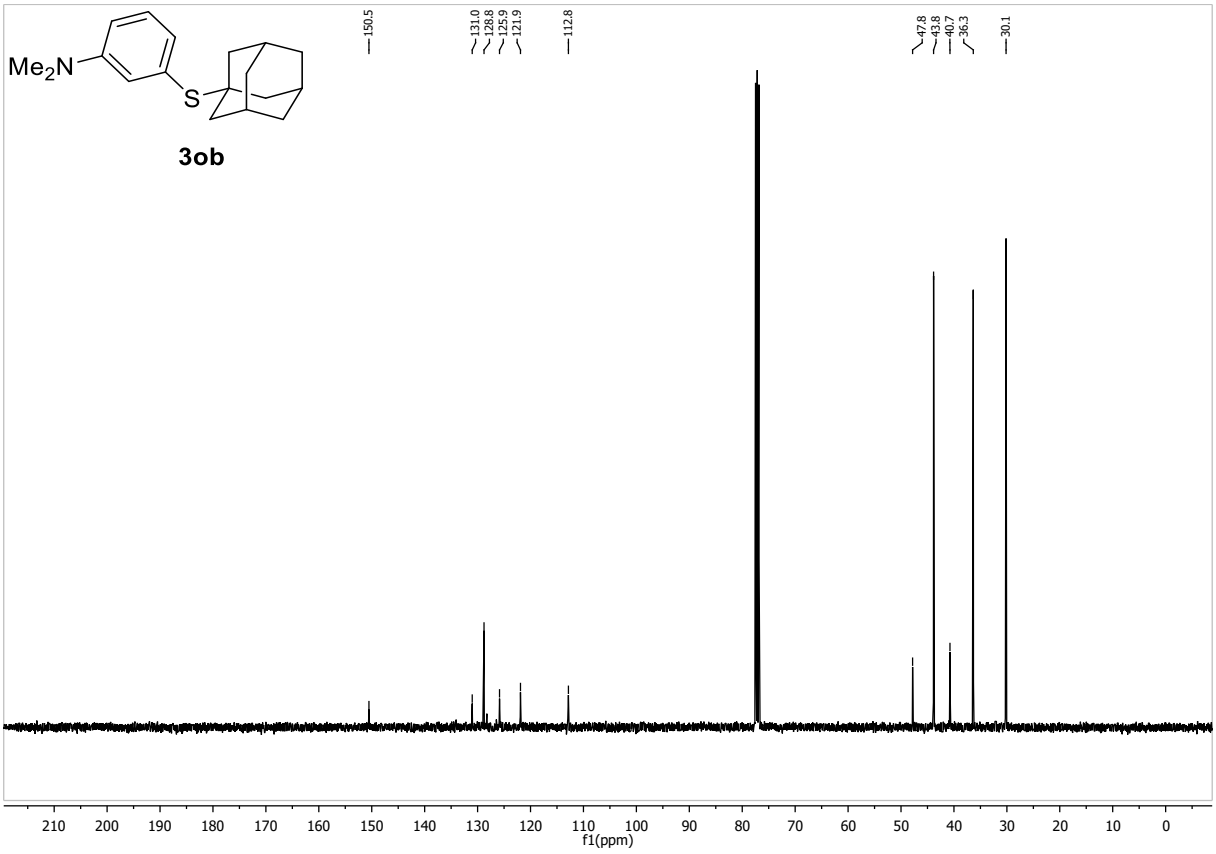
Me2N
S
3ob
150.5
131.0
128.8
125.9
121.9
112.8
47.8
43.8
40.7
36.3
30.1
210 200 190 180 170 160 150 140 130 120 110 100 90 80 70 60 50 40 30 20 10 0
f1(ppm)

1-(3-(((3s,5s,7s)-adamantan-1-yl)thio)phenyl)ethan-1-ol (3pb)

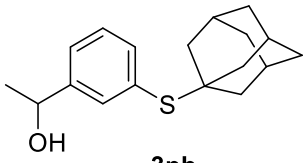

3pb

$C_{18}H_{24}OS$ (288.45 g/mol)

Following GP-B, **3pb** was synthesized using 1-(3-chlorophenyl)ethan-1-ol (134 µL 1.00 mmol, 1.0 equiv.) and 1-adamantanethiol (185 mg, 1.10 mmol, 1.1 equiv.). Purification by FC (SiO_2, gradient to 8:2 Hex:EtOAc over 20 CV) afforded **3pb** (244 mg, 847 µmol, 85%) as colorless solid.

R_f: 0.24 (Hex:EtOAc 9:1)

m.p.: 95.0 – 96.2 °C

^{1}H-NMR (400 MHz, $CDCl_3$, δ): 7.49 (t, *J* = 1.5 Hz, 1H), 7.42 – 7.36 (m, 2H), 7.30 (t, *J* = 7.6 Hz, 1H), 4.90 (q, *J* = 6.5 Hz, 1H), 2.01 (s, 3H), 1.81 (d, *J* = 2.6 Hz, 6H), 1.62 (q, *J* = 12.3 Hz, 6H), 1.50 (d, *J* = 6.5 Hz, 3H).

^{13}C-NMR (101 MHz, $CDCl_3$, δ): 146.1, 136.8, 134.8, 130.8, 128.5, 125.8, 70.2, 48.0, 43.8, 36.3, 30.1, 25.4.

HR-MS (ESI): m/z calc. for [M + Na^+] 311.14401, found 311.14432.

IR (ATR, $\tilde{\nu}$ [cm^{-1}]): 3299 (w), 2899 (m), 2846 (w), 1581 (w), 1448 (w), 1418 (w), 1370 (w), 1337 (w), 1299 (m), 1258 (w), 1202 (w), 1079 (m), 1034 (m), 971 (w), 907 (m), 825 (w), 792 (m), 770 (w), 702 (s).

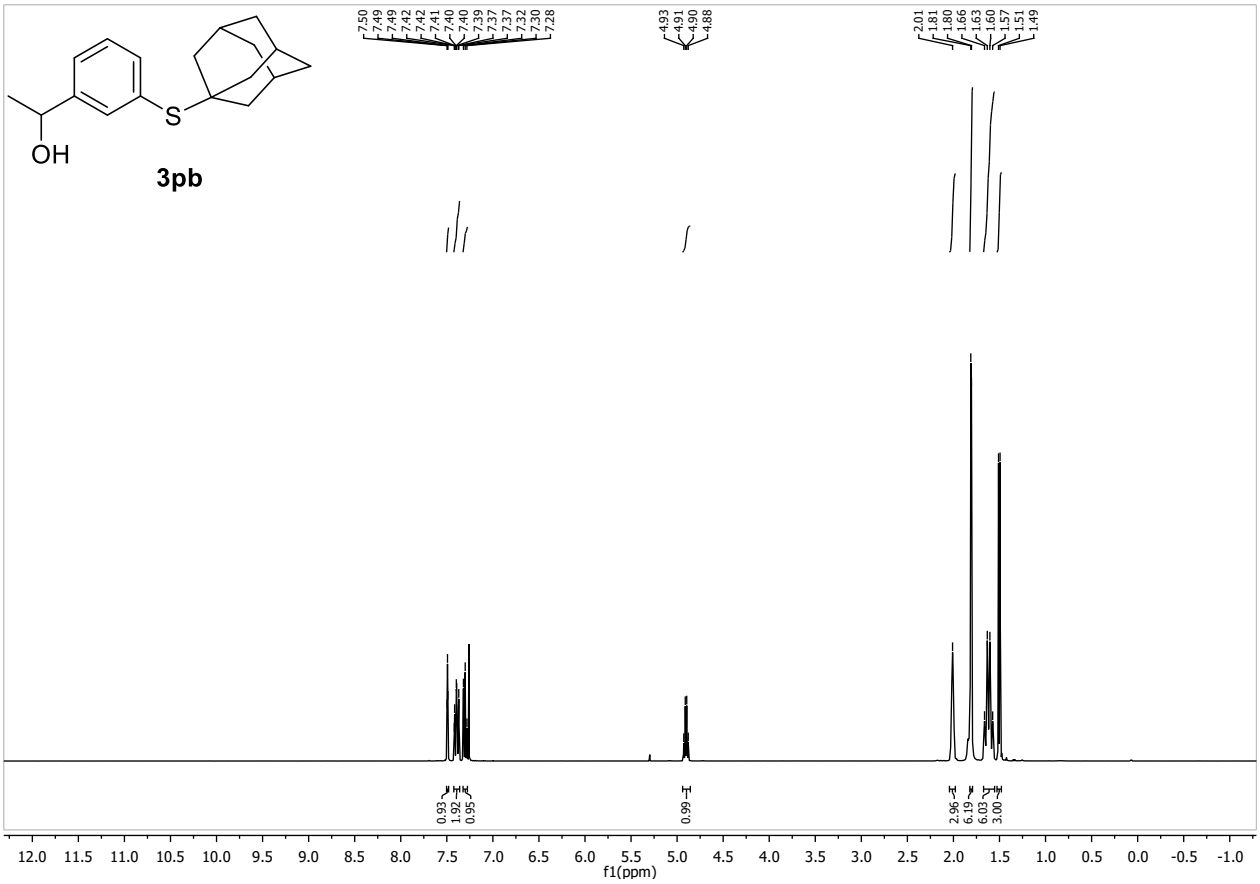
7.50
7.49
7.49
7.42
7.42
7.41
7.40
7.40
7.39
7.37
7.37
7.32
7.30
7.28
4.93
4.91
4.90
4.88
2.01
1.81
1.80
1.66
1.63
1.60
1.57
1.51
1.49
S
OH
3pb
0.93
1.92
0.95
0.99
2.96
6.19
6.03
3.00
12.0 11.5 11.0 10.5 10.0 9.5 9.0 8.5 8.0 7.5 7.0 6.5 6.0 5.5 5.0 4.5 4.0 3.5 3.0 2.5 2.0 1.5 1.0 0.5 0.0 -0.5 -1.0
f1(ppm)

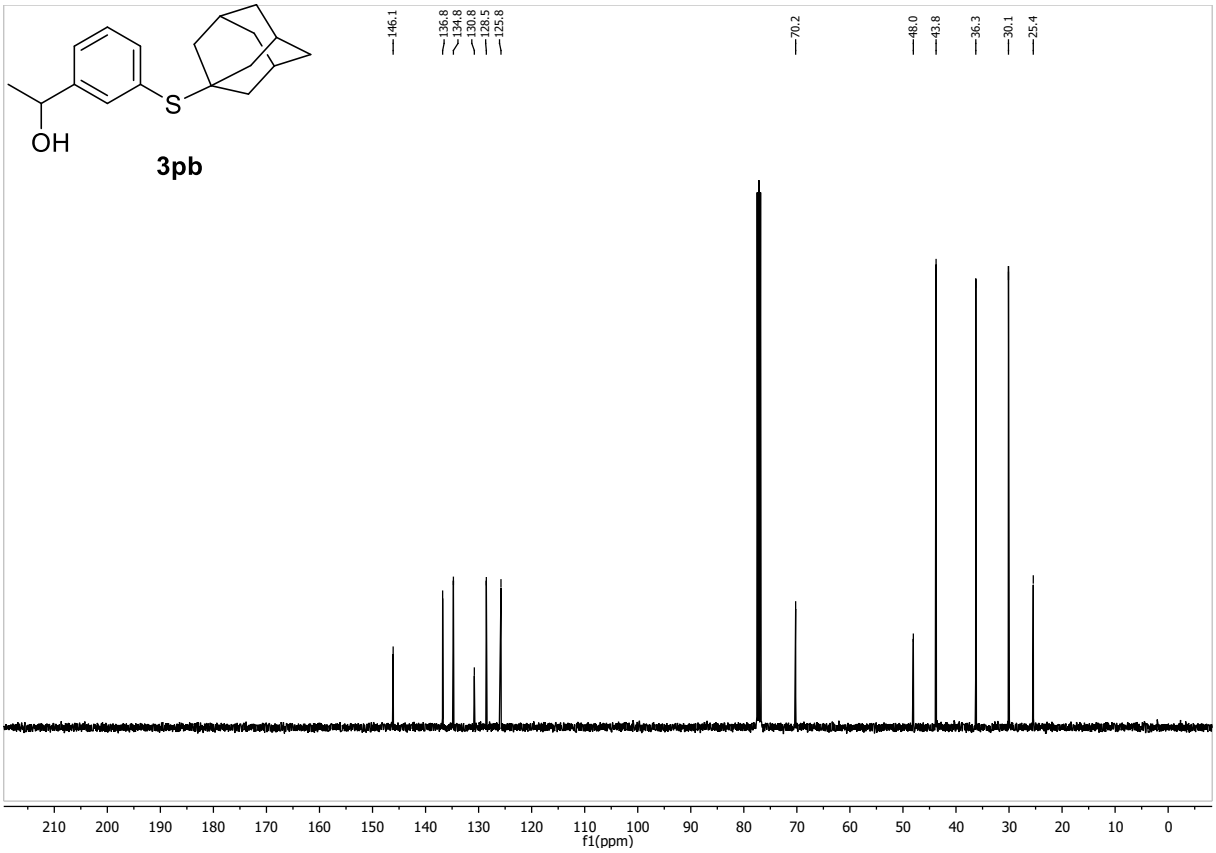
146.1
136.8
134.8
130.8
128.5
125.8
70.2
48.0
43.8
36.3
30.1
25.4
S
OH
3pb
210 200 190 180 170 160 150 140 130 120 110 100 90 80 70 60 50 40 30 20 10 0
f1(ppm)

((3s,5s,7s)-adamantan-1-yl)(3,4-dimethylphenyl)sulfane (3qb)

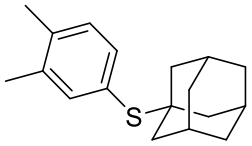

3qb

$C_{18}H_{24}S$ (272.45 g/mol)

Following GP-B, **3qb** was synthesized using 4-chloro-o-xylene (134 µL 1.00 mmol, 1.0 equiv.) and 1-adamantanethiol (185 mg, 1.10 mmol, 1.1 equiv.) Purification by FC (SiO_2, 5 CV Hex, gradient to 8:2 Hex:EtOAc over 15 CV) afforded **3qb** (247 mg, 906 µmol, 91%) as colorless solid.

R_f: 0.80 (Hex:EtOAc 9:1)

m.p.: 78.8 – 80.6 °C

^{1}H-NMR (400 MHz, $CDCl_3$, δ): 7.27 (s, 1H), 7.22 (dd, *J* = 7.8, 1.6 Hz, 1H), 7.07 (d, *J* = 7.8 Hz, 1H), 2.264 (s, 3H), 2.257 (s, 3H) 2.00 (s, 3H), 1.80 (d, *J* = 2.6 Hz, 6H), 1.62 (q, *J* = 7.9 Hz, 6H).

^{13}C-NMR (101 MHz, $CDCl_3$, δ): 138.9, 137.4, 136.7, 135.2, 129.7, 127.3, 47.6, 43.7, 36.3, 30.1, 19.8, 19.7.

HR-MS (EI): m/z calc. for $[M]^+$ 272.159322, found 272.15695.

IR (ATR, $\tilde{\nu}$ [cm^{-1}]): 2894 (s), 2846 (m), 1590 (w), 1560 (w), 1481 (w), 1445 (m), 1377 (w), 1343 (m), 1295 (m), 1255 (w), 1225 (w), 1180 (w), 1128 (w), 1098 (w), 1034 (m), 986 (w), 965 (w), 885 (m), 822 (s), 758 (w), 710 (w), 684 (w).

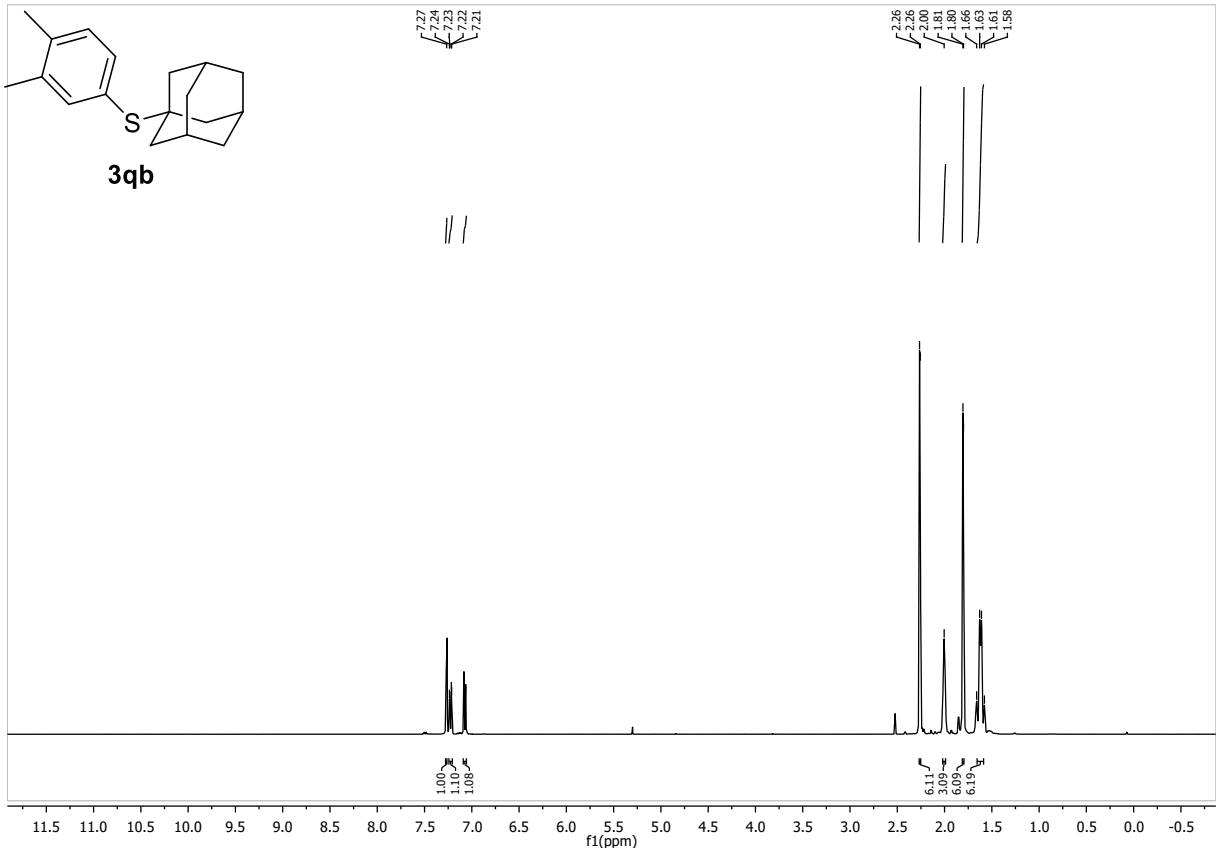
S
3qb
7.27
7.24
7.23
7.22
7.21
2.26
2.26
2.00
1.81
1.80
1.66
1.63
1.61
1.58
1.00
1.10
1.08
6.11
3.09
6.09
6.19
11.5 11.0 10.5 10.0 9.5 9.0 8.5 8.0 7.5 7.0 6.5 6.0 5.5 5.0 4.5 4.0 3.5 3.0 2.5 2.0 1.5 1.0 0.5 0.0 -0.5
f1(ppm)

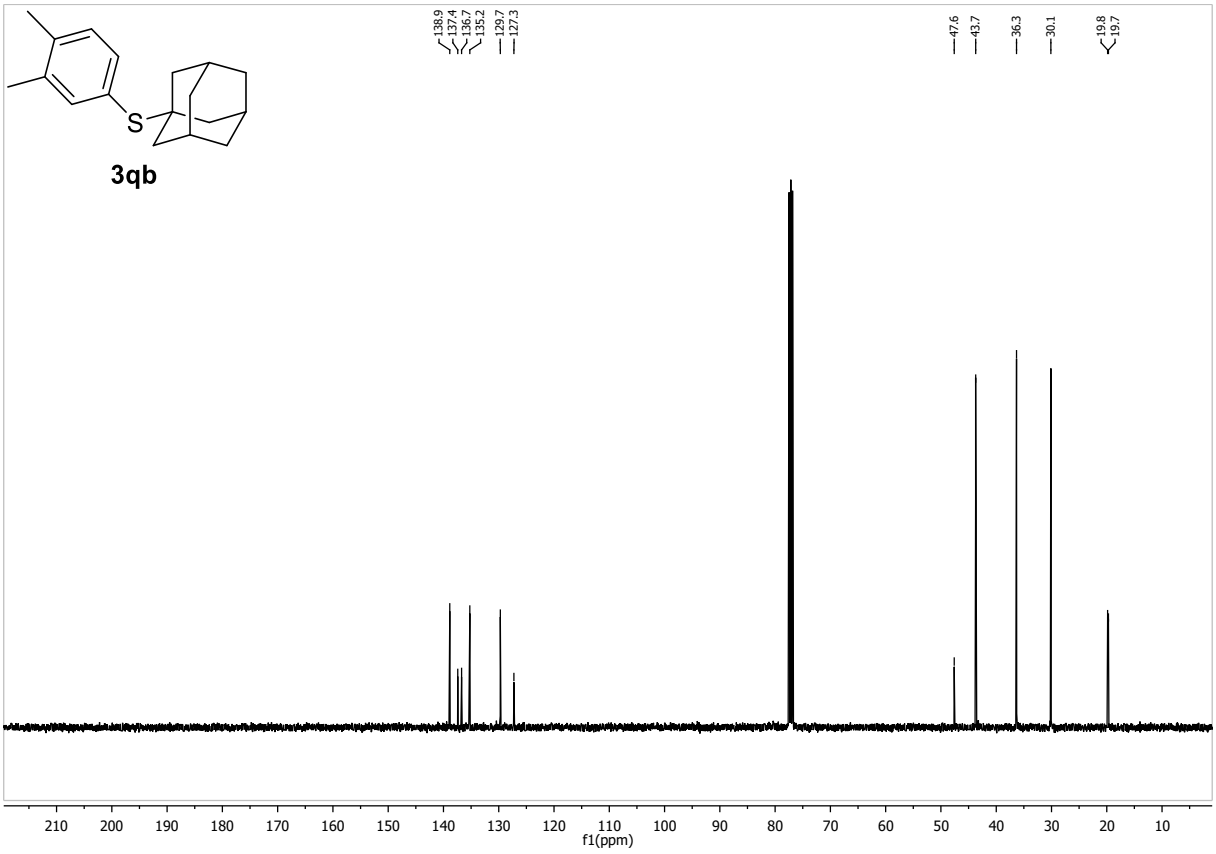
S
3qb
138.9
137.4
136.7
135.2
129.7
127.3
47.6
43.7
36.3
30.1
19.8
19.7
210 200 190 180 170 160 150 140 130 120 110 100 90 80 70 60 50 40 30 20 10
f1(ppm)

((3s,5s,7s)-adamantan-1-yl)(o-tolyl)sulfane(3rb)

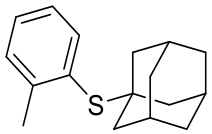

3rb

$C_{17}H_{22}S$ (258.42 g/mol)

Following GP-B, 3rb was synthesized using 1-chloro-2-methylbenzene (117 µL 1.00 mmol, 1.0 equiv.) and 1-adamantanethiol (185 mg, 1.10 mmol, 1.1 equiv.) Purification by FC (SiO_2, 5 CV Hex, gradient to 9:1 Hex:EtOAc over 15 CV) afforded **3rb** (39 mg, 150 µmol, 15%) as white solid. Conforms to reported analytical data.[24]

R_f: 0.64 (Hex:EtOAc 95:5)

^{1}H-NMR (400 MHz, $CDCl_3$, δ): 7.49 (dd, *J* = 7.5, 1.3 Hz, 1H), 7.29 – 7.22 (m, 2H), 7.17 – 7.10 (m, 1H), 2.52 (s, 3H), 2.00 (s, 3H), 1.85 (d, *J* = 3.1 Hz, 6H), 1.63 (d, *J* = 3.6 Hz, 6H).

^{13}C-NMR (101 MHz, $CDCl_3$, δ): 144.1, 139.3, 130.3, 130.2, 128.8, 125.5, 49.4, 43.8, 36.2, 30.0, 22.1.

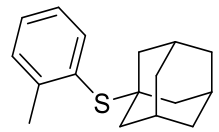

3rb

7.50
7.50
7.48
7.48
7.29
7.28
7.27
7.26
7.25
7.24
7.23
7.22
7.15
7.15
7.13
7.13
7.13
7.12
7.11
2.52
2.00
1.85
1.85
1.67
1.66
1.63
1.62
1.61
1.58
1.58
0.97
2.47
0.98
3.00
3.13
6.05
6.15
f1 (ppm)

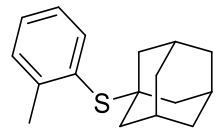

3rb

144.1
139.3
130.3
130.2
128.8
125.5
49.4
43.8
36.2
30.0
22.1
f1 (ppm)

((3s,5s,7s)-adamantan-1-yl)(3-chloro-4-methylphenyl)sulfane (3sb)

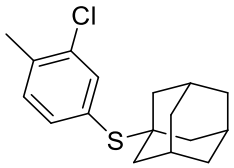

3sb

$C_{17}H_{21}ClS$ (292.87 g/mol)

Following GP-B, **3sb** was synthesized using 2,4-dichlorotoluene (161 mg, 1.00 mmol, 1.0 equiv.) and 1-adamantanethiol (185 mg, 1.10 mmol, 1.1 equiv.). Purification by FC (SiO_2, Hex 5 CV, gradient to 9:1 Hex:EtOAc over 20 CV) afforded **3sb** (250 mg, 293 µmol, 85%) as colorless solid.

R_f: 0.84 (Hex:EtOAc 9:1)

m.p.: 93.7 – 95.6 °C

^{1}H-NMR (400 MHz, $CDCl_3$, δ): 7.49 (d, *J* = 1.8 Hz, 1H), 7.26 (dd, *J* = 1.8 Hz, 7.8 Hz, 1H), 7.17 (d, *J* = 7.8 Hz, 1H), 2.38 (s, 3H), 2.02 (s, 3H), 1.79 (d, *J* = 2.7 Hz, 6H), 1.62 (q, *J* = 12.3 Hz, 6H).

^{13}C-NMR (101 MHz, $CDCl_3$, δ): 137.7, 136.8, 136.0, 134.0, 130.7, 129.3, 48.3, 43.7, 36.3, 36.3, 30.2, 30.1, 20.0.

HR-MS (EI): m/z calc. for [M] 292.104700, found 292.10531.

IR (ATR, $\tilde{\nu}$ [cm^{-1}]): 2911 (m), 2900 (m), 2849 (m), 1582 (w), 1545 (w), 1444 (m), 1370 (w), 1340 (w), 1295 (m), 1254 (w), 1180 (w), 1142 (w), 1102 (w), 1038 (m), 978 (w), 956 (w), 930 (w), 885 (w), 822 (s), 755 (w), 699 (m).

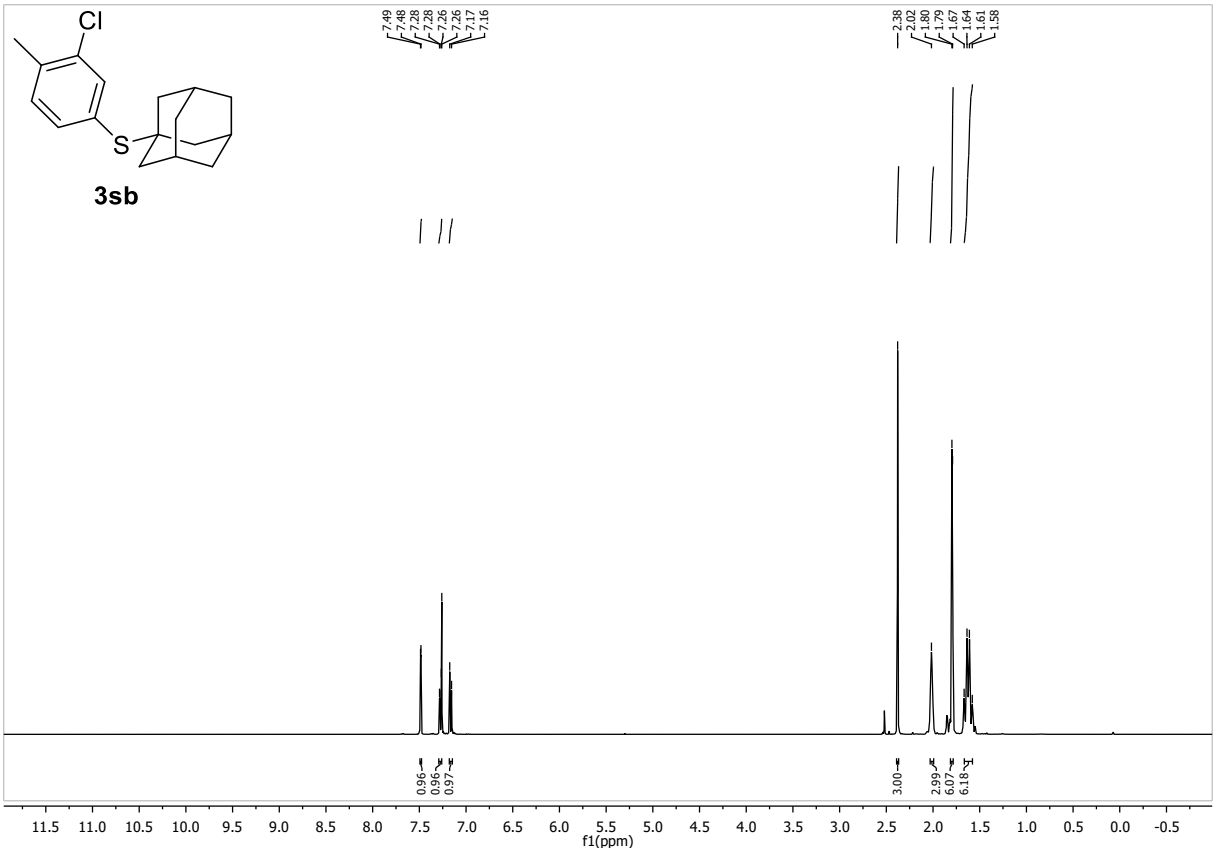
Cl
S
3sb
7.49
7.48
7.28
7.28
7.26
7.26
7.17
7.16
2.38
2.02
1.80
1.79
1.67
1.64
1.61
1.58
0.96
0.96
0.97
3.00
2.99
6.07
6.18
f1(ppm)

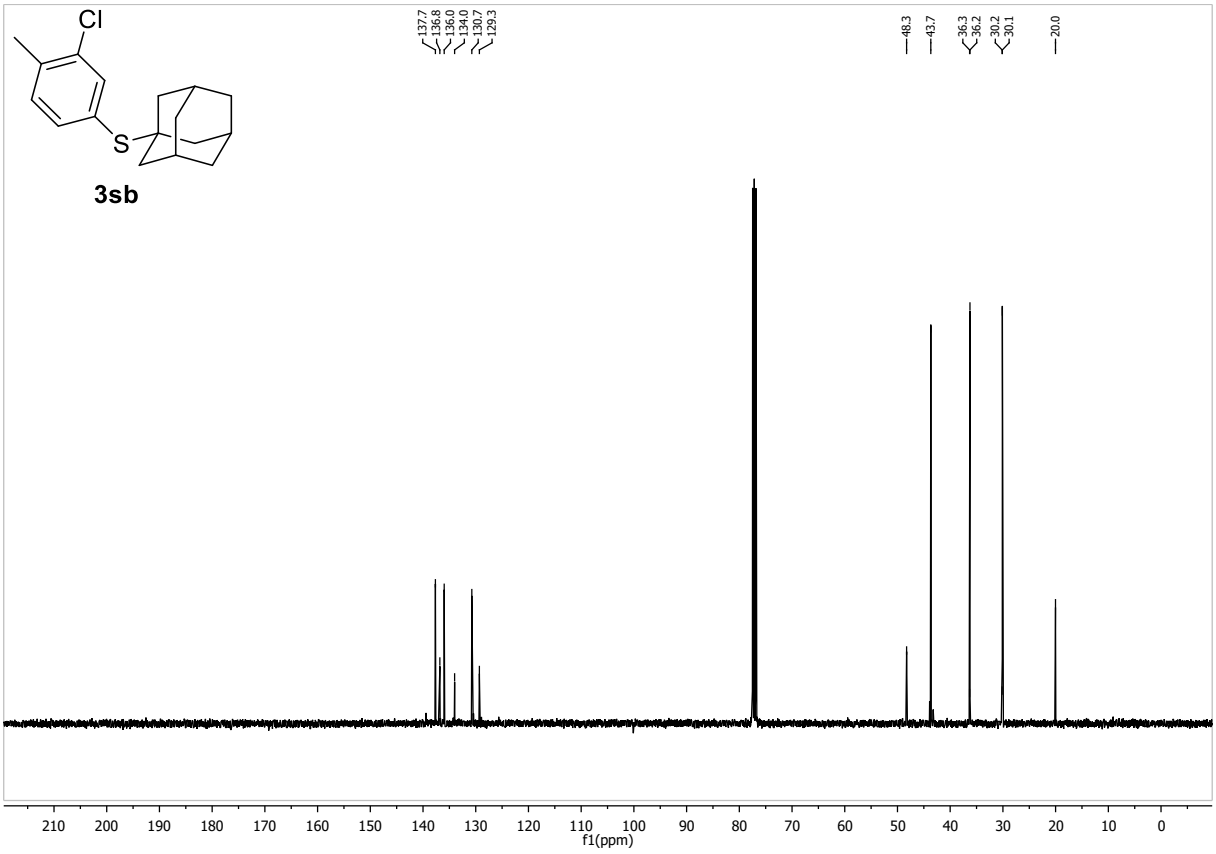
Cl
S
3sb
137.7
136.8
136.0
134.0
130.7
129.3
48.3
43.7
36.3
36.2
30.2
30.1
20.0
f1(ppm)

1,3-bis(((3S,5S,7S)-adamantan-1-yl)thio)benzene (3tb)

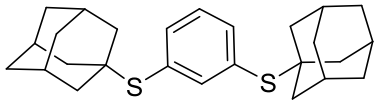

3tb

$C_{26}H_{34}S_2$ (410.68g/mol)

Following GP-B, **3tb** was synthesized using 1,3-dichlorbenzene (74 mg, 0.50 mmol, 1.0 equiv.) and 1-adamantanethiol (185 mg, 1.10 mmol, 1.1 equiv.). Purification by FC (SiO_2, 99:1 Hex:EtOAc 20 CV) afforded **3tb** (153 mg, 374 µmol, 75%) as colorless solid.

R_f: 0.78 (Hex:EtOAc 9:1)

m.p.: 170.1 – 171.8 °C

^{1}H-NMR (400 MHz, $CDCl_3$, δ): 7.68 (t, *J* = 1.7 Hz, 1H), 7.49 (dd, *J* = 7.7, 1.7 Hz, 2H), 7.27 (t, *J* = 7.7 Hz, 1H), 2.00 (s, 6H), 1.81 (d, *J* = 2.6 Hz, 12H), 1.61 (q, *J* = 12.1 Hz, 12H).

^{13}C-NMR (101 MHz, $CDCl_3$, δ): 146.6, 138.0, 130.7, 128.2, 48.4, 43.8, 36.3, 30.1.

HR-MS (EI): m/z calc. for [M] 410.209643, found 410.21066.

IR (ATR, $\tilde{\nu}$ [cm^{-1}]): 2895 (m), 2846 (m), 1746 (w), 1720 (w), 1556 (w), 1445 (m), 1381 (w), 1340 (w), 1291 (w), 1254 (w), 1176 (w), 1101 (w), 1068 (w), 1034 (m), 1005 (w), 968 (w), 915 (w), 885 (w), 822 (w), 792 (m), 744 (w), 692 (m).

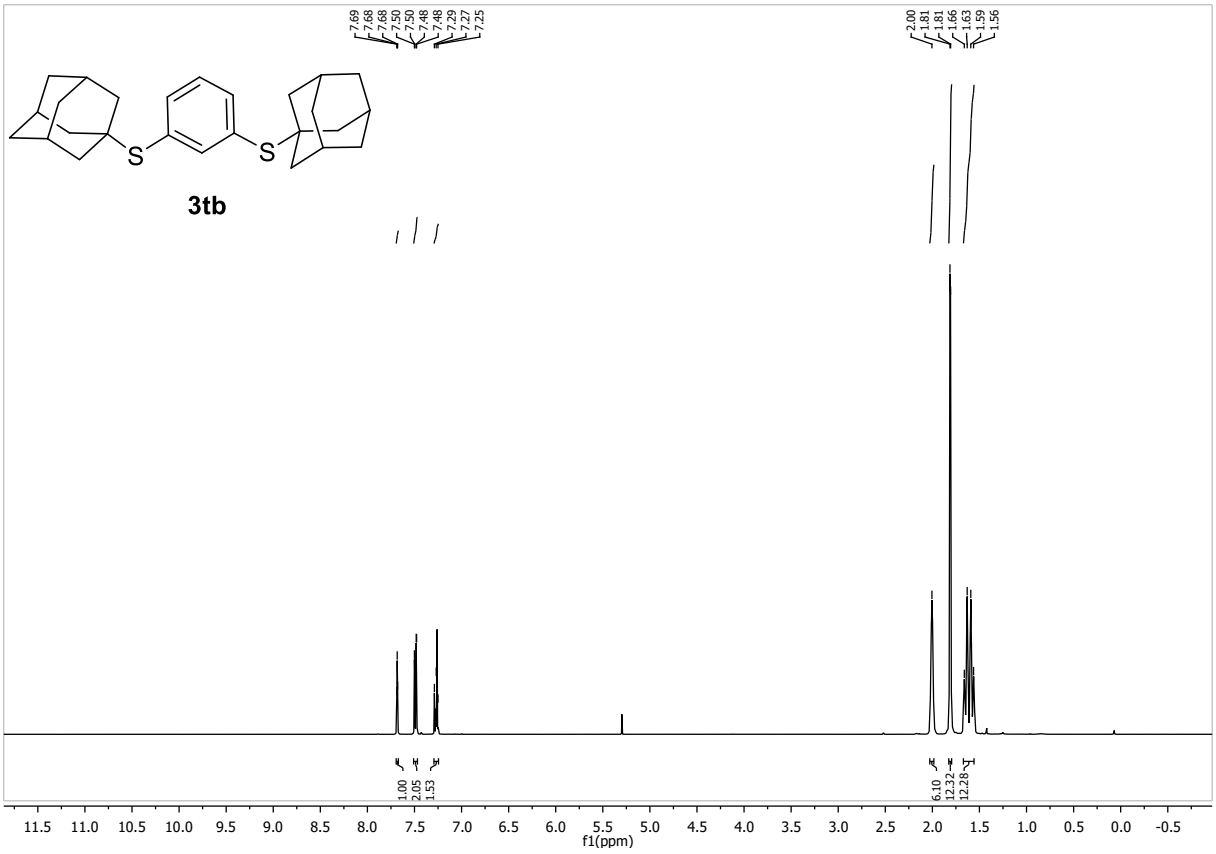
7.69
7.68
7.68
7.50
7.50
7.48
7.48
7.29
7.27
7.25
2.00
1.81
1.81
1.66
1.63
1.59
1.56
S
S
3tb
1.00
2.05
1.53
6.10
12.32
12.28
11.5 11.0 10.5 10.0 9.5 9.0 8.5 8.0 7.5 7.0 6.5 6.0 5.5 5.0 4.5 4.0 3.5 3.0 2.5 2.0 1.5 1.0 0.5 0.0 -0.5
f1(ppm)

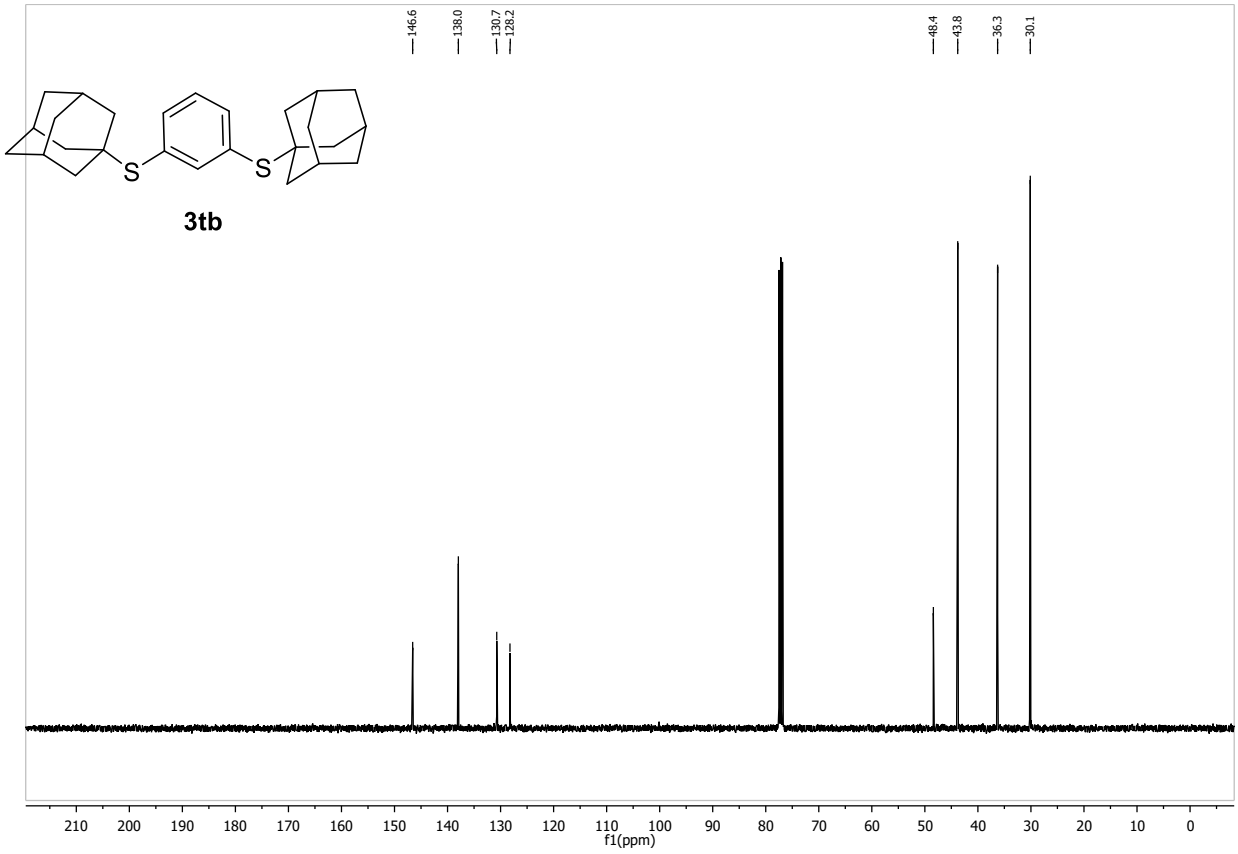
146.6
138.0
130.7
128.2
48.4
43.8
36.3
30.1
S
S
3tb
210 200 190 180 170 160 150 140 130 120 110 100 90 80 70 60 50 40 30 20 10 0
f1(ppm)

3-(((3s,5s,7s)-adamantan-1-yl)thio)pyridine (3ub)

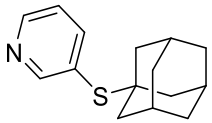

3ub

$C_{15}H_{19}NS$ (245.38 g/mol)

Following GP-B, **3ub** was synthesized using 3-chloropyridine (94 µL 1.0 mmol, 1.0 equiv.) and 1-adamantanethiol (185 mg, 1.10 mmol, 1.1 equiv.). Purification by FC (SiO_2, gradient to 8:2 Hex:EtOAc over 15 CV) afforded **3ub** (91 mg, 0.37 mmol, 37%) as colorless solid.

R_f: 0.22 (Hex:EtOAc 9:1)

m.p.: 92.2 – 93.3 °C

^{1}H-NMR (400 MHz, $CDCl_3$, δ): 8.68 (dd, *J* = 2.1, 0.7 Hz, 1H), 8.58 (dd, *J* = 4.8, 1.6 Hz, 1H), 7.84 – 7.79 (m, 1H), 7.30 – 7.25 (m, 1H), 2.02 (s, 3H), 1.79 (d, *J* = 2.6 Hz, 6H), 1.62 (q, *J* = 12.4 Hz, 6H).

^{13}C-NMR (101 MHz, $CDCl_3$, δ): 156.9, 149.4, 145.1, 128.0, 123.5, 48.7, 43.7, 36.1, 30.1.

HR-MS (ESI): m/z calc. for $[M+H]^+$ 246.13110, found 246.13112.

IR (ATR, $\tilde{\nu}$ [cm^{-1}]): 2898 (m), 2846 (w), 1560 (w), 1449 (w), 1396 (w), 1343 (w), 1292 (w), 1254 (w), 1184 (w), 1104 (w), 1025 (m), 1016 (w), 969 (w), 956 (w), 930 (w), 889 (w), 807 (m), 770 (w), 732 (w), 703 (m).

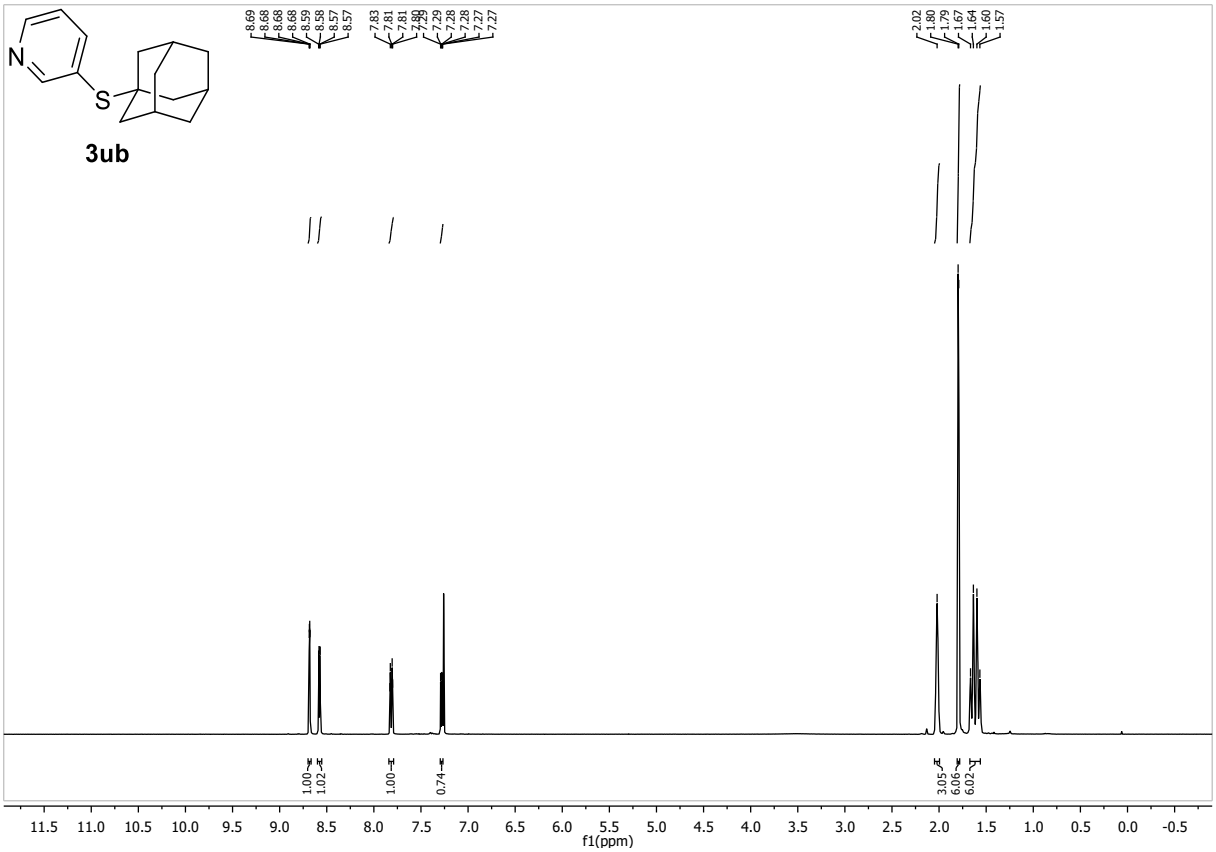
3ub
8.69
8.68
8.68
8.68
8.59
8.58
8.57
8.57
7.83
7.81
7.81
7.29
7.28
7.28
7.27
7.27
2.02
1.80
1.79
1.67
1.64
1.60
1.57
1.00
1.02
1.00
0.74
3.05
6.06
6.02
f1(ppm)

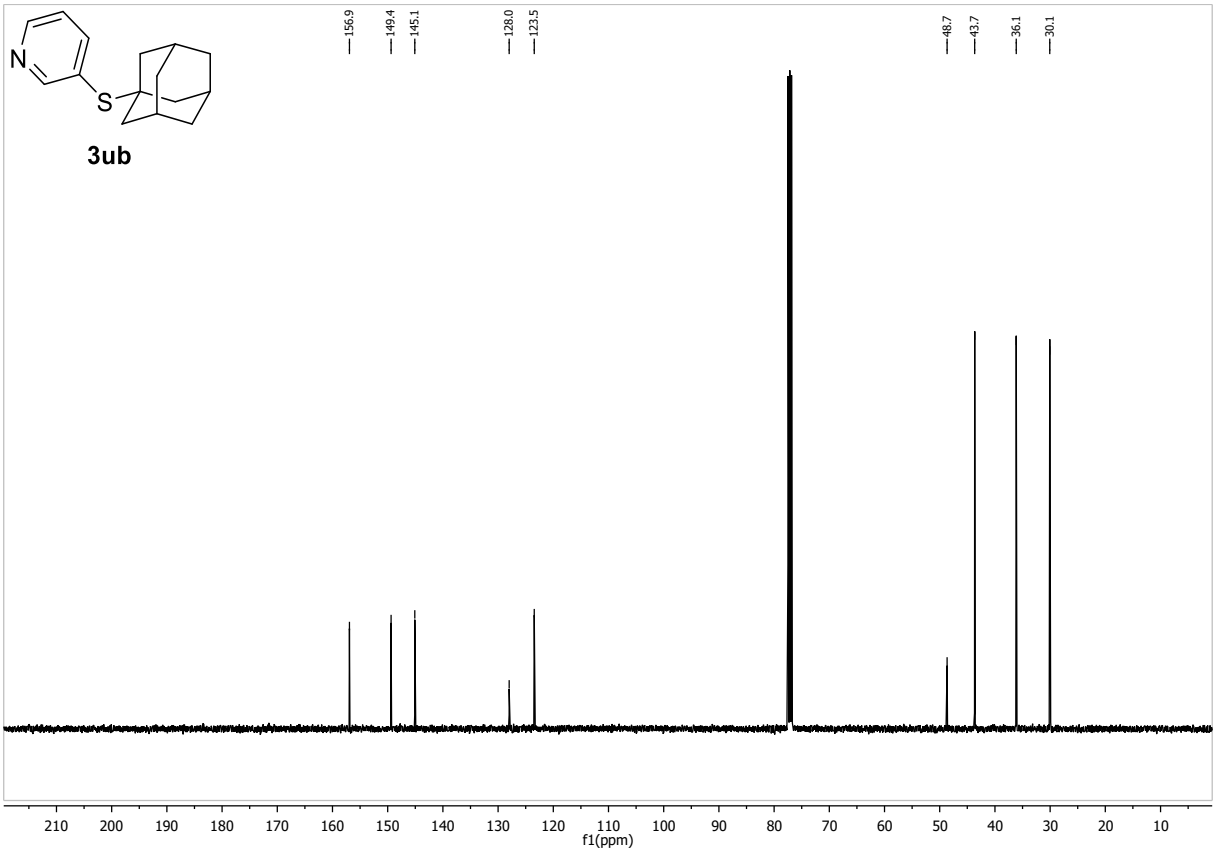
3ub
156.9
149.4
145.1
128.0
123.5
48.7
43.7
36.1
30.1
f1(ppm)

7-(((3s,5s,7s)-adamantan-1-yl)thio)quinoline (3vb)

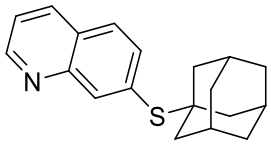

3vb

$C_{19}H_{21}NS$ (295.44 g/mol)

Following GP-B, **3vb** was synthesized using 6-chloroquinoline (164 mg, 1.00 mmol, 1.0 equiv.) and 1-adamantanethiol (185 mg, 1.10 mmol, 1.1 equiv.). Purification by FC (SiO_2, gradient to 7:3 Hex:EtOAc over 20 CV) afforded **3vb** (230 mg, 778 µmol, 78%) as colorless solid.

R_f: 0.15 (Hex:EtOAc 9:1)

m.p.: 115.2 – 116.7 °C

^{1}H-NMR (400 MHz, $CDCl_3$, δ): 8.94 (d, *J* = 4.7 Hz, 1H), 8.16 (d, *J* = 8.3 Hz, 1H), 8.05 (d, *J* = 8.7 Hz, 1H), 8.01 (d, *J* = 1.9 Hz, 1H), 7.80 (dd, *J* = 8.7, 1.9 Hz, 1H), 7.44 (dd, *J* = 8.3, 4.2 Hz, 1H), 2.05 – 1.98 (m, 3H), 1.87 (d, *J* = 2.9 Hz, 6H), 1.62 (q, *J* = 12.3 Hz, 6H).

^{13}C-NMR (101 MHz, $CDCl_3$, δ): 150.8, 147.8, 138.4, 136.9, 136.1, 129.5, 129.0, 128.1, 121.4, 48.8, 43.7, 36.1, 30.0.

HR-MS (ESI): m/z calc. for $[M+H]^+$ 296,14675, found 296,14692.

IR (ATR, $\tilde{\nu}$ [cm^{-1}]): 2909 (w), 2891 (w), 2849 (w), 1642 (s), 1597 (m), 1560 (w), 1489 (w), 1448 (m), 1422 (m), 1343 (s), 1288 (m), 1250 (m), 1217 (w), 1180 (w), 1135 (w), 1098 (w), 1071 (w), 1029 (m), 997 (w), 971 (w), 907 (w), 878 (w), 841 (m), 818 (m), 770 (s), 684 (s).

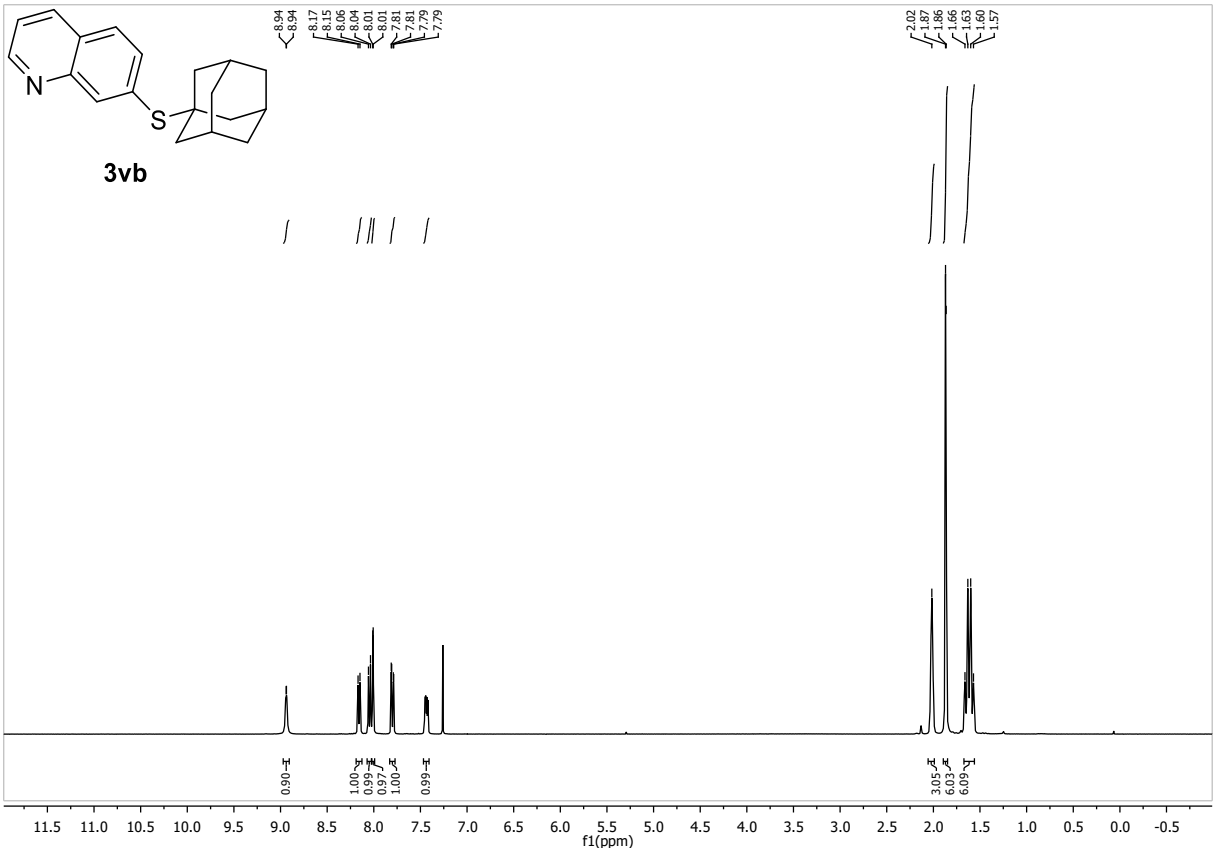
3vb
8.94
8.94
8.17
8.15
8.06
8.04
8.01
8.01
7.81
7.81
7.79
7.79
2.02
1.87
1.86
1.66
1.63
1.60
1.57
0.90
1.00
0.99
0.97
1.00
0.99
3.05
6.03
6.09
f1(ppm)

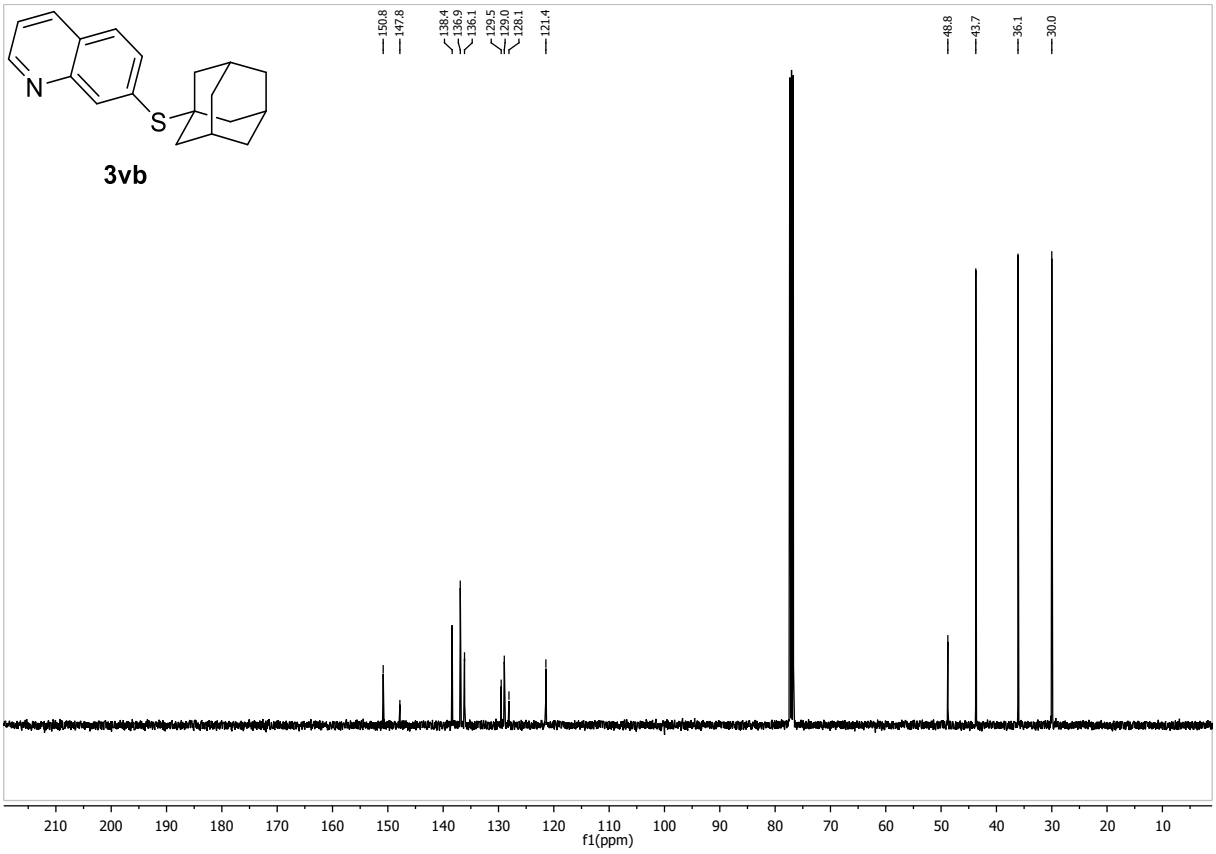
3vb
150.8
147.8
138.4
136.9
136.1
129.5
129.0
128.1
121.4
48.8
43.7
36.1
30.0
f1(ppm)

5-(((3s,5s,7s)-adamantan-1-yl)thio)-1*H*-indole (3wb)

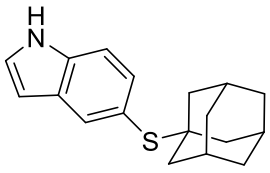

3wb

$C_{18}H_{21}NS$ (283.43 g/mol)

Following GP-B, **3wb** was synthesized using 5-chloro-1*H*-indole (152 mg, 1.00 mmol, 1.0 equiv.) and 1-adamantanethiol (185 mg, 1.10 mmol, 1.1 equiv.). Purification by FC (SiO_2, gradient to 8:2 Hex:EtOAc over 15 CV) afforded **3wb** (238 mg, 840 µmol, 84%) as colorless solid.

R_f: 0.27 (Hex:EtOAc 9:1)

m.p.: 170.1 – 171.3 °C

^{1}H-NMR (400 MHz, $CDCl_3$, δ): 8.21 (br. s, 1H), 7.81 (s, 1H), 7.33 (s, 2H), 7.24 – 7.22 (m, 1H), 6.57 – 6.55 (m, 1H), 1.99 (s, 3H), 1.83 (d, *J* = 2.6 Hz, 6H), 1.61 (q, *J* = 12.2 Hz, 6H).

^{13}C-NMR (101 MHz, $CDCl_3$, δ): 136.0, 131.7, 130.6, 128.3, 124.8, 120.6, 110.7, 102.9, 47.4, 43.6, 36.4, 30.1.

HR-MS (ESI): m/z calc. for [M + Na^+] 306.12869, found 306.12929.

IR (ATR, $\tilde{\nu}$ [cm^{-1}]): 3389 (w), 2895 (m), 2846 (w), 1746 (w), 1646 (w), 1608 (w), 1448 (m), 1407 (w), 1336 (w), 1299 (m), 1254 (w), 1191 (w), 1135 (w), 1094 (w), 1064 (w), 1034 (m), 975 (w), 893 (w), 807 (m), 770 (m), 736 (m), 688 (w).

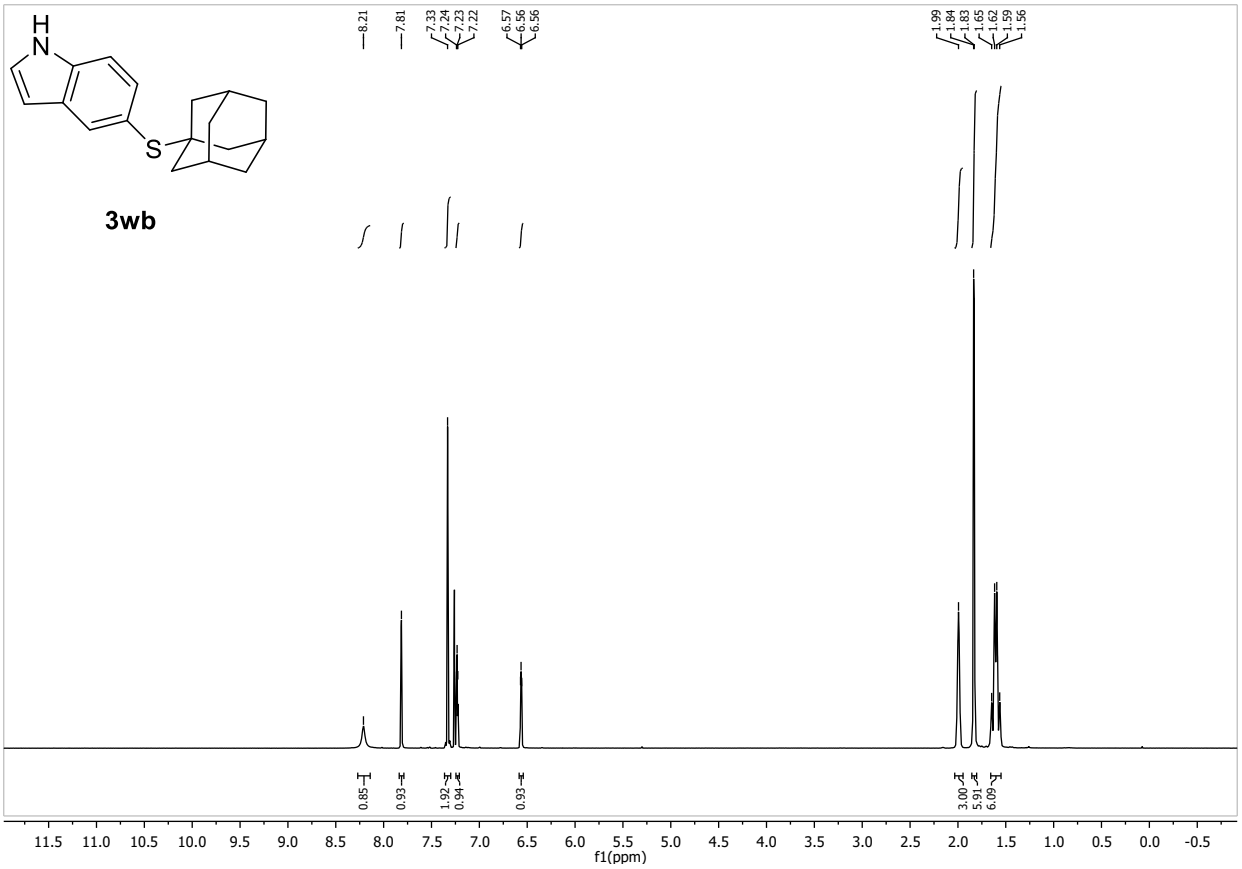
3wb
8.21
7.81
7.33
7.24
7.23
7.22
6.57
6.56
6.56
1.99
1.84
1.83
1.65
1.62
1.59
1.56
0.85
0.93
1.92
0.94
0.93
3.00
5.91
6.09
f1(ppm)

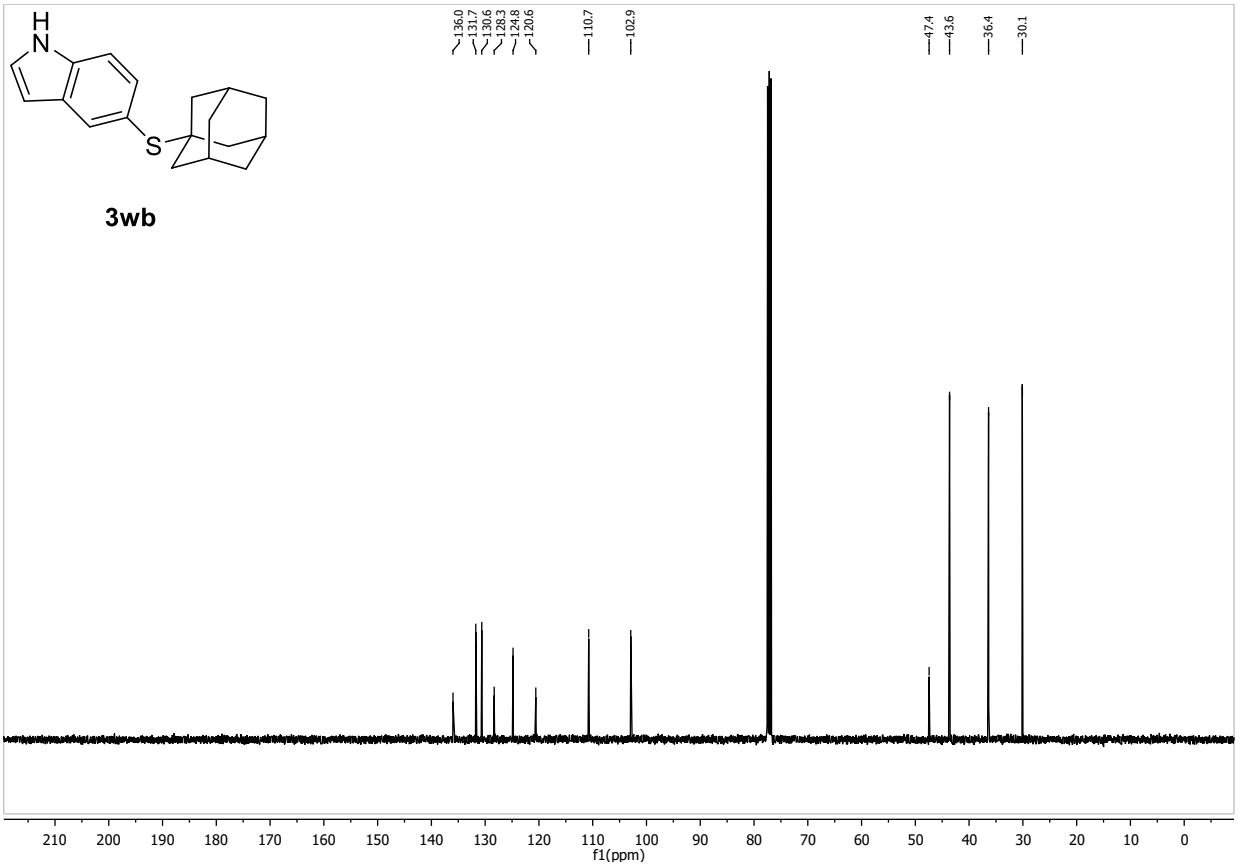
3wb
136.0
131.7
130.6
128.3
124.8
120.6
110.7
102.9
47.4
43.6
36.4
30.1
f1(ppm)

6-(((3s,5s,7s)-adamantan-1-yl)thio)-2-methylbenzo-thiazole (3xb)

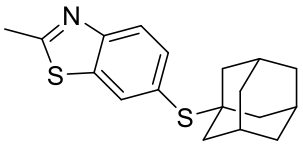

3xb

$C_{18}H_{21}NS_2$ (315.49 g/mol)

Following GP-B, **3xb** was synthesized using 5-chloro-2-methylbenzothiazole (184 mg, 1.00 mmol, 1.0 equiv.) and 1-adamantanethiol (185 mg, 1.10 mmol, 1.1 equiv.). Purification by FC (SiO_2, gradient to 8:2 Hex:EtOAc over 25 CV) afforded **3xb** (256 mg, 811 µmol, 81%) as colorless solid.

R_f: 0.38 (Hex:EtOAc 9:1)

m.p.: 196.7 – 198.8 °C

^{1}H-NMR (400 MHz, $CDCl_3$, δ): 8.11 (d, *J* = 1.4 Hz, 1H), 7.75 (d, *J* = 8.2 Hz, 1H), 7.47 (dd, *J* = 8.2, 1.4 Hz, 1H), 2.85 (s, 3H), 2.00 (s, 3H), 1.83 (d, *J* = 2.4 Hz, 6H), 1.60 (d, *J* = 11.6 Hz, 6H).

^{13}C-NMR (101 MHz, $CDCl_3$, δ): 167.9, 153.6, 136.4, 134.0, 131.4, 128.3, 120.9, 48.3, 43.7, 36.3, 30.1, 20.4.

HR-MS (ESI): m/z calc. for $[M+H]^+$ 316.11882, found 316.11899.

IR (ATR, $\tilde{\nu}$ [cm^{-1}]): 2887 (m), 2849 (w), 1780 (w), 1750 (w), 1649 (w), 1523 (w), 1433 (w), 1403 (w), 1370 (w), 1340 (w), 1291 (w), 1254 (w), 1232 (w), 1228 (w), 1162 (m), 1102 (w), 1034 (m), 1001 (w), 966 (w), 904 (w), 878 (m), 819 (m), 766 (w), 736 (w), 680 (w).

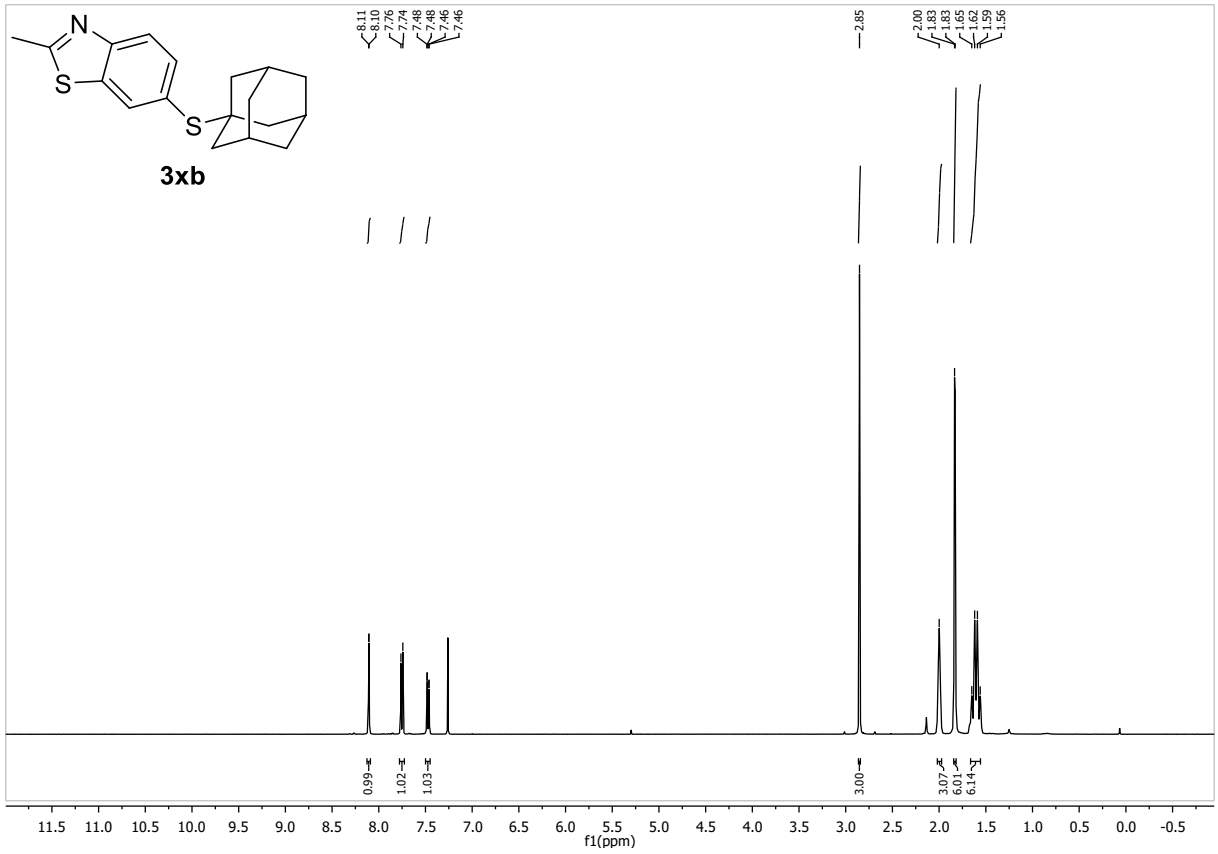
3xb
8.11
8.10
7.76
7.74
7.48
7.48
7.46
7.46
2.85
2.00
1.83
1.83
1.65
1.62
1.59
1.56
0.99
1.02
1.03
3.00
3.07
6.01
6.14
f1(ppm)

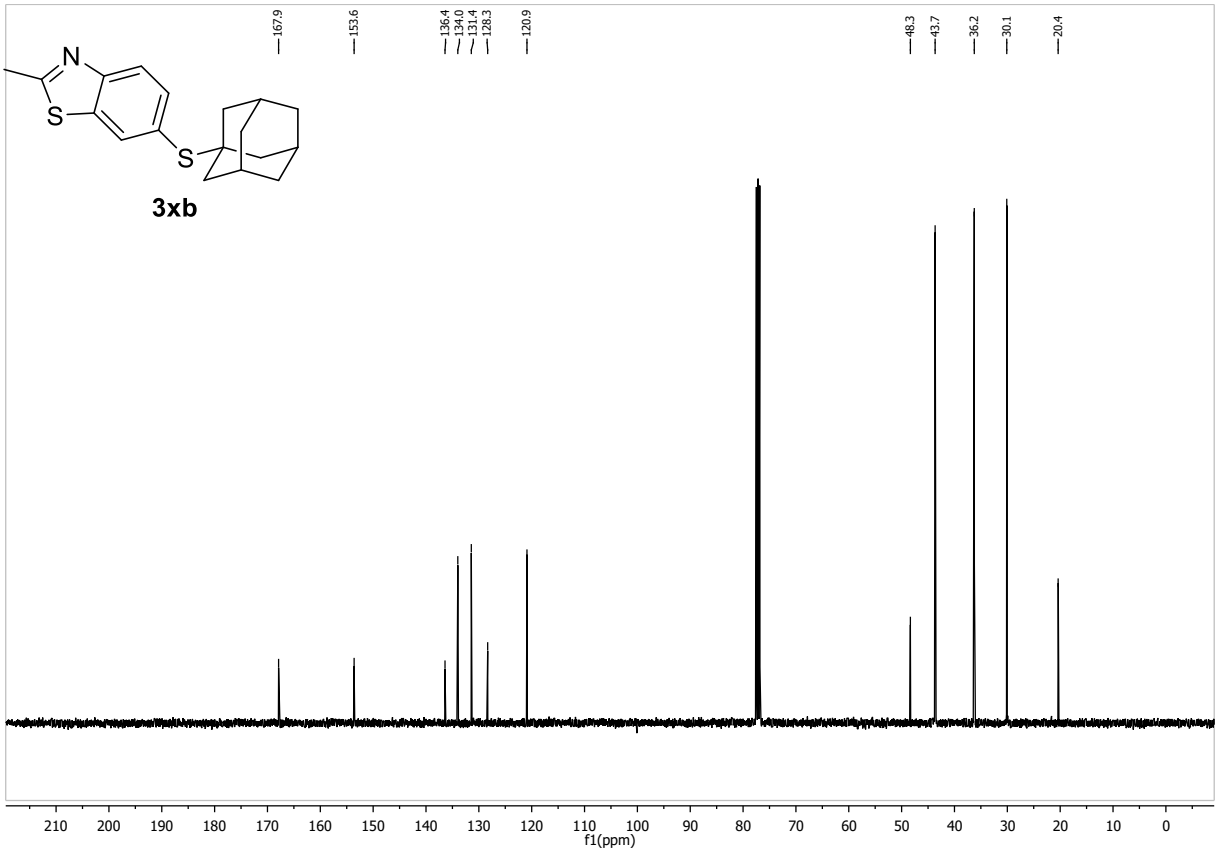
3xb
167.9
153.6
136.4
134.0
131.4
128.3
120.9
48.3
43.7
36.2
30.1
20.4
f1(ppm)

5-(((3s,5s,7s)-adamantan-1-yl)thio)benzo[d][1,3]dioxole (3yb)

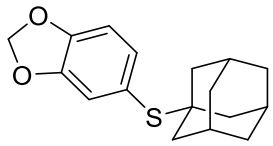

3yb

$C_{17}H_{20}O_2S$ (288.41 g/mol)

Following GP-B, **3yb** was synthesized using 5-chloro-1,3-benzodioxole (157 mg, 117 µL, 1.00 mmol, 1.0 equiv.) and 1-adamantanethiol (185 mg, 1.10 mmol, 1.1 equiv.). Purification by FC (SiO_2, gradient to 9:1 Hex:EtOAc over 20 CV) afforded **3yb** (193 mg, 669 µmol, 67%) as colorless solid.

R_f: 0.62 (Hex:EtOAc 9:1)

m.p.: 80.6 – 81.7 °C

^{1}H-NMR (400 MHz, $CDCl_3$, δ): 6.99 (dd, *J* = 7.9, 1.7 Hz, 1H), 6.95 (d, *J* = 1.6 Hz, 1H), 6.76 (d, *J* = 7.9 Hz, 1H), 5.99 (s, 2H), 2.01 (s, 3H), 1.79 (d, *J* = 2.6 Hz, 6H), 1.62 (d, *J* = 10.4 Hz, 6H).

^{13}C-NMR (101 MHz, $CDCl_3$, δ): 148.5, 147.4, 131.9, 122.9, 117.6, 108.2, 101.5, 47.9, 43.6, 36.3, 30.1.

HR-MS (EI): m/z calc. for [M] 288.117852, found 288.11442.

IR (ATR, $\tilde{\nu}$ [cm^{-1}]): 2902 (m), 2846 (w), 1504 (w), 1467 (s), 1407 (w), 1332 (w), 1299 (w), 1224 (s), 1158 (w), 1102 (m), 1030 (s), 978 (w), 930 (s), 889 (m), 859 (m), 807 (s), 721 (w), 684 (w).

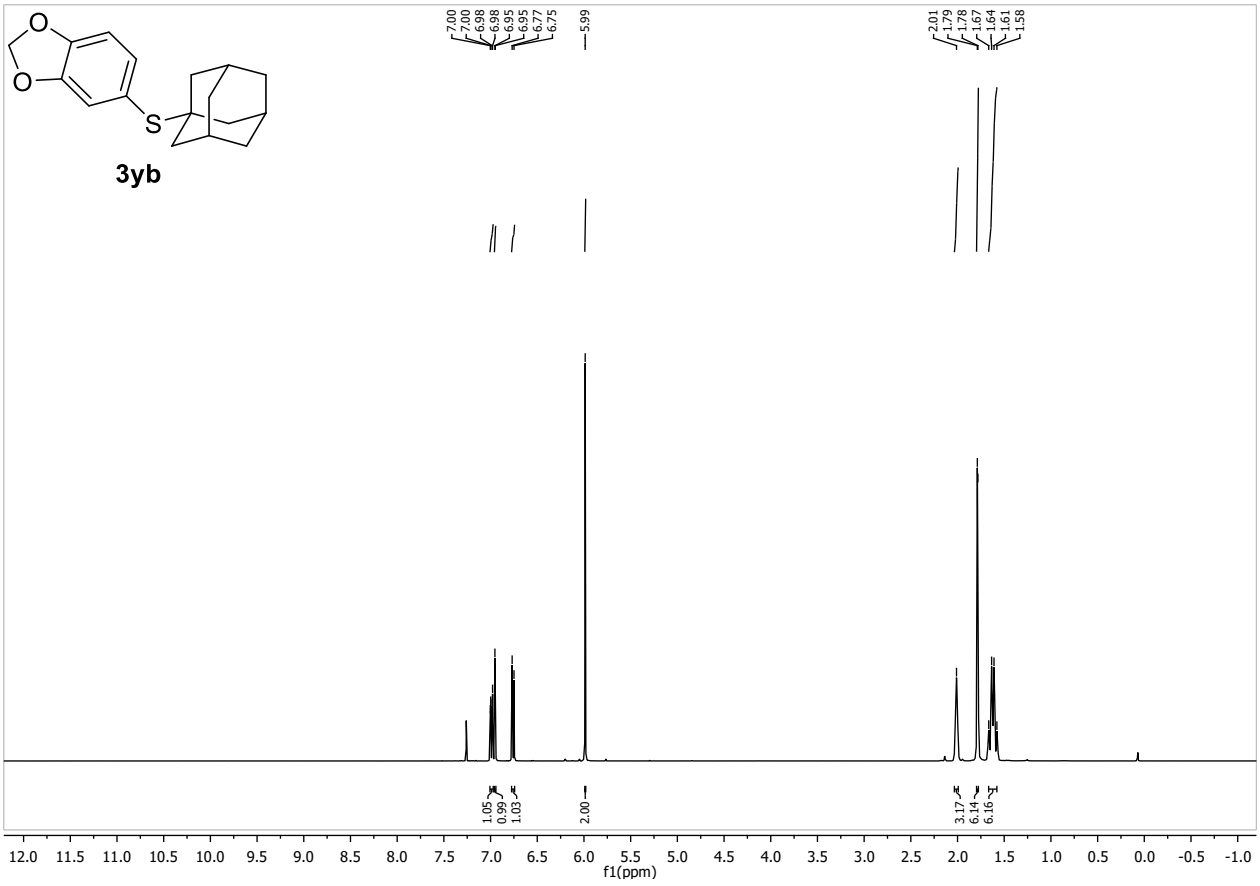
3yb
7.00
7.00
6.98
6.98
6.95
6.95
6.77
6.75
5.99
2.01
1.79
1.78
1.67
1.64
1.61
1.58
1.05
0.99
1.03
2.00
3.17
6.14
6.16
f1(ppm)

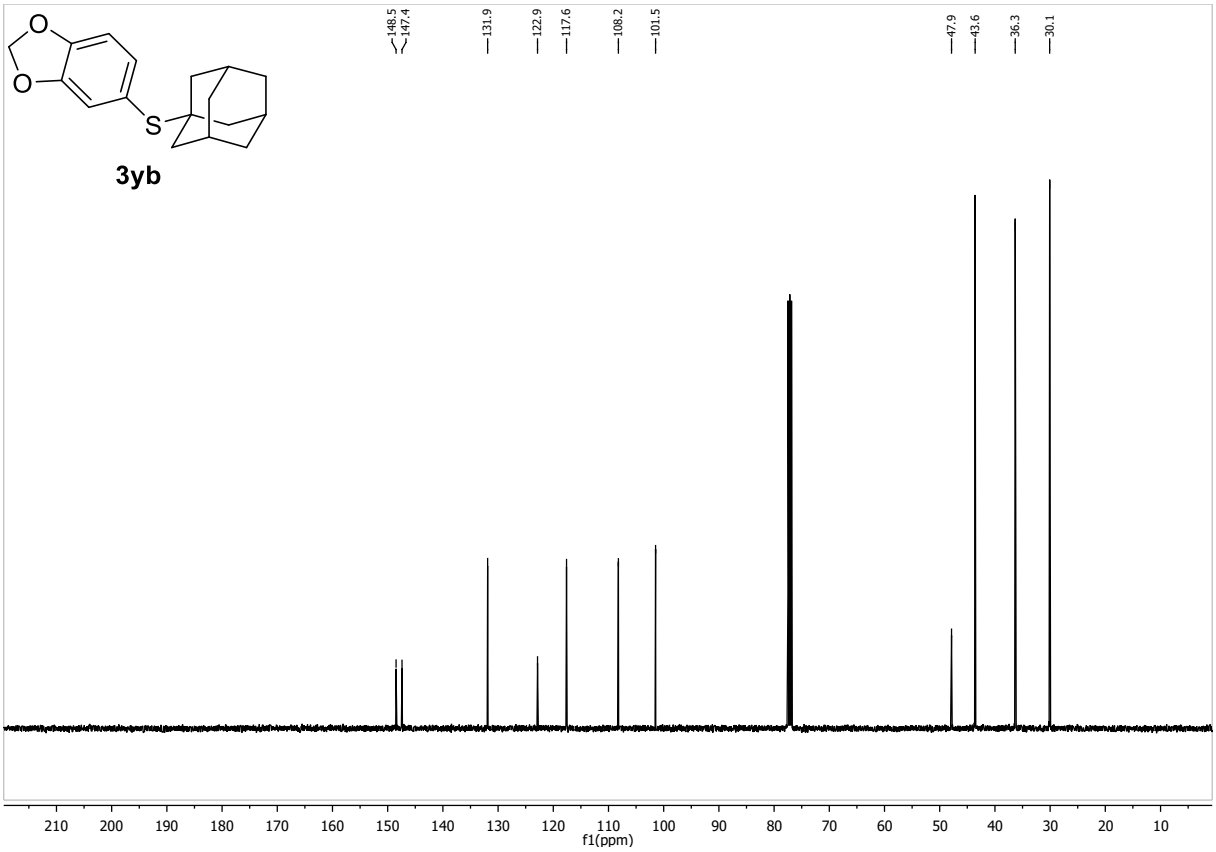
3yb
148.5
147.4
131.9
122.9
117.6
108.2
101.5
47.9
43.6
36.3
30.1
f1(ppm)

2-(((3s,5s,7s)-adamantan-1-yl)thio)-10-ethyl-10H-phenothiazine (3zb)

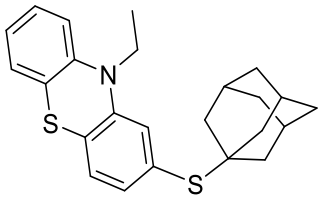

3zb

$C_{24}H_{27}NS_2$ (393.61 g/mol)

Following GP-B, **3zb** was synthesized using 2-chloro-10-ethylphenothiazine (131 mg, 500 µmol, 1.0 equiv.) and 1-adamantanethiol (93 mg, 0.55 mmol, 1.1 equiv.). Purification by FC (SiO_2, 99:1 Hex:EtOAc 15 CV) afforded **3zb** (174 mg, 441 µmol, 88%) as yellow solid.

R_f: 0.64 (Hex:EtOAc 9:1)

m.p.: 145.9 – 147.7 °C

^{1}H-NMR (400 MHz, $CDCl_3$, δ): 7.19 – 7.10 (m, 2H), 7.04 (s, 2H), 6.98 (s, 1H), 6.94 – 6.86 (m, 2H), 3.91 (q, *J* = 7.0 Hz, 2H), 2.02 (s, 3H), 1.81 (d, *J* = 2.6 Hz, 6H), 1.63 (q, *J* = 8.9 Hz, 6H), 1.42 (t, *J* = 7.0 Hz, 3H).

^{13}C-NMR (101 MHz, $CDCl_3$, δ): 144.8, 131.6, 129.4, 127.5, 126.9, 125.7, 124.2, 124.1, 122.7, 115.4, 48.3, 43.8, 42.05, 36.3, 30.1, 13.1.

HR-MS (ESI): m/z calc. for $[M]^+$ 394.15794, found 394.15856.

IR (ATR, $\tilde{\nu}$ [cm^{-1}]): 2906 (w), 2876 (w), 2846 (w), 1582 (w), 1550 (w), 1445 (s), 1393 (m), 1344 (w), 1314 (w), 1284 (m), 1238 (m), 1173 (w), 1131 (w), 1105 (m), 1034 (m), 971 (w), 949 (w), 916 (w), 881 (w), 807 (m), 744 (s), 680 (w).

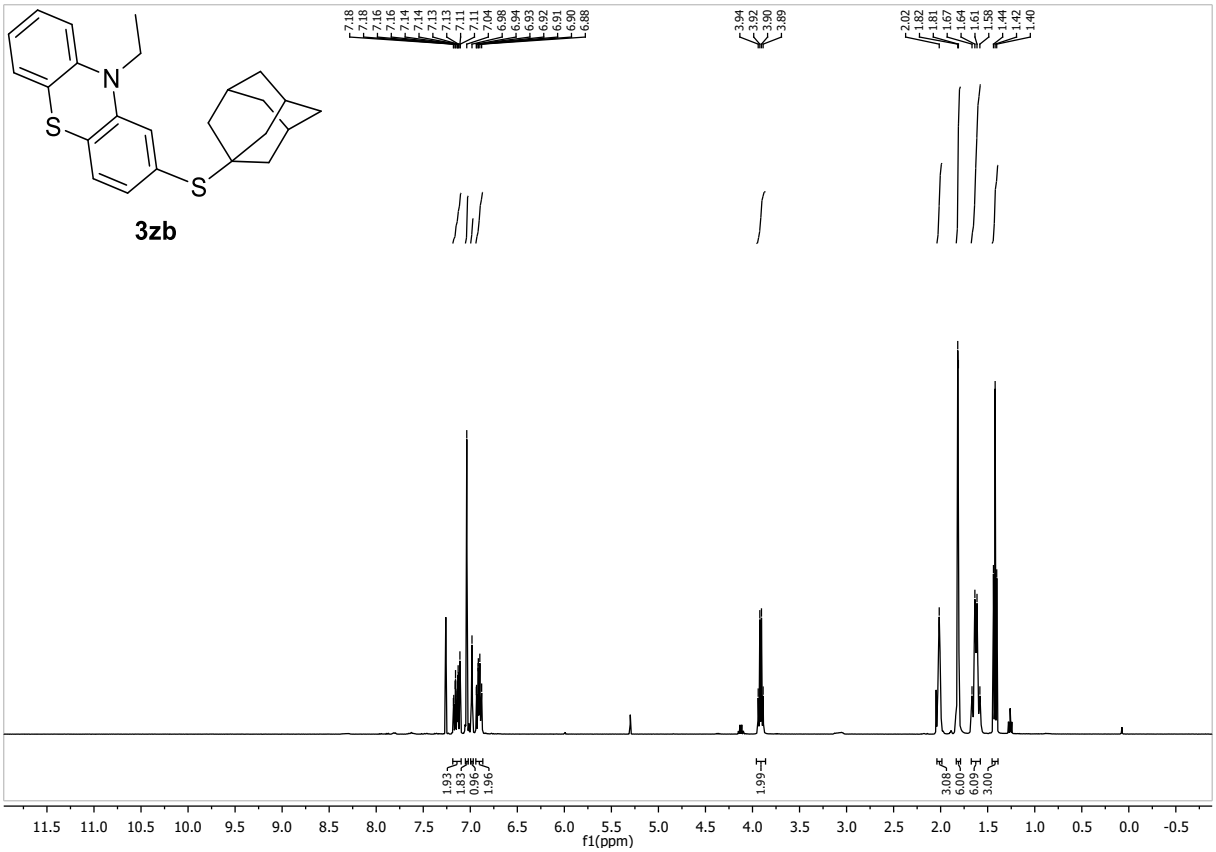
3zb
7.18
7.18
7.16
7.16
7.14
7.14
7.13
7.13
7.11
7.11
7.04
6.98
6.94
6.93
6.92
6.91
6.90
6.88
3.94
3.92
3.90
3.89
2.02
1.82
1.81
1.67
1.64
1.61
1.58
1.44
1.42
1.40
1.93
1.83
0.96
1.96
1.99
3.08
6.00
6.09
3.00
f1(ppm)

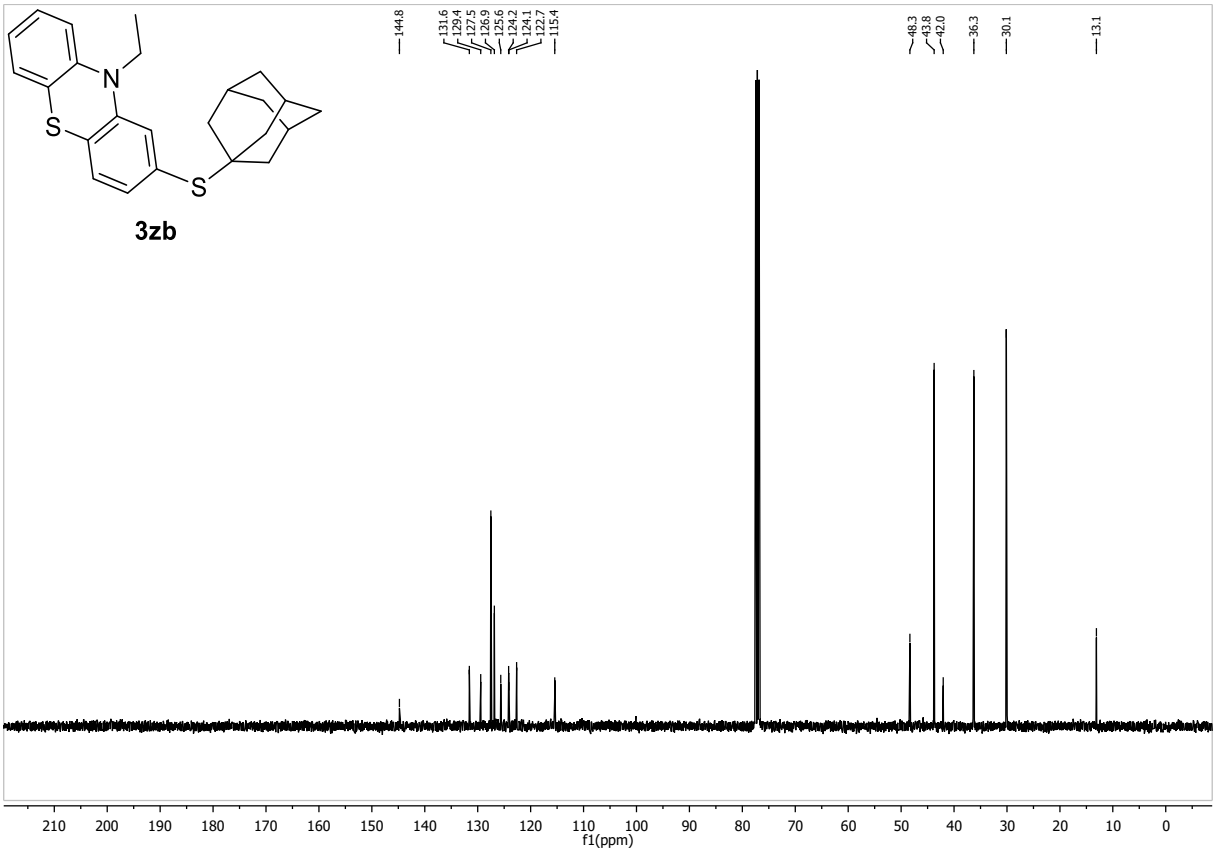
3zb
144.8
131.6
129.4
127.5
126.9
125.6
124.2
124.1
122.7
115.4
48.3
43.8
42.0
36.3
30.1
13.1
f1(ppm)

2-(((3s,5s,7s)-adamantan-1-yl)thio)-10H-phenothiazine (3Ab)

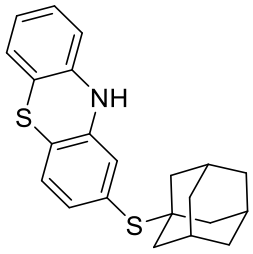

3Ab

$C_{22}H_{23}NS_2$ (365.55 g/mol)

Following GP-B, **3Ab** was synthesized using 2-chlorophenothiazine (234 mg, 1.00 mmol, 1.0 equiv.) and 1-adamantanethiol (185 mg, 1.1 mmol, 1.1 equiv.). Purification by FC (SiO_2, gradient to 9:1 Hex:EtOAc over 20 CV) afforded **3Ab** (330 mg, 903 µmol, 90%) off-white solid.

R_f: 0.44 (Hex:EtOAc 9:1)

m.p.: 176.0 – 178.1 °C

^{1}H-NMR (400 MHz, DMSO, δ): 8.63 (s, 1H), 7.02 – 6.96 (m, 2H), 6.93 – 6.85 (m, 2H), 6.82 – 6.72 (m, 3H), 6.67 – 6.62 (m, 1H), 1.97 (s, 3H), 1.73 (d, *J* = 2.9 Hz, 6H), 1.58 (q, *J* = 12.3 Hz, 6H).

^{13}C-NMR (101 MHz, DMSO, δ): 141.7, 141.4, 130.1, 128.5, 128.1, 127.5, 126.1, 125.8, 122.1, 121.8, 117.6, 115.6, 114.4, 47.3, 43.0, 35.4, 29.1.

HR-MS (ESI): m/z calc. for [M + Na^+], found.

IR (ATR, $\tilde{\nu}$ [cm^{-1}]): 3379 (w), 2897 (w), 2846 (w), 1585 (w), 1552 (w), 1458 (m), 1426 (m), 1349 (w), 1295 (m), 1247 (m), 1180 (w), 1157 (w), 1124 (w), 1098 (w), 1061 (w), 1034 (m), 972 (w), 923 (w), 859 (w), 807 (m), 736 (s), 680 (m).

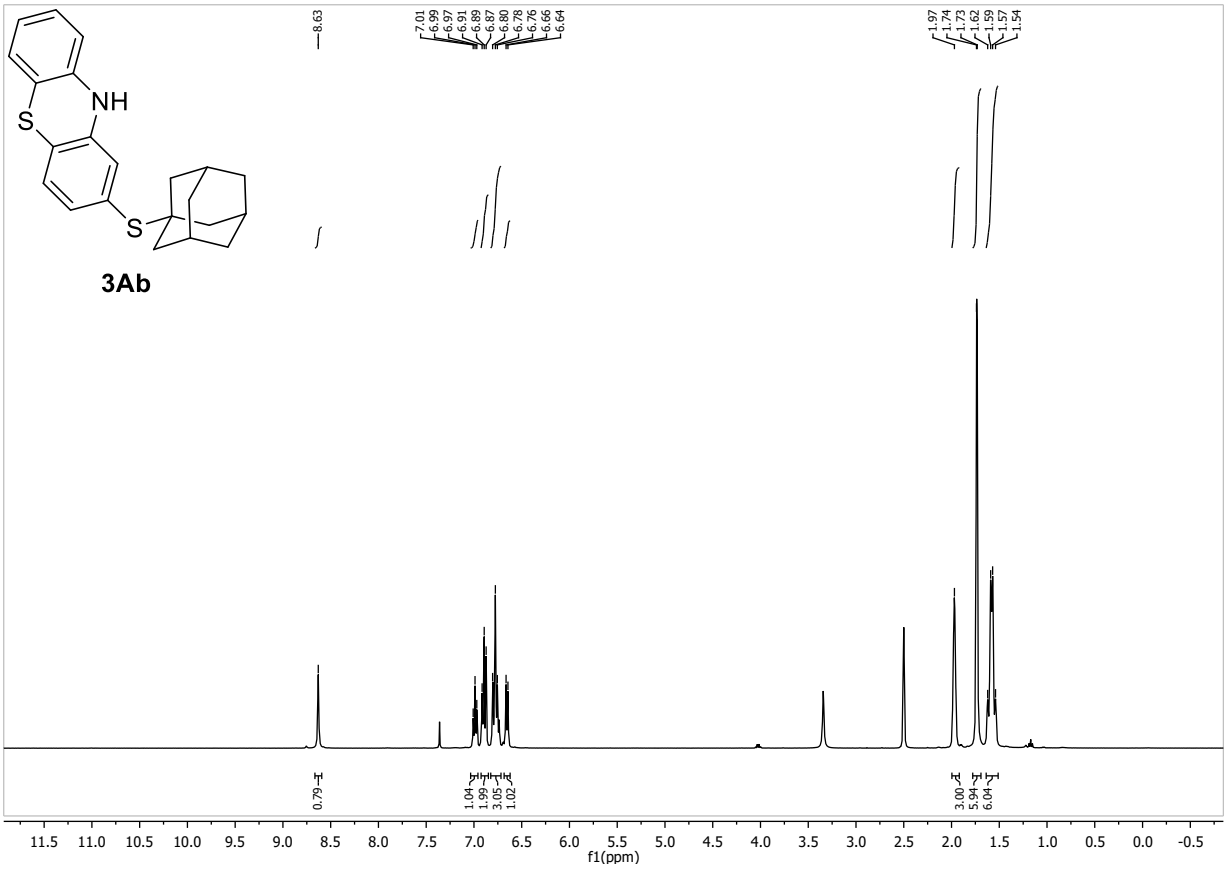
NH
S
S
3Ab
8.63
7.01
6.99
6.97
6.91
6.89
6.87
6.80
6.78
6.76
6.66
6.64
1.97
1.74
1.73
1.62
1.59
1.57
1.54
0.79
1.04
1.99
3.05
1.02
3.00
5.94
6.04
f1(ppm)

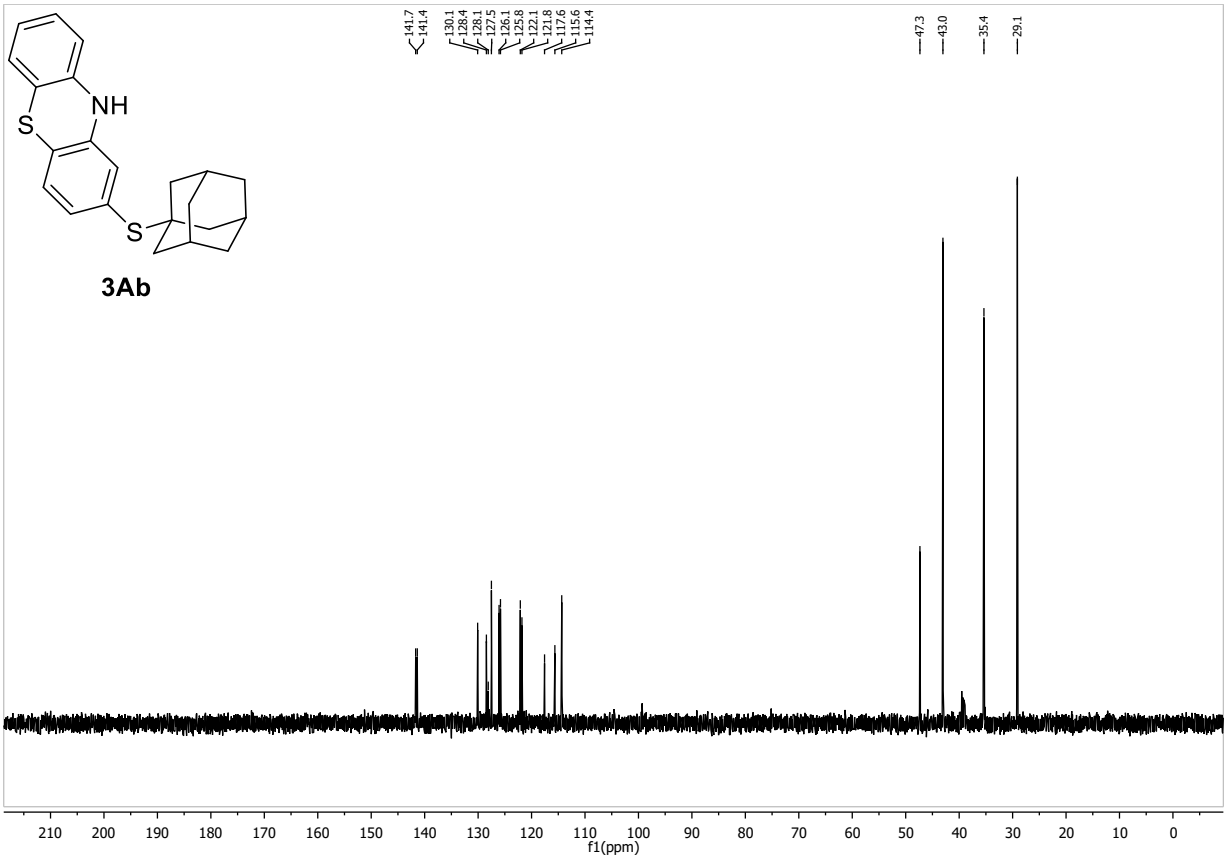
NH
S
S
3Ab
141.7
141.4
130.1
128.4
128.1
127.5
126.1
125.8
122.1
121.8
117.6
115.6
114.4
47.3
43.0
35.4
29.1
f1(ppm)

7-(((3s,5s,7s)-adamantan-1-yl)thio)-3-phenyl-4*H*-chromen-4-one (3Bb)

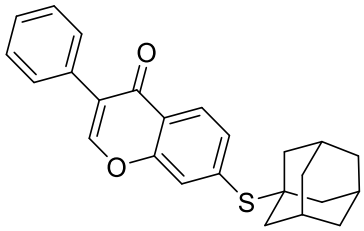

3Bb

$C_{25}H_{24}O_2S$ (388.53 g/mol)

Following GP-B, **3Bb** was synthesized using 6-chloroflavone (257 mg, 1.00 mmol, 1.0 equiv.) and 1-adamantanethiol (185 mg, 1.10 mmol, 1.1 equiv.). Purification by FC (SiO_2, gradient to 8:2 Hex:EtOAc over 5 CV, gradient to 5:5 Hex:EtOAc over 20 CV) afforded **3Bb** (345 mg, 888 µmol, 89%) as colorless solid.

R_f: 0.20 (Hex:EtOAc 9:1)

m.p.: 212.3 – 214.0 °C

^{1}H-NMR (400 MHz, $CDCl_3$, δ): 8.36 (d, *J* = 2.1 Hz, 1H), 7.93 (dd, *J* = 7.2, 1.5 Hz, 2H), 7.79 (dd, *J* = 8.6, 2.1 Hz, 1H), 7.57 – 7.50 (m, 4H), 6.85 (s, 1H), 2.02 (s, 3H), 1.83 (d, *J* = 2.3 Hz, 6H), 1.62 (q, *J* = 12.3 Hz, 6H).

^{13}C-NMR (101 MHz, $CDCl_3$, δ): 178.1, 163.6, 156.5, 142.9, 134.7, 131.9, 131.8, 129.2, 128.3, 126.5, 123.9, 118.2, 107.9, 48.6, 43.7, 36.2, 30.1.

HR-MS (ESI): m/z calc. for $[M+H]^+$ 389.15698 , found 389.15704.

IR (ATR, $\tilde{\nu}$ [cm^{-1}]): 2909 (w), 2891 (w), 2849 (w), 1642 (s), 1597 (m), 1560 (w), 1489 (w), 1448 (m), 1422 (m), 1343 (s), 1288 (m), 1250 (m), 1217 (w), 1180 (w), 1135 (w), 1098 (w), 1071 (w), 1029 (m), 997 (w), 971 (w), 907 (w), 878 (w), 841 (m), 818 (m), 770 (s), 684 (s).

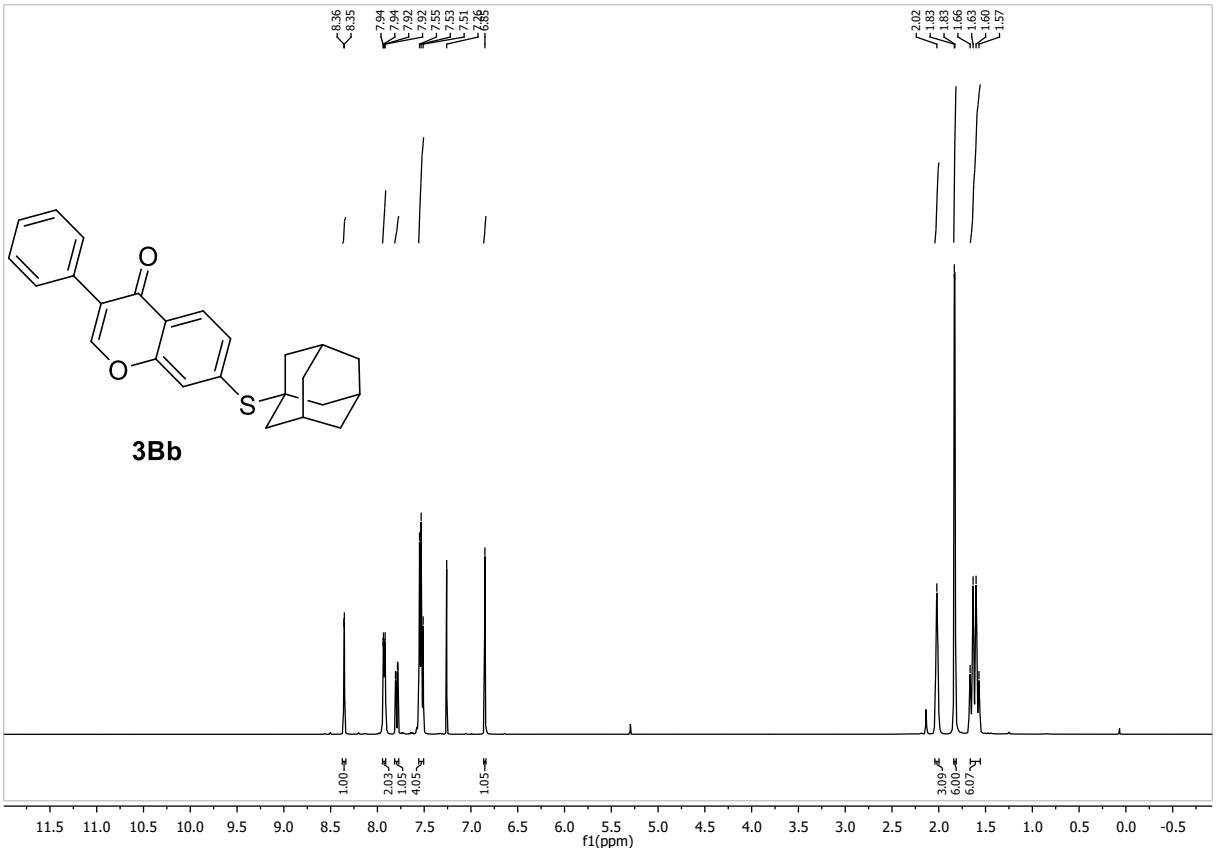
8.36
8.35
7.94
7.94
7.92
7.92
7.55
7.53
7.51
7.26
6.85
2.02
1.83
1.83
1.66
1.63
1.60
1.57
O
O
S
3Bb
1.00
2.03
1.05
4.05
1.05
3.09
6.00
6.07
11.5 11.0 10.5 10.0 9.5 9.0 8.5 8.0 7.5 7.0 6.5 6.0 5.5 5.0 4.5 4.0 3.5 3.0 2.5 2.0 1.5 1.0 0.5 0.0 -0.5
f1(ppm)

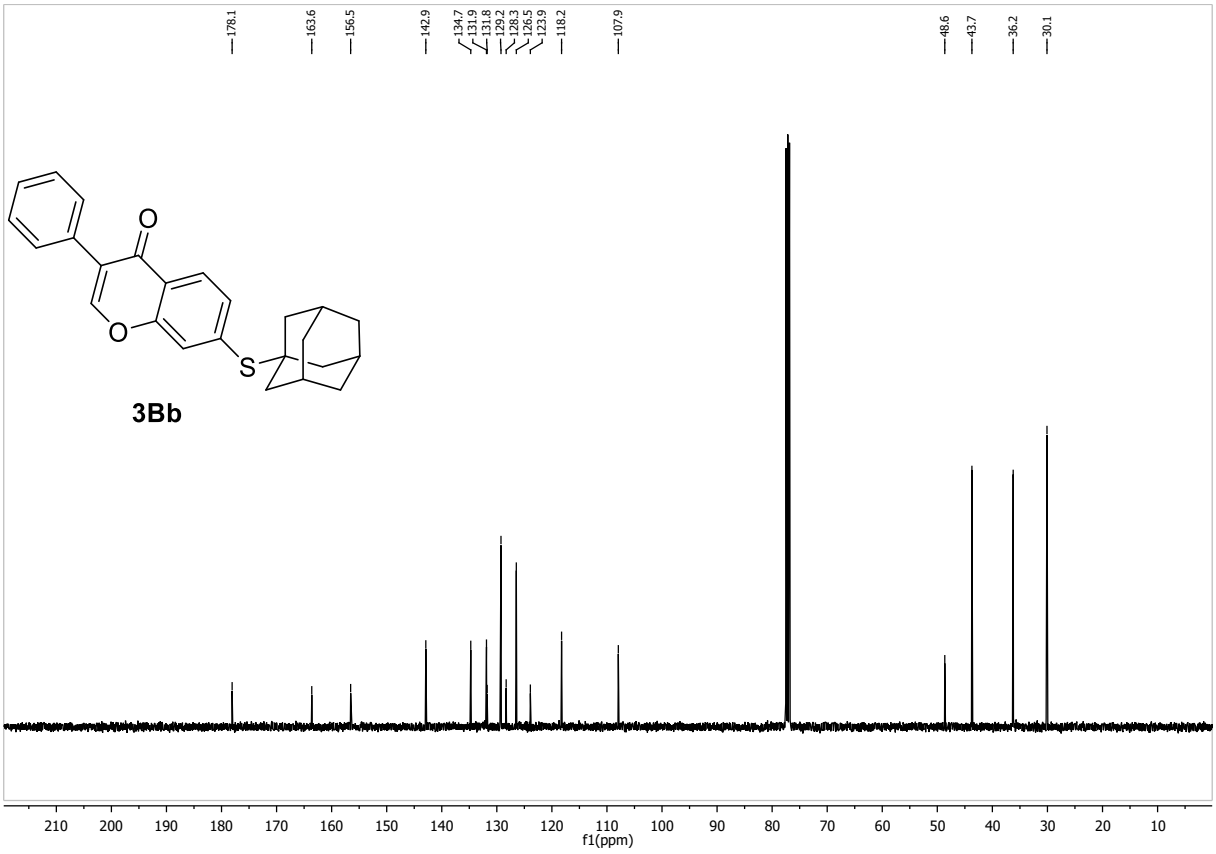
178.1
163.6
156.5
142.9
134.7
131.9
131.8
129.2
128.3
126.5
123.9
118.2
107.9
48.6
43.7
36.2
30.1
O
O
S
3Bb
210 200 190 180 170 160 150 140 130 120 110 100 90 80 70 60 50 40 30 20 10
f1(ppm)

Ethyl 4-(8-(((3s,5s,7s)-adamantan-1-yl)thio)-5,6-dihydro-11H-benzo[5,6]cyclohepta[1,2-b]pyridin-11-ylidene)piperidine-1-carboxylate (3Cb)

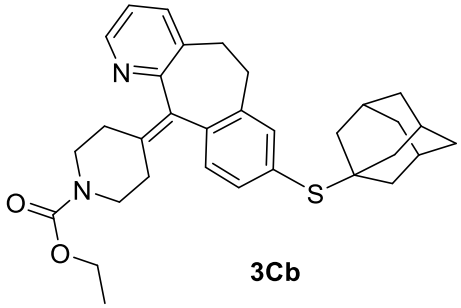

3Cb

$C_{32}H_{38}N_2O_2S$ (514.73 g/mol)

Following GP-B, **3Cb** was synthesized using Loratadine (191 mg, 0.50 mmol, 1.0 equiv.) and 1-adamantanethiol (93 mg, 0.55 mmol, 1.1 equiv.). Purification by FC (SiO_2, gradient to 5:5 Hex:EtOAc over 20 CV) afforded **3Cb** (179 mg, 348 µmol, 70%) as colorless solid.

R_f: 0.32 (Hex:EtOAc 5:5)

m.p.: 121.4 – 123.8 °C (starts melting at 100°C)

^{1}H-NMR (400 MHz, $CDCl_3$, δ): 8.43 – 8.40 (m, 1H), 7.49 – 7.44 (m, 1H), 7.31 – 7.26 (m, 2H), 7.16 – 7.08 (m, 2H), 4.19 – 4.08 (m, 2H), 3.81 (s, 2H), 3.46 – 3.31 (m, 2H), 3.21 – 3.08 (m, 2H), 2.91 – 2.76 (m, 2H), 2.55 – 2.44 (m, 1H), 2.42 – 2.24 (m, 3H), 2.00 (s, 3H), 1.80 (d, *J* = 2.2 Hz, 6H), 1.61 (q, *J* = 12.3 Hz, 6H), 1.24 (t, *J* = 7.1 Hz, 3H).

^{13}C-NMR (101 MHz, $CDCl_3$, δ): 155.6, 139.5, 138.3, 137.8, 135.3, 129.4, 122.4, 61.5, 48.1, 45.0, 44.9, 43.7, 36.3, 31.9, 31.8, 30.7, 30.7, 30.1, 14.8.

HR-MS (ESI): m/z calc. for $[M+H]^+$ 515.27268, found 515.27245.

IR (ATR, $\tilde{\nu}$ [cm^{-1}]): 2976 (w), 2901 (w), 2846 (w), 1694 (m), 1564 (w), 1470 (w), 1426 (m), 1381 (w), 1347 (w), 1325 (w), 1276 (w), 1221 (m), 1172 (w), 1109 (m), 1060 (w), 1034 (w), 993 (w), 926 (w), 889 (w), 833 (w), 769 (w), 718 (w), 684 (w).

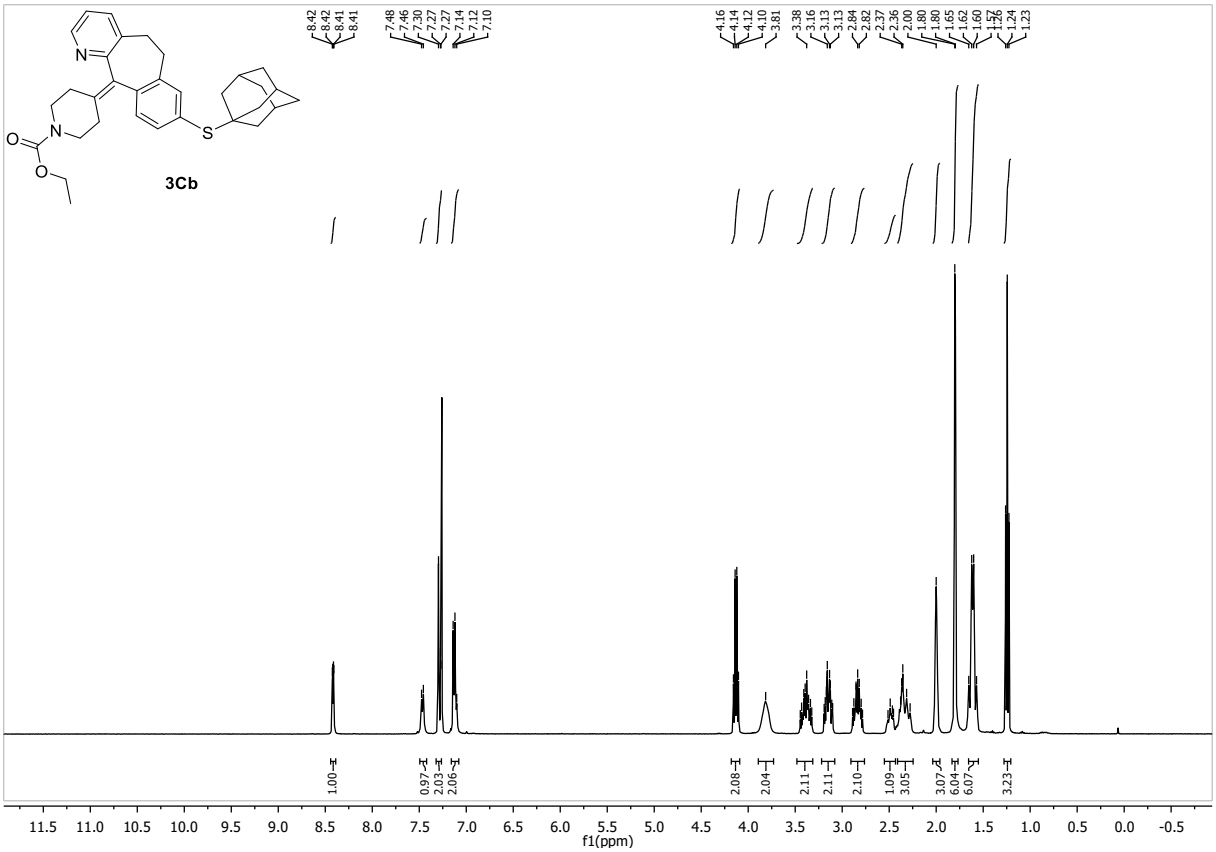
3Cb
8.42
8.42
8.41
8.41
7.48
7.46
7.30
7.27
7.27
7.14
7.12
7.10
4.16
4.14
4.12
4.10
3.81
3.38
3.16
3.13
3.13
2.84
2.82
2.37
2.36
2.00
1.80
1.80
1.65
1.62
1.60
1.26
1.24
1.23
1.00
0.97
2.03
2.06
2.08
2.04
2.11
2.11
2.10
1.09
3.05
3.07
6.04
6.07
3.23
f1(ppm)

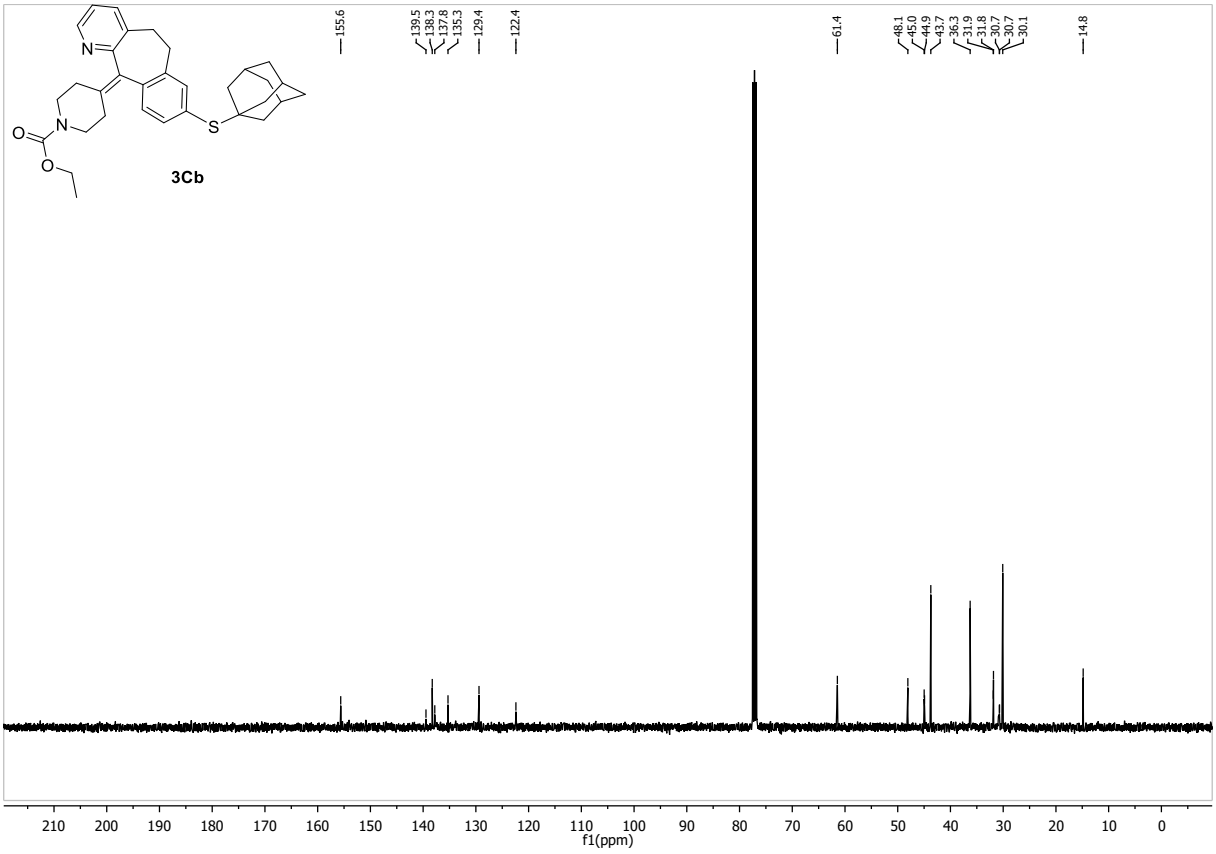
3Cb
155.6
139.5
138.3
137.8
135.3
129.4
122.4
61.4
48.1
45.0
44.9
43.7
36.3
31.9
31.8
30.7
30.7
30.1
14.8
f1(ppm)

Ethyl 2-(1-(4-(((3s,5s,7s)-adamantan-1-yl)thio)benzoyl)-5-methoxy-2-methyl-1H-indol-3-yl)acetate (3Db)

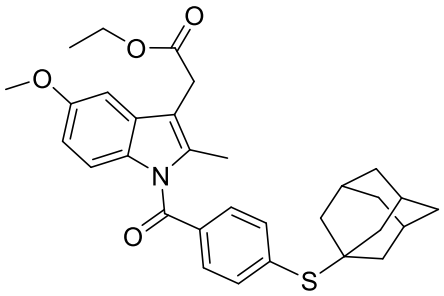

3Db

$C_{31}H_{35}NO_4S$ (517.68 g/mol)

Following GP-B, **3Db** was synthesized using Indometacine-o-ethylester (186 mg, 500 µmol, 1.0 equiv.) and 1-adamantanethiol (93 mg, 0.55 mmol, 1.1 equiv.). Purification by FC (SiO_2, 85:15 Hex:EtOAc over 15 CV) afforded **3Db** (194 mg, 374 µmol, 75%) as yellow solid.

R_f: 0.22 (Hex:EtOAc 9:1)

m.p.: could not be measured due to consistency

^{1}H-NMR (400 MHz, $CDCl_3$, δ): 7.65 – 7.58 (m, 4H), 6.97 (d, *J* = 2.5 Hz, 1H), 6.86 (d, *J* = 9.0 Hz, 1H), 6.64 (dd, *J* = 9.0, 2.5 Hz, 1H), 4.16 (q, *J* = 7.1 Hz, 2H), 3.83 (s, 3H), 3.65 (s, 2H), 2.38 (s, 3H), 2.04 (s, 3H), 1.85 (d, *J* = 2.5 Hz, 6H), 1.64 (q, *J* = 12.1 Hz, 6H), 1.26 (t, *J* = 7.1 Hz, 3H).

^{13}C-NMR (101 MHz, $CDCl_3$, δ): 171.0, 169.2, 156.1, 137.6, 136.9, 136.0, 135.7, 131.0, 130.8, 129.4, 115.2, 112.8, 111.7, 101.3, 61.1, 55.8, 49.3, 43.9, 36.2, 30.6, 30.2, 14.4, 13.6.

HR-MS (ESI): m/z calc. for $[M + Na]^+$ 540.21790, found 540.21865.

IR (ATR, $\tilde{\nu}$ [cm^{-1}]): 2902 (w), 2846 (w), 1732 (m), 1679 (s), 1593 (w), 1471 (m), 1452 (m), 1392 (w), 1358 (m), 1311 (s), 1254 (s), 1220 (s), 1164 (s), 1142 (s), 1094 (m), 1064 (s), 1031 (s), 919 (m), 833 (s), 800 (m), 755 (m), 695 (m), 669 (w).

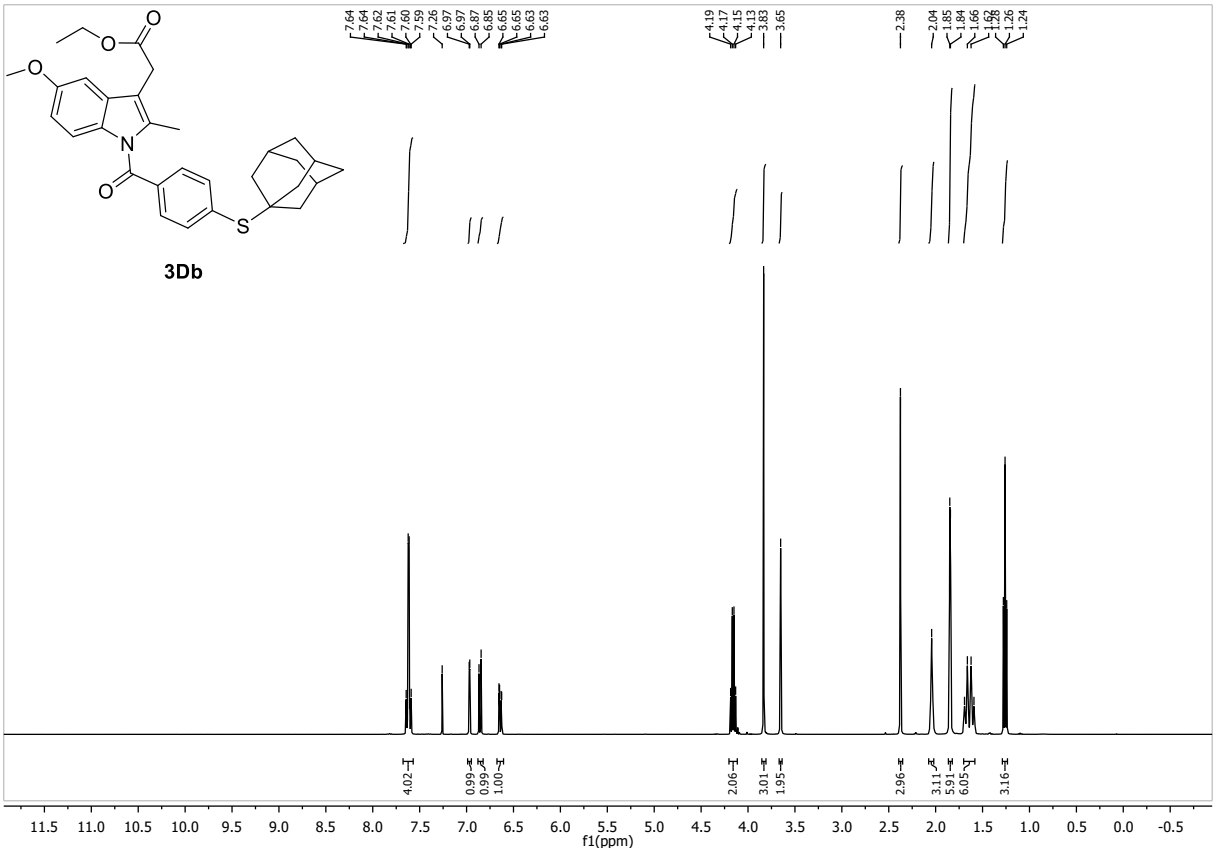
3Db
7.64
7.64
7.62
7.61
7.60
7.59
7.26
6.97
6.97
6.87
6.85
6.65
6.65
6.63
6.63
6.63
4.19
4.17
4.15
4.13
3.83
3.65
2.38
2.04
1.85
1.84
1.66
1.62
1.28
1.26
1.24
4.02
0.99
0.99
1.00
2.06
3.01
1.95
2.96
3.11
5.91
6.05
3.16
11.5 11.0 10.5 10.0 9.5 9.0 8.5 8.0 7.5 7.0 6.5 6.0 5.5 5.0 4.5 4.0 3.5 3.0 2.5 2.0 1.5 1.0 0.5 0.0 -0.5
f1(ppm)

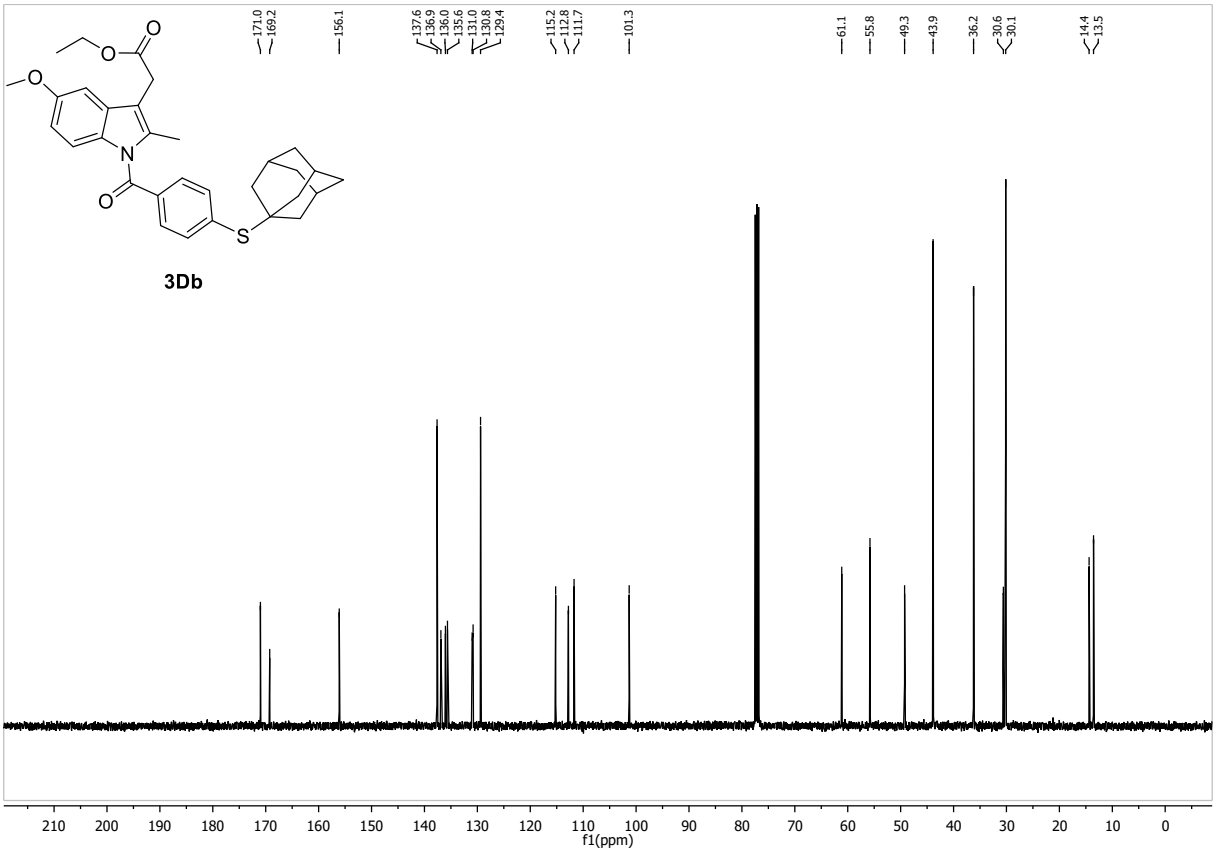
3Db
171.0
169.2
156.1
137.6
136.9
136.0
135.6
131.0
130.8
129.4
115.2
112.8
111.7
101.3
61.1
55.8
49.3
43.9
36.2
30.6
30.1
14.4
13.5
210 200 190 180 170 160 150 140 130 120 110 100 90 80 70 60 50 40 30 20 10 0
f1(ppm)

Isopropyl 2-(4-(4-(((3s,5s,7s)-adamantan-1-yl)thio)benzoyl)phenoxy)-2-methylpropanoate (3Eb)

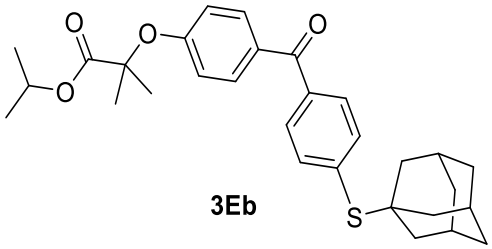

3Eb

$C_{30}H_{36}O_4S$ (492.67 g/mol)

Following GP-B, **3Eb** was synthesized using Fenofibrat (180 mg, 500 µmol, 1.0 equiv.) and 1-adamantanethiol (93 mg, 550 µmol, 1.1 equiv.). Purification by FC (SiO_2, gradient to 9:1 Hex:EtOAc over 20 CV) afforded **3Eb** (216 mg, 438 µmol, 88%) as colorless solid.

R_f: 0.36 (Hex:EtOAc 9:1)

m.p.: 93.6 – 96.7 °C

^{1}H-NMR (400 MHz, $CDCl_3$, δ): 7.79 – 7.74 (m, 2H), 7.70 – 7.66 (m, 2H), 7.59 (d, *J* = 8.2 Hz, 2H), 6.89 – 6.84 (m, 2H), 5.08 (hept, *J* = 6.3 Hz, 1H), 2.03 (s, 3H), 1.854 (s, 3H), 1.847 (s, 3H), 1.69 – 1.58 (m, 12H), 1.20 (d, *J* = 6.2 Hz, 6H).

^{13}C-NMR (101 MHz, $CDCl_3$, δ): 195.2, 173.3, 159.8, 138.1, 137.2, 135.9, 132.2, 132.1, 131.3, 130.5, 129.6, 128.7, 117.4, 117.3, 79.5, 69.5, 49.1, 43.9, 36.2, 30.2, 25.5, 21.7.

HR-MS (ESI): m/z calc. for $[M + Na]^+$ 515.22265, found 515.22318.

IR (ATR, $\tilde{\nu}$ [cm^{-1}]): 2977 (w), 2902 (w), 2850 (w), 1728 (m), 1638 (w), 1593 (s), 1504 (w), 1459 (w), 1382 (w), 1344 (w), 1280 (s), 1250 (s), 1173 (s), 1146 (s), 1098 (s), 1035 (m), 1012 (m), 971 (m), 926 (s), 848 (s), 759 (s), 680 (m).

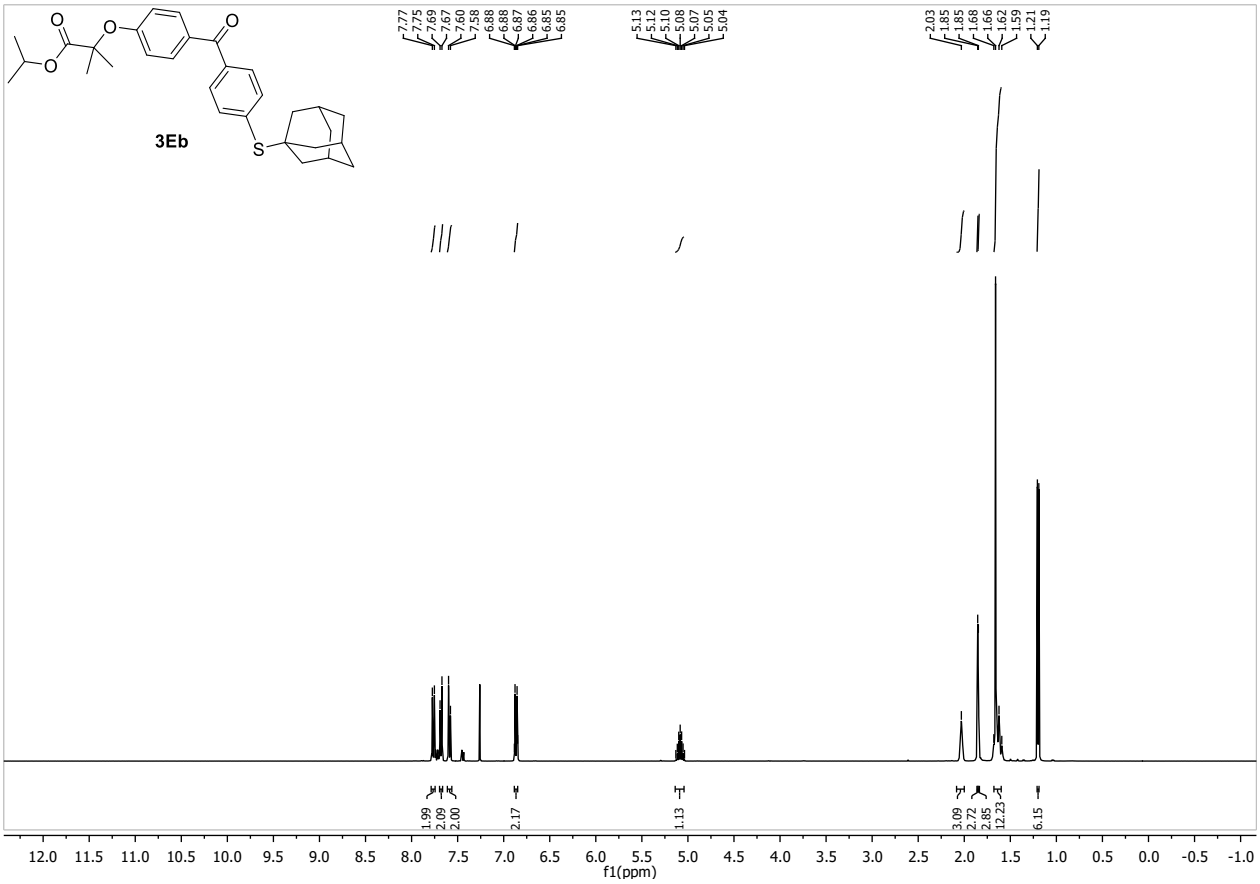
3Eb
7.77
7.75
7.69
7.67
7.60
7.58
6.88
6.87
6.86
6.85
5.13
5.12
5.10
5.08
5.07
5.05
5.04
2.03
1.85
1.85
1.68
1.66
1.62
1.59
1.21
1.19
1.99
2.09
2.00
2.17
1.13
3.09
2.72
2.85
12.23
6.15
f1(ppm)

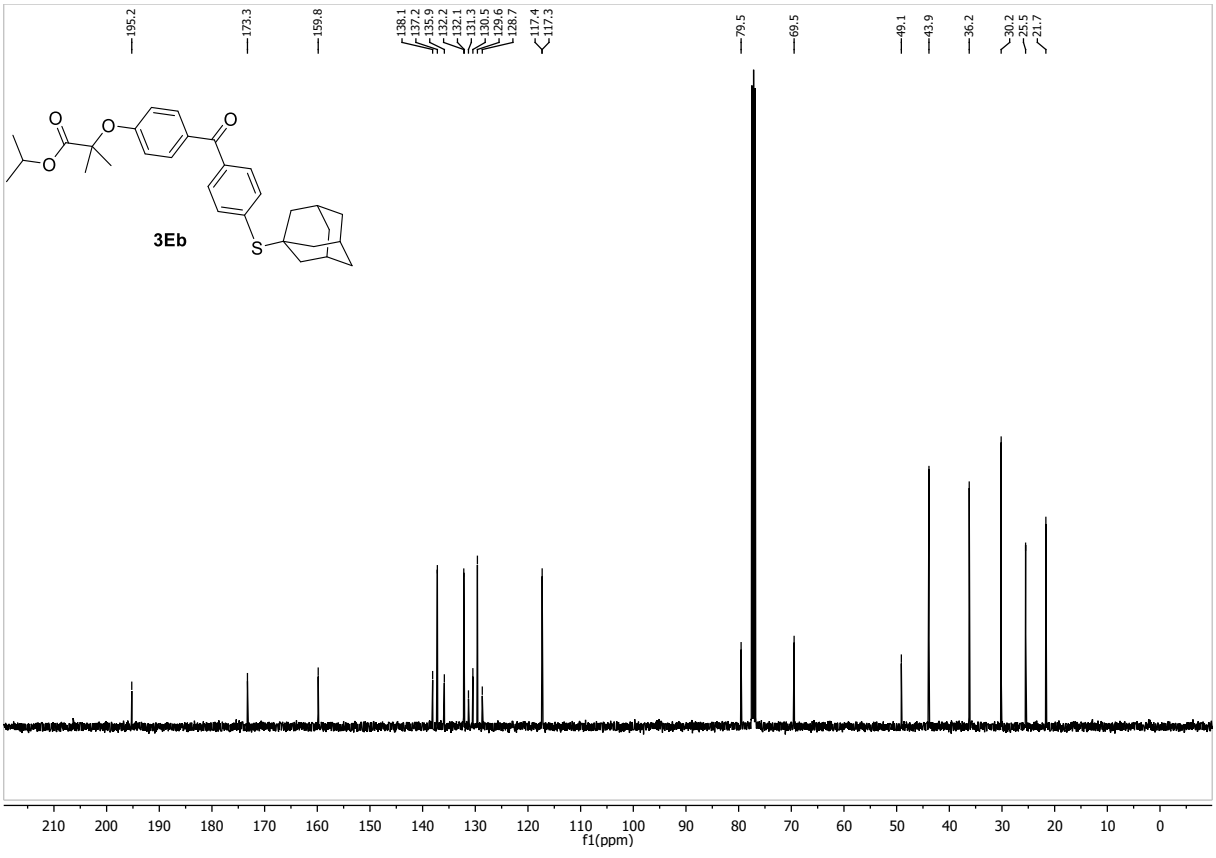
3Eb
195.2
173.3
159.8
138.1
137.2
135.9
132.2
132.1
131.3
130.5
129.6
128.7
117.4
117.3
79.5
69.5
49.1
43.9
36.2
30.2
25.5
21.7
f1(ppm)

Ethyl 4-(heptylthio)benzoate (3ac)

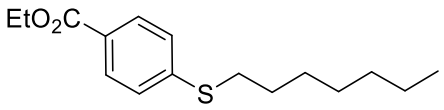

3ac

$C_{16}H_{24}O_2S$ (280.43 g/mol)

Following GP-B, **3ac** was synthesized using ethyl 4-chlorobenzoate (157 µL, 1.00 mmol, 1.0 equiv.) and 1-heptanethiol (172 µL, 1.10 mmol, 1.1 equiv.) Purification by FC (SiO_2, 5 CV Hex, gradient to 9:1 Hex:EtOAc over 15 CV) afforded **3ac** (265 mg, 943 µmol, 94 %) as colorless oil. Conforms to reported analytical data.[1]

R_f: 0.62 (Hex:EtOAc 9:1).

^{1}H-NMR (400 MHz, $CDCl_3$, δ): 7.93 (d, *J* = 8.5 Hz, 2H), 7.28 (d, *J* = 8.5 Hz, 2H), 4.36 (q, *J* = 7.1 Hz, 2H), 3.01 – 2.97 (t, *J* = 7.4 Hz, 2H), 1.69 (p, *J* = 7.3 Hz, 2H), 1.49 – 1.24 (m, 11H), 0.87 (t, *J* = 6.8 Hz, 3H).

^{13}C-NMR (101 MHz, $CDCl_3$, δ): 166.5, 144.4, 130.0, 126.4, 61.0, 32.2, 31.8, 29.0, 29.0, 28.9, 22.7, 14.5, 14.2.

HR-MS (ESI): m/z calc. for $[M+Na]^+$ 303.13892, found 303.13936.

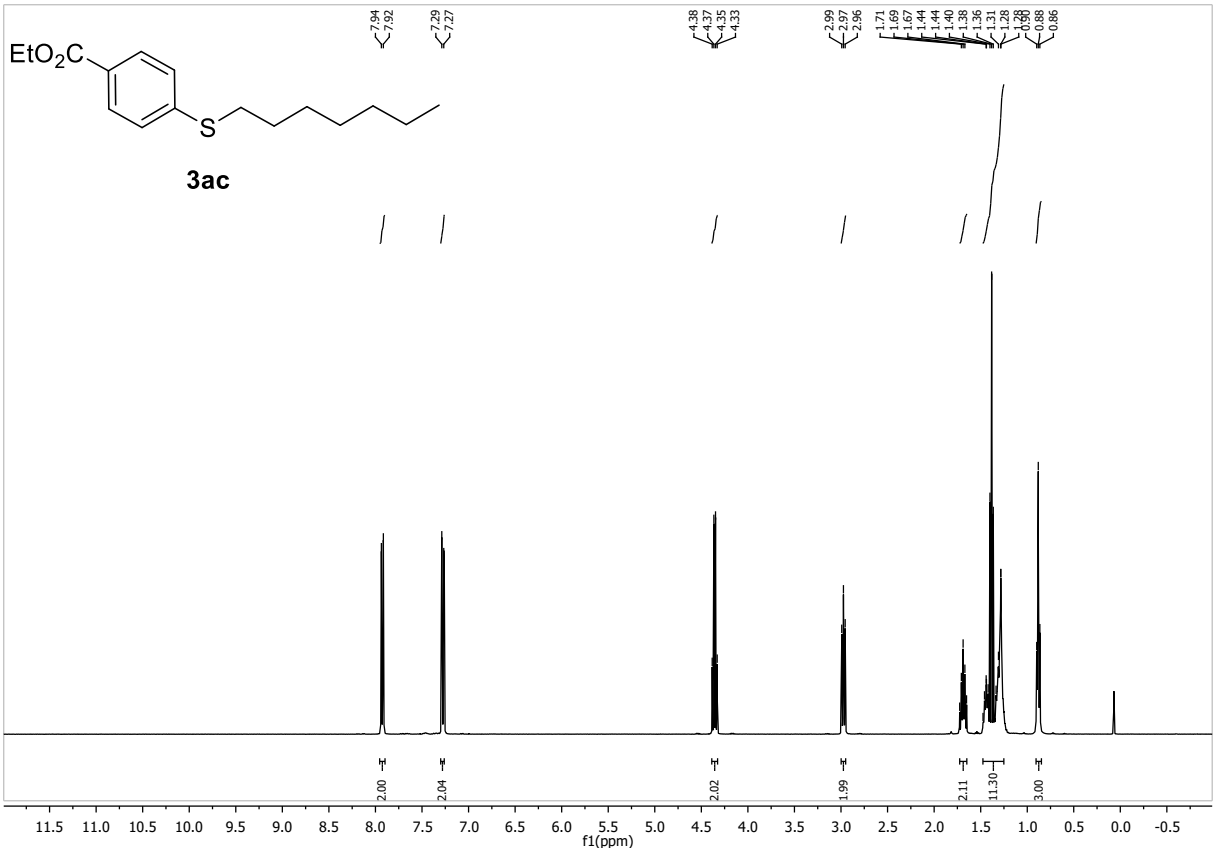
EtO2C
S
3ac
7.94
7.92
7.29
7.27
4.38
4.37
4.35
4.33
2.99
2.97
2.96
1.71
1.69
1.67
1.44
1.40
1.38
1.36
1.31
1.28
0.91
0.88
0.86
2.00
2.04
2.02
1.99
2.11
11.30
3.00
f1(ppm)

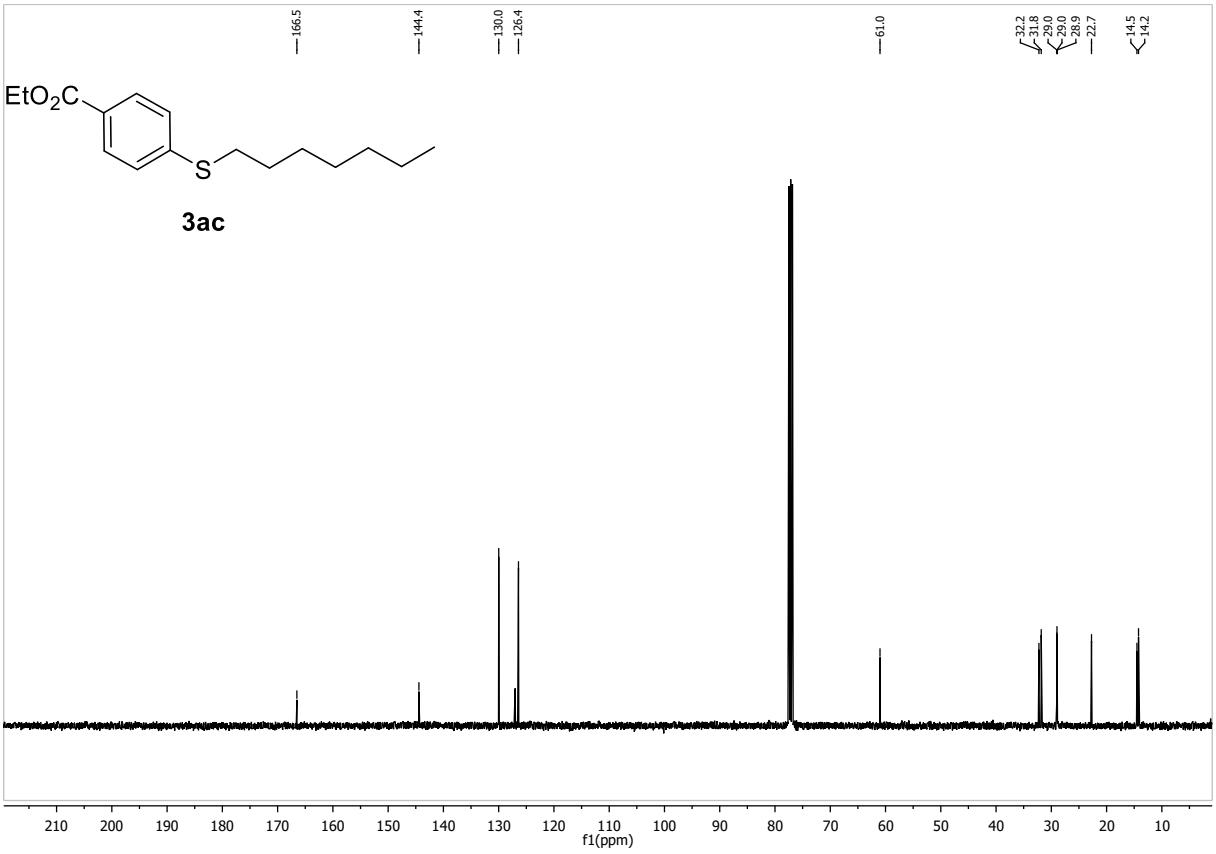
EtO2C
S
3ac
166.5
144.4
130.0
126.4
61.0
32.2
31.8
29.0
29.0
28.9
22.7
14.5
14.2
f1(ppm)

Ethyl 4-(dodecylthio)benzoate (3ad)

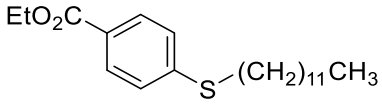

3ad

$C_{21}H_{34}O_2S$ (350.56 g/mol)

Following GP-B, **3ad** was synthesized using ethyl 4-chlorobenzoate (157 µL, 1.00 mmol, 1.0 equiv.) and 1-dodecanethiol (264 µL, 1.10 mmol, 1.1 equiv.). Purification by FC (SiO_2, 5 CV Hex, gradient to 8:2 Hex:EtOAc over 20 CV) afforded **3ad** (337 mg, 961 µmol, 96%) as off-white solid. Conforms to reported analytical data.[25]

R_f: 0.64 (Hex:EtOAc 9:1)

^{1}H-NMR (400 MHz, $CDCl_3$, δ): 7.93 (d, *J* = 8.5 Hz, 2H), 7.28 (d, *J* = 8.5 Hz, 2H), 4.36 (q, *J* = 7.2 Hz, 2H), 2.97 (t, *J* = 7.2 Hz, 2H), 1.69 (p, *J* = 7.2 Hz, 2H), 1.49 – 1.22 (m, 21H), 0.87 (t, *J* = 7.2 Hz, 3H).

^{13}C-NMR (101 MHz, $CDCl_3$, δ): 166.5, 144.4, 130.0, 127.0, 126.4, 61.0, 32.2, 32.1, 29.8, 29.8, 29.7, 29.6, 29.5, 29.3, 29.0, 28.9, 22.8, 14.5, 14.3.

HR-MS (ESI): m/z calc. for $[M+Na]^+$ 373,21717, found 373,21705.

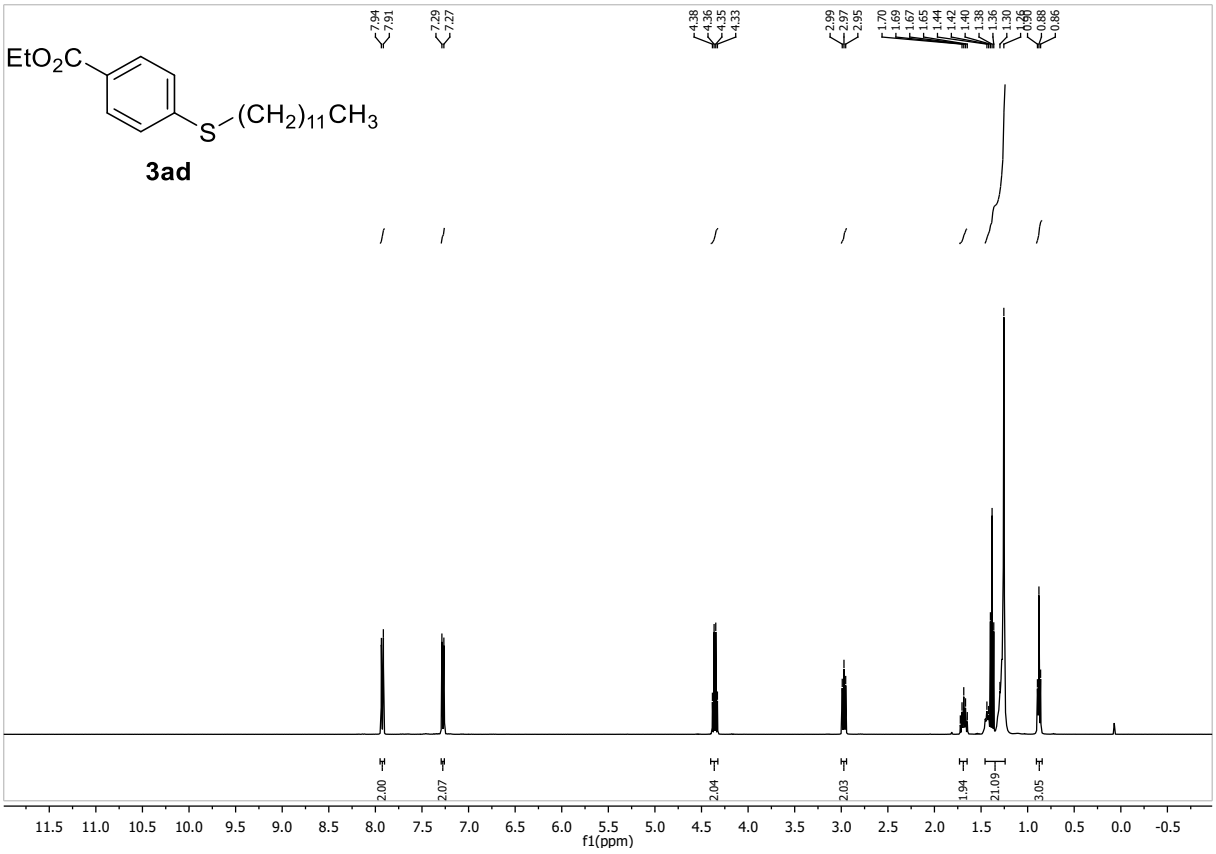
EtO2C
S
(CH2)11CH3
3ad
7.94
7.91
7.29
7.27
4.38
4.36
4.35
4.33
2.99
2.97
2.95
1.70
1.69
1.67
1.65
1.44
1.42
1.40
1.38
1.36
1.30
0.88
0.86
2.00
2.07
2.04
2.03
1.94
21.09
3.05
f1(ppm)

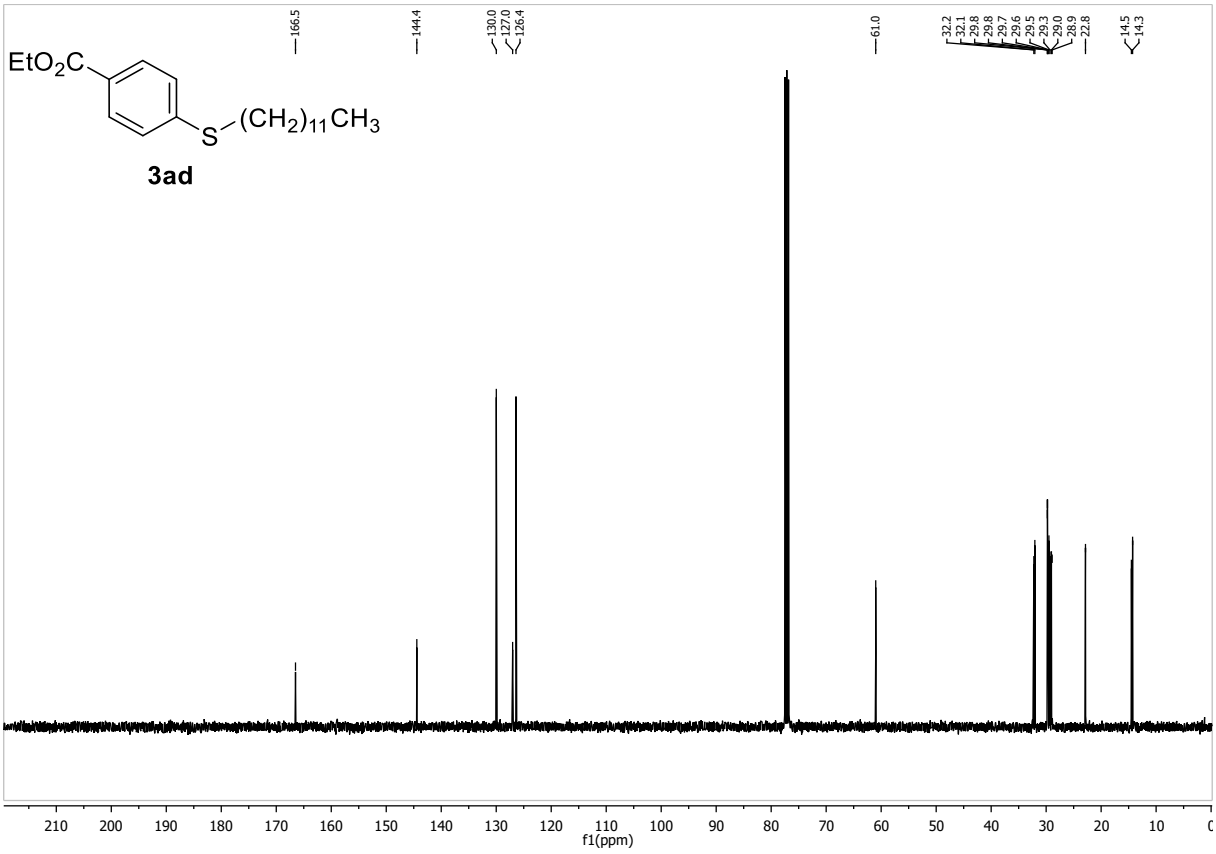
EtO2C
S
(CH2)11CH3
3ad
166.5
144.4
130.0
127.0
126.4
61.0
32.2
32.1
29.8
29.8
29.7
29.6
29.5
29.3
29.0
28.9
22.8
14.5
14.3
f1(ppm)

Ethyl 4-(2-ethylhexylthio) benzoate (3ae)

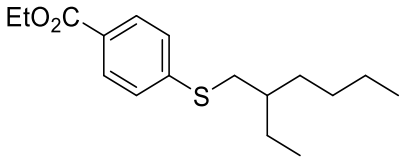

3ae

$C_{17}H_{26}O_2S$ (294.45 g/mol)

Following GP-B, **3ae** was synthesized using ethyl 4-chlorobenzoate (157 µL, 1.00 mmol, 1.0 equiv.) and 2-ethylhexanethiol (191 µL, 1.10 mmol, 1.1 equiv.). Purification by FC (SiO_2, 5 CV Hex, gradient to 9:1 Hex:EtOAc over 15 CV) afforded **3ae** (283 mg, 960 µmol, 96%) as colorless oil, which solidified upon standing.

R_f: 0.64 (Hex:EtOAc 9:1)

m.p.: ambient temperature

^{1}H-NMR (400 MHz, $CDCl_3$, δ): 7.92 (d, *J* = 8.5 Hz, 2H), 7.29 (d, *J* = 8.5 Hz, 2H), 4.35 (q, *J* = 7.1 Hz, 2H), 2.95 (d, *J* = 6.3 Hz, 2H), 1.62 (p, *J* = 6.2 Hz, 1H), 1.55 – 1.35 (m, 7H), 1.34 – 1.24 (m, 4H), 0.94 – 0.86 (m, 6H).

^{13}C-NMR (101 MHz, $CDCl_3$, δ): 166.5, 145.0 129.9, 126.9, 126.5, 61.0, 38.8, 36.6, 32.6, 28.9, 25.8, 23.1, 14.5, 14.2, 10.9.

HR-MS (ESI): m/z calc. for $[M+Na]^+$ 317.15457, found 317.15497.

IR (ATR, $\tilde{\nu}$ [cm^{-1}]): 3058 (w), 2957 (m), 2924 (m), 2862 (w), 1713 (s), 1593 (m), 1564 (w), 1459 (w), 1433 (w), 1396 (m), 1369 (w), 1310 (w), 1269 (vs), 1232 (m), 1176 (m), 1101 (s), 1019 (m), 877 (w), 844 (w), 785 (w), 755 (s), 691 (m).

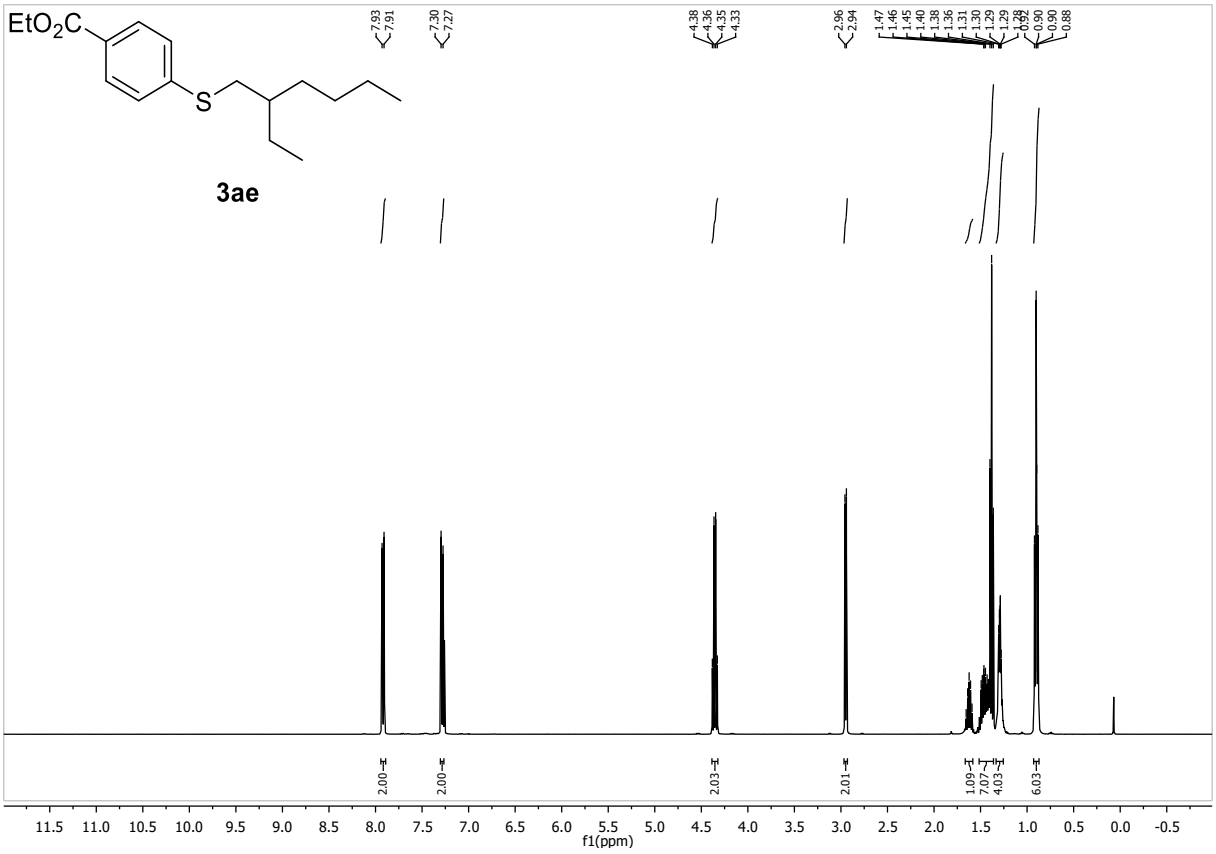
EtO2C
S
3ae
7.93
7.91
7.30
7.27
4.38
4.36
4.35
4.33
2.96
2.94
1.47
1.46
1.45
1.40
1.38
1.36
1.31
1.30
1.29
0.92
0.90
0.90
0.88
2.00
2.00
2.03
2.01
1.09
7.07
4.03
6.03
f1(ppm)

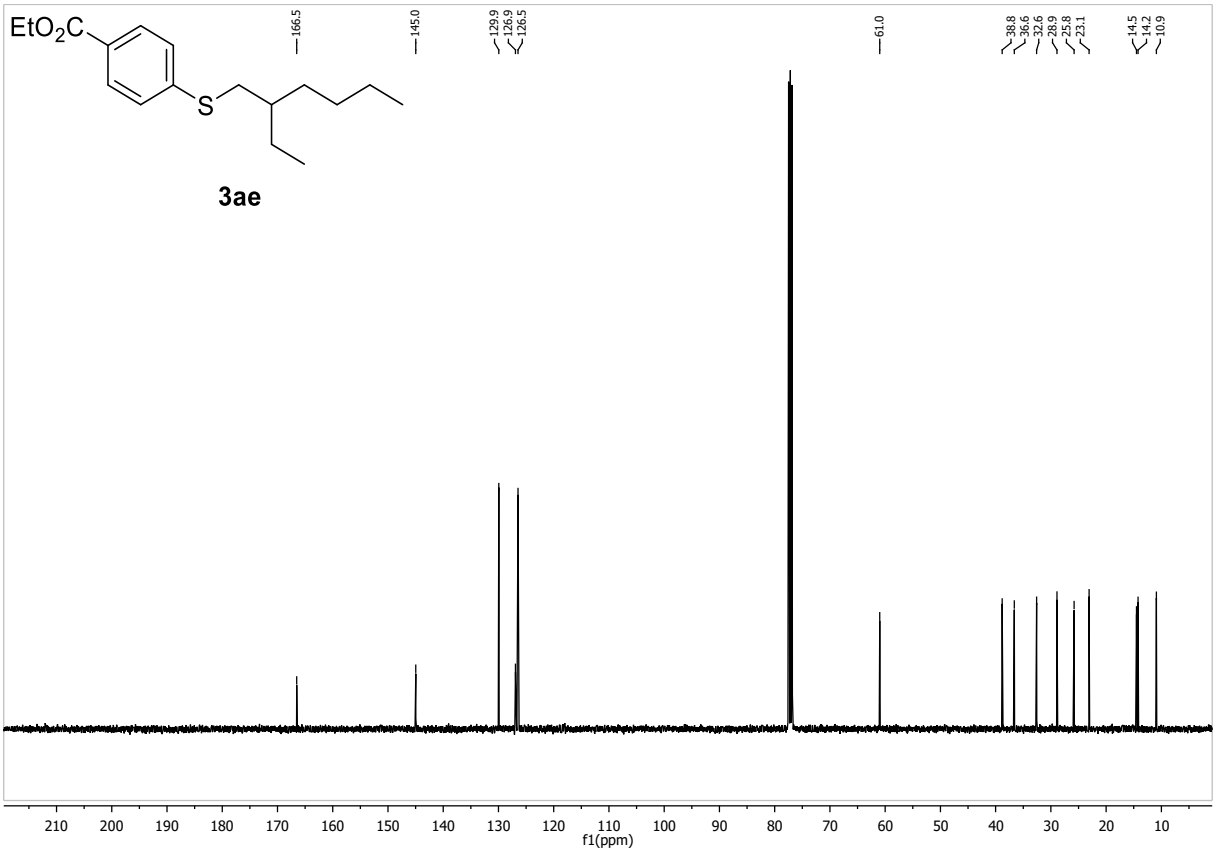
EtO2C
S
3ae
166.5
145.0
129.9
126.9
126.5
61.0
38.8
36.6
32.6
28.9
25.8
23.1
14.5
14.2
10.9
f1(ppm)

Ethyl 4-(cyclopentylthio)benzoate (3af)

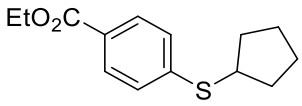

3af

$C_{14}H_{18}O_2S$ (250.36 g/mol)

Following GP-B, **3af** was synthesized using ethyl 4-chlorobenzoate (157 µL, 1.00 mmol, 1.0 equiv.) and cyclopentanethiol (118 µL, 1.10 mmol, 1.1 equiv.). Purification by FC (SiO_2, 5 CV Hex, gradient to 9:1 Hex:EtOAc over 15 CV) afforded **3af** (224 mg, 893 µmol, 89%) as colorless oil.

R_f: 0.57 (Hex:EtOAc 9:1)

^{1}H-NMR (400 MHz, $CDCl_3$, δ): 7.92 (d, *J* = 8.5 Hz, 2H), 7.30 (d, *J* = 8.5 Hz, 2H), 4.35 (q, *J* = 7.1 Hz, 2H), 3.75 – 3.66 (m, 1H), 2.19 – 2.07 (m, 2H), 1.85 – 1.74 (m, 2H), 1.71 – 1.59 (m, 4H), 1.38 (t, *J* = 7.1 Hz, 3H).

^{13}C-NMR (101 MHz, $CDCl_3$, δ): 166.5, 144.9, 129.9, 127.1, 127.0, 61.0, 44.4, 33.6, 25.1, 14.5.

HR-MS (ESI): m/z calc. for $[M+Na]^+$ 273.09197, found 273.09239.

IR (ATR, $\tilde{\nu}$ [cm^{-1}]): 2954 (w), 2865 (w), 1709 (s), 1590 (m), 1560 (w), 1480 (w), 1448 (w), 1396 (w), 1366 (w), 1310 (w), 1270 (s), 1176 (m), 1102 (s), 1019 (m), 964 (w), 934 (w), 904 (w), 874 (w), 844 (m), 788 (w), 758 (m), 721 (w), 691 (w).

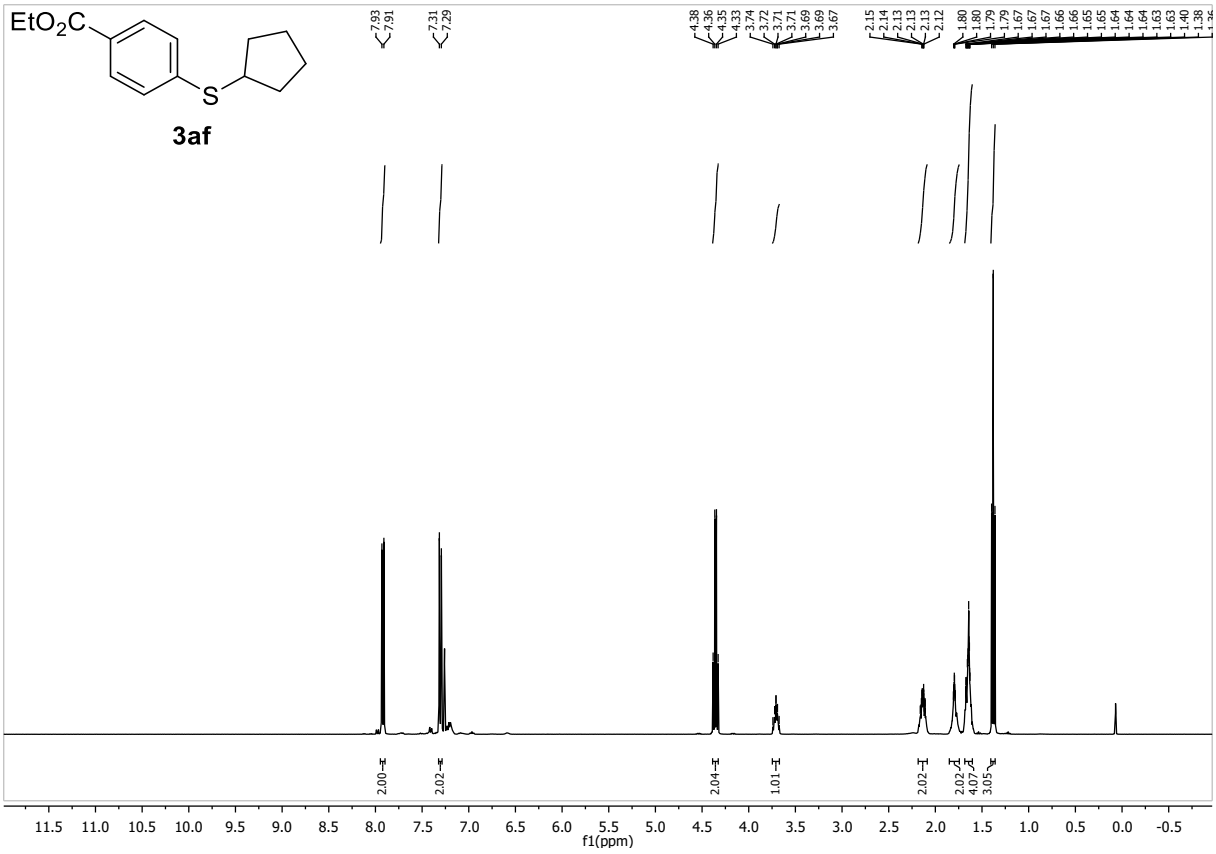
EtO2C
S
3af
7.93
7.91
7.31
7.29
4.38
4.36
4.35
4.33
3.74
3.72
3.71
3.71
3.69
3.69
3.67
2.15
2.14
2.13
2.13
2.13
2.12
1.80
1.80
1.79
1.79
1.67
1.67
1.67
1.66
1.66
1.65
1.65
1.64
1.64
1.63
1.63
1.40
1.38
2.00
2.02
2.04
1.01
2.02
2.02
4.07
3.05
11.5 11.0 10.5 10.0 9.5 9.0 8.5 8.0 7.5 7.0 6.5 6.0 5.5 5.0 4.5 4.0 3.5 3.0 2.5 2.0 1.5 1.0 0.5 0.0 -0.5
f1(ppm)

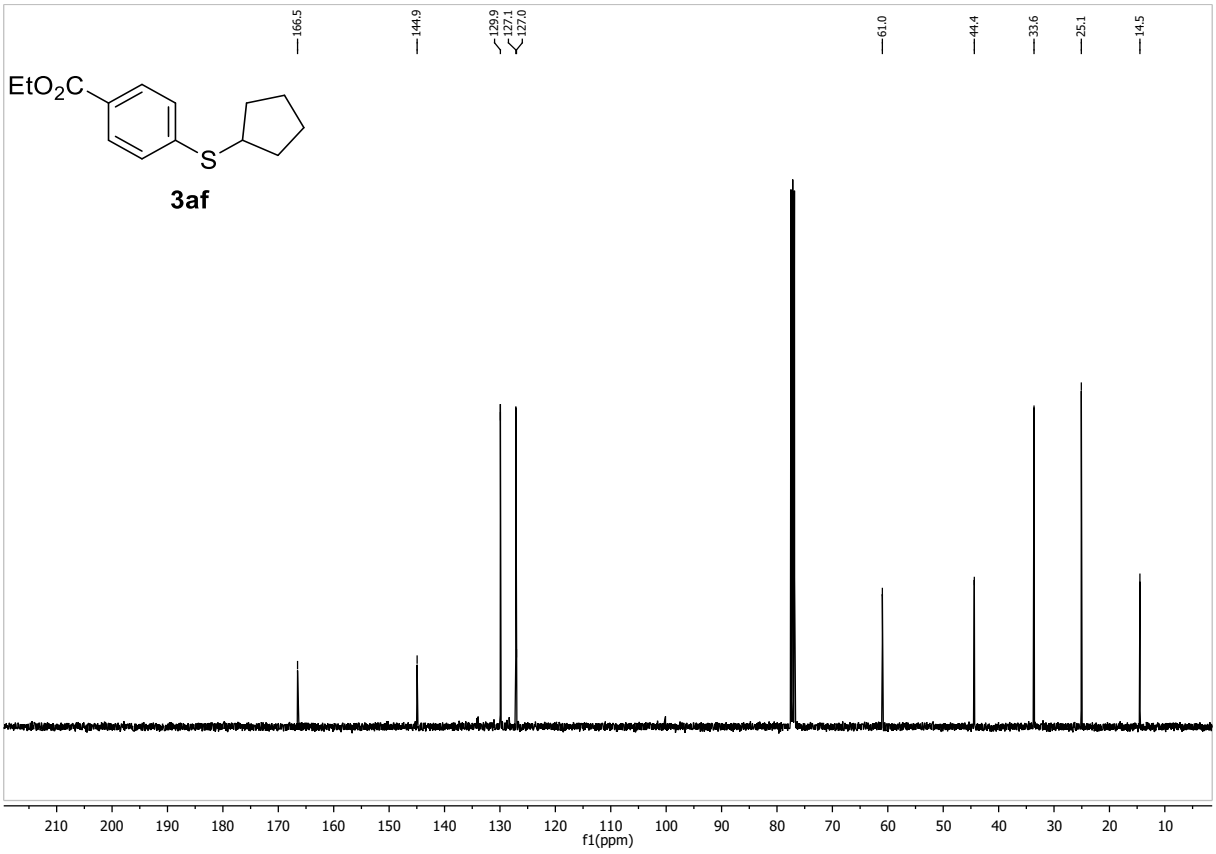
EtO2C
S
3af
166.5
144.9
129.9
127.1
127.0
61.0
44.4
33.6
25.1
14.5
210 200 190 180 170 160 150 140 130 120 110 100 90 80 70 60 50 40 30 20 10
f1(ppm)

Ethyl 4-(cyclohexylthio)benzoate (3aa)

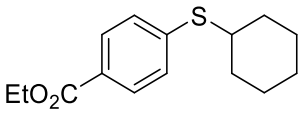

3aa

$C_{15}H_{20}O_2S$ (264.38 g/mol)

Following GP-B, **3aa** was synthesized using ethyl 4-chlorobenzoate (157 µL, 1.00 mmol, 1.0 equiv.) and cyclohexanethiol (135 µL, 1.10 mmol, 1.1 equiv.) Purification by FC (SiO_2, 5 CV Hex, gradient to 9:1 Hex:EtOAc over 15 CV) afforded **3aa** (259 mg, 980 µmol, 98%) as colorless oil. Conforms to reported analytical data.[25]

Upscale:
An inert, flame-dried and septum-caped Schlenk-tube equipped with a stirring bar was charged with KOAc (736 mg, 7.5 mmol, 1.5 equiv.), **C1** (3 mol%), ethyl 4-chlorobenzoate (778 µL, 5.00 mmol, 1.0 equiv.), cyclohexanethiol (673 µL, 5.50 mmol, 1.1 equiv.) and dissolved in THF (15 mL) and stirred at rt for 30 minutes. Work-up was done according to GP-B. Purification by manual column chromatography (SiO_2, Hex, gradient to 8:2 Hex:EtOAc) afforded **3aa** (1.30 g, 4.92 mmol, 98%) as colorless oil. Conforms to reported analytical data. [25]

R_f: 0.57 (Hex:EtOAc 9:1)

^{1}H-NMR (400 MHz, $CDCl_3$, δ): 7.93 (d, *J* = 8.5 Hz, 2H), 7.34 (d, *J* = 8.5 Hz, 2H), 4.36 (q, *J* = 7.1 Hz, 2H), 3.34 – 3.21 (m, 1H), 2.07 – 1.99 (m, 2H), 1.76 – 1.83 (m, 2H), 1.69 – 1.60 (m, 1H), 1.44 – 1.25 (m, 8H).

^{13}C-NMR (101 MHz, $CDCl_3$, δ): 166.5, 142.9, 130.0, 128.7, 127.7, 61.0, 45.3, 33.2, 26.1, 25.8, 14.5.

HR-MS (ESI): m/z calc. for $[M+Na]^+$ 287.10762, found 287.10808.

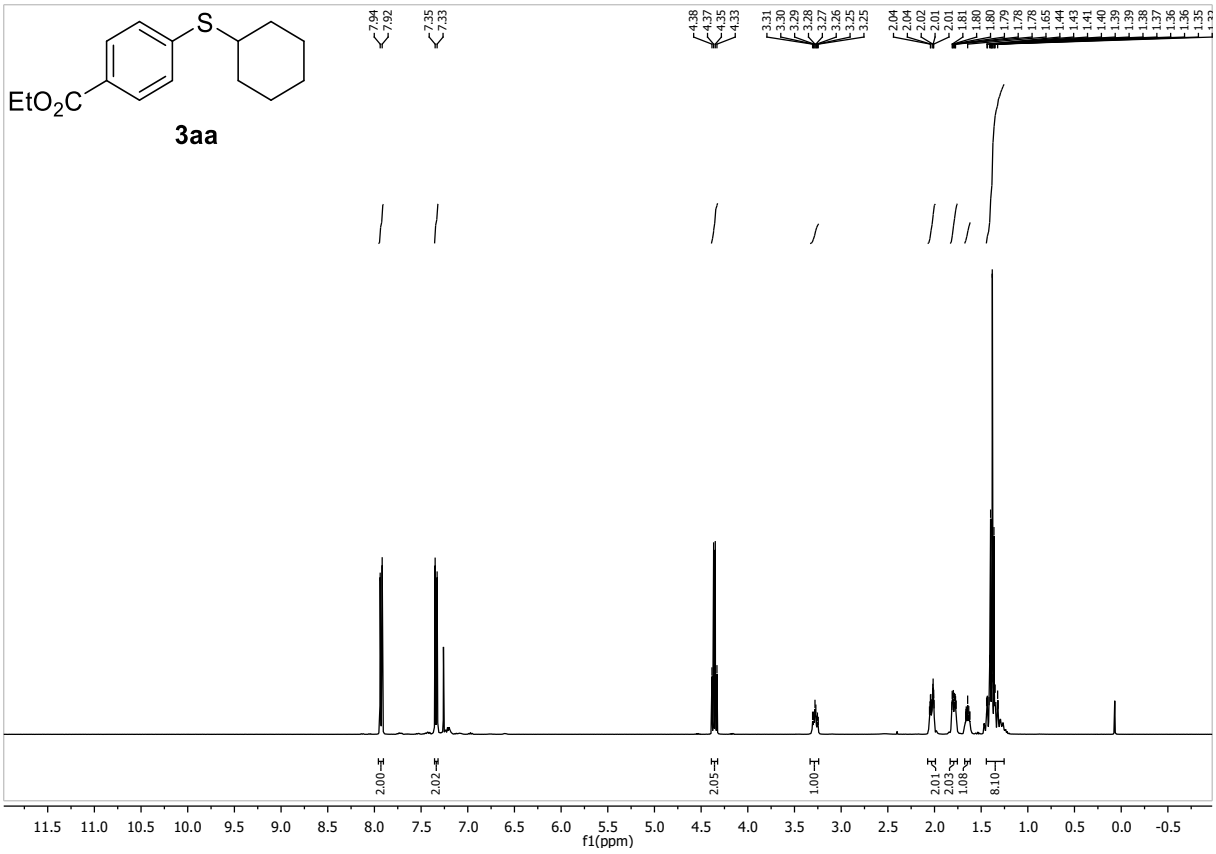
EtO2C
S
3aa
7.94
7.92
7.35
7.33
4.38
4.37
4.35
4.33
3.31
3.30
3.29
3.28
3.27
3.26
3.25
2.04
2.04
2.02
2.01
2.01
1.81
1.80
1.80
1.79
1.78
1.78
1.65
1.44
1.43
1.41
1.40
1.39
1.39
1.38
1.37
1.36
1.36
1.35
2.00
2.02
2.05
1.00
2.01
2.03
1.08
8.10
11.5 11.0 10.5 10.0 9.5 9.0 8.5 8.0 7.5 7.0 6.5 6.0 5.5 5.0 4.5 4.0 3.5 3.0 2.5 2.0 1.5 1.0 0.5 0.0 -0.5
f1(ppm)

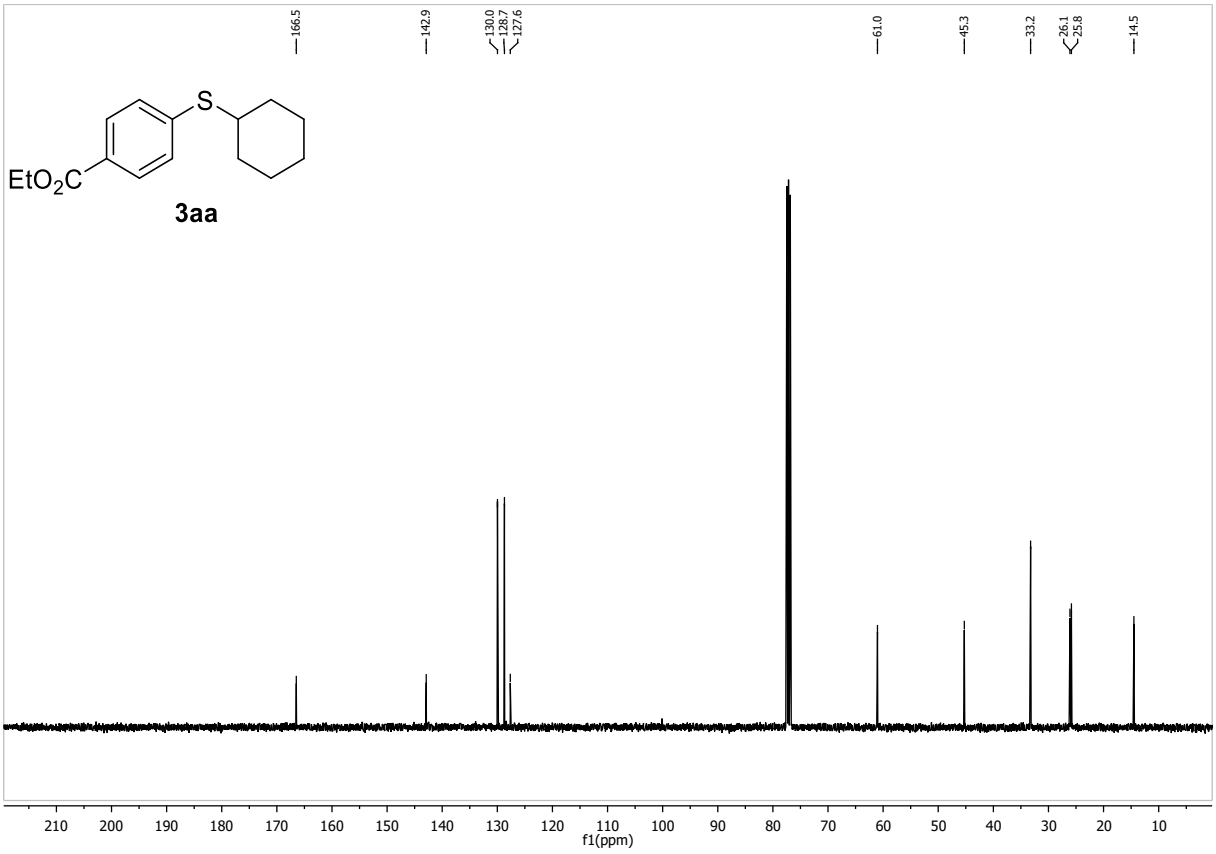
EtO2C
S
3aa
166.5
142.9
130.0
128.7
127.6
61.0
45.3
33.2
26.1
25.8
14.5
210 200 190 180 170 160 150 140 130 120 110 100 90 80 70 60 50 40 30 20 10
f1(ppm)

Ethyl 4-(tert-butylthio)benzoate (3ag)

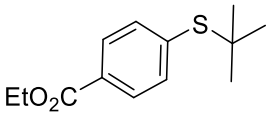

3ag

$C_{13}H_{18}O_2S$ (238.35 g/mol)

Following GP-B, **3ag** was synthesized using ethyl 4-chlorobenzoate (157 µL, 1.00 mmol, 1.0 equiv.) and 2-methyl-2-propanethiol (120 µL, 1.10 mmol, 1.1 equiv.) Purification by FC (SiO_2, 5 CV Hex, gradient to 9:1 Hex:EtOAc over 15 CV) afforded **3ag** (213 mg, 894 µmol, 89%) as colorless oil. Conforms to reported analytical data.[1]

R_f: 0.62 (Hex:EtOAc 9:1)

^{1}H-NMR (400 MHz, $CDCl_3$, δ): 7.99 (d, *J* = 8.3 Hz, 2H), 7.59 (d, *J* = 8.3 Hz, 2H), 4.38 (q, *J* = 7.1 Hz, 2H), 1.40 (t, *J* = 7.1 Hz, 3H), 1.31 (s, 9H).

^{13}C-NMR (101 MHz, $CDCl_3$, δ): ^{13}C NMR (101 MHz, $CDCl_3$) δ 166.4, 138.9, 136.9, 130.6, 129.6, 61.3, 46.9, 31.2, 14.5.

HR-MS (ESI): m/z calc. for $[M+Na]^+$ 261.09197, found 261.09249.

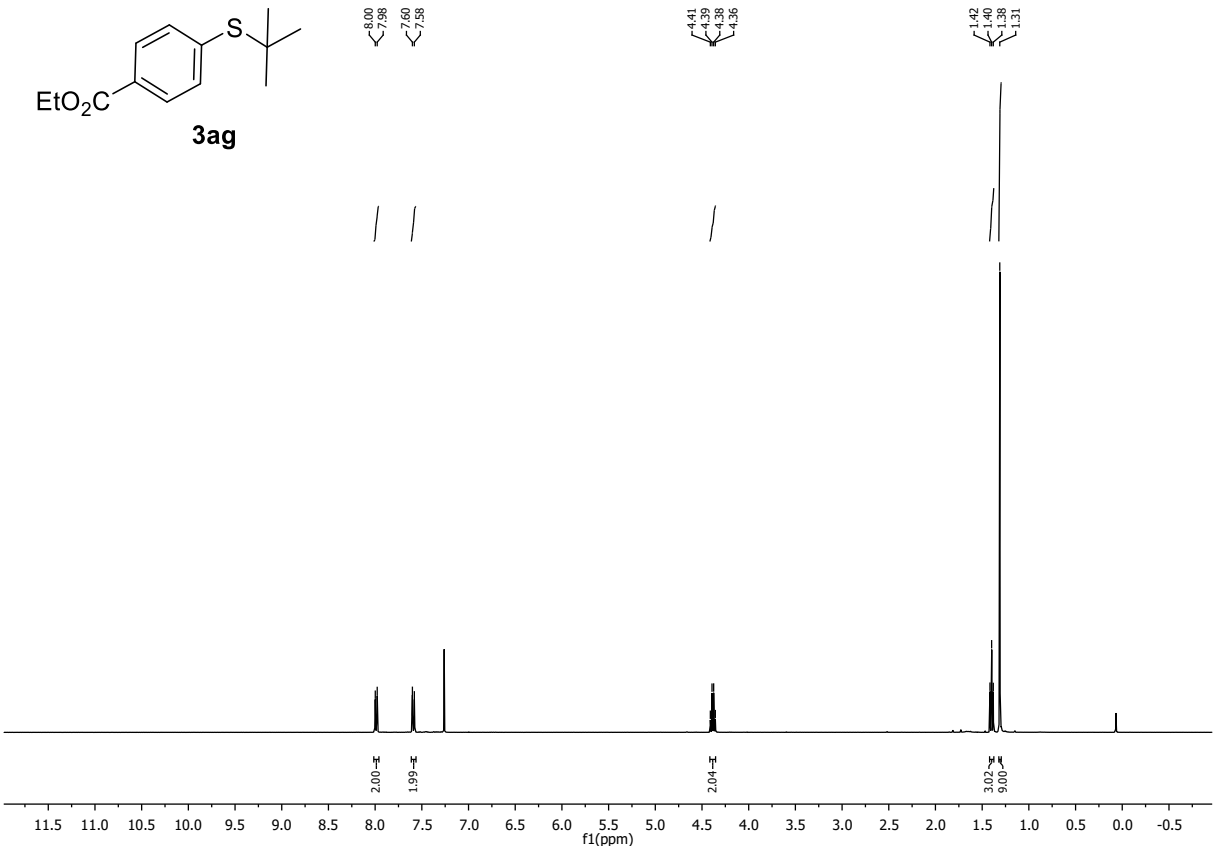
EtO2C
S
3ag
8.00
7.98
7.60
7.58
4.41
4.39
4.38
4.36
1.42
1.40
1.38
1.31
2.00
1.99
2.04
3.02
9.00
f1(ppm)

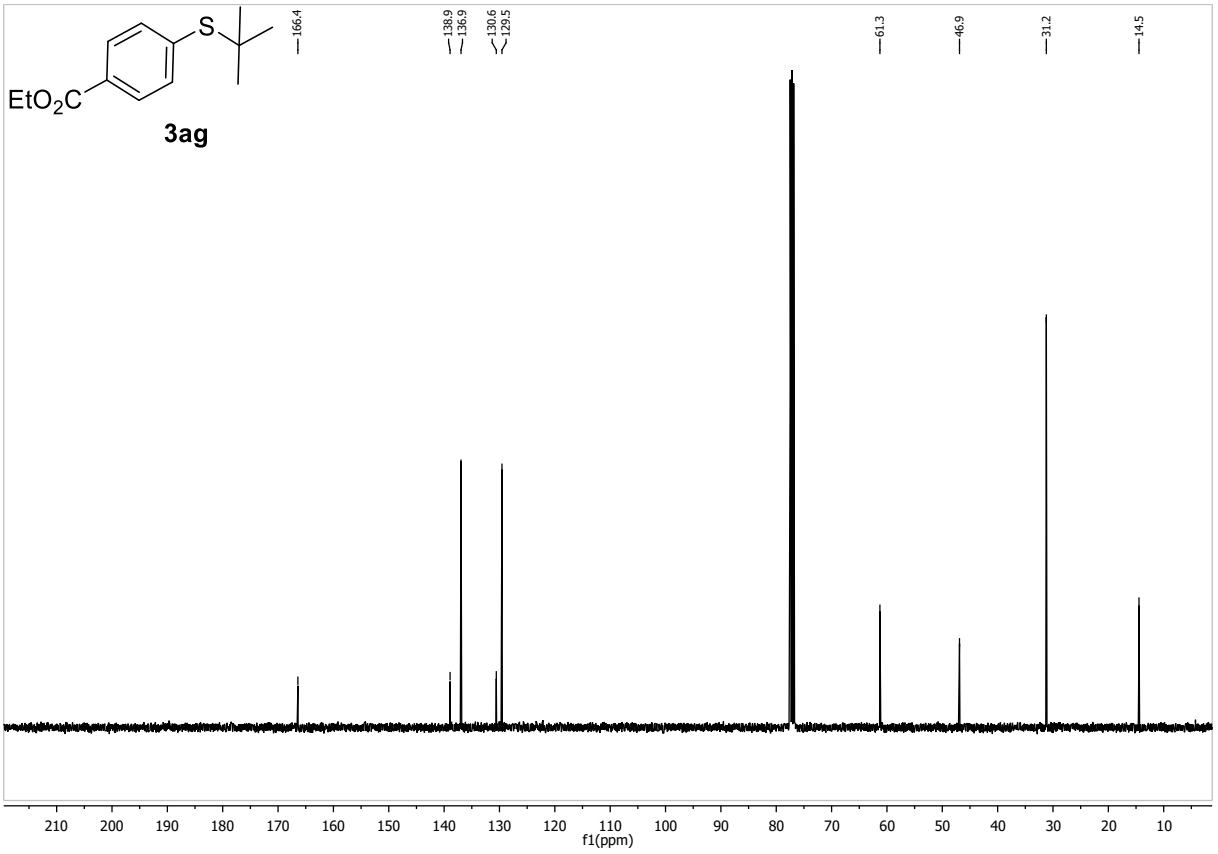
EtO2C
S
3ag
166.4
138.9
136.9
130.6
129.5
61.3
46.9
31.2
14.5
f1(ppm)

Ethyl 4-((2,2,4,6,6-pentamethylheptan-4-yl)thio)benzoate (3ah)

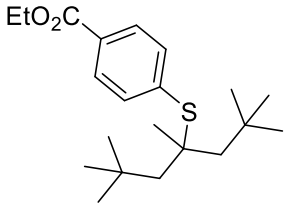

3ah

$C_{21}H_{34}O_2S$ (350.56 g/mol)

Following GP-B, **3ah** was synthesized using ethyl 4-chlorobenzoate (157 µL, 1.00 mmol, 1.0 equiv.) and *tert*-dodecanethiol (mixture of isomers,[26] 259 µL, 1.10 mmol, 1.1 equiv.). Purification by FC (SiO_2, 5 CV Hex, gradient to 9:1 Hex:EtOAc over 15 CV) afforded **3ah** (314 mg, 895 µmol, 90%, mixture of isomers according to the constitution of the starting material) as colorless oil.

R_f: 0.67 (Hex:EtOAc 9:1)

^{1}H-NMR (400 MHz, $CDCl_3$, δ): 8.01 – 7.89 (m, 2H), 7.61 – 7.51 (m, 2H), 4.44 – 4.31 (m, 2H), 1.67 – 0.58 (m, 28H).

^{13}C-NMR (101 MHz, $CDCl_3$, δ): 166.4, 137.0, 137.0, 136.9, 130.0, 129.5, 129.4, 129.4, 61.3, 61.2, 14.5.

HR-MS (ESI): m/z calc. for $[M+Na]^+$ 373.21717, found 373.21735.

IR (ATR, $\tilde{\nu}$ [cm^{-1}]): 2958 (m), 2928 (m), 2868 (w), 1717 (s), 1593 (w), 1459 (w), 1370 (w), 1269 (s), 1172 (w), 1102 (s), 1019 (m), 852 (w), 807 (w), 792 (w), 762 (m), 725 (w), 695 (w).

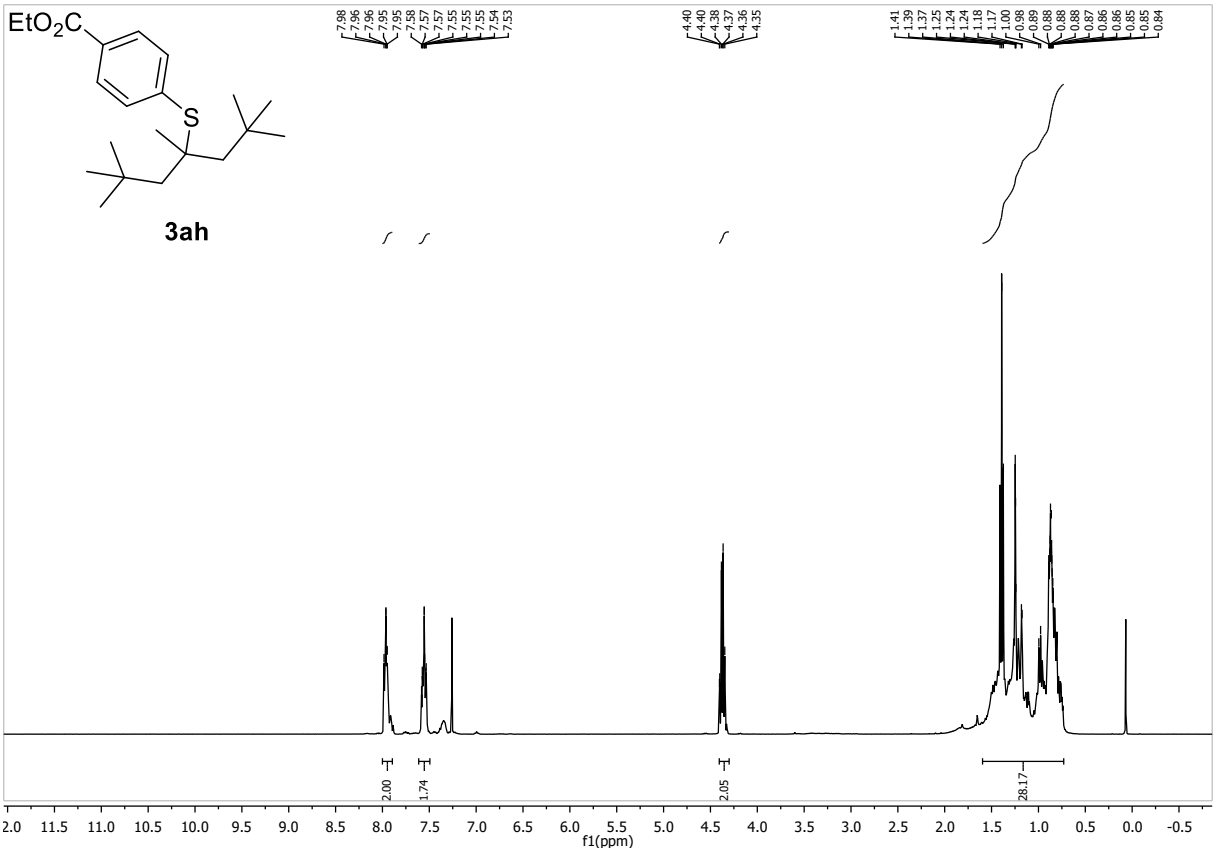
EtO2C
S
3ah
7.98
7.96
7.96
7.95
7.95
7.58
7.57
7.57
7.55
7.55
7.55
7.54
7.53
4.40
4.40
4.38
4.37
4.36
4.35
1.41
1.39
1.37
1.25
1.24
1.24
1.18
1.17
1.00
0.98
0.89
0.88
0.88
0.88
0.87
0.86
0.86
0.85
0.85
0.84
2.00
1.74
2.05
28.17
f1(ppm)

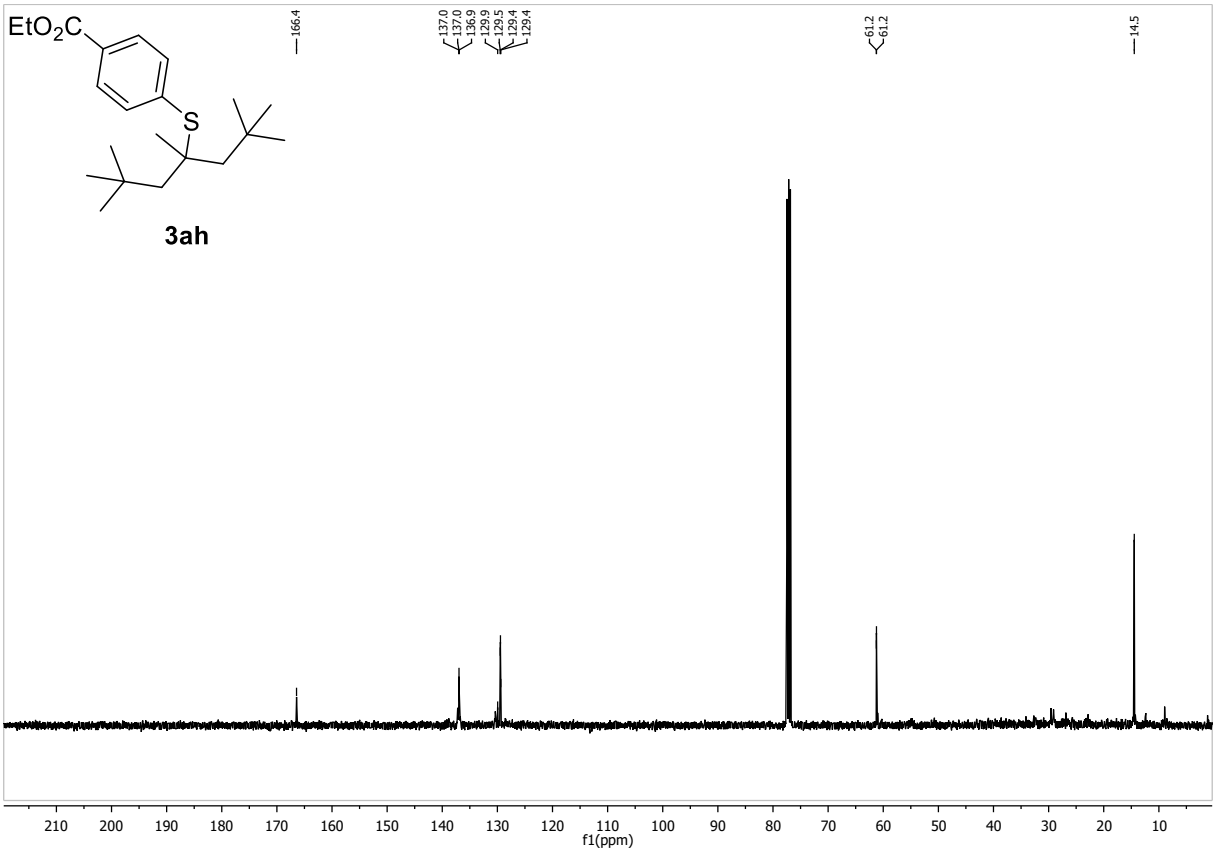
EtO2C
S
3ah
166.4
137.0
137.0
136.9
129.9
129.5
129.4
129.4
61.2
61.2
14.5
f1(ppm)

Ethyl 4-(((1S,2S,5R)-2,6,6-trimethylbicyclo[3.1.1]heptan-2-yl)thio)benzoate (3ai)

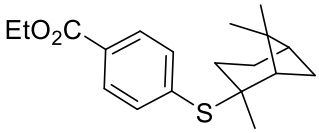

3ai

$C_{19}H_{26}O_2S$ (318.48 g/mol)

Following GP-B, **3ai** was synthesized using ethyl 4-chlorobenzoate (157 µL, 1.00 mmol, 1.0 equiv.) and 2-,3-,10-mercaptopiane (mixture of isomers,[26] 191 µL, 1.10 mmol, 1.1 equiv.). Purification by FC (SiO_2, 5 CV Hex, gradient to 9:1 Hex:EtOAc over 15 CV) afforded **3ai** (247 mg, 776 µmol, 78%, mixture of isomers according to the constitution of the starting material) as brown oil.

R_f: 0.62 (Hex:EtOAc 9:1)

^{1}H-NMR (400 MHz, $CDCl_3$, δ): 7.92 (d, *J* = 8.5 Hz, 2H), 7.26 (d, *J* = 8.5 Hz, 2H), 4.35 (q, *J* = 7.2 Hz, 2H), 3.11 – 2.84 (m, 2H), 2.42 – 2.21 (m, 2H), 2.14 – 1.53 (m, 6H), 1.38 (t, *J* = 7.2 Hz, 3H), 1.21 (d, *J* = 4.5 Hz, 3H), 1.05 (s, 2H), 0.89 (d, *J* = 9.7 Hz, 1H), 0.80 (s, 1H).

^{13}C-NMR (101 MHz, $CDCl_3$, δ): 166.5, 144.6, 123.0, 129.9, 127.0, 126.5, 126.3, 61.0, 45.7, 45.2, 41.3, 40.9, 40.4, 39.7, 39.4, 38.8, 38.6, 34.6, 33.4, 28.1, 26.8, 26.2, 24.4, 23.5, 23.4, 22.4, 22.2, 20.2, 14.5.

HR-MS (ESI): m/z calc. for $[M+Na]^+$ 341.15457, found 341.15500.

IR (ATR, $\tilde{\nu}$ [cm^{-1}]): 2980 (w), 2906 (m), 2869 (w), 1712 (s), 1590 (m), 1564 (w), 1560 (w), 1466 (w), 1396 (w), 1366 (w), 1310 (w), 1270 (s), 1176 (m), 1102 (s), 1019 (m), 956 (w), 911 (w), 874 (w), 844 (w), 785 (w), 755 (m), 691 (w).

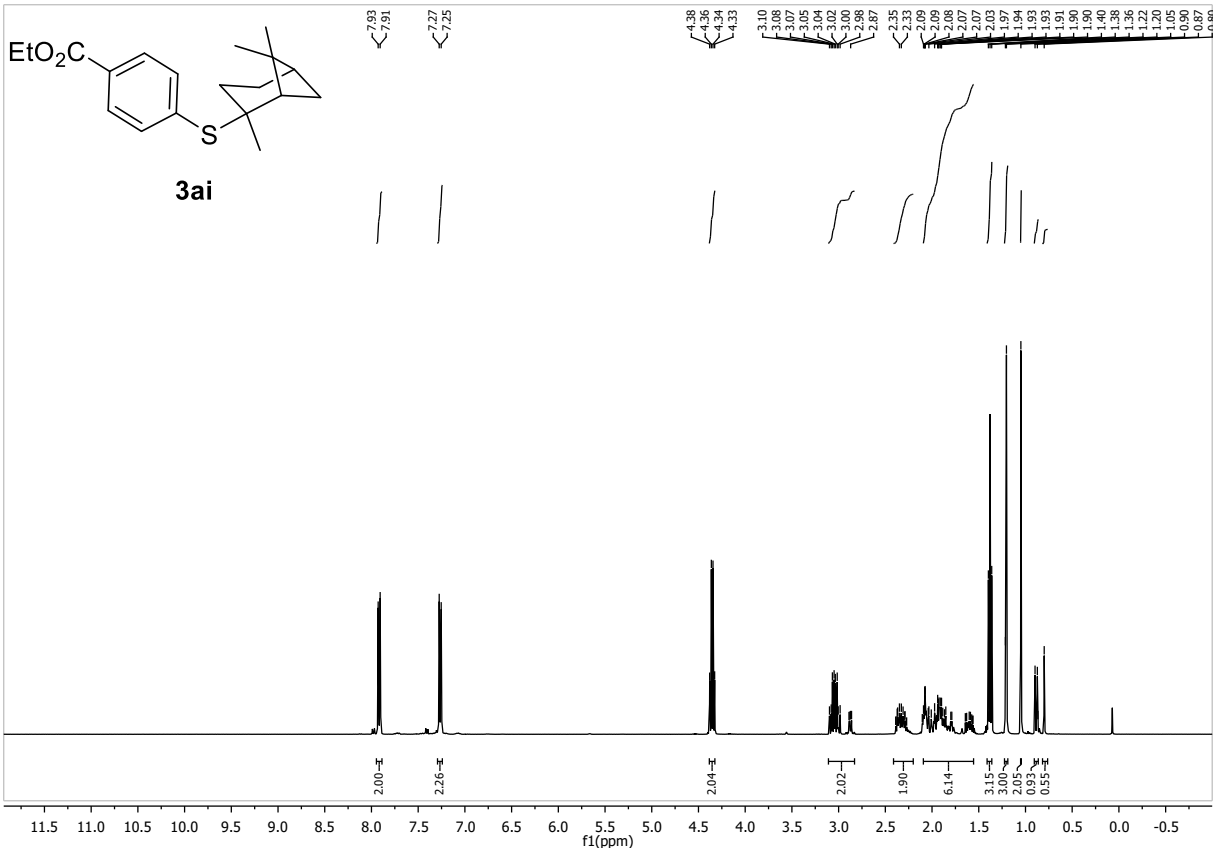
EtO2C
S
3ai
f1(ppm)

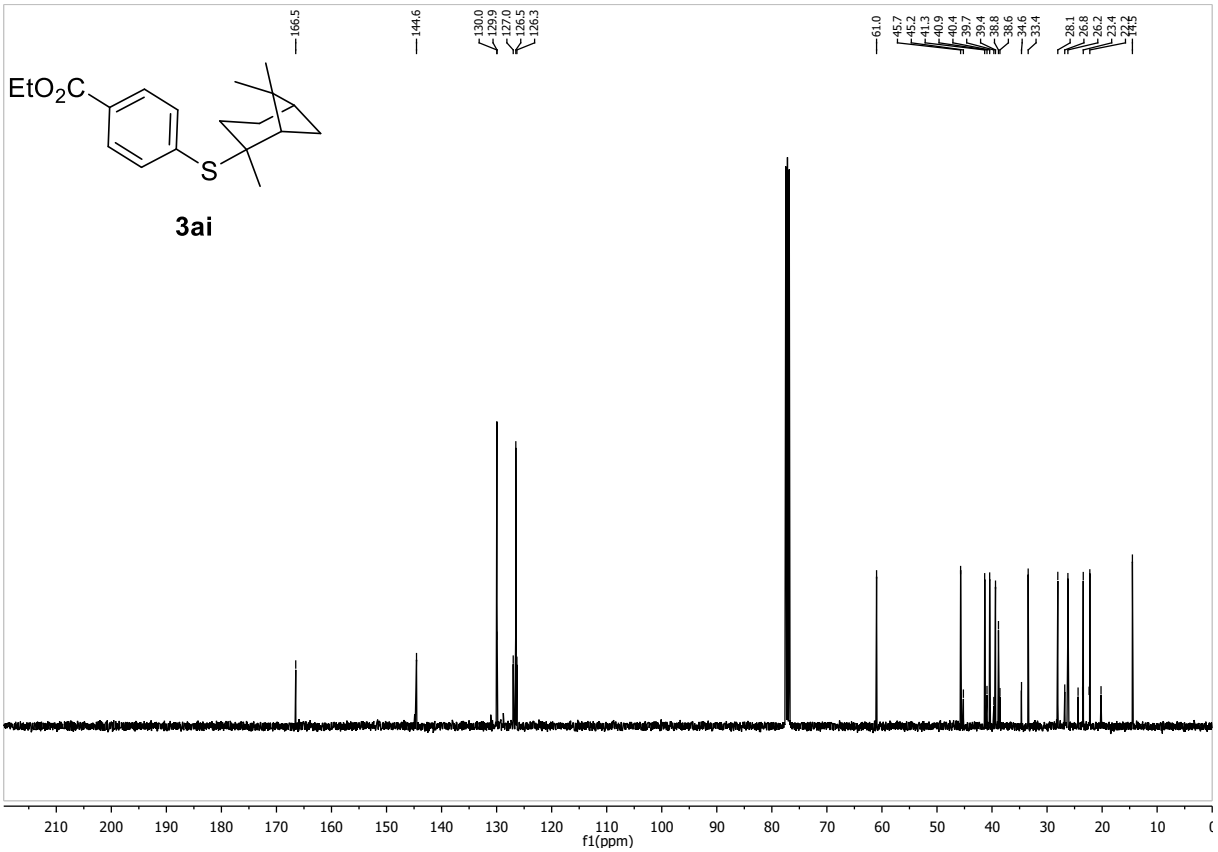
EtO2C
S
3ai
f1(ppm)

Ethyl 4-((2-methyloctan-2-yl)thio)benzoate (3aj)

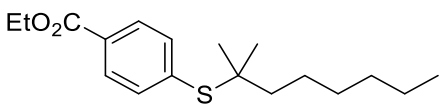

3aj

$C_{18}H_{28}O_2S$ (308.48 g/mol)

Following GP-B, **3aj** was synthesized using ethyl 4-chlorobenzoate (157 µL, 1.00 mmol, 1.0 equiv.) and 2-methyloctane-2-thiol (mixture of isomers,[26] 206 µL, 1.10 mmol, 1.1 equiv.) Purification by FC (SiO_2, 5 CV Hex, gradient to 9:1 Hex:EtOAc over 15 CV) afforded **3aj** (269 mg, 873 µmol, 87%, mixture of isomers according to the constitution of the starting material) as colorless oil. Conforms to reported analytical data.[1]

R_f: 0.67 (Hex:EtOAc 9:1)

^{1}H-NMR (400 MHz, $CDCl_3$, δ): 8.00 – 7.92 (m, 2H), 7.60 – 7.51 (m, 2H), 4.37 (q, *J* = 7.1 Hz, 2H), 1.53 – 0.80 (m, 22H).

^{13}C-NMR (101 MHz, $CDCl_3$, δ) all isomers: 166.4, 137.3, 137.3, 137.2, 137.2, 137.1, 137.1, 137.0, 136.9, 136.9, 136.8, 136.8, 130.4, 130.3, 130.3, 129.5, 129.5, 129.4, 129.4, 129.4, 61.2, 55.5, 55.2, 54.7, 51.2, 50.2, 48.9, 46.9, 46.8, 43.1, 42.4, 41.7, 40.2, 39.5, 37.3, 35.0, 34.3, 33.8, 33.4, 33.3, 33.1, 32.4, 31.8, 31.8, 31.8, 30.9, 30.9, 30.8, 29.6, 29.6, 29.5, 29.4, 29.1, 29.1, 28.7, 27.2, 27.0, 26.7, 26.5, 26.3, 25.8, 25.3, 25.3, 24.7, 23.1, 22.9, 22.8, 22.3, 21.7, 21.7, 20.3, 19.4, 17.9, 14.9, 14.5, 14.5, 14.5, 14.3, 14.3, 11.6, 11.6, 11.5, 9.2, 8.9.

HR-MS (ESI): m/z calc. for $[M+Na]^+$ 331.17022, found 331.17077.

IR (ATR, $\tilde{\nu}$ [cm^{-1}]): 2958 (m), 2928 (m), 2868 (w), 1717 (s), 1593 (w), 1459 (w), 1388 (w), 1370 (m), 1269 (s), 1172 (w), 1102 (s), 1016 (m), 852 (w), 807 (w), 792 (w), 762 (m), 725 (w), 695 (w).

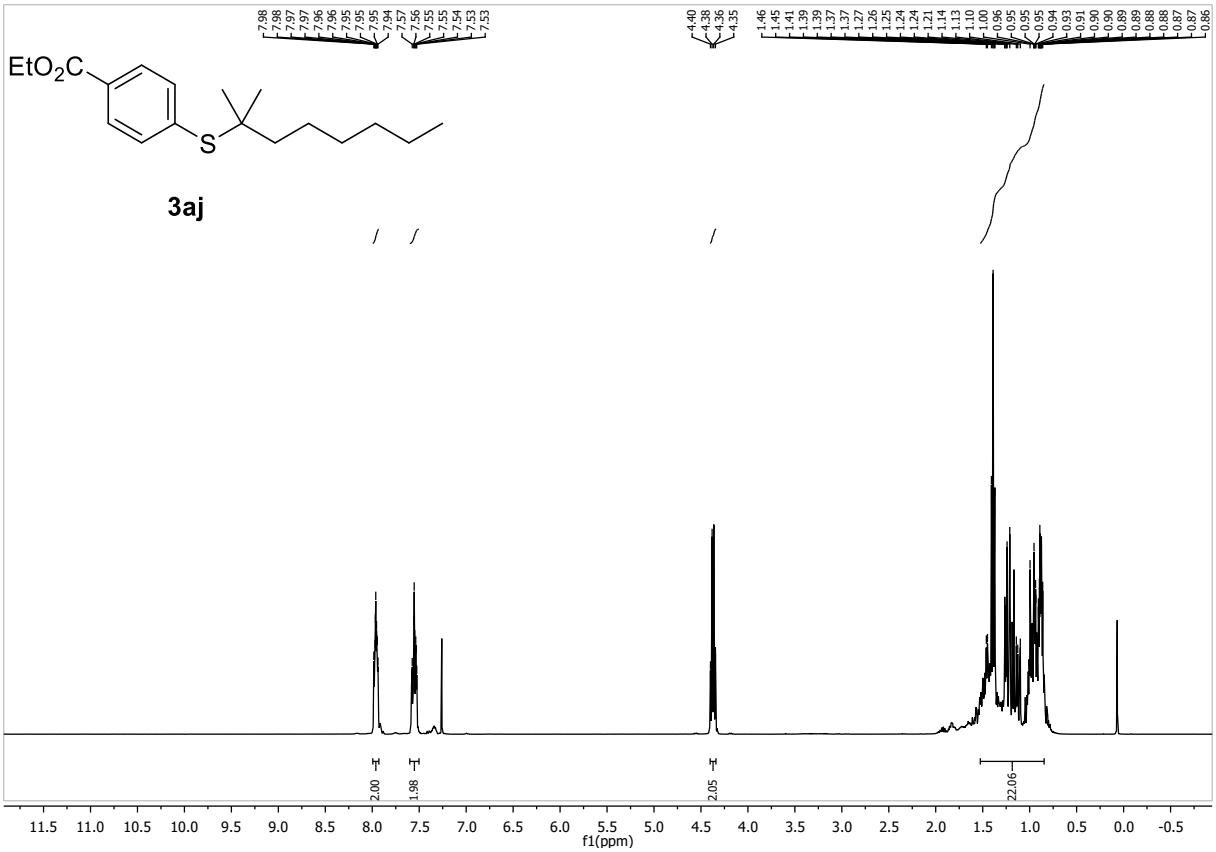
EtO2C
S
3aj
2.00
1.98
2.05
22.06
f1(ppm)

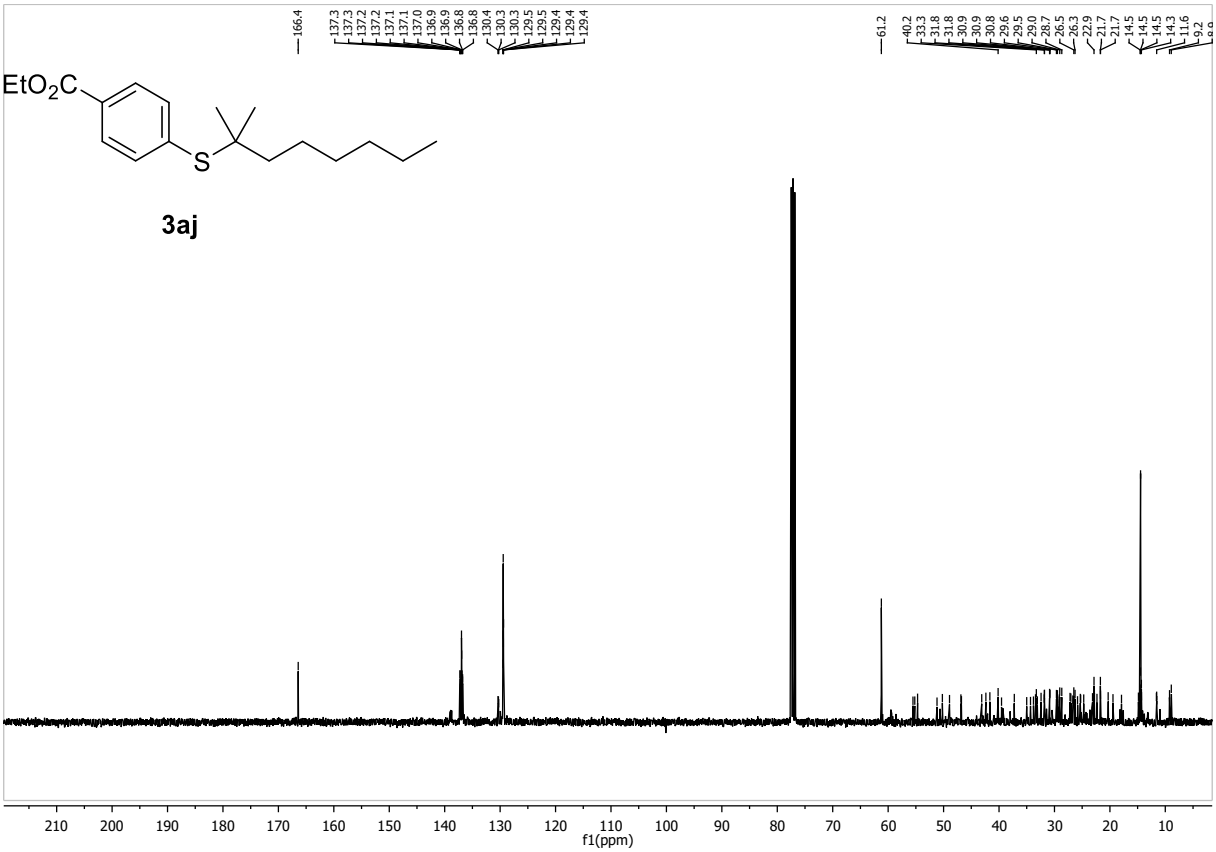
EtO2C
S
3aj
f1(ppm)

Ethyl 4-((2-phenylpropan-2-yl)thio)benzoate (3ak)

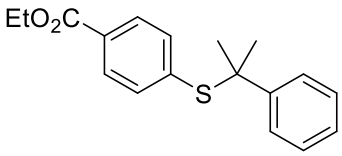

3ak

$C_{18}H_{20}O_2S$ (300.42 g/mol)

Following GP-B, **3ak** was synthesized using ethyl 4-chlorobenzoate (157 µL, 1.00 mmol, 1.0 equiv.) and 2-phenylpropane-2-thiol (166 µL, 1.10 mmol, 1.1 equiv.). Purification by FC (SiO_2, 5 CV Hex, gradient to 9:1 Hex:EtOAc over 15 CV) afforded **3ak** (45 mg, 149 µmol, 15%) as colorless solid.

R_f: 0.16 (Hex:EtOAc 99:1)

^{1}H-NMR (400 MHz, $CDCl_3$, δ): 7.82 – 7.78 (m, 2H), 7.45 – 7.40 (m, 2H), 7.31 – 7.24 (m, 2H), 7.23 – 7.18 (m, 1H), 7.14 – 7.09 (m, 2H), 4.33 (q, J = 7.1 Hz, 2H), 1.71 (s, 6H), 1.35 (t, J = 7.1 Hz, 3H).

^{13}C-NMR (101 MHz, $CDCl_3$, δ): 166.4, 146.2, 139.4, 135.0, 123.0, 129.3, 128.2, 126.9, 126.6, 61.1, 51.9, 30.1, 14.4.

HR-MS (ESI): m/z calc. for $[M+Na]^+$ 323.10762 found 323.10759.

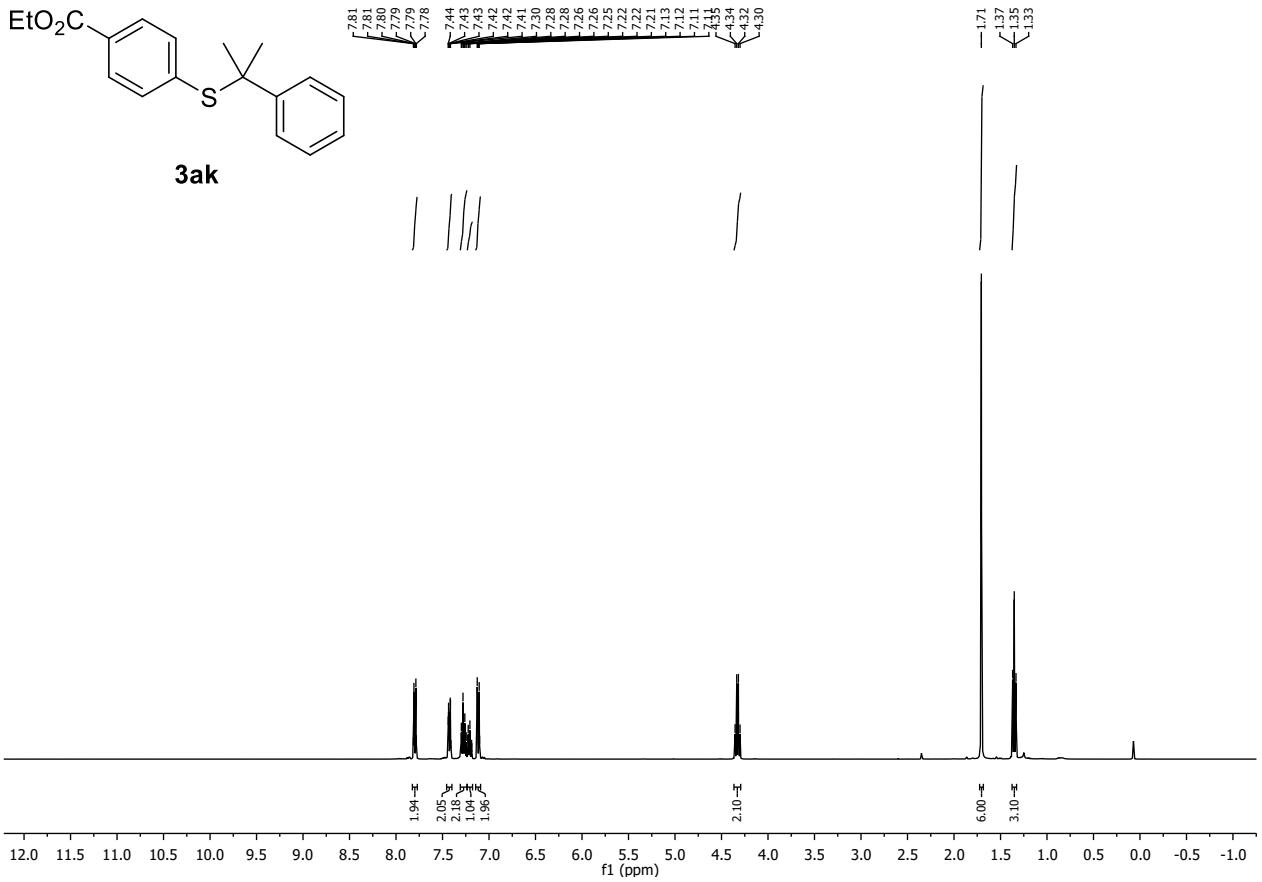
EtO2C
S
3ak
7.81
7.81
7.80
7.79
7.79
7.78
7.44
7.43
7.43
7.42
7.42
7.41
7.30
7.28
7.28
7.26
7.25
7.22
7.22
7.21
7.13
7.12
7.11
7.11
4.35
4.34
4.32
4.30
1.71
1.37
1.35
1.33
1.94
2.05
2.18
1.04
1.96
2.10
6.00
3.10
12.0 11.5 11.0 10.5 10.0 9.5 9.0 8.5 8.0 7.5 7.0 6.5 6.0 5.5 5.0 4.5 4.0 3.5 3.0 2.5 2.0 1.5 1.0 0.5 0.0 -0.5 -1.0
f1 (ppm)

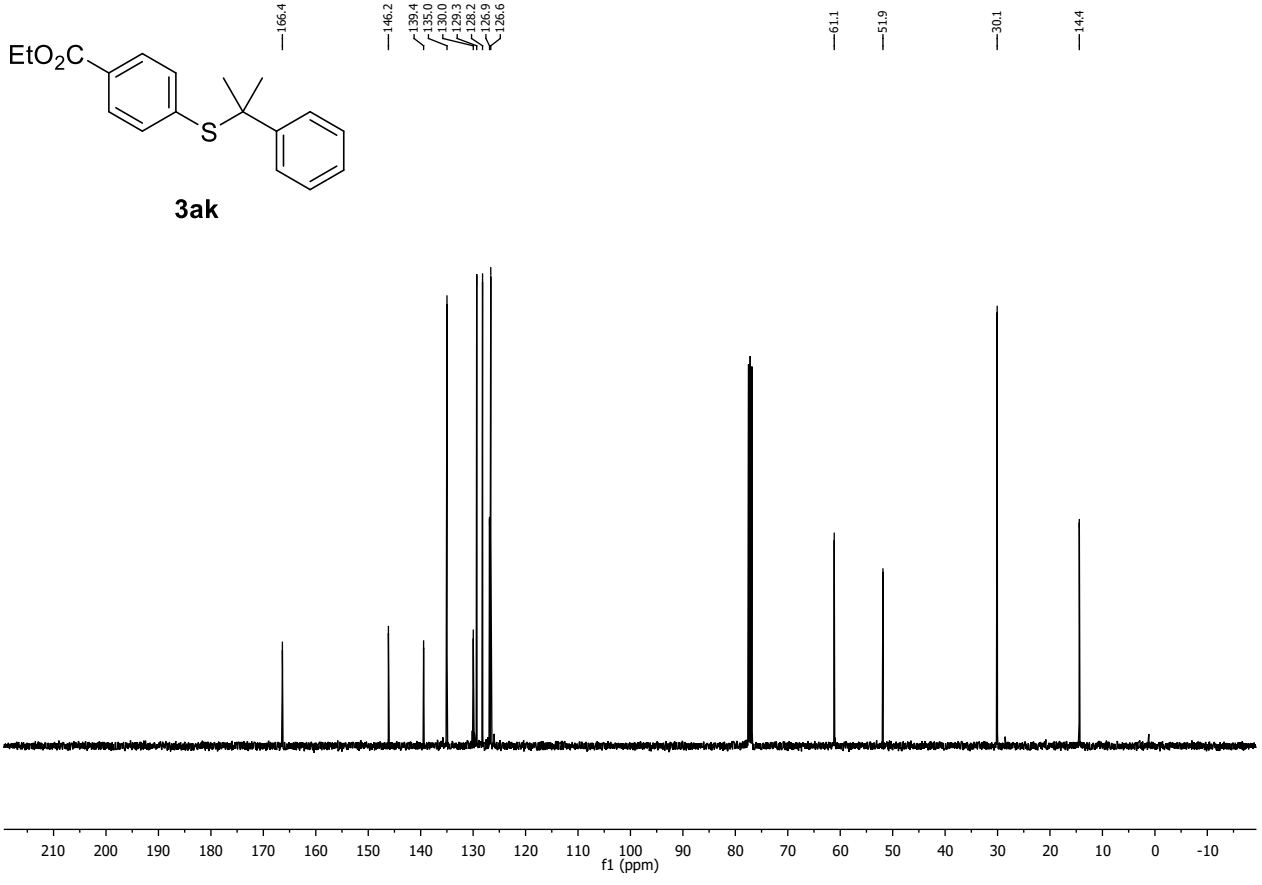
EtO2C
S
3ak
166.4
146.2
139.4
135.0
130.0
129.3
128.2
126.9
126.6
61.1
51.9
30.1
14.4
210 200 190 180 170 160 150 140 130 120 110 100 90 80 70 60 50 40 30 20 10 0 -10
f1 (ppm)

Ethyl 4-((2-(4-methyl-2-oxocyclohexyl)propan-2-yl)thio)benzoate (3al)

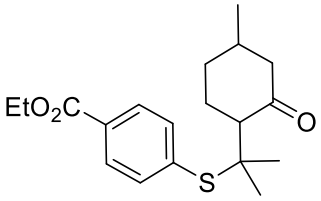

3al

$C_{19}H_{26}O_3S$ (334.47 g/mol)

Following GP-B, **3am** was synthesized using ethyl 4-chlorobenzoate (157 µL, 1.00 mmol, 1.0 equiv.) and 2-(2-mercaptopropan-2-yl)-5-methylcyclohexan-1-one (mixture of *cis* and *trans* isomers, 205 µL, 1.10 mmol, 1.1 equiv.). Purification by FC (SiO_2, 5 CV Hex, gradient to 9:1 Hex:EtOAc over 15 CV) afforded **3al** (299 mg, 896 µmol, 90%, 1:10 mixture of diastereomers according to the constitution of the starting material) as colorless oil.

R_f: 0.48 (Hex:EtOAc 9:1)

^{1}H-NMR (400 MHz, $CDCl_3$, δ): 7.99 (d, *J* = 8.2 Hz, 2H), 7.55 (d, *J* = 8.2 Hz, 2H), 4.42 – 4.35 (m, 2H), 2.79 – 2.69 (m, 1H), 2.36 – 2.22 (m, 2H), 2.08 – 1.84 (m, 3H), 1,67 – 1.53 (m, 1H), 1.45 – 1.36 (m, 9H), 1.30 – 1.21 (m, 1H), 1.00 (d, *J* = 5.8 Hz, 3H).

^{13}C-NMR (101 MHz, $CDCl_3$, δ): 210.7, 166.3, 138.0, 137.25, 130.9, 129.6, 61.3, 57.7, 52.5, 52.2, 37.0, 34.7, 30.0, 28.3, 24.3, 22.3, 14.5.

HR-MS (ESI): m/z calc. for $[M+Na]^+$ 357.14949, found 357.14978.

IR (ATR, $\tilde{\nu}$ [cm^{-1}]): 2954 (w), 2928 (w), 2869 (w), 1712 (s), 1593 (w), 1560 (w), 1452 (w), 1386 (w), 1366 (m), 1270 (s), 1202 (w), 1169 (w), 1103 (s), 1045 (w), 1016 (m), 990 (w), 930 (w), 852 (w), 792 (w), 762 (m), 729 (w), 695 (w).

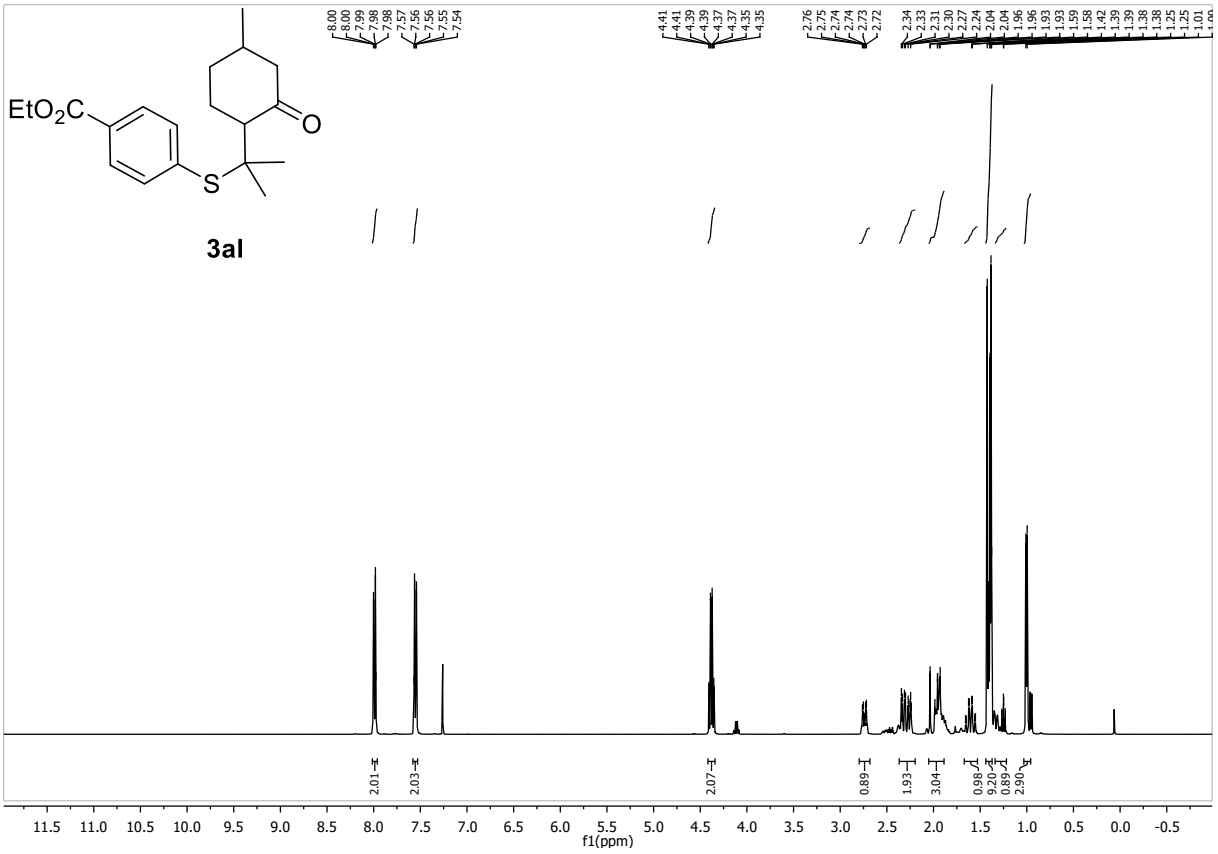
EtO2C
O
S
3al
f1(ppm)

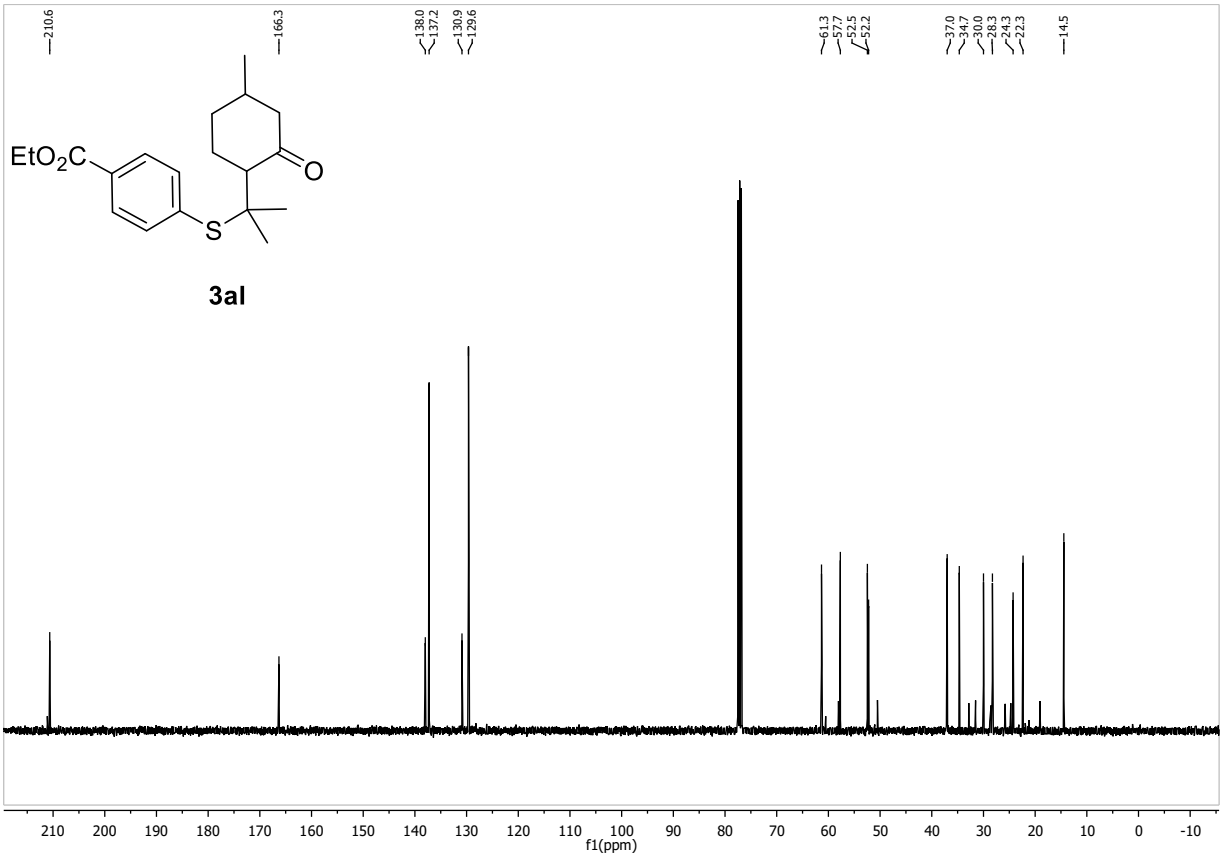
EtO2C
O
S
3al
f1(ppm)

Ethyl 4-((2-methyl-4-oxopentan-2-yl)thio)benzoate (3am)

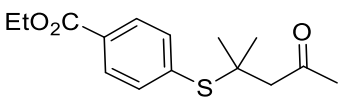

3am

$C_{15}H_{20}O_3S$ (280.38 g/mol)

Following GP-B, **3al** was synthesized using ethyl 4-chlorobenzoate (157 µL, 1.00 mmol, 1.0 equiv.) and 4-mercapto-4-methylpentan-2-one (152 µL, 1.10 mmol, 1.1 equiv.). Purification by FC (SiO_2, 5 CV Hex, gradient to 9:1 Hex:EtOAc over 15 CV) afforded **3am** (262 mg, 934 µmol, 93%) as colorless oil.

R_f: 0.29 (Hex:EtOAc 9:1)

^{1}H-NMR (400 MHz, $CDCl_3$, δ): 8.00 (d, *J* = 8.3 Hz, 2H), 7.59 (d, *J* = 8.3 Hz, 2H), 4.38 (q, *J* = 7.1 Hz, 2H), 2.68 (s, 2H), 2.14 (s, 3H), 1.45 – 1.34 (m, 9H).

^{13}C-NMR (101 MHz, $CDCl_3$, δ): 06.4, 166.3, 137.5, 137.3, 131.1, 129.7, 61.4, 54.6, 48.1, 32.3, 28.5, 14.5.

HR-MS (ESI): m/z calc. for $[M+Na]^+$ 303.10254, found 303.10287.

IR (ATR, $\tilde{\nu}$ [cm^{-1}]): 2972 (w), 2928 (w), 2872 (w), 1712 (s), 1626 (w), 1593 (w), 1560 (w), 1459 (w), 1392 (w), 1359 (m), 1270 (s), 1198 (w), 1172 (m), 1104 (s), 1016 (m), 941 (w), 855 (w), 792 (w), 762 (m), 725 (w), 695 (w), 673 (w).

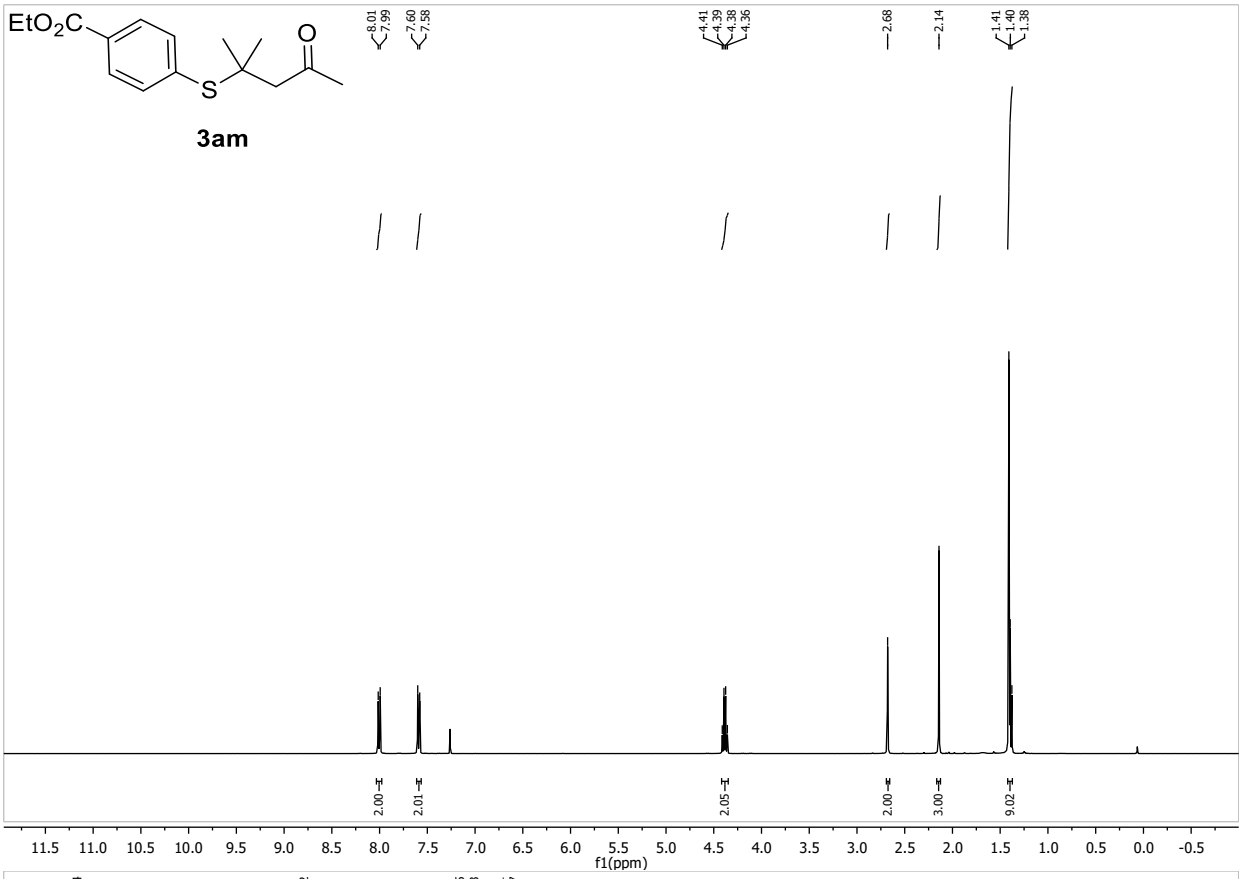
EtO2C
O
S
3am
8.01
7.99
7.60
7.58
4.41
4.39
4.38
4.36
2.68
2.14
1.41
1.40
1.38
2.00
2.01
2.05
2.00
3.00
9.02
f1(ppm)

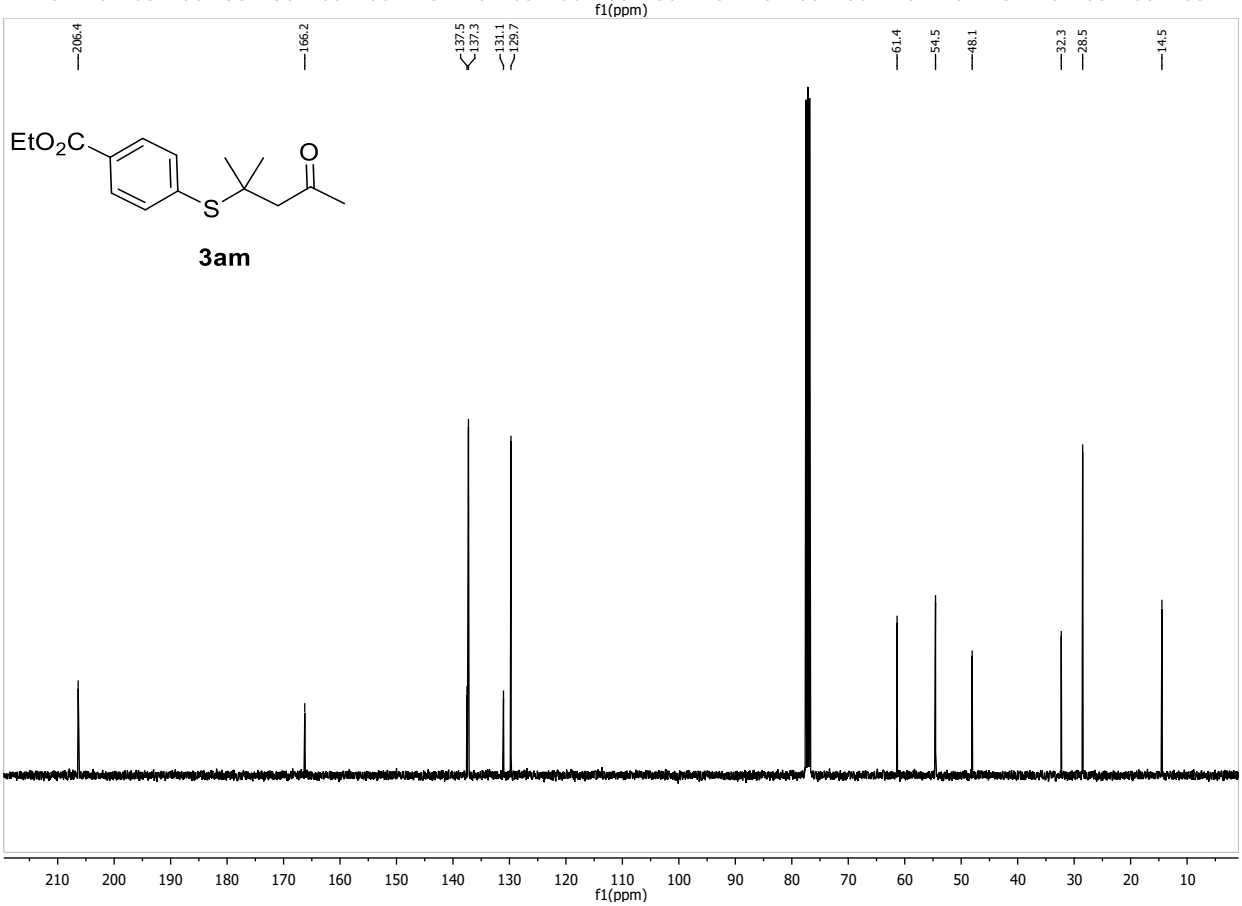
206.4
166.2
137.5
137.3
131.1
129.7
61.4
54.5
48.1
32.3
28.5
14.5
EtO2C
O
S
3am
f1(ppm)

Ethyl 4-((3-methoxy-3-oxopropyl)thio)benzoate (3an)

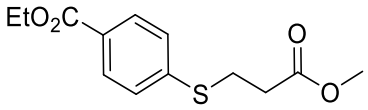

3an

$C_{13}H_{16}O_4S$ (268.33 g/mol)

Following GP-B, **3an** was synthesized using ethyl 4-chlorobenzoate (157 µL, 1.00 mmol, 1.0 equiv.) and methyl 3-mercaptopropionate (122 µL, 1.10 mmol, 1.1 equiv.). Purification by FC (SiO_2, 5 CV Hex, gradient to 7:3 Hex:EtOAc over 20 CV) afforded **3an** (191 mg, 713 µmol, 71%) as colorless liquid. Conforms to reported analytical data.[27]

R_f: 0.24 (Hex:EtOAc 9:1)

^{1}H-NMR (400 MHz, $CDCl_3$, δ): 7.95 (d, *J* = 8.5 Hz, 2H), 7.32 (d, *J* = 8.5 Hz, 2H), 4.36 (q, *J* = 7.1 Hz, 2H), 3.70 (s, 3H), 3.25 (t, *J* = 7.4 Hz, 2H), 2.68 (t, *J* = 7.4 Hz, 2H), 1.38 (t, *J* = 7.1 Hz, 3H).

^{13}C-NMR (101 MHz, $CDCl_3$, δ): 172.0, 166.3, 142.5, 130.2, 127.9, 127.3, 61.1, 52.1, 33.9, 27.5, 14.5.

HR-MS (ESI): m/z calc. for $[M + Na]^+$ 291.06615, found 291.06666.

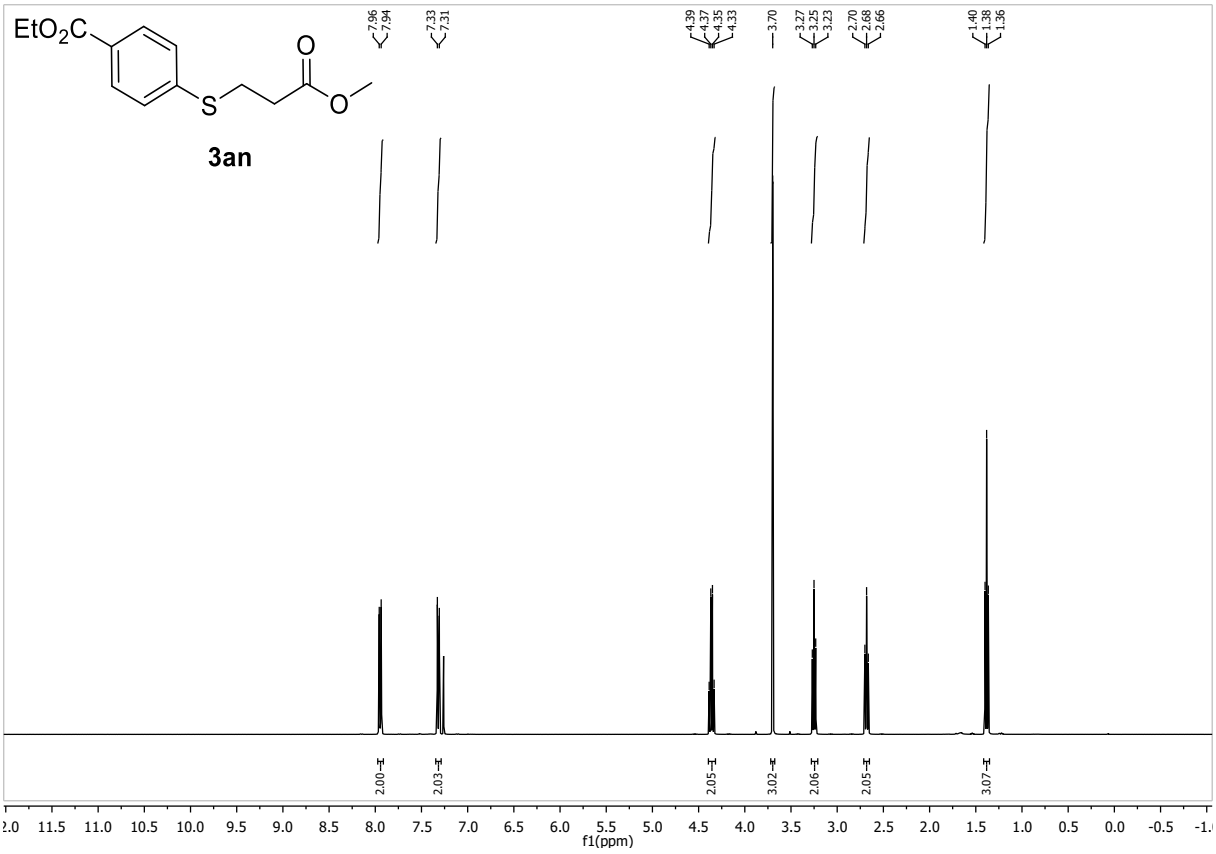
EtO2C
O
S
O
3an
7.96
7.94
7.33
7.31
4.39
4.37
4.35
4.33
3.70
3.27
3.25
3.23
2.70
2.68
2.66
1.40
1.38
1.36
2.00
2.03
2.05
3.02
2.06
2.05
3.07
f1(ppm)

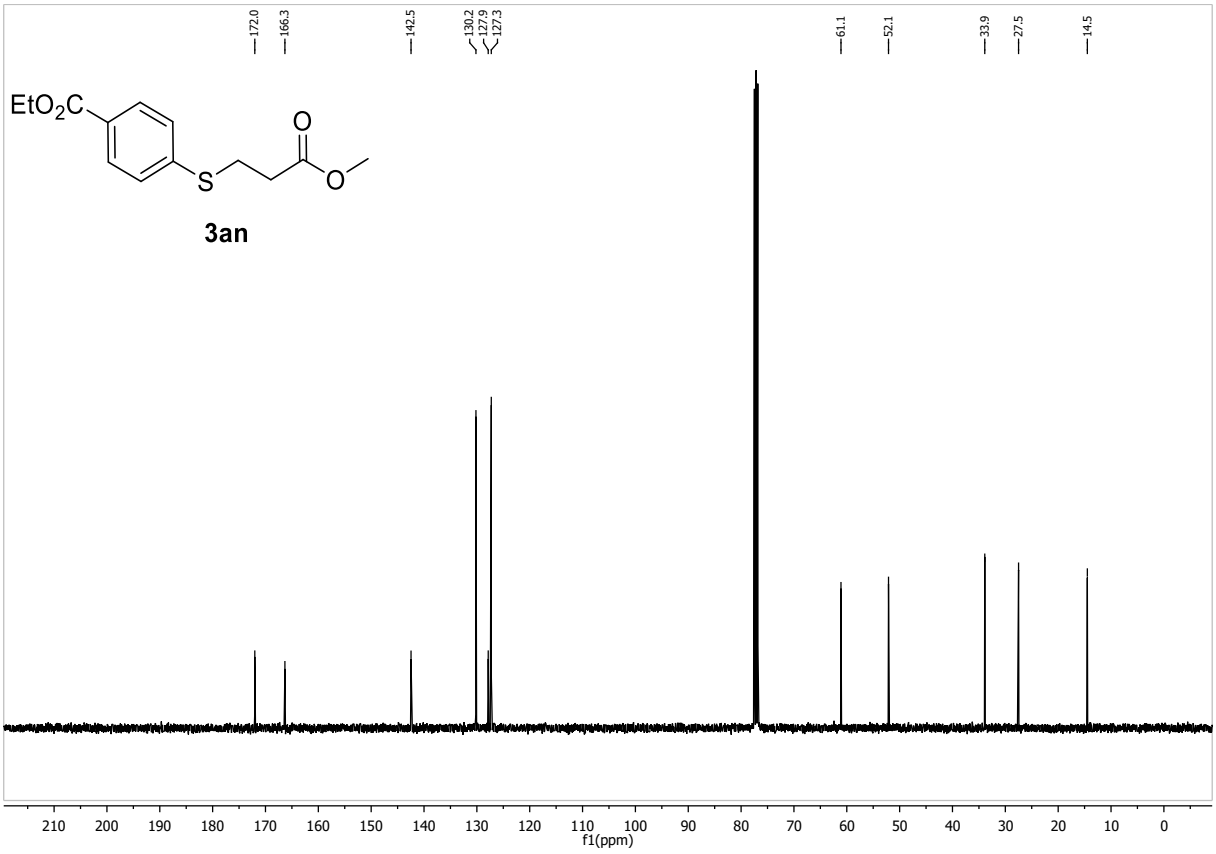
EtO2C
O
S
O
3an
172.0
166.3
142.5
130.2
127.9
127.3
61.1
52.1
33.9
27.5
14.5
f1(ppm)

Diethyl 4,4'-(hexane-1,6-diylbis(sulfanediyl))dibenzoate (3ao)

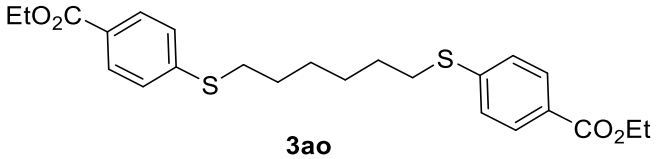

3ao

$C_{24}H_{30}O_4S_2$ (446.62 g/mol)

Following GP-B, **3ao** was synthesized using ethyl 4-chlorobenzoate (157 µL, 1.00 mmol, 2.0 equiv.) and 1,6-hexanedithiol (84 µL, 0.55 mmol, 1.1 equiv.). Purification by FC (SiO_2, gradient to 9:1 Hex:EtOAc over 10 CV, to 8:2 Hex:EtOAc over 10 CV) afforded **3ao** (185 mg, 415 µmol, 83%) as colorless solid.

R_f: 0.25 (Hex:EtOAc 9:1)

m.p.: 98.3 – 99.3 °C

^{1}H-NMR (400 MHz, $CDCl_3$, δ): 7.92 (d, *J* = 8.5 Hz, 4H), 7.27 (d, *J* = 8.7 Hz, 4H), 4.35 (q, *J* = 7.1 Hz, 4H), 2.97 (t, *J* = 7.3 Hz, 4H), 1.75 – 1.64 (m, 4H), 1.51 – 1.45 (m, 4H), 1.38 (t, *J* = 7.1 Hz, 6H).

^{13}C-NMR (101 MHz, $CDCl_3$, δ): 166.5, 144.1, 130.0, 127.2, 126.5, 61.0, 32.1, 28.7, 28.5, 14.5.

HR-MS (ESI): m/z calc. for [M + Na^+] 469.14777, found 469.14794.

IR (ATR, $\tilde{\nu}$ [cm^{-1}]): 2980 (w), 2928 (w), 2857 (w), 1705 (s), 1590 (s), 1463 (m), 1441 (w), 1396 (w), 1363 (w), 1314 (w), 1272 (vs), 1176 (s), 1101 (vs), 1016 (s), 955 (w), 877 (w), 859 (w), 833 (m), 788 (w), 751 (s), 721 (m), 684 (s).

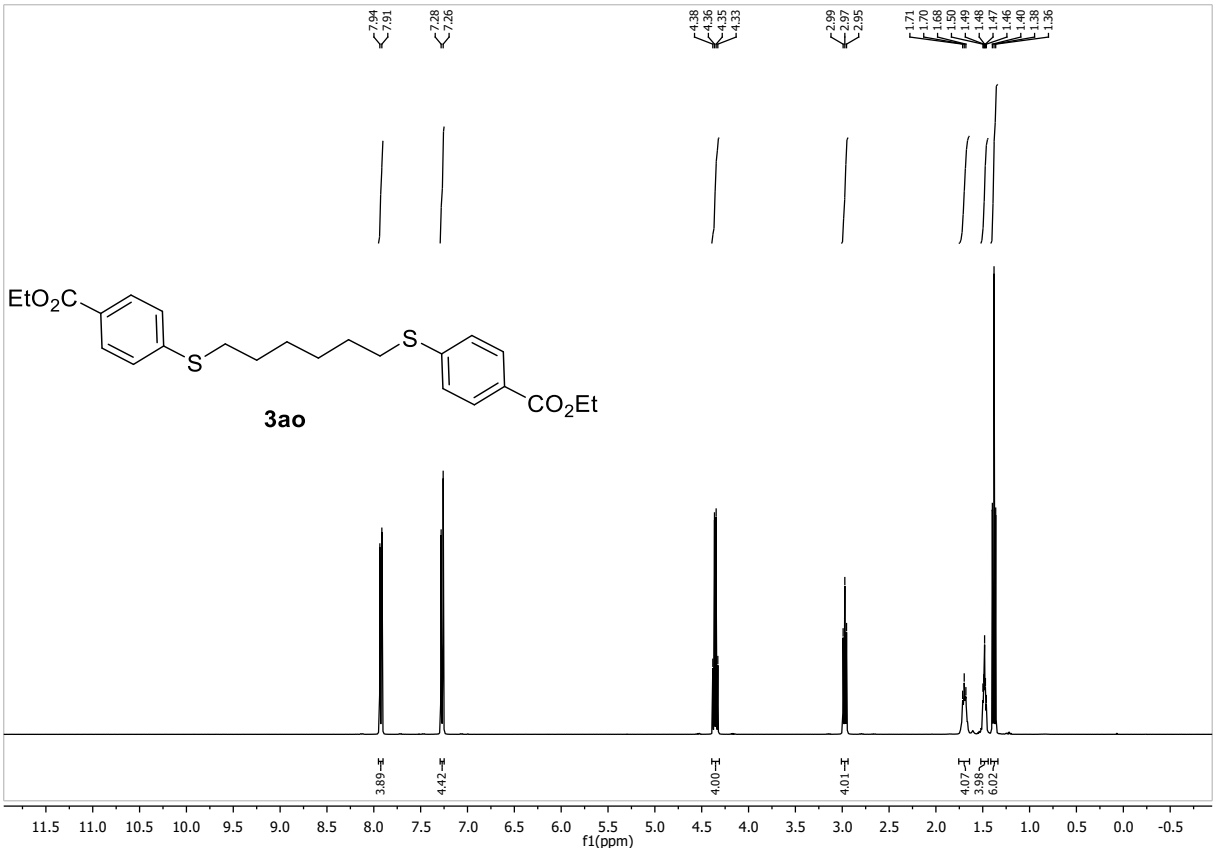
7.94
7.91
7.28
7.26
4.38
4.36
4.35
4.33
2.99
2.97
2.95
1.71
1.70
1.68
1.50
1.49
1.48
1.47
1.46
1.40
1.38
1.36
EtO2C
S
S
CO2Et
3ao
3.89
4.42
4.00
4.01
4.07
3.98
6.02
f1(ppm)

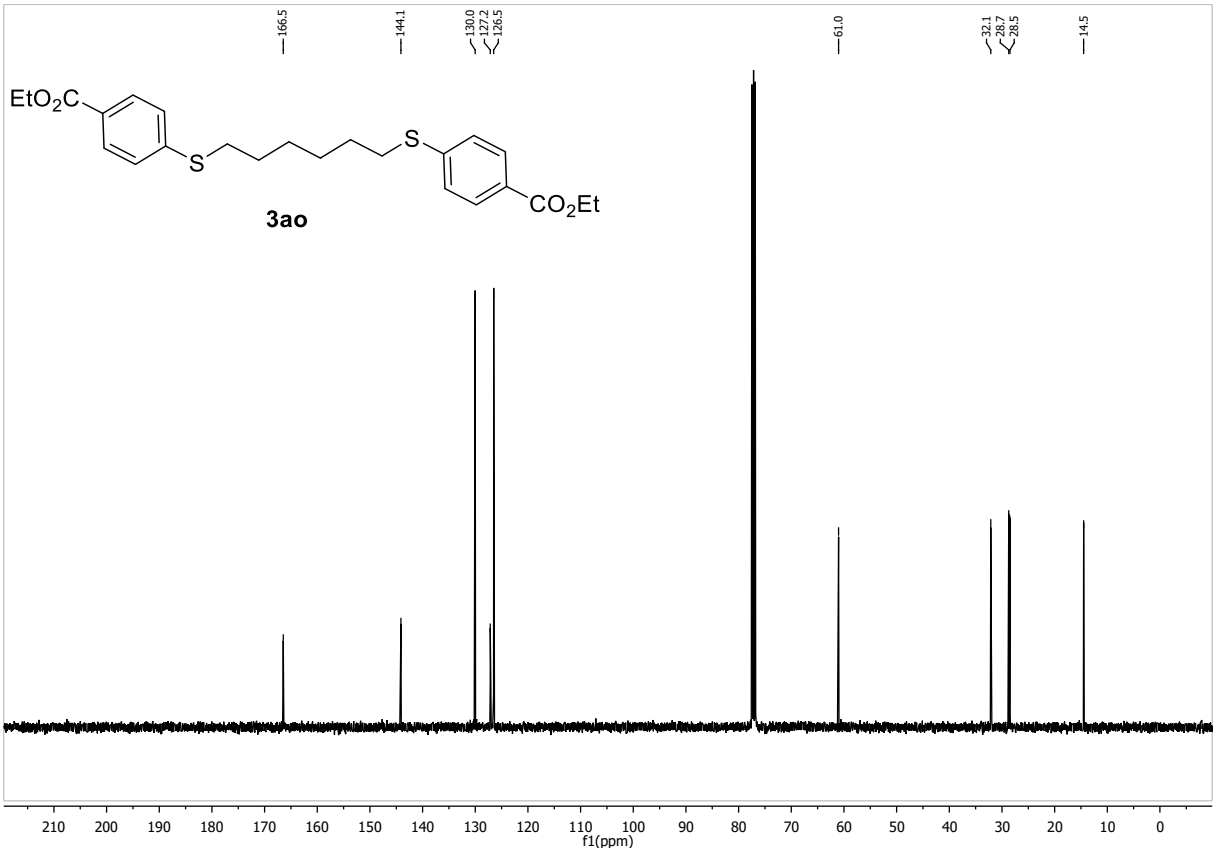
166.5
144.1
130.0
127.2
126.5
61.0
32.1
28.7
28.5
14.5
EtO2C
S
S
CO2Et
3ao
f1(ppm)

Ethyl 4-(((3S,10R,13R)-10,13-dimethyl-17-((R)-6-methylheptan-2-yl)-2,3,4,7,8,9,10,11,12,13,14,15,16,17-tetradecahydro-1H-cyclopenta[a]phenanthren-3-yl)thio)benzoate (3ap)

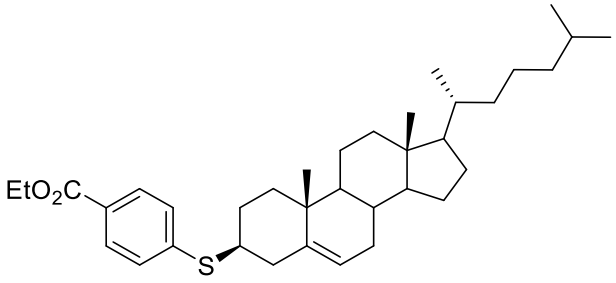

3ap

$C_{36}H_{54}O_2S$ (550.89 g/mol)

Following GP-B, **3ap** was synthesized using ethyl 4-chlorobenzoate (78 µL, 0.50 mmol, 1.0 equiv.) and thiocholesterol (222 mg, 1.10 mmol, 1.1 equiv.). Purification by FC (SiO_2, gradient to 9:1 Hex:EtOAc over 20 CV) afforded **3ap** (197 mg, 358 µmol, 72%) as colorless solid.

R_f: 0.60 (Hex:EtOAc 9:1)

m.p.: 96.2 – 98.0 °C

^{1}H-NMR (400 MHz, $CDCl_3$, δ): 7.83 (d, *J* = 8.4 Hz, 2H), 7.23 (d, *J* = 8.4 Hz, 2H), 5.24 (dd, *J* = 4.9, 1.9 Hz, 1H), 4.26 (q, *J* = 7.1 Hz, 2H), 3.15 – 3.02 (m, 1H), 2.25 (dd, *J* = 9.4, 2.6 Hz, 2H), 1.96 – 1.66 (m, 5H), 1.59 – 0.74 (m, 36H), 0.57 (s, 3H).

^{13}C-NMR (101 MHz, $CDCl_3$, δ): 166.6, 142.7, 141.5, 130.1, 128.8, 127.8, 121.8, 61.1, 57.0, 56.4, 50.5, 46.3, 42.5, 40.0, 39.8, 39.8, 39.6, 37.1, 36.4, 36.0, 32.1, 32.0, 29.5, 28.5, 28.3, 24.5, 24.1, 23.1, 22.8, 21.1, 19.6, 19.0, 14.6, 12.1.

HR-MS (ESI): m/z calc. for $[M+Na]^+$ 573,37367, found 573,37428.

IR (ATR, $\tilde{\nu}$ [cm^{-1}]): 2931 (m), 2902 (m), 2858 (w), 1712 (m), 1590 (m), 1460 (w), 1440 (w), 1396 (w), 1369 (w), 1336 (w), 1310 (w), 1269 (s), 1236 (m), 1176 (m), 1102 (s), 1017 (m), 956 (w), 930 (w), 878 (w), 841 (m), 796 (w), 755 (s), 691 (m).

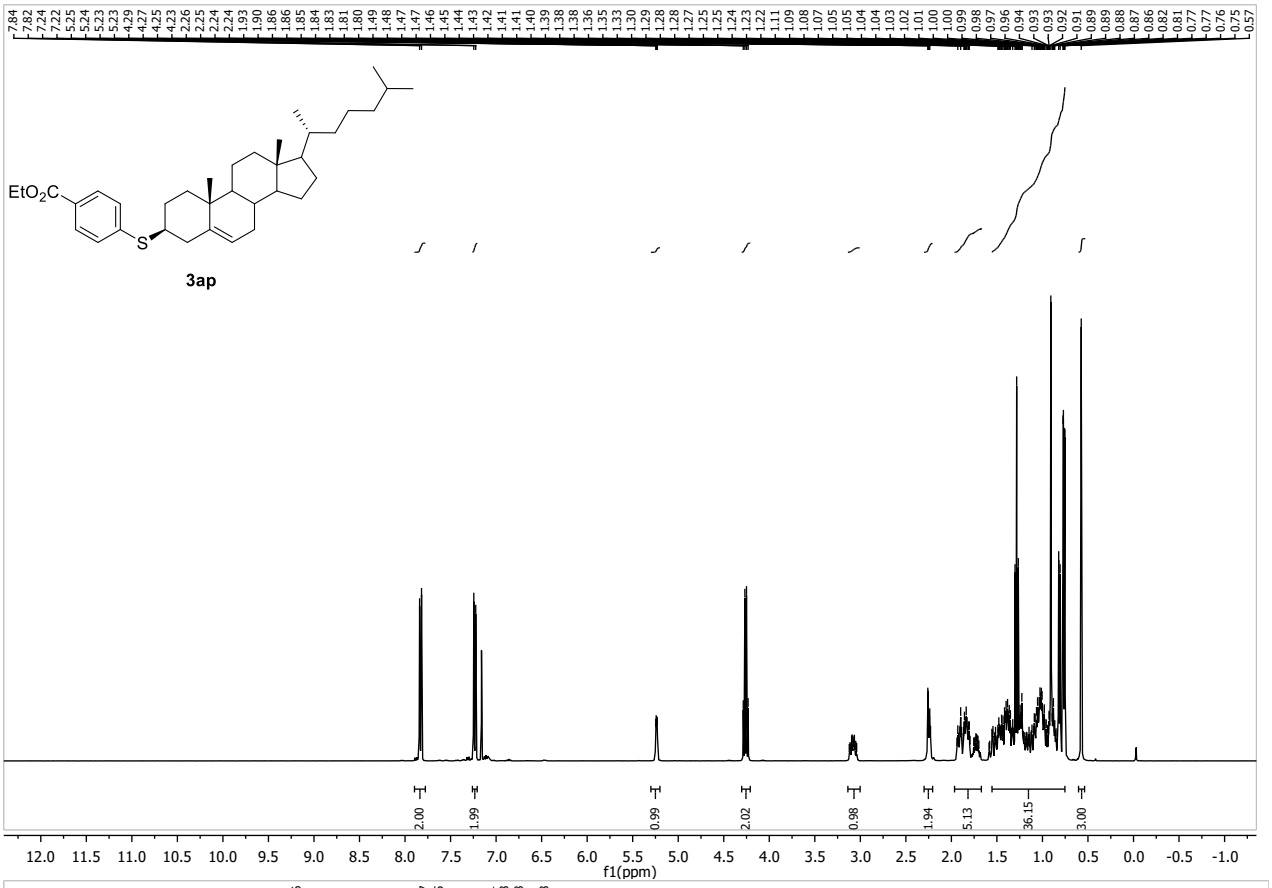
EtO2C
S
3ap
f1(ppm)

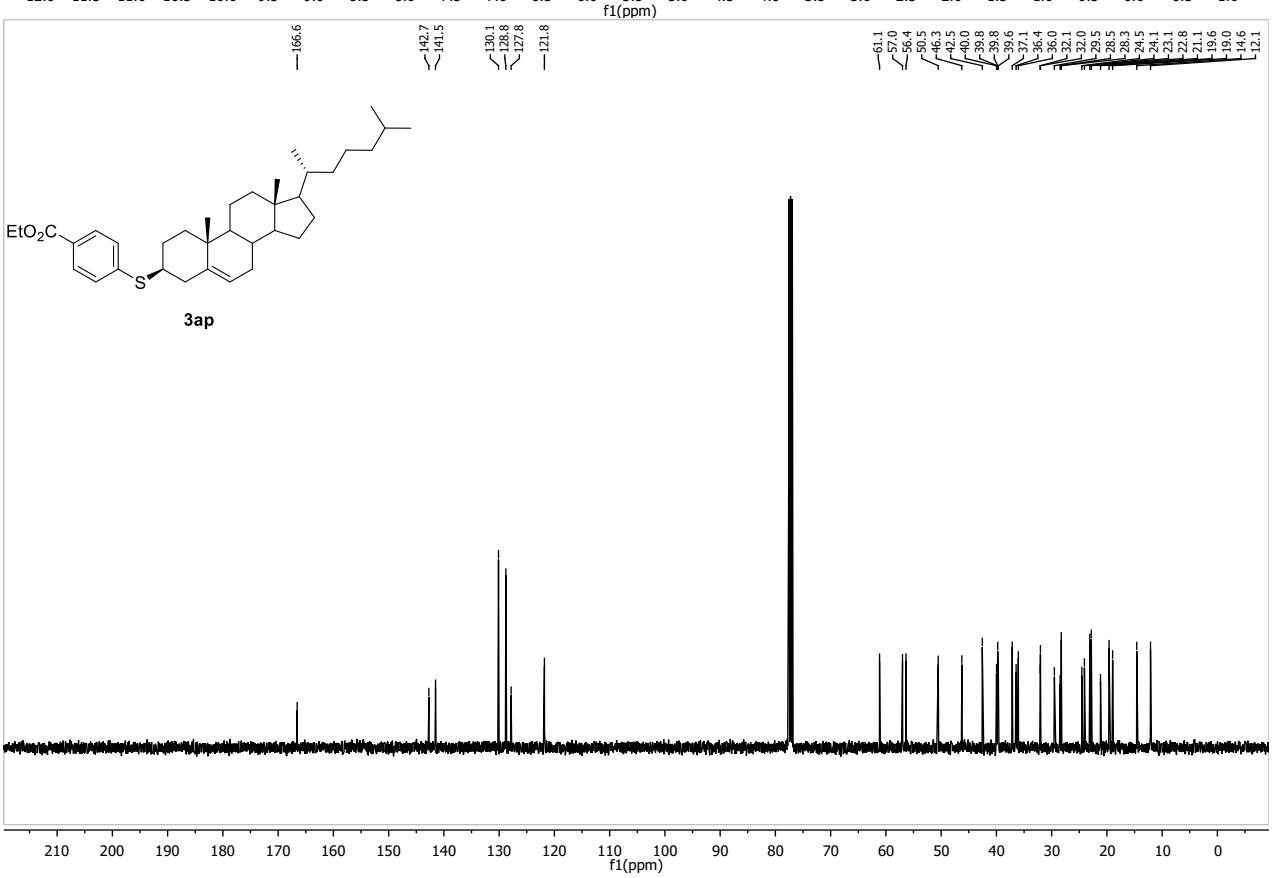
EtO2C
S
3ap
f1(ppm)

4-(((3s,5s,7s)-adamantan-1-yl)thio)phenyl 4-methylbenzenesulfonate (3Gb)

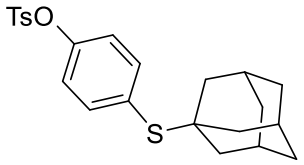

3Gb

$C_{23}H_{26}O_3S_2$ (414.58 g/mol)

Following GP-B, **3Gb** was synthesized using 4-chlorophenyl 4-methylbenzenesulfonate (282 mg, 1 mmol, 1.0 equiv.) and 1-adamantanethiol (185 mg, 1.10 mmol, 1.1 equiv.). Purification by FC (SiO_2, gradient to 8:2 Hex:EtOAc over 20 CV) afforded **3Gb** (368 mg, 889 µmol, 89%) as colorless solid.

Following GP-B, **3Gb** was synthesized using 4-(((trifluoromethyl)sulfonyl)oxy)phenyl 4-methylbenzenesulfonate (198 mg, 0.50 mmol, 1.0 equiv.) and 1-adamantanethiol (93 mg, 0.55 mmol, 1.1 equiv.). Purification by FC (SiO_2, gradient to 8:2 Hex:EtOAc over 20 CV) afforded **3Hb** (194 mg, 468 µmol, 94%) as colorless solid.

R_f: 0.4 (Hex:EtOAc 9:1)

^{1}H-NMR (400 MHz, $CDCl_3$, δ): 7.69 (d, *J* = 8.3 Hz, 2H), 7.41 – 7.37 (m, 2H), 7.30 (d, *J* = 8.0 Hz, 2H), 6.97 – 6.91 (m, 2H), 2.44 (s, 3H), 2.01 (s, 3H), 1.75 (d, *J* = 2.5 Hz, 6H), 1.68 – 1.54 (m, 6H).

^{13}C-NMR (101 MHz, $CDCl_3$, δ): 150.2, 145.6, 138.9, 132.3, 129.9, 129.8, 128.7, 122.3, 48.4, 43.7, 36.2, 30.1, 21.9.

HR-MS (ESI): m/z calc. for $[M+Na]^+$ 437.12156, found 437.12161.

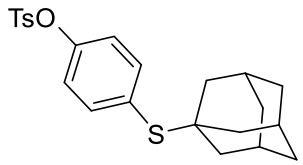
TsO
S

3Gb

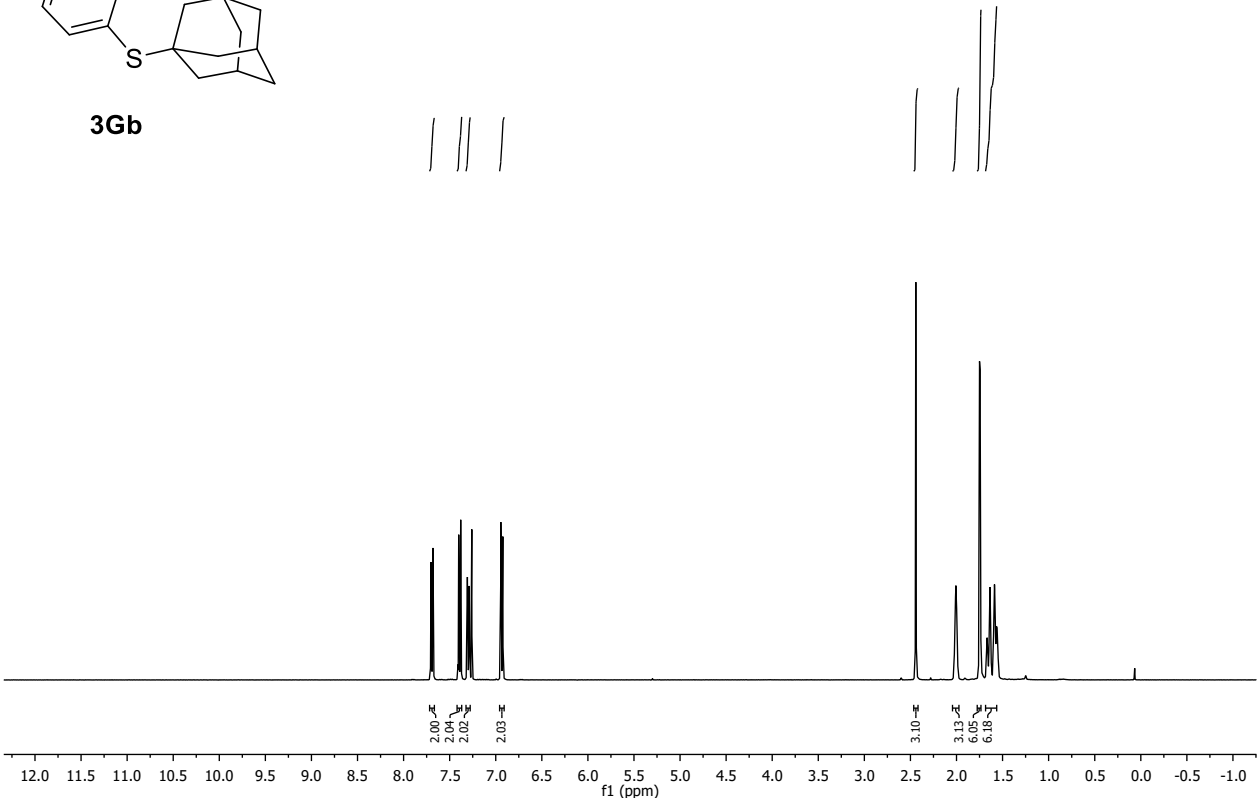
2.00
2.04
2.02
2.03
3.10
3.13
6.05
6.18
12.0 11.5 11.0 10.5 10.0 9.5 9.0 8.5 8.0 7.5 7.0 6.5 6.0 5.5 5.0 4.5 4.0 3.5 3.0 2.5 2.0 1.5 1.0 0.5 0.0 -0.5 -1.0
f1 (ppm)

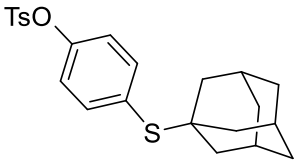
TsO
S

3Gb

150.2
145.6
138.9
132.3
129.9
129.8
128.7
122.3
48.4
43.6
36.2
30.1
21.9
210 200 190 180 170 160 150 140 130 120 110 100 90 80 70 60 50 40 30 20 10 0 -10
f1 (ppm)

(3s,5s,7s)-adamantan-1-yl)(4-chlorophenyl)sulfane (3Fb)

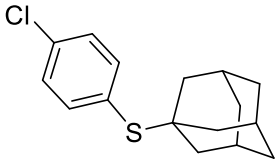

3Fb

$C_{16}H_{19}ClS$ (278.84 g/mol)

Following GP-B, **3Fb** was synthesized using 1,4-dichlorobenzene (221 mg, 1.50 mmol, 1.0 equiv.) and 1-adamantanethiol (278 mg, 1.65 mmol, 1.1 equiv.). Purification by FC (SiO_2, gradient to 8:2 Hex:EtOAc over 20 CV) afforded **3Fb** (130 mg, 466 µmol, 30%) as colorless solid. Conforms to reported analytical data.[21]

R_f: 0.73 (Hex:EtOAc 9:1)

^{1}H-NMR (400 MHz, $CDCl_3$, δ): 7.48 – 7.36 (m, 2H), 7.31 – 7.27 (m, 2H), 2.01 (s, 3H), 1.79 (d, *J* = 2.6 Hz, 6H), 1.62 (m, 6H).

^{13}C-NMR (101 MHz, $CDCl_3$, δ): 139.0, 135.2, 129.2, 128.7, 48.3, 43.7, 36.2, 30.1.

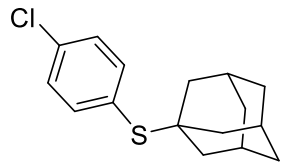
Cl
S

3Fb

7.43
7.43
7.42
7.41
7.41
7.40
7.30
7.30
7.29
7.28
7.28
7.27
2.01
1.79
1.78
1.67
1.64
1.60
1.57
2.00
2.02
3.11
6.09
6.14
12.0 11.5 11.0 10.5 10.0 9.5 9.0 8.5 8.0 7.5 7.0 6.5 6.0 5.5 5.0 4.5 4.0 3.5 3.0 2.5 2.0 1.5 1.0 0.5 0.0 -0.5 -1.0
f1 (ppm)

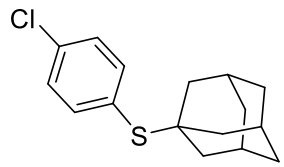
Cl
S

3Fb

139.0
135.2
129.2
128.6
48.3
43.7
36.2
30.1
210 200 190 180 170 160 150 140 130 120 110 100 90 80 70 60 50 40 30 20 10 0 -10
f1 (ppm)

1,4-bis(((3s,5s,7s)-adamantan-1-yl)thio)benzene (4)

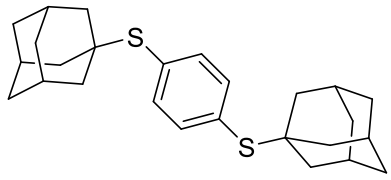

4

$C_{26}H_{34}S_2$ (410.68 g/mol)

Following GP-B, **4** was synthesized using 1,4-dichlorobenzene (221 mg, 1.50 mmol, 1.0 equiv.) and 1-adamantanethiol (278 mg, 1.65 mmol, 1.1 equiv.). Purification by FC (SiO_2, gradient to 8:2 Hex:EtOAc over 20 CV) afforded **4** (55 mg, 134 µmol, 9%) as colorless solid.

^{1}H-NMR (400 MHz, $CDCl_3$, δ): 7.43 (s, 4H), 2.02 (s, 6H), 1.81 (d, *J* = 2.6 Hz, 12H), 1.62 (q, *J* = 12.1 Hz, 12H).

^{13}C-NMR (101 MHz, $CDCl_3$, δ): 137.4, 131.5, 48.5, 43.8, 36.3, 30.1.

HR-MS (ESI): m/z calc. for $[M]^+$ 410.209643, found 410.21039.

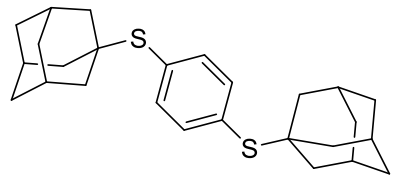

4

7.43
2.02
1.81
1.81
1.67
1.64
1.60
1.57
4.00
6.05
11.87
12.20
f1 (ppm)

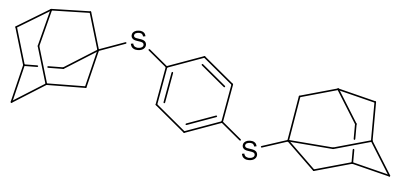

4

137.4
131.5
48.5
43.8
36.3
30.1
f1 (ppm)

((3s,5s,7s)-adamantan-1-yl)(4-(tert-butylthio)phenyl)sulfane (5)

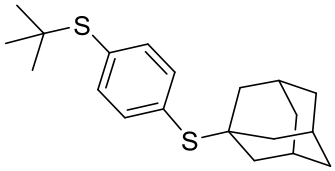

5

$C_{20}H_{28}S_2$ (332.56 g/mol)

5 was synthesized using 4-chlorophenyl trifluoromethanesulfonate (261 mg, 1.00 mmol, 1.0 equiv.), 1-adamantanethiol (185 mg, 1.10 mmol, 1.1 equiv.), 2-methyl-2-propanethiol (116 µL, 1.00 mmol, 1.1 equiv.). Purification by FC (SiO_2, gradient to 9:1 Hex:EtOAc over 20 CV) afforded **5** (115 mg, 344 µmol, 34%) as colorless solid.

R_f: 0.50 (Hex:EtOAc 98:02)

^{1}H-NMR (400 MHz, $CDCl_3$, δ): 7.49 – 7.41 (m, 4H), 2.02 (s, 3H), 1.81 (d, *J* = 2.5 Hz, 6H), 1.62 (q, *J* = 16.8, 14.6 Hz, 6H), 1.29 (s, 9H).

^{13}C-NMR (101 MHz, $CDCl_3$, δ): 137.5, 137.3, 137.2, 137.1, 48.4, 46.3, 43.7, 36.2, 31.0, 30.01.

HR-MS (ESI): m/z calc. for $[M]^+$ 332.1693, found 332.16373.

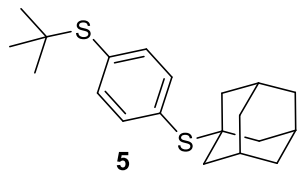

5

7.48
7.45
7.45
7.43
2.02
1.81
1.81
1.67
1.64
1.60
1.56
1.29
0.92
2.05
0.81
3.03
6.00
6.24
9.10
f1 (ppm)

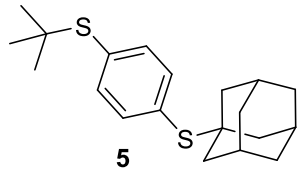

5

137.5
137.3
137.2
137.1
48.4
46.3
43.7
36.2
31.0
30.0
f1 (ppm)

6. Mechanistic investigations

6.1. Kinetic experiments and Hammett study

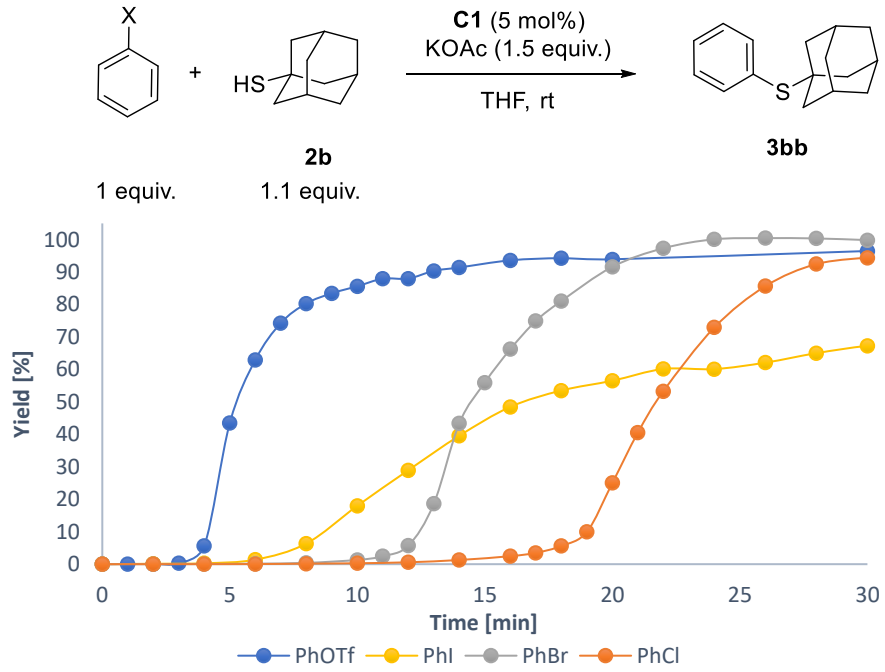

Figure S1: Kinetic analysis for the yield of **3bb** with a variety of electrophiles (PhCl, PhBr, PhI, PhOTf).

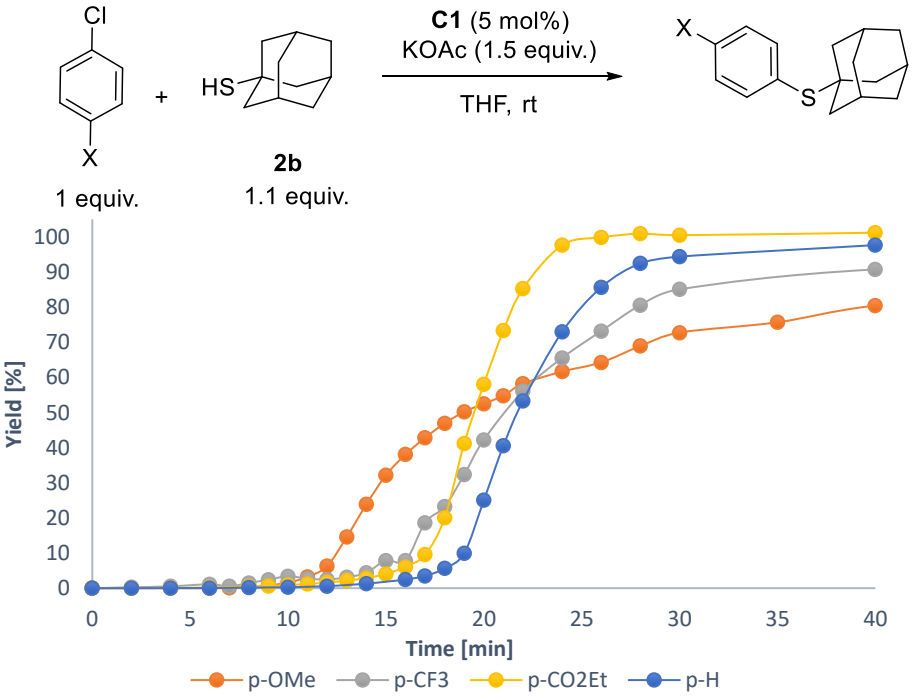

Figure S2: Kinetic analysis for the yield of the corresponding thioether with a variety of *para* substituted aryl chlorides.

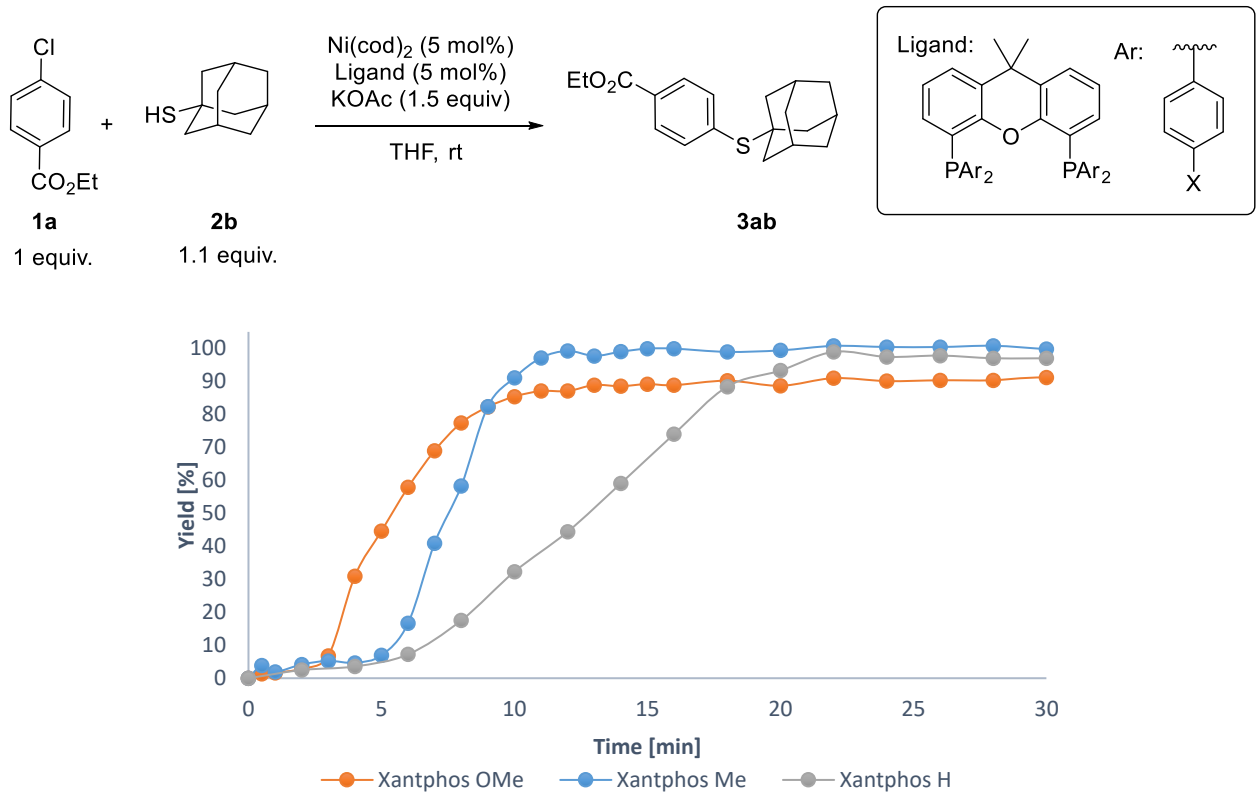

Figure S3: Kinetic analysis for the yield of **3ab** with a variety of *para* substituted Xantphos ligands.

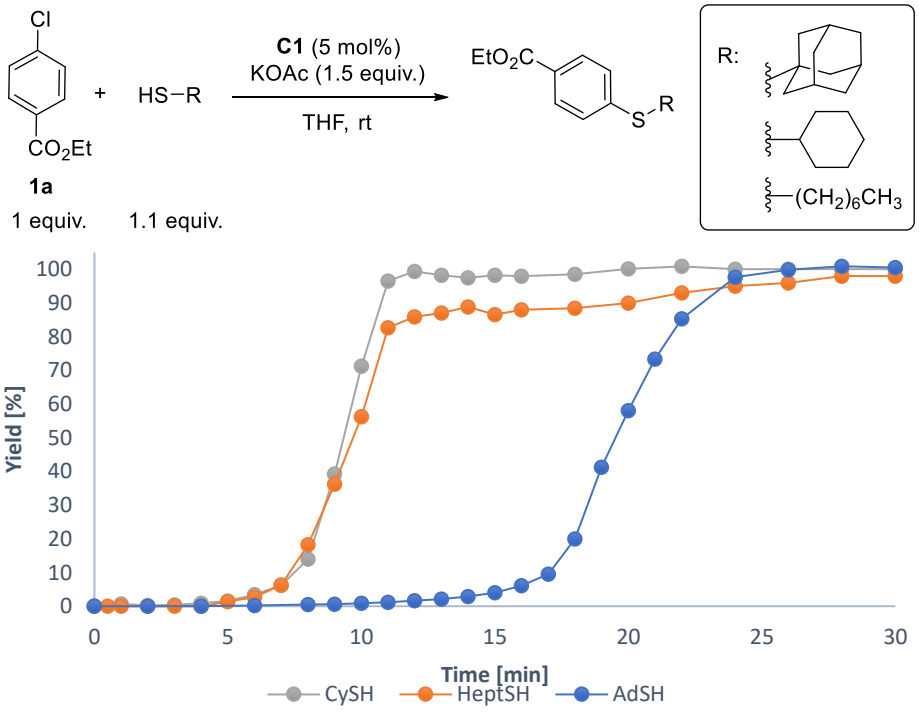

Figure S4: Kinetic analysis for the yield of the corresponding thioether with primary (heptanethiol), secondary (cyclohexanethiol) and tertiary (adamantanethiol) thiols.

The relative rate, k_{rel}, for each *p*-substituted aryl chloride or Xantphos ligand was fitted to the literature σ values[28] by using the Hammett expression $\log(k_X/k_H)=\rho\sigma$. The reaction rates **k** were determined after the initial period (catalyst preactivation) when the yield started to increase in a linear fashion till the slope decreased.

Table S6: Reaction rates **k** and **σ** values[28] for different *para* substituents on the aryl chloride.

Entry	Para Substituent X	σ_p	k_{rel}	$\log(k_{rel})$
1	OMe	- 0.27	0.64	-0.19
2	Me	-0.17	0.74	-0.13
3	H	0	1	0
4	CO_2Et	+0.45	1.40	0.15
5	CF_3	+0.54	0.65	-0.19

Table S7: Reaction rates **k** and **σ** values[28] for different *para* substituents on the Xantphos ligand.

Entry	Para Substituent X	σ_p	k_{rel}	$\log(k_{rel})$
1	OMe	- 0.27	2.64	0.42
2	Me	-0.17	2.80	0.45
3	H	0	1	0
4	CF_3	+0.54	-	-

Table S8: Reaction rates **k** for different electrophiles.

Entry	Ph-X	k_X (min^{-1})
1	Cl	12.62
2	Br	17.56
3	I	5.53
4	OTf (C-O)	28.64

Table S9: Reaction rates **k** for different thiols $k_{rel} = k_x / k_{tertiary.}$

Entry	Thiol		k_X (min^{-1})	k_{rel}
1	primary	Heptanethiol	16.80	0.95
2	seconday	Cyclohexanethiol	16.82	0.95
4	teritary	Adamantanethiol	17.69	1

6.2. NMR Experiments

^{31}P NMR experiments were conducted without internal standard. Small changes in shifts are possible.

a) Monitoring of the catalysis *via* NMR spectroscopy - ^{31}P NMR reaction control of the standard reaction conditions.

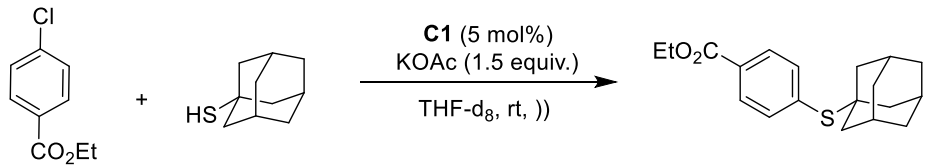

In a glovebox, a NMR tube was charged with KOAc (29.4 mg, 300 µmol, 1.5 equiv.), 1-adamantanethiol (37.0 mg, 220 µmol, 1.1 equiv.), C1 (7.64 mg, 10.0 µmol, 5 mol%), 4-chlorobenzoate (31.2 µL, 200 µmol, 1.0 equiv.) and THF- d_8 (0.6 mL). The reaction mixture was put into an ultrasonic bath and NMR measurements were recorded after 5, 10, 15, 30, 45 and 60 minutes.

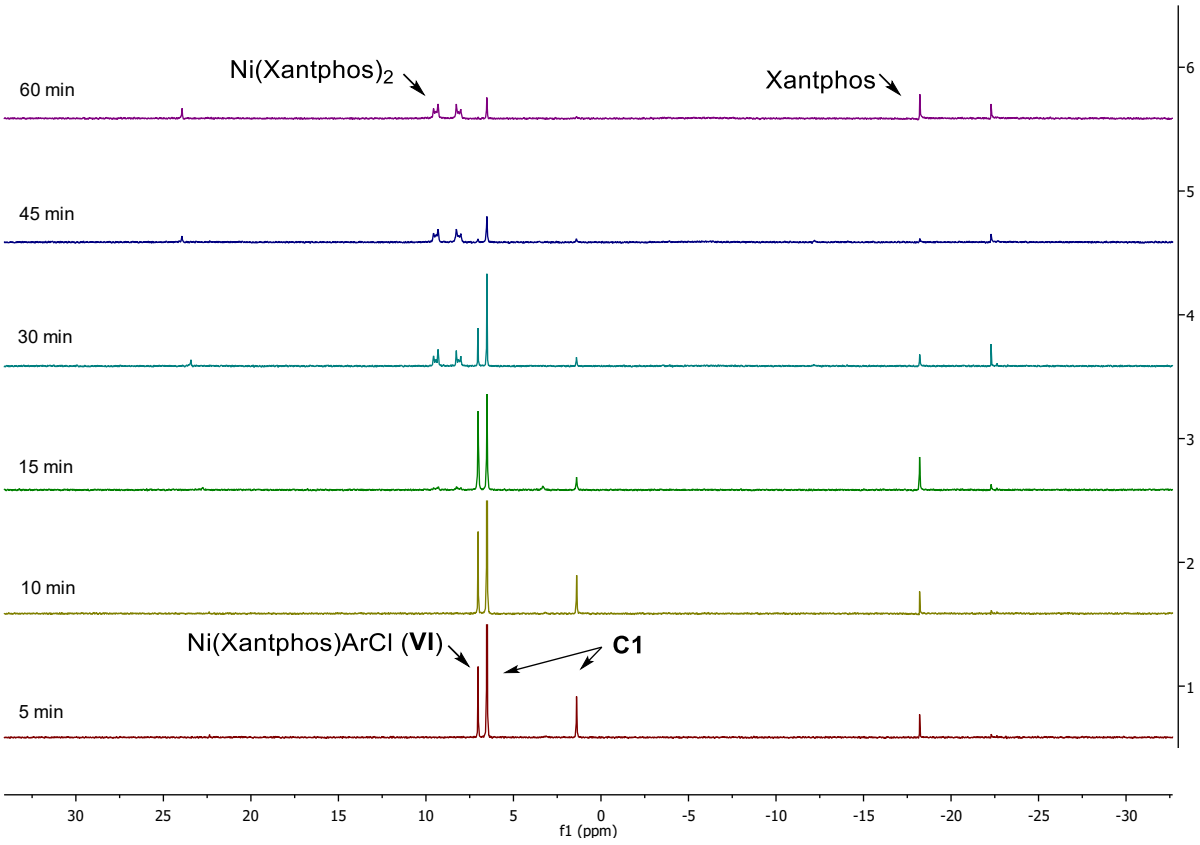

b) Oxidative addition product VI formation *via* alternative $Ni(cod)_2$ route to verify the observed ^{31}P NMR Signals during the reaction control experiments under standard conditions.

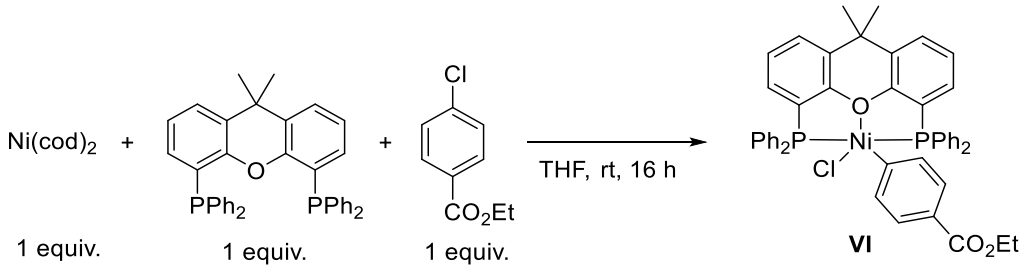

In a glovebox $Ni(cod)_2$ (68.77 mg, 250.00 µmol, 1 equiv.) was dissolved in THF (4 mL), under stirring Xantphos (144.66 mg, 250.00 µmol, 1 equiv.) was added slowly and the reaction mixture was stirred shortly at room temperature. 4-chlorobenzoate (39.1 µL, 250 µmol, 1.0 equiv.) was added and the mixture was stirred at room temperature for 16 h. The solvent was removed via filtration and the product was washed with cold (- 40 °C) hexane (3 x 1 mL) and THF (1 x 0.5 mL) and dried under reduced pressure.

^{31}P-NMR (162 MHz, THF-D_8, δ): 7.04.

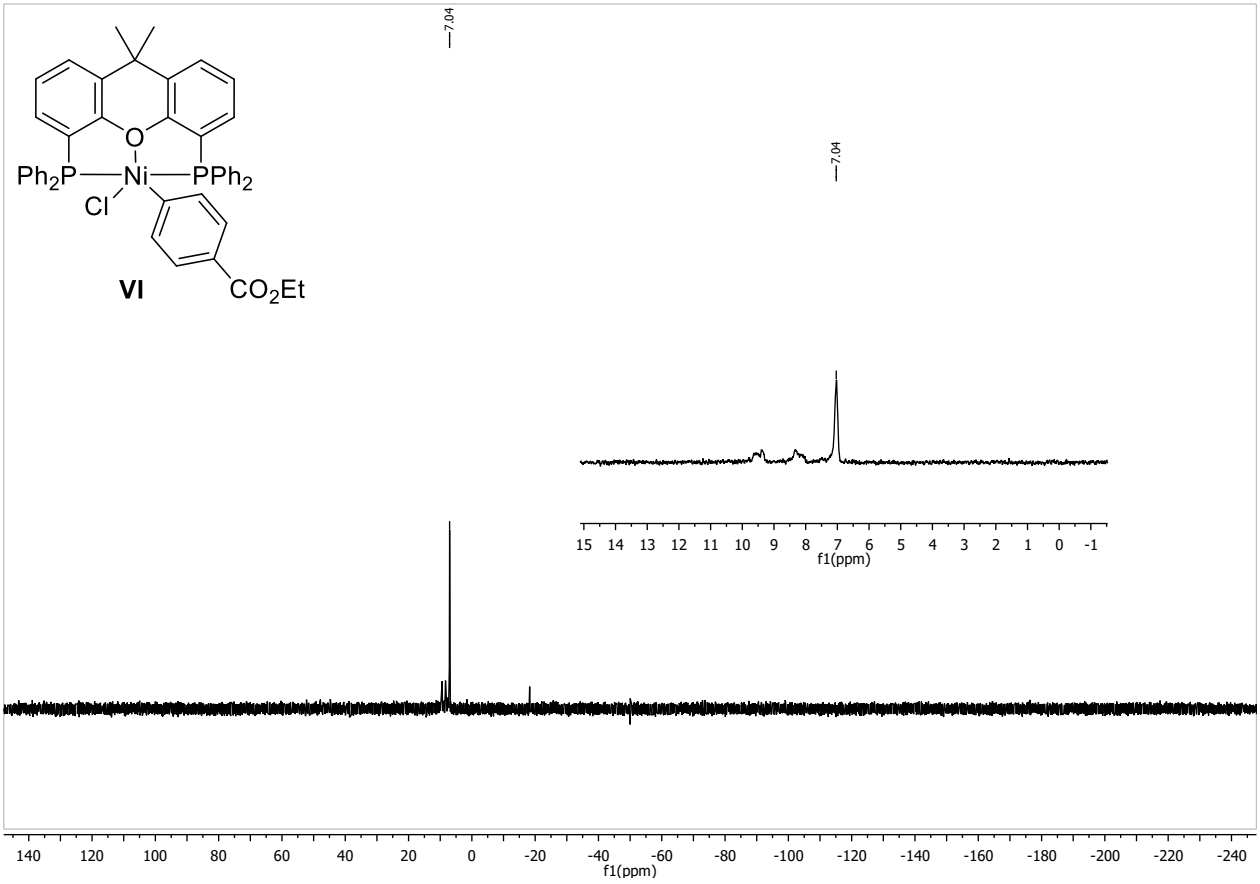

c) Oxidative addition product formation during ^{31}P NMR reaction control experiments / monitoring under standard conditions.

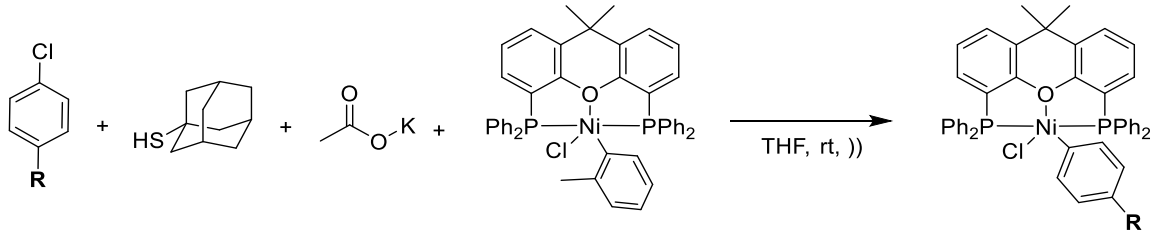

In a glovebox an NMR tube was charged with KOAc (29.4 mg, 300 µmol, 1.5 equiv.), 1-adamantanethiol (37.0 mg, 220 µmol, 1.1 equiv.), C1 (7.64 mg, 10.0 µmol, 5 mol%), the respective aryl chloride (200 µmol, 1.0 equiv.) and THF- d_8 (0.6 mL). The reaction mixture was put into an ultrasonic bath and NMR measurements were recorded.

VI R: CO_2Et: **^{31}P-NMR** (162 MHz, THF-$D_{8,}$ δ): 7.02.

VI-2 R: CF_3: **31P-NMR** (162 MHz, THF-$D_{8,}$ δ): 7.47.

VI-3 R: SO_2Me: **^{31}P-NMR** (162 MHz, THF-$D_{8,}$ δ): 7.69.

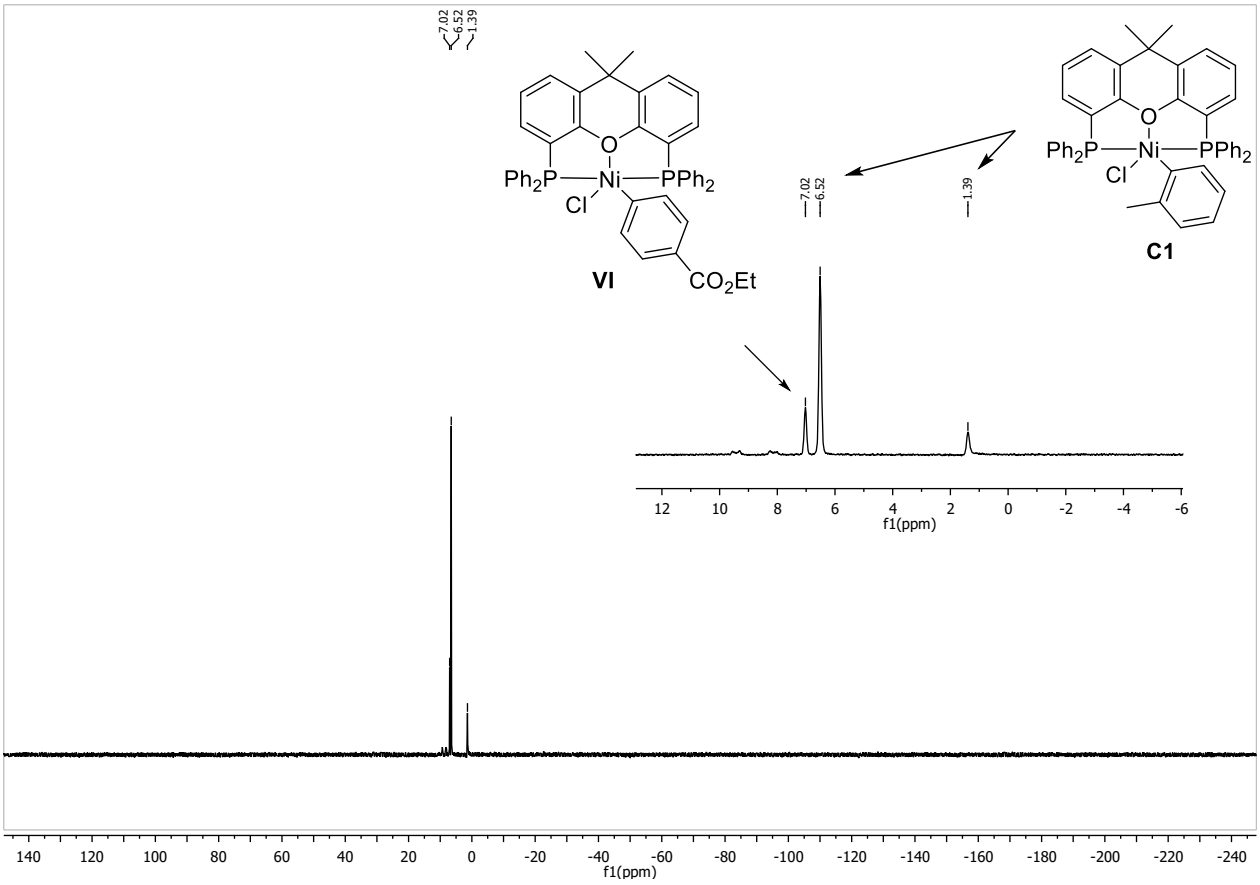

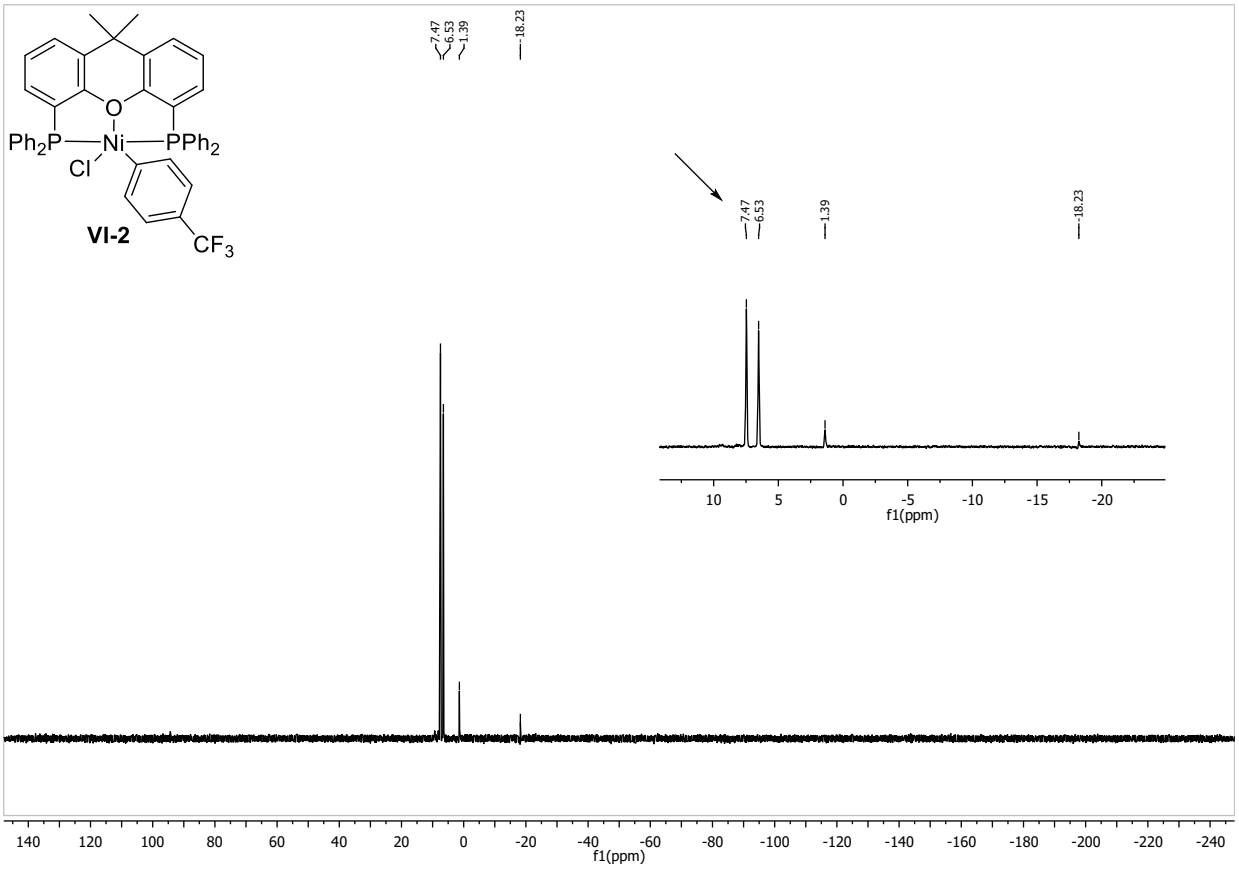
7.47
6.53
1.39
18.23
Ph2P
Ni
PPh2
Cl
CF3
VI-2
f1(ppm)

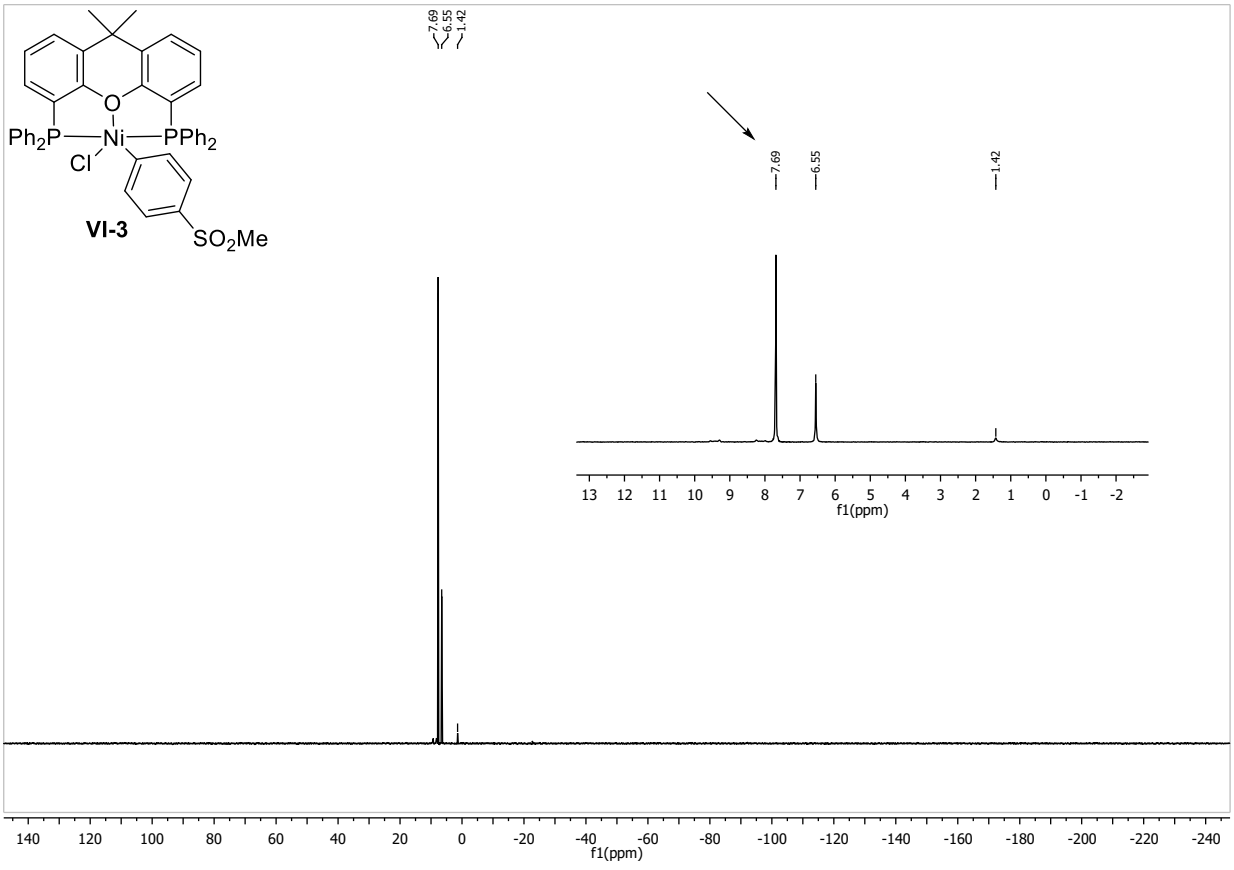
7.69
6.55
1.42
Ph2P
Ni
PPh2
Cl
SO2Me
VI-3
f1(ppm)

d) Ni(Xantphos)$_2$ formation *via* alternative Ni(cod)$_2$route.

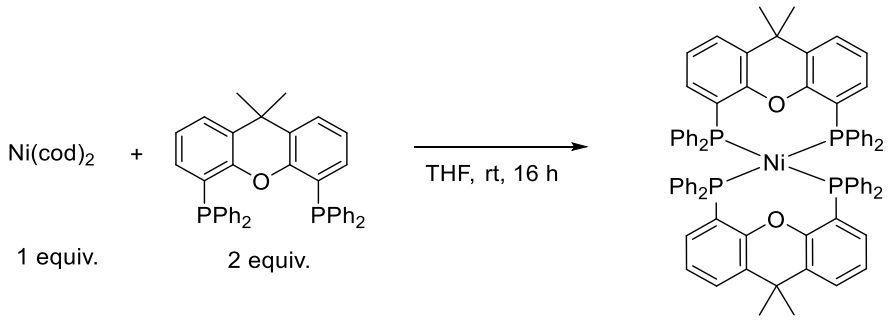

In a glovebox Ni(cod)$_2$ (27.51 mg, 100.0 µmol, 1 equiv.) was dissolved in THF (2 mL), Xantphos (115.7 mg, 200 µmol, 2 equiv.) was added slowly and the reaction mixture was stirred for 16 h at room temperature. The solvent was removed via filtration, the bright orange complex was washed with cold hexane (3 x 1 mL) and dried under reduced pressure. Crystallization was not successful yet. NMR data corresponds to similar complexes.[29 30]

^{31}P-NMR (162 MHz, THF-D$_8$, δ): 9.48 (d, *J* = 58.5 Hz), 8.21 (d, *J* = 54.4 Hz).

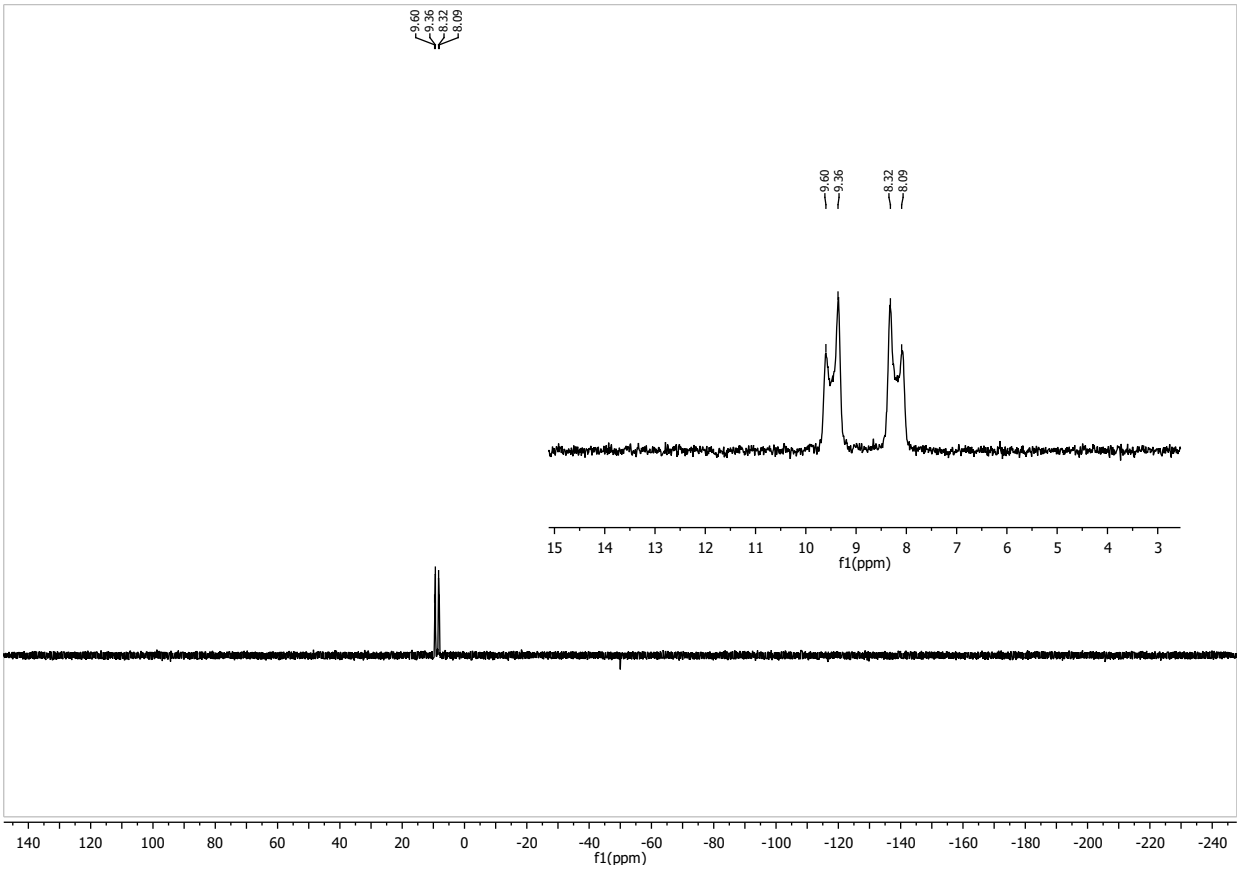

e) Catalyst C1 in THF-d_8.

^{31}P-NMR (162 MHz, THF-D_8, δ): 6.57 (major), 1.42 (minor).

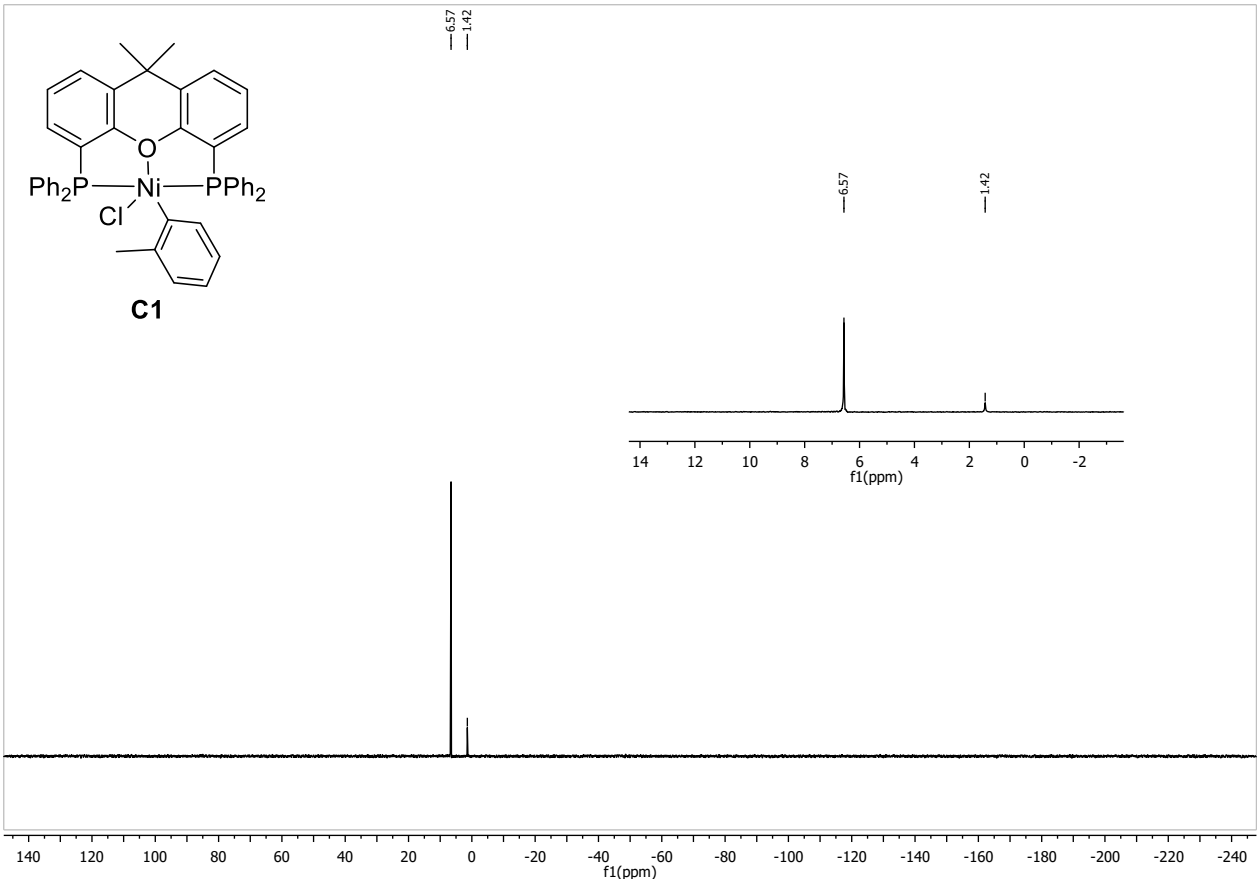

6.3. Computational Data

Cartesian Coordinates (in Å) and Energies (in E_h)

η^1-**I**

6	-1.509961000	3.491902000	-0.740925000
6	-0.362340000	4.457401000	-0.424322000
6	-1.364884000	2.158599000	-0.325785000
8	-0.166951000	1.755584000	0.215267000
6	0.985924000	2.343315000	-0.257419000
6	0.952251000	3.696816000	-0.631581000
6	-2.391397000	1.205906000	-0.453486000
6	2.152912000	1.563148000	-0.334498000
15	2.128269000	-0.219695000	0.159594000
15	-2.143886000	-0.519641000	0.161321000
28	0.034723000	-0.946535000	0.199307000
6	0.136473000	-0.974327000	-1.698065000
6	0.000867000	0.033917000	-2.664949000
6	0.401133000	-2.284417000	-2.151684000
6	0.093081000	-0.253298000	-4.034849000
6	0.492088000	-2.576830000	-3.514373000
6	0.332439000	-1.560547000	-4.465787000
1	-0.194959000	1.064730000	-2.364483000
1	0.556656000	-3.087665000	-1.423084000
1	-0.025951000	0.552203000	-4.765937000
1	0.697995000	-3.601419000	-3.837576000
1	0.403931000	-1.786544000	-5.533211000
6	-0.461818000	4.841158000	1.078848000
1	-1.415144000	5.355619000	1.278780000
1	-0.410964000	3.948254000	1.719381000
1	0.367174000	5.510997000	1.356281000
6	-0.432604000	5.734062000	-1.271652000
1	-0.366618000	5.510462000	-2.347184000
1	-1.371402000	6.274673000	-1.084337000
1	0.381089000	6.424300000	-1.007383000
6	-3.381191000	-1.479183000	-0.814934000
6	-4.601455000	-1.904694000	-0.261668000
6	-3.098493000	-1.787106000	-2.159271000
6	-5.516477000	-2.626918000	-1.034125000
6	-4.017863000	-2.506137000	-2.925801000
6	-5.227768000	-2.930576000	-2.367246000
1	-4.845040000	-1.671903000	0.776163000
1	-2.162723000	-1.464966000	-2.613323000
1	-6.460795000	-2.949790000	-0.588056000
1	-3.778947000	-2.737723000	-3.966707000
1	-5.943853000	-3.495954000	-2.969428000
6	3.012237000	-0.092219000	1.770267000
6	2.284161000	0.455528000	2.842232000
6	4.351588000	-0.459239000	1.965582000
6	2.890273000	0.629274000	4.087425000
6	4.952316000	-0.288248000	3.217171000
6	4.225233000	0.255519000	4.279655000
1	1.233795000	0.716897000	2.703953000
1	4.932072000	-0.881970000	1.143840000
1	2.313506000	1.050982000	4.914651000

1	5.995685000	-0.581565000	3.359033000
1	4.696734000	0.386873000	5.257144000
6	-2.866565000	-0.466366000	1.851560000
6	-3.452408000	0.679582000	2.407483000
6	-2.778218000	-1.635528000	2.627966000
6	-3.951603000	0.654159000	3.715043000
6	-3.287822000	-1.662735000	3.925468000
6	-3.872290000	-0.515060000	4.474830000
1	-3.523960000	1.598755000	1.822913000
1	-2.297282000	-2.523332000	2.214371000
1	-4.406015000	1.554053000	4.137652000
1	-3.214204000	-2.579171000	4.516562000
1	-4.262434000	-0.533227000	5.495686000
6	3.237191000	-1.107073000	-0.993242000
6	3.635696000	-2.405560000	-0.622099000
6	3.507719000	-0.649976000	-2.292766000
6	4.341321000	-3.204107000	-1.524402000
6	4.204905000	-1.459687000	-3.192722000
6	4.632015000	-2.733585000	-2.809186000
1	3.346854000	-2.803561000	0.352955000
1	3.146834000	0.324564000	-2.622546000
1	4.646302000	-4.210204000	-1.225619000
1	4.399580000	-1.094851000	-4.204295000
1	5.174348000	-3.366500000	-3.516569000
6	-3.593765000	1.618156000	-1.047876000
1	-4.405055000	0.898115000	-1.171063000
6	-3.753599000	2.929279000	-1.497175000
1	-4.691292000	3.232746000	-1.968196000
6	2.139890000	4.275034000	-1.091457000
1	2.153184000	5.321981000	-1.395732000
6	3.326237000	3.536351000	-1.140288000
1	4.249738000	4.011514000	-1.478810000
6	-2.719956000	3.857539000	-1.341655000
6	3.333472000	2.197269000	-0.752717000
1	-2.868764000	4.881069000	-1.686827000
1	4.263863000	1.626598000	-0.787117000
8	0.026668000	-1.345651000	2.092743000
6	0.753726000	-2.382793000	2.349056000
8	1.371562000	-3.024956000	1.491835000
6	0.849363000	-2.744782000	3.821859000
1	-0.089396000	-2.514988000	4.346262000
1	1.644775000	-2.127289000	4.271442000
1	1.117820000	-3.803116000	3.940381000

B3LYP -4230.23083631337
M06-L -4232.58641239585
G-E 0.66842373

η^2-**I**

6	1.088118000	3.703941000	-0.690300000
6	-0.062258000	4.550537000	-0.129669000
6	1.123588000	2.358496000	-0.309767000
8	0.093524000	1.848198000	0.452781000
6	-1.165636000	2.318250000	0.153960000
6	-1.318507000	3.668887000	-0.188076000
6	2.123439000	1.460843000	-0.708885000

6	-2.220657000	1.392505000	0.157621000
15	-1.833400000	-0.385407000	0.460978000
15	1.932660000	-0.284074000	-0.155179000
28	-0.169864000	-1.347477000	-0.653263000
6	-0.601915000	-0.559836000	-2.331680000
6	-0.943997000	-1.511423000	-3.317115000
6	-0.578242000	0.785145000	-2.727463000
6	-1.246801000	-1.126729000	-4.628369000
6	-0.874412000	1.175610000	-4.039254000
6	-1.215293000	0.221200000	-4.999658000
1	-0.953533000	-2.573324000	-3.065318000
1	-0.319870000	1.564963000	-2.019143000
1	-1.506871000	-1.892426000	-5.365958000
1	-0.835676000	2.236809000	-4.303541000
1	-1.450977000	0.521865000	-6.024191000
6	0.248483000	4.869943000	1.358590000
1	1.161623000	5.481351000	1.432871000
1	-0.586825000	5.425965000	1.812967000
1	0.407361000	3.948320000	1.937785000
6	-0.243054000	5.864650000	-0.897394000
1	-0.465515000	5.686564000	-1.960359000
1	-1.061425000	6.458632000	-0.464803000
1	0.664892000	6.481626000	-0.830700000
6	-1.537470000	-0.479049000	2.280906000
6	-1.201876000	0.633880000	3.067585000
6	-1.606196000	-1.745583000	2.889314000
6	-0.946720000	0.484345000	4.433396000
6	-1.361453000	-1.888879000	4.255366000
6	-1.028857000	-0.774418000	5.032525000
1	-1.135664000	1.627195000	2.625440000
1	-1.840040000	-2.623355000	2.287014000
1	-0.678684000	1.360364000	5.028975000
1	-1.424672000	-2.879446000	4.713402000
1	-0.829427000	-0.888158000	6.101213000
6	3.386480000	-1.122157000	-0.906285000
6	4.687966000	-1.053963000	-0.381244000
6	3.149214000	-1.869688000	-2.072677000
6	5.739801000	-1.712087000	-1.023647000
6	4.206223000	-2.520335000	-2.715856000
6	5.500864000	-2.442756000	-2.193444000
1	4.877660000	-0.487888000	0.533863000
1	2.131351000	-1.953270000	-2.461005000
1	6.749771000	-1.656569000	-0.608679000
1	4.012603000	-3.098880000	-3.622601000
1	6.325174000	-2.958395000	-2.693225000
6	2.372810000	-0.115294000	1.635550000
6	3.077436000	0.994558000	2.136004000
6	1.962195000	-1.118606000	2.529866000
6	3.367603000	1.096353000	3.499553000
6	2.259410000	-1.013959000	3.891168000
6	2.960092000	0.091208000	4.381672000
1	3.399552000	1.790174000	1.461289000
1	1.383540000	-1.965980000	2.160300000
1	3.913976000	1.967019000	3.872467000
1	1.916966000	-1.794720000	4.573923000
1	3.181017000	0.174539000	5.449200000
6	-3.457016000	-1.231913000	0.281059000
6	-4.499833000	-1.077120000	1.211762000
6	-3.637490000	-2.077939000	-0.822942000

6	-5.708959000	-1.750841000	1.029373000
6	-4.851277000	-2.748129000	-1.005241000
6	-5.887098000	-2.585049000	-0.081440000
1	-4.360155000	-0.433804000	2.084049000
1	-2.819013000	-2.210014000	-1.533002000
1	-6.515180000	-1.627505000	1.757377000
1	-4.982664000	-3.403495000	-1.869896000
1	-6.834067000	-3.113065000	-0.221197000
6	-2.601409000	4.099443000	-0.545363000
1	-2.770818000	5.138723000	-0.829216000
6	-3.677590000	3.206723000	-0.545509000
1	-4.672252000	3.557897000	-0.829783000
6	3.137021000	1.952146000	-1.541564000
1	3.928605000	1.281780000	-1.881703000
6	3.125793000	3.289235000	-1.951473000
1	3.916139000	3.659000000	-2.608989000
6	-3.492209000	1.866327000	-0.199467000
6	2.112725000	4.157632000	-1.531727000
1	-4.338997000	1.179631000	-0.231049000
1	2.126749000	5.195645000	-1.866336000
8	0.316370000	-3.322730000	-1.364774000
6	0.409706000	-3.651825000	-0.157843000
8	0.129524000	-2.789921000	0.741356000
6	0.905240000	-5.013663000	0.255038000
1	1.984065000	-4.937437000	0.470885000
1	0.761741000	-5.739416000	-0.556206000
1	0.399644000	-5.346099000	1.172652000

B3LYP -4230.22798533799
M06-L -4232.5797861735
G-E 0.66809197

2

16	-0.047776000	-0.672371000	-0.000004000
1	1.295555000	-0.833447000	0.000005000
6	-0.048542000	1.159216000	-0.000001000
1	-1.104204000	1.466932000	0.000002000
1	0.433390000	1.568275000	0.900120000
1	0.433386000	1.568278000	-0.900123000

B3LYP -438.563257529146
M06-L -438.738625463962
G-E 0.02138121

TS-PT

6	1.454799000	3.380023000	-0.751669000
6	0.582939000	4.385530000	0.010512000
6	1.411405000	2.027081000	-0.391411000
8	0.459192000	1.569129000	0.487701000
6	-0.677624000	2.301938000	0.689012000
6	-0.697799000	3.684040000	0.472464000
6	2.322020000	1.070535000	-0.873645000

6	-1.813695000	1.581215000	1.100144000
15	-1.788919000	-0.247520000	0.930966000
15	2.190331000	-0.669198000	-0.238046000
28	-1.527258000	-1.040265000	-1.085366000
6	-1.547123000	0.628632000	-1.928657000
6	-2.584747000	1.575485000	-1.933655000
6	-0.432980000	0.868769000	-2.752411000
6	-2.507961000	2.733626000	-2.715121000
6	-0.345998000	2.029660000	-3.530970000
6	-1.381440000	2.970045000	-3.511885000
1	-3.468560000	1.416389000	-1.309840000
1	0.378491000	0.139099000	-2.789096000
1	-3.327939000	3.457834000	-2.695515000
1	0.543476000	2.202753000	-4.143197000
1	-1.312887000	3.879045000	-4.116016000
6	1.371358000	4.826525000	1.274091000
1	2.316852000	5.313814000	0.987387000
1	0.775053000	5.532656000	1.873887000
1	1.611521000	3.957601000	1.906289000
6	0.262557000	5.618259000	-0.851598000
1	-0.291412000	5.328142000	-1.756781000
1	-0.335079000	6.350627000	-0.290869000
1	1.183040000	6.138781000	-1.151178000
6	-0.677070000	-0.855814000	2.261601000
6	-0.064461000	0.008397000	3.180979000
6	-0.520053000	-2.245633000	2.408511000
6	0.679320000	-0.508676000	4.245021000
6	0.216759000	-2.754815000	3.478871000
6	0.812973000	-1.889315000	4.401754000
1	-0.167196000	1.089016000	3.074860000
1	-0.970529000	-2.918176000	1.676785000
1	1.166250000	0.173037000	4.945643000
1	0.329244000	-3.836677000	3.589065000
1	1.398553000	-2.290019000	5.232518000
6	3.517858000	-1.490605000	-1.242959000
6	4.882739000	-1.476211000	-0.903367000
6	3.116753000	-2.144460000	-2.422536000
6	5.825201000	-2.101919000	-1.723873000
6	4.065315000	-2.759657000	-3.246549000
6	5.419500000	-2.743246000	-2.899452000
1	5.212631000	-0.970571000	0.006696000
1	2.055734000	-2.178611000	-2.686581000
1	6.882697000	-2.084242000	-1.445926000
1	3.739547000	-3.261655000	-4.161645000
1	6.158268000	-3.231193000	-3.540879000
6	3.044678000	-0.517013000	1.402238000
6	3.410092000	0.697319000	2.005287000
6	3.312355000	-1.712897000	2.092257000
6	4.028661000	0.713358000	3.259923000
6	3.950736000	-1.698486000	3.332826000
6	4.307590000	-0.482967000	3.925690000
1	3.226274000	1.642216000	1.490988000
1	3.020641000	-2.669619000	1.650019000
1	4.304513000	1.669834000	3.712442000
1	4.155884000	-2.641100000	3.846934000
1	4.799241000	-0.469148000	4.901815000
6	-3.448005000	-0.743610000	1.569671000
6	-3.738082000	-0.779715000	2.943932000
6	-4.451818000	-1.070841000	0.645706000

6	-5.017940000	-1.127460000	3.381913000
6	-5.731871000	-1.418758000	1.086626000
6	-6.016923000	-1.446688000	2.454702000
1	-2.960383000	-0.539051000	3.672458000
1	-4.219396000	-1.062542000	-0.421353000
1	-5.235951000	-1.153631000	4.452804000
1	-6.503955000	-1.677509000	0.357747000
1	-7.016015000	-1.723638000	2.801271000
6	-1.894217000	4.359609000	0.750403000
1	-1.951543000	5.438349000	0.601684000
6	-3.016956000	3.682065000	1.227600000
1	-3.932572000	4.233860000	1.451983000
6	3.251665000	1.491717000	-1.834063000
1	3.964743000	0.776184000	-2.245142000
6	3.269492000	2.817063000	-2.274203000
1	3.989999000	3.127881000	-3.034589000
6	-2.982140000	2.295900000	1.390763000
6	2.391667000	3.752643000	-1.724368000
1	-3.878648000	1.763781000	1.711476000
1	2.448940000	4.790599000	-2.052767000
8	-0.098219000	-2.349073000	-2.297598000
6	-0.315050000	-3.163088000	-1.362838000
8	-1.232235000	-2.925742000	-0.507431000
6	0.537229000	-4.395182000	-1.192996000
1	-0.017333000	-5.190822000	-0.677483000
1	1.404361000	-4.114120000	-0.572279000
1	0.916607000	-4.742328000	-2.163182000
16	-3.230409000	-1.992938000	-2.992226000
1	-2.074524000	-2.564032000	-3.398833000
6	-3.331373000	-0.727283000	-4.308560000
1	-3.630407000	-1.184434000	-5.262297000
1	-4.090099000	-0.000048000	-3.991769000
1	-2.373558000	-0.200364000	-4.404101000

B3LYP -4668.80388962274
M06-L 0.71211815
G-E -4671.32148744443

II

6	1.833107000	3.247771000	-1.602040000
6	0.772945000	4.350975000	-1.541394000
6	1.606639000	2.085804000	-0.845977000
8	0.413407000	1.930281000	-0.181884000
6	-0.709896000	2.498810000	-0.733825000
6	-0.597437000	3.667383000	-1.497381000
6	2.540524000	1.040420000	-0.754149000
6	-1.936830000	1.863088000	-0.481483000
15	-1.910863000	0.368598000	0.603653000
15	2.096924000	-0.479439000	0.212036000
28	-0.983403000	-1.454759000	-0.087992000
6	-1.196298000	-0.962712000	-1.927259000
6	-2.217343000	-1.685001000	-2.579132000
6	-0.410699000	-0.115115000	-2.722354000
6	-2.454905000	-1.551059000	-3.952912000
6	-0.635698000	0.023646000	-4.098175000
6	-1.664537000	-0.688617000	-4.720582000

1	-2.842155000	-2.381415000	-2.007512000
1	0.405152000	0.448769000	-2.273825000
1	-3.259028000	-2.124255000	-4.425396000
1	0.000529000	0.694828000	-4.683382000
1	-1.846715000	-0.577080000	-5.792996000
6	0.960502000	5.120403000	-0.203293000
1	1.954343000	5.594803000	-0.171598000
1	0.190936000	5.901960000	-0.101214000
1	0.873550000	4.441142000	0.658177000
6	0.893055000	5.338190000	-2.709108000
1	0.767880000	4.834662000	-3.679663000
1	0.135846000	6.131146000	-2.628053000
1	1.871834000	5.839162000	-2.699284000
6	-1.249842000	1.125554000	2.149989000
6	-1.722052000	2.377116000	2.581999000
6	-0.225680000	0.496015000	2.865809000
6	-1.179997000	2.978770000	3.719964000
6	0.325885000	1.103743000	3.996302000
6	-0.151365000	2.344131000	4.426743000
1	-2.512099000	2.886930000	2.024989000
1	0.147986000	-0.464266000	2.521224000
1	-1.557328000	3.949536000	4.051949000
1	1.143224000	0.609122000	4.525071000
1	0.281024000	2.822019000	5.309851000
6	3.162648000	-1.735876000	-0.624381000
6	4.420266000	-2.165175000	-0.169795000
6	2.640034000	-2.290126000	-1.808275000
6	5.140652000	-3.129994000	-0.882972000
6	3.369459000	-3.240290000	-2.526021000
6	4.619770000	-3.667491000	-2.063524000
1	4.845293000	-1.745174000	0.744278000
1	1.652692000	-1.983960000	-2.159247000
1	6.117339000	-3.456335000	-0.515603000
1	2.954081000	-3.653807000	-3.449071000
1	5.186248000	-4.417358000	-2.622154000
6	2.961752000	-0.160189000	1.812478000
6	3.416714000	1.110926000	2.198895000
6	3.043808000	-1.213275000	2.744146000
6	3.943470000	1.321499000	3.477405000
6	3.579996000	-1.005240000	4.016139000
6	4.029901000	0.266994000	4.389836000
1	3.357397000	1.947773000	1.500247000
1	2.686034000	-2.207906000	2.468808000
1	4.288211000	2.319799000	3.759481000
1	3.640574000	-1.838873000	4.720772000
1	4.443241000	0.433295000	5.387736000
6	-3.683666000	0.018167000	0.949873000
6	-4.213949000	0.067975000	2.247589000
6	-4.495476000	-0.437982000	-0.105409000
6	-5.542258000	-0.302415000	2.479864000
6	-5.823228000	-0.798994000	0.130233000
6	-6.351004000	-0.730795000	1.424359000
1	-3.588432000	0.384287000	3.083135000
1	-4.084344000	-0.516045000	-1.114058000
1	-5.942503000	-0.261462000	3.496192000
1	-6.444249000	-1.145562000	-0.699697000
1	-7.388345000	-1.020831000	1.609887000
6	-1.765328000	4.171585000	-2.083540000
1	-1.721883000	5.068787000	-2.701862000

6	-2.997371000	3.550921000	-1.868207000
1	-3.900722000	3.961690000	-2.324734000
6	3.748626000	1.184555000	-1.454230000
1	4.493422000	0.387831000	-1.407343000
6	3.994367000	2.319746000	-2.226592000
1	4.934236000	2.411867000	-2.775926000
6	-3.086680000	2.416544000	-1.057408000
6	3.041369000	3.340349000	-2.301334000
1	-4.060339000	1.960765000	-0.877582000
1	3.252392000	4.221820000	-2.907860000
8	-0.116603000	-3.111470000	-0.791612000
6	-0.583902000	-4.254643000	-0.855796000
8	-1.582599000	-4.676330000	-0.133660000
6	-0.015595000	-5.241963000	-1.834426000
1	1.066468000	-5.077191000	-1.927118000
1	-0.472320000	-5.035952000	-2.816785000
1	-0.242029000	-6.275254000	-1.543212000
16	-1.559201000	-2.507408000	1.917194000
1	-1.804674000	-3.951803000	0.576604000
6	-0.005148000	-3.303983000	2.491147000
1	0.680228000	-3.477486000	1.647737000
1	0.500821000	-2.665004000	3.230540000
1	-0.236820000	-4.267321000	2.970886000

B3LYP -4668.81068103292
M06-L -4671.32588392537
G-E 0.71476886

HOAc

8	-0.211902000	1.343587000	-0.000001000
8	1.246679000	-0.362063000	0.000000000
6	-0.001540000	0.157175000	-0.000002000
6	-1.048665000	-0.927157000	0.000000000
1	-0.920097000	-1.568309000	0.885742000
1	-2.047188000	-0.475019000	0.000001000
1	-0.920100000	-1.568310000	-0.885743000
1	1.862410000	0.390884000	0.000002000

B3LYP -228.920526463914
M06-L -229.175940208135
G-E 0.03486924

III

6	-1.149104000	3.800283000	-0.454666000
6	0.114329000	4.485640000	-0.987876000
6	-1.123773000	2.404498000	-0.328449000
8	0.038934000	1.726822000	-0.627629000
6	1.236656000	2.334840000	-0.329226000
6	1.329341000	3.732086000	-0.432065000
6	-2.243942000	1.656549000	0.071253000
6	2.318299000	1.525920000	0.061417000
15	2.138882000	-0.312955000	0.210296000

15	-2.114859000	-0.179376000	0.235172000
28	-0.013474000	-0.738870000	0.558307000
16	-0.120119000	0.686232000	2.469328000
6	-0.159319000	-2.348863000	-0.472840000
6	-0.061119000	-2.557182000	-1.858471000
6	-0.424175000	-3.482394000	0.328566000
6	-0.220694000	-3.826815000	-2.425347000
6	-0.574415000	-4.758213000	-0.229005000
6	-0.477545000	-4.935628000	-1.613728000
1	0.167854000	-1.717389000	-2.517223000
1	-0.515266000	-3.372685000	1.415483000
1	-0.136529000	-3.948486000	-3.509525000
1	-0.772084000	-5.615835000	0.421601000
1	-0.601411000	-5.928840000	-2.054179000
6	0.151388000	5.979746000	-0.640821000
1	-0.711525000	6.503043000	-1.076739000
1	0.145977000	6.142908000	0.447441000
1	1.048196000	6.456562000	-1.061515000
6	0.123764000	4.325497000	-2.534584000
1	0.095485000	3.263458000	-2.820589000
1	-0.754403000	4.822775000	-2.975890000
1	1.035998000	4.772893000	-2.960216000
6	-2.955994000	-0.642181000	-1.342550000
6	-4.221312000	-1.233732000	-1.451215000
6	-2.250302000	-0.317624000	-2.515059000
6	-4.763687000	-1.510227000	-2.711885000
6	-2.794637000	-0.588119000	-3.769495000
6	-4.053099000	-1.192578000	-3.871363000
1	-4.797866000	-1.475524000	-0.557061000
1	-1.267192000	0.153904000	-2.436023000
1	-5.750698000	-1.974420000	-2.783614000
1	-2.232061000	-0.333736000	-4.671479000
1	-4.478878000	-1.412050000	-4.853845000
6	3.438215000	-0.734020000	1.455026000
6	3.228837000	-0.308148000	2.780621000
6	4.607379000	-1.447041000	1.144453000
6	4.169117000	-0.598928000	3.770341000
6	5.542249000	-1.741236000	2.143206000
6	5.326459000	-1.320910000	3.457764000
1	2.328116000	0.266920000	3.017294000
1	4.803038000	-1.772329000	0.122162000
1	3.994669000	-0.257762000	4.794141000
1	6.446669000	-2.298519000	1.885313000
1	6.059379000	-1.550948000	4.235535000
6	-3.218065000	-0.712552000	1.591619000
6	-3.546320000	0.119139000	2.674937000
6	-3.551256000	-2.079752000	1.651329000
6	-4.238819000	-0.399317000	3.772865000
6	-4.247736000	-2.590504000	2.749296000
6	-4.598350000	-1.749667000	3.810657000
1	-3.225417000	1.160448000	2.678573000
1	-3.244658000	-2.753263000	0.847260000
1	-4.487657000	0.257615000	4.610126000
1	-4.503365000	-3.652617000	2.780601000
1	-5.138185000	-2.150035000	4.672642000
6	2.821669000	-0.925312000	-1.384839000
6	2.955425000	-2.314266000	-1.564337000
6	3.123855000	-0.070740000	-2.456712000
6	3.413877000	-2.832656000	-2.775821000

6	3.564209000	-0.594068000	-3.677246000
6	3.717004000	-1.974058000	-3.837633000
1	2.677480000	-2.996607000	-0.758599000
1	3.018327000	1.009841000	-2.341988000
1	3.509077000	-3.914389000	-2.896973000
1	3.794156000	0.083294000	-4.503828000
1	4.064118000	-2.381364000	-4.790750000
6	-3.446413000	2.344518000	0.286927000
1	-4.346150000	1.787231000	0.555085000
6	-3.496409000	3.735030000	0.182494000
1	-4.434141000	4.261668000	0.374418000
6	2.551573000	4.328189000	-0.103179000
1	2.660791000	5.411906000	-0.155796000
6	3.648197000	3.550987000	0.280679000
1	4.597485000	4.032428000	0.526472000
6	-2.352305000	4.456654000	-0.170094000
6	3.534388000	2.162885000	0.352660000
1	-2.411526000	5.542908000	-0.245410000
1	4.393189000	1.563189000	0.659651000
6	-0.308072000	-0.760502000	3.583973000
1	-1.164106000	-1.384257000	3.282779000
1	0.599871000	-1.385922000	3.582588000
1	-0.487350000	-0.407230000	4.611520000

B3LYP -4439.86173355408
M06-L -4442.14462288195
G-E 0.65708471

TS-RE

6	2.083615000	3.709448000	-0.447388000
6	0.946589000	4.736713000	-0.576639000
6	1.737852000	2.356920000	-0.556669000
8	0.427654000	2.023666000	-0.774892000
6	-0.520790000	2.748417000	-0.108989000
6	-0.312932000	4.126304000	0.064987000
6	2.643807000	1.299624000	-0.407439000
6	-1.645223000	2.058462000	0.359745000
15	-1.733560000	0.216384000	0.120837000
15	1.919394000	-0.395175000	-0.191885000
28	-0.153135000	-0.708290000	-1.125384000
6	-0.777233000	-2.547159000	-1.514455000
6	0.104858000	-3.496718000	-0.935239000
6	-2.152970000	-2.878114000	-1.564630000
6	-0.385029000	-4.650827000	-0.323613000
6	-2.630365000	-4.049943000	-0.973027000
6	-1.757018000	-4.938157000	-0.333285000
1	1.180753000	-3.315673000	-0.969448000
1	-2.863080000	-2.186948000	-2.017103000
1	0.317372000	-5.345348000	0.146490000
1	-3.704599000	-4.255974000	-0.994181000
1	-2.136368000	-5.851745000	0.130929000
16	0.061797000	-1.472257000	-3.154150000
6	-1.451108000	-1.423890000	-4.187388000
1	-1.867895000	-2.435423000	-4.309726000
1	-2.215540000	-0.760156000	-3.765223000
1	-1.140697000	-1.036786000	-5.169413000

6	0.655427000	4.947824000	-2.088145000
1	0.386198000	3.997932000	-2.573006000
1	-0.180467000	5.652729000	-2.221126000
1	1.545234000	5.352581000	-2.595792000
6	1.318501000	6.082111000	0.060335000
1	2.206826000	6.511366000	-0.425341000
1	0.507141000	6.813407000	-0.067365000
1	1.526332000	5.976188000	1.135939000
6	-1.895409000	-0.444959000	1.836411000
6	-1.734443000	0.319012000	3.002093000
6	-2.105563000	-1.832431000	1.959440000
6	-1.822964000	-0.283367000	4.261566000
6	-2.215781000	-2.425337000	3.217326000
6	-2.080089000	-1.651300000	4.374972000
1	-1.531111000	1.388780000	2.936094000
1	-2.181342000	-2.453855000	1.065640000
1	-1.685991000	0.324996000	5.159197000
1	-2.391226000	-3.501903000	3.288236000
1	-2.155262000	-2.116720000	5.361233000
6	1.884615000	-0.523843000	1.653428000
6	2.352885000	0.465480000	2.532198000
6	1.303967000	-1.688387000	2.189756000
6	2.259818000	0.284152000	3.917156000
6	1.233349000	-1.875237000	3.569276000
6	1.709956000	-0.888361000	4.439221000
1	2.795451000	1.383755000	2.142884000
1	0.891701000	-2.445830000	1.518550000
1	2.624849000	1.066010000	4.588634000
1	0.776908000	-2.783836000	3.966842000
1	1.637679000	-1.028854000	5.520775000
6	3.353481000	-1.469581000	-0.638228000
6	4.261043000	-1.989191000	0.299617000
6	3.509792000	-1.803276000	-1.995853000
6	5.306248000	-2.821944000	-0.113723000
6	4.559539000	-2.627634000	-2.406386000
6	5.459653000	-3.141092000	-1.466062000
1	4.147832000	-1.748450000	1.358781000
1	2.795343000	-1.428885000	-2.732570000
1	6.003083000	-3.223834000	0.626665000
1	4.666076000	-2.880360000	-3.464510000
1	6.275055000	-3.794856000	-1.786647000
6	-3.457950000	0.096937000	-0.550938000
6	-4.540067000	-0.516999000	0.093781000
6	-3.641455000	0.602832000	-1.850968000
6	-5.776224000	-0.633949000	-0.554650000
6	-4.874720000	0.495497000	-2.492609000
6	-5.947788000	-0.132169000	-1.846539000
1	-4.423495000	-0.916936000	1.102379000
1	-2.797201000	1.072566000	-2.364827000
1	-6.609113000	-1.123149000	-0.042524000
1	-4.997868000	0.892723000	-3.503559000
1	-6.912575000	-0.228748000	-2.351069000
6	3.441967000	4.000035000	-0.267760000
1	3.773870000	5.035931000	-0.181611000
6	4.391880000	2.971730000	-0.207918000
6	-2.642130000	2.816705000	0.995683000
1	-3.548273000	2.320153000	1.351053000
6	-2.471261000	4.188221000	1.190852000
6	3.999077000	1.630951000	-0.264762000

6	-1.311411000	4.835197000	0.740501000
1	-1.204097000	5.908130000	0.907209000
1	-3.248268000	4.765247000	1.697954000
1	5.449040000	3.221549000	-0.089270000
1	4.741612000	0.836193000	-0.161272000

B3LYP -4439.83468867503
M06-L -4442.12578853791
G-E 0.65561066

IV

6	-0.915972000	3.659108000	-1.643018000
6	-2.221650000	3.491879000	-2.435484000
6	-0.331818000	2.491163000	-1.125922000
8	-0.970920000	1.294678000	-1.338957000
6	-2.337974000	1.308624000	-1.206214000
6	-3.044407000	2.407380000	-1.723332000
6	0.857924000	2.480357000	-0.388409000
6	-2.943954000	0.238246000	-0.537862000
15	-1.850036000	-1.042210000	0.271219000
15	1.421527000	0.887165000	0.396437000
28	0.224892000	-0.777577000	-0.199886000
6	2.773856000	-2.611480000	-1.262262000
6	3.627873000	-3.039722000	-2.285842000
6	3.271989000	-2.428095000	0.032866000
6	4.977202000	-3.282008000	-2.010626000
6	4.620001000	-2.667982000	0.304637000
6	5.475517000	-3.092462000	-0.717307000
1	3.237415000	-3.164516000	-3.299145000
1	2.588674000	-2.063465000	0.802981000
1	5.644634000	-3.607686000	-2.812868000
1	5.007420000	-2.506367000	1.313725000
1	6.533770000	-3.267610000	-0.507972000
16	1.054371000	-2.192990000	-1.627951000
6	0.349609000	-3.890345000	-1.559072000
1	0.900598000	-4.548096000	-2.246249000
1	0.397248000	-4.280711000	-0.533994000
1	-0.699447000	-3.811866000	-1.870463000
6	-1.864384000	2.975823000	-3.856973000
1	-1.302823000	2.031842000	-3.803749000
1	-2.782014000	2.799717000	-4.440302000
1	-1.244259000	3.716074000	-4.386824000
6	-2.993373000	4.811004000	-2.559809000
1	-2.393867000	5.565203000	-3.090154000
1	-3.912720000	4.670670000	-3.146852000
1	-3.267630000	5.214814000	-1.573391000
6	-2.455925000	-0.958397000	2.025331000
6	-3.673552000	-1.486542000	2.488986000
6	-1.625074000	-0.280048000	2.927572000
6	-4.053113000	-1.319952000	3.823418000
6	-2.005064000	-0.106922000	4.261761000
6	-3.222414000	-0.625407000	4.711528000
1	-4.324358000	-2.045105000	1.812139000
1	-0.672777000	0.104241000	2.564573000
1	-5.002559000	-1.734519000	4.173311000
1	-1.339140000	0.428755000	4.942400000

1	-3.523563000	-0.497267000	5.754817000
6	1.489043000	1.325706000	2.194708000
6	0.791022000	2.405180000	2.760023000
6	2.123122000	0.413198000	3.061203000
6	0.740757000	2.574928000	4.148072000
6	2.081557000	0.587601000	4.444738000
6	1.387390000	1.671895000	4.995909000
1	0.269149000	3.115632000	2.116369000
1	2.654532000	-0.446429000	2.643377000
1	0.188258000	3.420105000	4.567275000
1	2.585347000	-0.130463000	5.097227000
1	1.348009000	1.806782000	6.079897000
6	3.222922000	0.969752000	-0.077943000
6	4.269287000	1.400144000	0.751652000
6	3.531471000	0.533459000	-1.377263000
6	5.592846000	1.379249000	0.294656000
6	4.847157000	0.521489000	-1.838102000
6	5.886116000	0.938821000	-0.998094000
1	4.059782000	1.750689000	1.764172000
1	2.723444000	0.178411000	-2.022206000
1	6.397956000	1.710969000	0.956157000
1	5.065490000	0.164333000	-2.847481000
1	6.920882000	0.915514000	-1.349991000
6	-2.646649000	-2.608280000	-0.319951000
6	-2.515517000	-3.784523000	0.440913000
6	-3.203192000	-2.705899000	-1.607032000
6	-2.932870000	-5.016934000	-0.065580000
6	-3.614593000	-3.940737000	-2.118035000
6	-3.480467000	-5.102254000	-1.350790000
1	-2.074607000	-3.735025000	1.440164000
1	-3.308327000	-1.808957000	-2.222179000
1	-2.824814000	-5.917984000	0.544306000
1	-4.043873000	-3.994137000	-3.122172000
1	-3.802478000	-6.067321000	-1.750084000
6	-0.236731000	4.862565000	-1.430536000
1	-0.649026000	5.798484000	-1.810454000
6	0.985650000	4.882545000	-0.744855000
6	-4.344505000	0.261614000	-0.433430000
1	-4.860535000	-0.557493000	0.070433000
6	-5.081106000	1.327036000	-0.950985000
6	1.528681000	3.704396000	-0.231310000
6	-4.434888000	2.399608000	-1.580295000
1	-5.030370000	3.229053000	-1.964450000
1	-6.169698000	1.331682000	-0.855625000
1	1.512247000	5.830004000	-0.606540000
1	2.473781000	3.729340000	0.316479000

B3LYP -4439.83976000344
M06-L -4442.13785320213
G-E 0.65746051

1

6	0.000000000	0.000000000	0.511077000
6	0.000000000	1.217482000	-0.177154000
6	0.000000000	-1.217482000	-0.177154000
6	0.000000000	1.209479000	-1.574864000

6	0.000000000	-1.209479000	-1.574864000
6	0.000000000	0.000000000	-2.277054000
1	0.000001000	2.154765000	0.381750000
1	0.000001000	-2.154765000	0.381750000
1	0.000000000	2.158963000	-2.116228000
1	0.000000000	-2.158963000	-2.116228000
1	-0.000001000	0.000000000	-3.369672000
17	-0.000001000	0.000001000	2.261925000

B3LYP -691.558498876461
M06-L -691.943012485897
G-E 0.0612521

3

6	0.000962000	0.259161000	0.000100000
6	-1.318342000	0.754581000	-0.000006000
6	0.204098000	-1.130724000	0.000152000
6	-2.402330000	-0.121723000	-0.000066000
6	-0.891961000	-2.001022000	0.000095000
6	-2.197540000	-1.507033000	-0.000015000
1	-1.491278000	1.834456000	-0.000043000
1	1.210658000	-1.549582000	0.000240000
1	-3.418232000	0.282433000	-0.000148000
1	-0.714989000	-3.080075000	0.000137000
1	-3.048629000	-2.192006000	-0.000058000
16	1.300211000	1.472932000	0.000150000
6	2.816594000	0.473045000	-0.000103000
1	2.890315000	-0.155095000	0.900714000
1	2.890439000	-0.154452000	-0.901356000
1	3.647480000	1.192855000	0.000208000

B3LYP -669.457990947405
M06-L -669.859877281621
G-E 0.09699111

V

6	2.068323000	3.519340000	-0.872835000
6	1.092118000	4.644664000	-0.500644000
6	1.720488000	2.223137000	-0.473647000
8	0.526614000	2.021893000	0.173485000
6	-0.535052000	2.749761000	-0.308756000
6	-0.324357000	4.081835000	-0.689398000
6	2.506838000	1.089818000	-0.711170000
6	-1.763951000	2.086206000	-0.410842000
15	-1.801059000	0.258900000	-0.074531000
15	1.795379000	-0.538988000	-0.187738000
28	-0.253532000	-1.162471000	-0.761128000
17	-1.473999000	-2.356807000	-3.354679000
6	-1.237737000	-2.732375000	-1.597066000
6	0.096020000	-3.119055000	-1.199652000
6	-2.374974000	-3.291687000	-0.918130000
6	0.222681000	-3.957082000	-0.037539000

6	-2.194340000	-4.057399000	0.209451000
6	-0.879487000	-4.382732000	0.667435000
1	0.898329000	-3.156301000	-1.941416000
1	-3.373503000	-3.078760000	-1.301687000
1	1.226946000	-4.272719000	0.259754000
1	-3.065880000	-4.439169000	0.747583000
1	-0.755764000	-5.013994000	1.551081000
6	1.327643000	5.911373000	-1.331439000
1	1.202714000	5.719184000	-2.407784000
1	0.628479000	6.707290000	-1.036116000
1	2.341226000	6.303792000	-1.163351000
6	1.285370000	4.978409000	1.004669000
1	2.307829000	5.345978000	1.186029000
1	0.569835000	5.755294000	1.317143000
1	1.124421000	4.088252000	1.630638000
6	3.290104000	3.673604000	-1.538891000
1	3.609917000	4.660369000	-1.876674000
6	4.117346000	2.568565000	-1.770882000
6	-2.853574000	2.838301000	-0.881455000
1	-3.835525000	2.372633000	-0.974419000
6	-2.684137000	4.173343000	-1.257338000
6	-1.429997000	4.788702000	-1.175203000
6	3.735477000	1.288052000	-1.359727000
1	-3.540664000	4.740502000	-1.629466000
1	-1.322654000	5.827946000	-1.488591000
1	5.072275000	2.707671000	-2.283259000
1	4.389986000	0.437583000	-1.556592000
6	2.057180000	-0.494739000	1.638636000
6	2.922601000	0.410906000	2.272372000
6	1.344408000	-1.420030000	2.417521000
6	3.072390000	0.388805000	3.661999000
6	1.505454000	-1.448034000	3.804089000
6	2.366767000	-0.542492000	4.430343000
1	3.481928000	1.139038000	1.680898000
1	0.653665000	-2.113790000	1.933755000
1	3.744432000	1.102980000	4.145527000
1	0.937581000	-2.167732000	4.397408000
1	2.482056000	-0.557454000	5.517346000
6	-1.757601000	0.146213000	1.770779000
6	-1.437397000	1.215452000	2.617972000
6	-2.009073000	-1.118472000	2.334058000
6	-1.374482000	1.025088000	4.002894000
6	-1.969727000	-1.299391000	3.716290000
6	-1.647164000	-0.227671000	4.556524000
1	-1.236472000	2.204973000	2.205178000
1	-2.232565000	-1.965920000	1.681747000
1	-1.112108000	1.865460000	4.650735000
1	-2.175839000	-2.287069000	4.137399000
1	-1.599982000	-0.371324000	5.639081000
6	-3.576614000	-0.091085000	-0.454676000
6	-4.601339000	-0.069118000	0.504321000
6	-3.902666000	-0.369749000	-1.792402000
6	-5.924026000	-0.331810000	0.132759000
6	-5.224975000	-0.622427000	-2.164171000
6	-6.239699000	-0.608285000	-1.200954000
1	-4.369976000	0.150211000	1.548358000
1	-3.110886000	-0.417811000	-2.541946000
1	-6.711500000	-0.318283000	0.891125000
1	-5.459665000	-0.844455000	-3.208402000

1	-7.273914000	-0.814675000	-1.488953000
6	3.112224000	-1.694946000	-0.770824000
6	4.007679000	-2.353053000	0.084735000
6	3.162576000	-1.970726000	-2.150176000
6	4.935362000	-3.266919000	-0.429168000
6	4.097782000	-2.870387000	-2.663357000
6	4.985676000	-3.525489000	-1.801243000
1	3.982124000	-2.155381000	1.158250000
1	2.451868000	-1.481119000	-2.823105000
1	5.623921000	-3.776869000	0.249831000
1	4.125513000	-3.070543000	-3.737587000
1	5.711094000	-4.239514000	-2.199564000

B3LYP -4461.95233924168
M06-L -4464.22406477079
G-E 0.62168984

VI

6	-1.457330000	3.621070000	-0.435856000
6	-0.254443000	4.377111000	-1.010038000
6	-1.324376000	2.233604000	-0.270793000
8	-0.102600000	1.651432000	-0.541474000
6	1.027706000	2.373347000	-0.216125000
6	1.003546000	3.766898000	-0.383036000
6	-2.389887000	1.418520000	0.153778000
6	2.160246000	1.691018000	0.265791000
15	2.139963000	-0.147619000	0.471304000
15	-2.157516000	-0.405911000	0.352049000
28	0.007205000	-0.708702000	0.770964000
17	-0.133082000	0.749466000	2.590598000
6	0.117531000	-2.121071000	-0.490162000
6	0.153878000	-3.433561000	0.014698000
6	0.156401000	-1.954370000	-1.885539000
6	0.229015000	-4.538521000	-0.845045000
6	0.230215000	-3.050885000	-2.747349000
6	0.267447000	-4.351027000	-2.230452000
1	0.121833000	-3.602546000	1.096800000
1	0.127509000	-0.945389000	-2.304850000
1	0.256409000	-5.550063000	-0.427798000
1	0.258318000	-2.890056000	-3.828727000
1	0.325110000	-5.211781000	-2.902321000
6	-2.815674000	-1.082959000	-1.224714000
6	-2.992892000	-0.291218000	-2.367788000
6	-3.033349000	-2.469502000	-1.311645000
6	-3.381539000	-0.876497000	-3.578300000
6	-3.424316000	-3.049252000	-2.516801000
6	-3.597451000	-2.254080000	-3.655803000
1	-2.824338000	0.786607000	-2.319948000
1	-2.867736000	-3.102712000	-0.437526000
1	-3.515446000	-0.249196000	-4.463463000
1	-3.576155000	-4.129774000	-2.571978000
1	-3.895968000	-2.710645000	-4.602998000
6	3.380532000	-0.511533000	1.782641000
6	2.926982000	-0.730351000	3.094256000
6	4.756422000	-0.605136000	1.504995000
6	3.839389000	-1.025697000	4.110797000

6	5.663318000	-0.901444000	2.525777000
6	5.206573000	-1.111151000	3.831111000
1	1.860423000	-0.646924000	3.312920000
1	5.121370000	-0.457914000	0.486227000
1	3.475737000	-1.192316000	5.128031000
1	6.730266000	-0.972443000	2.298621000
1	5.916718000	-1.346167000	4.628364000
6	2.966851000	-0.748796000	-1.055802000
6	3.318278000	-2.108869000	-1.121431000
6	3.158734000	0.061239000	-2.183434000
6	3.856871000	-2.644430000	-2.289373000
6	3.694801000	-0.480379000	-3.357679000
6	4.044662000	-1.831245000	-3.413413000
1	3.141292000	-2.758613000	-0.261688000
1	2.887466000	1.118488000	-2.151818000
1	4.112612000	-3.705826000	-2.329280000
1	3.839072000	0.160388000	-4.231496000
1	4.459117000	-2.253466000	-4.332499000
6	-3.412020000	-0.937036000	1.589066000
6	-4.753076000	-1.177443000	1.239152000
6	-3.000321000	-1.136711000	2.917307000
6	-5.668772000	-1.601026000	2.205502000
6	-3.921357000	-1.560339000	3.879261000
6	-5.254428000	-1.792886000	3.527721000
1	-5.082060000	-1.045400000	0.206111000
1	-1.962416000	-0.937261000	3.191502000
1	-6.708447000	-1.785236000	1.922611000
1	-3.591461000	-1.711027000	4.910346000
1	-5.970936000	-2.127656000	4.282472000
6	-0.348859000	5.888676000	-0.769180000
1	-0.382914000	6.127334000	0.304496000
1	0.511128000	6.408422000	-1.215328000
1	-1.247083000	6.304352000	-1.247901000
6	-0.207094000	4.114711000	-2.541833000
1	-1.116838000	4.506070000	-3.024119000
1	0.669851000	4.610712000	-2.987288000
1	-0.139798000	3.037957000	-2.756880000
6	-2.691983000	4.203227000	-0.128996000
1	-2.826894000	5.280507000	-0.230240000
6	-3.765790000	3.419002000	0.299471000
1	-4.724094000	3.887549000	0.534901000
6	2.145778000	4.491179000	-0.025282000
1	2.157735000	5.576463000	-0.130044000
6	3.282702000	3.840537000	0.460112000
1	4.166926000	4.419377000	0.736447000
6	3.290449000	2.452481000	0.596194000
6	-3.616728000	2.038362000	0.430217000
1	-4.458403000	1.435797000	0.774892000
1	4.179156000	1.954269000	0.986560000

B3LYP -4461.9986057687
M06-L -4464.26866237656
G-E 0.62154284

7. Unsuccessful substrates/ low yield

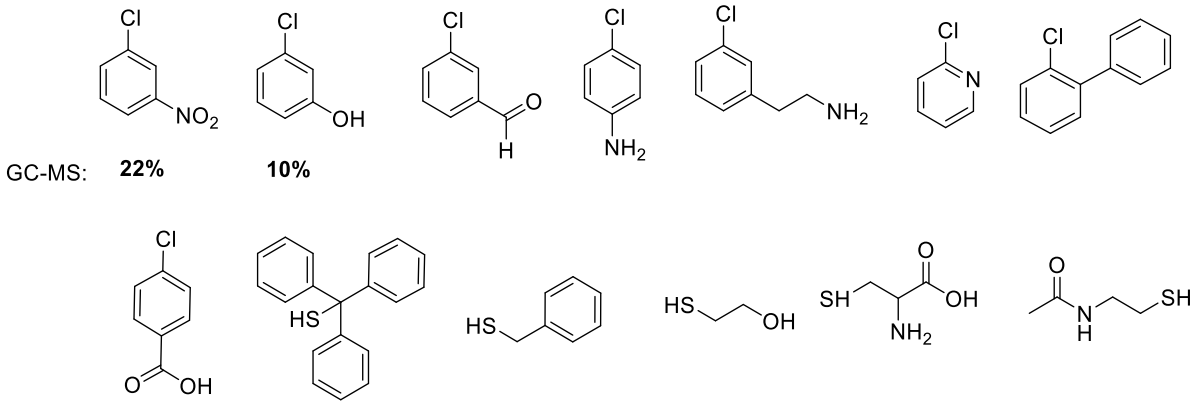

8. GC-FID calibration

The quantification of GC-yields was achieved by adding a standard compound (*n*-pentadecane) to reaction mixtures before quenching (usually 100 µL) and applying the general formula:

$$\frac{A(compound)}{A(standard)} = R \cdot \frac{m(compound)}{m(standard)}$$

R: Response factor of compound
A: Peak area determined by GC-FID
m: mass of compound

The R values were determined by GC calibrations of respective compounds with pentadecane in ethyl acetate and measuring different mass ratios.

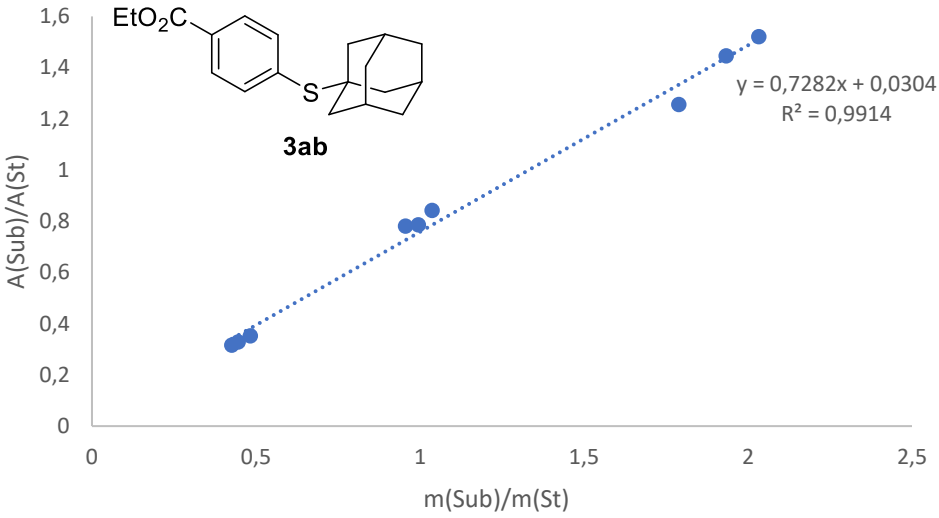

Mass ratio $\left[\frac{mg\ (Substrate)}{mg\ (Std)}\right]$	A (Substrate)	A (Std)	Area ratio $\left[\frac{A(Substrate)}{A\ (Std)}\right]$
0.43	7096.8	22481.0	0.31568
0.48	7290.0	20706.8	0.35206
0.45	8026.0	24412.7	0.32876
1.0	8924.9	11357.4	0.78582
0.96	8183.3	10477.1	0.78107
1.03	7865.3	9335.4	0.84252
1.93	16830.2	11642.3	1.44561
1.79	16569.6	13187.5	1.25646
2.03	15773.9	10371.3	1.52092

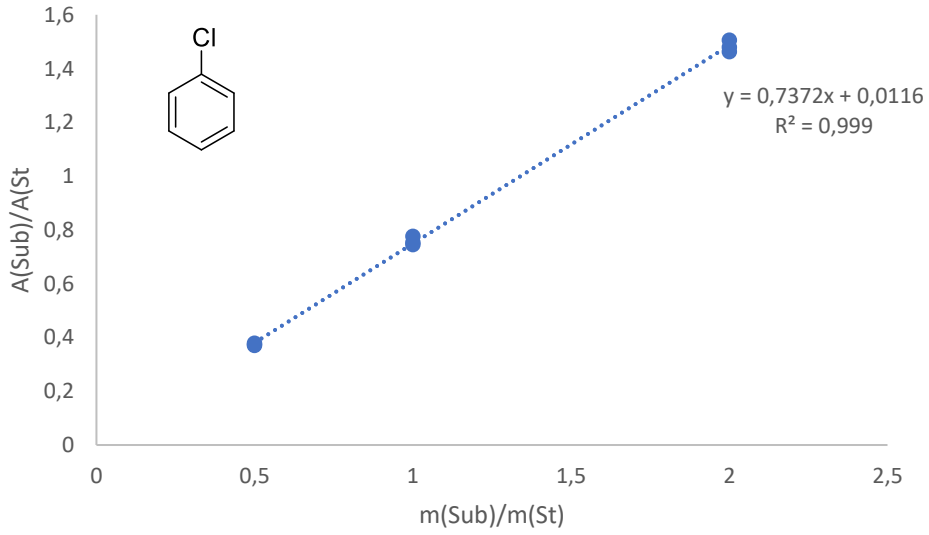

Mass ratio $\left[\frac{mg\ (Substrate)}{mg\ (Std)}\right]$	A (Substrate)	A (Std)	Area ratio $\left[\frac{A(Substrate)}{A\ (Std)}\right]$
0.50	9354.0	25297.0	0.36977
0.50	9627.0	25789.0	0.37330
0.50	8615.0	22769.0	0.37837
1.00	5206.0	6985.0	0.74531
1.00	7597.0	9787.0	0.77623
1.00	7922.0	10511.0	0.75369
2.00	15620.0	10557.0	1.47959
2.00	18607.0	12716.0	1.46327
2.00	16848.0	11190.0	1.50563

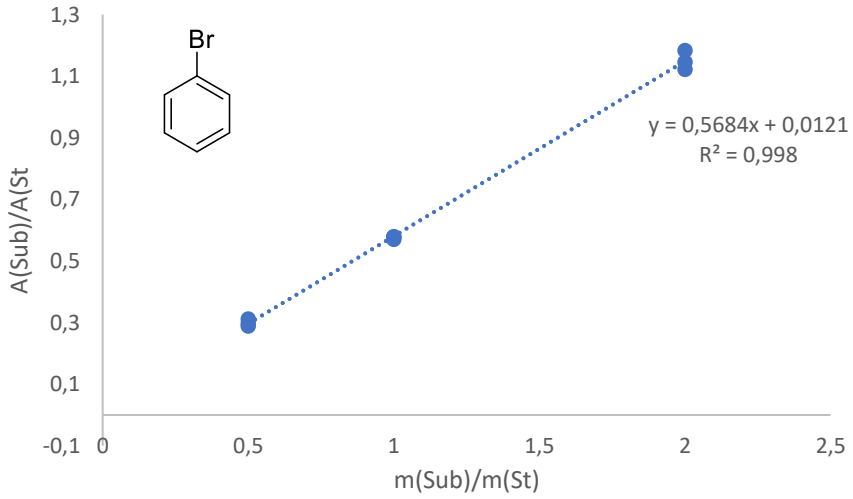

Mass ratio $\left[\frac{mg\ (Substrate)}{mg\ (Std)}\right]$	A (Substrate)	A (Std)	Area ratio $\left[\frac{A(Substrate)}{A\ (Std)}\right]$
0.50	7455.0	23918.0	0.31169
0.50	7573.0	25464.0	0.29740
0.50	5803.0	20099.0	0.28872
1.00	5984.0	10489.0	0.57050
1.00	6436.0	11113.0	0.57914
1.00	7312.0	12639.0	0.57853
2.00	12738.0	10765.0	1.18328
2.00	13517.0	11797.0	1.14580
2.00	12676.0	11295.0	1.12227

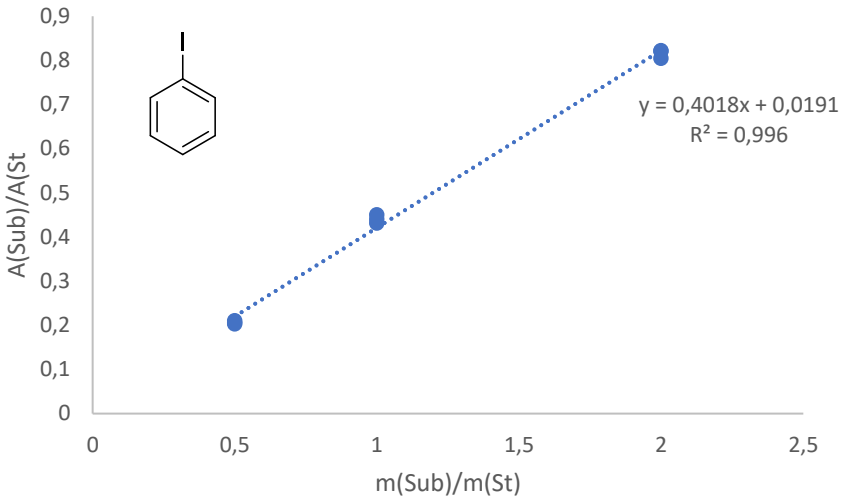

Mass ratio $\left[\frac{mg\ (Substrate)}{mg\ (Std)}\right]$	A (Substrate)	A (Std)	Area ratio $\left[\frac{A(Substrate)}{A\ (Std)}\right]$
0.50	4304.0	20879.0	0.20614
0.50	4927.0	24228.0	0.20336
0.50	4659.0	22138.0	0.21045
1.00	5472.0	12149.0	0.45041
1.00	5290.0	12250.0	0.43184
1.00	5446.0	12354.0	0.44083
2.00	10096.0	12278.0	0.82228
2.00	9326.0	11360.0	0.82095
2.00	9436.0	13017.0	0.80490

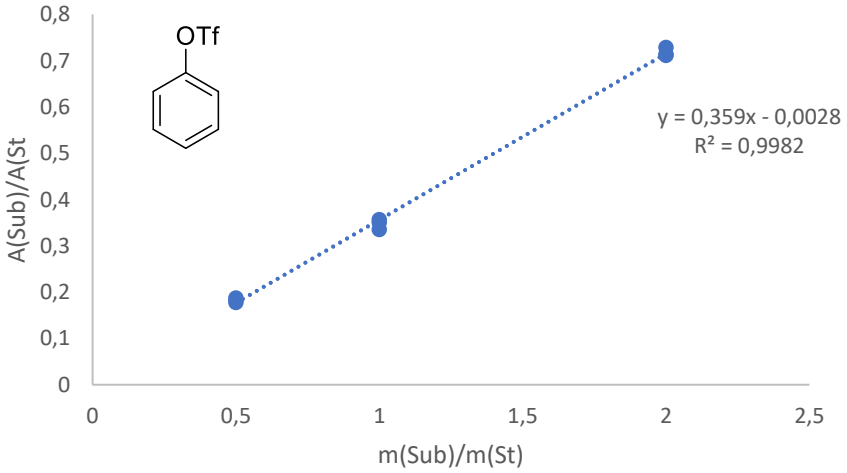

Mass ratio $\left[\frac{mg\ (Substrate)}{mg\ (Std)}\right]$	A (Substrate)	A (Std)	Area ratio $\left[\frac{A(Substrate)}{A\ (Std)}\right]$
0.50	4164.8	23377.7	0.17815
0.50	4742.3	25319.3	0.18730
0.50	4133.4	22685.3	0.18221
1.00	3901.2	11632.3	0.33538
1.00	3886.2	10895.3	0.35669
1.00	4388.4	12526.5	0.35033
2.00	8062.8	11288.5	0.71425
2.00	8029.2	11019.8	0.72862
2.00	8043.5	11304.6	0.71152

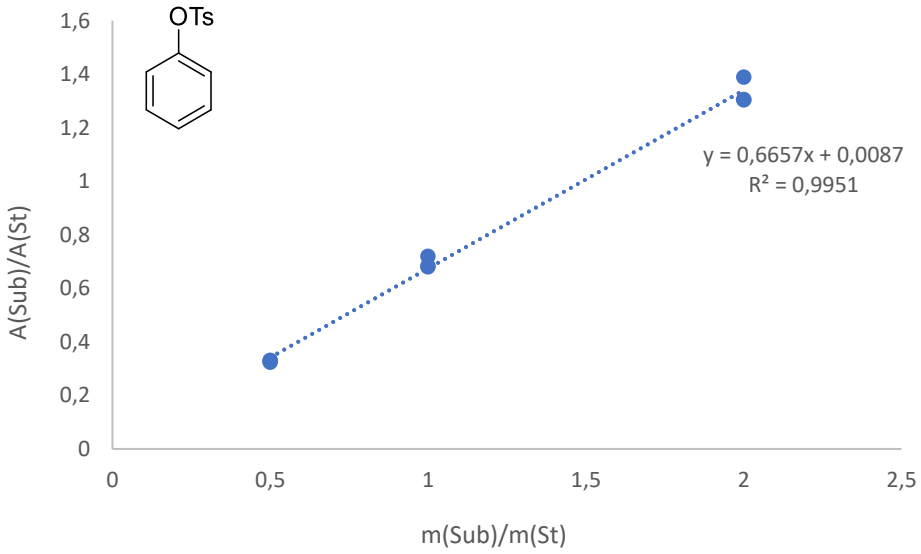

Mass ratio $\left[\frac{mg\ (Substrate)}{mg\ (Std)}\right]$	A (Substrate)	A (Std)	Area ratio $\left[\frac{A(Substrate)}{A\ (Std)}\right]$
0.5	3807.6	11738.1	0.32438
0.50	3771.8	11481.7	0.32851
0.50	3963.5	11968.7	0.33116
0.50	3875.2	5697.3	0.68018
1.00	3950.6	5780.5	0.68344
1.00	3847.5	5341.8	0.72026
1.00	7000.1	5040.4	1.38880
2.00	7446.5	5701.2	1.30613
2.00	7519.8	5763.0	1.30484

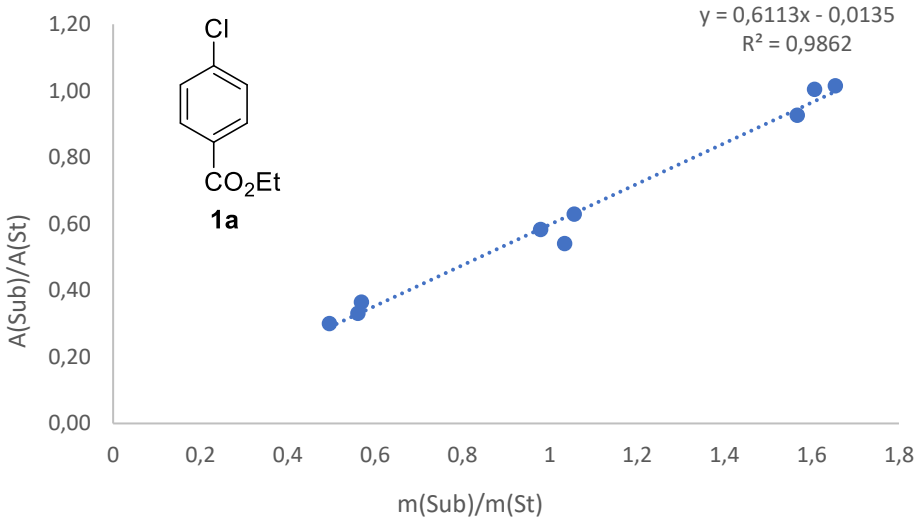

Mass ratio $\left[\frac{mg\ (Substrate)}{mg\ (Std)}\right]$	A (Substrate)	A (Std)	Area ratio $\left[\frac{A(Substrate)}{A\ (Std)}\right]$
0.49	6671.9	22176.1	0.30086
0.57	7535.6	20648.8	0.36494
0.56	8389.0	25275.9	0.33190
0.97	13711.5	23496.9	0.58355
1.06	15581.6	24742.7	0.62975
1.03	21462.4	39662.7	0.54112
1.65	12779.9	12591.4	1.01497
1.57	13370.8	14427.0	0.92679
1.61	12948.3	12884.1	1.00498

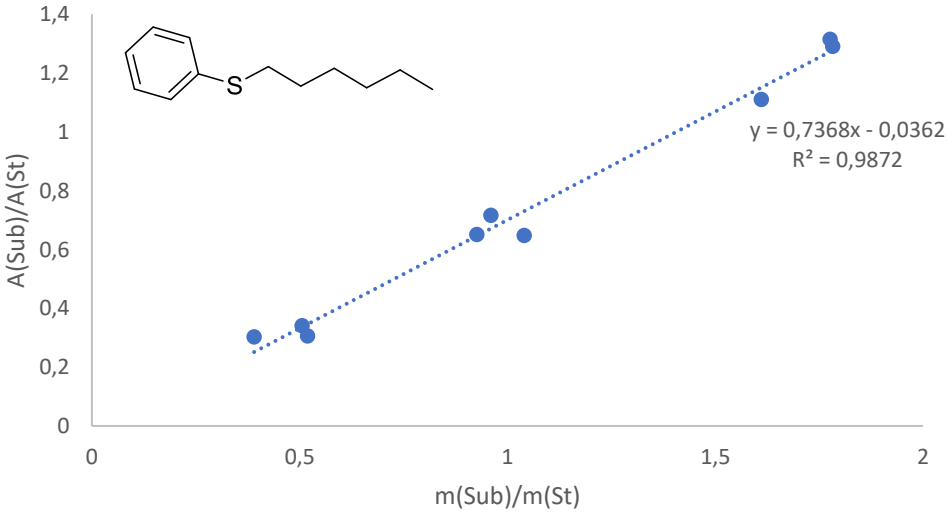

Mass ratio $\left[\frac{mg\ (Substrate)}{mg\ (Std)}\right]$	A (Substrate)	A (Std)	Area ratio $\left[\frac{A(Substrate)}{A\ (Std)}\right]$
0.39	7769.0	25616.6	0.30328
0.51	6528.8	19163.8	0.34068
0.52	6469.8	21164.9	0.30569
0.96	7232.8	10093.6	0.71657
1.04	7036.5	10870.5	0.64730
0.93	7032.9	10803.8	0.65097
1.78	13844.4	10726.0	1.29073
1.61	13505.5	12165.2	1.11017
1.78	15610.4	11868.1	1.31532

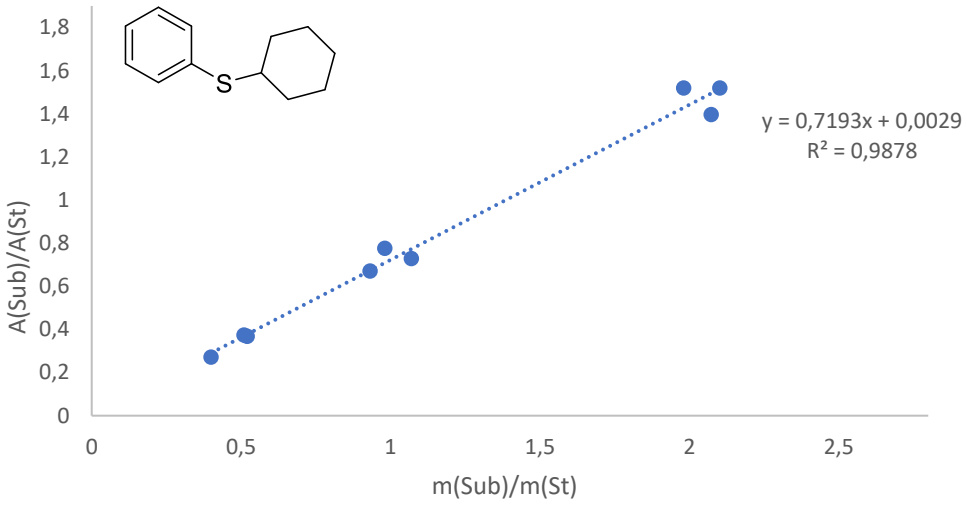

Mass ratio $\left[\frac{mg\ (Substrate)}{mg\ (Std)}\right]$	A (Substrate)	A (Std)	Area ratio $\left[\frac{A(Substrate)}{A\ (Std)}\right]$
0.40	5895.2	21634.9	0.27249
0.52	7658.4	20803.9	0.36812
0.51	7915.4	211282	0.37464
0.93	5786.7	8620.6	0.67126
0.98	8248.2	10613.5	0.77714
1.07	6410.7	8791.8	0.72917
1.98	1744.,5	11472.4	1.52021
2.10	13670.0	8993.8	1.51994
2.07	12843.8	9192.9	1.39714

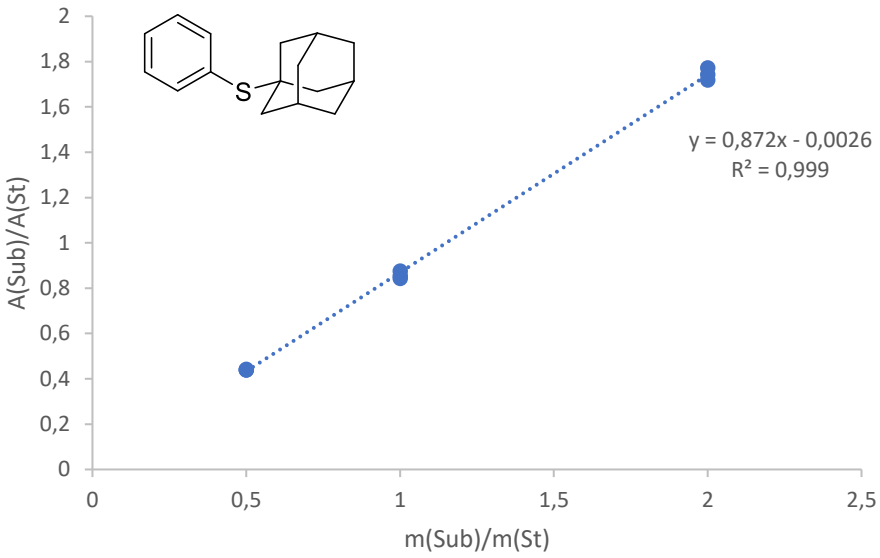

Mass ratio $\left[\frac{mg\ (Substrate)}{mg\ (Std)}\right]$	A (Substrate)	A (Std)	Area ratio $\left[\frac{A(Substrate)}{A\ (Std)}\right]$
0.50	10199.8	23172.0	0.44017
0.50	10364.2	23601.2	0.43913
0.50	9670.5	21866.0	0.44226
1.00	9733.8	11530.3	0.84419
1.00	10144.3	11858.2	0.85546
1.00	10757.7	12273.9	0.87647
2.00	19817.2	11370.5	1.74286
2.00	22510.6	13095.4	1.71897
2.00	21256.9	11988.2	1.77315

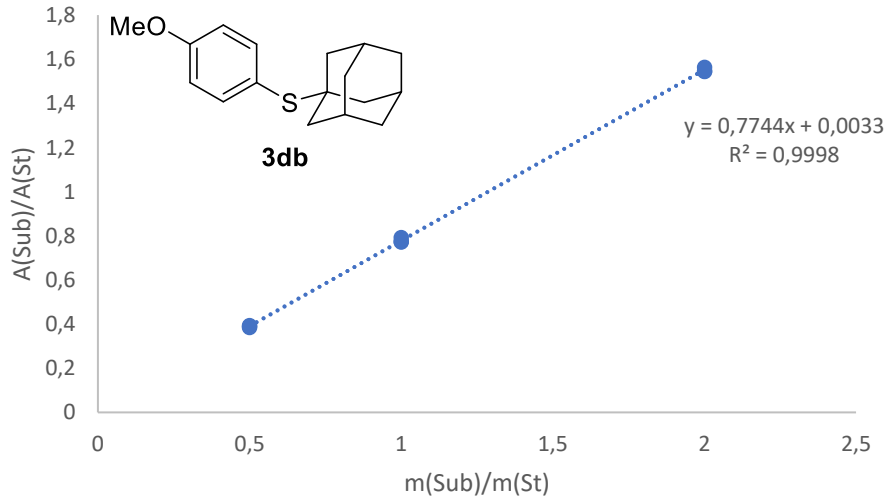

Mass ratio $\left[\frac{mg\ (Substrate)}{mg\ (Std)}\right]$	A (Substrate)	A (Std)	Area ratio $\left[\frac{A(Substrate)}{A\ (Std)}\right]$
0.50	10846.3	27564.4	0.39349
0.50	10710.2	27784.3	0.38548
0.50	10258.5	26396.0	0.38864
1.00	8823.1	11386.8	0.77485
1.00	8710.2	11280.7	0.77213
1.00	9111.9	11508.3	0.79177
2.00	17731.0	11339.8	1.56361
2.00	18921.4	12236.2	1.54635
2.00	19122.2	12382.9	1.54424

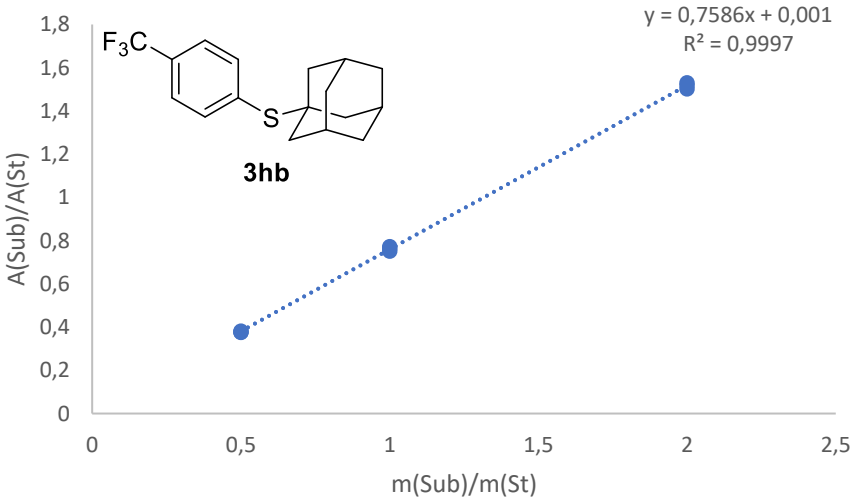

Mass ratio $\left[\frac{mg\ (Substrate)}{mg\ (Std)}\right]$	A (Substrate)	A (Std)	Area ratio $\left[\frac{A(Substrate)}{A\ (Std)}\right]$
0.50	10842.4	28751.2	0.37711
0.50	9458.4	24769.3	0.38186
0.50	9032.6	24021.1	0.37603
1.00	9881.3	13147.1	0.75160
1.00	10852.4	14200.9	0.76421
1.00	9749.9	12624.2	0.77232
2.00	19980.1	13159.1	1.51835
2.00	19309.8	12613.3	1.53091
2.00	23426.6	15590.4	1.50263

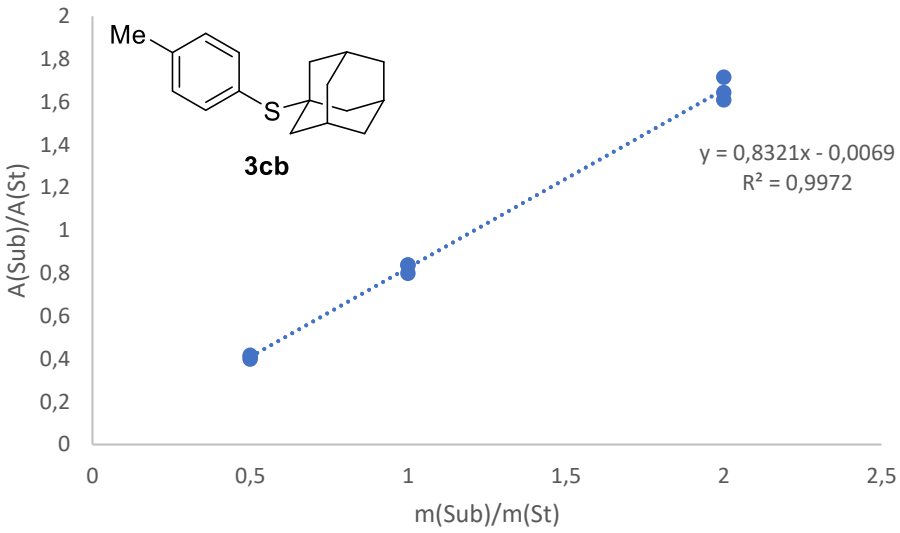

Mass ratio $\left[\frac{mg\ (Substrate)}{mg\ (Std)}\right]$	A (Substrate)	A (Std)	Area ratio $\left[\frac{A(Substrate)}{A\ (Std)}\right]$
0.50	5055.8	12380.0	0.40838
0.50	4786.9	11478.7	0.41702
0.50	4915.3	12284.3	0.40013
1.00	4835.2	6038.8	0.80069
1.00	5001.7	5965.5	0.83844
1.00	4865.8	5797.6	0.83928
2.00	9706.1	5657.0	1.71577
2.00	9917.7	6159.1	1.61025
2.00	9495.9	5773.2	1.64482

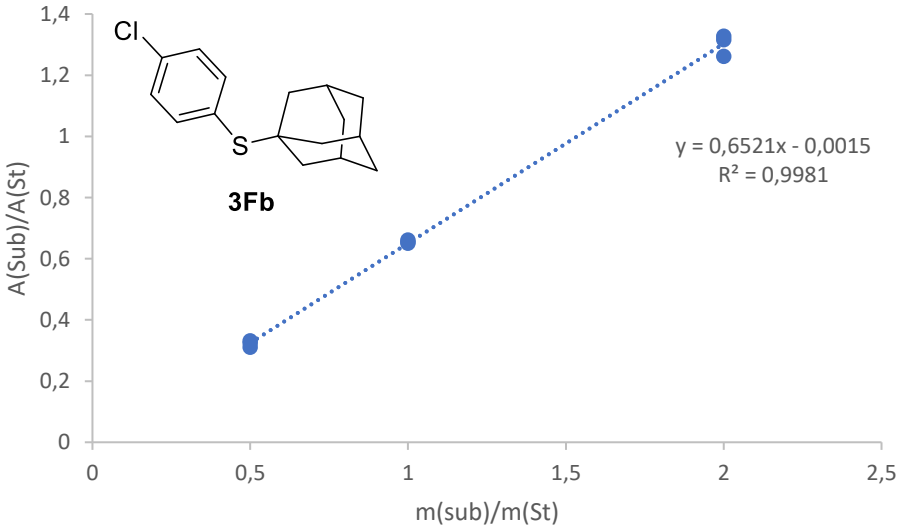

Mass ratio $\left[\frac{mg\ (Substrate)}{mg\ (Std)}\right]$	A (Substrate)	A (Std)	Area ratio $\left[\frac{A(Substrate)}{A\ (Std)}\right]$
0.50	4323.5	13347.9	0.32391
0.50	4384.1	13232.7	0.33131
0.50	4271.8	13780.1	0.31000
1.00	4333.2	6560.6	0.66049
1.00	4404.0	6775.9	0.64995
1.00	4388.3	6708.4	0.65415
2.00	8735.9	6580.1	1.32762
2.00	8623.3	6556.2	1.31529
2.00	9106.7	7222.7	1.26084

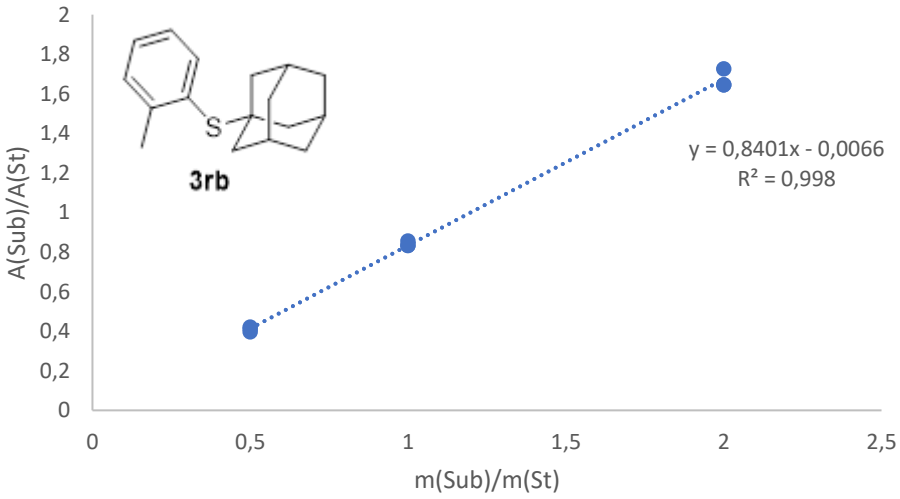

Mass ratio $\left[\frac{mg\ (Substrate)}{mg\ (Std)}\right]$	A (Substrate)	A (Std)	Area ratio $\left[\frac{A(Substrate)}{A\ (Std)}\right]$
0.50	5332.0	12967.0	0.41120
0.50	5179.9	12305.8	0.42093
0.50	4788.8	12094.9	0.39594
1.00	5355.2	6438.1	0.83180
1.00	5292.3	6187.9	0.85527
1.00	5188.8	6237.9	0.83182
2.00	10236.9	5936.0	1.72455
2.00	10067.1	6119.6	1.64506
2.00	10213.0	6207.9	1.64516

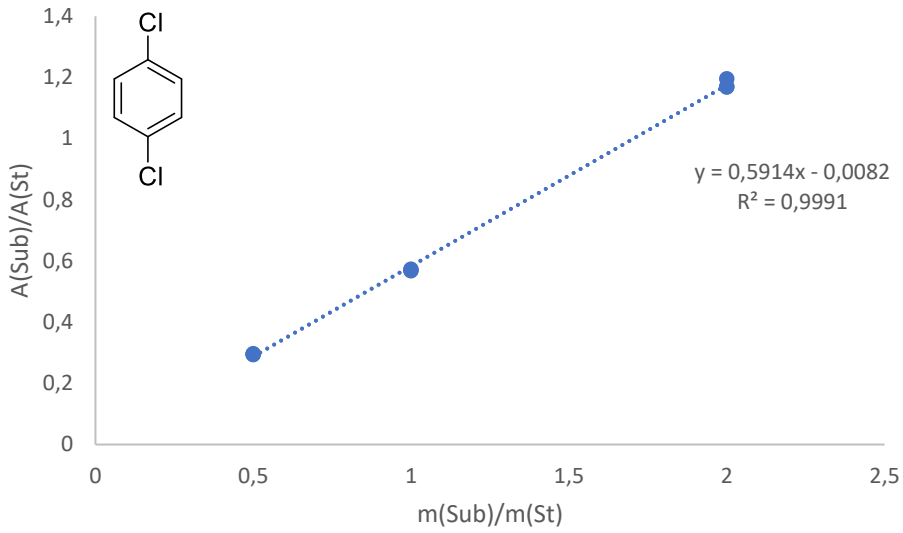

Mass ratio $\left[\frac{mg\ (Substrate)}{mg\ (Std)}\right]$	A (Substrate)	A (Std)	Area ratio $\left[\frac{A(Substrate)}{A\ (Std)}\right]$
0.50	3575.6	12095.8	0.29561
0.50	3607.2	12268.1	0.29403
0.50	3760.6	12661.5	0.29701
1.00	3369.7	5927.6	0.56848
1.00	3572.6	6222.0	0.57419
1.00	3619.8	6340.6	0.57089
2.00	6932.9	5798.0	1.19574
2.00	6790.4	5808.6	1.16903
2.00	6830.1	5831.8	1.17118

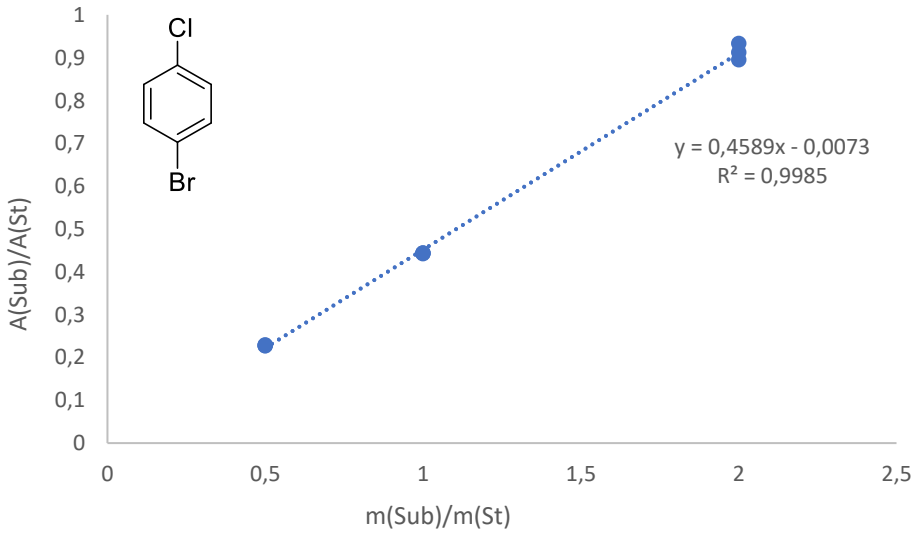

Mass ratio $\left[\frac{mg\ (Substrate)}{mg\ (Std)}\right]$	A (Substrate)	A (Std)	Area ratio $\left[\frac{A(Substrate)}{A\ (Std)}\right]$
0.50	2755.5	12119.1	0.22737
0.50	2630.5	11587.1	0.22702
0.50	2775.6	12116.2	0.22908
1.00	2950.2	6652.3	0.44349
1.00	2634.8	5959.6	0.44211
1.00	2555.7	5765.9	0.44324
2.00	5481.0	5874.3	0.93305
2.00	5533.9	6185.1	0.89471
2.00	5762.7	6318.8	0.91199

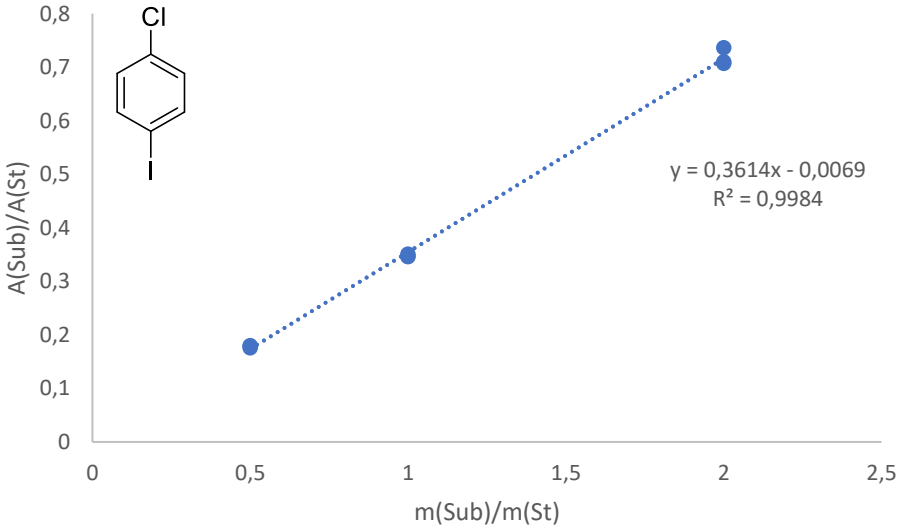

Mass ratio $\left[\frac{mg\ (Substrate)}{mg\ (Std)}\right]$	A (Substrate)	A (Std)	Area ratio $\left[\frac{A(Substrate)}{A\ (Std)}\right]$
0.50	2118.3	11840.7	0.17890
0.50	2147.0	12221.6	0.17567
0.50	2217.8	12342.5	0.17969
1.00	2112.4	6098.9	0.34636
1.00	2391.0	6895.2	0.34676
1.00	2016.5	5743.2	0.35111
2.00	4246.1	5765.8	0.73643
2.00	4316.3	6102.2	0.70734
2.00	4246.6	5977.3	0.71045

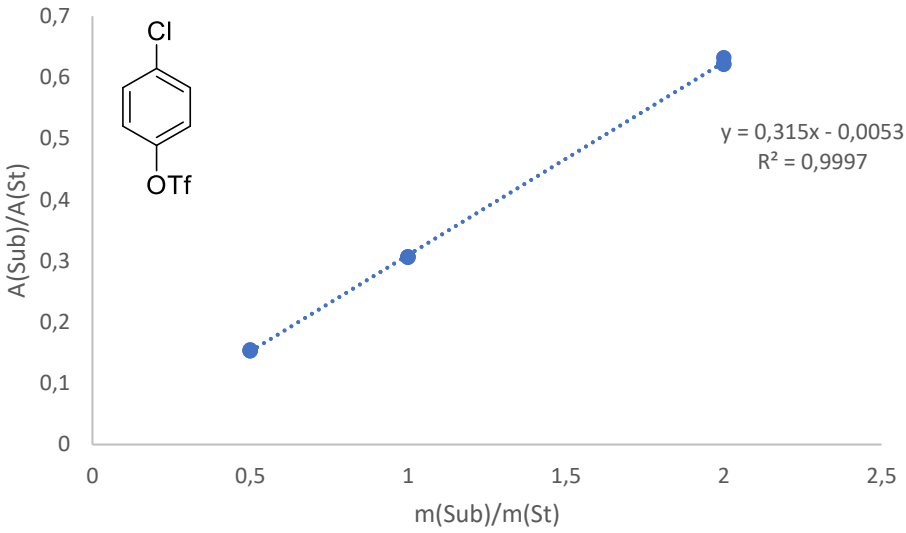

Mass ratio $\left[\frac{mg\ (Substrate)}{mg\ (Std)}\right]$	A (Substrate)	A (Std)	Area ratio $\left[\frac{A(Substrate)}{A\ (Std)}\right]$
0.50	1963.3	12790.9	0.15349
0.50	1843.9	11890.1	0.15508
0.50	1909.0	12443.8	0.15341
1.00	2165.3	7059.0	0.30674
1.00	1982.9	6451.7	0.30735
1.00	1827.1	5962.3	0.30644
2.00	3641.5	5757.0	0.63253
2.00	3663.2	5894.1	0.62150
2.00	3965.1	6369.4	0.62252

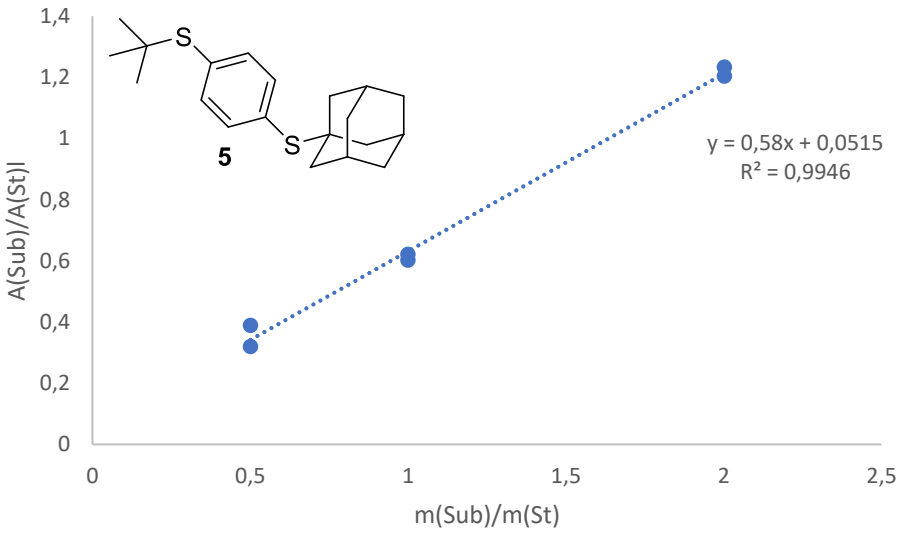

Mass ratio $\left[\frac{mg\ (Substrate)}{mg\ (Std)}\right]$	A (Substrate)	A (Std)	Area ratio $\left[\frac{A(Substrate)}{A\ (Std)}\right]$
0.50	2786.9	8711.2	0.31992
0.50	3334.6	8555.8	0.38975
1.00	3042.1	5049.4	0.60247
1.00	5517.1	8881.9	0.62116
2.00	5952.2	4943.4	1.20407
2.00	6282.7	5090.8	1.23413

9. References

1. Gehrtz, P. H.; Geiger, V.; Schmidt, T.; Srsan, L.; Fleischer, I., Cross-Coupling of Chloro(hetero)arenes with Thiolates Employing a Ni(0)-Precatalyst. *Org. Lett.* **2019,** *21* (1), 50-55.
2. Gottlieb, H. E.; Kotlyar, V.; Nudelman, A., NMR chemical shifts of common laboratory solvents as trace impurities. *J. Org. Chem.* **1997,** *62* (21), 7512-7515.
3. Neese, F., Software Update: the ORCA Program System, Version 4.0. *Wiley. Interdiscip. Rev. Comput. Mol. Sci.* **2018,** *8* (1), e1327.
4. Becke, A. D., Density-Functional Thermochemistry. III. The Role of Exact Exchange. *J. Chem. Phys.* **1993,** *98* (7), 5648-5652.
5. Stephens, P. J.; Devlin, F. J.; Chabalowski, C. F.; Frisch, M. J., Ab Initio Calculation of Vibrational Absorption and Circular Dichroism Spectra Using Density Functional Force Fields. *J. Phys. Chem.* **1994,** *98* (45), 11623-11627.
6. Weigend, F.; Ahlrichs, R., Balanced Basis Sets of Split Valence, Triple Zeta Valence and Quadruple Zeta Valence Quality for H to Rn: Design and Assessment of Accuracy. *Phys. Chem. Chem. Phys.* **2005,** *7* (18), 3297-3305.
7. Grimme, S., Supramolecular Binding Thermodynamics by Dispersion-Corrected Density Functional Theory. *Chem. Eur. J.* **2012,** *18* (32), 9955-9964.
8. Zhao, Y.; Truhlar, D. G., A New Local Density Functional for Main-Group Thermochemistry, Transition Metal Bonding, Thermochemical Kinetics, and Noncovalent Interactions. *J. Chem. Phys.* **2006,** *125* (19), 194101.
9. Marenich, A. V.; Cramer, C. J.; Truhlar, D. G., Universal Solvation Model Based on Solute Electron Density and on a Continuum Model of the Solvent Defined by the Bulk Dielectric Constant and Atomic Surface Tensions. *J. Phys. Chem. B* **2009,** *113* (18), 6378-6396.
10. Kranenburg, M.; van der Burgt, Y. E. M.; Kamer, P. C. J.; van Leeuwen, P. W. N. M.; Goubitz, K.; Fraanje, J., New Diphosphine Ligands Based on Heterocyclic Aromatics Inducing Very High Regioselectivity in Rhodium-Catalyzed Hydroformylation: Effect of the Bite Angle. *Organometallics* **1995,** *14* (6), 3081-3089.
11. Sergeev, A. G.; Artamkina, G. A.; Beletskaya, I. P., Variation of Xantphos-Based Ligands in the Palladium-Catalyzed Reaction of Aryl Halides with Ureas. *Russ. J. Org. Chem.* **2003,** *39* (12), 1741-1752.
12. Shaw, L.; Somisara, D. M. U. K.; How, R. C.; Westwood, N. J.; Bruijnincx, P. C. A.; Weckhuysen, B. M.; Kamer, P. C. J., Electronic and bite angle effects in catalytic C–O bond cleavage of a lignin model compound using ruthenium Xantphos complexes. *Catal. Sci. Technol.* **2017,** *7* (3), 619-626.
13. The coupling constants could not be determined due to complex C-F and C-P couplings and low intensity of signals.
14. Standley, E. A.; Smith, S. J.; Müller, P.; Jamison, T. F., A Broadly Applicable Strategy for Entry into Homogeneous Nickel(0) Catalysts from Air-Stable Nickel(II) Complexes. *Organometallics* **2014,** *33* (8), 2012-2018.
15. Goossen, L. J.; Rodríguez, N.; Linder, C., Decarboxylative Biaryl Synthesis from Aromatic Carboxylates and Aryl Triflates. *J. Am. Chem. Soc.* **2008,** *130* (46), 15248-15249.
16. Ogata, T.; Hartwig, J. F., Palladium-Catalyzed Amination of Aryl and Heteroaryl Tosylates at Room Temperature. *J. Am. Chem. Soc.* **2008,** *130* (42), 13848-13849.
17. Hu, J.; Lu, Y.; Li, Y.; Zhou, J., Highly active catalysts of bisphosphine oxides for asymmetric Heck reaction. *Chem. Commun.* **2013,** *49* (82), 9425-9427.
18. Cervi, A.; Vo, Y.; Chai, C. L. L.; Banwell, M. G.; Lan, P.; Willis, A. C., Gold(I)-Catalyzed Intramolecular Hydroarylation of Phenol-Derived Propiolates and Certain Related Ethers as a Route to Selectively Functionalized Coumarins and 2H-Chromenes. *J. Org. Chem.* **2021,** *86* (1), 178-198.
19. Dogga, B.; Kumar, C. S. A.; Joseph, J. T., Palladium-Catalyzed Reductive Carbonylation of (Hetero) Aryl Halides and Triflates Using Cobalt Carbonyl as CO Source. *Eur. J. Org. Chem.* **2021,** *2021* (2), 309-313.

20. Sämann, C.; Dhayalan, V.; Schreiner, P. R.; Knochel, P., Synthesis of Substituted Adamantylzinc Reagents Using a Mg-Insertion in the Presence of ZnCl2 and Further Functionalizations. *Organic Letters* **2014,** *16* (9), 2418-2421.
21. Wang, P. F.; Wang, X. Q.; Dai, J. J.; Feng, Y. S.; Xu, H. J., Silver-mediated decarboxylative C-S cross-coupling of aliphatic carboxylic acids under mild conditions. *Org Lett* **2014,** *16* (17), 4586-9.
22. Guo, S.-r.; He, W.-m.; Xiang, J.-n.; Yuan, Y.-q., Palladium-catalyzed thiolation of alkanes and ethers with arylsulfonyl hydrazides. *Chem. Commun.* **2014,** *50* (62), 8578-8581.
23. Delcaillau, T.; Bismuto, A.; Lian, Z.; Morandi, B., Nickel-Catalyzed Inter- and Intramolecular Aryl Thioether Metathesis by Reversible Arylation. *Angew. Chem. Int. Ed.* **2020,** *59,* 2110-2114.
24. Maurin, J. K.; Lasek, W.; Górska, A.; Świtaj, T.; Jakubowska, A. B.; Kazimierczuk, Z., Adamantylsulfanyl- and N-Adamantylcarboxamido-Derivatives of Heterocycles and Phenoles: Synthesis, Crystal Structure, Tumor Necrosis Factor-α Production-Enhancing Properties, and Theoretical Considerations. *Chem. Biodiv.* **2004,** *1* (10), 1498-1512.
25. Chen, C.-K.; Chen, Y.-W.; Lin, C.-H.; Lin, H.-P.; Lee, C.-F., Synthesis of CuO on mesoporous silica and its applications for coupling reactions of thiols with aryl iodides. *Chem. Commun.* **2010,** *46* (2), 282-284.
26. Mixture of isomers is not specified according to supplier.
27. Gehrtz, P. H.; Kathe, P.; Fleischer, I., Nickel-Catalyzed Coupling of Arylzinc Halides with Thioesters. *Chem. Eur. J.* **2018,** *24* (35), 8774-8778.
28. Hansch, C.; Leo, A.; Taft, R. W., A survey of Hammett substituent constants and resonance and field parameters. *Chem. Rev.* **1991,** *91* (2), 165-195.
29. Klingensmith, L. M.; Strieter, E. R.; Barder, T. E.; Buchwald, S. L., New Insights into Xantphos/Pd-Catalyzed C–N Bond Forming Reactions: A Structural and Kinetic Study. *Organometallics* **2006,** *25* (1), 82-91.
30. Goertz, W.; Keim, W.; Vogt, D.; Englert, U.; D. K. Boele, M.; A. van der Veen, L.; C. J. Kamer, P.; W. N. M. van Leeuwen, P., Electronic effects in the nickel-catalysed hydrocyanation of styrene applying chelating phosphorus ligands with large bite angles‡. *J. Chem. Soc., Dalton Trans.* **1998,** (18), 2981-2988.

OL Organic Letters

pubs.acs.org/OrgLett

Letter

Nickel Catalyzed Cross-Coupling of Aryl and Alkenyl Triflates with Alkyl Thiols

Regina M. Oechsner,[†] Ivo H. Lindenmaier,[†] and Ivana Fleischer*

Cite This: *Org. Lett.* 2023, 25, 1655−1660

Read Online

ACCESS | Metrics & More | Article Recommendations | Supporting Information

ABSTRACT: We report a nickel catalyzed C−S cross-coupling of aryl and alkenyl triflates with alkyl thiols. A variety of the corresponding thioethers were synthesized using an air-stable nickel precatalyst under mild reaction conditions with short reaction times. A broad substrate scope, including pharmaceutically relevant compounds, could be demonstrated.

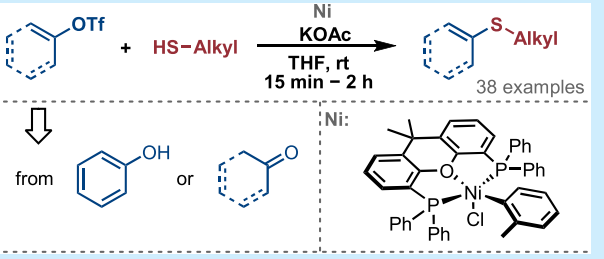

Thioethers are common motifs in agrochemicals,[1] materials,[2] and pharmaceutical compounds.[3] They can be conveniently synthesized via a variety of transformations.[4] One of the most prominent and versatile methods is the metal-catalyzed coupling of thiols with aryl and alkenyl (pseudo)-halides, also referred to as Migita-coupling.[5] Catalysts for this transformation are often based on palladium, but nickel as a low-cost and abundant metal has developed into an attractive alternative. In this case, aryl bromides and iodides[6] are typically employed as electrophiles, but recently the less reactive and more abundant aryl chlorides could be coupled.[7] In comparison to aryl (pseudo)halides, alkenyl electrophiles have been much less systematically explored, regardless of the employed catalyst.[8]

One of the disadvantages of halides is the synthesis of noncommercially available substrates, which may require multiple steps[9] and forcing reaction conditions[10] restricting the functional group tolerance. In contrast, aryl and alkenyl triflates, representatives of pseudohalides, can easily be synthesized in a simple one-step procedure from phenols[11] and ketones,[12] rendering them excellent alternative electrophiles. Phenols and ketones are both abundant, available as well as low-cost, and thus attractive building blocks, especially for more complex pharmaceutically active compounds.[13] In particular alkenyl halides, for which even simple compounds are not widely commercially available, triflates are an excellent alternative. This point is supported by a variety of publications reporting the transformation of alkenyl triflates to the corresponding alkenyl halides,[14] showcasing the synthetic potential and advantages of triflates.

Not only their synthetic accessibility but also the reactivity of triflates in coupling reactions is appealing. In C−S couplings, palladium is the most represented catalyst.[15] The reported methods commonly show only a limited scope of triflates (1−6 examples), utilize bidentate ligands such as Xantphos ((9,9-dimethyl-9*H*-xanthene-4,5-diyl)bis(diphenylphosphane), and require elevated temperatures (80−140 °C) to couple aryl triflates with mainly aryl thiols (Scheme 1a).

Nickel catalyzed methods remain rare for aryl sulfonates in general, with limited examples for the coupling of aryl thiols with aryl tosylates[7d] and mesylates,[16] but no examples for aryl triflates. Regarding alkenyl electrophiles, only a few reports were dedicated to the palladium catalyzed C−S coupling of tosylates[8f] and triflates,[8e] while nickel catalyzed couplings are even more underrepresented. The most recent example is the electrochemically promoted coupling of alkenyl triflates with thiols employing air-sensitive $Ni(cod)_2$ (15 mol %) reported by Pan and co-workers (Scheme 1b).[8j] They demonstrated an extensive substrate scope for aryl thiols, but only a limited scope for alkyl thiols (3 examples) providing moderate yields.

The inefficient coupling of alkyl thiols, especially tertiary ones, is a typical limitation of many C−S coupling methodologies. Our group closed this gap in a study on cross-coupling of aryl chlorides with tertiary alkyl thiols.[7e] A promising reactivity of triflates was observed in electrophile competition experiments, which led us to expand the scope of the methodology to aryl and alkenyl triflates (Scheme 1c).[17] To the best of our knowledge this is the first nickel catalyzed coupling of aryl as well as alkenyl triflates with challenging tertiary alkyl thiols showing a wide scope as well as functional group tolerance under mild conditions without the need for high temperatures, additives, reducing agents, reactive organometallic bases, or electrochemistry.

Received: January 20, 2023
Published: March 6, 2023

Scheme 1. Literature Examples for the Coupling of Triflates[8j,15c] and Our Objective

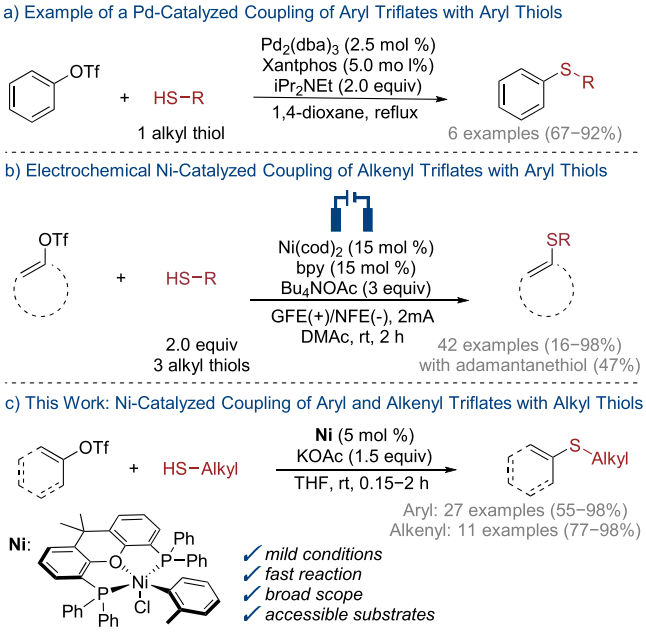

The mild reaction conditions (room temperature) and the catalytic system consisting of (Xantphos)Ni(*o*-tolyl)Cl (**Ni**)[18] as an air-stable precatalyst,[19] and KOAc as base from our previous work could directly be employed for the coupling of triflates. The substrate scope and functional group tolerance were explored using the sterically challenging adamantanethiol as the model nucleophile. First, various electron-neutral, -rich, and -deficient aryl triflates could be coupled in good to excellent yields (Scheme 2). Thioether **3aa** was obtained in excellent yield from PhOTf and in slightly diminished yields from PhCl, PhBr, and PhI, whereas less reactive pseudo halides such as tosylates and mesylates provided only low to moderate yields under standard conditions. Functional groups like nitrile, ester, trifluoromethyl, methoxy, and amide were tolerated, and thioethers **3ca**–**ga** were furnished in excellent yield (89–97%). Electrophiles containing heterocyclic moieties, often present in biologically active compounds for pharmaceutical or agrochemical applications, like pyridine, dioxole, or 4-methyl-2*H*-chromen-2-one, yielded the corresponding aryl thioethers **3ia**–**3ka** in good yields. In contrast to using aryl chlorides as substrates, where sterically hindered electrophiles showed low reactivity, *ortho*-methylsubstituted thioether **3la** and the 1-naphthyl-based product **3ma** were obtained via the coupling of aryl triflates in excellent yields.

Additionally, high chemoselectivity was observed for bis-electrophiles with chloro and tosyloxy groups providing the monocoupled products via a selective C−OTf functionalization in the presence of a C−Cl bond **3na** and in the presence of a C−OTs bond **3oa** in excellent yields. Dithioether **3pa** was obtained from the corresponding ditriflate.

Moreover, the potential of the methodology for late stage sulfenylation of triflates synthesized from more complex biorelevant phenols was demonstrated on two examples.

Scheme 2. Substrate Scope with Respect to Aryl Triflates[a]

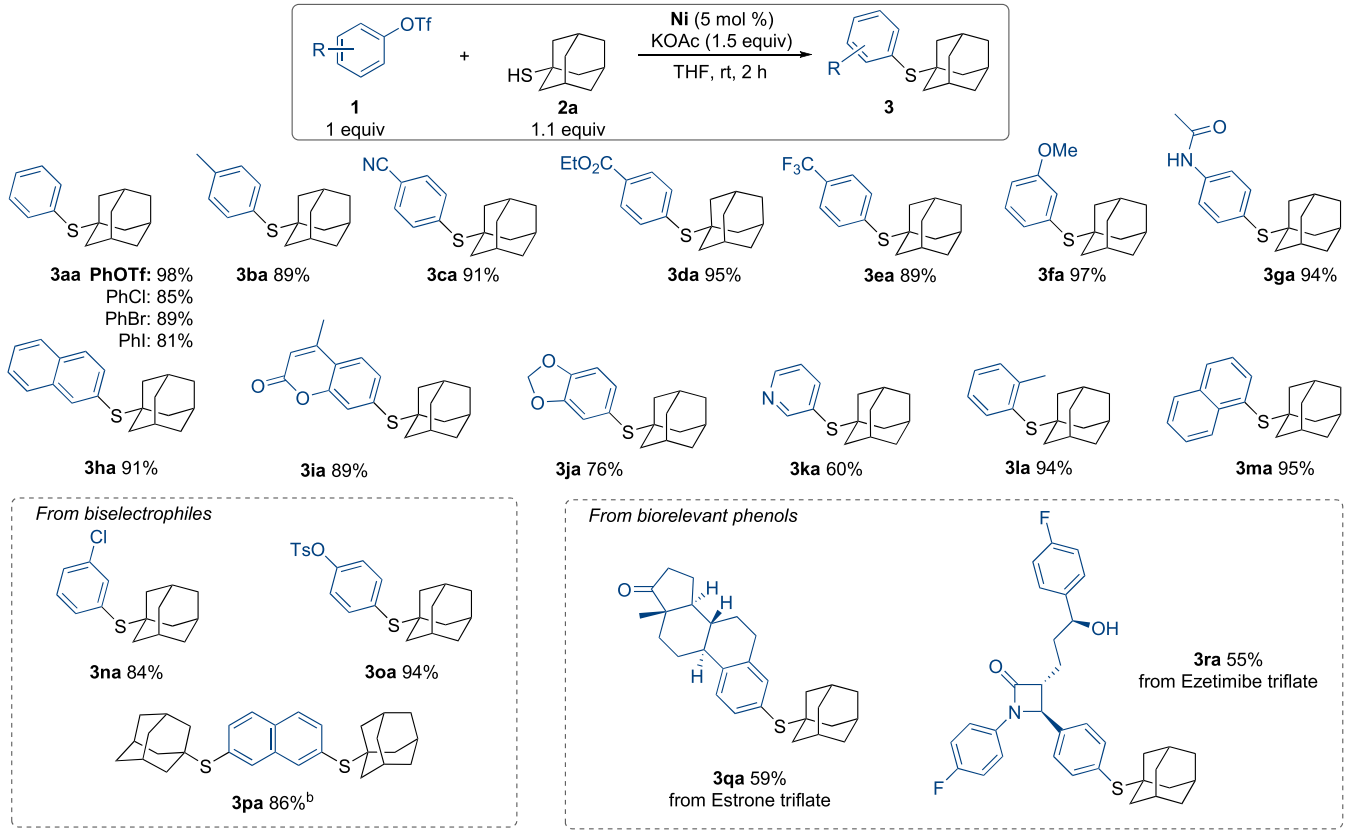

[a]Standard reaction conditions: **1** (1.0 or 0.5 mmol), **2a** (1.1 equiv), KOAc (1.5 equiv), **Ni** (5 mol %), THF (3 mL), rt, 2 h. Yields of isolated products. [b]With 2 equiv of **2a**.

https://doi.org/10.1021/acs.orglett.3c00218
Org. Lett. 2023, 25, 1655−1660

Scheme 3. Substrate Scope with Respect to Alkyl Thiols[a]

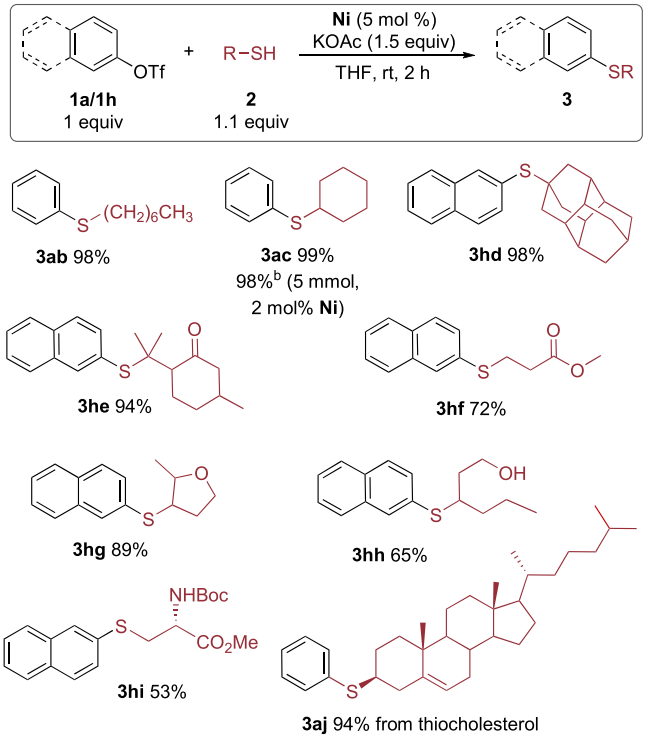

[a]Standard reaction conditions: **1a**/**1h** (1.0 or 0.5 mmol), **2** (1.1 equiv), KOAc (1.5 equiv), **Ni** (5 mol %), THF (3 mL), rt, 2 h. Yields of isolated products. [b]**1a** (5 mmol), **2c** (5.5 mmol), **Ni** (2 mol %).

Electrophiles derived from Estrone **1q** and Ezetimibe **1r** were successfully coupled and furnished the corresponding thioethers in 59% and 55% yields.

Then a variety of primary, secondary, and tertiary thiols were coupled (Scheme 3). Alkyl thiols, including the sterically challenging diadamantanethiol **2d**,[20] as well as thiols with functional groups such as ether, ester, and ketone were coupled in good to excellent yields (**3ab**−**3hg**, 72−99%). Selective C−S coupling provided **3hh** in 65% yield in the presence of a free hydroxyl group and **3hi** in 53% yield in the presence of a protected cysteine. Thiocholesterol (**2j**), as another representative of bioactive thiols, could be coupled in 94% yield. In comparison, the related coupling with aryl chloride furnished 72% yield, showcasing the superior performance of triflates. Upscaling the reaction to 5 mmol in the case of **3ac**, while decreasing the catalyst loading to 2 mol % highlights the applicability of the low-cost catalytic system on a larger scale.

Next, the coupling of alkenyl triflates with 1-adamantanethiol (**2a**) as the model substrate was demonstrated (Scheme 4). The reaction products, alkenyl thioethers, are valuable synthetic intermediates and often present in biorelevant compounds.[21] Various cyclic six-membered alkenyl moieties, including heterocycles, were coupled yielding the corresponding thioethers **5aa**−**5da** in 74−86% yields. The ester and amide functionalities in **5ba** and **5ca** were tolerated. Similar results were obtained for triflates with a fused benzene ring, such as 3,4-dihydronaphthalenyl triflates **5ea**, **5fa** and 2*H*-chromene derivative **5ga**. Moreover, the five- and seven-membered cycloalkenyl thioethers **5ha** and **5ia** as well as the acyclic compound **5ja** could be synthesized in excellent yields. The successful coupling of a

Scheme 4. Coupling of Alkenyl Triflates with 1-Adamantanethiol[a]

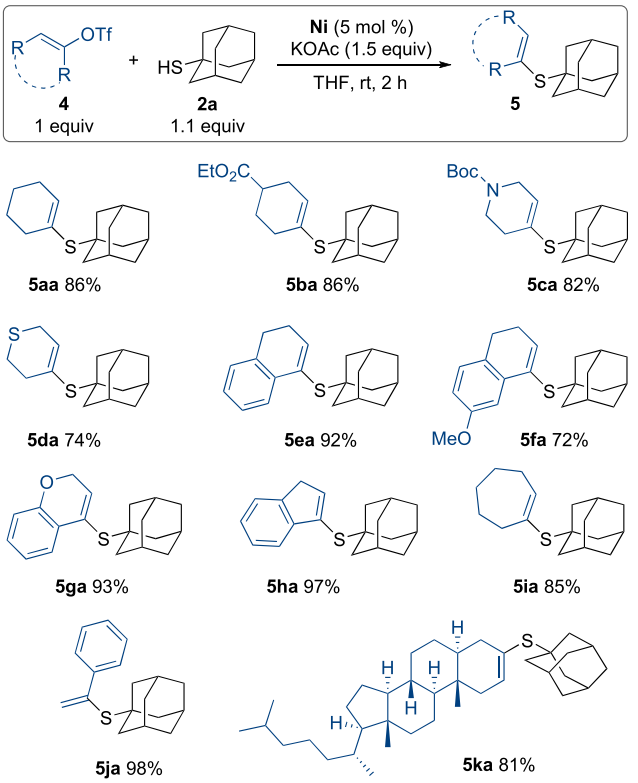

[a]Standard reaction conditions: **4** (1.0 or 0.5 mmol) **2a** (1.1 equiv), KOAc (1.5 equiv), **Ni** (5 mol %), THF (3 mL), rt, 2 h. Yields of isolated products.

Scheme 5. Postulated Catalytic Cycle and Precatalyst Activation

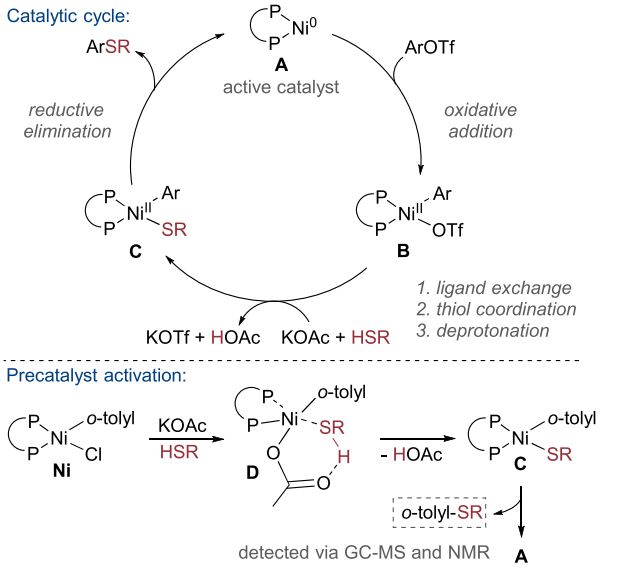

cholestane-3-one derived triflate **4k** highlights the possibility to convert more complex biorelevant structures.

We showed in our previous work on the sulfenylation of aryl chlorides that the reaction most likely proceeds through a Ni(0)/Ni(II) mechanism and acetate-assisted deprotonation of thiols, which is also plausible for the reaction of triflates (Scheme

https://doi.org/10.1021/acs.orglett.3c00218
Org. Lett. 2023, 25, 1655−1660

5).[17] The activation of the precatalyst, which is structurally related to the product of the oxidative addition, occurs via the same steps as the catalytic reaction (coordination of thiol, deprotonation, and reductive elimination of the thioether).

Subsequently, the reaction profiles of different electrophiles were compared (Scheme 6). An increase of the induction period

Scheme 6. Reaction Progress of Different Electrophiles

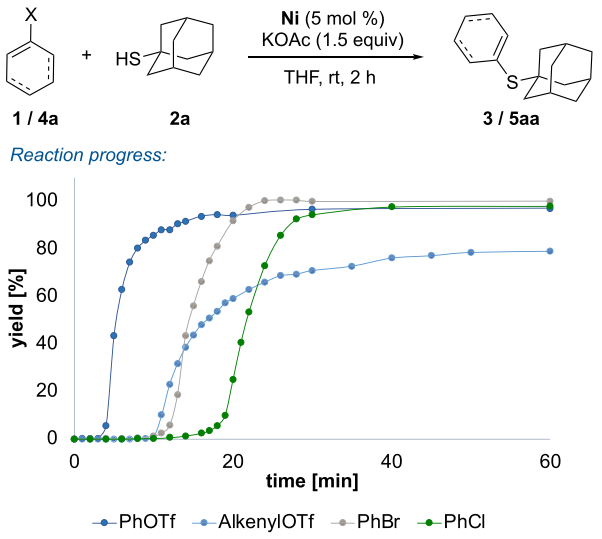

from PhOTf < AlkenylOTf ~ PhBr < PhCl and a decrease of the reaction rate from PhOTf > PhBr > PhCl > AlkenylOTf could be observed. The kinetic curves for the aryl electrophiles (PhOTf, PhBr, PhCl) are similar and identify PhOTf as the most reactive with the shortest induction period and highest reaction rate. This indicates a fast catalyst activation as well as catalysis, which might be explained by a more facile oxidative addition of aryl triflates. AlkenylOTf has a slightly different reaction profile with a lower reaction rate and longer induction period compared to the aryl counterpart. The current theory for the superiority of aryl triflates is an easier oxidative addition, facilitated by the initial π-coordination of the electrophile to Ni(0), which is stronger for the aromatic moiety. This is supported by DFT computations from our work with aryl chlorides.[7e]

In summary, we developed a mild and convenient, as well as scalable method for the nickel catalyzed C−S cross-coupling of aryl and alkenyl triflates with alkyl thiols employing the air stable and low-cost precatalyst (Xantphos)Ni(*o*-tolyl)Cl and KOAc as base at room temperature in THF for 15 min to 2 h. The method is characterized by good chemoselectivity and functional group tolerance, which was demonstrated on numerous substrates, including pharmaceutically relevant examples.

■ ASSOCIATED CONTENT

Data Availability Statement

The data underlying this study are available in the published article and its Supporting Information.

Supporting Information

The Supporting Information is available free of charge at https://pubs.acs.org/doi/10.1021/acs.orglett.3c00218.

General procedures, analytical data, and NMR spectra (PDF)

■ AUTHOR INFORMATION

Corresponding Author

Ivana Fleischer − *Institute of Organic Chemistry, Faculty of Science, Eberhard Karls Universität Tübingen, 72076 Tübingen, Germany;* orcid.org/0000-0002-2609-6536; Email: ivana.fleischer@uni-tuebingen.de

Authors

Regina M. Oechsner − *Institute of Organic Chemistry, Faculty of Science, Eberhard Karls Universität Tübingen, 72076 Tübingen, Germany*

Ivo H. Lindenmaier − *Institute of Organic Chemistry, Faculty of Science, Eberhard Karls Universität Tübingen, 72076 Tübingen, Germany*

Complete contact information is available at: https://pubs.acs.org/10.1021/acs.orglett.3c00218

Author Contributions

†R.M.O. and I.H.L. contributed equally.

Funding

This work was supported by the University of Tübingen and DFG (Deutsche Forschungsgemeinschaft).

Notes

The authors declare no competing financial interest.

■ ACKNOWLEDGMENTS

We thank Prof. Andrey Fokin and Prof. Peter Schreiner (both University of Gießen, Germany) for providing thiol **2d**. We thank the analytics department of the University of Tübingen for their excellent work. The financial support from the University of Tübingen and DFG (Grant FL 878/9-1) is gratefully acknowledged.

■ REFERENCES

(1) Hilton, H. W.; Nomura, N. S.; Yauger, W. L.; Kameda, S. S. Absorption, translocation, and metabolism of metribuzin (BAY-94337) in sugarcane. *J. Agric. Food. Chem.* **1974**, *22*, 578−582.

(2) Hill, H. W., Jr; Brady, D. G. Properties, environmental stability, and molding characteristics of polyphenylene sulfide. *Polym. Eng. Sci.* **1976**, *16*, 831−835.

(3) Scott, K. A.; Njardarson, J. T. Analysis of US FDA-Approved Drugs Containing Sulfur Atoms. *Top. Curr. Chem.* **2018**, *376*, 5.

(4) Geiger, V. J.; Oechsner, R. M.; Gehrtz, P. H.; Fleischer, I. Recent Metal-Catalyzed Methods for Thioether Synthesis. *Synthesis* **2022**, *54*, 5139−5167.

(5) Kosugi, M.; Shimizu, T.; Migita, T. Reactions of aryl halides with thiolate anions in the presence of catalytic amounts of tetrakis-(triphenylphosphine)palladium. Preparation of aryl sulfides. *Chem. Lett.* **1978**, *7*, 13−14.

(6) (a) Takagi, K. Nickel(0)-catalyzed Synthesis of Diaryl Sulfides from Aryl Halides and Aromatic Thiols. *Chem. Lett.* **1987**, *16*, 2221−2224. (b) Zhang, Y.; Ngeow, K. C.; Ying, J. Y. The First N-Heterocyclic Carbene-Based Nickel Catalyst for C−S Coupling. *Org. Lett.* **2007**, *9*, 3495−3498. (c) Iglesias, M. J.; Prieto, A.; Nicasio, M. C. Well-Defined Allylnickel Chloride/N-Heterocyclic Carbene [(NHC)Ni(allyl)Cl] Complexes as Highly Active Precatalysts for CN and CS Cross-Coupling Reactions. *Adv. Synth. Catal.* **2010**, *352*, 1949−1954. (d) Martin, A. R.; Nelson, D. J.; Meiries, S.; Slawin, A. M. Z.; Nolan, S. P. Efficient C−N and C−S Bond Formation Using the Highly Active [Ni(allyl)Cl(IPr*OMe)] Precatalyst. *Eur. J. Org. Chem.* **2014**, *2014*, 3127−3131. (e) Cristau, H. J.; Chabaud, B.; Chêne, A.; Christol, H. Synthesis of Diaryl Sulfides by Nickel(II)-Catalyzed Arylation of Arenethiolates. *Synthesis* **1981**, *1981*, 892−894. (f) Talukder, M. M.;

Miller, J. T.; Cue, J. M. O.; Udamulle, C. M.; Bhadran, A.; Biewer, M. C.; Stefan, M. C. Mono- and Dinuclear α-Diimine Nickel(II) and Palladium(II) Complexes in C−S Cross-Coupling. *Organometallics* **2021**, *40*, 83−94. (g) Yu, T. Y.; Pang, H.; Cao, Y.; Gallou, F.; Lipshutz, B. H. Safe, Scalable, Inexpensive, and Mild Nickel-Catalyzed Migita-Like C-S Cross-Couplings in Recyclable Water. *Angew. Chem., Int. Ed.* **2021**, *60*, 3708−3713. (h) Liu, D.; Ma, H.-X.; Fang, P.; Mei, T.-S. Nickel-Catalyzed Thiolation of Aryl Halides and Heteroaryl Halides through Electrochemistry. *Angew. Chem., Int. Ed.* **2019**, *58*, 5033−5037.

(7) (a) Jones, K. D.; Power, D. J.; Bierer, D.; Gericke, K. M.; Stewart, S. G. Nickel Phosphite/Phosphine-Catalyzed C−S Cross-Coupling of Aryl Chlorides and Thiols. *Org. Lett.* **2018**, *20*, 208−211. (b) Yin, G.; Kalvet, I.; Englert, U.; Schoenebeck, F. Fundamental Studies and Development of Nickel-Catalyzed Trifluoromethylthiolation of Aryl Chlorides: Active Catalytic Species and Key Roles of Ligand and Traceless MeCN Additive Revealed. *J. Am. Chem. Soc.* **2015**, *137*, 4164−4172. (c) Gehrtz, P. H.; Geiger, V.; Schmidt, T.; Srsan, L.; Fleischer, I. Cross-Coupling of Chloro(hetero)arenes with Thiolates Employing a Ni(0)-Precatalyst. *Org. Lett.* **2019**, *21*, 50−55. (d) Martín, M. T.; Marín, M.; Maya, C.; Prieto, A.; Nicasio, M. C. Ni(II) Precatalysts Enable Thioetherification of (Hetero)Aryl Halides and Tosylates and Tandem C−S/C−N Couplings. *Chem.—Eur. J.* **2021**, *27*, 12320−12326. (e) Oechsner, R. M.; Wagner, J. P.; Fleischer, I. Acetate Facilitated Nickel Catalyzed Coupling of Aryl Chlorides and Alkyl Thiols. *ACS Catal.* **2022**, *12*, 2233−2243.

(8) (a) Bates, C. G.; Saejueng, P.; Doherty, M. Q.; Venkataraman, D. Copper-Catalyzed Synthesis of Vinyl Sulfides. *Org. Lett.* **2004**, *6*, 5005−5008. (b) Kabir, M. S.; Van Linn, M. L.; Monte, A.; Cook, J. M. Stereo- and Regiospecific Cu-Catalyzed Cross-Coupling Reaction of Vinyl Iodides and Thiols: A Very Mild and General Route for the Synthesis of Vinyl Sulfides. *Org. Lett.* **2008**, *10*, 3363−3366. (c) Kao, H. L.; Lee, C. F. Efficient Copper-Catalyzed S-Vinylation of Thiols with Vinyl Halides. *Org. Lett.* **2011**, *13*, 5204. (d) Lin, Y.-Y.; Wang, Y.-J.; Lin, C.-H.; Cheng, J.-H.; Lee, C.-F. Synthesis of Alkenyl Sulfides Through the Iron-Catalyzed Cross-Coupling Reaction of Vinyl Halides with Thiols. *J. Org. Chem.* **2012**, *77*, 6100−6106. (e) Martínez, A. G.; Barcina, J. O.; de Fresno Cerezo, A.; Subramanian, L. R. Regioselective Synthesis of Alkenyl Sulfides from Alkenyl Triflates Using Palladium(0) as Catalyst. *Synlett* **1994**, *1994*, 561−562. (f) Velasco, N.; Virumbrales, C.; Sanz, R.; Suárez-Pantiga, S.; Fernández-Rodríguez, M. A. General Synthesis of Alkenyl Sulfides by Palladium-Catalyzed Thioetherification of Alkenyl Halides and Tosylates. *Org. Lett.* **2018**, *20*, 2848−2852. (g) Imazaki, Y.; Shirakawa, E.; Hayashi, T. Ruthenium-catalyzed reaction of alkenyl triflates with zinc thiolates. *Tetrahedron* **2011**, *67*, 10212−10215. (h) Yatsumonji, Y.; Okada, O.; Tsubouchi, A.; Takeda, T. Stereo-recognizing transformation of (*E*)-alkenyl halides into sulfides catalyzed by nickel(0) triethyl phosphite complex. *Tetrahedron* **2006**, *62*, 9981−9987. (i) Marchese, A. D.; Mirabi, B.; Larin, E. M.; Lautens, M. A Simplified Protocol for the Stereospecific Nickel-Catalyzed C−S Vinylation Using NiX2 Salts and Alkyl Phosphites. *Synthesis* **2020**, *52*, 311−319. (j) Zhang, F.; Wang, Y.; Wang, Y.; Pan, Y. Electrochemical Deoxygenative Thiolation of Preactivated Alcohols and Ketones. *Org. Lett.* **2021**, *23*, 7524−7528.

(9) Kang, H.; Facchetti, A.; Stern, C. L.; Rheingold, A. L.; Kassel, W. S.; Marks, T. J. Efficient Synthesis and Structural Characteristics of Zwitterionic Twisted π-Electron System Biaryls. *Org. Lett.* **2005**, *7*, 3721−3724.

(10) Wiley, G.; Hershkowitz, R.; Rein, B.; Chung, B. Studies in organophosphorus chemistry. I. Conversion of alcohols and phenols to halides by tertiary phosphine dihalides. *J. Am. Chem. Soc.* **1964**, *86*, 964−965.

(11) (a) Goossen, L. J.; Rodríguez, N.; Linder, C. Decarboxylative Biaryl Synthesis from Aromatic Carboxylates and Aryl Triflates. *J. Am. Chem. Soc.* **2008**, *130*, 15248−15249. (b) Huang, Z.; Liu, Z.; Zhou, J. An Enantioselective, Intermolecular α-Arylation of Ester Enolates To Form Tertiary Stereocenters. *J. Am. Chem. Soc.* **2011**, *133*, 15882−15885.

(12) (a) Martínez, A. G.; Herrera, A.; Martínez, R.; Teso, E.; García, A.; Osío, J.; Pargada, L.; Unanue, R.; Subramanian, L. R.; Hanack, M. A new and convenient synthesis of alkyl and aryl pyrimidines. *J. Heterocycl. Chem.* **1988**, *25*, 1237−1241. (b) Su, X.; Huang, H.; Yuan, Y.; Li, Y. Radical Desulfur-Fragmentation and Reconstruction of Enol Triflates: Facile Access to α-Trifluoromethyl Ketones. *Angew. Chem., Int. Ed.* **2017**, *56*, 1338−1341. (c) Collins, C. J.; Martínez, A. G.; Alvarez, R. M.; Aguirre, J. A. Über die stereoelektronischen Bedingungen der 1,2-Umlagerungen bei Vinylkationen. *Chem. Ber.* **1984**, *117*, 2815−2824. (d) Duan, J.; Du, Y.-F.; Pang, X.; Shu, X.-Z. Ni-catalyzed cross-electrophile coupling between vinyl/aryl and alkyl sulfonates: synthesis of cycloalkenes and modification of peptides. *Chem. Sci.* **2019**, *10*, 8706−8712.

(13) Corma, A.; Iborra, S.; Velty, A. Chemical Routes for the Transformation of Biomass into Chemicals. *Chem. Rev.* **2007**, *107*, 2411−2502.

(14) (a) Hofstra, J. L.; Poremba, K. E.; Shimozono, A. M.; Reisman, S. E. Nickel-Catalyzed Conversion of Enol Triflates into Alkenyl Halides. *Angew. Chem., Int. Ed.* **2019**, *58*, 14901−14905. (b) Shirakawa, E.; Imazaki, Y.; Hayashi, T. Ruthenium-catalyzed transformation of alkenyl triflates to alkenyl halides. *Chem. Commun.* **2009**, 5088−5090. (c) Shen, X.; Hyde, A. M.; Buchwald, S. L. Palladium-Catalyzed Conversion of Aryl and Vinyl Triflates to Bromides and Chlorides. *J. Am. Chem. Soc.* **2010**, *132*, 14076−14078. (d) Imazaki, Y.; Shirakawa, E.; Ueno, R.; Hayashi, T. Ruthenium-Catalyzed Transformation of Aryl and Alkenyl Triflates to Halides. *J. Am. Chem. Soc.* **2012**, *134*, 14760−14763. (e) Pan, J.; Wang, X.; Zhang, Y.; Buchwald, S. L. An Improved Palladium-Catalyzed Conversion of Aryl and Vinyl Triflates to Bromides and Chlorides. *Org. Lett.* **2011**, *13*, 4974−4976.

(15) (a) Fernández-Rodríguez, M. A.; Shen, Q.; Hartwig, J. F. A General and Long-Lived Catalyst for the Palladium-Catalyzed Coupling of Aryl Halides with Thiols. *J. Am. Chem. Soc.* **2006**, *128*, 2180−2181. (b) Zheng, N.; McWilliams, J. C.; Fleitz, F. J.; Armstrong, J. D.; Volante, R. P. Palladium-Catalyzed Synthesis of Aryl Sulfides from Aryl Triflates. *J. Org. Chem.* **1998**, *63*, 9606−9607. (c) Itoh, T.; Mase, T. A General Palladium-Catalyzed Coupling of Aryl Bromides/Triflates and Thiols. *Org. Lett.* **2004**, *6*, 4587−4590. (d) Mispelaere-Canivet, C.; Spindler, J.-F.; Perrio, S.; Beslin, P. $Pd_2(dba)_3$/Xantphos-Catalyzed Cross-Coupling of Thiols and Aryl Bromides/Triflates. *Tetrahedron* **2005**, *61*, 5253−5259. (e) Ma, F.; Li, J.; Zhang, S.; Gu, Y.; Tan, T.; Chen, W.; Wang, S.; Xu, H.; Yang, G.; Lerner, R. A. Metal-Catalyzed One-Pot On-DNA Syntheses of Diarylmethane and Thioether Derivatives. *ACS Catal.* **2022**, *12*, 1639−1649. (f) Kreis, M.; Bräse, S. A General and Efficient Method for the Synthesis of Silyl-Protected Arenethiols from Aryl Halides or Triflates. *Adv. Synth. Catal.* **2005**, *347*, 313−319.

(16) Percec, V.; Bae, J.-Y.; Hill, D. H. Aryl Mesylates in Metal Catalyzed Homo- and Cross-Coupling Reactions. 4. Scope and Limitations of Aryl Mesylates in Nickel Catalyzed Cross-Coupling Reactions. *J. Org. Chem.* **1995**, *60*, 6895−6903.

(17) Oechsner, R. M.; Lindenmaier, I. H.; Fleischer, I. Nickel Catalyzed Cross Coupling of Aryl and Alkenyl Triflates with Alkyl Thiols. *ChemRxiv* 2023, DOI: 10.26434/chemrxiv-2023-7632g. This content is a preprint and has not been peer-reviewed.

(18) Standley, E. A.; Smith, S. J.; Müller, P.; Jamison, T. F. A Broadly Applicable Strategy for Entry into Homogeneous Nickel(0) Catalysts from Air-Stable Nickel(II) Complexes. *Organometallics* **2014**, *33*, 2012−2018.

(19) Gehrtz, P. H.; Kathe, P.; Fleischer, I. Nickel-Catalyzed Coupling of Arylzinc Halides with Thioesters. *Chem.—Eur. J.* **2018**, *24*, 8774−8778.

(20) Tkachenko, B. A.; Fokina, N. A.; Chernish, L. V.; Dahl, J. E. P.; Liu, S.; Carlson, R. M. K.; Fokin, A. A.; Schreiner, P. R. Functionalized Nanodiamonds Part 3: Thiolation of Tertiary/Bridgehead Alcohols. *Org. Lett.* **2006**, *8*, 1767−1770.

(21) (a) Johannesson, P.; Lindeberg, G.; Johansson, A.; Nikiforovich, G. V.; Gogoll, A.; Synnergren, B.; Le Grèves, M.; Nyberg, F.; Karlén, A.; Hallberg, A. Vinyl Sulfide Cyclized Analogues of Angiotensin II with High Affinity and Full Agonist Activity at the AT1 Receptor. *J. Med. Chem.* **2002**, *45*, 1767. (b) Trost, B. M.; Lavoie, A. C. Enol thioethers as enol substitutes. An alkylation sequence. *J. Am. Chem. Soc.* **1983**, *105*,

https://doi.org/10.1021/acs.orglett.3c00218
Org. Lett. 2023, 25, 1655−1660

5075−5090. (c) Sader, H. S.; Johnson, D. M.; Jones, R. N. In Vitro Activities of the Novel Cephalosporin LB 11058 against Multidrug-Resistant Staphylococci and Streptococci. *Antimicrob. Agents Chemother.* **2004**, *48*, 53−62. (d) Marcantoni, E.; Massaccesi, M.; Petrini, M.; Bartoli, G.; Bellucci, M. C.; Bosco, M.; Sambri, L. A Novel Route to the Vinyl Sulfide Nine-Membered Macrocycle Moiety of Griseoviridin†. *J. Org. Chem.* **2000**, *65*, 4553−4559.

https://doi.org/10.1021/acs.orglett.3c00218
Org. Lett. 2023, 25, 1655−1660

Nickel Catalyzed Cross Coupling of Aryl and Alkenyl Triflates with Alkyl Thiols

SUPPORTING INFORMATION

Regina M. Oechsner[†], Ivo H. Lindenmaier[†] and Ivana Fleischer*

Institute of Organic Chemistry, Faculty of Science,
Eberhard Karls Universität Tübingen, Auf der Morgenstelle 18, 72076 Tübingen, Germany
*ivana.fleischer@uni-tuebingen.de

Table of Contents

1. General information

1.1. Chemicals and General Techniques

All cross-coupling reactions were carried out under an argon atmosphere using standard Schlenk techniques or an argon atmosphere Glovebox (GS MEGA E-Line, Glovebox Systemtechnik) and pre-dried glassware, unless noted otherwise. Dry THF was distilled over Na/benzophenone, stored over 3 Å MS and degassed. Solvents for reactions were dry and degassed. Solvents for chromatography were distilled prior to use. Column chromatography was carried out either manually or by a Puriflash system (Interchim XS420) using silica gel (0.04–0.063 mm) from Machery&Nagel. Thin Layer Chromatography was performed on silica gel coated glass plates (0.25 mm) with fluorescence indicator UV254 (Macherey-Nagel, TLC plates SIL G-25 UV254). For detection of spots, irradiation of UV light at 254 nm was used. Chemicals were purchased from abcr, Acros, Alfa Aesar, BLDChem, Carbolution Chemicals, Carl Roth, Fluorochem, Sigma-Aldrich or TCI. KOAc was dried prior to use at 110 °C under high vacuum. Adamantanethiol was stored and handled in a glovebox at room temperature. Other thiols were stored as received at -15 °C and handled under Argon flow. Substrates **1a**, **1b**, **1h**, **1l**, **1m**, **1n** and **1p** were commercially available.

1.2. Analytical Techniques

NMR spectra were recorded using Bruker Avance III HD 400 or Bruker Avance III HDX 600 at room temperature (400 MHz for ^{1}H experiments; 101 MHz for ^{13}C experiments; 162 MHz; 376 MHz for ^{19}F experiments) in commercially available deuterated solvents. ^{13}C-NMR experiments were performed in proton-decoupled mode. Chemical shifts (*δ)* are reported in ppm relative to the residual NMR solvent signals [1] (chloroform: ^{1}H 7.26 ppm and ^{13}C 77.16 ppm). The coupling constants (*J* values) are given in Hz and spin multiplicity with the usual designations for splitting patterns (s = singlet, d = doublet, t = triplet, q = quartet, m = multiplet, br s = broad singlet).

HR-MS (ESI, APCI, EI) measurements were carried out by the mass spectrometry department of the Institute of Organic Chemistry, University of Tübingen. Measurements were carried out using maXis 4G from Bruker (ESI, APCI) or by a MAT95 from Finnegan (EI). The molecular ion $[M]^+$, $[M+H]^+$ and $[M+Na]^+$ respectively are given in m/z units.

GC-FID (flame ionization detection) analysis was carried out on an Agilent 7820A system using dry hydrogen as carrier gas. An Agilent 19091J-431 column (30 m × 320 µm × 0.25 µm) was used. Program 50-280M15: heating from 50 °C to 280 °C within 15 minutes. Conversion and yield were determined via calibration against the internal standard pentadecane.

Melting point determination was achieved by using a Büchi B-540 machine with a visual detection (heating rate 5 °C/min). FT-IR spectra were recorded using a Cary 630 FTIR by applying the sample neat on a diamond ATR sampler.

2. General Procedures

General Procedure A (GP-A): Synthesis of aryl triflates.[2, 3]

In a 100 mL Schlenk-flask equipped with a stirring bar, the corresponding phenol (10 mmol, 1 equiv.) was dissolved in dry DCM (30 mL) and pyridine (3.0 equiv.) was added. After cooling the solution to 0 °C, trifluoromethanesulfonic anhydride (1.2 equiv.) was added dropwise under vigorous stirring, followed by removal of the ice-bath. The resulting mixture was stirred for 18 h at rt, diluted with DCM (10 mL), quenched with aqueous HCl (1 M, 10 mL), or, in the case of basic substrates, water (10 mL) and extracted with DCM (3 × 10 mL). The combined organic phases were washed with water (20 mL), saturated aqueous solution of $NaHCO_3$ (20 mL) and brine (20 mL), dried over anhydrous $MgSO_4$, concentrated *in vacuo* and purified by column chromatography (*n*-hexane/EtOAc).

General Procedure B1 (GP-B1): Synthesis of alkenyl triflates using trifluoromethanesulfonic anhydride.[4, 5]

In a 100 mL Schlenk-flask equipped with a stirring bar, dry sodium carbonate (1.6 equiv.) was suspended in dry DCM (30 mL) and the corresponding ketone (10 mmol, 1.0 equiv.) was added. After cooling to 0 °C, trifluoromethanesulfonic anhydride (1.5 equiv.) was added dropwise under vigorous stirring. The reaction mixture was slowly warmed to rt and stirred for 18 h, followed by dilution with DCM (10 mL), quenching with water (10 mL) and extraction with DCM (3 × 10 mL). The combined organic phases were washed with saturated aqueous solution of $NaHCO_3$ (2 × 10 mL) and brine (2 × 10 mL). The organic phase was dried over anhydrous $MgSO_4$, concentrated *in vacuo,* and purified by column chromatography (*n*-hexane/EtOAc).

General Procedure B2 (GP-B2): Synthesis of alkenyl triflates using LiHMDS.[6]

In a 100 mL Schlenk-flask equipped with a stirring bar, the corresponding ketone (10.0 mmol. 1 equiv.) was dissolved in dry THF (30 mL), cooled to –78 °C and LiHMDS (1.0 M in THF, 1.1 equiv.) was added. After stirring the mixture for 90 minutes $PhNTf_2$ (1.05 equiv.) was added. After stirring for 15 minutes the mixture was allowed to warm to room temperature followed by stirring for another 18 h. Subsequently, the reaction was quenched with water (10 mL) and extracted with EtOAc (3 × 10 mL). The combined organic phases were washed with saturated aqueous solution of NH_4Cl (1 × 10 mL), saturated aqueous solution of $NaHCO_3$ (1 × 10 mL) and brine (1 × 10 mL). The organic phase was dried over anhydrous $MgSO_4$, concentrated *in vacuo* and purified by column chromatography (*n*-hexane/EtOAc).

General Procedure B3 (GP-B3): Synthesis of alkenyl triflates using LDA.[6]

In a 100 mL Schlenk-flask equipped with a stirring bar, DIPEA (1.1 equiv.) was dissolved in dry THF (30 mL), cooled to –78 °C and *n*-butyllithium (2.5 M in hexane, 1.1 equiv.) was added dropwise. After stirring the solution for 15 minutes, the corresponding ketone (10.0 mmol. 1.0 equiv.), was added portion- or dropwise and the reaction was stirred for 90 minutes. Subsequently, $PhNTf_2$ (1.05 equiv.) was added, the mixture was stirred for 15 minutes and afterwards allowed to warm to room temperature followed by stirring for 18 h. The reaction was quenched with water (10 mL) and extracted with EtOAc (3 × 10 mL). The combined organic phases were washed with saturated aqueous solution of NH_4Cl (1 × 10 mL), saturated aqueous solution of $NaHCO_3$ (1 × 10 mL) and brine (1 × 10 mL). The organic phase was dried over anhydrous $MgSO_4$, concentrated *in vacuo* and purified by column chromatography (*n*-hexane/EtOAc).

General Procedure C (GP-C): Nickel-catalyzed C–S cross-coupling of aryl/alkenyl triflates and thiols for product isolation.

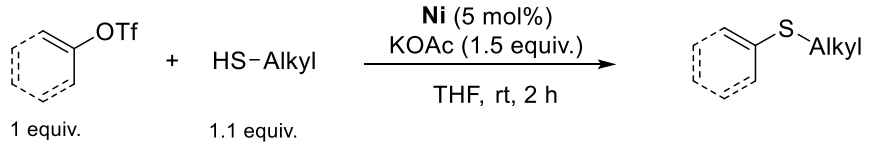

A 25 mL inert, flame-dried and septum-caped Schlenk-tube equipped with a stirring bar was charged with KOAc (1.5 equiv.) and precatalyst XantphosNi(*o*-tolyl)Cl **Ni** (5 mol%). After addition of the respective thiol (1.1 equiv.) and the corresponding aryl/alkenyl triflate (1 mmol, 1.0 equiv.) the mixture was dissolved in dry THF (3 mL) under stirring. After 2 h at room temperature, the reaction mixture was quenched with brine (3 mL) and diluted with EtOAc (8 mL). The organic phase was washed with brine (5 mL) and the combined aqueous phases were re-extracted with EtOAc (3 × 10 mL). The combined organic phases were dried over $MgSO_4$, concentrated *in vacuo* and purified by flash column chromatography (*n*-hexane/EtOAc).

General Procedure D (GP-D): Nickel-catalyzed C–S cross-coupling of aryl/alkenyl triflates and thiols for GC-FID analysis (screening).

A 10 mL inert, flame-dried and septum-caped Schlenk-tube equipped with a stirring bar was charged with KOAc (1.5 equiv.) and precatalyst XantphosNi(*o*-tolyl)Cl **Ni** (5 mol%). After addition of the respective thiol (1.1 equiv.) and the corresponding aryl/alkenyl triflate (0.2 mmol, 1.0 equiv.) the mixture was dissolved in dry THF (1 mL) under stirring. After 2 h at room temperature the internal standard *n*-pentadecane (50 µL) was added, the reaction mixture was quenched with brine (1 mL) and diluted with EtOAc (3 mL). A sample of the organic phase was filtered (glass pipette filled with cotton, celite, Al_2O_3 and Mg_2SO_4) and analyzed via GC-FID. Yields and conversion were determined through the internal standard method for quantitative analysis.

General Procedure E (GP-E): Reaction progress of nickel-catalyzed C-S cross-coupling with different electrophiles (kinetic studies).

A 10 mL inert, flame-dried and septum-caped Schlenk-tube equipped with a stirring bar was charged with KOAc (1.5 equiv.) and precatalyst XantphosNi(*o*-tolyl)Cl **Ni** (5 mol%). After addition of the internal standard n-pentadecane (100 µL), the respective thiol (1.1 equiv.), and corresponding aryl/alkenyl triflate (1.00 mmol, 1.0 equiv.) the mixture was dissolved in THF (3 mL) under stirring. The time was started with the addition of THF. After defined intervals (e.g. 1, 2, 3, 5 min) 0.1 µL samples of the reaction mixture were removed from the reaction mixture with inert syringes. The probes were diluted with EtOAc and quenched with brine. A sample of the organic phase was filtered (glass pipette filled with cotton, celite, Al_2O_3 and Mg_2SO_4) and analyzed via GC-FID. Yields and conversion were determined through the internal standard method for quantitative analysis.

3. Analytical Data

3.1. Precatalyst

(Xantphos)Ni(*o*-tolyl)Cl (Ni):

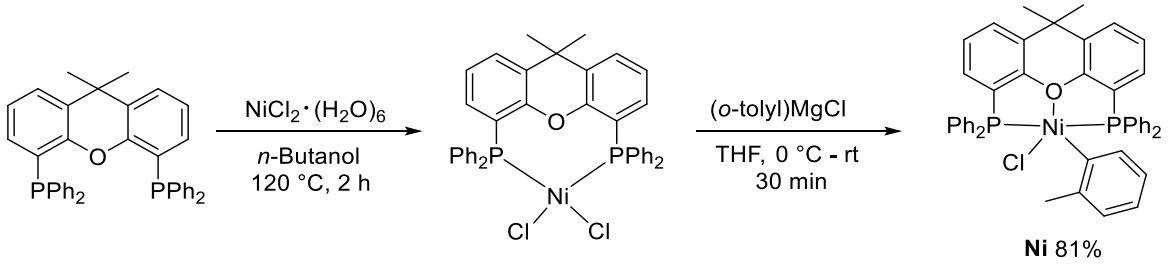

$C_{46}H_{39}ClNiOP_2$ (763.91 g/mol)

Step1: Synthesis of (Xantphos)$NiCl_2$

The precatalyst was synthesized following a literature procedure.[7, 8] $NiCl_2$ hexahydrate (513 mg, 2.16 mmol, 1.0 equiv.) was placed in an inert, flame-dried and septum-capped 100 mL round bottom flask equipped with a stir bar. *N*-Butanol (20 mL) was added, the bright green solution was sparged with argon for 20 minutes and added to Xantphos (1.25 g, 2.16 mmol, 1.00 equiv.), which was placed in an oven and flame-dried three necked round bottom flask equipped with a stir bar and reflux condenser. The reaction mixture was heated to 120 °C for 2 h. The purple-grey suspension was cooled to room temperature and shortly before filtration to 0 °C. The product was filtered with an inert Schlenk frit and placed under high vacuum. The grey-purple solid, which was presumed to be (Xantphos)$NiCl_2$ (1.38 g, 1.94 mmol, 90%) was carried on to the next step without further analysis.

Step2: Synthesis of (Xantphos)Ni(*o*-tolyl)Cl

(Xantphos)$NiCl_2$ (1.38 g, 1.94 mmol, 1.0 equiv.) was placed in an inert, flame-dried and septum-capped 100 mL round bottom flask equipped with a stir bar, suspended in dry THF (30 mL) and cooled to 0 °C. While stirring vigorously a freshly titrated *o*-tolylmagnesium chloride (1.15 M in THF/Toluene from Acros, 1.69 mL) was added dropwise. During the addition the color changed to dark red. Once the addition was completed the reaction mixture was stirred for 15 minutes at 0 °C and the solvent was removed by vacuum evaporation using a tepid water bath. The orange-red residue was suspended in MeOH (5 mL, HPLC grade, 15 min sparged with argon), cooled to 0 °C and filtered with an inert Schlenk frit. The orange filter cake was washed with cold Et_2O (2 x 15 mL, -20 °C) and dried in high vacuum to yield (Xantphos)Ni(*o*-tolyl)Cl (1.19 g, 1.94 mmol, 81%) as a fine orange powder. Analytical data corresponds to literature.[7, 8]

^{1}H-NMR (400 MHz, THF-D_8, δ): 8.32 – 8.24 (m, 4H), 7.64 (dd, *J* = 7.4, 1.5 Hz, 2H), 7.42 – 7.36 (m, 2H), 7.35 – 7.28 (m, 4H), 7.12 – 7.02 (m, 4H), 6.94 (t, *J* = 7.4 Hz, 2H), 6.72 (t, *J* = 7.7 Hz, 4H), 6.31 – 6.24 (m, 5H), 6.01 – 5.95 (m, 1H), 5.20 (d, *J* = 3.8 Hz, 2H), 3.40 (s, 3H), 1.94 (s, 3H), 1.63 (s, 3H).

^{31}P-NMR (162 MHz, THF-D_8, δ): 6.6 (s, major), 1.4 (s, minor).

^{1}H-NMR (400 MHz, THF-D_8) of precatalyst **Ni**:

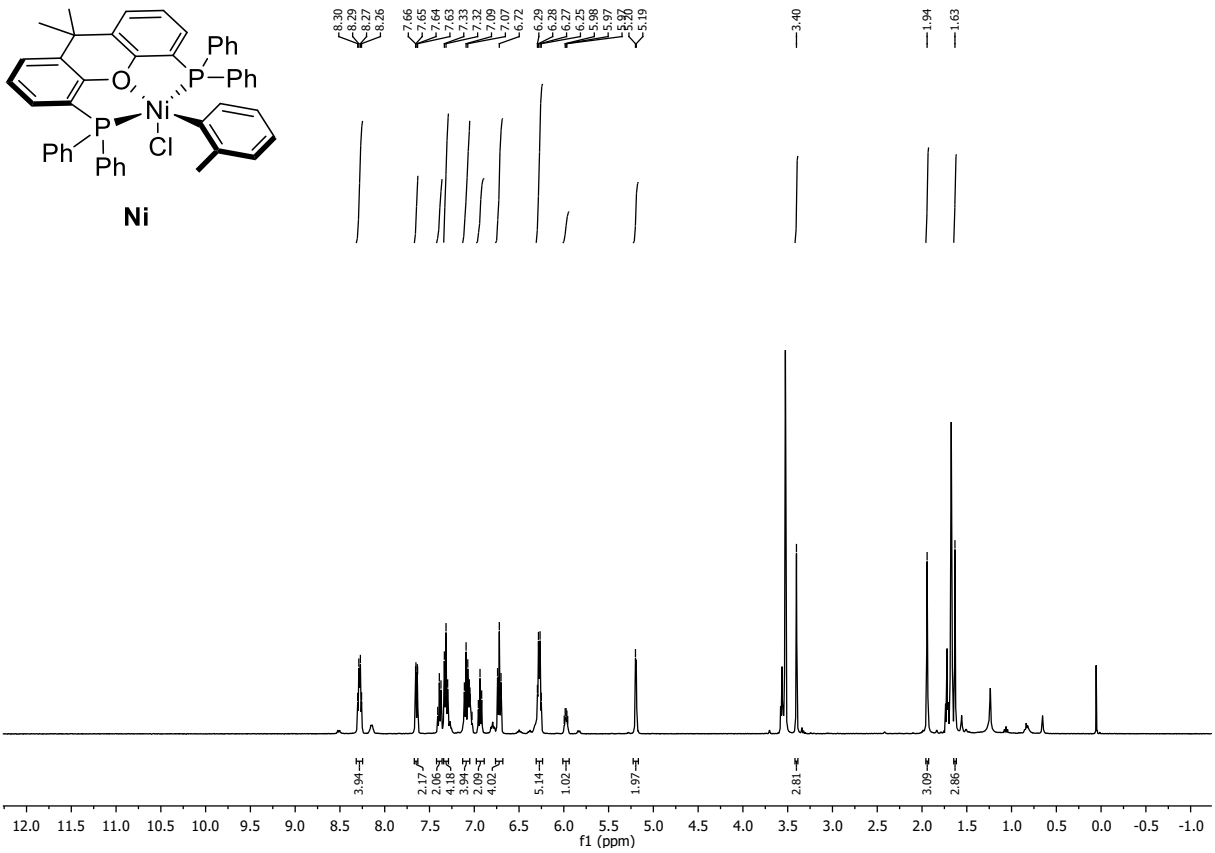

Ni

^{31}P-NMR (162 MHz, THF-D_8) of precatalyst **Ni**:

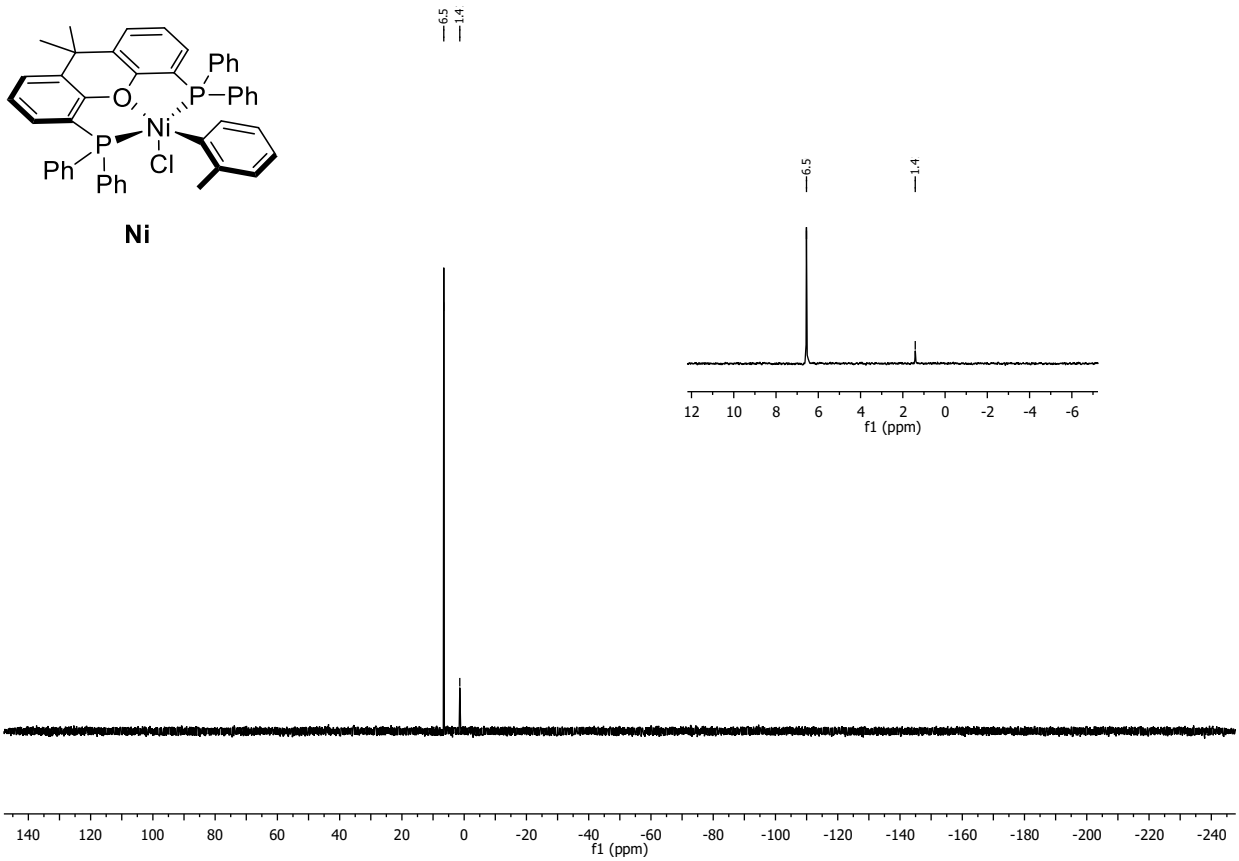

Ni

3.2. Substrates

3.2.1. Aryltriflates

4-Cyanophenyl trifluoromethanesulfonate (1c):

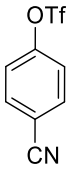

1c

$C_8H_4F_3NO_3S$ (251.18 g/mol)

Following **GP-A**, **1c** was synthesized using 4-hydroxybenzonitrile (1.19 g, 10.0 mmol, 1.0 equiv.). Purification by column chromatography (SiO_2, *n*-hexane/EtOAc 9:1) afforded **1c** (2.36 g, 9.40 mmol, 94%) as colorless oil. Conforms to reported analytical data.[9]

R_f: 0.37 (*n*-hexane/EtOAc 9:1).

^{1}H-NMR (400 MHz, $CDCl_3$, δ): 7.84 – 7.75 (m, 2H), 7.47 – 7.38 (m, 2H).

^{13}C-NMR (101 MHz, $CDCl_3$, δ): 152.1, 134.6, 122.8, 118.8 (q, *J* = 320.8 Hz), 117.2, 113.1.

^{19}F-NMR (376 MHz, $CDCl_3$, δ): -72.6.

^{1}H-NMR (400 MHz, $CDCl_3$) of compound **1c**:

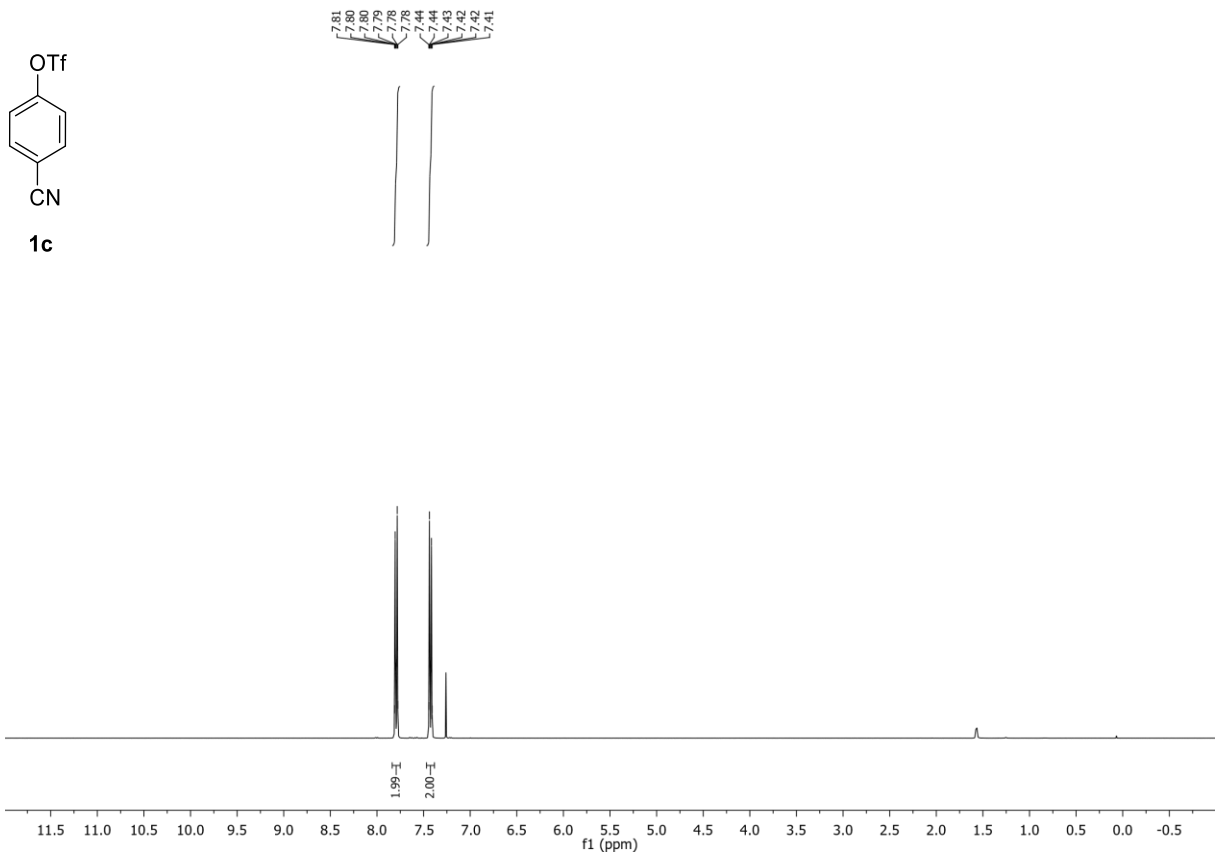

^{13}C-NMR (101 MHz, $CDCl_3$) of compound **1c**:

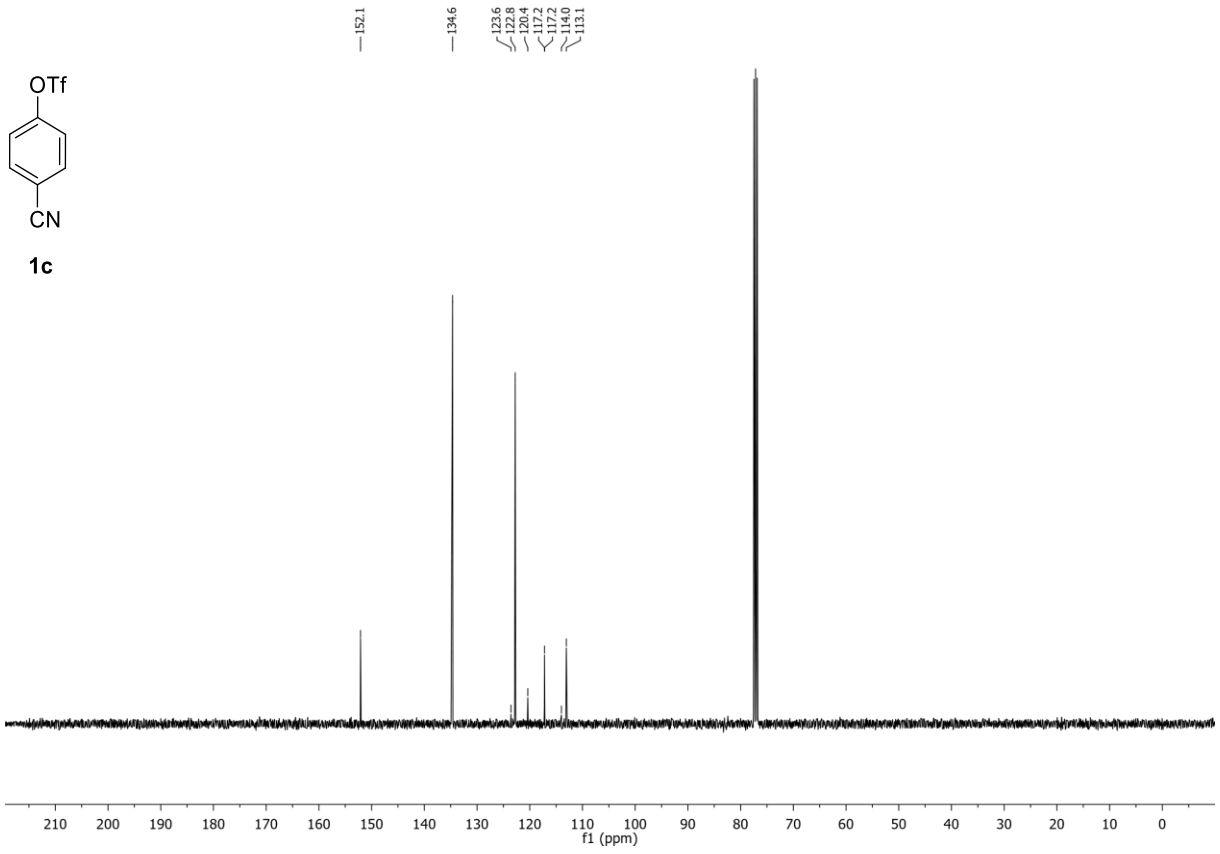

^{19}F-NMR (376 MHz, $CDCl_3$) of compound **1c**:

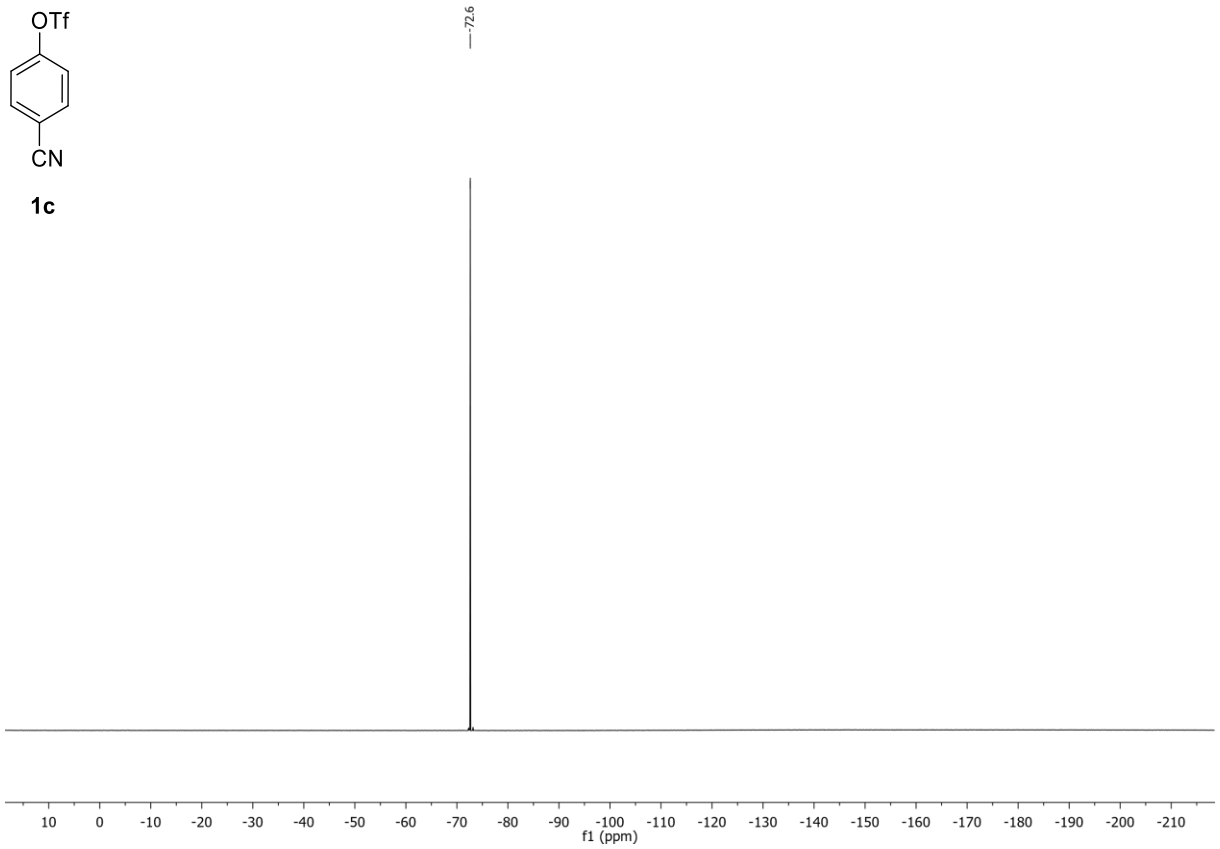

Ethyl 4-(((trifluoromethyl)sulfonyl)oxy)benzoate (1d):

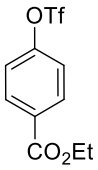

1d

$C_{10}H_9F_3O_5S$ (298.23 g/mol)

Following **GP-A**, **1d** was synthesized using ethyl 4-hydroxybenzoate (1.62 g, 10.0 mmol, 1.0 equiv.). Purification by column chromatography (SiO_2, *n*-hexane/EtOAc 95:5) afforded **1d** (2.30 g, 7.71 mmol, 77%) as a colorless liquid. Conforms to reported analytical data.[2]

^{1}H-NMR (400 MHz, $CDCl_3$, δ): 8.13 (dd, *J* = 9.3, 2.4 Hz, 2H), 7.39 – 7.29 (m, 2H), 4.38 (q, *J* = 7.1 Hz, 2H), 1.38 (t, *J* = 7.1 Hz, 3H).

^{13}C-NMR (101 MHz, $CDCl_3$, δ): 165.0, 152.5, 131.9, 130.8, 121.5, 118.9 (q, *J* = 320.8 Hz), 61.7, 14.3.

^{19}F-NMR (376 MHz, $CDCl_3$, δ): -72.9.

^{1}H-NMR (400 MHz, $CDCl_3$) of compound **1d**:

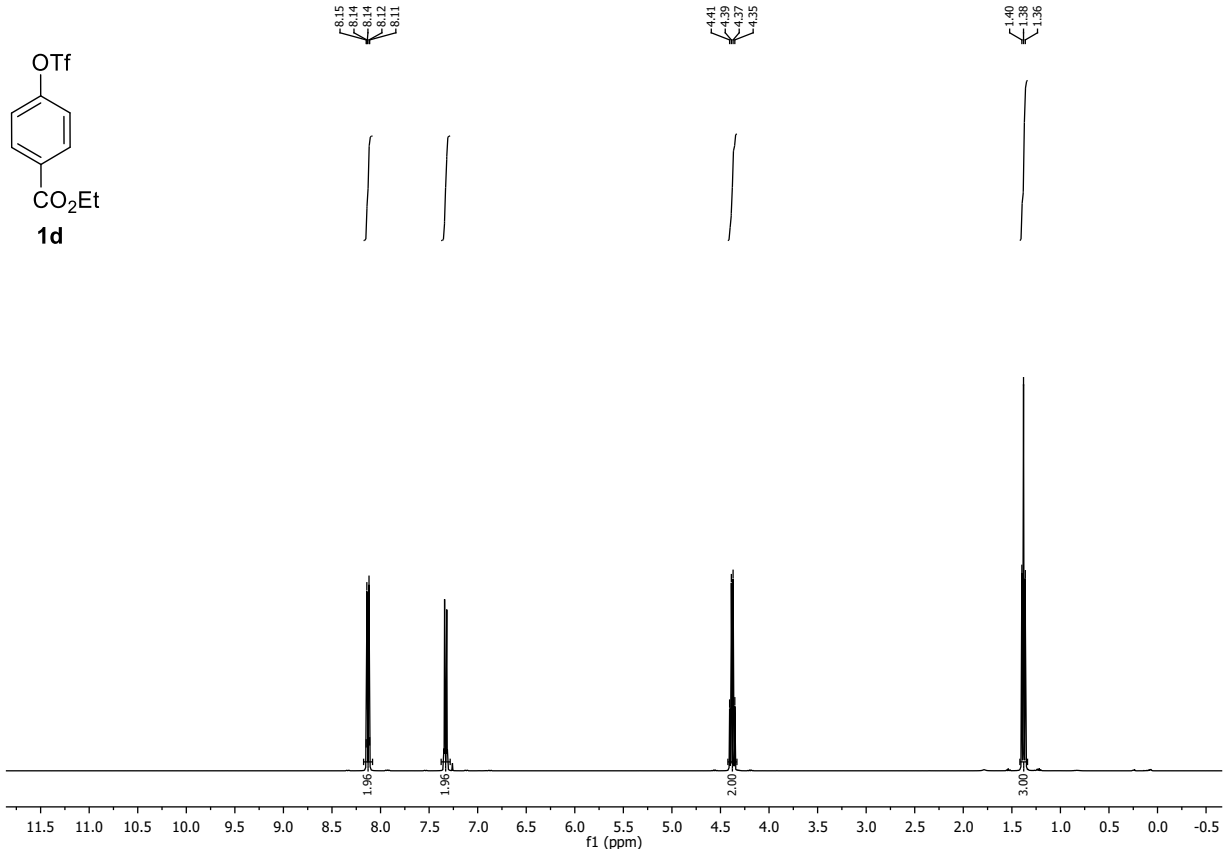

^{13}C-NMR (101 MHz, $CDCl_3$) of compound **1d**:

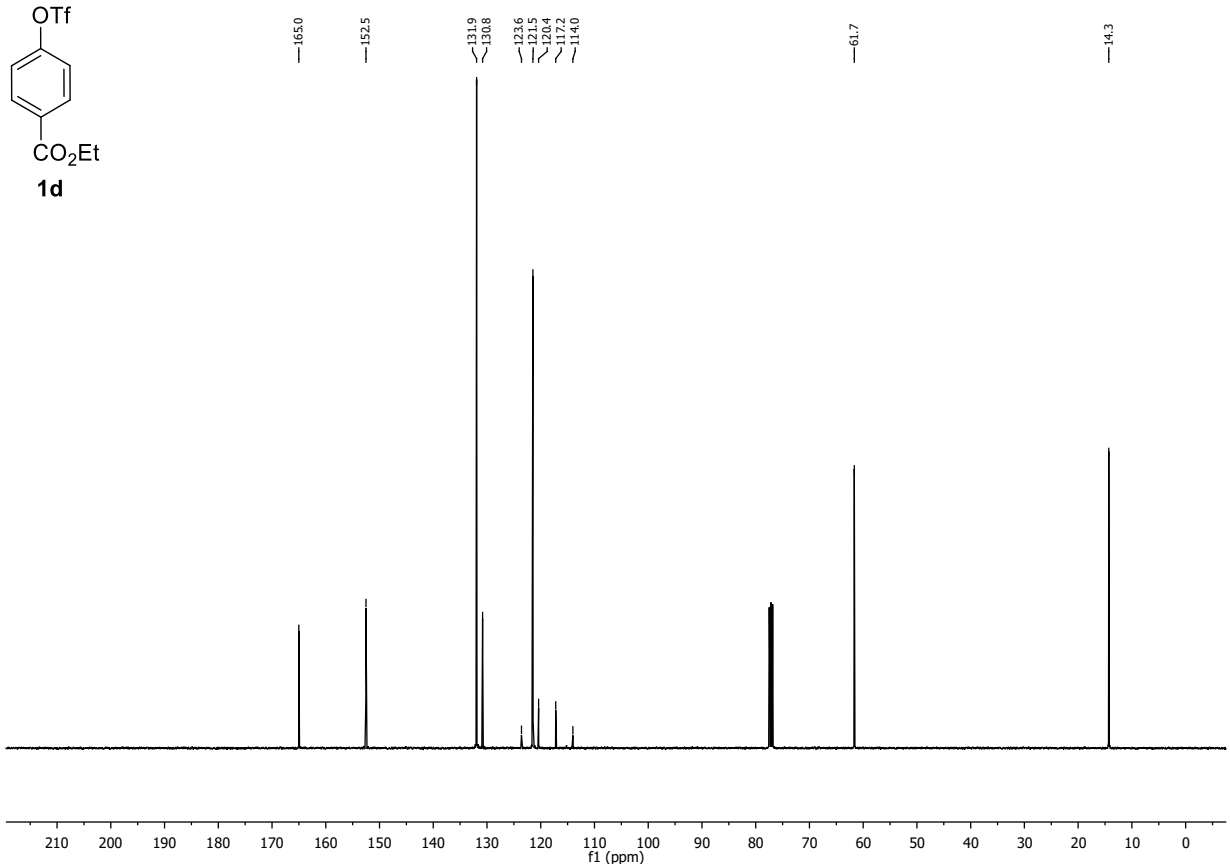

^{19}F-NMR (376 MHz, $CDCl_3$) of compound **1d**:

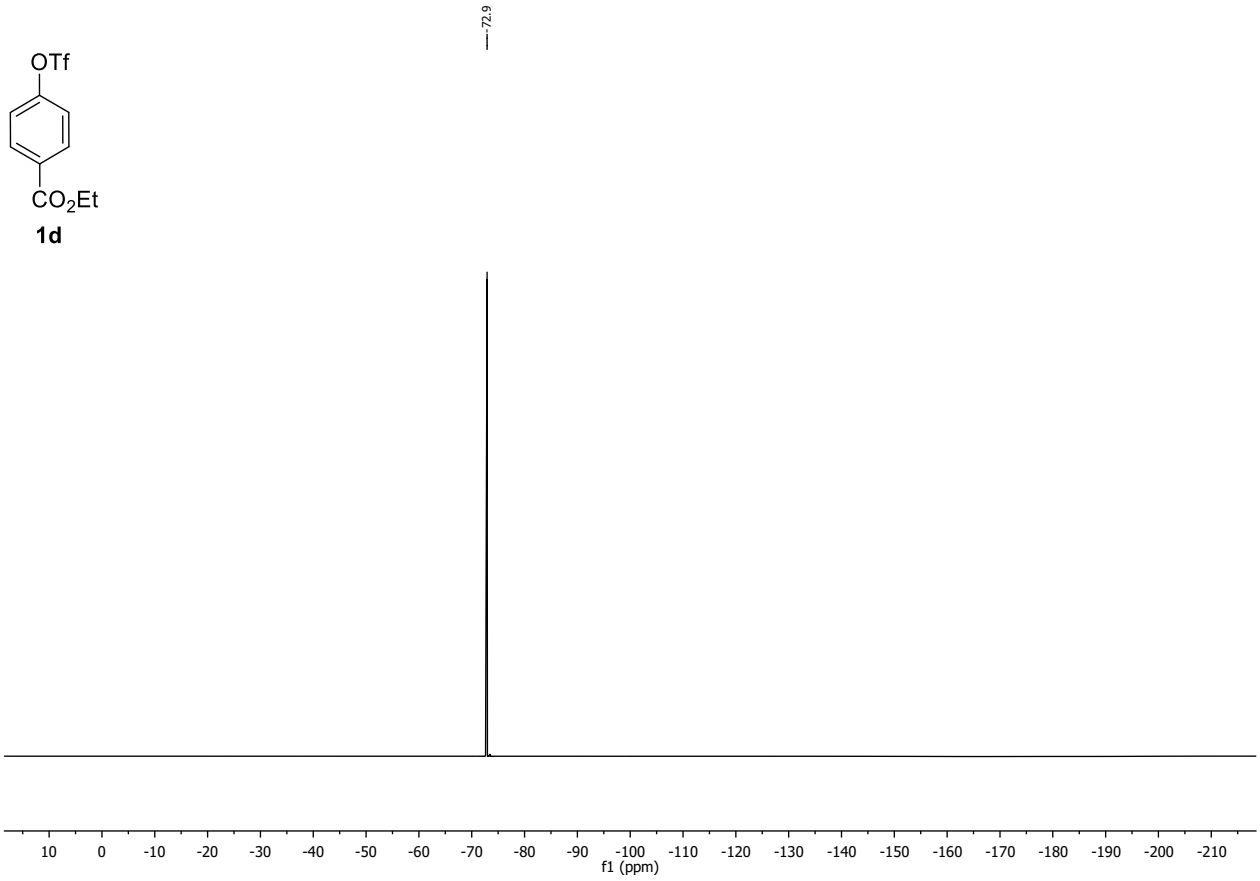

4-(Trifluoromethyl)phenyl trifluoromethanesulfonate (1e):

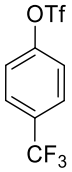

1e

$C_8H_4F_6O_3S$ (294.17 g/mol)

Following **GP-A**, **1e** was synthesized using 4-(trifluoromethyl)phenol (1.62 g, 10.0 mmol, 1.0 equiv.). Purification by column chromatography (SiO_2, *n*-hexane) afforded **1e** (1.74 g, 5.91 mmol, 59%) as colorless oil. Conforms to reported analytical data.[10]

R_f: 0.24 (*n*-hexane).

^{1}H-NMR (400 MHz, $CDCl_3$, δ): 7.75 (d, *J* = 8.7 Hz, 2H), 7.42 (d, *J* = 8.7 Hz, 2H).

^{13}C-NMR (101 MHz, $CDCl_3$, δ): 151.7, 131.0 (q, *J* = 33.5 Hz), 127.9 (q, *J* = 3.7 Hz), 123.4 (q, *J* = 272.7 Hz), 122.2, 118.9 (q, *J* = 320.6 Hz).

^{19}F-NMR (376 MHz, $CDCl_3$, δ): -62.7, -72.7.

^{1}H-NMR (400 MHz, $CDCl_3$) of compound **1e**:

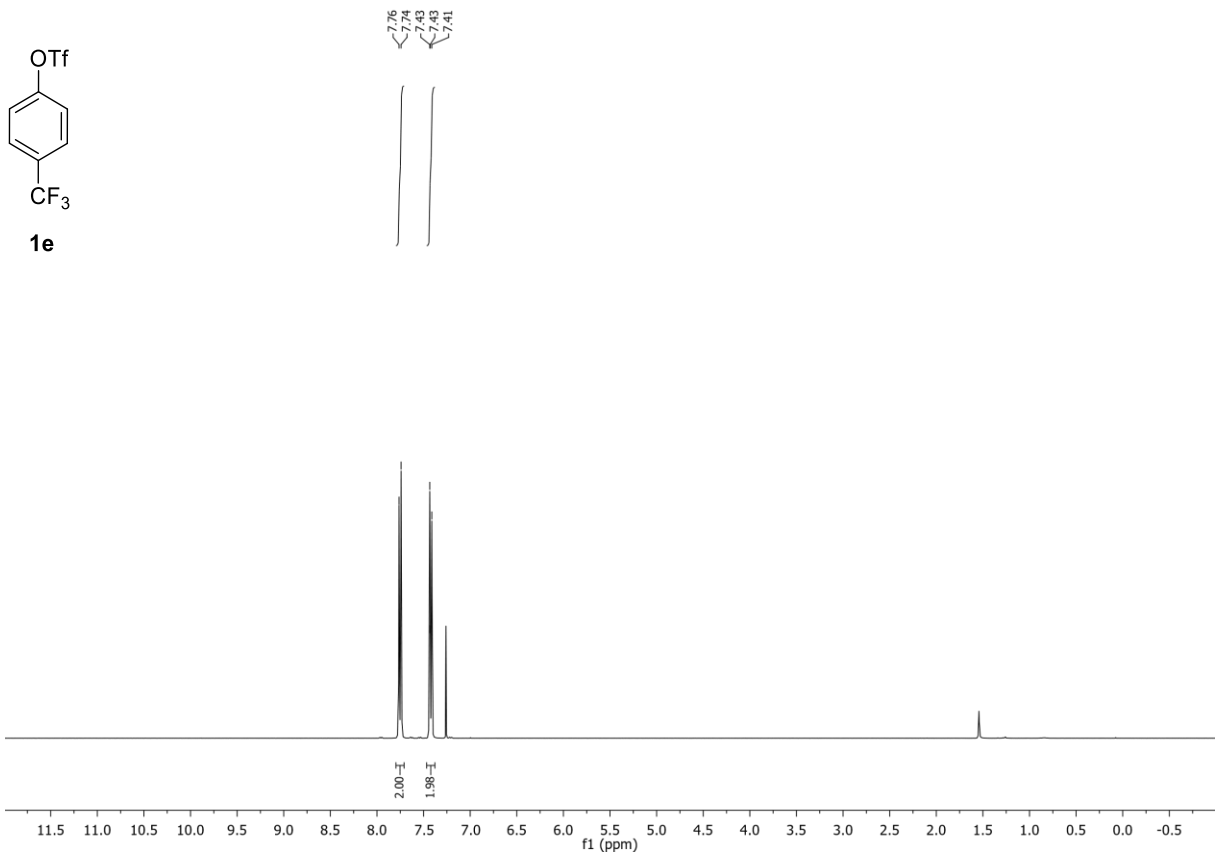

^{13}C-NMR (101 MHz, $CDCl_3$) of compound **1e**:

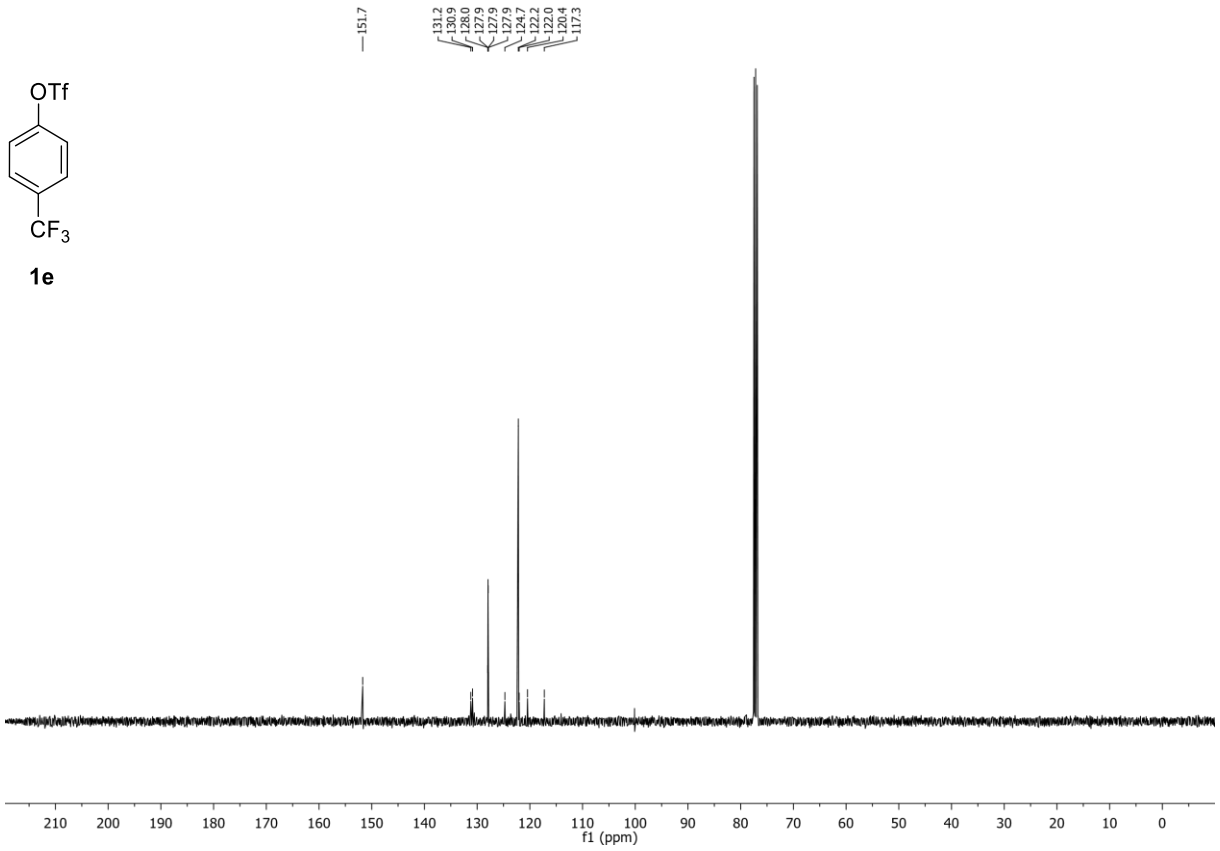

^{19}F-NMR (376 MHz, $CDCl_3$) of compound **1e**:

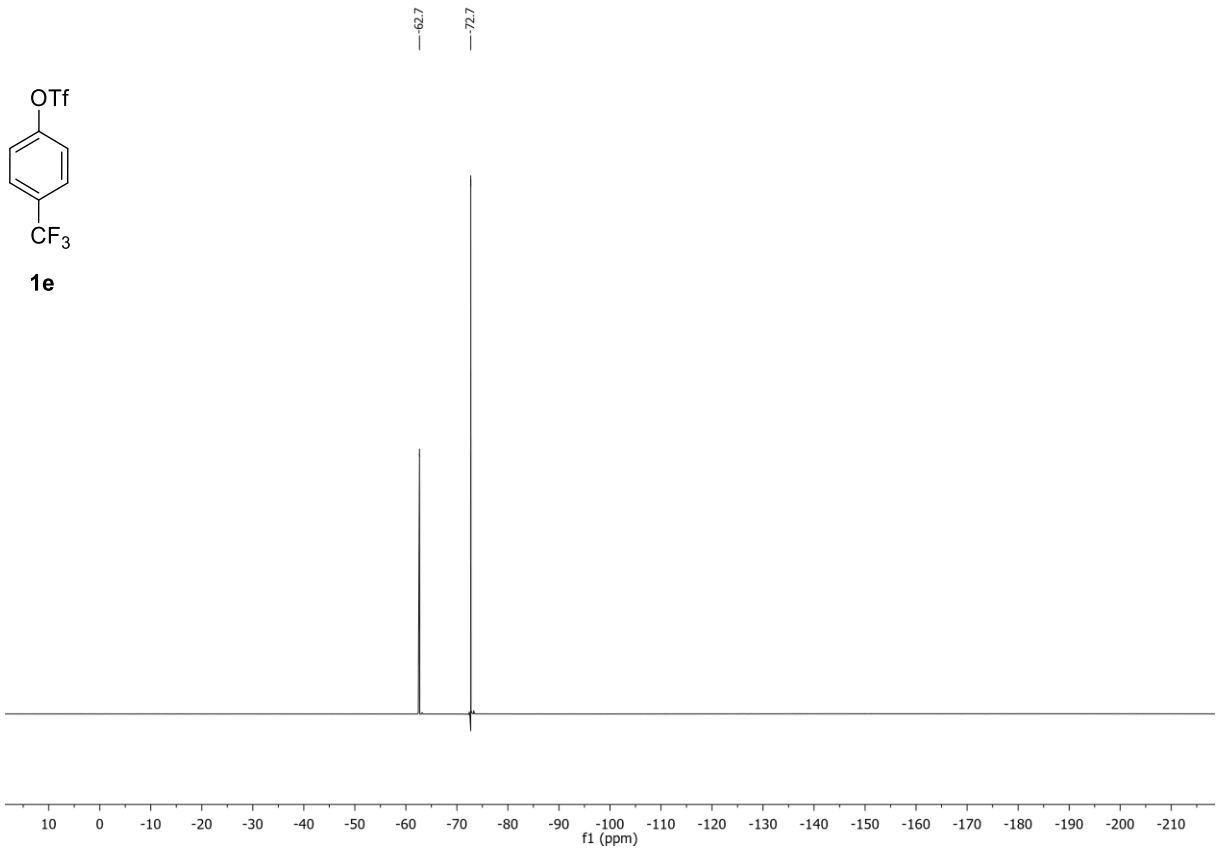

3-Methoxyphenyl trifluoromethanesulfonate (1f):

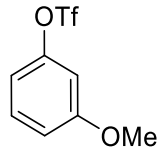

1f

$C_8H_7F_3O_4S$ (256.20 g/mol)

Following **GP-A**, **1f** was synthesized using 3-methoxyphenol (2.56 g, 10.0 mmol, 1.0 equiv.). Purification by column chromatography (SiO_2, *n*-hexane/EtOAc 95:5) afforded **1f** (2.12 g, 8.27 mmol, 83%) as a colorless liquid. Conforms to reported analytical data.[11]

R_f: 0.39 (*n*-hexane/EtOAc 98:2).

^{1}H-NMR (400 MHz, $CDCl_3$, δ): 7.34 (t, *J* = 8.3 Hz, 1H), 6.93 (dd, *J* = 8.3, 2.4 Hz, 1H), 6.87 (dd, *J* = 8.3, 2.4 Hz, 1H), 6.81 (t, *J* = 2.4 Hz, 1H).

^{13}C-NMR (101 MHz, $CDCl_3$, δ): 161.0, 150.4, 130.7, 118.9 (q, *J* = 319.8 Hz), 114.3, 113.4, 107.6, 55.8.

^{19}F-NMR (376 MHz, $CDCl_3$, δ): -72.9.

^{1}H-NMR (400 MHz, $CDCl_3$) of compound **1f**:

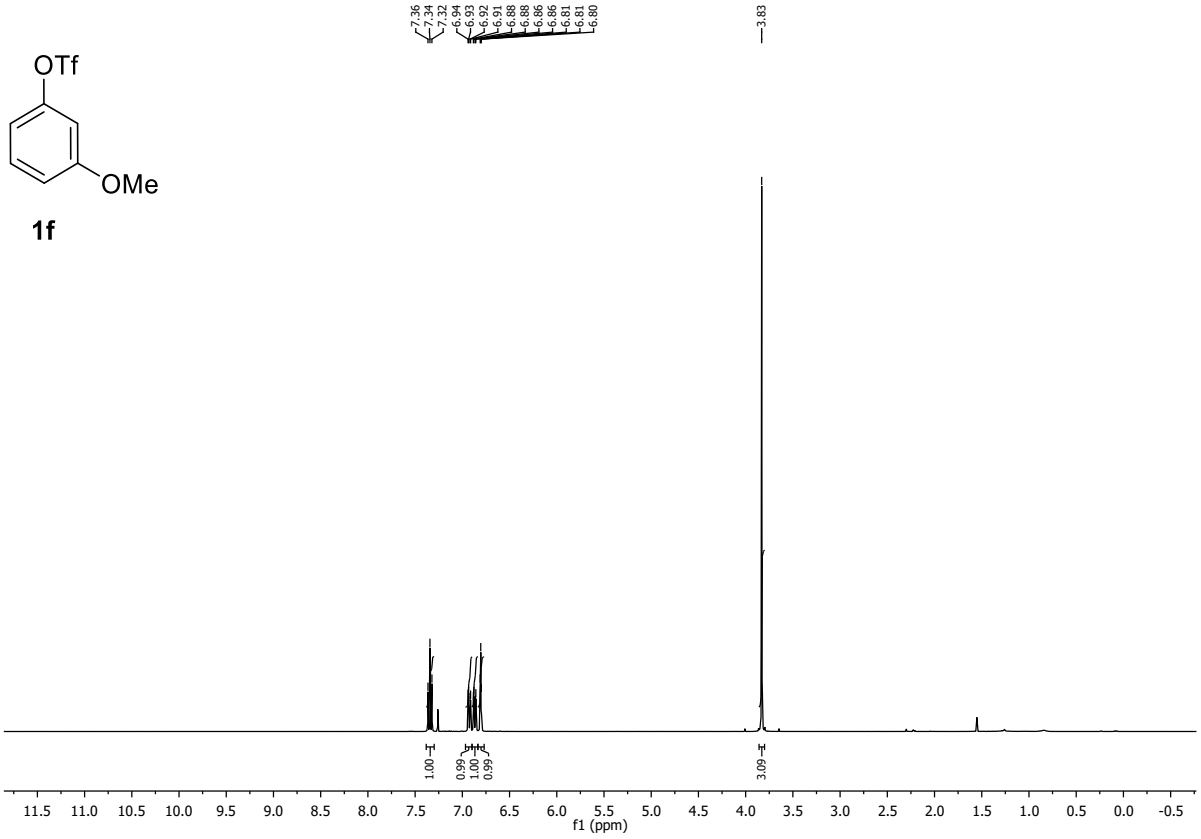

^{13}C-NMR (101 MHz, $CDCl_3$) of compound **1f**:

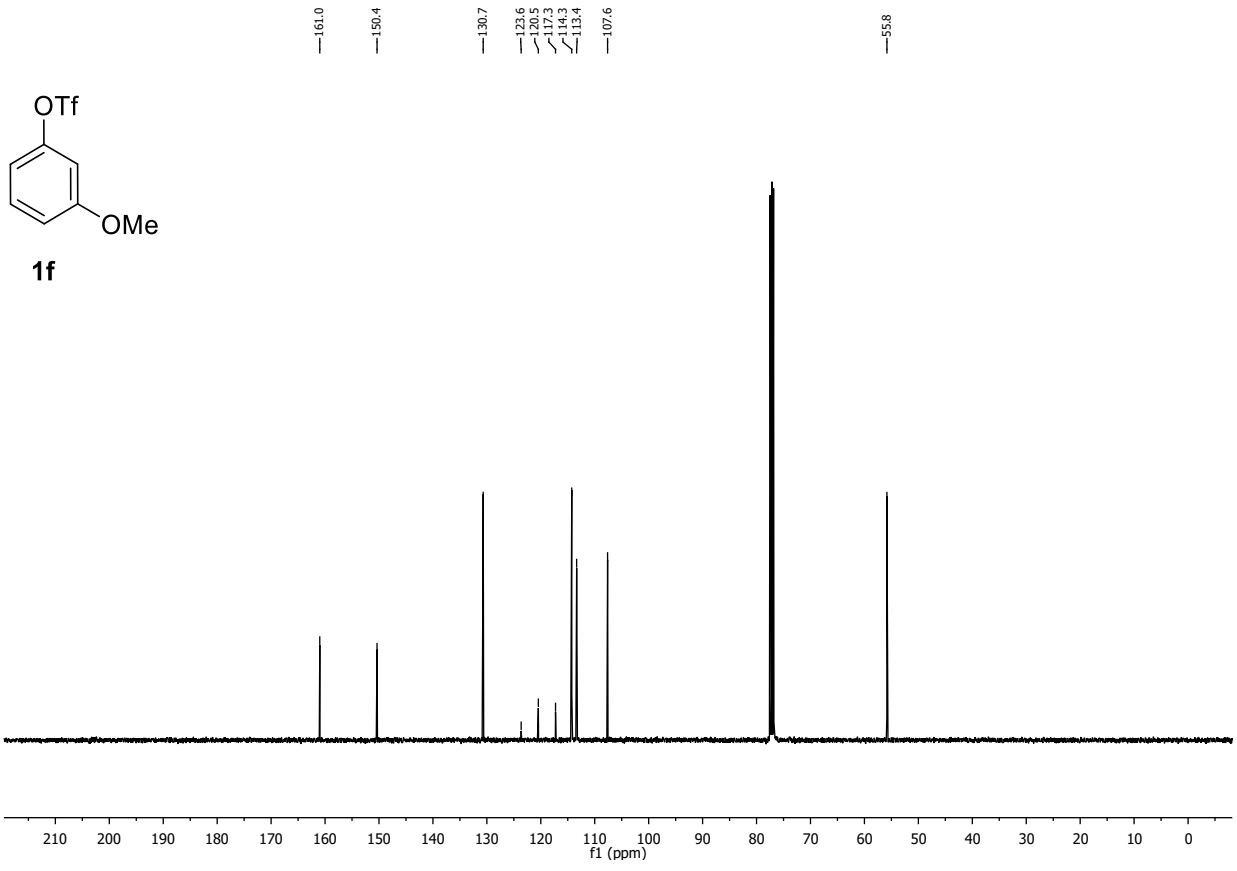

^{19}F-NMR (376 MHz, $CDCl_3$) of compound **1f**:

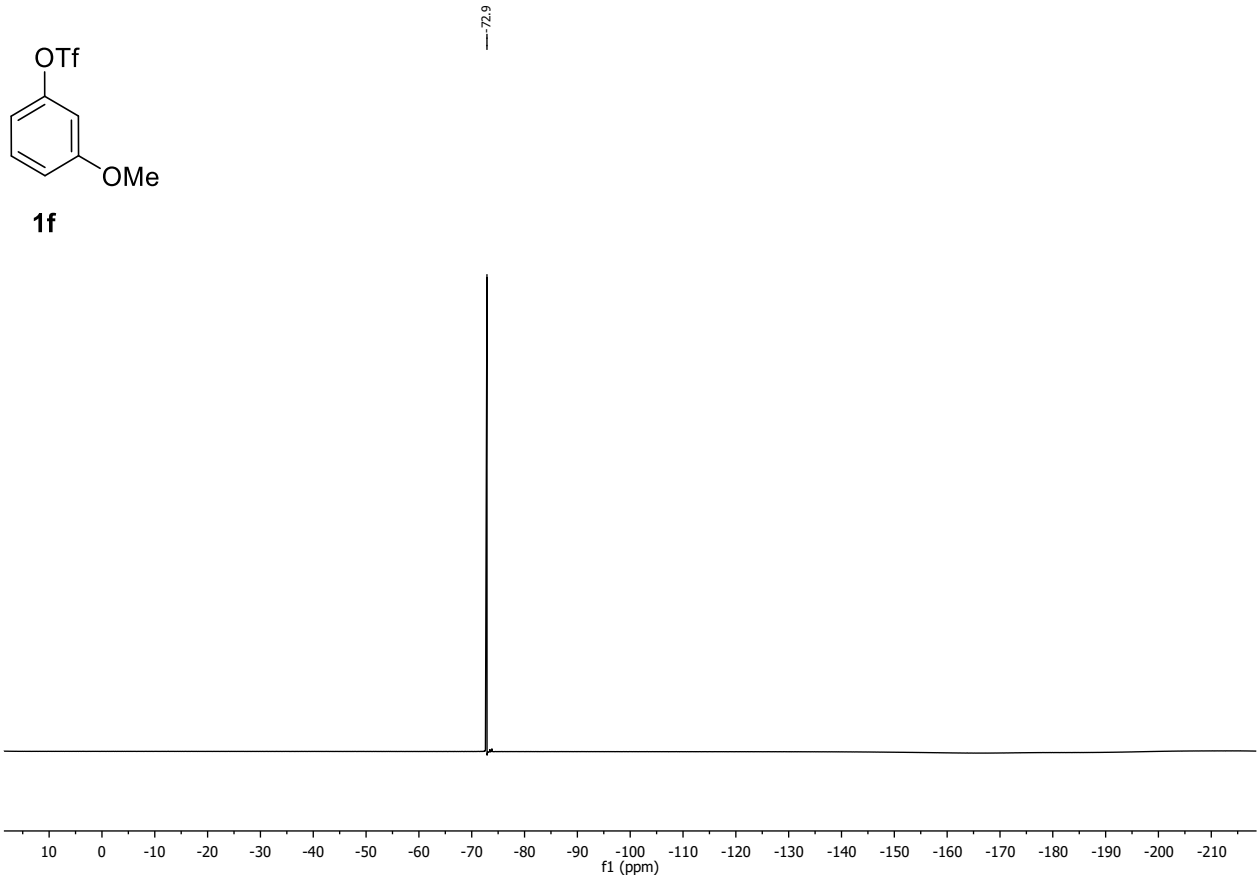

4-Acetamidophenyl trifluoromethanesulfonate (1g):

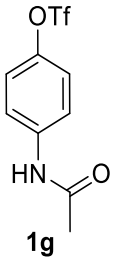

1g

$C_9H_8F_3NO_4S$ (283.22 g/mol)

Following **GP-A**, **1g** was synthesized using *N*-(4-hydroxyphenyl)acetamide (1.51 g, 10.0 mmol, 1.0 equiv.). Purification by column chromatography (SiO_2, *n*-hexane/EtOAc 50:50) afforded **1g** (1.4 g, 4.9 mmol, 48%) as a colorless liquid. Conforms to reported analytical data.[12]

R_f: 0.34 (*n*-hexane/EtOAc 50:50).

^{1}H-NMR (400 MHz, $CDCl_3$, δ): 7.60 (d, *J* = 8.9 Hz, 2H), 7.45 (br s, 1H), 7.22 (d, *J* = 8.9 Hz, 2H), 2.19 (s, 3H).

^{13}C-NMR (101 MHz, $CDCl_3$, δ): 168.6, 145.4, 138.0, 122.1, 121.2, 118.8 (q, *J* = 321.5 Hz), 24.7.

^{19}F-NMR (376 MHz, $CDCl_3$, δ): -72.7.

^{1}H-NMR (400 MHz, $CDCl_3$) of compound **1g**:

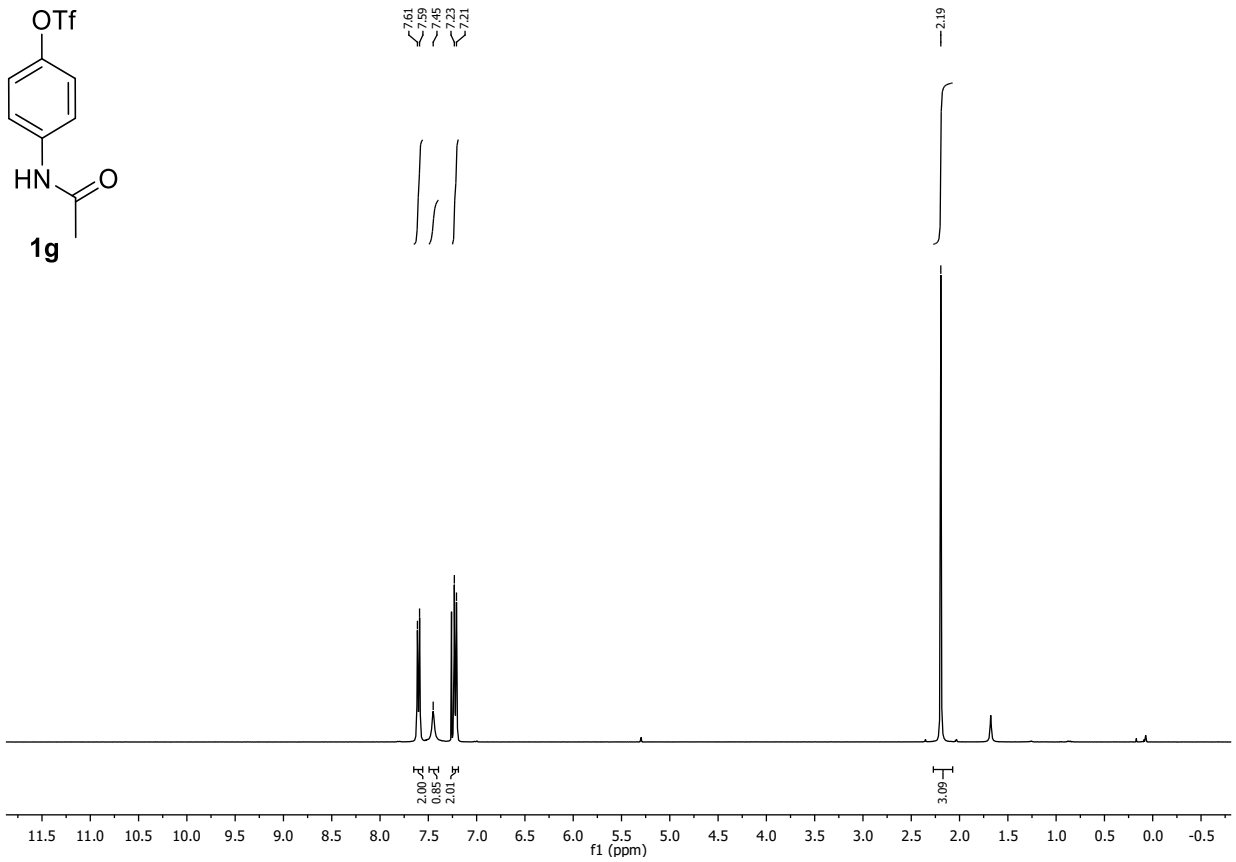

^{13}C-NMR (101 MHz, $CDCl_3$) of compound **1g**:

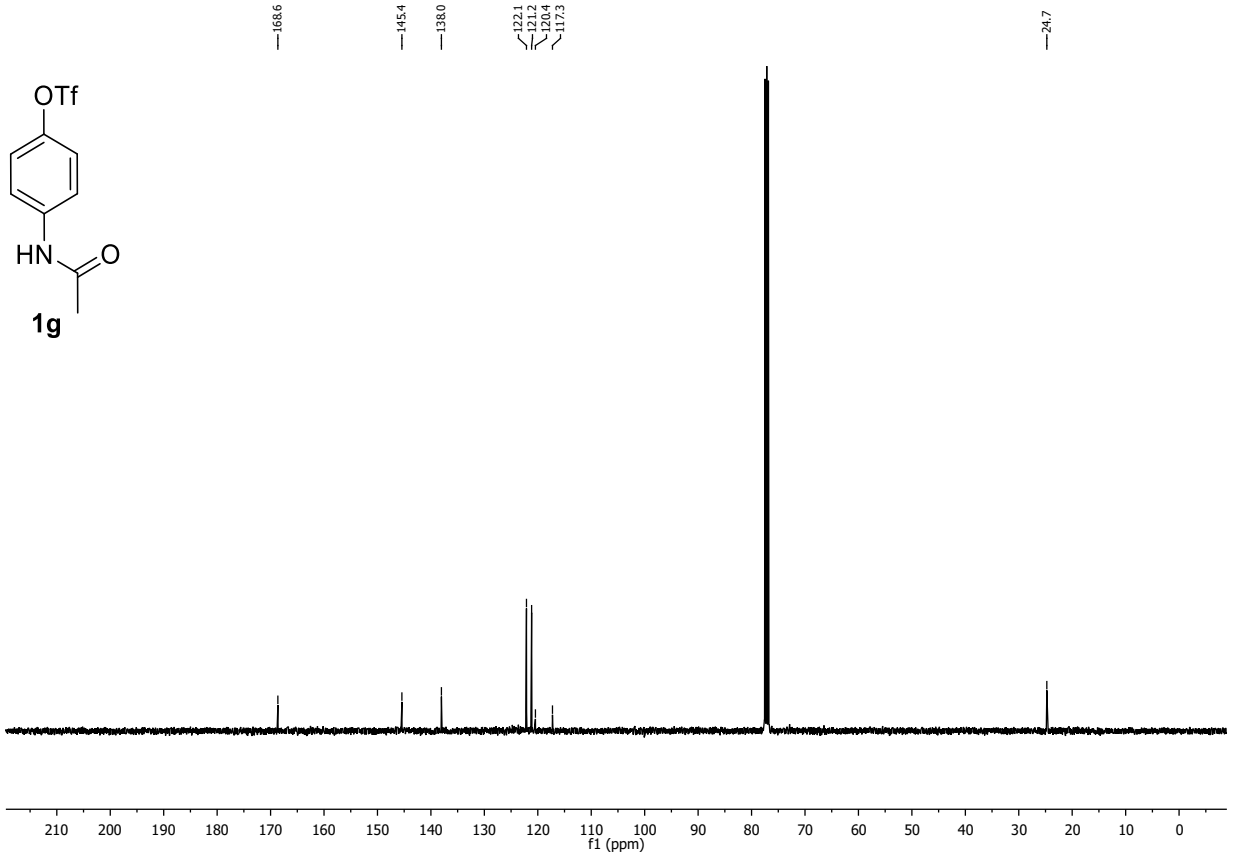

^{19}F-NMR (376 MHz, $CDCl_3$) of compound **1g**:

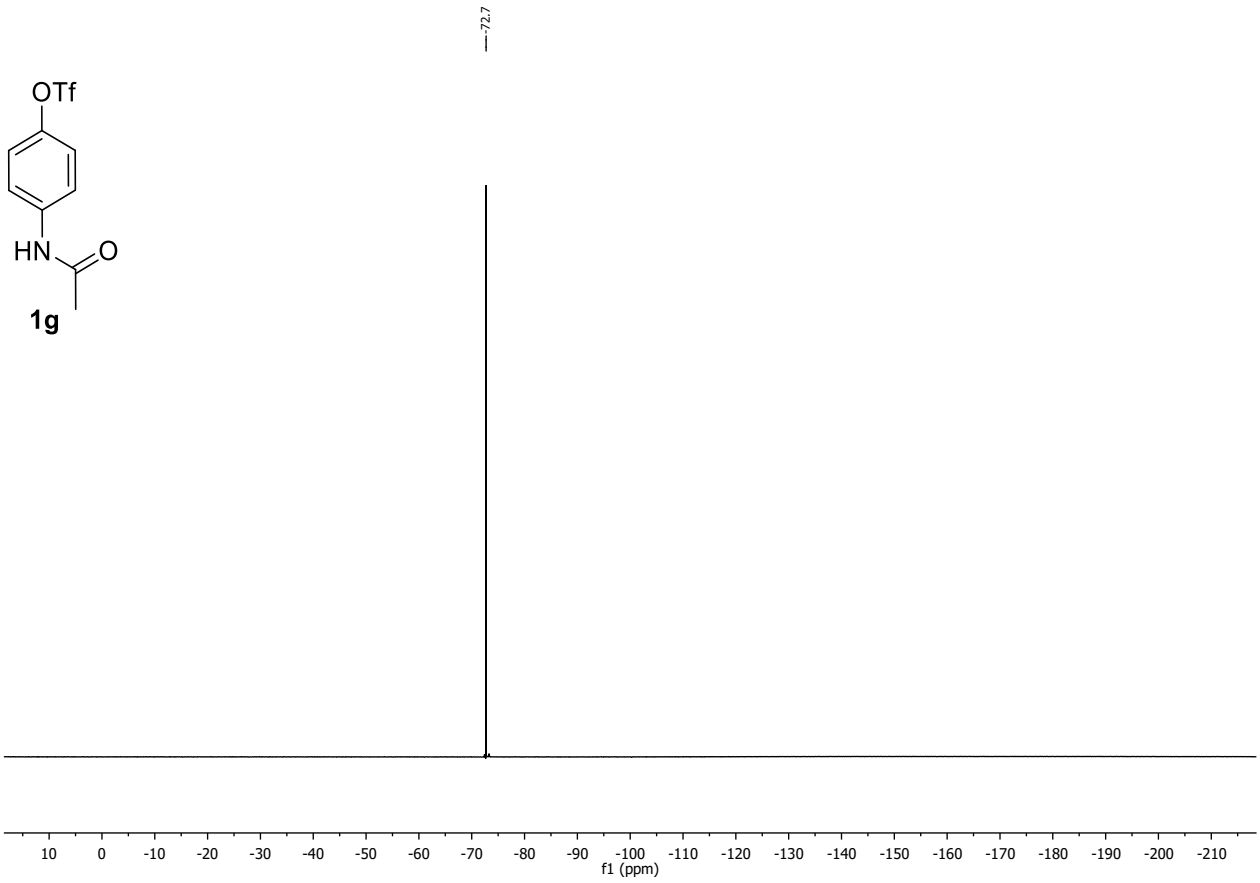

4-Methyl-2-oxo-2*H*-chromen-7-yl trifluoromethanesulfonate (1i):

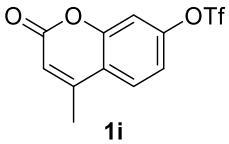

1i

$C_{11}H_7F_3O_5S$ (308.23 g/mol)

Following **GP-A**, **1i** was synthesized using 4-methylumbelliferone (1.76 g, 10.0 mmol, 1.0 equiv.). Purification by column chromatography (SiO_2, *n*-hexane/EtOAc 8:2) afforded **1i** (1.57 g, 5.09 mmol, 51%) as an off-white solid. Conforms to reported analytical data.[13]

R_f: 0.34 (*n*-hexane/EtOAc 8:2).

^{1}H-NMR (400 MHz, $CDCl_3$, δ): 7.70 (d, *J* = 8.7 Hz, 1H), 7.28 (d, *J* = 2.4 Hz, 1H), 7.26 – 7.23 (m, 1H), 6.36 (d, *J* = 1.3 Hz, 1H), 2.46 (d, *J* = 1.3 Hz, 3H).

^{13}C-NMR (101 MHz, $CDCl_3$, δ): 159.6, 154.3, 151.3, 150.9, 126.5, 120.2, 118.8 (q, *J* = 320.9 Hz), 117.6, 116.1, 110.7, 18.9.

^{19}F-NMR (376 MHz, $CDCl_3$, δ): -72.5.

^{1}H-NMR (400 MHz, $CDCl_3$) of compound **1i**:

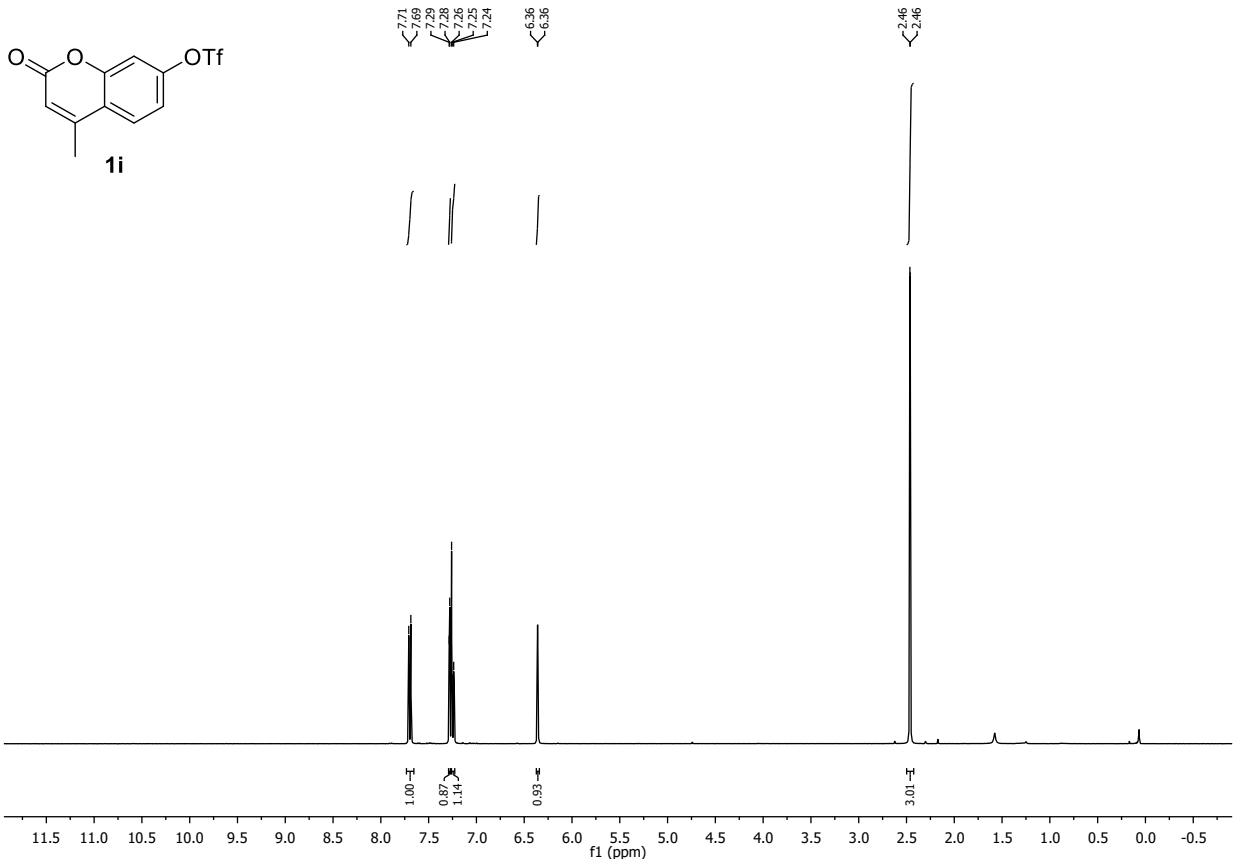

^{13}C-NMR (101 MHz, $CDCl_3$) of compound **1i**:

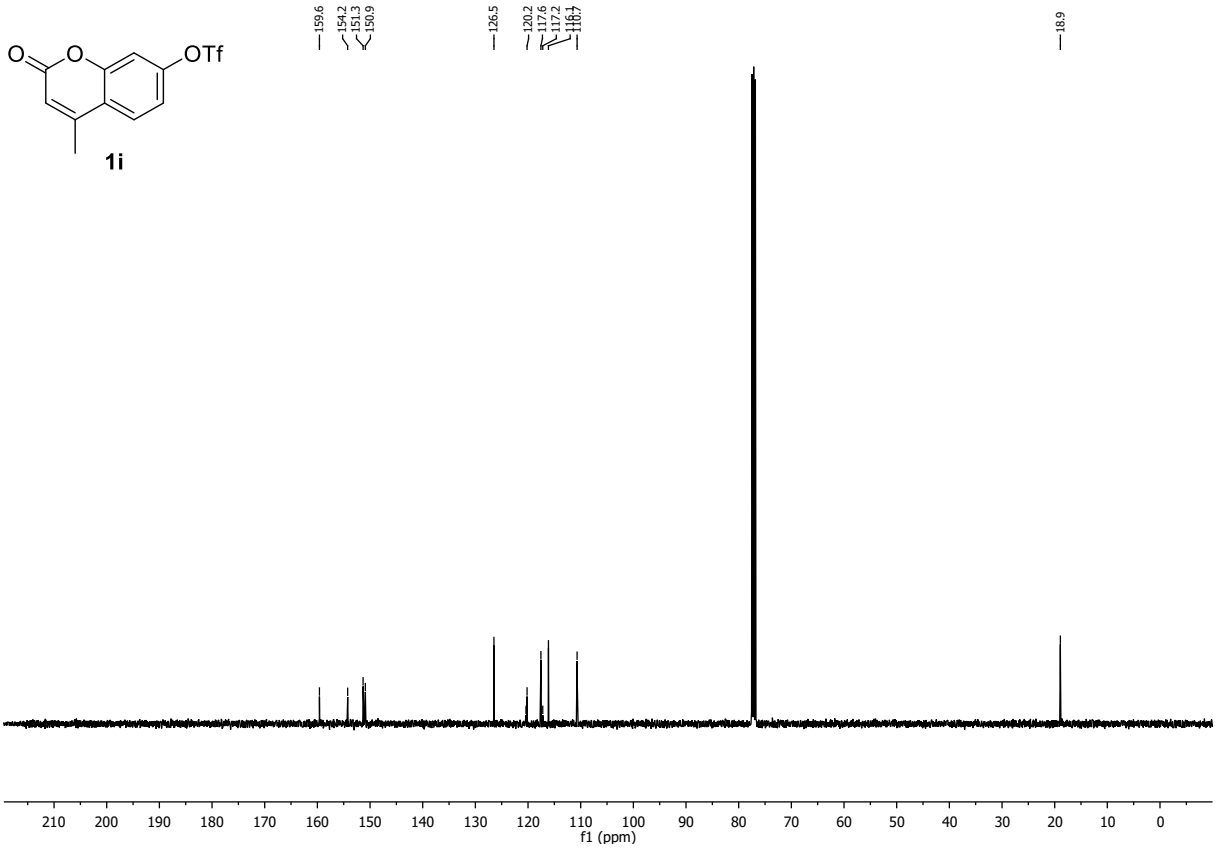

^{19}F-NMR (376 MHz, $CDCl_3$) of compound **1i**:

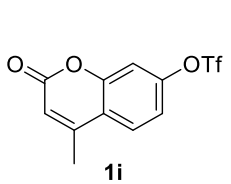

1i

Benzo[*d*][1,3]dioxol-5-yl trifluoromethanesulfonate (1j):

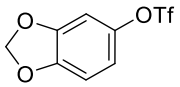

1j

$C_8H_5F_3O_5S$ (270.18 g/mol)

Following **GP-A**, **1j** was synthesized using benzo[*d*][1,3]dioxol-5-ol (1.38 g, 10.0 mmol, 1.0 equiv.). Purification by column chromatography (SiO_2, *n*-hexane/EtOAc 9:1) afforded **1j** (2.43 g, 8.99 mmol, 90%) as a colorless oil. Conforms to reported analytical data.[14]

R_f: 0.45 (*n*-hexane/EtOAc 9:1).

^{1}H-NMR (400 MHz, $CDCl_3$, δ): 6.84 – 6.71 (m, 3H), 6.05 (s, 2H).

^{13}C-NMR (101 MHz, $CDCl_3$, δ): 148.7, 147.6, 143.6, 118.9 (q, *J* = 320.6 Hz), 114.5, 108.4, 103.5, 102.6.

^{19}F-NMR (376 MHz, $CDCl_3$, δ): -72.7.

^{1}H-NMR (400 MHz, $CDCl_3$) of compound **1j**:

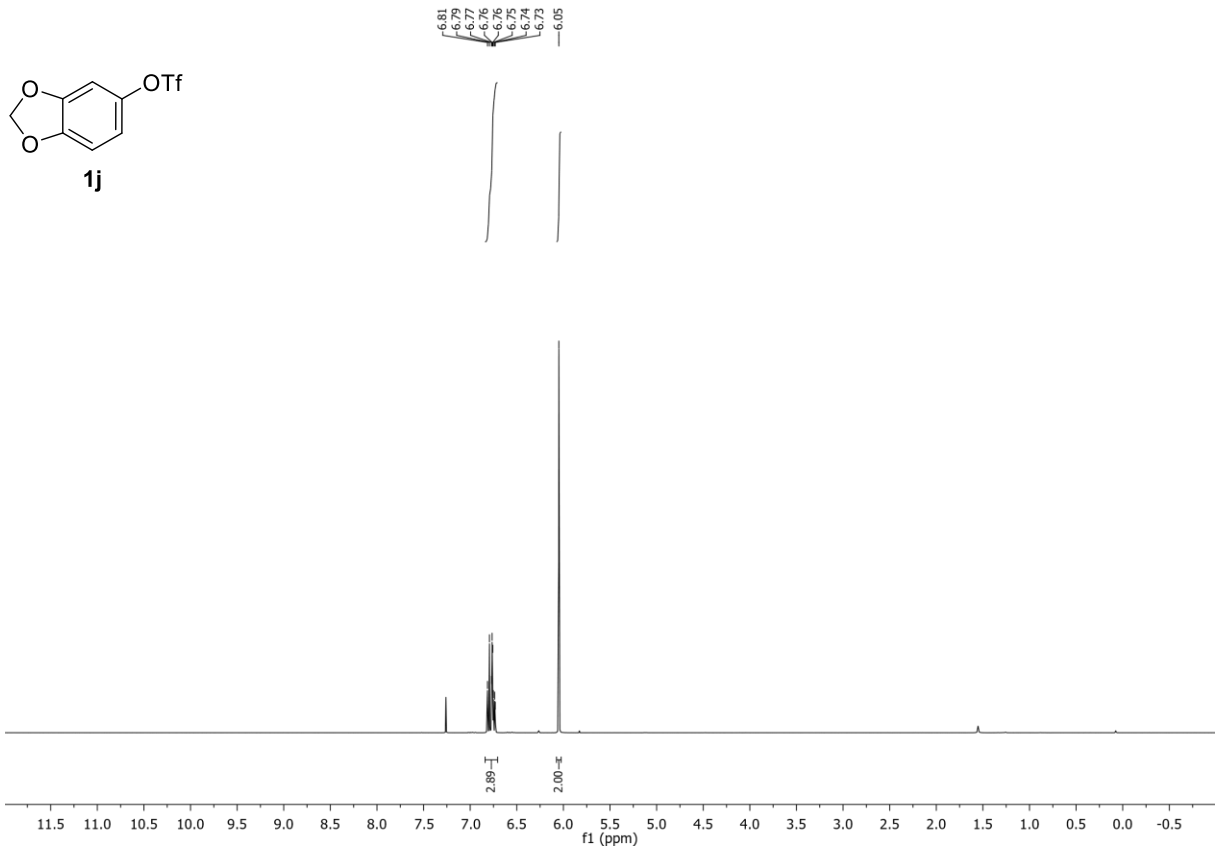

^{13}C-NMR (101 MHz, $CDCl_3$) of compound **1j**:

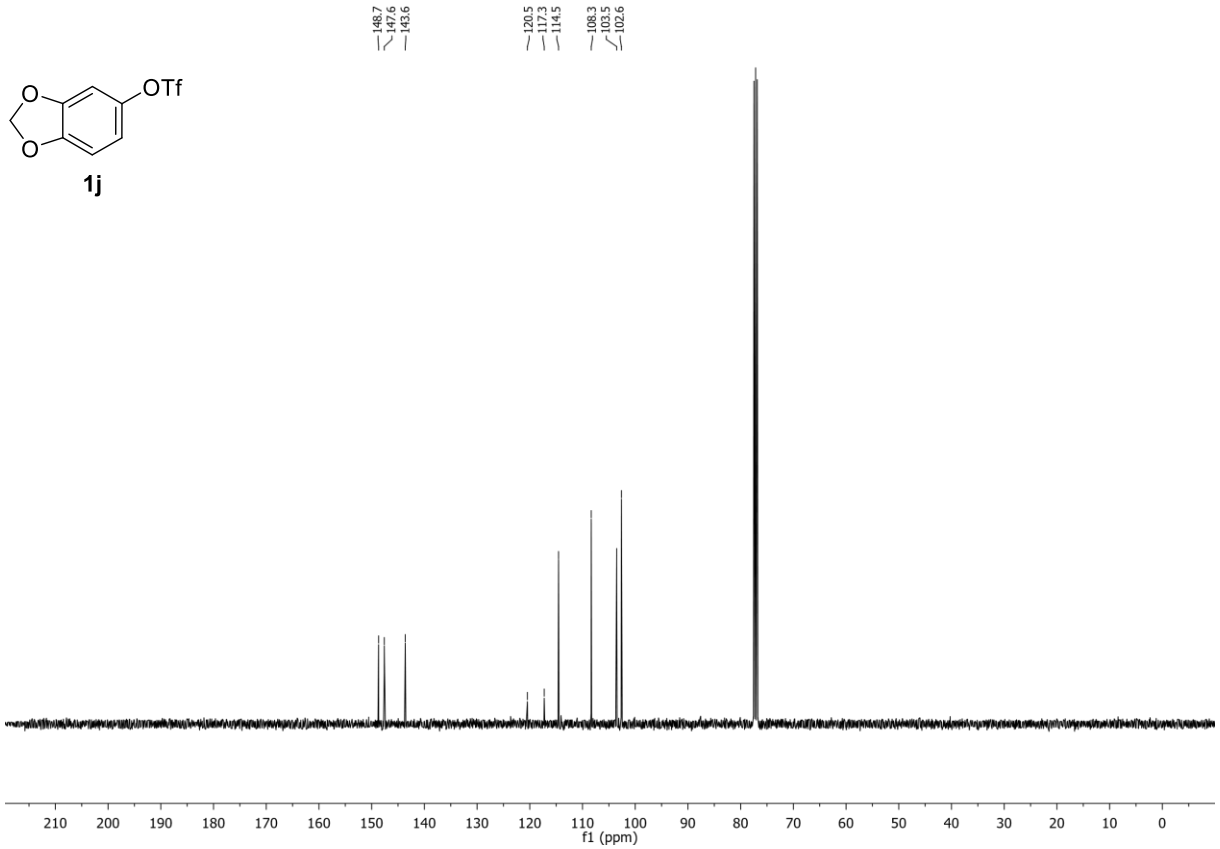

^{19}F-NMR (376 MHz, $CDCl_3$) of compound **1j**:

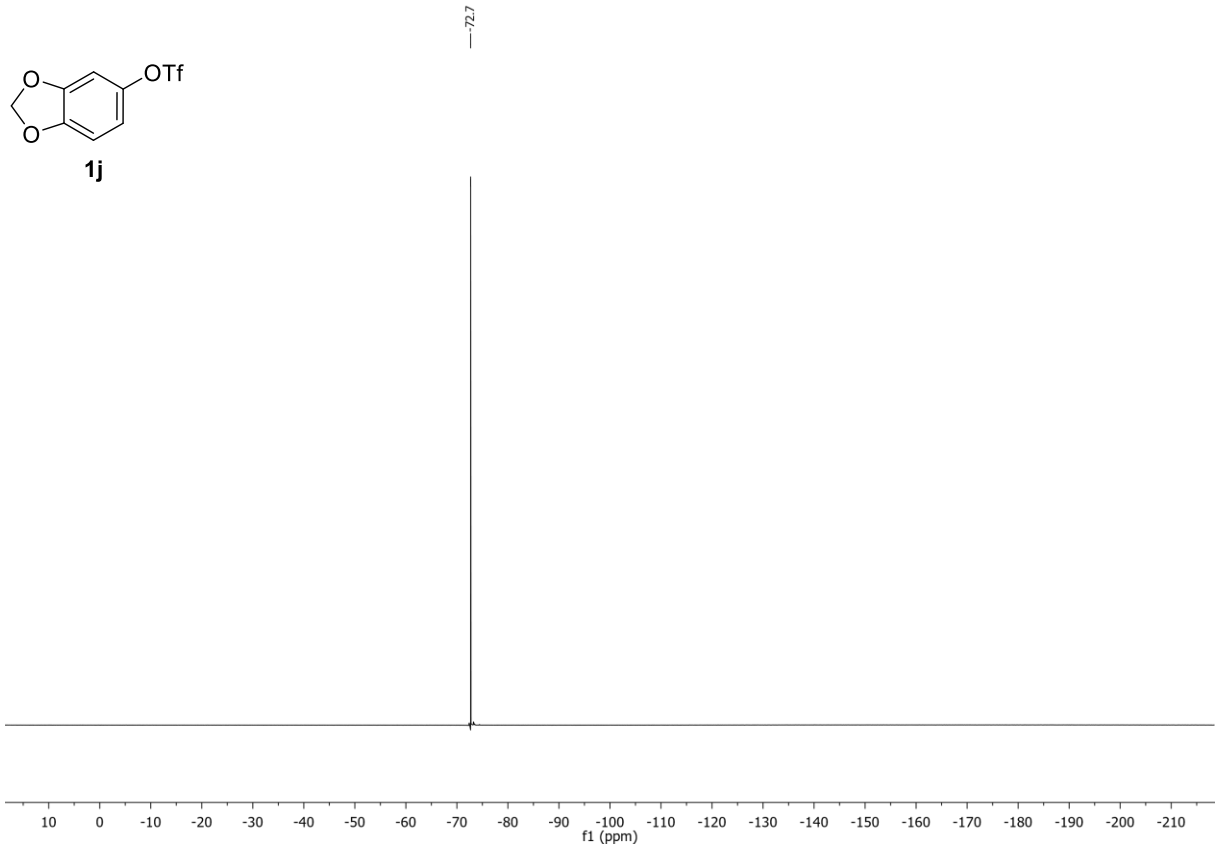

1j

Pyridin-3-yl trifluoromethanesulfonate (1k):

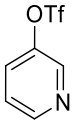

1k

$C_6H_4F_3NO_3S$ (227.16 g/mol)

Following **GP-A**, **1k** was synthesized using pyridine-3-ol (951 mg, 10.0 mmol, 1.0 equiv.). Purification by column chromatography (SiO_2, *n*-hexane/EtOAc 8:2) afforded **1k** (1.73 g, 7.62 mmol, 76%) as pale-yellow oil. Conforms to reported analytical data.[9]

R_f: 0.25 (*n*-hexane/EtOAc 8:2).

^{1}H-NMR (400 MHz, $CDCl_3$, δ): 8.70 – 8.63 (m, 1H), 8.61 (d, *J* = 2.8 Hz, 1H), 7.65 (ddd, *J* = 8.5, 2.8, 1.2 Hz, 1H), 7.43 (dd, *J* = 8.5, 4.7 Hz, 1H).

^{13}C-NMR (101 MHz, $CDCl_3$, δ): 149.6, 146.9, 143.0, 129.2, 118.8 (q, *J* = 321.0 Hz).

^{19}F-NMR (376 MHz, $CDCl_3$, δ): -72.6.

^{1}H-NMR (400 MHz, $CDCl_3$) of compound **1k**:

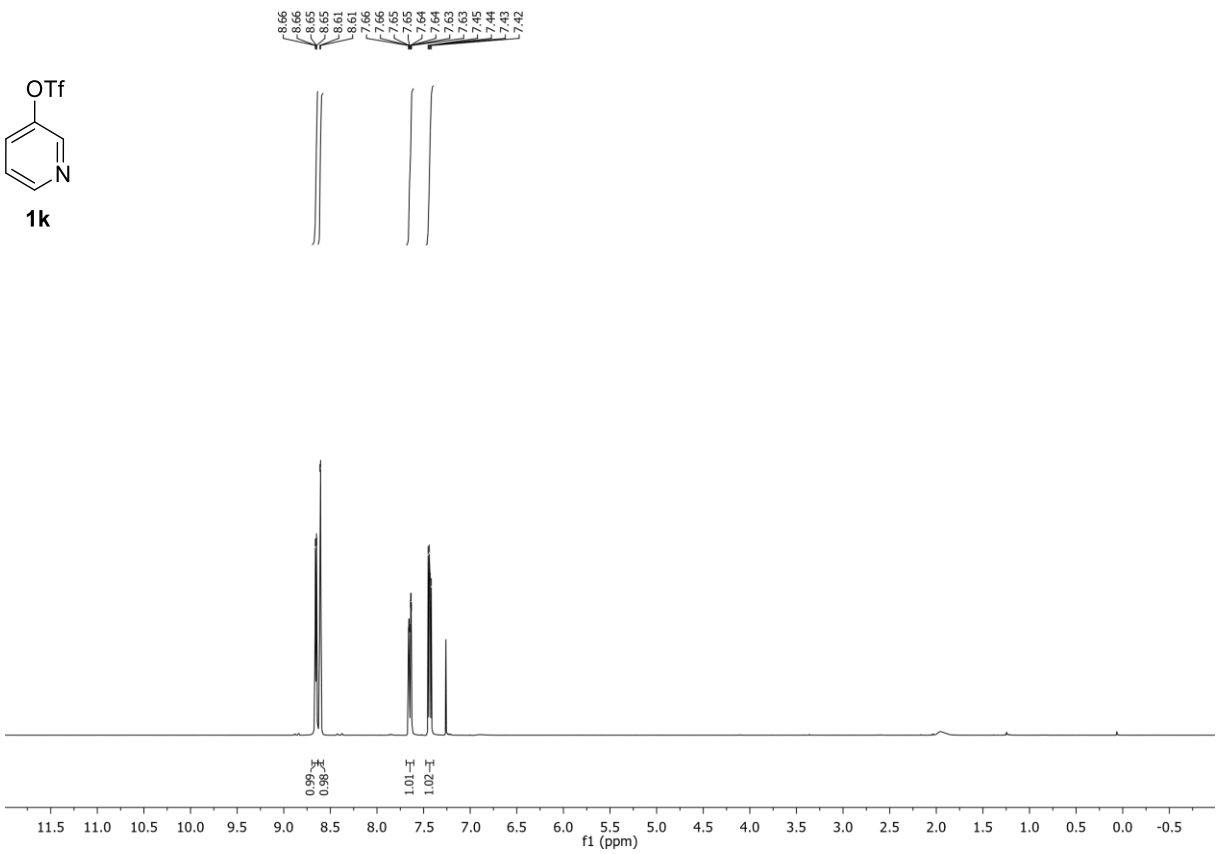

^{13}C-NMR (101 MHz, $CDCl_3$) of compound **1k**:

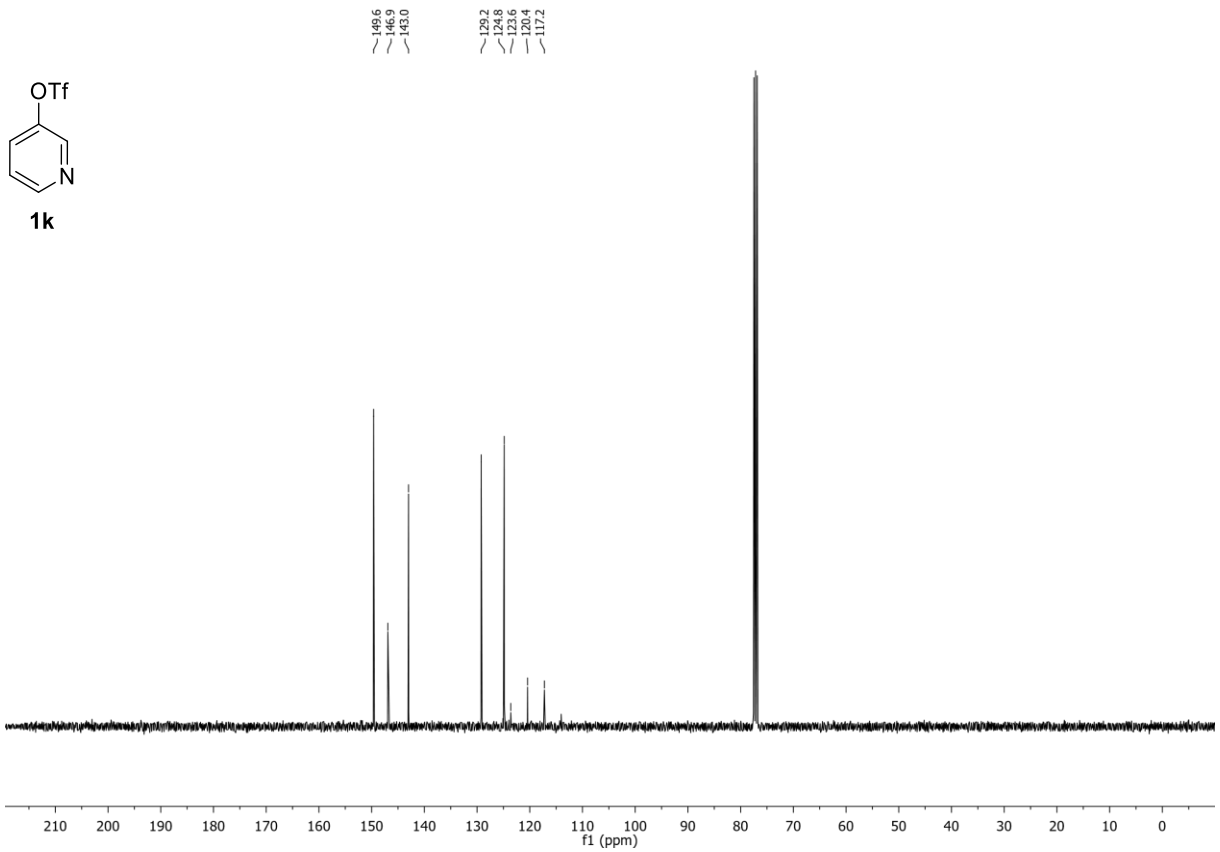

^{19}F-NMR (376 MHz, $CDCl_3$) of compound **1k**:

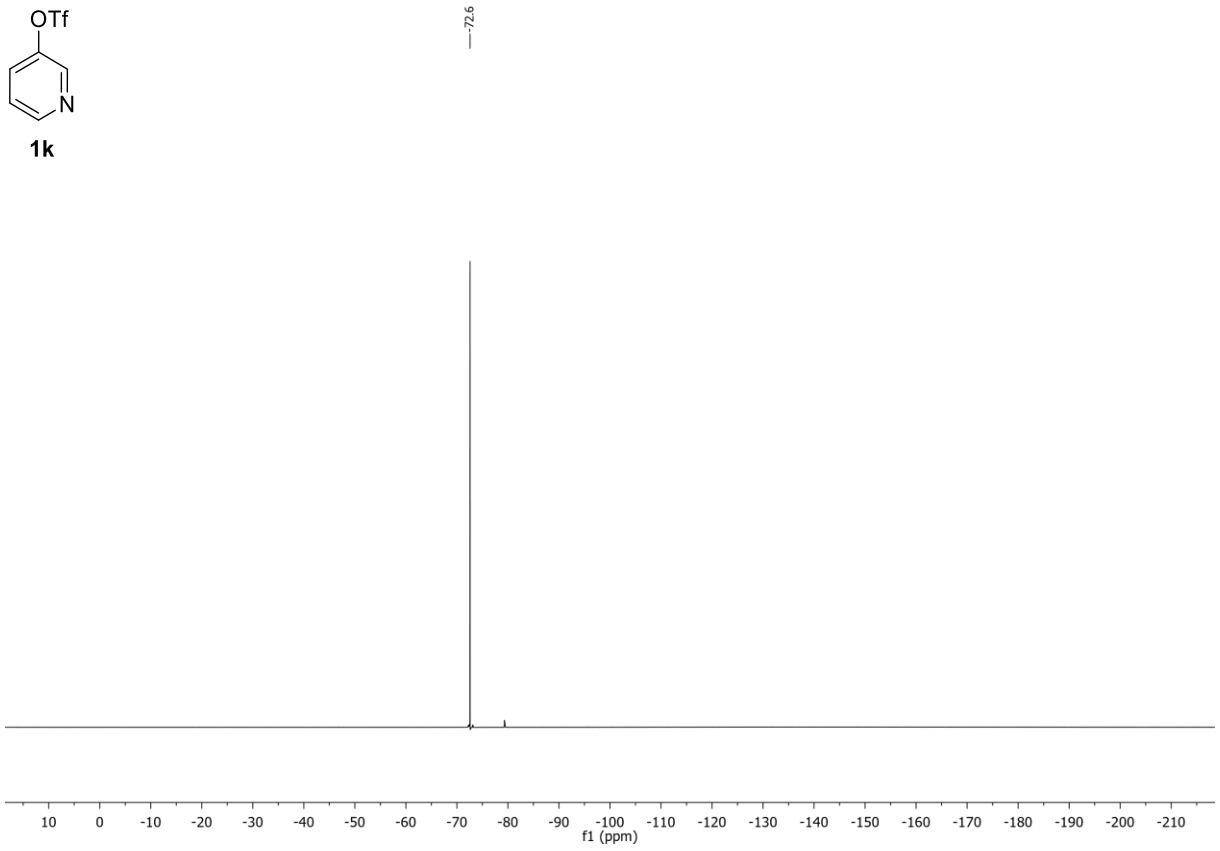

4-(((Trifluoromethyl)sulfonyl)oxy)phenyl 4-methylbenzenesulfonate (1o):

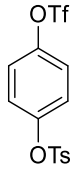

1o

$C_{14}H_{11}F_3O_6S_2$ (396.35 g/mol)

1o was synthesized following literature procedure.[7] Hydrochinone (1,1 g, 10 mmol, 1.0 equiv.) was dissolved in dry DCM (20 mL). Analytical grade pyridine (1.6 mL, 20 mmol, 2.0 equiv.) was added and the stirred solution was cooled to 0 °C. Trifluoromethanesulfonic anhydride (1.7 mL, 10 mmol, 1.0 equiv.) dissolved in dry DCM (10 mL) was added dropwise to the reaction mixture. After the addition was finished the reaction mixture was slowly warmed up to room temperature and stirred for 5 h. After dilution with DCM (15 mL) quenching with aqueous HCl (1M, 10 mL) the reaction mixture was washed with H_2O (10 mL), saturated aqueous solution of $NaHCO_3$ (10 mL) and brine (10 mL). The organic phase was dried over $MgSO_4$, concentrated under reduced pressure and the crude product was purified by column chromatography (SiO_2, *n*-hexane/EtOAc 9:1) to afford 4-hydroxyphenyl trifluoromethanesulfonate as colorless liquid (928 mg, 3.83 mmol, 38%).

To a stirred solution of 4-hydroxyphenyl trifluoromethanesulfonate (928 mg, 3.83 mmol, 1.0 equiv.) in DCM (1.5 mL) and triethylamine (1.5 mL) a solution of 4-toluenesulfonyl chloride (731 mg, 3.83 mmol, 1.0 equiv.) in DCM (1 mL) was added and the reaction mixture was stirred at room temperature for 16 h. Water (5 mL) was added and the reaction mixture was extracted with DCM (3 x 5 mL). The combined organic phases were washed with brine (5 mL), dried over $MgSO_4$ and concentrated under reduced pressure. Purification by FC (SiO_2, gradient to 8:2 *n*-hexane/EtOAc over 20 CV) afforded **1o** (1.15 g, 2.90 mmol, 76%) as colorless solid. Conforms to reported analytical data.[7, 15]

R_f: 0.25 (*n*-hexane/EtOAc 9:1).

^{1}H-NMR (400 MHz, $CDCl_3$, δ): 7.70 (d, *J* = 8.3 Hz, 2H), 7.34 (d, *J* = 8.0 Hz, 2H), 7.24 – 7.19 (m, 2H), 7.11 – 7.06 (m, 2H), 2.46 (s, 3H).

^{13}C-NMR (101 MHz, $CDCl_3$, δ): 149.0, 147.7, 146.1, 131.9, 130.1, 128.7, 124.5, 122.8, 118.6 (q, *J* = 320.7 Hz), 21.9.

^{19}F-NMR (376 MHz, $CDCl_3$, δ): -72.7.

^{1}H-NMR (400 MHz, $CDCl_3$) of compound **1o**:

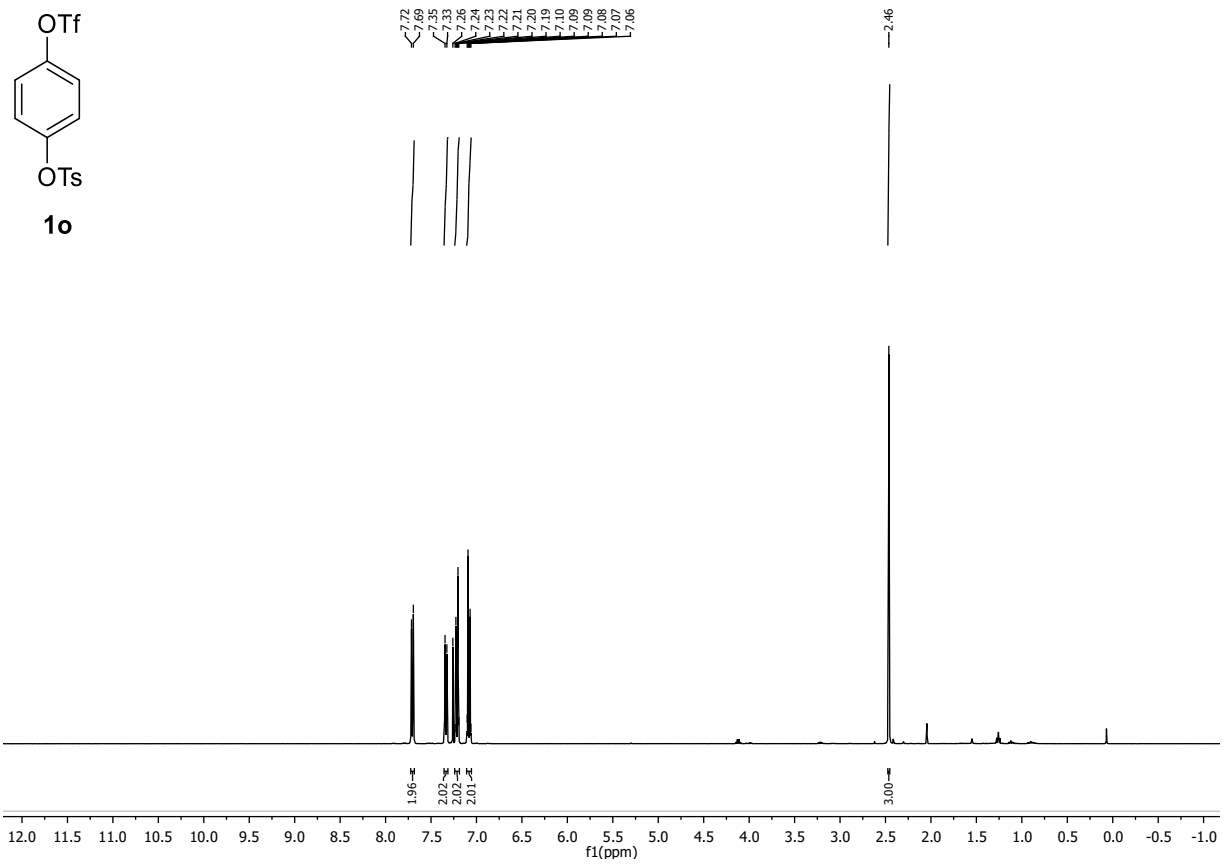

^{13}C-NMR (101 MHz, $CDCl_3$) of compound **1o**:

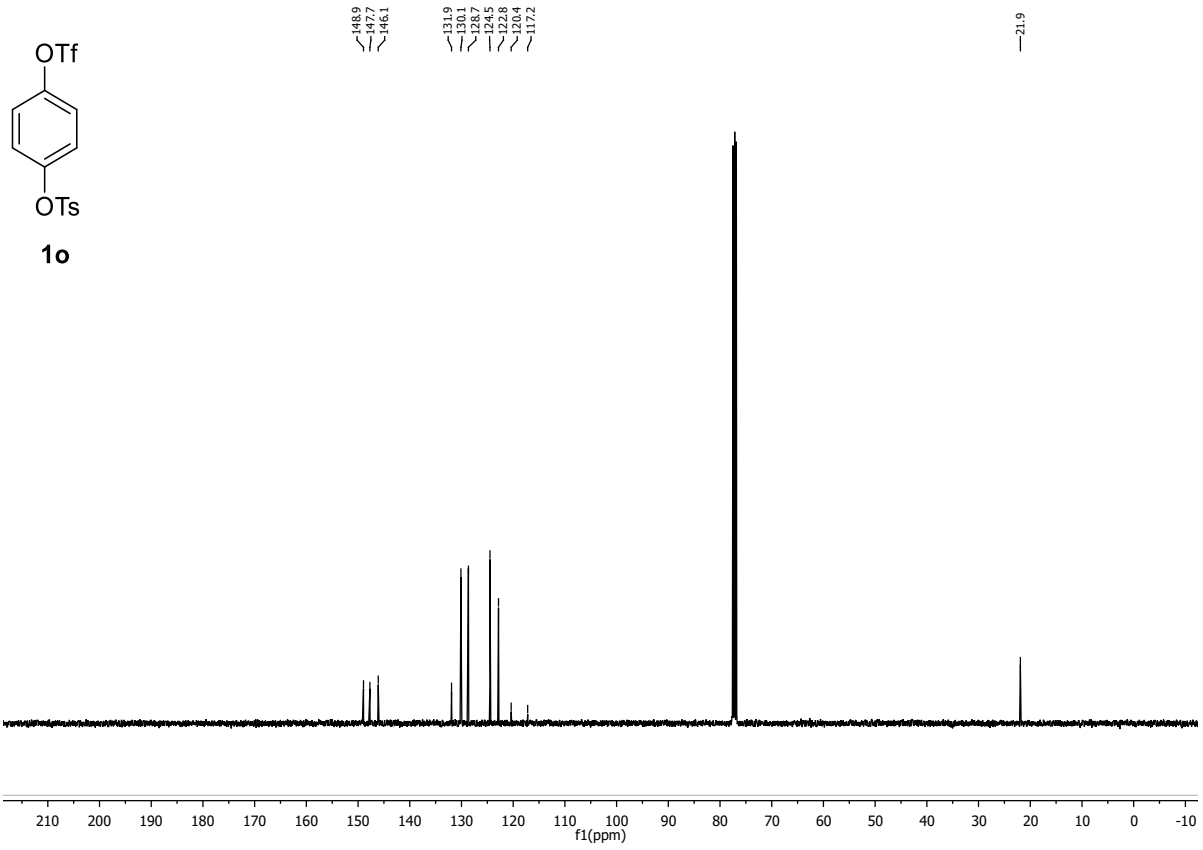

^{19}F-NMR (376 MHz, $CDCl_3$) of compound **1o**:

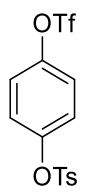

1o

(8*R*,9*S*,13*S*,14*S*)-13-Methyl-17-oxo-7,8,9,11,12,13,14,15,16,17-decahydro-6*H*-cyclopenta[*a*] phenanthrene-3-yl trifluoromethanesulfonate (1q):

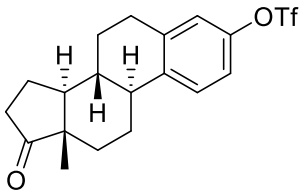

1q

$C_{19}H_{21}F_3O_4S$ (402.43 g/mol)

Following **GP-A**, **1q** was synthesized using Estrone (500 mg, 1.85 mmol, 1.0 equiv.). Purification by column chromatography (SiO_2, *n*-hexane/EtOAc 8:2) afforded **1q** (643 mg, 1.60 mmol, 86%) as a colorless solid. Conforms to reported analytical data.[16]

R_f: 0.72 (*n*-hexane/EtOAc 8:2).

^{1}H-NMR (400 MHz, $CDCl_3$, δ): 7.34 (d, *J* = 8.6 Hz, 1H), 7.04 (dd, *J* = 8.6, 2.7 Hz, 1H), 6.99 (d, *J* = 2.7 Hz, 1H), 2.98 – 2.90 (m, 2H), 2.58 – 2.46 (m, 1H), 2.45 – 2.24 (m, 2H), 2.21 – 1.92 (m, 4H), 1.63 – 1.47 (m, 6H), 0.92 (s, 3H).

^{13}C-NMR (101 MHz, $CDCl_3$, δ): 220.5, 147.7, 140.4, 139.4, 127.3, 121.4, 118.9 (q, *J* = 320.9 Hz), 118.4, 50.5, 48.0, 44.2, 37.9, 35.9, 31.6, 29.5, 26.2, 25.8, 21.7, 13.9.

^{19}F-NMR (376 MHz, $CDCl_3$, δ): -72.9.

^{1}H-NMR (400 MHz, $CDCl_3$) of compound **1q**:

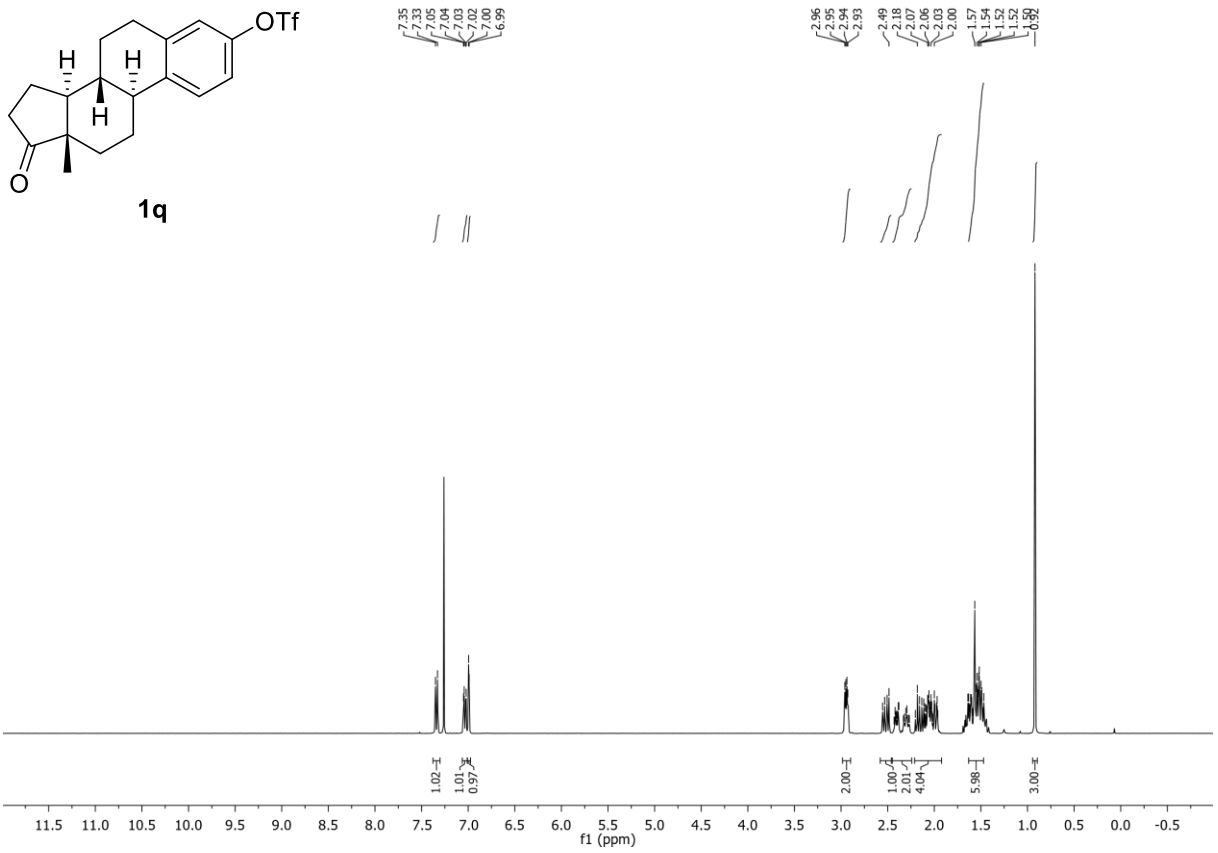

^{13}C-NMR (101 MHz, $CDCl_3$) of compound **1q**:

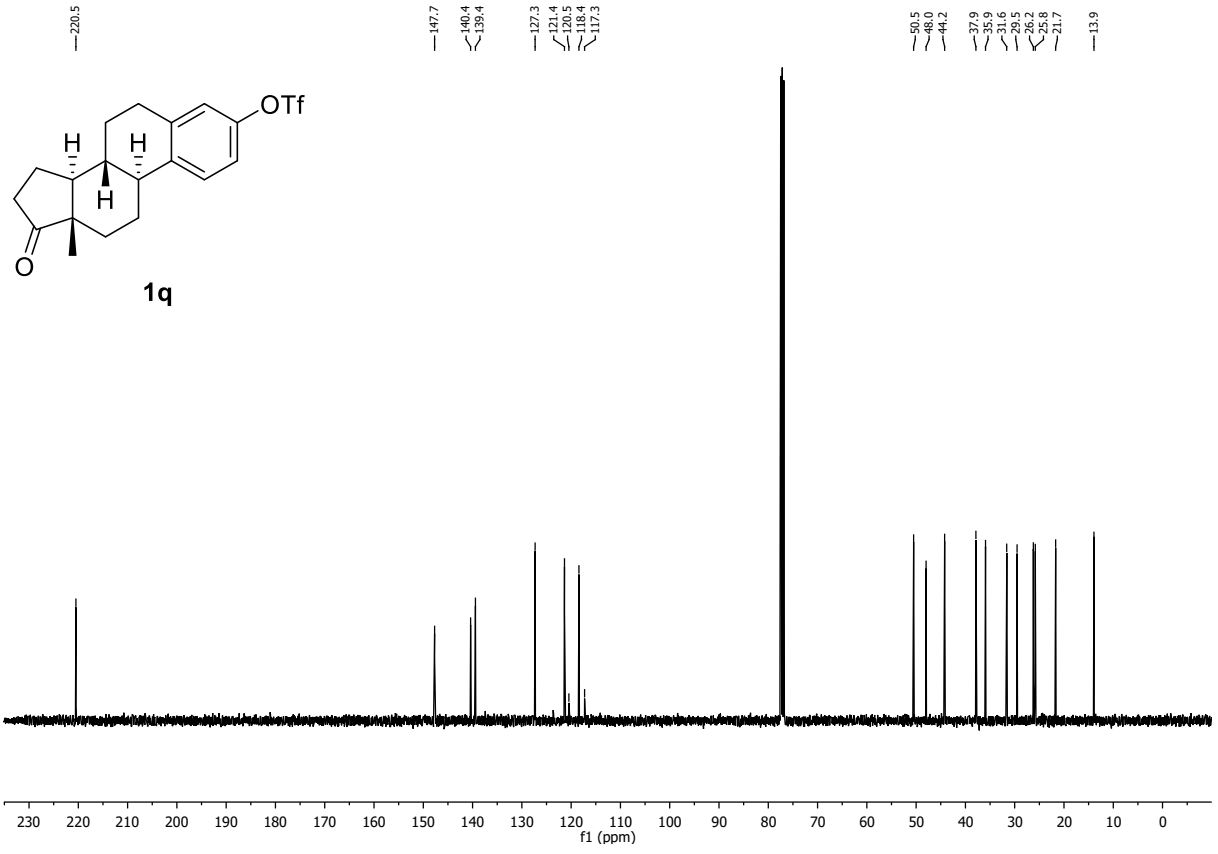

^{19}F-NMR (376 MHz, $CDCl_3$) of compound **1q**:

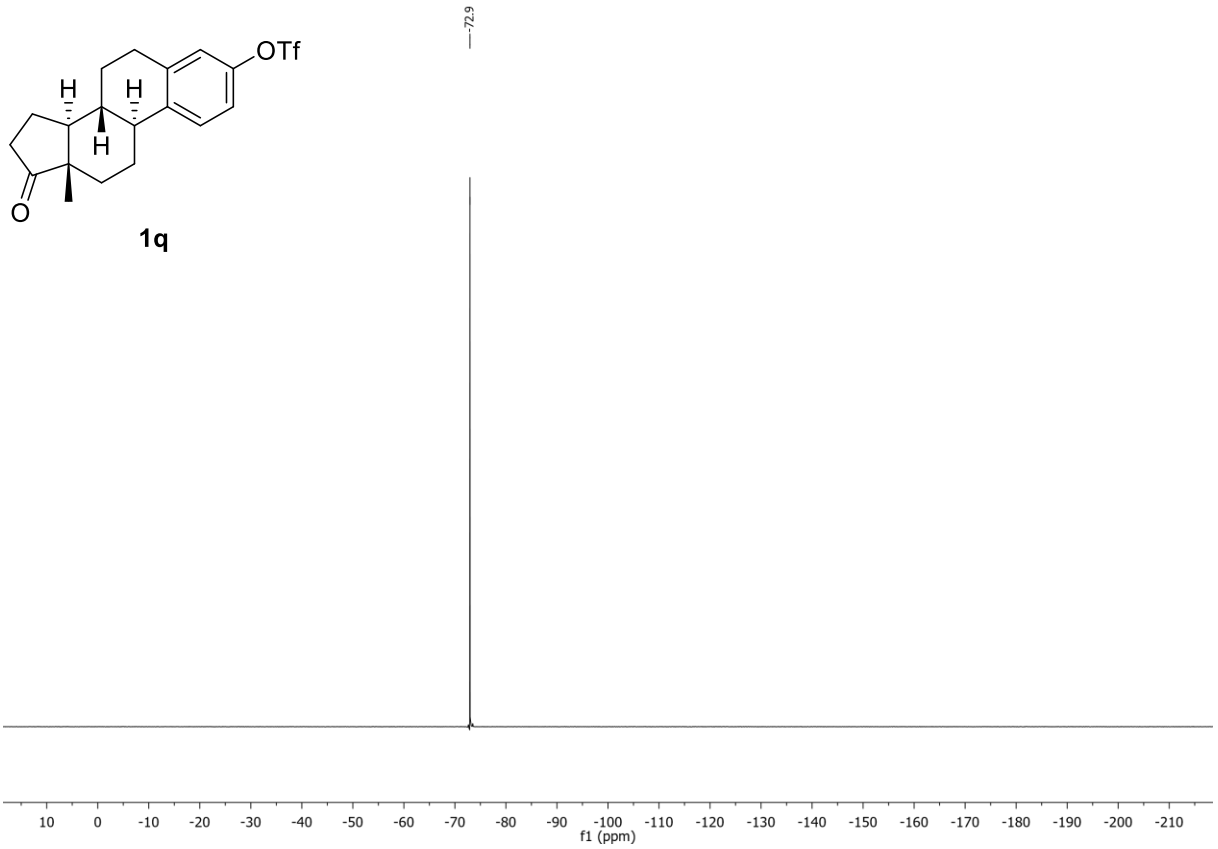

4-((2*S*,3*R*)-1-(4-Fluorophenyl)-3-((*S*)-3-(4-fluorophenyl)-3-hydroxypropyl)-4-oxoazetidin-2-yl)phenyl trifluoromethanesulfonate (1r):

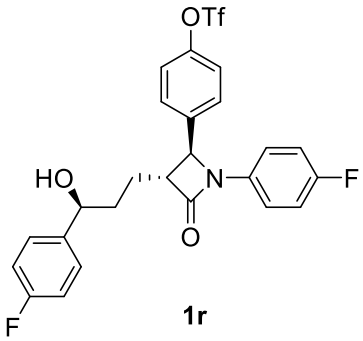

1r

$C_{25}H_{20}F_5NO_5S$ (541.49 g/mol)

Following **GP-A**, **1r** was synthesized using Ezetimibe (700 mg, 1.71 mmol, 1.0 equiv.). Purification by column chromatography (SiO_2, *n*-hexane/EtOAc 8:2) afforded **1r** (284 mg, 524 µmol, 31%) as a pale-yellow solid. Conforms to reported analytical data.[17]

R_f: 0.10 (*n*-hexane/EtOAc 8:2).

^{1}H-NMR (400 MHz, $CDCl_3$, δ): 7.44 – 7.38 (m, 2H), 7.31 – 7.27 (m, 4H), 7.23 – 7.16 (m, 2H), 7.07 – 6.91 (m, 4H), 4.73 (t, *J* = 6.1 Hz, 1H), 4.67 (d, *J* = 2.3 Hz, 1H), 3.02 – 3.11 (m, 1H), 2.06 – 1.85 (m, 4H).

^{13}C-NMR (101 MHz, $CDCl_3$, δ): 167.1, 162.2 (d, *J* = 245.5), 159.2 (d, *J* = 244.1 Hz), 149.4, 140.0 (d, *J* = 3.1 Hz), 138.2, 133.4 (d, *J* = 2.6 Hz), 127.8, 127.4 (d, *J* = 8.1 Hz), 122.4, 118.7 (q, *J* = 320.8 Hz), 118.4 (d, *J* = 8.0 Hz), 116.1 (d, *J* = 22.7 Hz), 115.4 (d, *J* = 21.3 Hz), 73.0, 60.4, 60.3, 36.5, 25.0.

^{19}F-NMR (376 MHz, $CDCl_3$, δ): -72.8, -114.6, -117.4.

^{1}H-NMR (400 MHz, $CDCl_3$) of compound **1r**:

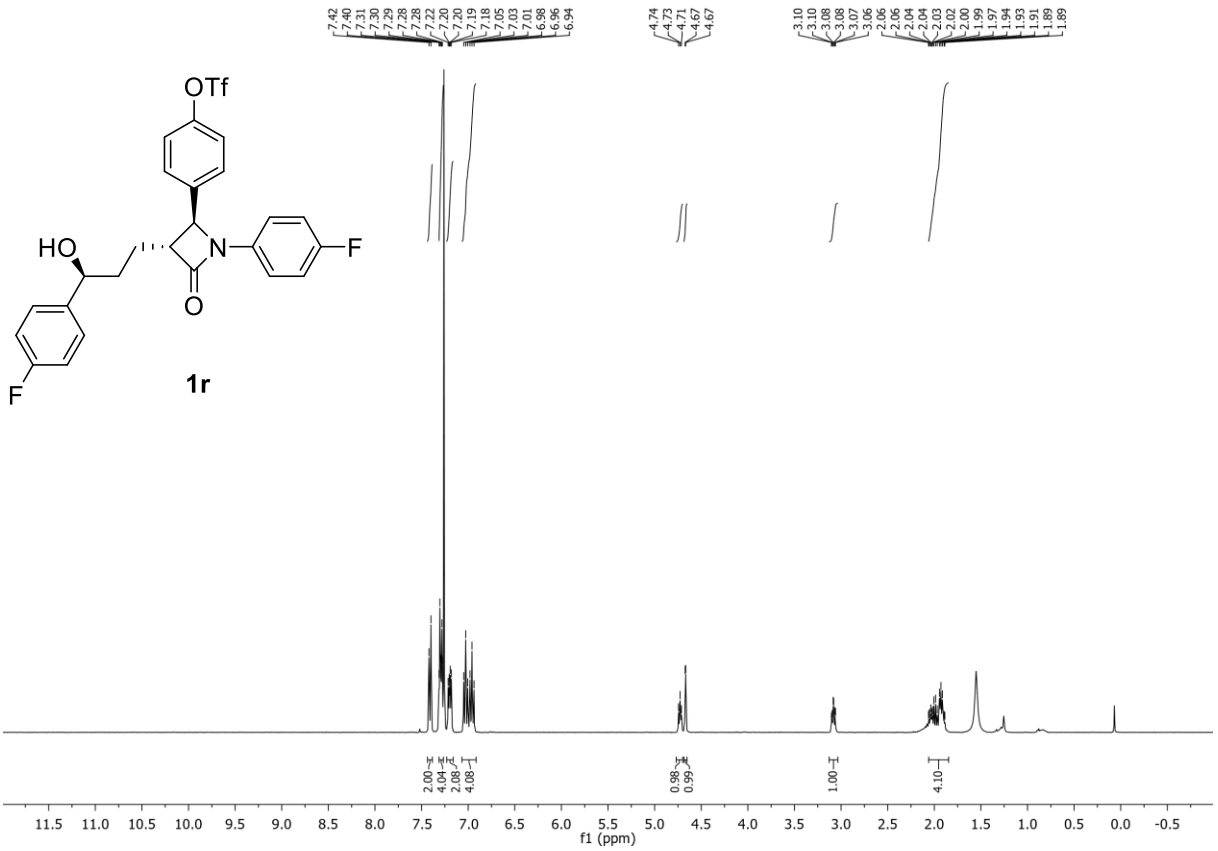

^{13}C-NMR (101 MHz, $CDCl_3$) of compound **1r**:

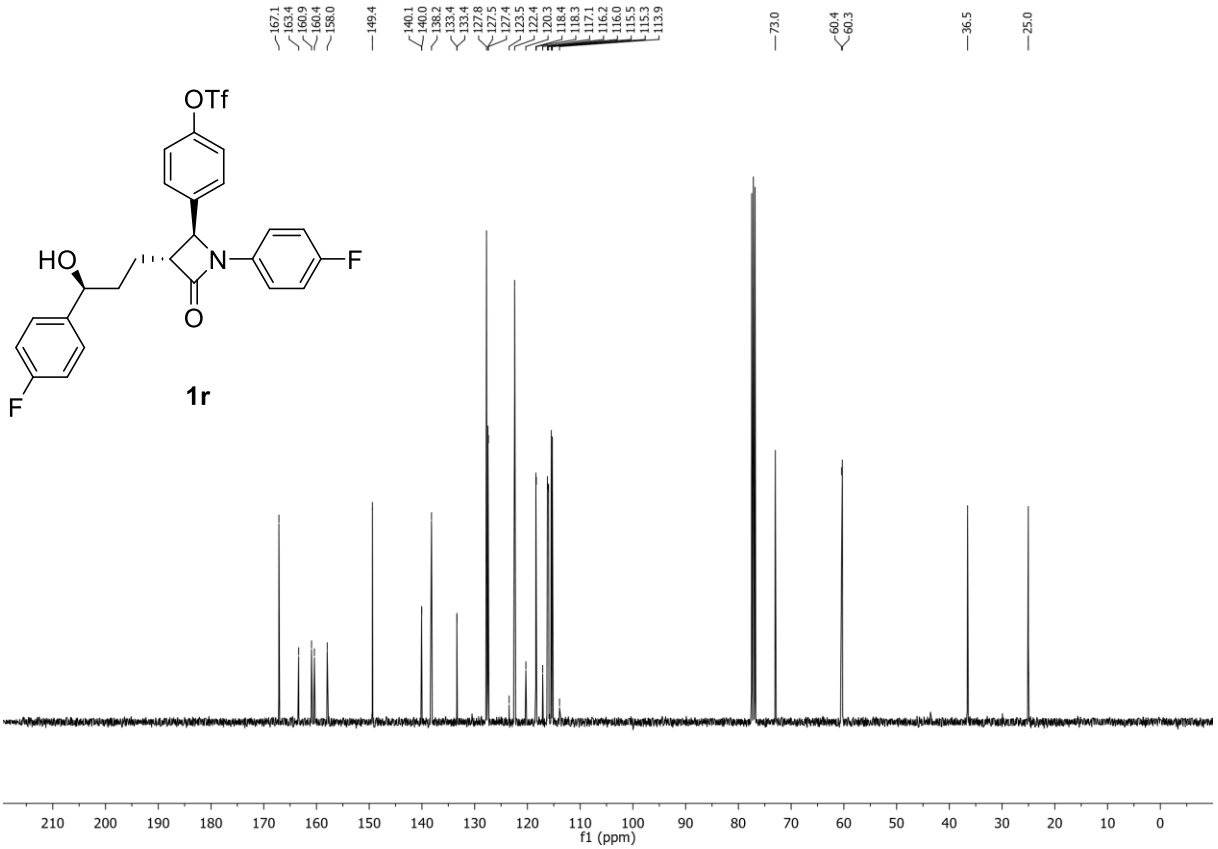

^{19}F-NMR (376 MHz, $CDCl_3$) of compound **1r**:

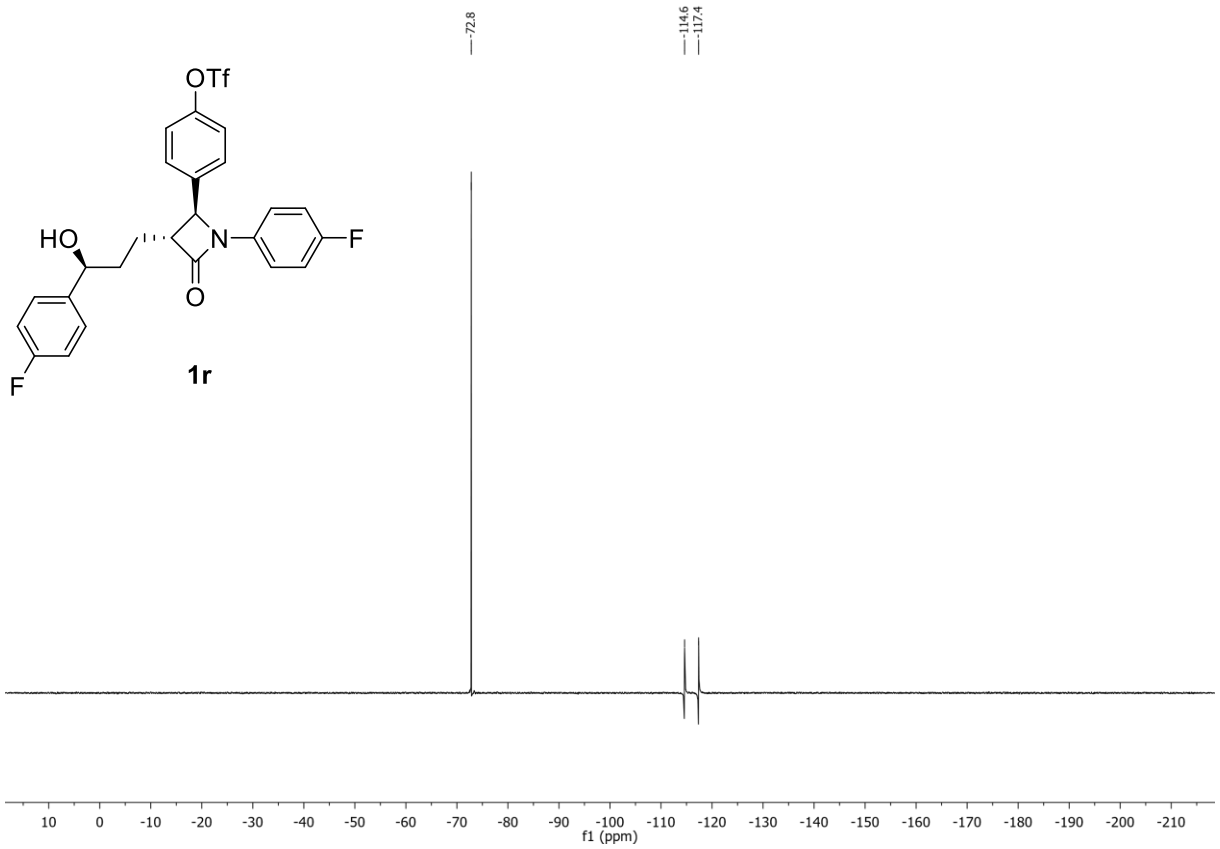

3.2.2. Alkenyltriflates

Cyclohex-1-en-1-yl trifluoromethanesulfonate (4a):

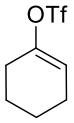

4a

$C_7H_9F_3O_3S$ (230.20 g/mol)

Following **GP-B1**, **4a** was synthesized using cyclohexanone (981 mg, 10.0 mmol, 1.0 equiv.). Purification by column chromatography (SiO_2, *n*-hexane) afforded **4a** (955 mg, 4.15 mmol, 42%) as a pale-green oil. Conforms to reported analytical data.[18]

R_f: 0.65 (*n*-hexane).

^{1}H-NMR (400 MHz, $CDCl_3$, δ): 5.76 (m, 1H), 2.31 (m, 2H), 2.21 – 2.15 (m, 2H), 1.82 – 1.75 (m, 2H), 1.64 – 1.57 (m, 2H).

^{13}C-NMR (101 MHz, $CDCl_3$, δ): 149.4, 118.6 (q, *J* = 319.9 Hz), 118.5, 27.6, 23.9, 22.7, 21.0.

^{19}F-NMR (376 MHz, $CDCl_3$, δ): -74.1.

^{1}H-NMR (400 MHz, $CDCl_3$) of compound **4a**:

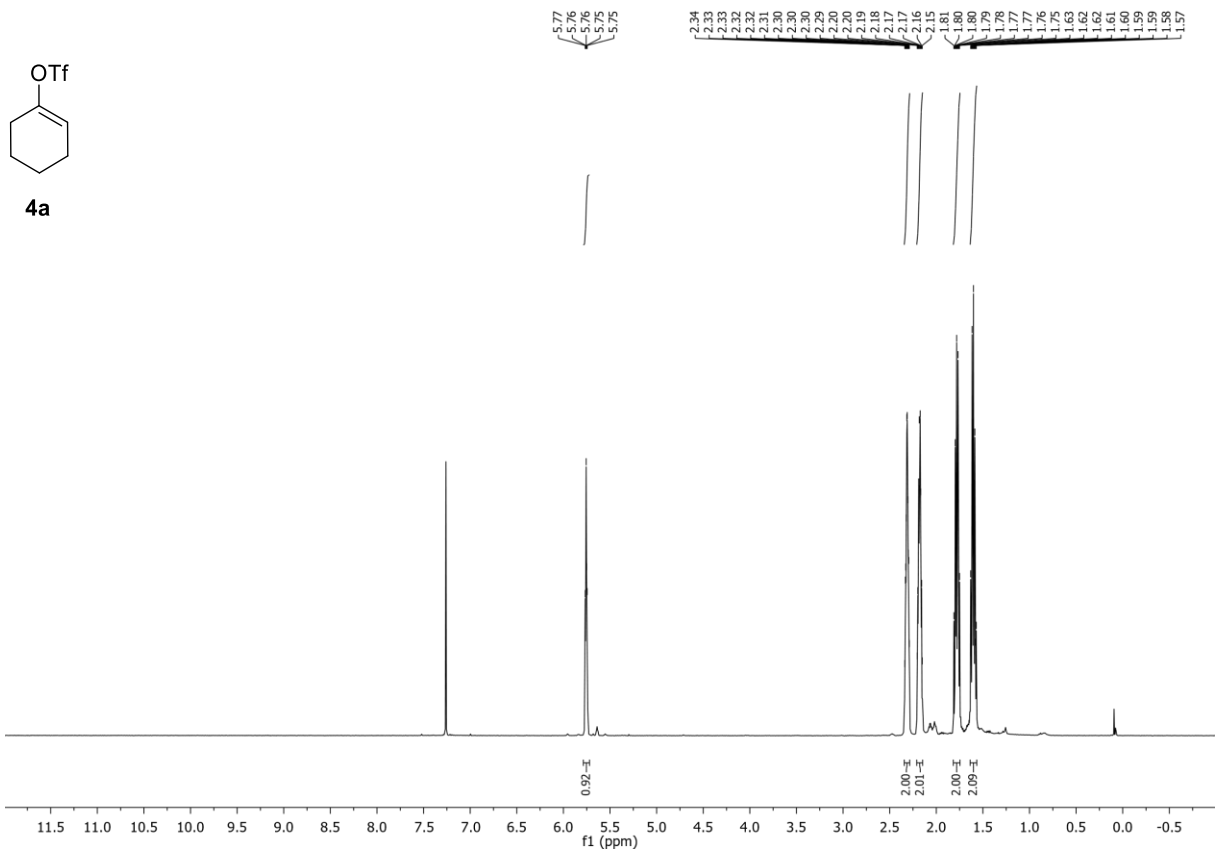

^{13}C-NMR (101 MHz, $CDCl_3$) of compound **4a**:

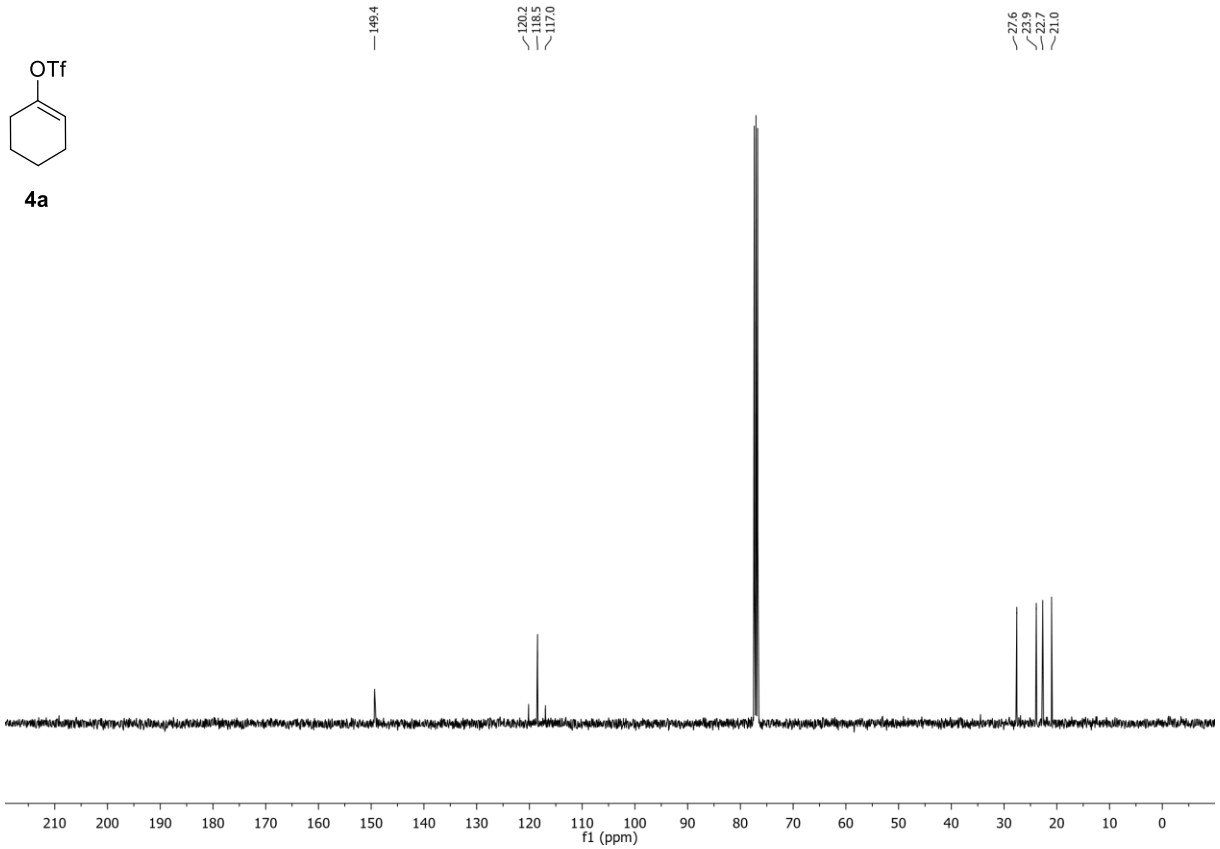

^{19}F-NMR (376 MHz, $CDCl_3$) of compound **4a**:

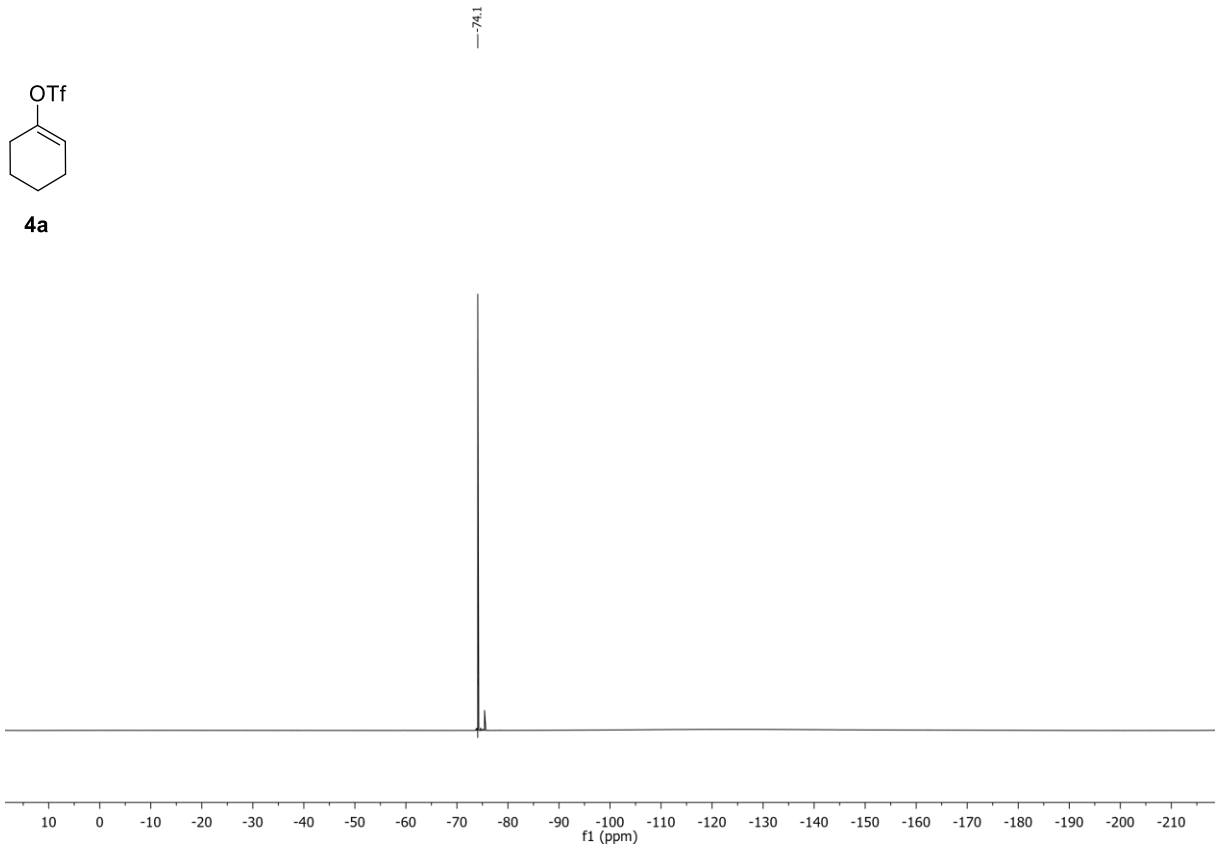

Ethyl 4-(((trifluoromethyl)sulfonyl)oxy)cyclohex-3-ene-1-carboxylate (4b):

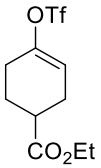

4b

$C_{10}H_{13}F_3O_5S$ (302.26 g/mol)

Following **GP-B2**, **4b** was synthesized using ethyl 4-oxocyclohexanecarboxylate (5.11 g, 30.0 mmol, 1.0 equiv.). Purification by column chromatography (SiO_2, *n*-hexane /EtOAc 95:5) afforded **4b** (4.53 g, 15.0 mmol, 50%) as a colorless oil. Conforms to reported analytical data.[19]

R_f: 0.31 (*n*-hexane/EtOAc 95:5).

^{1}H-NMR (400 MHz, $CDCl_3$, δ): 5.81 – 5.73 (m, 1H), 4.16 (q, *J* = 7.1 Hz, 2H), 2.65 – 2.54 (m, 1H), 2.48 – 2.37 (m, 4H), 2.19 – 2.07 (m, 1H), 1.98 – 1.85 (m, 1H), 1.26 (t, *J* = 7.1 Hz, 3H).

^{13}C-NMR (101 MHz, $CDCl_3$, δ): 174.1, 148.6, 118.6 (q, *J* = 320.1 Hz), 117.0, 61.0, 37.9, 26.7, 26.2, 25.2, 14.3.

^{19}F-NMR (376 MHz, $CDCl_3$, δ): -73.9.

^{1}H-NMR (400 MHz, $CDCl_3$) of compound **4b**:

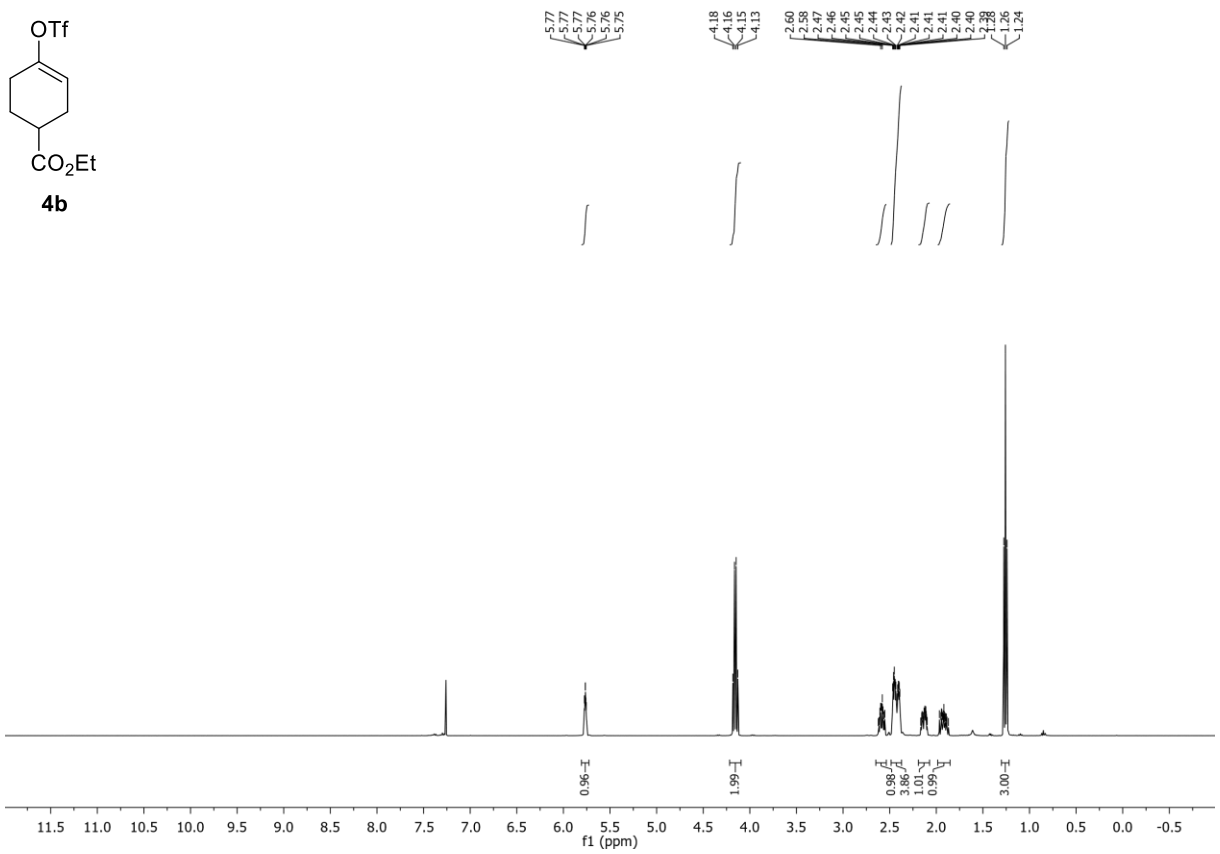

^{13}C-NMR (101 MHz, $CDCl_3$) of compound **4b**:

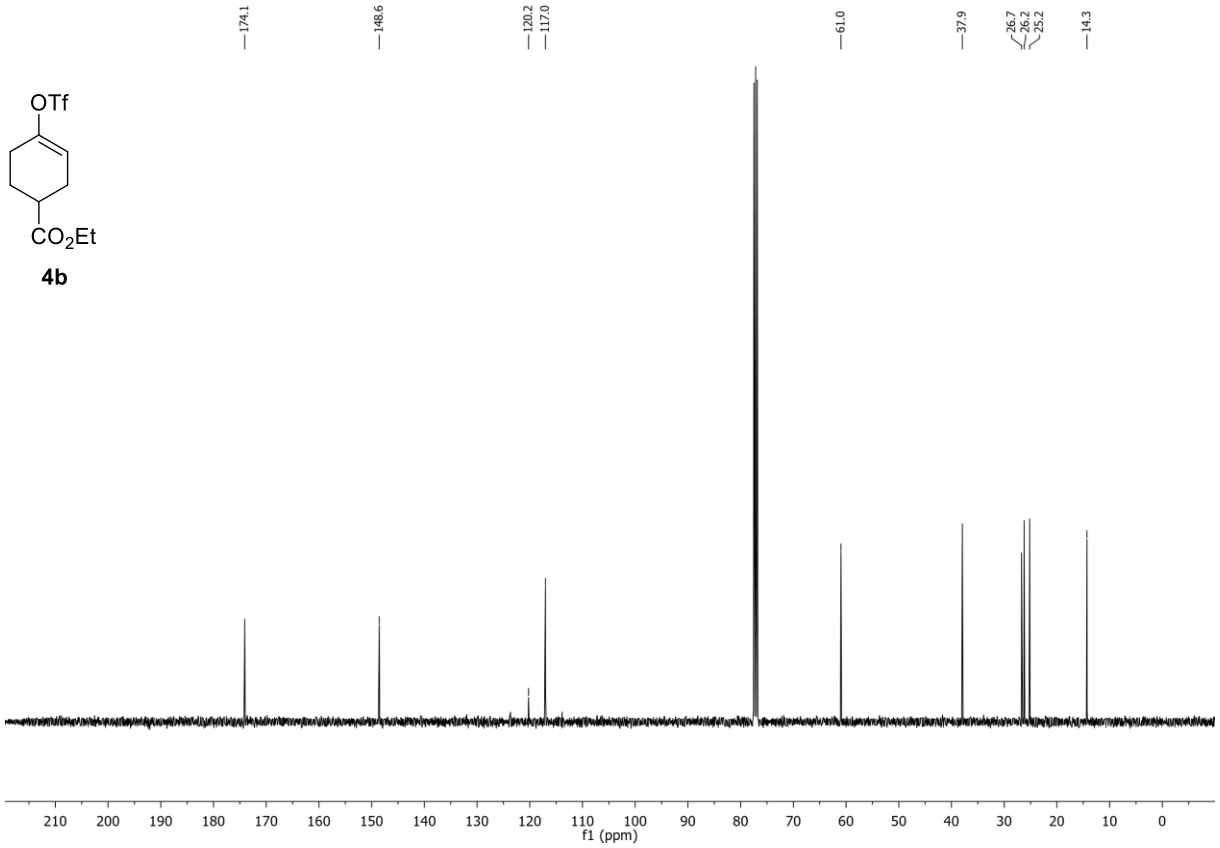

^{19}F-NMR (376 MHz, $CDCl_3$) of compound **4b**:

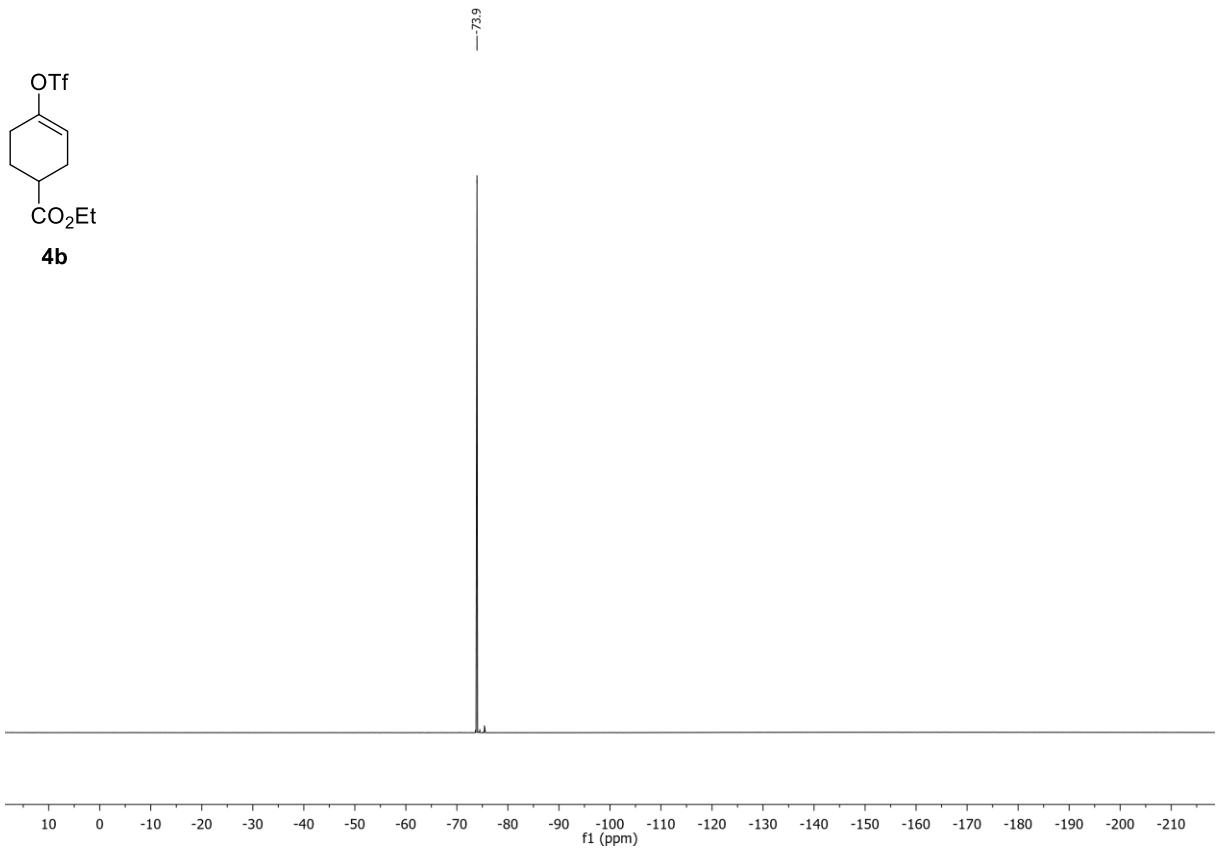

***tert*-Butyl 4-(((trifluoromethyl)sulfonyl)oxy)-3,6-dihydropyridine-1(2*H*)-carboxylate (4c):**

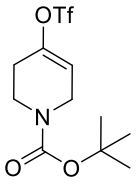

4c

$C_{11}H_{16}F_3NO_5S$ (331.31 g/mol)

Following **GP-B2**, **4c** was synthesized using *tert*-butyl 4-oxopiperidine-1-carboxylate (996 mg, 5.00 mmol, 1.0 equiv.). Purification by column chromatography (SiO_2, *n*-hexane/EtOAc 9:1) afforded **4c** (514 mg, 1.55 mmol, 31%) as a colorless oil. Conforms to reported analytical data.[20]

R_f: 0.22 (*n*-hexane/EtOAc 9:1).

^{1}H-NMR (400 MHz, $CDCl_3$, δ): 5.71 – 5.74 (m, 1H), 4.03 – 4.00 (m, 2H), 3.62 – 3.58 (m, 2H), 2.43 – 2.39 (m, 2H), 1.44 (s, 9H).

^{13}C-NMR (101 MHz, $CDCl_3$, δ): 154.4, 134.8, 129.5, 127.0, 123.4, 118.6 (q, *J* = 320.3 Hz), 80.7, 28.4.

^{19}F-NMR (376 MHz, $CDCl_3$, δ): -73.8.

^{1}H-NMR (400 MHz, $CDCl_3$) of compound **4c**:

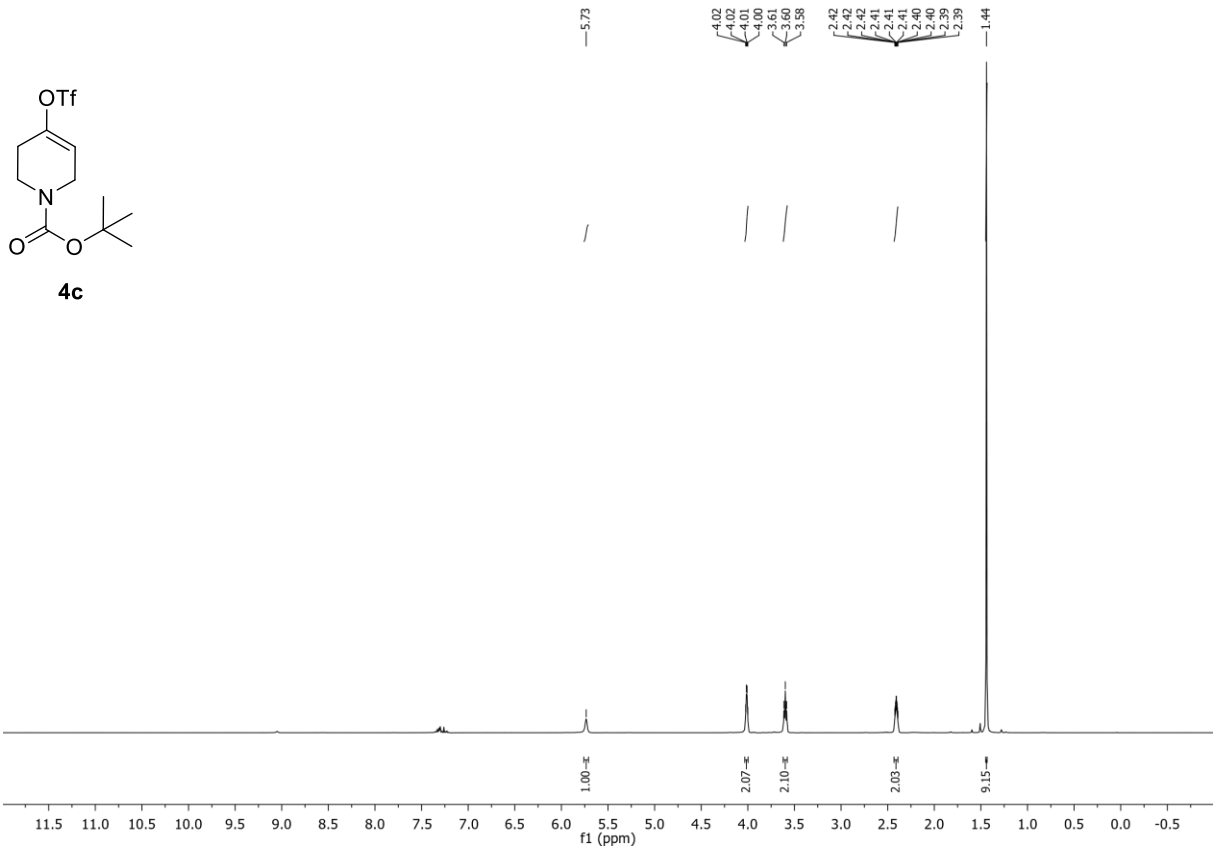

^{13}C-NMR (101 MHz, $CDCl_3$) of compound **4c**:

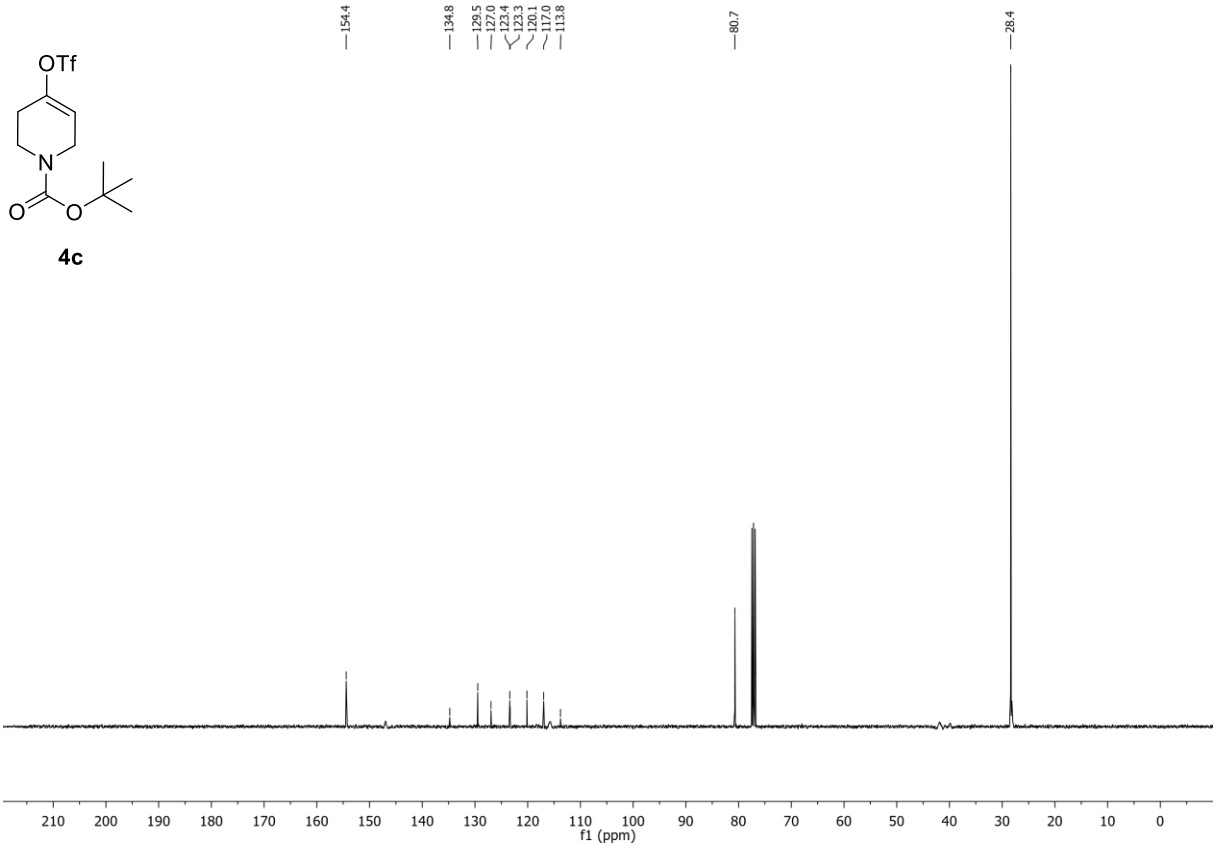

^{19}F-NMR (376 MHz, $CDCl_3$) of compound **4c**:

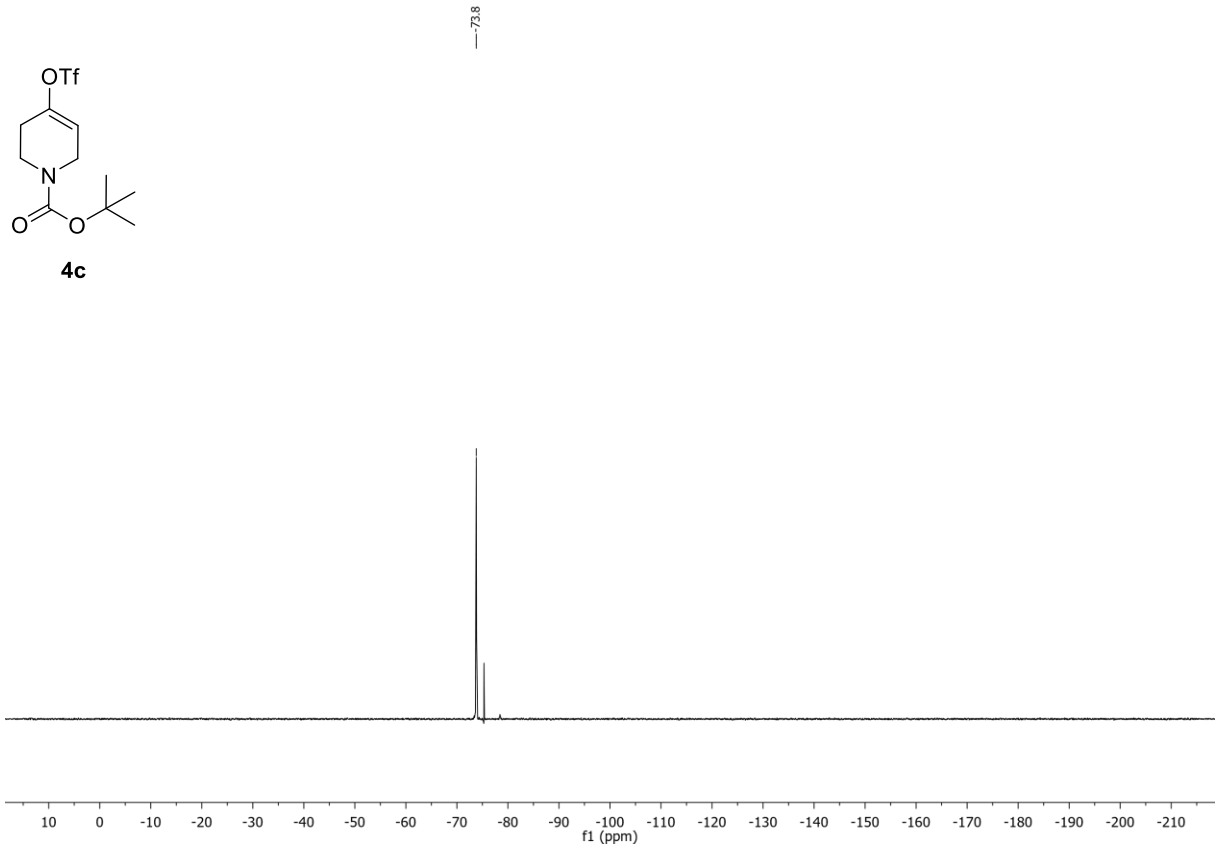

3,6-Dihydro-2*H*-thiopyran-4-yl trifluoromethanesulfonate (4d):

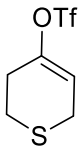

4d

$C_6H_7F_3O_3S_2$ (248.23 g/mol)

Following **GP-B2**, **4d** was synthesized using tetrahydro-4*H*-thiopyran-4-one (1.16 g, 10.0 mmol, 1.0 equiv.). Purification by column chromatography (SiO_2, *n*-hexane/EtOAc 98:2) afforded **4d** (1.41 g, 5.68 mmol, 57%) as a colorless oil. Conforms to reported analytical data.[21]

R_f: 0.32 (*n*-hexane/EtOAc 98:2).

^{1}H-NMR (400 MHz, $CDCl_3$, δ): 6.03 – 5.95 (m, 1H), 3.33 – 3.25 (m, 2H), 2.85 (t, *J* = 5.8 Hz, 2H), 2.66 – 2.56 (m, 2H).

^{13}C-NMR (101 MHz, $CDCl_3$, δ): 150.2, 118.6 (q, *J* = 320.2 Hz), 117.1, 29.4, 25.3, 25.0.

^{19}F-NMR (376 MHz, $CDCl_3$, δ): -73.9.

^{1}H-NMR (400 MHz, $CDCl_3$) of compound **4d**:

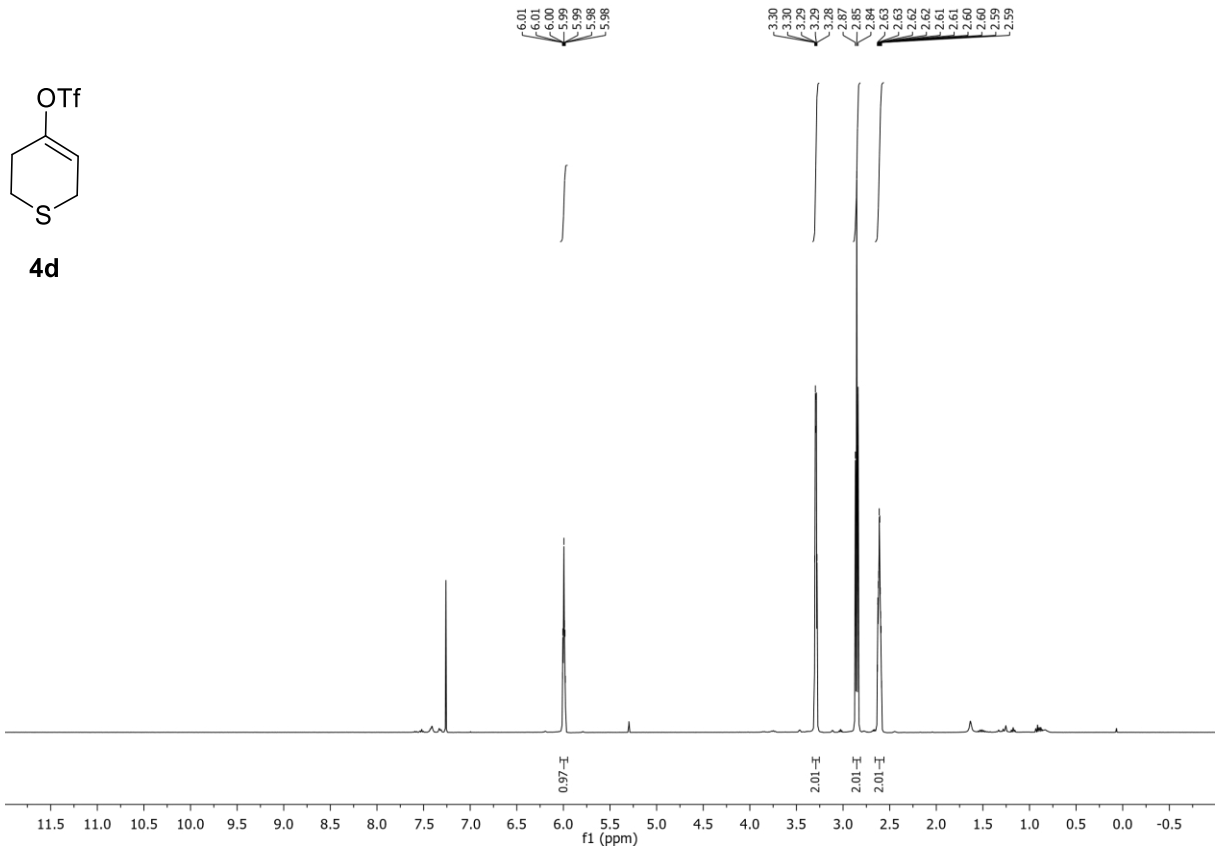

^{13}C-NMR (101 MHz, $CDCl_3$) of compound **4d**:

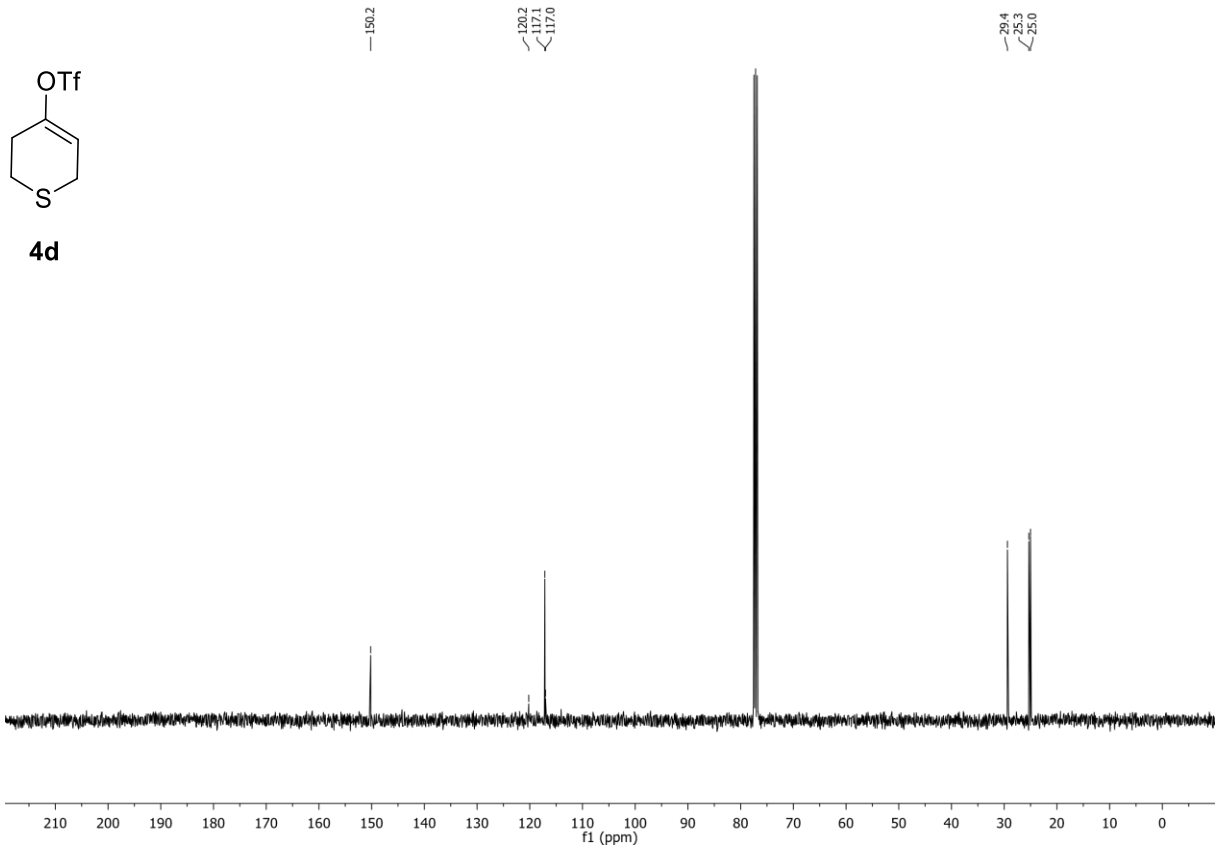

^{19}F-NMR (376 MHz, $CDCl_3$) of compound **4d**:

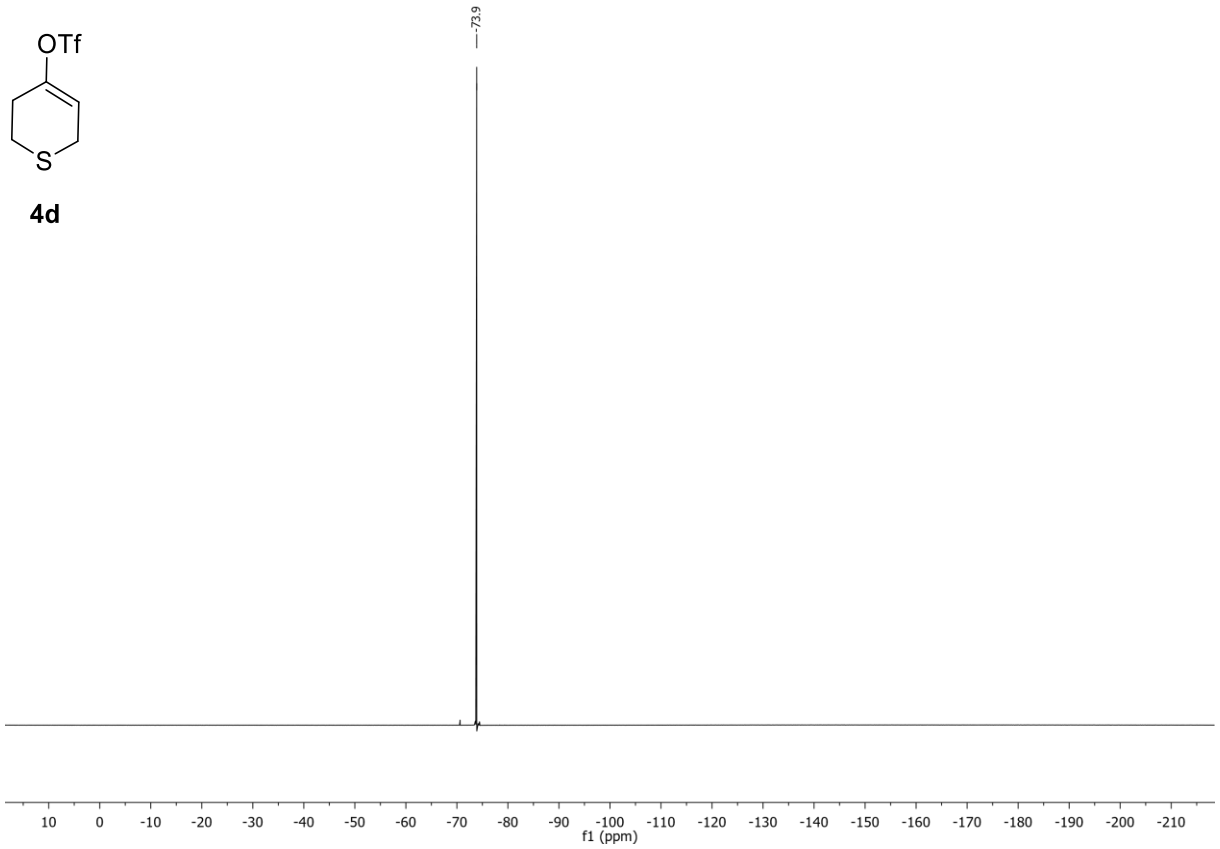

3,4-Dihydronaphthalen-1-yl trifluoromethanesulfonate (4e):

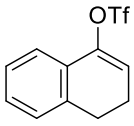

4e

$C_{11}H_9F_3O_3S$ (278.25 g/mol)

Following **GP-B1**, **4e** was synthesized using 1-tetralone (1.46 g, 10.0 mmol, 1.0 equiv.). Purification by column chromatography (SiO_2, *n*-hexane) afforded **4e** (2.08 g, 7.48 mmol, 75%) as a colorless oil. Conforms to reported analytical data.[18]

R_f: 0.35 (*n*-hexane).

^{1}H-NMR (400 MHz, $CDCl_3$, δ): 7.40 – 7.32 (m, 1H), 7.32 – 7.22 (m, 2H), 7.21 – 7.15 (m, 1H), 6.02 (t, *J* = 4.8 Hz, 1H), 2.88 (t, *J* = 8.2 Hz, 2H), 2.52 (td, *J* = 8.2, 4.8 Hz, 2H).

^{13}C-NMR (101 MHz, $CDCl_3$, δ): 146.5, 136.4, 129.3, 128.8, 127.9, 127.1, 121.4, 118.8 (q, *J* = 320.3 Hz), 117.9, 27.0, 22.5.

^{19}F-NMR (376 MHz, $CDCl_3$, δ): -73.7.

^{1}H-NMR (400 MHz, $CDCl_3$) of compound **4e**:

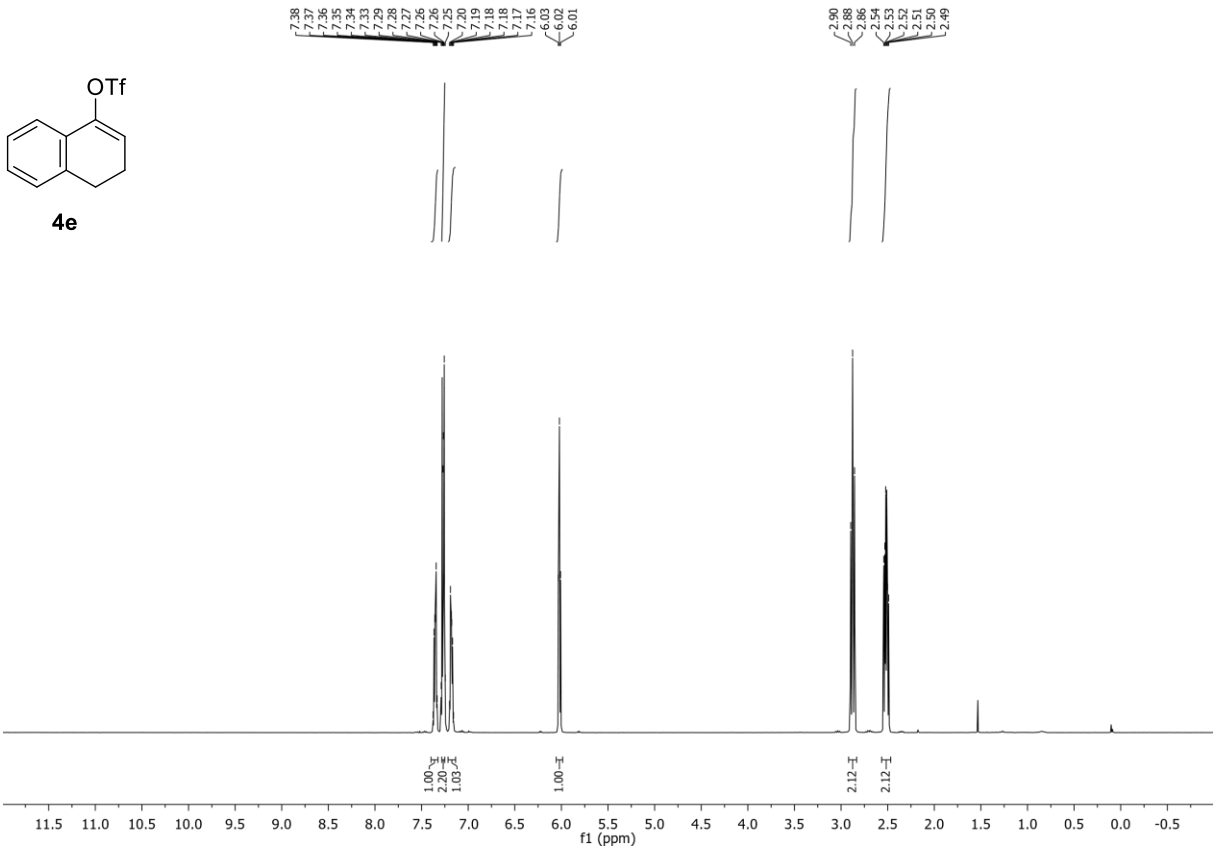

^{13}C-NMR (101 MHz, $CDCl_3$) of compound **4e**:

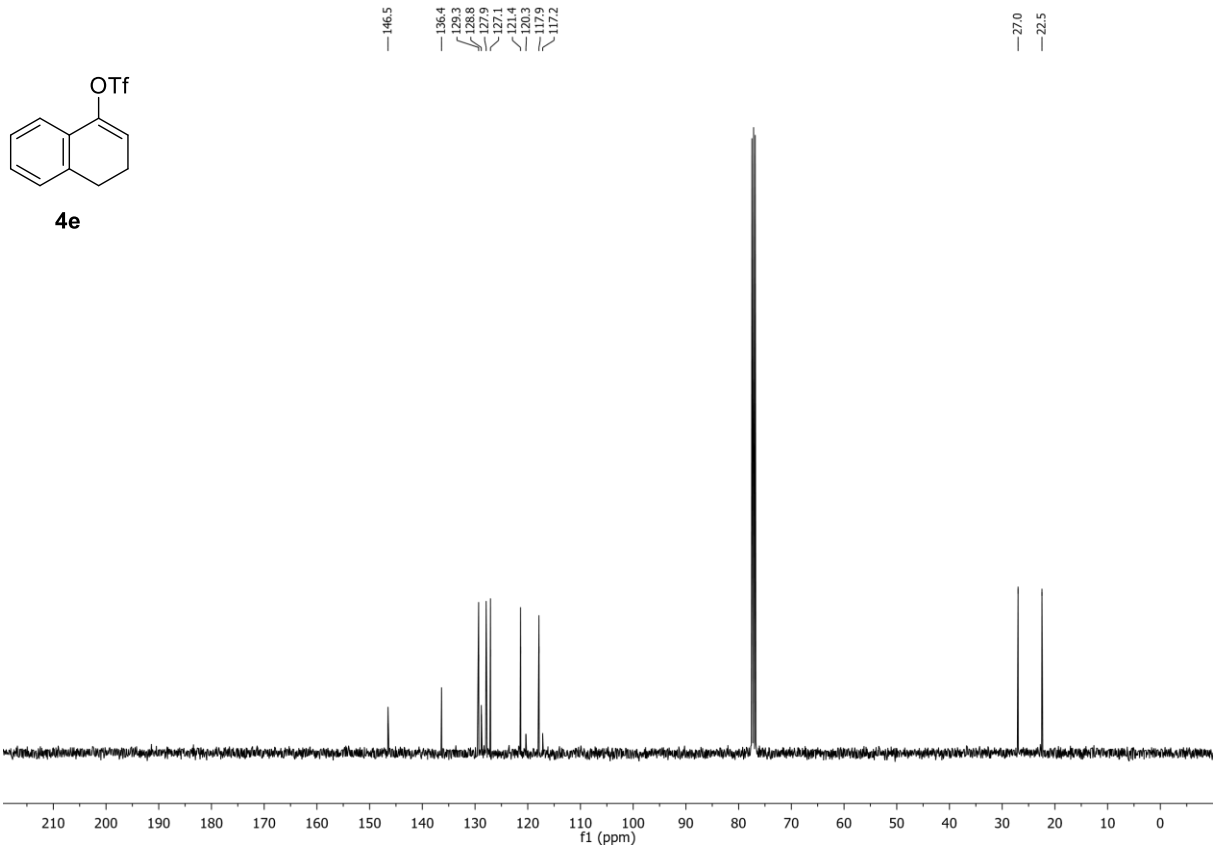

^{19}F-NMR (376 MHz, $CDCl_3$) of compound **4e**:

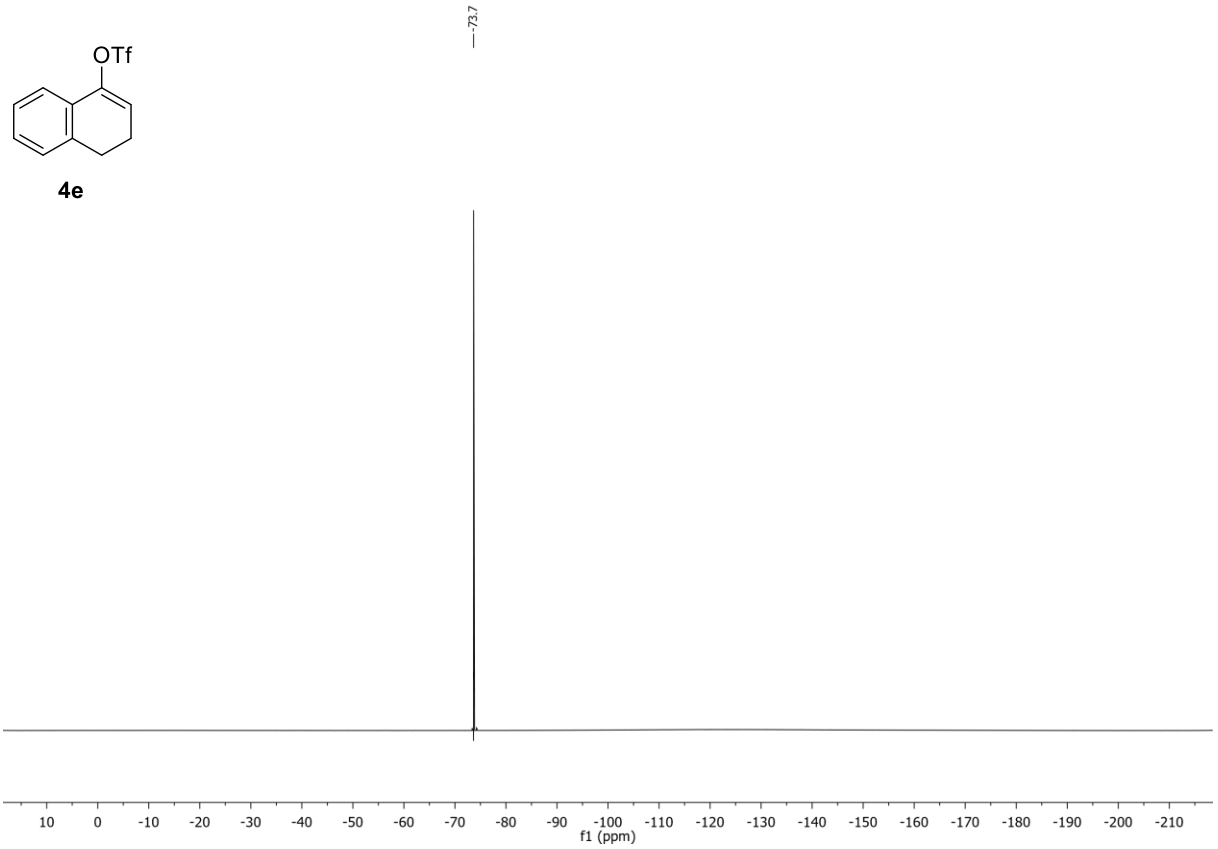

7-Methoxy-3,4-dihydronaphthalen-1-yl trifluoromethanesulfonate (4f):

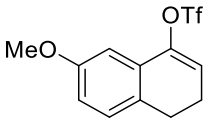

4f

$C_{12}H_{11}F_3O_4S$ (308.27 g/mol)

Following **GP-B3**, **4f** was synthesized using 7-methoxy-1-tetralone (1.76 g, 10.0 mmol, 1.0 equiv.). Purification by column chromatography (SiO_2, *n*-hexane/EtOAc 98:2) afforded **4f** (2.28 g, 7.40 mmol, 74%) as a colorless oil. Conforms to reported analytical data.[18]

R_f: 0.25 (*n*-hexane/EtOAc 98:2).

^{1}H-NMR (400 MHz, $CDCl_3$, δ): 7.09 (d, *J* = 8.3 Hz, 1H), 6.91 (d, *J* = 2.6 Hz, 1H), 6.80 (dd, *J* = 8.3, 2.6 Hz, 1H), 6.03 (t, *J* = 4.8 Hz, 1H), 3.81 (s, 3H), 2.84 – 2.75 (m, 2H), 2.49 (m, 2H).

^{13}C-NMR (101 MHz, $CDCl_3$, δ): 158.8, 146.4, 129.7, 128.8, 128.3, 118.8 (q, *J* = 320.3 Hz), 118.5, 114.6, 107.3, 55.5, 26.1, 22.9.

^{19}F-NMR (376 MHz, $CDCl_3$, δ): -73.7.

^{1}H-NMR (400 MHz, $CDCl_3$) of compound **4f**:

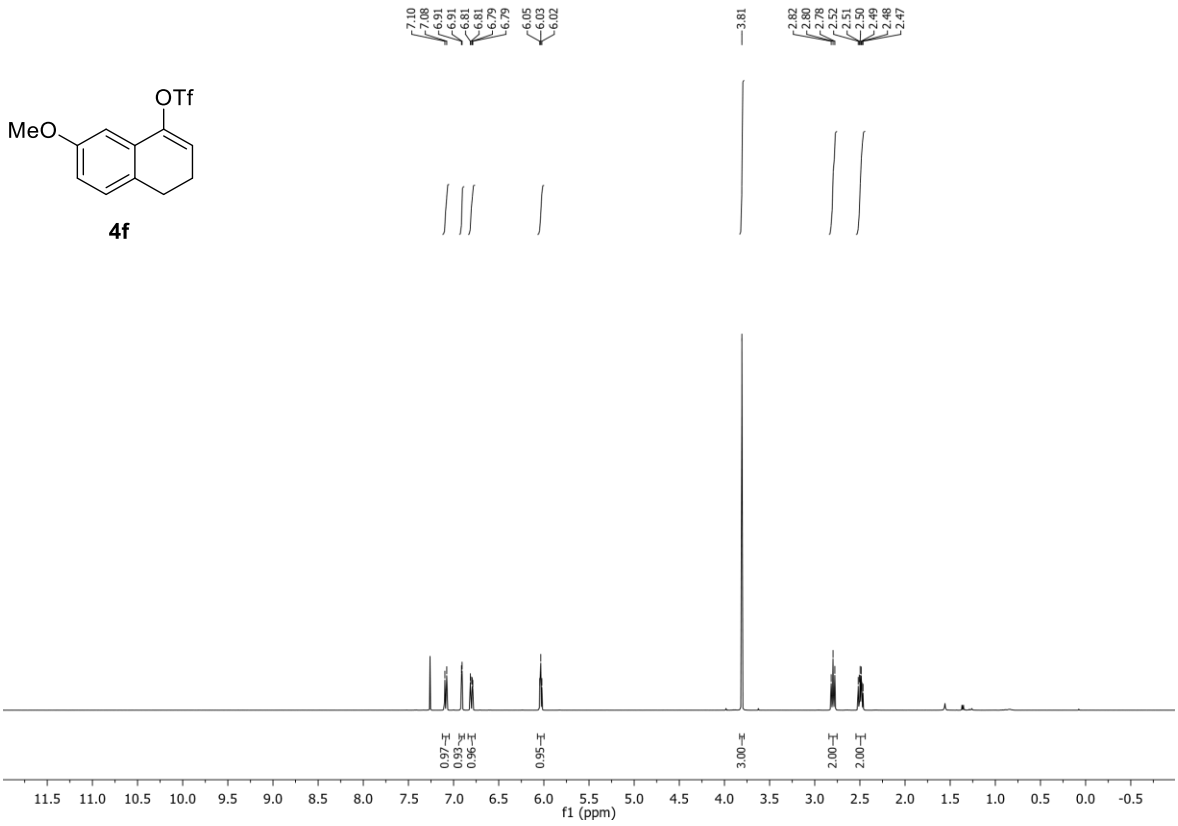

^{13}C-NMR (101 MHz, $CDCl_3$) of compound **4f**:

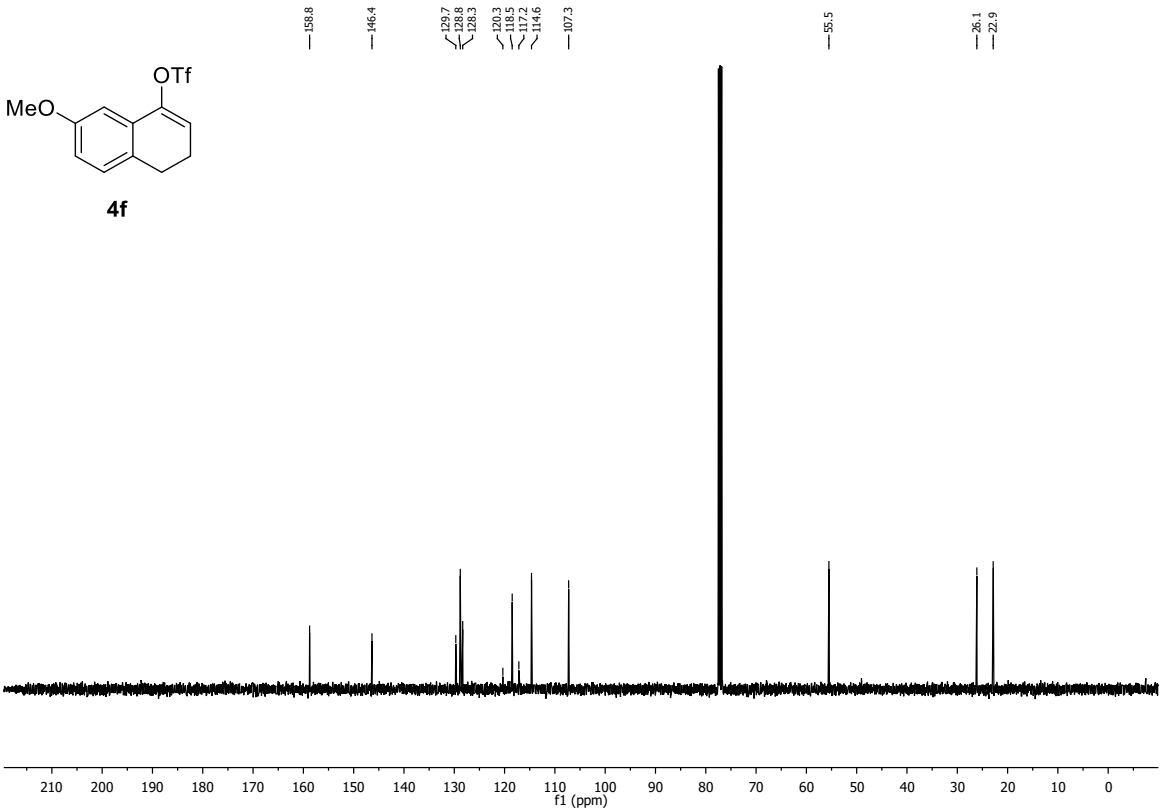

^{19}F-NMR (376 MHz, $CDCl_3$) of compound **4f**:

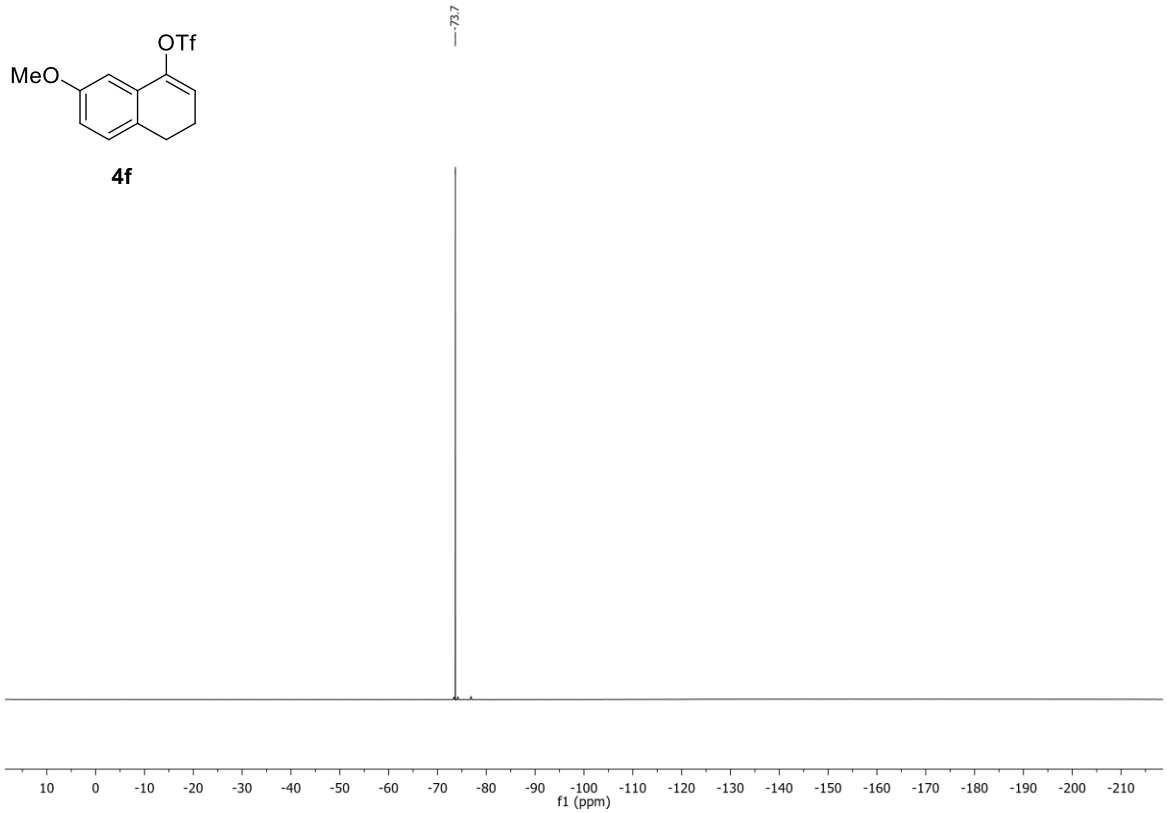

4f

2*H*-Chromen-4-yl trifluoromethanesulfonate (4g):

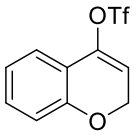

4g

$C_{10}H_7F_3O_4S$ (280.22 g/mol)

Following **GP-B3**, **4g** was synthesized using chromanone (1.48 g, 10.0 mmol, 1.0 equiv.). Purification by column chromatography (SiO_2, *n*-hexane/EtOAc 98:2) afforded **4g** (1.36 g, 4.85 mmol, 49%) as a yellow oil. Conforms to reported analytical data.[18]

R_f: 0.19 (*n*-hexane/EtOAc 98:2).

^{1}H-NMR (400 MHz, $CDCl_3$, δ): 7.26 – 7.22 (m, 2H), 6.97 (m, 1H), 6.85 (m, 1H), 5.76 (t, *J* = 3.9 Hz, 1H), 4.99 (d, *J* = 3.9 Hz, 2H).

^{13}C-NMR (101 MHz, $CDCl_3$, δ): 155.1, 143.3, 131.7, 122.0, 121.8, 118.7 (q, *J* = 319.8 Hz), 117.5, 116.4, 110.2, 65.2.

^{19}F-NMR (376 MHz, $CDCl_3$, δ): -73.5.

^{1}H-NMR (400 MHz, $CDCl_3$) of compound **4g**:

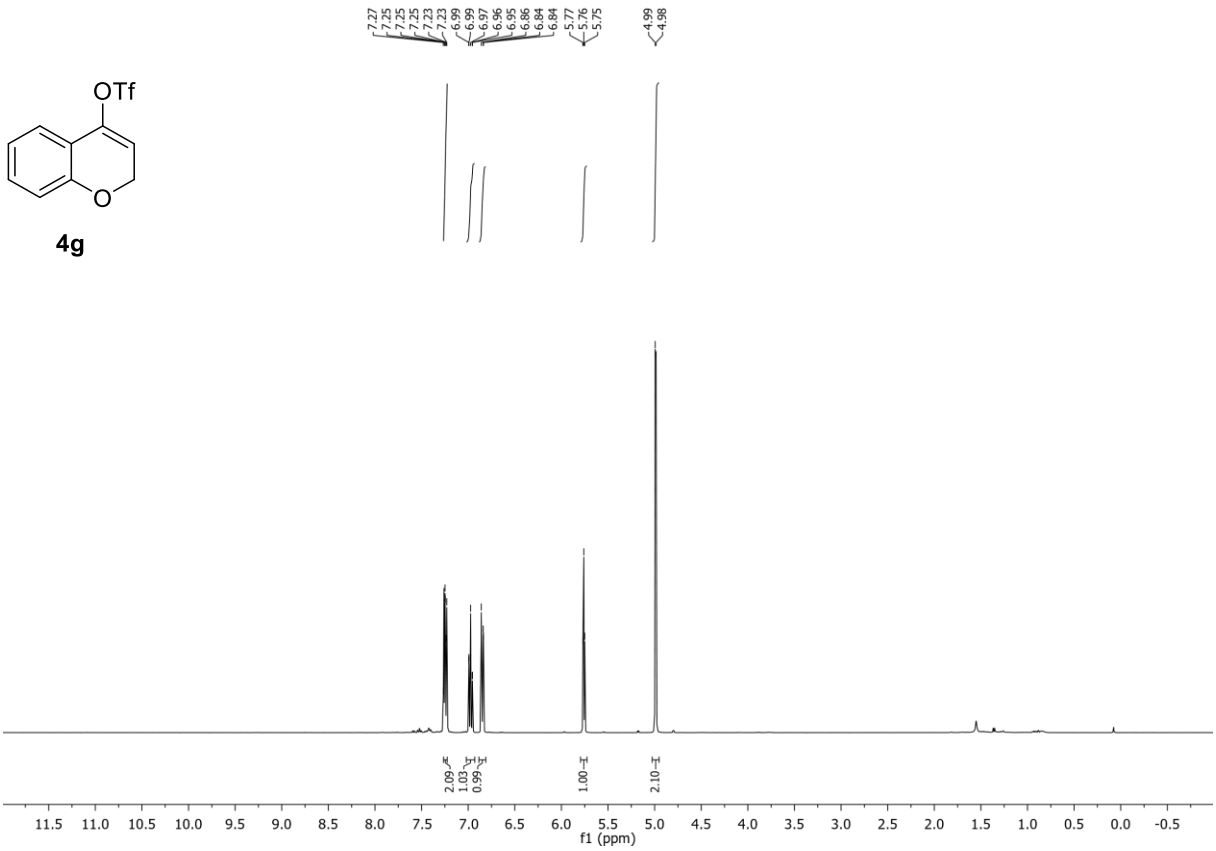

^{13}C-NMR (101 MHz, $CDCl_3$) of compound **4g**:

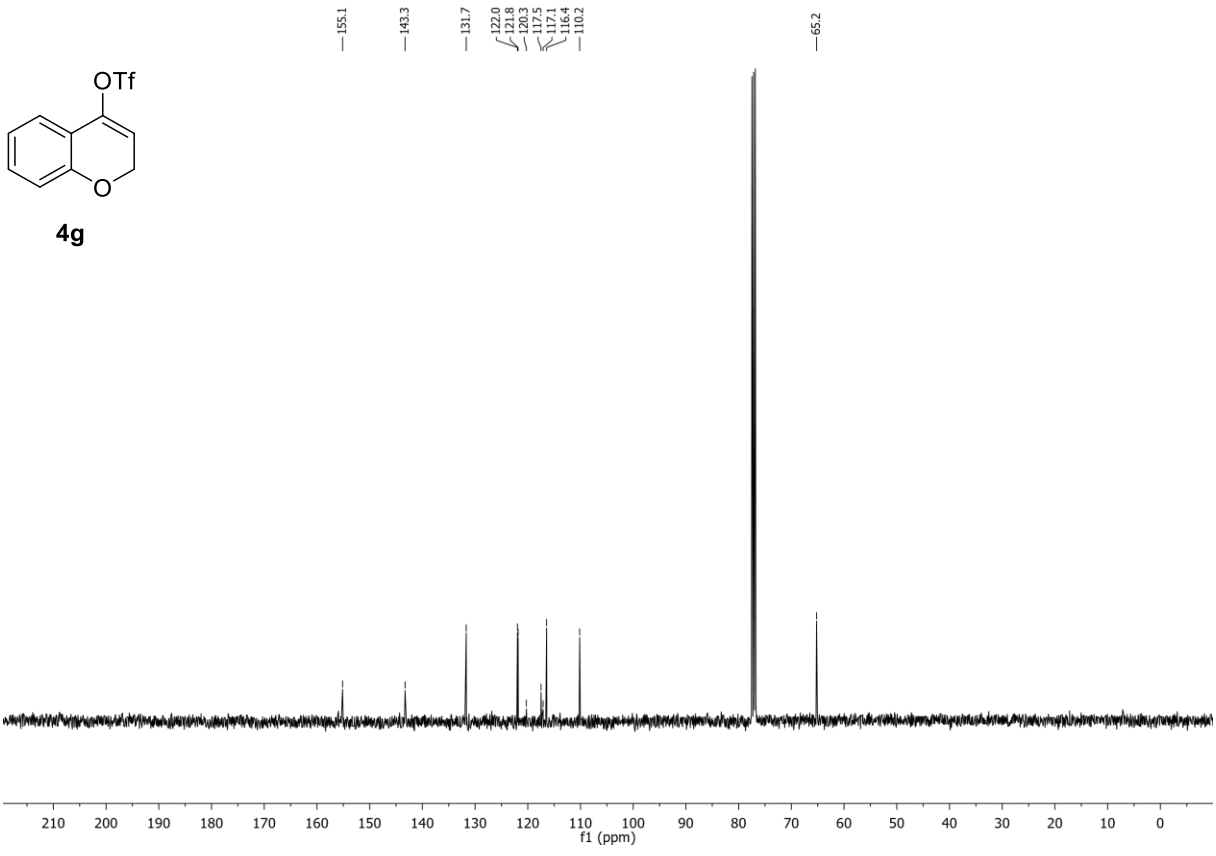

^{19}F-NMR (376 MHz, $CDCl_3$) of compound **4g**:

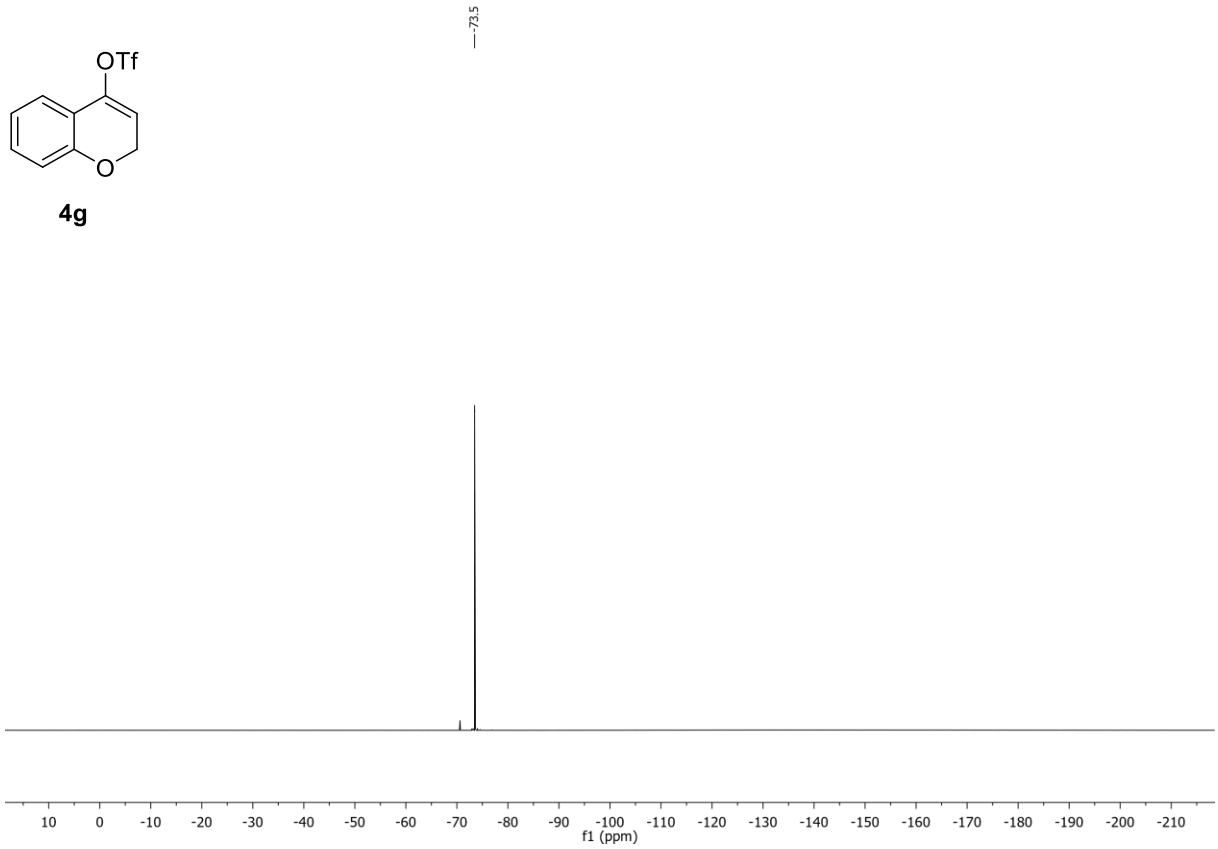

1*H*-Inden-3-yl trifluoromethanesulfonate (4h):

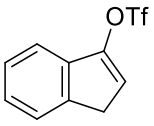

4h

$C_{10}H_7F_3O_3S$ (264.22 g/mol)

Following **GP-B1**, **4h** was synthesized using 1-indanone (1.32 g, 10.0 mmol, 1.0 equiv.). Purification by column chromatography (SiO_2, *n*-hexane) afforded **4h** (1.33 g, 5.03 mmol, 50%) as a colorless oil. Conforms to reported analytical data.[18]

R_f: 0.40 (*n*-hexane).

^{1}H-NMR (400 MHz, $CDCl_3$, δ): 7.52 – 7.30 (m, 4H), 6.39 (t, *J* = 2.4 Hz, 1H), 3.49 (d, *J* = 2.4 Hz, 2H).

^{13}C-NMR (101 MHz, $CDCl_3$, δ): 148.1, 141.3, 136.7, 127.1, 127.0, 124.6, 118.9 (q, *J* = 320.7 Hz), 118.4, 118.2, 35.0.

^{19}F-NMR (376 MHz, $CDCl_3$, δ): -73.1.

^{1}H-NMR (400 MHz, $CDCl_3$) of compound **4h**:

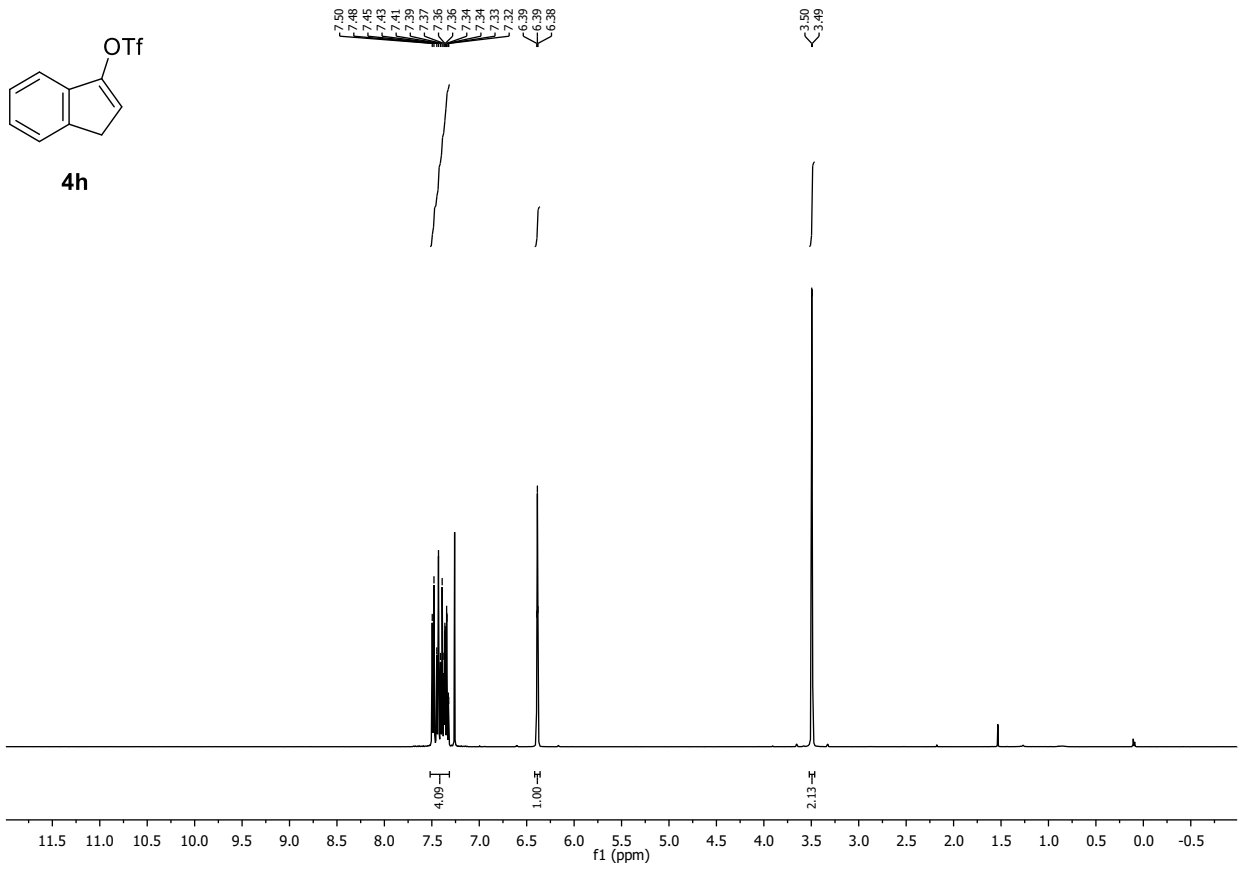

^{13}C-NMR (101 MHz, $CDCl_3$) of compound **4h**:

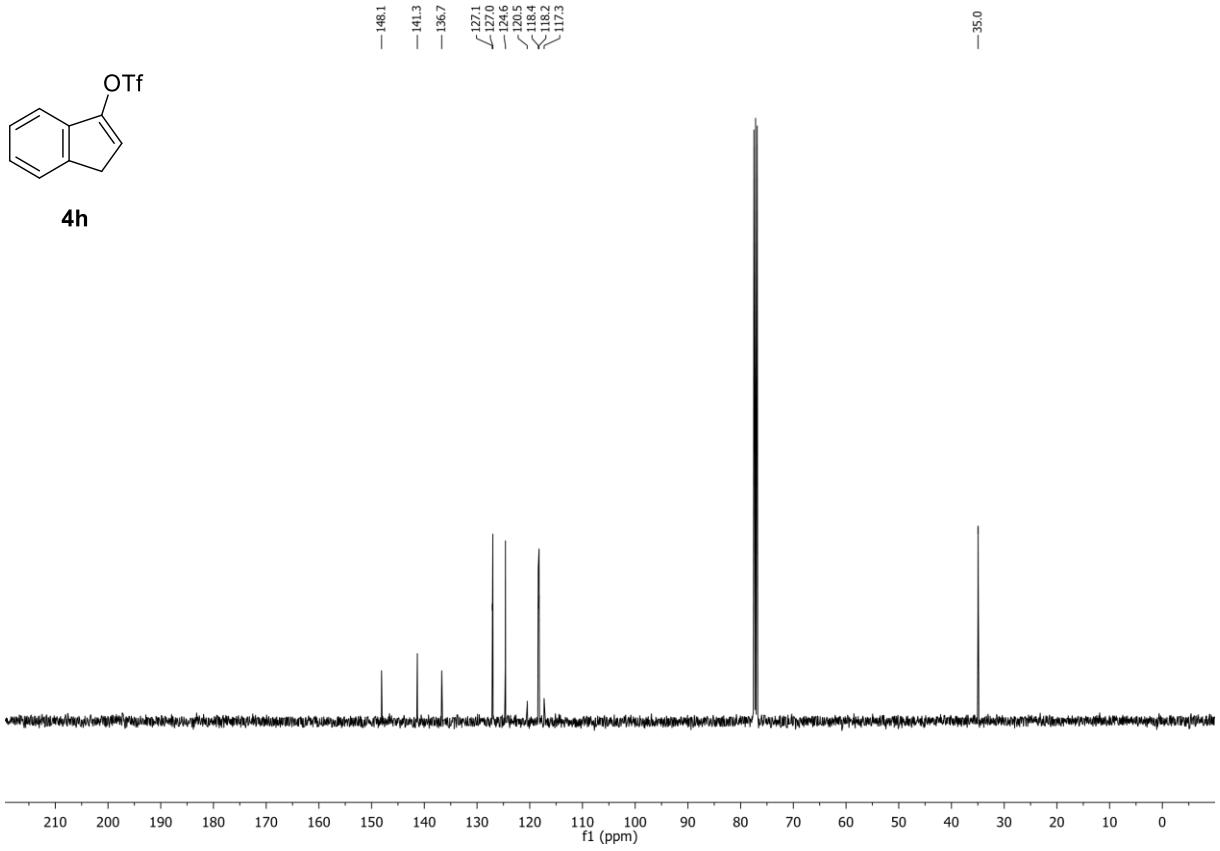

^{19}F-NMR (376 MHz, $CDCl_3$) of compound **4h**:

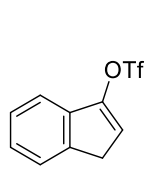

4h

Cyclohept-1-en-1-yl trifluoromethanesulfonate (4i):

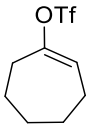

4i

$C_8H_{11}F_3O_3S$ (244.23 g/mol)

Following **GP-B1**, **4i** was synthesized using cycloheptanone (1.12 g, 10.0 mmol, 1.0 equiv.). Purification by column chromatography (SiO_2, *n*-hexane) afforded **4i** (1.26 g, 5.16 mmol, 52%) as a pale-yellow oil. Conforms to reported analytical data.[22]

R_f: 0.69 (*n*-hexane).

^{1}H-NMR (400 MHz, $CDCl_3$, δ): 5.88 (t, *J* = 6.4 Hz, 1H), 2.56 – 2.48 (m, 2H), 2.16 (m, 2H), 1.70 (m, 4H), 1.63 (m, 2H).

^{13}C-NMR (101 MHz, $CDCl_3$, δ): 153.2, 123.2, 118.7 (q, *J* = 320.4 Hz), 33.3, 30.0, 26.5, 24.92, 24.87.

^{19}F-NMR (376 MHz, $CDCl_3$, δ): -73.9.

^{1}H-NMR (400 MHz, $CDCl_3$) of compound **4i**:

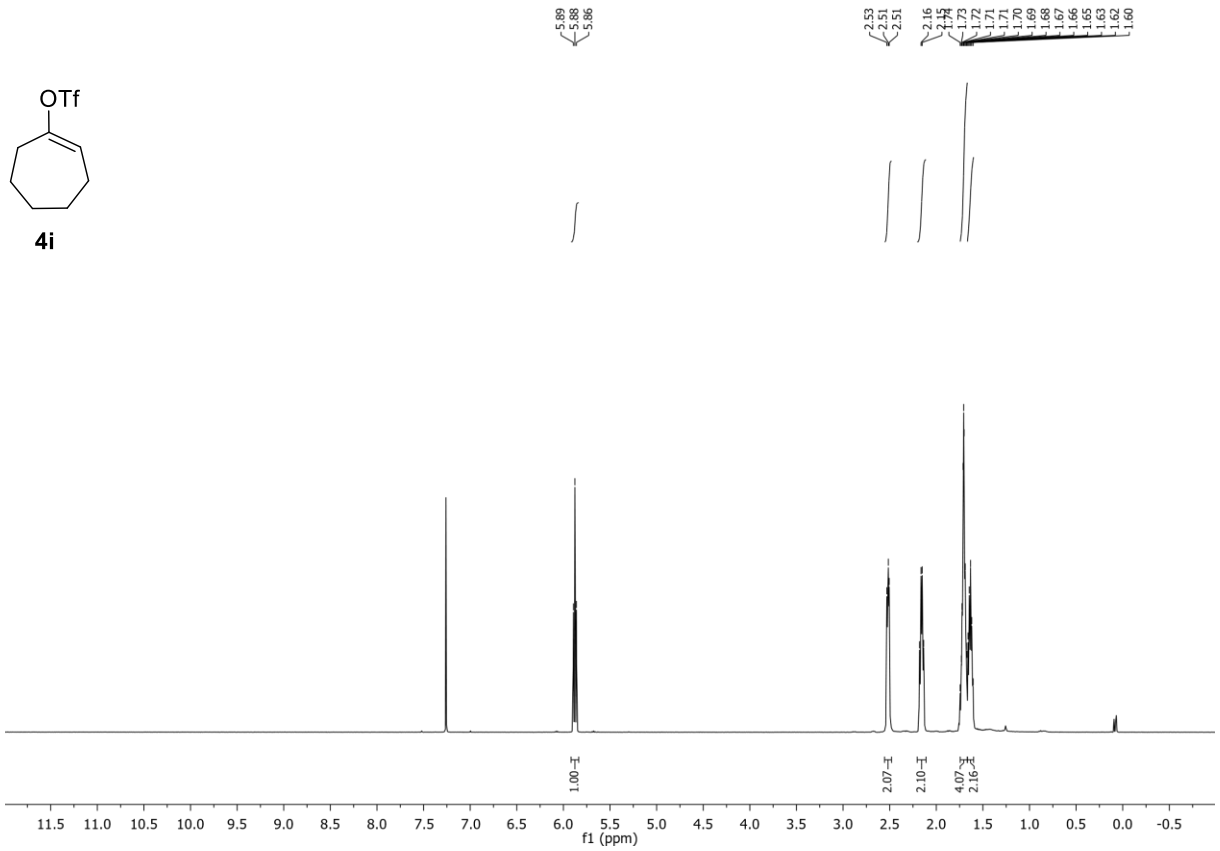

^{13}C-NMR (101 MHz, $CDCl_3$) of compound **4i**:

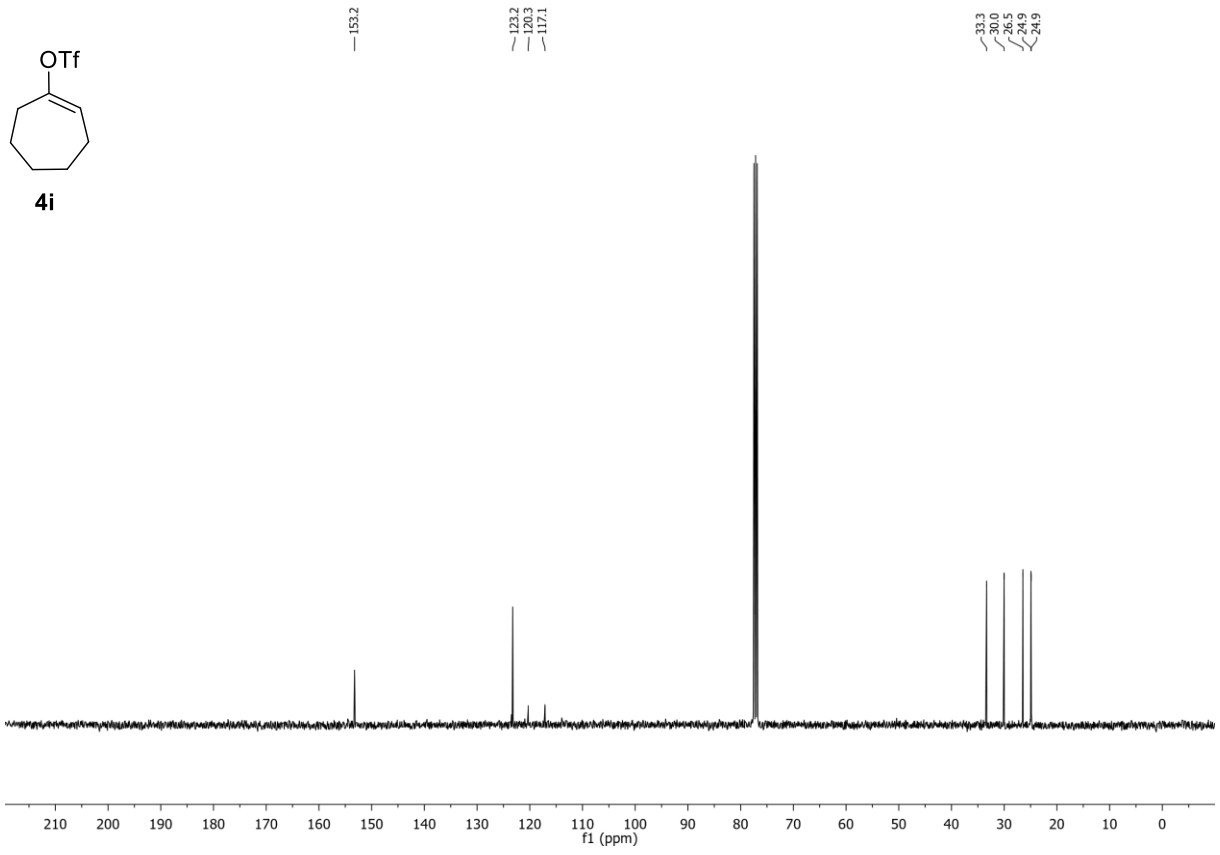

^{19}F-NMR (376 MHz, $CDCl_3$) of compound **4i**:

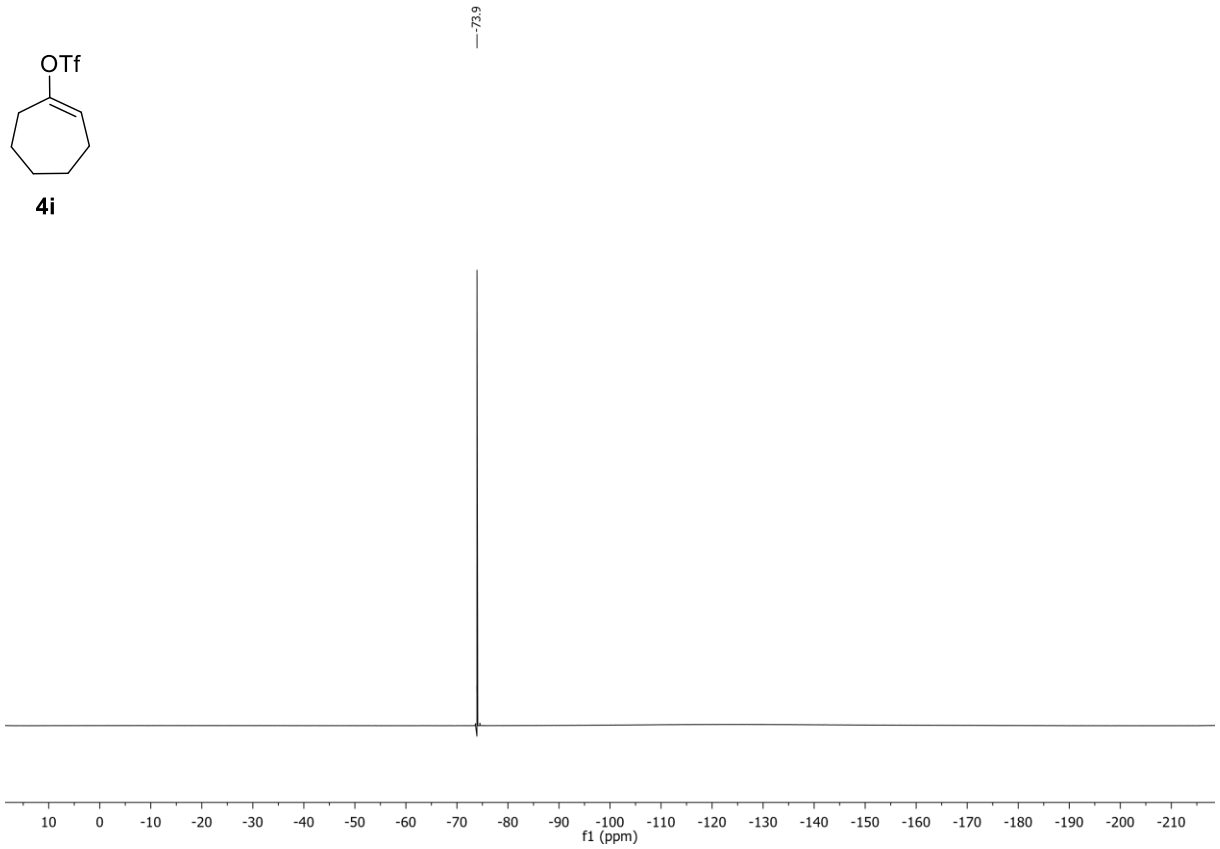

4i

1-Phenylvinyl trifluoromethanesulfonate (4j):

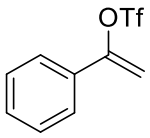

4j

$C_9H_7F_3O_3S$ (252.21 g/mol)

Following **GP-B1**, **4j** was synthesized using acetophenone (1.20 g, 10.0 mmol, 1.0 equiv.). Purification by column chromatography (SiO_2, *n*-hexane/EtOAc 95:5) afforded **4j** (1.07 g, 4.24 mmol, 42%) as a yellow oil. Conforms to reported analytical data.[23]

R_f: 0.67 (*n*-hexane/EtOAc 95:5).

^{1}H-NMR (400 MHz, $CDCl_3$, δ): 7.58 – 7.52 (m, 2H), 7.46 – 7.39 (m, 3H), 5.61 (d, *J* = 4.0 Hz, 1H), 5.38 (d, *J* = 4.0 Hz, 1H).

^{13}C-NMR (101 MHz, $CDCl_3$, δ): 153.6, 132.3, 132.2, 130.4, 129.0, 128.5, 125.5, 118.7 (q, *J* = 320.0 Hz), 104.4.

^{19}F-NMR (376 MHz, $CDCl_3$, δ): -73.8.

^{1}H-NMR (400 MHz, $CDCl_3$) of compound **4j**:

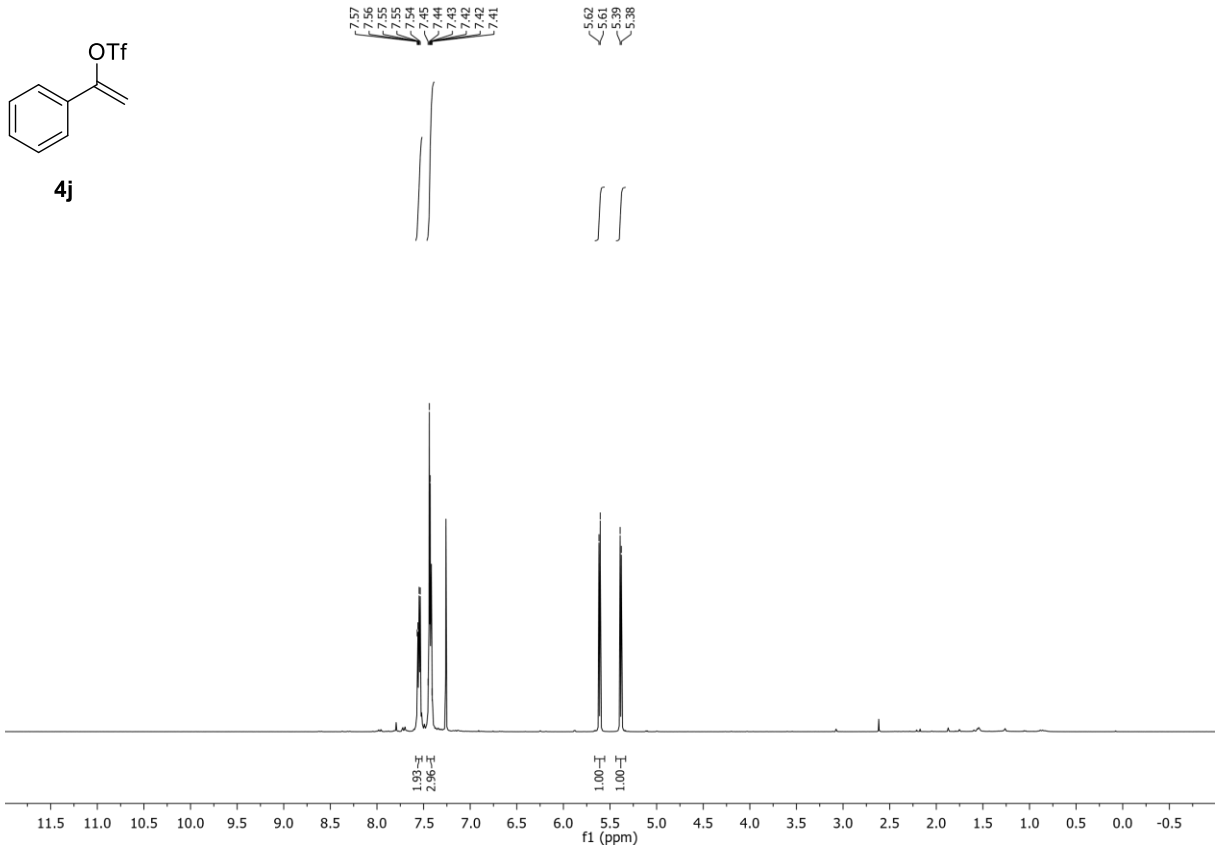

^{13}C-NMR (101 MHz, $CDCl_3$) of compound **4j**:

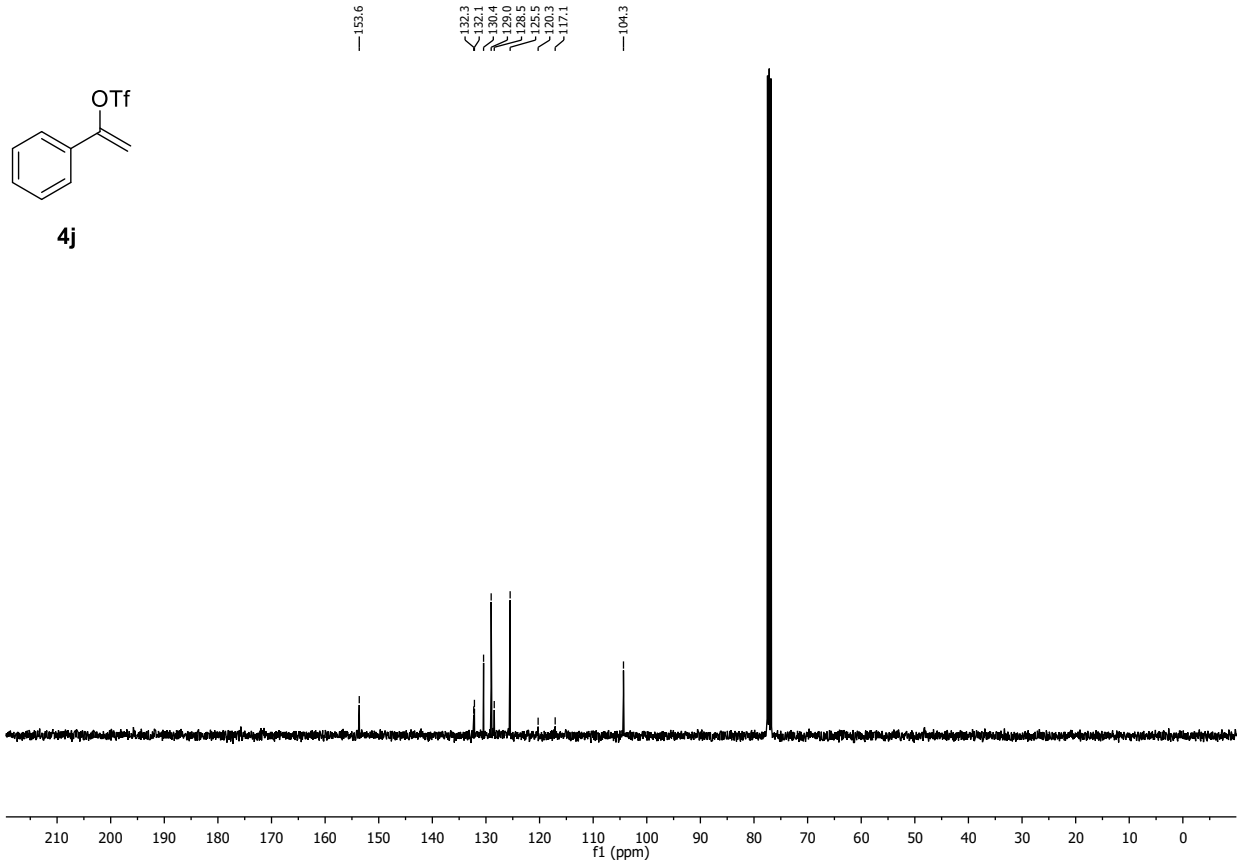

^{19}F-NMR (376 MHz, $CDCl_3$) of compound **4j**:

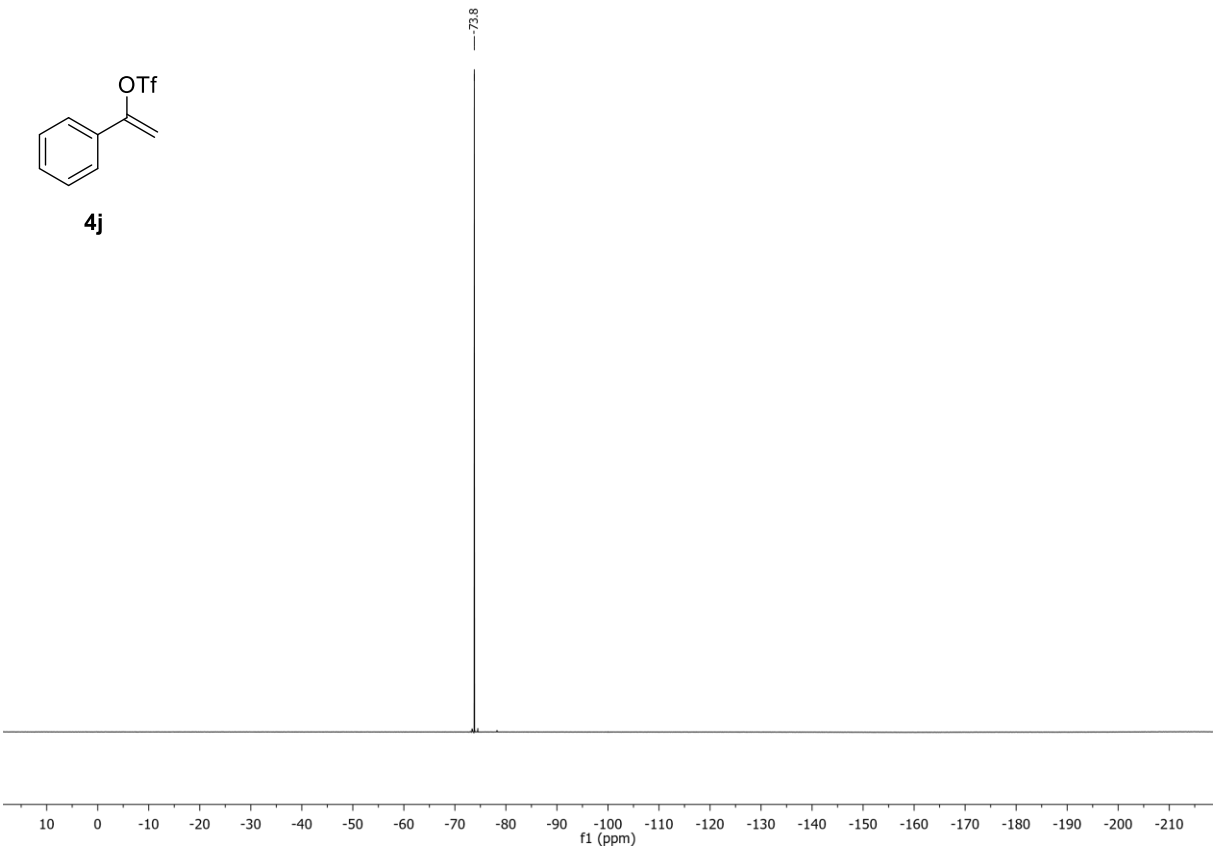

4j

(5*S*,10*S*,13*R*,17*R*)-10,13-Dimethyl-17-((*R*)-6-methylheptan-2-yl)-4,5,6,7,8,9,10,11,12,13,14,15,16,17-tetradecahydro-1*H*-cyclopenta[a]phenanthren-3-yl trifluoromethanesulfonate (4k):

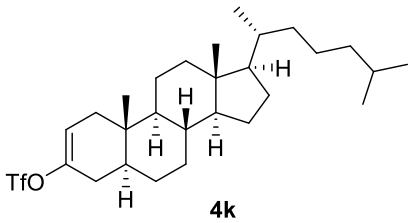

4k

$C_{28}H_{45}F_3O_3S$ (518.72 g/mol)

Following **GP-B2**, **4k** was synthesized using 5α-cholestan-3-one (1.00 g, 2.59 mmol, 1.0 equiv.). Purification by column chromatography (SiO_2, *n*-hexane) afforded **4k** (1.11 g, 2.14 mmol, 83%, dr = 85:15 (determined by ^{19}F-NMR)) as a colorless solid. Conforms to reported analytical data.[24]

R_f: 0.30 (*n*-hexane).

^{1}H-NMR (400 MHz, $CDCl_3$, δ): 5.66 – 5.37 (m, 1H), 2.14 – 1.97 (m, 3H), 1.90 – 1.65 (m, 3H), 1.58 – 1.19 (m, 14H), 1.17 – 0.94 (m, 8H), 0.92 – 0.84 (m, 10H), 0.80 (d, *J* = 11.0 Hz, 3H), 0.66 (s, 3H).

^{13}C-NMR (101 MHz, $CDCl_3$, δ): 148.1, 147.8, 122.3, 118.7 (q, *J* = 320.1 Hz), 117.3, 56.4, 53.5, 52.8, 45.5, 42.9, 42.6, 42.3, 40.1, 40.0, 39.7, 38.6, 36.3, 35.9, 35.6, 35.2, 34.6, 32.2, 32.0, 31.6, 28.40, 28.35, 28.2, 27.2, 25.8, 24.4, 24.3, 24.0, 23.0, 22.7, 21.6, 21.4, 18.8, 12.3, 12.14, 12.06, 11.8.

^{19}F-NMR (376 MHz, $CDCl_3$, δ): -74.0.

^{1}H-NMR (400 MHz, $CDCl_3$) of compound **4k** (both isomers):

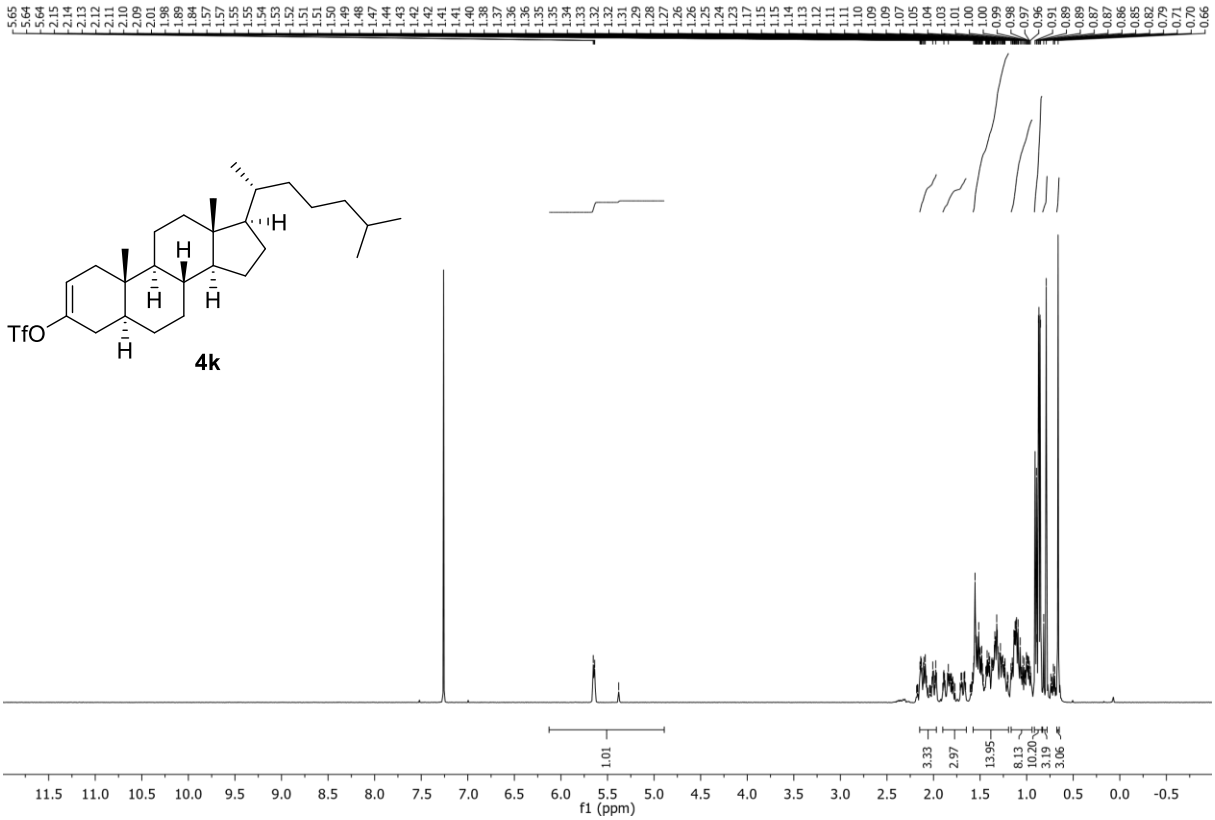

^{13}C-NMR (101 MHz, $CDCl_3$) of compound **4k** (both isomers):

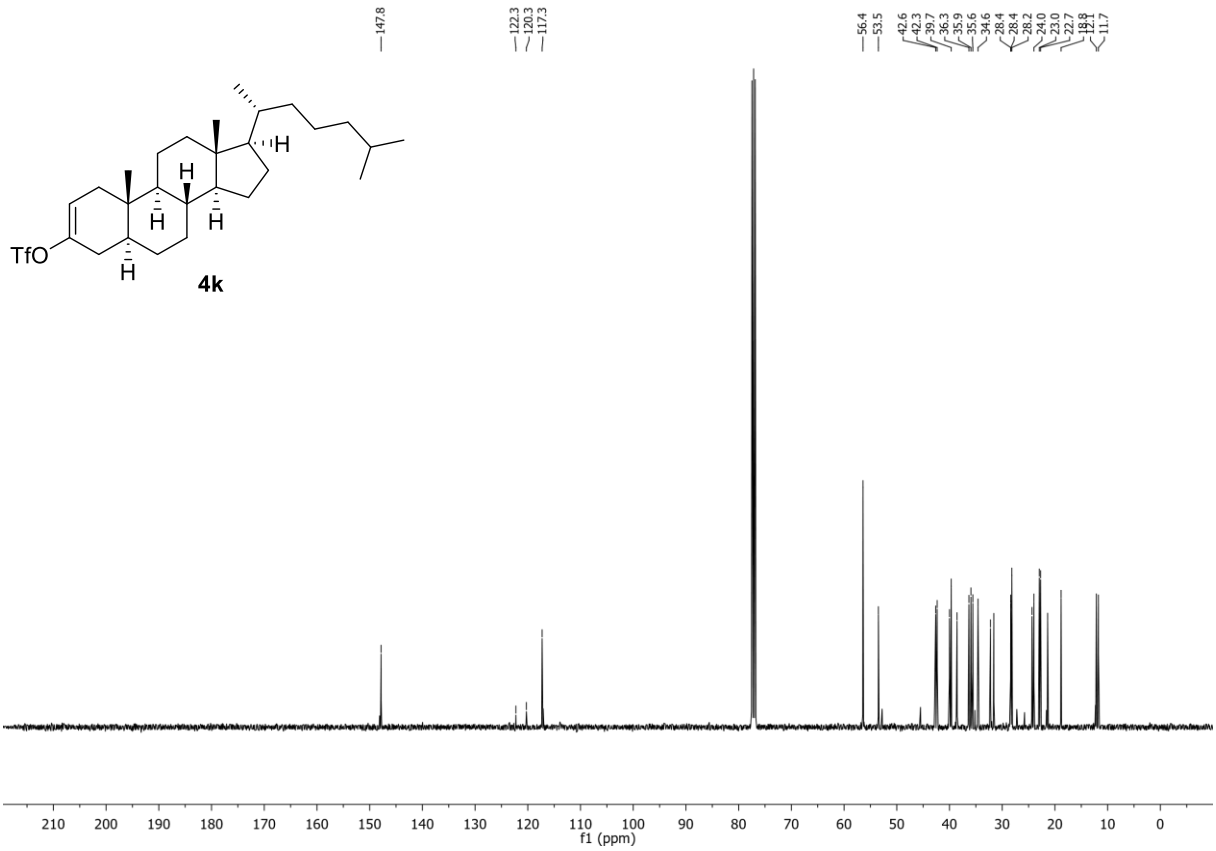

^{19}F-NMR (376 MHz, $CDCl_3$) of compound **4k** (both isomers):

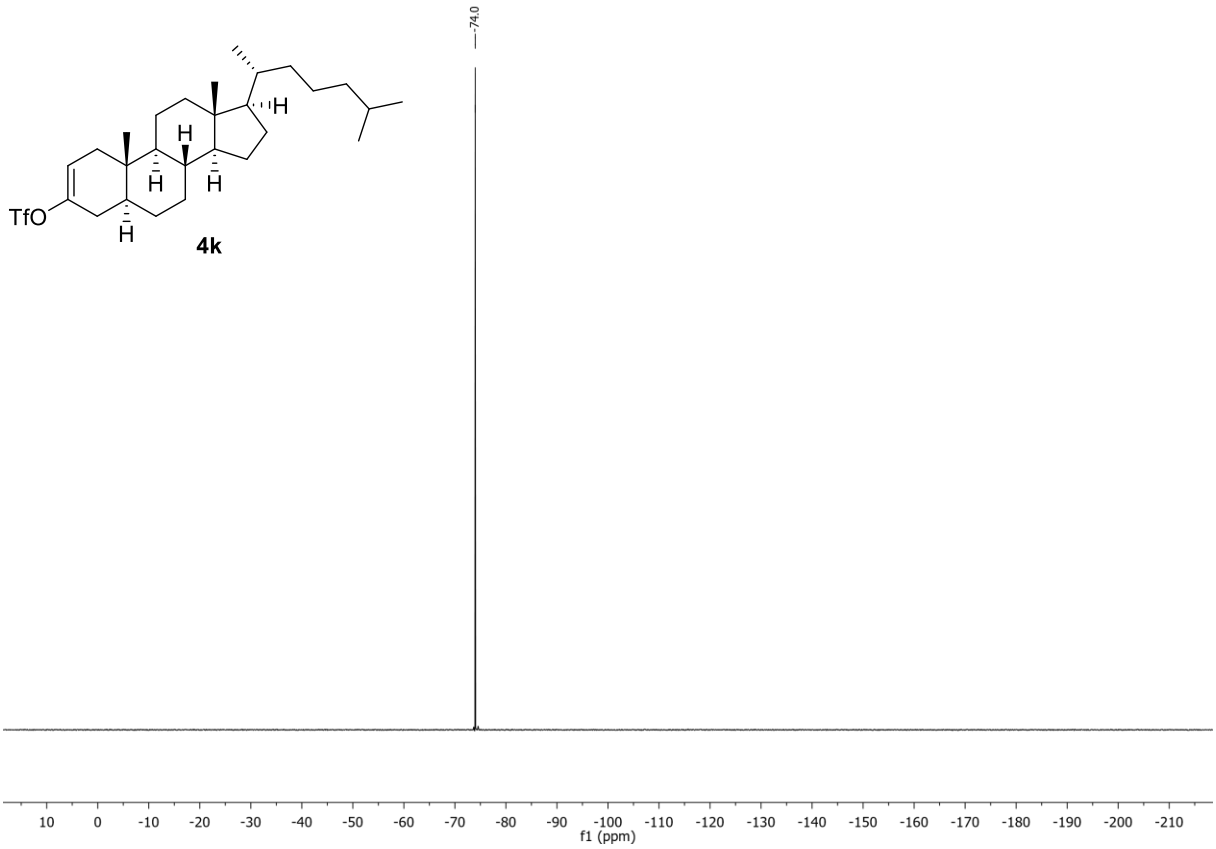

3.3. Products

3.3.1. Arylthioether

((1*s*,3*s*)-Adamantan-1-yl)(phenyl)sulfane (3aa):

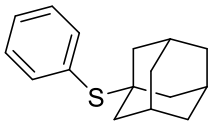

3aa

$C_{16}H_{20}S$ (244.40 g/mol)

Following **GP-C**, **3aa** was synthesized using phenyl trifluoromethanesulfonate (226 mg, 1.00 mmol, 1.0 equiv.) and 1-adamantanethiol (185 mg, 1.10 mmol, 1.1 equiv.). Purification by FC (SiO_2, gradient to 95:5 *n*-hexane/EtOAc over 15 CV) afforded **3aa** (240 mg, 982 µmol, 98%) as colorless solid. Conforms to reported analytical data.[25]

R_f: 0.78 (*n*-hexane/EtOAc 9:1).

^{1}H-NMR (400 MHz, $CDCl_3$, δ): 7.53 – 7.48 (m, 2H), 7.38 – 7.29 (m, 3H), 2.01 (s, 3H), 1.81 (d, *J* = 2.6 Hz, 6H), 1.62 (q, *J* = 12.3 Hz, 6H).

^{13}C-NMR (101 MHz, $CDCl_3$, δ): 137.8, 130.6, 128.7, 128.4, 48.0, 43.7, 36.3, 30.1.

^{1}H-NMR (400 MHz, $CDCl_3$) of compound **3aa**:

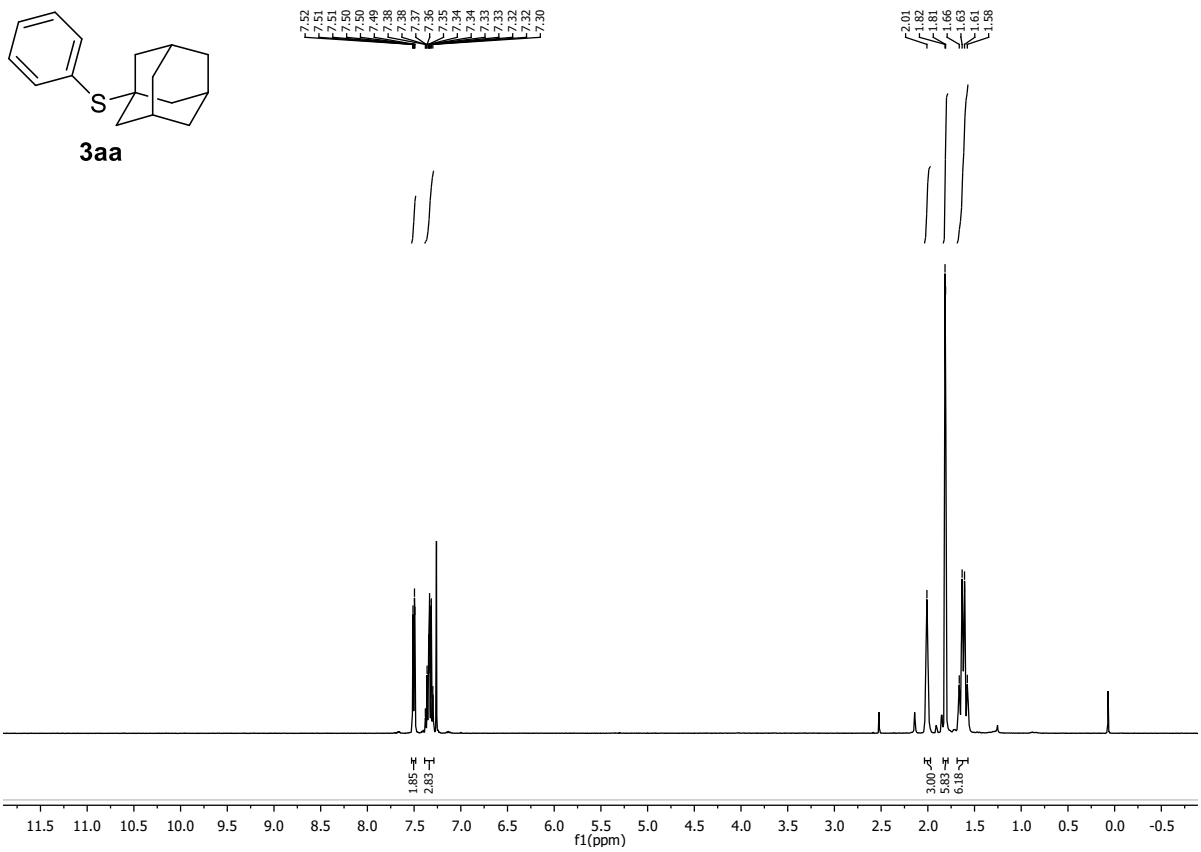

3aa

^{13}C-NMR (101 MHz, $CDCl_3$) of compound **3aa**:

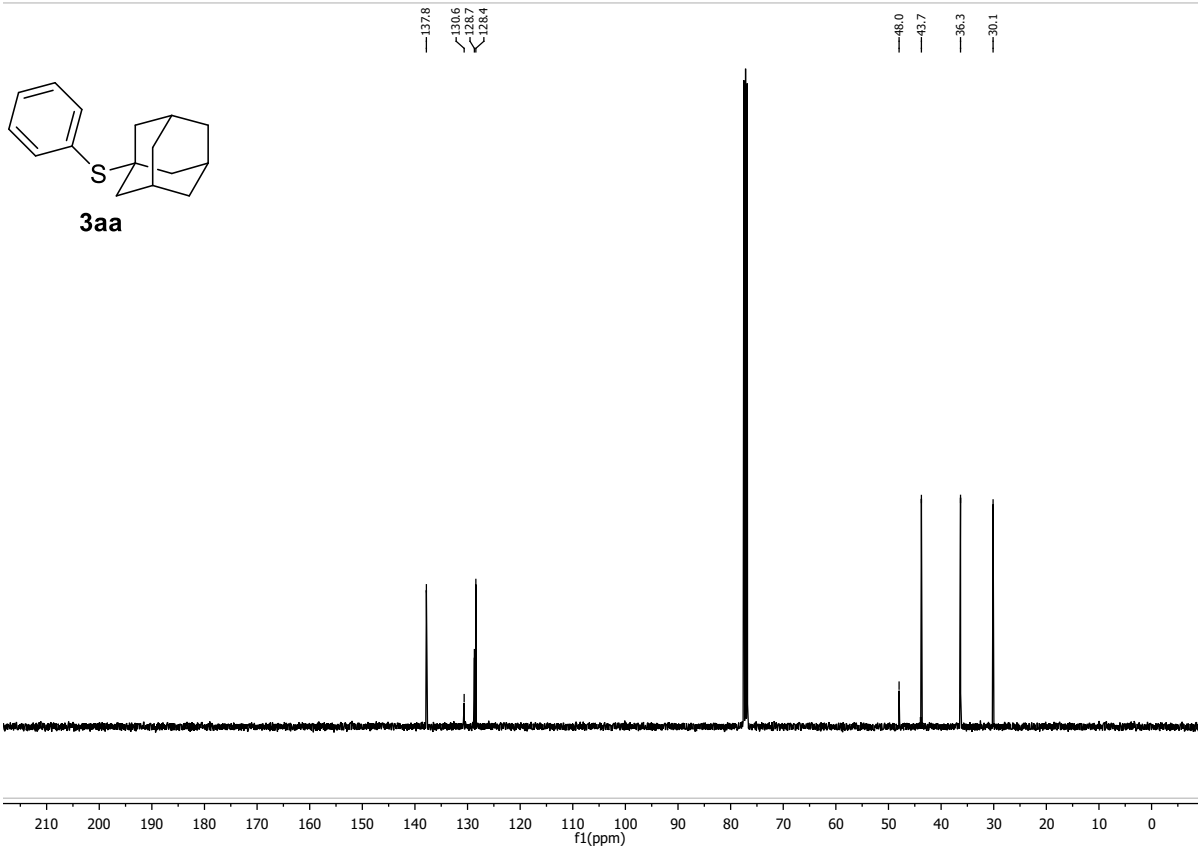

3aa

((1*s*,3*s*)-Adamantan-1-yl)(*p*-tolyl)sulfane (3ba):

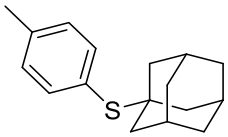

3ba

$C_{17}H_{22}S$ (258.42 g/mol)

Following **GP-C**, **3ba** was synthesized using *p*-tolyl trifluoromethanesulfonate (240 mg, 1.00 mmol, 1.0 equiv.) and 1-adamantanethiol (185 mg, 1.10 mmol, 1.1 equiv.). Purification by FC (SiO_2, gradient to 85:15 *n*-hexane /EtOAc over 20 CV) afforded **3ba** (231 mg, 894 µmol, 89%) as colorless solid. Conforms to reported analytical data.[25]

R_f: 0.27 (*n*-hexane).

^{1}H-NMR (400 MHz, $CDCl_3$, δ): 7.38 (d, *J* = 7.8 Hz, 2H), 7.12 (d, *J* = 7.8 Hz, 2H), 2.36 (s, 3H), 2.04 – 1.96 (m, 3H), 1.83 – 1.77 (m, 6H), 1.66 – 1.54 (m, 6H).

^{13}C-NMR (101 MHz, $CDCl_3$, δ): 138.7, 137.7, 129.2, 127.1, 47.7, 43.7, 36.3, 30.1, 21.4.

^{1}H-NMR (400 MHz, $CDCl_3$) of compound **3ba**:

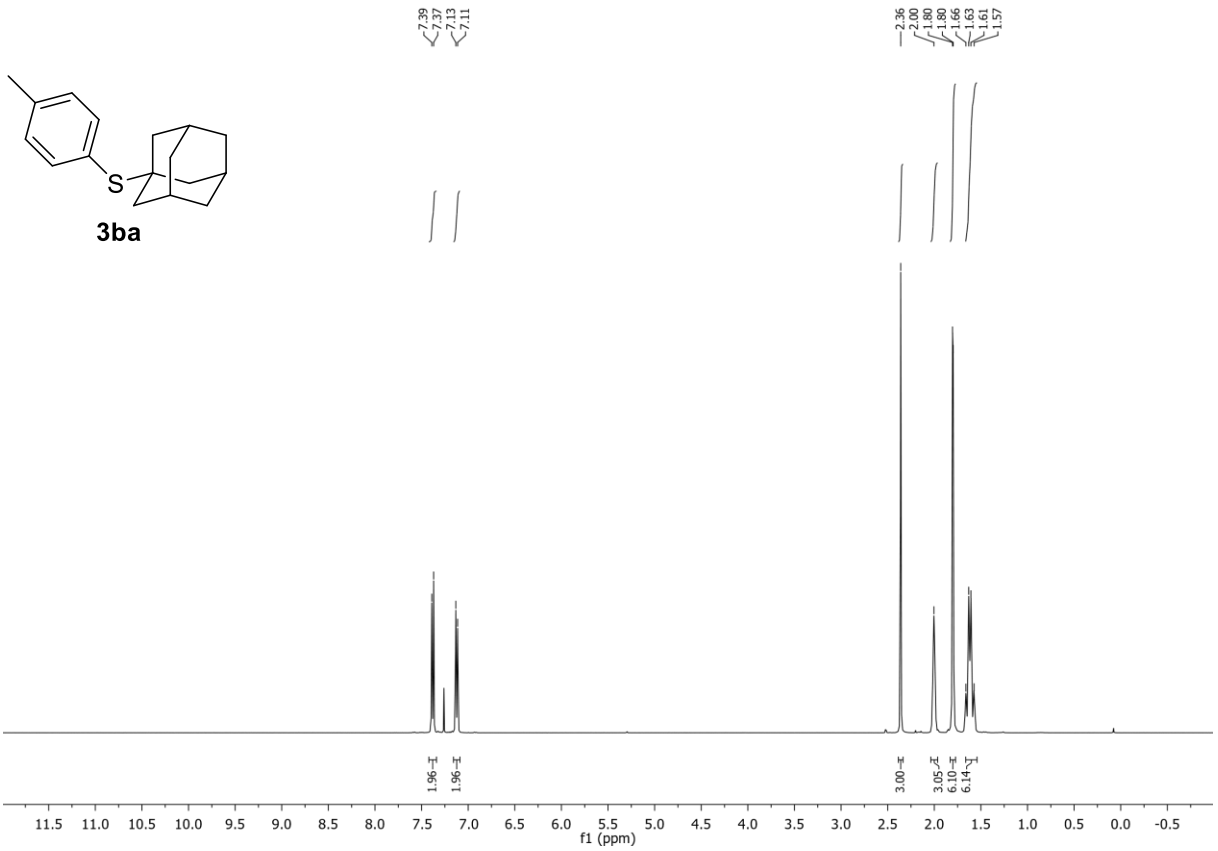

^{13}C-NMR (101 MHz, $CDCl_3$) of compound **3ba**:

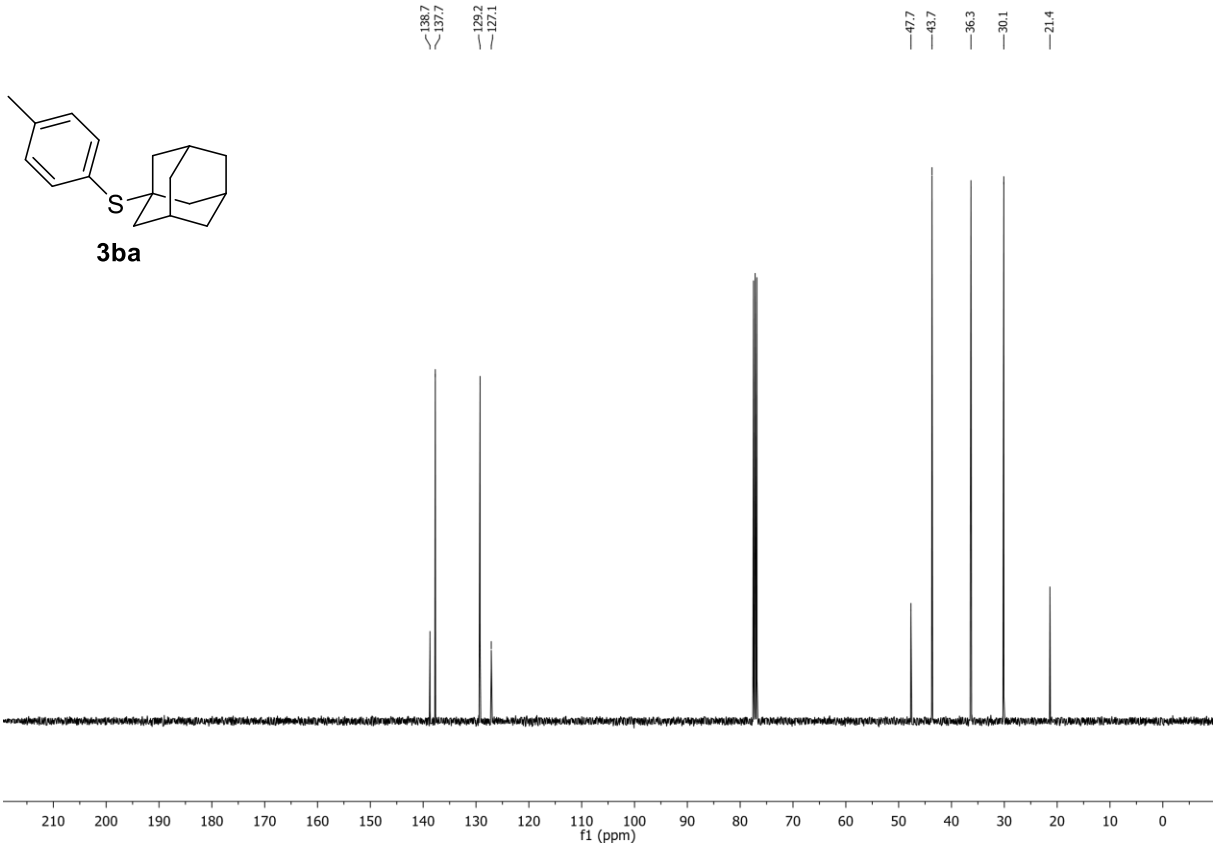

4-(((1*s*,3*s*)-Adamantan-1-yl)thio)benzonitrile (3ca):

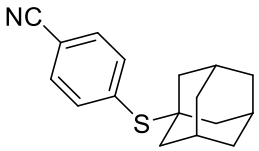

3ca

$C_{17}H_{19}NS$ (269.41 g/mol)

Following **GP-C**, **3ca** was synthesized using 4-cyanophenyl trifluoromethanesulfonate (251 mg, 1.00 mmol, 1.0 equiv.) and 1-adamantanethiol (185 mg, 1.10 mmol, 1.1 equiv.). Purification by FC (SiO_2, gradient to 6:4 *n*-hexane/EtOAc over 20 CV) afforded **3ca** (246 mg, 913 µmol, 91%) as colorless solid. Conforms to reported analytical data.[26]

R_f: 0.77 (*n*-hexane/EtOAc 95:5).

^{1}H-NMR (400 MHz, $CDCl_3$, δ): 7.59 (m, 4H), 2.07 – 2.01 (m, 3H), 1.85 – 1.81 (m, 6H), 1.68 – 1.59 (m, 6H).

^{13}C-NMR (101 MHz, $CDCl_3$, δ): 137.9, 137.7, 131.8, 118.7, 112.3, 49.8, 43.9, 36.1, 30.2.

^{1}H-NMR (400 MHz, $CDCl_3$) of compound **3ca**:

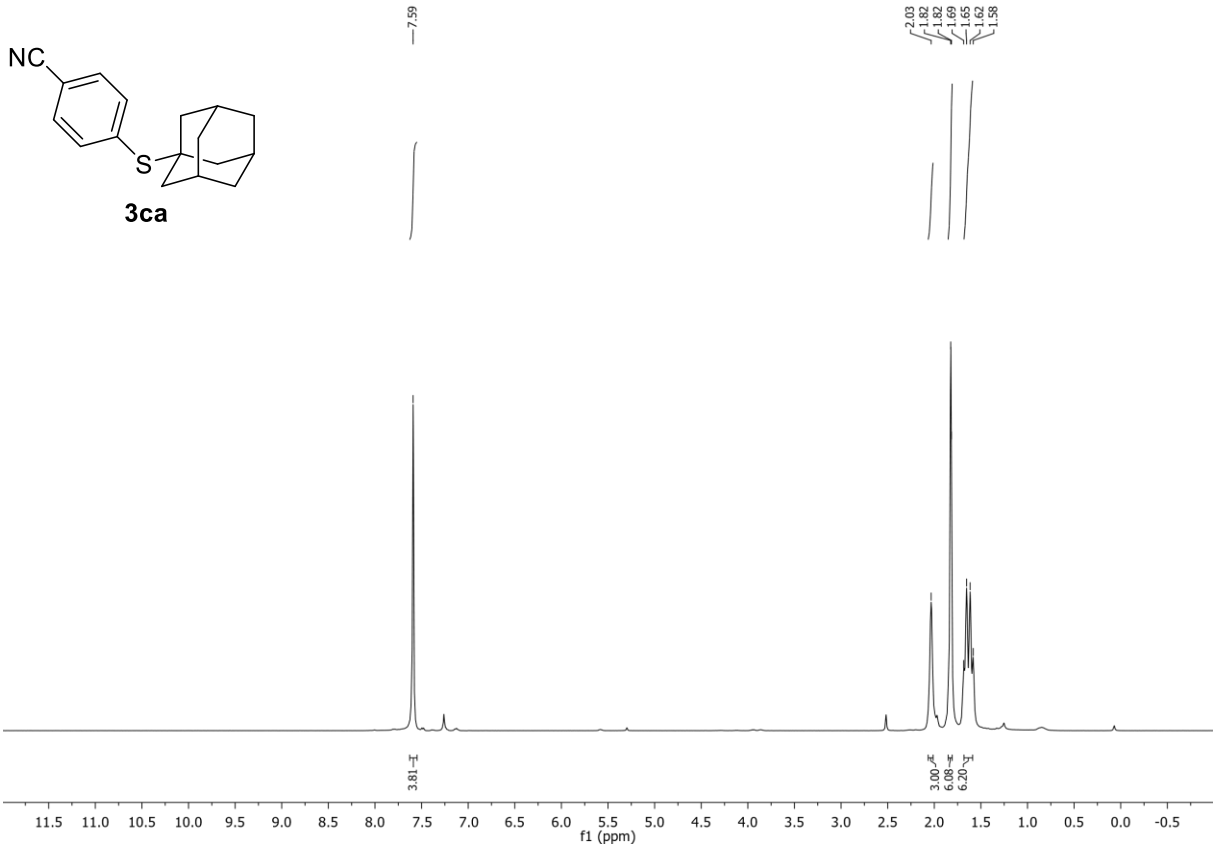

^{13}C-NMR (101 MHz, $CDCl_3$) of compound **3ca**:

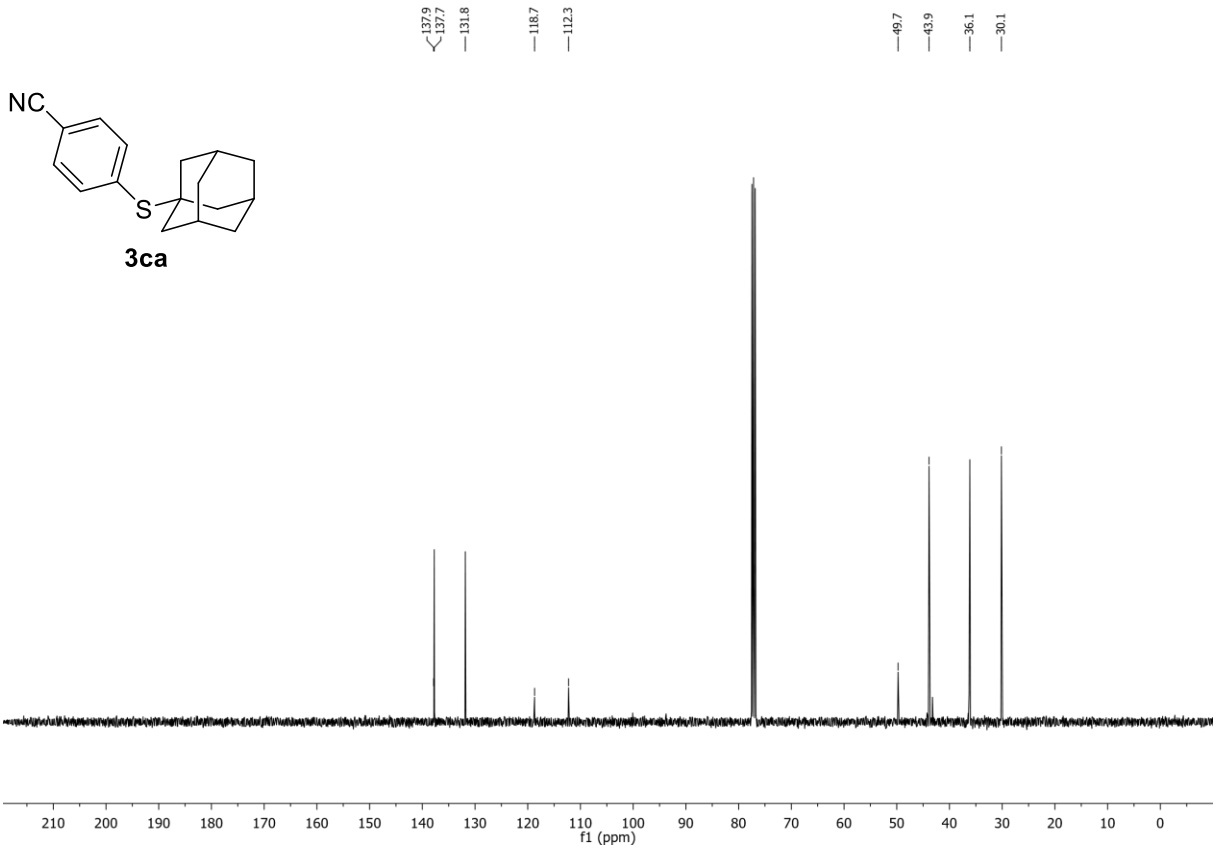

((1*s*,3*s*)-Adamantan-1-yl)(*o*-tolyl)sulfane (3da):

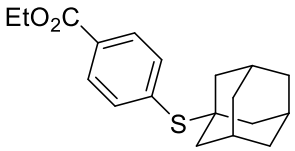

3da

$C_{19}H_{24}O_2S$ (316.46 g/mol)

Following **GP-C**, **3da** was synthesized using ethyl 4-(((trifluoromethyl)sulfonyl)oxy)benzoate (298 mg, 1.00 mmol, 1.0 equiv.) and 1-adamantanethiol (185 mg, 1.10 mmol, 1.1 equiv.). Purification by FC (SiO_2, gradient to 7:3 *n*-hexane/EtOAc over 20 CV) afforded **3da** (301 mg, 951 µmol, 95%) as colorless solid. Conforms to reported analytical data.[25]

R_f: 0.65 (*n*-hexane/EtOAc 9:1).

^{1}H-NMR (400 MHz, $CDCl_3$, δ): 7.97 (d, *J* = 8.2 Hz, 2H), 7.56 (d, *J* = 8.2 Hz, 2H), 4.38 (q, *J* = 7.1 Hz, 2H), 2.02 (m, 3H), 1.82 (m, 6H), 1.62 (m, 6H), 1.39 (t, *J* = 7.1 Hz, 3H).

^{13}C-NMR (101 MHz, $CDCl_3$, δ): 166.5, 137.3, 136.9, 130.6, 129.4, 61.3, 49.1, 43.9, 36.2, 30.2, 14.5.

^{1}H-NMR (400 MHz, $CDCl_3$) of compound **3da:**

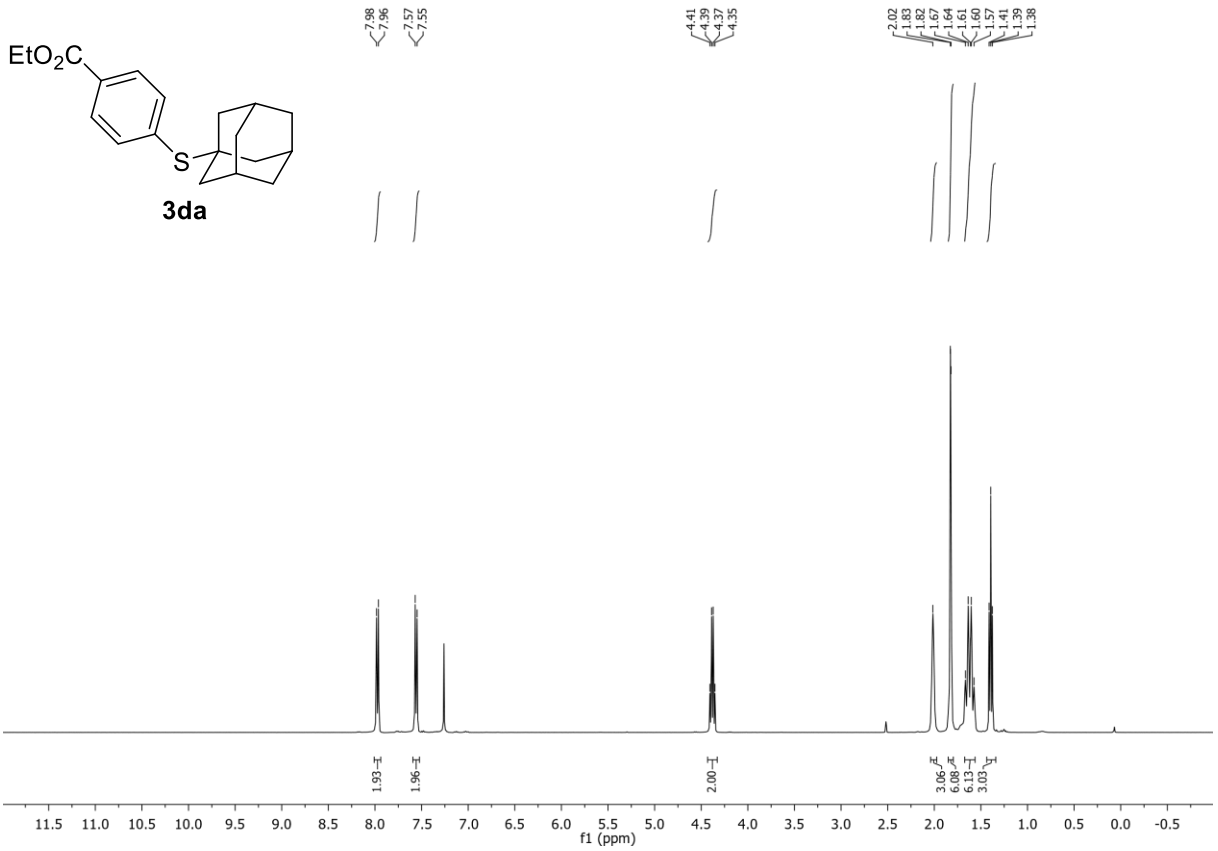

^{13}C-NMR (101 MHz, $CDCl_3$) of compound **3da**:

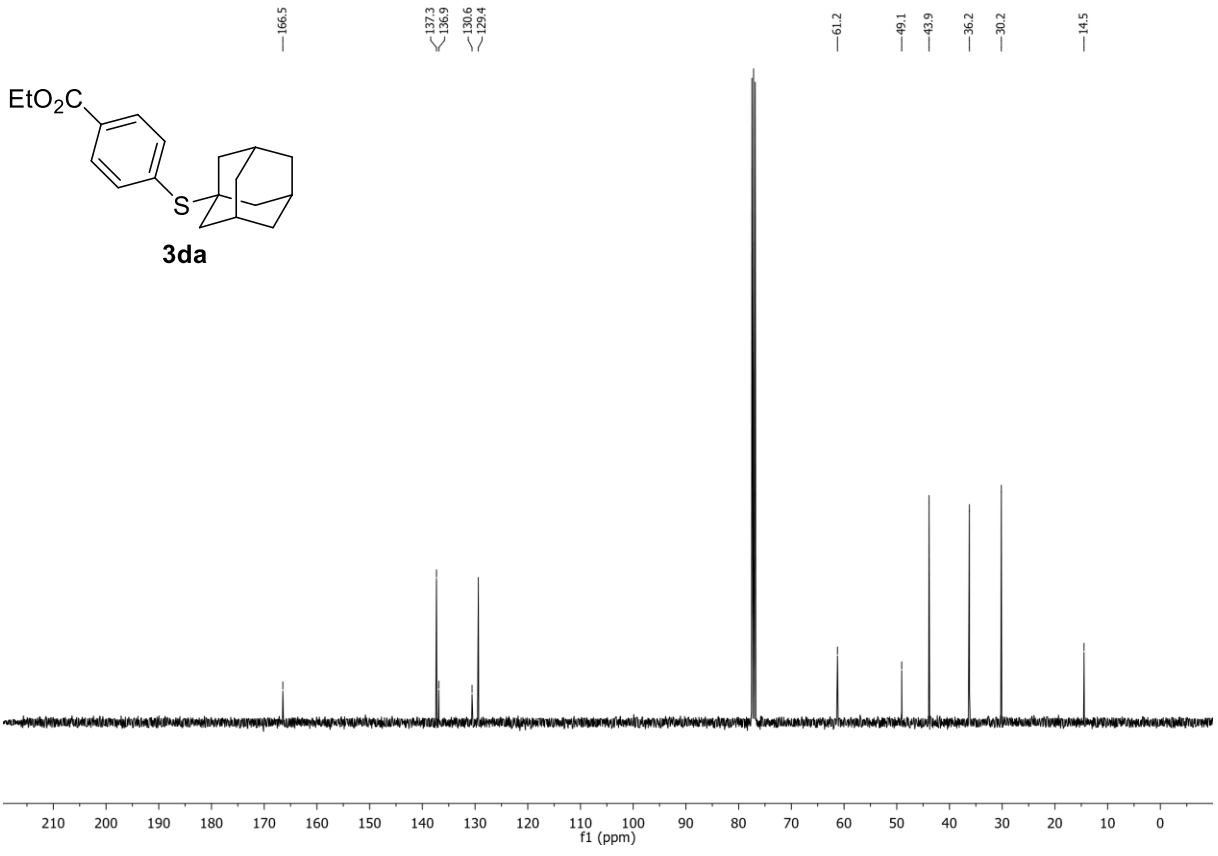

((1*s*,3*s*)-Adamantan-1-yl)(4-(trifluoromethyl)phenyl)sulfane (3ea):

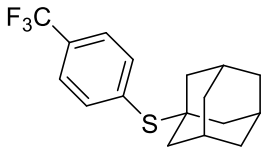

3ea

$C_{17}H_{19}F_3S$ (312.39 g/mol)

Following **GP-C**, **3ea** was synthesized using 4-(trifluoromethyl)phenyl trifluoromethanesulfonate (294 mg, 1.00 mmol, 1.0 equiv.) and 1-adamantanethiol (185 mg, 1.10 mmol, 1.1 equiv.). Purification by FC (SiO_2, gradient to 95:5 *n*-hexane/EtOAc over 12 CV, then to 8:2 over 5 CV) afforded **3ea** (277 mg, 888 µmol, 89%) as colorless solid. Conforms to reported analytical data.[25]

R_f: 0.77 (*n*-hexane/EtOAc 95:5).

^{1}H-NMR (400 MHz, $CDCl_3$, δ): 7.64 – 7.59 (m, 2H), 7.59 – 7.54 (m, 2H), 2.06 – 2.00 (m, 3H), 1.84 – 1.80 (m, 6H), 1.68 – 1.58 (m, 6H).

^{13}C-NMR (101 MHz, $CDCl_3$, δ): 137.8, 135.7, 130.7 (q, *J* = 32.6 Hz), 125.2 (q, *J* = 3.7 Hz), 124.2 (q, *J* = 272.2 Hz), 49.0, 43.8, 36.2, 30.1.

^{19}F-NMR (376 MHz, $CDCl_3$, δ): -62.6.

^{1}H-NMR (400 MHz, $CDCl_3$) of compound **3ea**:

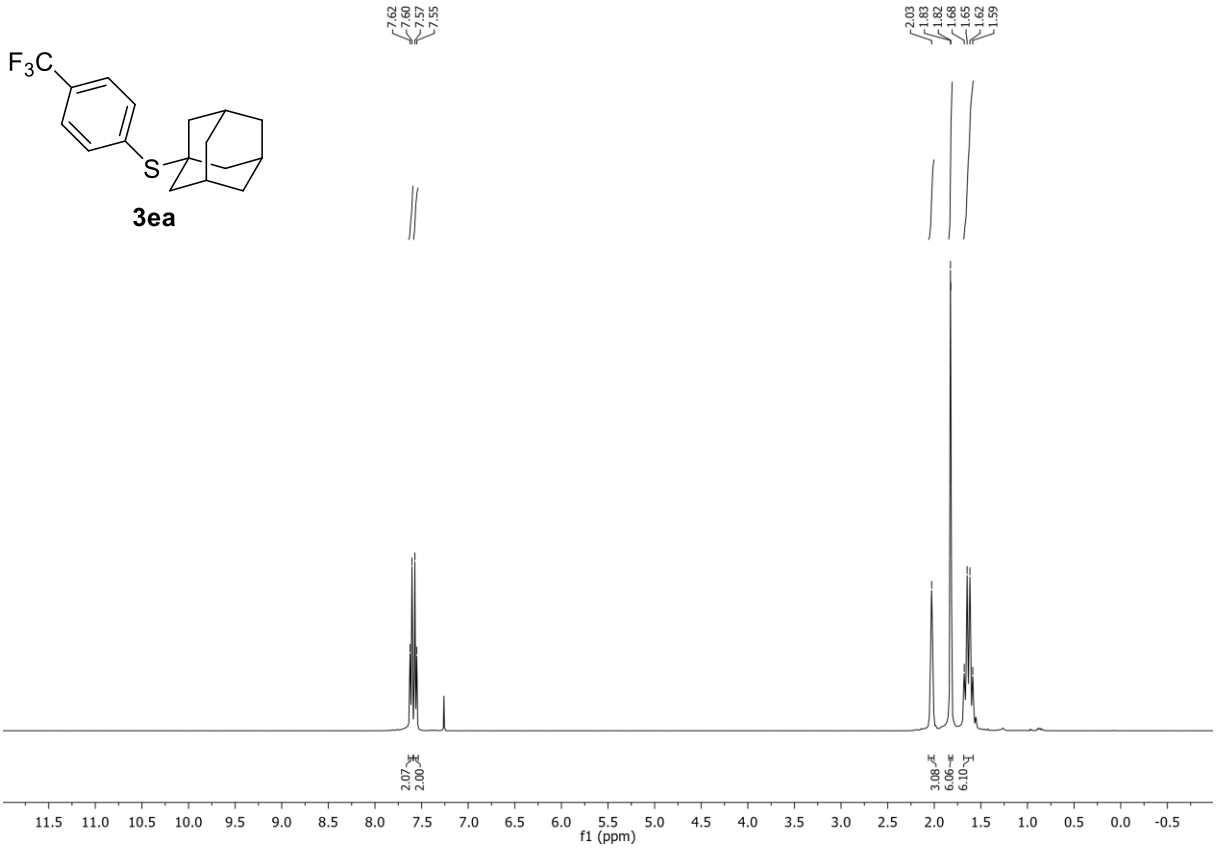

^{13}C-NMR (101 MHz, $CDCl_3$) of compound **3ea**:

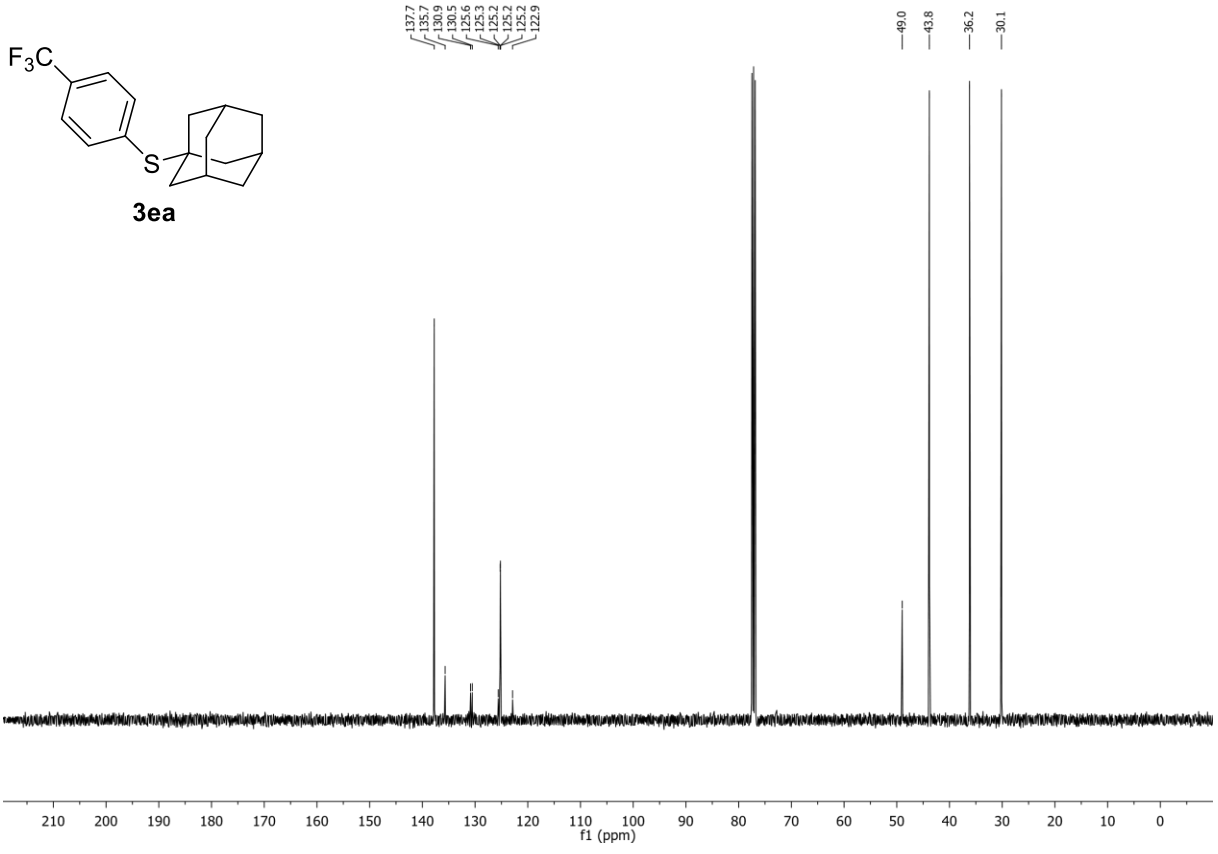

^{1}H-NMR (400 MHz, $CDCl_3$) of compound **3ea**:

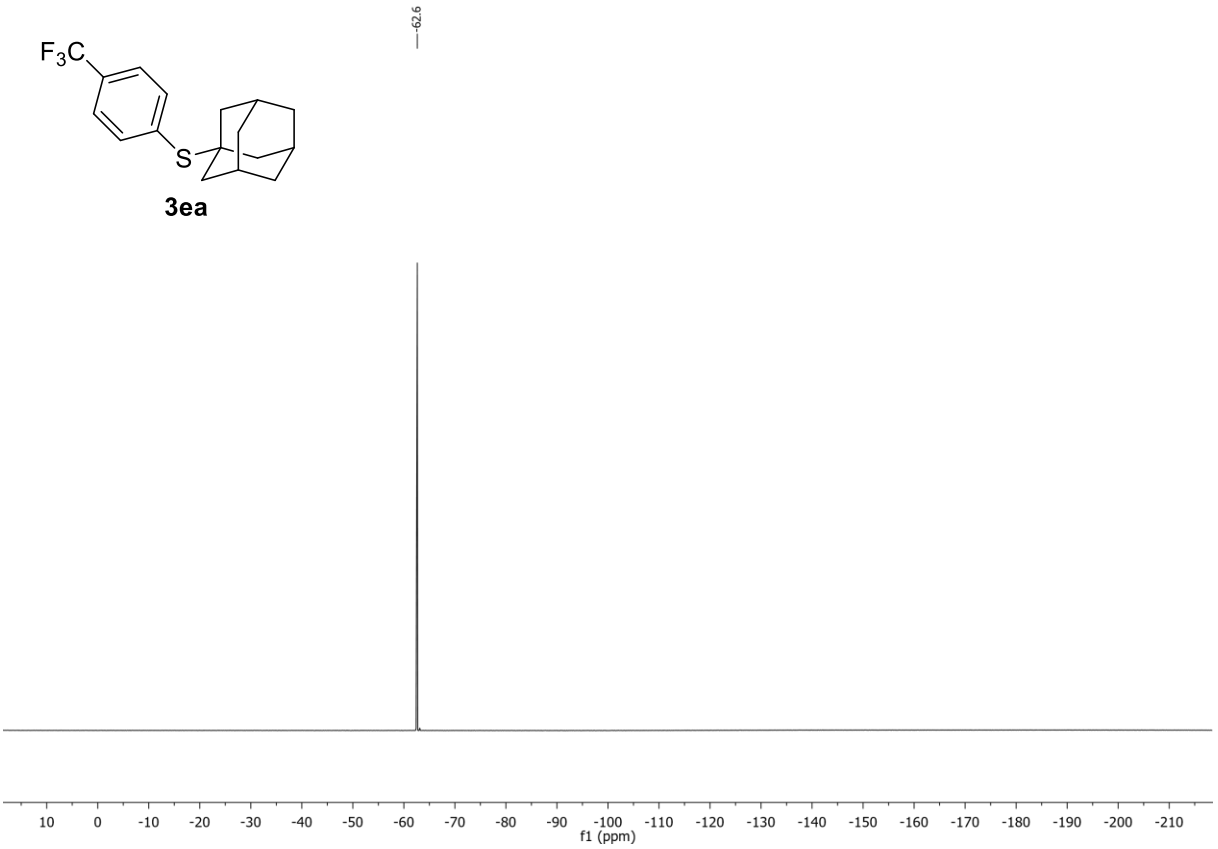

((3*s*,5*s*,7*s*)-Adamantan-1-yl)(3-methoxyphenyl)sulfane (3fa):

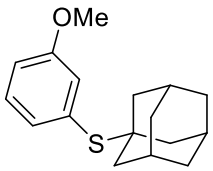

3fa

$C_{17}H_{22}OS$ (274.42 g/mol)

Following **GP-C**, **3fa** was synthesized using 3-methoxyphenyl trifluoromethanesulfonate (256 mg, 1.0 µmol, 1.0 equiv.) and 1-adamantanethiol (185 mg, 1.1 µmol, 1.1 equiv.). Purification by FC (SiO_2, 99:1 *n*-hexane/EtOAc for 20 CV) afforded **3fa** (267 mg, 973 µmol, 97%) as colorless solid. Conforms to reported analytical data.[25]

R_f: 0.53 (*n*-hexane/EtOAc 9:1).

^{1}H-NMR (400 MHz, $CDCl_3$, δ): 7.25 – 7.20 (m, 1H), 7.12 – 7.04 (m, 2H), 6.94 – 6.87 (m, 1H), 3.81 (s, 3H), 2.04 – 1.99 (m, 3H), 1.84 – 1.81 (m, 6H), 1.67 – 1.57 (m, 6H).

^{13}C-NMR (101 MHz, $CDCl_3$, δ): 159.3, 131.8, 130.1, 129.1, 122.9, 114.6, 100.1, 55.5, 48.2, 43.8, 36.3, 30.1.

^{1}H-NMR (400 MHz, $CDCl_3$) of compound **3fa**:

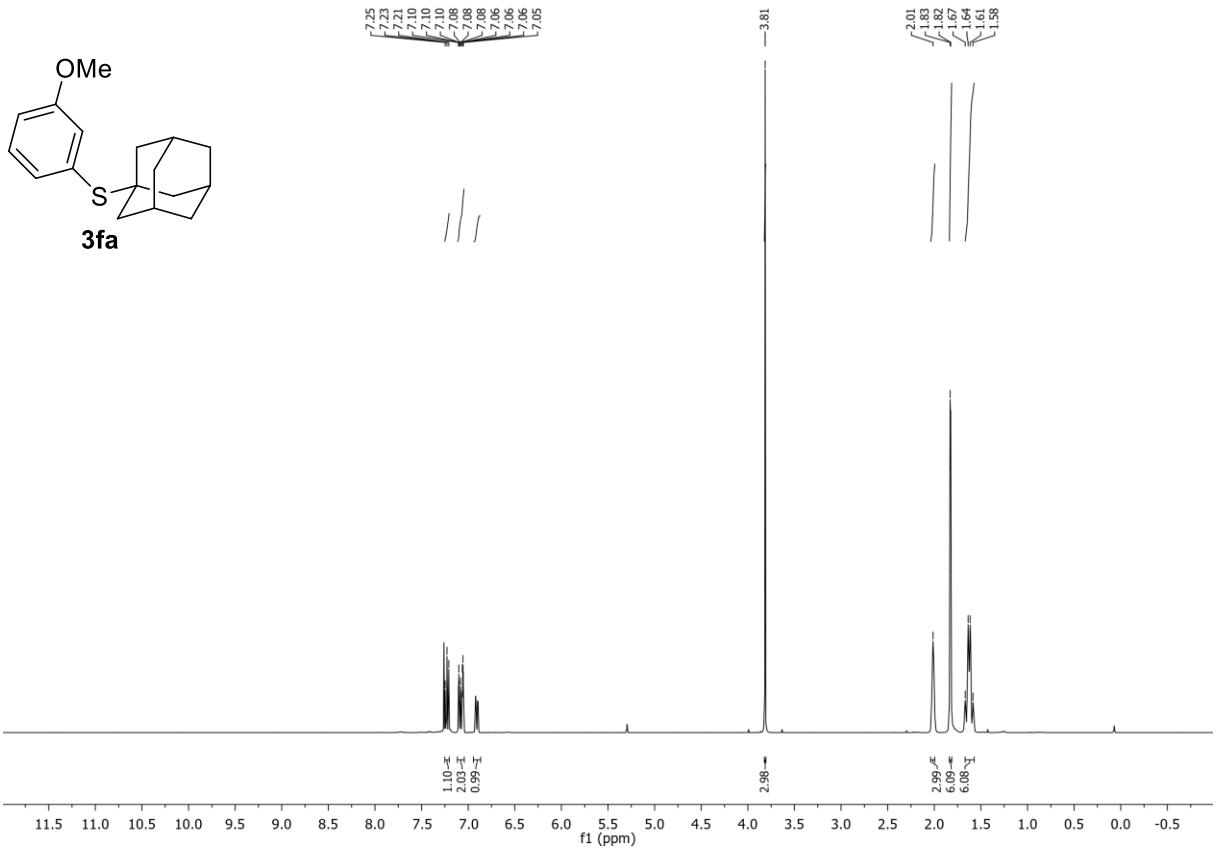

^{13}C-NMR (101 MHz, $CDCl_3$) of compound **3fa**:

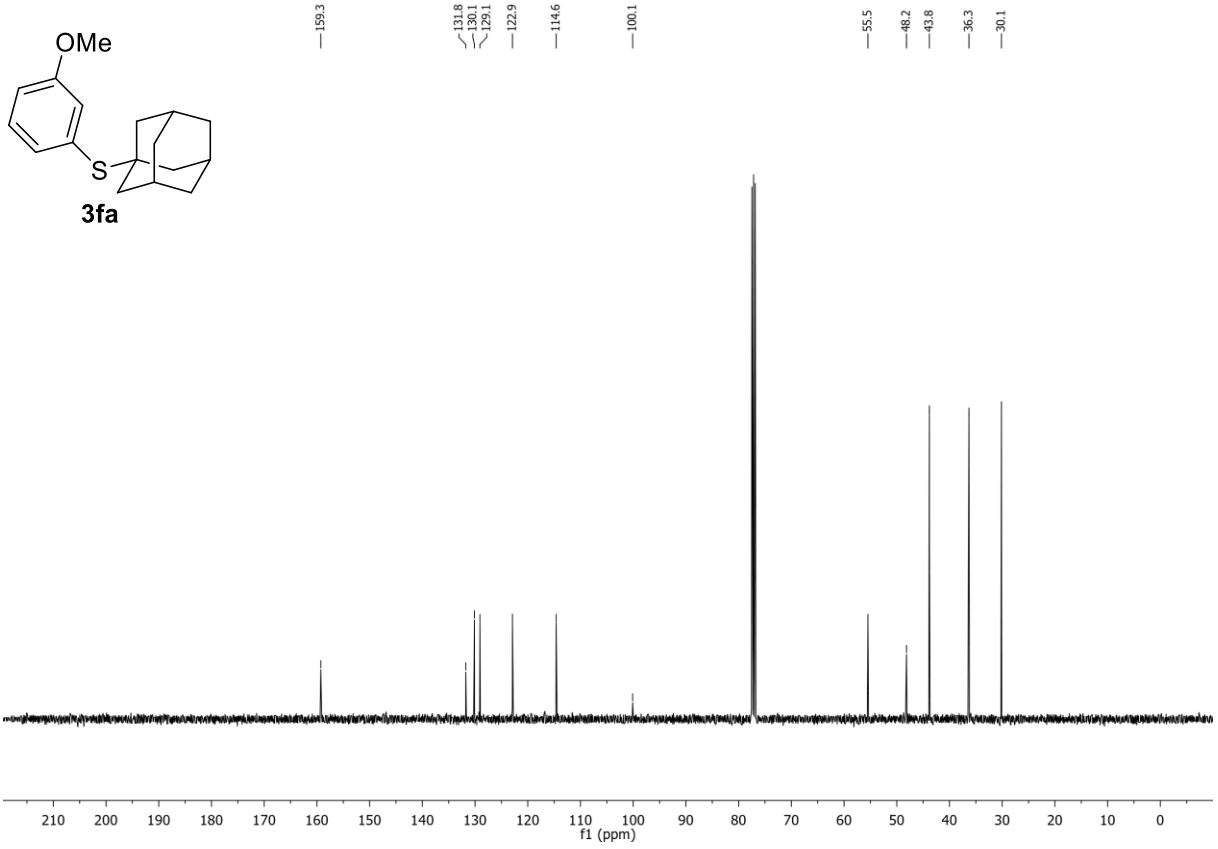

***N*-(4-(((1*s*,3*s*)-Adamantan-1-yl)thio)phenyl)acetamide (3ga):**

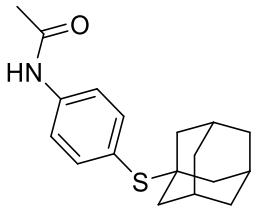

3ga

$C_{18}H_{23}NOS$ (301.45 g/mol)

Following **GP-C**, **3ga** was synthesized using 4-acetamidophenyl trifluoromethanesulfonate (283 mg, 1.00 mmol, 1.0 equiv.) and 1-adamantanethiol (185 mg, 1.10 mmol, 1.1 equiv.). Purification by FC (SiO_2, gradient to 50:50 *n*-hexane/EtOAc over 10 CV, then gradient to EtOAc over 5 CV) afforded **3ga** (283 mg, 939 µmol, 94%) as colorless solid. Conforms to reported analytical data.[25]

R_f: 0.38 (*n*-hexane/EtOAc 5:5).

^{1}H-NMR (400 MHz, $CDCl_3$, δ): 7.50 – 7.40 (m, 4H), 7.28 (br s, 1H), 2.19 (s, 3H), 2.00 (m, 3H), 1.78 (m, 6H), 1.63 (m, 6H).

^{13}C-NMR (101 MHz, $CDCl_3$, δ): 168.5, 138.5, 125.8, 119.5, 48.1, 43.7, 36.3, 30.1, 24.9.

^{1}H-NMR (400 MHz, $CDCl_3$) of compound **3ga**:

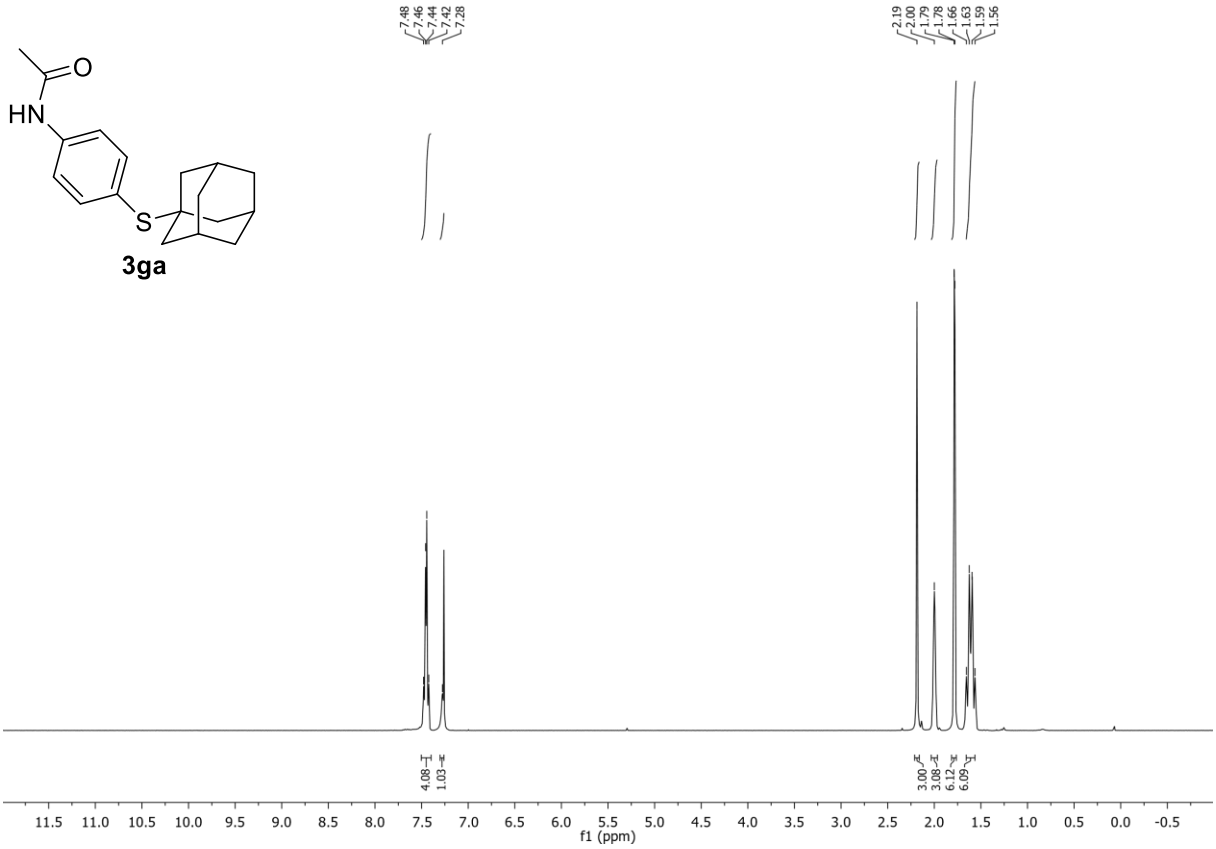

^{13}C-NMR (101 MHz, $CDCl_3$) of compound **3ga**:

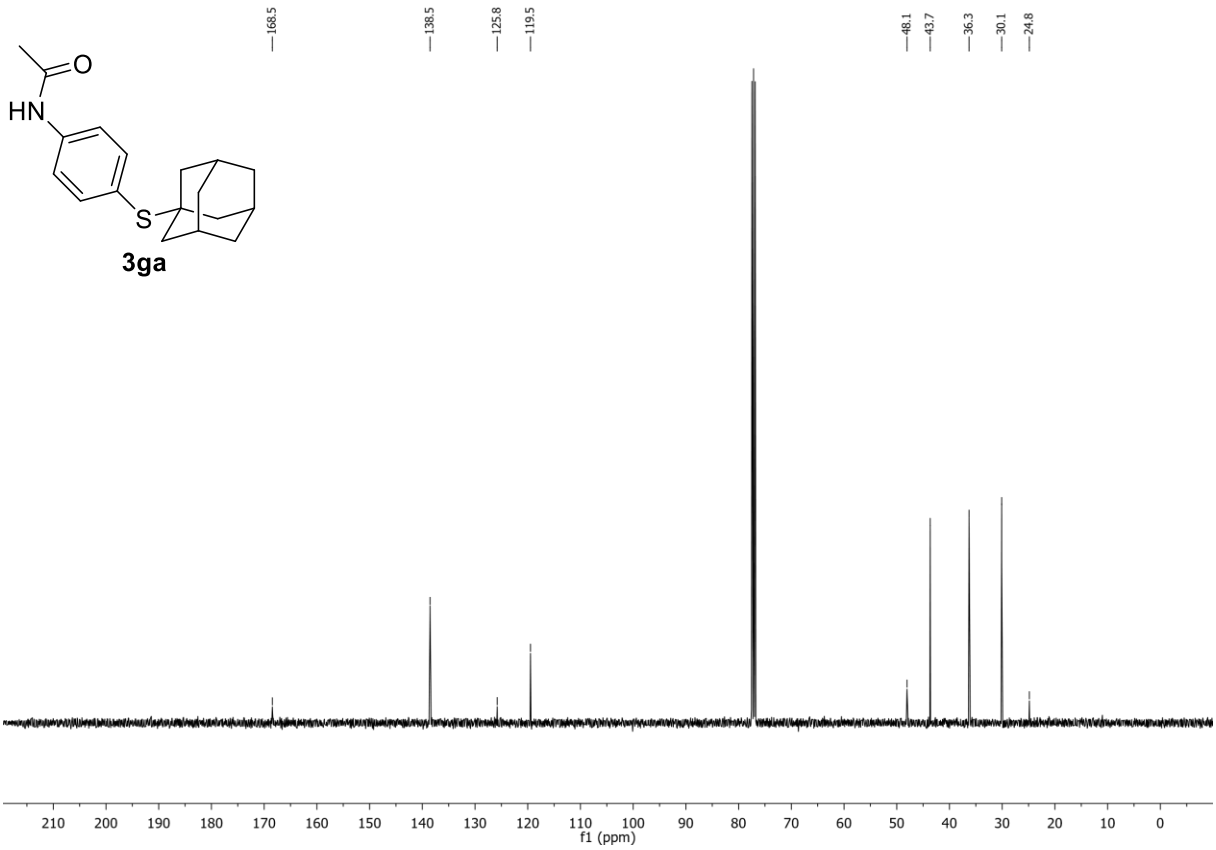

((1*s*,3*s*)-Adamantan-1-yl)(naphthalen-2-yl)sulfane (3ha):

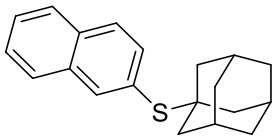

3ha

$C_{20}H_{22}S$ (294.46 g/mol)

Following **GP-C**, **3ha** was synthesized using naphthalen-2-yl trifluoromethanesulfonate (276 mg, 1.00 mmol, 1.0 equiv.) and 1-adamantanethiol (185 mg, 1.10 mmol, 1.1 equiv.). Purification by FC (SiO_2, gradient to 60:40 *n*-hexane/EtOAc over 20 CV) afforded **3ha** (267 mg, 907 µmol, 91%) as colorless solid. Conforms to reported analytical data.[27]

R_f: 0.30 (*n*-hexane).

^{1}H-NMR (400 MHz, $CDCl_3$, δ): 8.04 (s, 1H), 7.90 – 7.79 (m, 2H), 7.77 (d, *J* = 8.4 Hz, 1H), 7.57 (dd, *J* = 8.4, 1.7 Hz, 1H), 7.54 – 7.47 (m, 2H), 2.05 – 1.97 (m, 3H), 1.90 – 1.85 (m, 6H), 1.68 – 1.56 (m, 6H).

^{13}C-NMR (101 MHz, $CDCl_3$, δ): 137.4, 134.8, 133.4, 133.2, 128.2, 128.0, 127.7, 127.7, 126.7, 126.4, 48.5, 43.9, 36.3, 30.2.

^{1}H-NMR (400 MHz, $CDCl_3$) of compound **3ha**:

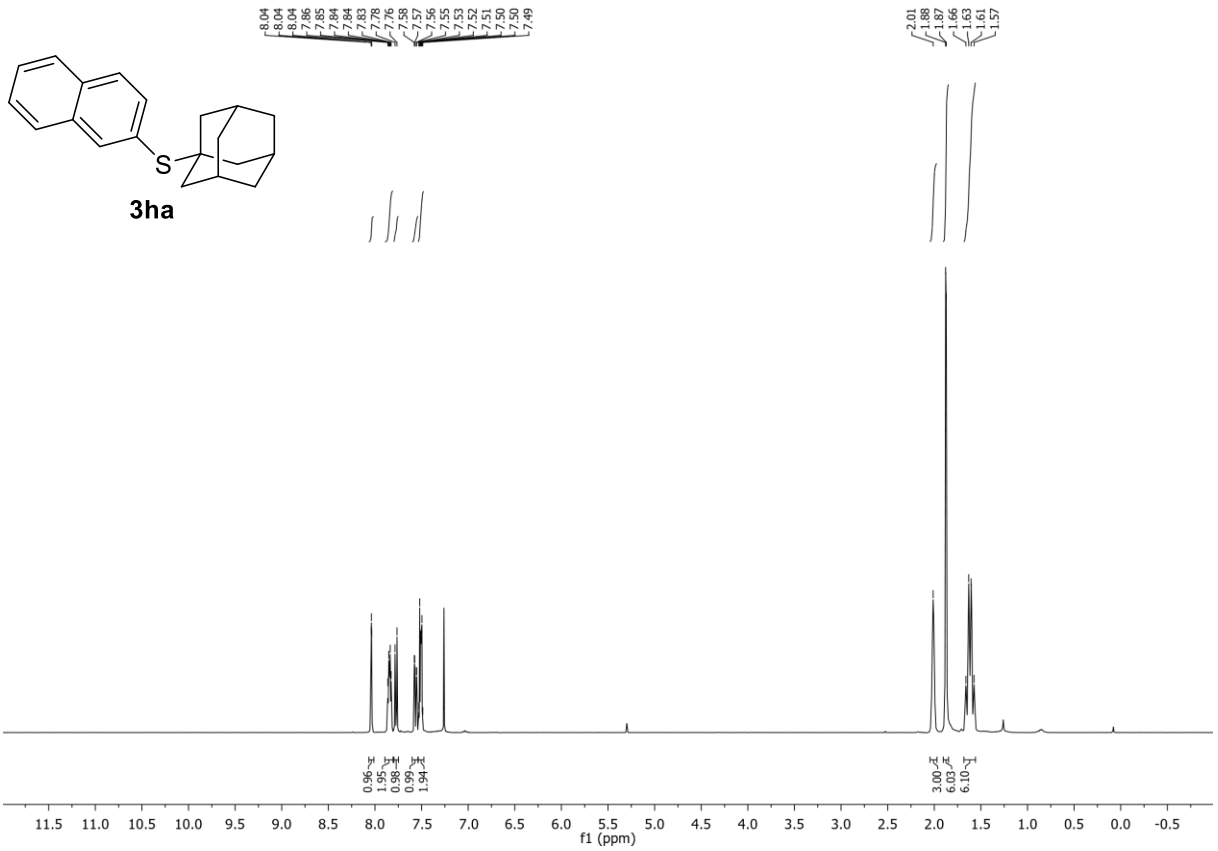

^{13}C-NMR (101 MHz, $CDCl_3$) of compound **3ha**:

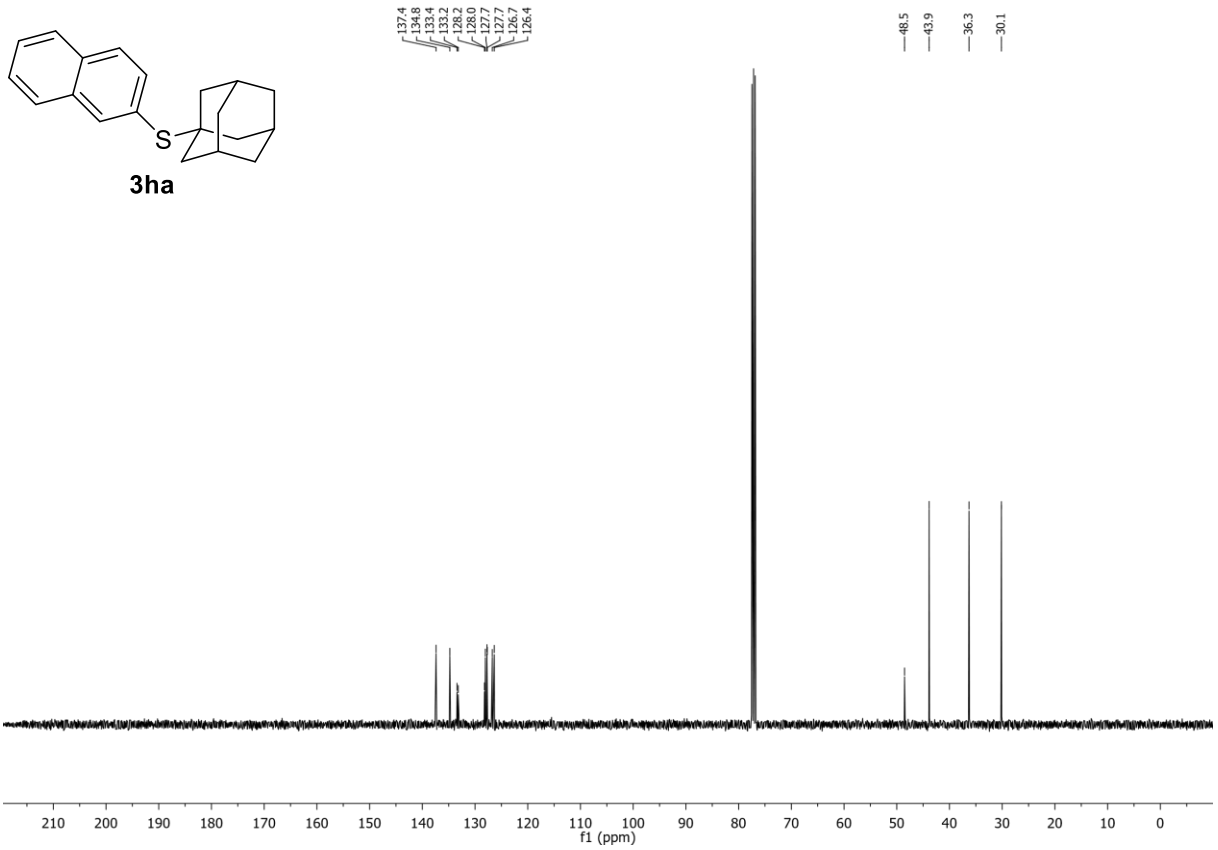

7-(((1*s*,3*s*)-Adamantan-1-yl)thio)-4-methyl-2*H*-chromen-2-one (3ia):

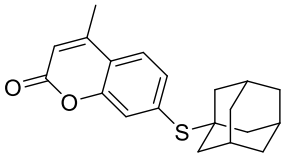

3ia

$C_{20}H_{22}O_2S$ (326.45 g/mol)

Following **GP-C**, **3ia** was synthesized using 4-methyl-2-oxo-2*H*-chromen-7-yl trifluoromethanesulfonate (308 mg, 1.00 mmol, 1.0 equiv.) and 1-adamantanethiol (185 mg, 1.10 mmol, 1.1 equiv.). Purification by FC (SiO_2, gradient to 75:15 *n*-hexane/EtOAc over 15 CV, then gradient to EtOAc over 5 CV) afforded **3ia** (289 mg, 885 µmol, 89%) as colorless solid.

R_f: 0.27 (*n*-hexane/EtOAc).

m.p.: 144.4 – 146.0 °C.

^{1}H-NMR (400 MHz, $CDCl_3$, δ): 7.52 (d, *J* = 8.1 Hz, 1H), 7.49 (d, *J* = 1.6 Hz, 1H), 7.40 (dd, *J* = 8.1, 1.6 Hz, 1H), 6.31 (q, *J* = 1.3 Hz, 1H), 2.44 (d, *J* = 1.3 Hz, 3H), 2.07 – 1.99 (m, 3H), 1.89 – 1.81 (m, 6H), 1.68 – 1.57 (m, 6H).

^{13}C-NMR (101 MHz, $CDCl_3$, δ): 160.6, 152.9, 152.1, 136.1, 133.0, 125.2, 124.0, 120.1, 115.6, 49.7, 43.9, 36.2, 30.2, 18.8.

HR-MS (APCI): m/z calc. for $[M+H]^+$ 327.1413, found 327.1412.

IR (ATR, $\tilde{\nu}$ [cm^{-1}]): 2900 (w), 2846 (w), 1717 (s), 1623 (w), 1593 (m), 1541 (w), 1482 (w), 1445 (w), 1385 (m), 1353 (w), 1349 (w), 1295 (w), 1262 (w), 1236 (w), 1217 (w), 1162 (m), 1105 (w), 1060 (w), 1034 (w), 1008 (w), 978 (w), 945 (m), 855 (s), 822 (m), 764 (m), 706 (m), 680 (w).

^{1}H-NMR (400 MHz, $CDCl_3$) of compound **3ia**:

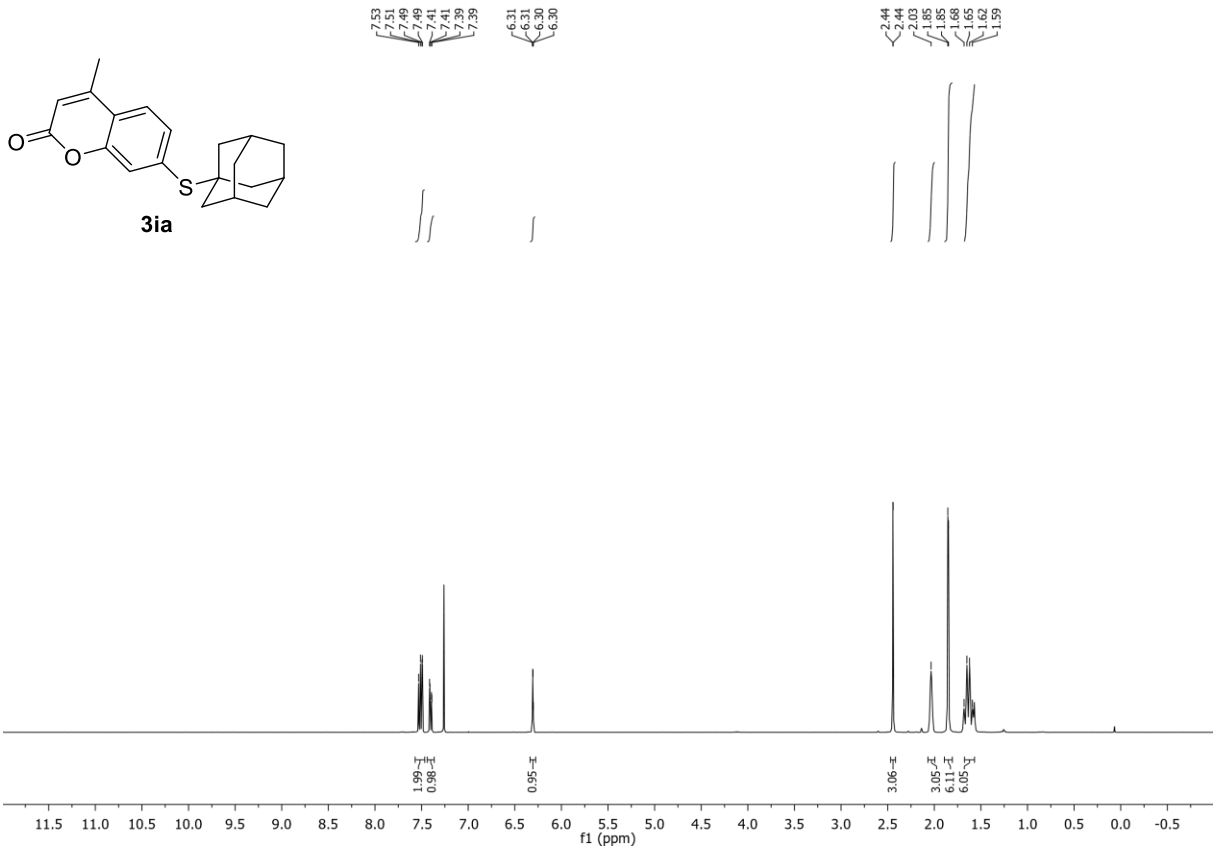

^{13}C-NMR (101 MHz, $CDCl_3$) of compound **3ia**:

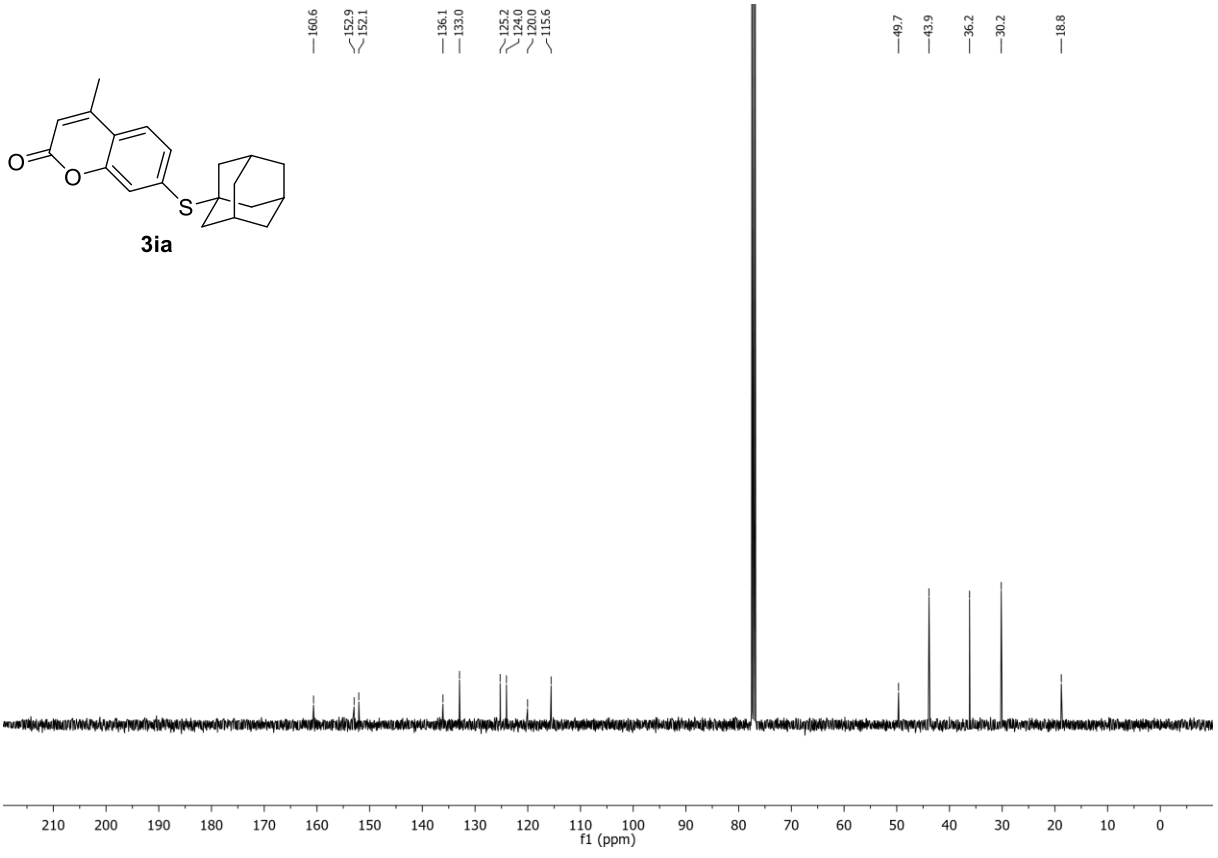

5-(((1*s*,3*s*)-Adamantan-1-yl)thio)benzo[d][1,3]dioxole (3ja):

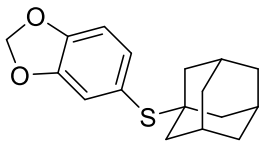

3ja

$C_{17}H_{20}O_2S$ (288.41 g/mol)

Following **GP-C**, **3ja** was synthesized using benzo[d][1,3]dioxol-5-yl trifluoromethanesulfonate (270 mg, 1.00 mmol, 1.0 equiv.) and 1-adamantanethiol (185 mg, 1.10 mmol, 1.1 equiv.). Purification by FC (SiO_2, gradient to 9:1 *n*-hexane/EtOAc over 15 CV) afforded **3ja** (218 mg, 756 µmol, 76%) as colorless solid. Conforms to reported analytical data.[25]

R_f: 0.70 (*n*-hexane/EtOAc 95:5).

^{1}H-NMR (400 MHz, $CDCl_3$, δ): 6.99 (dd, *J* = 7.9, 1.7 Hz, 1H), 6.95 (d, *J* = 1.7 Hz, 1H), 6.76 (d, *J* = 7.9 Hz, 1H), 5.99 (s, 2H), 2.05 – 1.98 (m, 3H), 1.81 – 1.76 (m, 6H), 1.67 – 1.57 (m, 6H).

^{13}C-NMR (101 MHz, $CDCl_3$, δ): 148.5, 147.4, 131.9, 122.9, 117.6, 108.2, 101.5, 47.9, 43.6, 36.3, 30.1.

^{1}H-NMR (400 MHz, $CDCl_3$) of compound **3ja**:

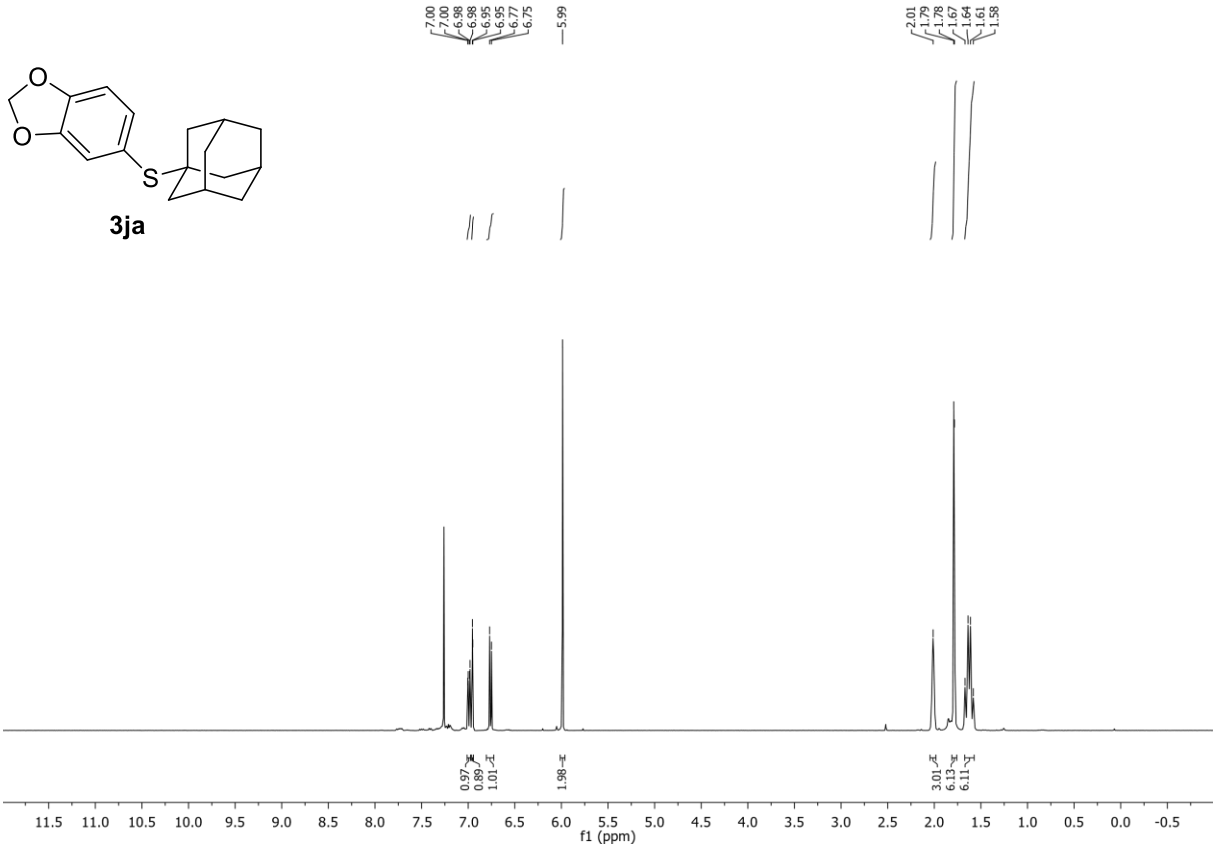

3ja

^{13}C-NMR (101 MHz, $CDCl_3$) of compound **3ja**:

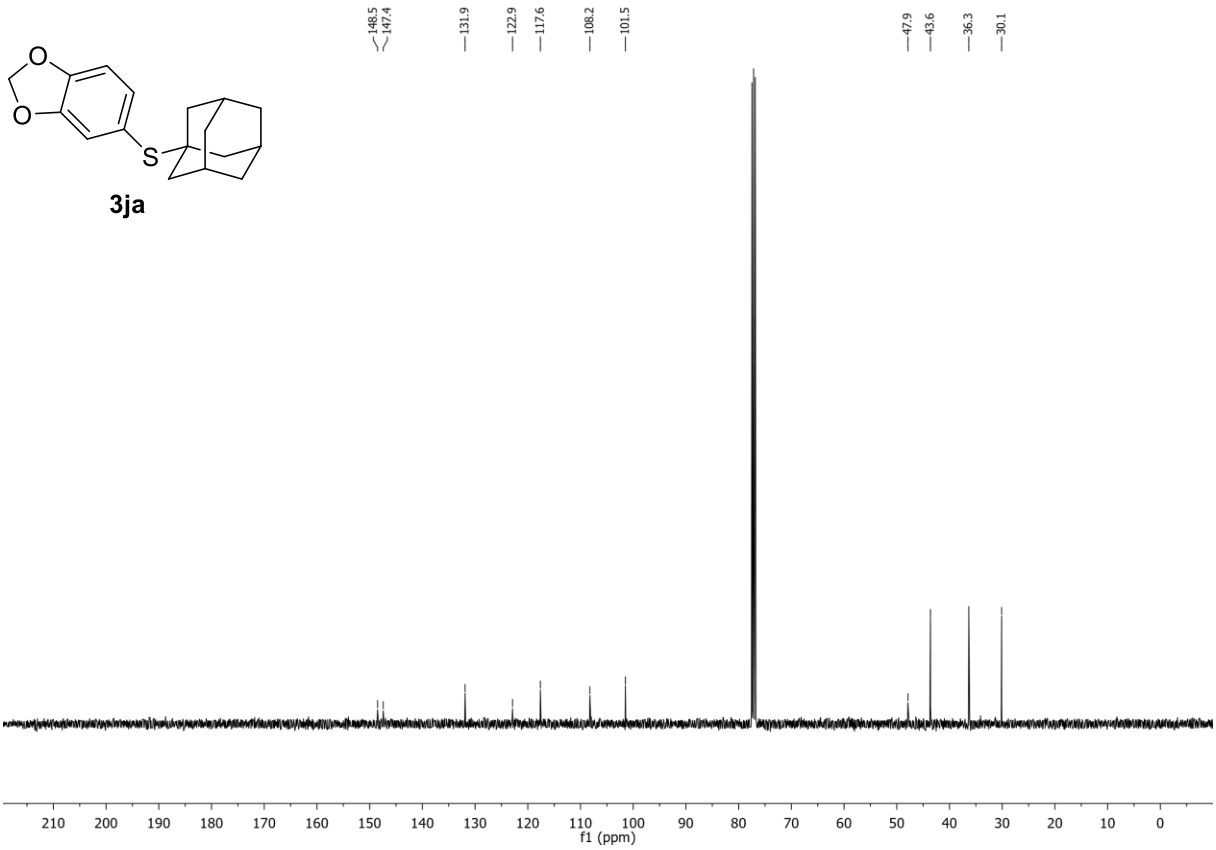

3ja

3-(((1*s*,3*s*)-Adamantan-1-yl)thio)pyridine (3ka):

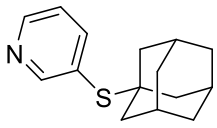

3ka

$C_{15}H_{19}NS$ (245.38 g/mol)

Following **GP-C**, **3ka** was synthesized using pyridin-3-yl trifluoromethanesulfonate (227 mg, 1.00 mmol, 1.0 equiv.) and 1-adamantanethiol (185 mg, 1.10 mmol, 1.1 equiv.). Purification by FC (SiO_2, gradient to 65:35 *n*-hexane/EtOAc over 15 CV) afforded **3ka** (146 mg, 595 µmol, 60%) as colorless solid. Conforms to reported analytical data.[25]

R_f: 0.31 (*n*-hexane/EtOAc 9:1).

^{1}H-NMR (400 MHz, $CDCl_3$, δ): 8.71 – 8.66 (m, 1H), 8.61 – 8.55 (m, 1H), 7.86 – 7.78 (m, 1H), 7.32 – 7.26 (m, 1H), 2.06 – 1.99 (m, 3H), 1.81 – 1.78 (m, 6H), 1.68 – 1.56 (m, 6H).

^{13}C-NMR (101 MHz, $CDCl_3$, δ): 156.9, 149.3, 145.1, 128.1, 123.5, 48.7, 43.7, 36.2, 30.1.

^{1}H-NMR (400 MHz, $CDCl_3$) of compound **3ka**:

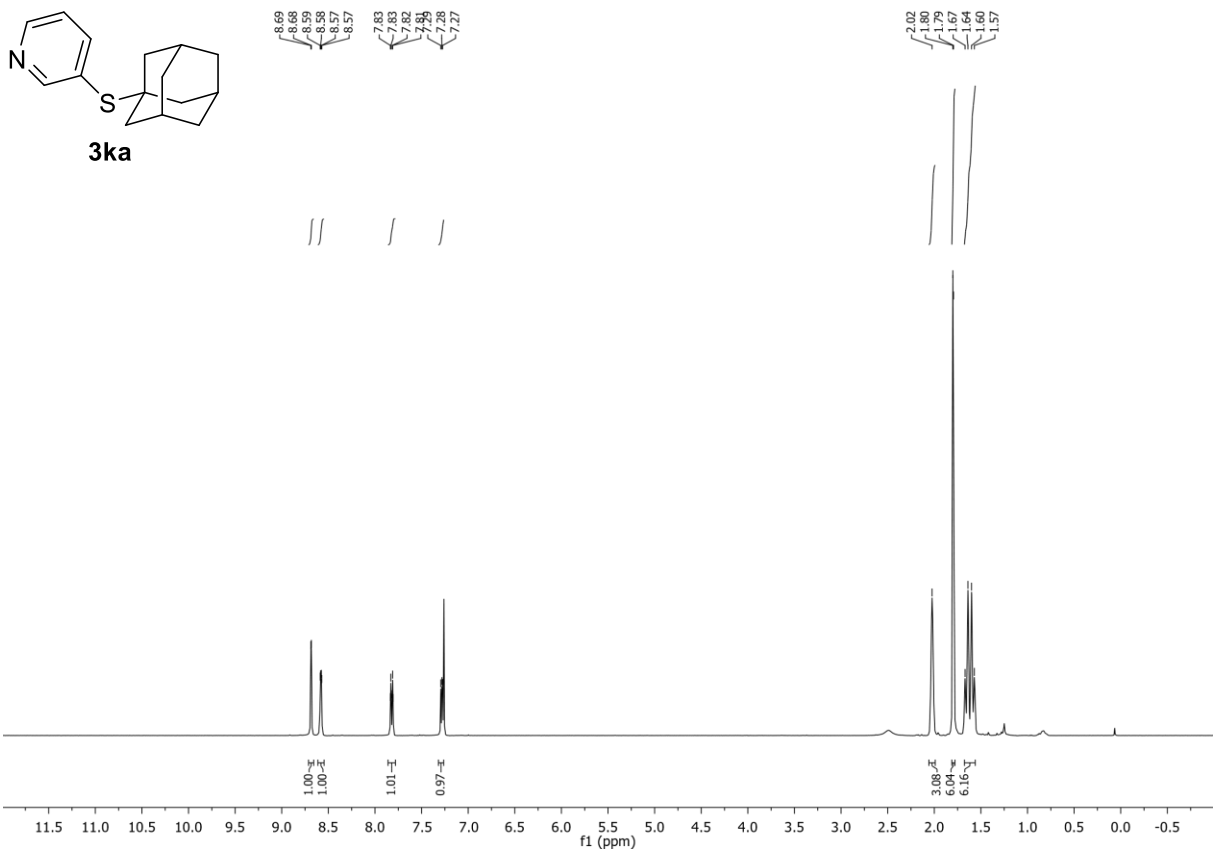

^{13}C-NMR (101 MHz, $CDCl_3$) of compound **3ka**:

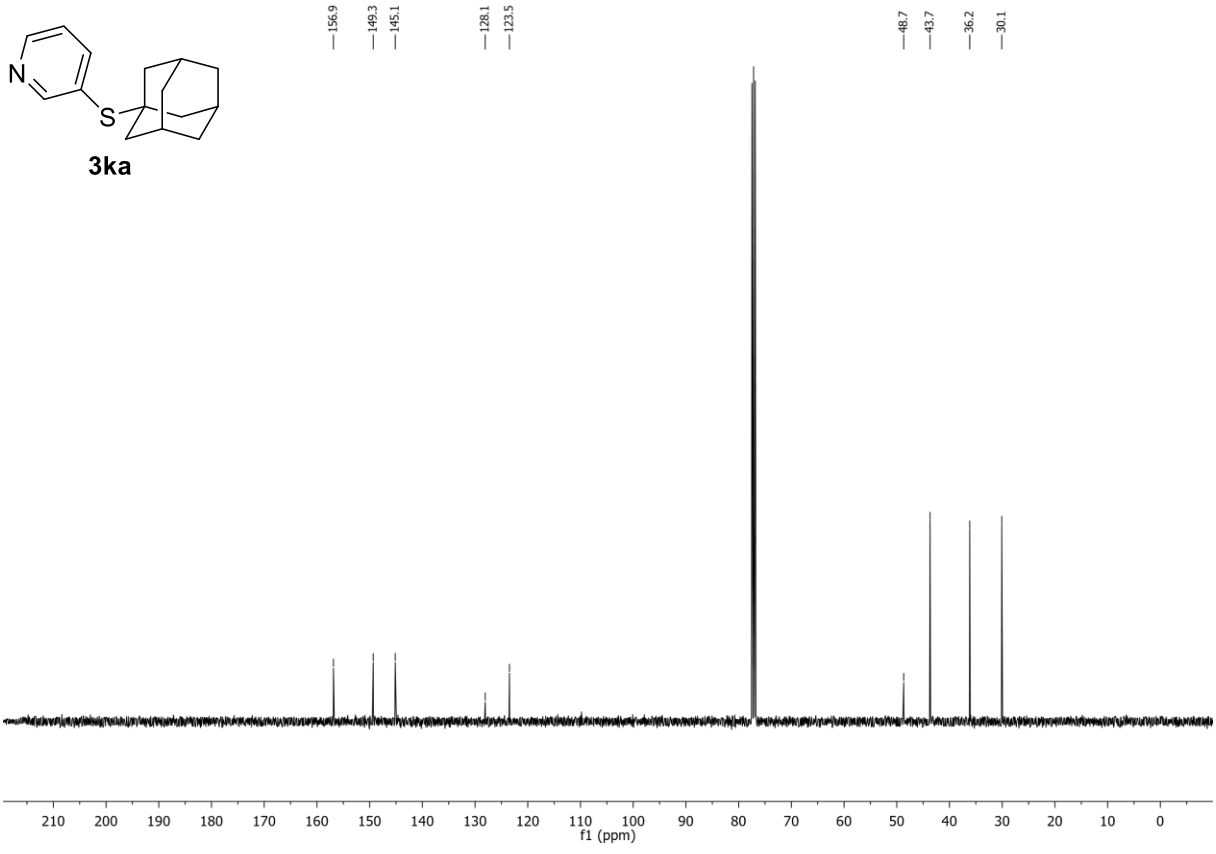

((1*s*,3*s*)-Adamantan-1-yl)(o-tolyl)sulfane (3la):

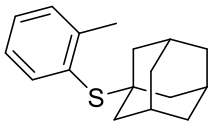

3la

$C_{17}H_{22}S$ (258.42 g/mol)

Following **GP-C**, **3la** was synthesized using *o*-tolyl trifluoromethanesulfonate (240 mg, 1.00 mmol, 1.0 equiv.) and 1-adamantanethiol (185 mg, 1.10 mmol, 1.1 equiv.). Purification by FC (SiO_2, gradient to 95:5 *n*-hexane/EtOAc over 10 CV, then 8:2 *n*-hexane/EtOAc over 10 CV) afforded **3la** (243 mg, 940 µmol, 94%) as colorless solid. Conforms to reported analytical data.[25]

R_f: 0.64 (*n*-hexane/EtOAc 95:5).

^{1}H-NMR (400 MHz, $CDCl_3$, δ): 7.53 – 7.46 (m, 1H), 7.29 – 7.26 (m, 1H), 7.26 – 7.22 (m, 1H), 7.18 – 7.09 (m, 1H), 2.52 (s, 3H), 2.03 – 1.98 (m, 3H), 1.87 – 1.83 (m, 6H), 1.67 – 1.57 (m, 6H).

^{13}C-NMR (101 MHz, $CDCl_3$, δ): 144.2, 139.4, 130.4, 130.3, 128.9, 125.7, 49.5, 43.9, 36.3, 30.2, 22.2.

^{1}H-NMR (400 MHz, $CDCl_3$) of compound **3la**:

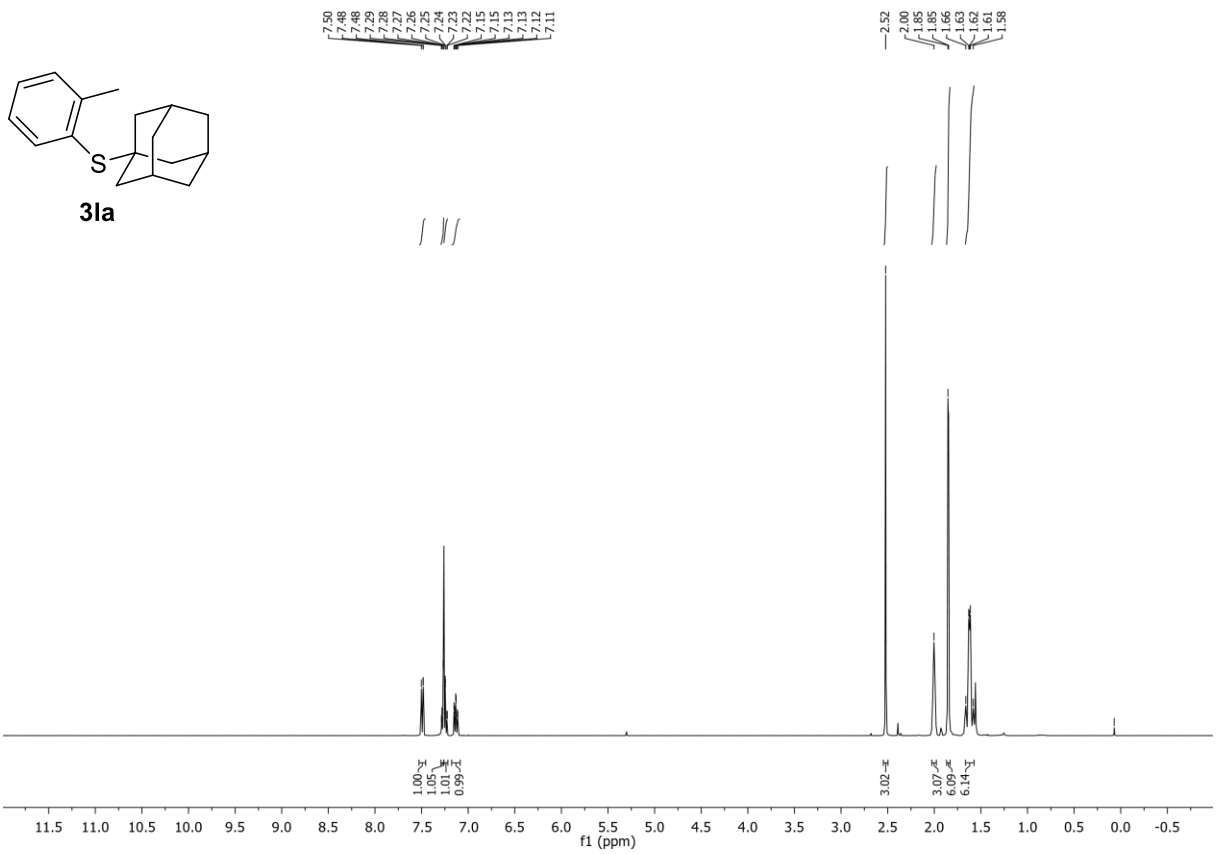

3la

^{13}C-NMR (101 MHz, $CDCl_3$) of compound **3la**:

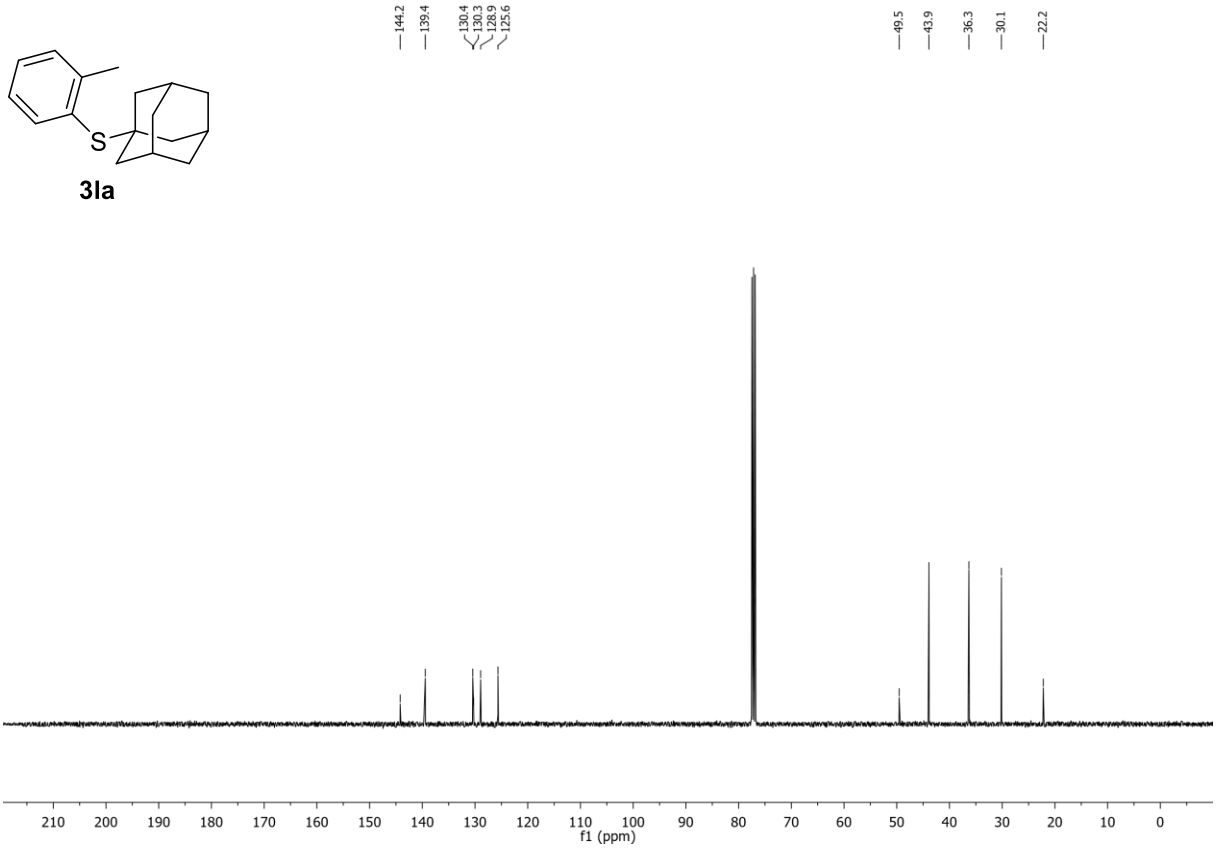

3la

((1*s*,3*s*)-Adamantan-1-yl)(naphthalen-1-yl)sulfane (3ma):

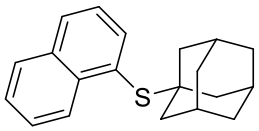

3ma

$C_{20}H_{22}S$ (294.46 g/mol)

Following **GP-C**, **3ma** was synthesized using naphthalen-1-yl trifluoromethanesulfonate (276 mg, 1.00 mmol, 1.0 equiv.) and 1-adamantanethiol (185 mg, 1.10 mmol, 1.1 equiv.). Purification by FC (SiO_2, Hex for 5 CV, then gradient to 9:1 *n*-hexane/EtOAc over 15 CV) afforded **3ma** (279 mg, 947 µmol, 95%) as colorless solid.

R_f: 0.32 (*n*-hexane/EtOAc 98:2).

m.p.: 96.2 – 101.1 °C.

^{1}H-NMR (400 MHz, $CDCl_3$, δ): 8.78 (d, *J* = 8.2 Hz, 1H), 7.92 – 7.82 (m, 2H), 7.82 – 7.75 (m, 1H), 7.60 – 7.40 (m, 3H), 2.00 – 1.95 (m, 3H), 1.88 – 1.86 (m, 6H), 1.64 – 1.55 (m, 6H).

^{13}C-NMR (101 MHz, $CDCl_3$, δ): 137.7, 137.3, 134.2, 129.9, 128.8, 128.3, 127.7, 126.4, 126.1, 125.2, 49.7, 44.1, 43.9, 36.34, 36.28, 30.21, 30.17.

HR-MS (APCI): m/z calc. for $[M+H]^+$ 295.1515, found 295.1514.

IR (ATR, $\tilde{\nu}$ [cm^{-1}]): 2898 (m), 2846 (m), 1586 (w), 1560 (w), 1497 (w), 1448 (w), 1373 (w), 1340 (w), 1299 (w), 1250 (w), 1206 (w), 1180 (w), 1135 (w), 1101 (w), 1034 (w), 967 (w), 863 (w), 822 (w), 796 (m), 766 (s), 684 (w), 678 (w).

^{1}H-NMR (400 MHz, $CDCl_3$) of compound **3ma**:

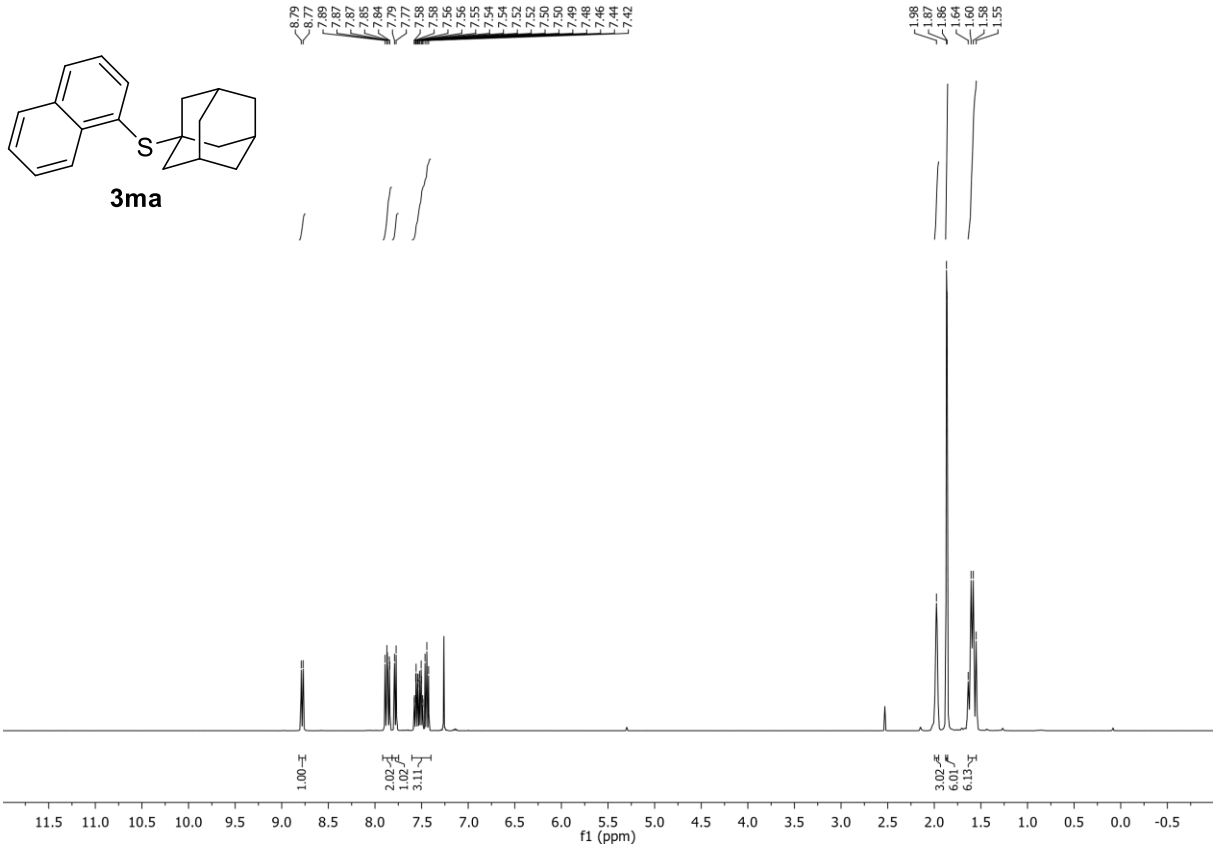

^{13}C-NMR (101 MHz, $CDCl_3$) of compound **3ma**:

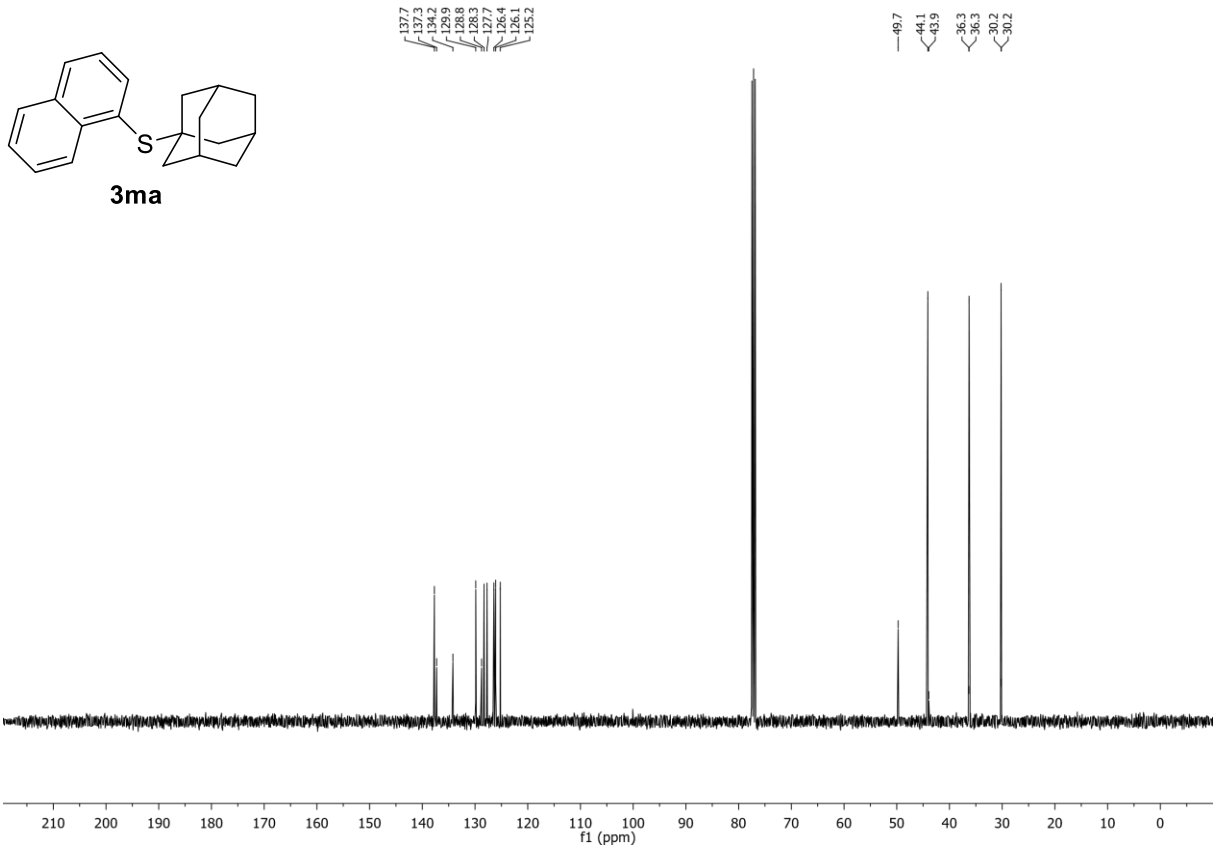

((1*s*,3*s*)-Adamantan-1-yl)(3-chlorophenyl)sulfane (3na):

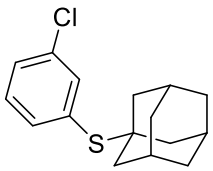

3na

$C_{16}H_{19}ClS$ (278.84 g/mol)

Following **GP-C**, **3na** was synthesized using 3-chlorophenyl trifluoromethanesulfonate (261 mg, 1.00 mmol, 1.0 equiv.) and 1-adamantanethiol (185 mg, 1.10 mmol, 1.1 equiv.). Purification by FC (SiO_2, Hex for 10 CV, then gradient to 5:5 *n*-hexane/EtOAc over 10 CV) afforded **3na** (235 mg, 843 µmol, 84%) as colorless solid.

R_f: 0.37 (*n*-hexane).

^{1}H-NMR (400 MHz, $CDCl_3$, δ): 7.52 – 7.48 (m, 1H), 7.39 – 7.32 (m, 2H), 7.26 – 7.22 (m, 1H), 2.05 – 2.00 (m, 3H), 1.82 – 1.80 (m, 6H), 1.68 – 1.58 (m, 6H).

^{13}C-NMR (101 MHz, $CDCl_3$, δ): 137.3, 135.9, 133.9, 132.7, 129.4, 128.9, 48.6, 43.8, 36.2, 30.1.

m.p.: 36.6 – 38.9 °C.

HR-MS (APCI): m/z calc. for $[M+H]^+$ 278.0891, found 278.0891.

IR (ATR, $\tilde{\nu}$ [cm^{-1}]): 2895 (s), 2846 (m), 1690 (w), 1564 (m), 1452 (m), 1396 (w), 1370 (w), 1340 (m), 1291 (m), 1251 (w), 1213 (w), 1168 (w), 1142 (w), 1111 (w), 1075 (w), 1034 (m), 1004 (w), 969 (w), 911 (w), 877 (m), 818 (w), 777 (s), 677 (s).

^{1}H-NMR (400 MHz, $CDCl_3$) of compound **3na**:

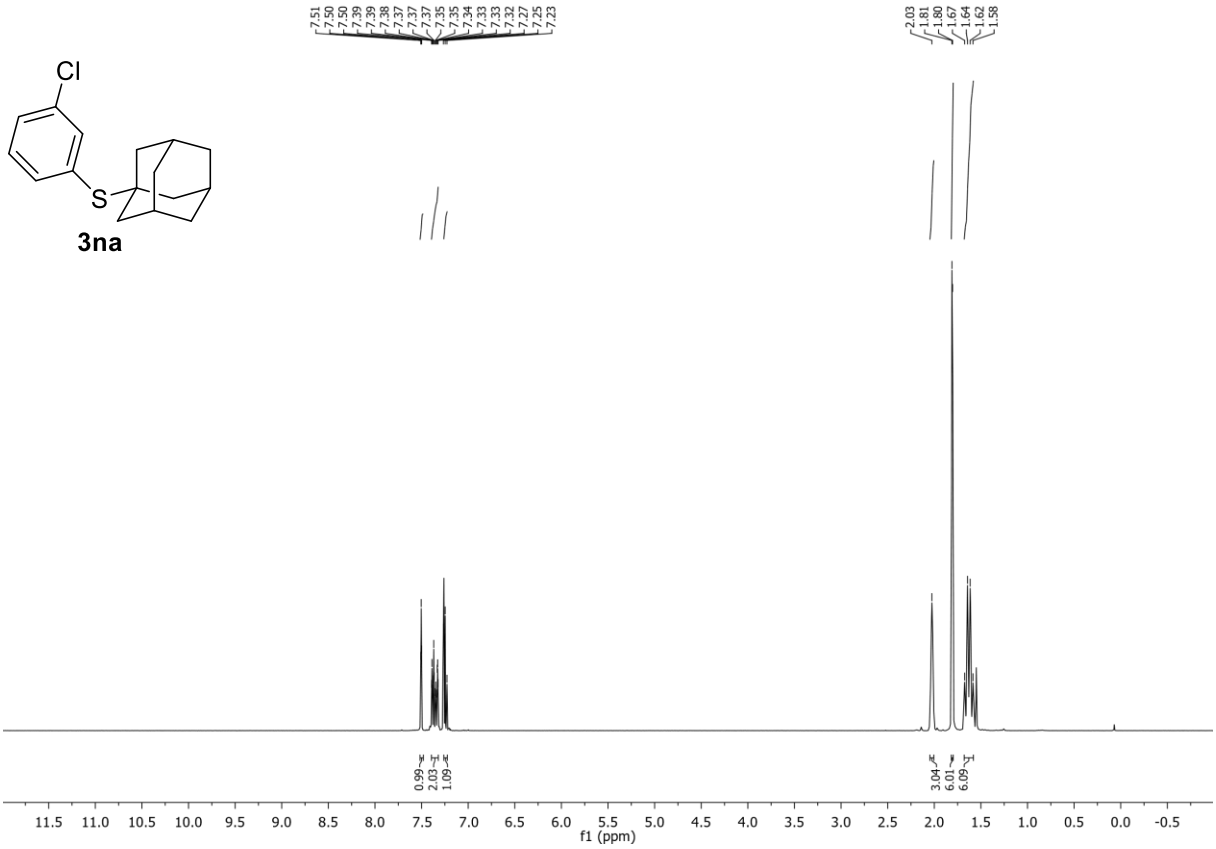

^{13}C-NMR (101 MHz, $CDCl_3$) of compound **3na**:

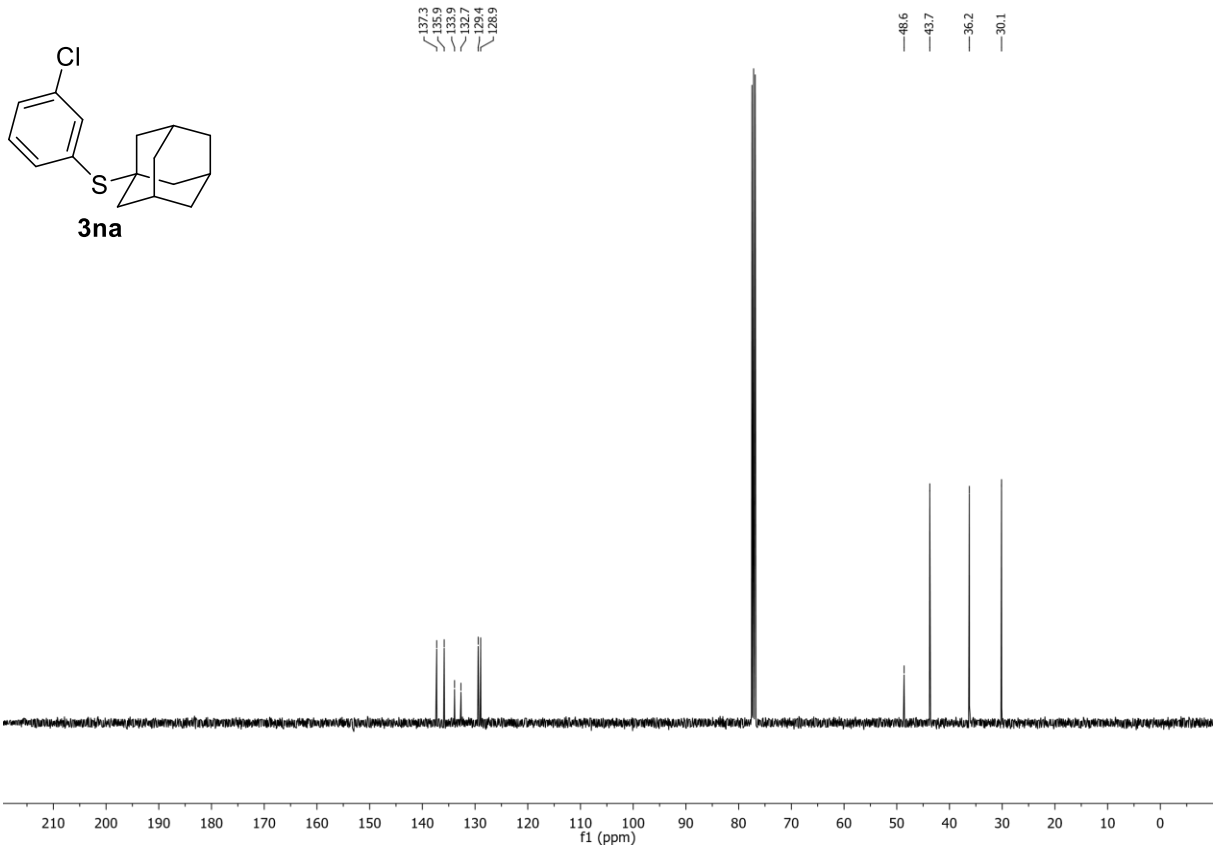

4-(((1*s*,3*s*)-Adamantan-1-yl)thio)phenyl 4-methylbenzenesulfonate (3oa):

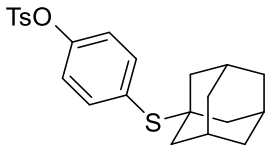

3oa

$C_{23}H_{26}O_3S_2$ (414.58 g/mol)

Following **GP-C**, **3oa** was synthesized using 4-(((trifluoromethyl)sulfonyl)oxy)phenyl 4-methylbenzenesulfonate (198 mg, 500 µmol, 1.0 equiv.) and 1-adamantanethiol (92.6 mg, 550 µmol, 1.1 equiv.). Purification by FC (SiO_2, gradient to 8:2 *n*-hexane/EtOAc over 20 CV) afforded **3oa** (194 mg, 468 µmol, 94%) as colorless solid. Conforms to reported analytical data.[25]

R_f: 0.38 (*n*-hexane/EtOAc 9:1).

^{1}H-NMR (400 MHz, $CDCl_3$, δ): 7.69 (d, *J* = 8.3 Hz, 2H), 7.43 – 7.35 (m, 2H), 7.30 (d, *J* = 8.1 Hz, 2H), 6.98 – 6.89 (m, 2H), 2.44 (s, 3H), 2.04 – 1.97 (m, 3H), 1.77 – 1.73 (m, 6H), 1.67 – 1.56 (m, 6H).

^{13}C-NMR (101 MHz, $CDCl_3$, δ): 150.2, 145.6, 138.9, 132.3, 129.9, 129.8, 128.7, 122.3, 48.4, 43.7, 36.2, 30.1, 21.9.

^{1}H-NMR (400 MHz, $CDCl_3$) of compound **3oa**:

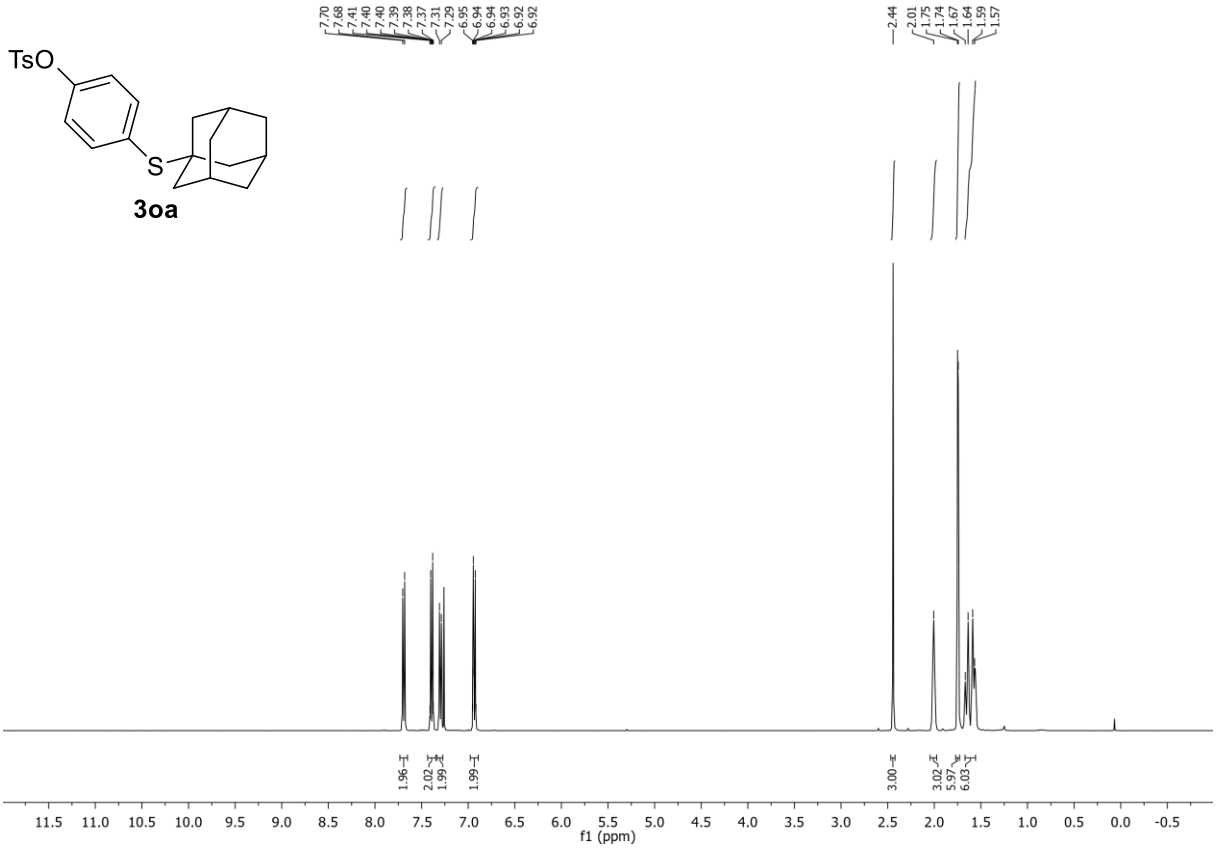

^{13}C-NMR (101 MHz, $CDCl_3$) of compound **3oa**:

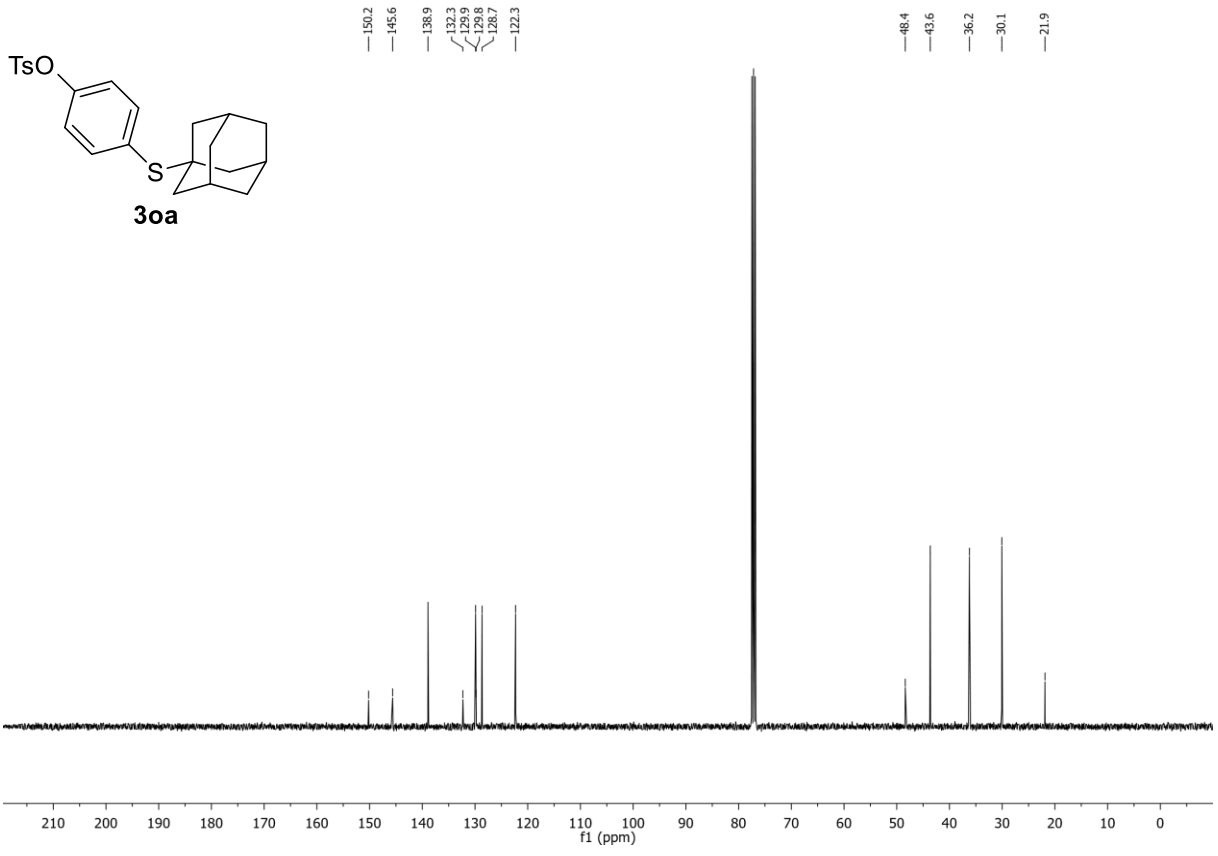

2,7-Bis(((1*s*,3*s*)-adamantan-1-yl)thio)naphthalene (3pa):

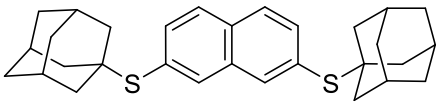

3pa

$C_{30}H_{36}S_2$ (460.74 g/mol)

Following **GP-C**, **3pa** was synthesized naphthalene-2,7-diyl bis(trifluoromethanesulfonate) (212 mg, 500 µmol, 1.0 equiv.) and 1-adamantanethiol (185 mg, 1.10 mmol, 2.2 equiv.). Purification by FC (SiO_2, gradient to 95:5 *n*-hexane/EtOAc over 15 CV) afforded **3pa** (197 mg, 428 µmol, 86%) as colorless solid.

R_f: 0.12 (*n*-hexane).

m.p.: 190.1 – 196.9 °C.

^{1}H-NMR (400 MHz, $CDCl_3$, δ): 8.01 (s, 2H), 7.77 (d, *J* = 8.4 Hz, 2H), 7.58 (d, *J* = 8.4 Hz, 2H), 2.04 – 1.99 (m, 6H), 1.90 – 1.85 (m, 12H), 1.67 – 1.58 (m, 12H).

^{13}C-NMR (101 MHz, $CDCl_3$, δ): 137.2, 135.5, 133.4, 132.7, 128.9, 127.4, 48.7, 43.9, 36.3, 30.2.

HR-MS (APCI): m/z calc. for $[M+H]^+$ 461.2331, found 461.2335.

IR (ATR, $\tilde{\nu}$ [cm^{-1}]): 2898 (m), 2846 (m), 1616 (w), 1579 (w), 1485 (w), 1444 (w), 1340 (w), 1295 (w), 1254 (w), 1213 (w), 1183 (w), 1139 (w), 1102 (w), 1034 (m), 970 (w), 945 (w), 904 (w), 844 (m), 818 (w), 766 (w), 736 (w), 684 (w).

^{1}H-NMR (400 MHz, $CDCl_3$) of compound **3pa**:

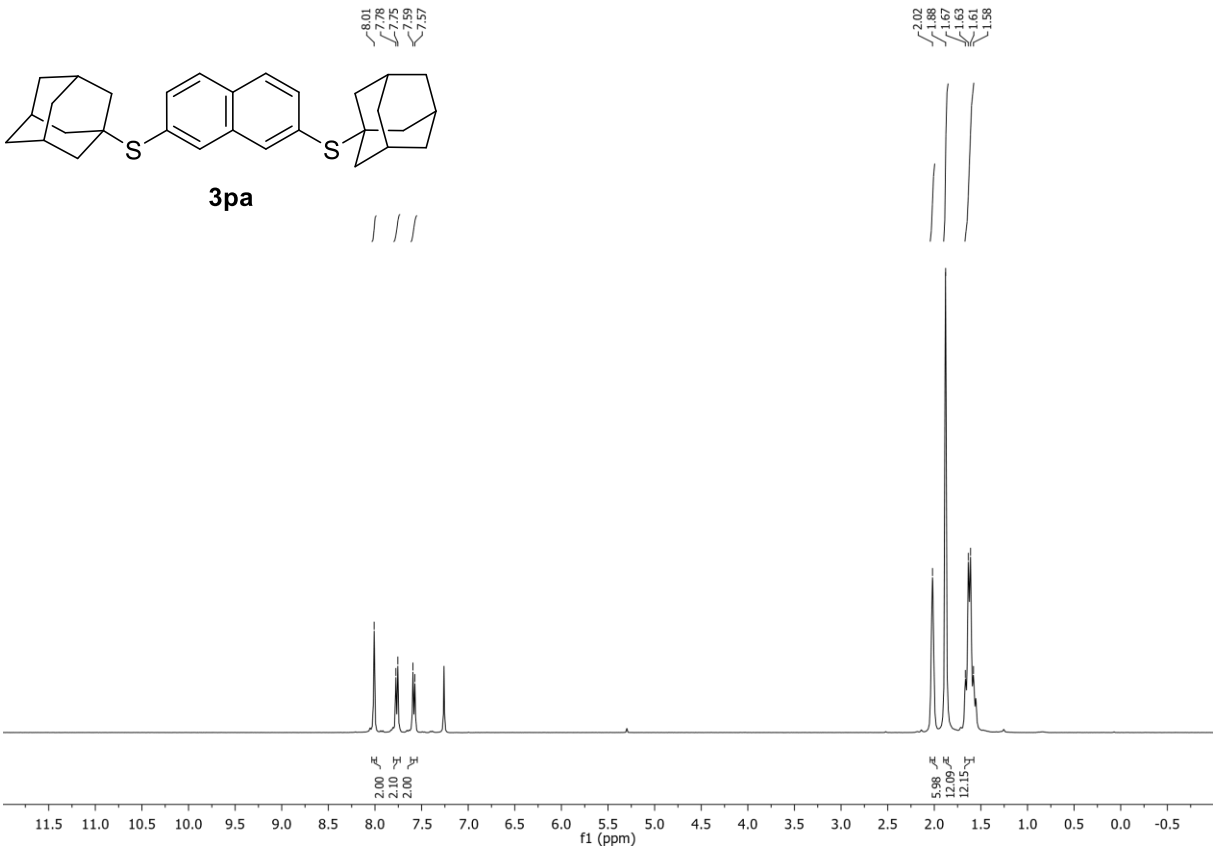

^{13}C-NMR (101 MHz, $CDCl_3$) of compound **3pa**:

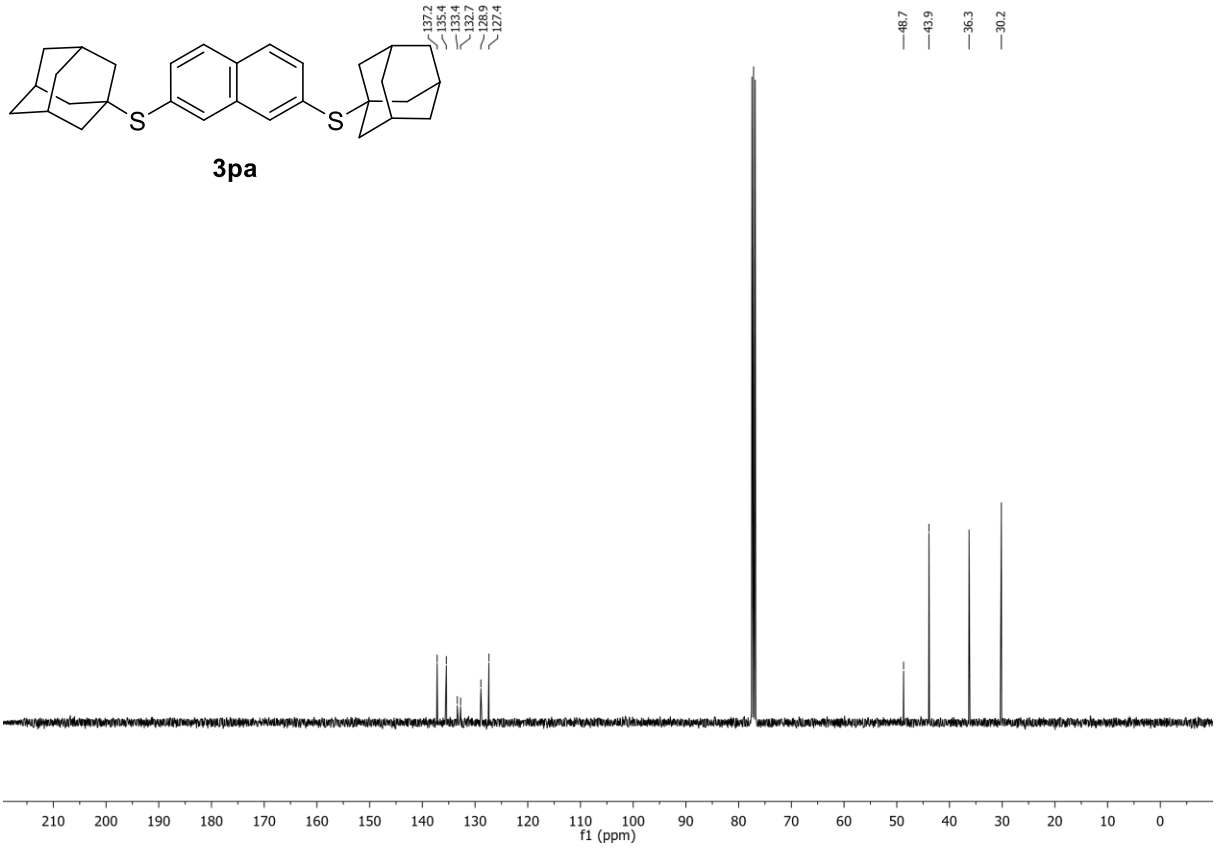

(8*R*,9*S*,13*S*,14*S*)-3-(((1*s*,3*R*)-Adamantan-1-yl)thio)-13-methyl-6,7,8,9,11,12,13,14,15,16-decahydro-17*H*-cyclopenta[a]phenanthren-17-one (3qa):

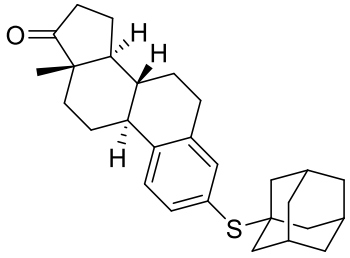

3qa

$C_{28}H_{36}OS$ (420.66 g/mol)

Following **GP-C**, **3qa** was synthesized using Estrone trifluoromethanesulfonate (201 mg, 500 µmol, 1.0 equiv.) and 1-adamantanethiol (92.6 mg, 550 µmol, 1.1 equiv.). Purification by FC (SiO_2, gradient to 9:1 *n*-hexane/EtOAc over 15 CV) afforded **3qa** (124 mg, 295 µmol, 59%) as colorless solid.

R_f: 0.44 (*n*-hexane/EtOAc 8:2).

m.p.: 172.2 – 174.8 °C.

^{1}H-NMR (400 MHz, $CDCl_3$, δ): 7.26 – 7.20 (m, 3H), 2.95 – 2.87 (m, 2H), 2.55 – 2.46 (m, 1H), 2.45 – 2.38 (m, 1H), 2.17 – 1.95 (m, 7H), 1.83 – 1.78 (m, 6H), 1.67 – 1.44 (m, 12H), 0.92 (s, 3H).

^{13}C-NMR (101 MHz, $CDCl_3$, δ): 220.9, 140.4, 138.2, 136.7, 135.1, 127.6, 125.4, 50.7, 48.1, 47.7, 44.5, 43.8, 38.1, 36.3, 36.0, 31.7, 30.1, 29.4, 26.6, 25.7, 21.8, 14.0.

HR-MS (APCI): m/z calc. for $[M+H]^+$ 421.2560, found 421.2560.

IR (ATR, $\tilde{\nu}$ [cm^{-1}]): 2909 (w), 2850 (w), 1735 (m), 1474 (w), 1451 (w), 1399 (w), 1370 (w), 1340 (w), 1295 (w), 1254 (w), 1213 (w), 1180 (w), 1083 (w), 1038 (w), 1005 (w), 975 (w), 893 (w), 818 (w), 777 (w), 710 (w), 684 (w).

^{1}H-NMR (400 MHz, $CDCl_3$) of compound **3qa**:

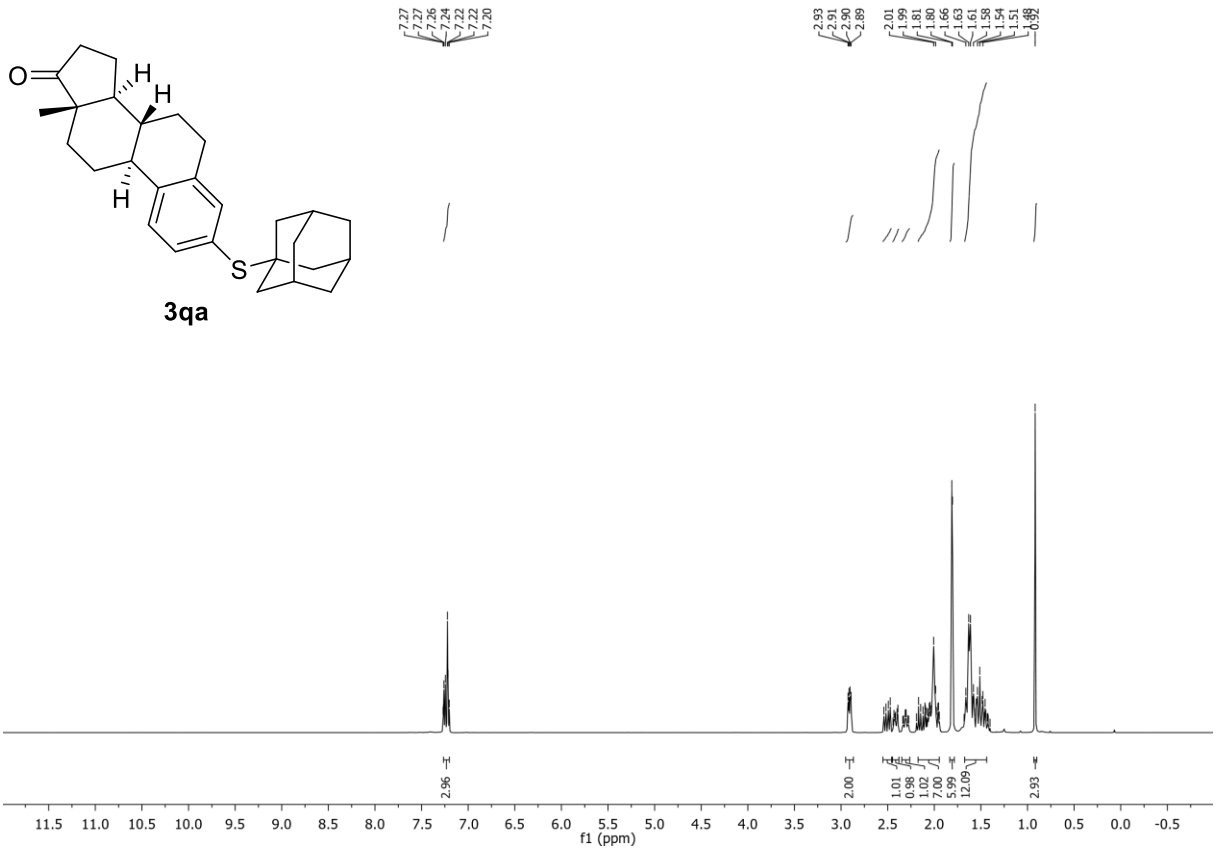

^{13}C-NMR (101 MHz, $CDCl_3$) of compound **3qa**:

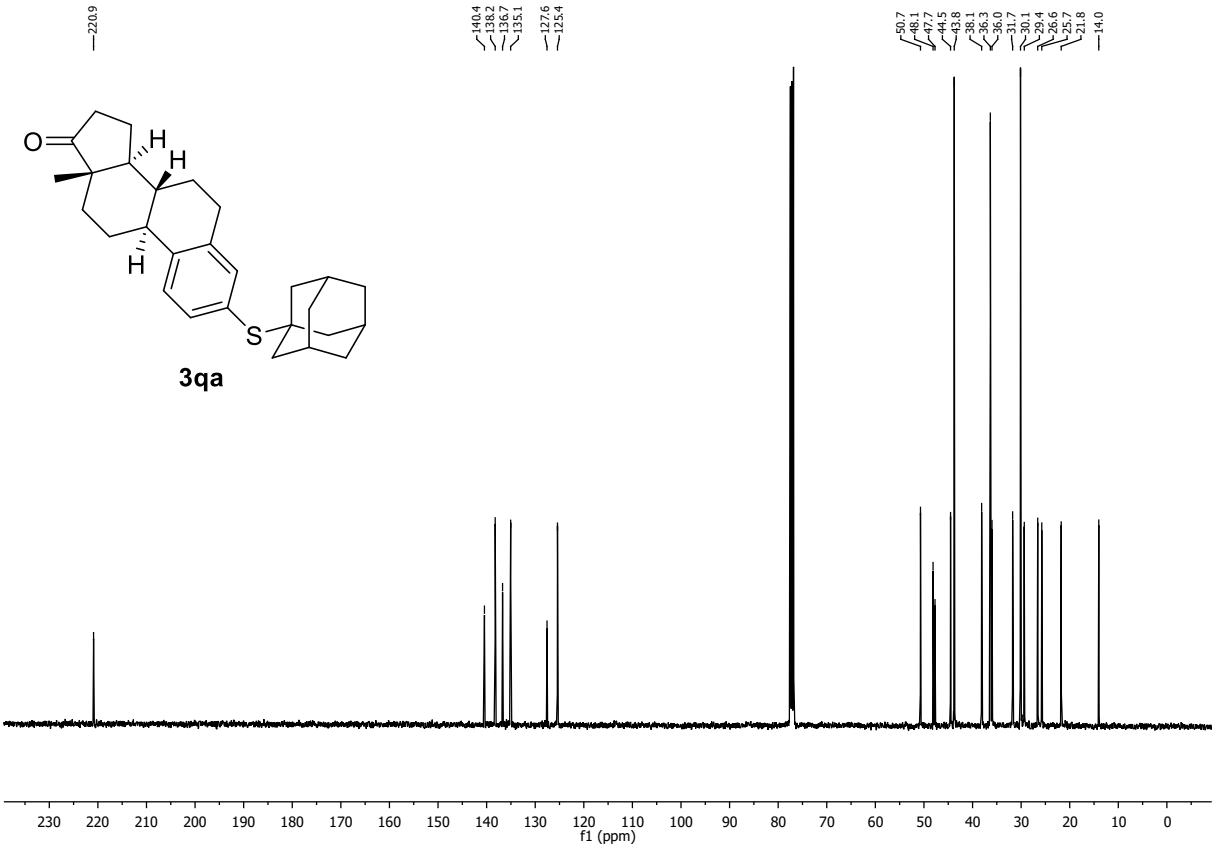

(3*R*,4*S*)-4-(4-(((1*s*,3*R*)-Adamantan-1-yl)thio)phenyl)-1-(4-fluorophenyl)-3-((*S*)-3-(4-fluorophenyl)-3-hydroxypropyl)azetidin-2-one (3ra):

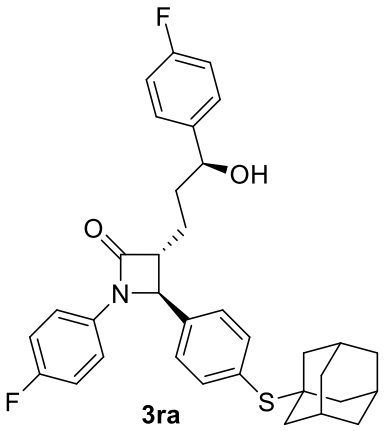

3ra

$C_{34}H_{35}F_2NO_2S$ (559.72 g/mol)

Following **GP-C**, **3ra** was synthesized using Ezetimibe trifluoromethanesulfonate (220 mg, 406 µmol, 1.0 equiv.) and 1-adamantanethiol (75.2 mg, 447 µmol, 1.1 equiv.). Purification by FC (SiO_2, gradient to 50:50 *n*-hexane/EtOAc over 15 CV, then gradient to EtOAc over 5 CV) afforded **3ra** (125 mg, 223 µmol, 55%) as colorless solid.

R_f: 0.26 (*n*-hexane/EtOAc 8:2).

m.p.: 143.2 – 146.5 °C.

^{1}H-NMR (400 MHz, $CDCl_3$, δ): 7.51 (d, *J* = 7.7 Hz, 2H), 7.36 – 7.27 (m, 4H), 7.25 – 7.20 (m, 2H), 7.06 – 6.92 (m, 4H), 4.73 (t, *J* = 5.9 Hz, 1H), 4.64 (d, *J* = 2.4 Hz, 1H), 3.18 – 3.09 (m, 1H), 2.06 – 1.90 (m, 8H), 1.84 – 1.79 (m, 6H), 1.69 – 1.58 (m, 6H).

^{13}C-NMR (101 MHz, $CDCl_3$, δ): 167.5, 163.6, 140.2, 140.1, 138.5, 138.1, 133.9, 131.5, 127.6, 127.5, 125.9, 118.5, 118.4, 116.1, 115.9, 115.6, 115.4, 73.3, 61.2, 60.4, 48.5, 43.8, 36.7, 36.2, 30.1, 25.3.

^{19}F-NMR (376 MHz, $CDCl_3$, δ): -114.7, -117.8.

HR-MS (ESI): m/z calc. for $[M+Na]^+$ 582.2249, found 582.2253.

IR (ATR, $\tilde{\nu}$ [cm^{-1}]): 3476 (w), 2905 (w), 2850 (w), 1731 (w), 1601 (w), 1504 (w), 1448 (w), 1388 (w), 1340 (w), 1296 (w), 1218 (w), 1153 (w), 1128 (w), 1101 (w), 1072 (w), 1038 (w), 1012 (w), 978 (w), 937 (w), 904 (w), 848 (w), 819 (w), 729 (w), 688 (w).

^{1}H-NMR (400 MHz, $CDCl_3$) of compound **3ra**:

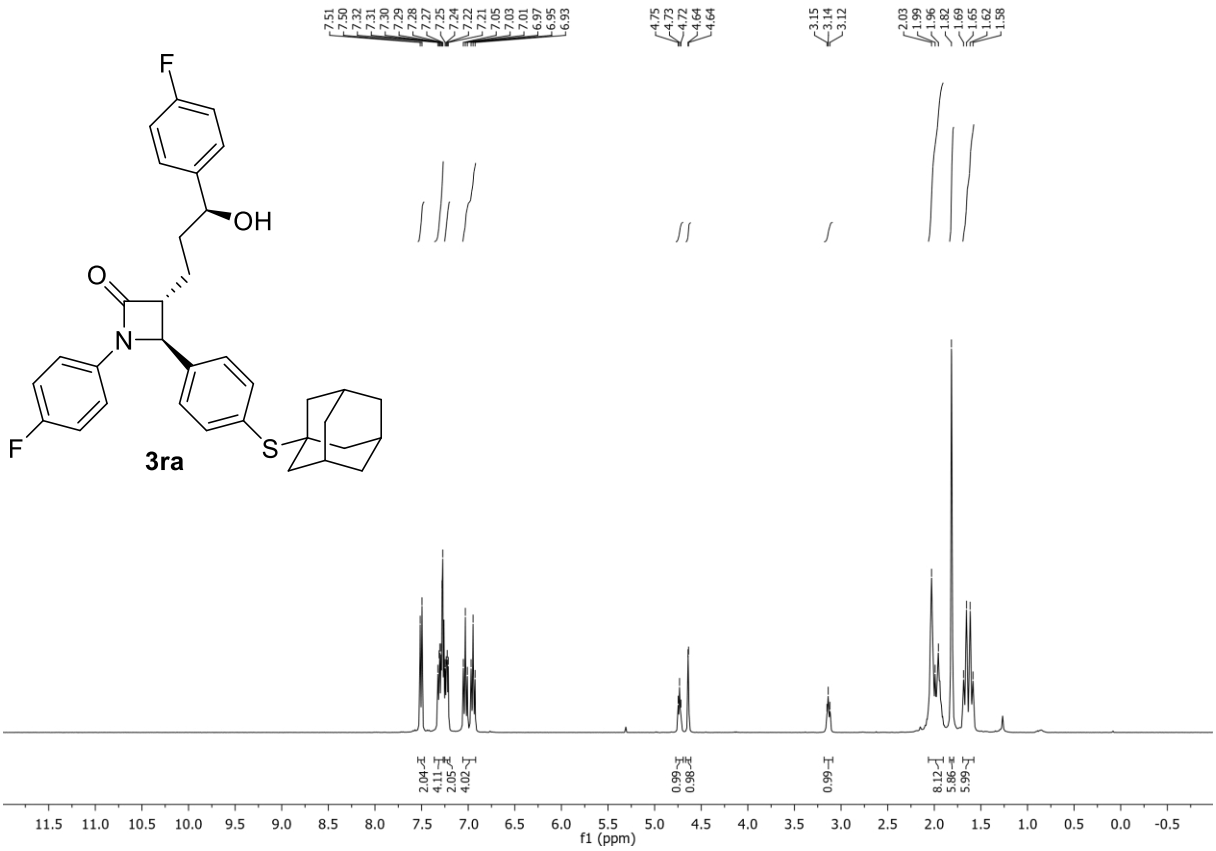

^{13}C-NMR (101 MHz, $CDCl_3$) of compound **3ra**:

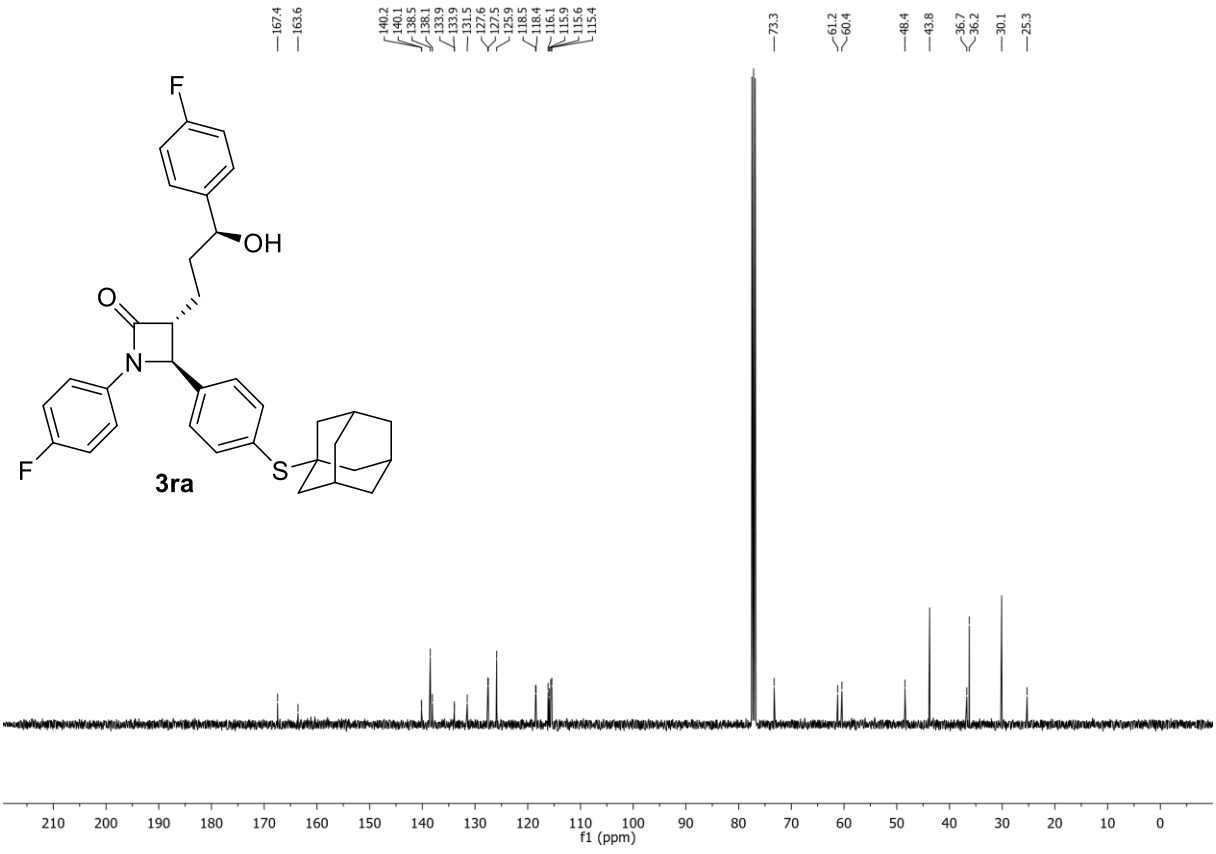

^{19}F-NMR (376 MHz, $CDCl_3$) of compound **3ra**:

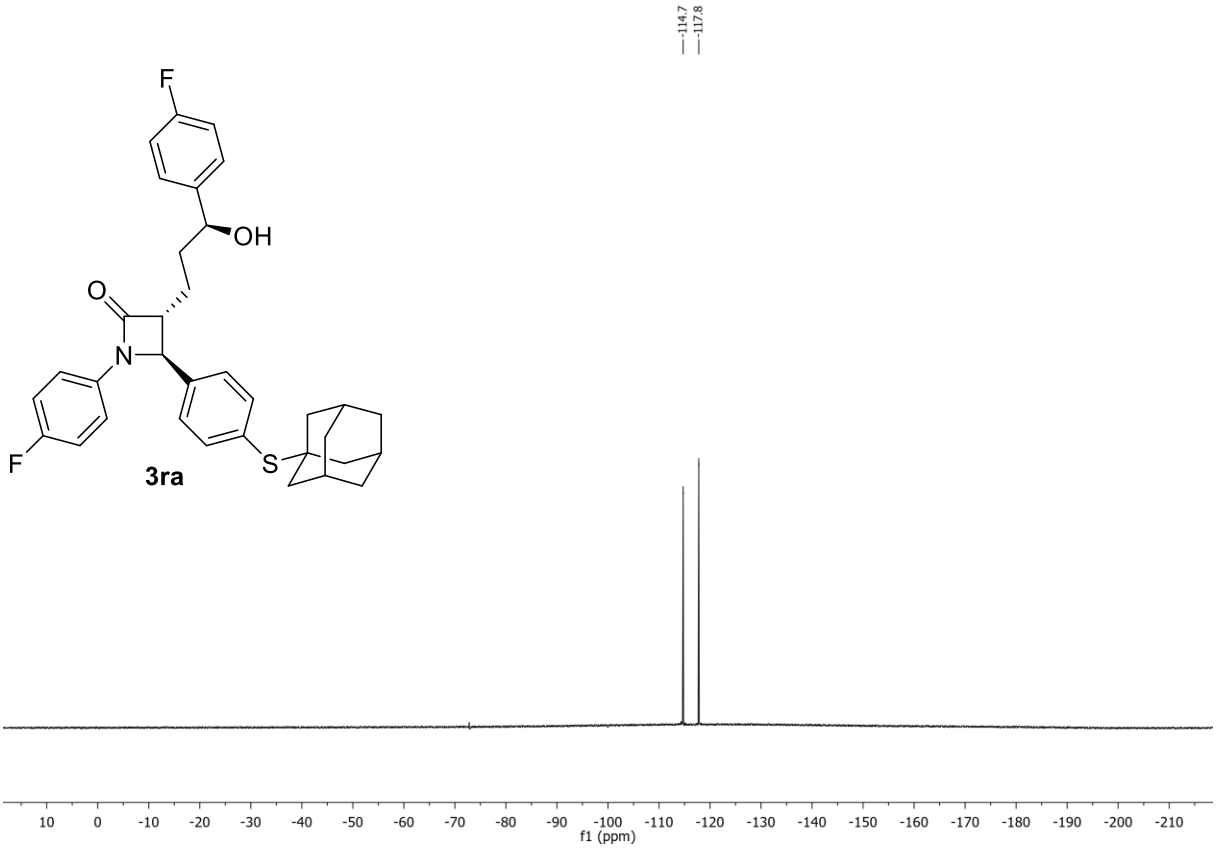

Heptyl(phenyl)sulfane (3ab):

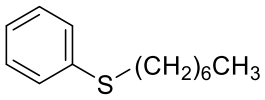

3ab

$C_{13}H_{20}S$ (208.36 g/mol)

Following **GP-C**, **3ab** was synthesized using phenyl trifluoromethanesulfonate (226 mg, 1.00 mmol, 1.0 equiv.) and 1-heptanethiol (145 mg, 1.10 mmol, 1.1 equiv.). Purification by FC (SiO_2, *n*-hexane for 15 CV) afforded **3ab** (205 mg, 983 µmol, 98%) as brown oil. Conforms to reported analytical data.[28]

R_f: 0.66 (*n*-hexane/EtOAc 99:1).

^{1}H-NMR (400 MHz, $CDCl_3$, δ): 7.30 – 7.19 (m, 4H), 7.15 – 7.06 (m, 1H), 2.91 – 2.80 (m, 2H), 1.66 – 1.53 (m, 2H), 1.43 – 1.20 (m, 8H), 0.87 – 0.79 (m, 3H).

^{13}C-NMR (101 MHz, $CDCl_3$, δ): 137.2, 129.0, 128.9, 125.7, 33.7, 31.9, 29.3, 28.98, 28.95, 22.7, 14.2.

^{1}H-NMR (400 MHz, $CDCl_3$) of compound **3ab**:

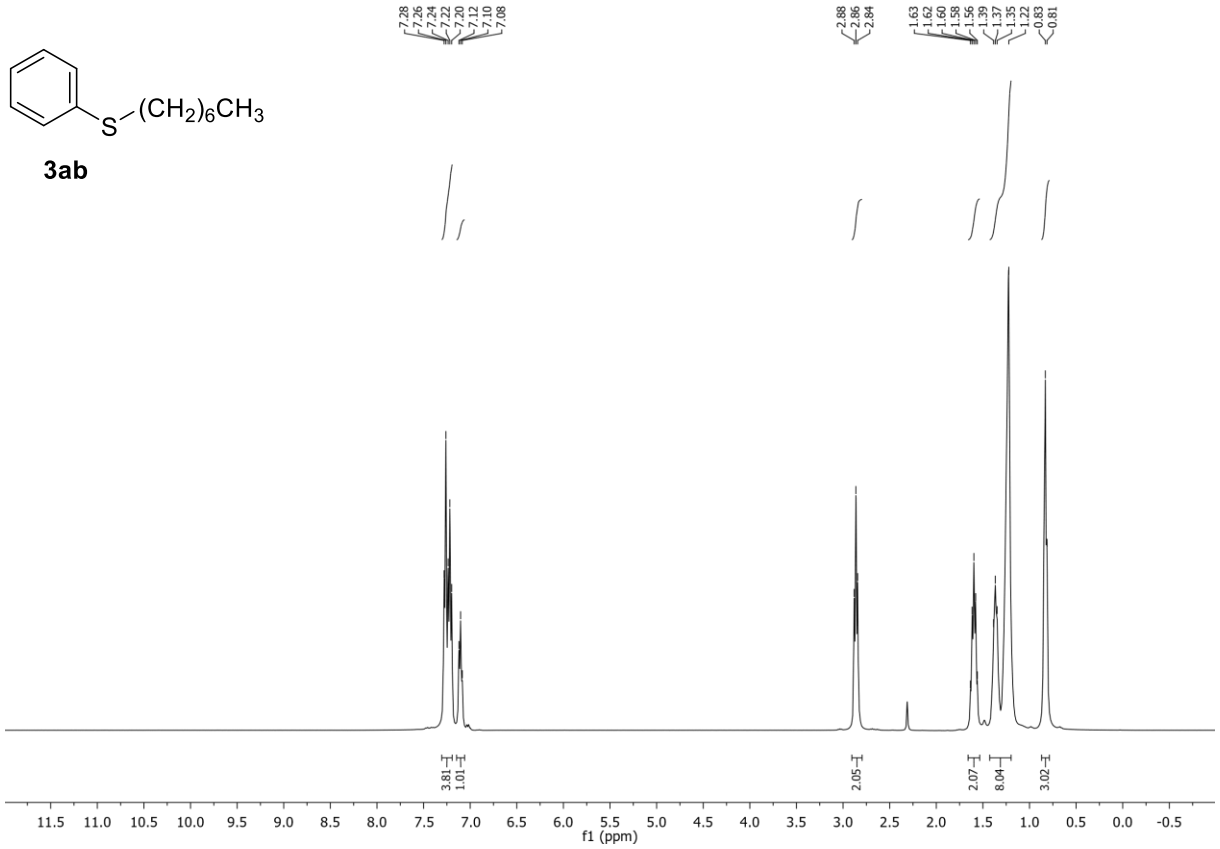

3ab

^{13}C-NMR (101 MHz, $CDCl_3$) of compound **3ab**:

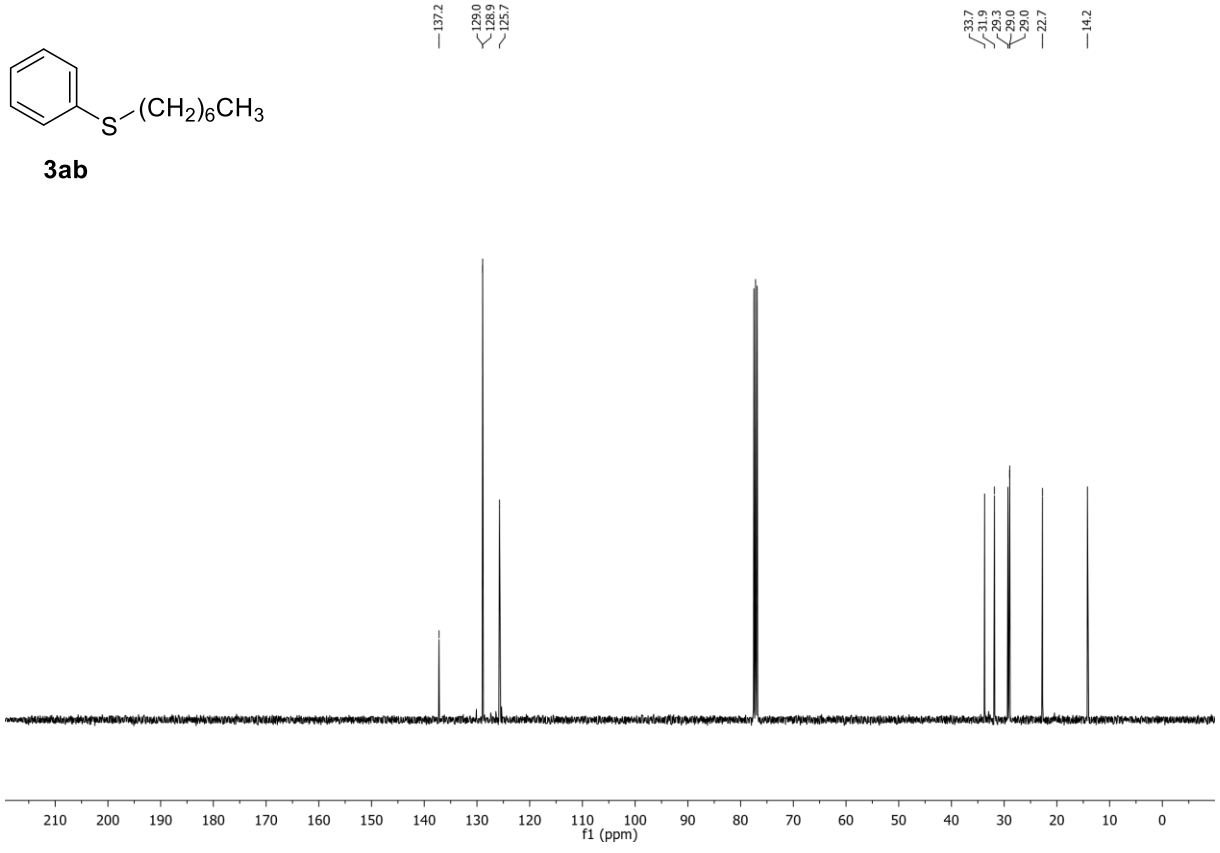

3ab

Cyclohexyl(phenyl)sulfane (3ac):

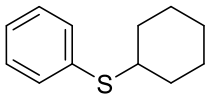

3ac

$C_{12}H_{16}S$ (192.32 g/mol)

Following **GP-C**, **3ac** was synthesized using phenyl trifluoromethanesulfonate (226 mg, 1.00 mmol, 1.0 equiv.) and cyclohexanethiol (128 mg, 1.10 mmol, 1.1 equiv.). Purification by FC (SiO_2, gradient to 9:1 *n*-hexane/EtOAc over 10 CV) afforded **3ac** (190 mg, 988 µmol, 99%) as colorless oil. Conforms to reported analytical data.[27]

Upscale:

An inert, flame-dried and septum-caped Schlenk-tube equipped with a stirring bar was charged with KOAc (736 mg, 7.5 mmol, 1.5 equiv.), XantphosNi(*o*-tolyl)Cl (2 mol%), phenyl trifluoromethanesulfonate (1.13 g, 5.00 mmol, 1.0 equiv.) and cyclohexanethiol (639 mg, 5.50 mmol, 1.1 equiv.). The reagents were dissolved in THF (15 mL) and stirred at room temperature for 2 h. Work-up was done according to **GP-C**. Purification by FC (SiO_2, gradient to 9:1 *n*-hexane/EtOAc over 10 CV) afforded **3ac** (941 mg, 4.89 mmol, 98%) as colorless oil.

R_f: 0.82 (*n*-hexane/EtOAc 9:1).

^{1}H-NMR (400 MHz, $CDCl_3$, δ): 7.43 – 7.39 (m, 2H), 7.32 – 7.19 (m, 3H), 3.18 – 3.06 (m, 1H), 2.05 – 1.92 (m, 2H), 1.86 – 1.70 (m, 2H), 1.68 – 1.60 (m, 1H), 1.45 – 1.22 (m, 5H).

^{13}C-NMR (101 MHz, $CDCl_3$, δ): 135.2, 131.9, 128.8, 126.7, 46.6, 33.4, 26.2, 25.9.

^{1}H-NMR (400 MHz, $CDCl_3$) of compound **3ac**:

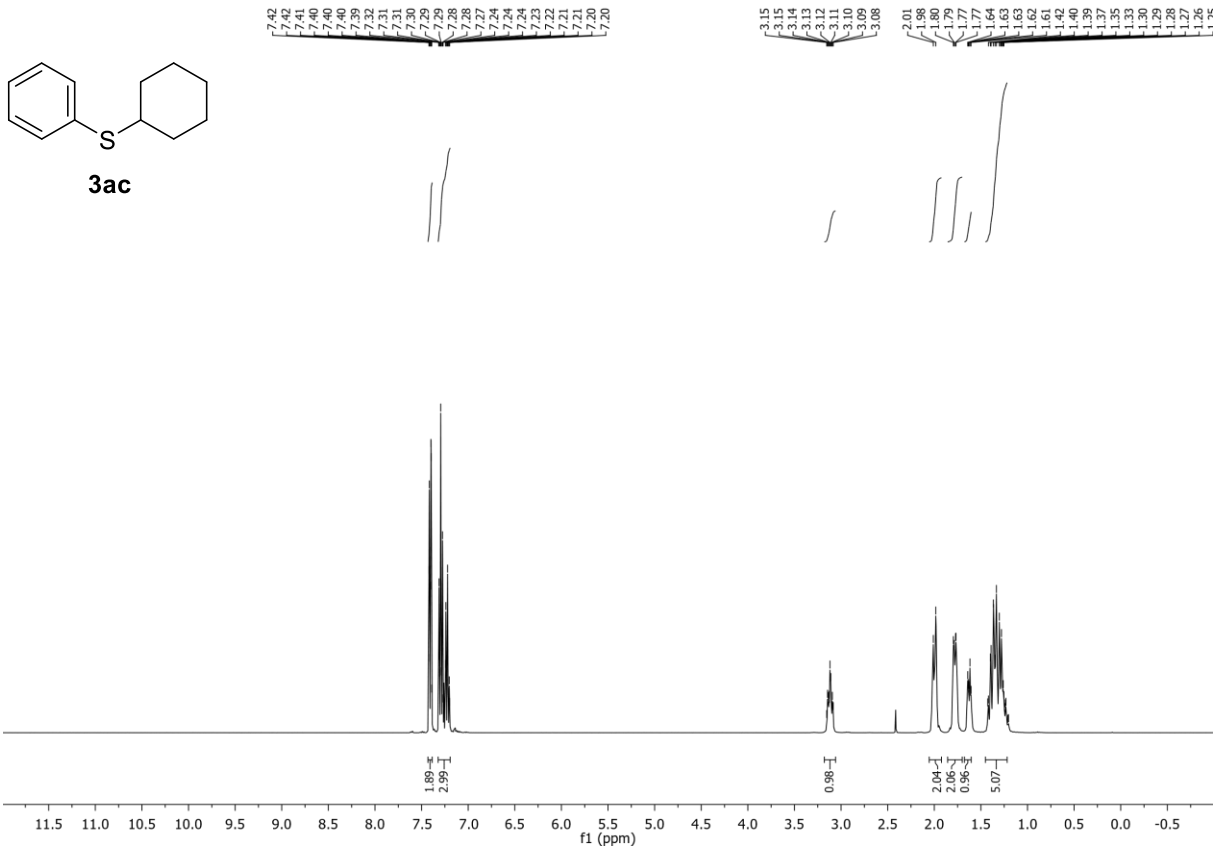

^{13}C-NMR (101 MHz, $CDCl_3$) of compound **3ac**:

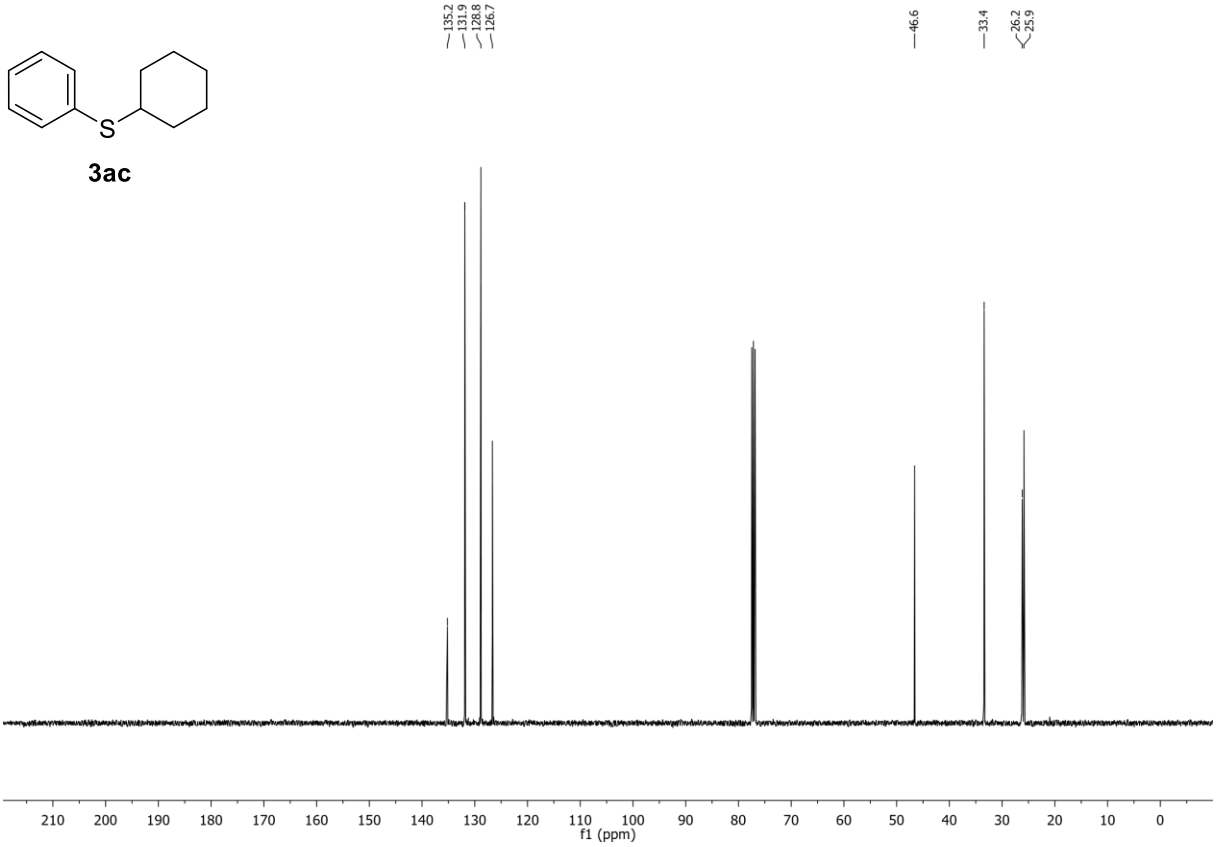

Naphthalen-2-yl((4*r*,4a*r*,8*r*,8a*r*,10*r*,11*r*)-octahydro-2,8,4,6-(epibutane[1,2,3,4]tetrayl)naphthalen-2(1*H*)-yl)sulfane (3hd):

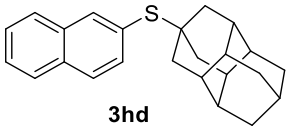

3hd

$C_{24}H_{26}S$ (346.53 g/mol)

Following **GP-C**, **3hd** was synthesized using naphthalen-2-yl trifluoromethanesulfonate (138 mg, 500 µmol, 1.0 equiv.) and (4*r*,4a*r*,8*r*,8a*r*,10*r*,11*r*)-octahydro-2,8,4,6-(epibutane[1,2,3,4]tetrayl) naphthalene-2(1*H*)-thiol[29] (121 mg, 550 µmol, 1.1 equiv.). Purification by FC (SiO_2, gradient to 8:2 *n*-hexane/EtOAc over 20 CV) afforded **3hd** (170 mg, 491 µmol, 98%) as colorless solid.

R_f: 0.26 (*n*-hexane).

m.p.: 145.1– 150.3 °C.

^{1}H-NMR (400 MHz, $CDCl_3$, δ): 8.04 (s, 1H), 7.88 – 7.73 (m, 3H), 7.61 – 7.46 (m, 3H), 1.85 – 1.81 (m, 9H), 1.77 – 1.73 (m, 1H), 1.69 – 1.63 (m, 9H).

^{13}C-NMR (101 MHz, $CDCl_3$, δ): 137.4, 134.8, 133.4, 133.2, 128.4, 128.0, 127.73, 127.67, 126.7, 126.3, 47.1, 44.5, 39.3, 37.5, 36.4, 25.6.

HR-MS (APCI): m/z calc. for $[M+H]^+$ 347.1828, found 347.1823.

IR (ATR, $\tilde{\nu}$ [cm^{-1}]):2903 (w), 2868 (m), 1795 (w), 1735 (w), 1679 (w), 1624 (w), 1582 (w), 1493 (w), 1456 (w), 1433 (w), 1403 (w), 1373 (w), 1318 (w), 1243 (w), 1195 (w), 1127 (w), 1109 (w), 1071 (w), 1042 (w), 979 (w), 941 (w), 889 (w), 848 (m), 822 (m), 736 (m), 707 (w).

^{1}H-NMR (400 MHz, $CDCl_3$) of compound **3hd**:

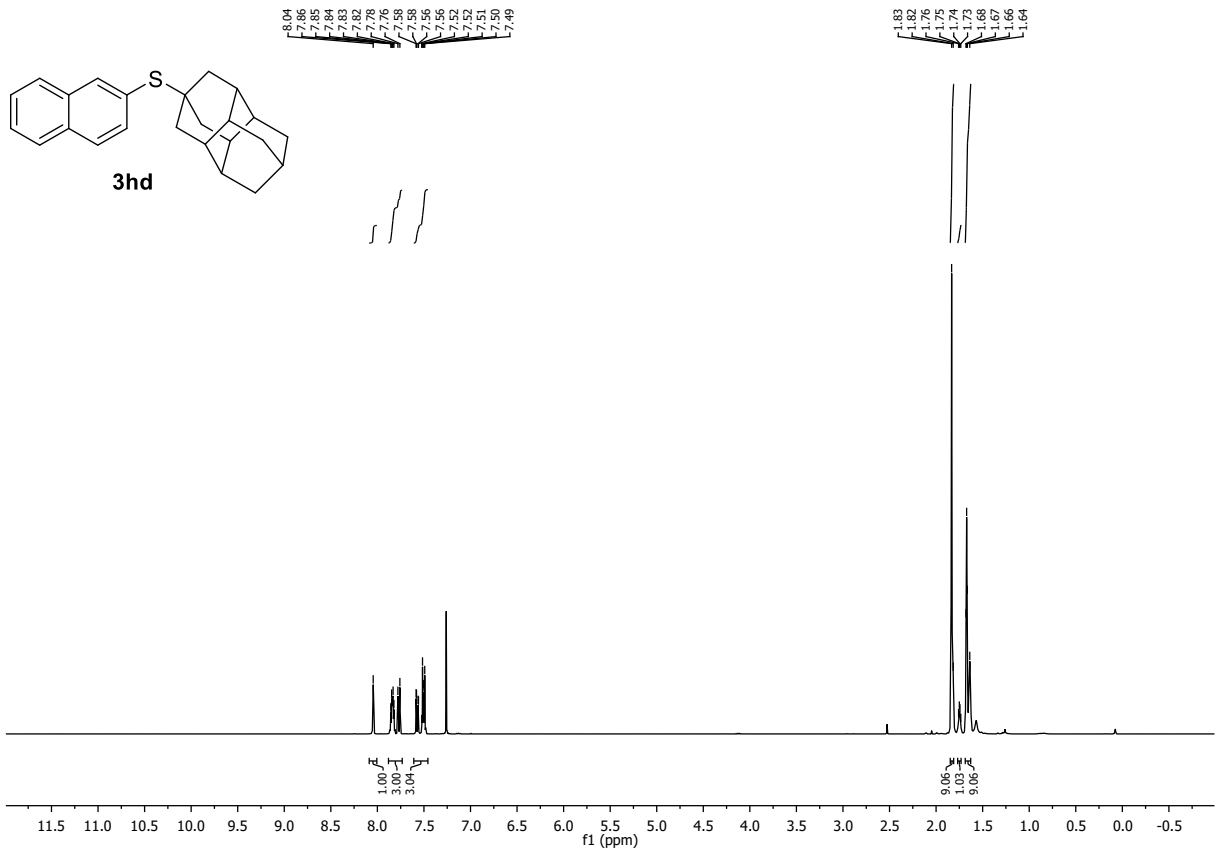

^{13}C-NMR (101 MHz, $CDCl_3$) of compound **3hd**:

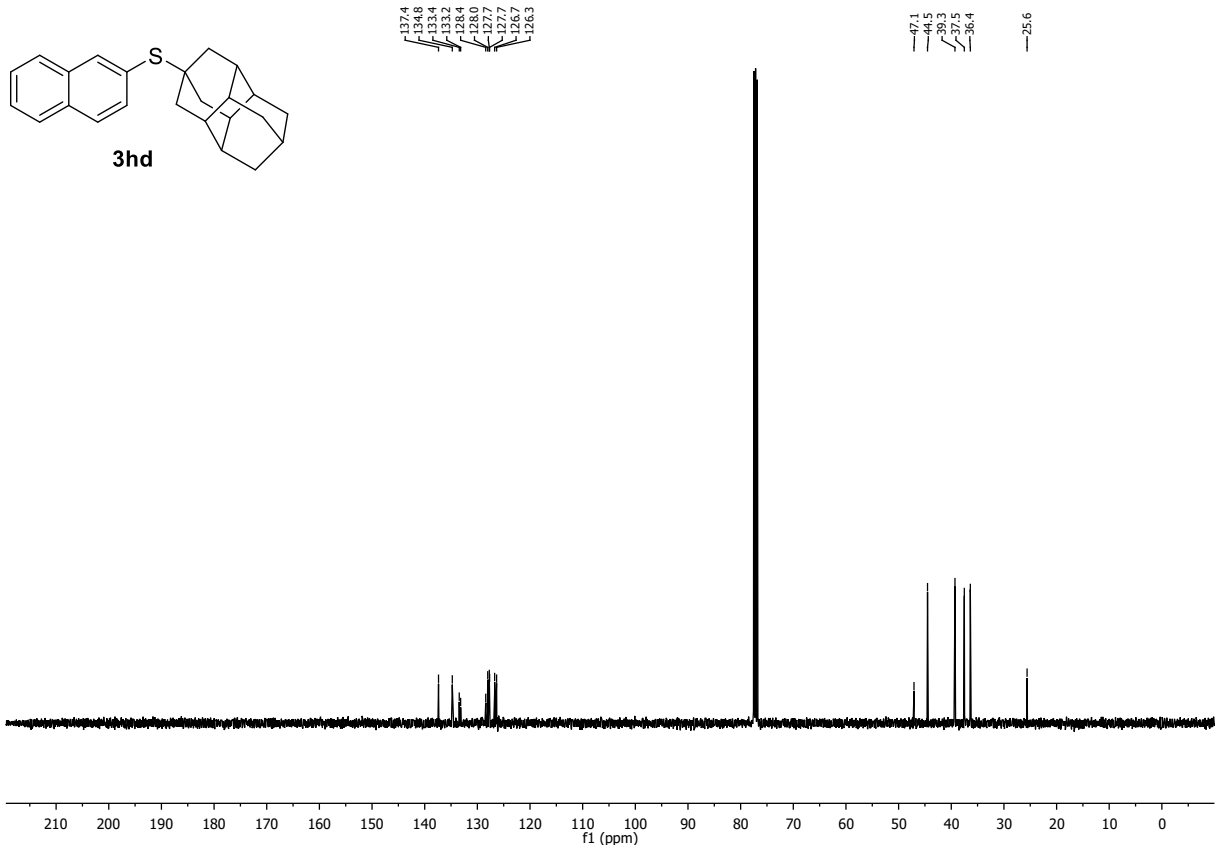

5-Methyl-2-(2-(naphthalen-2-ylthio)propan-2-yl)cyclohexan-1-one (3he):

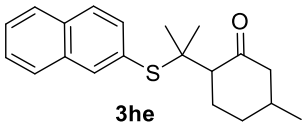

3he

$C_{20}H_{24}OS$ (312.47 g/mol)

Following **GP-C**, **3he** was synthesized using naphthalen-2-yl trifluoromethanesulfonate (276 mg, 1.00 mmol, 1.0 equiv.) and 8-mercaptomenthone (mixture of diastereomers ca. 8:2) (205 mg, 1.10 mmol, 1.1 equiv.). Purification by FC (SiO_2, gradient to 8:2 *n*-hexane/EtOAc over 15 CV) afforded **3he** (294 mg, 941 µmol, 94%, diastereomeric mixture according to starting material) as colorless solid.

R_f: 0.33 (*n*-hexane/EtOAc 95:5).

m.p.: 112.6 – 115.1 °C.

^{1}H-NMR (400 MHz, $CDCl_3$, δ): 8.04 – 8.02 (m, 1H), 7.87 – 7.79 (m, 3H), 7.56 – 7.51 (m, 3H), 2.92 – 2.81 (m, 1H), 2.41 – 2.35 (m, 1H), 2.28 – 2.23 (m, 1H), 2.09 – 1.86 (m, 4H), 1.67 – 1.61 (m, 1H), 1.47 (s, 3H), 1.42 (s, 3H), 1.00 (d, *J* = 5.8 Hz, 3H).

^{13}C-NMR (101 MHz, $CDCl_3$, δ): 211.1, 137.5, 134.3, 133.4, 133.2, 129.2, 128.1, 128.0, 127.7, 127.0, 126.5, 57.5, 52.5, 51.7, 37.1, 34.7, 30.1, 28.2, 24.0, 22.4.

HR-MS (ESI): m/z calc. for $[M+Na]^+$ 335.1440, found 335.1443.

IR (ATR, $\tilde{\nu}$ [cm^{-1}]): 3051 (w), 2950 (w), 2924 (w), 2865 (w), 1698 (s), 1582 (w), 1493 (w), 1452 (w), 1358 (m), 1320 (w), 1266 (w), 1228 (w), 1202 (w), 1161 (w), 1120 (m), 1091 (m), 1045 (m), 1016 (w), 986 (w), 945 (w), 893 (w), 852 (m), 815 (m), 740 (s), 699 (w).

^{1}H-NMR (400 MHz, $CDCl_3$) of compound **3he**:

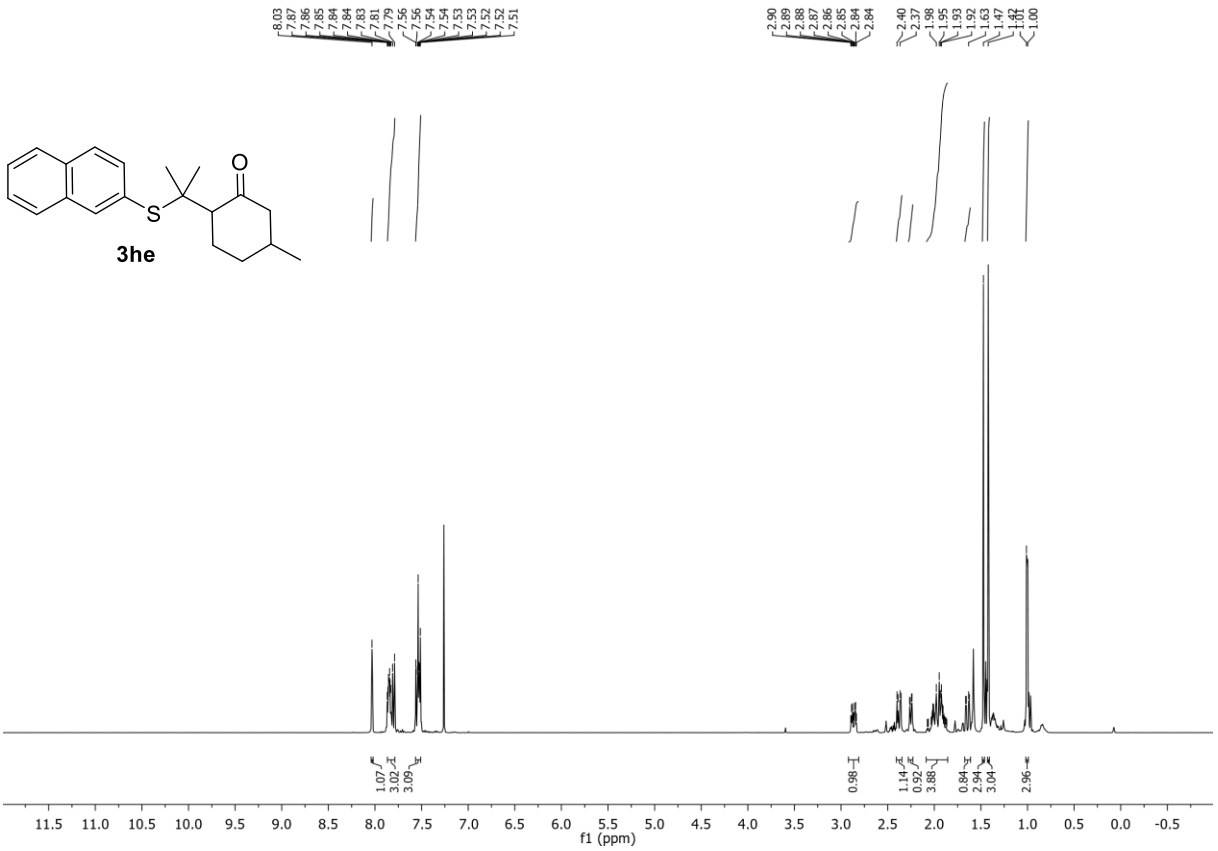

^{13}C-NMR (101 MHz, $CDCl_3$) of compound **3he**:

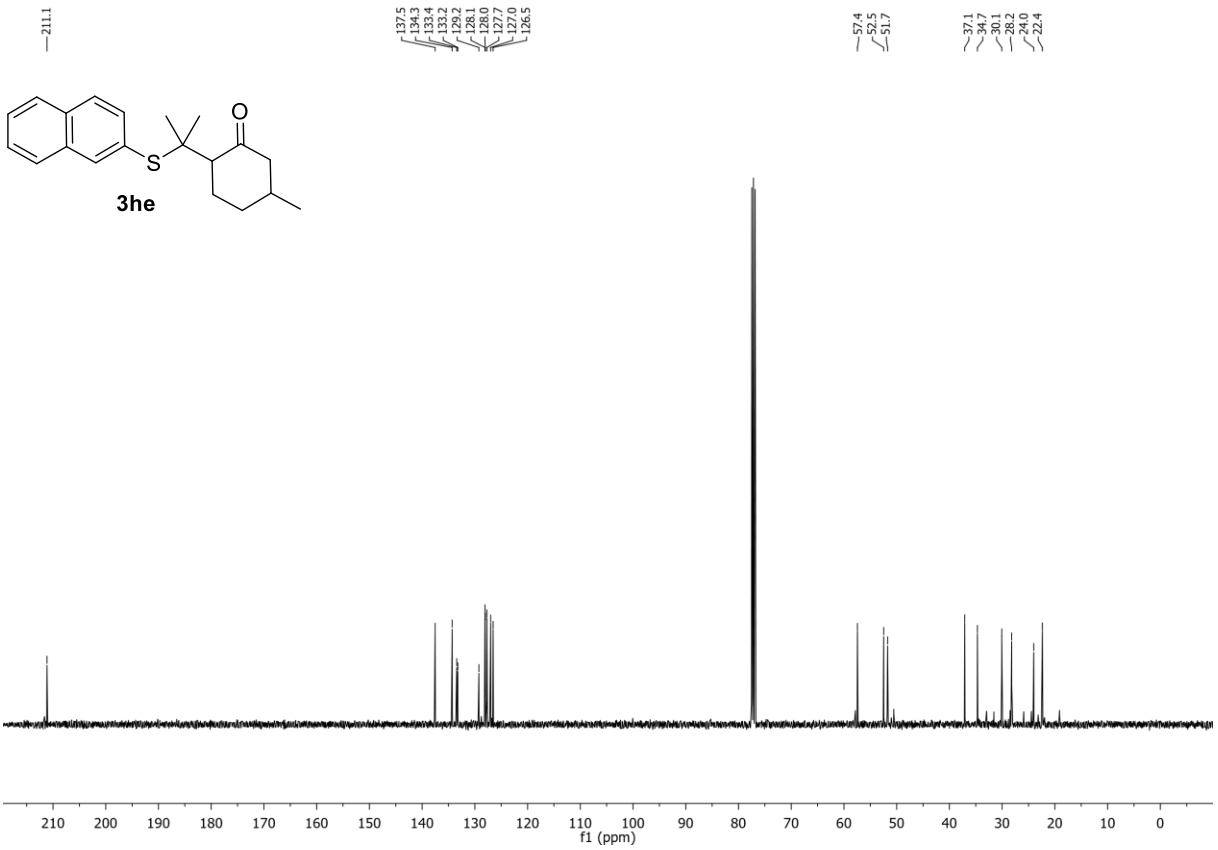

Methyl 3-(naphthalen-2-ylthio)propanoate (3hf):

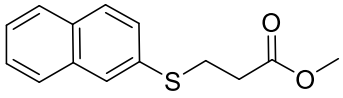

3hf

$C_{14}H_{14}O_2S$ (246.32 g/mol)

Following **GP-C**, **3hf** was synthesized using naphthalen-2-yl trifluoromethanesulfonate (276 mg, 1.00 mmol, 1.0 equiv.) and methyl 3-mercaptopropanoate (132 mg, 1.10 mmol, 1.1 equiv.). Purification by FC (SiO_2, gradient to 9:1 *n*-hexane/EtOAc over 15 CV, then gradient to 6:4 over 5 CV) afforded **3hf** (178 mg, 723 µmol, 72%) as colorless oil. Conforms to reported analytical data.[30]

R_f: 0.18 (*n*-hexane/EtOAc).

^{1}H-NMR (400 MHz, $CDCl_3$, δ): 7.84 – 7.71 (m, 4H), 7.53 – 7.40 (m, 3H), 3.68 (s, 3H), 3.27 (t, *J* = 7.4 Hz, 2H), 2.68 (t, *J* = 7.4 Hz, 2H).

^{13}C-NMR (101 MHz, $CDCl_3$, δ): 172.2, 133.8, 132.7, 132.0, 128.6, 128.1, 127.9, 127.7, 127.2, 126.7, 126.0, 51.9, 34.2, 28.9.

^{1}H-NMR (400 MHz, $CDCl_3$) of compound **3hf**:

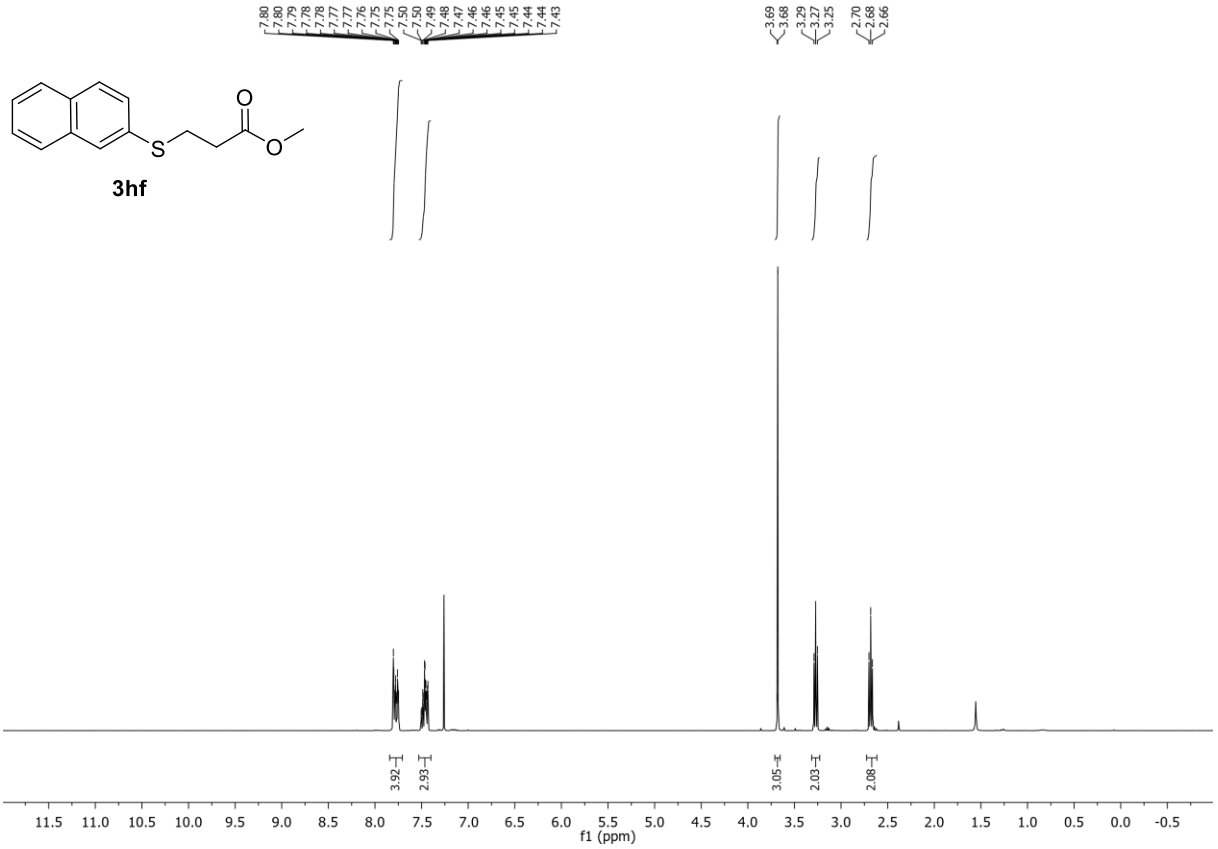

3hf

^{13}C-NMR (101 MHz, $CDCl_3$) of compound **3hf**:

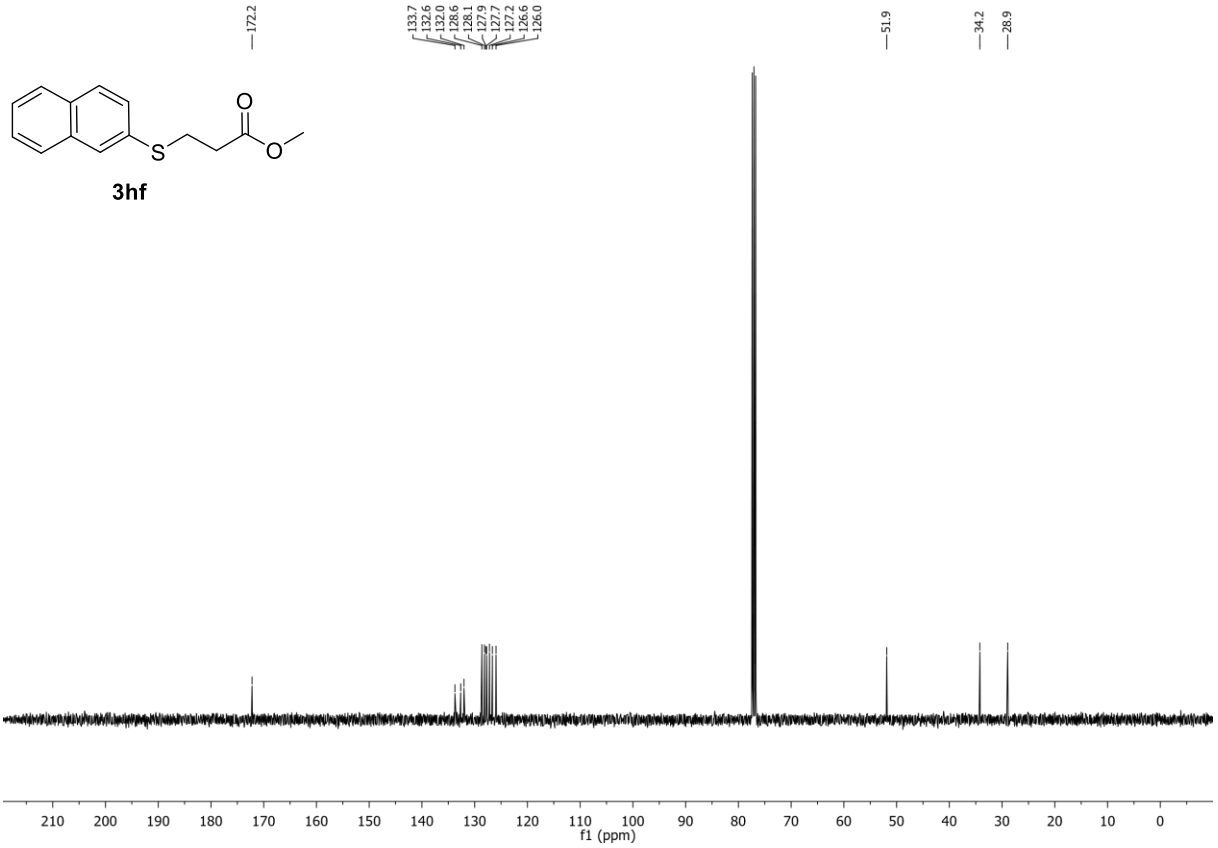

3hf

2-Methyl-3-(naphthalen-2-ylthio)tetrahydrofuran (3hg):

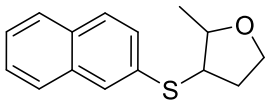

3hg

$C_{15}H_{16}OS$ (244.35 g/mol)

Following **GP-C**, **3hg** was synthesized using naphthalen-2-yl trifluoromethanesulfonate (276 mg, 1.00 mmol, 1.0 equiv.) and 2-methyltetrahydrofuran-3-thiol (mixture of diastereomers ca. 6:4) (130 mg, 1.10 mmol, 1.1 equiv.). Purification by FC (SiO_2, gradient to 8:2 *n*-hexane/EtOAc over 15 CV, then gradient to 60:40 over 5 CV) afforded **3hg** (217 mg, 888 µmol, 89%, diastereomeric mixture according to starting material) as colorless oil.

R_f: 0.25 (*n*-hexane/EtOAc 95:5).

Signals of both diastereomers:

^{1}H-NMR (400 MHz, $CDCl_3$, δ): 7.89 – 7.72 (m, 4H), 7.55 – 7.40 (m, 3H), 4.44 – 3.27 (m, 4H), 2.53 – 2.36 (m, 1H), 2.14 – 1.94 (m, 1H), 1.35 – 1.29 (d, *J* = 6.4/6.1 Hz, 3H).

^{13}C-NMR (101 MHz, $CDCl_3$, δ): 133.8, 133.7, 133.6, 132.6, 132.2, 131.9, 129.6, 128.9, 128.63, 128.61, 127.99, 127.99, 127.8, 127.4, 127.2, 126.8, 126.7, 126.2, 125.9, 80.6, 66.8, 66.1, 51.3, 49.6, 34.2, 33.5, 20.0, 17.1.

HR-MS (ESI): m/z calc. for $[M+Na]^+$ 267.0814, found 267.0811.

IR (ATR, $\tilde{\nu}$ [cm^{-1}]): 3051 (w), 2969 (w), 2928 (w), 2861 (w), 1620 (w), 1583 (w), 1496 (w), 1445 (w), 1377 (w), 1347 (w), 1318 (w), 1265 (w), 1232 (w), 1191 (w), 1105 (m), 1064 (m), 1016 (m), 941 (w), 889 (w), 848 (s), 810 (s), 740 (s).

^{1}H-NMR (400 MHz, $CDCl_3$) of compound **3hg**:

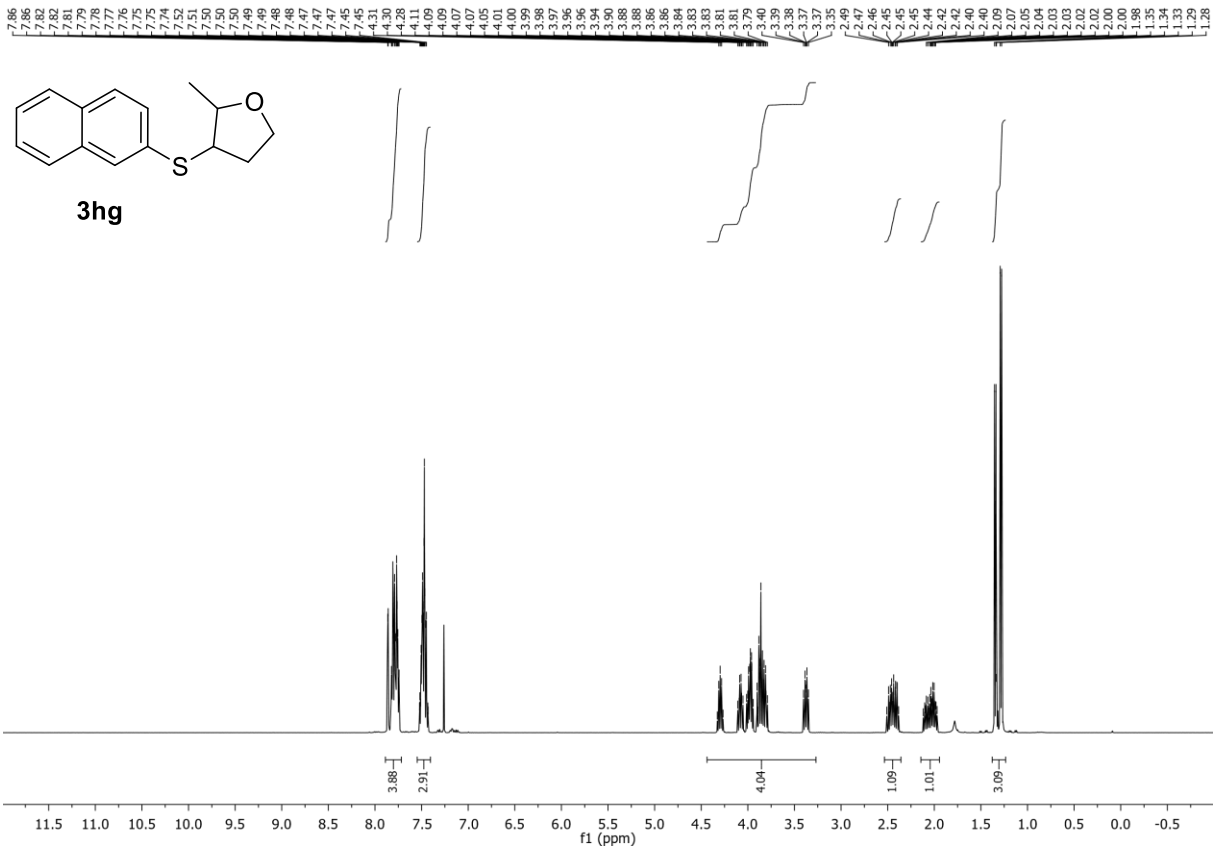

^{13}C-NMR (101 MHz, $CDCl_3$) of compound **3hg**:

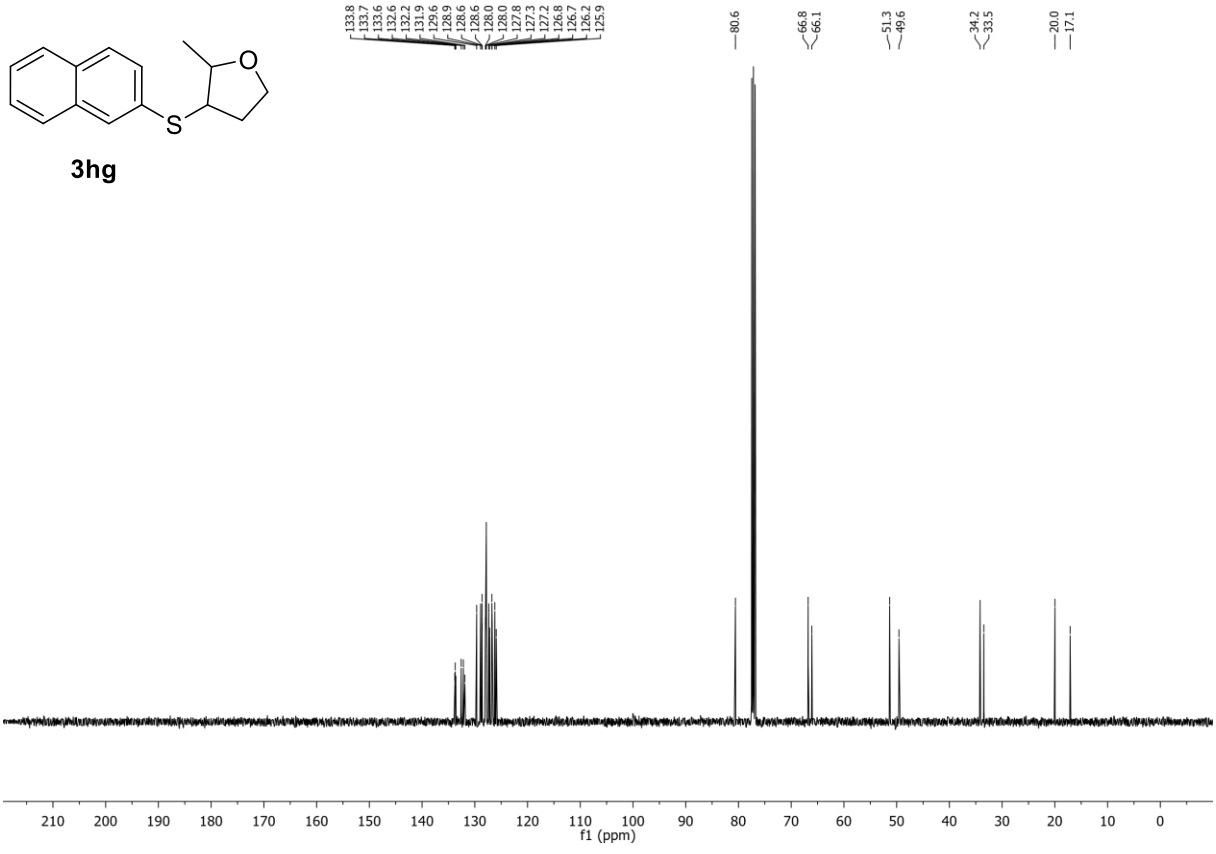

3-(Naphthalen-2-ylthio)hexan-1-ol (3hh):

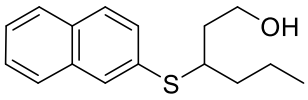

3hh

$C_{16}H_{20}OS$ (260.39 g/mol)

Following **GP-C**, **3hh** was synthesized using naphthalen-2-yl trifluoromethanesulfonate (276 mg, 1.00 mmol, 1.0 equiv.) and 3-mercaptohexan-1-ol (148 mg, 1.10 mmol, 1.1 equiv.). Purification by FC (SiO_2, gradient to 6:4 *n*-hexane/EtOAc over 20 CV) afforded **3hh** (168 mg, 645 µmol, 65% (85% purity) as colorless oil.

R_f: 0.19 (*n*-hexane/EtOAc 9:1).

^{1}H-NMR (400 MHz, $CDCl_3$, δ): 7.91 – 7.87 (m, 1H), 7.82 – 7.72 (m, 3H), 7.51 – 7.42 (m, 3H), 3.99 – 3.74 (m, 3H), 3.44 – 3.35 (m, 1H), 1.66 – 1.62 (m, 4H), 0.94 – 0.88 (m, 4H).

^{13}C-NMR (101 MHz, $CDCl_3$, δ): 133.8, 132.8, 132.3, 130.5, 129.7, 128.5, 127.8, 127.4, 126.6, 126.1, 60.9, 46.1, 37.54, 37.47, 20.2, 14.1.

HR-MS (ESI): m/z calc. for $[M+Na]^+$ 283.1127, found 283.1128.

IR (ATR, $\tilde{\nu}$ [cm^{-1}]): 3250 (br), 2951 (w), 2927 (w), 2868 (w), 1623 (w), 1583 (w), 1496 (w), 1456 (m), 1374 (w), 1344 (w), 1300 (w), 1265 (w), 1232 (w), 1201 (w), 1131 (w), 1041 (s), 945 (w), 889 (w), 851 (m), 811 (s), 740 (s).

^{1}H-NMR (400 MHz, $CDCl_3$) of compound **3hh**:

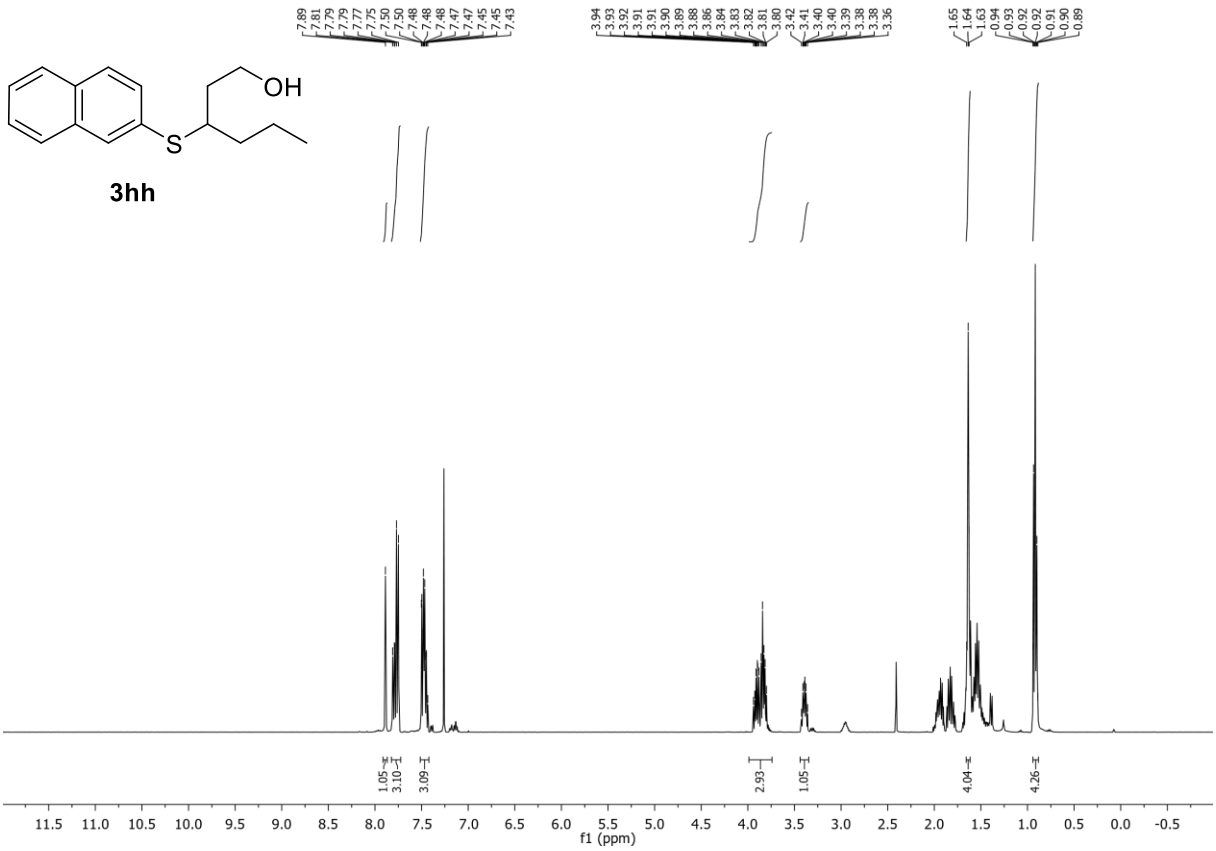

3hh

^{13}C-NMR (101 MHz, $CDCl_3$) of compound **3hh**:

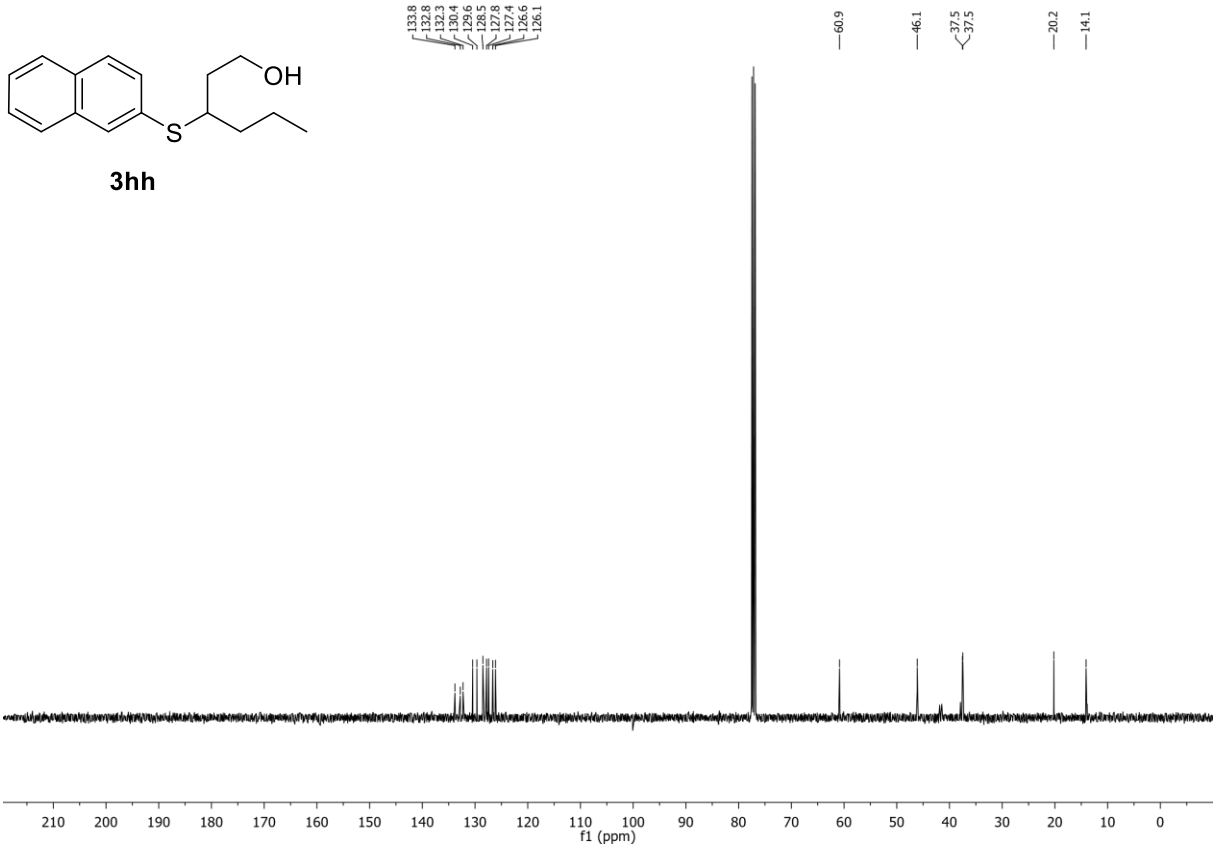

3hh

Methyl *N*-(*tert*-butoxycarbonyl)-*S*-(naphthalen-2-yl)-L-cysteinate (3hi):

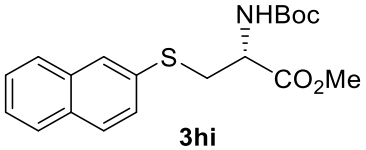

3hi

$C_{19}H_{23}NO_4S$ (361.6 g/mol)

Following GP-X, **3hi** was synthesized using naphthalen-2-yl trifluoromethanesulfonate (138 mg, 500 µmol, 1.0 equiv.) and methyl (*tert*-butoxycarbonyl)-L-cysteinate (129 mg, 550 µmol, 1.1 equiv.). Purification by FC (SiO_2, 85:15 *n*-hexane/EtOAc for 5 CV, then gradient to 3:7 over 10 CV) afforded **3hi** (95 mg, 263 µmol, 53%) as colorless solid.

R_f: 0.21 (Hex:EtOAc 90:10).

m.p.: 64.0 – 69.5 °C.

^{1}H-NMR (400 MHz, $CDCl_3$, δ): 7.90 – 7.84 (m, 1H), 7.82 – 7.72 (m, 3H), 7.52 – 7.40 (m, 3H), 5.45 – 5.29 (m, 1H), 4.67 – 4.57 (m, 1H), 3.48 (s, 3H), 1.47 – 1.44 (m, 2H), 1.36 (s, 9H).

^{13}C-NMR (101 MHz, $CDCl_3$, δ): 171.1, 133.8, 132.32, 132.26, 129.7, 128.8, 128.6, 127.8, 127.4, 126.8, 126.3, 53.5, 52.5, 37.3, 28.4, 28.3.

HR-MS (ESI): m/z calc. for $[M+Na]^+$ 384.1240, found 384.1242.

IR (ATR, $\tilde{\nu}$ [cm^{-1}]):3429.151 (w), 3060.144 (w), 3007.962 (w), 2970.688 (w), 2929.688 (w), 2870.05 (w), 2817.867 (w), 1736.939 (m), 1699.666 (s), 1625.119 (w), 1494.662 (m), 1438.752 (w), 1412.661 (w), 1390.297 (w), 1345.569 (s), 1315.75 (w), 1248.658 (w), 1211.385 (s), 1159.202 (s), 1062.291 (s), 1036.2 (w), 1006.381 (s), 965.38 (w), 950.471 (w), 920.652 (w), 902.016 (w), 861.015 (m), 820.014 (s), 797.65 (w), 779.014 (m), 741.74 (s), 670.921 (w).

^{1}H-NMR (400 MHz, $CDCl_3$) of compound **3hi**:

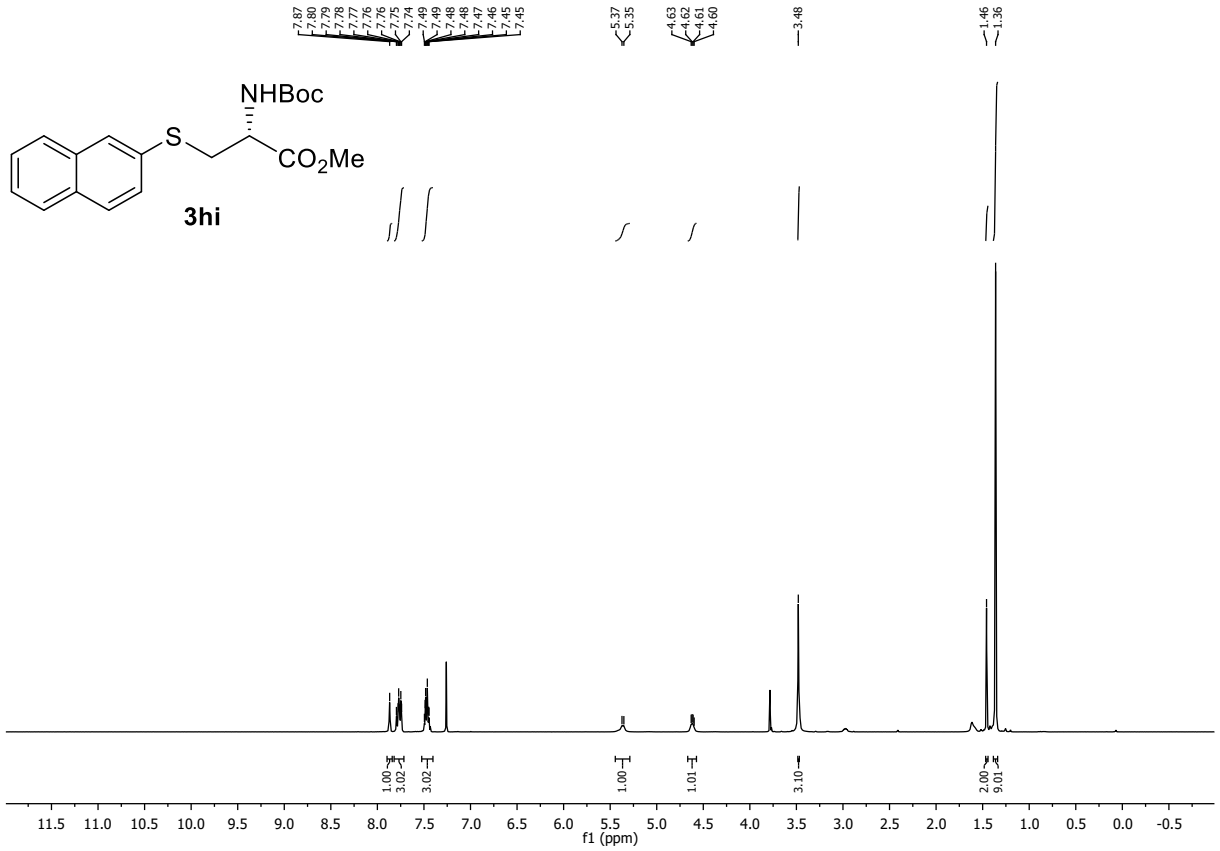

^{13}C-NMR (101 MHz, $CDCl_3$) of compound **3hi**:

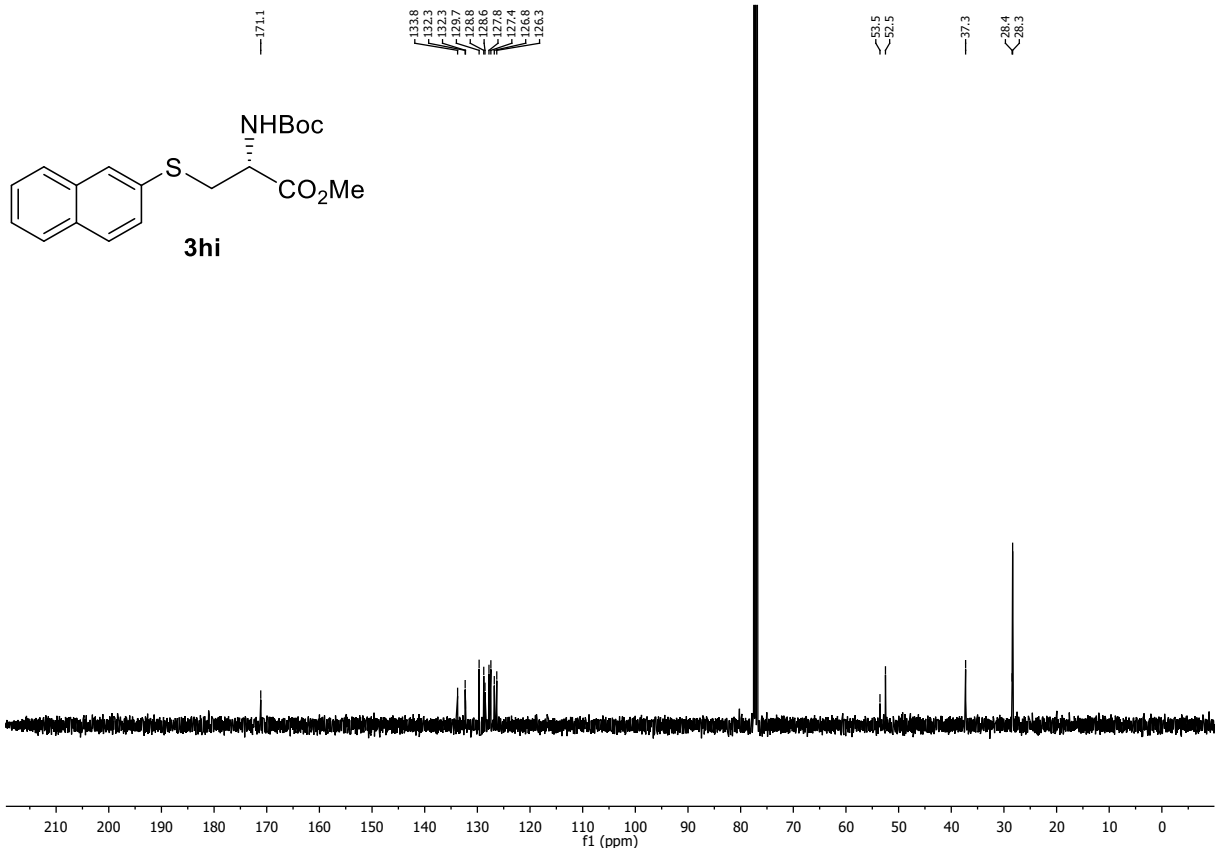

((3S,10R,13R)-10,13-Dimethyl-17-((*R*)-6-methylheptan-2-yl)-2,3,4,7,8,9,10,11,12,13,14,15,16,17-tetradecahydro-1*H*-cyclopenta[a]phenanthren-3-yl)(phenyl)sulfane (3aj):

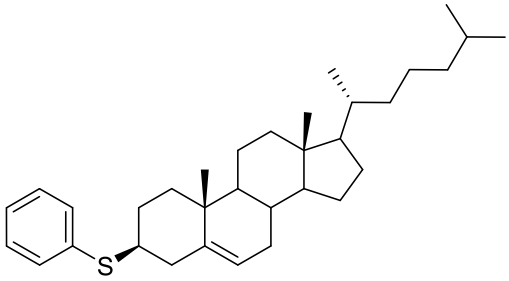

3aj

$C_{33}H_{50}S$ (478.82 g/mol)

Following **GP-C**, **3aj** was synthesized using phenyl trifluoromethanesulfonate (113 mg, 500 µmol, 1.0 equiv.) and thiocholesterol (222 mg, 550 µmol, 1.1 equiv.). Purification by FC (SiO_2, gradient to 9:1 *n*-hexane/EtOAc over 15 CV, then gradient to 5:5 over 5 CV) afforded **3aj** (226 mg, 472 µmol, 94%) as colorless solid. Conforms to reported analytical data.[31]

R_f: 0.52 (*n*-hexane).

^{1}H-NMR (400 MHz, $CDCl_3$, δ): 7.45 – 7.35 (m, 2H), 7.32 – 7.26 (m, 2H), 7.24 – 7.19 (m, 1H), 5.34 – 5.27 (m, 1H), 3.09 – 2.96 (m, 1H), 2.35 – 2.28 (m, 2H), 2.02 – 1.79 (m, 5H), 1.66 – 1.01 (m, 20H), 0.99 (s, 3H), 0.91 (d, *J* = 6.5 Hz, 3H), 0.86 (dd, *J* = 6.7, 1.9 Hz, 6H), 0.67 (s, 3H).

^{13}C-NMR (101 MHz, $CDCl_3$, δ): 141.8, 134.9, 131.8, 128.9, 126.7, 121.3, 56.8, 56.2, 50.4, 47.4, 42.4, 39.8, 39.7, 39.6, 37.0, 36.3, 35.9, 32.0, 31.9, 29.6, 28.4, 28.2, 24.4, 23.9, 23.0, 22.7, 21.0, 19.5, 18.8, 12.0.

^{1}H-NMR (400 MHz, $CDCl_3$) of compound **3aj**:

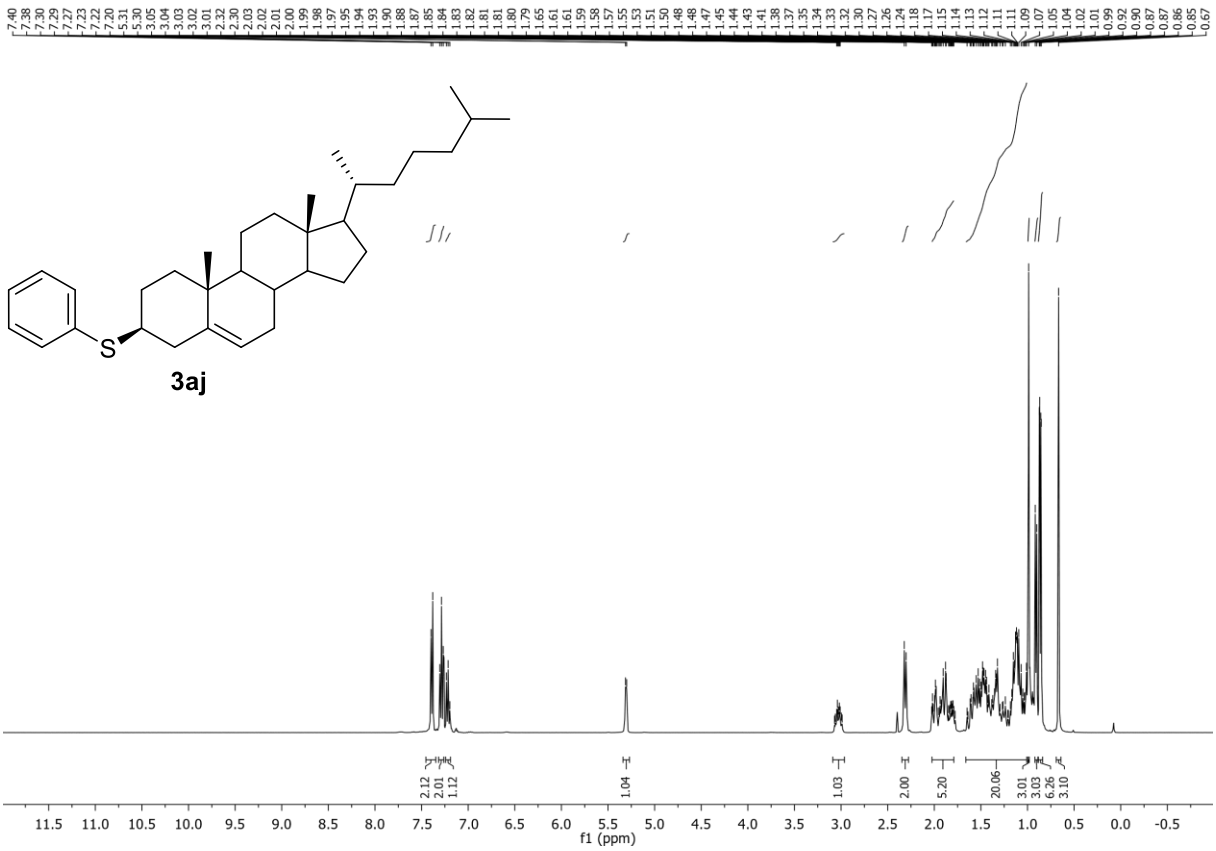

^{13}C-NMR (101 MHz, $CDCl_3$) of compound **3aj**:

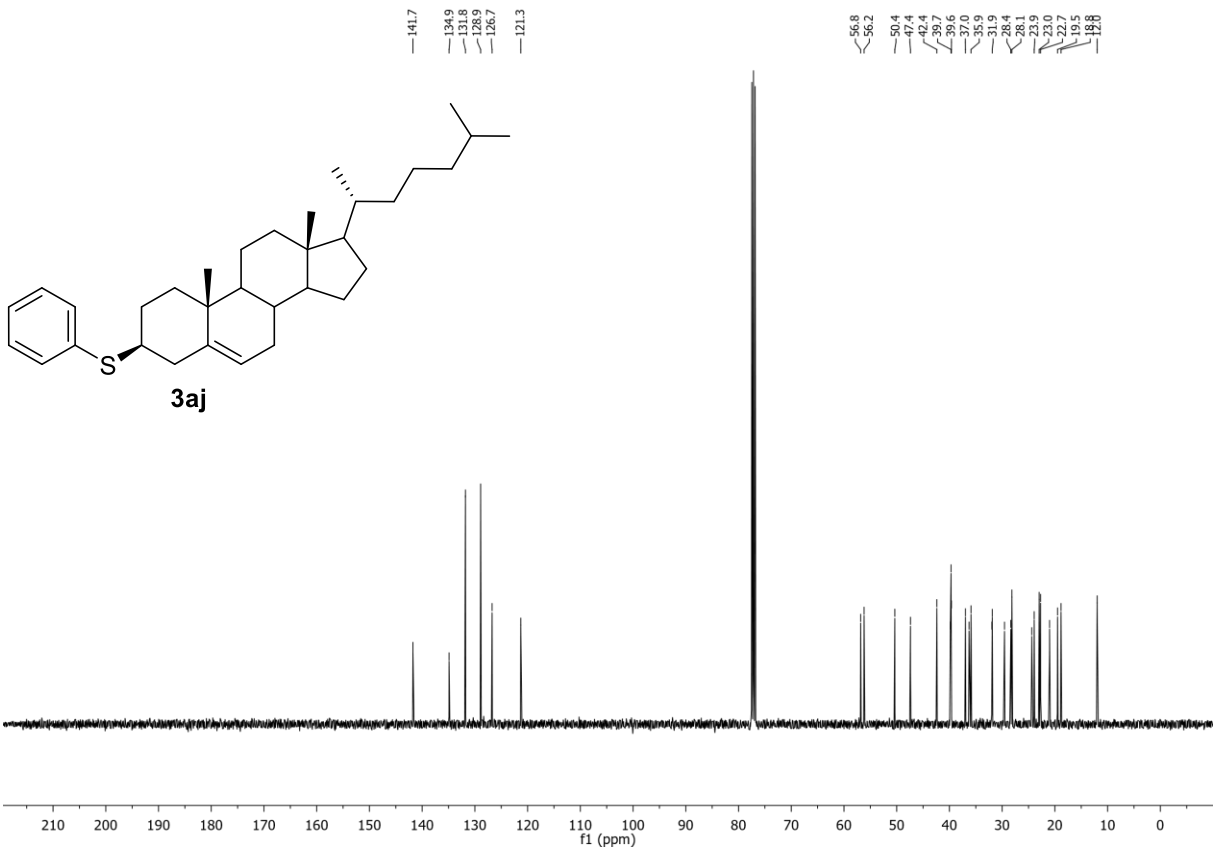

3.3.2. Alkenylthioether

((3*s*,5*s*,7*s*)-Adamantan-1-yl)(cyclohex-1-en-1-yl)sulfane (5aa):

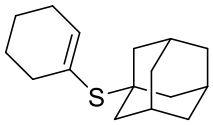

5aa

$C_{16}H_{24}S$ (248.43 g/mol)

Following **GP-C**, **5aa** was synthesized using cyclohex-1-en-1-yl trifluoromethanesulfonate (230 mg, 1.00 mmol, 1.0 equiv.) and 1-adamantanethiol (185 mg, 1.10 mmol, 1.1 equiv.). Purification by FC (SiO_2, gradient to 9:1 *n*-hexane/EtOAc over 20 CV) afforded **5aa** (231 mg, 857 µmol, 86%) as colorless solid.

R_f: 0.90 (*n*-hexane/EtOAc 9:1).

m.p.: 28.5 – 30.5 °C.

^{1}H-NMR (400 MHz, $CDCl_3$, δ): 6.13 – 6.08 (m, 1H), 2.28 – 2.22 (m, 2H), 2.18 – 2.11 (m, 2H), 2.05 – 2.01 (m, 3H), 1.87 – 1.84 (m, 6H), 1.68 – 1.65 (m, 6H), 1.60 – 1.54 (m, 2H).

^{13}C-NMR (101 MHz, $CDCl_3$, δ): 139.2, 129.1, 47.7, 44.3, 36.5, 35.8, 30.2, 27.3, 24.0, 21.6.

HR-MS (APCI): m/z calc. for $[M+H]^+$ 249.1672, found 249.1667.

IR (ATR, $\tilde{\nu}$ [cm^{-1}]): 2892 (s), 2846 (s), 1437 (m), 1340 (m), 1292 (m), 1254 (w), 1135 (w), 1101 (w), 1075 (w), 1064 (w), 1038 (m), 1016 (m), 975 (w), 914 (m), 833 (m), 800 (m), 770 (w), 725 (w), 684 (m).

^{1}H-NMR (400 MHz, $CDCl_3$) of compound **5aa**:

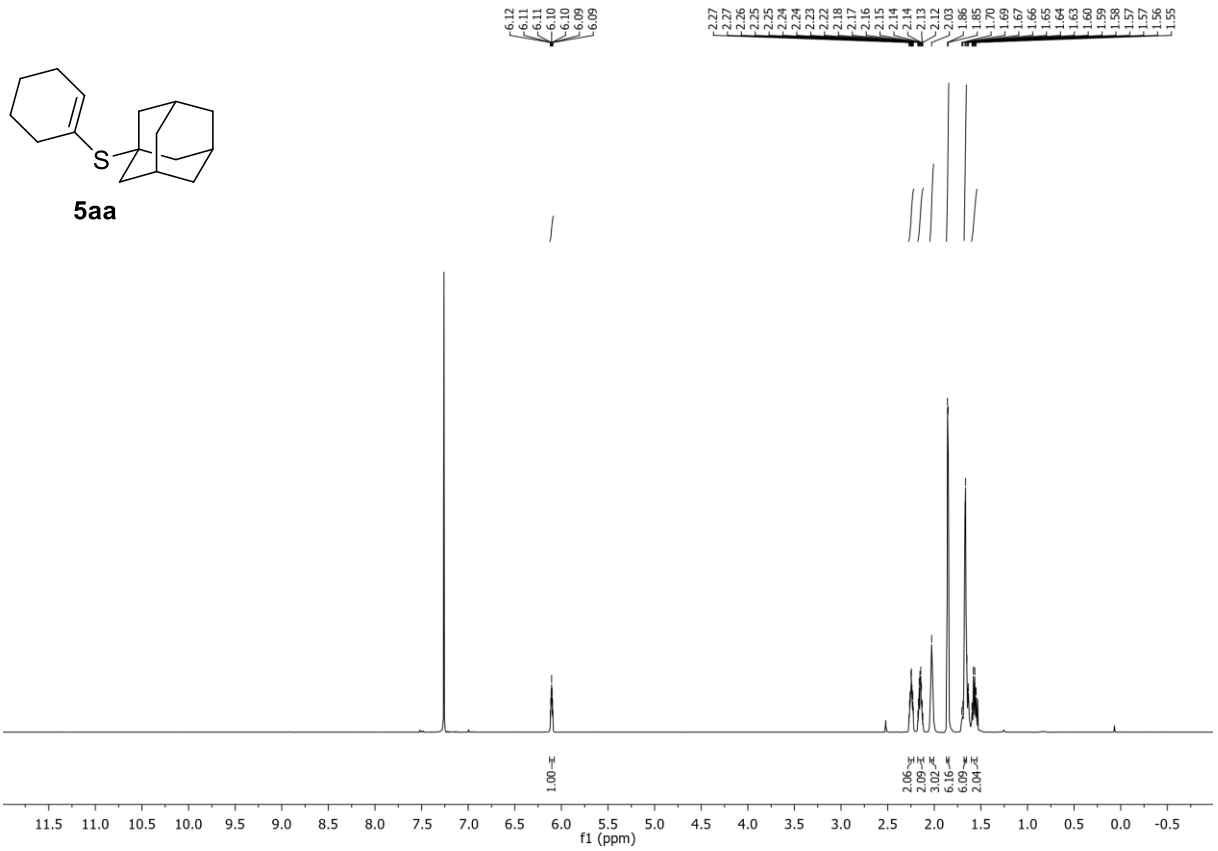

^{13}C-NMR (101 MHz, $CDCl_3$) of compound **5aa**:

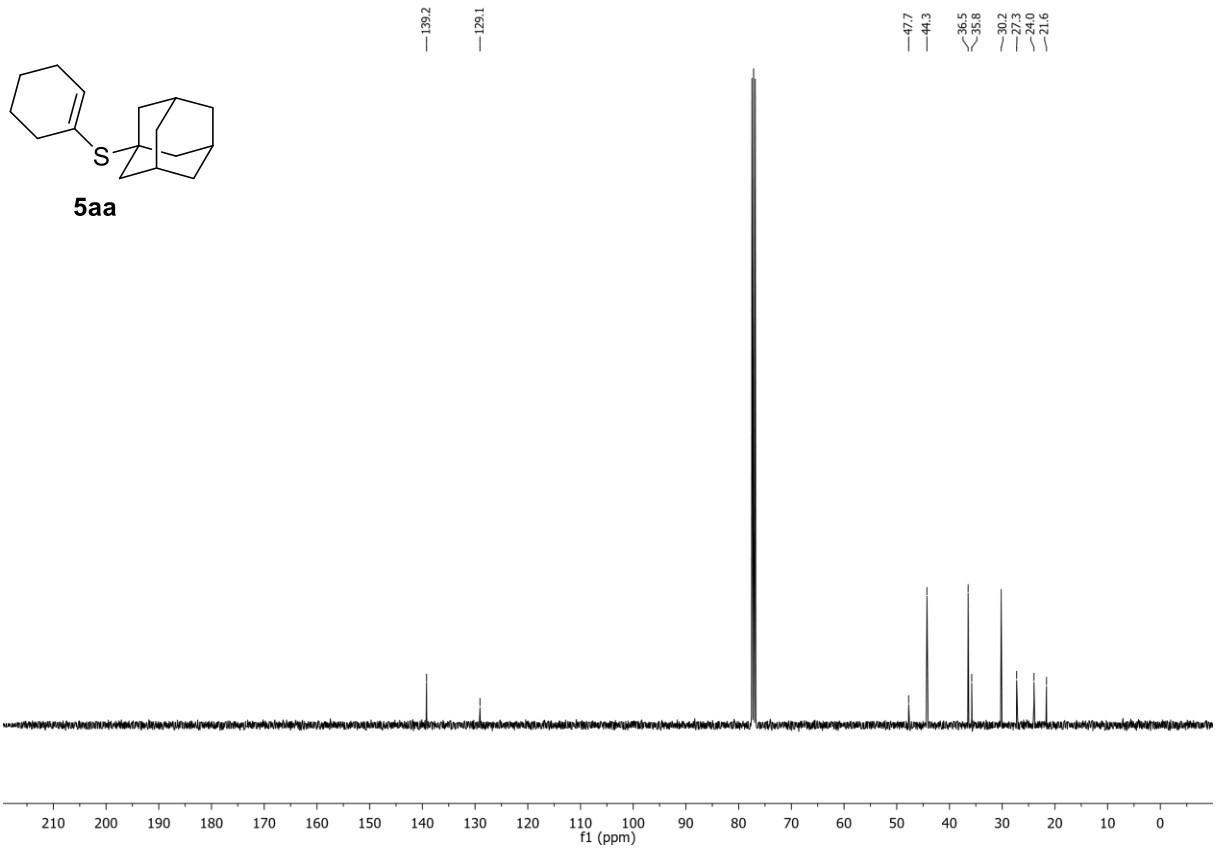

Ethyl 4-(((3*s*,5*s*,7*s*)-adamantan-1-yl)thio)cyclohex-3-ene-1-carboxylate (5ba):

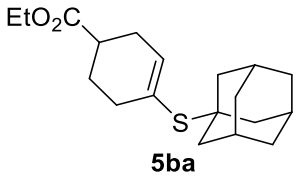

5ba

$C_{19}H_{28}O_2S$ (320.49 g/mol)

Following **GP-C**, **5ba** was synthesized using ethyl 4-(((trifluoromethyl)sulfonyl)oxy)cyclohex-3-ene-1-carboxylate (302 mg, 1.00 mmol, 1.0 equiv.) and 1-adamantanethiol (185 mg, 1.10 mmol, 1.1 equiv.). Purification by FC (SiO_2, gradient to 95:5 *n*-hexane/EtOAc over 15 CV) afforded **5ba** (276 mg, 861 µmol, 86%) as colorless oil.

R_f: 0.62 (*n*-hexane/EtOAc 95:5).

^{1}H-NMR (400 MHz, $CDCl_3$, δ): 6.13 – 6.07 (m, 1H), 4.14 (q, *J* = 7.2, 1.3 Hz, 2H), 2.58 – 2.49 (m, 1H), 2.47 – 2.29 (m, 4H), 2.04 – 2.01 (m, 3H), 1.87 – 1.83 (m, 6H), 1.82 – 1.74 (m, 2H), 1.69 – 1.63 (m, 6H), 1.26 (t, *J* = 7.1 Hz, 3H).

^{13}C-NMR (101 MHz, $CDCl_3$, δ): 175.6, 137.0, 128.9, 60.6, 48.0, 44.24, 44.20, 38.5, 36.4, 34.8, 30.3, 30.2, 29.5, 26.5, 14.4.

HR-MS (ESI): m/z calc. for $[M+Na]^+$ 343.1702, found 343.1703.

IR (ATR, $\tilde{\nu}$ [cm^{-1}]): 2972 (w), 2902 (s), 2846 (m), 1728 (s), 1444 (m), 1396 (w), 1373 (w), 1340 (w), 1299 (m), 1247 (m), 1217 (m), 1165 (s), 1101 (m), 1060 (m), 1031 (s), 971 (w), 922 (w), 859 (w), 807 (w), 744 (m), 692 (w).

^{1}H-NMR (400 MHz, $CDCl_3$) of compound **5ba**:

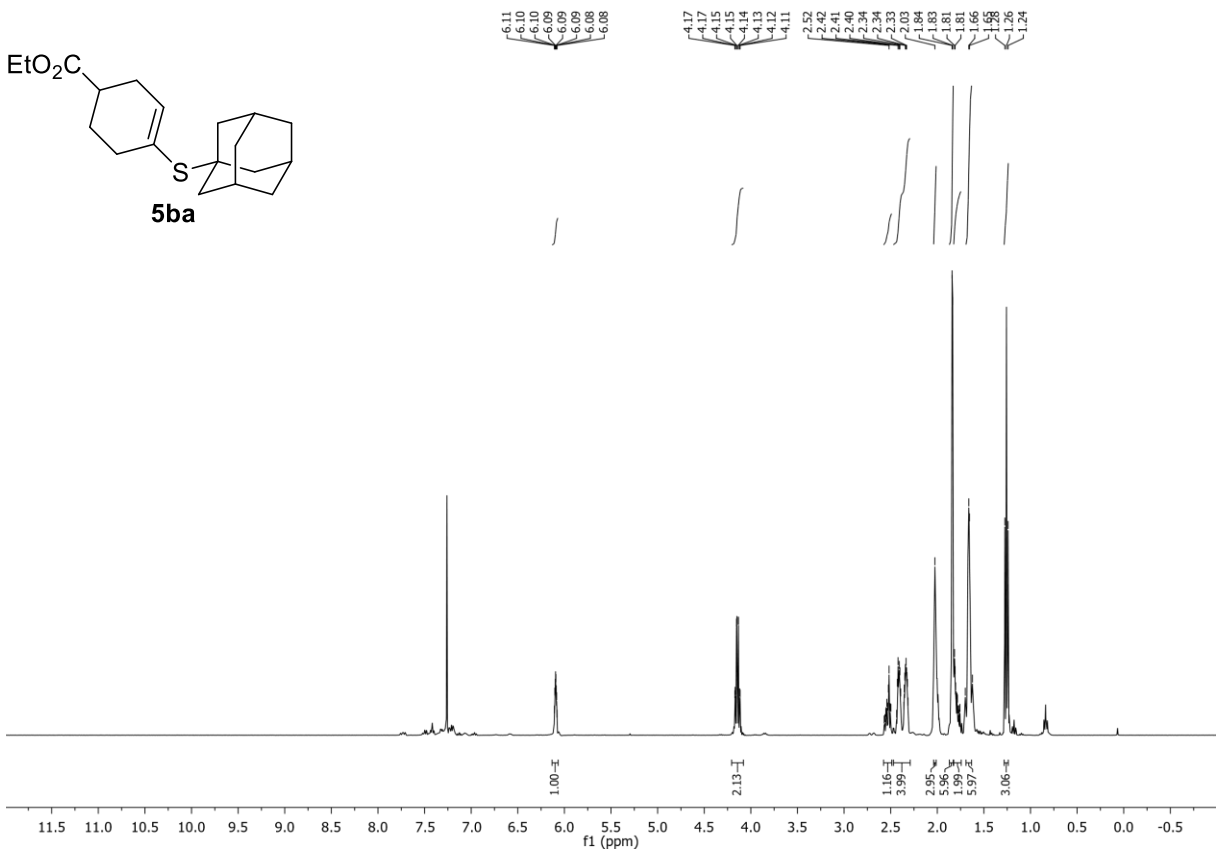

^{13}C-NMR (101 MHz, $CDCl_3$) of compound **5ba**:

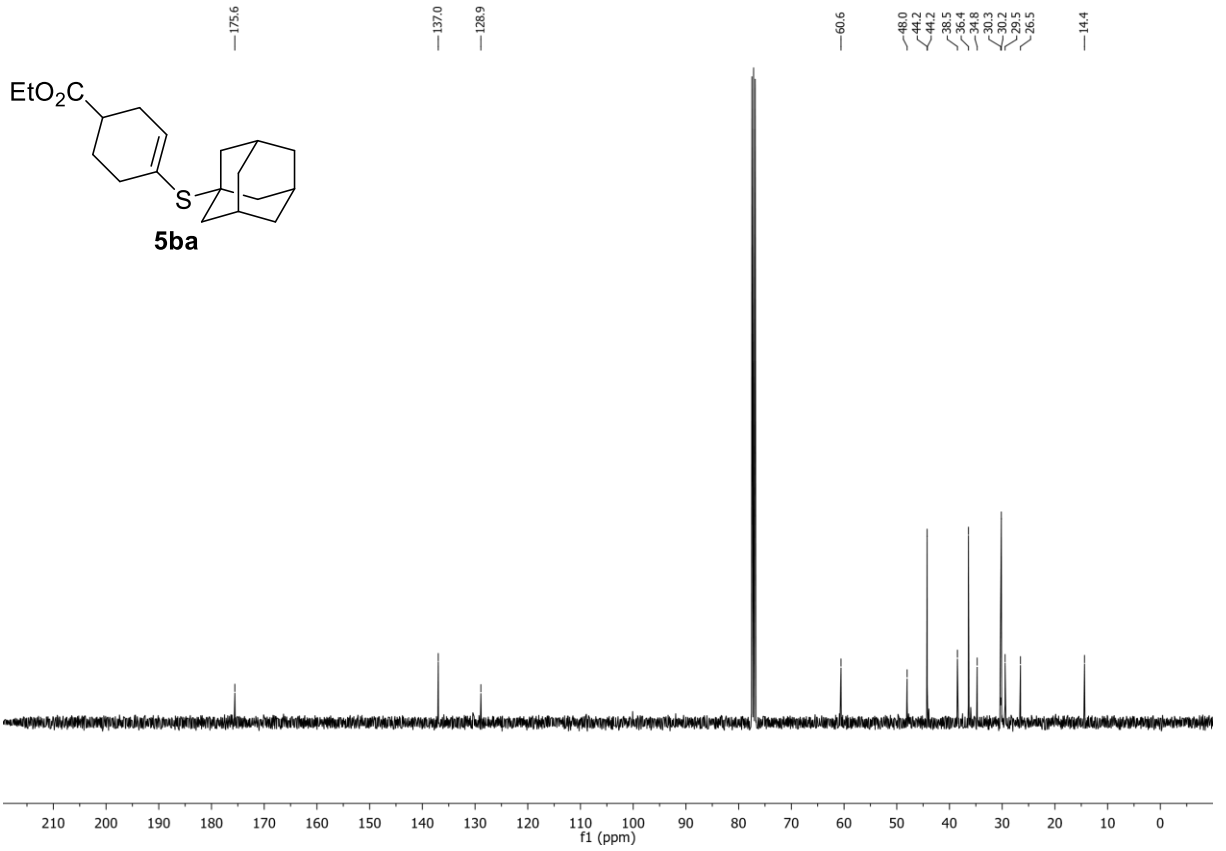

***tert*-Butyl 4-(((3*s*,5*s*,7*s*)-adamantan-1-yl)thio)-3,6-dihydropyridine-1(2*H*)-carboxylate (5ca):**

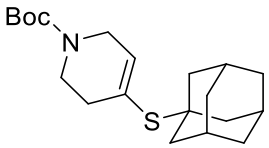

5ca

$C_{20}H_{31}NO_2S$ (349.53 g/mol)

Following **GP-C**, **5ca** was synthesized using *tert*-butyl 4-(((trifluoromethyl)sulfonyl)oxy)-3,6-dihydropyridine-1(2*H*)-carboxylate (331 mg, 1.00 mmol, 1.0 equiv.) and 1-adamantanethiol (185 mg, 1.10 mmol, 1.1 equiv.). Purification by FC (SiO_2, gradient to 8:2 *n*-hexane/EtOAc over 20 CV) afforded **5ca** (287 mg, 821 µmol, 82%) as colorless solid.

R_f: 0.23 (*n*-hexane/EtOAc 95:5).

m.p.: 78.3 – 80.7 °C.

^{1}H-NMR (400 MHz, $CDCl_3$, δ): 6.07 – 6.00 (m, 1H), 4.01 – 3.94 (m, 2H), 3.49 (t, *J* = 5.6 Hz, 2H), 2.41 – 2.31 (m, 2H), 2.06 – 2.01 (m, 3H), 1.87 – 1.84 (m, 6H), 1.70 – 1.63 (m, 6H), 1.48 – 1.46 (m, 9H).

^{13}C-NMR (101 MHz, $CDCl_3$, δ): 155.0, 100.1, 79.9, 48.4, 44.3, 36.3, 35.5, 30.1, 28.6.

HR-MS (ESI): m/z calc. for $[M+H]^+$ 372.1968, found 372.1972.

IR (ATR, $\tilde{\nu}$ [cm^{-1}]): 2973 (w), 2906 (m), 2850 (w), 1684 (s), 1449 (w), 1404 (s), 1362 (m), 1336 (m), 1269 (m), 1235 (m), 1172 (s), 1105 (m), 1044 (m), 978 (m), 945 (w), 859 (w), 829 (w), 766 (m), 684 (w).

^{1}H-NMR (400 MHz, $CDCl_3$) of compound **5ca**:

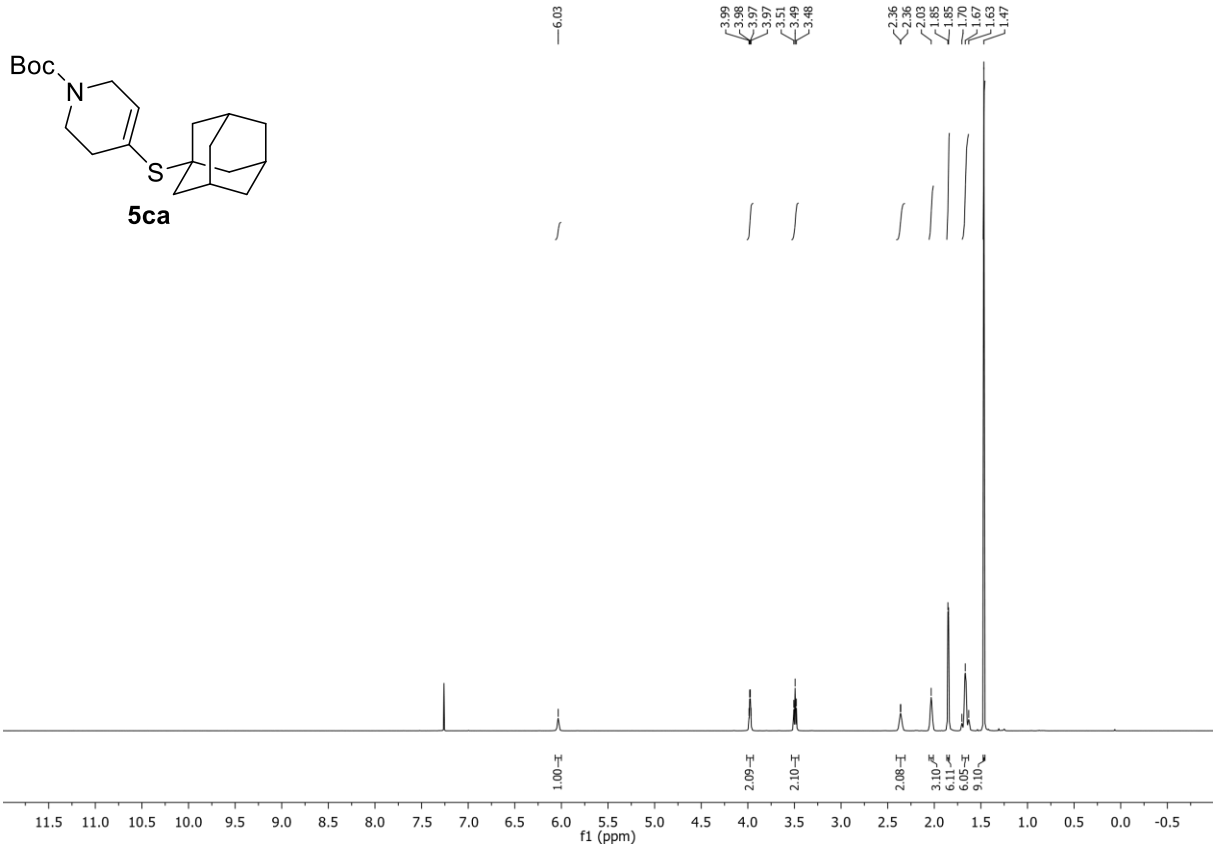

^{13}C-NMR (101 MHz, $CDCl_3$) of compound **5ca**:

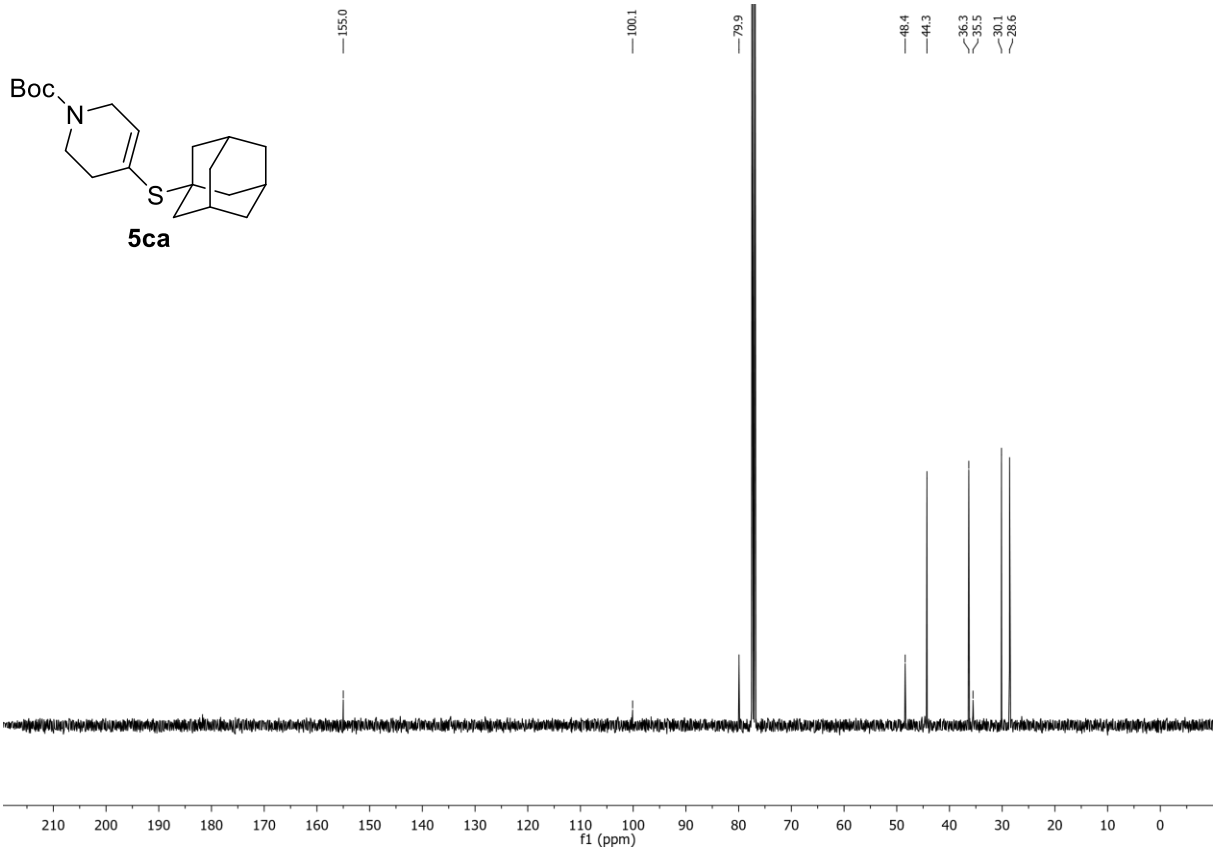

4-(((3*s*,5*s*,7*s*)-Adamantan-1-yl)thio)-3,6-dihydro-2*H*-thiopyran (5da):

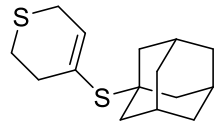

5da

$C_{15}H_{22}S_2$ (266.46 g/mol)

Following **GP-C**, **5da** was synthesized using 3,6-dihydro-2*H*-thiopyran-4-yl trifluoromethanesulfonate (248 mg, 1.00 mmol, 1.0 equiv.) and 1-adamantanethiol (185 mg, 1.10 mmol, 1.1 equiv.). Purification by FC (SiO_2, gradient to 97:3 *n*-hexane/EtOAc over 15 CV) afforded **5da** (198 mg, 743 µmol, 74%) as colorless solid.

R_f: 0.76 (*n*-hexane/EtOAc 95:5).

m.p.: 73.2 – 75.2 °C.

^{1}H-NMR (400 MHz, $CDCl_3$, δ): 6.34 – 6.26 (m, 1H), 3.28 (dt, *J* = 5.7, 2.7 Hz, 2H), 2.74 (t, *J* = 5.7 Hz, 2H), 2.56 (tt, *J* = 5.7, 2.7 Hz, 2H), 2.06 – 2.02 (m, 3H), 1.87 – 1.84 (m, 6H), 1.71 – 1.64 (m, 6H).

^{13}C-NMR (101 MHz, $CDCl_3$, δ): 135.1, 130.6, 48.5, 44.3, 36.44, 36.36, 30.2, 27.4, 26.2.

HR-MS (APCI): m/z calc. for $[M+H]^+$ 267.1236, found 267.1238.

IR (ATR, $\tilde{\nu}$ [cm^{-1}]): 2891 (m), 2846 (m), 2812 (w), 1620 (w), 1448 (w), 1414 (w), 1343 (w), 1295 (w), 1250 (w), 1191 (w), 1139 (w), 1101 (w), 1035 (m), 993 (w), 963 (m), 915 (w), 878 (w), 822 (w), 799 (m), 758 (w), 688 (w), 666 (w).

^{1}H-NMR (400 MHz, $CDCl_3$) of compound **5da**:

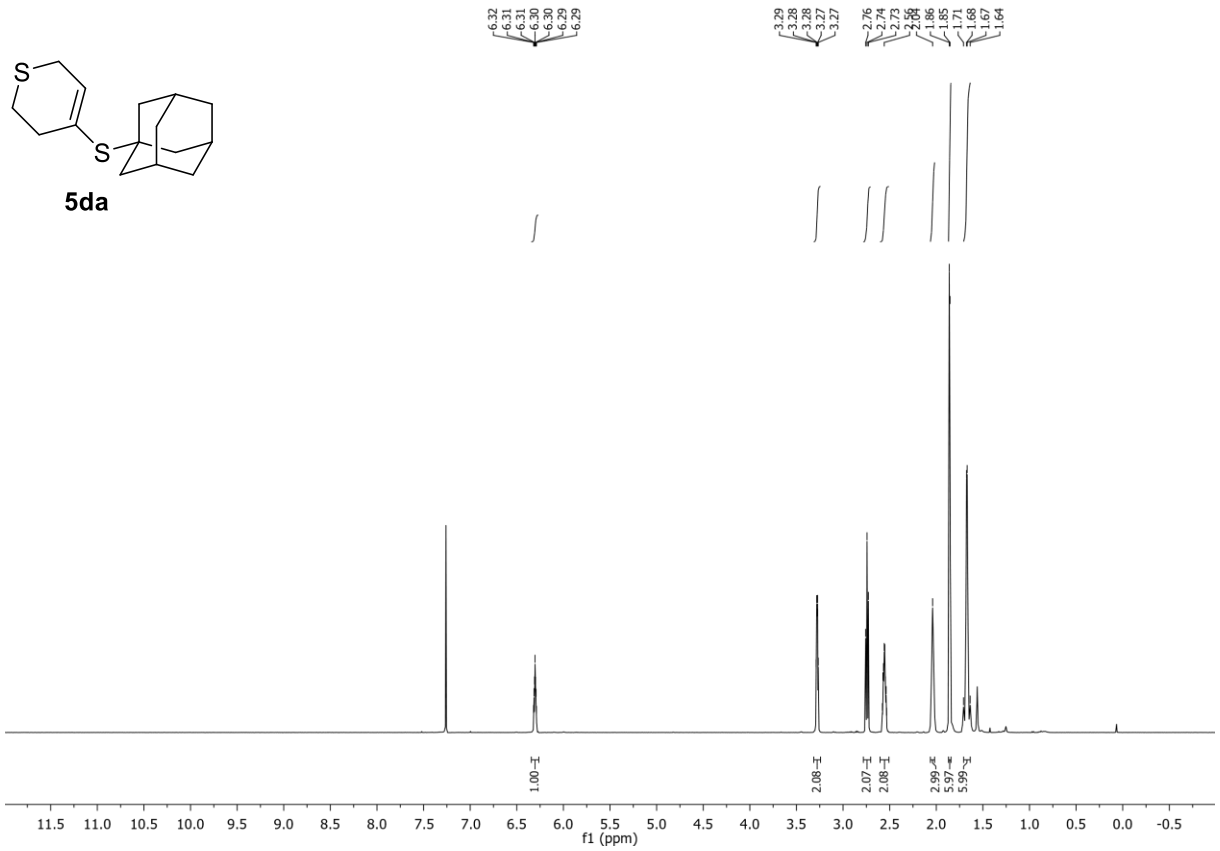

5da

^{13}C-NMR (101 MHz, $CDCl_3$) of compound **5da**:

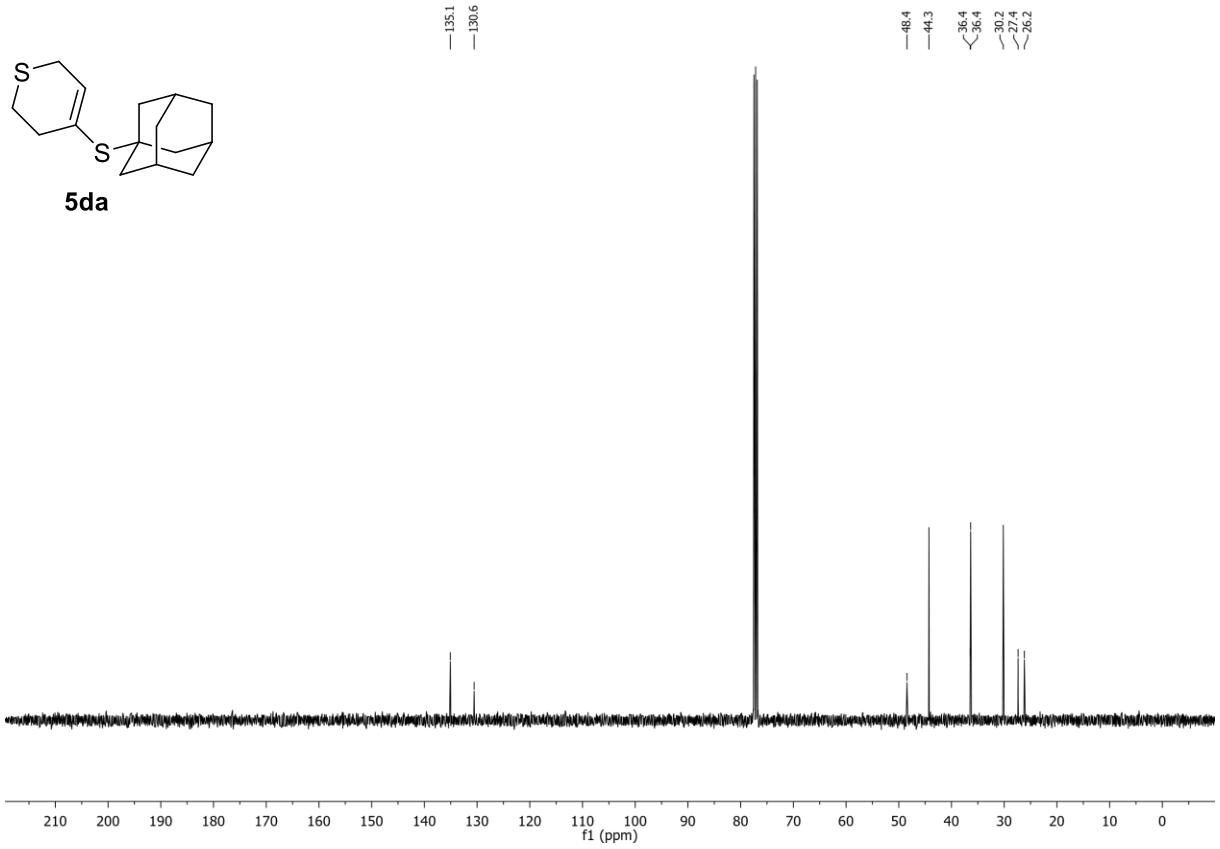

5da

((3*s*,5*s*,7*s*)-Adamantan-1-yl)(3,4-dihydronaphthalen-1-yl)sulfane (5ea):

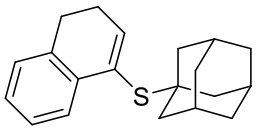

5ea

$C_{20}H_{24}S$ (296.47 g/mol)

Following **GP-C**, **5ea** was synthesized using 3,4-dihydronaphthalen-1-yl trifluoromethanesulfonate (278 mg, 1.00 mmol, 1.0 equiv.) and 1-adamantanethiol (185 mg, 1.10 mmol, 1.1 equiv.). Purification by FC (SiO_2, 99:1 *n*-hexane/EtOAc for 10 CV, then gradient to 95:5 over 10 CV) afforded **5ea** (274 mg, 924 µmol, 92%) as colorless solid.

R_f: 0.33 (*n*-hexane/EtOAc 98:2).

m.p.: 69.2 – 84.6 °C.

^{1}H-NMR (400 MHz, $CDCl_3$, δ): 7.92 (d, *J* = 7.5 Hz, 1H), 7.22 – 7.10 (m, 3H), 6.53 (t, *J* = 4.7 Hz, 1H), 2.81 (t, *J* = 8.0 Hz, 2H), 2.40 (td, *J* = 8.0, 4.7 Hz, 2H), 2.02 – 1.95 (m, 3H), 1.83 – 1.78 (m, 6H), 1.67 – 1.58 (m, 6H).

^{13}C-NMR (101 MHz, $CDCl_3$, δ): 142.0, 136.7, 135.9, 128.6, 127.3, 127.2, 126.5, 126.4, 48.0, 44.2, 36.4, 30.2, 28.2, 25.1.

HR-MS (APCI): m/z calc. for $[M+H]^+$ 297.1672, found 297.1674.

IR (ATR, $\tilde{\nu}$ [cm^{-1}]): 2897 (m), 2846 (m), 1680 (w), 1657 (w), 1653 (w), 1597 (w), 1474 (w), 1445 (m), 1412 (m), 1343 (w), 1292 (m), 1250 (w), 1210 (m), 1142 (m), 1105 (w), 1034 (m), 1009 (m), 967 (m), 900 (m), 878 (w), 825 (m), 758 (s), 733 (s), 688 (m).

^{1}H-NMR (400 MHz, $CDCl_3$) of compound **5ea**:

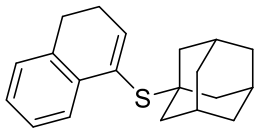

5ea

^{13}C-NMR (101 MHz, $CDCl_3$) of compound **5ea**:

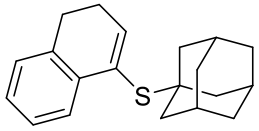

5ea

((3*s*,5*s*,7*s*)-Adamantan-1-yl)(7-methoxy-3,4-dihydronaphthalen-1-yl)sulfane (5fa):

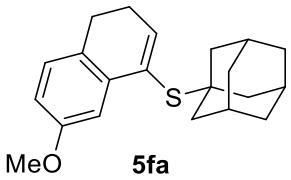

5fa

$C_{21}H_{26}OS$ (326.50 g/mol)

Following **GP-C**, **5fa** was synthesized using 7-methoxy-3,4-dihydronaphthalen-1-yl trifluoromethanesulfonate (308 mg, 1.00 mmol, 1.0 equiv.) and 1-adamantanethiol (185 mg, 1.10 mmol, 1.1 equiv.). Purification by FC (SiO_2, gradient to 98:2 *n*-hexane/EtOAc over 15 CV) afforded **5fa** (235 mg, 720 µmol, 72%) as colorless solid.

R_f: 0.17 (*n*-hexane/EtOAc 99:1).

m.p.: 77.2 – 80.6 °C.

^{1}H-NMR (400 MHz, $CDCl_3$, δ): 7.55 (d, *J* = 2.7 Hz, 1H), 7.02 (d, *J* = 8.1 Hz, 1H), 6.70 (dd, *J* = 8.1, 2.7 Hz, 1H), 6.55 (t, *J* = 4.6 Hz, 1H), 3.82 (s, 3H), 2.74 (t, *J* = 8.0 Hz, 2H), 2.38 (td, *J* = 8.0, 4.7 Hz, 2H), 2.02 – 1.94 (m, 3H), 1.83 – 1.79 (m, 6H), 1.66 – 1.58 (m, 6H).

^{13}C-NMR (101 MHz, $CDCl_3$, δ): 158.4, 142.7, 137.9, 128.6, 128.1, 128.0, 112.6, 112.4, 55.6, 48.0, 44.2, 36.4, 30.2, 27.3, 25.4

HR-MS (ESI): m/z calc. for $[M+Na]^+$ 349.1597, found 349.1596.

IR (ATR, $\tilde{\nu}$ [cm^{-1}]): 2901 (s), 2846 (w), 1601 (m), 1567 (w), 1485 (m), 1445 (m), 1412 (m), 1344 (w), 1314 (w), 1292 (w), 1269 (w), 1243 (s), 1209 (s), 1142 (s), 1105 (m), 1038 (s), 1012 (m), 975 (w), 896 (m), 874 (m), 837 (m), 807 (s), 736 (m), 684 (m).

^{1}H-NMR (400 MHz, $CDCl_3$) of compound **5fa**:

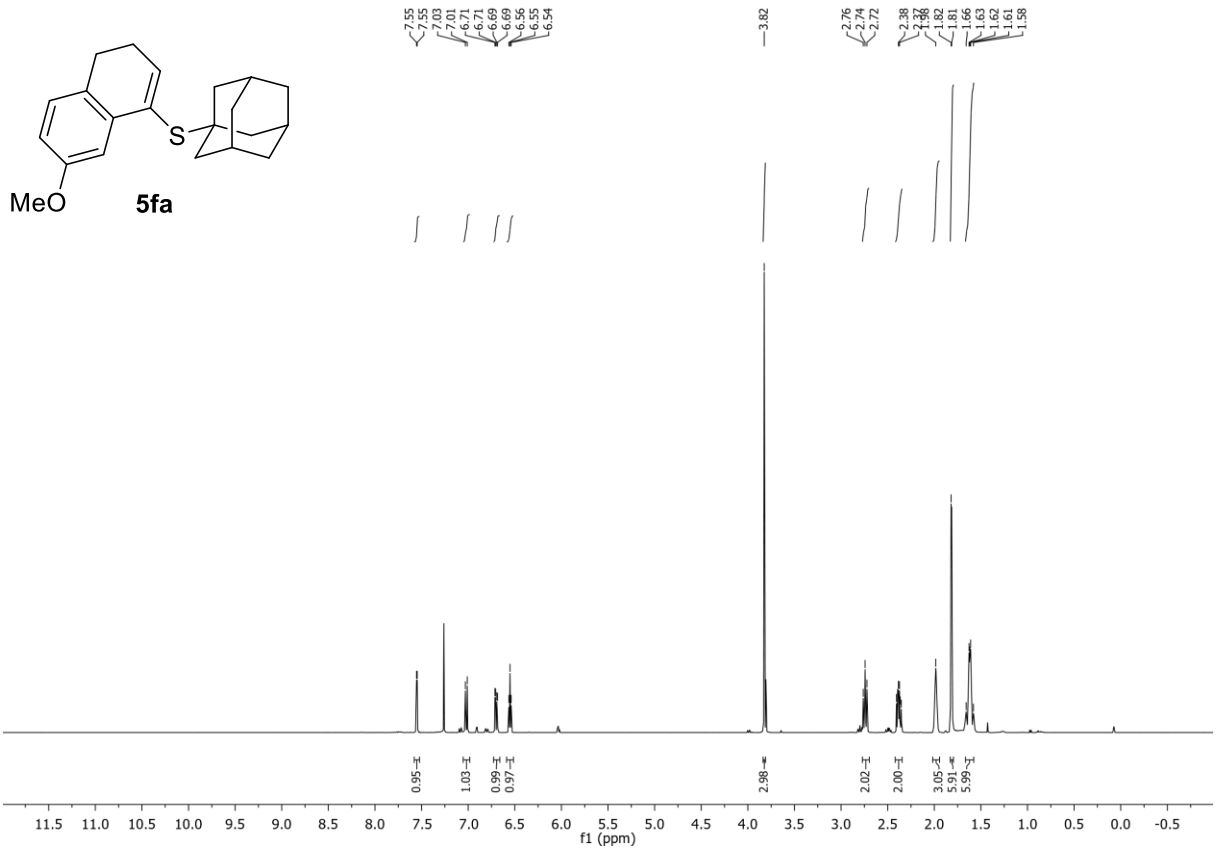

^{13}C-NMR (101 MHz, $CDCl_3$) of compound **5fa**:

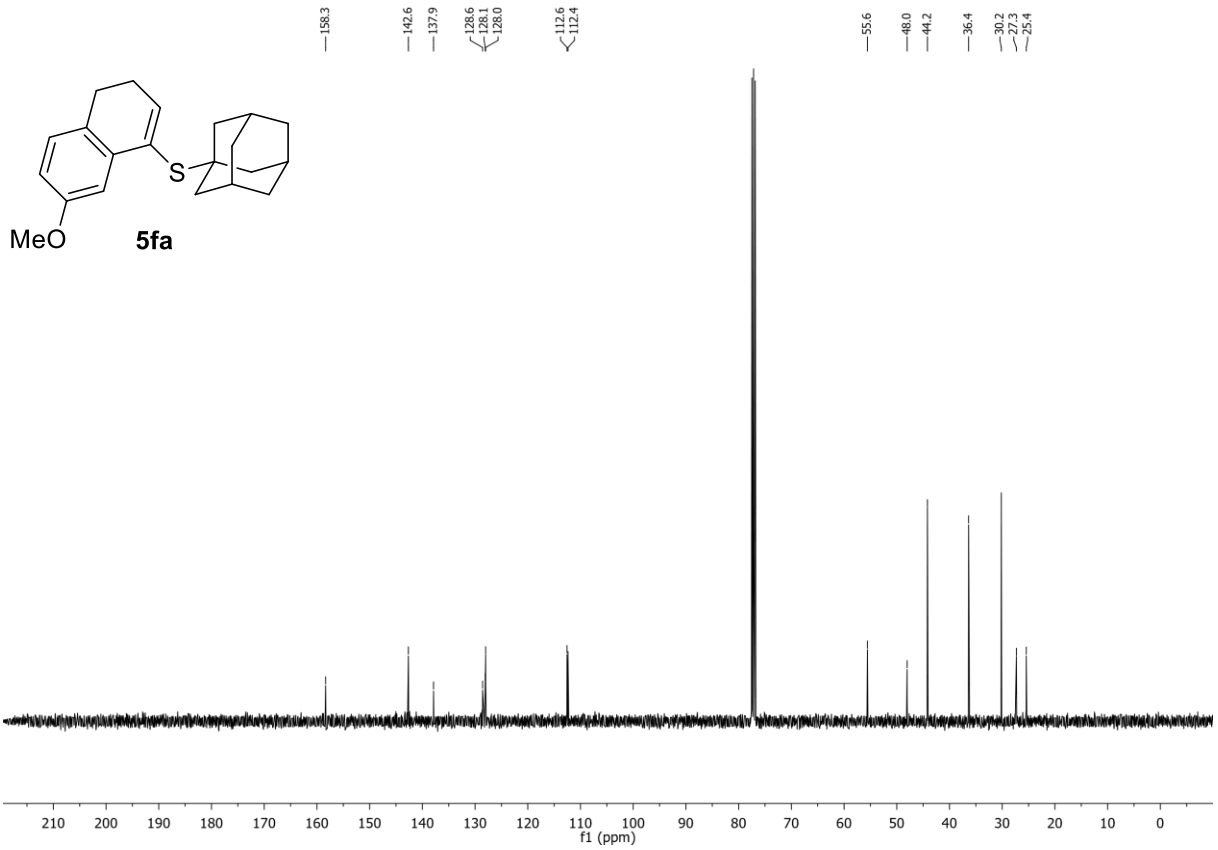

4-(((3*s*,5*s*,7*s*)-Adamantan-1-yl)thio)-2*H*-chromene (5ga):

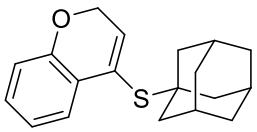

5ga

$C_{19}H_{22}OS$ (298.44 g/mol)

Following **GP-C**, **5ga** was synthesized using 2*H*-chromen-4-yl trifluoromethanesulfonate (280 mg, 1.00 mmol, 1.0 equiv.) and 1-adamantanethiol (185 mg, 1.10 mmol, 1.1 equiv.). Purification by FC (SiO_2, 99:1 *n*-hexane/EtOAc for 20 CV) afforded **5ga** (277 mg, 928 µmol, 93%) as colorless solid.

R_f: 0.21 (*n*-hexane/EtOAc 99:1).

m.p.: 54.8 – 58.1 °C.

^{1}H-NMR (400 MHz, $CDCl_3$, δ): 7.75 (d, *J* = 7.6 Hz, 1H), 7.13 (dd, *J* = 7.6 Hz, 1H), 6.92 (dd, *J* = 7.6 Hz, 1H), 6.79 (d, *J* = 8.0 Hz, 1H), 6.20 (t, *J* = 3.9 Hz, 1H), 4.82 (d, *J* = 3.9 Hz, 2H), 2.03 – 1.98 (m, 3H), 1.87 – 1.82 (m, 6H), 1.66 – 1.60 (m, 6H).

^{13}C-NMR (101 MHz, $CDCl_3$, δ): 154.1, 133.7, 129.6, 127.1, 126.5, 125.5, 121.3, 115.8, 66.0, 48.8, 44.1, 36.24, 36.19, 30.2.

HR-MS (ESI): m/z calc. for $[M+Na]^+$ 321.1284, found 321.1286.

IR (ATR, $\tilde{\nu}$ [cm^{-1}]): 2898 (m), 2846 (m), 2820 (w), 1601 (w), 1568 (w), 1474 (m), 1448 (m), 1400 (w), 1374 (w), 1343 (w), 1295 (w), 1247 (w), 1217 (s), 1176 (m), 1150 (w), 1112 (m), 1061 (m), 1034 (m), 1012 (m), 971 (m), 934 (w), 908 (w), 804 (m), 747 (s), 688 (m).

^{1}H-NMR (400 MHz, $CDCl_3$) of compound **5ga**:

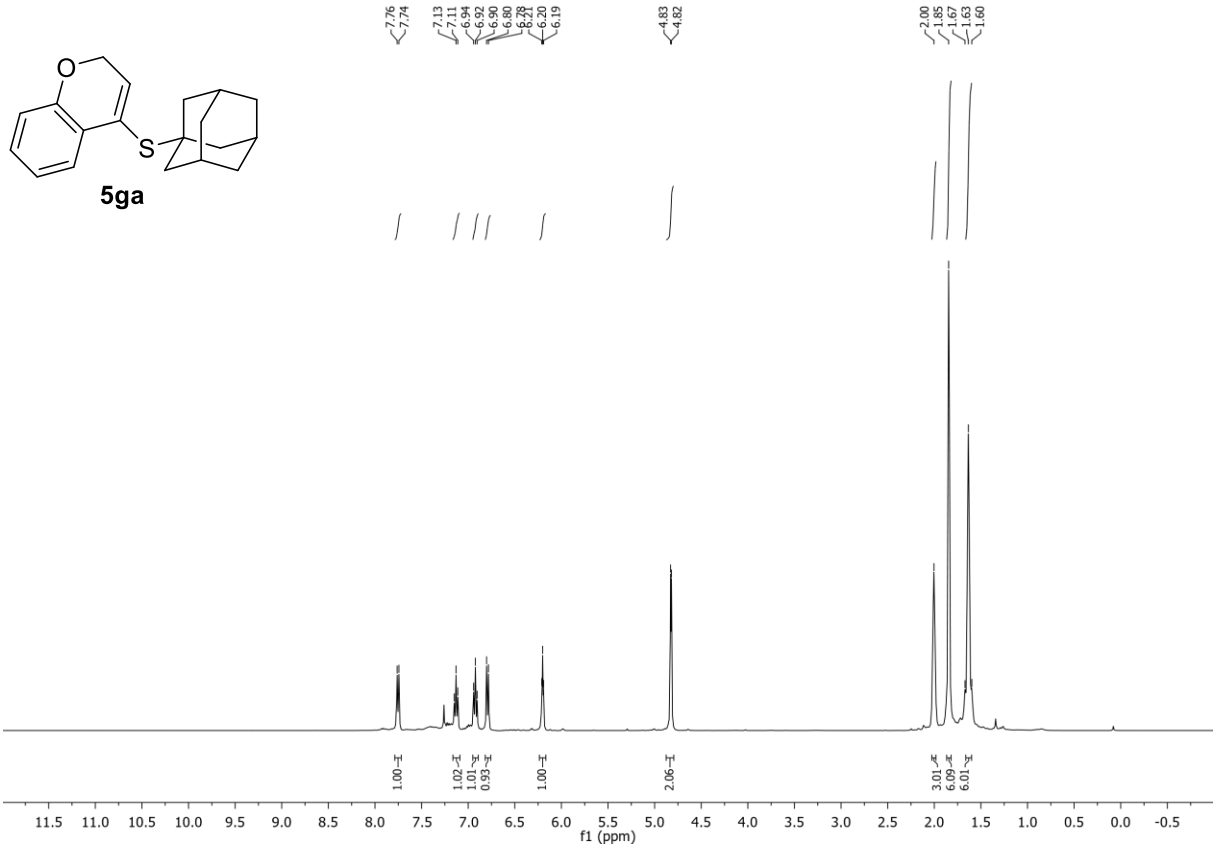

5ga

^{13}C-NMR (101 MHz, $CDCl_3$) of compound **5ga**:

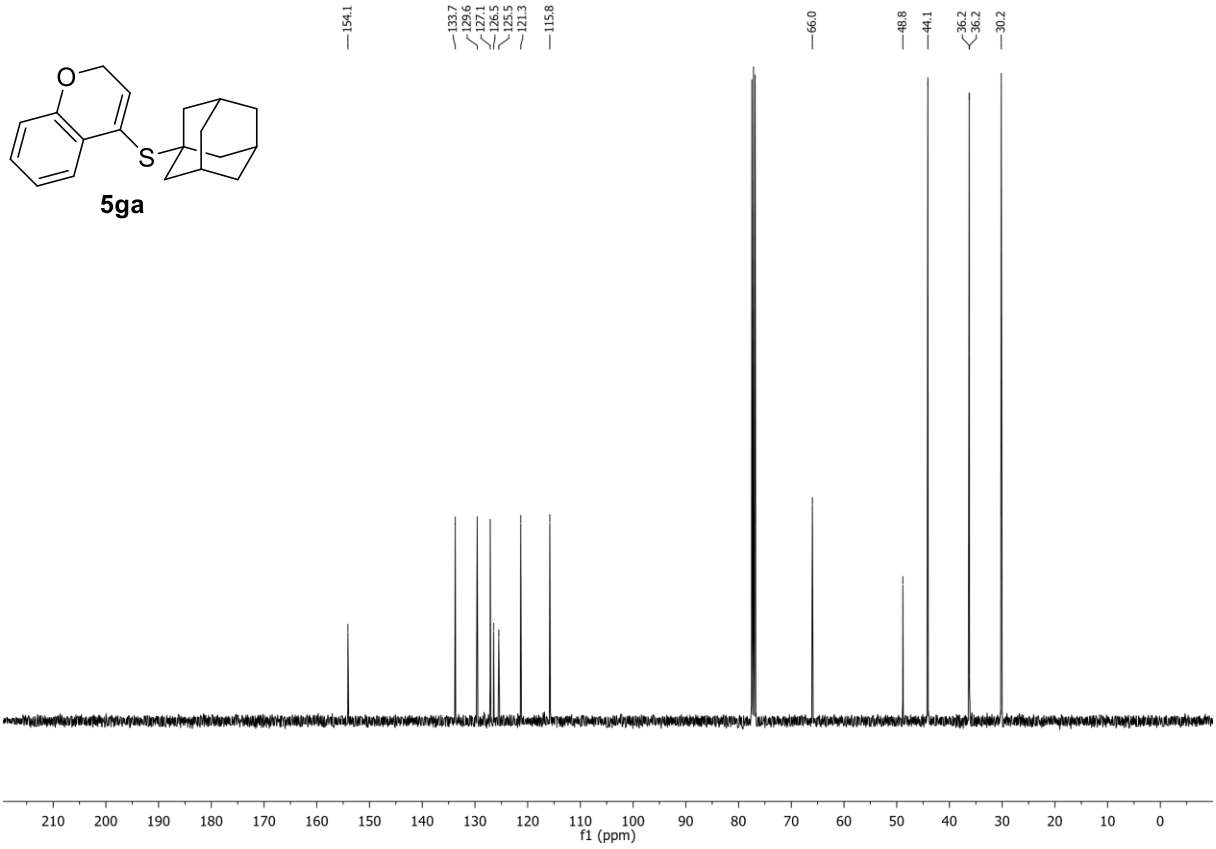

5ga

((3*s*,5*s*,7*s*)-Adamantan-1-yl)(1*H*-inden-3-yl)sulfane (5ha):

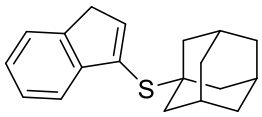

5ha

$C_{19}H_{22}S$ (282.45 g/mol)

Following **GP-C**, **5ha** was synthesized using 1*H*-inden-3-yl trifluoromethanesulfonate (264 mg, 1.00 mmol, 1.0 equiv.) and 1-adamantanethiol (185 mg, 1.10 mmol, 1.1 equiv.). Purification by FC (SiO_2, gradient to 95:5 *n*-hexane/EtOAc over 15 CV, then to 8:2 over 10 CV) afforded **5ha** (274 mg, 970 µmol, 97%) as colorless solid.

R_f: 0.55 (*n*-hexane/EtOAc 98:2).

m.p.: 79.6 – 80.5 °C.

^{1}H-NMR (400 MHz, $CDCl_3$, δ): 7.62 (d, *J* = 7.5 Hz, 1H), 7.46 (d, *J* = 7.3 Hz, 1H), 7.38 – 7.30 (m, 1H), 7.24 – 7.20 (m, 1H), 6.75 (t, *J* = 2.2 Hz, 1H), 3.50 (d, *J* = 2.2 Hz, 2H), 2.02 – 1.98 (m, 3H), 1.93 – 1.89 (m, 6H), 1.67 – 1.60 (m, 6H).

^{13}C-NMR (101 MHz, $CDCl_3$, δ): 146.9, 143.4, 143.0, 133.2, 126.5, 125.1, 123.7, 121.0, 48.6, 44.2, 38.8, 36.3, 30.2.

HR-MS (APCI): m/z calc. for $[M+H]^+$ 283.1515, found 283.1516.

IR (ATR, $\tilde{\nu}$ [cm^{-1}]): 2898 (m), 2846 (w), 1720 (w), 1657 (w), 1653 (w), 1582 (w), 1538 (w), 1448 (w), 1394 (w), 1318 (w), 1291 (w), 1265 (w), 1232 (w), 1198 (w), 1150 (w), 1098 (w), 1034 (w), 1012 (w), 975 (w), 949 (w), 911 (w), 885 (w), 821 (w), 755 (m), 710 (m), 688 (m).

^{1}H-NMR (400 MHz, $CDCl_3$) of compound **5ha**:

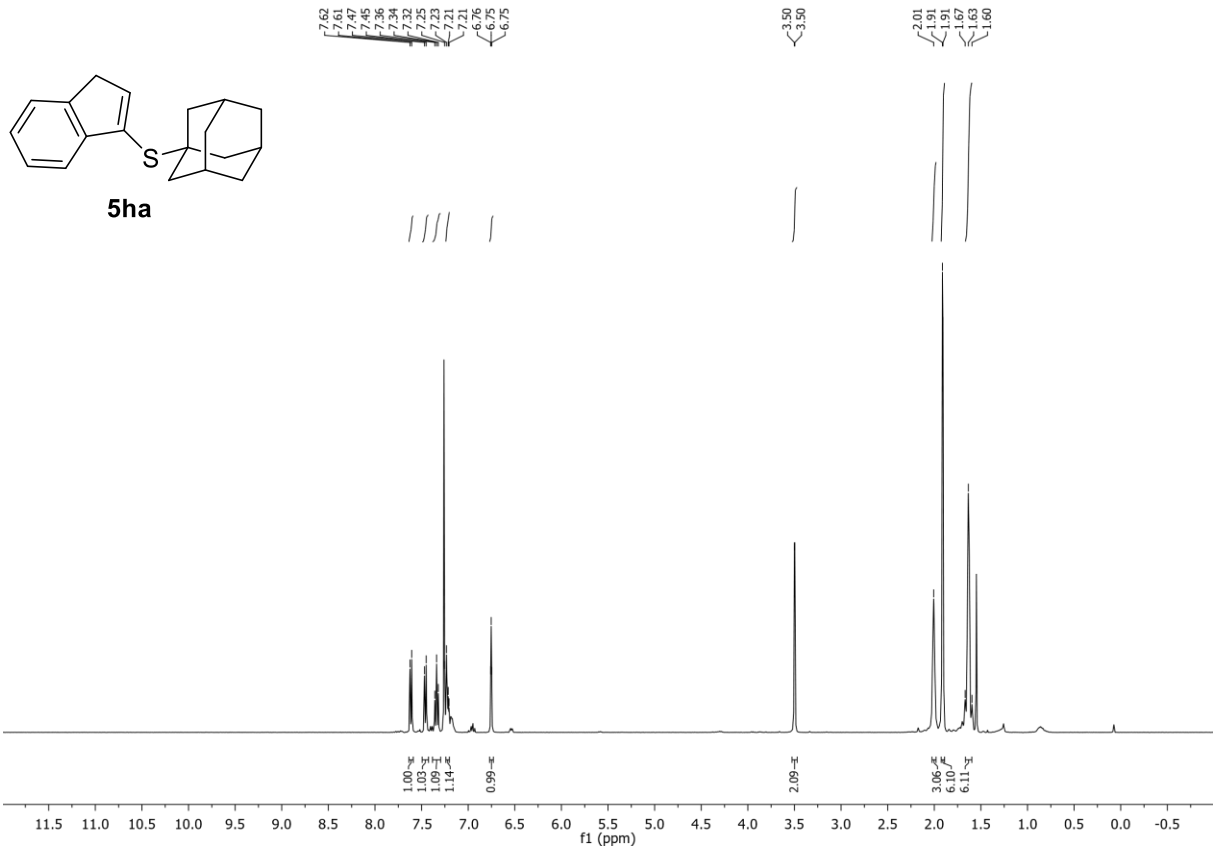

^{13}C-NMR (101 MHz, $CDCl_3$) of compound **5ha**:

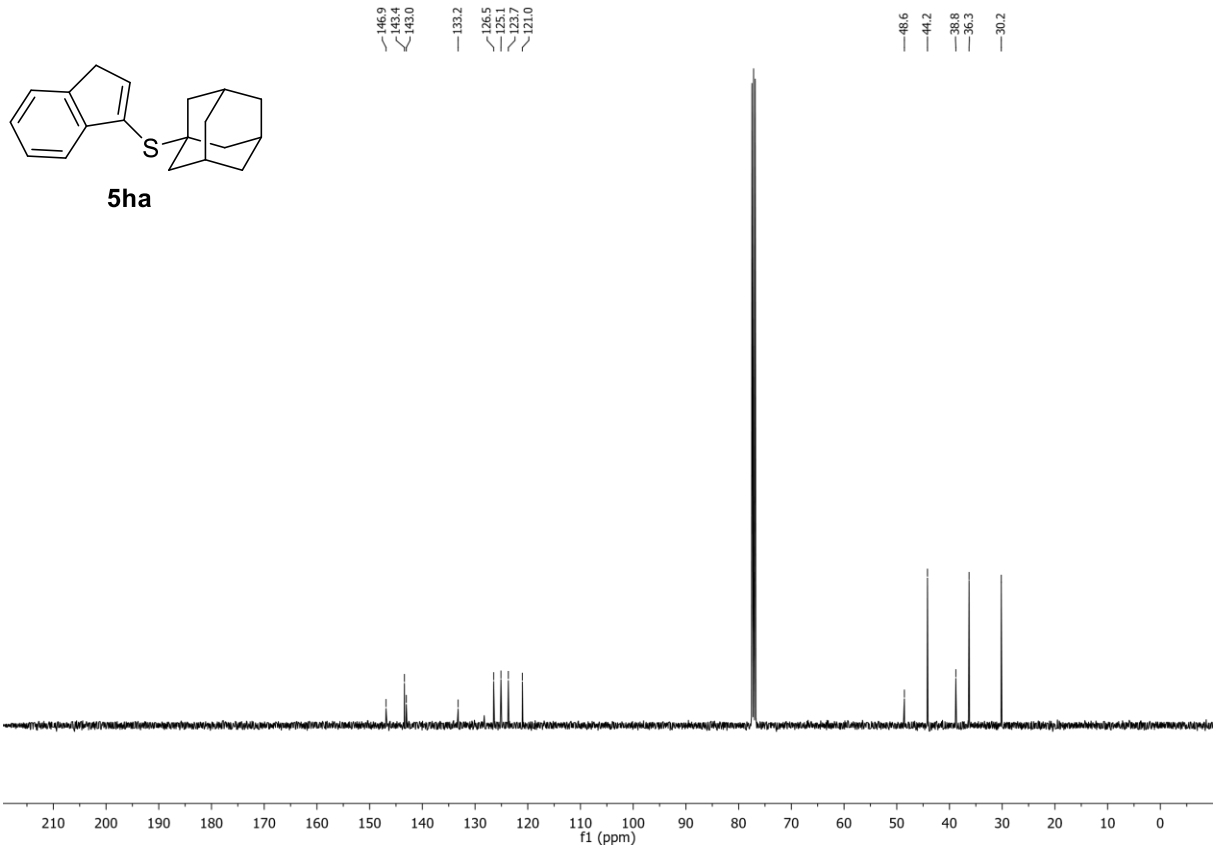

((3*s*,5*s*,7*s*)-Adamantan-1-yl)(cyclohex-1-en-1-yl)sulfane (5ia):

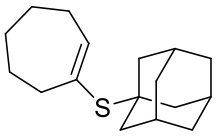

5ia

$C_{17}H_{26}S$ (262.46 g/mol)

Following **GP-C**, **5ia** was synthesized using cyclohept-1-en-1-yl trifluoromethanesulfonate (244 mg, 1.00 mmol, 1.0 equiv.) and 1-adamantanethiol (185 mg, 1.10 mmol, 1.1 equiv.). Purification by FC (SiO_2, 99:1 *n*-hexane/EtOAc for 20 CV, then gradient to 95:5 over 10 CV) afforded **5ia** (224 mg, 853 µmol, 85%) as colorless oil.

R_f: 0.82 (*n*-hexane/EtOAc 98:2).

^{1}H-NMR (400 MHz, $CDCl_3$, δ): 6.32 (t, *J* = 6.6 Hz, 1H), 2.55 – 2.51 (m, 2H), 2.21 – 2.13 (m, 2H), 2.04 – 2.00 (m, 3H), 1.86 – 1.84 (m, 6H), 1.76 – 1.64 (m, 8H), 1.60 – 1.50 (m, 4H).

^{13}C-NMR (101 MHz, $CDCl_3$, δ): 144.4, 135.1, 47.9, 44.2, 40.5, 36.5, 32.3, 30.2, 29.9, 26.7, 26.6.

HR-MS (APCI): m/z calc. for $[M+H]^+$ 263.1828, found 263.1826.

IR (ATR, $\tilde{\nu}$ [cm^{-1}]): 2902 (vs), 2846 (s), 1444 (s), 1343 (w), 1295 (m), 1258 (w), 1210 (w), 1101 (w), 1071 (w), 1038 (m), 969 (m), 930 (w), 889 (w), 852 (m), 811 (w), 754 (w), 687 (w).

^{1}H-NMR (400 MHz, $CDCl_3$) of compound **5ia**:

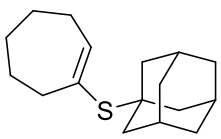

5ia

^{13}C-NMR (101 MHz, $CDCl_3$) of compound **5ia**:

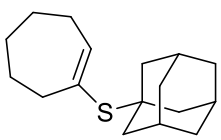

5ia

((3*s*,5*s*,7*s*)-Adamantan-1-yl)(1-phenylvinyl)sulfane (5ja):

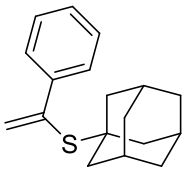

5ja

$C_{18}H_{22}S$ (270.43 g/mol)

Following **GP-C**, **5ja** was synthesized using 1-phenylvinyl trifluoromethanesulfonate (252 mg, 1.00 mmol, 1.0 equiv.) and 1-adamantanethiol (185 mg, 1.10 mmol, 1.1 equiv.). Purification by FC (SiO_2, *n*-hexane for 15 CV, then 99:1 *n*-hexane/EtOAc for 5 CV) afforded **5ja** (265 mg, 982 µmol, 98%) as colorless solid.

R_f: 0.41 (*n*-hexane).

m.p.: 52.3 – 54.6 °C.

^{1}H-NMR (400 MHz, $CDCl_3$, δ): 7.74 – 7.60 (m, 2H), 7.37 – 7.26 (m, 3H), 5.89 (s, 1H), 5.73 (s, 1H), 1.98 – 1.92 (m, 3H), 1.79 – 1.75 (m, 6H), 1.64 – 1.55 (m, 6H).

^{13}C-NMR (101 MHz, $CDCl_3$, δ): 142.7, 141.1, 128.1, 128.0, 127.5, 125.4, 48.5, 44.1, 36.3, 30.2, 30.1.

HR-MS (APCI): m/z calc. for $[M+H]^+$ 271.1515, found 271.1515.

IR (ATR, $\tilde{\nu}$ [cm^{-1}]): 2898 (s), 2846 (m), 1866 (w), 1799 (w), 1747 (w), 1683 (w), 1570 (w), 1482 (w), 1441 (m), 1374 (w), 1340 (w), 1295 (m), 1254 (w), 1217 (w), 1184 (w), 1101 (w), 1035 (m), 968 (w), 930 (m), 822 (w), 769 (s), 706 (s), 684 (s).

^{1}H-NMR (400 MHz, $CDCl_3$) of compound **5ja**:

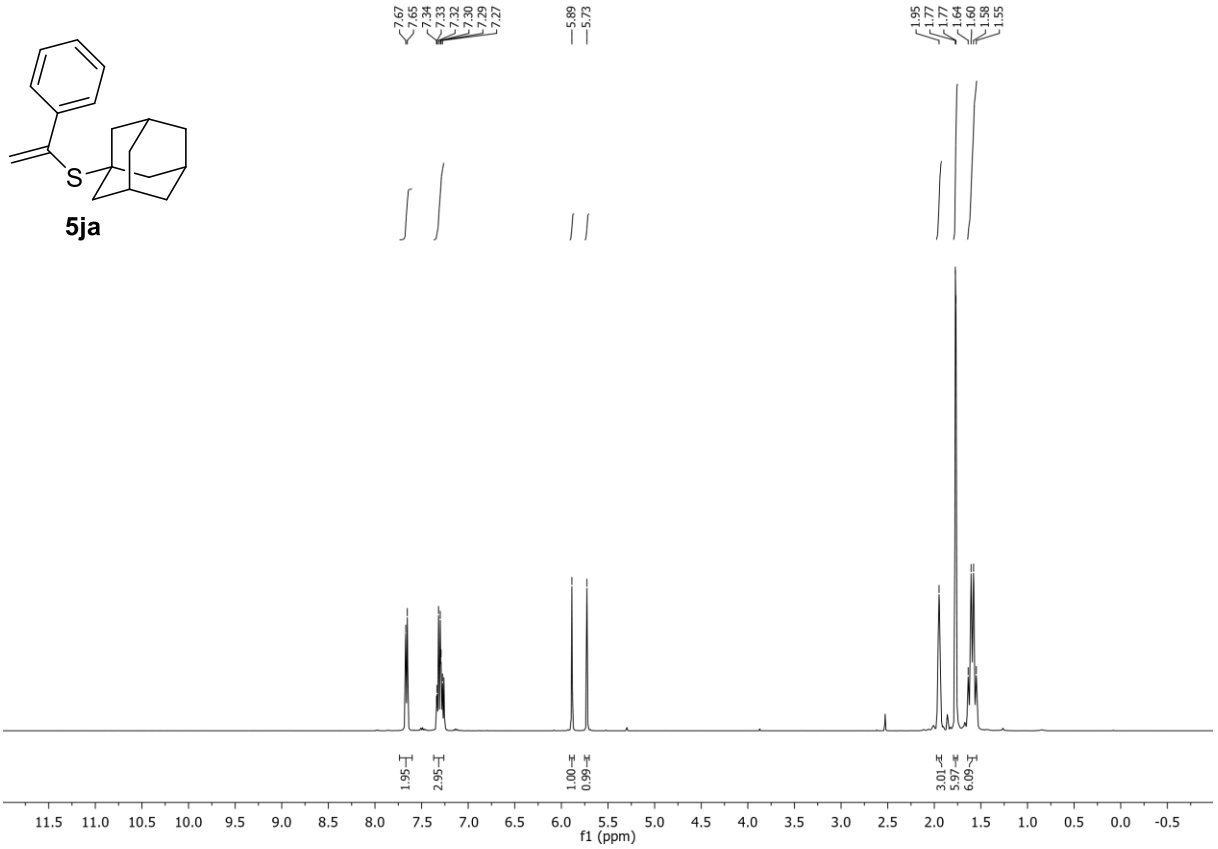

^{13}C-NMR (101 MHz, $CDCl_3$) of compound **5ja**:

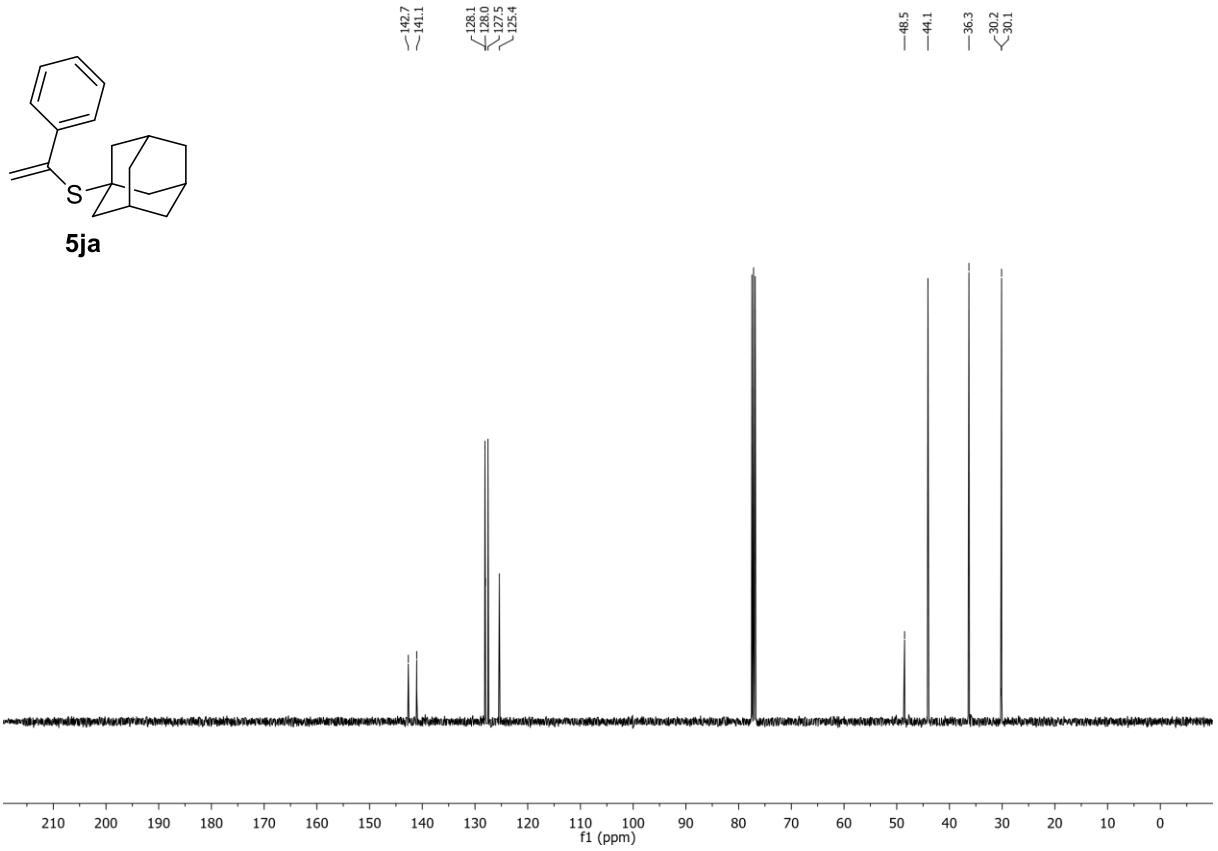

((1*s*,3*R*)-Adamantan-1-yl)((5*S*,8*R*,9*S*,10*S*,13*R*,14*S*,17*R*)-10,13-dimethyl-17-((*R*)-6-methylheptan-2-yl)-4,5,6,7,8,9,10,11,12,13,14,15,16,17-tetradecahydro-1*H*-cyclopenta[a]phenanthren-3-yl)sulfane (5ka):

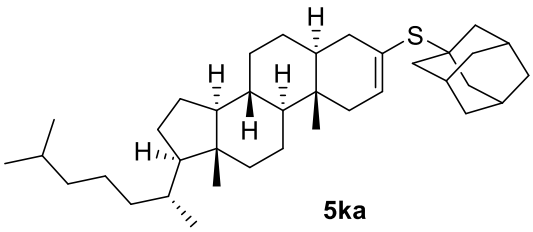

5ka

$C_{37}H_{60}S$ (536.95 g/mol)

Following **GP-C**, **5ka** was synthesized using 2-cholesten-3-yl trifluoromethanesulfonate (259 mg, 0.5 mmol, 1.0 equiv., mixture of regioisomers ca. 85:15) and 1-adamantanethiol (93 mg, 0.55 mmol, 1.1 equiv.). Purification by FC (SiO_2, *n*-hexane for 20 CV, then gradient to 8:2 *n*-hexane/EtOAc over 10 CV) afforded **5ka** (217 mg, 404 µmol, 81%, mixture of regioisomers according to starting material) as colorless solid.

R_f: 0.54 (*n*-hexane/EtOAc 99:1).

m.p.: 125.8 – 127.9 °C.

^{1}H-NMR (400 MHz, $CDCl_3$, δ): 6.05 – 5.69 (m, 1H), 2.32 – 1.90 (m, 8H), 1.87 – 1.75 (m, 8H), 1.68 – 1.63 (m, 6H), 1.60 – 0.93 (m, 22H), 0.90 (d, *J* = 6.4 Hz, 3H), 0.87 – 0.84 (m, 6H), 0.76 (s, 3H), 0.66 (s, 3H).

^{13}C-NMR (101 MHz, $CDCl_3$, δ): 143.7, 138.3, 127.5, 56.6, 56.4, 53.9, 53.2, 48.2, 47.8, 44.4, 42.92, 42.88, 42.6, 42.0, 40.6, 40.1, 39.7, 36.5, 36.3, 35.9, 35.7, 34.4, 33.8, 32.2, 31.9, 30.2, 28.6, 28.4, 28.2, 27.5, 24.4, 24.0, 23.0, 22.7, 21.4, 21.2, 18.8, 12.6, 12.31, 12.25, 12.1.

HR-MS (ESI): m/z calc. for $[M+Na]^+$ 559.4308, found 559.4310.

IR (ATR, $\tilde{\nu}$ [cm^{-1}]): 2902 (s), 2849 (m), 1448 (m), 1374 (w), 1340 (w), 1295 (w), 1250 (w), 1206 (w), 1172 (w), 1150 (w), 1101 (w), 1038 (w), 1001 (w), 969 (w), 956 (w), 930 (w), 889 (w), 806 (w), 770 (w), 732 (w), 684 (w).

^{1}H-NMR (400 MHz, $CDCl_3$) of compound **5ka**:

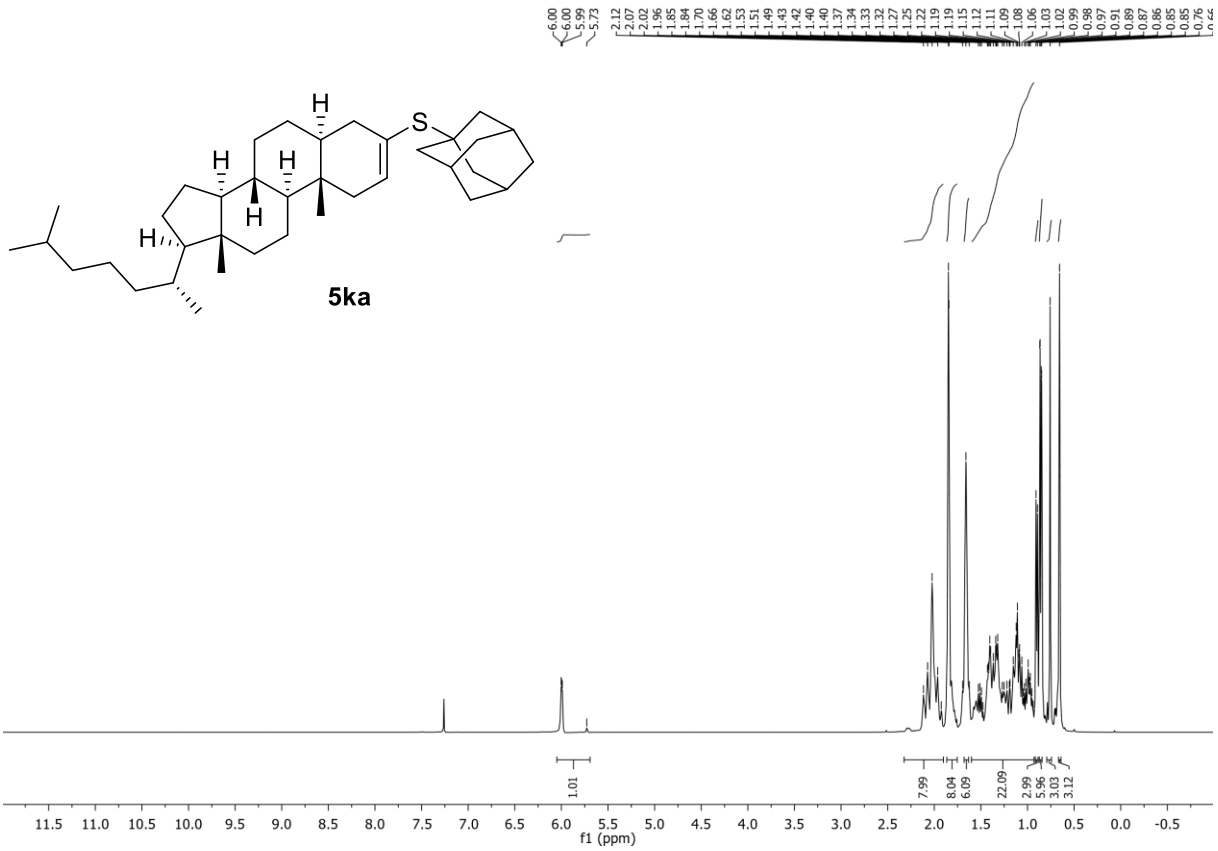

^{13}C-NMR (101 MHz, $CDCl_3$) of compound **5ka**:

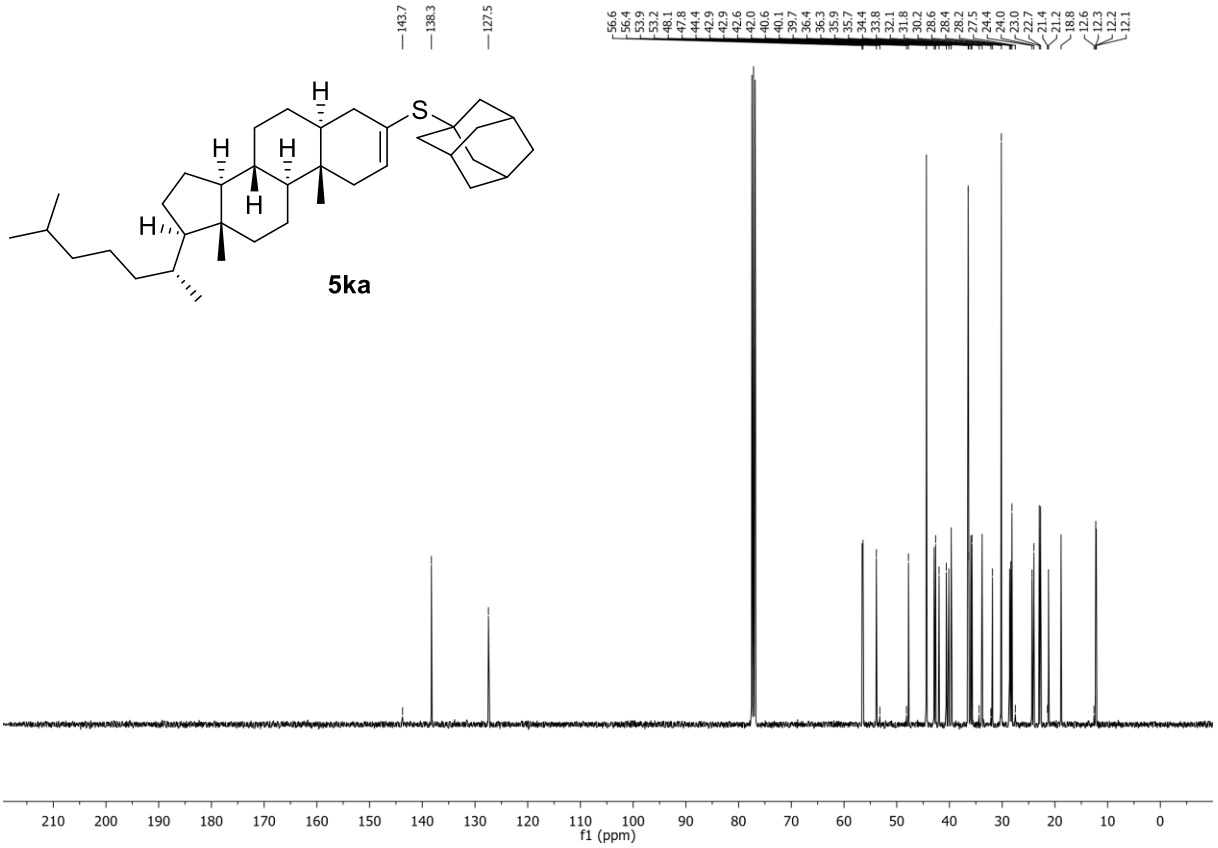

4. Kinetic experiments and GC-FID calibration

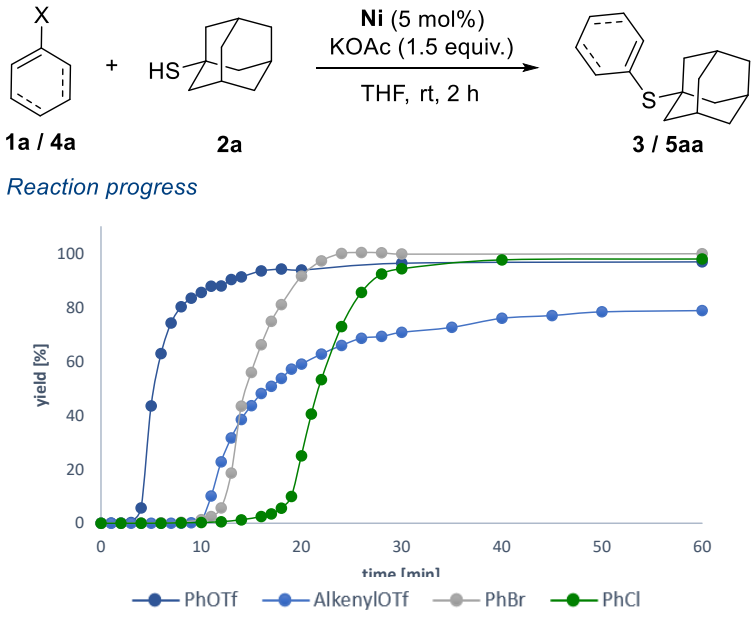

Figure S1: Kinetic analysis for the yield of **3aa/ 5aa** with a variety of electrophiles (PhOTf **1a**, AlkenylOTf **4a**, PhBr, PhCl).

The quantification of GC-yields was achieved by adding a standard compound (*n*-pentadecane) to reaction mixtures before quenching (usually 100 µL) and applying the general formula:

$$\frac{A(compound)}{A(standard)} = R \cdot \frac{m(compound)}{m(standard)}$$

R: Response factor of compound
A: Peak area determined by GC-FID
m: mass of compound

The R values were determined by GC calibrations of respective compounds with pentadecane in ethyl acetate and measuring different mass ratios.

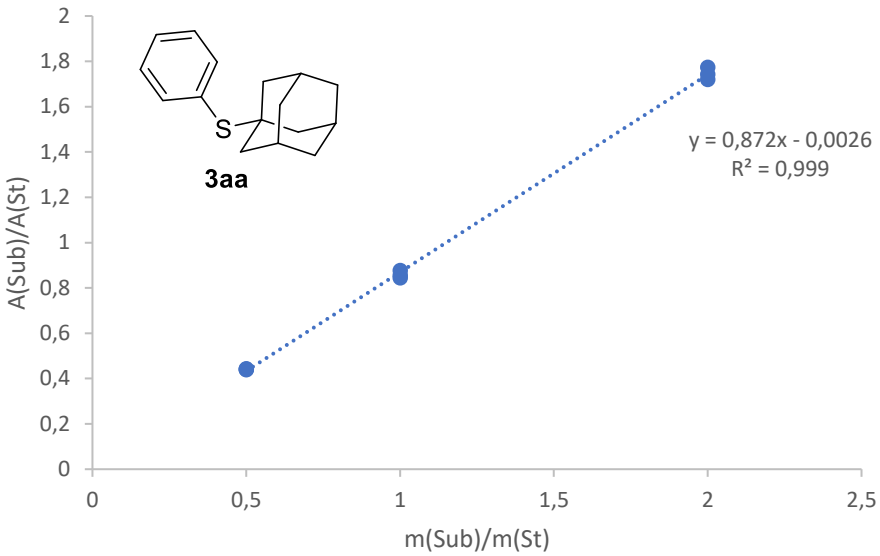

Mass ratio $\left[\frac{mg\ (Substrate)}{mg\ (Std)}\right]$	A (Substrate)	A (Std)	Area ratio $\left[\frac{A(Substrate)}{A\ (Std)}\right]$
0.50	10199.8	23172.0	0.44017
0.50	10364.2	23601.2	0.43913
0.50	9670.5	21866.0	0.44226
1.00	9733.8	11530.3	0.84419
1.00	10144.3	11858.2	0.85546
1.00	10757.7	12273.9	0.87647
2.00	19817.2	11370.5	1.74286
2.00	22510.6	13095.4	1.71897
2.00	21256.9	11988.2	1.77315

5. Unsuccessful Substrates/ low yields

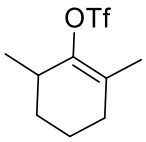

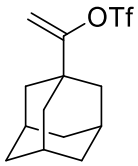

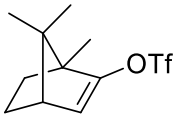

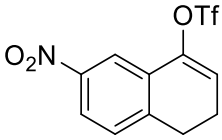

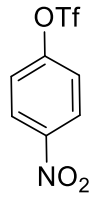

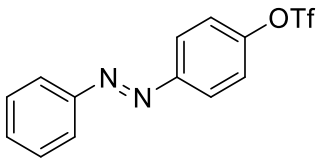

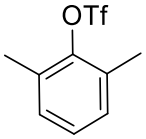

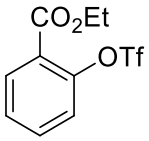

6. References

1. Gottlieb, H. E.; Kotlyar, V.; Nudelman, A., NMR chemical shifts of common laboratory solvents as trace impurities. *J. Org. Chem.* **1997**, *62*, 7512-7515.
2. Huang, Z.; Liu, Z.; Zhou, J., An Enantioselective, Intermolecular α-Arylation of Ester Enolates To Form Tertiary Stereocenters. *J. Am. Chem. Soc.* **2011**, *133*, 15882-15885.
3. Goossen, L. J.; Rodríguez, N.; Linder, C., Decarboxylative Biaryl Synthesis from Aromatic Carboxylates and Aryl Triflates. *J. Am. Chem. Soc.* **2008**, *130*, 15248-15249.
4. Olivares, A. M.; Weix, D. J., Multimetallic Ni- and Pd-Catalyzed Cross-Electrophile Coupling To Form Highly Substituted 1,3-Dienes. *J. Am. Chem. Soc.* **2018**, *140*, 2446-2449.
5. Martínez, A. G.; Herrera, A.; Martínez, R.; Teso, E.; García, A.; Osío, J.; Pargada, L.; Unanue, R.; Subramanian, L. R.; Hanack, M., A new and convenient synthesis of alkyl and aryl pyrimidines. *J. Heterocycl. Chem.* **1988**, *25*, 1237-1241.
6. Mc Murry, J. E.; Scott, W. J., A method for the regiospecific synthesis of enol triflates by enolate trapping. *Tetrahedron Lett.* **1983**, *24*, 979-982.
7. Oechsner, R. M.; Wagner, J. P.; Fleischer, I., Acetate Facilitated Nickel Catalyzed Coupling of Aryl Chlorides and Alkyl Thiols. *ACS Catal.* **2022**, 2233-2243.
8. Standley, E. A.; Smith, S. J.; Müller, P.; Jamison, T. F., A Broadly Applicable Strategy for Entry into Homogeneous Nickel(0) Catalysts from Air-Stable Nickel(II) Complexes. *Organometallics* **2014**, *33*, 2012-2018.
9. Seganish, W. M.; DeShong, P., Preparation and Palladium-Catalyzed Cross-Coupling of Aryl Triethylammonium Bis(catechol) Silicates with Aryl Triflates. *J. Org. Chem.* **2004**, *69*, 1137-1143.
10. Gill, D.; Hester, A. J.; Lloyd-Jones, G. C., On the preparation of ortho-trifluoromethyl phenyl triflate. *Org. Biomol. Chem.* **2004**, *2*, 2547-2548.
11. Mills, L. R.; Graham, J. M.; Patel, P.; Rousseaux, S. A. L., Ni-Catalyzed Reductive Cyanation of Aryl Halides and Phenol Derivatives via Transnitrilation. *J. Am. Chem. Soc.* **2019**, *141*, 19257-19262.
12. Maegawa, T.; Kitamura, Y.; Sako, S.; Udzu, T.; Sakurai, A.; Tanaka, A.; Kobayashi, Y.; Endo, K.; Bora, U.; Kurita, T.; Kozaki, A.; Monguchi, Y.; Sajiki, H., Heterogeneous Pd/C-Catalyzed Ligand-Free, Room-Temperature Suzuki–Miyaura Coupling Reactions in Aqueous Media. *Chem. Eur. J.* **2007**, *13*, 5937-5943.
13. Breed, D. R.; Thibault, R.; Xie, F.; Wang, Q.; Hawker, C. J.; Pine, D. J., Functionalization of Polymer Microspheres Using Click Chemistry. *Langmuir* **2009**, *25*, 4370-4376.
14. Smyth, L. A.; Phillips, E. M.; Chan, V. S.; Napolitano, J. G.; Henry, R.; Shekhar, S., Pd-Catalyzed Synthesis of Aryl and Heteroaryl Triflones from Reactions of Sodium Triflinate with Aryl (Heteroaryl) Triflates. *J. Org. Chem.* **2016**, *81*, 1285-1294.
15. Dogga, B.; Kumar, C. S. A.; Joseph, J. T., Palladium-Catalyzed Reductive Carbonylation of (Hetero) Aryl Halides and Triflates Using Cobalt Carbonyl as CO Source. *Eur. J. Org. Chem.* **2021**, *2021*, 309-313.
16. Cooper, P.; Crisenza, G. E. M.; Feron, L. J.; Bower, J. F., Iridium-Catalyzed α-Selective Arylation of Styrenes by Dual C−H Functionalization. *Angew. Chem. Int. Ed.* **2018**, *57*, 14198-14202.
17. Tang, P.; Furuya, T.; Ritter, T., Silver-Catalyzed Late-Stage Fluorination. *J. Am. Chem. Soc.* **2010**, *132*, 12150-12154.
18. Wu, D.-P.; He, Q.; Chen, D.-H.; Ye, J.-L.; Huang, P.-Q., A Stepwise Annulation for the Transformation of Cyclic Ketones to Fused 6 and 7-Membered Cyclic Enimines and Enones. *Chinese J. Chem.* **2019**, *37*, 315-322.
19. Lou, T. S.-B.; Bagley, S. W.; Willis, M. C., Cyclic Alkenylsulfonyl Fluorides: Palladium-Catalyzed Synthesis and Functionalization of Compact Multifunctional Reagents. *Angew. Chem. Int. Ed.* **2019**, *58*, 18859-18863.
20. Wurzer, N.; Klimczak, U.; Babl, T.; Fischer, S.; Angnes, R. A.; Kreutzer, D.; Pattanaik, A.; Rehbein, J.; Reiser, O., Heck-Type Coupling of Fused Bicyclic Vinylcyclopropanes: Synthesis of 1,2-Dihydropyridines, 2,3-Dihydro-1H-azepines, 1,4-Cyclohexadienes, and 2H-Pyrans. *ACS Catal.* **2021,** *11*, 12019-12028.

21. Liu, Y.; Lin, S.; Zhang, D.; Song, B.; Jin, Y.; Hao, E.; Shi, L., Photochemical Nozaki–Hiyama–Kishi Coupling Enabled by Excited Hantzsch Ester. *Org. Lett.* **2022**, *24*, 3331-3336.
22. Zhang, S.; Neumann, H.; Beller, M., Pd-Catalyzed Carbonylation of Vinyl Triflates To Afford α,β-Unsaturated Aldehydes, Esters, and Amides under Mild Conditions. *Org. Lett.* **2019**, *21*, 3528-3532.
23. Mahecha-Mahecha, C.; Lecornué, F.; Akinari, S.; Charote, T.; Gamba-Sánchez, D.; Ohwada, T.; Thibaudeau, S., Sequential Suzuki–Miyaura Coupling/Lewis Acid-Catalyzed Cyclization: An Entry to Functionalized Cycloalkane-Fused Naphthalenes. *Org. Lett.* **2020**, *22*, 6267-6271.
24. Cho, S.; McLaren, E. J.; Wang, Q., Three-Component Difunctionalization of Cyclohexenyl Triflates: Direct Access to Versatile Cyclohexenes via Cyclohexynes. *Angew. Chem. Int. Ed.* **2021**, *60*, 26332-26336.
25. Oechsner, R. M.; Wagner, J. P.; Fleischer, I., Acetate Facilitated Nickel Catalyzed Coupling of Aryl Chlorides and Alkyl Thiols. *ACS Catal.* **2022**, *12*, 2233-2243.
26. Jouffroy, M.; Kelly, C. B.; Molander, G. A., Thioetherification via Photoredox/Nickel Dual Catalysis. *Org. Lett.* **2016**, *18*, 876-879.
27. Delcaillau, T.; Bismuto, A.; Lian, Z.; Morandi, B., Nickel-Catalyzed Inter- and Intramolecular Aryl Thioether Metathesis by Reversible Arylation. *Angew. Chem. Int. Ed.* **2020**, *59*, 2110-2114.
28. Gehrtz, P. H.; Geiger, V.; Schmidt, T.; Sršan, L.; Fleischer, I., Cross-Coupling of Chloro(hetero)arenes with Thiolates Employing a Ni(0)-Precatalyst. *Org. Lett.* **2019**, *21*, 50-55.
29. Tkachenko, B. A.; Fokina, N. A.; Chernish, L. V.; Dahl, J. E. P.; Liu, S.; Carlson, R. M. K.; Fokin, A. A.; Schreiner, P. R., Functionalized Nanodiamonds Part 3: Thiolation of Tertiary/Bridgehead Alcohols. *Org. Lett.* **2006**, *8*, 1767-1770.
30. Zhou, J.-Y.; Zhu, Y.-M., Forging C−S(Se) Bonds by Nickel-catalyzed Decarbonylation of Carboxylic Acid and Cleavage of Aryl Dichalcogenides. *Eur. J. Org. Chem.* **2021**, *2021*, 2452-2461.
31. Lian, Z.; Bhawal, B. N.; Yu, P.; Morandi, B., Palladium-catalyzed carbon-sulfur or carbon-phosphorus bond metathesis by reversible arylation. *Science* **2017**, *356*, 1059-1063.

ACS Catalysis

pubs.acs.org/acscatalysis Letter

Flipping the Switch on Palladium-Catalyzed Carboiodination: Accessing Kinetic and Thermodynamic Products

Ramon Arora, Regina M. Oechsner, Clara Jans, Bijan Mirabi, Austin D. Marchese, and Mark Lautens*

Cite This: ACS Catal. 2023, 13, 6562−6567 Read Online

ACCESS | Metrics & More | Article Recommendations | Supporting Information

ABSTRACT: A palladium-catalyzed epimerization reaction of stereogenic alkyl iodides is reported. This transformation involves use of an air-stable precatalyst that efficiently epimerizes the C−I bond from the *exo* to the *endo* face of [2.2.1] bicyclic compounds. Mechanistic experiments support the stereoinversion of the C−I bond via reversible bond formation to generate the antiproduct bearing an *endo* iodide. Density functional theory studies were conducted to support a thermodynamically driven epimerization. Stoichiometric experiments suggested that irradiation of isolable alkyl−Pd(II) complexes promoted the C−I reductive elimination, which could even be applied to C−Br bond formation.

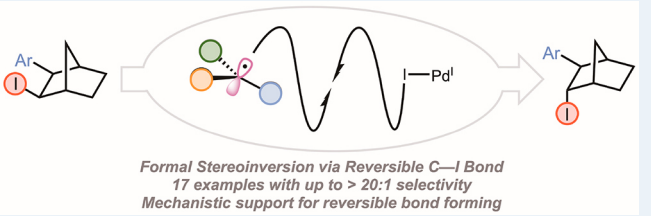

KEYWORDS: *palladium, blue lights, photoredox, epimerization, stereochemical editing*

Accessing all possible stereoisomers through common intermediates is an attractive approach in synthesis, as the physical and biological properties of each epimer may differ.[1−3] Typically, stereocenters are installed with the desired relative and absolute configuration at an early stage in a synthesis.[4,5] Consequently, accessing other stereoisomers may require restarting the synthetic sequence and modifying reagents or catalysts. Recently, the idea of accessing different diastereomers via stereochemical editing of a single stereocenter has been considered an attractive alternative.[6,7] Late-stage modification of select stereocenters has many advantages if high selectivity can be achieved.[8−11] The presence of reactive hydrogen atoms at the stereocenter of interest aids in the process, but also limits the scope of this strategy.

MacMillan and Wendlandt showcased the epimerization of a single carbon center through the in situ generation of a prochiral carbon-centered radical (Scheme 1A).[12−15] Most commonly, the thermodynamically favored product is formed. To date these methodologies typically involve C−H abstraction/recombination sequences, and thus exploiting this idea on a wider array of functionalized carbons was our objective. Our interest in the carbohalogenation reaction led us to focus on the epimerization of a class of rigid systems bearing carbon−halogen bonds.[16]

Molecules with C−X bonds are widely used electrophiles in organic synthesis, though their installation in a stereoselective manner remains nontrivial. Over the past decade, we devised numerous catalytic conditions for the carboiodination reaction, which represents a unique method to install C−I bonds.[17−23] Recently, we disclosed a Pd/blue-light-catalyzed carboiodination reaction to form 1° alkyl iodide bonds (Scheme 1B).[24] Notably, under photoirradiation, we found the C−I bond formation step to be reversible through a one-electron process. To capitalize on this mechanistic discovery, we hypothesized that this catalyst system may be sufficient to epimerize chiral C−I bonds and serve as a method for stereochemical editing of stereogenic C−X bonds (Scheme 1C).

In 2011, we reported an intermolecular carboiodination reaction that generated 1,2-disubstituted aryl-iodo-norbornanes.[25] This reaction required the use of high temperatures and expensive, air-sensitive ligands. We focused on the norbornyl scaffold as it provides a simple model system to study stereochemical editing, arising from sterically differentiated *exo* and *endo* faces. The classical thermal Pd-catalyzed carboiodination reaction yields the *syn* addition product in a stereospecific manner, wherein the migratory insertion occurs on the sterically more accessible *exo* face of norbornene (Scheme 1D). After forging the C−C bond, we speculated that the *exo* face would become more sterically crowded in the product. A catalytic system promoting reversible one-electron C−I bond abstraction/formation would enable the successful "editing" of the C−I stereocenter. The goal was to form the *endo* isomer via a thermodynamically driven stereoinvertive reductive elimination.

Literature examples of the addition of perfluoroalkyl iodides with a radical initiator yield the *anti* carboiodination product, lending support for our proposal.[26] Reversible C−I bond formation using a Pd/blue light approach would allow for the

Received: March 8, 2023
Revised: April 24, 2023

https://doi.org/10.1021/acscatal.3c01055
ACS Catal. 2023, 13, 6562−6567

Scheme 1. Precedented Work on Carbon Epimerization and Proposed Work

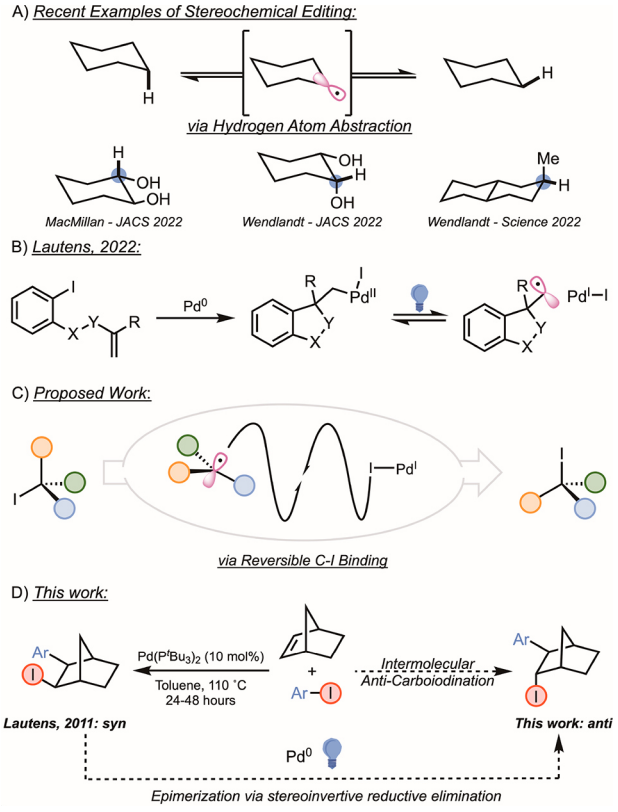

selective stereochemical epimerization of the *syn* iodides generated from the thermal Pd-carboiodination reaction to the *anti*-products. We explored the potential intermediacy of a Pd(I)/radical pair. Our results shed light on this radical pair by harnessing the blue light facilitated bond homolysis to epimerize C−I bonds via a formal stereoinvertive reductive elimination. This study showcases the effectiveness of this method with a prototypical scaffold for highly stereoselective epimerization with mild conditions and the use of cheap and air-stable palladium precatalyst.

We began by exploring a Pd/blue light-facilitated epimerization reaction utilizing *syn* carboiodinated products obtained from a thermal Pd-carboiodination reaction to the corresponding *anti* product under conditions with Pd/blue light. Following optimization, we discovered that 12.5 mol % of $Pd(OAc)_2$ and 1,5-bis(diphenylphosphino)pentane (DPPPent) in toluene with blue light irradiation for 24 h was optimal to epimerize the *exo* iodide to the *endo* iodide to yield product **3a** in 83% yield with >20:1 stereoselectivity (Table 1). The conditions we previously employed for Pd/blue light carboiodination worked, however in lower yield.[24] When the reaction was run with no light at 100 °C, we observed slight epimerization, in line with the thermal Pd-catalyzed carboiodination reactions reported by Tong in 2011.[27] Moreover, when subjecting the *syn* carboiodination product bearing an iodide on the *exo* face to UV light, which is well-established to induce C−I bond homolysis, we observed complete decomposition.[28] With the optimized conditions in hand, we explored the generality of this transformation (Scheme 2).

The reaction occurred with an iodo-indole scaffold, generating the epimerized product **3b** in excellent yield and

Table 1. Optimization of Conditions

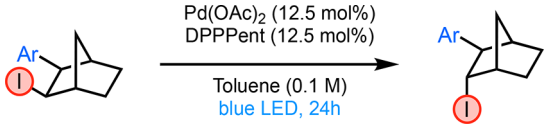

Entry	Deviation from Standard Conditions	% Yield[a]	endo/exo
1	10 mol % $Pd(OAc)_2$ and DPPPent	81	10:1
2	Adding 2.0 equiv of K_2CO_3	80	>20:1
3	10 mol % $Pd(PPh_3)_4$	38	1:1
4	10 mol % $Pd(PPh_3)_4$ w/2.0 equiv of K_2CO_3	80	8:1
5	3.75 mol % $[Pd(allyl)Cl]_2$ w/15% DPEPhos	25	1:2
6	10% $Pd(P^tBu_3)_2$	10	1:6
7	No light, 100 °C	18	1:3
8	270 nm light, no catalyst + ligand	0	-

[a]Yields are of the major diastereomer. Yields were determined by ^1H NMR analysis of the crude reaction mixture with 1,3,5-trimethoxybenzene as an internal standard. All reactions were run on 0.1 mmol scale.

>20:1 selectivity. The reaction tolerated various substituents on the aromatic ring, ranging from *p*-Me, *p*-OMe, *m*-F, *m*-CN, to give high yields and selectivity for the *endo* iodide (**3c**−**3f**). We tested the reaction with traditionally difficult functionalities in palladium catalysis and found equally good results. Substrates bearing aryl groups containing *p*-nitro-, *p*-OTBS, and lewis basic groups, such as free phenols, all underwent epimerization in excellent yields and high selectivity (**3g**−**3i**). This outcome suggested that stereoelectronic effects on the aryl system did not interfere with coordination of the arene to the norbornyl−Pd(II) species that was observed in a previous report in 2011.[29] The reaction was also amenable to substrates containing other halogens, generating good to excellent yields for the corresponding iodo-, bromo-, and chloro- groups (**3j**−**3l**). The reaction displays some steric constraints with substrates substituted at the *ortho* position. For example, an *o*-Me (**3m**) gave diminished yield and selectivity, while an *o*-^{i}Pr gave no epimerized product. This inhibition of product formation suggests that the increased steric hindrance inhibited an oxidative addition step into the crowded alkyl−iodide bond. This inhibition was also observed in the presence of naphthyl rings, which yielded the desired epimerized product in 64% yield and 10:1 stereoselectivity (**3n**).

To further probe steric effects, we prepared substrates stemming from an alkynyl iodination, developed by Tong in 2011.[27] The reduced size of the alkyne, when compared to substituted arenes, was predicted to reduce the *endo*/*exo* ratio based on lessened steric effects. Indeed, when subjected to our reaction conditions, products **3o**−**3q** were synthesized in good yields and moderate stereoselectivities.

To study the efficacy of a one-pot procedure to access *anti* carboiodinated products, we subjected iodobenzene (0.1 mmol) and norbornene (4.0 equiv) under similar conditions, and obtained product **3a** in 40% yield. Analogously, compounds **3c** and **3f** were also synthesized in moderated yields. Although this reaction demonstrates its applicability in a one pot-transformation, limitations arise with highly substituted aryl rings, where virtually no product can be observed. This outcome is complementary to our previous thermal carboiodination reaction,[25] as it serves a broader class of aryl rings, where visible light mediation can then facilitate the epimerization.

https://doi.org/10.1021/acscatal.3c01055
ACS Catal. 2023, 13, 6562−6567

Scheme 2. Substrate Scope of Epimerization[a]

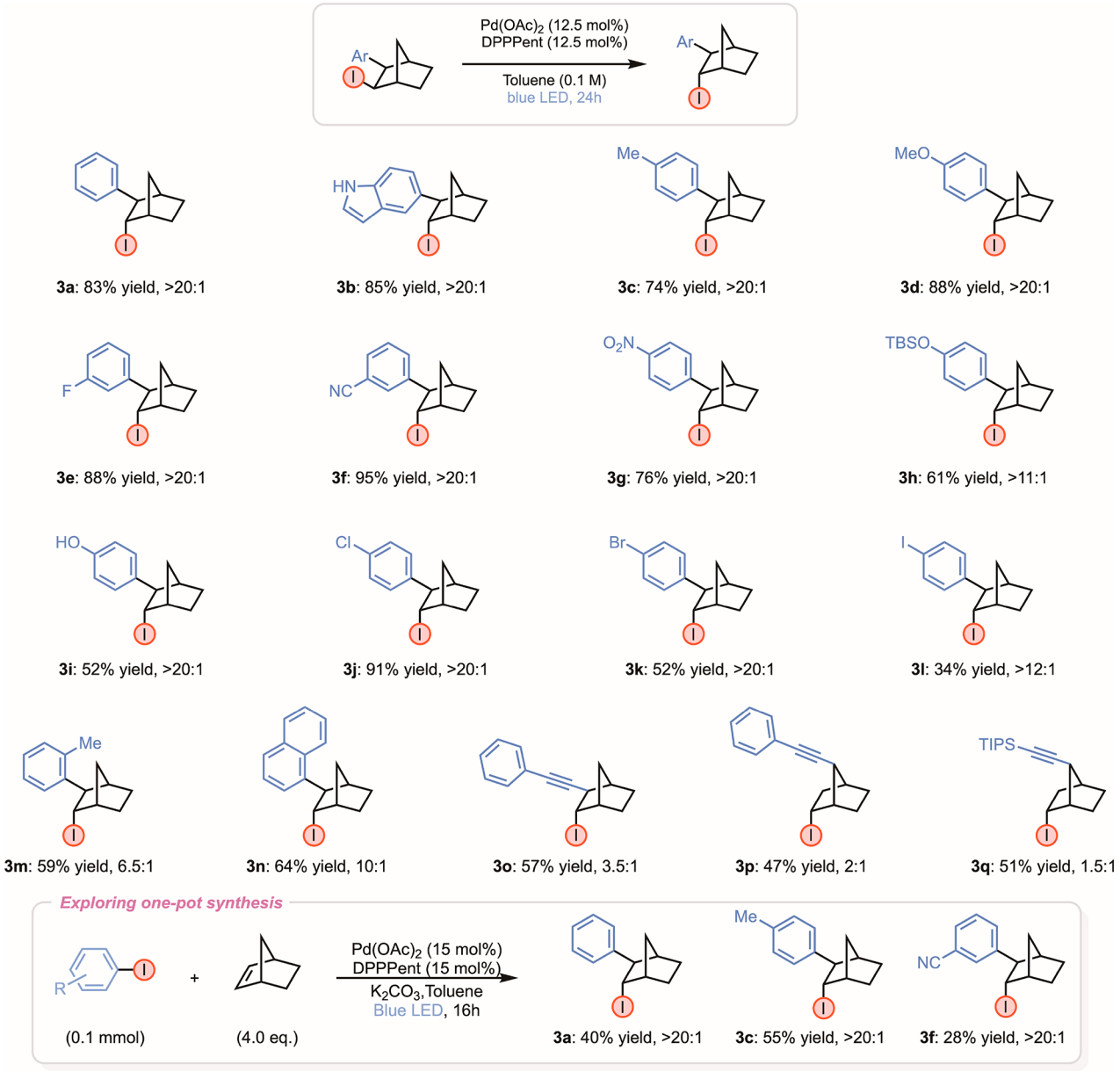

[a]All reactions were run on 0.1 mmol scale unless indicated otherwise in SI. All yields are isolated and are of the major diastereomer.

The next objective was to explore the reversibility of the C−I bond formation. The epimerization could follow two possible pathways (Scheme 3A). The first is through a traditional two-electron oxidative addition into the alkyl−iodide bond (**Path A**). The resulting complex could undergo a blue-light-mediated bond homolysis to generate the corresponding radical pair, ablating the stereochemical information (**int-B**). An identical intermediate can also be generated through a nonclassical mechanism that involves the excitation of the palladium catalyst with blue light (**Path B**). A subsequent one-electron oxidative addition would abstract the halide from the substrate to generate the same radical pair (**int-B**). At this point, **int-B** can either form the desired product via a direct halide abstraction from the Pd^{I}−I species to regenerate Pd^{0} (**Path C**), or it could recombine with the palladium catalyst to form the *endo* oxidative addition complex (**Path D**). Although a two-electron reductive elimination from **int-C** would provide the desired product, it seems unlikely, since neither PPh_3 nor DPPPent has been shown to enable the two-electron reductive elimination of the C−I bond.[25] Furthermore, we believe that **int-C** could lead to **4c**, which was observed in the crude reaction mixture, arising from *β*-hydride elimination. As a result, **int-C** is proposed to be in equilibrium with **int-B**, where product formation would still follow **Path C**.

Palladium complexes **I** and **II** bearing PPh_3 were synthesized according to a modified literature procedure (Scheme 3B,C).[29] These were isolated as the *syn* isomer, the diastereomer which arises from the thermal Pd-catalyzed reactions, which proceed via an oxidative addition followed by migratory insertion across the *exo* face of norbornene. Upon heating **I** at 100 °C in the absence of blue light, complete decomposition of the complex was observed, with no product being observed. Conversely, irradiation under blue light for 1 h provided the desired product in 39% yield. No change was observed after 16 h

https://doi.org/10.1021/acscatal.3c01055
ACS Catal. 2023, 13, 6562−6567

Scheme 3. Mechanistic Studies

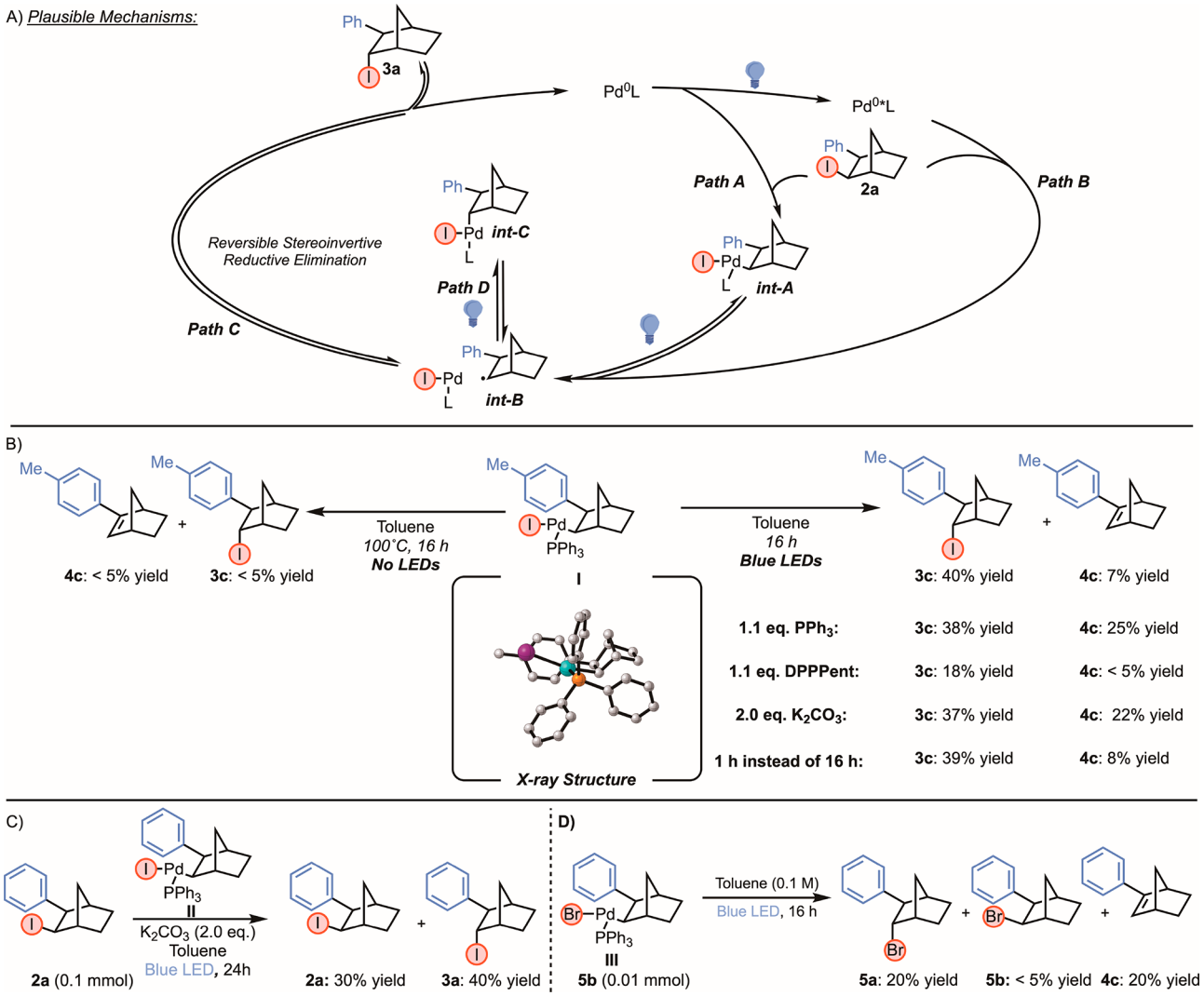

compared to 1 h. The efficiency of the stoichiometric reactions are identical to the catalytic reaction using $Pd(PPh_3)_4$, which gave the *endo* product in 38% yield (Table 1, entry 3). Other modifications to the reaction conditions were attempted, but no change in yield was observed (See Supporting Information for details). Complex **II** proved to be catalytically active in this reaction, which supports a reductive elimination with C−I bond formation and regeneration of a Pd (0) species (Scheme 3 C). Upon addition of 12.5 mol % of the complex to the starting material, the desired product was formed in 40% yield after 24 h.

To date, photoinduced $C(sp^3)$−X reductive elimination from alkyl−Pd(II) complexes has been limited to $C(sp^3)$−I bonds. To build on our previous work[24] as well as related studies from the Arndtsen group,[30,31] we explored the potential for a photoinduced reductive elimination of other C−X bonds, namely, $C(sp^3)$−Br. Complex **III** was prepared by a modified procedure and subjected to the reaction conditions (See Supporting Information for details). The corresponding brominated product was formed in 20% yield (Scheme 3D). Further studies are required to optimize the more challenging $C(sp^3)$−Br reductive elimination,[32−35] but this result suggests a visible-light-mediated palladium carbobromination reaction may be possible.

On/off experiments were conducted to determine if the reaction occurred through a chain propagation mechanism (Scheme 4A). This reaction was studied over the course of 6 h where photoirradiation occurred at 1 h intervals. It was evident that the reaction did not proceed in the absence of light, which indicates a chain propagation mechanism is unlikely. Blue light is required for bond homolysis/excitation of the palladium complex which enables the C−I bond cleavage. A reaction was conducted with 1.1 equiv of 2,2,6,6-tetramethyl-1-piperidinyloxy (TEMPO), which led to complete inhibition of the reaction, further supporting a radical mechanism (Scheme 4b).

To further probe the thermodynamic preference of the *endo isomer*, *exo*-iodide **2a** was subjected to traditional halogen atom transfer (XAT) conditions in the presence of acrylonitrile.[36] Addition occurred exclusively on the *endo* face, as might be anticipated based on steric effects. The origins for the selectivity were further confirmed by density functional theory (DFT) calculations at the SMD(toluene)/M06L/aug-cc-pvqz/sdd//wB97xd/6-311++g**/LANL2DZ level (Scheme 4C). The results indicated that the *endo* isomer of the products was thermodynamically favored, revealing that the *endo*-iodo isomer is favored by 1.7 kcal mol^{-1}. This effect is less pronounced when the norbornene is substituted with the smaller alkyne substituent, which showed a 1.5 kcal mol^{-1}

https://doi.org/10.1021/acscatal.3c01055
ACS Catal. 2023, 13, 6562−6567

Scheme 4. Experimental and Computational Studies

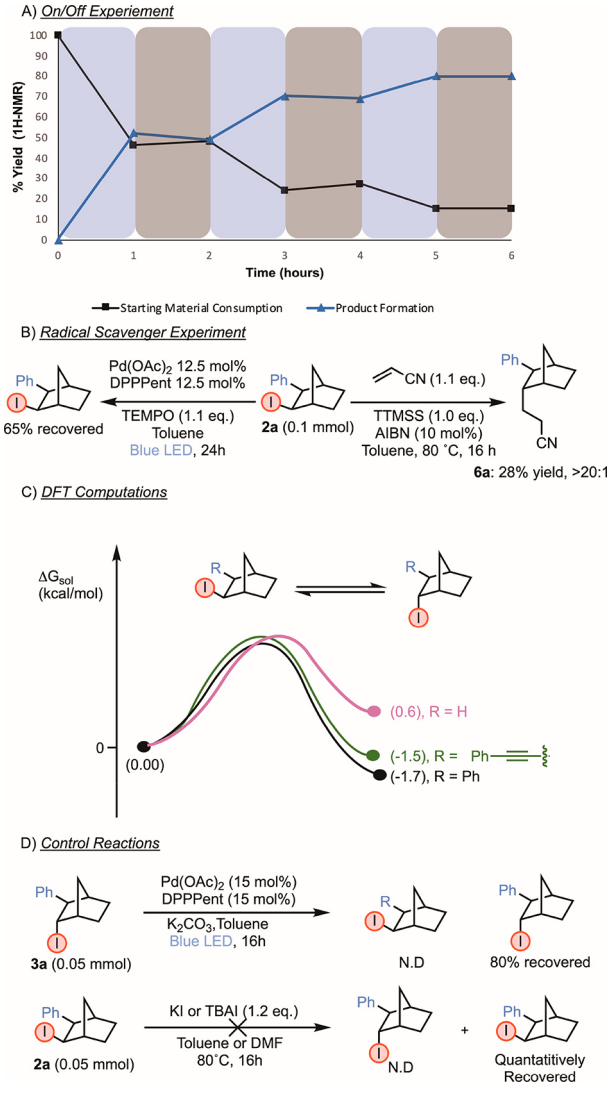

preference for the *endo* isomer.[37] These results are consistent with the experimental results, where the *endo* product was formed preferentially. The *exo*-iodonorbornane is more stable than the *endo* isomer in the absence of the aryl group. The steric hindrance of an aryl/alkynyl group on the *exo* face results in a thermodynamic preference to have the halogen on the *endo* face. Compound **3a** was resubjected to the catalytic conditions, but no epimerization was observed. Approximately 80% of **3a** was recovered. An S_N2-type pathway leading from *exo* to *endo* was also ruled out when the reaction was heated with exogenous iodide sources. The *exo* product was not observed under a variety of conditions, suggesting that this reaction occurs via a palladium blue light catalysis through a stereoinvertive reductive elimination.

In conclusion, we have identified a stereoselective epimerization in secondary aliphatic iodides via palladium/blue light catalysis. This transformation utilized an air-stable precatalyst that effectively epimerizes the C−I bond from the *exo* to the *endo* face of [2.2.1] bicyclic compounds. A variety of functionalized aryl moieties were tolerated. Mechanistic and computational studies suggested the epimerization favored the *endo* iodide, leading to a formal stereoinversion of the C−I bond via reversible bond formation. Studies involving the use of stoichiometric alkyl−Pd(II) complexes indicated the efficacy for this transformation and applicability to C−Br bond formation.

■ ASSOCIATED CONTENT

Supporting Information

The Supporting Information is available free of charge at https://pubs.acs.org/doi/10.1021/acscatal.3c01055.

Mechanistic Experiments and Characterization of all compounds (PDF)

Crystallographic data for ***Complex-I*** (CCDC 2235960) (CIF)

■ AUTHOR INFORMATION

Corresponding Author

Mark Lautens − *Davenport Research Laboratories, Department of Chemistry, University of Toronto, Toronto M5S 3H6 Ontario, Canada;* orcid.org/0000-0002-0179-2914; Email: mark.lautens@utoronto.ca

Authors

Ramon Arora − *Davenport Research Laboratories, Department of Chemistry, University of Toronto, Toronto M5S 3H6 Ontario, Canada;* orcid.org/0000-0003-4585-4328

Regina M. Oechsner − *Davenport Research Laboratories, Department of Chemistry, University of Toronto, Toronto M5S 3H6 Ontario, Canada*

Clara Jans − *Davenport Research Laboratories, Department of Chemistry, University of Toronto, Toronto M5S 3H6 Ontario, Canada*

Bijan Mirabi − *Davenport Research Laboratories, Department of Chemistry, University of Toronto, Toronto M5S 3H6 Ontario, Canada;* orcid.org/0000-0002-4852-3439

Austin D. Marchese − *Davenport Research Laboratories, Department of Chemistry, University of Toronto, Toronto M5S 3H6 Ontario, Canada;* orcid.org/0000-0002-3090-2748

Complete contact information is available at: https://pubs.acs.org/10.1021/acscatal.3c01055

Notes

The authors declare no competing financial interest.

■ ACKNOWLEDGMENTS

We thank the University of Toronto, the Natural Science and Engineering Research Council (NSERC), and Kennarshore Inc. for financial support. R.A. thanks OGS for a scholarship, A.D.M. thanks NSERC for an NSERC Vanier fellowship. B.M. thanks NSERC for a CGS-D scholarship. We thank Professor Fleischer for supporting a scientific exchange, and R.M.O. thanks the DAAD for a scholarship. C.J., A.G.D, and A.T. are thanked for insightful discussions. We thank Dr. Darcy Burns and Dr. Jack Sheng, University of Toronto, for their assistance with NMR experiments. We thank Dr. Ivan Franzoni and Bahman Mirabi for providing useful scripts that aided in the computational work. Computational support was provided in part by Compute Ontario (www.computeontario.ca) and Compute Canada (www.computecanada.ca). We thank Dr. Matt Forbes for the HRMS data. We thank Dr. Alan Lough for the X-ray data.

REFERENCES

(1) Eliel, E. L.; Wilen, S. H. *Stereochemistry of Organic Compounds;* Wiley, 1994.
(2) Gladysz, J.; Michl. *J.* Enantioselective Synthesis: Introduction. *Chem. Rev.* **1992**, *92* (5), 739−739.
(3) Xiang, S.-H.; Tan, B. Advances in Asymmetric Organocatalysis over the Last 10 Years. *Nat. Commun.* **2020**, *11*, 3786.
(4) Corey, E. J.; Cheng, X.-M. *The logic of chemical synthesis;* Wiley, 1989.
(5) Corey, E. J.; Kürti, L. *Enantioselective chemical synthesis: methods, logic and practice;* Direct Book Publishing, 2010.
(6) Wang, P.-Z.; Xiao, W.-J.; Chen, J.-R. Light Empowers Contra-thermodynamic Stereochemical Editing. *ChemRxiv* **2022**, DOI: 10.26434/chemrxiv-2022-g7sql.
(7) Tan, G.; Glorius, F. Stereochemical Editing. *Angew. Chem., Int. Ed.* **2023**, *62*
(8) Barton, L. M.; Edwards, J. T.; Johnson, E. C.; Bukowski, E. J.; Sausa, R. C.; Byrd, E. F. C.; Orlicki, J. A.; Sabatini, J. J.; Baran, P. S. Impact of Stereo- and Regiochemistry on Energetic Materials. *J. Am. Chem. Soc.* **2019**, *141*, 12531−12535.
(9) Macdougall, L. J.; Pérez-Madrigal, M. M.; Shaw, J. E.; Worch, J. C.; Sammon, C.; Richardson, S. M.; Dove, A. P. Using Stereochemistry to Control Mechanical Properties in Thiol-yne Click-hydrogels. *Angew. Chem., Int. Ed.* **2021**, *60* (49), 25856−25864.
(10) Worch, J. C.; Prydderch, H.; Jimaja, S.; Bexis, P.; Becker, M. L.; Dove, A. P. Stereochemical Enhancement of Polymer Properties. *Nat. Rev. Chem.* **2019**, *3* (9), 514−535.
(11) Walker, M. A. Improvement in aqueous solubility achieved via small molecular changes. *Bioorg. Med. Chem. Lett.* **2017**, *27* (23), 5100−5108.
(12) Zhang, Y.-A.; Palani, V.; Seim, A. E.; Wang, Y.; Wang, K. J.; Wendlandt, A. E. Stereochemical editing logic powered by the epimerization of unactivated tertiary stereocenters. *Science.* **2022**, *378* (6618), 383−390.
(13) Carder, H. M.; Wang, Y.; Wendlandt, A. E. Selective Axial-to-Equatorial Epimerization of Carbohydrates. *J. Am. Chem. Soc.* **2022**, *144* (26), 11870−11877.
(14) Zhang, Y.-A.; Gu, X.; Wendlandt, A. E. A Change from Kinetic to Thermodynamic Control Enables Trans-selective Stereochemical Editing of Vicinal Diols. *J. Am. Chem. Soc.* **2022**, *144* (1), 599−605.
(15) Oswood, C. J.; MacMillan, D. W. C. Selective Isomerization via Transient Thermodynamic Control: Dynamic Epimerization of trans to cis Diols. *J. Am. Chem. Soc.* **2022**, *144* (1), 93−98.
(16) Petrone, D. A.; Ye, J.; Lautens, M. Modern Transition-Metal-Catalyzed Carbon-Halogen Bond Formation. *Chem. Rev.* **2016**, *116* (14), 8003−8104.
(17) Marchese, A. D.; Adrianov, T.; Köllen, M. F.; Mirabi, B.; Lautens, M. Synthesis of Carbocyclic Compounds via a Nickel-Catalyzed Carboiodination Reaction. *ACS Catal.* **2021**, *11* (2), 925−931.
(18) Yoon, H.; Marchese, A. D.; Lautens, M. Carboiodination Catalyzed by Nickel. *J. Am. Chem. Soc.* **2018**, *140* (35), 10950−10954.
(19) Petrone, D. A.; Lischka, M.; Lautens, M. Harnessing Reversible Oxidative Addition: Application of Diiodinated Aromatic Compounds in the Carboiodination Process. *Angew. Chem., Int. Ed.* **2013**, *52* (40), 10635−10638.
(20) Marchese, A. D.; Kersting, L.; Lautens, M. Diastereoselective Nickel-Catalyzed Carboiodination Generating Six-Membered Nitrogen-Based Heterocycles. *Org. Lett.* **2019**, *21* (17), 7163−7168.
(21) Marchese, A. D.; Lind, F.; Mahon, Á. E.; Yoon, H.; Lautens, M. Forming Benzylic Iodides via a Nickel Catalyzed Diastereoselective Dearomative Carboiodination Reaction of Indoles. *Angew. Chem., Int. Ed.* **2019**, *58* (15), 5095−5099.
(22) Petrone, D. A.; Yoon, H.; Weinstabl, H.; Lautens, M. Additive Effects in the Palladium-Catalyzed Carboiodination of Chiral N-Allyl Carboxamides. *Angew. Chem., Int. Ed.* **2014**, *126* (30), 8042−8046.
(23) Petrone, D. A.; Malik, H. A.; Clemenceau, A.; Lautens, M. Functionalized Chromans and Isochromans via a Diastereoselective Pd(0)-Catalyzed Carboiodination. *Org. Lett.* **2012**, *14* (18), 4806−4809.
(24) Marchese, A. D.; Durant, A. G.; Reid, C. M.; Jans, C.; Arora, R.; Lautens, M. Pd(0)/Blue Light Promoted Carboiodination Reaction - Evidence for Reversible C-I Bond Formation via a Radical Pathway. *J. Am. Chem. Soc.* **2022**, *144* (45), 20554−20560.
(25) Newman, S. G.; Lautens, M. Palladium-Catalyzed Carboiodination of Alkenes: Carbon-Carbon Bond Formation with Retention of Reactive Functionality. *J. Am. Chem. Soc.* **2011**, *133* (6), 1778−1780.
(26) (a) Kirmse, W.; Wonner, A.; Allen, A. D.; Tidwell, T. T. Destabilized Carbocations: C2F5 Substituent Effects on Ground and Transition States in 2-Bicyclo[2.2.1]hepty 1 Brosylates. *J. Am. Chem. Soc.* **1992**, *114* (23), 8828. (b) Arceo, E.; Montroni, E.; Melchiorre, P. Photo-Organocatalysis of Atom-Transfer Radical Additions to Alkenes. *Angew. Chem., Int. Ed.* **2014**, *53* (45), 12064−12068. (c) Wallentin, C.-J.; Nguyen, J. D.; Finkbeiner, P.; Stephenson, C. R. J. Visible Light-Mediated Atom Transfer Radical Addition via Oxidative and Reductive Quenching of Photocatalysts. *J. Am. Chem. Soc.* **2012**, *134* (21), 8875−8884.
(27) Liu, H.; Chen, C.; Wang, L.; Tong, X. Pd(0)-Catalyzed Iodoalkynation of Norbornene Scaffolds: The Remarkable Solvent Effect on Reaction Pathway. *Org. Lett.* **2011**, *13* (19), 5072−5075.
(28) Clayden, J.; Warren, S. G.; Greeves, N. *Organic Chemistry,* 2nd ed.; Oxford University Press, 2012.
(29) Chai, D. I.; Thansandote, P.; Lautens, M. Mechanistic Studies of Pd-Catalyzed Regioselective Aryl C-H Bond Functionalization with Strained Alkenes: Origin of Regioselectivity. *Chem.-Eur. J.* **2011**, *17* (29), 8175−8188.
(30) Liu, Y.; Zhou, C.; Jiang, M.; Arndtsen, B. A. Versatile Palladium-Catalyzed Approach to Acyl Fluorides and Carbonylations by Combining Visible Light- and Ligand-Driven Operations. *J. Am. Chem. Soc.* **2022**, *144* (21), 9413−9420.
(31) Torres, G. M.; Liu, Y.; Arndtsen, B. A. A dual light-driven palladium catalyst: Breaking the barriers in carbonylation reactions. *Science.* **2020**, *368* (6488), 318−323.
(32) Roy, A. H.; Hartwig, J. F. Directly Observed Reductive Elimination of Aryl Halides from Monomeric Arylpalladium(II) Halide Complexes. *J. Am. Chem. Soc.* **2003**, *125* (46), 13944−13945.
(33) Roy, A. H.; Hartwig, J. F. Reductive Elimination of Aryl Halides from Palladium(II). *J. Am. Chem. Soc.* **2001**, *123* (6), 1232−1233.
(34) Chen, X.; Zhao, J.; Dong, M.; Yang, N.; Wang, J.; Zhang, Y.; Liu, K.; Tong, X. Pd(0)-Catalyzed Asymmetric Carbohalogenation: H-Bonding-Driven C(sp3)-Halogen Reductive Elimination under Mild Conditions. *J. Am. Chem. Soc.* **2021**, *143* (4), 1924.
(35) Lan, Y.; Liu, P.; Newman, S. G.; Lautens, M.; Houk, K. N. Theoretical study of Pd(0)-catalyzed carbohalogenation of alkenes: mechanism and origins of reactivities and selectivities in alkyl halide reductive elimination from Pd(II) species. *Chem. Sci.* **2012**, *3* (6), 1987−1995.
(36) Ballestri, M.; Chatgilialoglu, C.; Clark, K. B.; Griller, D.; Giese, B.; Kopping, B. Tris(trimethylsilyl)silane as a radical-based reducing agent in synthesis. *J. Org. Chem.* **1991**, *56* (2), 678.
(37) We note that an energy difference of 1.51 kcal mol^{-1} would suggest a product ratio of approximately 13:1 instead of the observed 3.5:1 (ΔG = −0.74 at T = 298.15 K). Given that small errors in Hartree can lead to large discrepancies in units of kcal mol^{-1}, we are using the computations to qualitatively describe the more favored isomer rather than quantitatively predict isomeric ratios.

https://doi.org/10.1021/acscatal.3c01055
ACS Catal. 2023, 13, 6562−6567

Supporting Information

Flipping the Switch on Palladium-Catalyzed Carboiodination: Accessing Kinetic and Thermodynamic Products

Ramon Arora, Regina M. Oechsner, Clara Jans, Bijan Mirabi, Austin Marchese, and Mark Lautens*.

Corresponding Authors:
*Prof. Mark Lautens. Email: mark.lautens@utoronto.ca Address: Davenport Research Laboratories, Department of Chemistry, University of Toronto, 80 St. George Street, Toronto, Ontario, Canada M5S 3H6

Author Affiliations:
Davenport Research Laboratories, Department of Chemistry, University of Toronto, 80 St. George Street, Toronto, Ontario, Canada M5S 3H6

Table of Contents

General Considerations

All reactions were performed in a dry environment under an inert atmosphere of argon unless otherwise stated. Reactions were monitored by thin layer chromatography (TLC) and visualized under UV light or by iodine staining. Flash column chromatography was performed with Silicycle 46- 60 µm silica gel. Catalytic reactions were performed in 2-dram vials equipped with a Teflon cap. THF was distilled over sodium/benzophenone. Toluene and DCM were distilled over CaH_2.

All reagents and organic building blocks were purchased from commercial suppliers (Sigma-Aldrich, Alfa Aesar, TCI, Combi-Blocks, Oakwood Chemical, AK Scientific) and used as received. NMR characterization data was collected at 296 K on a Varian Mercury 400 or an Agilent DD2 500 equipped with a 5mm Xses Cold Probe. Spectra were internally referenced to the residual solvent signal (1H NMR: $CDCl_3$ = 7.26 ppm, ^{13}C NMR: $CDCl_3$ = 77.0 ppm). Data for ^1H NMR is reported as follows: chemical shift (δ ppm), multiplicity (s = singlet, d = doublet, t = triplet, q = quartet, m = multiplet, br = broad), coupling constant (Hz), integration. Coupling constants were rounded to the nearest 0.5 Hz. Infrared (IR) spectra were recorded on a PerkinElmer Spectrum 100 instrument equipped with a single-bounce diamond / ZnSe ATR accessory. Melting point ranges were determined on a Fisher-Johns Melting Point Apparatus and are reported uncorrected. High resolution mass spectra (HRMS) were obtained on a Micromass 70S-250 spectrometer (EI) or an ABI/Sciex QStar Mass Spectrometer (ESI) or a JEOL AccuTOF model JMS-T1000LC mass spectrometer equipped with and IONICS® Direct Analysis in Real Time (DART) ion source at Advanced Instrumentation for Molecular Structure (AIMS) in the Department of Chemistry at the University of Toronto.

For details of the blue LED's: Sapphire Blue LED Tape -12vdc, Waterproof, Blue, Double Density 5050 - creativelightings.com.

Apparatus set-up: A pyrex dish was wrapped with 4-5 loops of the blue LEDs and placed on a magnetic stir plate. The apparatus was fitted with a fan which was placed ~3-5 cm above the vials. Multiple temperature readings of the internal temperature of the apparatus were taken, giving a temperature of 25-35˚C within a 1 cm distance from the lights. Reactions are generally placed ~2-3 cm away from the lights (the walls of the dish), by placing them in a grid from a test tube rack.

General Procedures

Synthesis of Starting Materials

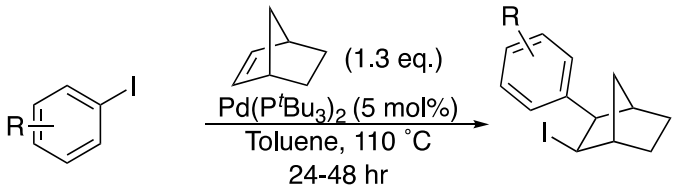

GP1A: General Procedure 1A: Synthesis according to Lautens.[1] To a flame-dried, argon backfilled flask equipped with a stir bar, aryl iodide (1.0 eq., if solid) and palladium tri-*tert*-butylphosphine (0.05 eq.) were added, followed by norbornene (1.3 eq.), and toluene (0.1 M). The vial was sealed and stirred at 110 ˚C for 24-48 hours. The reaction mixture was diluted with ethyl acetate, washed through a silica plug (3 cm) and concentrated *in vacuo*. The residue was dissolved in DCM (0.5 M), dry loaded with silica and purified using column chromatography.

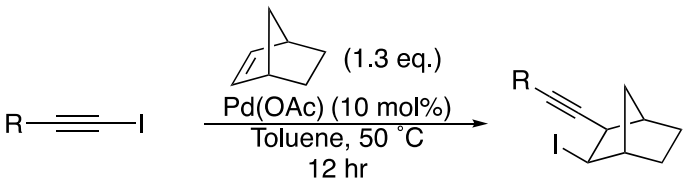

**Note: Liquid substrates were weighed in a separate oven-dried and argon-purged 2-dram vial before being transferred to the reaction flask with 2 aliquots of solvent.

GP1B: General Procedure 1B: Synthesis according to Tong.[2] To a flame-dried, argon backfilled flask, equipped with a stir bar, norbornene (1.3 eq.), $Pd(OAc)_2$ (0.1 eq.) and toluene (0.1 M) were added. The iodoalkyne (1 eq.) was then added and the reaction was sealed and stirred at 50 ˚C for 24-48 hours. The reaction mixture was diluted with ethyl acetate, washed through a silica plug (3 cm) and concentrated *in vacuo*. The residue was dissolved in DCM (0.5 M), dry loaded with silica and purified using column chromatography.

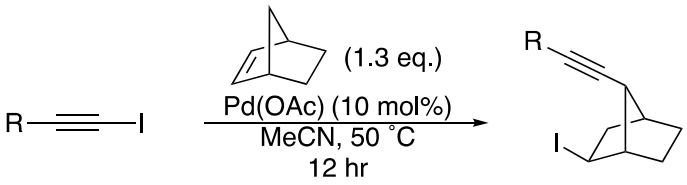

GP1C: General Procedure 1C: Synthesis according to Tong.[2] Norbornene (1.3 eq.), $Pd(OAc)_2$ (0.1 eq.) and acetonitrile (0.1 M) were added to a flame-dried, argon backfilled flask, equipped with a stir bar. The iodoalkyne (1 eq.) was then added and the reaction was sealed and stirred at 50 ˚C for 24-48 hours. The reaction mixture was diluted with ethyl acetate, washed through a silica plug (3 cm) and concentrated *in vacuo*. The residue was dissolved in DCM (0.5 M), dry loaded with silica and purified using column chromatography.

Catalytic Procedure

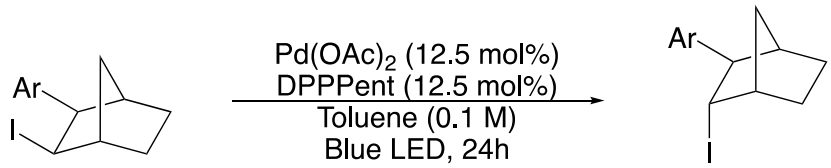

GP2A: General Procedure 2A: $Pd(OAc)_2$ (12.5 mol%), DPPPent (12.5 mol%) and substrate (1.0 eq., if solid) were added to an oven-dried, argon backfilled 2-dram vial, equipped with a stir bar. The reaction mixture was purged with argon for 5 minutes and toluene (0.1 M) was added. After sealing the vial with a teflon screw cap it was irradiated (465 nm) and stirred under a cooling fan for 24 hours. The reaction mixture was diluted with ethyl acetate, washed through a silica plug (3 cm) and concentrated *in vacuo.* Conversion was determined *via* ^1H NMR of the crude reaction mixture with 1,3,5-Trimethoxybenzene as internal standard. Afterwards the product was dissolved in DCM, dry loaded with silica and purified using column chromatography.

**Note: Liquid substrates were weighed in a separate oven-dried and argon-purged 2-dram vial before being transferred to the reaction flask with 2 aliquots of solvent.

Optimization

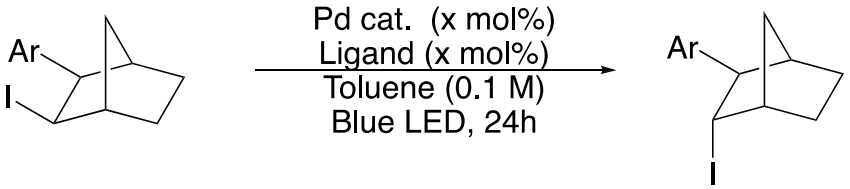

Table S1: Optimization of Palladium Epimerization

Entry	Pd source	Ligand	Base	Conditions	Yield, dr
1	10% $Pd(OAc)_2$	10% DPPPent		Blue LED	83 %, 10:1
2	10% $Pd(OAc)_2$	12.5% DPPPent		Blue LED	70% yield, 15:1
2	3.75% $Pd(allyl)Cl]_2$	15% DPEPhos	K_2CO_3 (2.0 eq.)	Blue LED	25%, 1:2
3*	12.5% $Pd(OAc)_2$	12.5% DPPPent		Blue LED	83 % >20:1
4	12.5% $Pd(OAc)_2$	12.5% DPPPent		100°C	18%, 1:3
5	12.5% $Pd(OAc)_2$	12.5% DPPPent	K_2CO_3 (2.0 eq.)	Blue LED	80%, >20:1
6	12.5% $Pd(OAc)_2$	12.5% ^{t}BuDavePhos		Blue LED	8%, 1:10
7	12.5% $Pd(OAc)_2$	12.5% DPPM		Blue LED	25%, 1:3
8	12.5% $Pd(OAc)_2$	12.5% DPPProp		Blue LED	49%, 1:1
9	12.5% $Pd(OAc)_2$	12.5% DPPF		Blue LED	23%. 4:1
10	$Pd(PPh_3)$ (10 mol%)			Blue LED	38% 1:1
11	$Pd(PPh_3)$ (10 mol%)		K_2CO_3 (2.0 eq.)	Blue LED	80% 8:1
12	$Pd(P^tBu_3)_2$ (10 mol%)			Blue LED	10% 1:6
13	-			270 nm LED	n.r.
14	12.5% $Pd(OAc)_2$		12.5% DPPPent	100 ˚C No LED	18, 1:3

*Entry 3 yielded optimized conditions, and was used to test the breadth of the reaction. Decreasing reaction times below 24 hours resulted in lower dr.

The remaining balance for all the reactions was observed as phenylnorbornane.

The active catalyst in this reaction presumably Pd(DPPPentO)$_2$, where one of the phosphines on the bidentate ligand have been oxidized to reduce Pd(OAc)$_2$.[3]

Ligands Screened

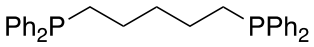

DPPPent

DPPProp

DPPM

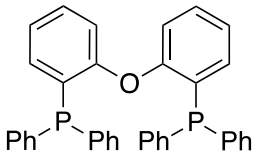

DPEPhos

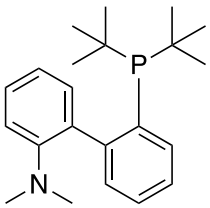

^{t}BuDavePhos

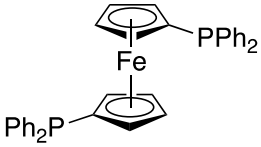

DPPF

Known Starting Materials:

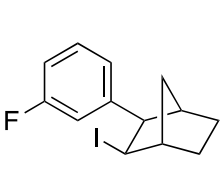

Compound 2e

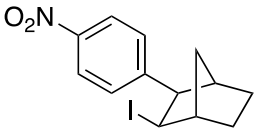

Compound 2g

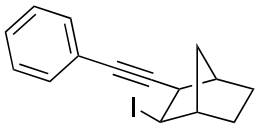

Compound 2o

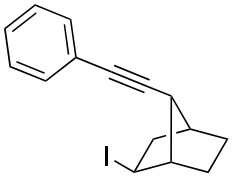

Compound 2p

2e,**g** were synthesized according to a literature procedure by Lautens.[1] **2o**,**p** were synthesized according to a literature procedure by Tong.[2]

Novel Starting Materials:

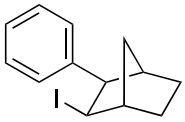

Compound 2a

***(1S,2R,3R,4R)-2-iodo-3-phenylbicyclo[2.2.1]heptane* (2a)**

Prepared according to **GP1A** using iodobenzene on 2 mmol scale. The product was isolated as a clear oil via column chromatography eluting with pentane (397 mg, 1.32 mmol, 66% yield).

^{1}H NMR (500 MHz, $CDCl_3$) δ 7.36 – 7.29 (m, 2H), 7.25 – 7.19 (m, 1H), 7.17 – 7.09 (m, 2H), 4.62 (ddd, *J* = 7.9, 2.2, 0.7 Hz, 1H), 2.91 – 2.76 (m, 2H), 2.62 (dq, *J* = 3.2, 1.3 Hz, 1H), 2.29 (dp, *J* = 10.3, 1.9 Hz, 1H), 1.76 – 1.58 (m, 2H), 1.60 – 1.21 (m, 3H).

^{13}C NMR (126 MHz, $CDCl_3$) δ 147.7, 128.4, 127.9, 126.5, 52.9, 49.4, 45.4 (d, *J* = 0.9 Hz), 42.4, 36.3, 31.2, 28.5.

IR (thin film, cm^{-1}) 2970, 2948, 1488, 1449, 1296, 1171, 1145, 1075, 958, 800.

HRMS (DART) [M+NH_4] calculated 298.02184 m/z (found 316.05521m/z for $C_{13}H_{15}I$).

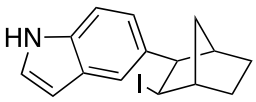

Compound 2b

***5-((1R,2R,3R,4S)-3-iodobicyclo[2.2.1]heptan-2-yl)-1H-indole* (2b)**

Prepared according to **GP1A** using 5-iodobenzene on a 0.5 mmol scale. The product was isolated as a brown solid via column chromatography, eluting with 95:5 pentane:EtOAc. (80 mg, 0.12 mmol, 24% yield).

^{1}H NMR (500 MHz, $CDCl_3$) (500 MHz, $CDCl_3$) δ 8.06 (s, 1H), 7.43 – 7.38 (m, 1H), 7.35 – 7.30 (m, 1H), 7.18 (dd, *J* = 3.2, 2.4 Hz, 1H), 6.95 (dd, *J* = 8.4, 1.8 Hz, 1H), 6.54 (ddd, *J* = 3.2, 2.1, 1.0 Hz, 1H), 4.69 (dd, *J* = 7.9, 2.1 Hz, 1H), 2.89 (dd, *J* = 20.1, 6.0 Hz, 2H), 2.69 (dt, *J* = 3.2, 1.6 Hz, 1H), 2.39 (dp, *J* = 10.2, 2.0 Hz, 1H), 1.74 – 1.62 (m, 2H), 1.59 – 1.48 (m, 1H), 1.48 – 1.35 (m, 2H).

^{13}C NMR (126 MHz, $CDCl_3$) δ 139.7, 134.5, 127.5, 124.4, 123.4, 119.6, 110.2, 102.8, 53.1, 49.5, 47.4, 42.8, 36.3, 31.4, 28.5.

IR (thin film, cm^{-1}) 3396, 2962, 2921, 2870, 1474, 1452, 1417, 1315, 1169, 1088.

HRMS (DART) [M+H] calculated m/z 337.03274 (found 338.04066 m/z for $C_{15}H_{16}IN$).

MP 160-162 ˚C.

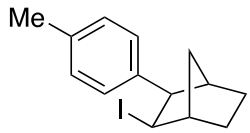

Compound 2c

***(1S,2R,3R,4R)-2-iodo-3-(p-tolyl)bicyclo[2.2.1]heptane* (2c)**

Prepared according to **GP1A** using 4-iodotoluene on a 0.5 mmol scale. The product was isolated as a clear oil via column chromatography, eluting with 100% pentane. (90 mg, 0.14 mmol, 28% yield).

^{1}H NMR (500 MHz, $CDCl_3$) δ 7.17 – 7.07 (m, 2H), 7.05 – 6.96 (m, 2H), 4.60 (ddd, *J* = 7.9, 2.2, 0.6 Hz, 1H), 2.86 – 2.81 (m, 1H), 2.77 (d, *J* = 7.9 Hz, 1H), 2.58 (dq, *J* = 3.3, 1.4 Hz, 1H), 2.34 (s, 3H), 2.27 (dp, *J* = 10.2, 1.9 Hz, 1H), 1.72 – 1.57 (m, 2H), 1.49 (ddt, *J* = 10.3, 3.8, 1.6 Hz, 1H), 1.44 – 1.39 (m, 1H), 1.39 – 1.30 (m, 1H).

^{13}C NMR (126 MHz, $CDCl_3$) δ 144.8, 135.9, 128.6, 128.2, 52.6, 49.4, 45.9, 42.5, 36.2, 31.2, 28.5, 21.1.

IR (thin film, cm^{-1}) 2965, 2918, 2873, 1491, 1453, 1167, 1296, 1144, 1000, 763.

HRMS (DART) [M+NH_4] calculated 312.03749 m/z (found 330.07160 m/z for $C_{14}H_{17}I$).

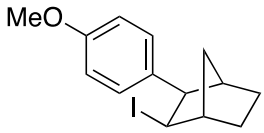

Compound 2d

***(1S,2R,3R,4R)-2-iodo-3-(4-methoxyphenyl)bicyclo[2.2.1]heptane* (2d)**

Prepared according to **GP1A** using 4-iodoanisole on a 0.5 mmol scale. The product was isolated as a clear oil via column chromatography, eluting with 99:1 pentane:EtOAc. (95 mg, 0.13o mmol, 29% yield).

^{1}H NMR (500 MHz, $CDCl_3$) δ 7.06 – 6.99 (m, 2H), 6.84 (d, *J* = 8.7 Hz, 2H), 4.61 (ddd, *J* = 7.9, 2.2, 0.7 Hz, 1H), 3.80 (s, 3H), 2.86 – 2.82 (m, 1H), 2.75 (d, *J* = 7.8 Hz, 1H), 2.55 (dt, *J* = 3.2, 1.5 Hz, 1H), 2.28 – 2.23 (m, 1H), 1.68 – 1.61 (m, 2H), 1.48 (ddt, *J* = 10.3, 3.7, 1.6 Hz, 1H), 1.41 – 1.28 (m, 2H).

^{13}C NMR (126 MHz, $CDCl_3$) δ 158.0, 140.3, 129.3, 113.1, 55.2, 52.2, 48.9, 46.6, 43.0, 36.1, 31.2, 28.5.

IR (thin film, cm^{-1}) 2948, 2867, 1670, 1580, 1511, 1452, 1267, 1178, 1037, 817.

HRMS (DART) [M+H] calculated 328.03241 m/z (found 329.03944 m/z for $C_{14}H_{17}IO$).

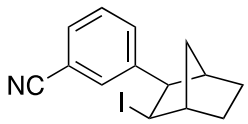

Compound 2f

***3-((1R,2R,3R,4S)-3-iodobicyclo[2.2.1]heptan-2-yl)benzonitrile* (2f)**

Prepared according to according to **GP1A** using 3-iodobenzonitrile on a 0.5 mmol scale. The product was isolated as an orange oil via column chromatography, eluting with 95:5 pentane:EtOAc (108 mg, 0.17 mmol, 33% yield).

^{1}H NMR (500 MHz, $CDCl_3$) δ 7.49 (dt, *J* = 7.7, 1.4 Hz, 1H), 7.44 – 7.35 (m, 2H), 7.32 (dt, *J* = 7.9, 1.5 Hz, 1H), 4.55 (dd, *J* = 8.2, 2.2 Hz, 1H), 2.87 – 2.82 (m, 2H), 2.56 (dt, *J* = 3.1, 1.6 Hz, 1H), 2.25 – 2.17 (m, 1H), 1.75 – 1.62 (m, 2H), 1.57 – 1.50 (m, 1H), 1.48 – 1.31 (m, 2H).

^{13}C NMR (126 MHz, $CDCl_3$) δ 148.8, 133.1, 131.8, 130.2, 128.7, 119.2, 111.9, 52.4, 49.3, 43.3, 42.3, 36.2, 31.0, 28.4.

IR (thin film, cm^{-1}) 2954, 2921, 2876, 2226, 1448, 1302, 1172, 1144, 1118, 917.

HRMS (DART) [M+H] calculated 323.17747 m/z (found 324.02450 m/z for $C_{14}H_{14}IN$).

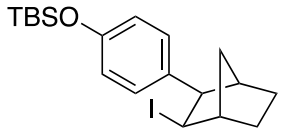

Compound 2h

***tert*-butyl(4-((1*R*,2*R*,3*R*,4*S*)-3-iodobicyclo[2.2.1]heptan-2-yl)phenoxy)dimethylsilane (2h)**

Prepared according to according to **GP1A** on a 1 mmol scale. The product was isolated as a grey oil via column chromatography, eluting with 92.5:7.5 pentane:DCM (143 mg, 0.34 mmol, 34% yield).

^{1}H NMR (500 MHz, $CDCl_3$) δ 6.98 – 6.91 (m, 2H), 6.81 – 6.72 (m, 2H), 4.59 (ddd, *J* = 7.8, 2.2, 0.7 Hz, 1H), 2.85 – 2.80 (m, 1H), 2.73 (d, *J* = 7.8 Hz, 1H), 2.55 (dt, *J* = 3.2, 1.6 Hz, 1H), 2.28 – 2.20 (m, 1H), 1.70 – 1.58 (m, 2H), 1.49 – 1.43 (m, 1H), 1.43 – 1.37 (m, 1H), 1.37 – 1.29 (m, 1H), 0.98 (s, 9H), 0.19 (s, 6H).

^{13}C NMR (126 MHz, $CDCl_3$) δ 154.1, 140.9, 129.2, 119.5, 52.3, 49.3, 46.5, 42.5, 36.1, 31.2, 28.5, 25.7, 18.2, -4.4 (d, *J* = 0.9 Hz).

IR (thin film, cm^{-1}) 2965, 2955, 2873, 1606, 1507, 1459, 1264, 1252, 1170, 938.

HRMS (DART) [M+H] calculated 428.10324 m/z (found 429.11147 m/z for $C_{19}H_{29}IOSi$).

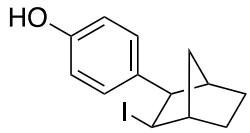

Compound 2i

4-((1*R*,2*R*,3*R*,4*S*)-3-iodobicyclo[2.2.1]heptan-2-yl)phenol (2i)

Prepared from **compound 2h** via deprotection of the TBDMS group. **Compound 2h** (0.126 mmol) was dissolved in dry THF and cooled to 0 ˚C. 1.1 eq. of TBAF (1M) was added dropwise and the reaction was stirred until completion. The reaction was then flushed through a pad of silica and solvent was removed *in vacuo*. The product was isolated as a yellow solid via column chromatography, eluting with a gradient from 95:5 pentane:EtOAc to 90:10 pentane:EtOAc. (98 mg, 0.31 mmol, 46% yield).

^{1}H NMR (500 MHz, $CDCl_3$) δ 7.03 – 6.94 (m, 2H), 6.82 – 6.68 (m, 2H), 4.70 – 4.51 (m, 2H), 2.85 – 2.80 (m, 1H), 2.73 (d, *J* = 7.8 Hz, 1H), 2.54 (dq, *J* = 3.3, 1.5 Hz, 1H), 2.24 (dp, *J* = 10.2, 1.9 Hz, 1H), 1.68 – 1.59 (m, 2H), 1.49 – 1.43 (m, 1H), 1.43 (s, 1H), 1.37 – 1.29 (m, 1H).

^{13}C NMR (126 MHz, $CDCl_3$) δ 153.9, 140.5, 129.5, 114.7, 52.2, 49.3, 46.5, 42.6, 36.1, 31.2, 28.5.

IR(thin film, cm^{-1}) 3209 (br), 2959, 2919, 2870, 1741, 1510, 1448, 1231, 1170, 1183.

HRMS (DART) [M+NH4] calculated 314.16647 m/z (found 332.05166 m/z for $C_{13}H_{15}IO$).

MP 160-162 °C.

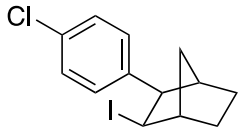

Compound 2j

(1*R*,2*R*,3*R*,4*S*)-2-(4-chlorophenyl)-3-iodobicyclo[2.2.1]heptane (2j)

Prepared according to according to **GP1A** using 4-cloroiodobenzene on a 1 mmol scale. The product was isolated as a yellow solid via column chromatography, eluting with 100% pentane (237 mg, 0.71 mmol, 71% yield).

^{1}H NMR (500 MHz, $CDCl_3$) δ 7.33 – 7.23 (m, 2H), 7.09 – 6.99 (m, 2H), 4.57 (ddd, *J* = 8.0, 2.2, 0.6 Hz, 1H), 2.89 – 2.82 (m, 1H), 2.78 (d, *J* = 7.9 Hz, 1H), 2.55 (dt, *J* = 3.2, 1.5 Hz, 1H), 2.24 (dp, *J* = 10.3, 1.9 Hz, 1H), 1.74 – 1.60 (m, 2H), 1.54 – 1.46 (m, 1H), 1.46 – 1.31 (m, 2H).

^{13}C NMR (126 MHz, $CDCl_3$) δ 146.1, 132.1, 129.7, 128.0, 52.3, 49.4, 44.7 (d, *J* = 0.9 Hz), 42.5, 36.2, 31.2, 28.5.

IR (thin film, cm^{-1}) 2966, 2917, 2933, 1491, 1456, 1297, 1167, 1144, 1088, 1011 .

HRMS (DART) [M+NH4] calculated 331.98287 m/z (found 350.01665 m/z for $C_{13}H_{14}ICl$).

MP 55-59 °C.

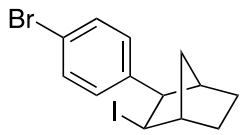

Compound 2k

***(1R,2R,3R,4S)-2-(4-bromophenyl)-3-iodobicyclo[2.2.1]heptane* (1w)**

Prepared according to according to **GP1A** using 4-bromoiodobenzene on a 1 mmol scale. The product was isolated as a grey oil via column chromatography, eluting with 100% pentane (121 mg, 0.32 mmol, 32% yield).

^{1}H NMR (500 MHz, $CDCl_3$) δ 7.49 – 7.32 (m, 2H), 7.03 – 6.93 (m, 2H), 4.56 (ddd, *J* = 7.9, 2.3, 0.6 Hz, 1H), 2.83 (ddq, *J* = 3.9, 1.5, 0.8 Hz, 1H), 2.76 (d, *J* = 7.9 Hz, 1H), 2.54 (dt, *J* = 3.3, 1.6 Hz, 1H), 2.22 (dt, *J* = 10.3, 2.1 Hz, 1H), 1.70 – 1.62 (m, 2H), 1.52 – 1.46 (m, 1H), 1.44 – 1.39 (m, 1H), 1.39 – 1.29 (m, 1H).

^{13}C NMR (126 MHz, $CDCl_3$) δ 146.5, 131.0, 130.1, 120.2, 52.4, 49.3, 44.3, 42.4, 36.2, 31.1, 28.4.

IR (thin film, cm^{-1}) 2954, 2918, 1487, 1260, 1169, 1069, 1008, 903, 845, 745.

HRMS (DART) [M+NH4] calculated 377.06347 m/z (found 393.96686 m/z for $C_{13}H_{14}IBr$).

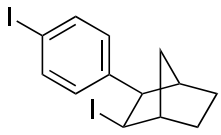

Compound 2l

***(1S,2R,3R,4R)-2-iodo-3-(4-iodophenyl)bicyclo[2.2.1]heptane* (2l)**

Prepared according to according to **GP1A** using 1,4-diiodobenzene on a 1 mmol scale. The product was isolated as a clear oil via column chromatography, eluting with 100% pentane (89 mg, 0.21 mmol, 21% yield).

^{1}H NMR (500 MHz, $CDCl_3$) (500 MHz, $CDCl_3$) δ 7.62 (d, *J* = 8.5 Hz, 2H), 7.00 – 6.73 (m, 2H), 4.55 (ddd, *J* = 7.9, 2.2, 0.6 Hz, 1H), 2.86 – 2.80 (m, 1H), 2.74 (d, *J* = 7.9 Hz, 1H), 2.53 (dt, *J* = 3.3, 1.6 Hz, 1H), 2.21 (dt, *J* = 10.3, 2.1 Hz, 1H), 1.69 – 1.61 (m, 2H), 1.49 (ddt, *J* = 10.3, 3.8, 1.6 Hz, 1H), 1.44 – 1.37 (m, 1H), 1.37 (s, 1H).

^{13}C NMR (126 MHz, $CDCl_3$) δ 147.2, 136.9, 130.4, 91.7, 52.5, 49.3, 44.2, 42.4, 36.2, 31.1, 28.4.

IR (thin film, cm^{-1}) 2950, 2245, 1601, 1459, 1254, 1205, 1152, 1067, 836, 700.

HRMS (DART) [M+NH4] calculated 423.91849 m/z (found 441.95230 m/z for $C_{13}H_{14}I_2$).

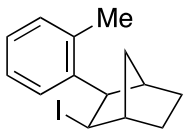

Compound 2m

(1*S*,2*R*,3*R*,4*R*)-2-iodo-3-(*o*-tolyl)bicyclo[2.2.1]heptane (2m)

Prepared according to according to **GP1A** using 2-iodotoluene on a 1 mmol scale. The product was isolated as a clear oil via column chromatography, eluting with 100% pentane (75 mg, 0.24 mmol, 24% yield).

^{1}H NMR (500 MHz, $CDCl_3$) δ 7.26 – 7.06 (m, 4H), 4.68 (dd, *J* = 8.0, 2.1 Hz, 1H), 2.86 (dt, *J* = 5.3, 1.6 Hz, 2H), 2.65 (dt, *J* = 3.1, 1.6 Hz, 1H), 2.33 – 2.25 (m, 1H), 2.23 (s, 3H), 1.72 – 1.64 (m, 2H), 1.57 – 1.40 (m, 2H), 1.40 – 1.28 (m, 1H).

^{13}C NMR (126 MHz, $CDCl_3$) δ 146.2, 136.3, 130.1, 126.4, 125.9, 125.6, 49.6, 44.0, 42.0, 36.1, 31.3, 28.6, 20.5.

IR (thin film, cm^{-1}) 2965, 2956, 2870, 1454, 1265, 1204, 1172, 1140, 1135, 833.

HRMS (DART) [M+NH4] calculated 312.03749 m/z (found 330.07130 m/z for $C_{14}H_{17}I$).

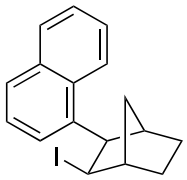

Compound 2n

1-((1*R*,2*R*,3*R*,4*S*)-3-iodobicyclo[2.2.1]heptan-2-yl)naphthalene (2n)

Prepared according to according to **GP1A** using 1-iodonapthalene on a 1 mmol scale. The product was isolated as a clear oil via column chromatography, eluting with 95:5 pentane:DCM (109 mg, 0.31 mmol, 31% yield).

^{1}H NMR (500 MHz, $CDCl_3$) δ 7.91 (ddq, *J* = 8.3, 1.2, 0.7 Hz, 1H), 7.87 – 7.81 (m, 1H), 7.75 (dt, *J* = 7.7, 1.2 Hz, 1H), 7.55 – 7.38 (m, 4H), 4.85 (ddd, *J* = 7.8, 2.2, 0.7 Hz, 1H), 3.51 (d, *J* = 7.8 Hz, 1H), 2.92 (s, 1H), 2.83 (d, *J* = 3.7 Hz, 1H), 2.50 – 2.36 (m, 1H), 1.82 – 1.73 (m, 2H), 1.62 – 1.56 (m, 2H), 1.50 – 1.42 (m, 1H).

^{13}C NMR (126 MHz, $CDCl_3$) δ 143.7, 133.6, 132.2, 128.9, 127.0, 125.9, 125.4, 125.1, 123.7, 123.2, 49.9, 48.8, 44.1, 42.2, 36.1, 31.4, 28.6.

IR(thin film, cm^{-1}) 2955, 2919, 2851, 1465, 1259, 1205, 1173, 1090, 1018, 859, 773.

HRMS (DART) [M+H] calculated 348.03749 m/z (found 349.04467 m/z for $C_{17}H_{17}I$).

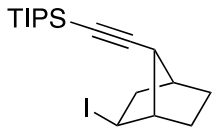

Compound 2q

***(((1S,2S,4S,7R)-2-iodobicyclo[2.2.1]heptan-7-yl)ethynyl)triisopropylsilane* (2q)**

Prepared according to according to **GP1C** on a 1 mmol scale. The product was isolated as a clear oil via column chromatography, eluting with 100% pentane (187 mg, 0.47 mmol, 47% yield).

^{1}H NMR (500 MHz, $CDCl_3$) δ 3.84 (ddd, *J* = 8.1, 5.4, 1.3 Hz, 1H), 2.73 – 2.69 (m, 1H), 2.65 (dddd, *J* = 13.7, 5.5, 4.2, 2.7 Hz, 1H), 2.60 (p, *J* = 1.5 Hz, 1H), 2.35 – 2.29 (m, 1H), 2.13 (ddd, *J* = 13.7, 8.1, 1.5 Hz, 1H), 1.60 (ddddd, *J* = 12.0, 7.6, 6.1, 4.5, 3.2 Hz, 1H), 1.55 – 1.45 (m, 1H), 1.31 – 1.24 (m, 1H), 1.20 – 1.12 (m, 1H), 1.12 – 1.05 (m, 21H).

^{13}C NMR (126 MHz, $CDCl_3$) δ 107.0, 86.0, 50.7, 44.6, 43.9, 40.7, 31.2, 26.6, 21.7, 18.8, 18.8, 11.3.

IR (thin film, cm^{-1}) 2940, 2896, 2172, 1462, 1365, 1343, 1223, 1073, 995, 882.

HRMS (DART) [M+H] calculated 402.12397 m/z (found 403.13148 m/z for $C_{18}H_{31}ISi$).

Products:

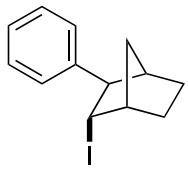

(1*S*,2*S*,3*R*,4*R*)-2-iodo-3-phenylbicyclo[2.2.1]heptane (3a)

Prepared according to **GP2A** on a 0.1 mmol scale. The product was isolated as a white solid via column chromatography, eluting with 100% pentane (average yield over 3 runs: 24.7 mg, 0.083 mmol, 83% yield).

^{1}H NMR (500 MHz, $CDCl_3$) δ 7.34 – 7.28 (m, 4H), 7.25 – 7.21 (m, 1H), 4.17 (ddd, *J* = 5.9, 3.7, 2.3 Hz, 1H), 2.95 (dd, *J* = 6.0, 2.1 Hz, 1H), 2.63 – 2.49 (m, 1H), 2.39 – 2.29 (m, 1H), 2.00 – 1.90 (m, 1H), 1.82 (dddd, *J* = 10.4, 4.0, 2.4, 1.5 Hz, 1H), 1.75 – 1.61 (m, 2H), 1.45 (dddd, *J* = 12.3, 9.6, 4.0, 2.9 Hz, 1H), 1.39 (dq, *J* = 10.4, 1.8 Hz, 1H).

^{13}C NMR (126 MHz, $CDCl_3$) δ 143.9, 128.6, 126.4, 126.4, 59.4, 45.6, 42.4, 41.4, 35.0, 30.7, 27.4.

IR (thin film, cm^{-1}) 2957, 2917, 1741, 1601, 1497, 1471, 1452, 1296, 1206, 1165, 1024.

HRMS (DART) [M+NH4] calculated 298.02184 m/z (found 316.05562 m/z for $C_{13}H_{15}I$).

MP 30-33 ˚C.

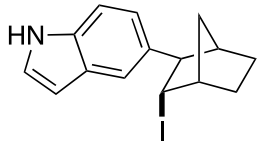

5-((1*R*,2*S*,3*R*,4*S*)-3-iodobicyclo[2.2.1]heptan-2-yl)-1*H*-indole (3b)

Prepared according to **GP2A** on a 0.1 mmol scale. The product was isolated as a brown solid via column chromatography, eluting with 100% pentane: 95:5 pentane:EtOAc (28.8mg, 0.085 mmol, 85% yield).

^{1}H NMR (500 MHz, $CDCl_3$) δ 8.07 (s, 1H), 7.58 (dq, *J* = 1.6, 0.8 Hz, 1H), 7.33 (dt, *J* = 8.4, 0.9 Hz, 1H), 7.25 – 7.16 (m, 2H), 6.54 (ddd, *J* = 3.1, 2.0, 1.0 Hz, 1H), 4.27 (ddd, *J* = 5.9, 3.6, 2.3 Hz, 1H), 3.07 (dd, *J* = 6.1, 2.1 Hz, 1H), 2.56 (dp, *J* = 4.3, 1.4 Hz, 1H), 2.46 – 2.34 (m, 1H), 2.03 – 1.91 (m, 2H), 1.80 – 1.59 (m, 2H), 1.59 – 1.45 (m, 1H), 1.42 (dq, *J* = 10.3, 1.8 Hz, 1H).

^{13}C NMR (126 MHz, $CDCl_3$) δ 135.5, 134.6, 128.0, 124.6, 121.4, 117.7, 111.2, 102.6, 59.7, 45.7, 43.2, 42.8, 35.1, 30.8, 27.5.

IR (thin film, cm^{-1}) 3416, 2955, 2919, 2848, 1467, 1299, 1169, 1191, 1063, 969 .

HRMS (DART) [M+H] calculated 337.03274 m/z (found 338.04028 m/z for $C_{15}H_{16}IN$).

MP 115-118 °C.

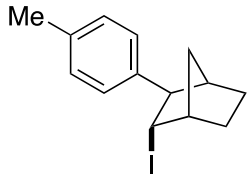

(1*S*,2*S*,3*R*,4*R*)-2-iodo-3-(*p*-tolyl)bicyclo[2.2.1]heptane (3c)

Prepared according to **GP2A** on a 0.1 mmol scale. The product was isolated as a yellow solid via column chromatography, eluting with 100% pentane (23.1, 0.074 mmol, 74% yield).

^{1}H NMR (500 MHz, $CDCl_3$) δ 7.25 – 7.19 (m, 2H), 7.16 – 7.09 (m, 2H), 4.17 (ddd, *J* = 5.9, 3.6, 2.3 Hz, 1H), 2.92 (dd, *J* = 6.1, 2.0 Hz, 1H), 2.53 (ddt, *J* = 5.7, 2.7, 1.4 Hz, 1H), 2.38 – 2.29 (m, 3H), 1.96 (dddd, *J* = 12.2, 8.6, 4.5, 2.3 Hz, 1H), 1.82 (dtt, *J* = 10.3, 2.5, 1.6 Hz, 1H), 1.77 – 1.59 (m, 2H), 1.51 – 1.31 (m, 3H).

^{13}C NMR (126 MHz, $CDCl_3$) δ 140.9, 136.0, 129.3, 126.3, 59.2, 45.6, 42.5 (d, *J* = 2.3 Hz), 41.8, 35.0, 30.7, 27.4, 21.0.

IR (thin film, cm^{-1}) 2957, 2809, 1514, 1456, 1346, 1380, 1189, 1145, 1167, 852.

HRMS (DART) [M+H] calculated 312.03749 m/z (found 313.04559 m/z for $C_{14}H_{17}I$).

MP 62-66 ˚C.

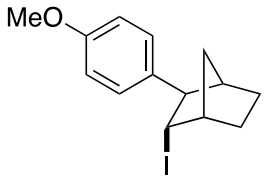

(1*S*,2*S*,3*R*,4*R*)-2-iodo-3-(4-methoxyphenyl)bicyclo[2.2.1]heptane (3d)

Prepared according to **GP2A** on a 0.1 mmol scale. The product was isolated as a yellow oil via column chromatography, eluting with a gradient of 100% pentane to 95:5 pentane:EtOAc (28.8 mg, 0.088 mmol, 88% yield).

^{1}H NMR (500 MHz, $CDCl_3$) δ 7.29 – 7.18 (m, 2H), 6.90 – 6.80 (m, 2H), 4.13 (ddd, *J* = 5.9, 3.6, 2.2 Hz, 1H), 3.79 (s, 3H), 2.89 (dd, *J* = 6.1, 2.1 Hz, 1H), 2.56 – 2.48 (m, 1H), 2.35 – 2.26 (m, 1H), 1.93 (dddd, *J* = 12.2, 8.6, 4.5, 2.3 Hz, 1H), 1.80 (dddd, *J* = 10.3, 4.0, 2.4, 1.5 Hz, 1H), 1.76 – 1.55 (m, 2H), 1.49 – 1.40 (m, 1H), 1.39 – 1.27 (m, 1H).

^{13}C NMR (126 MHz, $CDCl_3$) δ 158.2, 136.1, 127.4, 114.0, 58.8, 55.3, 45.6, 42.5, 42.1, 34.9, 30.7, 27.3.

IR (thin film, cm^{-1}) 2960, 2917, 2875, 2851, 1742, 1488, 1457, 1249, 1196, 1082.

HRMS (DART) [M+H] calculated 328.03241 m/z (found 329.04041 m/z for $C_{14}H_{17}OI$).

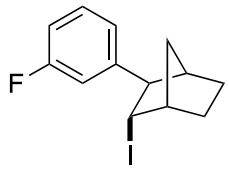

(1*R*,2*R*,3*S*,4*S*)-2-(3-fluorophenyl)-3-iodobicyclo[2.2.1]heptane (3e)

Prepared according to **GP2A** on a 0.1 mmol scale. The product was isolated as a yellow oil via column chromatography eluting with 100% pentane (27.7 mg, 0.088 mmol, 88% yield).

^{1}H NMR (500 MHz, $CDCl_3$) δ 7.31 – 7.23 (m, 1H), 7.11 (ddt, *J* = 7.7, 1.7, 0.8 Hz, 1H), 7.06 – 6.97 (m, 1H), 6.92 (tdd, *J* = 8.4, 2.6, 1.0 Hz, 1H), 4.12 (ddd, *J* = 5.9, 3.6, 2.2 Hz, 1H), 2.93 (dd, *J* = 6.0, 2.1 Hz, 1H), 2.60 – 2.50 (m, 1H), 2.39 – 2.30 (m, 1H), 1.95 (dddd, *J* = 11.9, 8.4, 4.4, 2.3 Hz, 1H), 1.84 – 1.58 (m, 3H), 1.53 – 1.37 (m, 2H).

^{13}C NMR (126 MHz, $CDCl_3$) δ 164.0, 162.0, 146.4, 130.1 (d, *J* = 8.5 Hz), 122.2 (d, *J* = 2.8 Hz), 113.3 (dd, *J* = 21.2, 2.5 Hz), 59.2 (d, *J* = 1.7 Hz), 45.6, 42.3, 40.6, 35.0, 30.6, 27.3.

^{19}F NMR (377 MHz, CDCl3-insert) δ -112.83.

IR (thin film, cm^{-1}) 2952, 2866, 1601, 1508, 1454, 1246, 1169, 905, 822, 960.

HRMS (DART) [M+NH_4] calculated 316.01242 m/z (found 334.04670 m/z for $C_{13}H_{14}FI$).

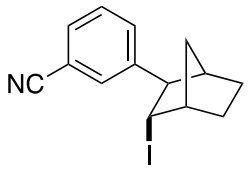

3-((1*R*,2*R*,3*S*,4*S*)-3-iodobicyclo[2.2.1]heptan-2-yl)benzonitrile (3f)

Prepared according to **GP2A** on a 0.1 mmol scale. The product was isolated as a yellow oil via column chromatography eluting with a gradient of 100% pentane to 95:5 pentane:EtOAc (31.3 mg, 0.095 mmol, 95% yield).

^{1}H NMR (500 MHz, $CDCl_3$) δ 7.63 – 7.55 (m, 2H), 7.53 (dt, *J* = 7.7, 1.4 Hz, 1H), 7.41 (td, *J* = 7.7, 0.7 Hz, 1H), 4.05 (ddd, *J* = 5.9, 3.6, 2.2 Hz, 1H), 2.94 (dd, *J* = 6.1, 2.0 Hz, 1H), 2.55 (tq, *J* = 4.6, 1.3 Hz, 1H), 2.34 (dt, *J* = 3.3, 1.6 Hz, 1H), 1.94 (dddd, *J* = 11.8, 8.2, 4.3, 2.3 Hz, 1H), 1.82 – 1.60 (m, 3H), 1.53 – 1.37 (m, 2H).

^{13}C NMR (126 MHz, $CDCl_3$) δ 145.2, 131.2, 130.2, 129.8, 129.5, 118.9, 112.7, 59.0, 45.6, 42.1, 39.8, 35.1, 30.6, 27.1.

IR (thin film, cm^{-1}) 2960, 2875, 2226, 1481, 1297, 1189, 1165, 1144, 932, 914, 781.

HRMS (DART) [M+NH4] calculated 323.01709 m/z (found 341.05124 m/z for $C_{14}H_{14}IN$).

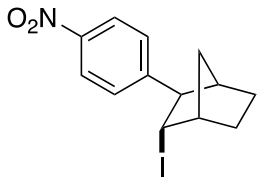

(1*S*,2*S*,3*R*,4*R*)-2-iodo-3-(4-nitrophenyl)bicyclo[2.2.1]heptane (3g)

Prepared according to **GP2A** on a 0.1 mmol scale. The product was isolated as a yellow oil via column chromatography, eluting with a gradient of 100% pentane to 95:5 pentane:EtOAc (32.6 mg, 0.076 mmol, 76% yield).

^{1}H NMR (500 MHz, $CDCl_3$) δ 8.42 – 7.92 (m, 2H), 7.48 (dd, *J* = 8.9, 0.7 Hz, 2H), 4.08 (ddd, *J* = 5.9, 3.6, 2.2 Hz, 1H), 3.01 (dd, *J* = 6.3, 2.0 Hz, 1H), 2.63 – 2.53 (m, 1H), 2.38 (dt, *J* = 3.2, 1.6 Hz, 1H), 1.95 (dddd, *J* = 11.7, 8.1, 4.3, 2.3 Hz, 1H), 1.82 – 1.63 (m, 3H), 1.53 – 1.41 (m, 2H).

^{13}C NMR (126 MHz, $CDCl_3$) δ 151.3, 127.2, 123.9, 123.2, 59.4, 45.6, 42.2, 39.4, 35.2, 30.6, 27.1.

IR (thin film, cm^{-1}) 2961, 2923, 2869, 1592, 1515, 1344, 1315, 1301, 1166, 1111, 955.

HRMS (DART) [M+H] calculated 343.00692 m/z (found 344.01494 m/z for $C_{13}H_{14}INO_2$).

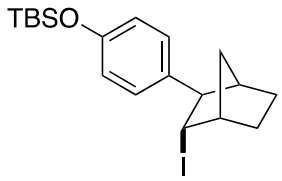

***tert-butyl(4-((1R,2R,3S,4S)-3-iodobicyclo[2.2.1]heptan-2-yl)phenoxy)dimethylsilane* (3h)**

Prepared according to **GP2A** on a 0.05 mmol scale. The product was isolated as an orange solid via column chromatography, eluting with a gradient of 100% pentane to 95:5 pentane:EtOAc (13.1 mg, 0.031 mmol, 61% yield, 11:1 ratio).

^{1}H NMR (500 MHz, $CDCl_3$) δ 7.20 – 7.11 (m, 2H), 6.81 – 6.72 (m, 2H), 4.13 (ddd, *J* = 5.9, 3.5, 2.3 Hz, 1H), 2.88 (dd, *J* = 6.0, 2.1 Hz, 1H), 2.54 – 2.48 (m, 1H), 2.31 – 2.27 (m, 1H), 1.93 (dddd, *J* = 12.1, 8.6, 4.5, 2.3 Hz, 1H), 1.79 (dddd, *J* = 10.4, 4.0, 2.4, 1.6 Hz, 1H), 1.75 – 1.57 (m, 2H), 1.46 – 1.33 (m, 2H), 0.98 (s, 9H), 0.19 (s, 6H).

^{13}C NMR (126 MHz, $CDCl_3$) δ 154.1, 136.6, 127.3, 120.0, 58.8, 45.6, 42.4, 42.3, 34.9, 30.6, 27.4, 25.7, 18.2, -4.4.

IR (thin film, cm^{-1}) 2955, 2857, 1504, 1245, 1169, 1094, 1013, 903, 840, 797.

HRMS (DART) [M+H] calculated 428.10324m/z (found 429.11027 m/z for $C_{19}H_{29}IOSi$).

MP 48-51 °C.

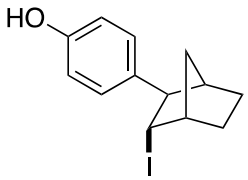

4-((1*R*,2*R*,3*S*,4*S*)-3-iodobicyclo[2.2.1]heptan-2-yl)phenol (3i)

Prepared according to **GP2A** on a 0.05 mmol scale. The product was isolated as a yellow solid via column chromatography, eluting with a gradient of 100% pentane to 80:20 pentane:EtOAc (8.1 mg, 0.026 mmol, 52% yield).

^{1}H NMR (500 MHz, $CDCl_3$) δ 7.23 – 7.13 (m, 2H), 6.82 – 6.71 (m, 2H), 4.11 (ddd, *J* = 5.9, 3.6, 2.3 Hz, 1H), 2.87 (dd, *J* = 6.0, 2.1 Hz, 1H), 2.56 – 2.45 (m, 1H), 2.31 – 2.26 (m, 1H), 1.93 (dddd, *J* = 12.1, 8.6, 4.5, 2.3 Hz, 1H), 1.79 (dddd, *J* = 10.3, 4.0, 2.4, 1.5 Hz, 1H), 1.74 – 1.59 (m, 2H), 1.47 – 1.33 (m, 2H).

^{13}C NMR (126 MHz, $CDCl_3$) δ 154.0, 136.3, 127.6, 115.4, 58.8, 45.6, 42.4, 42.1, 35.0, 30.7, 27.3.

IR (thin film, cm^{-1}) 3210 (br), 2954, 2921, 2869, 1601, 1509, 1452, 1233, 1175, 1164, 1104.

HRMS (DART) [M+NH4] calculated 314.01476 m/z (found 315.02600 m/z for $C_{13}H_{15}IO$).

MP 101-103 °C.

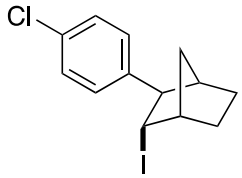

(1*R*,2*R*,3*S*,4*S*)-2-(4-chlorophenyl)-3-iodobicyclo[2.2.1]heptane (3j)

Prepared according to **GP2A** on a 0.1 mmol scale. The product was isolated as a yellow oil via column chromatography, eluting with 100% pentane (30.1 mg, 0.091 mmol, 91% yield).

^{1}H NMR (500 MHz, $CDCl_3$) δ 7.32 – 7.20 (m, 4H), 4.08 (ddd, *J* = 5.9, 3.6, 2.2 Hz, 1H), 2.90 (dd, *J* = 6.0, 2.1 Hz, 1H), 2.52 (tt, *J* = 3.3, 1.3 Hz, 1H), 2.36 – 2.28 (m, 1H), 1.94 (dddd, *J* = 12.1, 8.5, 4.4, 2.3 Hz, 1H), 1.81 – 1.58 (m, 3H), 1.50 – 1.36 (m, 2H).

^{13}C NMR (126 MHz, $CDCl_3$) δ 142.3, 132.2, 128.7, 127.8, 58.9, 45.6, 42.3, 40.9, 35.0, 30.6, 27.2.

IR (thin film, cm^{-1}) 2963, 2875, 1497, 1185, 1155, 1082, 1094, 1010, 816, 729.

HRMS (DART) [M+NH4] calculated 331.98287 m/z (found 350.01647 m/z for $C_{13}H_{14}ICl$).

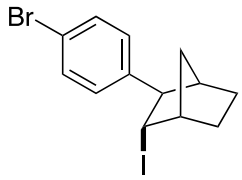

(1*R*,2*R*,3*S*,4*S*)-2-(4-bromophenyl)-3-iodobicyclo[2.2.1]heptane (3k)

Prepared according to **GP2A** on a 0.1 mmol scale. The product was isolated as a yellow oil via column chromatography, eluting with 100% pentane (21.1 mg, 0.052 mmol, 52% yield).

^{1}H NMR (500 MHz, $CDCl_3$) δ 7.47 – 7.39 (m, 2H), 7.24 – 7.14 (m, 2H), 4.08 (ddd, *J* = 5.9, 3.6, 2.2 Hz, 1H), 2.88 (dd, *J* = 6.1, 2.0 Hz, 1H), 2.55 – 2.49 (m, 1H), 2.32 – 2.27 (m, 1H), 1.93 (dddd, *J* = 12.1, 8.5, 4.5, 2.3 Hz, 1H), 1.81 – 1.57 (m, 3H), 1.44 – 1.36 (m, 2H).

^{13}C NMR (126 MHz, $CDCl_3$) δ 142.8, 131.7, 128.1, 120.3, 59.0, 45.6, 42.2, 40.8, 35.0, 30.6, 27.2.

IR (thin film, cm^{-1}) 2954, 2872, 1488, 1452, 1297, 1184, 1164, 1073, 1008, 910, 759.

HRMS (DART) [M+NH4] calculated 375.93236 m/z (found 393.96557 m/z for $C_{13}H_{14}IBr$).

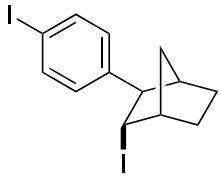

(1*S*,2*S*,3*R*,4*R*)-2-iodo-3-(4-iodophenyl)bicyclo[2.2.1]heptane (3l)

Prepared according to **GP2A** on a 0.05 mmol scale. The product was isolated as a clear oil via column chromatography, eluting with 100% pentane (7.1 mg, 0.017 mmol, 34% yield).

^{1}H NMR (500 MHz, $CDCl_3$) δ 7.65 – 7.55 (m, 2H), 7.12 – 7.03 (m, 2H), 4.11 – 4.05 (m, 1H), 2.86 (dd, *J* = 6.0, 2.0 Hz, 1H), 2.55 – 2.49 (m, 1H), 2.36 – 2.20 (m, 1H), 1.93 (dddd, *J* = 12.0, 8.4, 4.4, 2.3 Hz, 1H), 1.82 – 1.58 (m, 3H), 1.54 – 1.30 (m, 2H).

^{13}C NMR (126 MHz, $CDCl_3$) δ 143.5, 137.7, 128.5, 91.7, 59.0, 45.6, 42.2, 40.7, 35.0, 30.6, 27.2.

IR (thin film, cm^{-1}) 2953, 2920, 2850, 1484, 1452, 1164, 1064, 1004, 807, 738.

HRMS (DART) [M+NH4] calculated 423.91849 m/z (found 441.95158 m/z for $C_{13}H_{14}I_2$).

MP 55-59 °C.

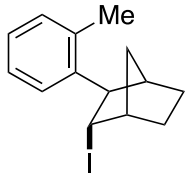

(1*S*,2*S*,3*R*,4*R*)-2-iodo-3-(*o*-tolyl)bicyclo[2.2.1]heptane (3m)

Prepared according to **GP2A** on a 0.1 mmol scale. The product was isolated as a yellow oil via column chromatography, eluting with 100% pentane (18.4 mg, 0.059 mmol, 59% yield, 6.5:1 ratio).

^{1}H NMR (500 MHz, $CDCl_3$) δ 7.24 – 6.98 (m, 4H), 4.53 (ddd, *J* = 6.1, 3.6, 2.3 Hz, 1H), 3.09 (dd, *J* = 6.3, 2.0 Hz, 1H), 2.58 (ddt, *J* = 4.7, 3.0, 1.5 Hz, 1H), 2.40 (d, *J* = 0.7 Hz, 3H), 2.03 – 1.93 (m, 2H), 1.85 (dddd, *J* = 10.5, 4.0, 2.4, 1.6 Hz, 1H), 1.74 (dddt, *J* = 16.9, 10.8, 4.3, 2.3 Hz, 1H), 1.62 (tddd, *J* = 12.1, 5.0, 4.0, 0.7 Hz, 1H), 1.52 (dddt, *J* = 11.9, 9.2, 4.0, 2.4 Hz, 1H), 1.34 – 1.23 (m, 1H).

^{13}C NMR (126 MHz, $CDCl_3$) δ 141.6, 136.4, 130.5, 126.3, 126.1, 124.3, 55.9, 45.4, 44.7, 38.3, 34.4, 31.2, 27.4, 20.6.

IR (thin film, cm^{-1}) 2951, 2868, 1602, 1507, 1470, 1243, 1169, 1098, 886, 719.

HRMS (DART) [M+NH4] calculated 312.03749 m/z (found 330.07051 m/z for $C_{14}H_{17}I$).

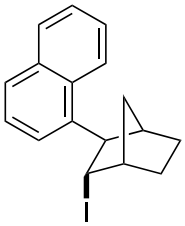

1-((1*R*,2*R*,3*S*,4*S*)-3-iodobicyclo[2.2.1]heptan-2-yl)naphthalene

Prepared according to **GP2A** on a 0.05 mmol scale. The product was isolated as a clear oil via column chromatography, eluting with 100% pentane (11.1 mg, 0.032 mmol, 64% yield, 10:1 ratio).

^{1}H NMR (500 MHz, $CDCl_3$) δ 8.09 (ddq, *J* = 8.5, 1.4, 0.7 Hz, 1H), 7.89 – 7.83 (m, 1H), 7.75 (dt, *J* = 8.2, 1.1 Hz, 1H), 7.71 – 7.40 (m, 3H), 7.36 (dt, *J* = 7.2, 1.0 Hz, 1H), 4.74 (ddd, *J* = 6.0, 3.7, 2.2 Hz, 1H), 3.65 (dd, *J* = 6.2, 1.9 Hz, 1H), 2.65 (td, *J* = 4.0, 1.3 Hz, 1H), 2.20 (dq, *J* = 3.2, 1.5 Hz, 1H), 2.14 – 2.05 (m, 1H), 1.87 – 1.65 (m, 4H), 1.32 (dq, *J* = 10.4, 1.8 Hz, 1H).

^{13}C NMR (126 MHz, $CDCl_3$) δ 138.7, 134.1, 132.0, 128.8, 127.2, 126.0, 125.6, 125.2, 124.2, 121.4, 55.5, 45.6, 45.0, 36.8, 34.4, 30.8, 27.7.

IR (thin film, cm^{-1}) 2951, 2871, 1508, 1470, 1243, 1169, 822, 885, 860, 774.

HRMS (DART) [M+H] calculated 348.03749 m/z (found 349.04578 m/z for $C_{17}H_{17}I$).

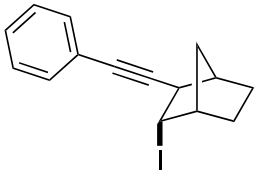

(1*S*,2*S*,3*R*,4*R*)-2-iodo-3-(phenylethynyl)bicyclo[2.2.1]heptane (3o)

Prepared according to **GP2A** on a 0.1 mmol scale. The product was isolated as a clear oil via column chromatography, eluting with 100% pentane (18.3 mg, 0.057 mmol, 57% yield, 3.5:1 ratio).

^{1}H NMR (500 MHz, $CDCl_3$) δ 7.43 – 7.34 (m, 2H), 7.34 – 7.23 (m, 3H), 4.23 (ddd, *J* = 5.0, 3.8, 2.1 Hz, 1H), 2.68 (dd, *J* = 5.1, 2.3 Hz, 1H), 2.48 (ddt, *J* = 4.0, 2.9, 1.2 Hz, 1H), 2.34 – 2.29 (m, 1H), 1.91 – 1.82 (m, 2H), 1.71 – 1.52 (m, 2H), 1.42 – 1.33 (m, 2H).

^{13}C NMR (126 MHz, $CDCl_3$) δ 131.5, 128.2, 127.8, 123.5, 91.1, 82.8, 47.5, 44.9, 44.4, 37.6, 34.8, 28.7, 27.7.

IR (thin film, cm^{-1}) 2965, 2923, 2874, 1595, 1451, 1439, 1333, 1277, 1227, 920.

HRMS (DART) [M+NH4] calculated 322.02184 m/z (found 323.02939 m/z for $C_{15}H_{15}I$).

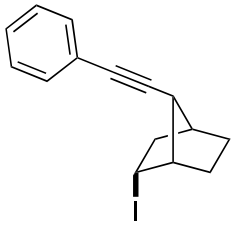

(1*S*,2*R*,4*S*,7*R*)-2-iodo-7-(phenylethynyl)bicyclo[2.2.1]heptane (3p)

Prepared according to **GP2A** on a 0.1 mmol scale. The product was isolated as a clear oil via column chromatography eluting with 100% pentane (15.1 mg, 0.047 mmol, 47% yield, 2:1 ratio).

^{1}H NMR (500 MHz, $CDCl_3$) δ 7.42 – 7.34 (m, 2H), 7.33 – 7.23 (m, 3H), 4.82 – 4.74 (m, 1H), 2.73 (dddd, *J* = 13.8, 11.0, 4.5, 3.1 Hz, 1H), 2.65 (q, *J* = 1.8 Hz, 1H), 2.55 – 2.50 (m, 1H), 2.24 (td, *J* = 4.4, 1.6 Hz, 1H), 2.06 – 1.95 (m, 1H), 1.80 – 1.60 (m, 3H), 1.38 (ddd, *J* = 12.1, 9.4, 4.3 Hz, 1H).

^{13}C NMR (126 MHz, $CDCl_3$) δ 131.5, 128.3, 127.9, 123.4, 88.7, 83.2, 49.8, 42.9, 41.6, 39.1, 30.0, 29.2, 28.6.

IR (thin film, cm^{-1}) 2962, 2871, 1597, 1488, 1442, 1344, 1215, 1158, 906, 774.

HRMS (DART) [M+NH4] calculated 322.02184 m/z (found 323.02907 m/z for $C_{15}H_{15}I$).

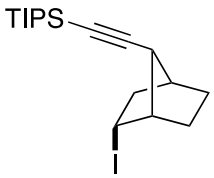

(((1*S*,2*R*,4*S*,7*R*)-2-iodobicyclo[2.2.1]heptan-7-yl)ethynyl)triisopropylsilane (3q)

Prepared according to **GP2A** on a 0.1 mmol scale. The product was isolated as a clear oil via column chromatography eluting with 100% pentane (20.7 mg, 0.051 mmol, 51% yield, 1.5:1 ratio).

^{1}H NMR (500 MHz, $CDCl_3$) δ 4.70 (dddd, *J* = 10.9, 4.6, 3.9, 2.3 Hz, 1H), 2.67 (dddd, *J* = 13.7, 10.9, 4.5, 3.1 Hz, 1H), 2.50 (q, *J* = 1.8 Hz, 1H), 2.46 – 2.41 (m, 1H), 2.15 (ddd, *J* = 4.5, 3.1, 1.4 Hz, 1H), 1.95 (ddd, *J* = 12.8, 9.4, 4.0 Hz, 1H), 1.74 – 1.51 (m, 3H), 1.33 (ddd, *J* = 12.2, 9.4, 4.3 Hz, 1H), 1.13 – 0.96 (m, 21H).

^{13}C NMR (126 MHz, $CDCl_3$) δ 107.37, 83.52, 49.75, 43.02, 41.72, 39.52, 29.89, 29.03, 28.70, 18.62, 11.22.

IR (thin film, cm^{-1}) 2940, 2863, 2169, 1462, 1339, 1216, 1158, 1069, 994, 882.

HRMS (DART) [M+NH4] calculated 402.12397 m/z (found 403.13106 m/z for $C_{18}H_{31}ISi$).

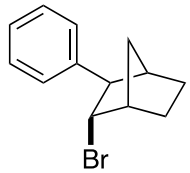

(1*S*,2*S*,3*R*,4*R*)-2-bromo-3-phenylbicyclo[2.2.1]heptane (5a)

Prepared according to **GP2A** on a 0.1 mmol scale. The product was isolated as a clear oil via column chromatography eluting with 100% pentane (5.1 mg, 0.020 mmol, 20% yield).

^{1}H NMR (500 MHz, $CDCl_3$) (500 MHz, $CDCl_3$) δ 7.31 (d, *J* = 5.2 Hz, 4H), 7.24 – 7.21 (m, 1H), 4.20 (ddd, *J* = 5.6, 3.8, 2.0 Hz, 1H), 2.84 (dd, *J* = 5.6, 2.4 Hz, 1H), 2.57 – 2.51 (m, 1H), 2.45 (d, *J* = 4.0 Hz, 1H), 2.13 – 1.91 (m, 1H), 1.78 (dddd, *J* = 10.4, 3.9, 2.4, 1.5 Hz, 1H), 1.75 – 1.56 (m, 2H), 1.50 – 1.41 (m, 2H).

^{13}C NMR (126 MHz, $CDCl_3$) δ 143.8, 128.6, 126.5, 126.4, 62.1, 57.9, 44.6, 42.6, 36.1, 30.6, 23.7.

IR (thin film, cm^{-1}) 2992, 2854, 1495, 1452, 1374, 1299, 1256, 1234, 1152, 1069.

HRMS (DART) [M+NH4] calculated 250.03571 m/z (found 268.07041 m/z for $C_{13}H_{15}Br$).

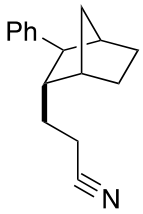

3-((1*S*,2*S*,3*S*,4*R*)-3-phenylbicyclo[2.2.1]heptan-2-yl)propanenitrile (6a)[3]

Prepared according to **GP2A** on a 0.1 mmol scale. The product was isolated as a clear oil via column chromatography eluting with a gradient of 100% pentane to 90:10 pentane:EtOAc (6.3 mg, 0.028 mmol, 28% yield).

^{1}H NMR ^{1}H NMR (500 MHz, $CDCl_3$) δ 7.30 – 7.23 (m, 2H), 7.22 – 7.12 (m, 3H), 2.96 – 2.90 (m, 1H), 2.47 (dd, *J* = 4.0, 1.6 Hz, 1H), 2.21 – 2.03 (m, 3H), 2.00 (dddd, *J* = 10.6, 9.0, 4.9, 1.6 Hz, 1H), 1.77 (dp, *J* = 10.2, 2.0 Hz, 1H), 1.75 – 1.66 (m, 1H), 1.61 (ddt, *J* = 12.1, 7.7, 4.1 Hz, 1H), 1.42 – 1.29 (m, 3H), 1.11 (dtd, *J* = 14.1, 7.8, 4.9 Hz, 1H), 0.98 (dddd, *J* = 14.0, 10.6, 7.3, 6.2 Hz, 1H).

^{13}C NMR (126 MHz, $CDCl_3$) δ 142.3, 128.5 (d, *J* = 7.4 Hz), 128.2, 125.9, 119.9, 51.5, 47.7, 42.4, 39.8, 35.3, 30.9, 29.0, 27.4, 16.4.

IR (thin film, cm^{-1}) 2953, 2871, 2244, 1741, 1600, 1492, 1453, 1259, 1075, 1031.

HRMS (DART) [M+NH4] calculated 225.15175 m/z (found 226.15828 m/z for $C_{16}H_{19}N$).

Stoichiometric Pd-Complex Experiments

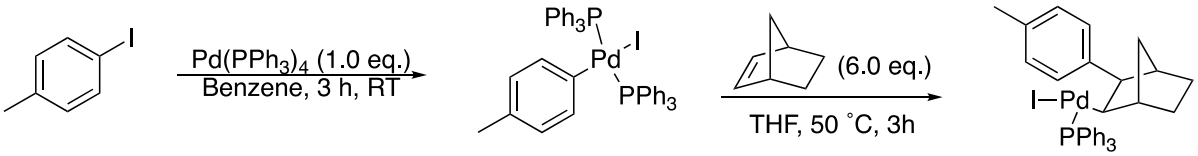

O.A complex ***Complex-I***

Procedure to Synthesize Complex-I[4-5]**:** $Pd(PPh_3)_4$ (1.0 eq.) was added to an oven-dried, argon backfilled 2-dram amber vial, equipped with a stir bar, followed by anhydrous, degassed benzene (0.01 M). 1-iodo-4-methylbenzene (1.0 eq.) was added, a septum screw cap was used to seal the vial and the reaction was stirred for 3 h at room temperature. The resulting mixtured was filtered through a vacuum frit and washed with hexane (3x). The resulting white powder was dried and subjected to the next step.

The **O.A complex**, norbornene (6.0 eq.) and anhydrous degassed THF (0.01M) were added to an oven-dried, argon backfilled 2-dram amber vial, equipped with a stir bar. A septum screw cap was used to seal the vial and the reaction was stirred for 3 h at 50 ˚C. During the reaction a colour change to orange was observed. The solvent was removed *in vacuo* and the residue was sonicated and washed 3 times with diethyl ether and 3 times with hexane to yield the desired **Complex-I** as yellow powder. The complex was crystalized in a 2 chamber diffusion of DCM:MeOH.

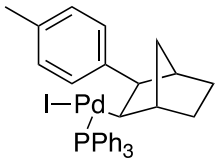

Complex-I

^{1}H NMR (500 MHz, $CDCl_3$) δ 7.87 (d, *J* = 7.7 Hz, 1H), 7.78 – 7.56 (m, 7H), 7.54 – 7.29 (m, 11H), 3.26 (d, *J* = 7.7 Hz, 1H), 2.70 (dt, *J* = 10.0, 1.9 Hz, 1H), 2.50 (d, *J* = 8.6 Hz, 3H), 1.75 – 1.69 (m, 1H), 1.49 – 1.38 (m, 2H), 1.34 – 1.23 (m, 3H), 0.97 (th, *J* = 9.1, 4.5 Hz, 2H).s

^{13}C NMR (126 MHz, $CDCl_3$) δ 143.2, 135.0 (d, *J* = 11.6 Hz), 132.0, 131.9, 131.6, 130.5 (d, *J* = 2.5 Hz), 128.1 (d, *J* = 10.9 Hz), 99.3, 99.2, 54.0 (d, *J* = 2.8 Hz), 43.6 (d, *J* = 3.9 Hz), 42.3 (d, *J* = 15.7 Hz), 40.7, 37.8, 31.6, 30.0 (d, *J* = 10.9 Hz), 27.9, 25.3, 22.6, 21.7, 14.1.

^{31}P NMR (121 MHz, $CDCl_3$) δ 38.3.

HRMS (ESI+) [M - I]+ calculated 942.12325 m/z (found 549.1277 m/z for $C_{32}H_{32}IPPd$).

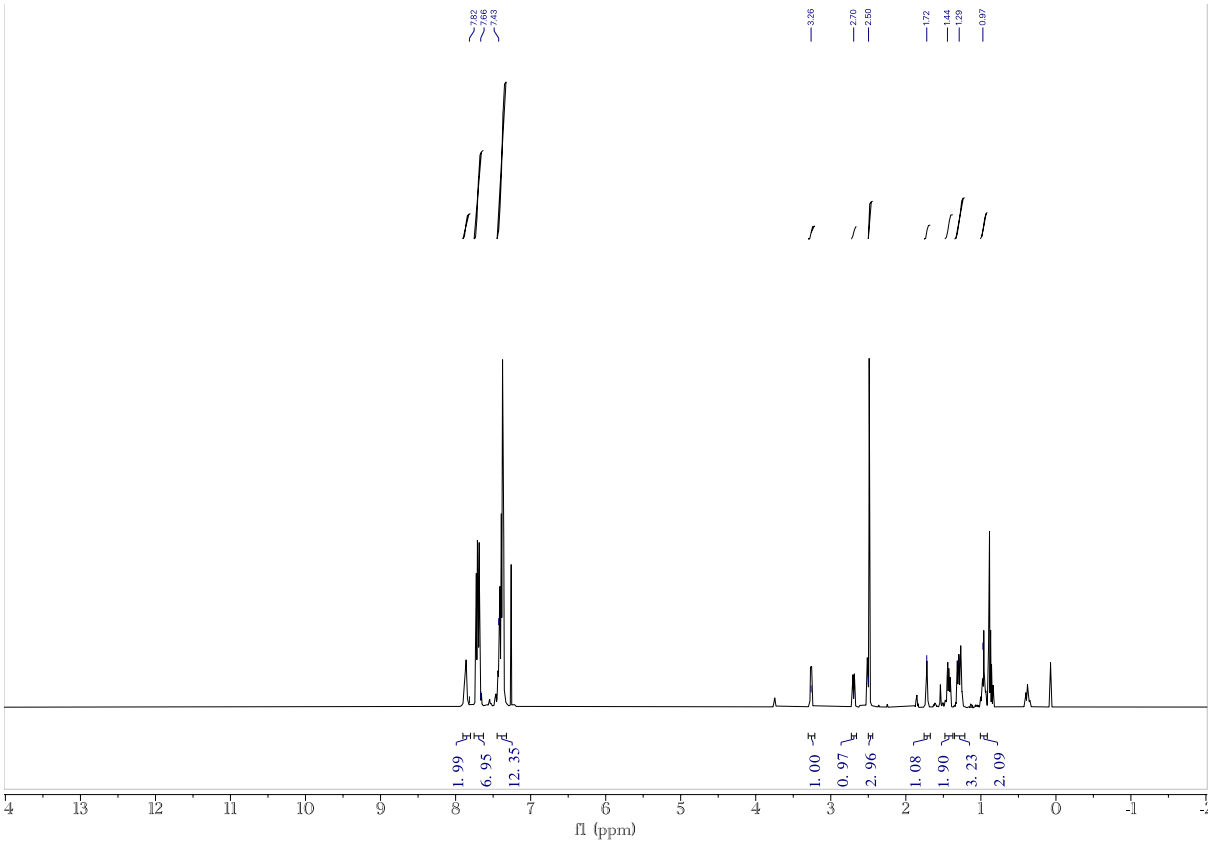
7.82
7.66
7.43
3.26
2.70
2.50
1.72
1.44
1.29
0.97
1.99
6.95
12.35
1.00
0.97
2.96
1.08
1.90
3.23
2.09
f1 (ppm)

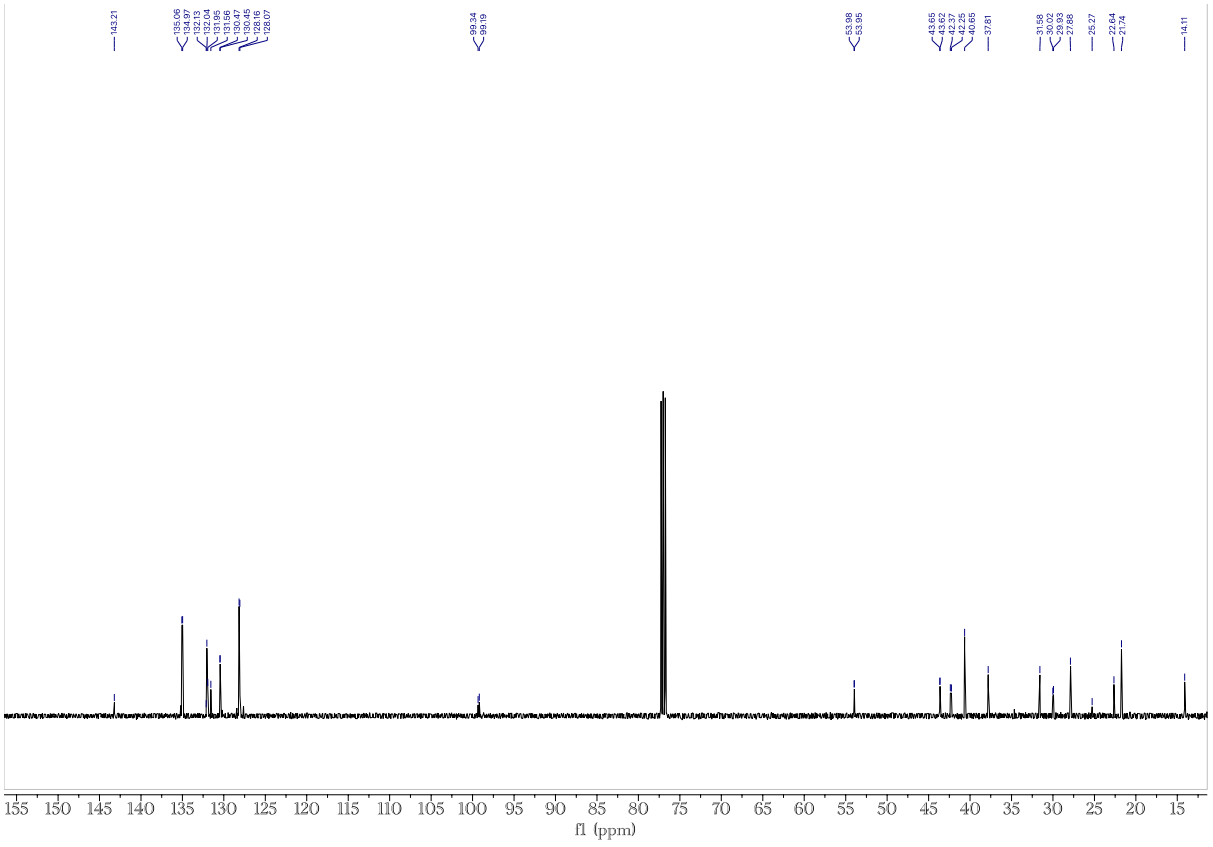
143.21
136.06
134.97
132.13
132.04
131.66
131.56
130.47
130.45
128.16
128.07
99.34
99.19
53.98
53.86
43.65
43.62
42.37
42.25
40.65
37.81
31.58
30.02
29.93
27.88
25.27
22.64
21.74
14.11
f1 (ppm)

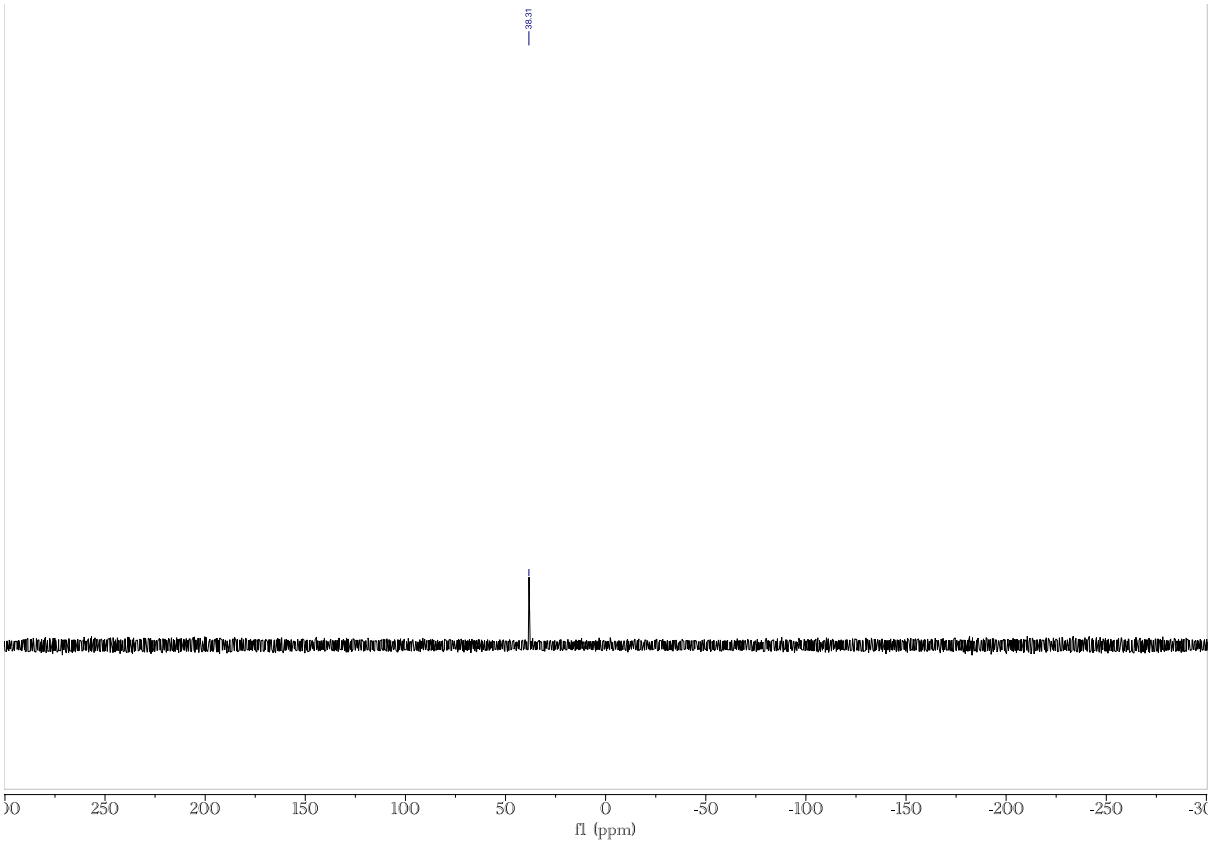

Target Ion Species

Ion Species	*m/z*	*Ionic Formula*
(M+H)+	549.1277	C32 H32 P Pd

MFG Calculator Results

Target m/z	*Ionic Formula*	*Calc m/z*	*+/- (mDa)*	*+/- (ppm)*	*MFG Score*
549.1277	C32 H32 P Pd	549.1292	-1.5	-2.7	99.24
549.1277	C22 H31 N4 O6 Pd	549.1294	-1.7	-3.1	96.41
549.1277	C21 H35 O10 Pd	549.1281	-0.4	-0.7	93.71
549.1277	C23 H27 N8 O2 Pd	549.1308	-3.1	-5.6	93.01
549.1277	C25 H37 O3 P2 Pd	549.1269	0.8	1.5	90.82
549.1277	C20 H36 N2 O7 P Pd	549.1311	-3.4	-6.2	87.02
549.1277	C27 H32 N2 O2 P Pd	549.1252	2.5	4.6	79.65
549.1277	C21 H32 N6 O3 P Pd	549.1324	-4.7	-8.6	79.50
549.1277	C21 H33 N6 O P2 Pd	549.1242	3.5	6.4	67.04

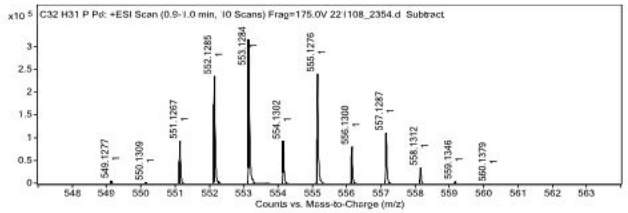

Predicted Isotope Match Table

Isotope	*m/z*	*Calc m/z*	Diff (mDa)	Abund (%)	Calc Abund (%)	+/-
1	549.1277	549.1292	-1.5	2.4	2.8	0.4
2	550.1309	550.1326	-1.7	0.9	1.0	0.1
3	551.1267	551.1277	-1.0	29.9	31.3	1.4
4	552.1285	552.1290	-0.5	72.9	73.3	0.4
5	553.1284	553.1283	0.1	100.0	100.0	0.0
6	554.1302	554.1311	-0.9	28.9	30.6	1.7
7	555.1276	555.1279	-0.3	76.4	78.9	2.5
8	556.1300	556.1310	-1.0	25.2	26.4	1.2
9	557.1287	557.1294	-0.7	35.0	37.2	2.2
10	558.1312	558.1324	-1.2	10.9	11.9	1.0
11	559.1346	559.1356	-1.0	1.7	2.0	0.3

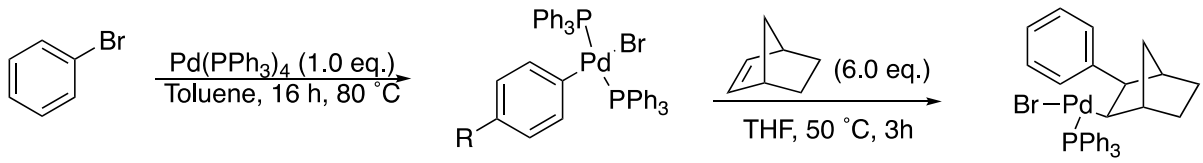

O.A complex ***Complex-III***

Procedure to Synthesize Complex-III[6]**:** $Pd(PPh_3)_4$ (1.0 eq.) was added to an oven-dried, argon backfilled 2-dram amber vial, equipped with a stir bar, followed by anhydrous degassed toluene (0.01 M). Bromobenzene (1.0 eq.) was added, a septum screw cap was used to seal the vial and the reaction was stirred at 80 °C for 16 h. Afterwards the solvent was removed *in vacuo* and the crude product washed with hexanes 3 times. The resulting white powder was dried and subjected to the next step.

To an oven-dried, argon backfilled 2-dram amber vial, equipped with a stir bar, was added the respective **O.A complex**, norbornene (6.0 eq.) and anhydrous degassed THF (0.01M). A septum screw cap was used to seal the vial and the reaction was stirred for 3 h at 50 ˚C. During the reaction a colour change to orange was observed. The solvent was removed *in vacuo* and the residue was sonicated and washed 3 times with diethyl ether and 3 times with hexane to yield the desired **Complex-III** as yellow powder.

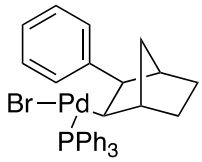

Complex-III

^{1}H NMR (300 MHz, $CDCl_3$) δ 7.99 – 7.75 (m, 5H), 7.75 – 7.61 (m, 10H), 7.47 – 7.33 (m, 5H), 3.82 – 3.71 (m, 1H), 3.31 (d, *J* = 7.6 Hz, 1H), 2.72 (d, *J* = 10.3 Hz, 1H), 2.54 (d, *J* = 4.3 Hz, 1H), 1.91 – 1.80 (m, 1H), 1.65 (s, 2H), 1.31 (t, *J* = 9.8 Hz, 3H), 0.99 (d, *J* = 8.7 Hz, 1H).

^{13}C NMR (126 MHz, $CDCl_3$) (126 MHz, $CDCl_3$) δ 135.7, 134.9, 134.8, 134.6, 134.5, 132.0, 131.5, 131.1, 130.9, 130.8, 130.5, 130.5, 128.3, 128.2, 58.4, 54.4, 43.3, 40.6, 38.2, 29.8, 29.7, 28.0, 25.2.

^{31}P NMR (162 MHz, $CDCl_3$) δ 37.04, 23.04. (23.04 is unreacted starting material).

HRMS (ESI+) [M +H]+ calculated 633.05381 m/z (found 630.063209 m/z for $C_{31}H_{30}BrPPd$).

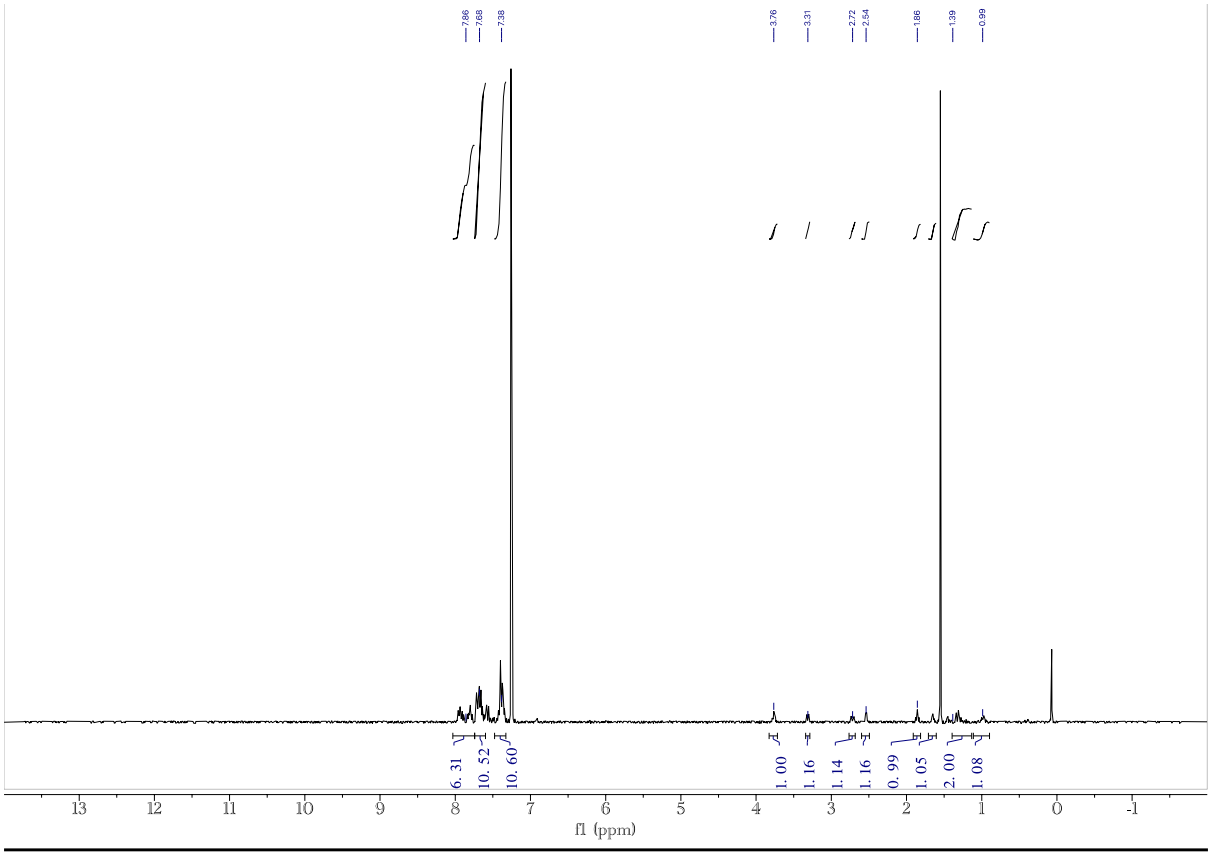
7.86
7.68
7.38
3.76
3.31
2.72
2.54
1.86
1.39
0.99
6.31
10.52
10.60
1.00
1.16
1.14
1.16
0.99
1.05
2.00
1.08
f1 (ppm)

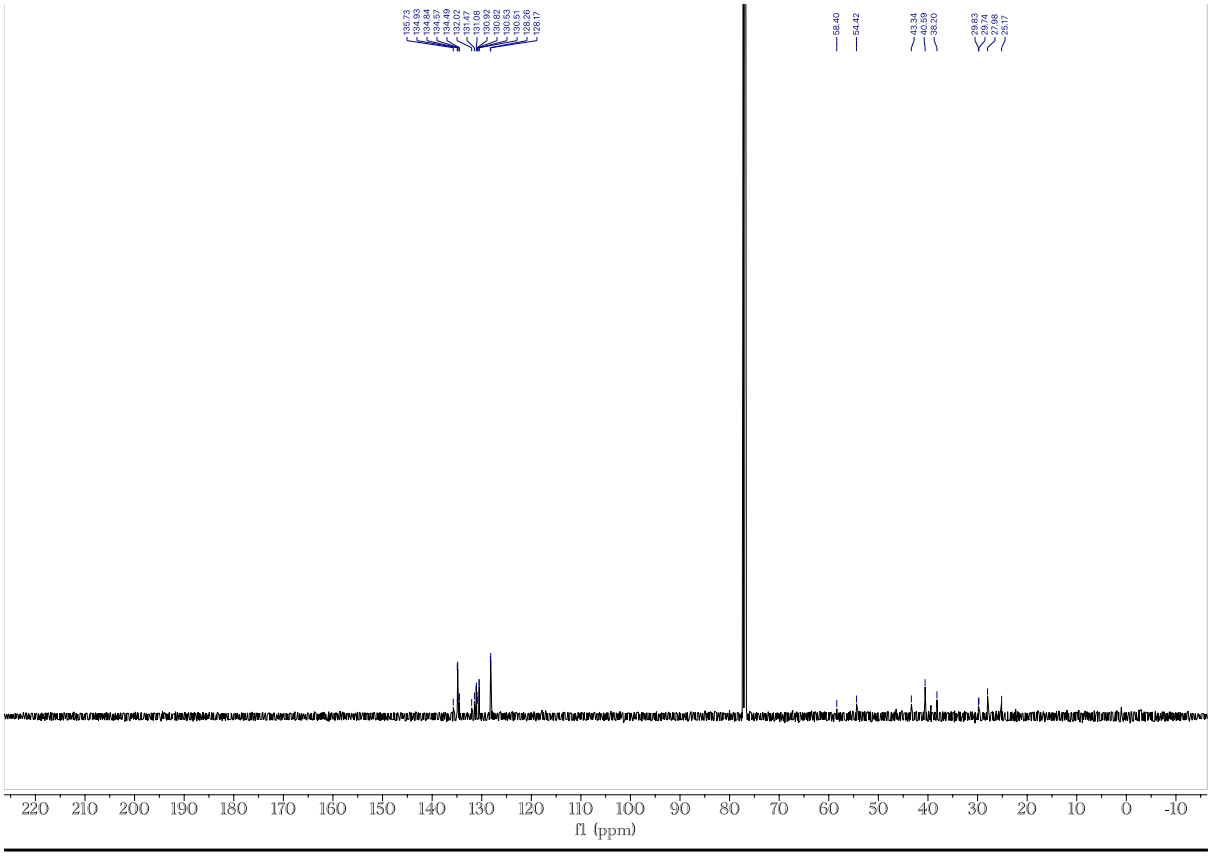
135.73
134.93
134.84
134.57
134.49
131.72
131.47
131.08
130.92
130.82
130.53
130.51
129.26
128.17
58.40
54.42
43.34
40.59
38.20
29.83
29.74
27.98
25.17
f1 (ppm)

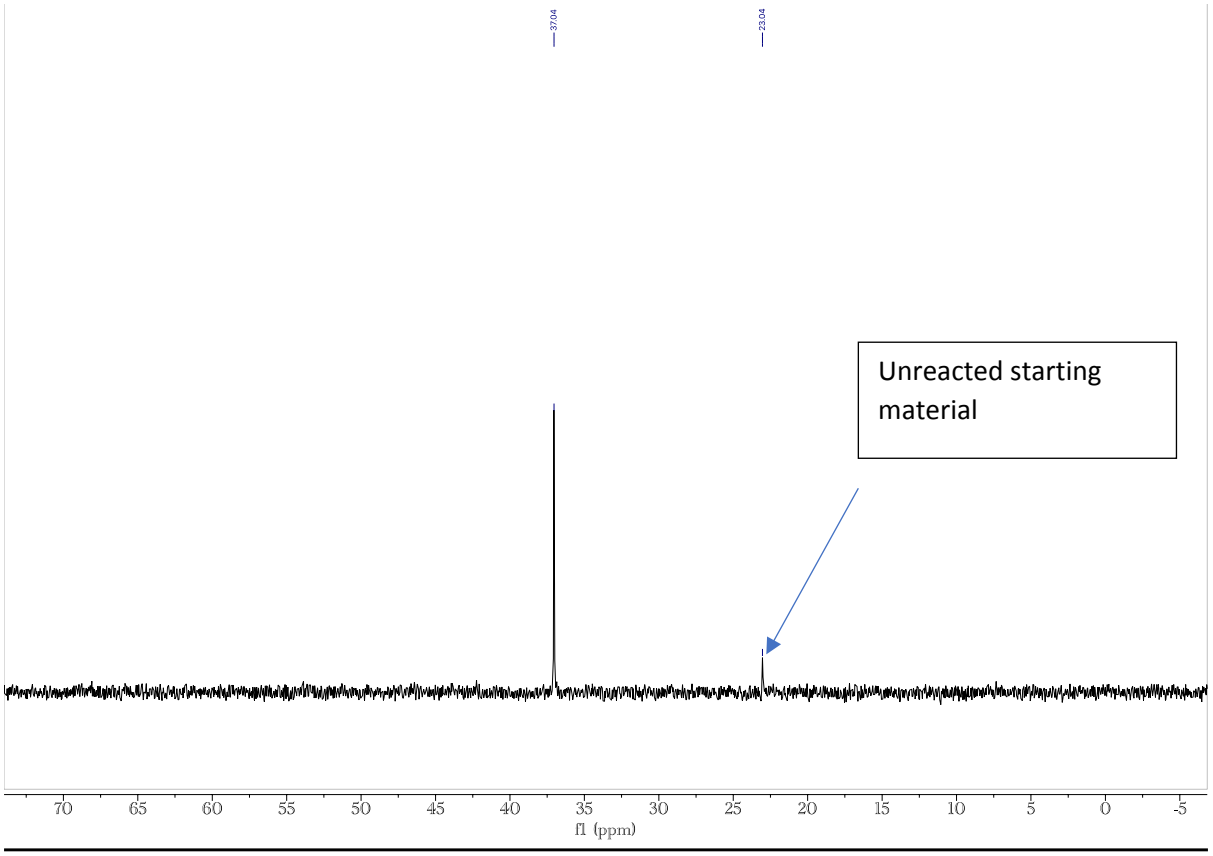
37.04
23.04
Unreacted starting material
70 65 60 55 50 45 40 35 30 25 20 15 10 5 0 -5
f1 (ppm)

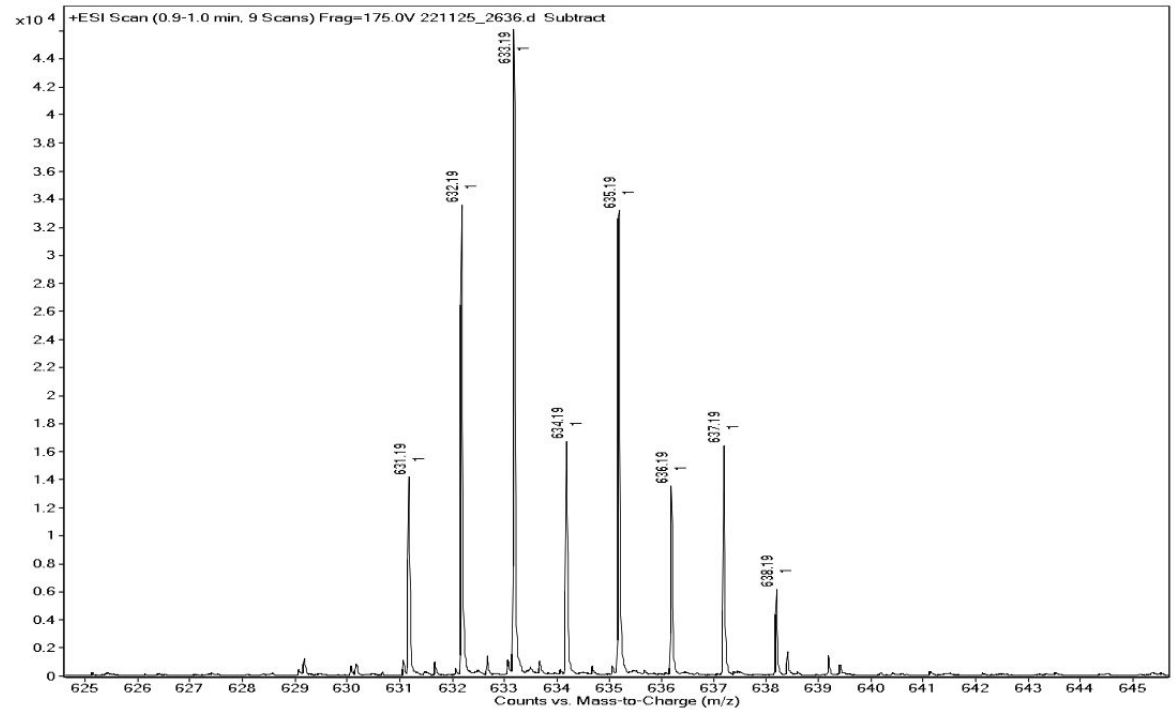
x10 4
+ESI Scan (0.9-1.0 min, 9 Scans) Frag=175.0V 221125_2636.d Subtract
633.19
632.19
635.19
634.19
631.19
637.19
636.19
638.19
Counts vs. Mass-to-Charge (m/z)

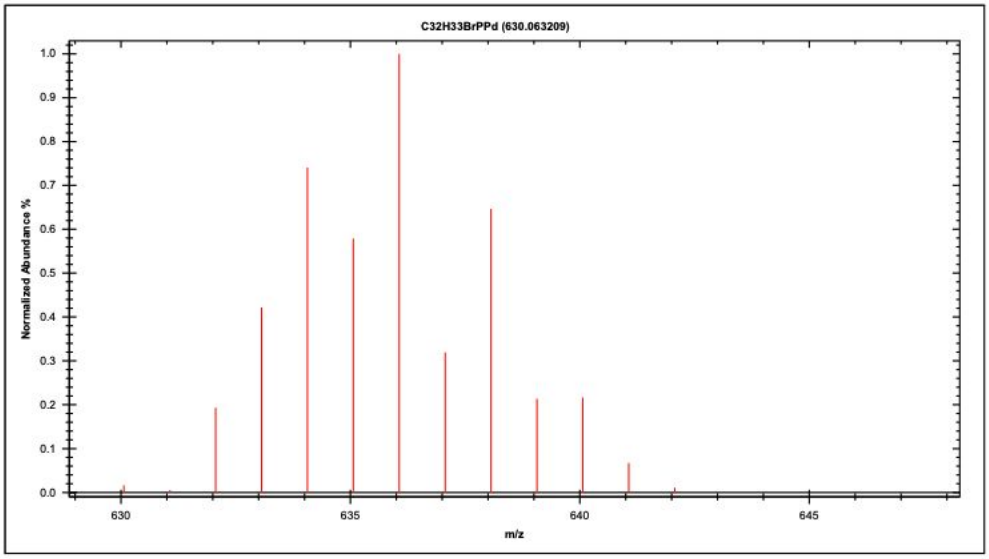

Product Formation via Complex-I:

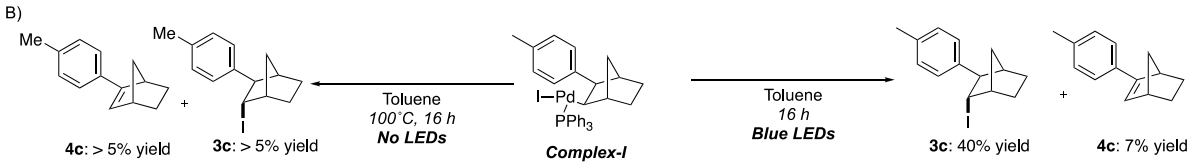

1.1 eq. PPh_3:	**3c**: 38% yield	**4c**: 25% yield
1.1 eq. DPPPent:	**3c**: 18% yield	**4c**: > 5% yield
2.0 eq. K_2CO_3:	**3c**: 37% yield	**4c**: 22% yield
1 h instead of 16 h:	**3c**: 29% yield	**4c**: 8% yield

Procedure: ***Complex-I*** (1 eq., 0.01 mmol), the respective ligand (0 or 1.1 eq.) and K_2CO_3 (0 or 2 eq.) were added to an oven-dried, argon backfilled 2-dram vial, equipped with a stir bar. The reaction vial was purged with argon for 5 minutes. Anhydrous and degassed toluene (1 mL) was added, a teflon tape and screw cap were used to seal the vial. The reaction mixture was either irradiated with Blue LEDs (465 nm) and stirred under a cooling fan for 1 or 16 h (right), or heated at 100 ˚C for 16 h (left). The crude reaction mixture was diluted with ethyl acetate, washed through a silica plug (3 cm) and concentrated *in vacuo.* Yields were determined using ^{1}H NMR with 1,3,5-trimethoxybenzene as internal standard in a 3mm NMR tube (0.2 mL $CDCl_3$).

Catalytic Competence of Complex-II

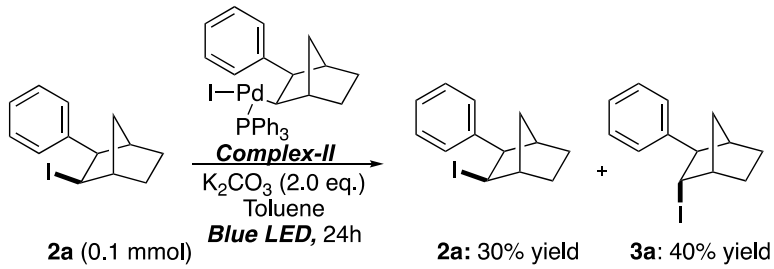

Procedure: ***Complex-II*** (12.5 mol%), and K_2CO_3 (2.0 eq.) were added to an oven-dried, argon backfilled 2-dram vial, equipped with a stir bar. The reaction vial was purged for 5 minutes. Anhydrous and degassed toluene was used to dissolve substrate **2a** (1.0 eq., 0.1 mmol) and were added (1 mL). Teflon tape and a screw cap were used to seal the vial and the reaction was irradiated with Blue LEDs (465 nm) and stirred under a cooling fan for 24 h. The crude reaction mixture was diluted with ethyl acetate, washed through a silica plug (3 cm) and concentrated *in vacuo.* Yields were determined using ^{1}H NMR with 1,3,5-trimethoxybenzene as internal standard in a 3mm NMR tube (0.2 mL $CDCl_3$).

Product formation via Complex-III:

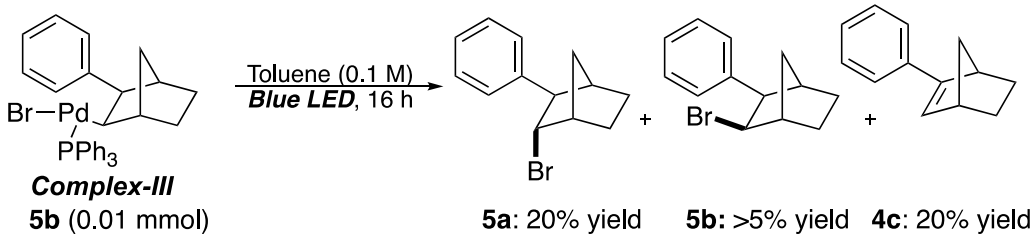

Procedure: ***Complex-III*** (1.0 eq., 0.01 mmol) was added to an oven-dried, argon backfilled 2-dram vial, equipped with a stir bar,. The reaction vial was purged with argon for 5 minutes, anhydrous and degassed toluene (1 mL) was added and a teflon screw cap was used to seal the vial. The reaction mixture was irradiated with Blue LEDs (465 nm) and stirred under a cooling fan for 16 h. The crude reaction mixture was diluted with ethyl acetate, washed through a silica plug (3 cm) and concentrated *in vacuo.* Yields were determined using ^{1}H NMR with 1,3,5-trimethoxybenzene as internal standard in a 3mm NMR tube (0.2 mL $CDCl_3$).

The anti-relationship of the bromide and the phenyl group was determined via 1D-NOE experiments.

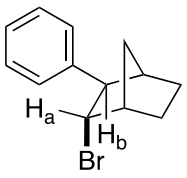

Compound 5a

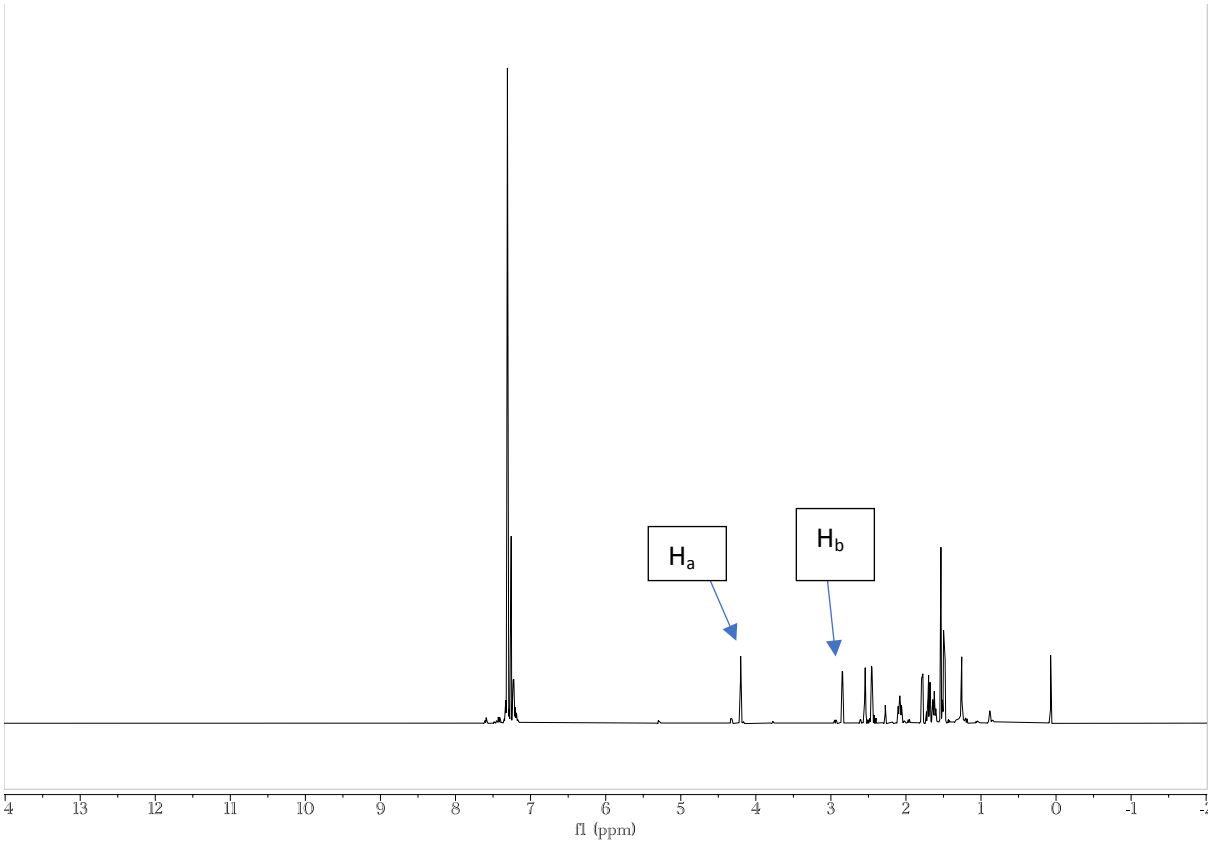

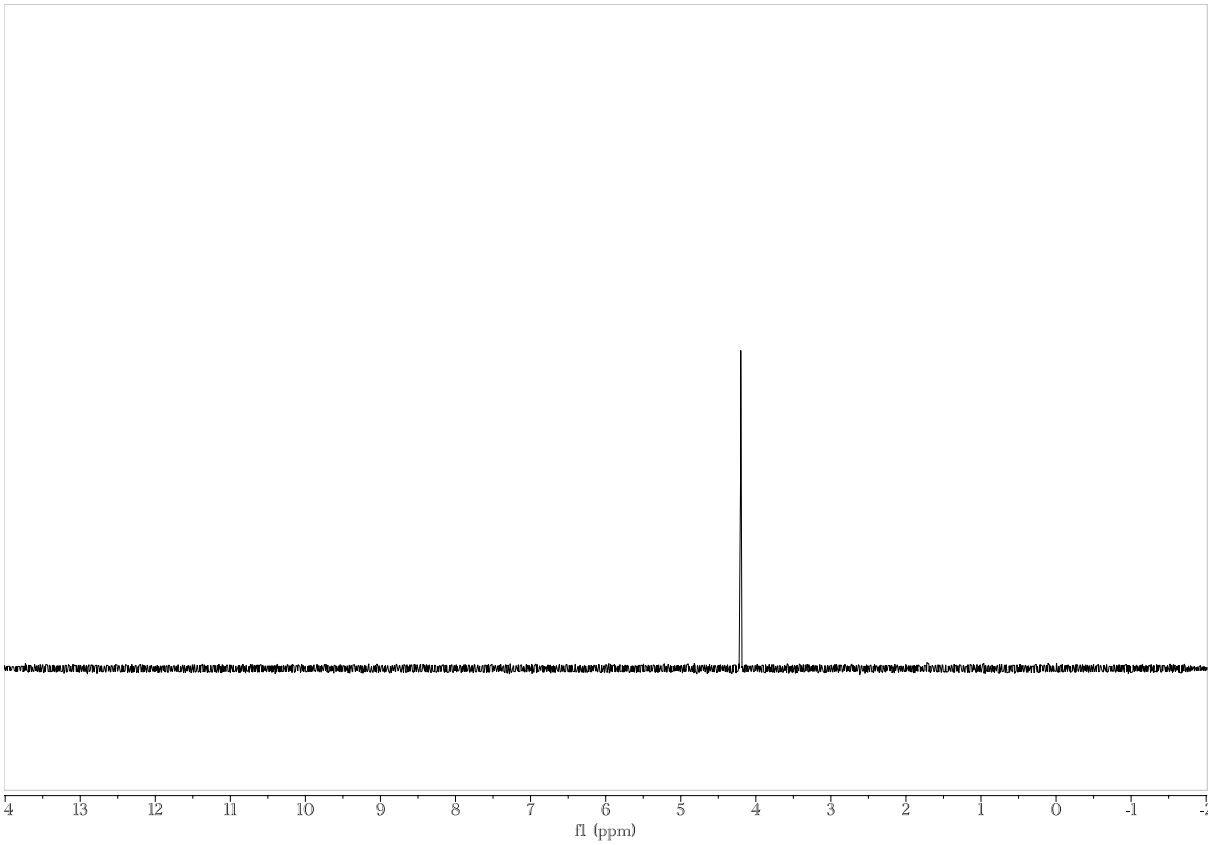

H_a shows no correlation to H_b

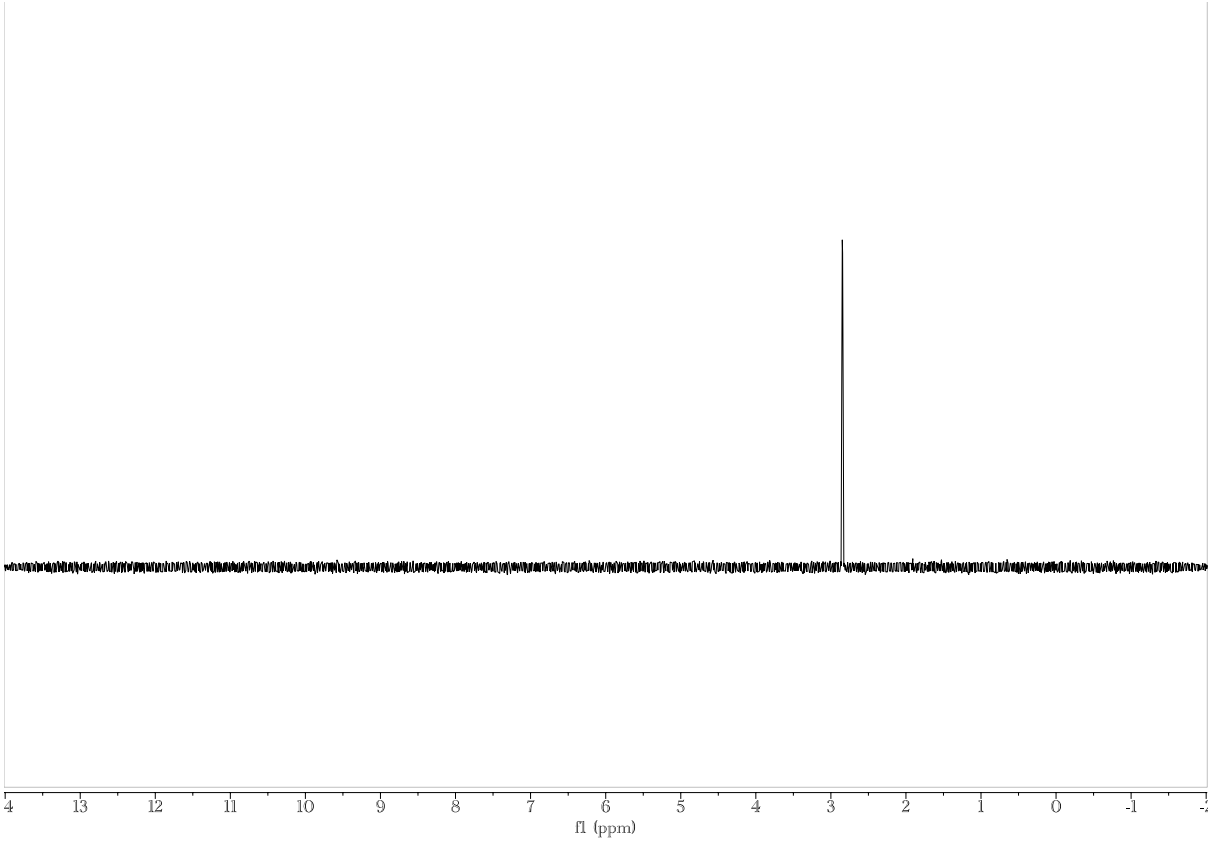

H_b shows no correlation to H_a

On/Off Experiment:

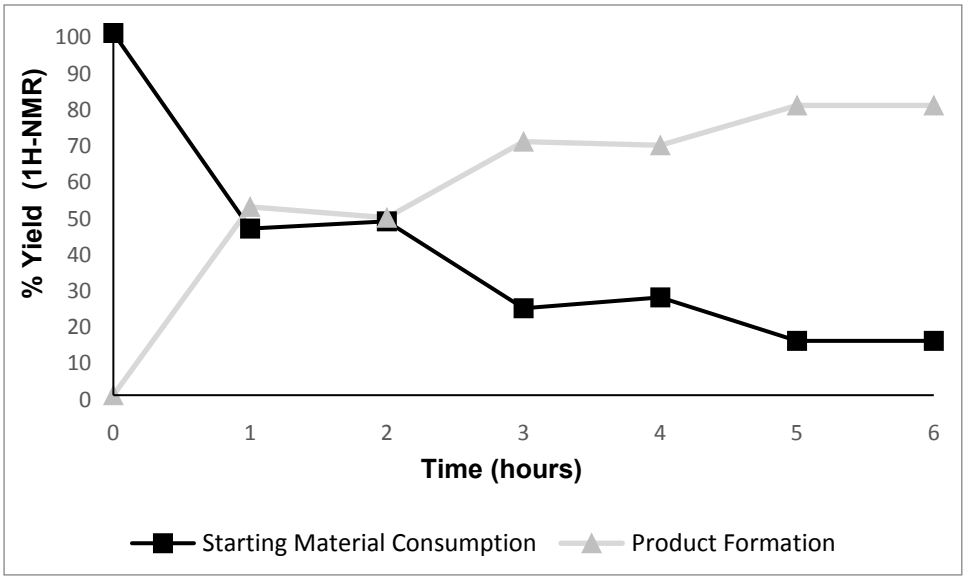

Procedure: Substrate **2a** (1.0 eq., 0.1 mmol), $Pd(OAc)_2$ (12.5 mol%) and DPPent (12.5 mol%) were added to an oven-dried, argon backfilled J-young tube. The reaction vial was purged for 5 minutes and d^8-Toluene (1 mL) was added. A J-young tube screw cap was used to seal the vial and the reaction was irradiated in intervals (1 h on, 1 h off) with Blue LEDs (465 nm). The reaction progress was monitored for 6 h using ^{1}H NMR with 1,3,5-trimethoxybenzene as internal standard.

Radical Scavenger Experiment:

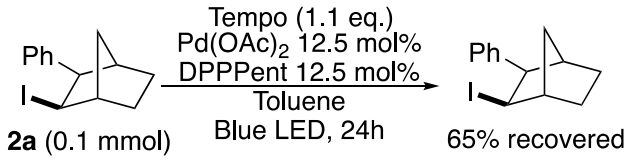

Procedure using TEMPO: Substrate **2a** (1.0 eq., 0.1 mmol), $Pd(OAc)_2$ (12.5 mol%), DPPent (12.5 mol%) and TEMPO (1.1 eq.) were added to an oven-dried, argon backfilled 2-dram vial, equipped with a stir bar. The reaction vial was purged with argon for 5 minutes, anhydrous and degassed toluene (1 mL) was added and a teflon screw cap was used to seal the vial. The reaction mixture was irradiated with Blue LEDs (465 nm) and stirred under a cooling fan for 24 h. The crude reaction mixture was diluted with ethyl acetate, washed through a silica plug (3 cm) and concentrated *in vacuo.* Yields were determined using ^{1}H NMR with 1,3,5-trimethoxybenzene as internal standard in a 3mm NMR tube (0.2 mL $CDCl_3$).

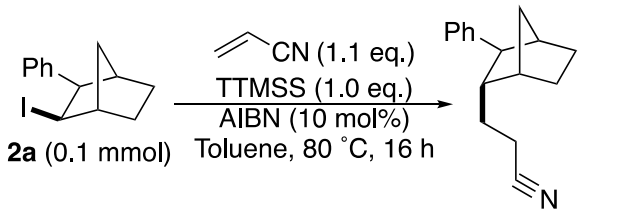

6a: 28% yield, >20:1

Procedure using Arylonitrile[3]**:** Substrate **2a** (1.0 eq., 0.1 mmol), TTMSS (1.0 eq.), AIBN (10 mol%) and acrylonitrile (1.1 eq.) were added to an oven-dried, argon backfilled 2-dram vial, equipped with a stir bar. The reaction vial was purged for 5 minutes and teflon tape was placed around it. Anhydrous and degassed toluene (1 mL) was added, a teflon screw cap was used to seal the vial and the reaction stirred at 80 ˚C for 24 h. The crude reaction mixture was diluted with ethyl acetate, washed through a silica plug (3 cm) and concentrated *in vacuo.* The product **6a** was isolated via column chromatography.

The product anti-relationship between the phenyl group and the acrylonitrile was determined via 1D-NOE.

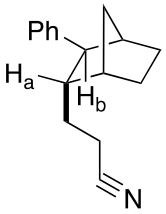

Compound 6a

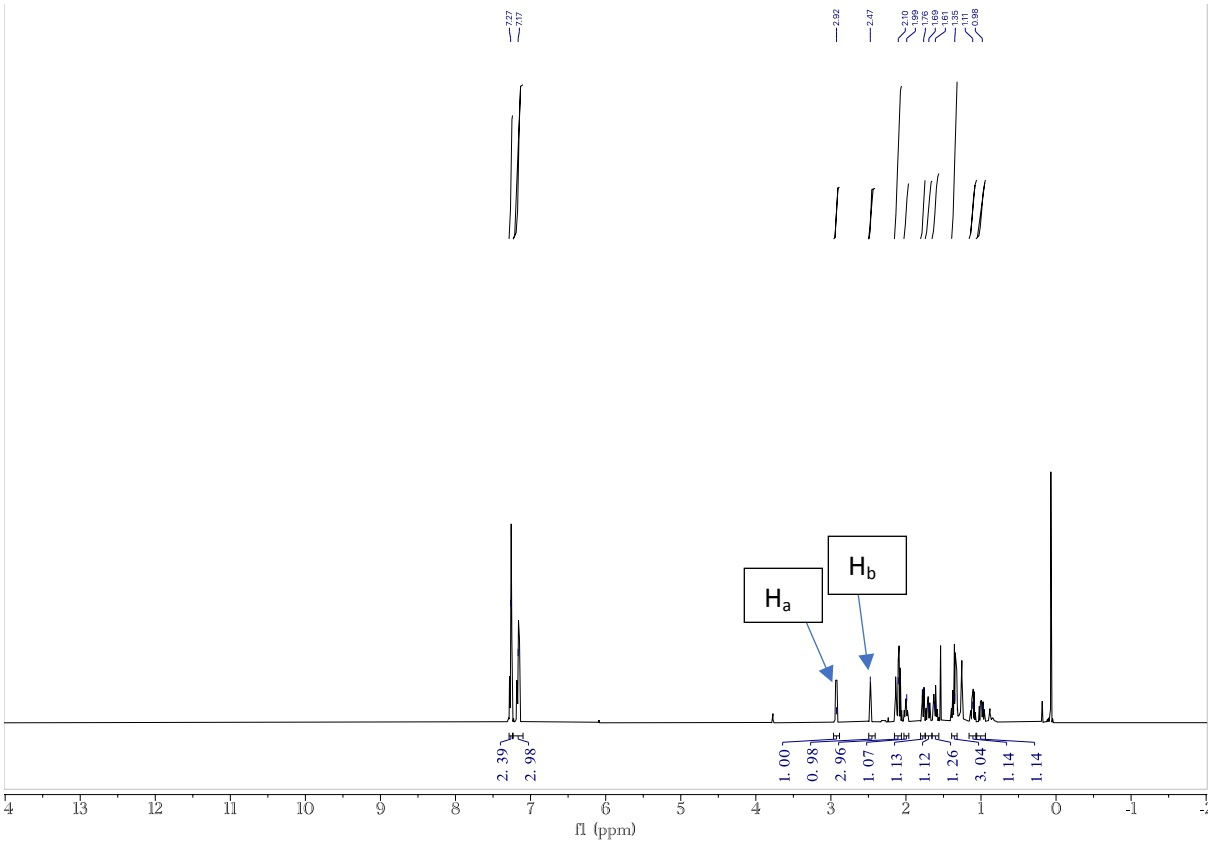

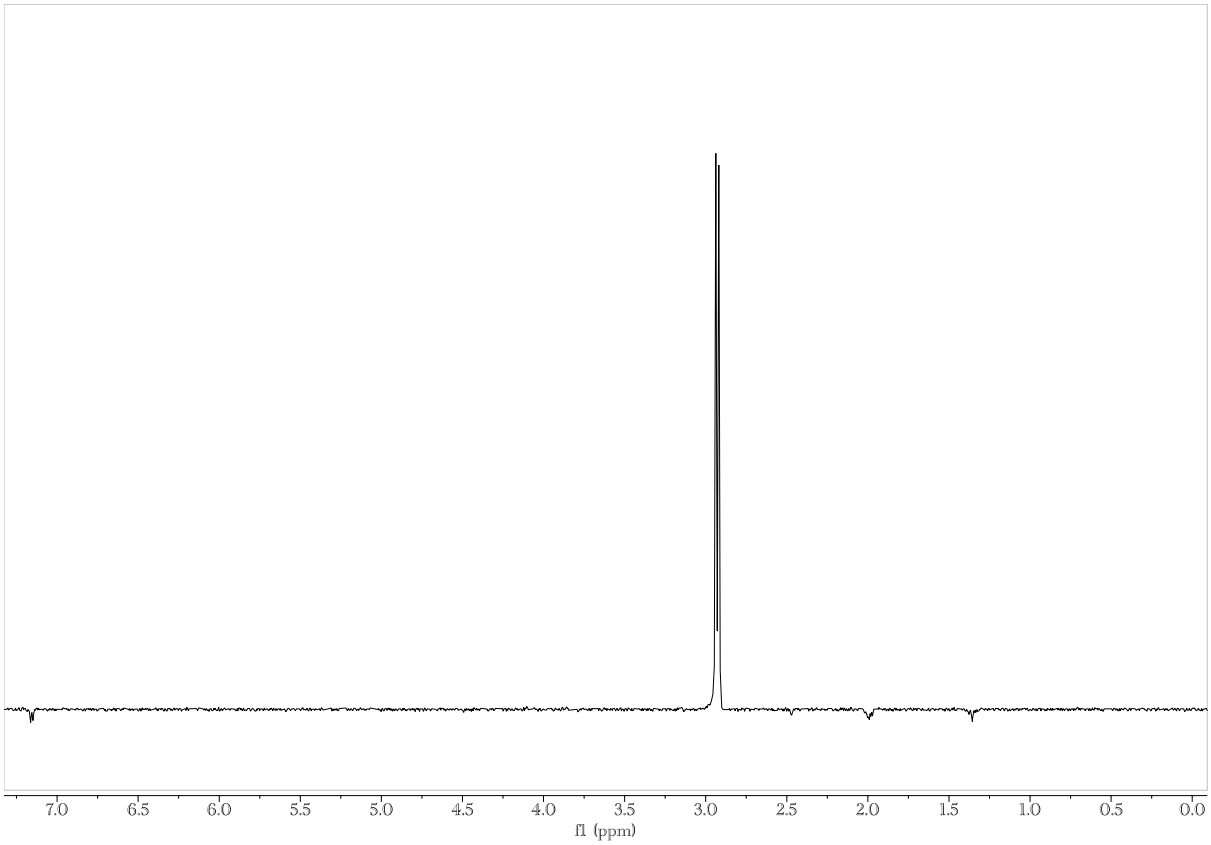

H_a shows no correlation to H_b

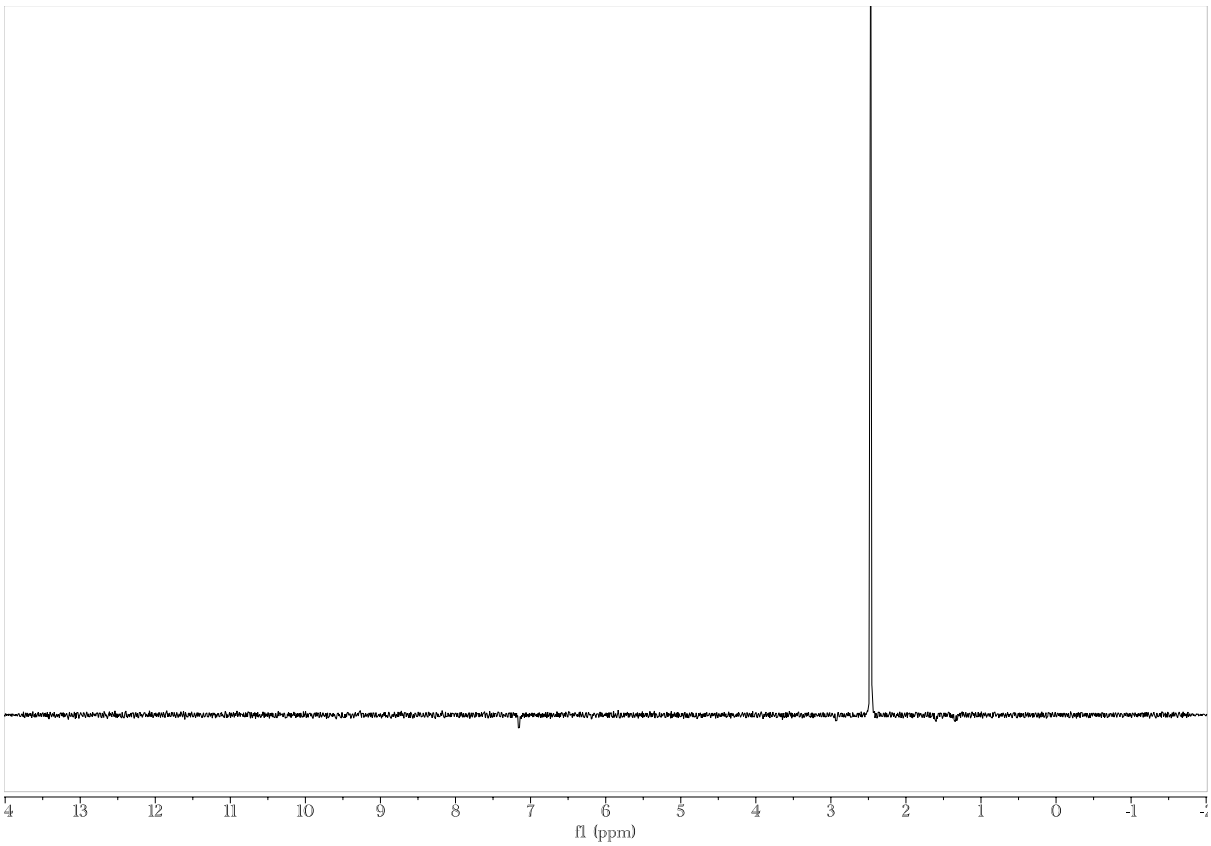

H_b shows no correlation to H_a

Control Studies

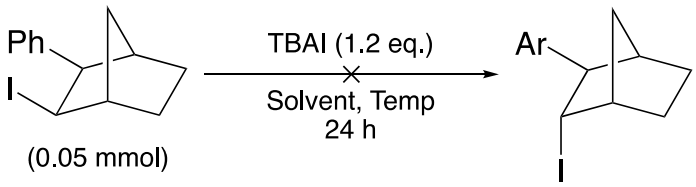

Procedure: Substrate **2a** (1.0 eq., 0.05 mmol), and TBAI (1.2 eq.) were added to an oven-dried, argon backfilled 2-dram vial, equipped with a stir bar. The reaction vial was purged for 5 minutes and teflon tape was placed around it. Anhydrous solvent (1 mL) was added, a teflon screw cap was used to seal the vial and the reaction stirred at reflux for 24 h. The crude reaction mixture was diluted with ethyl acetate, washed through a silica plug (3 cm) and concentrated *in vacuo.* The product **6a** was isolated via column chromatography.

The reaction was run separately with acetonitrile at 80˚C , DMF at 100 ˚C and acetone at 55 ˚C. In each case, there was no conversion to the anti-iodide product, ruling out the potential SN_2 pathway.

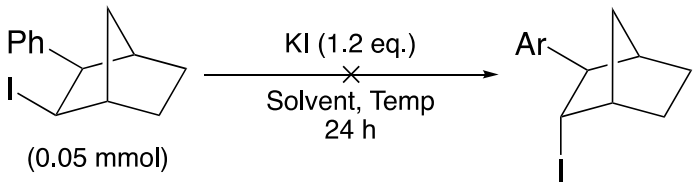

Procedure: Substrate **2a** (1.0 eq., 0.05 mmol), and KI (1.2 eq.) were added to an oven-dried, argon backfilled 2-dram vial, equipped with a stir bar. The reaction vial was purged for 5 minutes and teflon tape was placed around it. Anhydrous solvent (1 mL) was added, a teflon screw cap was used to seal the vial and the reaction stirred at reflux for 24 h. The crude reaction mixture was diluted with ethyl acetate, washed through a silica plug (3 cm) and concentrated *in vacuo.* The product **6a** was isolated via column chromatography.

The reaction was run separately with toluene at 80˚C , and DMF at 80 ˚C. In each case, there was no conversion to the anti-iodide product, ruling out the potential SN_2 pathway.

Computational Details

Density functional theory (DFT) calculations were performed using the Gaussian16 package.[7] All geometry optimizations were performed at the wB97XD level of theory without any constraints at 298 K and 1 atm, using an ultrafine integration grid. The wB97XD functional contains a version of Grimme's D2 dispersion model. The Berny algorithm was used for geometry optimizations.[8] The use of the standard double-ζ basis set (LANL2DZ) and its effective core potentials (ECPs) were used for I.[9] The 6-311+g(d,p) Pople basis set was used for all other atoms (C, H).[10] All frequency calculations were performed at the same level of theory for all intermediates to confirm minima (no imaginary frequencies). Following geometry optimization, electronic energies of the optimized structures were recalculated at the M06L level of theory with the addition of Grimme's D3 dispersion with the original damping function.[11-12] Dunning's augmented correlation consistent quadruple-ζ basis set aug-cc-pVQZ was used for C and H atoms.[13] The Stuttgart and Dresden basis set and its corresponding ECPs were used for I.[14] Solvent effects were assessed using the SMD model developed by Truhlar using the default parameters for toluene.[15] Solution-phase corrected zero-point energies, enthalpies, and Gibbs free energies were obtained by adding the respective gas phase thermodynamic contributions to the single-point energies. The solution phase Gibbs free energies were calculated using the following equations.

$$G_{sol} = G_{gas} + G_{solv} \quad (1)$$

$$G_{gas} = H_{gas} - TS_{gas} \quad (2)$$

$$H_{gas} = E_{SCF} + ZPE \quad (3)$$

Where G_{sol} represents the Gibbs free energy with solvation correction, G_{solv}, from the gas phase Gibbs free energy, G_{gas}. H_{gas} refers to the enthalpy of the species in the gas phase, T is temperature, and S_{gas} is the entropy of the molecule in the gas phase. E_{SCF} refers to the self-consistent field electronic energy and ZPE refers to the zero-point energy. Gibbs free energies are reported kcal mol^{-1}. The Gibbs free energies were converted to standard state by applying a correction of 1.89 kcal mol^{-1} to all species according to (RT ln (c/c_o) at 298.15 K).[16] Grimme's quasi-harmonic approximation was used with a frequency cutoff of 50 cm^{-1}, as recommended by Baik,[17] to correct for the effect of small frequency vibrational modes.[18] The images of the computed structures were created with CYLview (unimportant hydrogens omitted for clarity).[19]

Energies and Cartesian Coordinates

exo-iodonorbornene

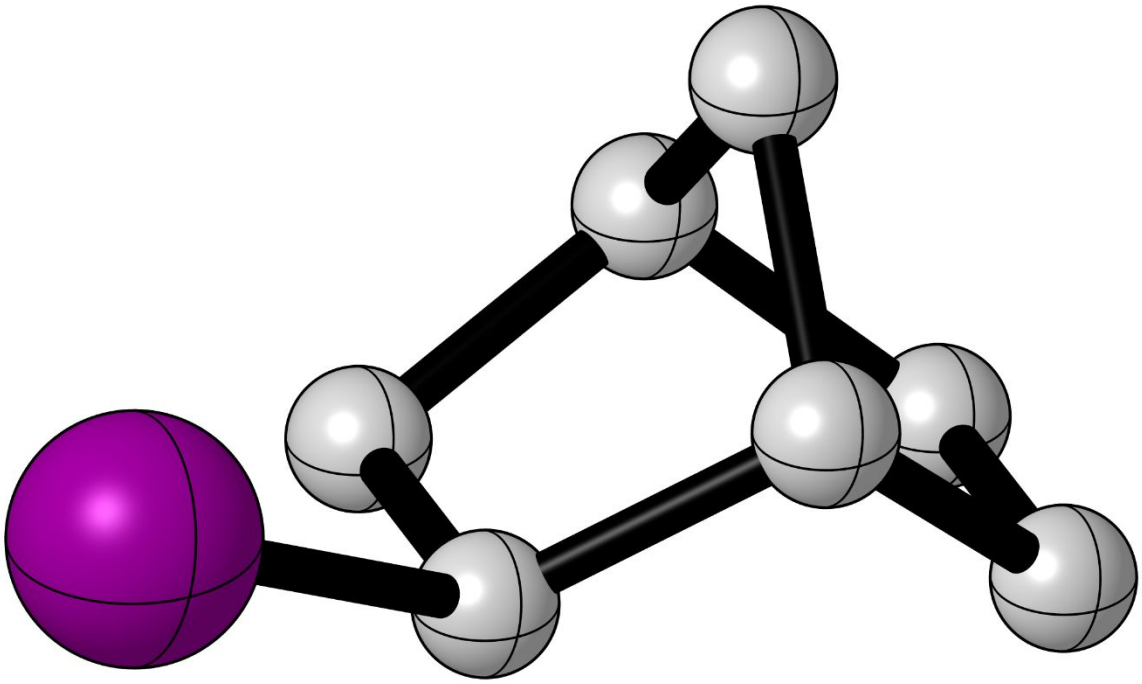

E_{SCF} (M06L/aug-cc-pVQZ) = -284.867166

Zero-point correction = 0.168026 (Hartree/particle)

Thermal correction to entropy = 0.03808

Thermal correction to entropy after Grimme's quasi-harmonic approximation = 0.038054

Gibbs free energy = -284.737194

1	2.329193000	-1.550769000	-1.507630000
6	2.501029000	-1.224626000	-0.478874000

6	2.228604000	1.016597000	0.385630000
6	0.325872000	-0.076742000	-0.620554000
6	1.018374000	1.305196000	-0.524209000
6	1.179255000	-0.976290000	0.282805000
6	3.231181000	0.146343000	-0.391557000
1	1.309329000	1.674567000	-1.510918000
1	0.679572000	-1.887299000	0.606974000
1	3.462050000	0.565423000	-1.374023000
1	3.072212000	-2.011581000	0.019352000
1	2.662083000	1.917541000	0.820411000
1	0.247705000	-0.455922000	-1.636318000
1	0.368107000	2.053594000	-0.070509000
1	4.172626000	0.056694000	0.155863000
6	1.633722000	0.002294000	1.376064000
1	2.379610000	-0.430955000	2.047088000
1	0.807636000	0.401820000	1.968849000
53	-1.777327000	-0.028108000	0.005755000

endo-iodonorbornene

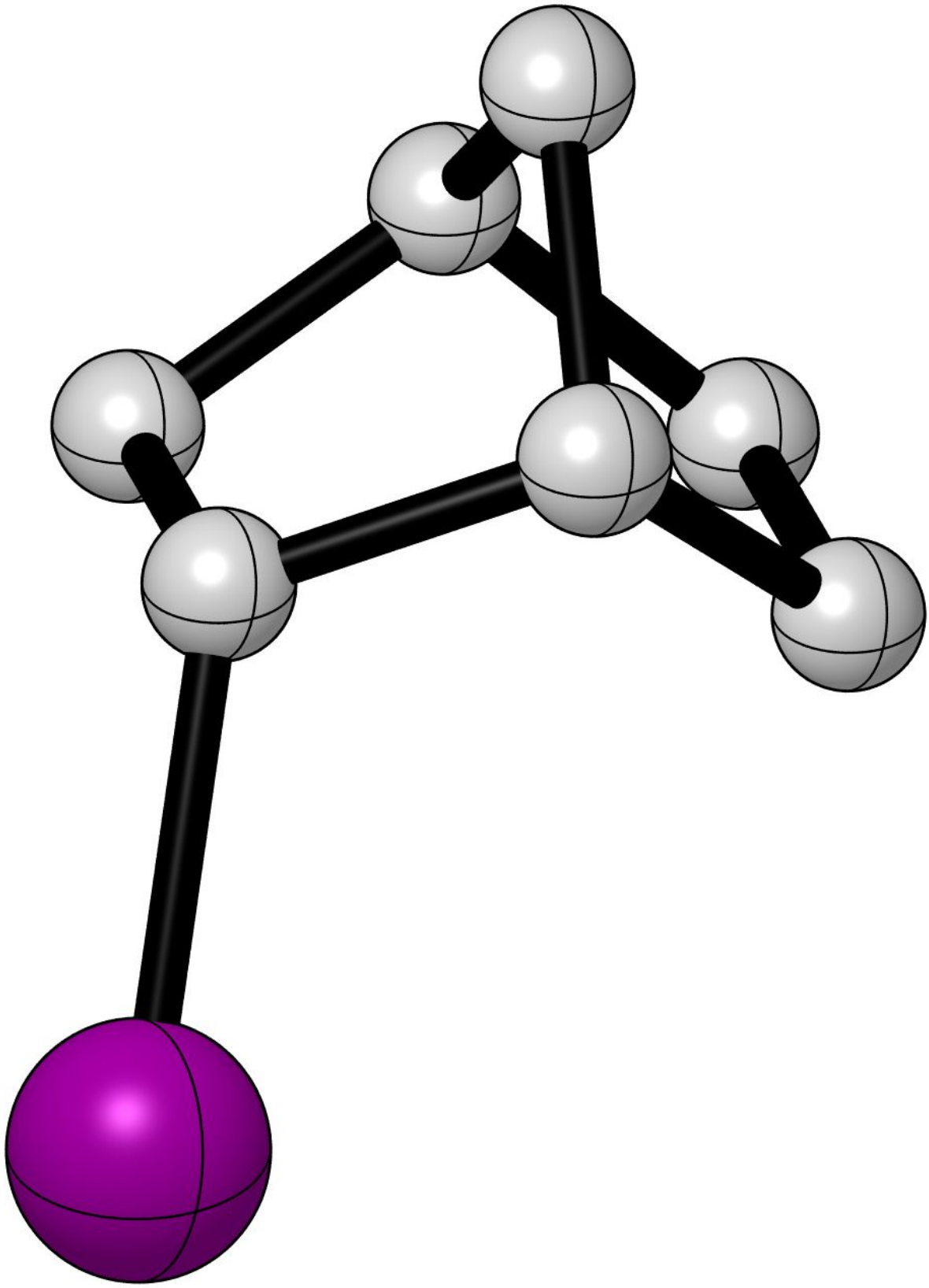

E_{SCF} (M06L/aug-cc-pVQZ) = -284.866471

Zero-point correction = 0.168167 (Hartree/particle)

Thermal correction to entropy = 0.038005

Thermal correction to entropy after Grimme's quasi-harmonic approximation = 0.037961

Gibbs free energy = -284.736265

1	-0.592539000	1.935786000	-0.350950000
6	-1.516287000	1.504650000	0.036777000
6	-2.473396000	-0.648435000	-0.527377000
6	-0.301461000	-0.672434000	0.510723000
6	-1.093220000	-1.323341000	-0.652049000
6	-1.253531000	0.393238000	1.067011000
6	-2.357970000	0.791155000	-1.059687000
1	-0.640550000	-1.146532000	-1.628272000
1	-0.960448000	0.754907000	2.052402000
1	-1.880339000	0.825325000	-2.041648000
1	-2.081476000	2.313070000	0.506335000
1	-3.282233000	-1.225266000	-0.976354000
1	-1.153539000	-2.404656000	-0.505468000
1	-3.346401000	1.247064000	-1.158299000
6	-2.570227000	-0.407911000	0.989572000
1	-3.440070000	0.187971000	1.277964000
1	-2.557902000	-1.327987000	1.580456000
1	-0.061101000	-1.397693000	1.284922000
53	1.686663000	0.045594000	-0.042093000

2a

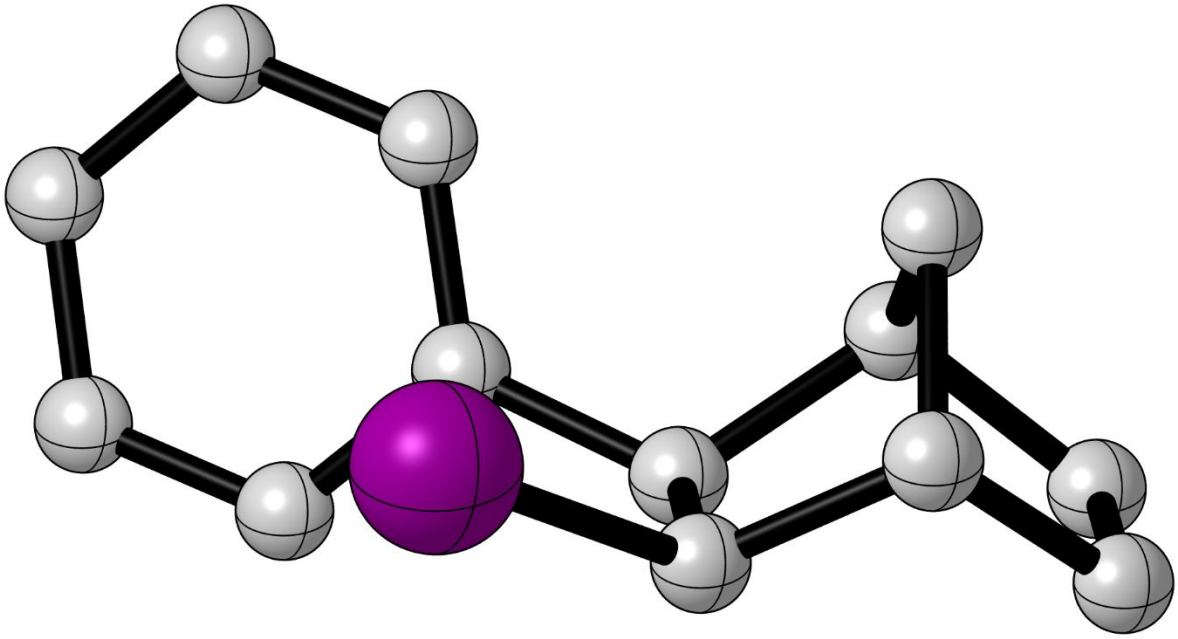

E_{SCF} (M06L/aug-cc-pVQZ) = -515.980337

Zero-point correction = 0.249699 (Hartree/particle)

Thermal correction to entropy = 0.048980

Thermal correction to entropy after Grimme's quasi-harmonic approximation = 0.048306

Gibbs free energy = -515.778944

1	-0.556911000	-2.921718000	0.804066000
6	-1.110162000	-2.097040000	0.348649000
6	-1.141979000	0.119177000	-0.650776000
6	-3.207523000	-1.313697000	-0.540314000
6	-2.372518000	-0.261987000	0.215545000
6	-2.352271000	-2.584156000	-0.424855000
6	-0.271054000	-1.176832000	-0.592881000
1	-4.175674000	-1.468146000	-0.049927000
1	-2.974436000	0.581789000	0.561456000
1	-2.107151000	-3.007270000	-1.404012000
1	-0.307137000	-1.645123000	-1.588489000
1	-1.451126000	0.306240000	-1.686859000
1	-3.393054000	-1.034272000	-1.581511000
1	-2.890184000	-3.348472000	0.147963000
6	-1.750601000	-1.110824000	1.325809000

1	-1.031766000	-0.570767000	1.945226000
1	-2.499248000	-1.578311000	1.976477000
6	1.206307000	-1.055800000	-0.278861000
6	3.973856000	-0.799979000	0.185482000
6	2.086243000	-0.695149000	-1.315340000
6	1.746208000	-1.287025000	0.994471000
6	3.118847000	-1.159347000	1.223696000
6	3.457873000	-0.566765000	-1.085416000
1	1.704299000	-0.503529000	-2.316424000
1	1.113691000	-1.563039000	1.832756000
1	3.519596000	-1.338102000	2.218874000
1	4.120136000	-0.283212000	-1.898415000
1	5.040482000	-0.698895000	0.368035000
53	-0.271903000	1.943573000	0.079991000

3a

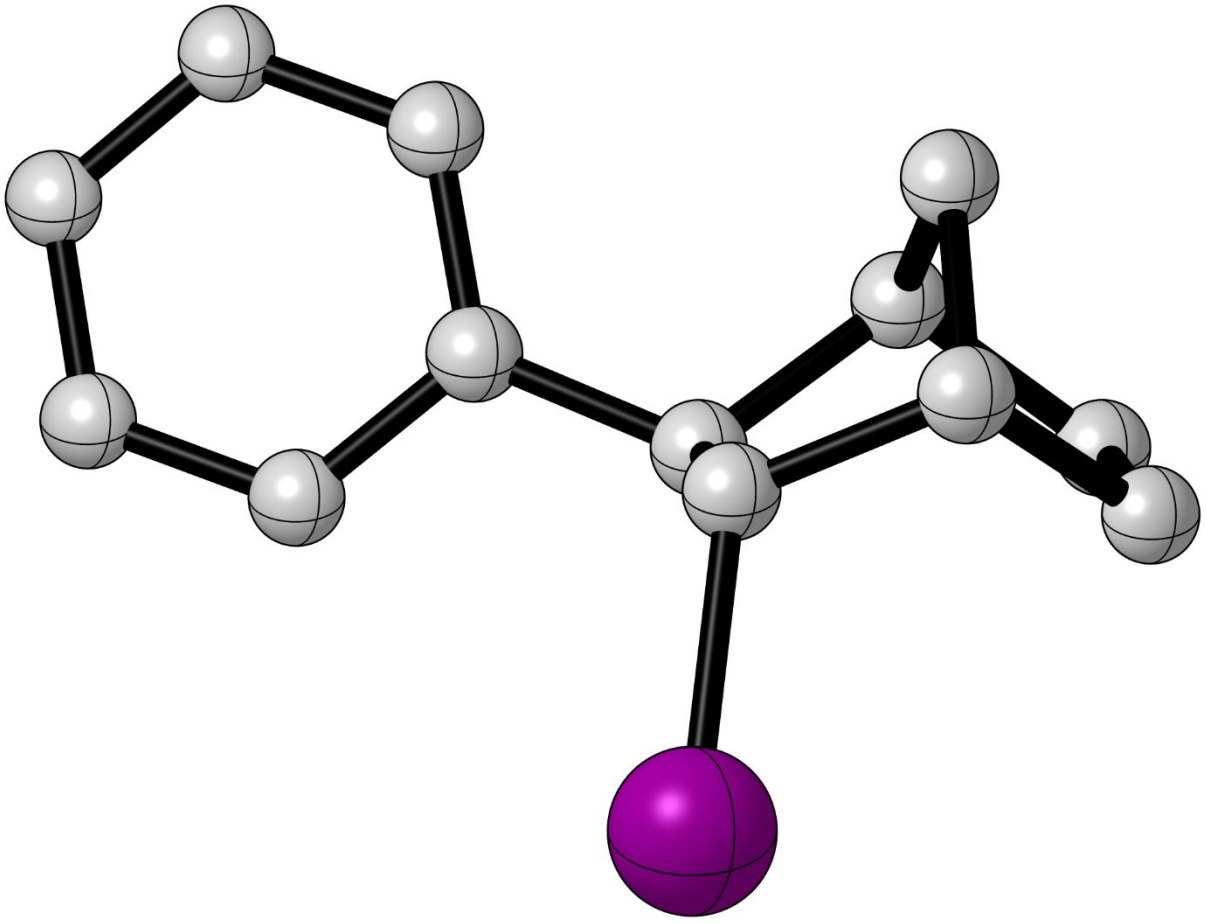

E_{SCF} (M06L/aug-cc-pVQZ) = -515.983147

Zero-point correction = 0.249921 (Hartree/particle)

Thermal correction to entropy = 0.049386

Thermal correction to entropy after Grimme's quasi-harmonic approximation = 0.048442

Gibbs free energy = -515.781668

1	1.147770000	2.772979000	0.894061000
6	0.288032000	2.218045000	0.512647000
6	-0.552184000	0.241111000	-0.592978000
6	-2.101614000	2.111624000	0.284146000
6	-1.300112000	1.558800000	-0.912778000
6	-1.012184000	2.568351000	1.261974000
6	0.444964000	0.666378000	0.521288000
1	-2.701077000	2.975320000	-0.027828000
1	-1.878643000	1.520647000	-1.838802000
1	-1.091021000	2.070532000	2.233076000
1	0.140350000	0.299414000	1.510996000
1	-2.785191000	1.391015000	0.738769000
1	-1.085048000	3.649635000	1.429930000
6	-0.120364000	2.535107000	-0.931263000
1	0.636392000	2.278650000	-1.677694000
1	-0.424734000	3.578018000	-1.074372000
6	1.846009000	0.125986000	0.277937000
6	4.398593000	-0.994641000	-0.145618000
6	2.133289000	-1.194839000	0.664390000
6	2.869341000	0.871859000	-0.324636000
6	4.134541000	0.315451000	-0.534762000
6	3.396978000	-1.750503000	0.453861000
1	1.370254000	-1.807356000	1.139910000
1	2.708481000	1.897581000	-0.642793000
1	4.915421000	0.909290000	-1.002490000
1	3.597329000	-2.774169000	0.761713000

1	5.382679000	-1.425034000	-0.309797000
1	0.000196000	-0.056446000	-1.494543000
53	-1.820470000	-1.375782000	-0.072554000

2o

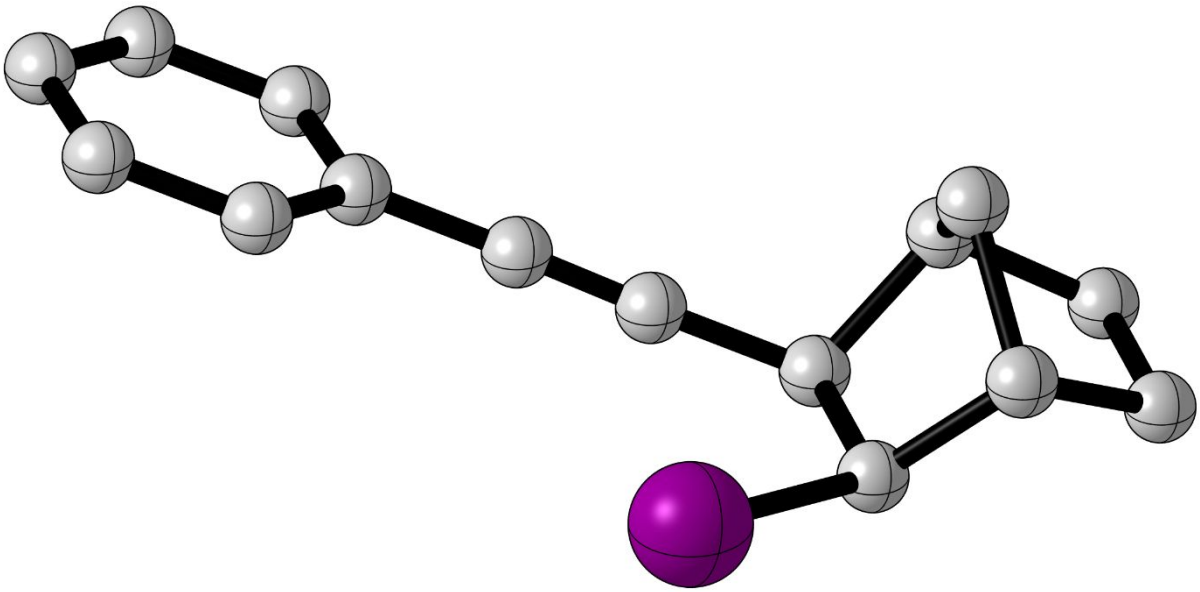

E_{SCF} (M06L/aug-cc-pVQZ) = -592.164792

Zero-point correction = 0.259637 (Hartree/particle)

Thermal correction to entropy = 0.056646

Thermal correction to entropy after Grimme's quasi-harmonic approximation = 0.053834

Gibbs free energy = -591.958989

1	4.414746000	1.165392000	-0.941870000
6	3.955910000	1.511359000	-0.012411000
6	1.678817000	2.265155000	0.290436000
6	2.057173000	0.014612000	-0.541297000
6	1.107313000	1.252005000	-0.745440000
6	2.995751000	0.463135000	0.589235000
6	3.045953000	2.755849000	-0.211217000
1	1.250119000	1.628843000	-1.763579000
1	3.502354000	-0.360375000	1.088392000
1	3.007319000	3.092955000	-1.250024000
1	4.765555000	1.719167000	0.691080000

1	0.969710000	3.058978000	0.520501000
1	2.593443000	-0.226469000	-1.455549000
1	3.391237000	3.598531000	0.392051000
6	2.071733000	1.337690000	1.448202000
1	2.603444000	1.857935000	2.248473000
1	1.226431000	0.791931000	1.872849000
6	-0.316043000	1.030191000	-0.548500000
6	-1.495745000	0.877310000	-0.371689000
6	-2.887107000	0.629314000	-0.148978000
6	-5.596592000	0.119352000	0.292191000
6	-3.310796000	-0.641631000	0.255870000
6	-3.835731000	1.640986000	-0.330585000
6	-5.181719000	1.384190000	-0.110277000
6	-4.658048000	-0.891052000	0.474035000
1	-2.572761000	-1.423085000	0.394139000
1	-3.508251000	2.625082000	-0.644942000
1	-5.909735000	2.174662000	-0.253754000
1	-4.976938000	-1.878817000	0.787163000
1	-6.648658000	-0.078590000	0.463379000
53	1.096354000	-1.891263000	-0.077844000

3o

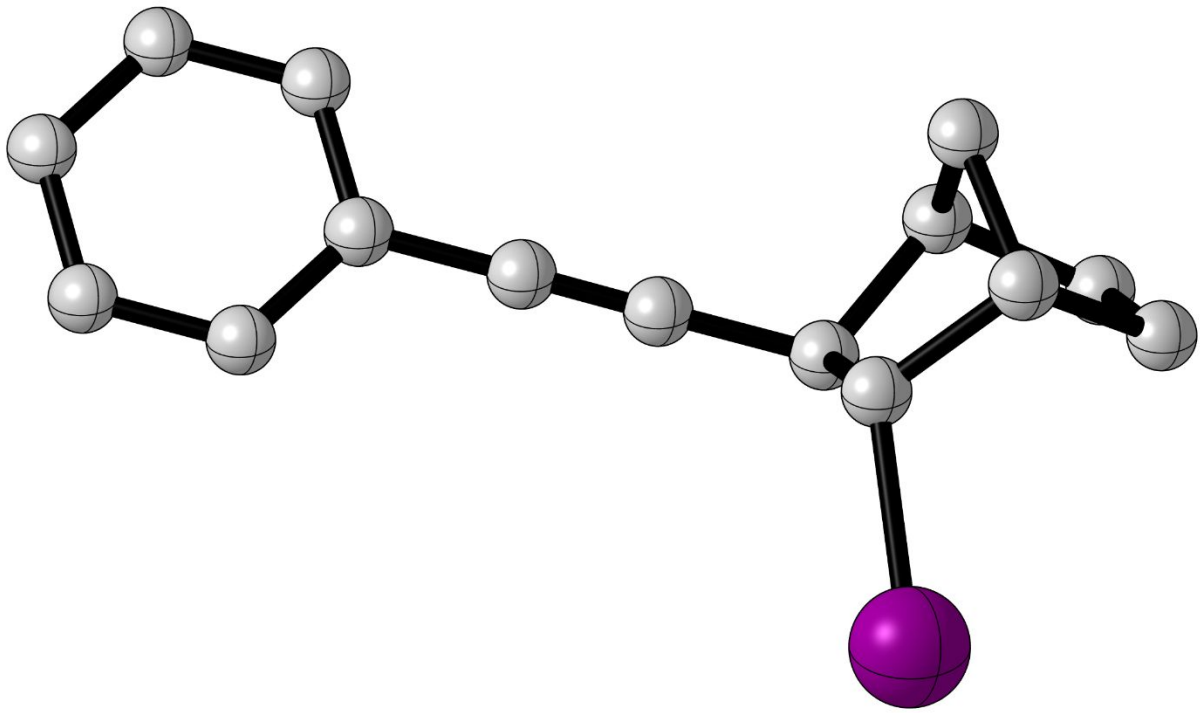

E_{SCF} (M06L/aug-cc-pVQZ) = -592.166970

Zero-point correction = 0.259736 (Hartree/particle)

Thermal correction to entropy = 0.057044

Thermal correction to entropy after Grimme's quasi-harmonic approximation = 0.054162

Gibbs free energy = -591.961396

1	3.809193000	1.085427000	-0.343297000
6	3.179867000	1.888245000	0.042701000
6	0.859197000	2.327004000	-0.501337000
6	1.347882000	0.206784000	0.548821000
6	0.511814000	0.816906000	-0.623473000
6	2.167036000	1.385666000	1.084444000
6	2.280898000	2.531874000	-1.050672000
1	0.843865000	0.431032000	-1.590037000
1	2.593360000	1.188189000	2.067638000
1	2.412820000	2.067376000	-2.030693000
1	3.839543000	2.629292000	0.499628000
1	0.103177000	2.968983000	-0.951402000
1	2.493692000	3.597721000	-1.161745000

6	1.081476000	2.479408000	1.011571000
1	1.461800000	3.465399000	1.289981000
1	0.191858000	2.257557000	1.606151000
6	-0.909845000	0.536319000	-0.468881000
6	-2.082259000	0.306684000	-0.322202000
6	-3.474023000	0.019701000	-0.148170000
6	-6.187867000	-0.546318000	0.194569000
6	-3.929507000	-1.303307000	-0.167376000
6	-4.394796000	1.055444000	0.044597000
6	-5.742308000	0.770895000	0.214430000
6	-5.278295000	-1.580823000	0.003355000
1	-3.216997000	-2.105930000	-0.317024000
1	-4.043667000	2.080605000	0.059051000
1	-6.447508000	1.580864000	0.362749000
1	-5.620617000	-2.609333000	-0.013202000
1	-7.241087000	-0.766011000	0.327519000
1	0.688696000	-0.177598000	1.323056000
53	2.482194000	-1.567179000	-0.005710000

X-Ray Crystallographic Data – Complex I

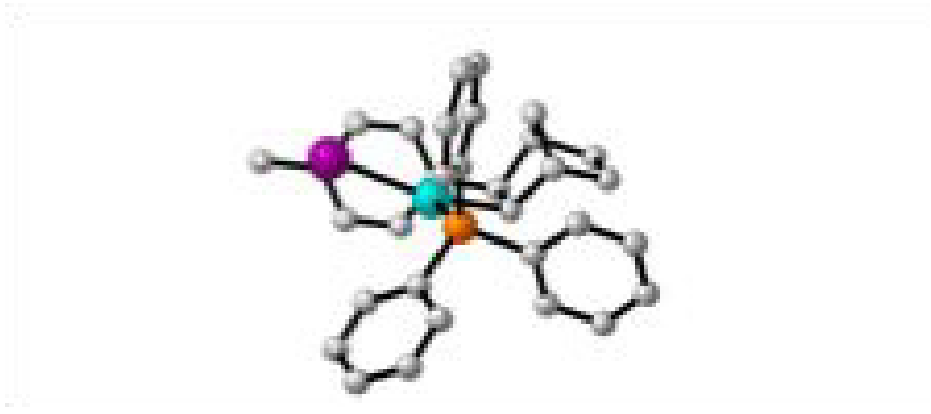

Table S2. Crystal data and structure refinement for d22147_a.

Identification code	d22147_a
Empirical formula	C32 H32 I P Pd
Formula weight	680.84
Temperature	150(2) K

Wavelength	0.71073 Å	
Crystal system	Monoclinic	
Space group	$P2_1/n$	
Unit cell dimensions	a = 12.021(2) Å	a= 90°.
	b = 18.049(3) Å	b= 94.218(5)°.
	c = 12.263(2) Å	g = 90°.
Volume	2653.4(8) $Å^3$	
Z	4	
Density (calculated)	1.704 Mg/m^3	
Absorption coefficient	1.943 mm^{-1}	
F(000)	1352	
Crystal size	0.100 x 0.050 x 0.020 mm^3	
Theta range for data collection	2.012 to 27.461°.	
Index ranges	-15<=h<=15, -23<=k<=23, -15<=l<=15	
Reflections collected	58965	
Independent reflections	6055 [R(int) = 0.1371]	
Completeness to theta = 25.242°	100.0 %	
Absorption correction	Semi-empirical from equivalents	
Max. and min. transmission	0.7456 and 0.6876	
Refinement method	Full-matrix least-squares on F^2	
Data / restraints / parameters	6055 / 0 / 317	
Goodness-of-fit on F^2	1.014	
Final R indices [I>2sigma(I)]	R1 = 0.0398, wR2 = 0.0637	
R indices (all data)	R1 = 0.0807, wR2 = 0.0718	
Extinction coefficient	n/a	
Largest diff. peak and hole	0.556 and -0.675 $e.Å^{-3}$	

Table S3. Atomic coordinates (x 10^4) and equivalent isotropic displacement parameters ($Å^2$x 10^3) for d22147_a. U(eq) is defined as one third of the trace of the orthogonalized U^{ij} tensor.

	x	y	z	U(eq)
I(1)	5512(1)	2130(1)	6776(1)	25(1)
Pd(1)	4112(1)	3225(1)	5976(1)	16(1)
P(1)	4602(1)	4041(1)	7328(1)	15(1)
C(15)	3826(3)	4919(2)	7318(3)	17(1)
C(9)	4184(3)	2861(2)	3944(3)	20(1)
C(1)	2782(3)	3860(2)	5378(3)	15(1)
C(2)	2309(3)	3343(2)	4456(3)	17(1)
C(25)	4839(4)	3548(2)	10634(4)	24(1)
C(11)	4683(4)	1561(2)	4006(3)	22(1)
C(20)	3071(3)	5093(2)	8101(3)	18(1)
C(16)	3939(4)	5408(2)	6447(3)	20(1)
C(3)	1153(3)	3126(2)	4827(3)	17(1)
C(10)	4924(3)	2292(2)	3763(3)	21(1)
C(6)	1854(3)	3896(2)	6155(3)	20(1)
C(7)	1363(3)	3107(2)	6075(3)	18(1)
C(32)	6830(4)	4018(2)	6751(3)	24(1)
C(13)	2902(4)	1962(2)	4590(3)	20(1)
C(27)	6040(3)	4372(2)	7350(3)	18(1)
C(30)	8203(4)	4925(2)	7321(4)	28(1)
C(8)	3139(3)	2702(2)	4357(3)	18(1)
C(12)	3654(4)	1410(2)	4412(3)	23(1)
C(22)	3481(3)	3200(2)	8780(3)	19(1)
C(26)	5080(4)	3836(2)	9615(3)	21(1)
C(28)	6365(4)	5010(2)	7929(4)	24(1)
C(21)	4389(3)	3663(2)	8685(3)	17(1)
C(5)	894(3)	4346(2)	5578(3)	19(1)
C(19)	2409(3)	5720(2)	7968(4)	24(1)
C(31)	7895(4)	4297(3)	6739(4)	31(1)
C(4)	392(3)	3812(2)	4690(3)	22(1)
C(29)	7440(4)	5282(2)	7925(4)	27(1)
C(18)	2511(4)	6193(2)	7087(4)	26(1)
C(24)	3923(4)	3101(2)	10718(4)	25(1)
C(23)	3229(4)	2922(2)	9795(4)	24(1)

C(14)	5525(4)	952(3)	3887(4)	33(1)
C(17)	3276(4)	6043(2)	6339(4)	23(1)

Table S4. Bond lengths [Å] and angles [°] for d22147_a.

I(1)-Pd(1)	2.7313(5)
Pd(1)-C(1)	2.058(4)
Pd(1)-P(1)	2.2625(11)
Pd(1)-C(8)	2.421(4)
Pd(1)-C(9)	2.584(4)
P(1)-C(27)	1.827(4)
P(1)-C(21)	1.834(4)
P(1)-C(15)	1.839(4)
C(15)-C(16)	1.399(6)
C(15)-C(20)	1.404(6)
C(9)-C(10)	1.388(6)
C(9)-C(8)	1.418(6)
C(9)-H(9A)	1.0000
C(1)-C(6)	1.520(5)
C(1)-C(2)	1.543(5)
C(1)-H(1A)	1.0000
C(2)-C(8)	1.539(5)
C(2)-C(3)	1.544(5)
C(2)-H(2A)	1.0000
C(25)-C(24)	1.375(6)
C(25)-C(26)	1.403(6)
C(25)-H(25A)	0.9500
C(11)-C(10)	1.387(6)
C(11)-C(12)	1.394(6)
C(11)-C(14)	1.509(6)
C(20)-C(19)	1.386(6)
C(20)-H(20A)	0.9500
C(16)-C(17)	1.397(6)
C(16)-H(16A)	0.9500
C(3)-C(7)	1.533(6)
C(3)-C(4)	1.541(5)
C(3)-H(3A)	1.0000
C(10)-H(10A)	0.9500
C(6)-C(5)	1.539(6)
C(6)-C(7)	1.543(5)
C(6)-H(6A)	1.0000

C(7)-H(7A)	0.9900
C(7)-H(7B)	0.9900
C(32)-C(31)	1.376(6)
C(32)-C(27)	1.397(6)
C(32)-H(32A)	0.9500
C(13)-C(12)	1.373(6)
C(13)-C(8)	1.399(5)
C(13)-H(13A)	0.9500
C(27)-C(28)	1.394(6)
C(30)-C(31)	1.376(6)
C(30)-C(29)	1.380(6)
C(30)-H(30A)	0.9500
C(12)-H(12A)	0.9500
C(22)-C(21)	1.386(6)
C(22)-C(23)	1.395(6)
C(22)-H(22A)	0.9500
C(26)-C(21)	1.396(6)
C(26)-H(26A)	0.9500
C(28)-C(29)	1.382(6)
C(28)-H(28A)	0.9500
C(5)-C(4)	1.544(5)
C(5)-H(5A)	0.9900
C(5)-H(5B)	0.9900
C(19)-C(18)	1.388(6)
C(19)-H(19A)	0.9500
C(31)-H(31A)	0.9500
C(4)-H(4A)	0.9900
C(4)-H(4B)	0.9900
C(29)-H(29A)	0.9500
C(18)-C(17)	1.373(6)
C(18)-H(18A)	0.9500
C(24)-C(23)	1.395(6)
C(24)-H(24A)	0.9500
C(23)-H(23A)	0.9500
C(14)-H(14A)	0.9800
C(14)-H(14B)	0.9800
C(14)-H(14C)	0.9800
C(17)-H(17A)	0.9500

C(1)-Pd(1)-P(1)	92.99(11)
C(1)-Pd(1)-C(8)	67.00(14)
P(1)-Pd(1)-C(8)	159.86(10)
C(1)-Pd(1)-C(9)	83.03(14)
P(1)-Pd(1)-C(9)	147.82(10)
C(8)-Pd(1)-C(9)	32.71(13)
C(1)-Pd(1)-I(1)	166.68(11)
P(1)-Pd(1)-I(1)	95.02(3)
C(8)-Pd(1)-I(1)	105.07(9)
C(9)-Pd(1)-I(1)	95.66(10)
C(27)-P(1)-C(21)	107.65(19)
C(27)-P(1)-C(15)	101.37(18)
C(21)-P(1)-C(15)	102.82(18)
C(27)-P(1)-Pd(1)	114.76(14)
C(21)-P(1)-Pd(1)	112.10(13)
C(15)-P(1)-Pd(1)	116.85(14)
C(16)-C(15)-C(20)	119.0(4)
C(16)-C(15)-P(1)	118.0(3)
C(20)-C(15)-P(1)	122.8(3)
C(10)-C(9)-C(8)	120.2(4)
C(10)-C(9)-Pd(1)	114.2(3)
C(8)-C(9)-Pd(1)	67.3(2)
C(10)-C(9)-H(9A)	115.5
C(8)-C(9)-H(9A)	115.5
Pd(1)-C(9)-H(9A)	115.5
C(6)-C(1)-C(2)	103.7(3)
C(6)-C(1)-Pd(1)	112.8(3)
C(2)-C(1)-Pd(1)	99.1(2)
C(6)-C(1)-H(1A)	113.3
C(2)-C(1)-H(1A)	113.3
Pd(1)-C(1)-H(1A)	113.3
C(8)-C(2)-C(1)	107.9(3)
C(8)-C(2)-C(3)	115.8(3)
C(1)-C(2)-C(3)	103.2(3)
C(8)-C(2)-H(2A)	109.9
C(1)-C(2)-H(2A)	109.9
C(3)-C(2)-H(2A)	109.9

C(24)-C(25)-C(26)	120.2(4)
C(24)-C(25)-H(25A)	119.9
C(26)-C(25)-H(25A)	119.9
C(10)-C(11)-C(12)	117.8(4)
C(10)-C(11)-C(14)	121.4(4)
C(12)-C(11)-C(14)	120.7(4)
C(19)-C(20)-C(15)	119.8(4)
C(19)-C(20)-H(20A)	120.1
C(15)-C(20)-H(20A)	120.1
C(17)-C(16)-C(15)	120.2(4)
C(17)-C(16)-H(16A)	119.9
C(15)-C(16)-H(16A)	119.9
C(7)-C(3)-C(4)	100.4(3)
C(7)-C(3)-C(2)	102.4(3)
C(4)-C(3)-C(2)	107.7(3)
C(7)-C(3)-H(3A)	114.9
C(4)-C(3)-H(3A)	114.9
C(2)-C(3)-H(3A)	114.9
C(11)-C(10)-C(9)	121.6(4)
C(11)-C(10)-H(10A)	119.2
C(9)-C(10)-H(10A)	119.2
C(1)-C(6)-C(5)	107.1(3)
C(1)-C(6)-C(7)	102.4(3)
C(5)-C(6)-C(7)	100.8(3)
C(1)-C(6)-H(6A)	114.9
C(5)-C(6)-H(6A)	114.9
C(7)-C(6)-H(6A)	114.9
C(3)-C(7)-C(6)	94.4(3)
C(3)-C(7)-H(7A)	112.9
C(6)-C(7)-H(7A)	112.9
C(3)-C(7)-H(7B)	112.9
C(6)-C(7)-H(7B)	112.9
H(7A)-C(7)-H(7B)	110.3
C(31)-C(32)-C(27)	120.5(4)
C(31)-C(32)-H(32A)	119.8
C(27)-C(32)-H(32A)	119.8
C(12)-C(13)-C(8)	120.9(4)
C(12)-C(13)-H(13A)	119.5

C(8)-C(13)-H(13A)	119.5
C(28)-C(27)-C(32)	118.0(4)
C(28)-C(27)-P(1)	120.5(3)
C(32)-C(27)-P(1)	121.4(3)
C(31)-C(30)-C(29)	119.9(4)
C(31)-C(30)-H(30A)	120.0
C(29)-C(30)-H(30A)	120.0
C(13)-C(8)-C(9)	117.7(4)
C(13)-C(8)-C(2)	124.0(4)
C(9)-C(8)-C(2)	118.2(3)
C(13)-C(8)-Pd(1)	107.4(3)
C(9)-C(8)-Pd(1)	80.0(2)
C(2)-C(8)-Pd(1)	85.3(2)
C(13)-C(12)-C(11)	121.8(4)
C(13)-C(12)-H(12A)	119.1
C(11)-C(12)-H(12A)	119.1
C(21)-C(22)-C(23)	121.1(4)
C(21)-C(22)-H(22A)	119.4
C(23)-C(22)-H(22A)	119.4
C(21)-C(26)-C(25)	119.7(4)
C(21)-C(26)-H(26A)	120.2
C(25)-C(26)-H(26A)	120.2
C(29)-C(28)-C(27)	121.2(4)
C(29)-C(28)-H(28A)	119.4
C(27)-C(28)-H(28A)	119.4
C(22)-C(21)-C(26)	119.4(4)
C(22)-C(21)-P(1)	117.7(3)
C(26)-C(21)-P(1)	122.9(3)
C(6)-C(5)-C(4)	103.6(3)
C(6)-C(5)-H(5A)	111.0
C(4)-C(5)-H(5A)	111.0
C(6)-C(5)-H(5B)	111.0
C(4)-C(5)-H(5B)	111.0
H(5A)-C(5)-H(5B)	109.0
C(20)-C(19)-C(18)	120.7(4)
C(20)-C(19)-H(19A)	119.6
C(18)-C(19)-H(19A)	119.6
C(30)-C(31)-C(32)	120.7(4)

C(30)-C(31)-H(31A)	119.6
C(32)-C(31)-H(31A)	119.6
C(3)-C(4)-C(5)	103.1(3)
C(3)-C(4)-H(4A)	111.1
C(5)-C(4)-H(4A)	111.1
C(3)-C(4)-H(4B)	111.1
C(5)-C(4)-H(4B)	111.1
H(4A)-C(4)-H(4B)	109.1
C(30)-C(29)-C(28)	119.6(4)
C(30)-C(29)-H(29A)	120.2
C(28)-C(29)-H(29A)	120.2
C(17)-C(18)-C(19)	120.0(4)
C(17)-C(18)-H(18A)	120.0
C(19)-C(18)-H(18A)	120.0
C(25)-C(24)-C(23)	120.6(4)
C(25)-C(24)-H(24A)	119.7
C(23)-C(24)-H(24A)	119.7
C(24)-C(23)-C(22)	118.9(4)
C(24)-C(23)-H(23A)	120.5
C(22)-C(23)-H(23A)	120.5
C(11)-C(14)-H(14A)	109.5
C(11)-C(14)-H(14B)	109.5
H(14A)-C(14)-H(14B)	109.5
C(11)-C(14)-H(14C)	109.5
H(14A)-C(14)-H(14C)	109.5
H(14B)-C(14)-H(14C)	109.5
C(18)-C(17)-C(16)	120.3(4)
C(18)-C(17)-H(17A)	119.9
C(16)-C(17)-H(17A)	119.9

Symmetry transformations used to generate equivalent atoms:

Table S5. Anisotropic displacement parameters ($Å^2 x\ 10^3$) for d22147_a. The anisotropic displacement factor exponent takes the form: $-2p^2[\ h^2\ a^{*2}U^{11} + ...\ + 2\ h\ k\ a^*\ b^*\ U^{12}\ ]$

	U^{11}	U^{22}	U^{33}	U^{23}	U^{13}	U^{12}
I(1)	29(1)	24(1)	21(1)	-1(1)	-2(1)	10(1)
Pd(1)	15(1)	16(1)	16(1)	-2(1)	0(1)	2(1)
P(1)	14(1)	16(1)	16(1)	-2(1)	1(1)	0(1)
C(15)	12(2)	21(2)	19(2)	-6(2)	-1(2)	-2(2)
C(9)	24(2)	29(2)	7(2)	1(2)	4(2)	-3(2)
C(1)	15(2)	13(2)	16(2)	2(2)	-3(2)	2(2)
C(2)	18(2)	17(2)	16(2)	1(2)	1(2)	2(2)
C(25)	27(3)	22(2)	21(3)	-6(2)	-3(2)	8(2)
C(11)	22(2)	28(3)	18(2)	-9(2)	2(2)	3(2)
C(20)	14(2)	18(2)	22(2)	-4(2)	0(2)	-4(2)
C(16)	20(2)	18(2)	23(2)	-2(2)	5(2)	-5(2)
C(3)	15(2)	20(2)	17(2)	2(2)	0(2)	0(2)
C(10)	16(2)	31(3)	17(2)	-4(2)	7(2)	-1(2)
C(6)	16(2)	19(2)	24(2)	-3(2)	1(2)	2(2)
C(7)	13(2)	21(2)	20(2)	1(2)	4(2)	0(2)
C(32)	24(3)	29(3)	20(2)	-4(2)	2(2)	-2(2)
C(13)	23(2)	19(2)	18(2)	-4(2)	2(2)	-3(2)
C(27)	16(2)	21(2)	19(2)	1(2)	-2(2)	3(2)
C(30)	17(2)	35(3)	32(3)	15(2)	4(2)	-5(2)
C(8)	19(2)	22(2)	12(2)	-3(2)	-1(2)	-2(2)
C(12)	30(3)	15(2)	25(3)	-2(2)	2(2)	-1(2)
C(22)	19(2)	19(2)	18(2)	-2(2)	-1(2)	-3(2)
C(26)	17(2)	20(2)	26(3)	-10(2)	0(2)	0(2)
C(28)	18(2)	21(2)	34(3)	-5(2)	2(2)	1(2)
C(21)	18(2)	16(2)	17(2)	-4(2)	1(2)	6(2)
C(5)	13(2)	18(2)	26(3)	-4(2)	2(2)	2(2)
C(19)	15(2)	25(2)	31(3)	-9(2)	6(2)	0(2)
C(31)	19(3)	47(3)	30(3)	7(2)	12(2)	1(2)
C(4)	14(2)	27(2)	24(2)	2(2)	1(2)	-2(2)
C(29)	23(3)	24(2)	34(3)	4(2)	-4(2)	-4(2)
C(18)	25(3)	14(2)	38(3)	-5(2)	-7(2)	2(2)
C(24)	27(3)	29(3)	19(2)	-1(2)	4(2)	2(2)
C(23)	26(3)	24(2)	24(2)	-1(2)	3(2)	-2(2)

C(14)	29(3)	34(3)	37(3)	-7(2)	6(2)	4(2)
C(17)	31(3)	13(2)	25(3)	4(2)	-3(2)	0(2)

Table S6. Hydrogen coordinates (x 10^4) and isotropic displacement parameters (Å^{2}x 10^3) for d22147_a.

	x	y	z	U(eq)
H(9A)	4187	3284	3418	24
H(1A)	3006	4358	5110	18
H(2A)	2219	3622	3750	20
H(25A)	5309	3662	11268	29
H(20A)	3013	4782	8719	22
H(16A)	4467	5307	5928	24
H(3A)	831	2661	4492	21
H(10A)	5611	2405	3465	25
H(6A)	2093	4064	6913	24
H(7A)	1907	2721	6330	22
H(7B)	668	3056	6454	22
H(32A)	6631	3582	6349	29
H(13A)	2212	1840	4875	24
H(30A)	8940	5113	7307	33
H(12A)	3468	912	4570	28
H(22A)	3023	3071	8145	23
H(26A)	5710	4148	9559	26
H(28A)	5838	5263	8334	29
H(5A)	1177	4803	5247	23
H(5B)	334	4483	6096	23
H(19A)	1881	5828	8485	28
H(31A)	8423	4053	6325	38
H(4A)	-390	3685	4816	26
H(4B)	416	4030	3952	26
H(29A)	7652	5712	8335	33
H(18A)	2050	6620	7002	31
H(24A)	3761	2912	11412	30
H(23A)	2594	2615	9855	29
H(14A)	5157	469	3932	50
H(14B)	6120	992	4475	50
H(14C)	5845	998	3178	50
H(17A)	3355	6372	5746	28

Table S7. Torsion angles [°] for d22147_a.

C(27)-P(1)-C(15)-C(16)	60.0(4)
C(21)-P(1)-C(15)-C(16)	171.3(3)
Pd(1)-P(1)-C(15)-C(16)	-65.5(3)
C(27)-P(1)-C(15)-C(20)	-124.6(3)
C(21)-P(1)-C(15)-C(20)	-13.4(4)
Pd(1)-P(1)-C(15)-C(20)	109.8(3)
C(6)-C(1)-C(2)-C(8)	-124.1(3)
Pd(1)-C(1)-C(2)-C(8)	-7.8(3)
C(6)-C(1)-C(2)-C(3)	-1.1(4)
Pd(1)-C(1)-C(2)-C(3)	115.3(3)
C(16)-C(15)-C(20)-C(19)	3.5(6)
P(1)-C(15)-C(20)-C(19)	-171.8(3)
C(20)-C(15)-C(16)-C(17)	-2.5(6)
P(1)-C(15)-C(16)-C(17)	173.0(3)
C(8)-C(2)-C(3)-C(7)	84.0(4)
C(1)-C(2)-C(3)-C(7)	-33.6(4)
C(8)-C(2)-C(3)-C(4)	-170.7(3)
C(1)-C(2)-C(3)-C(4)	71.7(4)
C(12)-C(11)-C(10)-C(9)	1.8(6)
C(14)-C(11)-C(10)-C(9)	-175.4(4)
C(8)-C(9)-C(10)-C(11)	-1.9(6)
Pd(1)-C(9)-C(10)-C(11)	74.9(5)
C(2)-C(1)-C(6)-C(5)	-70.4(4)
Pd(1)-C(1)-C(6)-C(5)	-176.7(2)
C(2)-C(1)-C(6)-C(7)	35.2(4)
Pd(1)-C(1)-C(6)-C(7)	-71.1(3)
C(4)-C(3)-C(7)-C(6)	-57.5(3)
C(2)-C(3)-C(7)-C(6)	53.5(3)
C(1)-C(6)-C(7)-C(3)	-54.4(4)
C(5)-C(6)-C(7)-C(3)	56.0(3)
C(31)-C(32)-C(27)-C(28)	0.0(6)
C(31)-C(32)-C(27)-P(1)	177.0(3)
C(21)-P(1)-C(27)-C(28)	-71.8(4)
C(15)-P(1)-C(27)-C(28)	35.7(4)
Pd(1)-P(1)-C(27)-C(28)	162.6(3)
C(21)-P(1)-C(27)-C(32)	111.2(4)

C(15)-P(1)-C(27)-C(32)	-141.3(3)
Pd(1)-P(1)-C(27)-C(32)	-14.4(4)
C(12)-C(13)-C(8)-C(9)	-0.7(6)
C(12)-C(13)-C(8)-C(2)	175.5(4)
C(12)-C(13)-C(8)-Pd(1)	-88.3(4)
C(10)-C(9)-C(8)-C(13)	1.3(6)
Pd(1)-C(9)-C(8)-C(13)	-104.4(4)
C(10)-C(9)-C(8)-C(2)	-175.1(4)
Pd(1)-C(9)-C(8)-C(2)	79.2(3)
C(10)-C(9)-C(8)-Pd(1)	105.8(4)
C(1)-C(2)-C(8)-C(13)	114.4(4)
C(3)-C(2)-C(8)-C(13)	-0.6(6)
C(1)-C(2)-C(8)-C(9)	-69.5(4)
C(3)-C(2)-C(8)-C(9)	175.6(3)
C(1)-C(2)-C(8)-Pd(1)	6.6(3)
C(3)-C(2)-C(8)-Pd(1)	-108.4(3)
C(8)-C(13)-C(12)-C(11)	0.7(7)
C(10)-C(11)-C(12)-C(13)	-1.2(6)
C(14)-C(11)-C(12)-C(13)	176.0(4)
C(24)-C(25)-C(26)-C(21)	-0.4(6)
C(32)-C(27)-C(28)-C(29)	-0.8(6)
P(1)-C(27)-C(28)-C(29)	-177.8(3)
C(23)-C(22)-C(21)-C(26)	1.8(6)
C(23)-C(22)-C(21)-P(1)	-176.6(3)
C(25)-C(26)-C(21)-C(22)	-0.8(6)
C(25)-C(26)-C(21)-P(1)	177.5(3)
C(27)-P(1)-C(21)-C(22)	-162.5(3)
C(15)-P(1)-C(21)-C(22)	91.0(3)
Pd(1)-P(1)-C(21)-C(22)	-35.4(3)
C(27)-P(1)-C(21)-C(26)	19.2(4)
C(15)-P(1)-C(21)-C(26)	-87.4(4)
Pd(1)-P(1)-C(21)-C(26)	146.3(3)
C(1)-C(6)-C(5)-C(4)	73.0(4)
C(7)-C(6)-C(5)-C(4)	-33.7(4)
C(15)-C(20)-C(19)-C(18)	-2.1(6)
C(29)-C(30)-C(31)-C(32)	0.1(7)
C(27)-C(32)-C(31)-C(30)	0.4(7)
C(7)-C(3)-C(4)-C(5)	37.7(4)

C(2)-C(3)-C(4)-C(5)	-69.0(4)
C(6)-C(5)-C(4)-C(3)	-2.3(4)
C(31)-C(30)-C(29)-C(28)	-0.8(7)
C(27)-C(28)-C(29)-C(30)	1.2(7)
C(20)-C(19)-C(18)-C(17)	-0.3(7)
C(26)-C(25)-C(24)-C(23)	0.6(6)
C(25)-C(24)-C(23)-C(22)	0.4(6)
C(21)-C(22)-C(23)-C(24)	-1.6(6)
C(19)-C(18)-C(17)-C(16)	1.4(7)
C(15)-C(16)-C(17)-C(18)	0.1(6)

Symmetry transformations used to generate equivalent atoms:

Spectra

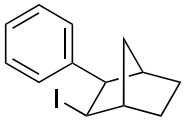

Compound 2a

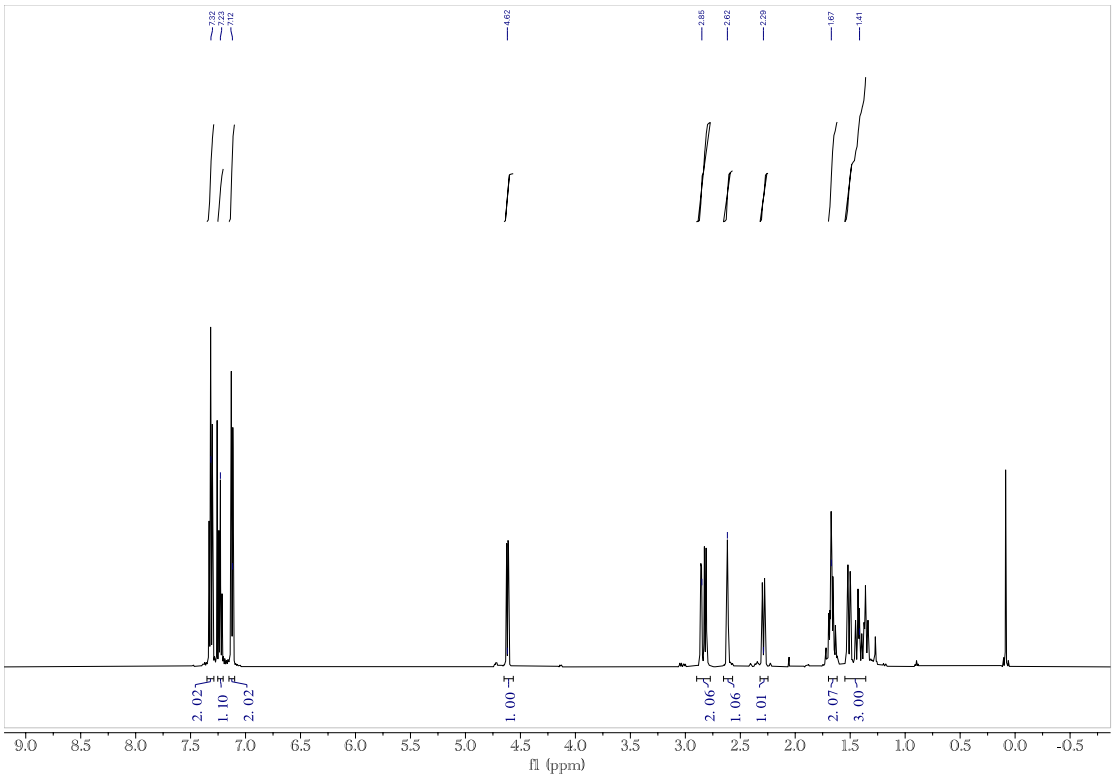

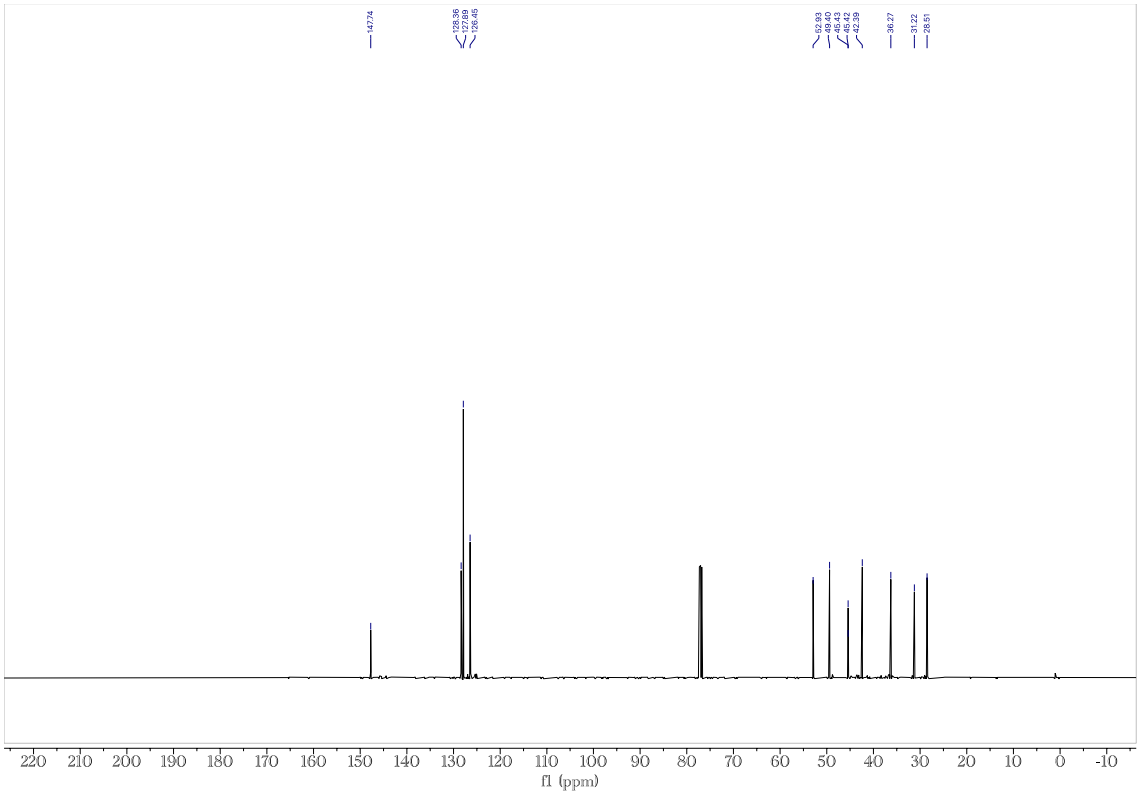

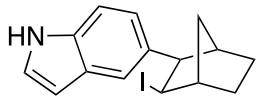
HN
I

Compound 2b

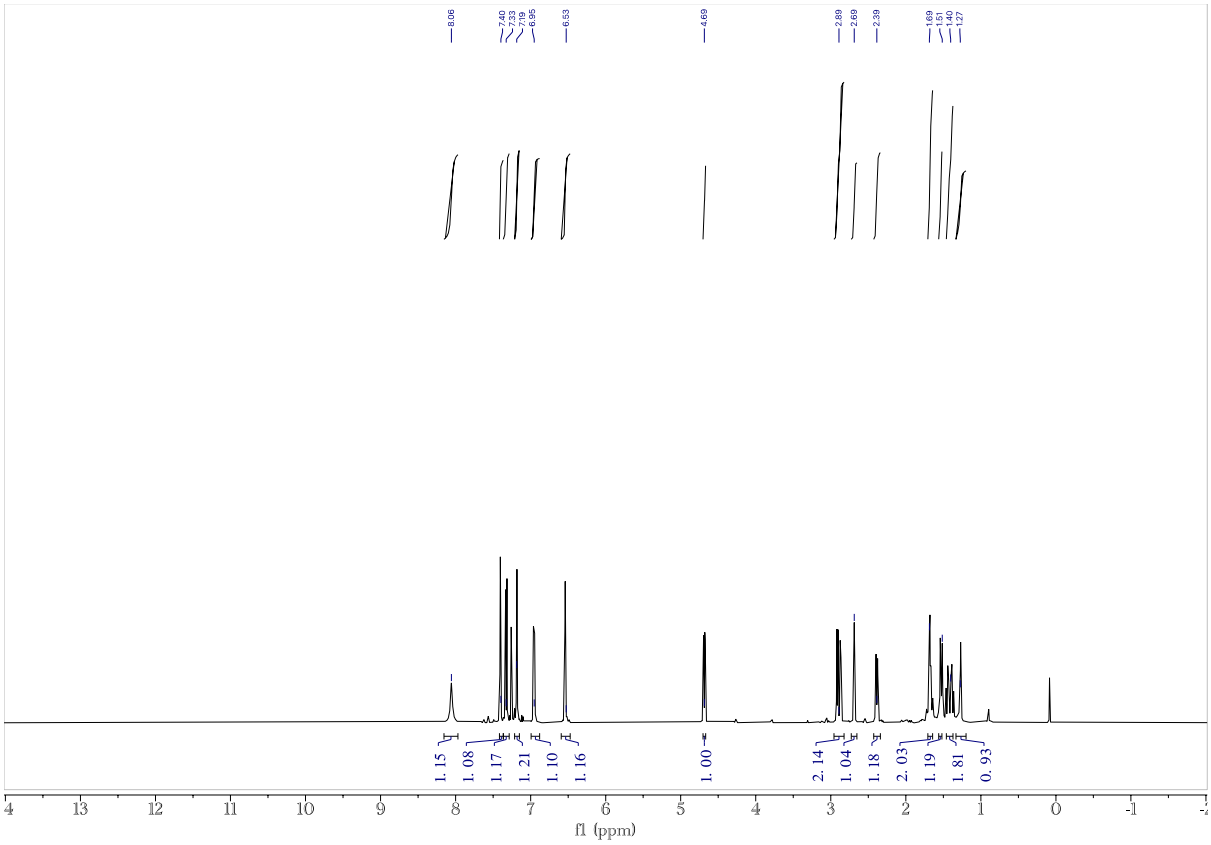
8.06
7.40
7.33
7.19
6.95
6.53
4.69
2.89
2.69
2.39
1.69
1.51
1.40
1.27
1.15
1.08
1.17
1.21
1.10
1.16
1.00
2.14
1.04
1.18
2.03
1.19
1.81
0.93
f1 (ppm)

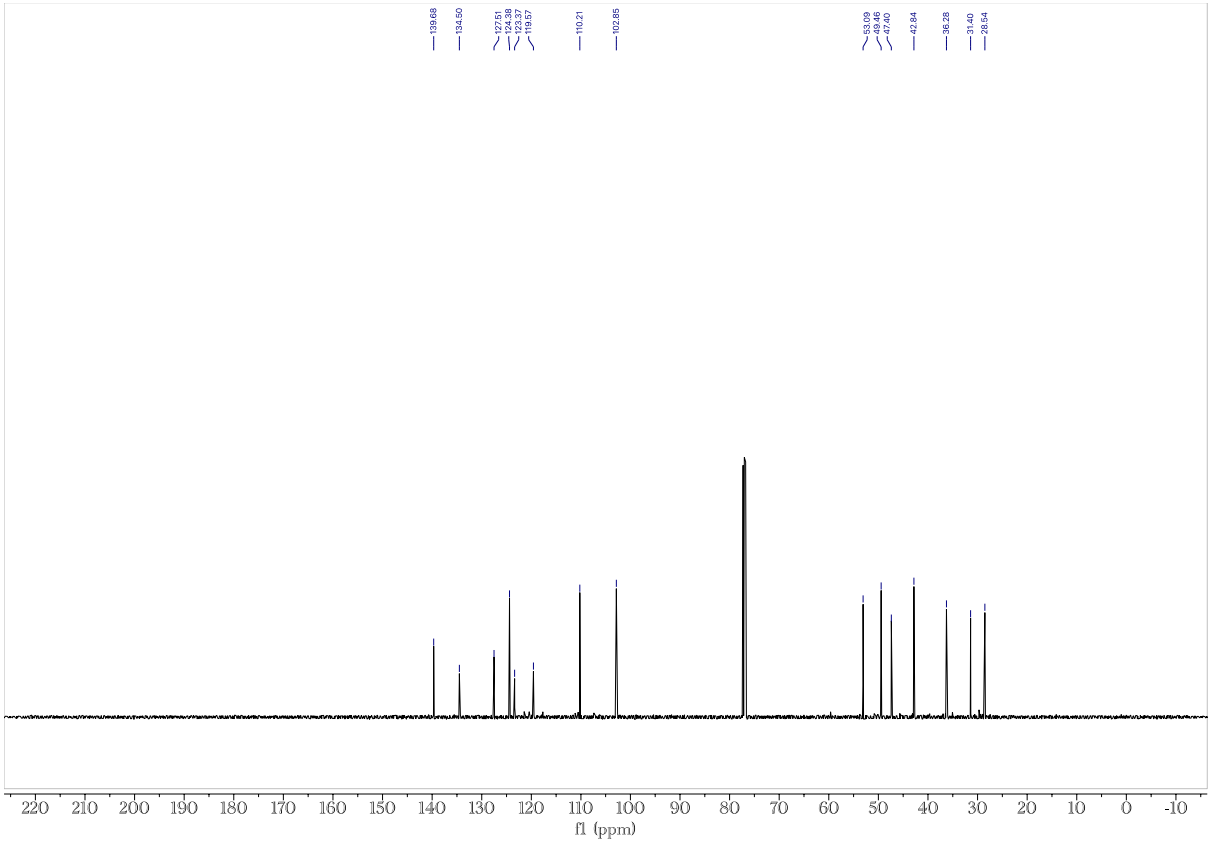
139.68
134.90
127.51
124.38
123.37
119.57
110.21
102.85
53.09
49.46
47.40
42.84
36.28
31.40
28.54
f1 (ppm)

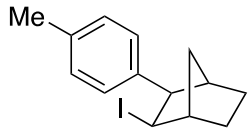
Me
I

Compound 2c

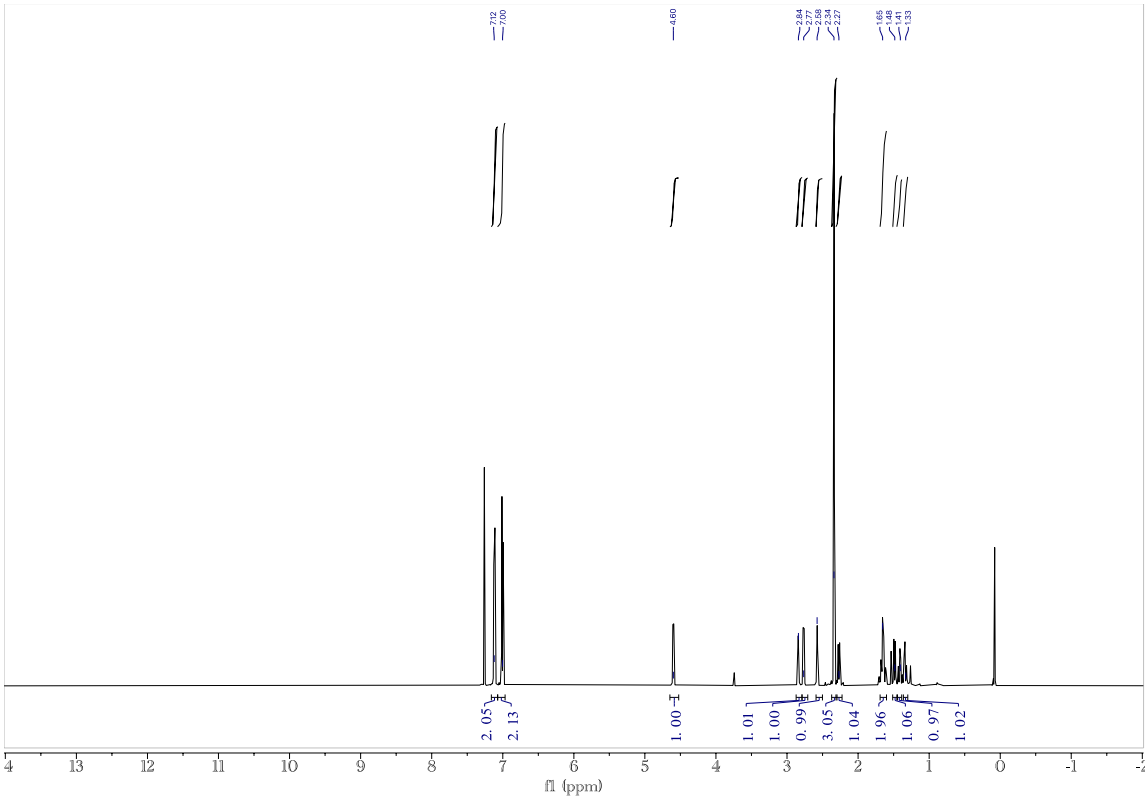
7.12
7.00
4.60
2.84
2.77
2.58
2.34
2.27
1.65
1.48
1.41
1.33
2.05
2.13
1.00
1.01
1.00
0.99
3.05
1.04
1.96
1.06
0.97
1.02
f1 (ppm)

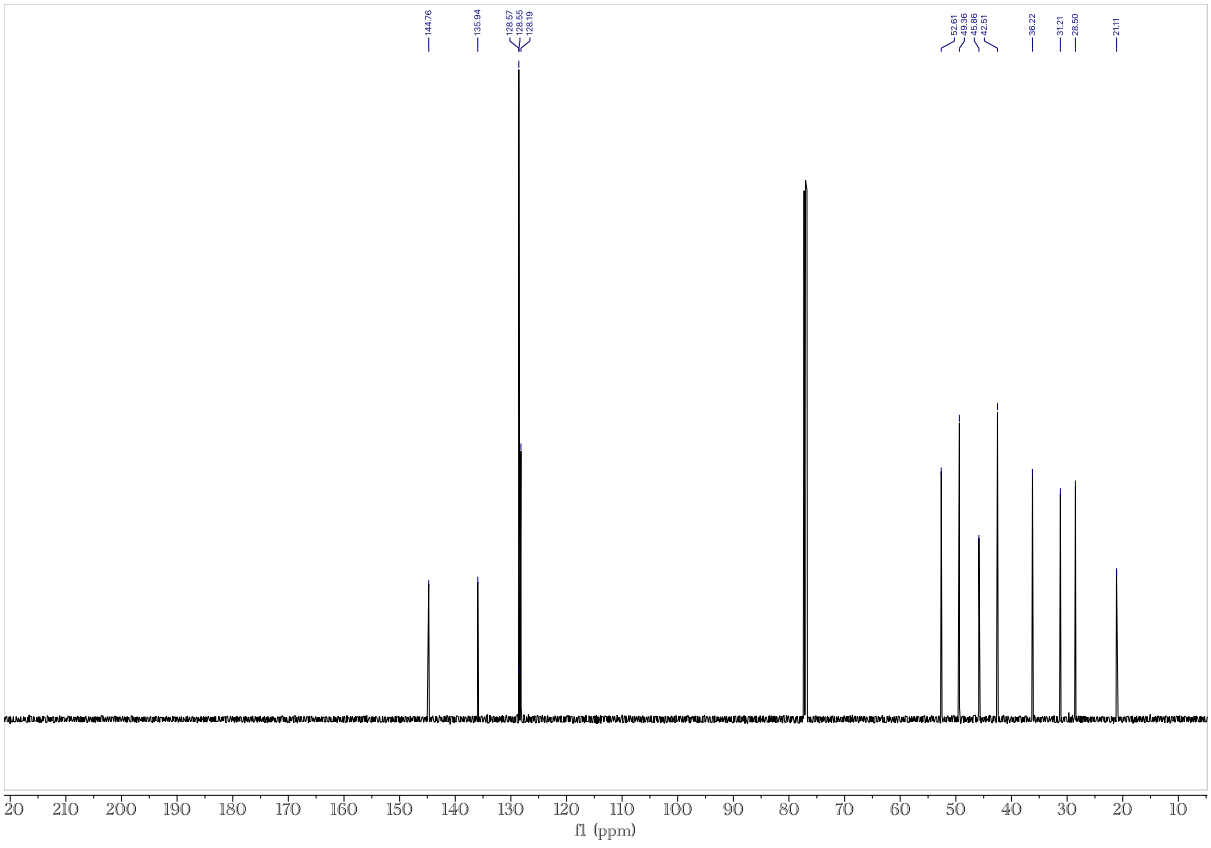
144.76
135.94
128.57
128.55
128.19
52.61
49.36
45.86
42.61
36.22
31.21
28.50
21.11
f1 (ppm)

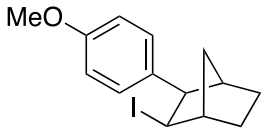
MeO

Compound 2d

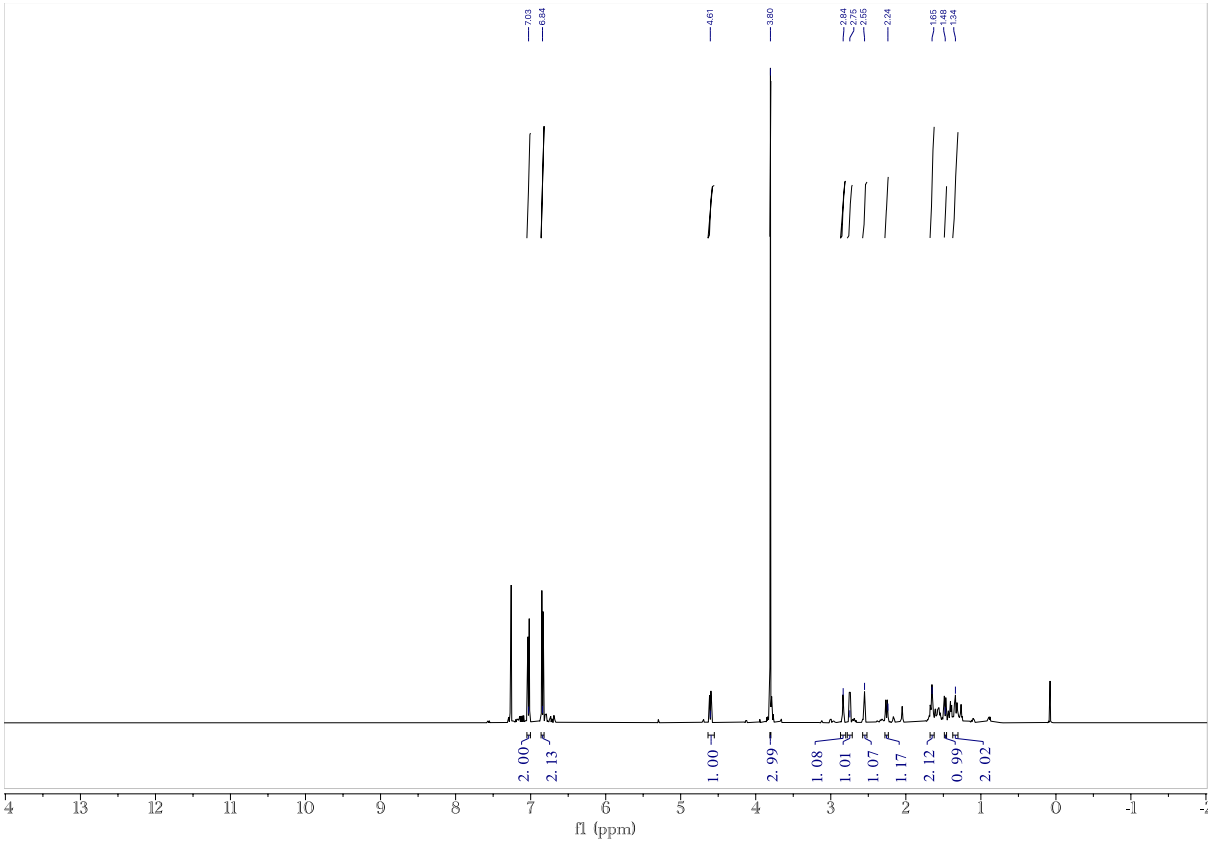
7.03
6.84
4.61
3.80
2.84
2.75
2.65
2.24
1.65
1.48
1.34
2. 00
2. 13
1. 00
2. 99
1. 08
1. 01
1. 07
1. 17
2. 12
0. 99
2. 02
f1 (ppm)

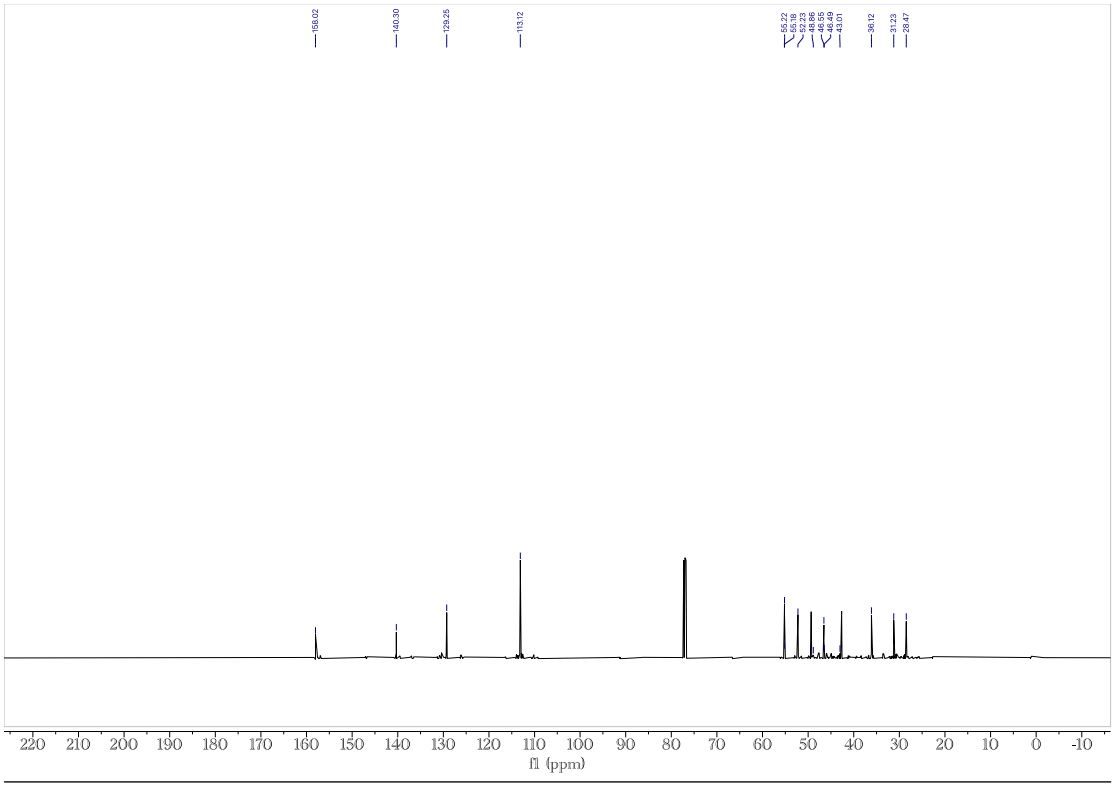
158.02
140.30
129.25
113.12
55.22
55.18
52.93
48.86
48.55
46.49
43.01
36.12
31.23
28.47
f1 (ppm)

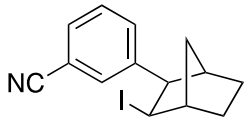
NC
I

Compound 2f

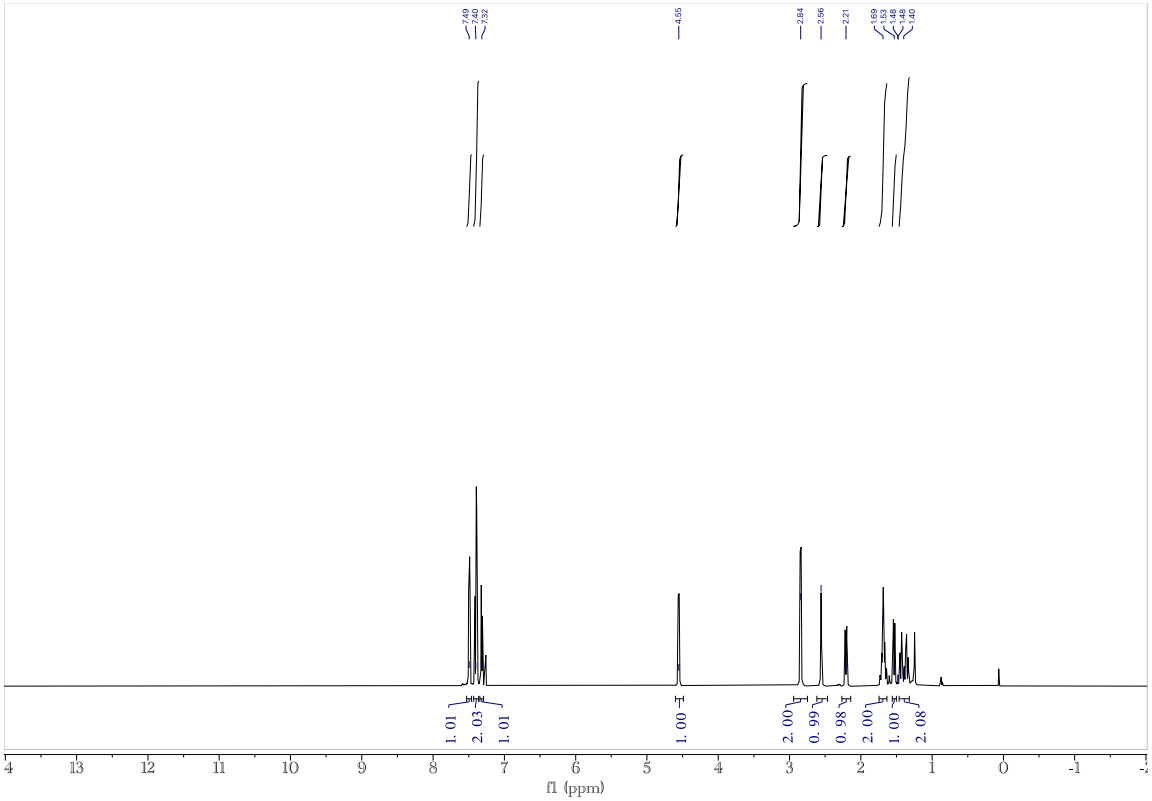
7.49
7.40
7.32
4.55
2.84
2.56
2.21
1.69
1.53
1.48
1.46
1.40
1.01
2.03
1.01
1.00
2.00
0.99
0.98
2.00
1.00
2.08
f1 (ppm)

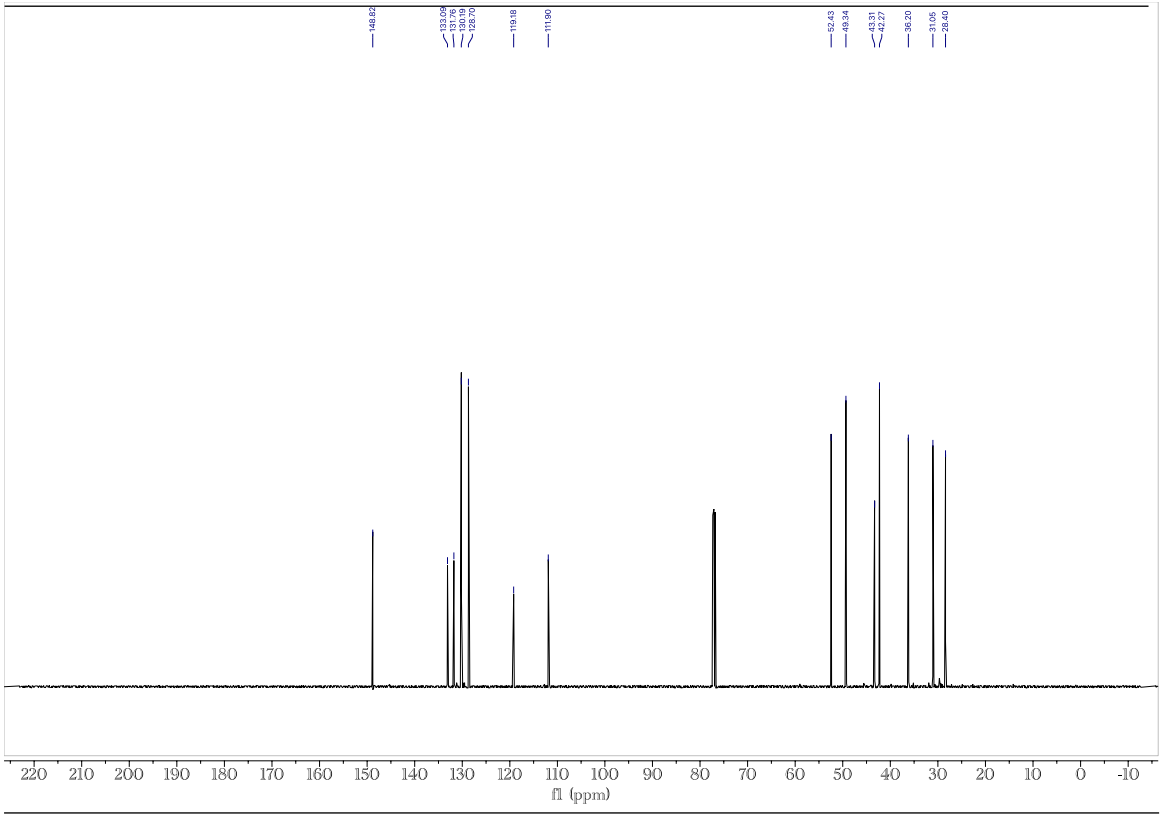
148.62
133.08
131.76
130.19
128.70
119.18
111.90
52.43
49.34
43.31
42.27
36.20
31.05
28.40
f1 (ppm)

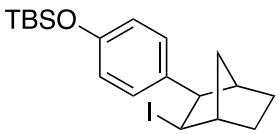
TBSO
I

Compound 2h

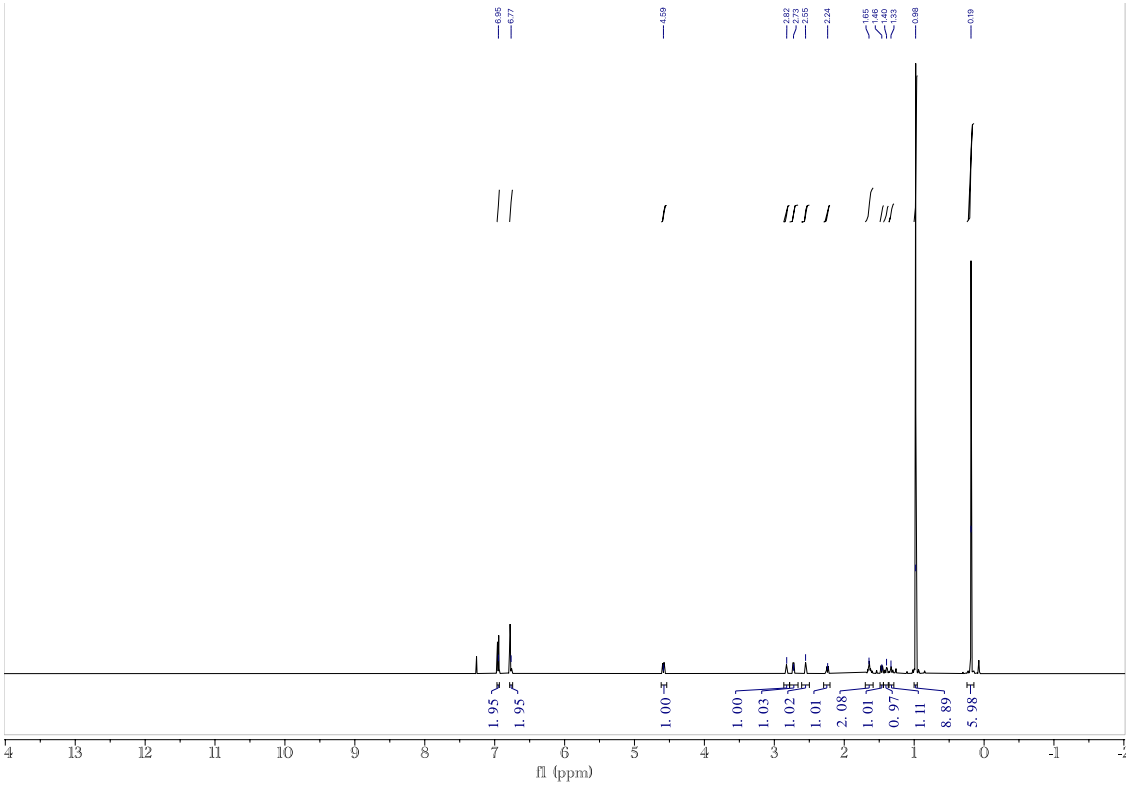
6.96
6.77
4.59
2.82
2.73
2.55
2.24
1.65
1.46
1.40
1.33
0.98
0.19
1.95
1.95
1.00
1.00
1.03
1.02
1.01
2.08
1.01
0.97
1.11
8.89
5.98
f1 (ppm)

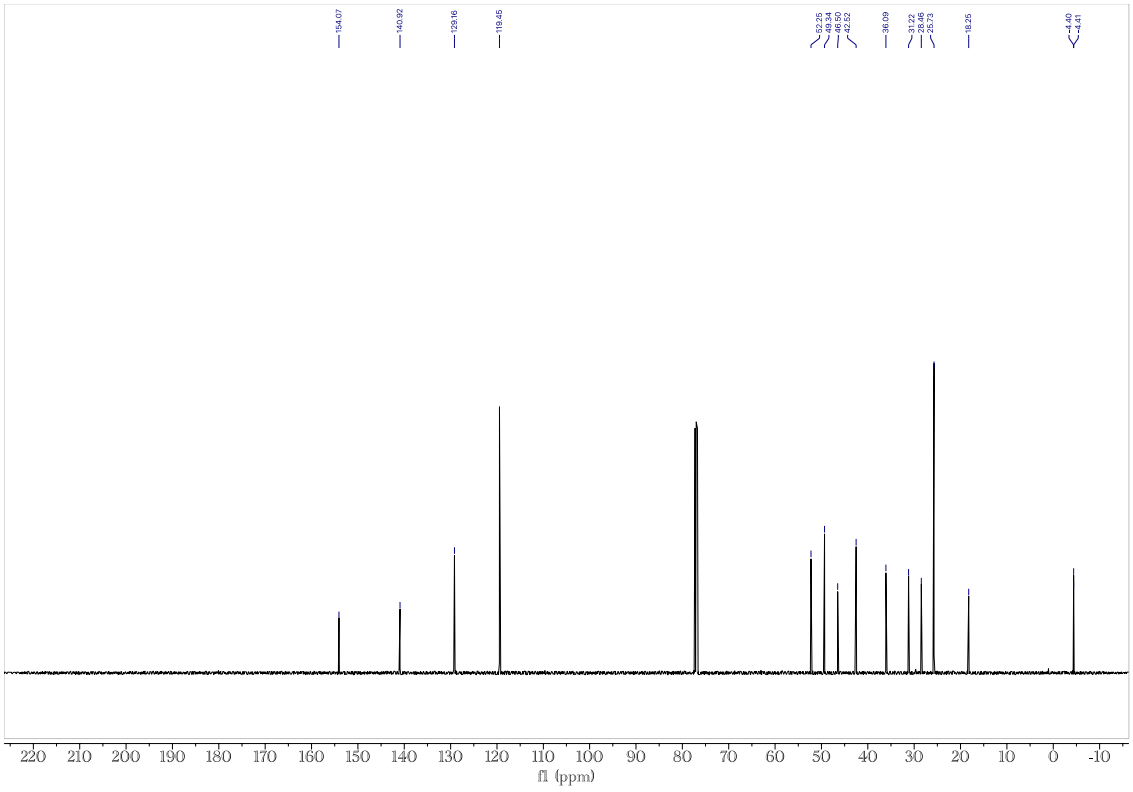
154.07
140.92
128.16
119.45
52.25
49.34
46.50
42.52
36.09
31.22
28.48
20.52
18.25
-4.40
-4.41
f1 (ppm)

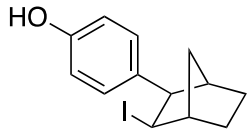
HO
I

Compound 2i

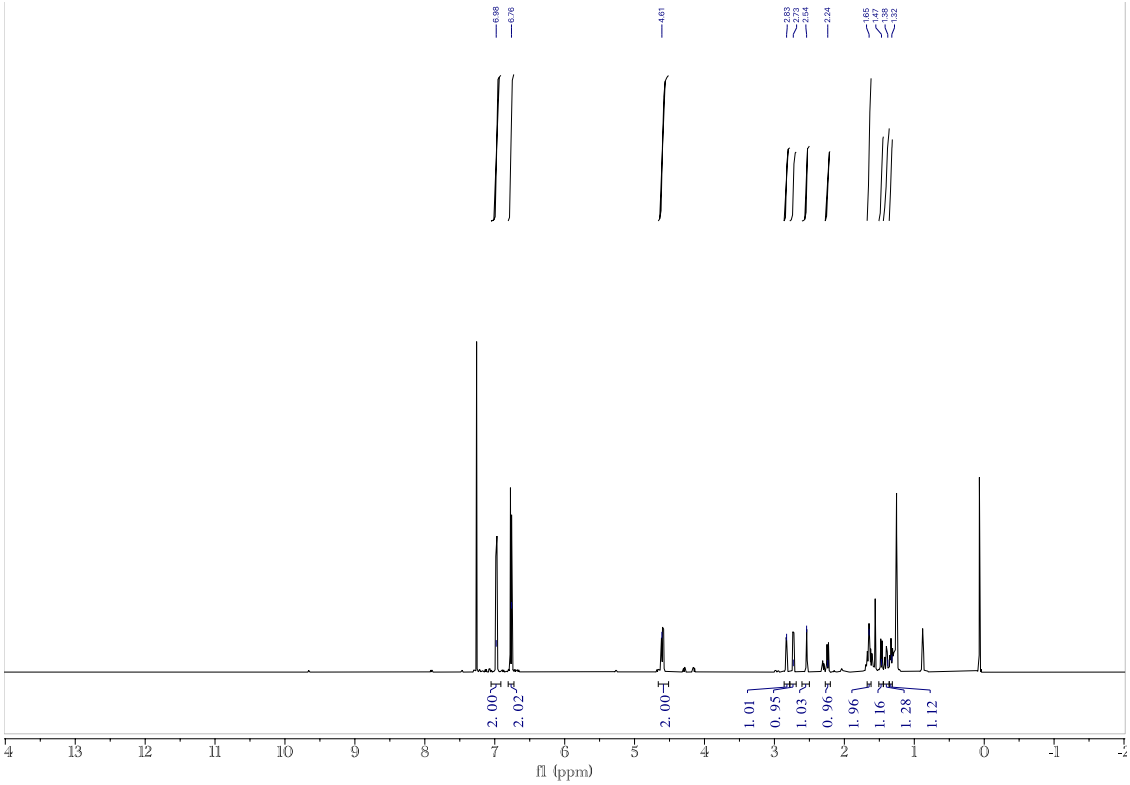
6.98
6.76
4.61
2.83
2.73
2.54
2.24
1.65
1.47
1.38
1.32
2.00
2.02
2.00
1.01
0.95
1.03
0.96
1.96
1.16
1.28
1.12
f1 (ppm)

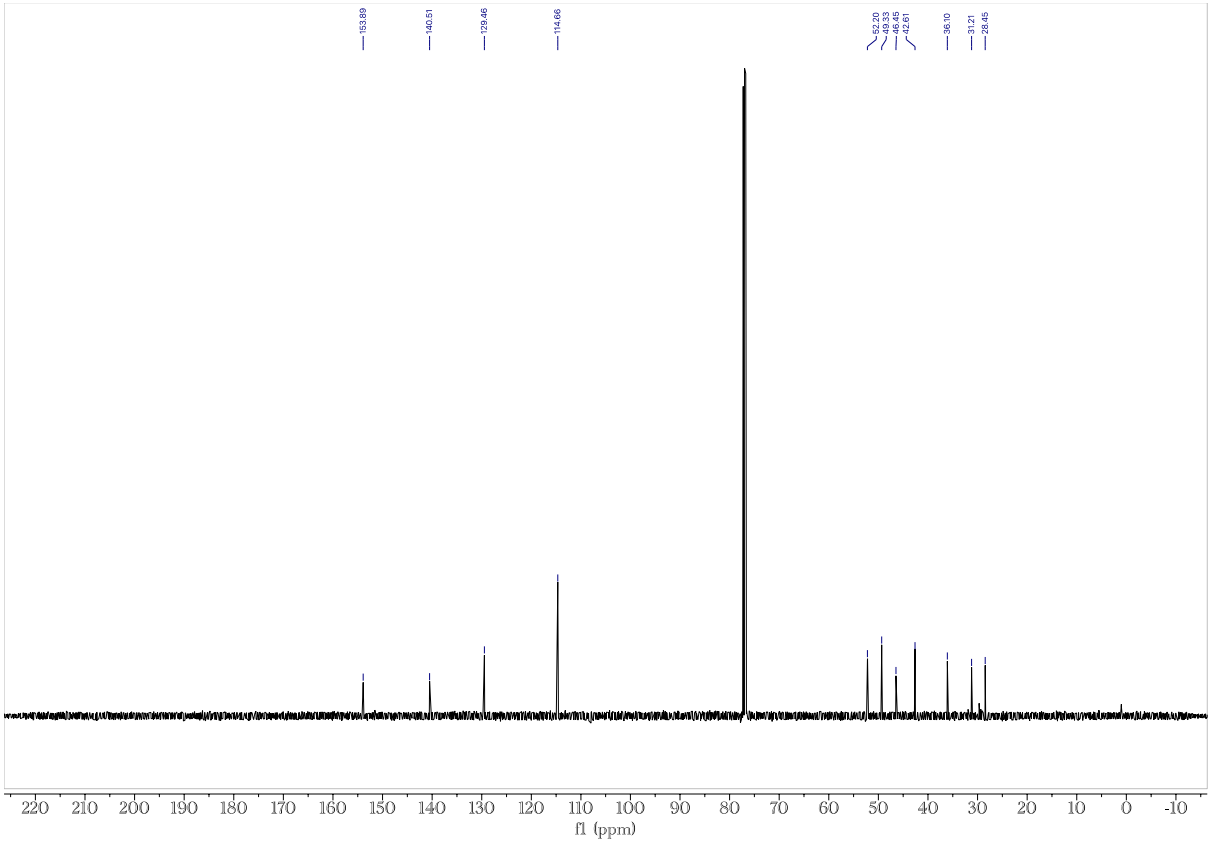
153.89
140.51
129.46
114.66
52.20
49.33
45.45
42.61
36.10
31.21
28.45
f1 (ppm)

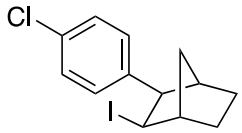
Cl
I

Compound 2j

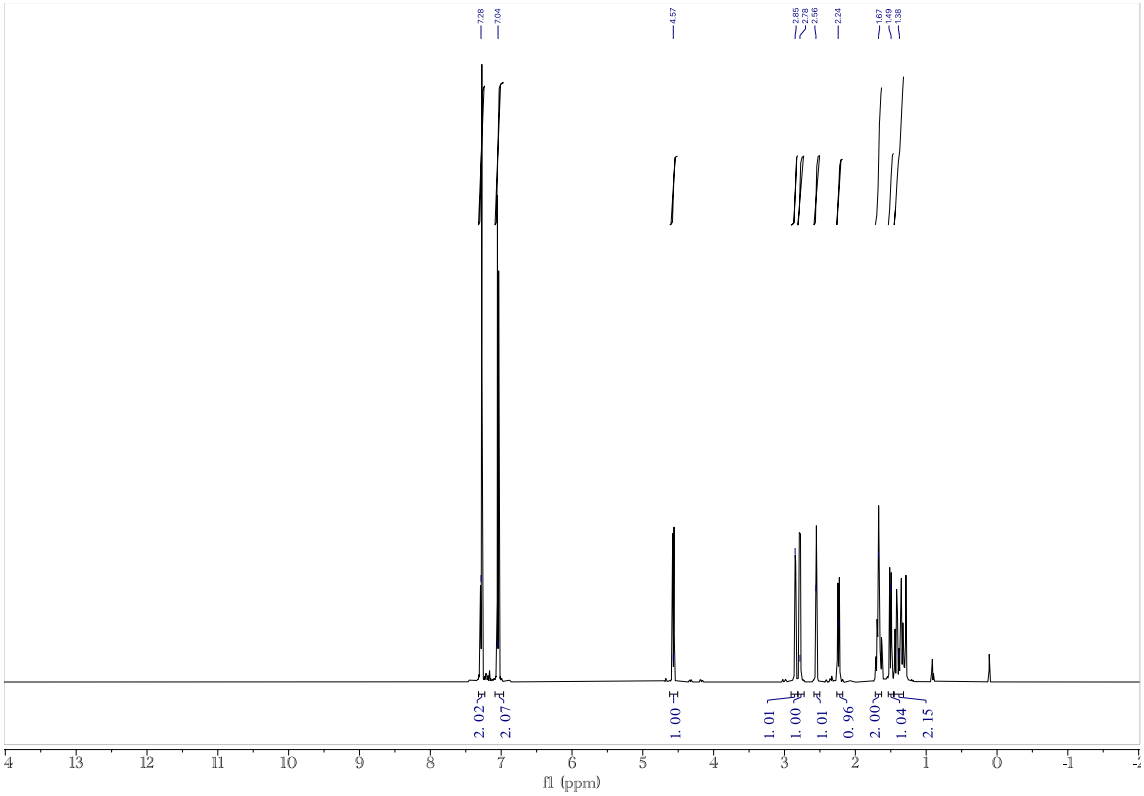
7.28
7.04
4.57
2.85
2.83
2.66
2.24
1.67
1.49
1.38
2.02
2.07
1.00
1.01
1.00
1.01
0.96
2.00
1.04
2.15
f1 (ppm)

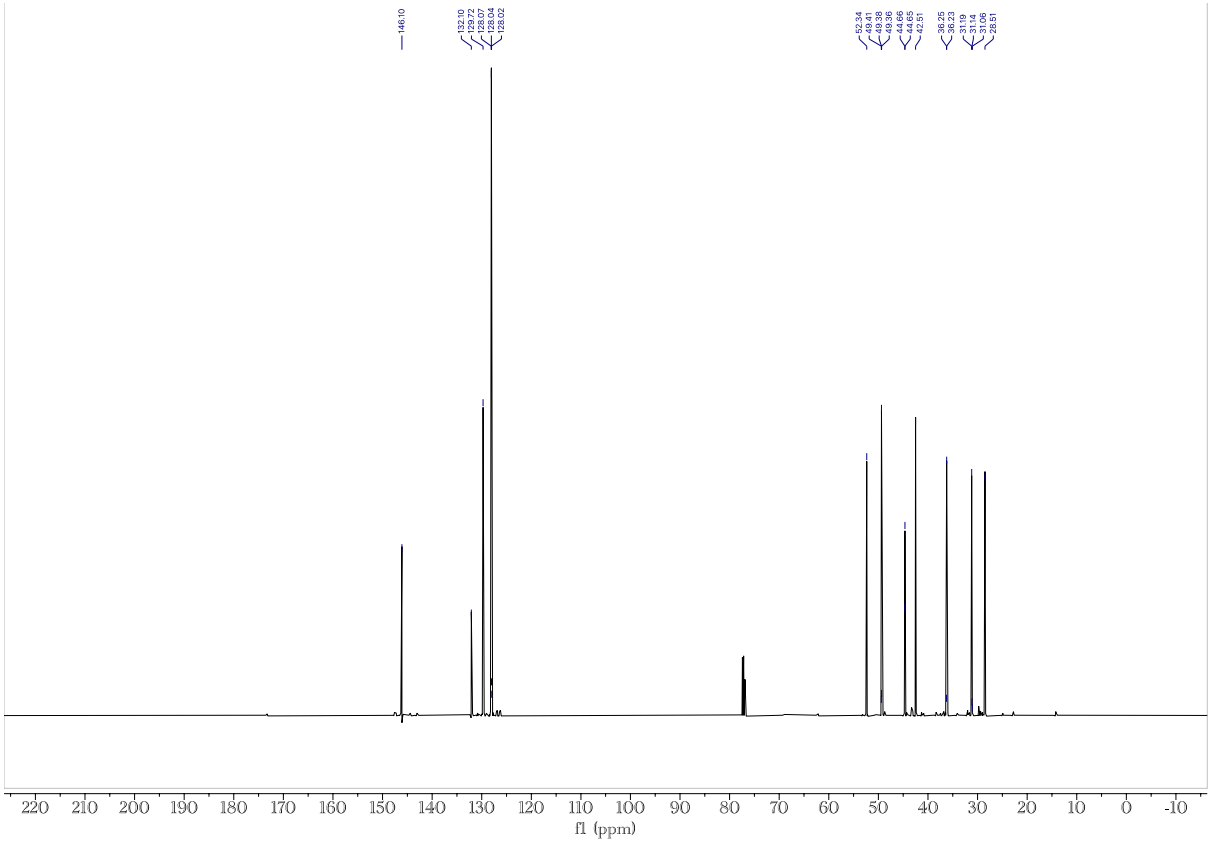
146.10
132.10
128.72
128.02
128.04
128.02
52.34
49.41
49.38
49.36
44.66
44.65
42.51
36.25
36.23
31.19
31.14
31.06
28.51
f1 (ppm)

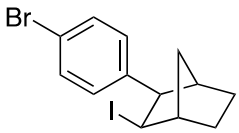
Br
I

Compound 2k

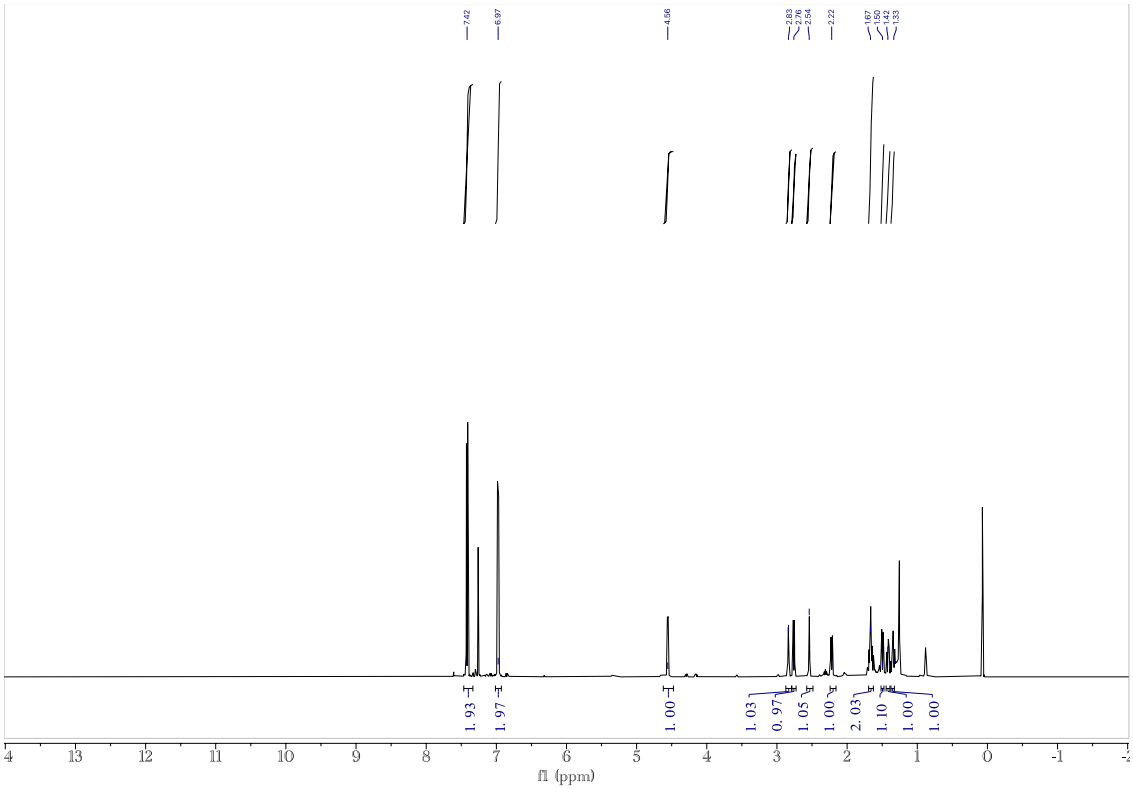
7.42
6.97
4.56
2.83
2.76
2.54
2.22
1.67
1.59
1.42
1.33
1.93
1.97
1.00
1.03
0.97
1.05
1.00
2.03
1.10
1.00
1.00
f1 (ppm)

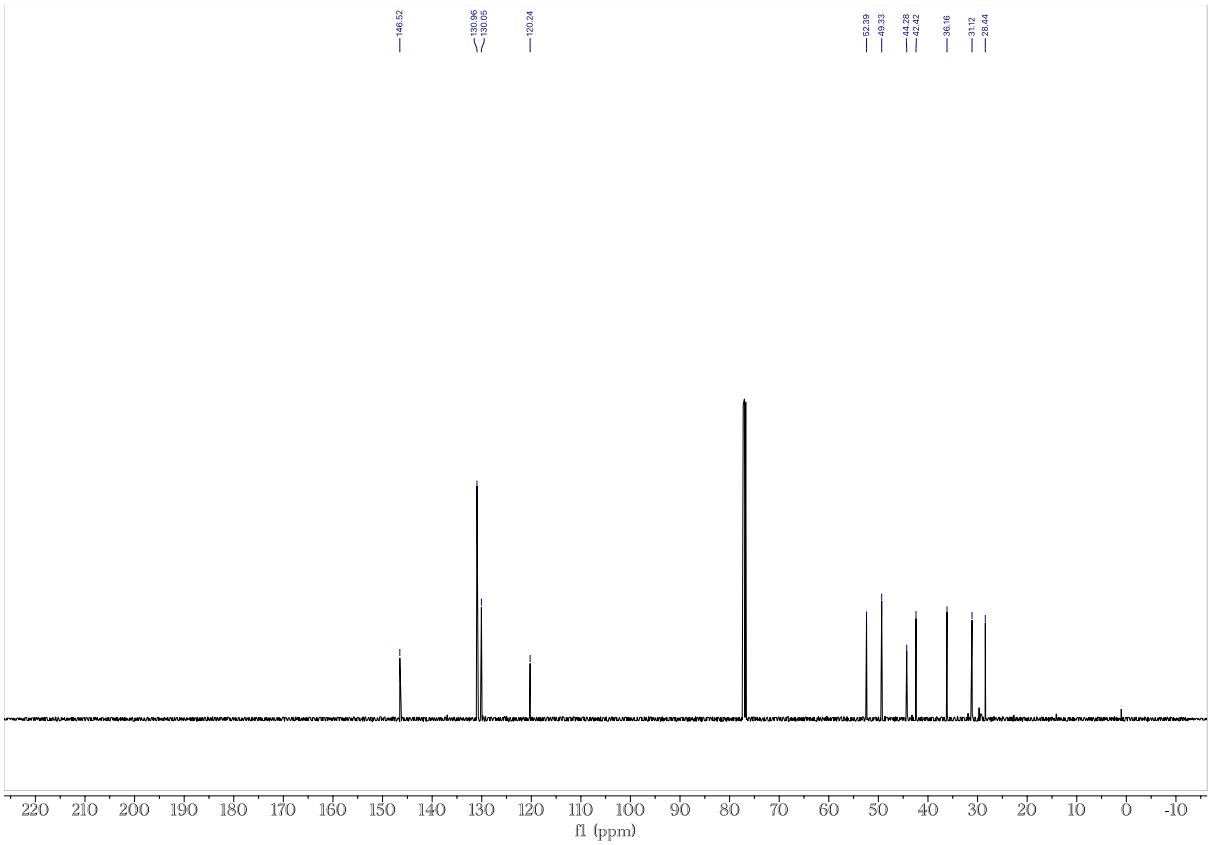
146.52
130.96
130.85
120.24
52.39
49.33
44.28
42.42
36.16
31.12
28.44
f1 (ppm)

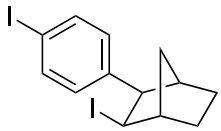

Compound 2l

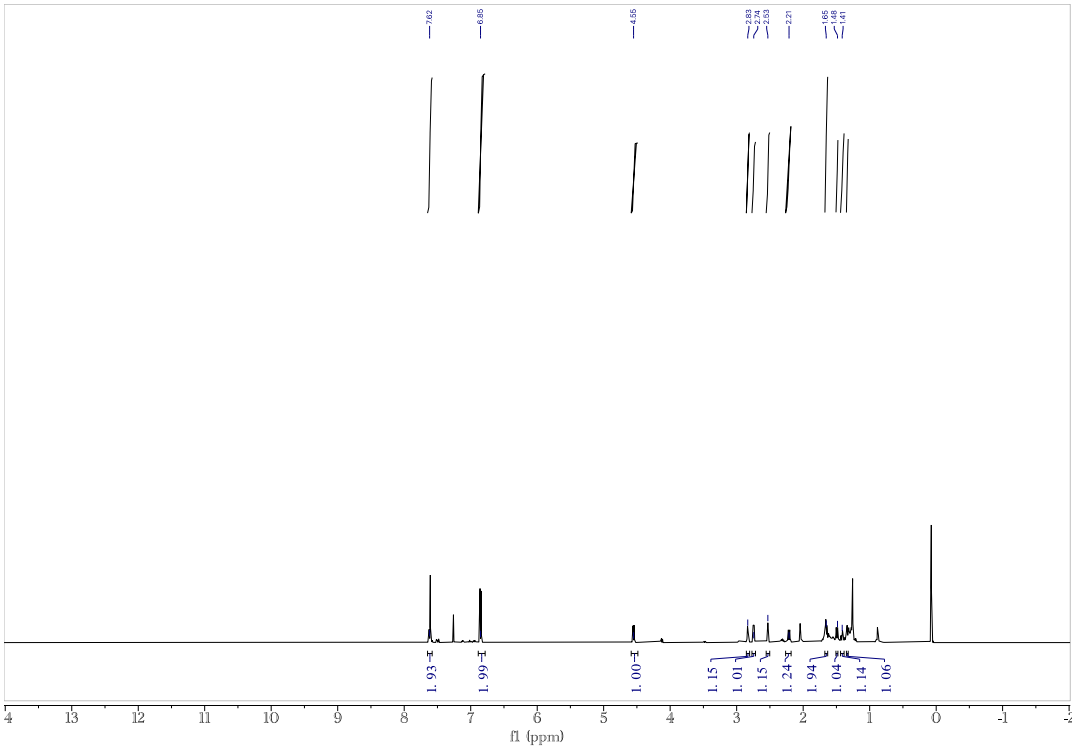
7.62
6.85
4.55
2.83
2.74
2.53
2.21
1.65
1.48
1.41
1.93
1.99
1.00
1.15
1.01
1.15
1.24
1.94
1.04
1.14
1.06
f1 (ppm)

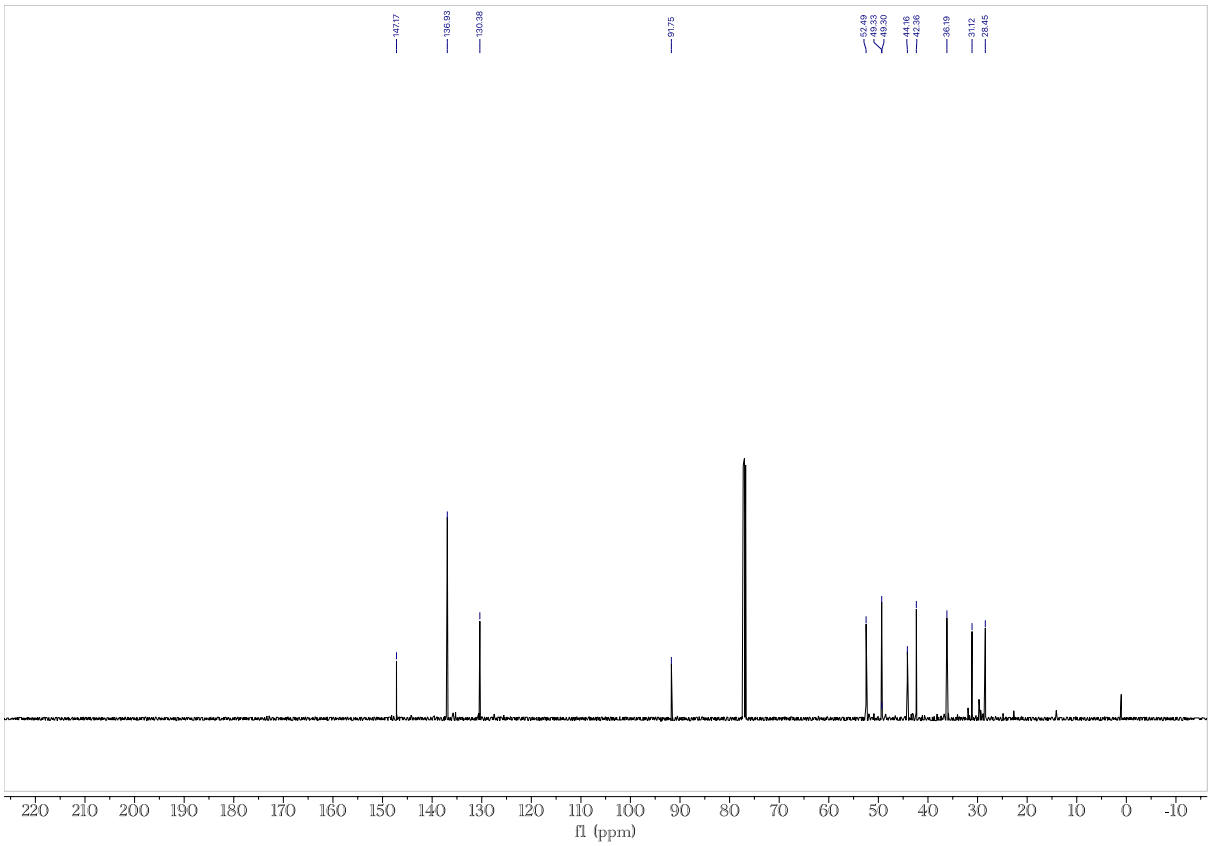
147.17
136.93
130.38
91.75
50.49
49.33
49.30
44.16
42.36
36.19
31.12
28.45
f1 (ppm)

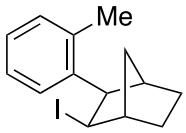
Me
I

Compound 2m

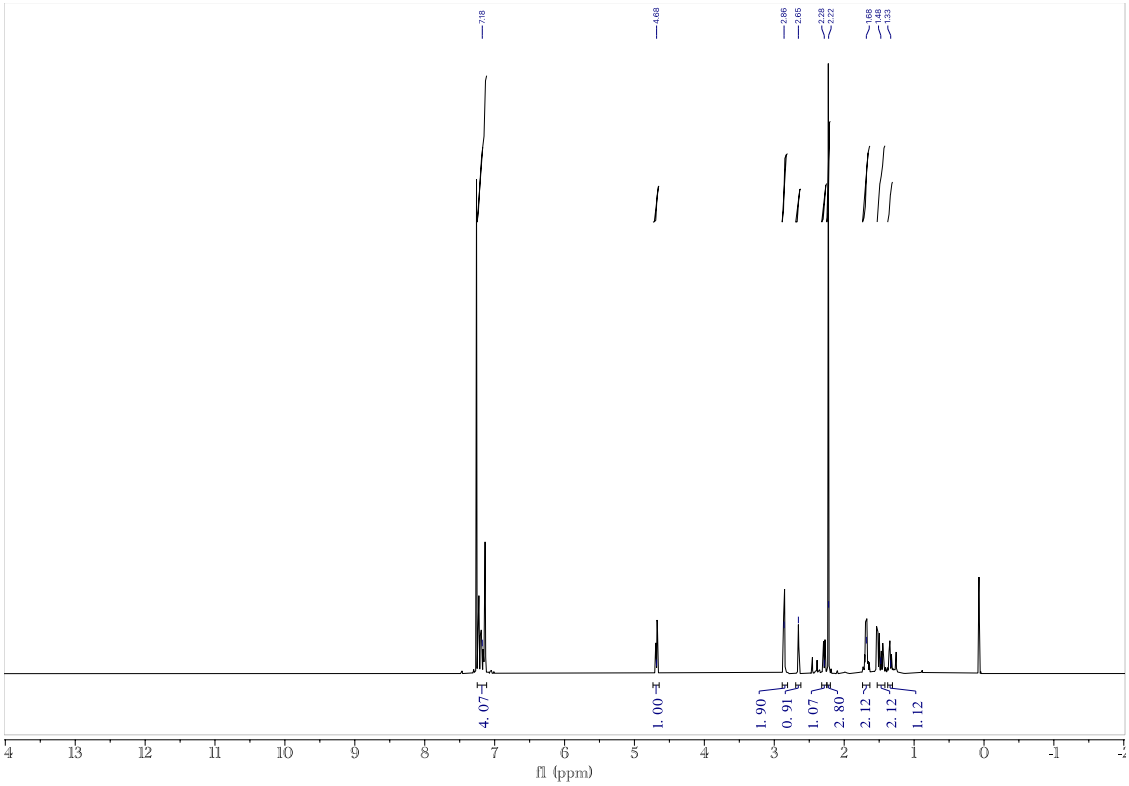
7.18
4.68
2.86
2.65
2.28
2.22
1.68
1.48
1.33
4.07
1.00
1.90
0.91
1.07
2.80
2.12
2.12
1.12
f1 (ppm)

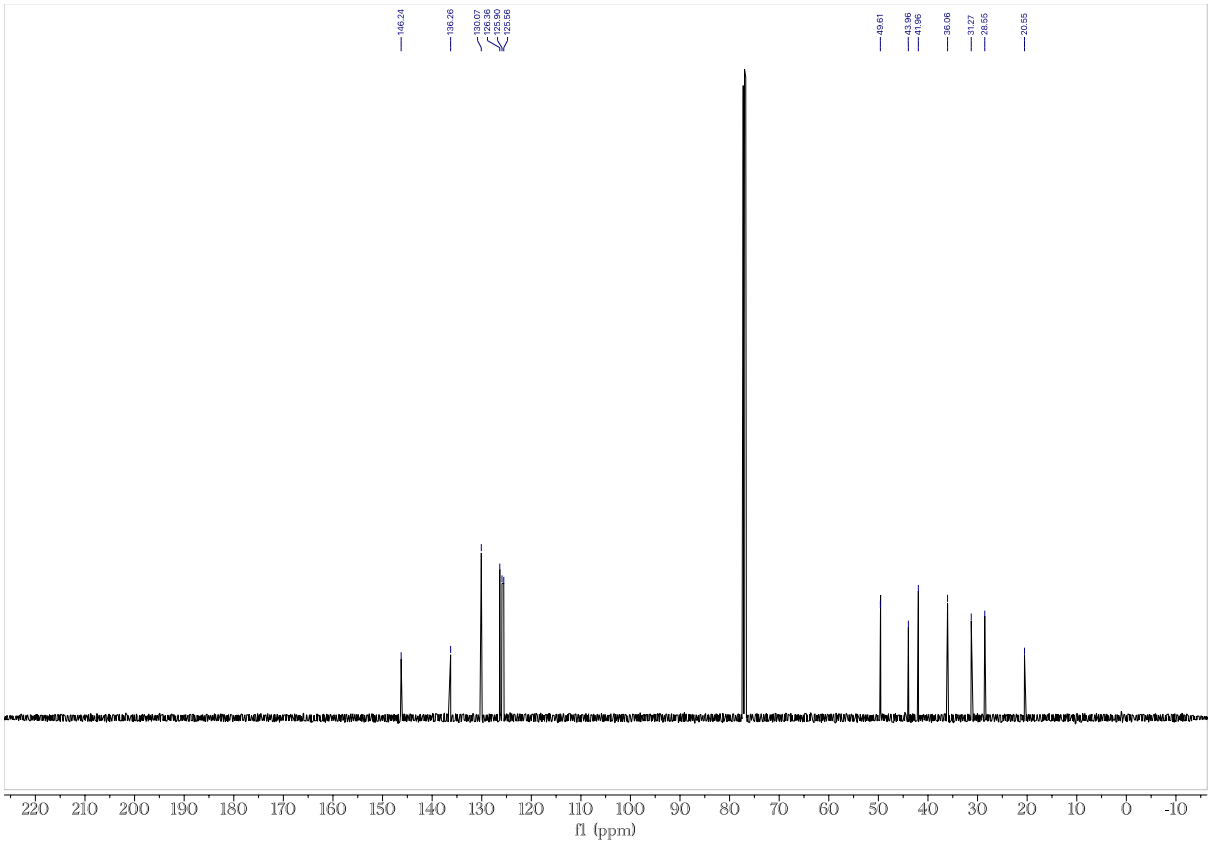
146.24
136.26
130.07
126.36
125.99
125.56
49.61
43.96
41.96
36.06
31.27
28.55
20.55
f1 (ppm)

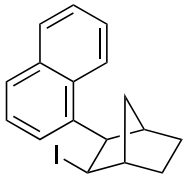

Compound 2n

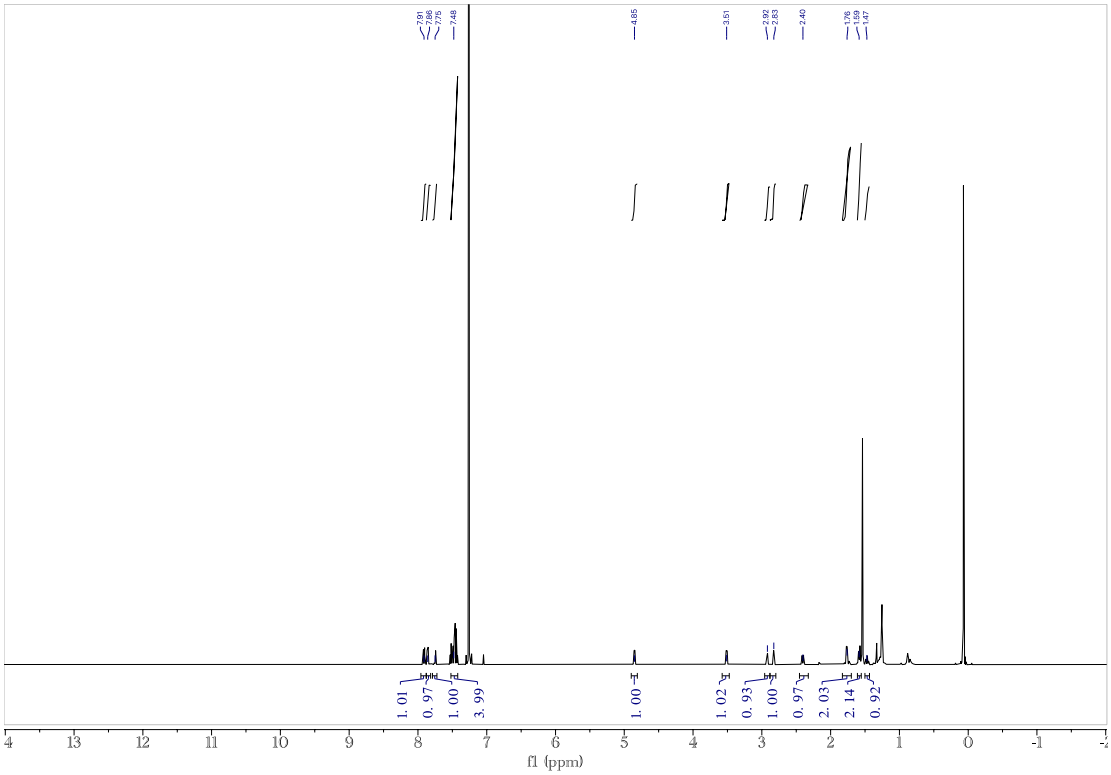
7.91
7.88
7.75
7.48
4.85
3.51
2.92
2.83
2.40
1.76
1.69
1.47
1.01
0.97
1.00
3.99
1.00
1.02
0.93
1.00
0.97
2.03
2.14
0.92
f1 (ppm)

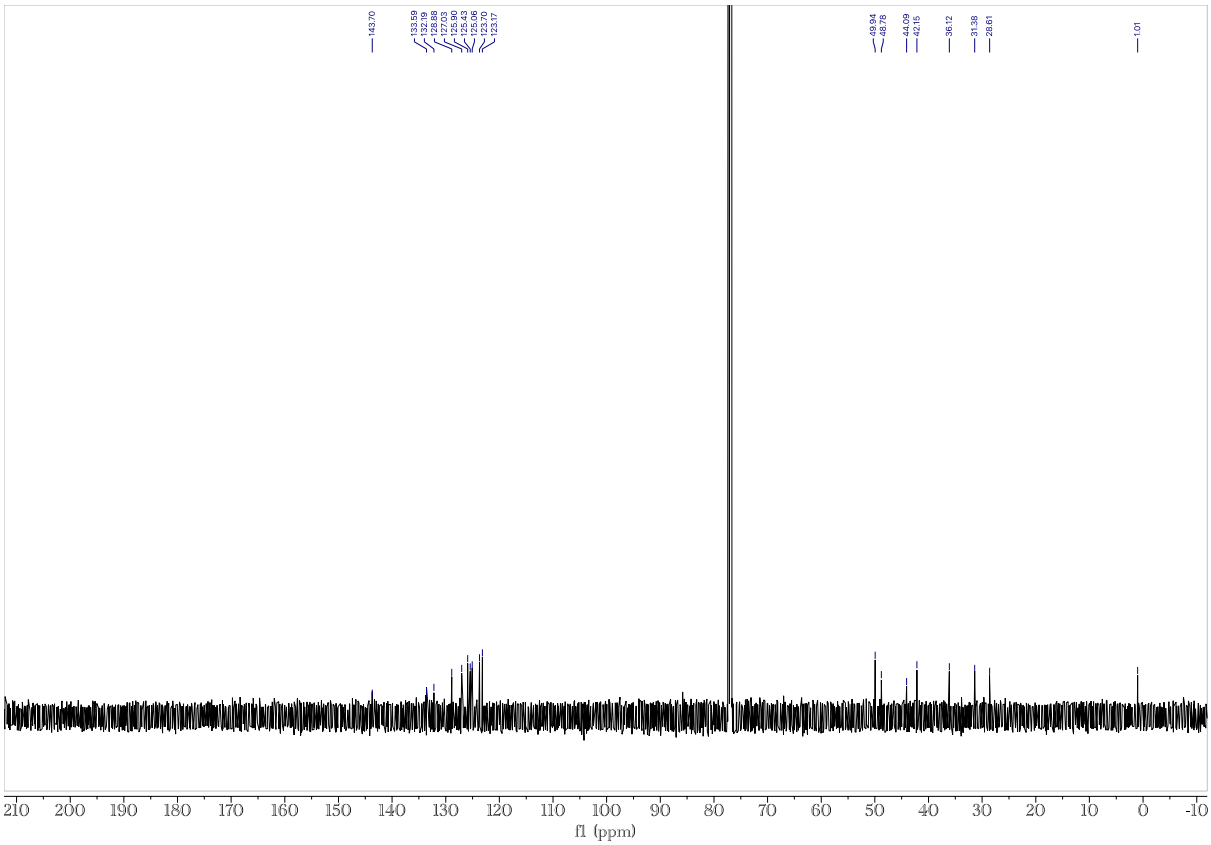
143.70
133.50
132.19
128.88
127.03
126.60
125.43
125.06
123.70
123.17
69.94
48.78
44.09
42.16
36.12
31.38
28.61
1.01
f1 (ppm)

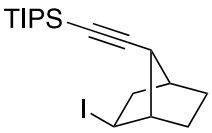
TIPS
I

Compound 2q

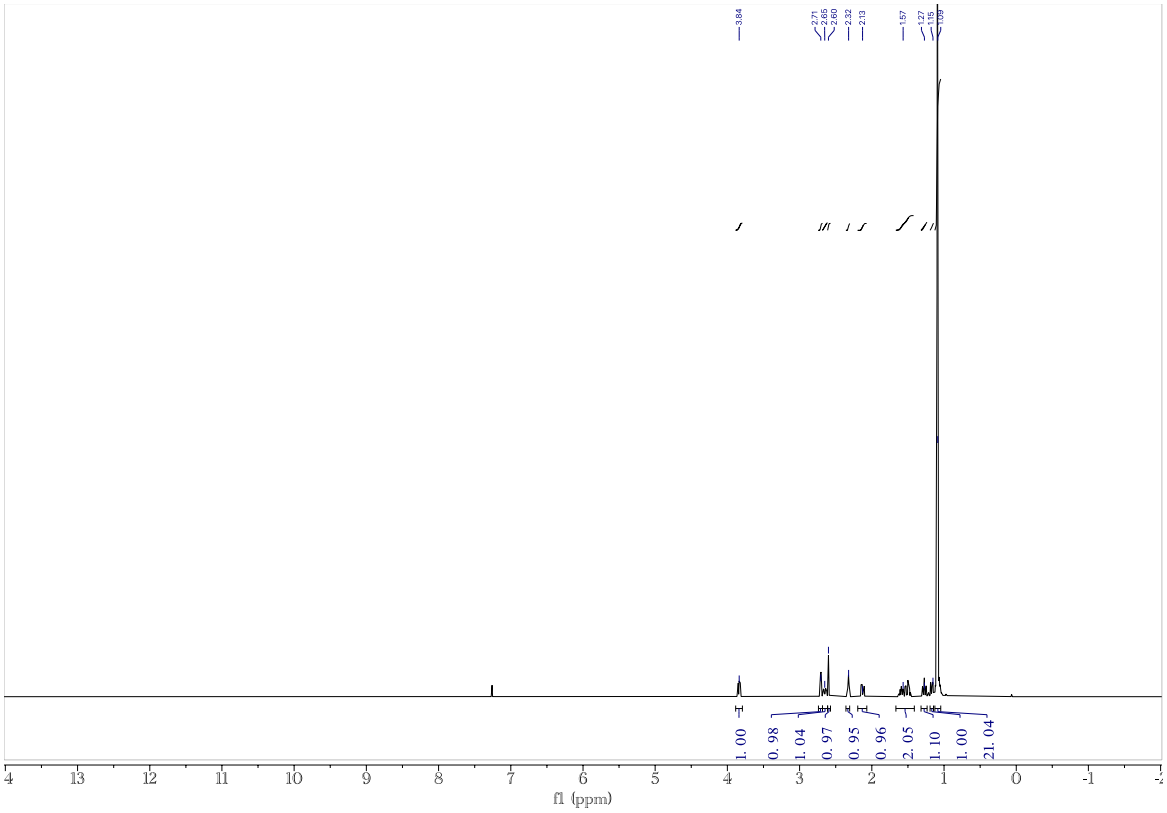
3.84
2.71
2.65
2.60
2.32
2.19
1.57
1.27
1.15
1.03
1.00
0.98
1.04
0.97
0.95
0.96
2.05
1.10
1.00
21.04
f1 (ppm)

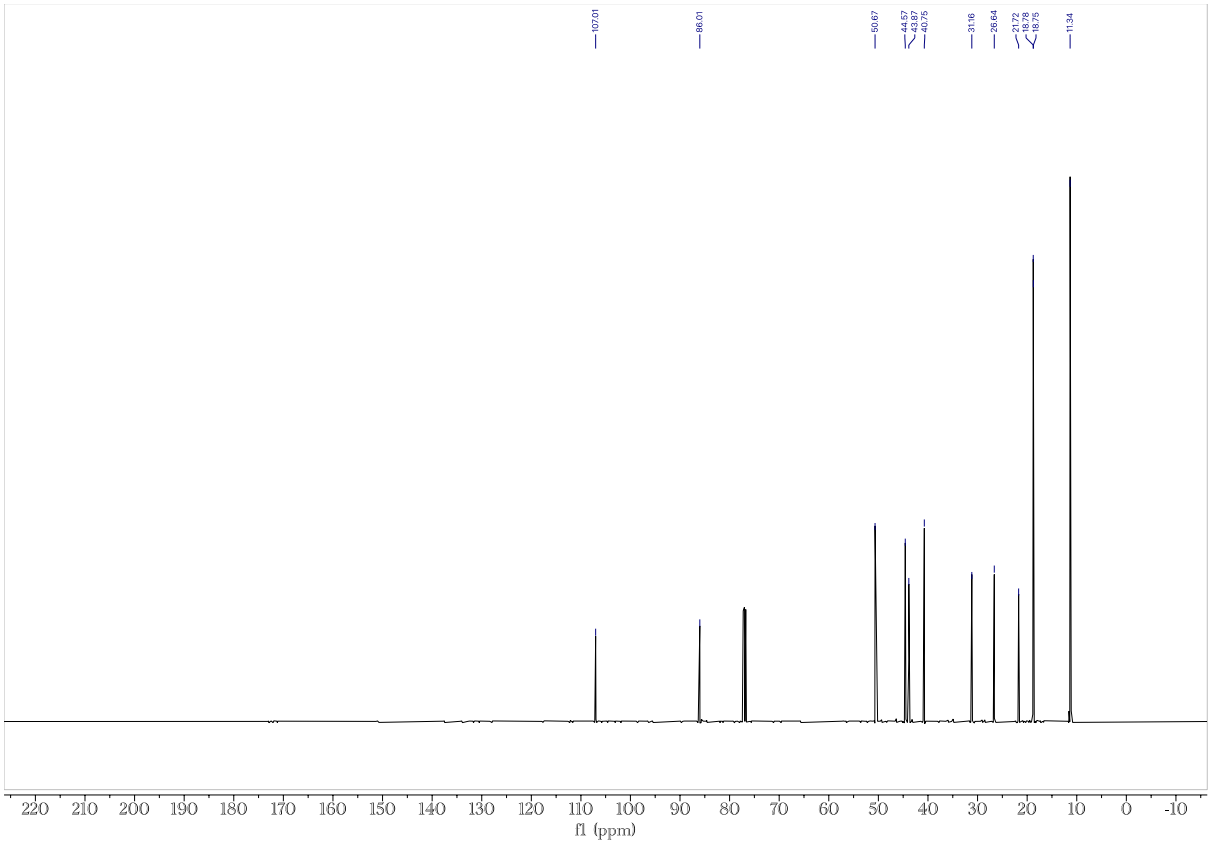
107.01
86.01
50.67
44.57
43.87
40.75
31.16
26.64
21.72
18.78
18.75
11.34
f1 (ppm)

Product Characterization

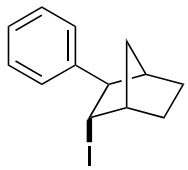

Compound 3a

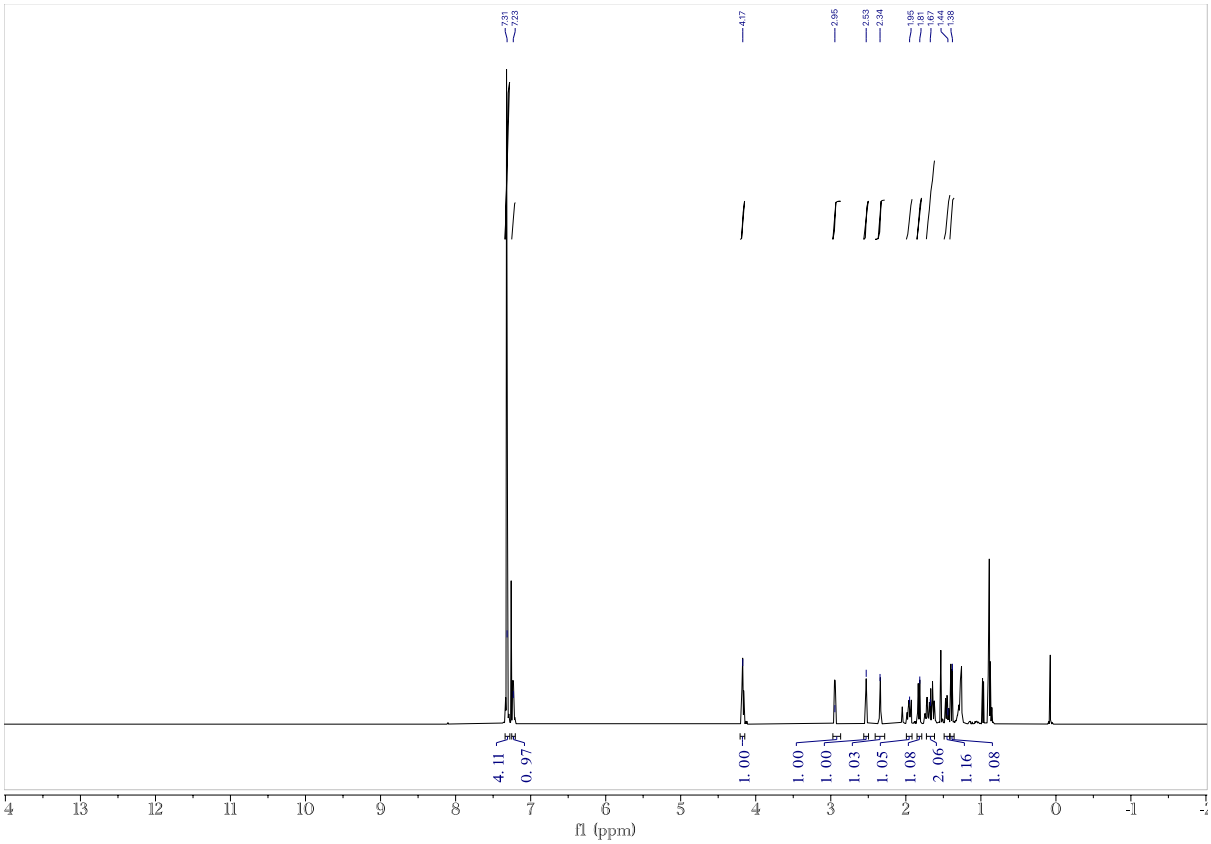

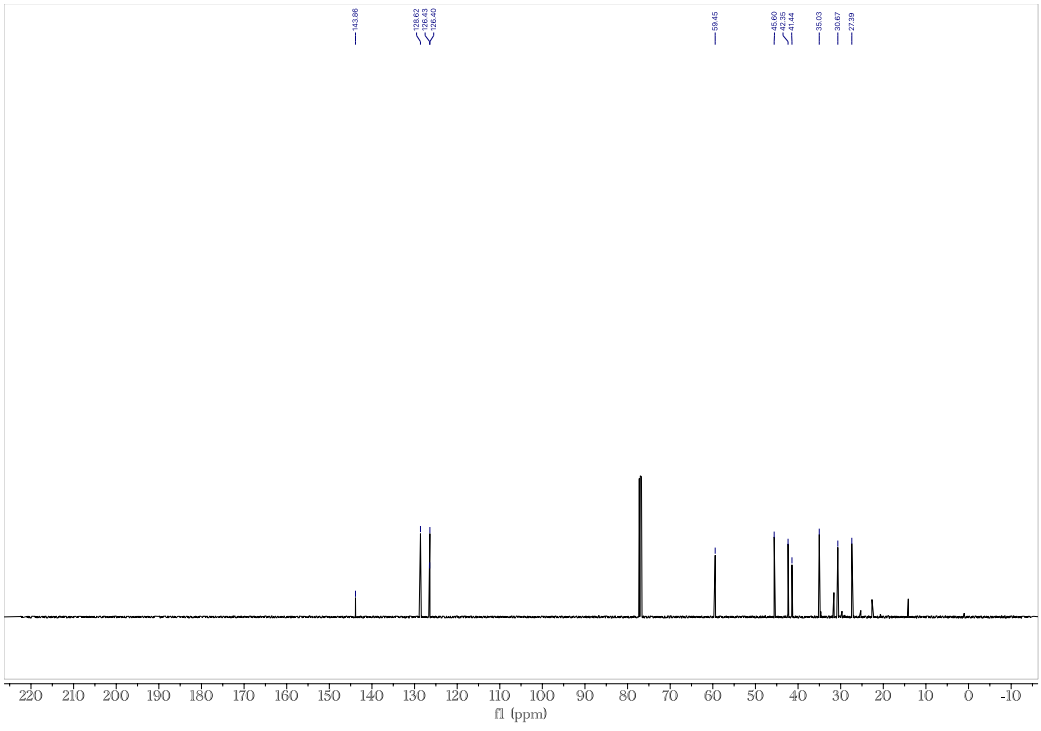

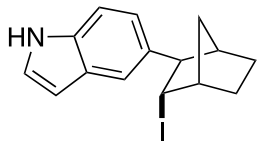
HN

Compound 3b

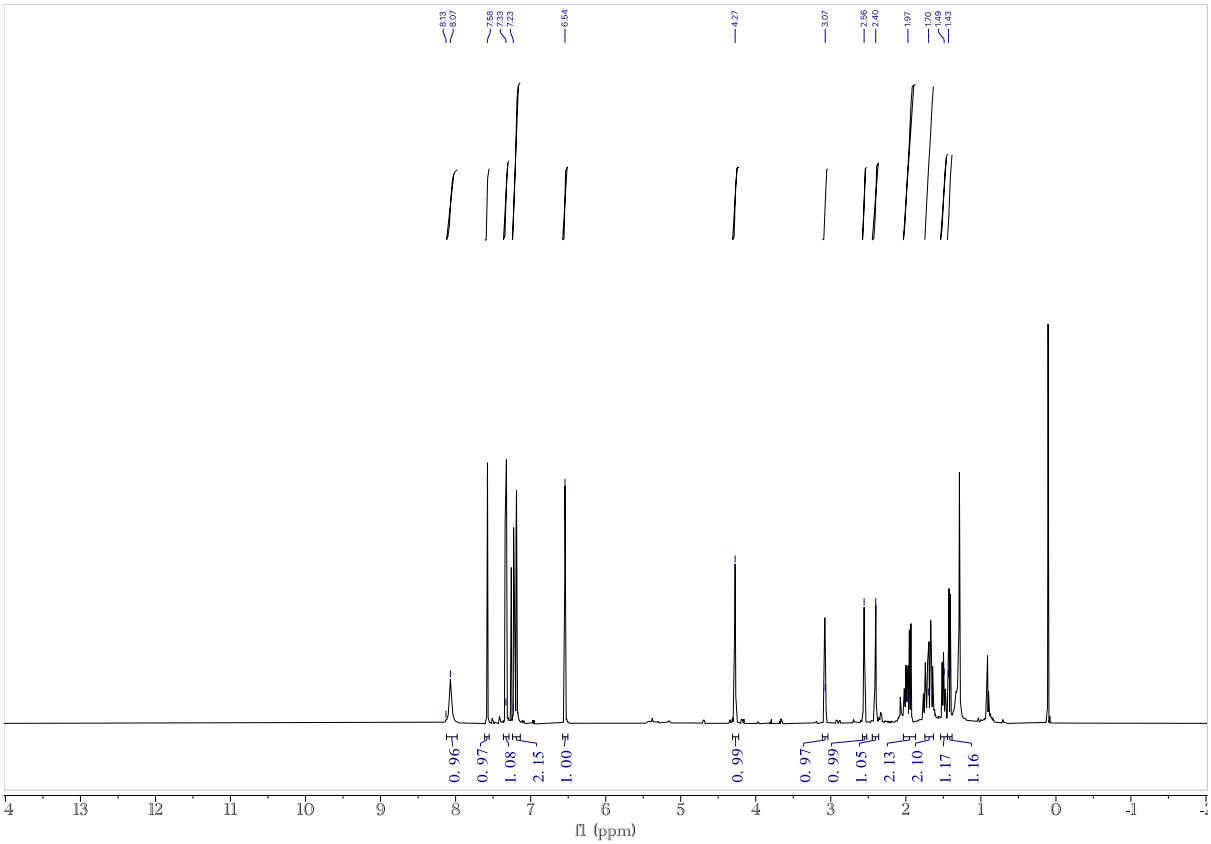
8.13
8.07
7.58
7.33
7.23
6.54
4.27
3.07
2.56
2.40
1.97
1.70
1.49
1.43
0.96
0.97
1.08
2.15
1.00
0.99
0.97
0.99
1.05
2.13
2.10
1.17
1.16
f1 (ppm)

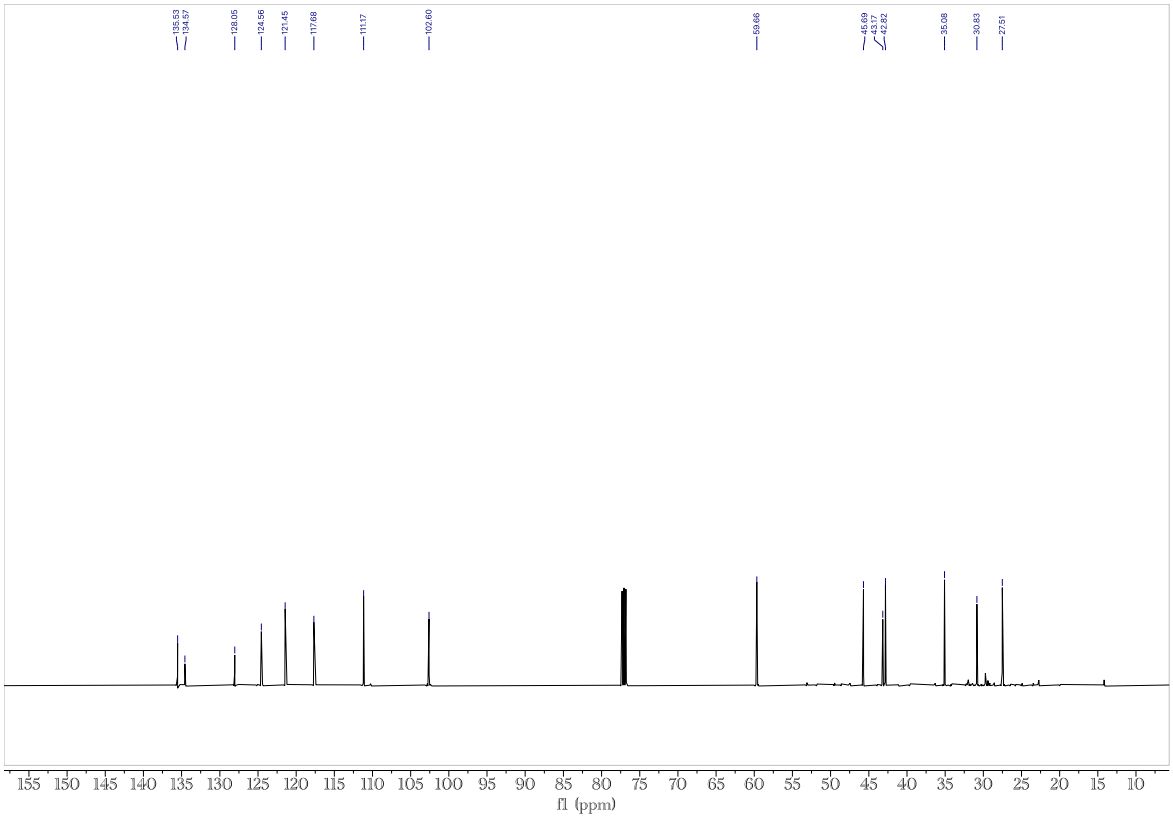
135.53
134.57
128.05
124.56
121.45
117.68
111.17
102.60
59.66
45.69
43.57
42.82
35.08
30.83
27.51
f1 (ppm)

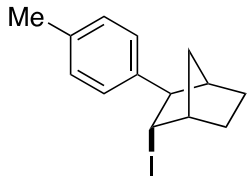
Me

Compound 3c

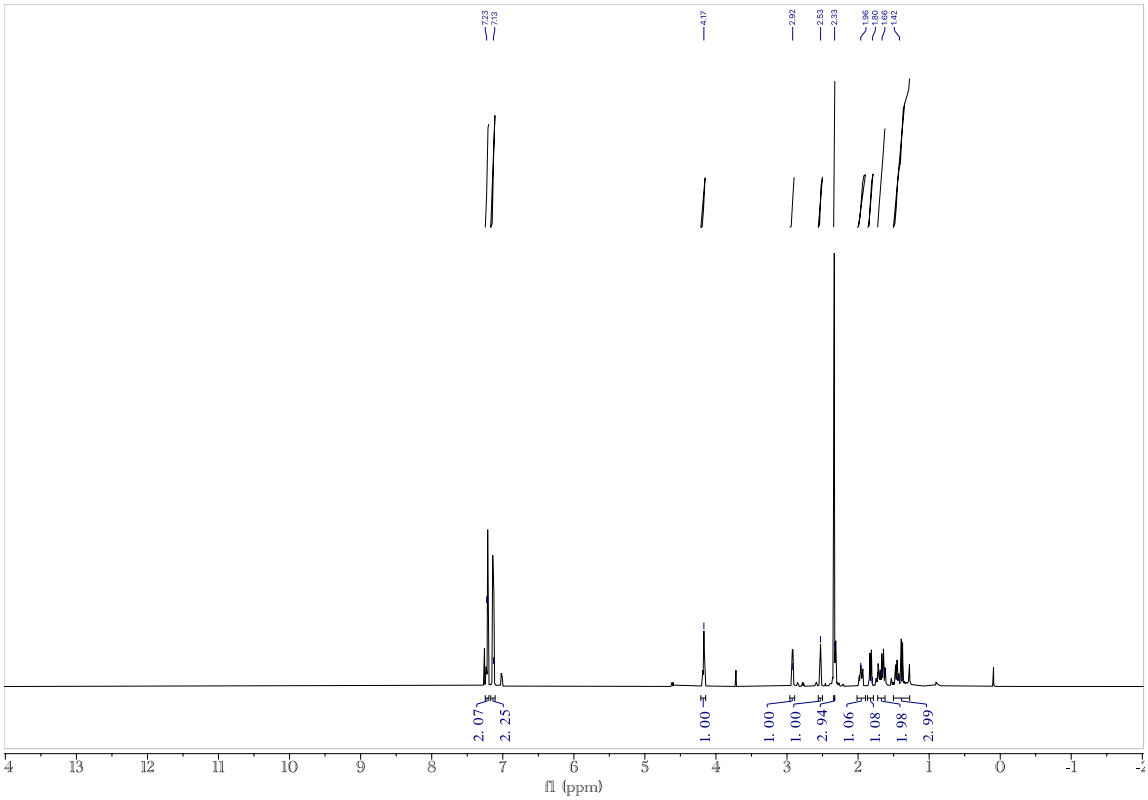
7.23
7.19
4.17
2.92
2.53
2.33
1.96
1.86
1.66
1.42
2.07
2.25
1.00
1.00
1.00
2.94
1.06
1.08
1.98
2.99
f1 (ppm)

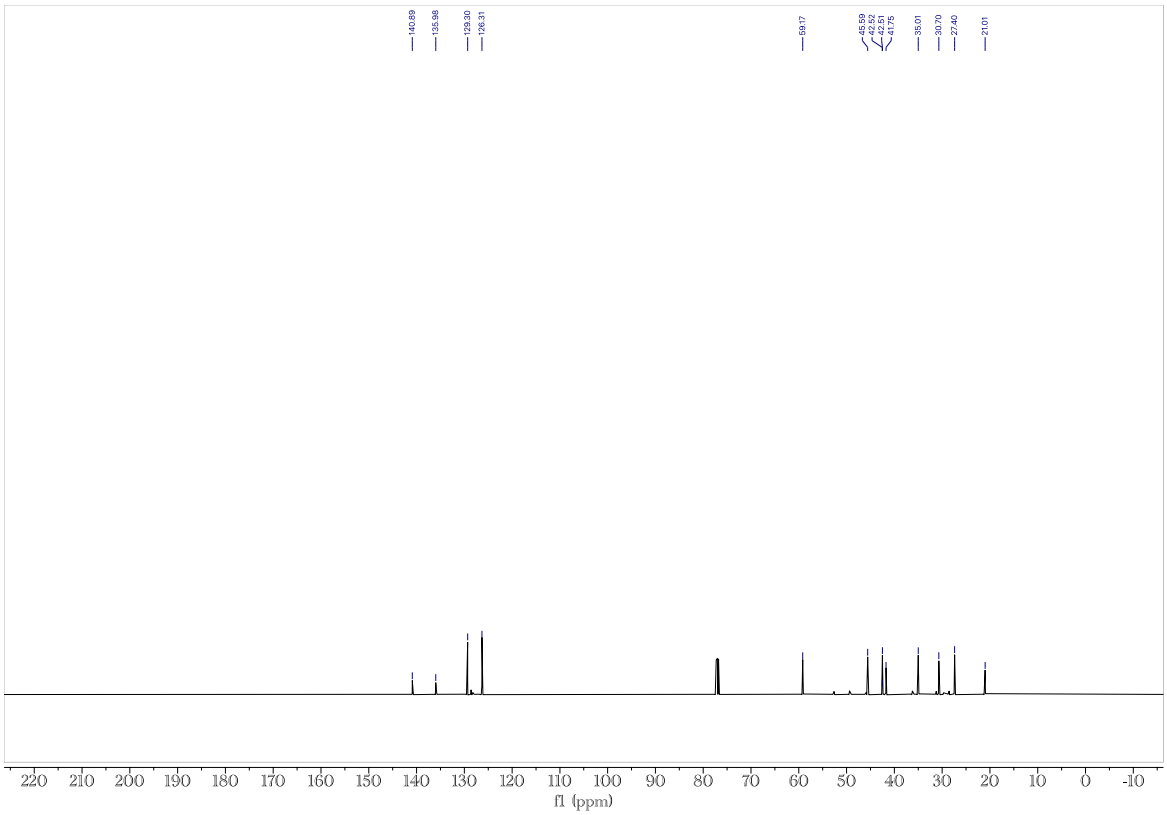
140.89
135.98
129.30
126.31
59.17
45.59
42.52
42.51
41.75
35.01
30.70
27.40
21.01
f1 (ppm)

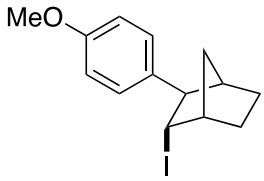
MeO

Compound 3d

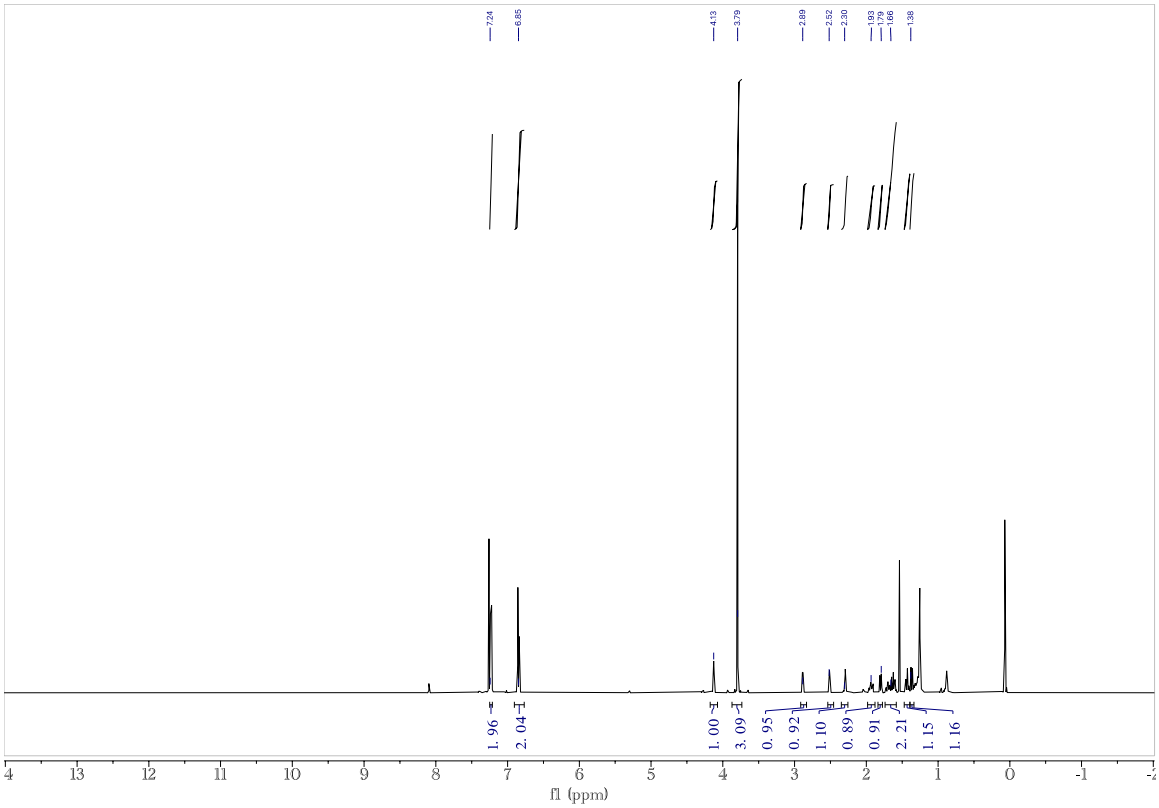
7.24
6.85
4.13
3.79
2.89
2.52
2.30
1.93
1.79
1.66
1.38
1.96
2.04
1.00
3.09
0.95
0.92
1.10
0.89
0.91
2.21
1.15
1.16
f1 (ppm)

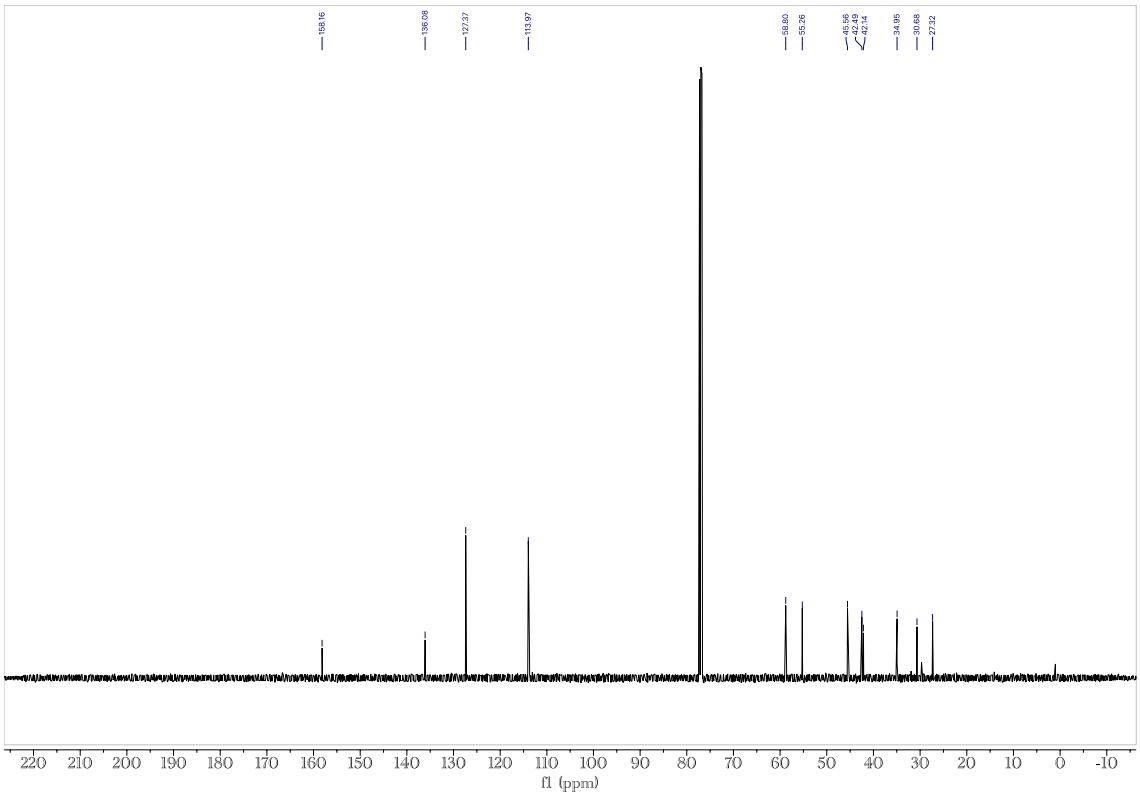
158.16
136.08
127.37
113.97
58.80
55.26
46.56
42.49
42.14
34.85
30.68
27.32
f1 (ppm)

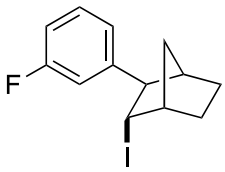
F
I

Compound 3e

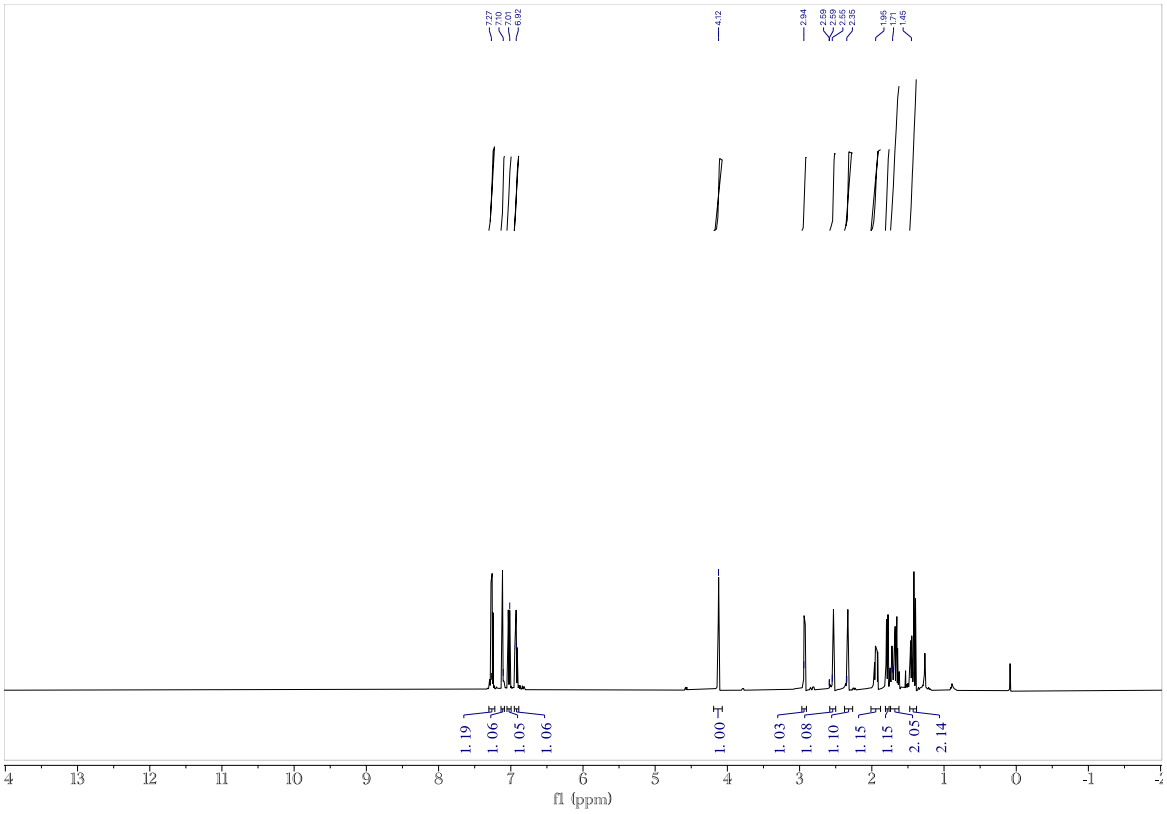
7.27
7.00
7.01
6.92
4.12
2.94
2.89
2.69
2.55
2.35
1.95
1.71
1.45
1.19
1.06
1.05
1.06
1.00
1.03
1.08
1.10
1.15
1.15
2.05
2.14
f1 (ppm)

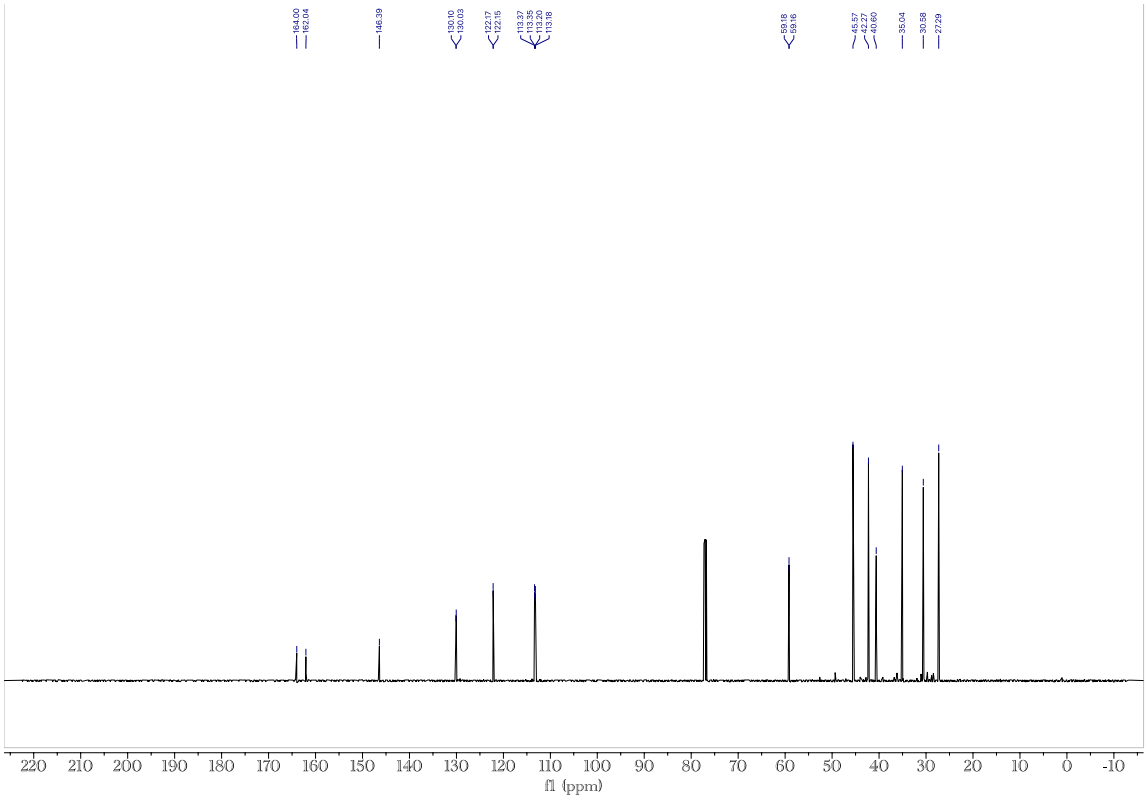
164.00
162.04
146.39
130.10
130.03
122.17
122.15
113.37
113.35
113.20
113.18
59.18
59.16
45.57
42.27
40.66
35.04
30.58
27.29
220 210 200 190 180 170 160 150 140 130 120 110 100 90 80 70 60 50 40 30 20 10 0 -10
f1 (ppm)

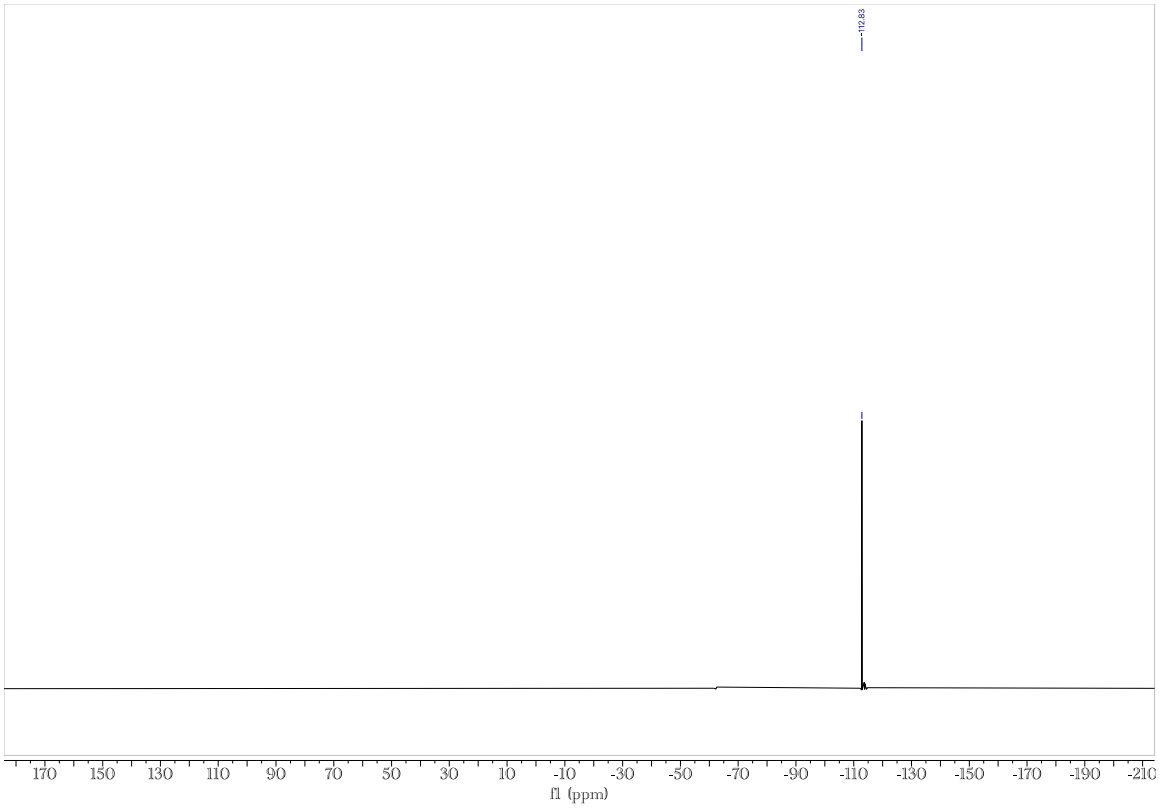
-112.63
170 150 130 110 90 70 50 30 10 -10 -30 -50 -70 -90 -110 -130 -150 -170 -190 -210
f1 (ppm)

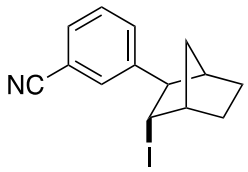
NC
I

Compound 3f

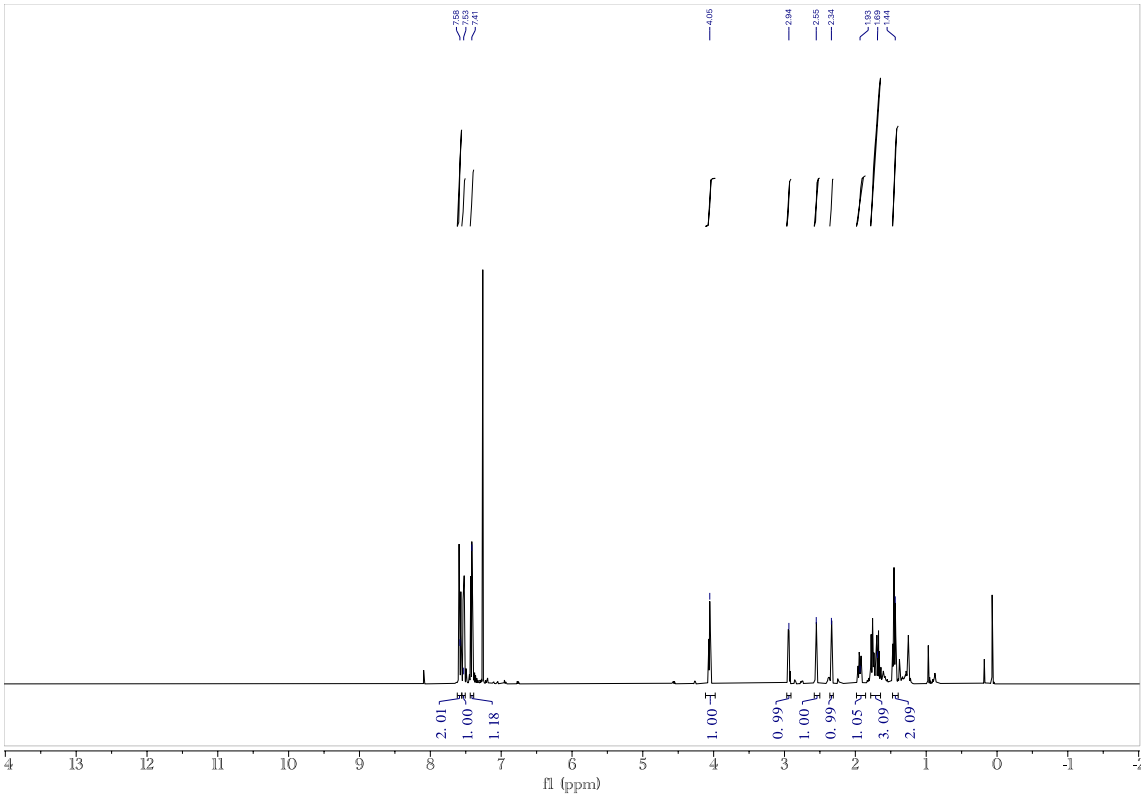
7.58
7.53
7.41
4.06
2.94
2.55
2.34
1.93
1.69
1.44
2. 01
1. 00
1. 18
1. 00
0. 99
1. 00
0. 99
1. 05
3. 09
2. 09
f1 (ppm)

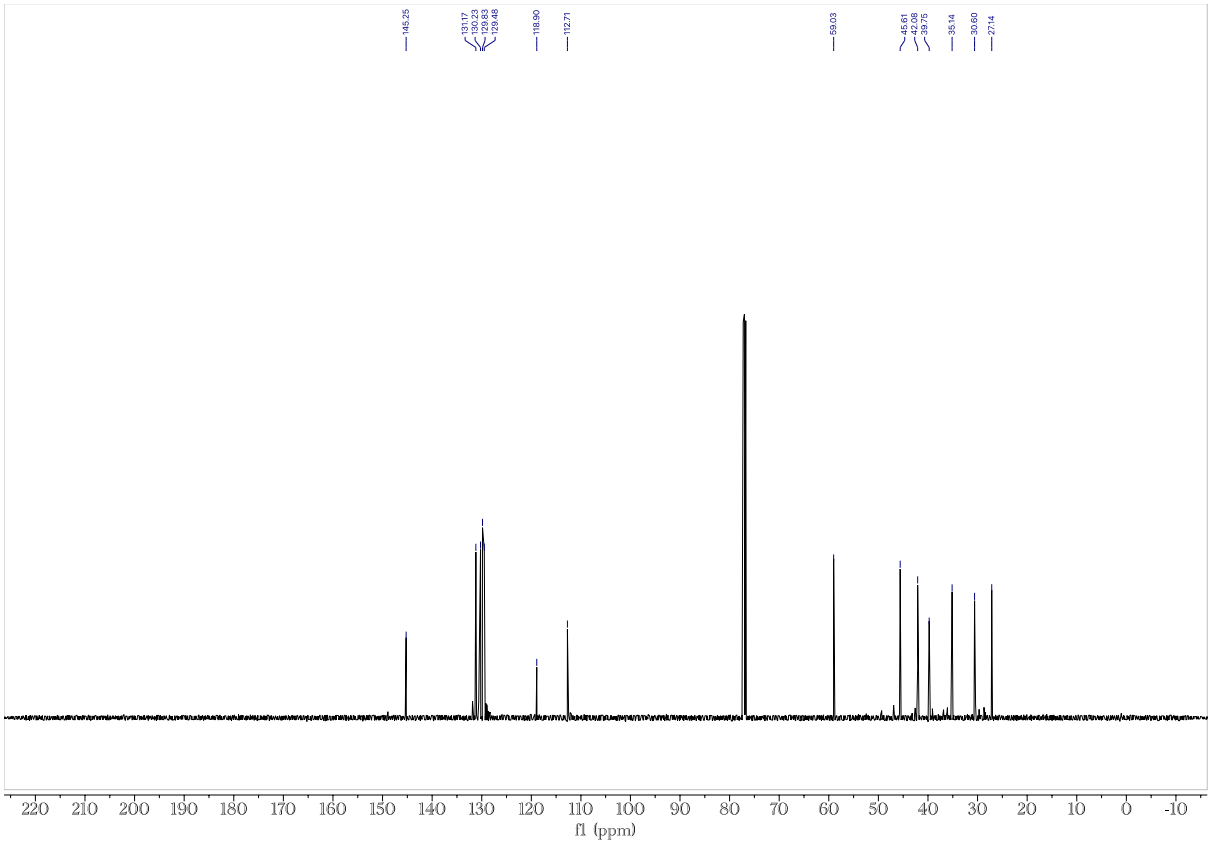
145.25
131.17
130.23
129.93
129.48
118.90
112.71
59.03
45.61
42.08
39.75
35.14
30.60
27.14
f1 (ppm)

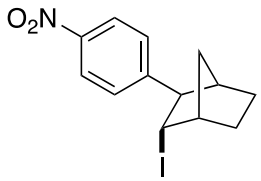
O2N

Compound 3g

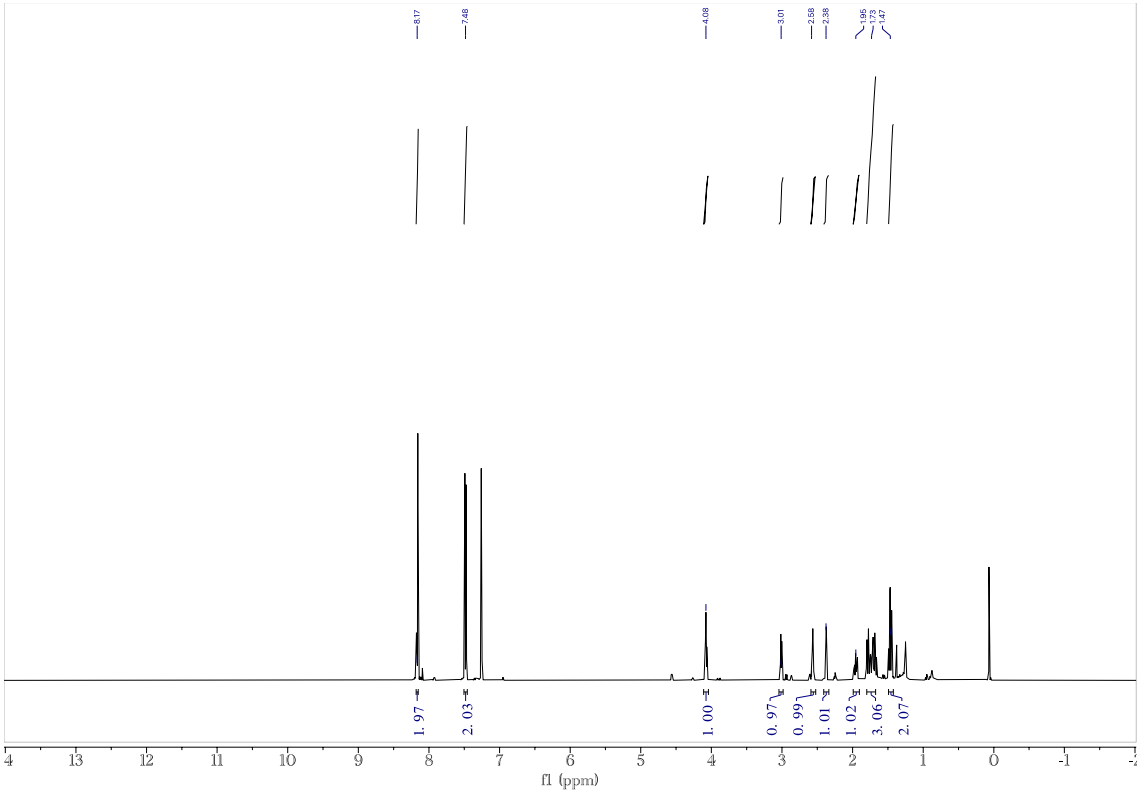
8.17
7.48
4.08
3.01
2.58
2.38
1.66
1.75
1.47
1.97
2.03
1.00
0.97
0.99
1.01
1.02
3.06
2.07
f1 (ppm)

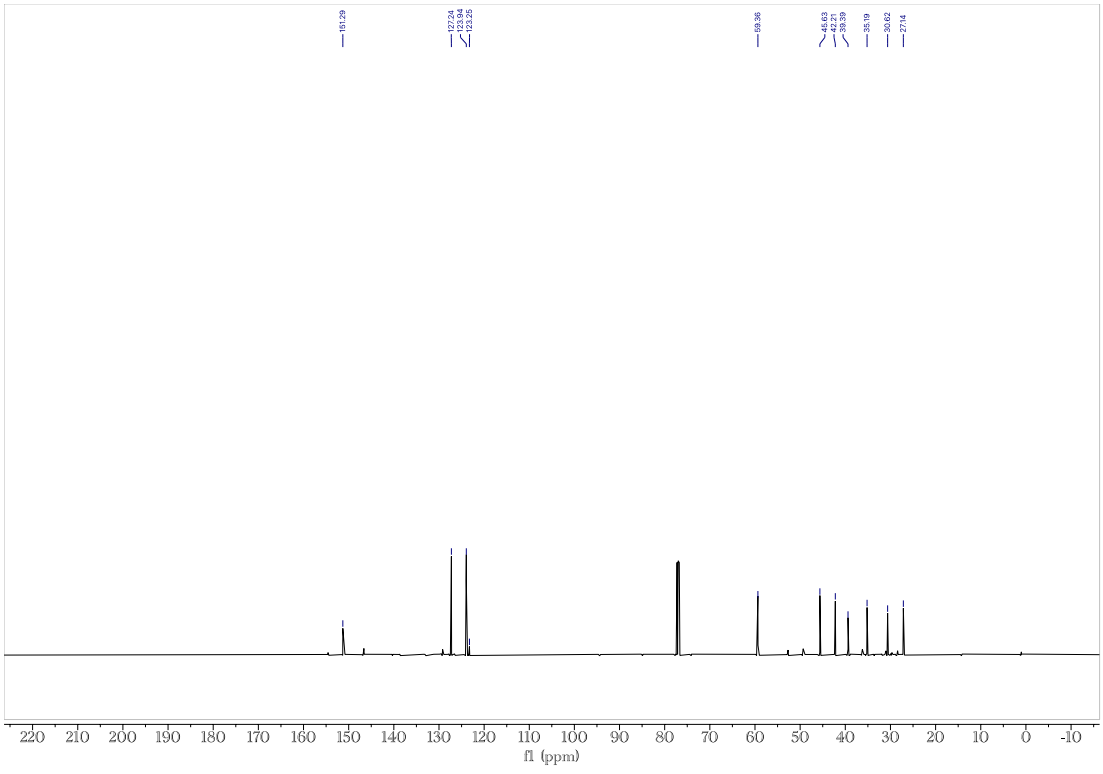
151.29
127.24
123.94
122.85
69.36
45.63
42.31
39.39
35.19
30.62
27.14
f1 (ppm)

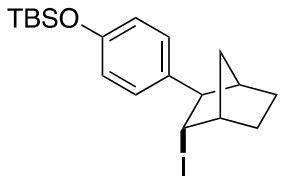
TBSO

Compound 3h

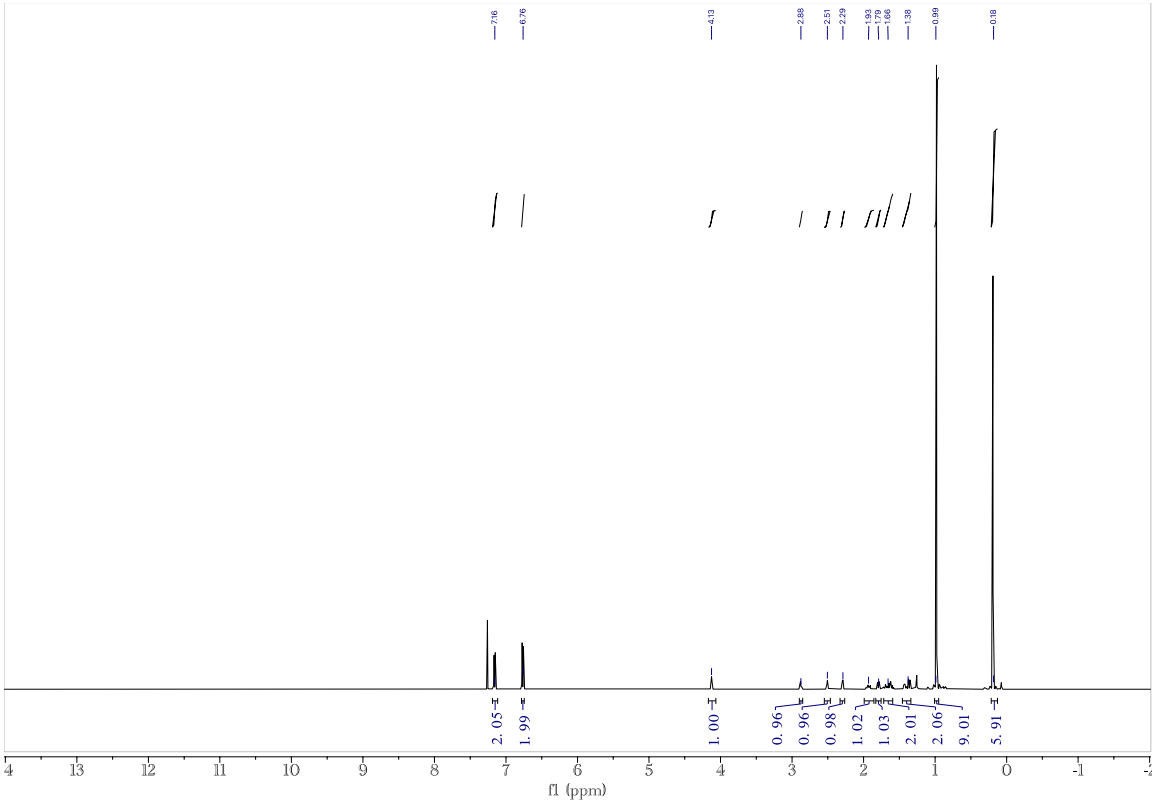
7.16
6.76
4.13
2.88
2.51
2.29
1.93
1.79
1.66
1.38
0.99
0.18
2.05
1.99
1.00
0.96
0.96
0.98
1.02
1.03
2.01
2.06
9.01
5.91
f1 (ppm)

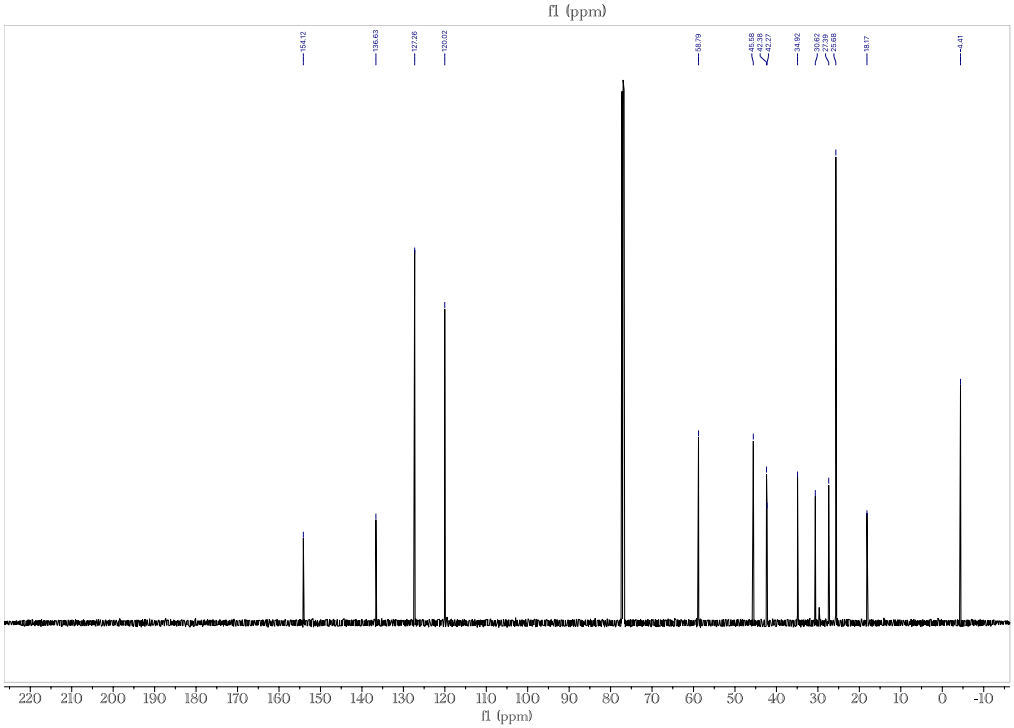
154.12
136.63
127.26
120.02
58.79
46.58
42.38
42.27
34.92
30.62
27.39
26.68
18.17
-4.41
f1 (ppm)

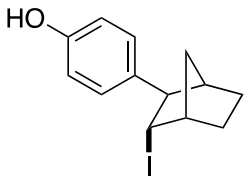
HO

Compound 3i

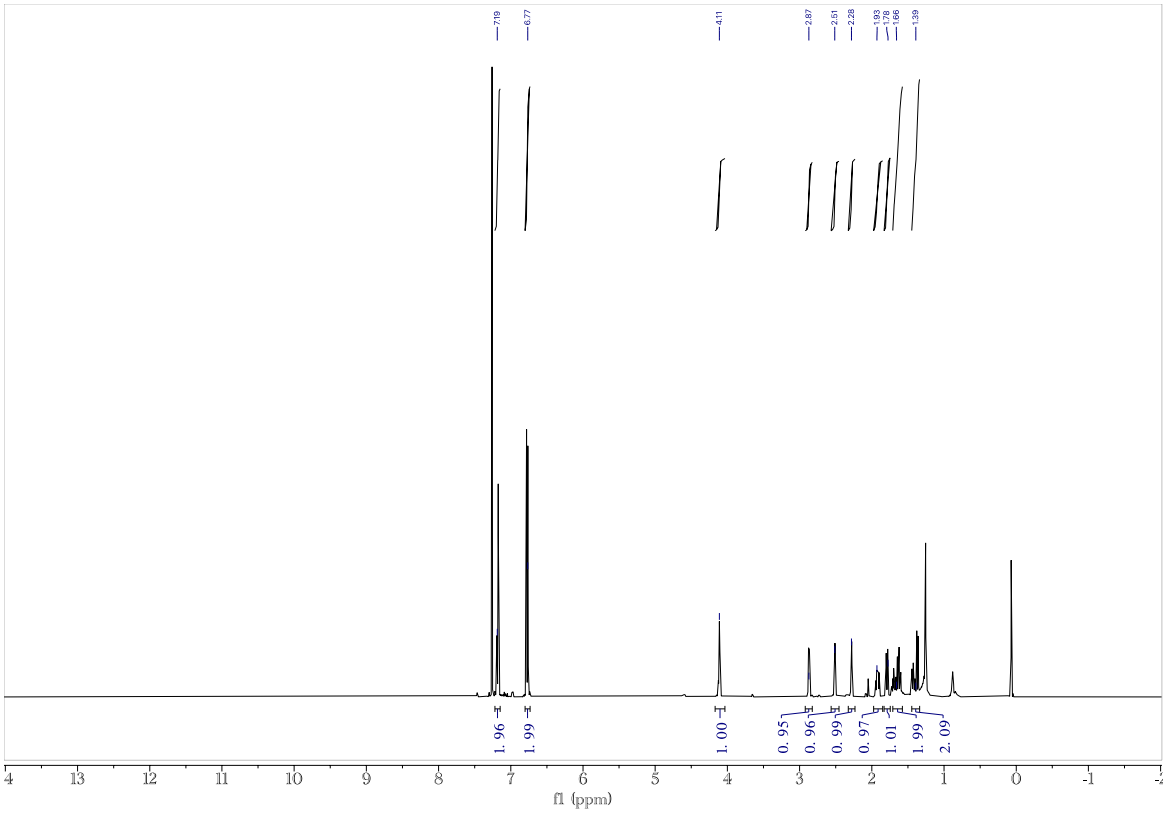
7.19
6.77
4.11
2.87
2.61
2.28
1.93
1.79
1.66
1.39
1.96
1.99
1.00
0.95
0.96
0.99
0.97
1.01
1.99
2.09
f1 (ppm)

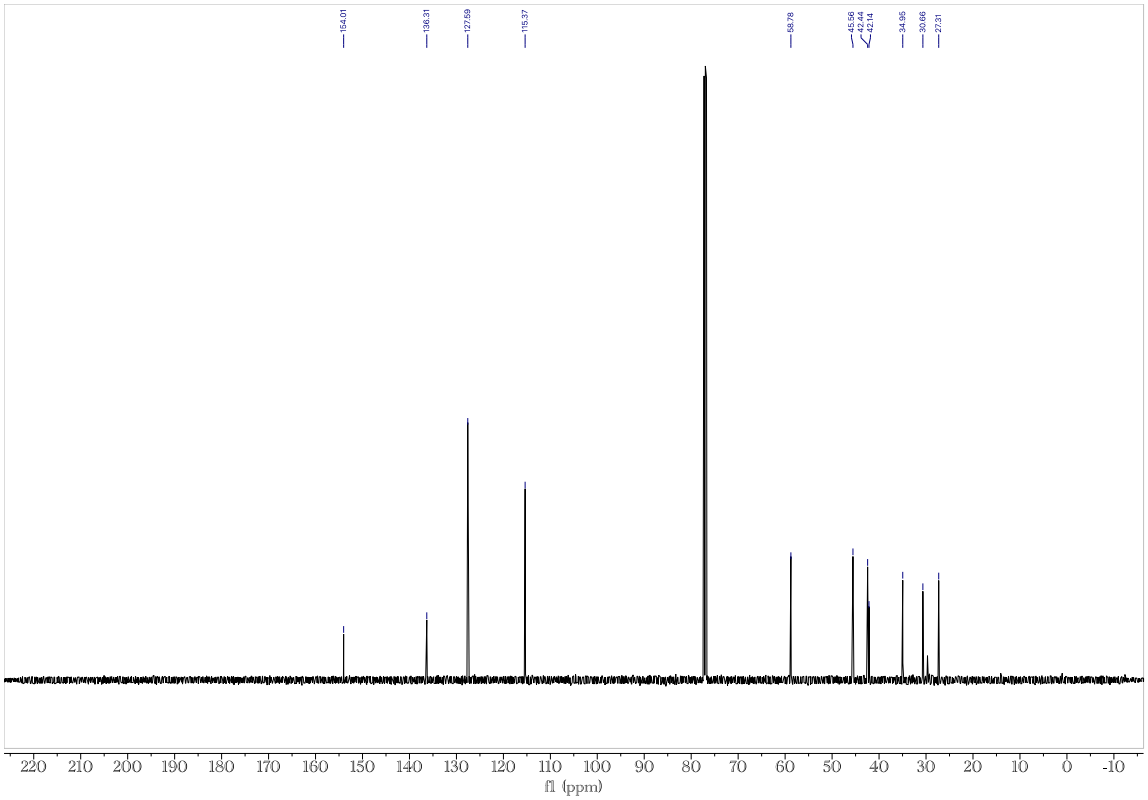
154.01
136.31
127.59
115.37
58.78
45.56
42.44
42.14
34.95
30.66
27.31
f1 (ppm)

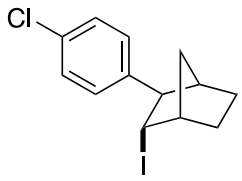
Cl
I

Compound 3j

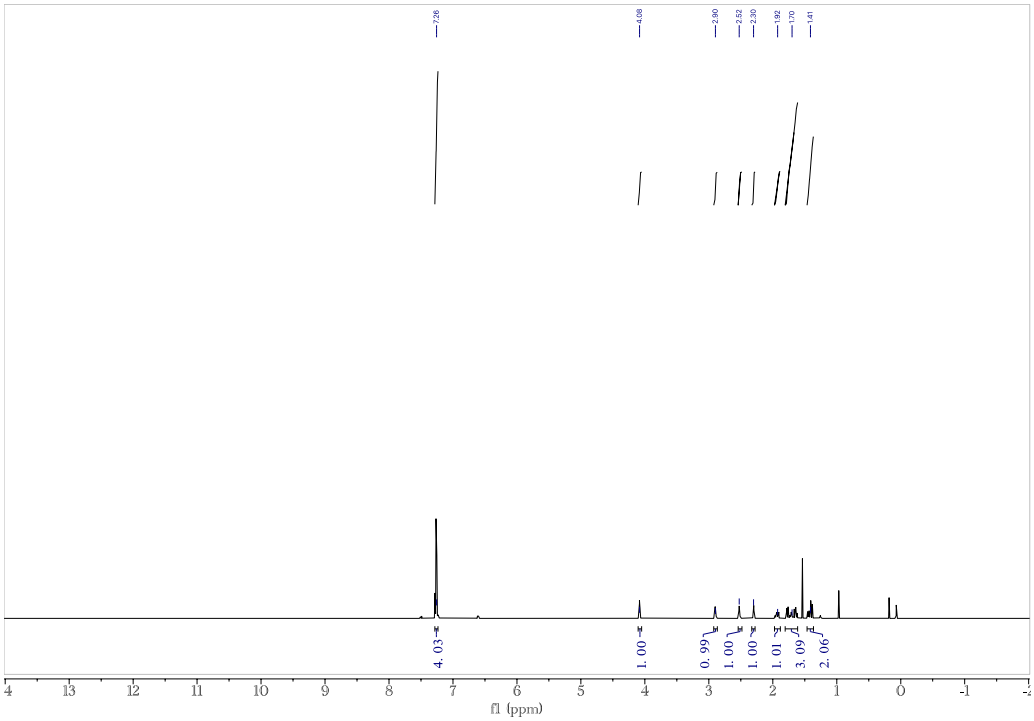
7.26
4.08
2.90
2.52
2.30
1.92
1.70
1.41
4.03
1.00
0.99
1.00
1.00
1.01
3.09
2.06
f1 (ppm)

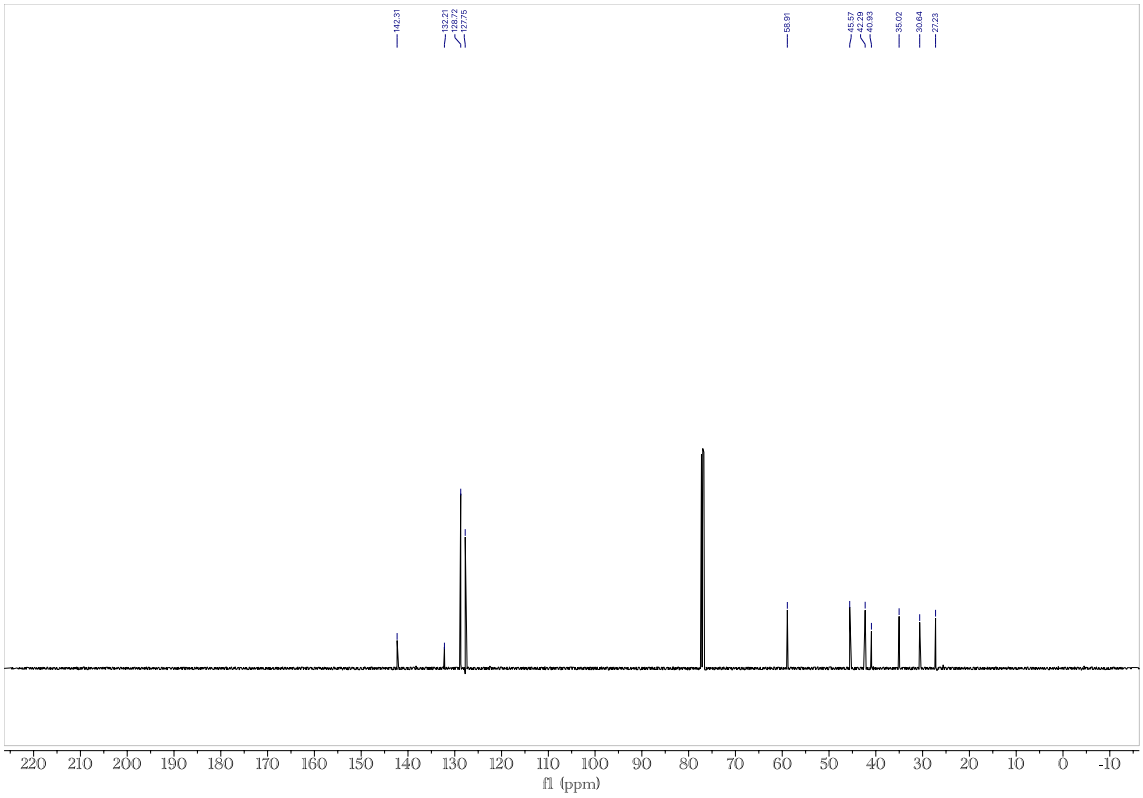
142.31
132.23
129.72
127.75
58.91
45.57
42.58
40.93
35.02
30.64
27.23
f1 (ppm)

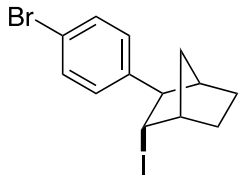
Br
I

Compound 3k

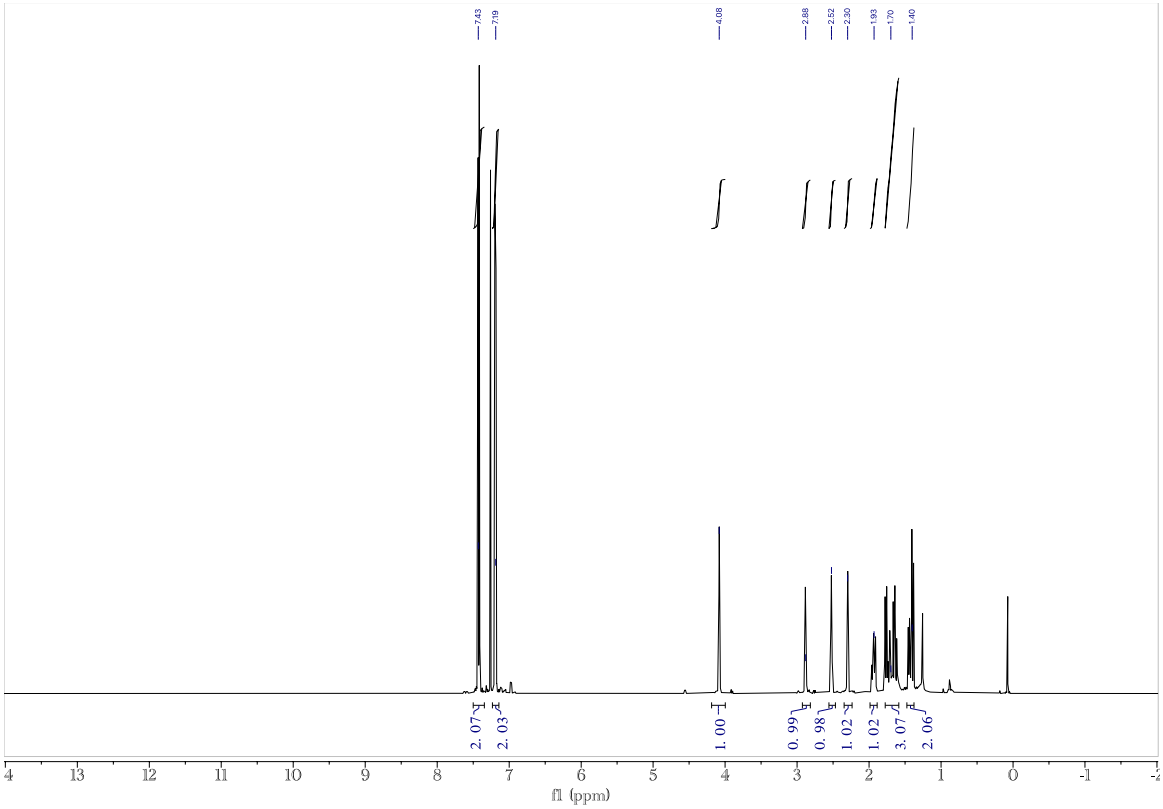
7.43
7.19
4.08
2.88
2.52
2.30
1.93
1.70
1.40
2.07
2.03
1.00
0.99
0.98
1.02
1.02
3.07
2.06
f1 (ppm)

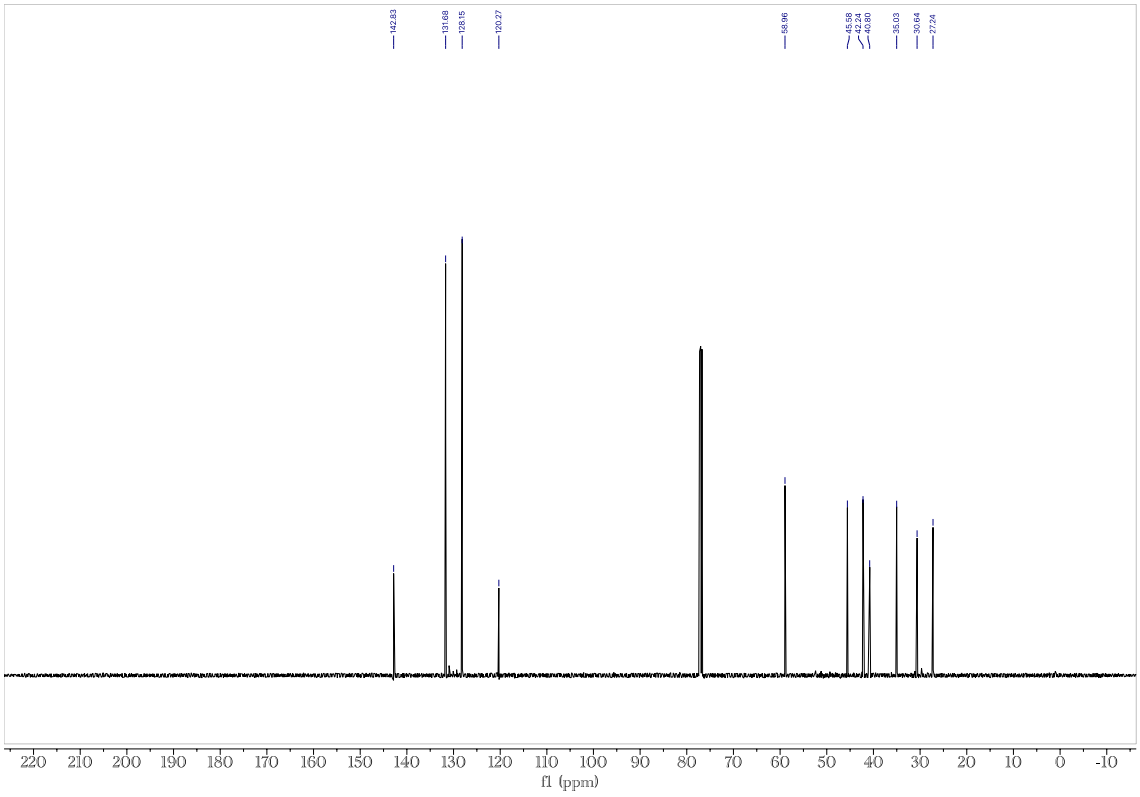
142.83
131.68
128.15
120.27
58.96
45.58
42.24
40.80
35.03
30.64
27.24
f1 (ppm)

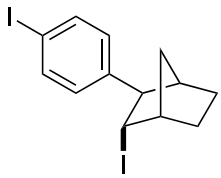

Compound 3l

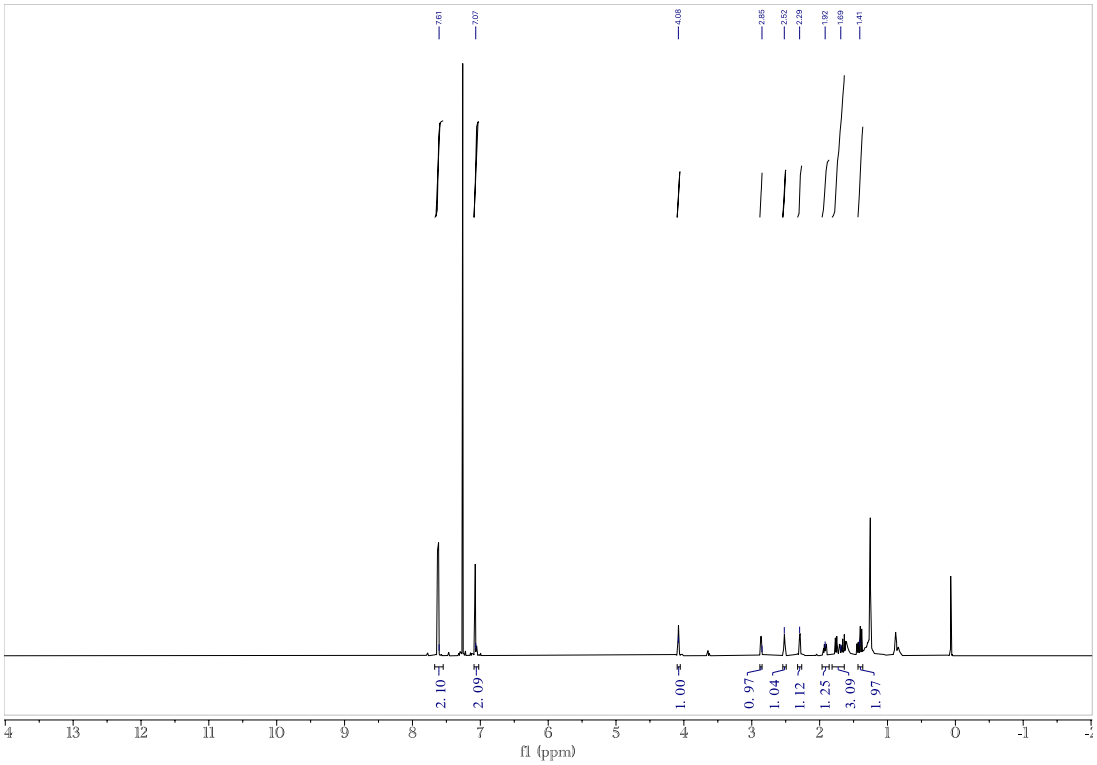
7.61
7.07
4.08
2.85
2.52
2.29
1.92
1.69
1.41
2.10
2.09
1.00
0.97
1.04
1.12
1.25
3.09
1.97
f1 (ppm)

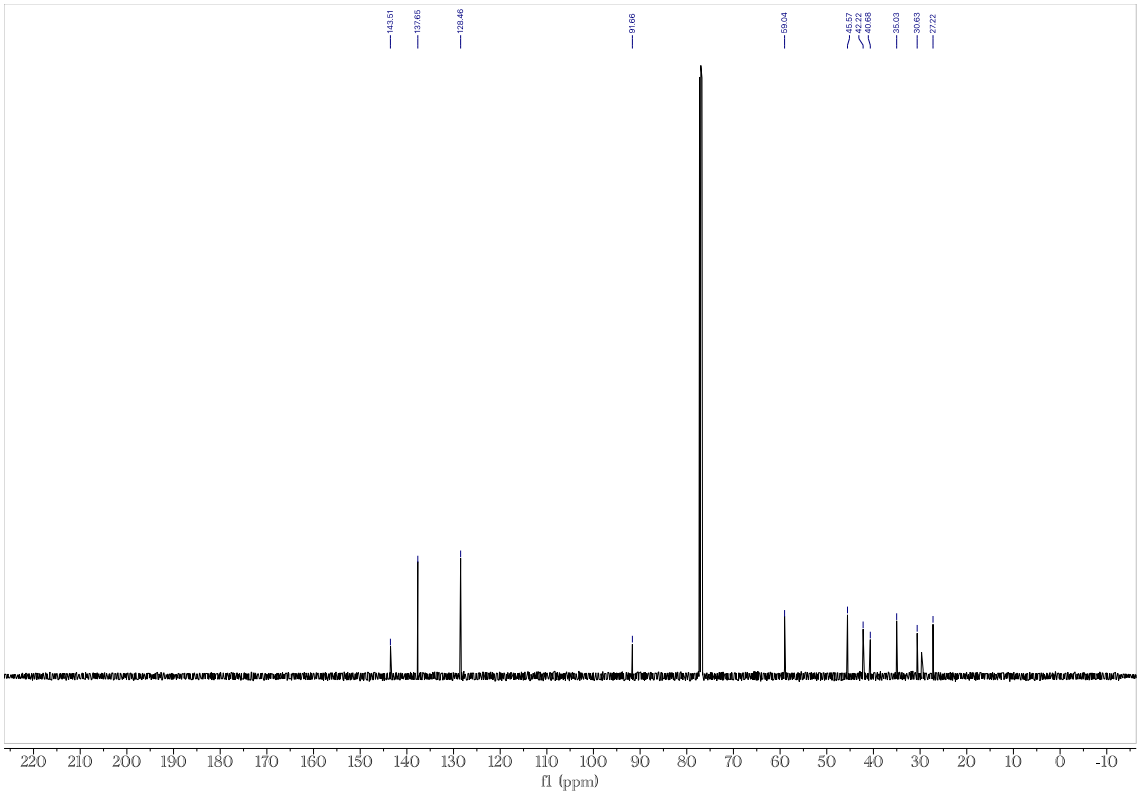
143.51
137.65
128.46
91.66
59.04
45.57
42.22
40.68
35.03
30.63
27.22
f1 (ppm)

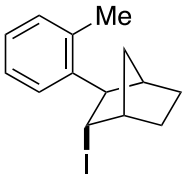
Me
I

Compound 3m

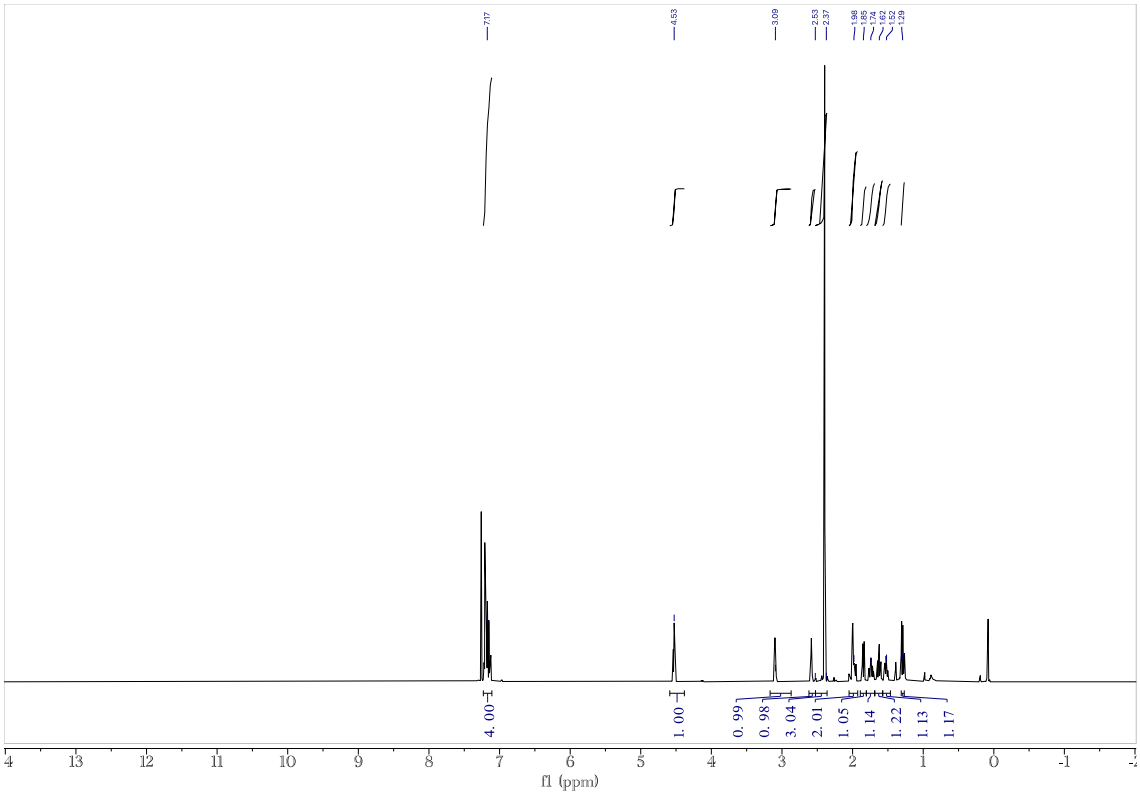
7.17
4.53
3.09
2.53
2.37
1.98
1.95
1.74
1.62
1.52
1.30
4.00
1.00
0.99
0.98
3.04
2.01
1.05
1.14
1.22
1.13
1.17
f1 (ppm)

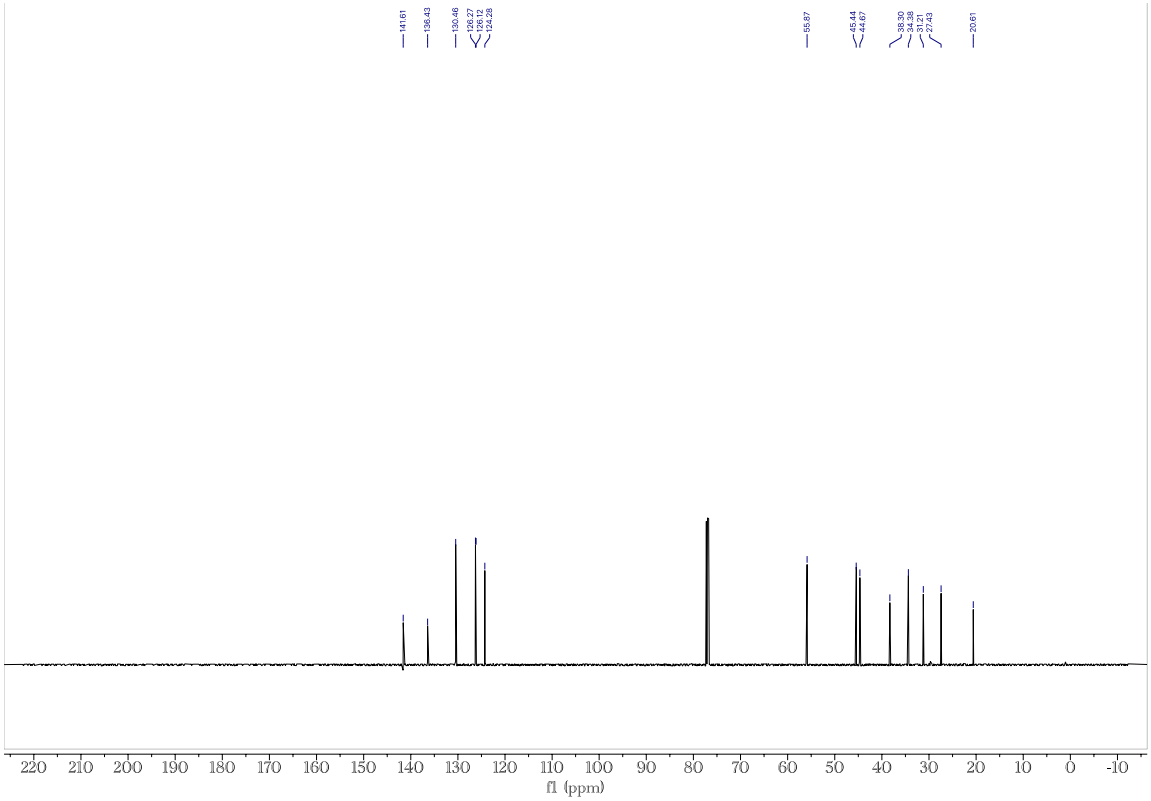
141.61
138.43
130.46
126.27
126.12
124.28
55.87
45.44
44.67
38.30
34.38
31.21
27.43
20.61
f1 (ppm)

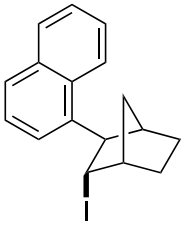

Compound 3n

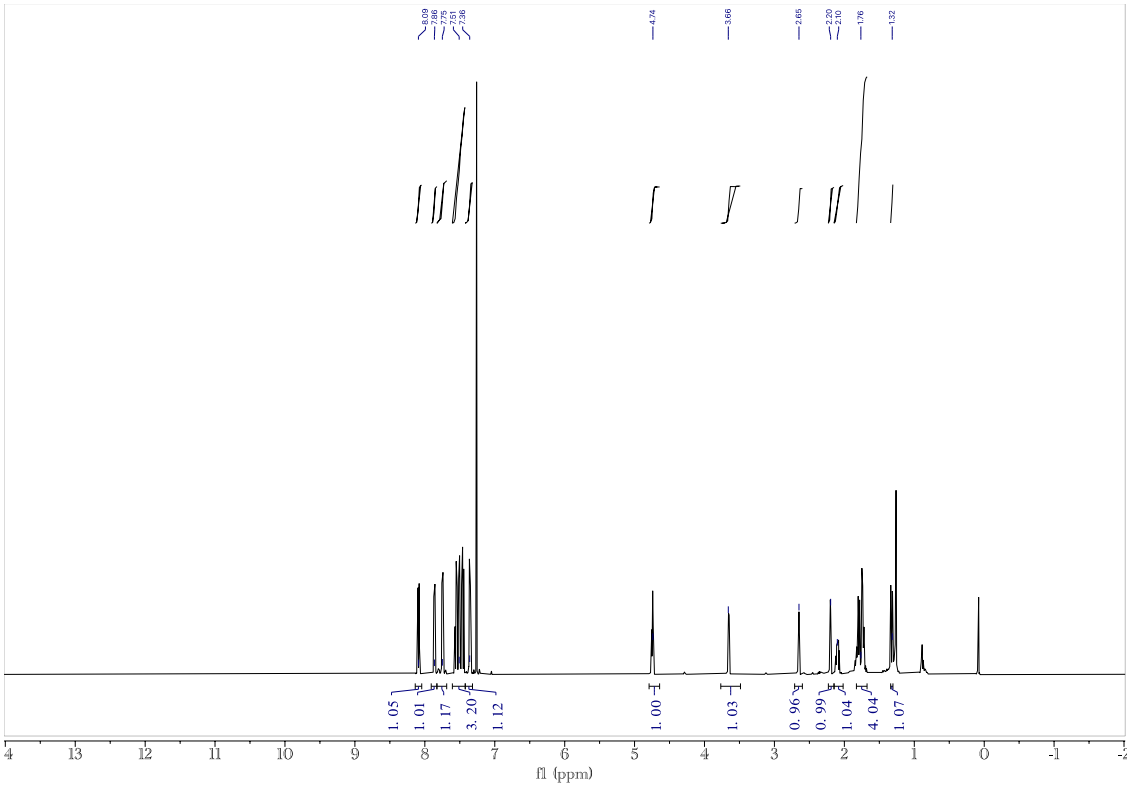
8.09
7.86
7.75
7.53
7.36
4.74
3.66
2.65
2.20
2.10
1.76
1.32
1.05
1.01
1.17
3.20
1.12
1.00
1.03
0.96
0.99
1.04
4.04
1.07
f1 (ppm)

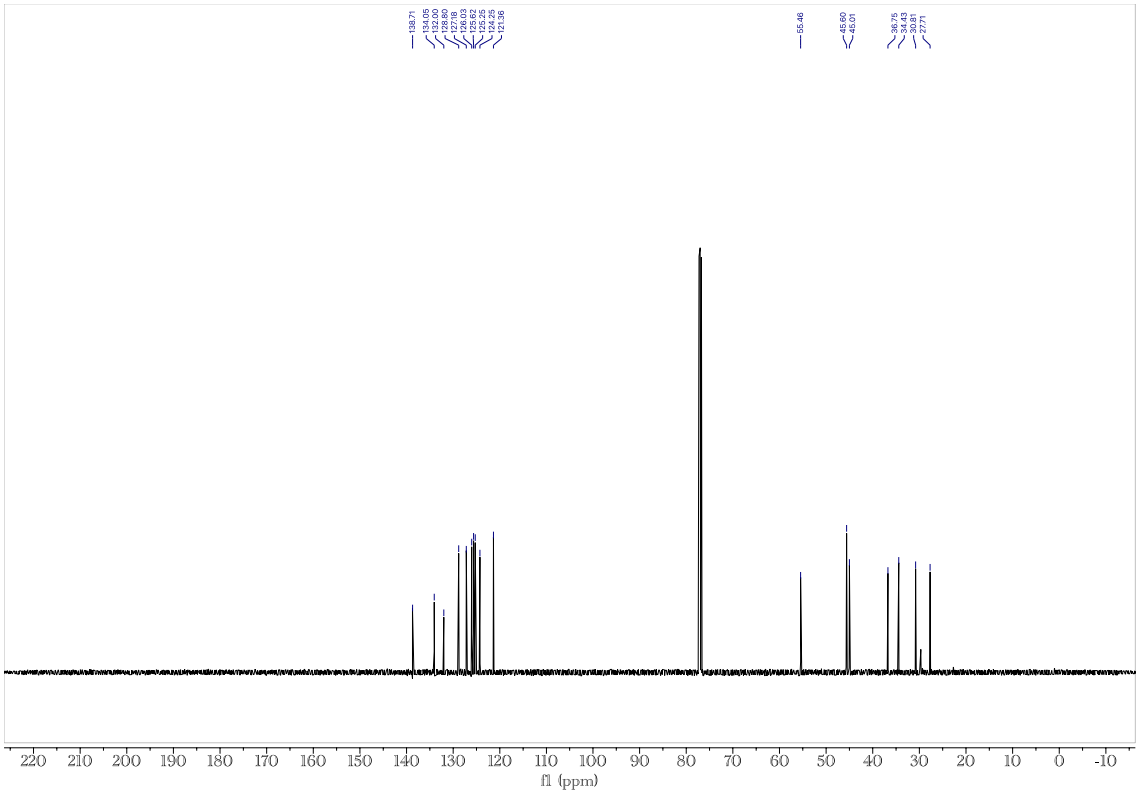
138.71
134.05
132.00
129.80
129.70
126.03
125.62
125.45
124.25
121.36
55.46
45.60
45.01
38.75
34.43
30.81
27.71
f1 (ppm)

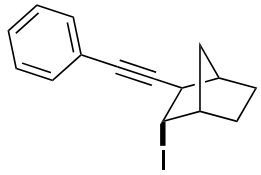

Compound 3o

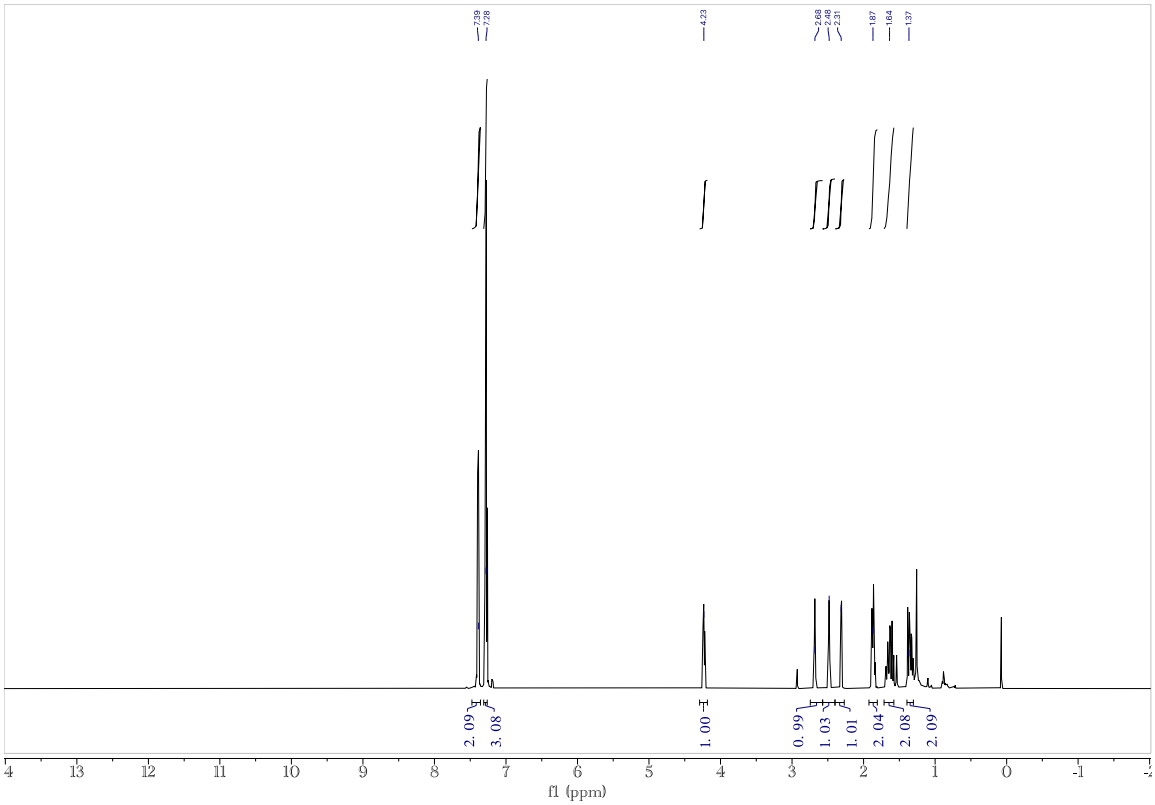
7.39
7.28
4.23
2.68
2.48
2.31
1.87
1.64
1.37
2. 09
3. 08
1. 00
0. 99
1. 03
1. 01
2. 04
2. 08
2. 09
f1 (ppm)

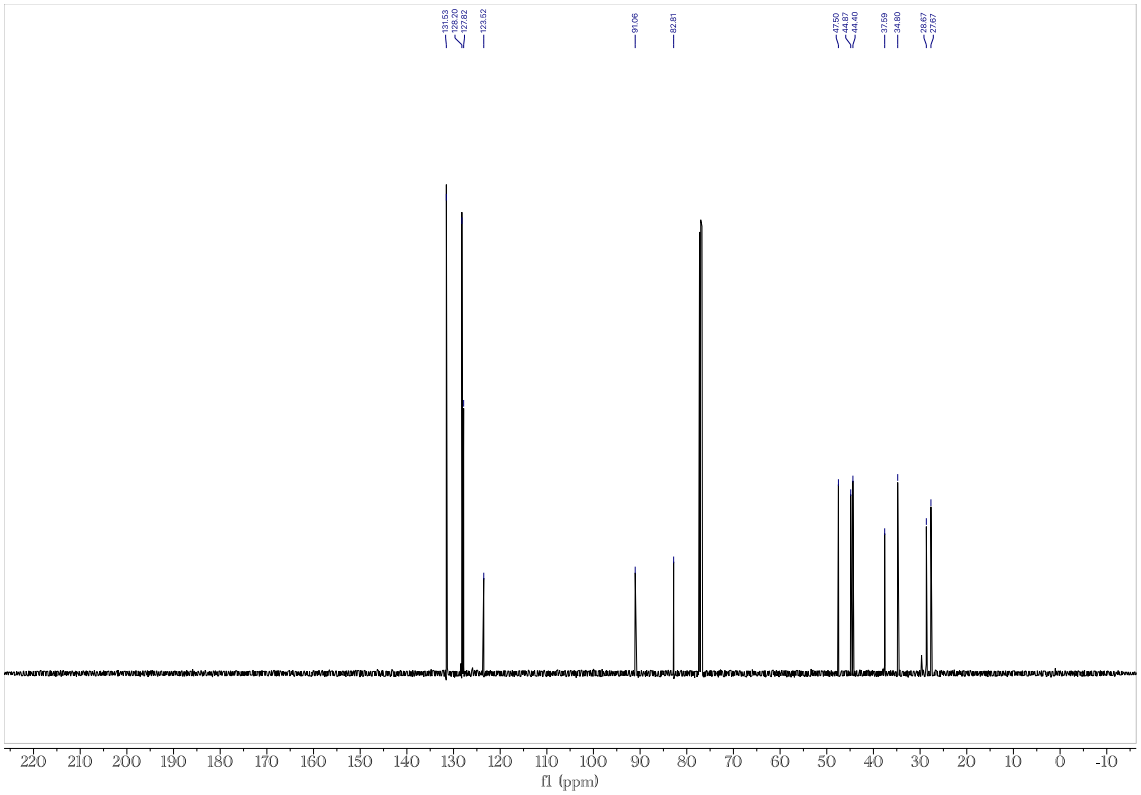
131.53
129.20
127.82
123.52
91.06
82.81
47.50
44.59
44.40
37.59
34.80
28.67
27.67
f1 (ppm)

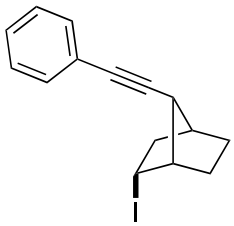

Compound 3p

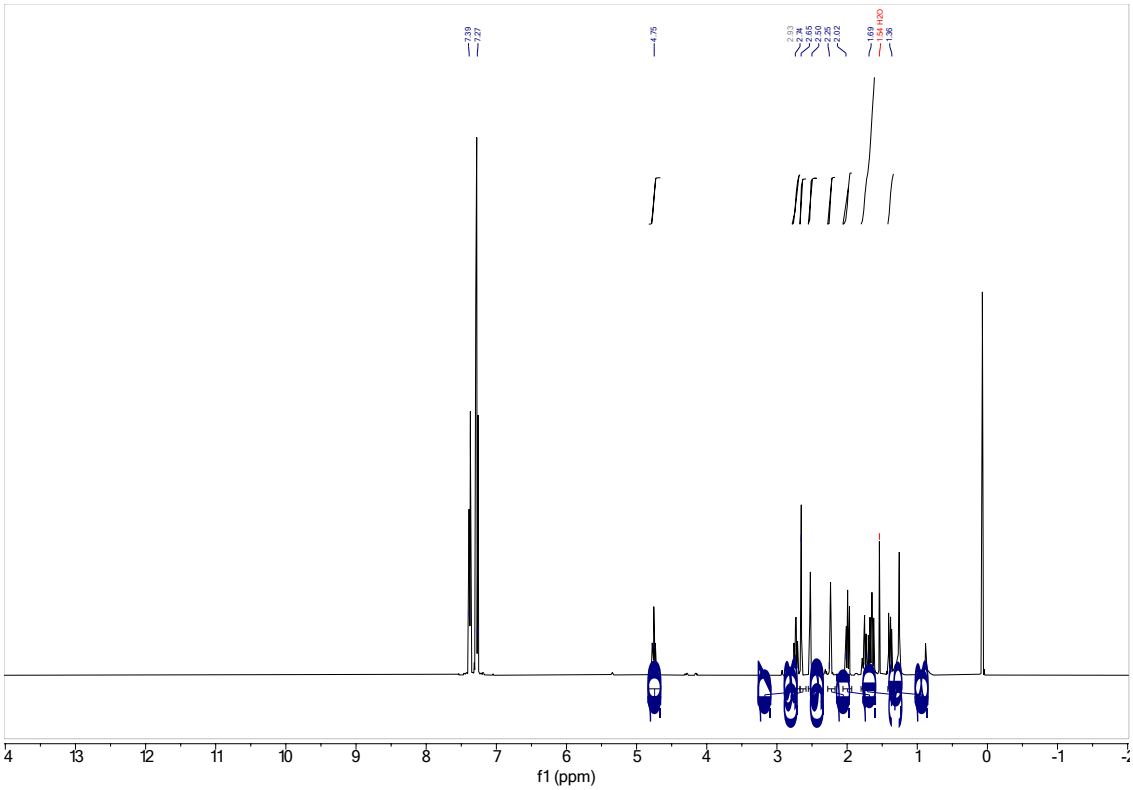
7.39
7.27
4.75
2.93
2.74
2.65
2.59
2.25
2.02
1.69
1.54 H2O
1.36
f1 (ppm)

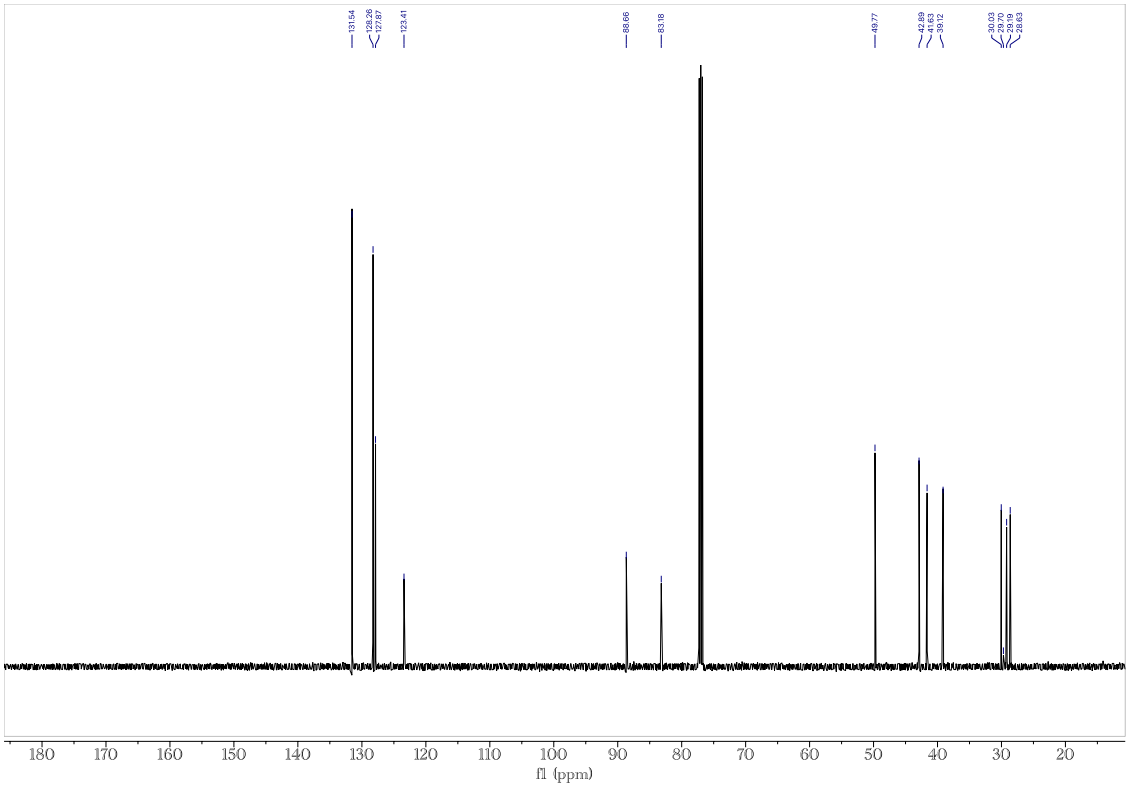
131.54
128.26
127.67
123.41
88.66
83.18
49.77
42.89
42.63
39.12
30.03
29.20
29.19
28.83
f1 (ppm)

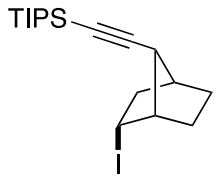
TIPS

Compound 3q

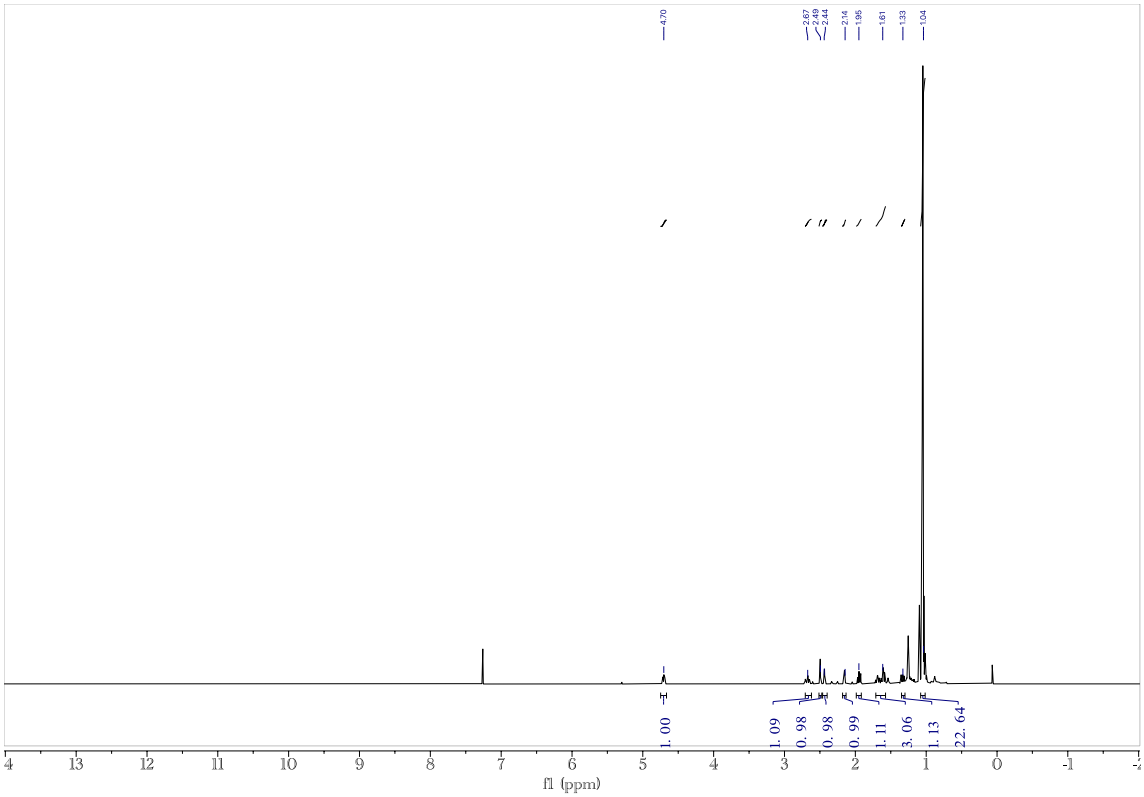
4.70
2.67
2.49
2.44
2.14
1.95
1.61
1.33
1.04
1.00
1.09
0.98
0.98
0.99
1.11
3.06
1.13
22.64
f1 (ppm)

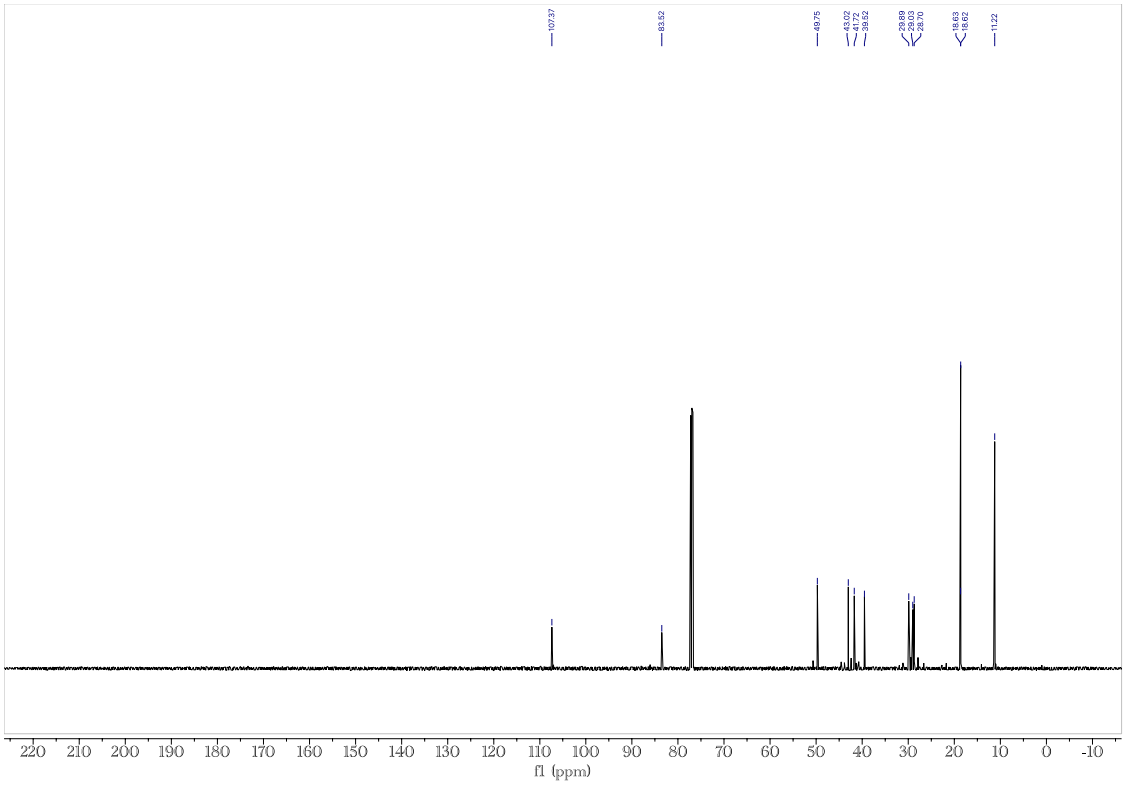
107.37
83.52
69.75
43.02
41.72
39.52
29.89
29.03
28.70
18.63
18.62
11.22
f1 (ppm)

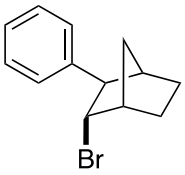
Br

Compound 5a

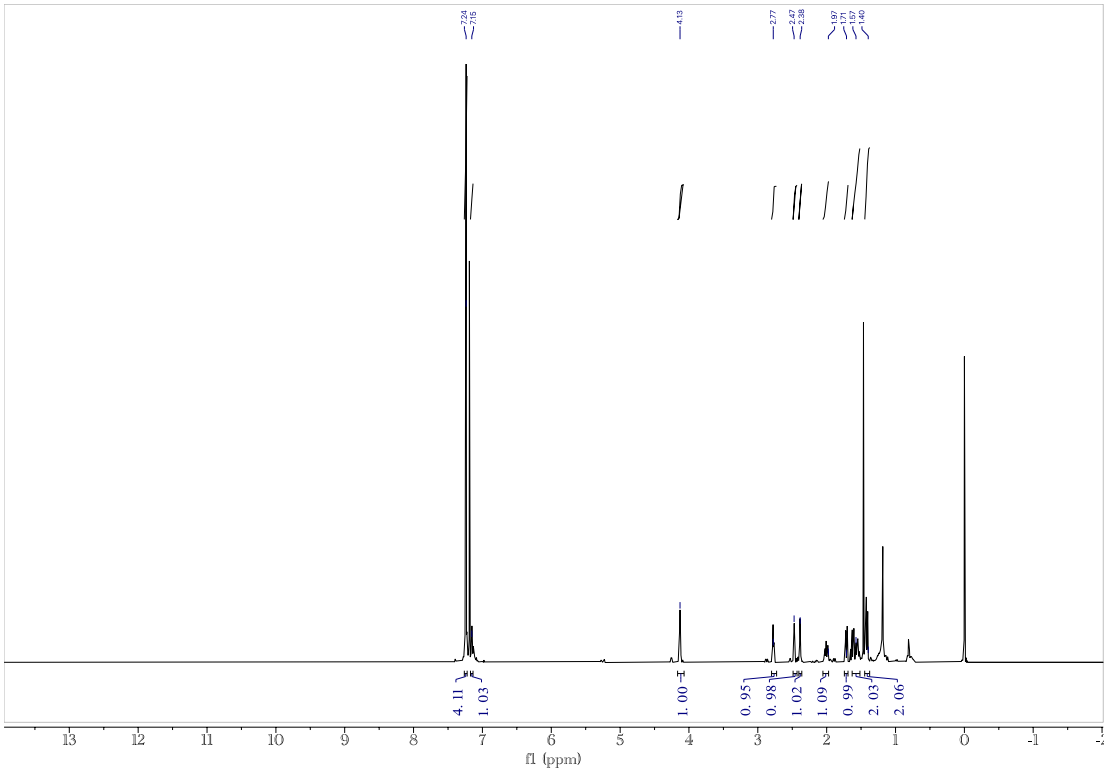
7.24
7.15
4.13
2.77
2.47
2.38
1.97
1.71
1.57
1.40
4.11
1.03
1.00
0.95
0.98
1.02
1.09
0.99
2.03
2.06
f1 (ppm)

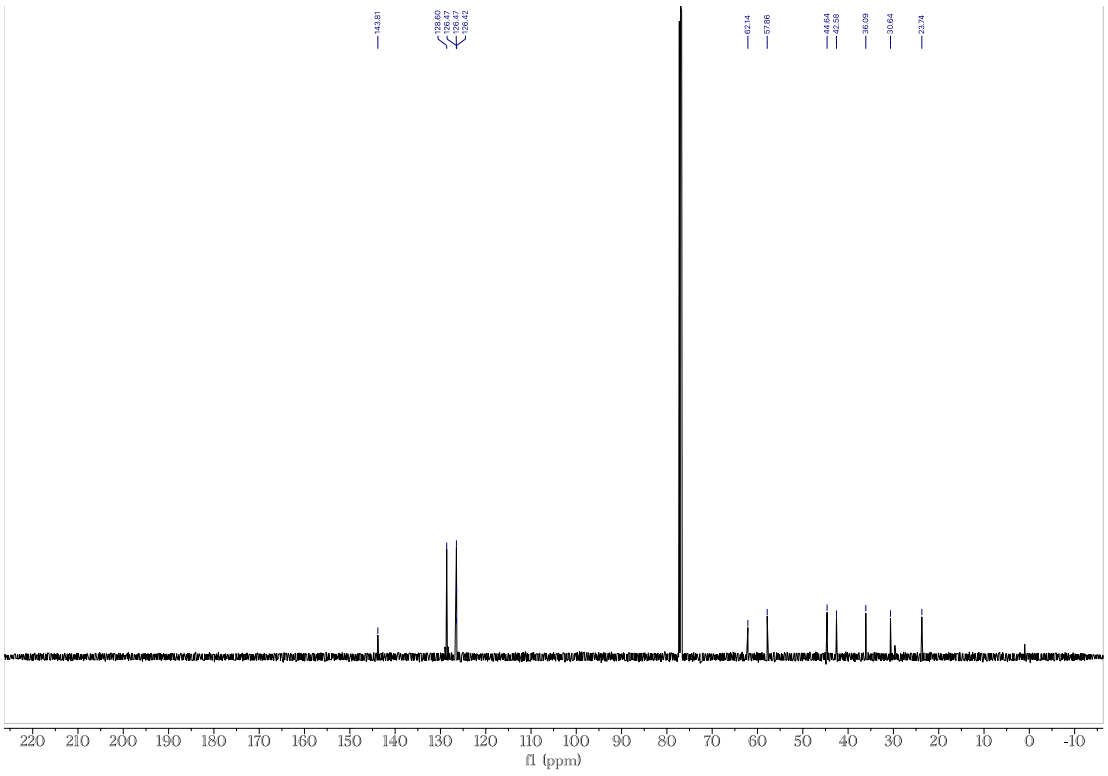
143.81
128.60
126.47
126.07
125.42
62.14
57.86
44.64
42.58
36.09
30.64
23.74
f1 (ppm)

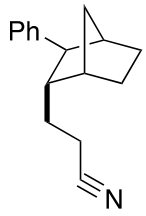
Ph
N

Compound 6a

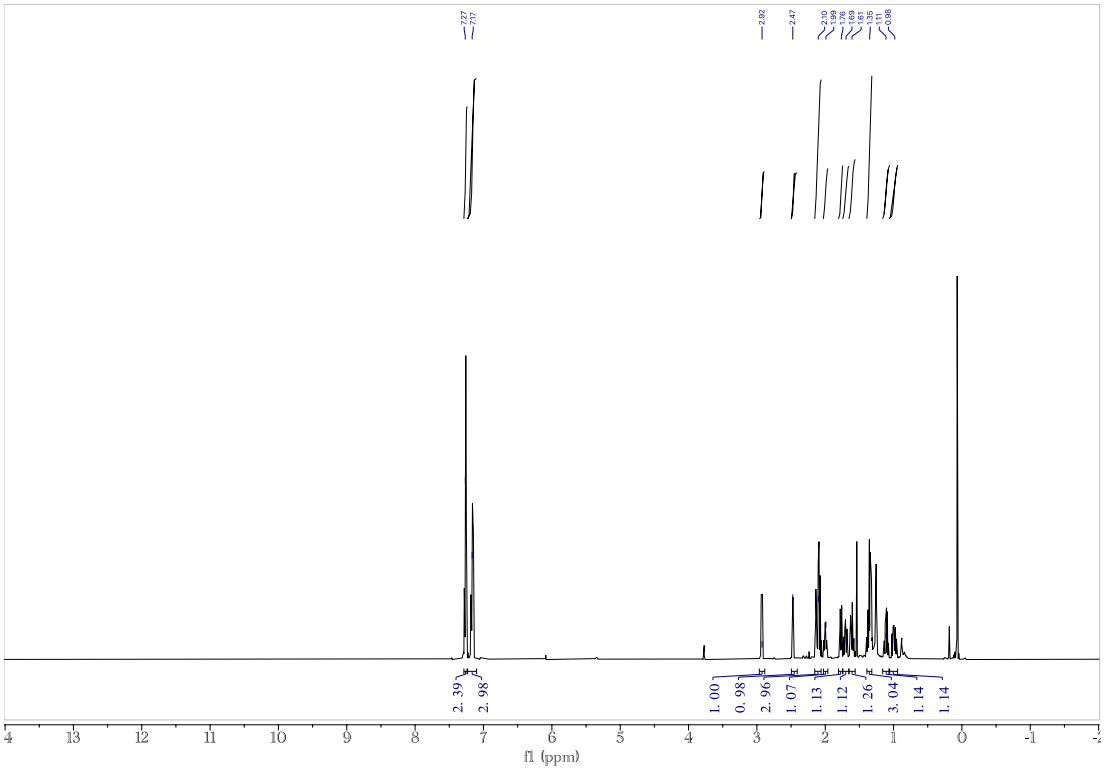
7.27
7.17
2.92
2.47
2.10
1.69
1.76
1.69
1.65
1.35
1.11
1.08
2.39
2.98
1.00
0.98
2.96
1.07
1.13
1.12
1.26
3.04
1.14
1.14
f1 (ppm)

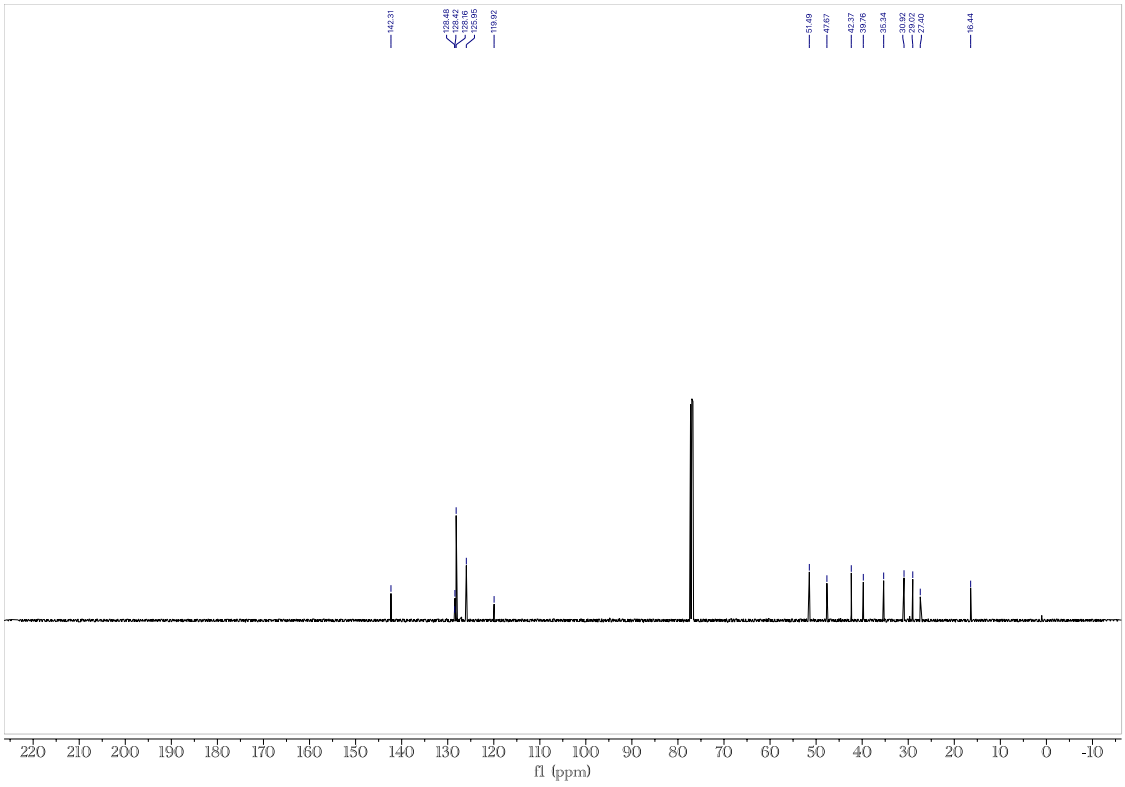
142.31
128.48
128.47
128.16
125.95
119.92
51.49
47.67
42.37
39.76
35.34
30.92
29.02
27.40
16.44
f1 (ppm)

References

1) Newman, S. G.; Lautens, M. Palladium-Catalyzed Carboiodination of Alkenes: Carbon−Carbon Bond Formation with Retention of Reactive Functionality. *J. Am. Chem. Soc.* **2011**, *133* (6), 1778-1780.
2) Liu, H.; Chen, C.; Wang, L.; Tong, X. Pd(0)-Catalyzed Iodoalkynation of Norbornene Scaffolds: The Remarkable Solvent Effect on Reaction Pathway. *Org. Lett.* **2011**, *13* (19), 5072-5075.
3) a) Amatore, C.; Jutand, A.; Thuilliez, A.. Formation of Palladium(0) Complexes from Pd(oac)2 and a Bidentate Phosphine Ligand (dppp) and Their Reactivity in Oxidative Addition. Organometallics **2001**, *20* (15), 3241–3249.
   b) Johansson Seechurn, C. C. C.; Sperger, T.; Scrase, T. G.; Schoenebeck, F.; Colacot, T. J.. Understanding the Unusual Reduction Mechanism of Pd(ii) to Pd(i): Uncovering Hidden Species and Implications in Catalytic Cross-coupling Reactions. *Journal of the American Chemical Society* **2017**, *139* (14), 5194–5200.
   c) Ballestri, M.; Chatgilialoglu, C.; Clark, K. B.; Griller, D.; Giese, B.; Kopping, B. Tris(trimethylsilyl)silane as a radical-based reducing agent in synthesis. *J. Org. Chem.* **1991**, *56* (2), 678-683.
4) Chai, D. I.; Thansandote, P.; Lautens, M. Mechanistic Studies of Pd-Catalyzed Regioselective Aryl C-H Bond Functionalization with Strained Alkenes: Origin of Regioselectivity European *J. Org. Chem.* **2011**, *17* (29), 8175-8188.
5) Catellani, M.; Mealli, C.; Motti, E.; Paoli, P.; Perez-Carreño, E.; Pregosin, P. S. Palladium−Arene Interactions in Catalytic Intermediates: An Experimental and Theoretical Investigation of the Soft Rearrangement between η^1 and η^2 Coordination Modes. *J. Am. Chem. Soc.* **2002**, *124* (16), 4336.
6) Fitton, P.; Rick, EA. *J. The addition of aryl halides to tetrakis(triphenylphosphine)palladium(0) Organomet. Chem.* **1971**, *28* (2), 287- 291.
7) Frisch, M. J.; Trucks, G. W.; Schlegel, H. B.; Scuseria, G. E.; Robb, M. A.; Cheeseman, J. R.; Scalmani, G.; Barone, V.; Petersson, G. A.; Nakatsuji, H.; Li, X.; Caricato, M.; Marenich, A. V.; Bloino, J.; Janesko, B. G.; Gomperts, R.; Mennucci, B.; Hratchian, H. P.; Ortiz, J. V.; Izmaylov, A. F.; Sonnenberg, J. L.; Williams-Young, D.; Ding, F.; Lipparini, F.; Egidi, F.; Goings, J.; Peng, B.; Petrone, A.; Henderson, T.; Ranasinghe, D.; Zakrzewski, V. G.; Gao, J.; Rega, N.; Zheng, G.; Liang, W.; Hada, M.; Ehara, M.; Toyota, K.; Fukuda, R.; Hasegawa, J.; Ishida, M.; Nakajima, T.; Honda, Y.; Kitao, O.; Nakai, H.; Vreven, T.; Throssell, K.; Montgomery, J. A., Jr.; Peralta, J. E.; Ogliaro, F.; Bearpark, M. J.; Heyd, J. J.; Brothers, E. N.; Kudin, K. N.; Staroverov, V. N.; Keith, T. A.; Kobayashi, R.; Normand, J.; Raghavachari, K.; Rendell, A. P.; Burant, J. C.; Iyengar, S. S.; Tomasi, J.; Cossi, M.; Millam, J. M.; Klene, M.; Adamo, C.; Cammi, R.; Ochterski, J. W.; Martin, R. L.; Morokuma, K.; Farkas, O.; Foresman, J. B.; Fox, D. J. Gaussian, Inc., Wallingford CT, 2016.
8) Li, X.; Frisch, M. J. Energy-Represented Direct Inversion in the Iterative Subspace within a Hybrid Geometry Optimization Method. J. Chem. Theory Comput., 2006, 2 (3), 835–839.
9)
   a) Dunning Jr, T. H.; Hay, P. J. Modern Theoretical Chemistry, Ed. III; H. F. Schaefer, Ed.; Plenum: New York, 1997.
   b) Hay, P. J.; Wadt, W. R. Ab Initio Effective Core Potentials for Molecular Calculations. Potentials for the Transition Metal Atoms Sc to Hg. J. Chem. Phys. 1985, 82 (1), 270–283.
   c) Wadt, W. R.; Hay, P. J. Ab Initio Effective Core Potentials for Molecular Calculations. Potentials for Main Group Elements Na to Bi. J. Chem. Phys. 1985, 82 (1), 284–298

d) Hay, P. J.; Wadt, W. R. Ab Initio Effective Core Potentials for Molecular Calculations. Potentials for K to Au Including the Outermost Core Orbitale. J. Chem. Phys. 1985, 82 (1), 299–310.

10)
a) McLean, A.D. Contracted Gaussian Basis Sets for Molecular Calculations. I. Second Row Atoms, Z=11-18. *J. Chem. Phys.*, **1980**, 72, 5639-5648
b) Krishnan, R.; Binkley, J.S.; Seeger, R.; Pople, J.A. Self-consistent Molecular Orbital Methods. XX. A Basis Set for Correlated Wave Functions. *J. Chem. Phys.*, **1980**, 72, 650-654
c) McGrath, M.P.; Radom, L. Extension of Gaussian-1 (G1) Theory to Bromine-containing Molecules. *J. Chem. Phys.*, **1991**, 94, 511-516
d) Curtiss, L.A. Extension of Gaussian-2 Theory to Molecules containing Third-row Atoms Ga-Kr. *J. Chem. Phys.*, **1995**, 103, 6104-6113
e) Binning Jr., R.C.; Curtiss, L.A. Compact Contracted Basis Sets for Third-row Atoms: Ga-Kr. *J. Comp. Chem.*, **1990**, 11, 1206-1216
f) Frisch, M. J.; Pople, J. A.; Binkley, J. S. Self-Consistent Molecular Orbital Methods 25. Supplementary Functions for Gaussian Basis Sets. *J. Chem. Phys.* **1984**, *80* (7), 3265–3269
g) Clark, T.; Chandrasekhar, J.; Spitznagel, G.W.; Schleyer, P.v.R. Efficient Diffuse Function-augmented Basis-sets for Anion Calculations. III. The 3-21+G Basis Set for First-row Elements Li-F. *J. Comp. Chem.*, **1983**, 4, 294-301

11) Clark, T.; Chandrasekhar, J.; Spitznagel, G.W.; Schleyer, P.v.R. Efficient Diffuse Function-augmented Basis-sets for Anion Calculations. III. The 3-21+G Basis Set for First-row Elements Li-F. *J. Comp. Chem.*, **1983**, 4, 294-301

12) Clark, T.; Chandrasekhar, J.; Spitznagel, G.W.; Schleyer, P.v.R. Efficient Diffuse Function-augmented Basis-sets for Anion Calculations. III. The 3-21+G Basis Set for First-row Elements Li-F. *J. Comp. Chem.*, **1983**, 4, 294-301

13) Clark, T.; Chandrasekhar, J.; Spitznagel, G.W.; Schleyer, P.v.R. Efficient Diffuse Function-augmented Basis-sets for Anion Calculations. III. The 3-21+G Basis Set for First-row Elements Li-F. *J. Comp. Chem.*, **1983**, 4, 294-301

14)
a) Dunning, T. H.; Hay, P. J. Modern Theoretical Chemistry, Ed. H. F. Schaefer III, Vol. 3 (plenum, New York, 1977) 1-28
b) Bergner, A.; Dolg, M.; Kuechle, W.; Stoll, H.; Preuss, H. Mol. Phys. **1993**, *80*, 1431-1441

15) Marenich, A. V.; Cramer, C. J.; Truhlar, D. G. Universal Solvation Model Based on Solute Electron Density and on a Continuum Model of the Solvent Defined by the Bulk Dielectric Constant and Atomic Surface Tensions. *J. Phys. Chem.* **2009**, *113* (18), 6378–6396.

16) Hopmann, K. H. How Accurate Is DFT for Iridium-Mediated Chemistry? *Organometallics* **2016**, *35* (22), 3795–3807.

17) Ryu, H.; Park, J.; Kim, H. K.; Park, J. Y.; Kim, S. -T.; Baik, M. -H. *Organometallics*, **2018**, *37*, 3228-3239

18) These calculations were carried out with the Python script GoodVibes. I. Funes-Ardoiz and R. S. Paton GoodVibes.py, DOI: 10.5281/zeonodo.124756

19) C. Y. Legault, CYLview, 1.0b; Université de Sherbrooke, Sherbrooke, Quebec, Canada, 2009; http://www.cylview.org.

Acetate Facilitated Nickel Catalyzed Cross-Coupling of Aryl Chlorides and Alkyl Thiols

Regina M. Oechsner, J. Philipp Wagner, Ivana Fleischer*

*Institut of Organic Chemistry, University of Tübingen, Auf der Morgenstelle 18, DE-72076 Tübingen, Germany

Through the Migita reaction, a metal catalyzed C-S cross-coupling of aryl halides and thiols under basic conditions, thioethers can be efficiently generated.[1] The bioisoster of ethers is an attractive structural motif in pharmaceutical compounds. So far mainly palladium catalyzed reactions are of industrial use, but low-cost nickel-catalyzed methods could replace them in the future. Previously reported nickel-catalyzed methods for the coupling of challenging aryl chlorides commonly employ expensive, air sensitive transmetalation reagents (e.g. PhZnCl)[2] or high temperatures. Herein, we report a mild and convenient catalytic system for the coupling of aryl chlorides and primary, secondary as well as previously challenging tertiary alkyl thiols using an air-stable Ni(II) precatalyst in combination with the low-cost base KOAc at room temperature.[3] It enables the generation of thioethers from a wide range of substrates in good to excellent yields, tolerating a variety of functional groups and pharmaceutical compounds. Chemoselective functionalization of disubstituted substrates was demonstrated. Kinetic and NMR studies, as well as DFT computations support a Ni(0)/Ni(II) catalytic cycle with the oxidative addition product as resting state and acetate playing a key role in the formation of a thiolate complex via internal deprotonation.

Nickel Catalyzed C-S Coupling: Challenges

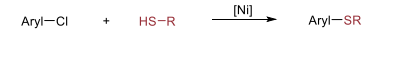

ArylCl as substrate
- *high BDE of C-Cl*
- *less reactive*
- *but available and cheap*

aliphatic 3° thiols
- *often low yields*
- *side reactions*
- *unexplored*

reaction conditions
- *high-cost*
- *high temperature*
- *long reaction time*

This Work

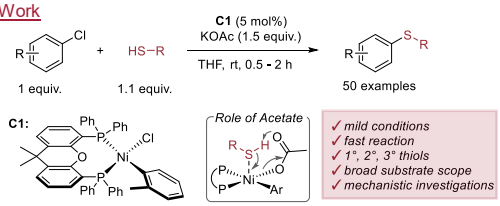

- ✓ *mild conditions*
- ✓ *fast reaction*
- ✓ *1°, 2°, 3° thiols*
- ✓ *broad substrate scope*
- ✓ *mechanistic investigations*

Base Screening

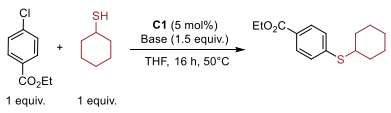

Base	Conv. [%]	Yield [%]
NaO^{t}Bu	81	62
KO^{t}Bu	75	25
Li_2CO_3	13	10
Na_2CO_3	60	56
K_2CO_3	56	52
Cs_2CO_3	12	9
$Zn(OPiv)_2$	34	33
$Zn(OAc)_2$	60	54
Na_2HPO_4	65	62
Sodiumcitrate	44	42
NaOAc	89	85

Acetate Screening

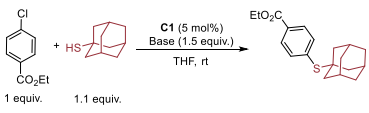

Base	time [h]	Conv. [%]	Yield [%]
LiOAc	2	4	0
LiOAc	16	5	2
NaOAc	2	20	14
NaOAc	16	86	83
KOAc	2	95	95
CsOAc	2	95	93

Substrate Scope

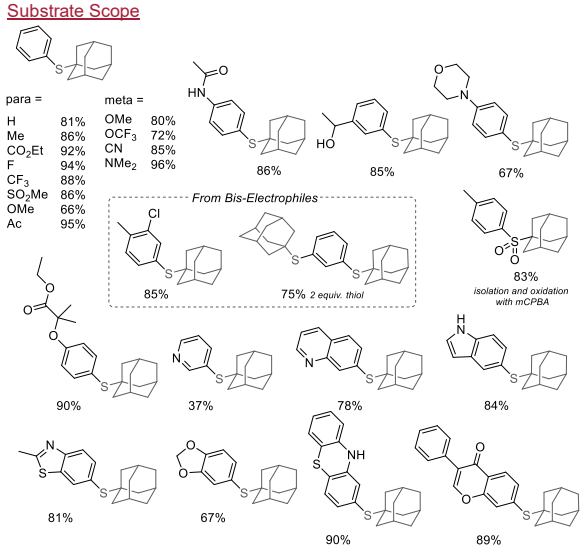

From Biorelevant Substrates

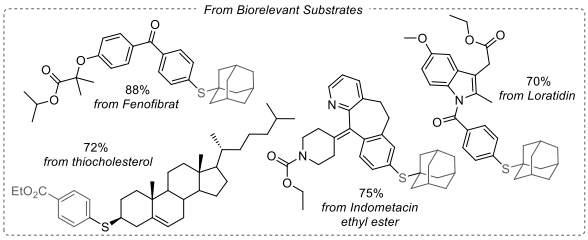

Comparison of 1°, 2°, 3° Thiols

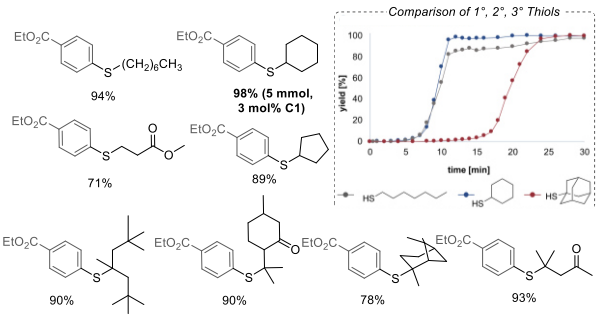

Alternative Electrophiles

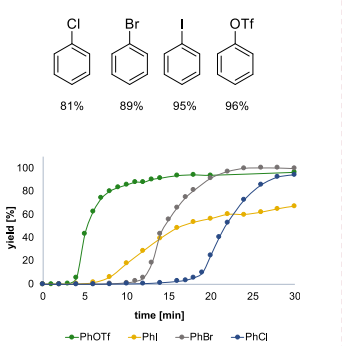

Chemoselective Monosubstitution

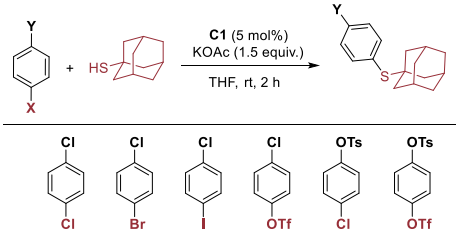

One-Pot Chemoselective Disubstitution

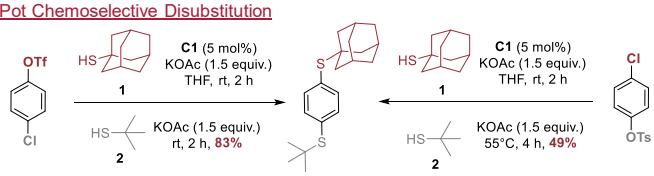

Postulated Mechanism

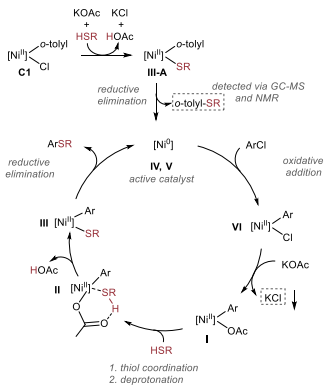

Oxidative-Addition Intermediate ^{31}P NMR

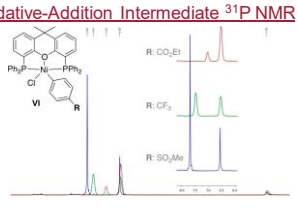

DFT Computations

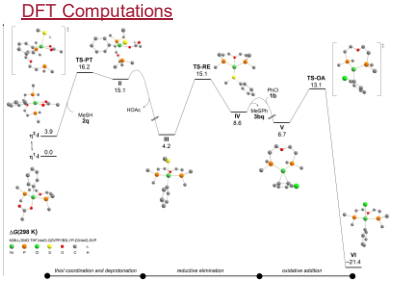

[1] Kosugi, M.; Shimizu, T.; Migita, T. *Chem. Lett.* **1978,** 7, *13.* Migita, T.; Shimizu, T.; Asami, Y.; Shiobara, J.-i.; Kato, Y.; Kosugi, M. *Bull. Chem. Soc. Jpn.* **1980,** 53, *1385.*
[2] P. Gehrtz, V. Geiger, T. Schmidt, L. Sršan, I. Fleischer, *Org. Lett.* **2019**, 21, *50 - 55.* [3] R. M. Oechsner, J. P. Wagner, I. Fleischer, *ACS Catal.* **2022**, 12, *2233−2243.*

Chapter 6

APPENDIX

6. Appendix

List of Abbreviations

Å	Ångström
acac	Acetylacetonate
Acety-CoA	Acetyl-Coenzyme A
Ar	Aryl
ArX	Aryl halide
BCE	Before common era
BDE	Bond dissociation energy
BINAP	2,2'-Bis(diphenylphosphino)-1,1'-binapthyl
BINOL	1,1'-Bi-2-naphthol
BOX	Bis(oxazoline)
Bpy (**L11**)	2,2'-Bipyridine
CMD	Concerted metalation-deprotonation
cod	1,5-Cyclooctadiene
conv.	Conversion
ΔG	Gibbs free energy
DABCO	1,4-Diazabicyclo[2.2.2]octane
dba	Dibenzylideneacetone
DCM	Dichloromethane
DFT	Density functional theory
DMA	N,N-Dimethylacetamide
DMAP	4-N,N-Dimethylaminopyridine
DME	1,2-Dimethoxyethane
DMEDA (**L15**)	N,N-Dimethylethylenediamine
DMF	N,N-Dimethylformamide
DMI	1,3-Dimethyl-2-imidazolidinone
DMSO	Dimethyl sulfoxide
DNA	Deoxyribonucleic acid
DPEPhos	Bis((2-dipenylphosphino)phenyl)ether
dppb	1,4-Bis(diphenylphosphino)butane
dppbz	1,2-Bis(diphenylphosphino)benzene
dppe	1,2-Bis(diphenylphosphino)ethane
dppf (**L7**)	1,1'-Bis(diphenylphosphino)ferrocene
dpppe (**L22**)	1,5-Bis(diphenylphosphino)pentane
e.g.	Exempli gratia
E_A	Activation energy
equiv.	Equivalents
et al.	et alii

EtOH	Ethanol
FID	Flame ionization detector
GC	Gas chromatography
h	Hours
η	Hapticity
HPLC	High-performance liquid chromatography
Hz	Hertz
^{i}Pent	Isopentyl
^{i}Pr	Isopropyl
κ	Denticity
LDA	Lithium diisopropylamide
LED	Light-emitting diode
LiHMDS	Lithium bis(trimethylsilyl)amide
mA	Milliampere
Me	Methyl
MeCN	Acetonitrile
min	Minutes
none	No yield
NHC	N-Heterocyclic carbene
NMP	N-Methyl-2-pyrrolidone
NMR	Nuclear magnetic resonance
OAc	Acetate
OMs	Mesylate (methanesulfonate)
OTf	Triflate (trifluoromethanesulfonate)
OTs	Tosylate (4-methylbenzenesulfonate)
$P(O^{i}Pr)_3$	Triisopropylphosphine
PCy_3	Tricyclohexylphosphine
Pd(0)*	Exited state palladium complex
PEPPSI	Pyridine-enhanced pre-catalyst preparation stabilization and initiation
Ph	Phenyl
phen (**L8**)	Phenanthroline
PMe_3	Trimethylphosphine
PPh_3	Triphenylphosphine
PTABS (**L4**)	1,3,5-Triaza-7-phosphaadamantane
$P^{t}Bu_3$	Tri-tert-butylphosphine
Q-Phos (**L20**)	Pentaphenyl(di-tert-butylphosphino)ferrocene
quant.	Quantitative conversion (> 99% yield)
ROH	Alcohol
rt	Room temperature
ρ	Hammett reaction rate constant
SET	Single-electron-transfer

σ_p	Hammett substituent constant (para)
$t^{1/2}$	Half-life
TBHP	tert-Butyl hydroperoxide
traces	< 5% yield
^{t}BuBrettPhos (**L3**)	Bis(2-methyl-2-propanyl)(2',4',6'-triisopropyl-3,6-dimethoxy-2-biphenylyl)phosphine
^{t}BuXPhos (**L2**)	Bis(2-methyl-2-propanyl)(2',4',6'-triisopropyl-2-biphenylyl)phosphine
Tf_2O	Trifluoromethanesulfonic anhydride
THF	Tetrahydrofuran
UV	Ultraviolet
wt%	Percentage by weight
X	Halide
Xantphos (**L6**)	4,5-Bis-(diphenylphosphino)-9,9-dimethylxanthen
1°, 2°, 3°	Primary, secondary, tertiary
((( )))	Ultrasonic
(R)-Tol-BINAP (**L5**)	(*R*)-(+)-2,2′-Bis(di-p-tolylphosphino)-1,1′-binaphthyl
†	Co-author
	Irradiation of the reaction mixture with blue light (465 nm LED)

Table 6. Cost for catalyst precursors (Sigma-Aldrich price, 14.06.2023).

Catalyst precursor	CAS	Sigma-Aldrich	Purity [%]	Weight [g]	Price [€]	Price per g [€]
$NiCl_2 \cdot 6H_2O$	7791-20-2	223387	> 99	25	62.40	2.50
$PdCl_2$	7647-10-1	921033	> 99	25	1780.00	71.20
$Ni(OAc)_2 \cdot 4H_2O$	6018-89-9	244066	98	100	27.90	0.28
$(Pd(OAc)_2)_3$	3375-31-3	205869	98	100	6320.00	63.20
$Ni(cod)_2$	1295-35-8	244988	-	2	128.80	64.40
$Pd_2(dba)_3$	51364-51-3	328774	97	1	83.80	83.80